DEEP SUBSURFACE MICROBIOLOGY

EDITED BY: Andreas Teske, Jennifer F. Biddle, Virginia P. Edgcomb and Axel Schippers

PUBLISHED IN: Frontiers in Microbiology

frontiers Research Topics

frontiers

ISSN 1664-8714
ISBN 978-2-88919-536-7
DOI 10.3389/978-2-88919-536-7

About Frontiers

Frontiers is more than just an open-access publisher of scholarly articles: it is a pioneering approach to the world of academia, radically improving the way scholarly research is managed. The grand vision of Frontiers is a world where all people have an equal opportunity to seek, share and generate knowledge. Frontiers provides immediate and permanent online open access to all its publications, but this alone is not enough to realize our grand goals.

Frontiers Journal Series

The Frontiers Journal Series is a multi-tier and interdisciplinary set of open-access, online journals, promising a paradigm shift from the current review, selection and dissemination processes in academic publishing. All Frontiers journals are driven by researchers for researchers; therefore, they constitute a service to the scholarly community. At the same time, the Frontiers Journal Series operates on a revolutionary invention, the tiered publishing system, initially addressing specific communities of scholars, and gradually climbing up to broader public understanding, thus serving the interests of the lay society, too.

Dedication to Quality

Each Frontiers article is a landmark of the highest quality, thanks to genuinely collaborative interactions between authors and review editors, who include some of the world's best academicians. Research must be certified by peers before entering a stream of knowledge that may eventually reach the public - and shape society; therefore, Frontiers only applies the most rigorous and unbiased reviews.
Frontiers revolutionizes research publishing by freely delivering the most outstanding research, evaluated with no bias from both the academic and social point of view.
By applying the most advanced information technologies, Frontiers is catapulting scholarly publishing into a new generation.

What are Frontiers Research Topics?

Frontiers Research Topics are very popular trademarks of the Frontiers Journals Series: they are collections of at least ten articles, all centered on a particular subject. With their unique mix of varied contributions from Original Research to Review Articles, Frontiers Research Topics unify the most influential researchers, the latest key findings and historical advances in a hot research area! Find out more on how to host your own Frontiers Research Topic or contribute to one as an author by contacting the Frontiers Editorial Office: **researchtopics@frontiersin.org**

DEEP SUBSURFACE MICROBIOLOGY

Topic Editors:
Andreas Teske, University of North Carolina at Chapel Hill, USA
Jennifer F. Biddle, University of Delaware, USA
Virginia P. Edgcomb, Woods Hole Oceanographic Institution, USA
Axel Schippers, Federal Institute for Geosciences and Natural Resources, Germany

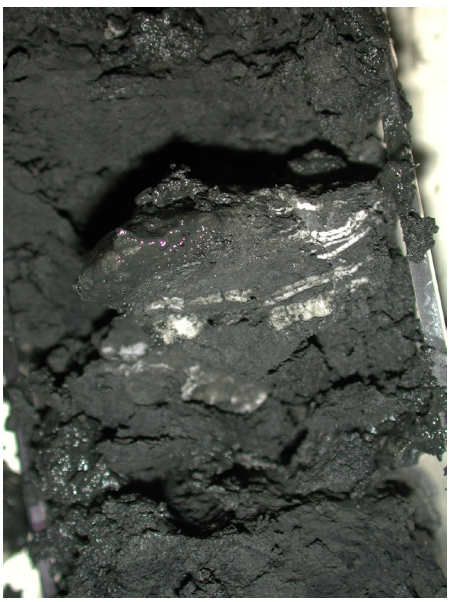

Methane hydrate in deep subsurface sediment of the Peru Trench, drilling site 1230 of the Ocean Drilling Program. This subsurface hydrate sample was dissolving within minutes after shipboard recovery from over 5000 m water depth and ca. 100 m sediment depth. The microbial communities and geochemical parameters of the highly reducing, sulfidic and methane-rich sediments of ODP site 1230 are included in this research topic (Durbin and Teske, doi: 10.3389/fmicb.2012.00168). Image by courtesy of the Leg 201 shipboard Party

Deep subsurface microbiology is a highly active and rapidly advancing research field at the interface of microbiology and the geosciences; it focuses on the detection, identification, quantification, cultivation and activity measurements of bacteria, archaea and eukaryotes that permeate the subsurface biosphere of deep marine sediments and the basaltic ocean and continental crust. The deep subsurface biosphere abounds with uncultured, only recently discovered and – at best – incompletely understood microbial populations. In spatial extent and volume, Earth's subsurface biosphere is only rivaled by the deep sea water column.

So far, no deep subsurface sediment has been found that is entirely devoid of microbial life; microbial cells and DNA remain detectable at sediment depths of more than 1 km; microbial life permeates deeply buried hydrocarbon reservoirs, and is also found several kilometers down in continental crust aquifers. Severe energy limitation, either as electron acceptor or donor shortage, and scarcity of microbially degradable organic carbon sources are among the evolutionary pressures that have shaped the genomic and physiological repertoire of the deep subsurface biosphere. Its biogeochemical role as long-term organic carbon repository, inorganic electron and energy source, and subduction recycling engine continues to be explored by current research at the interface of microbiology, geochemistry and biosphere/geosphere evolution.

This Research Topic addresses some of the central research questions about deep subsurface microbiology and biogeochemistry: phylogenetic and physiological microbial diversity in the deep subsurface; microbial activity and survival strategies in severely energy-limited subsurface habitats; microbial activity as reflected in process rates and gene expression patterns; biogeographic isolation and connectivity in deep subsurface microbial communities; the ecological standing of subsurface biospheres in comparison to the surface biosphere – an independently flourishing biosphere, or mere survivors that tolerate burial (along with organic carbon compounds), or a combination of both? Advancing these questions on Earth's deep subsurface biosphere redefines the habitat range, environmental tolerance, activity and diversity of microbial life.

Citation: Teske, A., Biddle, J. F., Edgcomb, V. P., Schippers, A., eds. (2015). Deep Subsurface Microbiology. Lausanne: Frontiers Media. doi: 10.3389/978-2-88919-536-7

Table of Contents

frontiers in MICROBIOLOGY

ORIGINAL RESEARCH ARTICLE
published: 19 July 2011
doi: 10.3389/fmicb.2011.00156

The deep biosphere in terrestrial sediments in the Chesapeake Bay area, Virginia, USA

Anja Breuker[1,2], Gerrit Köweker[1], Anna Blazejak[1†] and Axel Schippers[1,2]*

[1] *Geomicrobiology, Federal Institute for Geosciences and Natural Resources, Hannover, Germany*
[2] *Faculty of Natural Sciences, Leibniz Universität Hannover, Hannover, Germany*

Edited by:
Andreas Teske, University of North Carolina at Chapel Hill, USA

Reviewed by:
Marco J. L. Coolen, Woods Hole Oceanographic Institution, USA
Karine Alain, Centre National de la Recherche Scientifique, France

***Correspondence:**
Axel Schippers, Bundesanstalt für Geowissenschaften und Rohstoffe, Stilleweg 2, 30655 Hannover, Germany.
e-mail: axel.schippers@bgr.de

†Current Address
Anna Blazejak, Max Planck Institute for Marine Microbiology, Bremen, Germany.

For the first time quantitative data on the abundance of *Bacteria, Archaea,* and *Eukarya* in deep terrestrial sediments are provided using multiple methods (total cell counting, quantitative real-time PCR, Q-PCR and catalyzed reporter deposition–fluorescence *in situ* hybridization, CARD–FISH). The oligotrophic (organic carbon content of ∼0.2%) deep terrestrial sediments in the Chesapeake Bay area at Eyreville, Virginia, USA, were drilled and sampled up to a depth of 140 m in 2006. The possibility of contamination during drilling was checked using fluorescent microspheres. Total cell counts decreased from 10^9 to 10^6 cells/g dry weight within the uppermost 20 m, and did not further decrease with depth below. Within the top 7 m, a significant proportion of the total cell counts could be detected with CARD–FISH. The CARD–FISH numbers for *Bacteria* were about an order of magnitude higher than those for *Archaea*. The dominance of *Bacteria* over *Archaea* was confirmed by Q-PCR. The down core quantitative distribution of prokaryotic and eukaryotic small subunit ribosomal RNA genes as well as functional genes involved in different biogeochemical processes was revealed by Q-PCR for the uppermost 10 m and for 80–140 m depth. *Eukarya* and the Fe(III)- and Mn(IV)-reducing bacterial group *Geobacteriaceae* were almost exclusively found in the uppermost meter (arable soil), where reactive iron was detected in higher amounts. The bacterial candidate division JS-1 and the classes *Anaerolineae* and *Caldilineae* of the phylum *Chloroflexi*, highly abundant in marine sediments, were found up to the maximum sampling depth in high copy numbers at this terrestrial site as well. A similar high abundance of the functional gene *cbbL* encoding for the large subunit of RubisCO suggests that autotrophic microorganisms could be relevant in addition to heterotrophs. The functional gene *aprA* of sulfate reducing bacteria was found within distinct layers up to ca. 100 m depth in low copy numbers. The gene *mcrA* of methanogens was not detectable. Cloning and sequencing data of 16S rRNA genes revealed sequences of typical soil *Bacteria*. The closest relatives of the archaeal sequences were *Archaea* recovered from terrestrial and marine environments. Phylogenetic analysis of the *Crenarchaeota* and *Euryarchaeota* revealed new members of the uncultured South African Gold Mine Group, Deep Sea Hydrothermal Vent Euryarchaeotal Group 6, and Miscellaneous Crenarcheotic Group clusters.

Keywords: CARD–FISH, Chesapeake Bay, *Crenarchaeota*, deep biosphere, *Euryarchaeota*, real-time PCR, sediments, subsurface

INTRODUCTION

The Earth's deep biosphere includes a variety of subsurface habitats, such as mines and deep aquifer systems in the continental realm, and sediments and igneous rock in the marine realm. It has been estimated that nearly half of total biomass on Earth resides in the deep biosphere (Whitman et al., 1998). However, the existing data used to generate this global census are highly skewed and in reality reflect habitat accessibility. Deeply buried marine sediments are among the best studied deep biosphere habitats. They are populated by a huge number of prokaryotes mainly belonging to uncultivated phylogenetic lineages (Parkes et al., 2000; Teske, 2006; Biddle et al., 2008; Fry et al., 2008; Teske and Sørensen, 2008). The abundance of particular phylogenetic and physiological prokaryotic groups, i.e., *Archaea* and *Bacteria*, methanogens or sulfate reducers, in deeply buried marine sediments has been quantified based on 16S rRNA and functional gene analysis by quantitative, real-time PCR (Q-PCR), FISH, and catalyzed reporter deposition–fluorescence *in situ* hybridization (CARD–FISH; Schippers et al., 2005; Biddle et al., 2006; Inagaki et al., 2006; Schippers and Neretin, 2006; Engelen et al., 2008; Nunoura et al., 2009; Webster et al., 2009).

The terrestrial deep subsurface biosphere has been studied so far only by total cell counting, cultivation techniques as well as by molecular 16S rRNA gene diversity analyses. The hard rock terrestrial deep biosphere in, e.g., granite, basalt, or metabasalt has been mainly explored by groundwater analyses rather than by deep

rock drilling (Pedersen, 1993, 1997; Stevens and McKinley, 1995; Fredrickson et al., 1997; Chapelle et al., 2002; Moser et al., 2003; Lin et al., 2006; Hallbeck and Pedersen, 2008; Sahl et al., 2008; Borgonie et al., 2011; Itävaara et al., 2011).

Deep subsurface terrestrial sediments defined as deeper than 30–35 m (Balkwill et al., 1989) have just begun to be studied by molecular techniques. Cell numbers determined by total cell counting or cultivation indicate that a correlation of cell numbers with depth as described for marine sediments (Parkes et al., 1994, 2000) does not exist. Fry et al. (2009) did not find a decrease in cell numbers with depth in a terrestrial drill core of 148 m length including an interbedded coal deposit in New Zealand. Hoos and Schweisfurth (1982) also did not find a decreasing number of colony forming units (CFU) with depth after analyzing cultivable aerobic and anaerobic bacteria up to a sediment depth of 90 m in Lower Saxony, Germany. The lack of decreasing cell numbers with sediment depth is also supported by AODC and CFU numbers in coastal plain and fluvial sediment cores from South Carolina (Savannah River Site) and Washington State (Hanford Site), USA, sampled up to 265 m depth (Balkwill et al., 1989; Sinclair and Ghiorse, 1989; Fredrickson et al., 1991; Kieft et al., 1995) and Cretaceous sedimentary rock in New Mexico, USA at 190 m depth (Takai et al., 2003).

Analysis of the microbial diversity by 16S rRNA gene sequencing revealed the dominance of the following prokaryotic groups in deep terrestrial sediments. Most abundant among the *Bacteria* were *Proteobacteria, Actinobacteria, Firmicutes, Chloroflexi*, members of the *Geobacteraceae* family, sulfate reducers, denitrifiers, fermenters, and acetogens. The most frequently occurring *Archaea* were the Miscellaneous Crenarchaeotic Group, *Methanosarcinales* and *Methanobacteriales* (Boivin-Jahns et al., 1996; Chandler et al., 1997; Detmers et al., 2001, 2004; Takai et al., 2003; Inagaki et al., 2005; Kovacik et al., 2006; Brown and Balkwill, 2009; Fry et al., 2009).

Organic carbon seems to be most important for the long term survival of microorganisms in the terrestrial deep biosphere because a correlation was found between total organic carbon (TOC) and direct counts, basal respiration as well as aerobic glucose mineralization (e.g., Kieft et al., 1995).

The aim of this study was a comprehensive microbial community analysis of deep terrestrial sediments in order to provide missing quantitative data on the abundance of prokaryotes in the terrestrial deep biosphere. As terrestrial study site, deep sediments up to a depth of 140 m in the Chesapeake Bay area at Eyreville, Virginia, USA, were chosen. Total cells stained with SYBR Green were counted with three different methods and the microbial diversity was explored by 16S rRNA gene cloning and sequencing. In addition, Q-PCR and CARD–FISH were applied for the first time to study the deep biosphere in terrestrial sediments. With these quantitative methods, 16S rRNA and functional genes of phylogenetic and physiological prokaryotic groups relevant in deeply buried marine sediments were analyzed.

MATERIALS AND METHODS

SITE AND SEDIMENT DESCRIPTION

The Chesapeake Bay impact structure (CBIS), Virginia, USA, was formed during the late Eocene meteoric impact approximately 35.5 million years (Ma) ago. It has been explored by an international team of scientists in a project of the International Continental Scientific Drilling Program (ICDP) and the U.S. Geological Survey (USGS, Gohn et al., 2006, 2008, 2009). A cross-section figure showing main features of the CBIS and the drill site location is shown elsewhere (Gohn et al., 2008). The CBIS project acquired continuously cored sections from three holes drilled to a composite depth of 1766 m at a site within the central zone of the structure at the Eyreville drill site near Cape Charles, Virginia, USA. The drill bit penetrated a 1322-m-thick section of impact-related rocks and sediments and an overlying 444-m-thick section of post-impact sandy and clayish sediments. The latter consist of upper Eocene to Pliocene (∼5.3 to ∼1.8 Ma) continental-shelf sediments and Pleistocene (∼1.8 to ∼0.01 Ma) non-marine sediments. The upper 140 m (Miocene to Pleistocene) studied here were cored in Eyreville hole C during April and May 2006. In this depth interval, the porosity is between 36 and 54%, and the pore water chemistry indicates freshwater conditions, however the NaCl concentration is ∼0.2% at 100 m depth and increases to ∼1% at the bottom of the core (Gohn et al., 2006, 2008, 2009). In this study only post-impact sediments up to 140 m depth not influenced by the meteoric impact were analyzed.

SEDIMENT SAMPLING

In this study, cores from Eyreville hole C were sampled for terrestrial microbial community analysis. Fifty sediment samples were taken from the surface (arable soil) down to a depth of up to 140 m. To avoid contamination, samples for microbiological analysis were only taken from the center of each sediment core (63.5 mm diameter) using sterilized cut 5 mL syringes or sterilized spatulas. Depth intervals for sampling were selected based on the quality of the cores with a higher depth resolution near the surface and a lower one at greater depth. As a contamination control, fluorescent microspheres were applied during coring for every second core and samples were taken from the periphery as well as the center of the cores for microscopic inspection as previously described (Kallmeyer et al., 2006; Gohn et al., 2009). Four samples could be identified as potentially contaminated and were not further analyzed.

For CARD–FISH and counting total cells with fluorescence microscopy, sediment samples were fixed in 4% formaldehyde–PBS (phosphate buffered saline) as described by Llobet-Brossa et al. (1998) and finally stored at −20°C in PBS–ethanol (1:1). For DNA based molecular as well as geochemical analysis, a parallel set of samples was directly frozen at −20°C. All samples were transported to BGR frozen with dry ice as air-freight, and afterward stored at −20°C until analysis.

GEOCHEMICAL ANALYSIS

The elemental composition of the solid material was determined by XRF analysis (Philips PW 2400). TOC and the total amount of carbon (TC) and sulfur (TS) were measured with the instrument LECO CS 200 (LECO Corporation). TC and TS were measured after acid removal of carbonates. Reactive iron was extracted with buffered citrate–dithionite as described by Canfield (1989), and measured by ICP-OES (Jobin Yvon Emission 166 Ultrace HR 1000).

TOTAL CELL COUNTS AND CARD–FISH

Total cell numbers were determined in formaldehyde fixed samples by staining with SYBR Green II following three different protocols. Cells were counted in the sediment matrix as described by Weinbauer et al. (1998) and were detached from sediment particles before counting as described by Kallmeyer et al. (2008) and Lunau et al. (2005). The latter protocol was modified by replacing the ultrasonic bath with an ultrasonic probe. CARD–FISH was carried out as described (Pernthaler et al., 2002; Schippers et al., 2005) and filters were hybridized for *Archaea* and *Bacteria* using probes ARCH915 or EUB338 I-III as a mixture. As a negative hybridization control the probe NON-338 was applied. For contamination control fluorescent beads of bacterial size were used and counted.

QUANTITATIVE REAL-TIME PCR ANALYSIS

The quantitative composition of the microbial community was analyzed by Q-PCR after DNA extraction. High-molecular-weight DNA was extracted from 0.5 g of a frozen sediment sample following a modified FastDNA Spin Kit for Soil (Bio101) protocol (Webster et al., 2003). Sterilized quartz sand treated in a muffle furnace for organic carbon removal was used as negative control in the extraction procedure. Extracted DNA was amplified by Q-PCR using the device ABI Prism 7000 (Applied Biosystems) and master mixes from the companies Applied Biosystems, Eurogentec, or Invitrogen. Each DNA extract was measured in triplicate. After each Q-PCR, melting curves were measured for SYBR Green I assays. The copy numbers of the 16S rRNA gene were quantified for *Archaea* (Takai and Horikoshi, 2000), *Bacteria* (Nadkarni et al., 2002), the JS-1- and *Chloroflexi*-related bacteria (Blazejak and Schippers, 2010), and the Fe(III)- and Mn(IV)-reducing family *Geobacteraceae* (Holmes et al., 2002). The 18S rRNA gene of *Eukarya* was determined as previously described (Schippers and Neretin, 2006). Functional genes were quantified as described: *mcrA* for methyl coenzyme M reductase subunit A (Wilms et al., 2007), *aprA* for adenosine 5′-phosphosulfate reductase subunit A (Blazejak and Schippers, submitted), and *cbbL* for the large subunit of the enzyme ribulose-1.5-bisphosphate carboxylase/oxygenase (RubisCO, form I "red-like"; Selesi et al., 2007).

CLONING AND SEQUENCING

High-molecular-weight DNA was extracted from 0.5 g of a frozen sediment sample as described above. Four depths (75–108 m) were analyzed for bacterial 16S rRNA gene sequences and two depths (108–125 m) were analyzed for archaeal 16S rRNA gene sequences. PCR reactions were carried out with the 1.1 or 2 Master Mix® (Thermo Scientific). PCR for *Bacteria* was carried out with the universal primers GM3f (AGA GTT TGA TCM TGG C) and GM4r (TAC CTT GTT ACG ACT T; Muyzer et al., 1995). The following thermocycling conditions were used: one cycle at 95 or 96°C for 5 min; 26–30 cycles at 95 or 96°C for 1 min, 42°C for 1 min, and 72°C for 3 min; and one cycle at 72°C for 7 min. PCR for *Archaea* was carried out with the primers 109f (ACK GCT CAG TAA CAC GT; Grosskopf et al., 1998) and 912r (CTC CCC CGC CAA TTC CTT TA; Lueders and Friedrich, 2000). These thermocycling conditions were used: one cycle at 95°C for 5 min; 26–30 cycles at 95°C for 1 min, 52°C for 1 min, and 72°C for 3 min; and one cycle at 72°C for 6 min. Cloning in *Escherichia coli* was carried out with the pGEM-t-Easy Vector Systems (Promega®) Kit following the instruction manual. For screening of 16S rRNA genes, 96 clones per sample were randomly picked. For template DNA, a small amount of cells from each clone colony was picked with a sterile toothpick and suspended in 20 μL of sterile water. One or two microliter of this template DNA, after preheating to 95°C for 2 min, were amplified by PCR as described above by using a 25- to 50-μL (total volume) mixture. PCR products of the correct size (∼1500 bp resp. 850 bp) were purified with the QIAquick PCR Purification Kit (Quiagen®) or directly send for sequencing. Sequencing reactions were carried out by Seqlab Laboratories, Göttingen, Germany. Sequences were edited with BioEdit[1]. A negative DNA extraction control without sediment was treated in parallel. For *Bacteria*, PCR products were also obtained for this negative control (presumably contaminants). The negative control of the PCR reaction itself was negative. In conclusion presumably contamination happened during the DNA extraction procedure. Fifty clones resulting from the negative control were analyzed using BLAST. Partial sequences from sediment samples which exhibited more than 98% similarity to the assumed contaminants were not included in the analysis of bacterial 16S rRNA gene sequences. For *Archaea*, the negative DNA extraction control did not result in a PCR product. All archaeal sequences were aligned by using the SINA Webaligner[2] or the integrated Aligner of the ARB software[3] (Ludwig et al., 2004) and were manually adjusted. Closest relatives of all bacterial and archaeal 16S rDNA sequences found with BLAST[4] were also included in the phylogenetic analysis. For tree construction, sequences were grouped together in a clone family if they exhibited 99% sequence identity using similarity matrix in the ARB software.

Rarefaction curves were calculated with the mothur software[5] (Schloss et al., 2009).

PHYLOGENETIC ANALYSIS

Chimera check was done with the Greengenes Bellerophon program[6]. The closest sequence relatives of the 16S rRNA gene sequences based on BLAST searches were imported into ARB and aligned using the integrated aligner and manually adjusted. The 16S rRNA gene sequence data were analyzed with the ARB software package (see text footnote 3). Phylogenetic trees were calculated by performing distance matrix methods (Neighbor Joining with 1000 bootstrap values, both with the Jukes–Cantor correction, Jukes and Cantor, 1969), maximum parsimony analysis and Maximum-Likelihood analysis. For tree reconstruction only sequences with more than 800 bp were used. Phylogenetic trees were calculated via ARB using the Maximum-Likelihood method. The closest sequence relatives and representatives of the major taxonomic groups were included (Baker et al., 2003). Similarity analysis and clone grouping was done with the ARB similarity matrix with Jukes–Cantor correction (Jukes and Cantor, 1969).

[1] www.mbio.ncsu.edu/BioEdit/bioedit.html
[2] www.arb-silva.de/aligner
[3] www.arb-home.de
[4] www.ncbi.nlm.nih.gov
[5] www.mothur.org
[6] greengenes.lbl.gov/cgi-bin/nph-index.cgi

The phylogenetic groups were arranged according to Teske and Sørensen (2008) and Spang et al. (2010).

RESULTS

In this study, we analyzed the microbial ecology and bulk geochemistry of 50 samples from the post-impact CBIS terrestrial sediment from land surface (arable soil) up to a depth of 140 m.

GEOCHEMICAL RESULTS

Data for the geochemical solid phase analysis of 48 sediment samples are summarized in **Table 1**. TOC as substrate for heterotrophic microorganisms remained low in the complete sediment depth range with a mean value of ∼0.2% and a maximum value of 0.9% (w/w) characterizing the sediments as oligotrophic. Reactive iron, relevant for Fe(III)-reducing microorganisms, was more than twice as high in the uppermost meter than the mean for the total 140 m (data not shown).

MICROBIOLOGICAL RESULTS

TOTAL CELL COUNTS AND CARD–FISH

Total cells stained with SYBR Green were counted following three different protocols. Depth profiles of total cell counts are shown in **Figure 1**. For all three protocols, the maximal cell counts were detected near the surface. The total cell counts indicate a logarithmic decline with depth within the upper 20 m, and show no significant depth correlation between 20 and 140 m. The method comparison shows that the highest cell counts for all depths were obtained with the protocol without detaching cells from sediment particles after Weinbauer et al. (1998). Maximum cell counts of more than 10^9 cells/g at the surface declined to about 10^6 cells/g at 20 m depth. Below 20 m, counts were highly variable and not correlated with depth. In comparison, the overall counts obtained with protocols in which the cells were detached from sediment particles before counting gave about half an order of magnitude (Kallmeyer et al., 2008) and about one order of magnitude (Lunau et al., 2005, modified) lower cell counts.

A comparison of the highest total cell counts after Weinbauer et al. (1998) with numbers of living *Bacteria* and *Archaea* obtained by CARD–FISH is given in **Figure 2** for the top 7 m sediment depth. A significant proportion of the total cell counts could be detected with CARD–FISH. Interestingly, the CARD–FISH numbers for *Bacteria* were about an order of magnitude higher than those for the *Archaea*. At some depth *Archaea* were not detectable at all. Below 7 m sediment depth the CARD–FISH cell signals were below the detection limit of 10^5 cells/g.

Table 1 | Geochemical solid phase analysis of 48 sediment samples.

Total organic C	Total C	Total P	Total S	Total Fe	Reactive Fe
0.18 (0.2)	0.61 (0.62)	0.03 (0.02)	0.65 (0.77)	2.02 (1.6)	0.32 (0.4)

Mean and (SD) are given in % (w/w).

QUANTITATIVE MICROBIAL COMMUNITY ANALYSIS BY Q-PCR

Results of Q-PCR analysis for the uppermost 10 m depth and for 80–140 m depth are shown in **Figure 3**. The Q-PCR data on bacterial 16S rRNA gene copy numbers matched well with the total cell counts after Weinbauer et al. (1998). *Archaea* were found in lower copy numbers than the *Bacteria* in the top 10 m. At 80–140 m depth, *Archaea* were detected only at a few depths, and always in lower copy numbers using Q-PCR. Thus, the dominance of *Bacteria* over *Archaea* in the CBIS post-impact sediment was confirmed by Q-PCR and CARD–FISH.

In addition to the prokaryotic domains *Bacteria* and *Archaea*, *Eukarya* and specific prokaryotic groups were quantified via Q-PCR by 16S rRNA or functional gene quantification. *Eukarya* and the Fe(III)- and Mn(IV)-reducing bacterial group *Geobacteraceae* were found in the uppermost meter (arable soil) only (besides at 4 m). In the uppermost meter, reactive iron was detected in higher amounts as a potential electron acceptor for the *Geobacteraceae*. The bacterial candidate division JS-1 and the classes *Anaerolineae* and *Caldilineae* of the phylum *Chloroflexi*, highly abundant in marine sediments (Blazejak and Schippers, 2010), were found in high copy numbers up to the maximum sampling depth of 140 m. A similar high abundance was found for the functional gene *cbbL* coding for the large subunit of the form I "red-like" ribulose-1.5-bisphosphate carboxylase/oxygenase (RubisCO) occurring in autotrophic *Proteobacteria* that fix CO_2 via the Calvin–Benson–Bassham (CBB) cycle (Selesi et al., 2007; Badger and Bek, 2008). The functional gene *aprA* coding for adenosine 5′-phosphosulfate reductase occurring in sulfate reducing bacteria was found within distinct layers up to ca. 100 m depth. The gene *mcrA* for methyl coenzyme M reductase of methanogenic *Archaea* could not be detected.

MICROBIAL DIVERSITY

In order to reveal the prokaryotic diversity in the CBIS sediment, a phylogenetic analysis of 16S rRNA gene sequences from four depths for *Bacteria* and two depths for *Archaea* was performed. The results for the *Bacteria* are shown in **Table 2**, those for the *Archaea* in **Figures 4–7**. Overall, the bacterial diversity seems to be very low. This finding may partly be a result of the limited number of reported bacterial clone data. Many bacterial clones had to be excluded since their 16S RNA gene sequences exhibited more than 98% similarity (checked with BLAST) to the 16S rRNA gene sequences obtained from the negative DNA extraction control with no sediment (contaminants). Sequences of the remaining bacterial 16S rRNA genes revealed typical soil bacteria (**Table 2**).

The analysis of 16S rRNA gene sequences of *Archaea* from two depths, 109 and 125 m, resulted in 13 and 103 clones which could be allocated to the phyla *Euryarchaeota* or *Crenarchaeota*, respectively. The rarefaction curves of the 16S rRNA gene sequences indicate a good coverage of the archaeal diversity as can be seen in the flattening of the two curves (**Figure 4**). The composition of the archaeal community shows a similar ratio of euryarcheotic and crenarcheotic contingents (109 m: 5 euryarchaeotal sequences, 58 crenarchaeotal sequences, 125 m: 8 euryarchaeotal sequences, 57 crenarchaeotal sequences) for the two analyzed sediment depths (**Figure 5**).

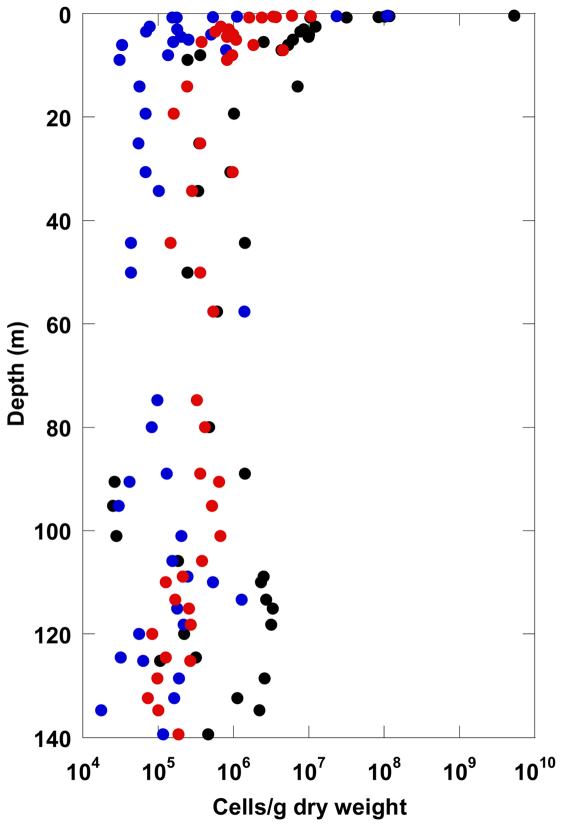

FIGURE 1 | Total cell counts for the terrestrial CBIS post-impact sediment obtained with three different methods (black: method Weinbauer et al., 1998; red: method Kallmeyer et al., 2008; blue: method Lunau et al., 2005).

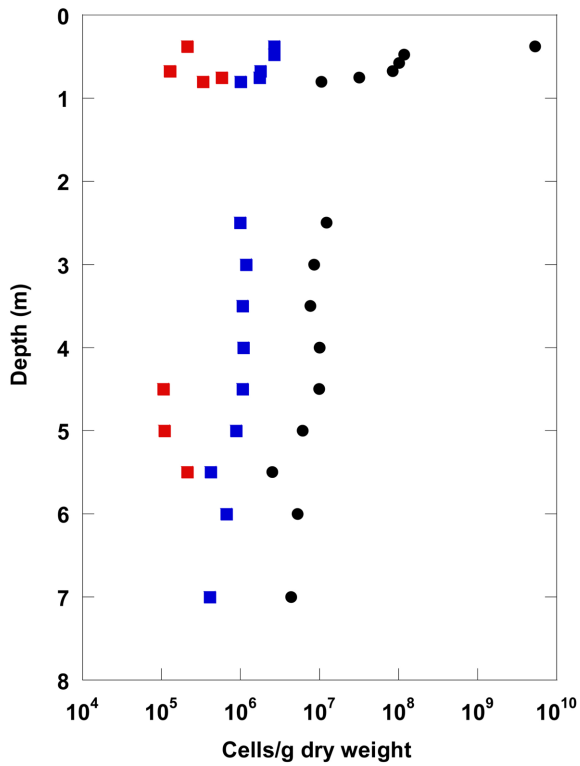

FIGURE 2 | Catalyzed reporter deposition–fluorescence *in situ* hybridization numbers for *Bacteria* (blue) and *Archaea* (red) displayed with total cell counts (black: Weinbauer et al., 1998) for the uppermost 8 m of the terrestrial CBIS post-impact sediment.

The phylogenetic analysis with different methods (ARB neighbor joining with 1000 bootstraps, maximum parsimony method, data not shown) gave similar results as the maximum-likelihood analysis. Phylogenetic trees for the two archaeal phyla, *Euryarchaeota* and *Crenarchaeota,* are shown in **Figures 6** and **7**. Two euryarcheotic clone groups, E1 and E2, could be allocated to the South African Gold Mine Group (SAGMEG). Group E1 clustered together with a clone received from deeply buried sediments of the Peru margin (AB177011). Group E2 represents a novel phylogenetic subgroup of archaeal sequences with less than 98% similarity to its closest sequence, AY093454. A third clone group, E3 could be allocated to the Deep Sea Hydrothermal Vent Euryarchaeotal Group 6 (DHVE6). The 16S rRNA gene sequence similarity to its closest sequence EU750878 is less than 89%. Both SAGMEG and DHVE6 contain 16S rRNA gene sequences of terrestrial as well as of marine origin (Teske and Sørensen, 2008). The three clone groups could be allocated to the two different depths. Group E1 includes only sequences from 109 m depth while group E2 and E3 include only sequences from 125 m depth.

All 16S rRNA gene sequences from the phylum *Crenarchaeota* belong to the Miscellaneous Crenarcheotic Group (MCG). Sequences received could be grouped into eight different clone groups. Five groups (C1, C2, C3, C6, C7) represent new phylogenetic clusters with less than 99% similarity to their closest related sequences in GenBank. Some clone groups were found in one sample only (e.g., C7, 109 m; C4, 125 m), while others occurred in both samples. Interestingly, the clone groups C3a (125 m) and C3b (109 m) are related to each other and belong together to a new cluster, but the similarity between C3a and C3b is 96.7% and thus below the species level.

DISCUSSION

ABUNDANCE OF TOTAL AND LIVING CELLS

The microbial community in terrestrial sediments up to a depth of 140 m in the Chesapeake Bay area, Virginia, USA, was thoroughly analyzed by SYBR Green total cell counting, Q-PCR, and CARD–FISH, and 16S rRNA gene cloning. The organic carbon content is low (mean ~0.2%) in these oligotrophic deep terrestrial sediments, thus little substrate is available for sustaining a thriving heterotrophic microbial community. Nevertheless total cell counts after Weinbauer et al. (1998) and Q-PCR data exhibited an average of about 10^6 cells/g between 20 and 140 m depth without a decrease with depth. In comparison, the overall counts obtained with protocols that detached cells from sediment particles before counting resulted in one (Lunau et al., 2005) to half (Kallmeyer et al., 2008) an order of magnitude lower cell counts. This difference between the protocols can be explained by a loss of

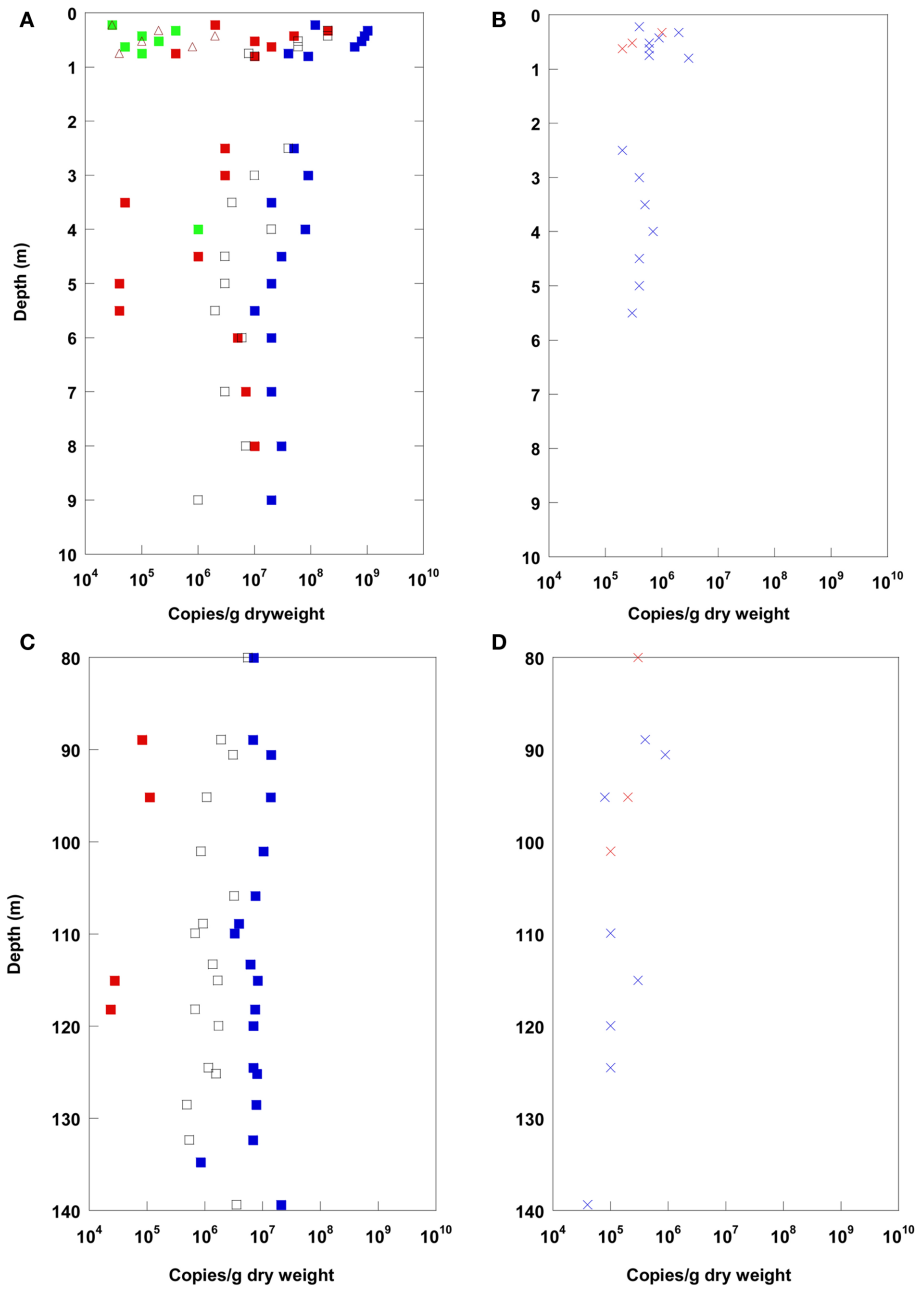

FIGURE 3 | Real-time PCR (Q-PCR) data for the terrestrial CBIS post-impact sediment in the uppermost 10 m depth (A,B), and in 80–140 m depth (C,D). Different phylogenetic groups, blue: *Bacteria*, red: *Archaea*, green: *Eukarya*, brown: *Geobacteriaceae*, black: JS-1-*Chloroflexi* **(A,C)**; functional genes, red: *aprA*, blue: *cbbL* **(B,D)**.

cells during the detachment procedure and/or counting of unspecific signals without detaching cells from sediment particles. A comparison of the total cell counts with the 16S rRNA gene copy numbers of *Bacteria* obtained by Q-PCR gives the best match with the highest cell counts (Weinbauer et al., 1998). Thus, cell loss during the cell detachment procedures seemed to be more relevant than an overestimation by counting unspecific signals. Although the detachment protocols likely result in an underestimate of total cell numbers, the protocols are suitable for sediments in which the numbers of microorganisms are below 10^5 cells/mL sediment (D'Hondt et al., 2009; Schippers et al., 2010).

The CARD–FISH bacterial cell numbers reflecting living cells were lower than the total cell numbers (Weinbauer et al., 1998) which may indicate a minor proportion of living cells or overlooked CARD–FISH cells due to insufficient cell staining. More evidence for living cells was provided by cultivation experiments (unpublished). In these experiments, fresh samples from various depths were incubated for several months. A strong CO_2 release

Table 2 | Summary of the phylogenetic analysis of bacterial 16S rRNA genes in terrestrial CBIS post-impact sediment.

Clone group	Number of clones	Depth (m)	Class	Next cultivated neighbour	Similarity (%)
Bact 1	21	101, 109, 125	*Gammaproteobacteria*	*Pseudomonas stutzeri*, strain ATCC 17588, AF094748	>98.8
Bact 2	2	101, 109	*Gammaproteobacteria*	*Pseudomonas guineae*, strain LMG 24016^T, AM491810	>99
Bact 3	12	109, 125	*Gammaproteobacteria*	*Acinetobacter lwoffii*, strain DSM 2403, X81665	>98.8
Bact 4	2	125	*Alphaproteobacteria*	*Mesorhizobium amorphae*, strain ACCC19665, AF041442	>99
Bact 5	2	75, 101	*Alphaproteobacteria*	*Acidocella aluminiidurans*, strain AL46, AB362219	>98.8
Bact 6	16	109	*Actinobacteria*	*Arthrobacter humicola*, strain KV-653, AB279890	>99

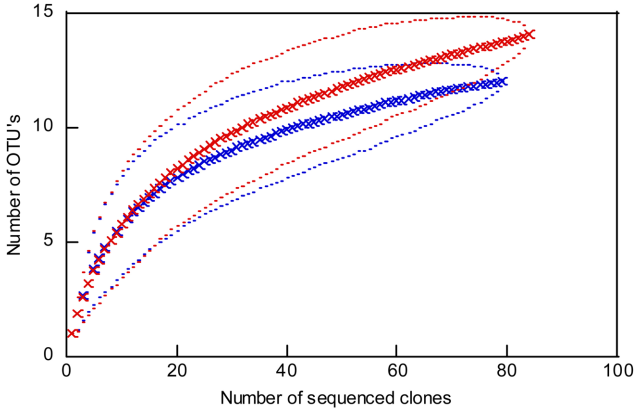

FIGURE 4 | Rarefaction curves for the archaeal 16S rRNA gene sequences from 109 m depth (red) to 125 m depth (blue). Outer and inner lines: high and low confidence interval (95%). OTU, operational taxonomic unit; cut off of OTU's = 1%.

was observed in aerobic and in anaerobic cultures with or without addition of Fe(III) as a terminal electron acceptor, indicating microbial activity under these conditions. Assays with additional sulfate and nitrate did not show evolution of CO_2 (Michael Siegert and Martin Krüger, personal communication).

In a previous study of the deeper sediments of the terrestrial CBIS at the same drill site total cell counts were obtained after staining with DAPI and exhibited significantly higher numbers, between 10^6 and 10^8 cells/g with high variation over the depth interval 140–444 m of the post-impact CBIS sediment (Gohn et al., 2008). The total cell counts increased with depth below 140 m of the post-impact sediment. One explanation for this finding might be the changing lithology connected to a dramatically changing TOC content with depth. The post-impact CBIS sediments from 140 to 444 m consist of a generally fine-grained upper Eocene to upper Miocene sediment with about a 10 times higher TOC content than the coarser grained upper Miocene to Pleistocene section above 140 m (Gohn et al., 2009). Most likely the higher TOC content at greater depth sustains significantly more cells than in the upper oligotrophic sediment. These data represent the first observation of a significant increase of cell counts with depth in deep terrestrial sediment. The relevance for a lithological control on the deep biosphere has been previously pointed out for deeply buried marine sediments (Coolen et al., 2002; Inagaki et al., 2003; Parkes et al., 2005). Below the post-impact CBIS terrestrial sediments in the geologically different zones of sediment breccias, schist, pegmatite, and granite (444–1766 m depth) the total cell numbers were considerably lower (10^4 and 10^6 cells/g or not detectable; Gohn et al., 2008). The novel actinobacterium *Tessaracoccus profundi* was isolated and described from a depth of 940 m (Finster et al., 2009).

The average total cell numbers of about 10^6 cells/g between 20 and 140 m depth found in this study are in the same order of magnitude or somewhat higher than those found in other deep terrestrial sediments in a similar depth range by total cell counting or by cultivation (Hoos and Schweisfurth, 1982; Balkwill et al., 1989; Fredrickson et al., 1991; Kieft et al., 1995; Takai et al., 2003; Fry et al., 2009). These studies are in agreement with our study, and did not find a decrease in cell numbers with depth. This is in contrast to marine sediments for which a correlation of cell numbers with depth was described (Parkes et al., 1994, 2000; Schippers et al., 2005). The reason for the difference in cell numbers vs. depth in marine and terrestrial sediments is unknown but has considerable importance for the estimation of the global abundance of prokaryotes on Earth (Whitman et al., 1998) as previously stated (Fry et al., 2009).

ABUNDANCE OF *BACTERIA* VS. *ARCHAEA*

This study is the first providing quantitative data on the abundance of *Bacteria* and *Archaea* in deep terrestrial sediment. The dominance of *Bacteria* over *Archaea* in the CBIS post-impact terrestrial sediment was confirmed by Q-PCR and CARD–FISH. The proportions of *Bacteria* and *Archaea* in marine sediments have shown to be highly variable in different sediments and sediment layers and conflicting results have been published for analyses of nucleic-acids (Q-PCR and CARD–FISH) and intact polar lipids (IPL) of cell membranes (Inagaki et al., 2003, 2006; Schippers et al., 2005, 2010; Biddle et al., 2006; Schippers and Neretin, 2006; Wilms et al., 2007; Engelen et al., 2008; Lipp et al., 2008; Nunoura et al., 2009; Webster et al., 2009). Schouten et al. (2010) and Logemann et al. (2011) reported about a fossilization of archaeal IPL biomarkers in marine sediments indicating that IPL biomarkers detect fossil signals rather than living *Archaea*, thus putting their proposed dominance in the marine deep biosphere into question.

Another explanation for the conflicting results is given by mismatches of archaeal primers and probes with 16S rRNA gene sequences of the dominant archaeal groups in marine sediments and therefore a potential underestimation of archaeal cell numbers by nucleic-acid based methods (Teske and Sørensen, 2008). A comparison of our archaeal Q-PCR results with our clone library data for the samples at 109 and 125 m revealed a discrepancy of the

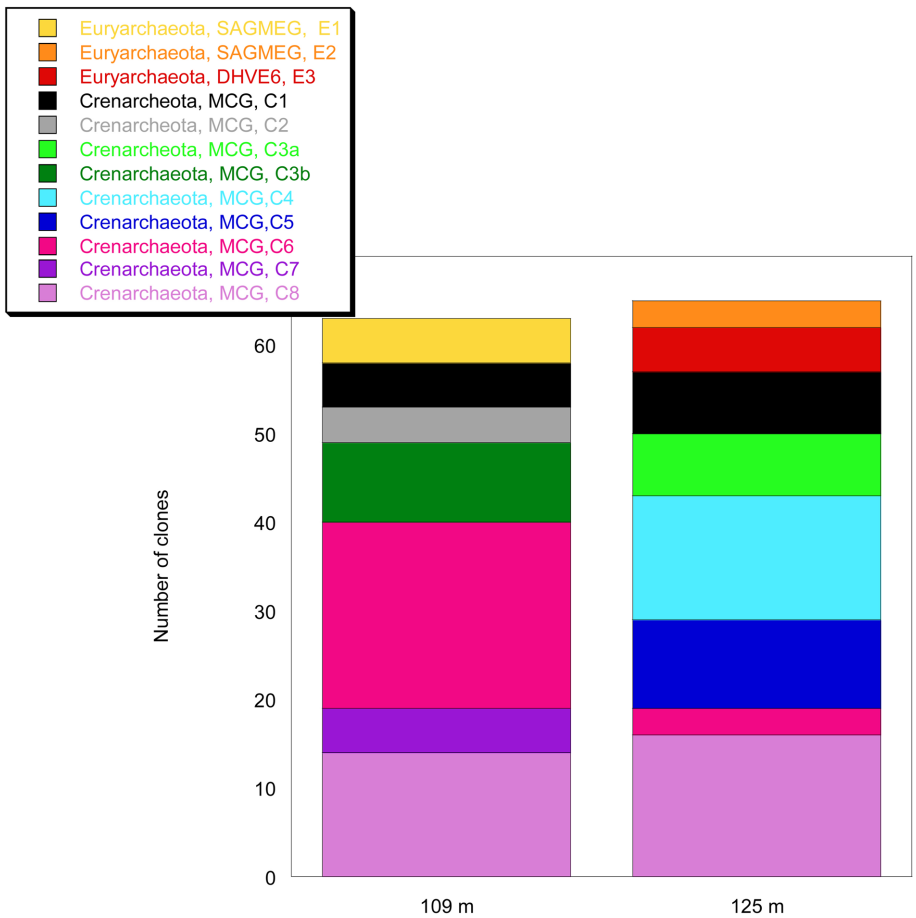

FIGURE 5 | Analysis of the composition of the archaeal community in the terrestrial CBIS post-impact sediment at 109 and 125 m depth.

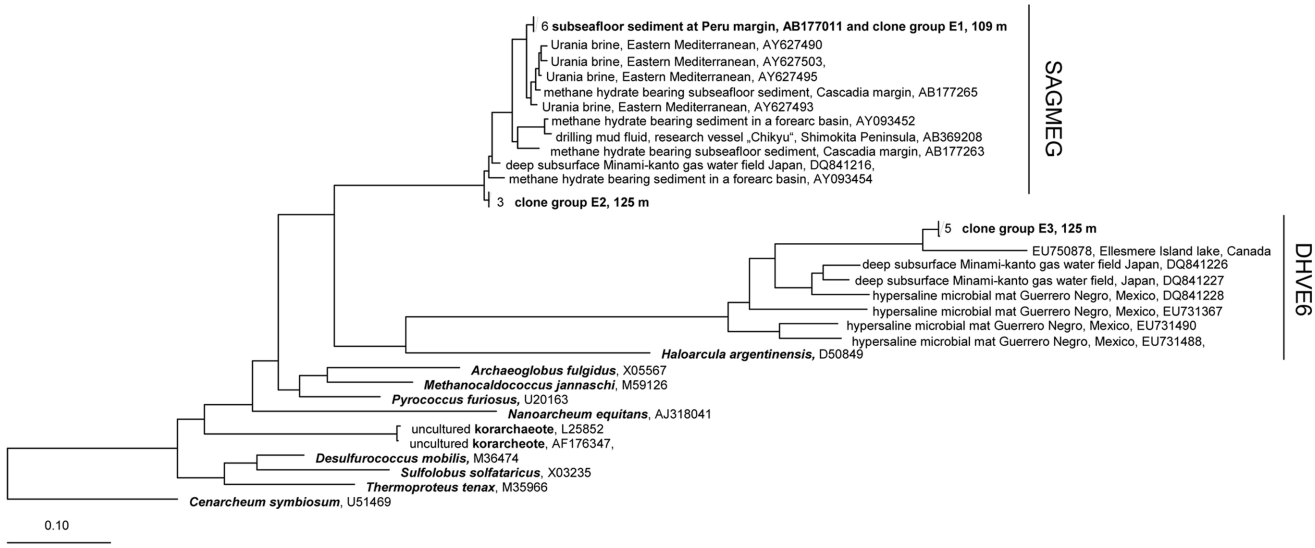

FIGURE 6 | Maximum-Likelihood phylogenetic tree of the *Euryarcheota* showing clades found in terrestrial CBIS post-impact sediment. The tree was rooted with *Cenarchaeum symbiosum* as a representative of the deeply branched group "*Thaumarcheota*." SAGMEG, South African Gold Mine Group, DHVE6, Deep Sea Hydrothermal Vent Euryarchaeotal Group 6.

FIGURE 7 | Maximum-Likelihood phylogenetic tree of the *Crenarcheota* showing clades found in terrestrial CBIS post-impact sediment. The tree was rooted with *Cenarchaeum symbiosum* as a representative of the deeply branched group "*Thaumarcheota*." MCG, Miscellaneous Crenarcheotic Group.

two methods which used different primers and probes. While in the clone library several different groups were found, Q-PCR did not result in archaeal 16S rRNA gene amplification. For Q-PCR, we used the primers Arch349F and Arch806R, and the TaqMan probe Arch516 (Takai and Horikoshi, 2000). According to Teske and Sørensen (2008) the primer Arch349F has several mismatches within the groups SAGMEG, DHVE6, and MCG. We checked the primer Arch349F against our sequences and found more than five mismatches with some sequences. Similarly, probe Arch516 and primer Arch806R matched only when at least three (probe Arch516F) and two (primer Arch806R) mismatches were allowed. This finding elucidates the necessity for the development of novel archaeal Q-PCR assays.

ABUNDANCE OF SPECIFIC TAXA AND OF FUNCTIONAL GENES

The detection of the functional gene *cbbL* coding for the large subunit of the form I "red-like" RubisCO in many samples in relatively high copy numbers in our study indicates that autotrophic *Proteobacteria* are relevant in the deep terrestrial sediments as well. However, their abundance is at least an order of magnitude lower

than the 16S rRNA gene copy number of the dominant *Bacteria*, thus heterotrophic bacteria play the mayor role in the deep terrestrial sediment despite the low content of organic carbon. However, heterotrophs were also found in oligotrophic deeply buried marine sediments (D'Hondt et al., 2004).

The bacterial candidate division JS-1 and the classes *Anaerolineae* and *Caldilineae* of the phylum *Chloroflexi* comprised a higher proportion of the *Bacteria*, but these specific groups with almost no cultivated representatives are less abundant than in marine sediments where almost identical 16S rRNA gene copy numbers for the specific groups and the *Bacteria* were found (Webster et al., 2004, 2011; Blazejak and Schippers, 2010).

Fe(III)-, Mn(IV)-, and sulfate-reducers, methanogens as well as *Eukarya* quantified via general 18S rRNA genes (*Eukarya*), specific 16S rRNA genes (*Geobacteraceae*), or functional genes (*aprA*, *mcrA*) play a minor or no role in the deep post-impact CBIS terrestrial sediment while these groups were regularly detected in subsurface marine sediments (Schippers and Neretin, 2006; Wilms et al., 2007; Engelen et al., 2008; Nunoura et al., 2009; Webster et al., 2009; Schippers et al., 2010). *Eukarya* and *Geobacteraceae* were found in the uppermost meter of the CBIS drill site where reactive iron and presumably eukaryotic DNA from farming in the arable soil is available. Deeper eukaryotic DNA was detected in one sample only. Due to the low TOC and sulfate content of the terrestrial sediment, sulfate reduction, and methanogenesis are expected to be less relevant than in deeply buried marine continental margin sediments with a higher TOC content (D'Hondt et al., 2004; Parkes et al., 2005; Schippers et al., 2005; Schippers and Neretin, 2006; Teske, 2006). Both processes are also less relevant in oligotrophic deeply buried marine sediments (D'Hondt et al., 2004; Sørensen et al., 2004; Teske, 2006; Nunoura et al., 2009) in agreement with our terrestrial study.

DIVERSITY OF *BACTERIA* AND *ARCHAEA*

The bacterial 16S rRNA gene sequences belong to three classes: *Alphaproteobacteria*, *Gammaproteobacteria*, and *Actinobacteria*. All bacterial 16S rRNA gene sequences have more than 98.9% similarity to sequences of cultivated heterotrophic bacteria. Almost all of the identified bacteria were previously found in other deep terrestrial sediments (Balkwill et al., 1989; Boivin-Jahns et al., 1996).

The phylogenetic analysis of the *Archaea* identified euryarcheotic as well as crenarcheotic 16S rRNA gene sequences including novel phylogenetic clusters related to lineages that do not yet contain cultivated representatives. The euryarcheotic clone groups E1 and E2 belong to the SAGMEG. This group includes 16S rRNA gene sequences found in a South African gold mine and sequences from the deep marine subsurface (Teske and Sørensen, 2008). Fry et al. (2009) also found euryarcheotic sequences belonging to SAGMEG in deep terrestrial sediments including an interbedded coal deposit. Sequences isolated from hot springs (Greece) or dolomite aquifers (South Africa) also belong to the SAGMEG (**Figure 6**). In conclusion this group seems not to be restricted to the deep subsurface biosphere, and occurs in marine and terrestrial environments. Similarly, the DHVE6 to which clone group E3 belongs includes terrestrial and marine sequences. The DHVE6 group defined by Takai and Horikoshi (1999) includes sequences from deep sea hydrothermal vents in the Eastern Pacific Ocean. Successively, sequences from different habitats could be affiliated to this group; examples are from a hydrothermal field at 13°N, 141°W in the South Pacific Rise (Nercessian et al., 2003) and from ODP Site 1231 at the Peru Basin (Sørensen et al., 2004). The closest relative to the group E3 is a sequence from a highly stratified meromictic lake on Ellesmere Island that is characterized by a high salinity in deeper layers (Poliot et al., 2009). Further related 16S rRNA sequences derive from habitats with high salinity: from a hypersaline microbial mat at Guerrero Negro, Mexico (Robertson et al., 2009) and from a commercial gas–water-producing well water in Japan which contains ancient seawater at depths of 347–1132 m (Mochimaru et al., 2007). In conclusion the novel group E3 seems to be related to clones that derive from environments with higher salinity (**Figure 6**). The DHVE6 group is affiliated with reduced (metal-) sulfides at vent structures (Takai and Horikoshi, 1999), reduced iron and manganese species (Sørensen et al., 2004), hydrogen sulfide (Robertson et al., 2009), and/or high salinity (Poliot et al., 2009; Robertson et al., 2009).

All crenarcheotic clones found in this study belong to the MCG. This group contains a huge number of diverse phylogenetic lineages from different, partially extreme habitats from terrestrial and marine origin (Teske and Sørensen, 2008). We identified clone groups which have closely related sequences from other environments (C5, C8, **Figure 7**), and also several novel groups with a relatively high distance to the closest related sequences (C1, C2). As summarized by Teske and Sørensen (2008), the MCG appears to be heterotrophic, which corroborates our Q-PCR data on the dominance of heterotrophic prokaryotes (see above), despite the low TOC content (in particular 0.24% for 109 m and 0.28% for 125 m depth).

CONCLUSION

For the first time quantitative data on the abundance of *Bacteria*, *Archaea*, and *Eukarya* in deep terrestrial sediments are provided using multiple methods (total cell counting, CARD–FISH, and Q-PCR). This was done together with the description of the bacterial and archaeal lineages and the quantification of specific taxa and of functional genes. The presence of a significant fraction of rRNA containing, viable bacterial and archaeal cells as revealed by CARD–FISH despite low levels of organic carbon is a relevant finding in this study. The dominance of *Bacteria* over *Archaea* resulted from CARD–FISH and Q-PCR data. Other major findings are the discovery of new sequence clusters within previously described cren- and euryarchaeotal lineages and the presence of high copy numbers of *cbbL* encoding for the large subunit of the form I "red-like" RubisCO suggesting that autotrophic *Proteobacteria* could be relevant in addition to heterotrophs in the terrestrial deep subsurface.

ACKNOWLEDGMENTS

We thank the ICDP, the USGS, and the drilling team for drilling and providing samples, and Mary A. Voytek for giving advice to the application of fluorescent microspheres. We also thank Eastern Shore Laboratory (ESL) in Wachapreague, Virginia, for laboratory space and support during sampling. The 16S rRNA gene sequences of the CBIS post-impact sediment were submitted to NCBI with the accession numbers JF500169-JF500398. This work was funded by the DFG research grant SCHI 535/6 to Axel Schippers.

REFERENCES

Badger, M. R., and Bek, E. J. (2008). Multiple Rubisco forms in proteobacteria: their functional significance in relation to CO2 acquisition by the CBB cycle. *J. Exp. Bot.* 59, 1525–1541.

Baker, G. C., Smith, J. J., and Cowan, D. A. (2003). Review and re-analysis of domain-specific 16S primers. *J. Microbiol. Methods* 55, 541–555.

Balkwill, D. L., Fredrickson, J. K., and Thomas, J. M. (1989). Vertical and horizontal variations in the physiological diversity of the aerobic chemoheterotrophic bacterial microflora in deep southeast coastal-plain subsurface sediments. *Appl. Environ. Microbiol.* 55, 1058–1065.

Biddle, J. F., Fitz-Gibbon, S., Schuster, S. C., Brenchley, J. E., and House, C. H. (2008). Metagenomic signatures of the Peru Margin subseafloor biosphere show a genetically distinct environment. *Proc. Natl. Acad. Sci. U.S.A.* 105, 10583–10588.

Biddle, J. F., Lipp, J. S., Lever, M., Lloyd, K. G., Sørensen, K. B., Anderson, R., Fredricks, H. F., Elvert, M., Kelly, T. J., Schrag, D. P., Sogin, M. L., Brenchley, J. E., Teske, A, House, C. H., and Hinrichs, K. U. (2006). Heterotrophic Archaea dominate sedimentary subsurface ecosystems off Peru. *Proc. Natl. Acad. Sci. U.S.A.* 103, 3846–3851.

Blazejak, A., and Schippers, A. (2010). High abundance of JS-1- and Chloroflexi-related bacteria in deeply buried marine sediments revealed by quantitative, real-time PCR. *FEMS Microbiol. Ecol.* 72, 198–207.

Boivin-Jahns, V., Ruimy, R., Bianchi, A., Daumas, S., and Christen, R. (1996). Bacterial diversity in a deep-subsurface clay environment. *Appl. Environ. Microbiol.* 62, 3405–3412.

Borgonie, G., García-Moyano, A., Litthauer, D., Bert, W., Bester, A., van Heerden, E., Möller, C., Erasmus, M., and Onstott, T. C. (2011). Nematoda from the terrestrial deep subsurface of South Africa. *Nature* 474, 79–82.

Brown, M. G., and Balkwill, D. L. (2009). Antibiotic resistance in bacteria from the deep terrestrial subsurface. *Microb. Ecol.* 57, 484–493.

Canfield, D. E. (1989). Reactive iron in marine sediments. *Geochim. Cosmochim. Acta* 53, 619–632.

Chandler, D. P., Li, S.-M., Spadoni, C. M., Drake, G. R., Balkwill, D. L., Fredrickson, J. K., and Brockman, F. J. (1997). A molecular comparison of culturable aerobic heterotrophic bacteria and 16S rDNA clones derived from a deep subsurface sediment. *FEMS Microbiol. Ecol.* 23, 131–144.

Chapelle, F. H., O'Neill, K., Bradley, P. M., Methé, B. A., Ciufo, S. A., Knobel, L. L., and Lovley, D. R. (2002). A hydrogen-based subsurface microbial community dominated by methanogens. *Nature* 415, 312–315.

Coolen, M. J. L., Cypionka, H., Sass, A. M., Sass, H., and Overmann, J. (2002). Ongoing modification of Mediterranean Pleistocene sapropels mediated by prokaryotes. *Science* 296, 2407–2410.

Detmers, J., Schulte, U., Strauss, H., and Kuever, J. (2001). Sulfate reduction at a lignite seam: microbial abundance and activity. *Microb. Ecol.* 42, 238–247.

Detmers, J., Strauss, H., Schulte, U., Bergmann, A., Knittel, K., and Kuever, J. (2004). FISH shows that *Desulfotomaculum* spp. are the dominating sulfate-reducing bacteria in a pristine aquifer. *Microb. Ecol.* 47, 236–242.

D'Hondt, S., Spivack, A. J., Pockalny, R., Ferdelman, T. G., Fischer, J. P., Kallmeyer, J., Abrams, L. J., Smith, D. C., Graham, D., Hasiuk, F., Schrum, H., and Stancin, M. A. (2009). Subseafloor sedimentary life in the South Pacific Gyre. *Proc. Natl. Acad. Sci. U.S.A.* 106, 11651–11656.

D'Hondt, S. L., Jørgensen, B. B., Miller, D. J., Batzke, A., Blake, R., Cragg, B. A., Cypionka, H., Dickens, G. R., Ferdelman, T. G., Hinrichs, K. U., Holm, N. G., Mitterer, R., Spivack, A., Wang, G., Bekins, B., Engelen, B., Ford, K., Gettemy, G., Rutherford, S. D., Sass, H., Skilbeck, C. G., Aiello, I. W., Guèrin, G., House, C. H., Inagaki, F., Meister, P., Naehr, T., Niitsuma, S., Parkes, R. J., Schippers, A., Smith, D. C., Teske, A., Wiegel, J., Padilla, C. N., and Solis Acosta, J. L. (2004). Distributions of microbial activities in deep subseafloor sediments. *Science* 306, 2216–2221.

Engelen, B., Ziegelmüller, K., Wolf, L., Köpke, B., Gittel, A., Cypionka, H., Treude, T., Nakagawa, S., Inagaki, F., Lever, M. A., and Steinsbu, B. O. (2008). Fluids from the oceanic crust support microbial activities within the deep biosphere. *Geomicrobiol. J.* 25, 55–66.

Finster, K. W., Cockell, C. S., Voytek, M. A., Gronstal, A. L., and Kjeldsen, K. U. (2009). Description of *Tessaracoccus profundi* sp. nov., a deep-subsurface actinobacterium isolated from a Chesapeake impact crater drill core (940 m depth). *Antonie Van Leeuwenhoek* 96, 515–526.

Fredrickson, J. K., Balkwill, D. L., Zachara, J. M., Li, S. M. W., Brockman, F. J., and Simmons, M. A. (1991). Physiological diversity and distributions of heterotrophic bacteria in deep cretaceous sediments of the Atlantic coastal plain. *Appl. Environ. Microbiol.* 57, 402–411.

Fredrickson, J. K., McKinley, J. P., Bjornstad, B. N., Long, P. E., Ringelberg, D. B., White, D. C., Krumholz, L. R., Suflita, J. M., Colwell, F. S., Lehman, R. M., Phelps, T. J., and Onstott, T. C. (1997). Pore-size constraints on the activity and survival of subsurface bacteria in a late Cretaceous shale-sandstone sequence, northwestern New Mexico. *Geomicrobiol. J.* 14, 183–202.

Fry, J. C., Horsfield, B., Sykes, R., Cragg, B. A., Heywood, C., Kim, G. T., Mangelsdorf, K., Mildenhall, D. C., Rinna, J., Vieth, A., Zink, K. G., Sass, H., Weightman, A. J., and Parkes, R. J. (2009). Prokaryotic populations and activities in an interbedded coal deposit, including a previously deeply buried section (1.6-2.3 km) above ~150 Ma basement rock. *Geomicrobiol. J.* 26, 163–178.

Fry, J. C., Parkes, R. J., Cragg, B. A., Weightman, A. J., and Webster, G. (2008). Prokaryotic diversity and activity in the deep subseafloor biosphere. *FEMS Microbiol. Ecol.* 66, 181–196.

Gohn, G. S., Koeberl, C., Miller, K. G., and Reimold, W. U. (2009). *The ICDP-USGS Deep Drilling Project in the Chesapeake Bay Impact Structure: Results from the Eyreville Core Holes.* Boulder, CO: The Geological Society of America Special Paper 458.

Gohn, G. S., Koeberl, C., Miller, K. G., Reimold, W. U., Browning, J. V., Cockell, C. S., Horton, J. W. Jr., Kenkmann, T., Kulpecz, A. A., Powars, D. S. Sanford, W. E., and Voytek, M. A. (2008). Deep drilling into the Chesapeake Bay impact structure. *Science* 320, 1740–1745.

Gohn, G. S., Koeberl, C., Miller, K. G., Reimold, W. U., Cockell, C. S., Horton, J. W. Jr., Sanford, W. E., and Voytek, M. A. (2006). Chesapeake Bay impact structure drilled. *EOS* 87, 349, 355.

Grosskopf, R., Janssen, P. H., and Liesack, W. (1998). Diversity and structure of the methanogenic community in anoxic rice paddy soil microcosms as examined by cultivation and direct 16S rRNA gene sequence retrieval. *Appl. Environ. Microbiol.* 64, 960–969.

Hallbeck, L., and Pedersen, K. (2008). Characterization of microbial processes in deep aquifers of the Fennoscandian Shield. *Appl. Geochem.* 23, 1796–1819.

Holmes, D. E., Finneran, K. T., O'Neil, R. A., and Lovley, D. R. (2002). Enrichment of members of the family Geobacteraceae associated with stimulation of dissimilatory metal reduction in uranium-contaminated aquifer sediments. *Appl. Environ. Microbiol.* 68, 2300–2306.

Hoos, E., and Schweisfurth, R. (1982). Untersuchungen über die Verteilung von Bakterien von 10 bis 90 Meter unter Bodenoberkante. *Vom Wasser* 58, 103–112.

Inagaki, F., Nunoura, T., Nakagawa, S., Teske, A., Lever, M., Lauer, A., Suzuki, M., Takai, K., Delwiche, M., Colwell, F. S., Nealson, K. H., Horikoshi, K., D'Hondt, S., and Jørgensen, B. B. (2006). Biogeographical distribution and diversity of microbes in methane hydrate-bearing deep marine sediments on the Pacific ocean margin. *Proc. Natl. Acad. Sci. U.S.A.* 103, 2815–2820.

Inagaki, F., Okada, H., Tsapin, A. I., and Nealson, K. H. (2005). The paleome: a sedimentary genetic record of past microbial communities. *Astrobiology* 5, 141–153.

Inagaki, F., Suzuki, M., Takai, K., Oida, H., Sakamoto, T., Aoki, K., Nealson, K. H., and Horikoshi, K. (2003). Microbial communities associated with geological horizons in coastal subseafloor sediments from the Sea of Okhotsk. *Appl. Environ. Microbiol.* 69, 7224–7235.

Itävaara, M., Nyyssönen, M., Kapanen, A., Nousiainen, A., Ahonen, L., and Kukkonen, I. (2011). Characterization of bacterial diversity to a depth of 1500m in the Outokumpu deep borehole, Fennoscandian Shield. *FEMS Microbiol. Ecol.* 77, 295–309.

Jukes, T. H., and Cantor, C. R. (1969). *Evolution of Protein Molecules.* New York: Academic Press.

Kallmeyer, J., Mangelsdorf, K., Cragg, B. A., and Horsfield, B. (2006). Techniques for contamination assessment during drilling for terrestrial subsurface sediments. *Geomicrobiol. J.* 23, 227–239.

Kallmeyer, J., Smith, D. C., Spivack, A. J., and D'Hondt, S. L. (2008). New cell extraction procedure applied to deep subsurface sediments. *Limnol. Oceanogr. Methods* 6, 236–245.

Kieft, T. L, Fredrickson, J. K., McKinley, J. P., Bjornstad, B. N., Rawson, S. A., Phelps, T. J., Brockman, F. J., and Pfiffner, S. M. (1995). Microbiological comparisons within and across contiguous lacustrine, paleosol, and fluvial subsurface sediments. *Appl. Environ. Microbiol.* 61, 749–757.

Kovacik, W. P. Jr., Takai, K., Mormile, M. R., McKinley, J. P., Brockman, F. J., Fredrickson, J. K., and Holben, W. E. (2006). Molecular analysis of deep subsurface Cretaceous rock indicates abundant Fe(III)- and S°-reducing bacteria in a sulfate-rich environment. *Environ. Microbiol.* 8, 141–155.

Lin, L. H., Wang, P. L., Rumble, D., Lippmann-Pipke, J., Boice, E., Pratt, L. M., Sherwood Lollar, B., Brodie, E. L., Hazen, T. C., Andersen, G. L., DeSantis, T. Z., Moser, D. P., Kershaw, D., and Onstott, T. C. (2006). Long term sustainability of a high energy, low diversity crustal biome. *Science* 314, 479–482.

Lipp, J. S., Morono, Y., Inagaki, F., and Hinrichs, K. U. (2008). Significant contribution of Archaea to extent biomass in marine subsurface sediments. *Nature* 454, 991–994.

Llobet-Brossa, E., Rossello-Mora, R., and Amann, R. (1998). Microbial community composition of Wadden Sea sediments as revealed by fluorescence in situ hybridization. *Appl. Environ. Microbiol.* 64, 2691–2696.

Logemann, J., Graue, J., Köster, J., Engelen, B., Rullkötter, J., and Cypionka, H. (2011). A laboratory experiment of intact polar lipid degradation in sandy sediments. *Biogeosci. Discuss.* 8, 3289–3321.

Ludwig, W., Strunk, O., Westram, R., Richter, L., Meiser, H., Yadhukumar, Buchner, A., Lai, T., Steppi, S., Jobb, G., Förster, W., Brettske, I., Gerber, S., Ginhart, A. W., Gross, O., Grumann, S., Hermann, S., Jost, R., König, A., Liss, T., Lüßmann, R., May, M., Nonhoff, B., Reichel, B., Strehlow, R., Stamatakis, A., Stuckmann, N., Vilbig, A., Lenke, M., Ludwig, T., Bode, A., and Schleifer, K. H. (2004). ARB: a software environment for sequence data. *Nucleic Acids Res.* 32, 1363–1371.

Lueders, T., and Friedrich, M. (2000). Archaeal population dynamics during sequential reduction processes in rice field soil. *Appl. Environ. Microbiol.* 66, 2732–2742.

Lunau, M., Lemke, A., Walther, K., Martens-Habbena, W., and Simon, M. (2005). An improved method for counting bacteria from sediments and turbid environments by epifluorescence microscopy. *Environ. Microbiol.* 7, 961–968.

Mochimaru, H., Yoshioka, H., Tamaki, H., Nakamura, K., Kaneko, N., Sakata, S., Imachi, H., Sekiguchi, Y., Uchiyama, H., and Kamagata, Y. (2007). Microbial diversity and methanogenic potential in a high temperature natural gas field in Japan. *Extremophiles* 11, 453–461.

Moser, D. P., Onstott, T. C., Fredrickson, J. K., Brockman, F. J., Balkwill, D. L., Drake, G. R., Pfiffner, S. M., White, D. C., Takai, K., Pratt, L. M., Fong, J., Sherwood Lollar, B., Slater, G., Phelps, T. J., Spoelstra, N., Deflaun, M., Southam, G., Welty, A. T., Baker, B. J., and Hoek, J. (2003). Temporal shifts in the geochemistry and microbial community structure of an ultradeep mine borehole following isolation. *Geomicrobiol. J.* 20, 517–548.

Muyzer, G., Teske, A., Wirsen, C. O., and Jannasch, H. W. (1995). Phylogenetic relationships of *Thiomicrospira* species and their identification in deep-sea hydrothermal vent samples by denaturing gradient gel electrophoresis of 16S rDNA fragments. *Arch. Microbiol.* 164, 165–172.

Nadkarni, M., Martin, F. E., Jacques, N. A., and Hunter, N. (2002). Determination of bacterial load by real-time PCR using a broad range (universal) probe and primer set. *Microbiology* 148, 257–266.

Nercessian, O., Reysenbach, A. L., Prieur, D., and Jeanthon, C. (2003). Archaeal diversity associated with in situ samplers deployed on hydrothermal vents on the East Pacific Rise (13°N). *Environ. Microbiol.* 5, 492–502.

Nunoura, T., Soffientino, B., Blazejak, A., Kakuta, J., Oida, H., Schippers, A., and Takai, K. (2009). Subseafloor microbial communities associated with rapid turbidite deposition in the Gulf of Mexico continental slope (IODP Expedition 308). *FEMS Microbiol. Ecol.* 69, 410–424.

Parkes, R. J., Cragg, B. A., Bale, S. J., Getliff, J. M., Goodman, K., Rochelle, P. A., Fry, J. C., Weightman, A. J., and Harvey, S. M. (1994). Deep bacterial biosphere in Pacific Ocean sediments. *Nature* 371, 410–413.

Parkes, R. J., Cragg, B. A., and Wellsbury, P. (2000). Recent studies on bacterial populations and processes in subseafloor sediments: a review. *Hydrogeology J.* 8, 11–28.

Parkes, R. J., Webster, G., Cragg, B. A., Weightman, A. J., Newberry, C. J., Ferdelman, T. G., Kallmeyer, J., Jørgensen, B. B., Aiello, I. W., and Fry, J. C. (2005). Deep sub-seafloor prokaryotes stimulated at interfaces over geological time. *Nature* 436, 390–394.

Pedersen, K. (1993). The deep subterranean biosphere. *Earth Sci. Rev.* 34, 243–260.

Pedersen, K. (1997). Microbial life in deep granitic rock. *FEMS Microbiol. Rev.* 20, 399–414.

Pernthaler, A., Pernthaler, J., and Amann, R. (2002). Fluorescence in situ hybridization and catalyzed reporter deposition for the identification of marine bacteria. *Appl. Environ. Microbiol.* 68, 3094–3101.

Poliot, J., Galand, P. E., Loveley, C., and Vincent, W. F. (2009). Vertical structure of archaeal communities and the distribution of ammonia monooxygenase A gene variants in two merocmictic high Arctic lakes. *Environ. Microbiol.* 11, 687–699.

Robertson, C. E., Spear, J. R., Harris, K., and Pac, N. R. (2009). Diversity and stratification of Archaea in a hypersaline microbial mat. *Appl. Environ. Microbiol.* 75, 1801–1810.

Sahl, J. W., Schmidt, R., Swanner, E. D., Mandernack, K. W., Templeton, A. S., Kieft, T. L., Smith, R. L., Sanford, W. E., Callaghan, R. L., Mitton, J. B., and Spear, J. R. (2008). Subsurface microbial diversity in deep-granitic-fracture water in Colorado. *Appl. Environ. Microbiol.* 74, 143–152.

Schippers, A., Köweker, G., Höft, C., and Teichert, B. (2010). Quantification of microbial communities in three forearc sediment basins off Sumatra. *Geomicrobiol. J.* 27, 170–182.

Schippers, A., and Neretin, L. N. (2006). Quantification of microbial communities in near-surface and deeply buried marine sediments on the Peru continental margin using real-time PCR. *Environ. Microbiol.* 8, 1251–1260.

Schippers, A., Neretin, L. N., Kallmeyer, J., Ferdelman, T. G., Cragg, B. A., Parkes, R. J., and Jørgensen, B. B. (2005). Prokaryotic cells of the deep sub-seafloor biosphere identified as living bacteria. *Nature* 433, 861–864.

Schloss, P. D., Westcott, S., Ryabin, T., Hall, J. R., Hartmann, M., Hollister, E. B., Lesniewski, R. A., Oakley, B. B., Parks, D. H., Robinson, C. L., Sahl, J. W., Stres, B., Thallinger, G. G., Van Horn, D. L., and Weber, C. F. (2009). Introducing mothur: open-source, platform-independent community-supported software for describing and comparing microbial communities. *Appl. Environ. Microbiol.* 75, 7537–7541.

Schouten, S., Middelburg, J. J., Hopmans, E. C., and Sinninghe Damste, J. S. (2010). Fossilization and degradation of intact polar lipids in deep subsurface sediments: a theoretical approach. *Geochim. Cosmochim. Acta* 74, 3806–3814.

Selesi, D., Pattis, I., Schmid, M., Kandeler, E., and Hartmann, A. (2007). Quantification of bacterial RubisCO genes in soils by cbbL targeted real-time PCR. *J. Microbiol. Methods* 69, 497–503.

Sinclair, J. L., and Ghiorse, W. C. (1989). Distribution of aerobic bacteria, protozoa, algae and fungi in deep subsurface sediments. *Geomicrobiol. J.* 7, 15–31.

Sørensen, K. B., Lauer, A., and Teske, A. P. (2004). Archaeal phylotypes in a metal-rich and low-activity deep subsurface sediment of the Peru Basin, ODP Leg 201, Site 1231. *Geobiology* 2, 151–161.

Spang, A., Hatzenpichler, R., Brochier-Armanet, C., Ratei, T., Tischler, P., Spieck, E., Streit, W., Stahl, D., Wagner, M., and Schleper, C. (2010). Distinct gene set in two different lineges of ammonia oxidizing archaea supports the phylum Thaumarcheota. *Trends Microbiol.* 18, 331–340.

Stevens, T. O., and McKinley, J. P. (1995). Lithoautotrophic microbial ecosystems in deep basalt aquifers. *Science* 270, 450–454.

Takai, K., and Horikoshi, K. (1999). Genetic diversity of Archaea in deep-sea hydrothermal vent environments. *Genetics* 152, 1285–1297.

Takai, K., and Horikoshi, K. (2000). Rapid detection and quantification of members of the archaeal community by quantitative PCR using fluorogenic probes. *Appl. Environ. Microbiol.* 66, 5066–5072.

Takai, K., Mormile, M. R., McKinley, J. P., Brockman, F. J., Holben, W. E., Kovacik, W. P., and Fredrickson, J. K. (2003). Shifts in archaeal communities associated with lithological and geochemical variations in subsurface Cretaceous rock. *Environ. Microbiol.* 5, 309–320.

Teske, A. P. (2006). Microbial communities of deep marine subsurface sediments: molecular and cultivation surveys. *Geomicrobiol. J.* 23, 357–368.

Teske, A. P., and Sørensen, K. B. (2008). Uncultured archaea in deep marine marine subsurface sediments: have we caught them all? *ISME J.* 2, 3–18.

Webster, G., Blazejak, A., Cragg, B. A., Schippers, A., Sass, H., Rinna, J., Tang, X., Mathes, F., Ferdelman, T. G., Fry, J. C., Weightman, A. J., and Parkes, R. J. (2009). Subsurface microbiology and biogeochemistry of a deep, cold-water carbonate mound from the Porcupine Seabight (IODP Expedition 307). *Environ. Microbiol.* 11, 239–257.

Webster, G., Newberry, C. J., Fry, J. C., and Weightman, A. J. (2003). Assessment of bacterial community structure in the deep sub-seafloor biosphere by 16S rDNA-based techniques: a cautionary tale. *J. Microbiol. Methods* 55, 155–164.

Webster, G., Parkes, R. J., Fry, J. C., and Weightman, A. J. (2004).

Widespread occurrence of a novel division of bacteria identified by 16S rDNA gene sequences originally found in deep marine sediments. *Appl. Environ. Microbiol.* 70, 5708–5713.

Webster, G., Sass, H., Cragg, B. A., Gorra, R., Knab, N. J., Green, C. J., Mathes, F., Fry, J. C., Weightman, A. J., and Parkes, R. J. (2011). Enrichment and cultivation of prokaryotes associated with the sulphate-methane transition zone of diffusion-controlled sediments of Aarhus Bay, Denmark, under heterotrophic conditions. *FEMS Microbiol. Ecol.* 77, 248–263.

Weinbauer, M. G., Beckmann, C., and Höfle, M. G. (1998). Utility of green fluorescent nucleic acid dyes and aluminium oxide membrane filters for rapid epifluorescence enumeration of soil and sediment bacteria. *Appl. Environ. Microbiol.* 64, 5000–5003.

Whitman, W. B., Coleman, D. C., and Wiebe, W. J. (1998). Prokaryotes: the unseen majority. *Proc. Natl. Acad. Sci. U.S.A.* 95, 6578–6583.

Wilms, R., Sass, H., Köpke, B., Cypionka, H., and Engelen, B. (2007). Methane and sulfate profiles within the subsurface of a tidal flat are reflected by the distribution of sulfate-reducing bacteria and methanogenic archaea. *FEMS Microbiol. Ecol.* 59, 611–621.

Conflict of Interest Statement: The authors declare that the research was conducted in the absence of any commercial or financial relationships that could be construed as a potential conflict of interest.

Received: 31 March 2011; paper pending published: 23 May 2011; accepted: 05 July 2011; published online: 19 July 2011.

Citation: Breuker A, Köweker G, Blazejak A and Schippers A (2011) The deep biosphere in terrestrial sediments in the Chesapeake Bay area, Virginia, USA. Front. Microbio. ***2****:156. doi: 10.3389/fmicb. 2011.00156*

This article was submitted to Frontiers in Extreme Microbiology, a specialty of Frontiers in Microbiology.

frontiers in
MICROBIOLOGY

HYPOTHESIS AND THEORY ARTICLE
published: 09 November 2011
doi: 10.3389/fmicb.2011.00219

Is the genetic landscape of the deep subsurface biosphere affected by viruses?

Rika E. Anderson[1]*, William J. Brazelton[1,2] and John A. Baross[1]

[1] School of Oceanography and Astrobiology Program, University of Washington, Seattle, WA, USA
[2] Department of Biology, East Carolina University, Greenville, NC, USA

Edited by:
Jennifer F. Biddle, University of Delaware, USA

Reviewed by:
Elizaveta Bonch-Osmolovskyaya, Winogradsky Institute of Microbiology Russian Academy of Sciences, Russia
Jens Kallmeyer, University of Potsdam, Germany

****Correspondence:***
Rika E. Anderson, School of Oceanography, Box 357940, University of Washington, Seattle, WA 98195, USA.
e-mail: rikander@u.washington.edu

Viruses are powerful manipulators of microbial diversity, biogeochemistry, and evolution in the marine environment. Viruses can directly influence the genetic capabilities and the fitness of their hosts through the use of fitness factors and through horizontal gene transfer. However, the impact of viruses on microbial ecology and evolution is often overlooked in studies of the deep subsurface biosphere. Subsurface habitats connected to hydrothermal vent systems are characterized by constant fluid flux, dynamic environmental variability, and high microbial diversity. In such conditions, high adaptability would be an evolutionary asset, and the potential for frequent host–virus interactions would be high, increasing the likelihood that cellular hosts could acquire novel functions. Here, we review evidence supporting this hypothesis, including data indicating that microbial communities in subsurface hydrothermal fluids are exposed to a high rate of viral infection, as well as viral metagenomic data suggesting that the vent viral assemblage is particularly enriched in genes that facilitate horizontal gene transfer and host adaptability. Therefore, viruses are likely to play a crucial role in facilitating adaptability to the extreme conditions of these regions of the deep subsurface biosphere. We also discuss how these results might apply to other regions of the deep subsurface, where the nature of virus–host interactions would be altered, but possibly no less important, compared to more energetic hydrothermal systems.

Keywords: viral ecology, microbial evolution, hydrothermal vents, deep subsurface biosphere

INTRODUCTION

Viruses play a crucial role in marine biogeochemical cycles, microbial ecology, and evolution. Several recent reviews (Suttle, 2005; Rohwer and Thurber, 2009; Kristensen et al., 2010) have highlighted our current understanding of the viral impact on the marine environment. Generally, viruses influence the marine environment in three ways: first, through altering biogeochemical cycles by "shunting" the microbial loop through lysis of hosts (Suttle, 2005); second, by modifying the diversity and abundance of their hosts, particularly those that are most abundant, through what is dubbed "kill the winner" (Thingstad and Lignell, 1997); and third, by altering the genetic content of their hosts. Via the latter mechanism, viruses can fundamentally alter the course of evolution in their microbial hosts.

One means by which viruses can manipulate the genetic content of their hosts is by facilitating the process of horizontal gene transfer through transduction. This occurs when, in the process of virion synthesis, host genetic material is also incorporated into the viral genome. The newly synthesized viruses can then transfer the previous host's genetic material into a new host upon infection. It has been suggested that this could be an important mechanism for horizontal gene transfer in the marine environment: one study estimated that up to 10^{14} transduction events per year occur in Tampa Bay Estuary alone (Jiang and Paul, 1998). Additionally, viral-like transducing particles known as gene transfer agents (GTAs) are increasingly recognized as an important mechanism for horizontal gene transfer: it has been estimated that GTA transduction rates are over one million times higher than previously reported viral transduction rates in the marine environment (McDaniel et al., 2010). GTAs and their potential impact on the deep subsurface biosphere will be discussed below.

Viruses may be particularly important in facilitating horizontal gene transfer between phylogenetically distinct lineages. Fully sequenced genomes of archaea and bacteria indicate that horizontal gene transfer does occur between lineages that are distantly related, including between domains. Overall, it is thought that interdomain horizontal gene transfer is a relatively common phenomenon, with approximately 3% of genes in bacterial genomes and 4–8% of genes in archaeal genomes involved in transfer events (Yutin and Koonin, 2009). The genome of *Methanosarcina mazei*, for example, contains many genes of possible bacterial origin including a bacterial chaperonin system (Deppenmeier et al., 2002). Thermophiles appear to have a particularly high percentage of transferred genes (Beiko et al., 2005; Yutin and Koonin, 2009), though it is unclear if this is due to a propensity for acquiring distantly related genes or to the close proximity of archaea and bacteria in high temperature habitats like vents. For example, up to 16.2% of the genes in *Aquifex aeolicus* had a best hit to archaeal species (Deckert et al., 1998; Yutin and Koonin, 2009), which is much higher than the average for bacteria. The genome of *Thermotoga maritima*, isolated from geothermally heated sediment, contains genes related to oxygen reduction that are likely to have

been transferred through a single transfer event from a member of the *Thermococcales* (Nelson et al., 1999). Several *Thermococcales* strains have been found to contain mobile genetic elements or virus-like particles (Prieur et al., 2004), and thus there is a strong possibility that viruses are responsible for these transfer events. Viral transduction and GTAs are attractive as possible mechanisms for transfer events such as these because other mechanisms of genetic transfer do not seem capable of explaining the observed genomic similarities among distantly related species. Conjugation is a specialized process limited to particular lineages, and transformation often transfers only small amounts of genetic material, rather than multi-gene cassettes. While viral host range varies depending on viral type, some, especially GTAs, are thought to be capable of infecting distantly related hosts.

Viruses can manipulate the genetic content of their hosts not only by horizontal gene transfer, but also by expression of viral-encoded genes during the course of infection. The life cycle of lysogenic viruses involves a stage in which the virus integrates its own genome into the host genome, lying latent within the host genome for several generations until it is induced by an environmental stressor or other signal. Many integrated prophage have been found to encode what are termed fitness factors or lysogenic conversion genes: genes expressed by the prophage that can promote host fitness (Paul, 2008). These fitness factors can enhance host survivability in various environmental conditions. The cholera toxin genes in *Vibrio cholerae*, for example, are expressed by a filamentous bacteriophage that has integrated into the *V. cholerae* genome (Waldor and Mekalanos, 1996). Studies have shown that prophage genes are upregulated in response to changing environmental conditions (Smoot et al., 2001) or during biofilm formation (Whiteley et al., 2001). Even cryptic prophage, which have been integrated in the host genome for so long that they have decayed and are no longer active as phage, can carry genes that improve survivability during osmotic, oxidative, and acid stresses, and influence biofilm formation (Wang et al., 2010). Viruses infecting marine cyanobacteria, or cyanophage, have been found to carry genes for both photosystems I and II (Mann et al., 1993; Lindell et al., 2004, 2005; Millard et al., 2004; Sullivan et al., 2005; Sharon et al., 2009). These genes are expressed during viral infection, and are thought to enhance phage fitness by supplementing the host's photosynthetic machinery (Lindell et al., 2005).

While a large amount of work has been dedicated to understanding the viral impact on the marine environment, the implications for the deep subsurface biosphere have been barely explored. **Table 1** summarizes current research on viral abundance, production, and diversity in the deep subsurface biosphere, as well as shallow sediments, methane hydrates, and the deep-water column to provide a basis for comparison.

As can be seen in **Table 1**, only a few studies have focused on deep subsurface viruses. Most research to date in the deep ocean has focused on viral production and abundance in the water column and surface sediments. None of these studies, to our knowledge, has focused on the genetic and evolutionary implications of viral infection on the deep subsurface biosphere. Yet the viral impact on the evolution of bacterial and archaeal hosts could have even more profound implications in the deep subsurface than in the upper water column. A primary reason for this is that it is generally accepted that lysogeny is a more important viral lifestyle under suboptimal conditions, when host or nutrient abundance is low (Paul, 2008). This has been demonstrated in laboratory conditions, in which lysogenic viruses have a competitive advantage over lytic viruses in nutrient-limited media (Levin and Lenski, 1983). In natural populations, lysogeny becomes a more common lifestyle during seasons or in regions where host abundance is low (Jiang

Table 1 | Summary of previous work on viral abundance, activity, and diversity in various environments of the deep subsurface biosphere, deep ocean, and sediments.

Environment	Work on viruses to date	Reference
Surface marine sediments	High viral production in benthic ecosystems: may be responsible for up to 80% of cell mortality, thus releasing large amounts of carbon through the "viral shunt." Viral diversity in sediments is fairly high, and showed a higher incidence of lysogenic than lytic phages	Danovaro et al. (2008), Middelboe et al. (2006), Siem-Jørgensen et al. (2008), Breitbart et al. (2004)
Deep sediments	Viral and bacterial abundance and production decrease exponentially with depth in sediments, up to 96 mbsf Mitomycin C experiments revealed that 46% of isolates contained inducible prophage	Middelboe et al. (2011), Bird et al. (2001), Engelhardt et al. (2011)
Deep basalt	None known	
Deep granitic groundwater	Viruses are present and correlated with bacterial abundance (ratio of ∼10:1), similar to many surface environments	Kyle et al. (2008)
Diffuse flow hydrothermal fluid	Lysogeny appears to be a dominant lifestyle among vent viruses; viruses in diffuse flow are capable of infecting a wide range of hosts across domains and thermal regimes	Williamson et al. (2008), Anderson et al. (2011)
Cold seeps/methane hydrates	Viral activity and abundance vary among seeps, with a virus to prokaryote ratio ranging between relatively low (<0.1) to relatively high (66.36)	Middelboe et al. (2006), Kellogg (2010)
Deep-water column	Viral abundance generally tracks bacterial abundance, but the virus:cell ratio at depth varies. In some areas, the ratio increases with depth Metagenomic work characterizing viral diversity found most viral sequences had matches to bacteriophages in the *Podo-*, *Sipho-*, and *Myoviridae*, with a few hits to eukaryotic sequences	Hara et al. (1996), Parada et al. (2007), Steward and Preston (2011)

and Paul, 1998; McDaniel et al., 2002; Williamson et al., 2002; Weinbauer, 2004). Therefore, lysogeny may be a favored lifestyle in the deep subsurface due to difficulties in finding a new host after newly synthesized virions are released. In deep sediments, the main difficulties are likely to be low cell abundance and immobility. In extreme environments, lysogeny may be favored because of reduced viability of viral particles outside the cell. As shown in **Table 1**, lysogeny appears to be a common lifestyle in sediments and hydrothermal vents. If lysogeny is indeed more common in the deep subsurface biosphere, this would increase the proportion of cells harboring prophage, potentially increasing the number of cells expressing fitness factors encoded by the prophage.

The impact of viruses on the genetic landscape of their hosts may be particularly pronounced in diffuse flow fluids of hydrothermal systems. In these environments, high temperature hydrothermal fluid mixes with seawater both in the subsurface and above the seafloor, resulting in gradients of temperature, pH, and chemical and mineralogical composition (Baross and Hoffman, 1985). A schematic representation of the vent environment, and the accompanying gradients, is shown in **Figure 1A**. The constant fluid flux through these gradients enables potentially frequent contact between diverse microbial communities.

The microorganisms inhabiting diffuse flow fluids are tremendously diverse in terms of taxonomy, metabolism, and thermal

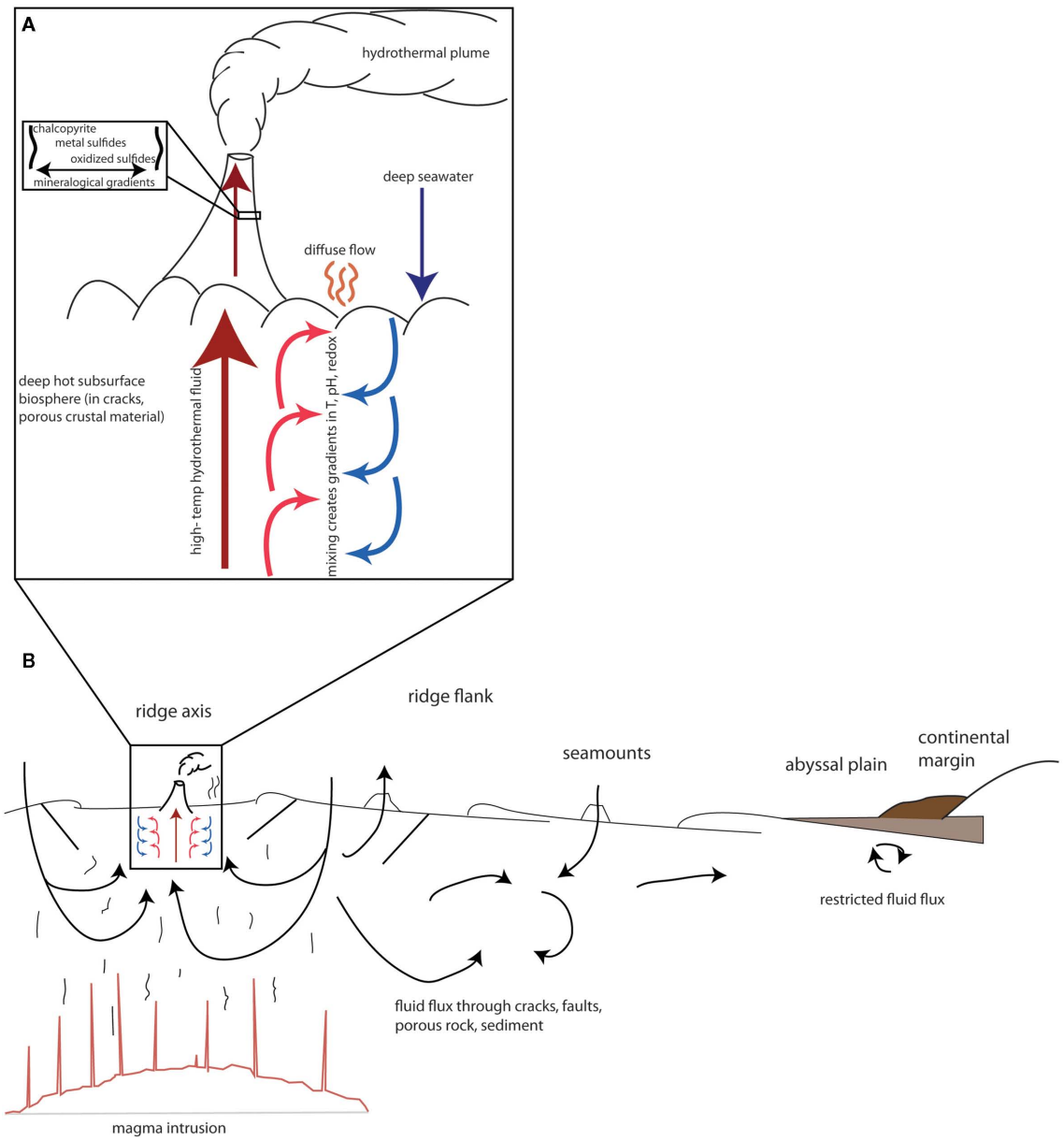

FIGURE 1 | Schematic of fluid flux and gradient formation in (A) hydrothermal systems and (B) various regimes of the deep biosphere. Arrows represent fluid flux. Based on figures in Edwards et al. (2011), Huber et al. (2003), and Baross and Hoffman (1985).

regime. Studies of the population structures of archaea and bacteria in diffuse fluids have found thousands of phylotypes within both domains (Huber et al., 2007). The abundance of reduced compounds in vent fluids allows microbial metabolisms to take advantage of a wide range of energy sources, including hydrogen, reduced iron, sulfur, as well as organic compounds. There is, therefore, a wide range of potential hosts for viruses to infect in diffuse flow fluids.

In the extreme and dynamic conditions of hydrothermal vents, genetic exchange could provide a fitness advantage to any organism able to acquire a novel function that is useful in a changing environment. Evidence already exists suggesting that vent habitats are conducive for genetic exchange. As mentioned above, genomic studies have shown that rates of horizontal gene transfer between thermophiles are higher than between other groups, including between domains. This may be due to the predominant physiology of vent organisms: microbial communities often form biofilms on the surfaces of or within vent structures (Jannasch and Wirsen, 1981; Schrenk et al., 2003). Subsurface sediments and crustal habitats also provide abundant surfaces for biofilm formation. The high cell density in a biofilm increases rates of host contact, thus facilitating higher rates of viral infection, and can also foster genetic exchange through transformation. A recent metagenomics study found that transposase sequences in biofilms in the Lost City hydrothermal field are 10 times more abundant than in metagenomes from other environments (Brazelton and Baross, 2009). If this result is characteristic of subsurface biofilms, then genetic exchange in the deep subsurface biosphere is likely to be of great importance.

It has been suggested that viruses may act as a reservoir of genes that can be used as a mechanism for adaptation by their cellular hosts (Goldenfeld and Woese, 2007), effectively expanding the "pan-genome" to include the viral assemblage. Here, we argue that viral-mediated genetic exchange is particularly important as a means to adapt to frequently changing conditions in the diffuse flow vent environment. We will review what is known about viruses in the vent environment, and examine what evidence exists that viruses play a role in modifying the genetic content (and therefore the fitness) of their cellular hosts. We conclude by discussing the larger implications for viruses in the deep subsurface biosphere in general.

VIRUSES AS A "GENETIC REPOSITORY" IN HYDROTHERMAL VENT SYSTEMS

EVIDENCE FOR VIRAL ACTIVITY IN DIFFUSE FLOW SYSTEMS

The few studies that have focused on viruses in diffuse flow vent environments have indicated that viruses play an important role in influencing microbial ecology in these ecosystems. One study quantified viral abundance in diffuse flow fluids, finding that on average there were approximately 10^7 viral-like particles (VLPs) per milliliter of fluid, or about 10 times as many viruses as cells, which is comparable to other marine ecosystems (Ortmann and Suttle, 2005). Another study, focusing on VLP counts at shallow hydrothermal vents, found that viruses were about five times more abundant than cells, though found that VLP counts increased with distance from the vents (Manini et al., 2008). The authors suggested that one possible explanation for this trend was a change in viral lifestyle from lysogenic to lytic, resulting in an increase in the number of apparent viruses. Additionally, diffuse fluids from 9° North, a hydrothermal vent field on the East Pacific Rise, have been found to harbor a higher incidence of inducible prophage than nearby ambient seawater, indicating that lysogeny is a more common lifestyle for vent phage than those in other marine environments (Williamson et al., 2008). A viral metagenome at Hulk vent on the Juan de Fuca Ridge showed that vent viruses are relatively diverse and have the potential to infect hosts from a wide range of taxonomic groups and thermal regimes (Anderson et al., 2011).

Genome sequences of bacteria and archaea may also show evidence of extensive viral activity in diffuse flow hydrothermal vents. Within bacterial and archaeal genomes are regions called clustered regularly interspaced palindromic repeats (CRISPRs), which are thought to facilitate the immune response to viral infection (Barrangou et al., 2007; Brouns et al., 2008; Sorek et al., 2008; van der Oost et al., 2009; Hovarth and Barrangou, 2010; Labrie et al., 2010; Marraffini and Sontheimer, 2010). These loci consist of a series of short repeats, about 20–50 bp long, and are interspersed by a series of spacer regions, each about 25–75 bp in length. These spacer regions are created to match a short sequence on an invading element, such as a virus or a plasmid. The newly synthesized spacers are then inserted between direct repeats on the CRISPR locus (Makarova et al., 2003; Bolotin et al., 2005; Haft et al., 2005; Mojica et al., 2005; Pourcel et al., 2005; Marraffini and Sontheimer, 2008; Hale et al., 2009). If a virus or plasmid invades a cell that possesses a CRISPR spacer matching a sequence on that invader, the CRISPR system will mobilize the immune response. This occurs through the formation of a Cascade complex from nearby *Cas* (CRISPR-associated) genes in conjunction with small RNAs derived from the CRISPR spacers, which recognize and bind target DNA (Jore et al., 2011). The invading nucleic acid is cleaved as a result (Garneau et al., 2010).

Each of these CRISPR regions therefore acts as a record of previous viral infection, with each spacer thought to represent at least one independent infection event in the history of that strain. Interestingly, it has been observed that thermophilic strains, on average, have a higher number of CRISPR loci in their genomes than mesophiles or psychrophiles (Makarova et al., 2003; Anderson et al., 2011; **Figure 2**). While there is no definitive explanation for the abundance of CRISPRs in thermophiles, this does indicate that viral infection plays an important role in the evolution and ecology of thermophilic microbial communities. Moreover, the CRISPR immune mechanism itself is unique among viral immunity systems in that it responds in a sequence-specific manner to the invasion of foreign genetic material, rather than through prevention of phage adsorption, blocking phage DNA entry, or random restriction modification. Thus, the abundance of CRISPRs in thermophiles indicates that at least the entry, if not the successful takeover, of foreign genetic material between different hosts is a relatively common phenomenon in high temperature environments. CRISPR loci can also be found in the genomes of bacteria and archaea isolated from other environments in the deep ocean and sediments (**Table 2**), though there is a clear correlation with temperature. This may serve as evidence that viruses play a particularly important role in the evolution of microbes in high temperature

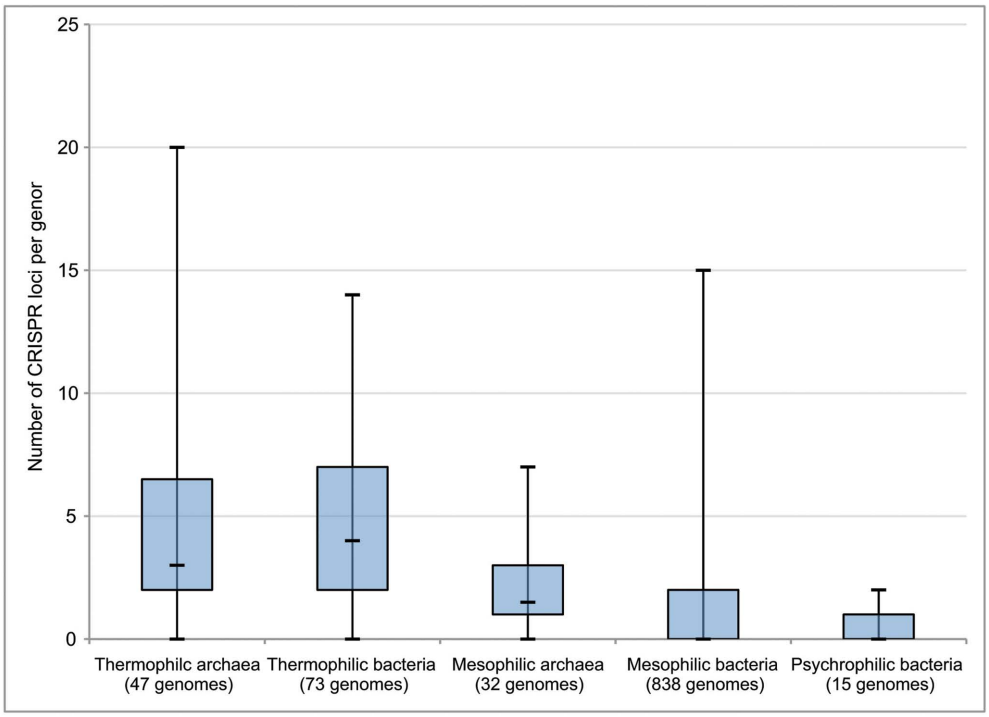

FIGURE 2 | Number of CRISPR loci per genome in thermophilic, mesophilic, and psychrophilic archaea and bacteria. Box boundaries represent first and third quartiles, and markers on lines represent minimum, median, and maximum, respectively. Modified from Anderson et al. (2011).

environments. This includes diffuse flow hydrothermal vents but could also include other regions in the subsurface with broad temperature gradients.

A further piece of evidence for the important role of viruses, one that is not restricted to high temperature organisms, is the presence of prophage in the genomes of sequenced archaea and bacteria. As mentioned above, lysogenic phage can provide supplementary metabolic functions while integrated into the genome as prophage. **Table 2** lists the bacteria and archaea from diffuse flow fluids and other deep ocean habitats that have been found with integrated prophage in their genomes. Two of the listed bacterial isolates, one from the deep-water column and one from marine sediments, each possess seven prophage in their genomes. This represents a significant amount of genetic material. Considering the tendency of bacteria to select for faster reproduction rates and thus for smaller genomes (Carlile, 1982), the presence of seven prophage regions on the genome represents a potential fitness cost (through slower replication rates) that must be offset by a fitness benefit, such as the presence of fitness factors expressed by the prophage. Considering the prevalence of prophage in the genomes of isolates from diffuse flow fluids and deep sediments, it would not be surprising if prophage are present in most subsurface organisms.

EVIDENCE FOR VIRAL-MEDIATED HORIZONTAL GENE TRANSFER

Having established that viruses are abundant and likely to be active in diffuse flow hydrothermal fluids, we now turn to evidence that viruses mediate the exchange of genes between hosts in these regions. Here, we will do this primarily through analysis of a marine hydrothermal vent viral metagenome, or virome, collected from Hulk vent in the Main Endeavor Field on the Juan de Fuca Ridge, previously described in Anderson et al. (2011). We examine evidence for viral-mediated horizontal gene transfer in the vent environment first by searching the marine vent virome for genes related to lysogeny and gene insertion; and then by using comparative metagenomics to determine which genes are selected to be maintained in the viral gene pool.

GENES RELATED TO LYSOGENY AND GENE INSERTION

As mentioned above, a higher proportion of bacteria and archaea in diffuse flow hydrothermal vents appear to contain inducible prophage within their genomes than bacteria and archaea from other marine environments (Williamson et al., 2008), indicating that lysogeny is an important lifestyle for viruses in diffuse flow fluids. To test whether this finding is supported by publicly available metagenomic data, we searched for genes associated with lysogeny in the marine vent virome from Hulk and compared the number of matches with that of metagenomes from other environments. It is important to note that while most lysogenic phage are integrated into cellular genomes as prophage, the Hulk vent sample would have experienced substantially colder temperatures as well as decreased pressures prior to the filtration steps that removed cells and captured viral-sized particles. This environmental shock may have induced many of the prophage within the microbial community, resulting in their being captured in the viral size fraction. While this has not yet been demonstrated experimentally, it

Table 2 | Habitat, thermal regime, number of CRISPR loci, and number of prophage for archaea and bacteria isolated from the deep-water column, marine sediments, or hydrothermal systems whose genomes have been sequenced.

Name	No. CRISPR loci	No. prophage	Optimal growth temperature (°C)	Habitat	Reference
ARCHAEA					
Aciduliprofundum boonei	2	2	70	Hydrothermal chimney	Reysenbach et al. (2006)
Methanocaldococcus jannaschii DSM 2661	20	0	85	Hydrothermal chimney	Jones et al. (1983)
Methanocaldococcus sp. FS406-22	23	0	85	Hydrothermal fluid	Mehta and Baross (2006)
Methanopyrus kandleri strain 116	5	0	122	Hydrothermal fluid	Takai et al. (2008)
Methanothermococcus okinawensis	7	1	60–65	Hydrothermal chimney	Takai et al. (2002)
Thermococcus barophilus	4	0	85	Hydrothermal chimney	Marteinsson et al. (1999)
Thermococcus gammatolerans	3	3	88	Hydrothermal chimney	Jolivet et al., 2003
BACTERIA					
Deferribacter desulfuricans	4	1	60–65	Hydrothermal chimney	Takai et al. (2003)
Idiomarina loihiensis L2TR	0	3	43	Hydrothermal fluid	Hou et al. (2004)
Marinithermus hydrothermalis	5	2	67.5	Hydrothermal chimney	Sako et al. (2003)
Nautilia profundicola	0	1	41–45	Polychaete worm	Campbell et al. (2001)
Nitratifractor salsuginis	2	3	37	Hydrothermal chimney	Nakagawa et al. (2005)
Oceanithermus profundus	1	1	60	Hydrothermal chimney	Miroshnichenko et al. (2003)
Oceanobacillus iheyensis HTE831	0	4	30	Deep sea sediment	Lu et al. (2001)
Photobacterium profundum	2	3	10	Deep sea sediment	Nogi et al. (1998)
Shewanella piezotolerans WP3	1	5	15–20	Deep sea sediment	Wang et al. (2008)
Shewanella violacea DSS12	1	1	8	Deep sea sediment	Kato et al. (1995)
Sulfurimonas autotrophica	0	1	25	High temperature sediment	Inagaki et al. (2003)
Thermosediminibacter oceani DSM 16646	6	7	68	Deep sea sediment	Lee et al. (2005)
Zunongwangia profunda SM-A87	2	2	25–30	Deep sea sediment	Qin et al. (2010)

CRISPR loci were identified with CRISPRFinder (Grissa et al., 2007a,b) and prophage were identified with ProphageFinder (Bose and Barber, 2006). Modified from a table in Orcutt et al. (2011).

is an important consideration in the sampling of metagenomes from relatively extreme environments.

To determine the overall abundance of genes related to lysogeny, we first created a database of lysogeny-associated proteins with Pfam seed sequences (Finn et al., 2010). These proteins include phage integrases, repressors, and antirepressors expressed during the prophage stage, regulatory proteins that trigger the switch between the lysogenic and lytic stages, and proteins involved in phage integration and excision. We queried this database with the marine vent virome using BLASTX, as well as a set of other viral and cellular metagenomes from the MG-RAST database (Meyer et al., 2008).

Metagenomes with the highest percentages of sequencing reads matching lysogeny domains were cellular rather than viral (**Table 3**). These hits were most likely matches to prophage incorporated into cellular genomes. Two of the top three metagenomes were sampled from environments that are considered "extreme," namely, a highly acidic mine drainage and the high-pH, high temperature Lost City hydrothermal field. This supports the hypothesis stated earlier that lysogeny becomes a more common viral lifestyle in extreme environments because viruses have a higher chance of survival as prophage than as virions under harsh conditions. Also in the top three was the whale fall cellular metagenome. While it is unclear exactly why this metagenome had a relatively high percentage of lysogeny-related domains, one possibility is that since whale falls are relatively rare events, the organisms colonizing whale falls must endure extreme periods of relative starvation, followed by periods of plenty. Any viruses infecting these taxa would benefit from a lysogenic lifestyle in order to survive these extreme periods of starvation, during which cells would most likely either be dormant or replicating extremely slowly.

Fourth on the list was a cellular metagenome sampled from farm soil, in which lysogeny may be the favored lifestyle for viruses as a result of the difficulties in encountering a new host within the sediment matrix, an environment in which mobility is likely to be significantly impaired. However, sequences matching lysogeny domains were not particularly abundant in cellular metagenomes derived from deep Peru Margin sediments, though some depth horizons had a higher abundance than others (**Table 3**). At this point it is unclear whether this is due to differences in viral lifestyle or simply to a lower abundance of viruses in Peru Margin sediments.

In contrast, the sequences matching lysogeny domains in the Yellowstone hot springs and marine vent viromes (fifth and sixth

Table 3 | Percent of reads matching a DNA ligase and a transposase domain in 19 sequenced metagenomes.

Metagenome	Type of metagenome	Percent of reads matching a lysogeny domain (rank)	Percent of reads matching a DNA ligase	MG-RAST ID number	Reference
Marine vent virome (subset)	Viral	0.073 (6)	1.245	Subset of 4448187.3	Anderson et al. (2011)
Marine vent virome (full)	Viral	0.067 (7)	0.594	4448187.3	Anderson et al. (2011)
Farm soil	Microbial	0.192 (4)	0.131	4441091.3	Tringe et al. (2005)
Acid mine drainage	Microbial	0.468 (1)	0.109	4441137.3, 444138.3	Tyson et al. (2004)
Yellowstone hot springs	Viral	0.104 (5)	0.085	4443745.3, 4443746.3, 4443747.3, 4443762.3, 4443749.3, 4443750.3	Bhaya et al. (2007)
Whale fall	Microbial	0.332 (2)	0.070	4441619.3, 4441656.4, 4441620.3	Tringe et al. (2005)
Lost city hydrothermal field	Microbial	0.291 (3)	0.069	4461585.3	Brazelton and Baross (2009)
Alvinella symbionts	Microbial	0.044 (9)	0.068	4441102.3	Grzymski et al. (2008)
Peru margin sediments, 32 mbsf	Microbial	0.020 (11)	0.047	4459940.3	Biddle et al. (2008)
Peru margin sediments, 1 mbsf	Microbial	0.017 (13)	0.044	4440961.3	Biddle et al. (2008)
Arctic Ocean	Viral	0.020 (12)	0.018	4441622.3	Angly et al. (2006)
Peru margin sediments, 16 mbsf	Microbial	0.005 (18)	0.018	4440973.3	Biddle et al. (2008)
Peru margin sediments, 50 mbsf	Microbial	0.016 (14)	0.016	4459941.3	Biddle et al. (2008)
Fishgut	Microbial	0.023 (10)	0.010	4441695.3	Dinsdale et al. (2008)
Gulf of Mexico	Viral	0.008 (15)	0.006	4441625.4	Angly et al. (2006)
Bay of British Columbia	Viral	0.006 (17)	0.004	4441623.3	Angly et al. (2006)
Microbialites	Viral	0.063 (8)	0.003	4440320.3, 4440321.3, 4440323.3	Desnues et al. (2008)
Sargasso Sea	Viral	0.004 (19)	0.002	4441624.3	Angly et al. (2006)
Microbialites	Microbial	0.008 (16)	0	4440061.3	Breitbart et al. (2009)

Metagenomes are ordered according to the percent of reads matching a DNA ligase, with the highest percentage at the top. Column 3 lists the percentage of reads to a lysogeny-related domain, followed by the rank according to the percentage of reads with a hit among other metagenomes. The marine vent virome subset consists of all reads within contigs with a coverage of eight or greater plus all reads within contigs labeled "unknown" (Anderson et al., 2011). Marine vent virome reads were dereplicated prior to analysis. Mbsf, meters below seafloor. Metagenomes were downloaded from the MG-RAST database (www.metagenomics.anl.gov) and compared to a list of lysogeny-related sequences derived from Pfam seed sequences using blastx with a minimum e-value of 10^{-5}.

on the list, respectively) are most likely derived from lysogenic viruses that entered the lytic stage due to an environmental stressor, possibly resulting from the sampling process. Interestingly, these two viromes, both sampled from high temperature environments, had the highest proportion of sequencing reads matching lysogeny domains of all the viromes analyzed here. In contrast, viromes from more temperate environments, such as the Bay of British Columbia or the Sargasso Sea, had a much lower abundance of lysogeny sequences. This parallels the relative abundance of lysogeny-related domains in extreme cellular metagenomes, and again may indicate that natural selection favors lysogenic viruses in extreme environments.

The lysogeny-associated domains chosen for this analysis were selected from genes that are uniquely associated with prophage. However, this would exclude genes that serve other roles in both viruses and cells but may also be crucial in facilitating horizontal gene transfer. This includes genes required for integration of DNA into host or viral genomes, such as DNA ligases. Interestingly, 1.25% of the sequencing reads in the marine vent virome had a match to a DNA ligase, which is almost 10 times higher than any of the 17 other cellular or viral metagenomes analyzed here (**Table 3**). Moreover, these ligases were especially enriched in the subset of the marine vent virome considered more likely to be "viral" – that is, those reads that were assembled into contigs with an average coverage of at least eight, or within contigs in which a majority of reads were categorized as either "unknown" or "viral" by MG-RAST (Anderson et al., 2011). Therefore, the abundance of ligases appears to be distinctly viral in character.

Most of the potential ligase sequences in the marine vent virome had matches to NAD-dependent ligases rather than ATP-dependent ligases. ATP-dependent ligases are fairly widespread among eukaryotes, bacteria, and archaea, while NAD-dependent ligases are generally characteristic of bacteria, though they have been seen in some viruses, eukaryotes, and archaea (Doherty and Suh, 2000; Tomkinson et al., 2006). Furthermore, they appear to be characteristic of marine rather than terrestrial metagenomes, for unknown reasons. To determine whether the ligases in the marine vent virome were most closely related to ligases from a particular group of organisms, we constructed a phylogenetic tree of NAD-dependent DNA ligases including ligase-matching

sequences from the marine vent virome, using a reference tree of previously characterized DNA ligases as a constraint (**Figure 3**). The reference viral ligases do not necessarily group together on this tree, suggesting there is not a viral ligase type that is necessarily distinct from bacterial, archaeal, or eukaryotic ligases. Similarly, the sequences from the marine vent virome are scattered across the tree, with some closely related to ligases found in viruses, and others more closely related to bacterial or archaeal ligases. Yutin and Koonin (2009) have previously highlighted the non-monophyletic nature of viral DNA ligases. This may attest to the fluid nature of viral genomes in that they frequently pick up genes from their hosts and may also be a further indication of the high diversity of the marine vent viral assemblage. While several vent virome sequences were grouped with DNA ligases found in viruses, the majority grouped most closely with a DNA ligase from *Rickettsia felis*, a Gram-negative bacterium in the Alphaproteobacteria group. *R. felis* is closely related to SAR11, one of the most common bacterial lineages in marine environments. While SAR11 sequences were not common in the marine vent virome, it is possible that ancestral viruses in the marine vent environment had acquired ligases from SAR11 or similar groups, which then became more abundant in the viral gene pool due to positive selection.

While it is unclear exactly what ecological role these ligases play, their high abundance suggests that they play a uniquely important role in the vent viral assemblage. DNA ligases repair double-stranded breaks in DNA by catalyzing the synthesis of phosphodiester bonds between 5′-phosphoryl and 3′-hydroxyl groups (Lehnman, 1974). DNA ligases are thus important for DNA replication, recombination, and repair across all domains as well as viruses. However, the high abundance of DNA ligases in the vent virome is unusual and may reflect a specific role in the vent ecosystem, possibly in the integration of viral genomes into the host genome through recombination. It is therefore plausible that the abundance of these genes is indicative of prevalent horizontal gene transfer in these regions of the deep subsurface biosphere.

Finally, GTAs may act as an important mechanism for viral-mediated horizontal gene transfer. These phage-like particles were originally discovered in marine *Rhodobacteria*, but have since been discovered in various other bacterial and archaeal species, particularly in the marine environment (Lang and Beatty, 2000; Matson et al., 2005; Stanton, 2007; Biers et al., 2008, Leung et al., 2010). GTAs randomly incorporate segments of the host genome into a viral capsid, then transfer this to new hosts, including phylogenetically unrelated organisms, without resulting in lysis of the host cell. It has been suggested that GTAs are defective phage

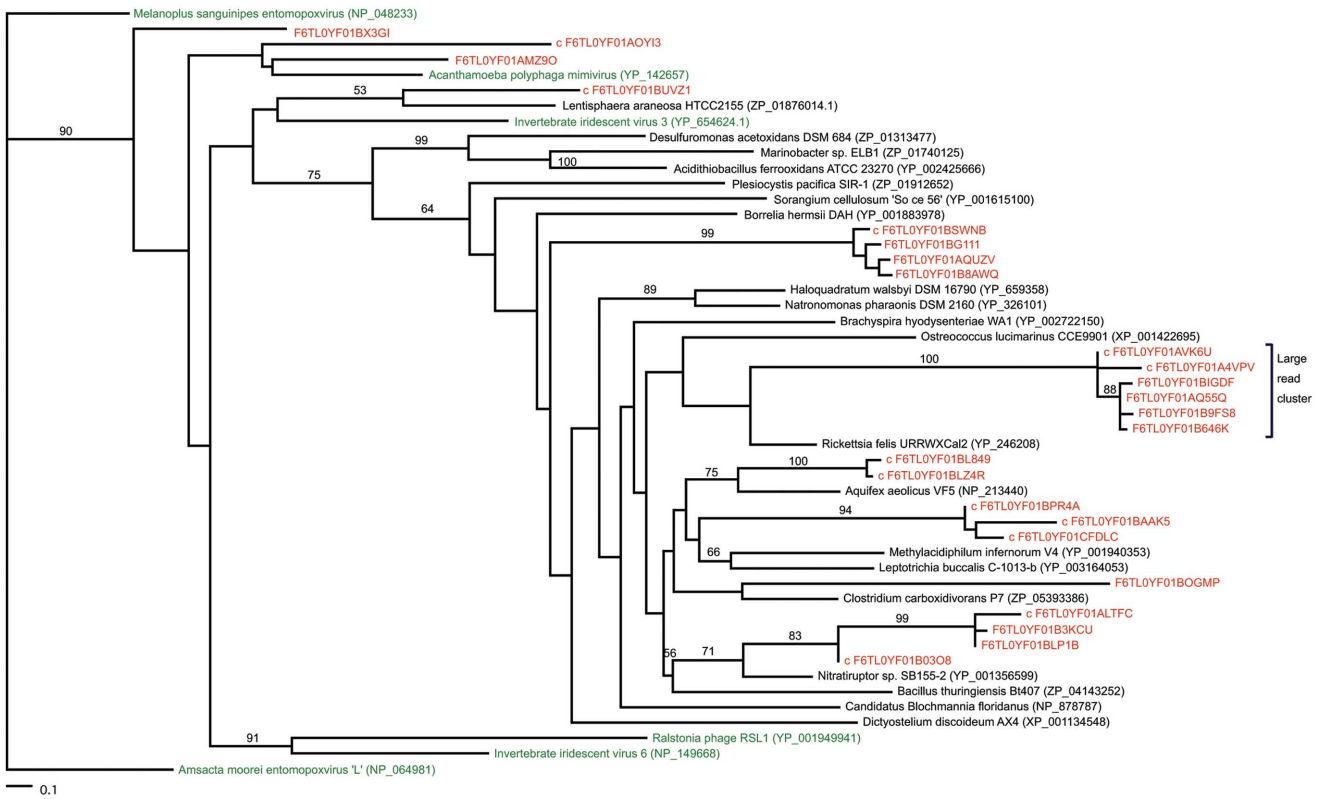

FIGURE 3 | Maximum-likelihood phylogenetic tree of NAD-dependent DNA ligases with metagenomic reads from the marine vent virome. The "large read cluster" denotes the branch in which the majority of metagenomic reads matching ligases grouped on the tree. Numbers indicate the bootstrap values of internal nodes (where $n = 100$). Metagenomic reads are colored red. All ligase protein sequences were obtained from NCBI (accession numbers listed). Trees were constructed in RAxML by incorporating metagenomic sequences into a constraint tree of references sequences based on the phylogeny of Yutin and Koonin (2009). Trees imaged with TreeViewX.

(Lang and Beatty, 2000; Matson et al., 2005; Stanton, 2007); if so, it would seem that GTAs have effectively lost their parasitic nature and have instead been usurped by the host for the purposes of gene exchange. While the only sequenced GTA genes are from the *Rhodobacter capsulatus* (Lang and Beatty, 2000) and *Brachyspira hyodysentariae* (Matson et al., 2005) GTAs, the marine vent virome included six sequencing reads with matches to known GTA genes. While these are few, the scarcity of sequences from GTAs in public databases to date prohibits a larger-scale search for GTAs in viral metagenomes. Nevertheless, GTAs may play a significant role in transferring genes between hosts in the marine environment and appear to be present in diffuse flow fluids. In the dynamic, extreme conditions of the deep subsurface, selection may be particularly strong for cells that harbor GTAs as a mechanism for obtaining advantageous genes. It has been hypothesized that a large portion of marine viromes may consist of GTAs carrying poorly conserved bacterial genes (Kristensen et al., 2010) and may thus contribute a large portion of the poorly conserved "cloud" of genes in the viral gene pool.

ENRICHMENT FOR FUNCTIONAL GENES IN THE VENT VIROME

This "cloud" of genes, or genetic reservoir, consists of an overlapping pool of genes derived from both viruses and cells. Genes in the viral genetic reservoir are expressed in cellular hosts through either horizontal gene transfer or prophage insertion, and then maintained in the gene pool through positive selection. Thus, the genes maintained in the viral metagenome, in addition to genes for viral synthesis, packaging, and maintenance, are likely to consist of non-housekeeping genes that provide a selective advantage in the event of a shift in environmental conditions. This is expected to be particularly the case in the gradient-dominated, dynamic vent environment.

An initial example of this can be found through analysis of assembled contigs of the marine vent virome from Hulk (assembly and contig analysis described in Anderson et al., 2011). Among the lysogeny domains matching sequences in the marine vent virome was the XerD tyrosine recombinase protein, commonly associated with lysogenic phage and transposases. This gene was assembled onto a contig that also contains the universal stress protein UspA. UspA is known to be phosphorylated in response to stasis stress in *Escherichia coli* (Nyström and Neidhardt, 1994; Freestone et al., 1997), and thus is induced when growth conditions are not optimal. It would be advantageous to both host and prophage for the prophage-encoded protein to induce a response in the host when growth conditions are poor. As mentioned, prophage have been found to encode genes to enhance host survivability in stressful conditions, and this sequence may be one example of many such instances in the vent ecosystem.

While this is one example of a potential fitness factor encoded by a lysogenic phage, comparative metagenomics can give a more large-scale picture of which functional genes are enriched in the viral fraction. To do this we compared the relative enrichment of several gene categories in the marine vent virome and a cellular metagenome sampled from a sulfide chimney at Mothra hydrothermal field on the Juan de Fuca Ridge (Xie et al., 2011; **Figure 4**). Each metagenome was analyzed through the MG-RAST pipeline and annotated using the KEGG Orthology database (Meyer et al., 2008). For this analysis, as before, we used only the vent virome subset that we consider to be convincingly viral: that is, sequencing reads assembled into contigs with an average coverage of at least eight or composed of reads identified as "unknown" or "viral" by MG-RAST. The virome was relatively enriched in gene categories such as replication and repair, nucleotide metabolism, and translation, which are important for the synthesis of viral genetic material during the lytic stage. Interestingly, however, the virome was particularly enriched in genes related to energy metabolism, with nearly 12% of all identifiable sequencing reads matching this category in the virome, compared to 7% in the cellular metagenome. Genes in this category include genes used for oxidative phosphorylation, photosynthesis, methane metabolism, carbon fixation, and sulfur and nitrogen metabolism. It seems plausible that these genes are maintained in the viral genetic reservoir through positive selection. For example, if a cell were to be flushed into a region in which the abundance of its conventional electron donor was limited, the acquisition of a gene allowing it to utilize an alternative electron donor, via either transduction or prophage expression, would increase the fitness of that cell. The relative enrichment of genes related to energy metabolism in the virome may be evidence of this type of selection.

Other sequences in the marine vent virome had matches to metabolic genes that have also been found in viruses from other environments. For example, 11 sequencing reads in the marine vent virome had close matches to PhoH, a phosphate starvation-inducible protein that has previously been found in *Prochlorococcus* and *Synechococcus* phage genomes (Sullivan et al., 2009). It has been hypothesized that PhoH, when expressed by phage, could aid the host in phosphorus scavenging during the infection stage. In hydrothermal systems, phosphate is removed from seawater through water–rock reactions in the deep subsurface, thus limiting phosphate availability to native microbial communities (Wheat et al., 1996). The presence of PhoH in the marine vent virome suggests that vent viruses may, in a manner similar to the cyanophage, assist in phosphate acquisition during the course of infection. Similarly, eight reads closely matching transaldolases, also found on cyanophage genomes, were found in the marine vent virome. It is thought that these transaldolases may play a role in metabolizing carbon substrates to assist in energy production and synthesis of important compounds, and thus may be yet another example of fitness factors expressed by phage (Sullivan et al., 2005).

This positive selection for genes that can increase host fitness would suggest that the genes found in the marine vent virome can give an indication of the unique environmental conditions from which it was sampled, such as limitations or extremes in factors such as nutrients, energy availability, temperature, or pH. For example, 301 sequencing reads in the marine vent virome were annotated by MG-RAST as uptake [NiFe]-hydrogenases, enzymes involved in the oxidation of hydrogen to produce energy (Vignais and Billoud, 2007). Hydrogen oxidation is known to be an important metabolic strategy in hydrothermal vent systems, where it provides a greater energy return than the oxidation of methane or sulfur (Amend and Shock, 2001), which are also common reduced compounds in vent environments. The [NiFe]-hydrogenases encoded in the marine vent virome could enable

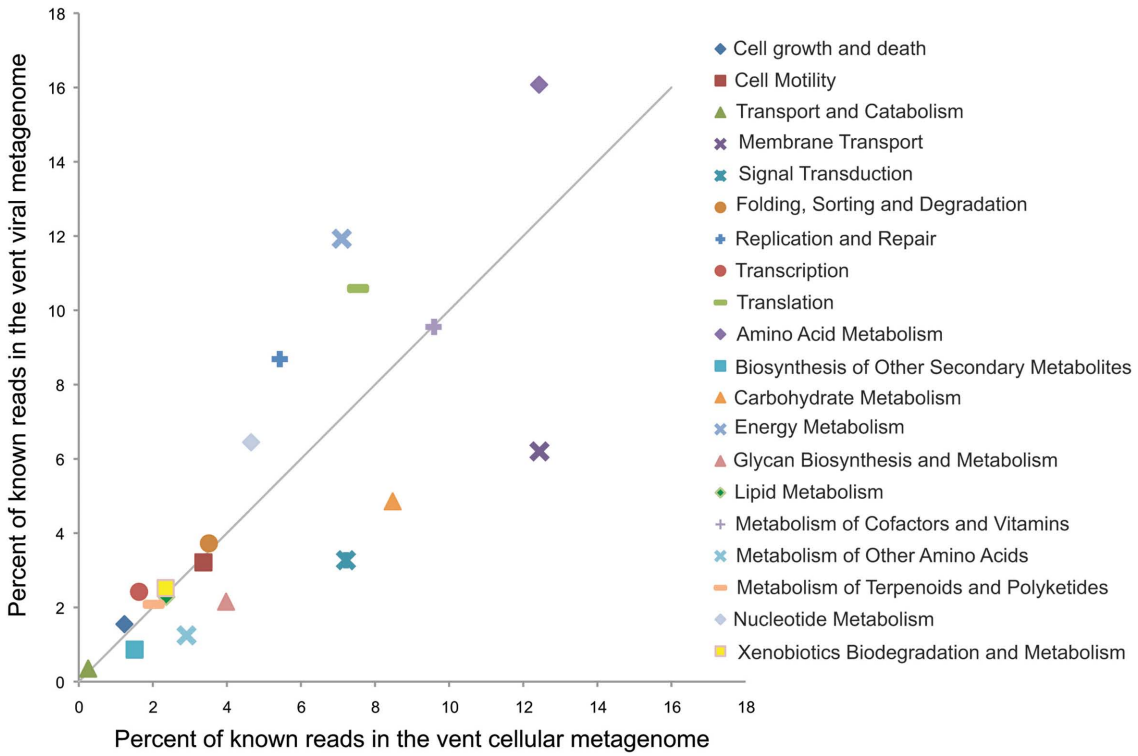

FIGURE 4 | Relative percentages of reads matching gene categories in the marine vent virome (Anderson et al., 2011) and the hydrothermal vent cellular metagenome by Xie et al. (2011). The solid line indicates a 1:1 ratio between the viral and cellular metagenomes. Metagenomes were analyzed with MG-RAST (Meyer et al., 2008), and reads were annotated with the KEGG Orthology database, release 56.

utilization of an important alternative energy source for viral hosts if transferred into their genome via transduction, or if expressed by prophage as a fitness factor, which could bolster host metabolism during viral infection.

To present a larger-scale illustration of how the genetic profile of a virome might act as a signature of the environment from which it was sampled, we compared the relative enrichment of functional gene categories in the marine vent virome with a set of 42 other viromes, initially analyzed by Dinsdale et al., 2008; **Figure 5**). As in the previous analysis, only the convincingly viral subset of the marine vent virome from Hulk was used. In this analysis, genes were annotated with the SEED subsystems in MG-RAST to make a more direct comparison with the study by Dinsdale et al. (2008). The results show that the marine vent virome is particularly enriched in genes related to regulation and cell signaling (enriched by 300%) and RNA metabolism (enriched by 230%). The genes assigned to the "cell signaling" category include those related to biofilm formation and quorum sensing, regulation of virulence, and sensing environmental stimuli. For example, 118 sequencing reads in the marine vent virome have close matches to genes in the "regulation of virulence" category. Most of these matched the BarA–UvrY two-component system, a system regulating virulence in pathogenic *E. coli* (Herren et al., 2006). The BarA–UvrY system functions by sensing changes in environmental conditions to induce a metabolic switch, a function that would be useful in the rapidly changing conditions of the vent environment.

We expect that the pool of genes undergoing positive selection for retention in the virus genetic reservoir would represent those genes that may be occasionally necessary, though not strictly required, in the environment from which it was sampled. Thus, we expect accessory genes such as those related to secondary metabolisms to be selected for maintenance in the virome, rather than housekeeping genes such as ribosomal proteins. In addition to representing the "cloud" of poorly conserved genes from both cellular and viral pangenomes (Kristensen et al., 2010), we expect positive selection to customize this "genetic reservoir" to match the needs of the hosts drawing from it.

EXTRAPOLATING THE VIRAL IMPACT FROM HYDROTHERMAL VENTS TO OTHER REGIMES OF THE DEEP SUBSURFACE BIOSPHERE

We have suggested here that viruses are likely to play an important role in modifying the genetic content of their hosts in diffuse flow fluids of hydrothermal systems. We now turn to a discussion of whether the characteristics of viruses in diffuse fluids is likely to be the case for other regimes of the deep subsurface biosphere. The vent ecosystem has several unique attributes that distinguish it from other deep subsurface habitats, so extrapolation from the vent subsurface to the rest of the deep subsurface biosphere must be done cautiously. The two most distinctive attributes of the vent system are the extreme gradients in temperature, pH, redox state, chemical composition, and mineralogy, and the constant fluid flux

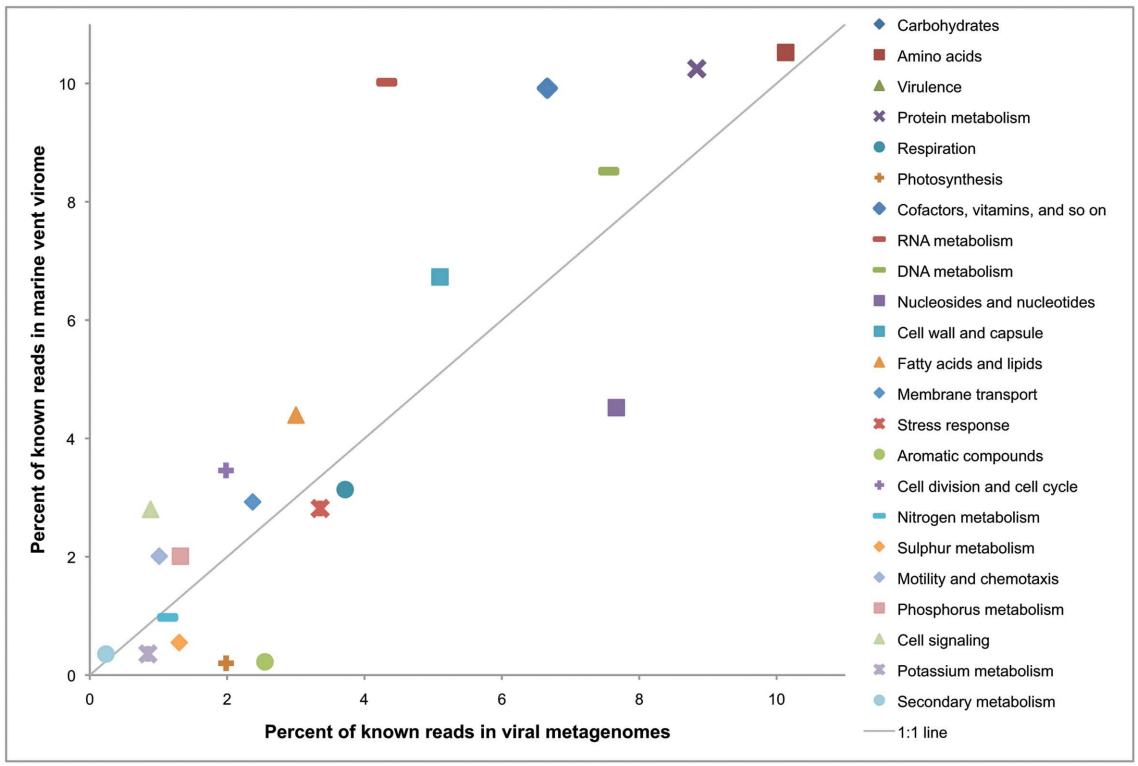

FIGURE 5 | Relative percentages of reads matching gene categories in the marine vent virome and a set of 42 viral metagenomes isolated from other environments (listed in Dinsdale et al., 2008). The solid line indicates a 1:1 ratio between the vent metagenome and the other viral metagenomes. Metagenomes were analyzed with MG-RAST (Meyer et al., 2008) and annotated using the SEED subsystems database.

between microenvironments. On the ridge axis, hot hydrothermal fluid mixing with cool, oxygenated seawater facilitates interaction among diverse cellular communities and their accompanying viral assemblages. For this reason, we have argued that this environment may be conducive to gene flow from one microenvironment to the next via viral transfer. However, the impact of viruses is likely to extend to other provinces of the deep subsurface biosphere, which we detail below.

CRUSTAL ENVIRONMENTS: UNSEDIMENTED RIDGE FLANKS, CRUSTAL OUTCROPS, SEAMOUNTS, ARC SYSTEMS

This fluid flux from one environment to the next is characteristic of many regimes in the deep subsurface biosphere. As sediments covering the seafloor tend to be relatively impermeable, fluid flux depends on outcropping of igneous crust (Edwards et al., 2011). Fluids flux most vigorously at mid-ocean ridges at the hydrothermal systems discussed above, and degree of fluid flux decreases with distance from the ridge axis, as shown in **Figure 1B**. However, these environments are not completely stagnant. On ridge flanks and recharge zones, which can extend hundreds of kilometers from the ridge axis, oxygenated seawater flows into the ocean floor, with residence times of days to years (Johnson et al., 2010). Some of this fluid emerges in discharge zones in the form of hydrothermal vents on ridge axes, while some fluids may circulate more locally. Off-axis, fluid flows through seamounts; and farther afield, fluids may circulate in a more restricted manner (Edwards et al., 2005). Overall, however, the volume of fluid flux is large, as at least 60% of the oceanic crust is hydrologically active, and the fluid-crust reservoir in which these processes might be expected to occur is approximately 10 times the size of the sedimentary reservoir (Edwards et al., 2011). Fluid-flux-dominated environments, therefore, constitute the majority of the deep subsurface. This fluid flux facilitates transfer of chemicals throughout the crust, thus exposing microbial communities to varying conditions and also transporting microorganisms from one region to the next. The regions of the oceanic crust dominated by fluid flux are therefore analogous to the hydrothermal systems described above, though characterized by fewer extremes in temperature, pH, and redox conditions.

By means of this flux, viruses or their accompanying hosts are transported between biomes, and can facilitate horizontal gene transfer between organisms native to drastically different environments. Viral metagenomics has suggested that while local diversity of viral assemblages is high, global diversity may be low, suggesting that viruses frequently migrate between biomes (Breitbart and Rohwer, 2005). One study found that viruses from sediments, soils, and lakes were able to propagate in marine waters, suggesting that viruses have a broad enough host range that they can successfully move between biomes (Sano et al., 2004). Fluid flux between the seafloor–ocean interface, within sediments, and within cracks in the Earth's crust may act as a conduit for viruses or the microbes that bear them, thus potentially sharing genes among habitats. Moreover, if biofilms are hotspots for horizontal gene transfer and viral infection (as discussed above), we may expect that regions of the subsurface characterized by biofilm formation, which could

include any habitat with surfaces available for attachment, will be exposed to higher rates of gene transfer than in environments with lower cell density.

SEDIMENTED ENVIRONMENTS: ABYSSAL PLAINS, CONTINENTAL MARGINS

As shown in **Figure 1B**, some provinces of the deep subsurface biosphere, particularly those characterized by deep sedimentation, experience more restricted fluid flux and therefore have potentially limited contact between hosts of different environment niches. Yet even in these regions, viruses may alter host fitness through lysogeny. As stated above, lysogeny appears to become a more predominant lifestyle in regions with suboptimal conditions, such as low nutrient abundance, low host replication rates, or low host contact rates. Some sedimented regions of the deep subsurface are characterized by particularly low cell abundance, such as in sediments within oligotrophic gyres (D'Hondt et al., 2009), or are exposed to extremely limited organic matter, nutrient, or free energy availability (Schrenk et al., 2010). Moreover, the lack of mobility in the sediment matrix may encourage a lysogenic lifestyle as well, as viruses may have difficulty in contacting a new host within a sediment matrix, especially in regions with low cell abundance. Therefore, the lysogenic lifestyle is likely to be much more common among viruses in these regions, and the archaeal and bacterial inhabitants of these regions have an even higher likelihood of expressing fitness factors encoded by prophage. Initial studies of prophage in the deep subsurface biosphere seem to support this case (Engelhardt et al., 2011). These prophage may aid in host survivability. For example, in deeply buried marine sediments with limited organic carbon or other nutrients, viruses may carry genes to aid in scavenging these compounds or in providing secondary metabolisms to take advantage of alternative energy or nutrient sources. However, more work needs to be done on sequencing viral or cellular isolates from these regions to gain further support for this hypothesis.

One final viral influence that is likely to impact all provinces of the deep subsurface biosphere is the input of viruses from surface waters. Marine sediments receive large inputs of allochthonous material daily, much of it bearing particle-associated microbes that sink through the water column. If these microbes carry prophage or lytic viruses in the process of replicating, these viruses could potentially encounter a different host in its new sediment-bound habitat. These viruses, delivered from the upper water column, could then deliver genes from more pelagic habitats to the deep subsurface. One might even expect induction of prophage to occur more frequently in sinking microbes as they are exposed to increased pressures, which has been found to induce prophage in *E. coli* (Aertsen et al., 2004). In this sense, viruses may serve as a highway for gene exchange between the surface marine realm and the deep subsurface biosphere.

CONCLUSION

The presence of lysogeny-related genes as well as potentially advantageous cellular functional genes in the virome of a marine, diffuse flow hydrothermal vent bolster the hypothesis that viruses modify the genetic landscape of the hydrothermal habitat, both through expression of prophage genes during lysogenic infection and through the process of transduction. Indeed, this habitat – as well as several others in the deep subsurface biosphere – is uniquely poised for fostering an almost symbiotic relationship between viruses and their hosts. As mentioned above, deep sea microbes have higher numbers of integrated prophage and transposable elements in their genomes (Campanaro et al., 2005; Vezzi et al., 2005; Ivars-Martinez et al., 2008), and lysogeny appears to be favored over lysis in the extreme regions of the marine realm (Paul, 2008). In regions of the deep subsurface biosphere with low host contact rates, low nutrient flux, or rapidly changing conditions, expression by latent prophage or viral transduction may play a crucial role in bolstering host fitness.

More work certainly remains to be done to determine the scope of the viral impact on the deep subsurface biosphere. Sequencing the genomes of archaeal and bacterial isolates from various regions of the deep subsurface can indicate what prophage elements are present. Viral metagenomics can indicate what types of genes are harbored by viruses, and therefore can indicate which genes may either be transferred into host genomes or expressed during the prophage stage. Thus far, the evidence suggests that viruses play a crucial role in enhancing the fitness of their hosts by modifying their genetic content. They may help their hosts adapt to the unique challenges of the various habitats of the deep subsurface biosphere, acting as a genetic repository for new, adaptive functions. Viruses are emerging as a profound evolutionary force whose impact we have yet to fully assess, particularly in the realms of the deep.

ACKNOWLEDGMENTS

The authors thank Jon Kaye at the Gordon and Betty Moore Foundation for help with virome sequencing. Sequencing of virome sample G2810 was funded by the Gordon and Betty Moore Foundation through a grant to the Broad Institute. Rika E. Anderson was funded by an NSF Graduate Research Fellowship through NSF grant number DGE-0718124, an NSF IGERT grant to the University of Washington Astrobiology Program, and the ARCS Foundation. William J. Brazelton was funded by a NASA Astrobiology Institute Postdoctoral Fellowship. Research funding was provided through a NASA Astrobiology Institute grant through Cooperative Agreement NNA04CC09A to the Geophysical Laboratory at the Carnegie Institution for Science.

REFERENCES

Aertsen, A., Van Houdt, R., Vanoirbeek, K., and Michiels, C. W. (2004). An SOS response induced by high pressure in *Escherichia coli*. *J. Bacteriol.* 186, 6133–6141.

Amend, J. P., and Shock, E. L. (2001). Energetics of overall metabolic reactions of thermophilic and hyperthermophilic archaea and bacteria. *FEMS Microbiol. Rev.* 25, 175–243.

Anderson, R. E., Brazelton, W. J., and Baross, J. A. (2011). Using CRISPRs as a metagenomic tool to identify microbial hosts of a diffuse flow hydrothermal vent viral assemblage. *FEMS Microbiol. Ecol.* 77, 120–133.

Angly, F. E., Felts, B., Breitbart, M., Salamon, P., Edwards, R. A., Carlson, C., Chan, A. M., Haynes, M., Kelley, S., Liu, H., Mahaffy, J. M., Mueller, J. E., Nulton, J., Olson, R., Parsons, R., Rayhawk, S., Suttle, C. A., and Rohwer, F. (2006). The marine viromes of four oceanic regions. *PLoS Biol.* 4, e368. doi:10.1371/journal.pbio.0040368

Baross, J. A., and Hoffman, S. E. (1985). Submarine hydrothermal vents and associated gradient environments as sites for the origin and evolution of life. *Orig. Life Evol. Biosph.* 15, 327–345.

Barrangou, R., Fremaux, C., Deveau, H., Richards, M., Boyaval, P., Moineau, S., Romero, D. A., and Horvath, P. (2007). CRISPR provides acquired resistance against viruses in prokaryotes. *Science* 315, 1709–1712.

Beiko, R. G., Harlow, T. J., and Ragan, M. A. (2005). Highways of gene sharing in prokaryotes. *Proc. Natl. Acad. Sci. U.S.A.* 102, 14332–14337.

Bhaya, D., Grossman, A. R., Steunou, A.-S., Khuri, N., Cohan, F. M., Hamamura, N., Melendrez, M. C., Bateson, M. M., Ward, D. M., and Heidelberg, J. F. (2007). Population level functional diversity in a microbial community revealed by comparative genomic and metagenomic analyses. *ISME J.* 1, 703–713.

Biddle, J. F., Fitz-Gibbon, S., Schuster, S. C., Brenchley, J. E., and House, C. H. (2008). Metagenomic signatures of the Peru Margin subseafloor biosphere show a genetically distinct environment. *Proc. Natl. Acad. Sci. U.S.A.* 105, 10583–10588.

Biers, E. J., Wang, K., Pennington, C., Belas, R., Chen, F., and Moran, M. A. (2008). Occurrence and expression of gene transfer agent (GTA) genes in marine bacterioplankton. *Appl. Environ. Microbiol.* 74, 2933–2939.

Bird, D. F., Juniper, S. K., Ricciardi-Regault, M., Martineu, P., Prairie, Y. T., and Calvert, S. E. (2001). Subsurface viruses and bacteria in Holocene/Late Pleistocene sediments of Saanich Inlet, BC: ODP Holes 1033B and 1034B, Leg 169S. *Mar. Geol.* 174, 227–239.

Bolotin, A., Quinquis, B., Sorokin, A., and Ehrlich, S. D. (2005). Clustered regularly interspaced short palindrome repeats (CRISPRs) have spacers of extrachromosomal origin. *Microbiology* 151, 2551–2561.

Bose, M., and Barber, R. (2006). Prophage finder: a prophage loci prediction tool for prokaryotic genome sequences. *In Silico Biol.* 6, 0020.

Brazelton, W. J., and Baross, J. A. (2009). Abundant transposases encoded by the metagenome of a hydrothermal chimney biofilm. *ISME J.* 3, 1420–1424.

Breitbart, M., Felts, B., Kelley, S., Mahaffy, J. M., Nulton, J., Salamon, P., and Rohwer, F. (2004). Diversity and population structure of a near-shore marine-sediment viral community. *Proc. Biol. Sci.* 271, 565–574.

Breitbart, M., Hoare, A., Nitti, A., Siefert, J., Haynes, M., Dinsdale, E., Edwards, R., Souza, V., Rohwer, F., and Hollander, D. (2009). Metagenomic and stable isotopic analyses of modern freshwater microbialites in Cuatro Cienegas, Mexico. *Environ. Microbiol.* 11, 16–34.

Breitbart, M., and Rohwer, F. (2005). Here a virus, there a virus, everywhere the same virus? *Trends Microbiol.* 13, 278–284.

Brouns, S. J. J., Jore, M. M., Lundgren, M., Westra, E. R., Slijkhuis, R. J. H., Snijders, A. P. L., Dickman, M. J., Makarova, K. S., Koonin, E. V., and Van der Oost, J. (2008). Small CRISPR RNAs guide antiviral defense in prokaryotes. *Science* 321, 960–964.

Campanaro, S., Vezzi, A., Vitulo, N., Lauro, F., D'Angelo, M., Simonato, F., Cestaro, A., Malacrida, G., Bertoloni, G., Valle, G., and Bartlett, D. H. (2005). Laterally transferred elements and high pressure adaptation in *Photobacterium profundum* strains. *BMC Genomics* 6, 122. doi:10.1186/1471-2164-6-122

Campbell, B. J., Jeanthon, C., Kostka, J. E., Luther, G. W. III, and Cary, S. C. (2001). Growth and phylogenetic properties of novel bacteria belonging to the epsilon subdivision of the proteobacteria enriched from *Alvinella pompejana* and deep-sea hydrothermal vents. *Appl. Environ. Microbiol.* 67, 4566–4572.

Carlile, M. (1982). Prokaryotes and eukaryotes: strategies and successes. *Trends Biochem. Sci.* 7, 128–130.

Danovaro, R., Dell'Anno, A., Corinaldesi, C., Magagnini, M., Noble, R., Tamburini, C., and Weinbauer, M. (2008). Major viral impact on the functioning of benthic deep-sea ecosystems. *Nature* 454, 1084–1087.

Deckert, G., Warren, P. V., Gaasterland, T., Young, W. G., Lenox, A. L., Graham, D. E., Overbeek, R., Snead, M. A., Keller, M., Aujay, M., Huber, R., Feldman, R. A., Short, J. M., Olsen, G. J., and Swanson, R. V. (1998). The complete genome of the hyperthermophilic bacterium *Aquifex aeolicus*. *Nature* 392, 353–358.

Deppenmeier, U., Johann, A., Hartsch, T., Merkl, R., Schmitz, R. A., Martinez-Arias, R., Henne, A., Wiezer, A., Bäumer, S., Jacobi, C., Brügemann, H., Lienard, T., Christmann, A., Bömeke, M., Steckel, S., Bhattacharyya, A., Lykidis, A., Overbeek, R., Klenk, H. P., Gunsalus, R. P., Fritz, H. J., and Gottschalk, G. (2002). The genome of *Methanosarcina mazei*: evidence for lateral gene transfer between bacteria and archaea. *J. Mol. Microbiol. Biotechnol.* 4, 453–461.

Desnues, C., Rodriguez-Brito, B., Rayhawk, S., Kelley, S., Tran, T., Haynes, M., Liu, H., Furlan, M., Wegley, L., Chau, B., Ruan, Y., Hall, D., Angly, F. E., Edwards, R. A., Li, L., Thurber, R. V., Reid, R. P., Siefert, J., Souza, V., Valentine, D., Swan, B. K., Breitbart, M., and Rohwer, F. (2008). Biodiversity and biogeography of phages in modern stromatolites and thrombolites. *Nature* 452, 340–344.

D'Hondt, S., Spivack, A. J., Pockalny, R., Ferdelman, T. G., Fischer, J. P., Kallmeyer, J., Abrams, L. J., Smith, D. C., Graham, D., Hasiuk, F., Schrum, H., and Stancin, A. M. (2009). Subseafloor sedimentary life in the South Pacific Gyre. *Proc. Natl. Acad. Sci. U.S.A.* 106, 11651–11656.

Dinsdale, E. A., Edwards, R. A., Hall, D., Angly, F., Breitbart, M., Brulc, J. M., Furlan, M., Desnues, C., Haynes, M., Li, L., McDaniel, L., Moran, M. A., Nelson, K. E., Nilsson, C., Olson, R., Paul, J., Brito, B. R., Ruan, Y., Swan, B. K., Stevens, R., Valentine, D. L., Thurber, R. V., Wegley, L., White, B. A., and Rohwer, F. (2008). Functional metagenomic profiling of nine biomes. *Nature* 452, 629–632.

Doherty, A. J., and Suh, S. W. (2000). Structural and mechanistic conservation in DNA ligases. *Nucleic Acids Res.* 28, 4051–4058.

Edwards, K. J., Bach, W., and McCollom, T. M. (2005). Geomicrobiology in oceanography: microbe-mineral interactions at and below the seafloor. *Trends Microbiol.* 13, 449–456.

Edwards, K. J., Wheat, C. G., and Sylvan, J. B. (2011). Under the sea: microbial life in volcanic oceanic crust. *Nat. Rev. Microbiol.* 9, 703–712.

Engelhardt, T., Sahlberg, M., Cypionka, C., and Engelen, B. (2011). Induction of prophages from deep-subseafloor bacteria. *Environ. Microbiol. Rep.* 3, 459–465.

Finn, R. D., Mistry, J., Tate, J., Coggill, P., Heger, A., Pollington, J. E., Gavin, O. L., Gunasekaran, P., Ceric, G., Forslund, K., Holm, L., Sonnhammer, E. L., Eddy, S. R., and Bateman, A. (2010). The Pfam protein families database. *Nucleic Acids Res.* 38, D211–D222.

Freestone, P., Nyström, T., Trinei, M., and Norris, V. (1997). The universal stress protein, UspA, of *Escherichia coli* is phosphorylated in response to stasis. *J. Mol. Biol.* 274, 318–324.

Garneau, J. E., Dupuis, M. È., Villion, M., Romero, D. A., Barrangou, R., Boyaval, P., Fremaux, C., Horvath, P., Magadán, A. H., and Moineau, S. (2010). The CRISPR/Cas bacterial immune system cleaves bacteriophage and plasmid DNA. *Nature* 468, 67–71.

Goldenfeld, N., and Woese, C. (2007). Biology's next revolution. *Nature* 445, 369.

Grissa, I., Vergnaud, G., and Pourcel, C. (2007a). CRISPRFinder: a web tool to identify clustered regularly interspaced short palindromic repeats. *Nucleic Acids Res.* 35, W52–W57.

Grissa, I., Vergnaud, G., and Pourcel, C. (2007b). The CRISPRdb database and tools to display CRISPRs and to generate dictionaries of spacers and repeats. *BMC Bioinformatics* 8: 172. doi: 10.1186/1471-2105-8-172

Grzymski, J. J., Murray, A. E., Campbell, B. J., Kaplarevic, M., Gao, G. R., Lee, C., Daniel, R., Ghadiri, A., Feldman, R. A., and Cary, S. C. (2008). Metagenome analysis of an extreme microbial symbiosis reveals eurythermal adaptation and metabolic flexibility. *Proc. Natl. Acad. Sci. U.S.A.* 105, 17516–17521.

Haft, D. H., Selengut, J., Mongodin, E. F., and Nelson, K. E. (2005). A guild of 45 CRISPR-associated (Cas) protein families and multiple CRISPR/Cas subtypes exist in prokaryotic genomes. *PLoS Comput. Biol.* 1, e60. doi:10.1371/journal.pcbi.0010060

Hale, C. R., Zhao, P., Olson, S., Duff, M. O., Graveley, B. R., Wells, L., Terns, R. M., and Terns, M. P. (2009). RNA-guided RNA cleavage by a CRISPR RNA-Cas protein complex. *Cell* 139, 945–956.

Hara, S., Koike, I., Terauchi, K., Kamiya, H., and Tanoue, E. (1996). Abundance of viruses in deep oceanic waters. *Mar. Ecol. Prog. Ser.* 145, 269–277.

Herren, C. D., Mitra, A., Palaniyandi, S. K., Coleman, A., Elankumaran, S., and Mukhopadhyay, S. (2006). The BarA-UvrY two-component system regulates virulence in avian pathogenic *Escherichia coli* O78:K80:H9. *Infect. Immun.* 74, 4900–4909.

Hou, S., Saw, J. H., Lee, K. S., Freitas, T. A., Belisle, C., Kawarabayasi, Y., Donachie, S. P., Pikina, A., Galperin, M. Y., Koonin, E. V., Makarova, K. S., Omelchenko, M. V., Sorokin, A., Wolf, Y. I., Li, Q. X., Keum, Y. S., Campbell, S., Denery, J., Aizawa, S.-I., Shibata, S., Malahoff, A., and Alam, M. (2004). Genome sequence of the deep-sea gammaproteobacterium *Idiomarina loihiensis* reveals amino acid fermentation as a source of carbon and energy. *Proc. Natl. Acad. Sci. U.S.A.* 101, 18036–18041.

Hovarth, P., and Barrangou, R. (2010). CRISPR/Cas, the immune system of bacteria and archaea. *Science* 327, 167–170.

Huber, J. A., Butterfield, D. A., and Baross, J. A. (2003). Bacterial diversity in a subseafloor habitat following a deep-sea volcanic eruption. *FEMS Microbiol. Ecol.* 43, 393–309.

Huber, J. A., Mark Welch, D. B., Morrison, H. G., Huse, S. M., Neal, P. R., Butterfield, D. A., and Sogin, M. L. (2007). Microbial population structures in the deep marine biosphere. *Science* 318, 97.

Inagaki, F., Takai, K., Kobayashi, H., Nealson, K. H., and Horikoshi, K. (2003). *Sulfurimonas autotrophica* gen. nov., sp. nov., a novel sulfur-oxidizing ε-proteobacterium isolated from hydrothermal sediments in the Mid-Okinawa trough. *Int. J. Syst. Evol. Microbiol.* 53, 1801–1805.

Ivars-Martinez, E., Martin-Cuadrado, A.-B., D'Auria, G., Mira, A., Ferriera, S., Johnson, J., Friedman, R., and Rodriguez-Valera, F. (2008). Comparative genomics of two ecotypes of the marine planktonic copiotroph *Alteromonas macleodii* suggests alternative lifestyles associated with different kinds of particulate organic matter. *ISME J.* 2, 1194–1212.

Jannasch, H. W., and Wirsen, C. O. (1981). Morphological survey of microbial mats near deep-sea thermal vents. *Appl. Environ. Microbiol.* 41, 528–538.

Jiang, S. C., and Paul, J. H. (1998). Gene transfer by transduction in the marine environment. *Appl. Environ. Microbiol.* 64, 2780–2787.

Johnson, H. P., Tivey, M. A., Bjorklund, T. A., and Salmi, M. S. (2010). Hydrothermal circulation within the Endeavour segment, Juan de Fuca Ridge. *Geochem. Geophys. Geosyst.* 11, Q05002.

Jolivet, E., L'Haridon, S., Corre, E., Forterre, P., and Prieur, D. (2003). *Thermococcus gammatolerans* sp. nov., a hyperthermophilic archaeon from a deep-sea hydrothermal vent that resists ionizing radiation. *Int. J. Syst. Evol. Microbiol.* 53, 847–851.

Jones, W. J., Leigh, J. A., Mayer, F., Woese, C. R., and Wolfe, R. S. (1983). *Methanococcus jannaschii* sp. nov., an extremely thermophilic methanogen from a submarine hydrothermal vent. *Arch. Microbiol.* 136, 254–261.

Jore, M. M., Lundgren, M., van Duijn, E., Bultema, J. B., Westra, E. R., Waghmare, S. P., Wiedenheft, B., Pul, Ü., Wurm, R., Wagner, R., Beijer, M. R., Barendregt, A., Zhou, K., Snijders, A. P., Dickman, M. J., Doudna, J. A., Boekema, E. J., Heck, A. J., van der Oost, J., and Brouns, S. J. (2011). Structural basis for CRISPR RNA-guided DNA recognition by cascade. *Nat. Struct. Mol. Biol.* 18, 529–536.

Kato, C., Sato, T., and Horikoshi, K. (1995). Isolation and properties of barophilic and barotolerant bacteria from deep-sea mud samples. *Biodivers. Conserv.* 4, 1–9.

Kellogg, C. A. (2010). Enumeration of viruses and prokaryotes in deep-sea sediments and cold seeps of the Gulf of Mexico. *Deep Sea Res. Part 2 Top. Stud. Oceanogr.* 57, 2002–2007.

Kristensen, D. M., Mushegian, A. R., Dolja, V. V., and Koonin, E. V. (2010). New dimensions of the virus world discovered through metagenomics. *Trends Microbiol.* 18, 11–19.

Kyle, J. E., Eydal, H. S. C., Ferris, F. G., and Pedersen, K. (2008). Viruses in granitic groundwater from 69 to 450 m depth of the Äspö hard rock laboratory, Sweden. *ISME J.* 2, 571–574.

Labrie, S. J., Samson, J. E., and Moineau, S. (2010). Bacteriophage resistance mechanisms. *Nat. Rev. Microbiol.* 8, 317–327.

Lang, A. S., and Beatty, J. T. (2000). Genetic analysis of a bacterial genetic exchange element: the gene transfer agent of *Rhodobacter capsulatus*. *Proc. Natl. Acad. Sci. U.S.A.* 97, 859–864.

Lee, Y.-J., Wagner, I. D., Brice, M. E., Kevbrin, V. V., Mills, G. L., Romanek, C. S., and Wiegel, J. (2005). *Thermosediminibacter oceani* gen. nov., sp. nov. and *Thermosediminibacter litoriperuensis* sp. nov., new anaerobic thermophilic bacteria isolated from Peru Margin. *Extremophiles* 9, 375–383.

Lehnman, I. R. (1974). DNA ligase: structure, mechanism, and function. *Science* 186, 790–797.

Leung, M. M., Florizone, S. M., Taylor, T. A., Lang, A. S., and Beatty, J. T. (2010). The gene transfer agent of *Rhodobacter capsulatus*. *Adv. Exp. Med. Biol.* 675, 253–264.

Levin, B. R., and Lenski, R. E. (1983). "Coevolution in bacteria and their viruses and plasmids," in *Coevolution*, eds D. J. Futuyma and M. Slatkin (Sunderland, MA: Sinauer Associates), 99–127.

Lindell, D., Jaffe, J. D., Johnson, Z. I., Church, G. M., and Chisholm, S. W. (2005). Photosynthesis genes in marine viruses yield proteins during host infection. *Nature* 438, 86–89.

Lindell, D., Sullivan, M. B., Johnson, Z. I., Tolonen, A. C., Rohwer, F., and Chisholm, S. W. (2004). Transfer of photosynthesis genes to and from *Prochlorococcus* viruses. *Proc. Natl. Acad. Sci. U.S.A.* 101, 11013–11018.

Lu, J., Nogi, Y., and Takami, H. (2001). *Oceanobacillus iheyensis* gen. nov., sp. nov., a deep-sea extremely halotolerant and alkaliphilic species isolated from a depth of 1050 m on the Iheya Ridge. *FEMS Microbiol. Lett.* 205, 291–297.

Makarova, K. S., Wolf, Y. I., and Koonin, E. V. (2003). Potential genomic determinants of hyperthermophily. *Trends Genet.* 19, 172–176.

Manini, E., Luna, G. M., Corinaldesi, C., Zeppilli, D., Bortoluzzi, G., Caramanna, G., Raffa, F., and Danovaro, R. (2008). Prokaryote diversity and virus abundance in shallow hydrothermal vents of the Mediterranean Sea (Panarea Island) and the Pacific Ocean (North Sulawesi-Indonesia). *Microb. Ecol.* 55, 626–639.

Mann, N. H., Cook, A., Millard, A., Bailey, S., and Clokie, M. (1993). Bacterial photosynthesis genes in a virus. *Environ. Microbiol.* 59, 3736–3743.

Marraffini, L. A., and Sontheimer, E. J. (2008). CRISPR interference limits horizontal gene transfer in *Staphylococci* by targeting DNA. *Science* 322, 1843–1845.

Marraffini, L. A., and Sontheimer, E. J. (2010). Self versus non-self discrimination during CRISPR RNA-directed immunity. *Nature* 463, 568–571.

Marteinsson, V. T., Birrien, J. L., Reysenbach, A. L., Vernet, M., Marie, D., Gambacorta, A., Messner, P., Sleytr, U. B., and Prieur, D. (1999). *Thermococcus barophilus* sp. nov., a new barophilic and hyperthermophilic archaeon isolated under high hydrostatic pressure from a deep-sea hydrothermal vent. *Int. J. Syst. Bacteriol.* 49, 351–359.

Matson, E. G., Thompson, M. G., Humphrey, S. B., Zuerner, R. L., and Stanton, T. B. (2005). Identification of genes of VSH-1, a prophage-like gene transfer agent of *Brachyspira hyodysenteriae*. *J. Bacteriol.* 187, 5885–5892.

McDaniel, L., Houchin, L. A., Williamson, S. J., and Paul, J. H. (2002). Plankton blooms: lysogeny in marine *Synechococcus*. *Nature* 415, 496.

McDaniel, L. D., Young, E., Delaney, J., Ruhnau, F., Ritchie, K. B., and Paul, J. H. (2010). High frequency of horizontal gene transfer in the oceans. *Science* 330, 50.

Mehta, M. P., and Baross, J. A. (2006). Nitrogen fixation at 92°C by a hydrothermal vent archaeon. *Science* 314, 1783–1786.

Meyer, F., Paarmann, D., D'Souza, M., Olson, R., Glass, E., Kubal, M., Paczian, T., Rodriguez, A., Stevens, R., Wilke, A., Wilkening, J., and Edwards, R. A. (2008). The metagenomics RAST server – a public resource for the automatic phylogenetic and functional analysis of metagenomes. *BMC Bioinformatics* 9, 386. doi: 10.1186/1471-2105-9-386

Middelboe, M., Glud, R. N., and Filippini, M. (2011). Viral abundance and activity in the deep sub-seafloor biosphere. *Aquat. Microb. Ecol.* 63, 1–8.

Middelboe, M., Glud, R. N., Wenzhöfer, F., Oguri, K., and Kitazato, H. (2006). Spatial distribution and activity of viruses in the deep-sea sediments of Sagami Bay, Japan. *Deep Sea Res. Part 1 Oceanogr. Res. Pap.* 53, 1–13.

Millard, A., Clokie, M. R. J., Shub, D. A., and Mann, N. H. (2004). Genetic organization of the psbAD region in phages infecting marine *Synechococcus* strains. *Proc. Natl. Acad. Sci. U.S.A.* 101, 11007–11012.

Miroshnichenko, M. L., L'haridon, S., Jeanthon, C., Antipov, A. N., Kostrikina, N. A., Tindall, B. J., Schumann, P., Spring, S., Stackebrandt, E., and Bonch-Osmolovskaya, E. A. (2003). *Oceanithermus profundus* gen. nov., sp. nov., a thermophilic, microaerophilic, facultatively chemolithoheterotrophic bacterium from a deep-sea hydrothermal vent. *Int. J. Syst. Evol. Microbiol.* 53, 747–752.

Mojica, F. J. M., Díez-Villaseñor, C., García-Martínez, J., and Soria, E. (2005). Intervening sequences of regularly spaced prokaryotic repeats derive from foreign genetic elements. *J. Mol. Evol.* 60, 174–182.

Nakagawa, S., Takai, K., Inagaki, F., Horikoshi, K., and Sako, Y. (2005). *Nitratiruptor tergarcus* gen. nov., sp. nov. and *Nitratifractor salsuginis* gen. nov., sp. nov., nitrate-reducing chemolithoautotrophs of the Epsilonproteobacteria isolated from a deep-sea hydrothermal system in the Mid-Okinawa trough. *Int. J. Syst. Evol. Microbiol.* 55, 925–933.

Nelson, K. E., Clayton, R. A., Gill, S. R., Gwinn, M. L., Dodson, R. J., Haft, D. H., Hickey, E. K., Peterson, J. D., Nelson, W. C., Ketchum, K. A., McDonald, L., Utterback, T. R., Malek, J. A., Linher, K. D., Garrett, M. M., Stewart, A. M., Cotton, M. D., Pratt, M. S., Phillips, C. A., Richardson, D., Heidelberg, J., Sutton, G. G., Fleischmann, R. D., Eisen, J. A., White, O., Salzberg, S. L., Smith, H. O., Venter, J. C., and Fraser, C. M. (1999). Evidence for lateral gene transfer between archaea and bacteria from genome sequence of *Thermotoga maritima*. *Nature* 399, 323–329.

Nogi, Y., Masui, N., and Kato, C. (1998). *Photobacterium profundum* sp. nov., a new, moderately barophilic bacterial species isolated from a deep-sea sediment. *Extremophiles* 2, 1–8.

Nyström, T., and Neidhardt, F. C. (1994). Expression and role of the universal stress protein, UspA, of *Escherichia coli* during growth arrest. *Mol. Microbiol.* 11, 537–544.

Orcutt, B. N., Sylvan, J. B., Knab, N. J., and Edwards, K. J. (2011). Microbial ecology of the dark ocean above, at, and below the seafloor. *Microbiol. Mol. Biol. Rev.* 75, 361–422.

Ortmann, A. C., and Suttle, C. A. (2005). High abundances of viruses in a deep-sea hydrothermal vent system indicates viral mediated microbial mortality. *Deep Sea Res. Part 2 Top. Stud. Oceanogr.* 52, 1515–1527.

Parada, V., Sintes, E., Van Aken, H. M., Weinbauer, M. G., and Herndl, G. J. (2007). Viral abundance, decay, and diversity in the meso-and bathypelagic waters of the North Atlantic. *Appl. Environ. Microbiol.* 73, 4429–4438.

Paul, J. H. (2008). Prophages in marine bacteria: dangerous molecular time bombs or the key to survival in the seas? *ISME J.* 2, 579–589.

Pourcel, C., Salvignol, G., and Vergnaud, G. (2005). CRISPR elements in *Yersinia pestis* acquire new repeats by preferential uptake of bacteriophage DNA, and provide additional tools for evolutionary studies. *Microbiology* 151, 653–663.

Prieur, D., Erauso, G., Geslin, C., Lucas, S., Gaillard, M., Bidault, A., Mattenet, A. -C., Rouault, K., Flament, D., Forterre, P., and Le Romancer, M. (2004). Genetic elements of *Thermococcales*. *Biochem. Soc. T.* 32, 184–187.

Qin, Q.-L., Zhang, X.-Y., Wang, X.-M., Liu, G.-M., Chen, X.-L., Xie, B.-B., Dang, H.-Y., Zhou, B.-C., Yu, J., and Zhang, Y.-Z. (2010). The complete genome of *Zunongwangia profunda* SM-A87 reveals its adaptation to the deep-sea environment and ecological role in sedimentary organic nitrogen degradation. *BMC Genomics* 11, 247. doi:10.1186/1471-2164-11-247

Reysenbach, A. L., Liu, Y., Banta, A., Beveridge, T. J., Kirshtein, J. D., Schouten, S., Tivey, M. K., Von Damm, K. L., and Voytek, M. A. (2006). A ubiquitous thermoacidophilic archaeon from deep-sea hydrothermal vents. *Nature* 442, 444–447.

Rohwer, F., and Thurber, R. V. (2009). Viruses manipulate the marine environment. *Nature* 458, 207–212.

Sako, Y., Nakagawa, S., Takai, K., and Horikoshi, K. (2003). *Marinithermus hydrothermalis* gen. nov., sp. nov., a strictly aerobic, thermophilic bacterium from a deep-sea hydrothermal vent chimney. *Int. J. Syst. Evol. Microbiol.* 53, 59–65.

Sano, E., Carlson, S., Wegley, L., and Rohwer, F. (2004). Movement of viruses between biomes. *Appl. Environ. Microbiol.* 70, 5842–5846.

Schrenk, M. O., Huber, J. A., and Edwards, K. J. (2010). Microbial provinces in the subseafloor. *Ann. Rev. Mar. Sci.* 2, 279–304.

Schrenk, M. O., Kelley, D. S., Delaney, J. R., and Baross, J. A. (2003). Incidence and diversity of microorganisms within the walls of an active deep-sea sulfide chimney. *Appl. Environ. Microbiol.* 69, 3580–3592.

Sharon, I., Alperovitch, A., Rohwer, F., Haynes, M., Glaser, F., Atamna-Ismaeel, N., Pinter, R. Y., Partensky, F., Koonin, E. V., Wolf, Y. I., Nelson, N., and Béjà, O. (2009). Photosystem I gene cassettes are present in marine virus genomes. *Nature* 461, 258–262.

Siem-Jørgensen, M., Glud, R. N., and Middelboe, M. (2008). Viral dynamics in a coastal sediment: seasonal pattern, controlling factors and relations to the pelagic–benthic coupling. *Mar. Biol. Res.* 4, 165–179.

Smoot, L. M., Smoot, J. C., Graham, M. R., Somerville, G. A., Sturdevant, D. E., Migliaccio, C. A. L., Sylva, G. L., and Musser, J. M. (2001). Global differential gene expression in response to growth temperature alteration in group A *Streptococcus*. *Proc. Natl. Acad. Sci. U.S.A.* 98, 10416–10421.

Sorek, R., Kunin, V., and Hugenholtz, P. (2008). CRISPR – a widespread system that provides acquired resistance against phages in bacteria and archaea. *Nat. Rev. Microbiol.* 6, 181–186.

Stanton, T. B. (2007). Prophage-like gene transfer agents–Novel mechanisms of gene exchange for *Methanococcus*, *Desulfovibrio*, *Brachyspira*, and *Rhodobacter* species. *Anaerobe* 13, 43–49.

Steward, G. F., and Preston, C. M. (2011). Analysis of a viral metagenomic library from 200 m depth in Monterey Bay, California constructed by direct shotgun cloning. *Virol. J.* 8, 287.

Sullivan, M. B., Coleman, M. L., Weigele, P., Rohwer, F., and Chisholm, S. W. (2005). Three *Prochlorococcus cyanophage* genomes: signature features and ecological interpretations. *PLoS Biol.* 3, e144. doi:10.1371/journal.pbio.0030144

Sullivan, M. B., Krastins, B., Hughes, J. L., Kelly, L., Chase, M., Sarracino, D., and Chisholm, S. W. (2009). The genome and structural proteome of an ocean siphovirus: a new window into the cyanobacterial "mobilome." *Environ. Microbiol.* 11, 2935–2951.

Suttle, C. A. (2005). Viruses in the sea. *Nature* 437, 356–361.

Takai, K., Inoue, A., and Horikoshi, K. (2002). *Methanothermococcus okinawensis* sp. nov., a thermophilic, methane-producing archaeon isolated from a Western Pacific deep-sea hydrothermal vent system. *Int. J. Syst. Evol. Microbiol.* 52, 1089–1095.

Takai, K., Kobayashi, H., Nealson, K. H., and Horikoshi, K. (2003). *Deferribacter desulfuricans* sp. nov., a novel sulfur-, nitrate-and arsenate-reducing thermophile isolated from a deep-sea hydrothermal vent. *Int. J. Syst. Evol. Microbiol.* 53, 839–846.

Takai, K., Nakamura, K., Toki, T., Tsunogai, U., Miyazaki, M., Miyazaki, J., Hirayama, H., Nakagawa, S., Nunoura, T., and Horikoshi, K. (2008). Cell proliferation at 122°C and isotopically heavy CH4 production by a hyperthermophilic methanogen under high-pressure cultivation. *Proc. Natl. Acad. Sci. U.S.A.* 105, 10949–10954.

Thingstad, T., and Lignell, R. (1997). Theoretical models for the control of bacterial growth rate, abundance, diversity and carbon demand. *Aquat. Microb. Ecol.* 13, 19–27.

Tomkinson, A. E., Vijayakumar, S., Pascal, J. M., and Ellenberger, T. (2006). DNA ligases: structure, reaction mechanism, and function. *Chem. Rev.* 106, 687–699.

Tringe, S. G., von Mering, C., Kobayashi, A., Salamov, A. A., Chen, K., Chang, H. W., Podar, M., Short, J. M., Mathur, E. J., Detter, J. C., Bork, P., Hugenholtz, P., and Rubin, E. M. (2005). Comparative metagenomics of microbial communities. *Science* 22, 554–557.

Tyson, G. W., Chapmon, J., Hugenholtz, P., Allen, E. E., Ram, R. J., Richardson, P. M., Solovyev, V. V., Rubin, E. M., Rokhsar, D. S., and Banfield, J. F. (2004). Community structure and metabolism through reconstruction of microbial genomes from the environment. *Nature* 428, 37–43.

van der Oost, J., Jore, M. M., Westra, E. R., Lundgren, M., and Brouns, S. J. J. (2009). CRISPR-based adaptive and heritable immunity in prokaryotes. *Trends Biochem. Sci.* 34, 401–407.

Vezzi, A., Campanaro, S., D'Angelo, M., Simonato, F., Vitulo, N., Lauro, F. M., Cestaro, A., Malacrida, G., Simionati, B., Cannata, N.,Romualdi, C., Bartlett, D. H., and Valle, G. (2005). Life at depth: *Photobacterium profundum* genome sequence and expression analysis. *Science* 307, 1459–1461.

Vignais, P. M., and Billoud, B. (2007). Occurrence, classification, and biological function of hydrogenases: an overview. *Chem. Rev.* 107, 4206–4272.

Waldor, M. K., and Mekalanos, J. J. (1996). Lysogenic conversion by a filamentous phage encoding cholera toxin. *Science* 272, 1910–1914.

Wang, F., Wang, J., Jian, H., Zhang, B., Li, S., Wang, F., Zeng, X., Gao, L., Bartlett, D. H., Yu, J., Hu, S., and Xiao, X. (2008). Environmental adaptation: genomic analysis of the piezotolerant and psychrotolerant deep-sea iron reducing bacterium *Shewanella piezotolerans* WP3. *PLoS ONE* 3, e1937. doi:10.1371/journal.pone.0001937

Wang, X., Kim, Y., Ma, Q., Hong, S. H., Pokusaeva, K., Sturino, J. M., and Wood, T. K. (2010). Cryptic prophages help bacteria cope with adverse environments. *Nat. Commun.* 1, 147.

Weinbauer, M. G. (2004). Ecology of prokaryotic viruses. *FEMS Microbiol. Rev.* 28, 127–181.

Wheat, G. C., Feely, R. A., and Mottl, M. J. (1996). Phosphate removal by oceanic hydrothermal processes: an update of the phosphorus budget in the oceans. *Geochim. Cosmochim. Acta* 60, 3593–3608.

Whiteley, M., Bangera, M. G., Bumgarner, R. E., Parsek, M. R., Teitzel, G. M., Lory, S., and Greenberg, E. P. (2001). Gene expression in *Pseudomonas aeruginosa* biofilms. *Nature* 413, 860–864.

Williamson, S. J., Cary, S. C., Williamson, K. E., Helton, R. R., Bench, S. R., Winget, D., and Wommack, K. E. (2008). Lysogenic virus–host interactions predominate at deep-sea diffuse-flow hydrothermal vents. *ISME J.* 2, 1112–1121.

Williamson, S. J., Houchin, L. A., McDaniel, L., and Paul, J. H. (2002). Seasonal variation in lysogeny as depicted by prophage induction in Tampa Bay, Florida. *Appl. Environ. Microbiol.* 68, 4307–4314.

Xie, W., Wang, F., Guo, L., Chen, Z., Sievert, S. M., Meng, J., Huang, G., Li, Y., Yan, Q., Wu, S., Wang, X., Chen, S., He, G., Xiao, X., and Xu, A. (2011). Comparative metagenomics of microbial communities inhabiting deep-sea hydrothermal vent chimneys with contrasting chemistries. *ISME J.* 5, 414–426.

Yutin, N., and Koonin, E. V. (2009). Evolution of DNA ligases of nucleocytoplasmic large DNA viruses of eukaryotes: a case of hidden complexity. *Biol. Direct* 4, 51.

Conflict of Interest Statement: The authors declare that the research was conducted in the absence of any commercial or financial relationships that could be construed as a potential conflict of interest.

Received: 31 August 2011; accepted: 14 October 2011; published online: 09 November 2011.

Citation: Anderson RE, Brazelton WJ and Baross JA (2011) Is the genetic landscape of the deep subsurface biosphere affected by viruses? Front. Microbio. ***2****:219. doi: 10.3389/fmicb.2011.00219*

This article was submitted to Frontiers in Extreme Microbiology, a specialty of Frontiers in Microbiology.

frontiers in
MICROBIOLOGY

METHODS ARTICLE
published: 21 November 2011
doi: 10.3389/fmicb.2011.00233

A cell extraction method for oily sediments

Michael Lappé* and Jens Kallmeyer

Geomicrobiology Group, Institute of Earth and Environmental Science, University of Potsdam, Potsdam, Germany

Edited by:
Andreas Teske, University of North Carolina at Chapel Hill, USA

Reviewed by:
Slava Epstein, Northeastern University, USA
Casey R. J. Hubert, Newcastle University, UK

****Correspondence:***
Michael Lappé, Geomicrobiology Group, University of Potsdam, Karl-Liebknecht-Straße 24-25, 14476 Potsdam-Golm, Germany.
e-mail: lappe@geo.uni-potsdam.de

Hydrocarbons can be found in many different habitats and represent an important carbon source for microbes. As fossil fuels, they are also an important economical resource and through natural seepage or accidental release they can be major pollutants. DNA-specific stains and molecular probes bind to hydrocarbons, causing massive background fluorescence, thereby hampering cell enumeration. The cell extraction procedure of Kallmeyer et al. (2008) separates the cells from the sediment matrix. In principle, this technique can also be used to separate cells from oily sediments, but it was not originally optimized for this application. Here we present a modified extraction method in which the hydrocarbons are removed prior to cell extraction. Due to the reduced background fluorescence the microscopic image becomes clearer, making cell identification, and enumeration much easier. Consequently, the resulting cell counts from oily samples treated according to our new protocol are significantly higher than those treated according to Kallmeyer et al. (2008). We tested different amounts of a variety of solvents for their ability to remove hydrocarbons and found that *n*-hexane and – in samples containing more mature oils – methanol, delivered the best results. However, as solvents also tend to lyse cells, it was important to find the optimum solvent to sample ratio, at which hydrocarbon extraction is maximized and cell lysis minimized. A volumetric ratio of 1:2–1:5 between a formalin-fixed sediment slurry and solvent delivered highest cell counts. Extraction efficiency was around 30–50% and was checked on both oily samples spiked with known amounts of *E. coli* cells and oil-free samples amended with fresh and biodegraded oil. The method provided reproducible results on samples containing very different kinds of oils with regard to their degree of biodegradation. For strongly biodegraded oil MeOH turned out to be the most appropriate solvent, whereas for less biodegraded samples *n*-hexane delivered best results.

Keywords: cell enumeration, hydrocarbons, cell separation, subsurface microbiology

INTRODUCTION

Hydrocarbons in the environment constitute an important energy source for microorganisms (Bushnell and Haas, 1941). Phylogenetically diverse groups of microorganisms are present in and around oily sediments (Joynt et al., 2006), the oil coming from either natural seepage or man-made oil spills. The world's largest natural oil reserves are found on the flanks of foreland basins in the Americas (Head et al., 2003; Oil and Gas Journal, 2005), where the general capability for hydrocarbon oxidation was proven in the Athabasca River System (Wyndham and Costerton, 1981). Hydrocarbons enter natural ecosystems by either seepage from geologic reservoirs or through anthropogenic activities (Paisse et al., 2010). They act as environmental pollutants and can cause significant damage to their surrounding but also constitute a carbon source for microorganisms. Natural oils are a mixture of thousands of different compounds. Oil composition depends not just on its source material but also on its degree of biological degradation. Biodegradation preferentially removes *n*-alkanes, isoprenoid-alkanes, cyclo-alkanes, and aromatic compounds from the oil, with the residue containing increasing amounts of alcohols, acids and other water-soluble compounds (Huang et al., 2008; Head et al., 2010).

Oily sediments have received increased attention over the last few years, especially because of their microbial richness and diversity (Edgcomb et al., 2002). In order to obtain an accurate picture of the microbial community in oily sediments, it is important first to quantify the number of cells.

Unfortunately, enumeration of cells in oily sediments seems to be hampered by hydrocarbons, which tend to interact with the DNA-specific stains and molecular probes (Teske et al., 2002). This causes high background fluorescence and makes oily sediments hard to count, thereby lowering the number of detectable cells.

One possible way to overcome the problem of strong background fluorescence is to extract the cells from the sample. Such techniques are usually used in cases where cell abundance is too low for a direct cell count (Fry, 1988; Cragg et al., 1990). Kallmeyer et al. (2008) developed a method to efficiently extract cells from marine sediments and thereby lowering the minimum detection limit from around 10^5 cells cm^{-3} to 10^3 cells cm^{-3}. The method works well with oil-free sediments from the deep marine subsurface, but does not produce satisfactory results with oily sediments.

To overcome the problem of oil-induced background fluorescence, we developed a method that in a first step extracts hydrocarbons from the sediment and in a second step separates the cells from the sediment matrix prior to counting. Solvents not only dissolve hydrocarbons, they also tend to lyse cells. Different

solvents in a wide sample-to-solvent ratio were tested in order to find the most effective solvent and the optimal ratio at which cell lysis does not exceed the positive effect of hydrocarbon removal.

MATERIALS AND METHODS

SAMPLING LOCATIONS AND SAMPLES

Canadian oil sand and processed oil sand

The samples come from an oil sand mining site in the Athabasca Oil Sand area near Ft. McMurray (Alberta, Canada). The crude oil sand, consisting mainly of clays, silicates, water, and hydrocarbons, is dark brown to black and the particle size ranges from fine sand to silt. Clay lenses are common, which gives the sample a very inhomogeneous character. The oil sand sample has a total organic carbon (TOC) content of 13.2%. The extracted oil sand is medium brown and its particle size ranges from fine sand to very fine sand. It contains no clay lenses, but in between the sand, some black nodules are found. The extracted oil sand sample has a TOC content of 0.24%. The mature (biodegraded) oil is the residue of a secondary microbiological degradation (Strausz et al., 2010).

Oily sediments from the Gulf of Mexico

The samples from the Gulf of Mexico are highly diverse. Their total oil content varies significantly, also the sites are affected by either natural hydrocarbon seepage (Beggi Meadow, Orca Basin), or anthropogenic oil spill (Deep Water Horizon wellhead). Other samples are almost devoid of oil (Garden Banks). In contrast to the Canadian oil sand, the oil found in sediment samples from the Gulf of Mexico is rather light and immature (Anderson et al., 1983; Holba et al., 1996).

Beggi Meadow. The sampling site is located in the northern part of the Gulf of Mexico, east of the Mississippi delta (Cooper and Hart, 2002). The sediment sample was taken on Nov 23rd 2010 during Alvin Dive 4652 from the seafloor at 27°N 42.128′; 90°W 38.892′ in a water depth of 834 m. The ambient temperature was 6.3°C. The sediment is very fine-grained, dark gray to black, and very oily.

Orca Basin. The Orca Basin is located in the northern Gulf of Mexico, off the coasts of Texas and Louisiana (26°N 56.25′; 91°W 17.10′). This depression covers an area of about 400 km^2 and has a maximum depth of about 600 m below the surrounding seafloor. In the bottom 200 m it contains anoxic, hypersaline (about 250 $g\,kg^{-1}$) water. Its bathymetry is attributed to salt diapirism and resulting slump features. The salt diapirism is also responsible for the brine (Shokes et al., 1977; Van Cappellen et al., 1998). The sample was taken from the upper 20 cmbsf (cm below the sea floor) with a multicorer on Nov 21st 2010. Ambient water temperature was 3.6°C. The slightly oily sediment is red and very fine-grained.

Near deep water horizon wellhead (Macondo oilfield). The sample was taken from 1.5 nautical miles south of the wellhead of the Deep Water Horizon Drilling Platform (Macondo wellhead) in the Mississippi Canyon (28°N 43.35′; 88°W 21.77′). The drilling rig is now located in a water depth of 1.5 km, about 66 km off the coast of Louisiana (Kessler et al., 2011). The sample was taken with a multicorer on Nov 30th 2010 from a depth of 5–6 cmbsf. Ambient temperature was 4.3°C. The very fine-grained sediment is ochre to slightly greenish brown and only slightly oily.

Garden Banks. Garden Banks is located 170 km south southeast of Galveston, TX, USA, and is a topographic high (lowest water depth about 40 m) resulting from diapirism of Jurassic-age salt (Rezak et al., 1985). Massive, head-forming corals dominate the summits of both of the banks. Surrounding depths range between 100 m in the north and 150 m in the south. The sample was taken southeast of Garden Banks at 27°N 33.207′; 92°W 32.430′ in a water depth of 568 m with a multicorer on Nov 15th 2010 from a sediment depth of 0–10 cmbsf. Ambient temperature was 6.4°C. The sediment is gray and very fine-grained.

Lake Van

Lake Van is located on a plateau in eastern Anatolia, Turkey. It covers an area of 3570 km^2, has a maximum depth of 460 m (Litt et al., 2009), and is the largest soda lake in the world (Kadioglu et al., 1997). The samples were taken during the ICDP drilling operation PALEOVAN in summer 2010 using a hydraulic piston corer. The sample is from the Northern Basin site from a depth of about 3 m below the sea floor (mbsf). It is gray and fine-grained and does not contain any hydrocarbons.

REAGENTS AND MATERIALS

The materials used for the cell extraction have to be absolute cell-free. To achieve this, all glassware used during the cell extraction procedure is combusted before use. In order to increase turnover times, the glass filter towers for the preparation of the filters are not combusted but first washed in a sodium hypochlorite solution, then rinsed first with distilled water then ethanol, followed by a final flaming with a blow-torch directly before use. Reagents were autoclaved if possible and always 0.2 μm filter sterilized immediately before use to remove all cells. The following reagents were used:

- Sodium chloride/formalin solution for preparation of primary marine slurries. To avoid osmotic stress on the cells, the salinity is adjusted to *in situ* conditions, i.e., 25 $g\,L^{-1}$ NaCl for normal marine samples. 20 mL L^{-1} of formalin is added as a fixative.
- Sodium chloride/sodium azide ($NaCl/NaN_3$) solution for further dilution of the primary marine slurries. Salinity is identical to the respective primary slurry, i.e., 25 $g\,L^{-1}$ NaCl for normal marine samples. About 0.1% NaN_3 is added as a biocide to prevent growth of accidentally introduced foreign cells, it has the advantage over formalin of not forming any hazardous volatiles.
- Phosphate buffered saline (PBS) for preparation of the primary slurries from terrestrial samples: 8 $g\,L^{-1}$ NaCl, 0.2 $g\,L^{-1}$ KCl, 1.44 $g\,L^{-1}$ Na_2HPO_4, and 0.24 $g\,L^{-1}$ KH_2PO_4. When preparing primary slurries, 20 mL L^{-1} of formalin is added.
- Carbonate dissolution mix (CDM) for dissolution of carbonates: 20 mL L^{-1} (0.43 M) glacial acetic acid and 35 $g\,L^{-1}$ (0.43 M) sodium acetate. NaCl and PBS, respectively, are added to correspond to the salinity of the samples. After autoclaving, 20 mL L^{-1} of formalin is added.
- Tris-aminomethane–ethylenediaminetetraacetic acid buffer (TE-buffer): 1.211 $g\,L^{-1}$ tris-aminomethane and 0.372 $g\,L^{-1}$

ethylenediaminetetraacetic acid. TE-buffer is used for further dilution of terrestrial samples and for the final rinse of all samples after filtration before staining.

- Detergent mix (DM) for detachment of the cells from sediment particles: 37.2 g L^{-1} (100 mM) disodium EDTA dihydrate, 44.6 g L^{-1} (100 mM) sodium pyrophosphate decahydrate, and 10 mL L^{-1} Tween 80. After autoclaving, formalin is added to a final concentration of 20 mL L^{-1}. The solution is kept under constant stirring during cooling to avoid separation of Tween 80.
- Calcium chloride/sodium acetate ($CaCl_2$/NaAc) solution to neutralize the HF and buffer the pH: 110.984 g L^{-1} $CaCl_2$ and 82.04 g L^{-1} Na-acetate.
- Nycodenz for the density separation: 50 g 100 mL^{-1} Nycodenz.
- The following solvents were used: *n*-hexane, methanol (MeOH), propanol, *n*-octane, *n*-decane, ethanol (EtOH), dichloromethane (DCM), acetone.

METHODS

In order to prevent the DNA-specific stains to interact with the hydrocarbons and to increase the minimum detection limit for cell enumeration, hydrocarbons and cells have to be separated from the oily sediment in two consecutive extraction steps. The cell extraction method of Kallmeyer et al. (2008) serves as basis for the new method, therefore parts of the previous method are reiterated for clarity. **Figure 1** gives an overview of the complete procedure. The primary sediment slurry is prepared by suspending a sediment sample in a fixative solution of similar salinity and thoroughly shaken to form a homogenous slurry. For marine and terrestrial samples, 2.5% (w/v) sodium chloride solution and 1 × PBS solution are used, respectively. For the sample from the hypersaline Orca Basin, the sodium chloride concentration was increased to 250 g NaCl L^{-1}. Independent of the type and salinity of the samples, formalin is added to the solution to a final concentration of 2%.

Ratios between sediment and fixative solution vary widely between different users. For all our experiments we use slurries with a 1:5 (v:v) sediment to fixative ratio.

Prior to the actual cell extraction, the hydrocarbons have to be removed from the oily sediments, because they interact with DNA-specific stains used for marking the cells and cause high background fluorescence, thereby preventing exact cell enumeration. We found the optimal ratio of slurry to solvent to be between 1:2 and 1:5, i.e., one part of the slurry combined with two to five parts of the solvent. The slurry and solvent mixture is shaken (Vortex-Genie 2 shaker) for 20 min to allow for dissolution of oil compounds. After the oil extraction, the sample is centrifuged for 15 min at 12,000 × *g* in order to collect all free floating cells in the pellet. The solvent with the dissolved oil compounds remains in the supernatant and can be decanted off. The cells can then be extracted from the remaining sediment pellet.

Carbonates interfere with the dissolution of the extracellular polymers that bind the cells to the mineral grains. Therefore they have to be dissolved prior to cell detachment (Kallmeyer et al., 2008).

Before performing this time-consuming step, it is advisable to check all samples for their carbonate content under a low magnification stereomicroscope by adding some drops of HCl to a small amount of slurry. All samples used in this study were free of carbonates; we therefore did not perform this step.

After dissolution of hydrocarbons and carbonates, the remaining pellet is suspended with 350 µL of either TE-buffer for the terrestrial samples or with NaCl/NaN_3 solution for the marine samples. Then, 50 µL each of DM and methanol (MeOH) are added (Kallmeyer et al., 2008). The mixture of slurry, NaCl/NaN_3, or TE-buffer, DM, and MeOH is vortexed at maximum speed for 30 min.

A cushion of 500 µL 50% (wt/vol) Nycodenz is injected into the bottom of the vial according to Kallmeyer et al. (2008), followed by centrifugation at 2,000 × *g* for 15 min in a swing out rotor centrifuge. The cells are separated from the sediment particles by density centrifugation. The supernatant is treated according to Kallmeyer et al. (2008). The pellet is resuspended in 350 µL TE-buffer or NaCl/NaN_3 solution, and again 50 µL each of DM and MeOH are added. After sonicating for 10 min in a sonication bath (Bandelin Sonorex Digitec) at room temperature, the vials are vortexed for 15 min, followed by density separation as described above. The supernatants from the density separation and the carbonate dissolution step are pooled and can be used for cell counting or other applications (Kallmeyer et al., 2008). Prior to filtration, 100 µL of 1% hydrofluoric acid (HF) is added to the supernatant and left for 10 min to reduce non-specific background fluorescence from sediment particles. The filters are rinsed inside the filter towers with a few ml of TE-buffer to remove any remaining HF. One or two blank samples were processed with each batch of samples processed for cell extraction.

For cell counting, the supernatants are filtered onto 0.2 µm polycarbonate filters (Whatman Cyclopore Track Etched Membrane; Jones et al., 1989; Stockner et al., 1990). To ensure an even distribution of the cells on the filter, 5 mL of 0.2 µm filtered TE-buffer or NaCl/NaN_3, should be placed into the filter tower prior to the addition of supernatant. Staining and embedding is carried out according to Morono et al. (2009). Cell counting is performed using an epifluorescence microscope.

RESULTS

At the beginning of the experiments, we tried to count cells directly from completely untreated samples similar to the protocol of Cragg et al. (1990). No cells could be detected due to massive background fluorescence caused by the SYBR Green I stain binding to hydrocarbons. The same effect was observed using Acridine Orange instead of SYBR Green I. By using the cell extraction procedure of Kallmeyer et al. (2008) it was possible to see a few cells, but due to the hydrocarbons still being present, there was considerable background fluorescence (**Figure 2A**). We therefore developed a hydrocarbon extraction step prior to cell extraction, that effectively removed the oil from the sample, thereby drastically reducing background fluorescence (**Figure 2B**).

Due to the large range of total cell abundances in the different samples, all results are presented as percent values relative to cell counts obtained by the extraction procedure of Kallmeyer et al. (2008).

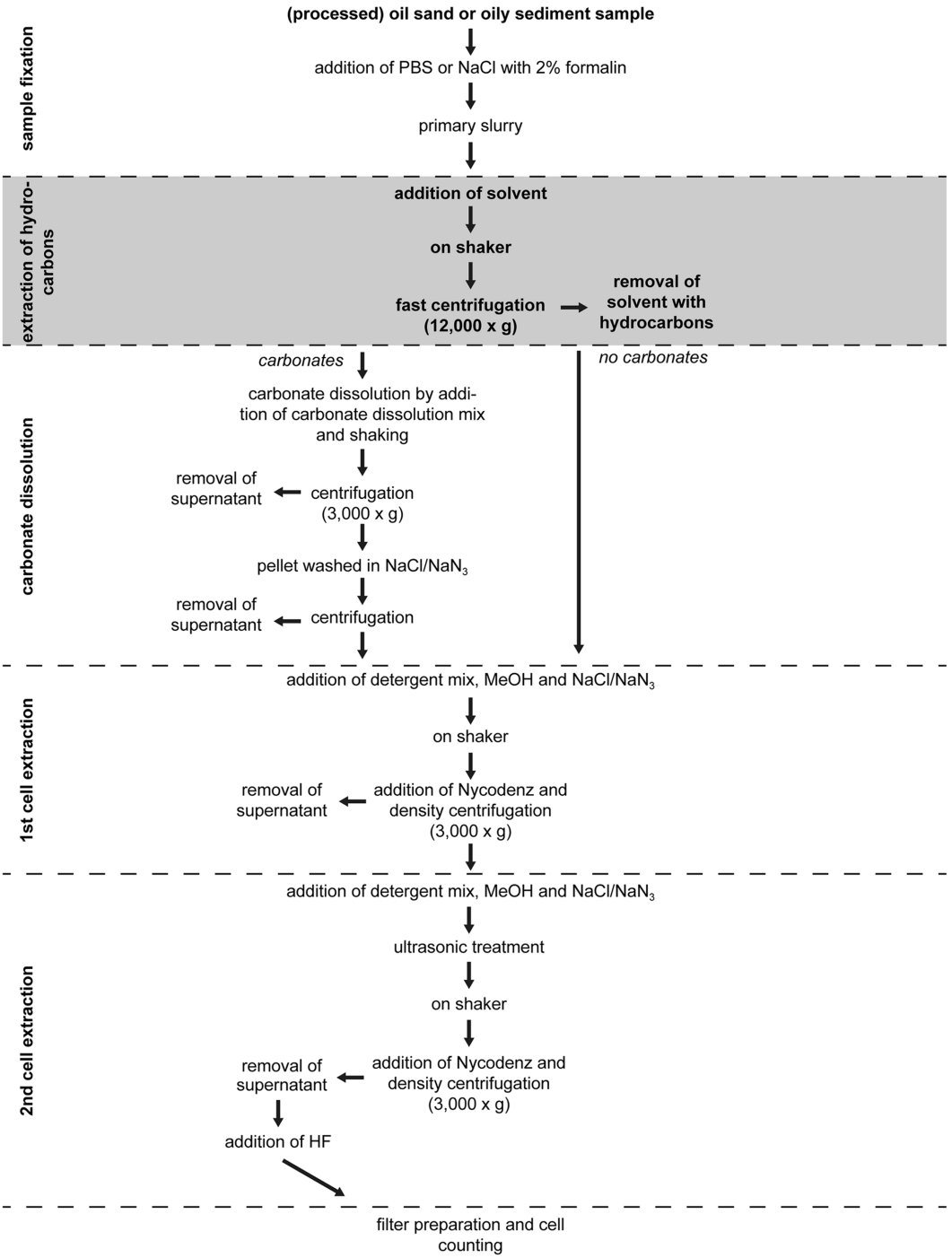

FIGURE 1 | The flow chart shows the complete hydrocarbon and cell extraction procedure for oily sediments. The method is based on the cell extraction procedure of Kallmeyer et al. (2008). The hydrocarbon extraction step is shaded. Details about incubation times and amounts of reagents are provided in the text.

For initial tests only a subset of samples (crude and processed oil sand, Garden Banks) was treated with a wide range of solvents: MeOH, *n*-hexane, propanol, acetone, EtOH, *n*-octane, *n*-decane, a mixture of *n*-hexane and MeOH, a mixture of *n*-hexane and DCM, and a double extraction with *n*-hexane. MeOH and *n*-hexane showed the most promising results (**Figures 3A–C**), because they delivered high and reproducible cell counts on all samples tested. The other solvents delivered results that were either consistently below 100% (EtOH, acetone, DCM) or did not show high extraction efficiency with all types of samples (*n*-octane and *n*-decane).

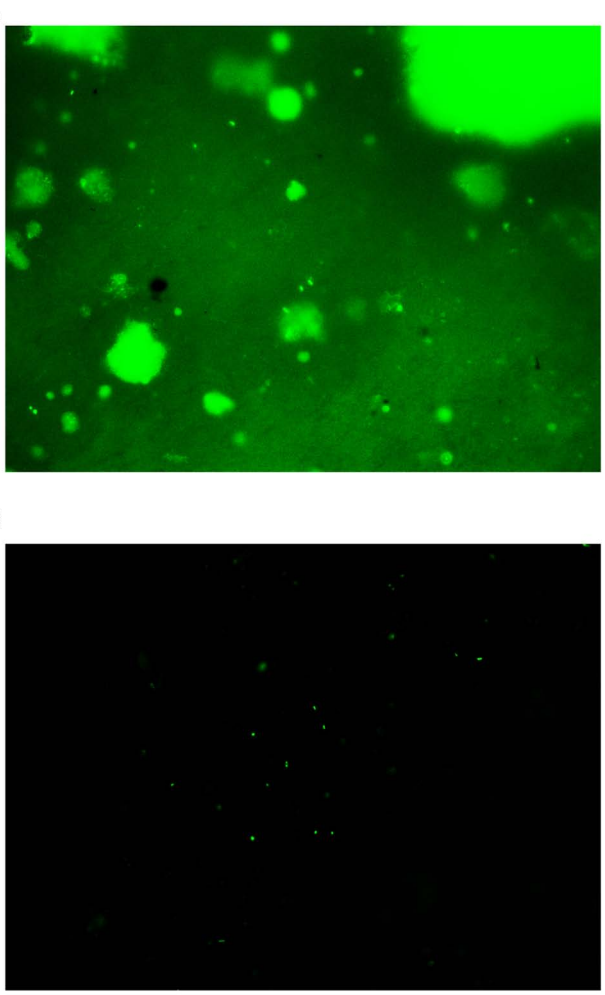

FIGURE 2 | Image of an oil sand sample under the fluorescence microscope. (A) Sample processed according to the extraction procedure of Kallmeyer et al. (2008) without hydrocarbon extraction. Cells are difficult to identify due to strong background fluorescence. **(B)** Sample after hydrocarbon extraction prior to cell extraction. Background fluorescence is drastically reduced and cells are much easier to detect.

MeOH and *n*-hexane were therefore tested on a greater variety of samples (**Figure 4**). For all samples, highest cell counts were achieved with solvent volumes between 100 and 250 μL (i.e., a ratio of primary slurry to solvent of 1:2–1:5). When using lower volumes, the filters still showed some background fluorescence, thereby hampering cell detection. Using higher volumes, the cell extraction efficiency decreased again toward efficiency values of the standard extraction procedure or even below that.

Two competing factors appear to control the efficiency of the solvent extraction. The first one is the gain in counting efficiency due to the removal of oil; the second one is lysis of cells by the solvents, which reduces the number of cells in the sample. It is therefore necessary to find the threshold at which the positive effect is maximized and the negative minimized. Therefore we exposed a formalin-fixed culture of *E. coli* to solvents, using the same sample-to-solvent ratios as for the sediment slurries. About 20% of the cells were lysed by the procedure. To test the efficiency of our new cell extraction method, we added a known amount of *E. coli* cells to the crude oil sand sample. Of these added cells, 55% could be recovered by the cell separation with solvent extraction (data not shown). This indicates that some of the added cells are either lysed or not extracted.

To further test the effect of solvents on cells in the sediment, we applied our method to a completely oil-free sample from Lake Van and one with very low, barely detectable, oil content (Garden Banks; **Figure 4**). On these two samples we expected little to no positive effect from the solvent addition and could therefore use them to test whether there is a certain threshold for addition of solvents, above which cell lysis occurs or if cell lysis starts even at very small additions of solvent.

The pattern of extraction efficiency vs. solvent addition in the *n*-hexane extracted Garden Banks sample follows the same general trend observed in all samples, just shifted to lower values (**Figure 4**). Maximum efficiency reached 100% at 200 μL of solvent addition. The MeOH extraction did not show any clear trend and remained <50% for all slurry to solvent ratios. The use of other solvents did not lead to higher extraction efficiencies for the Garden Banks sample (**Figure 3A**).

For the oil-free Lake Van sample the extraction with either solvent (MeOH and *n*-hexane) did not increase efficiency above the normal extraction, both solvents reached maximum values around 100%. However, for the *n*-hexane extraction the pattern is somewhat different; highest extraction efficiency (95%) is reached with the lowest amount of solvent added, all higher additions led to much lower efficiencies. For the MeOH extraction, efficiency is generally low (<50%), except for the addition of 200 μL, with which an efficiency of about 100% is achieved.

It appears that MeOH seems to work better in samples containing heavy, mature oil, or bitumen, whereas *n*-hexane is the most appropriate solvent to remove hydrocarbons in oily sediment samples containing light and rather immature oil (**Figure 4**).

There is large scatter in the range of best extraction efficiencies. In the sample from Beggi Meadow, all solvent to sample ratios tested delivered higher cell counts than the standard method, even up to 1,000 μL of *n*-hexane. Still, highest efficiencies were achieved with 100–250 μL of solvent (**Figure 4**).

To test whether there is a loss of cells from the centrifugation step after hydrocarbon extraction (12,000 × *g* for 15 min) some supernatants were filtered and counted. No cells were found on any filter indicating that the centrifugation step works well and that all cells remain in the pellet.

We also added light oil (non-biodegraded, API gravity of 32.9°), and heavy oil (strongly biodegraded, API gravity <10°) to oil-free Lake Van sediment. Due to very strong background fluorescence no cells could be detected using the standard method of Kallmeyer et al. (2008). The spiked samples were then processed according to our new solvent extraction method. In the sample spiked with the light oil, it was possible to detect 11 and 33% of the cells with MeOH and *n*-hexane, respectively, as compared to the oil-free sample. In the sample spiked with the heavy oil, MeOH extraction delivered higher cell counts (47%) than *n*-hexane (38%). This indicates that the choice of a solvent used depends on the biodegradative state of the oil.

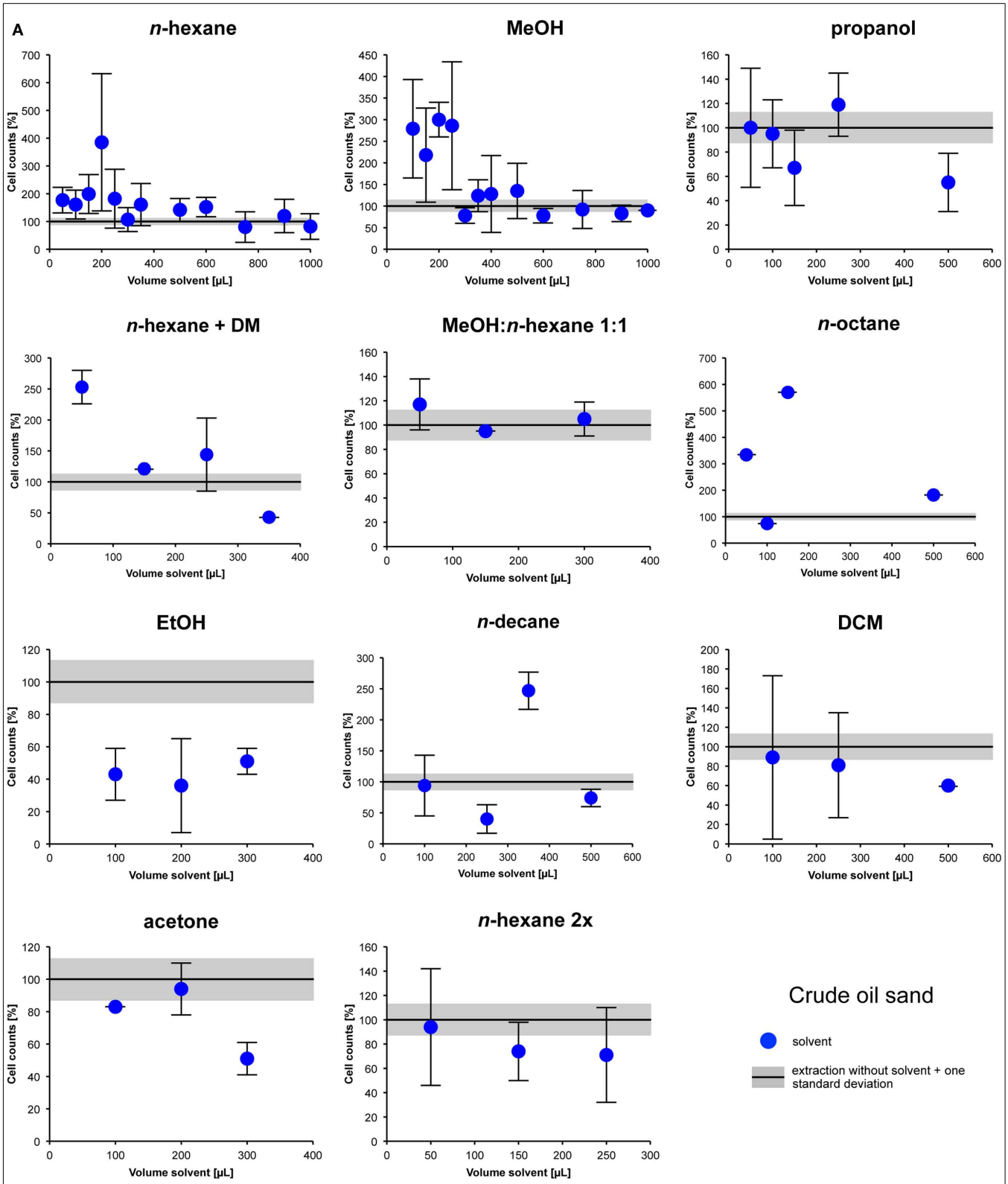

FIGURE 3 | Continued

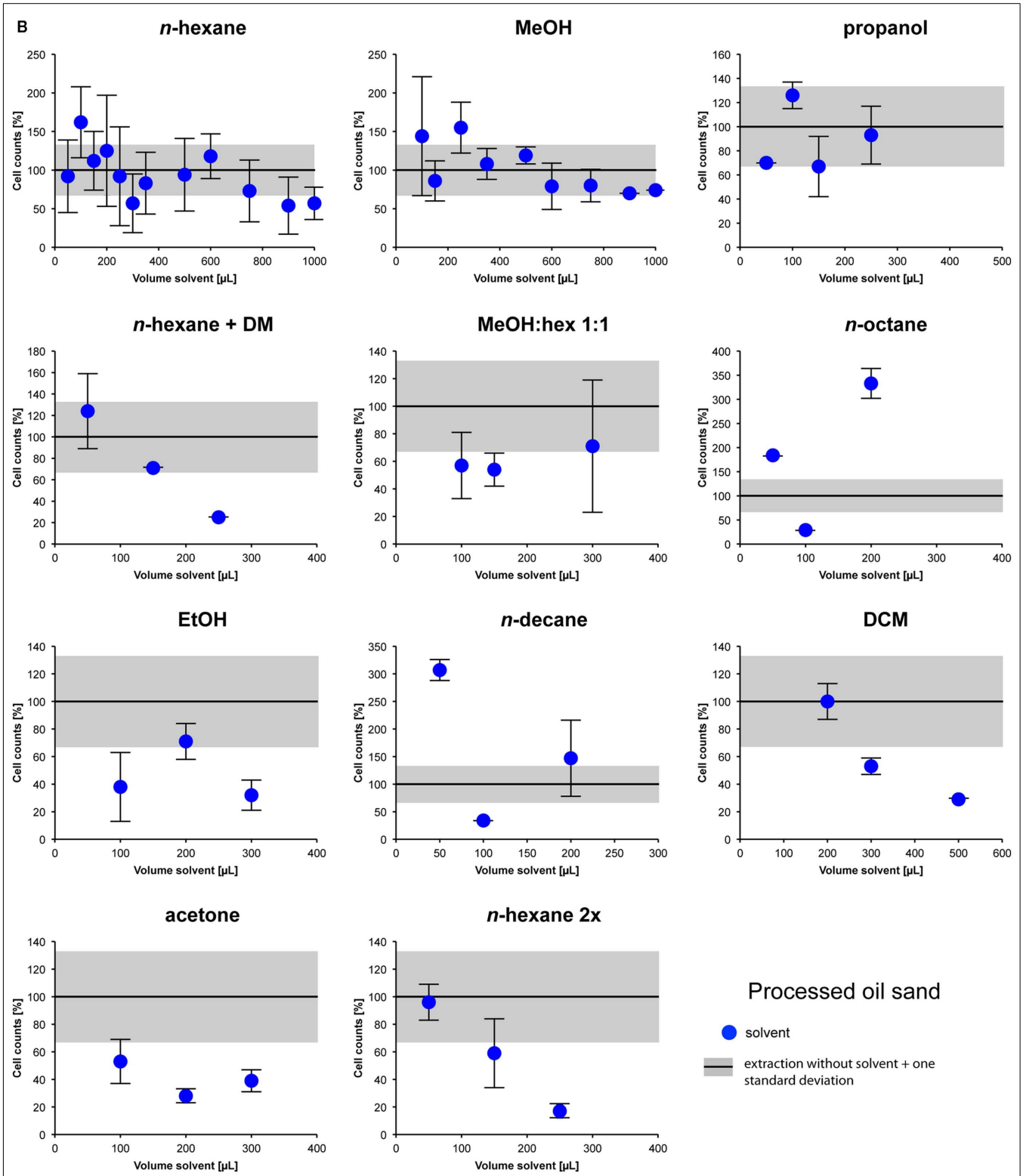

FIGURE 3 | Continued

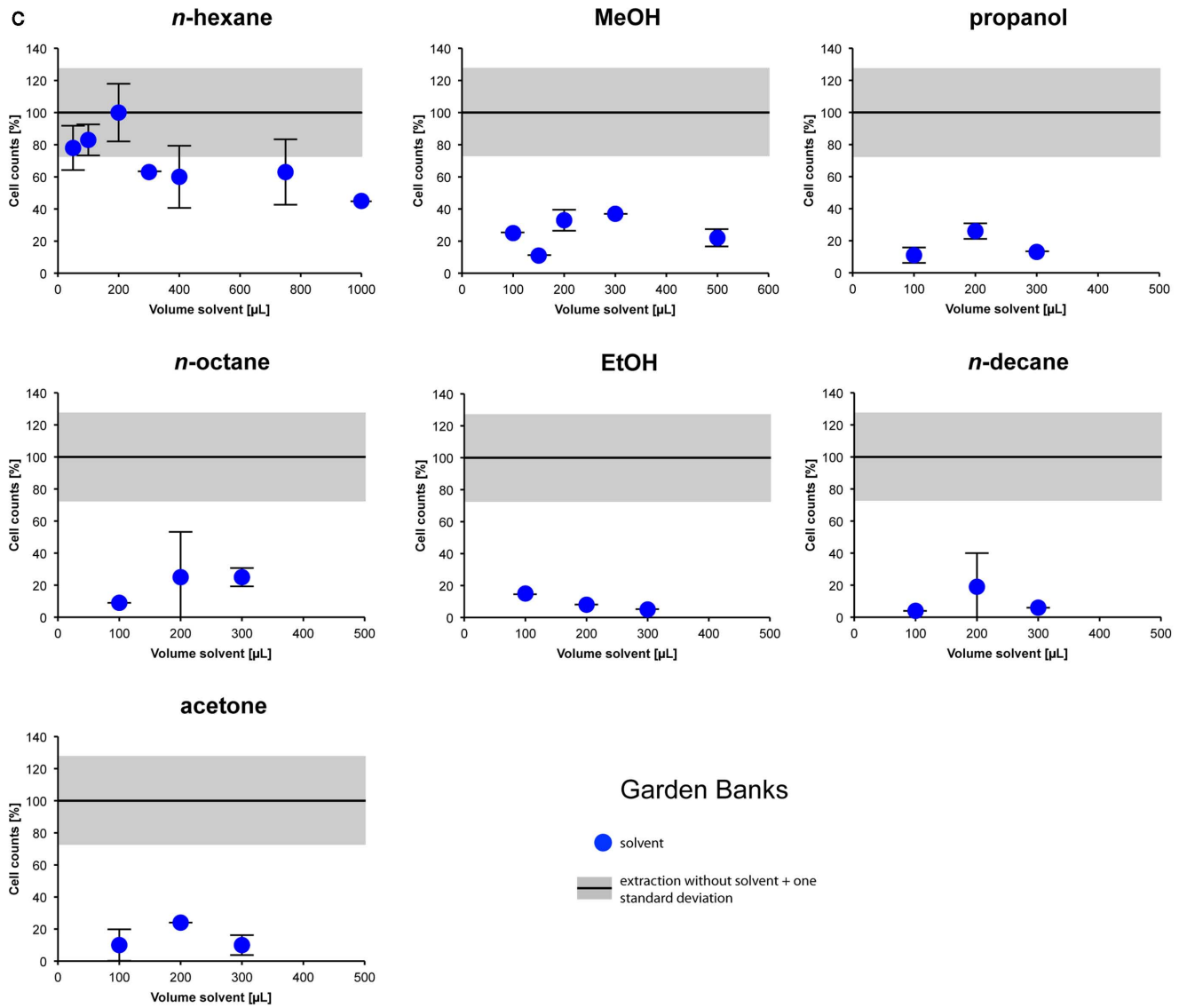

FIGURE 3 | (A) Extraction of hydrocarbons with different solvents applied to a crude oil sand from Athabasca, Canada. To compare the extraction results, cell counts are given as percentages of the results of the standard procedure of Kallmeyer et al. (2008). The obtained cell counts after counting cells from untreated (i.e., without solvent) samples is set to 100%. The shaded areas represent 1 × SD for standard cell extractions without solvent treatment. **(B)** Extraction of hydrocarbons with different solvents applied to a processed oil sand from Athabasca, Canada. To compare the extraction results, cell counts are given as percentages of the results of the standard procedure of Kallmeyer et al. (2008). The obtained cell counts after counting cells from untreated (i.e., without solvent) samples is set to 100%. The shaded areas represent 1 × SD for standard cell extractions without solvent treatment. **(C)** Extraction of hydrocarbons with different solvents applied to an oily marine sediment sample from Garden Banks. To compare the extraction results, cell counts are given as percentages of the results of the standard procedure of Kallmeyer et al. (2008). The obtained cell counts after counting cells from untreated (i.e., without solvent) samples is set to 100%. The shaded areas represent 1 × SD for standard cell extractions without solvent treatment. None of the indicated solvents worked well at this sample, because it was almost free of hydrocarbons.

DISCUSSION

By removal of hydrocarbons prior to cell extraction the microscopic image becomes much clearer, making it possible to detect significantly more cells on the filter. The remaining background fluorescence is very low (**Figure 2B**). Especially the use of *n*-hexane and MeOH in a slurry to solvent ratio of 1:2–1:5 (50 µL of primary slurry and 100–250 µL of solvent) delivers the best (i.e., highest) cell counts (**Figure 4**). When using a higher solvent to slurry ratio, cell counts decrease again. Apparently the effect of cell lysis is greater than the improvement of the microscope image by removing interfering hydrocarbons.

The concentration above which cell lysis exceeds the positive effect of hydrocarbon dissolution appears to be dependent on the type of solvent. This might be the reason why for DCM cell counts are lower than those from the standard cell extraction procedure, not just above a certain solvent to slurry ratio, but uniformly over

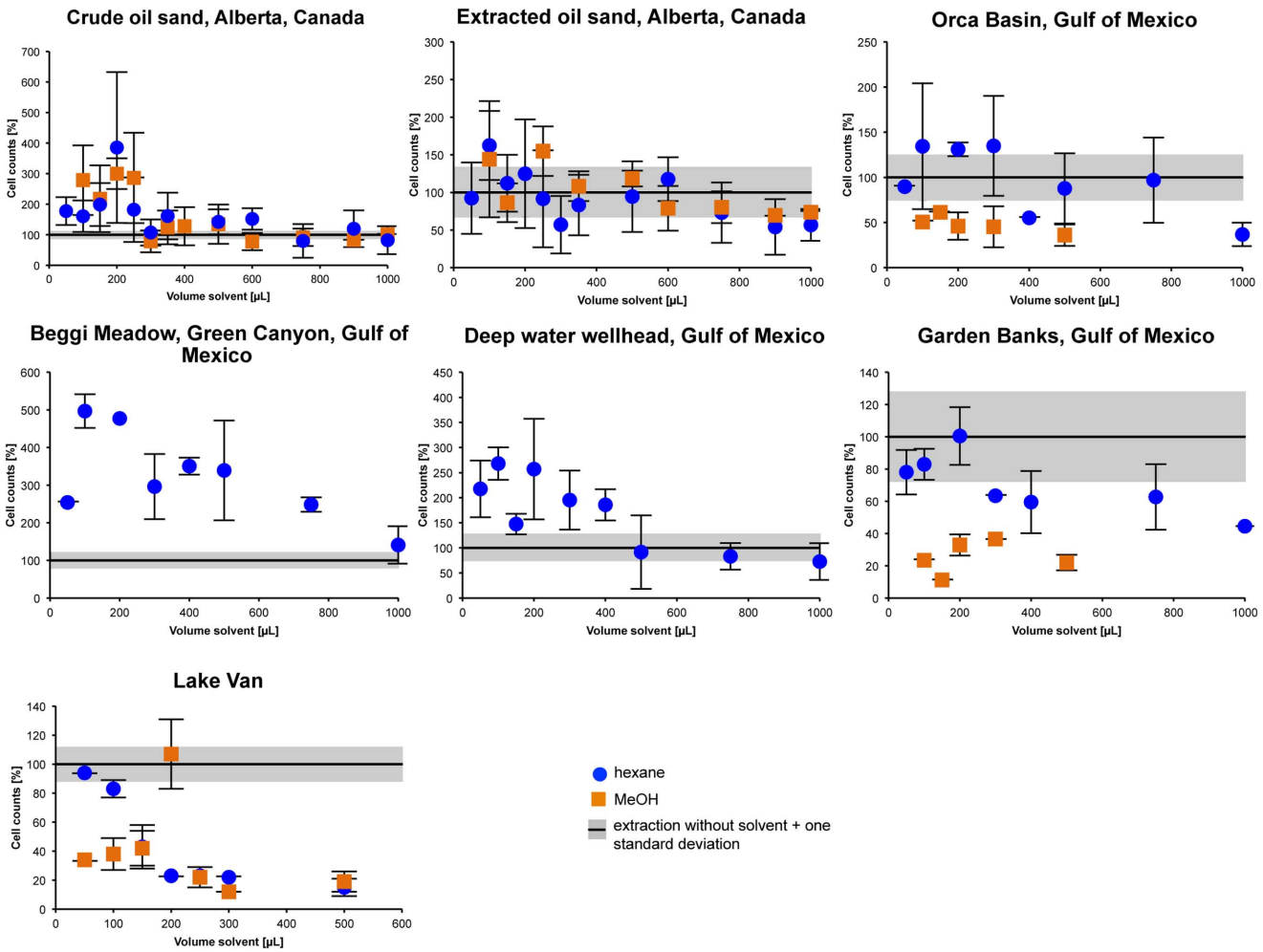

FIGURE 4 | Cell extraction efficiencies for different sample types treated with either *n*-hexane or MeOH. Cell counts are given as percentages of the results of the standard procedure of Kallmeyer et al. (2008). In most samples a typical pattern becomes obvious. Cell extraction efficiencies are highest for a slurry to solvent ratio of 1:2–1:5 (i.e., between 100 and 250 µL).

all ratios tested. DCM is also impractical to handle, as it needs special filters, vials and glass syringes, because it dissolves most plastics.

Some solvents might be less suitable than others to dissolve hydrocarbons, especially propanol, EtOH, or acetone. After the treatment with these solvents, the filters still showed background fluorescence, indicating that hydrocarbons were still present in the sample. Concomitantly, the supernatants of the propanol, EtOH, and acetone extraction were almost colorless. In contrary, the supernatants of the *n*-octane, *n*-decane, DCM, or *n*-hexane extraction were dark red to brown, indicating that hydrocarbon extraction was successful.

Although *n*-octane delivers high cell counts, we do not recommend its use. The samples extracted with *n*-octane and *n*-decane showed murky supernatants, containing small flocs of particulate (organic?) matter that settled on the filter and made cell enumerations difficult or even impossible. Given the difficulties with these filters, the reported cell numbers should be treated with caution.

Surprisingly, extractions with a mixture of the two best working solvents (*n*-hexane and MeOH) lead to lower results than with a single solvent. Also, two consecutive extractions with *n*-hexane did not lead to higher results either (**Figures 3A–C**). This is probably due to the fact that the cells were lysed by the long exposure to the solvent.

The discrepancy in the increase of the extraction efficiency between the samples (especially for MeOH) might result from the different compositions of the oils. The more biodegraded or mature the oil is, the less paraffinic compounds it contains (Huang et al., 2008; Head et al., 2010). MeOH – a more polar solvent than *n*-hexane – might be more useful in strongly mature samples, whereas *n*-hexane works better with light, more paraffinic oil. This might also explain, why in the terrestrial samples, containing heavy, mature oil, most solvents delivered results coming close to 100% extraction efficiency, whereas in marine samples, containing light oil, the results usually fell below 50% for most solvents (**Figures 3A–C**).

The increase in extraction efficiency after the solvent extraction is much higher for the original oil sand than for the processed one. This seems to be logical, because there are much more hydrocarbons in the fresh oil sand before the extraction of the oil (TOC of 13.2%) than after the extraction (TOC of 0.24%).

The solvent extraction did not improve cell counting in the oil-poor sediments from Garden Banks and in the oil-free sample from Lake Van. That was expected, because there is no oil in the sediment, which could hamper cell detection. We expected cell lysis to either start at a certain threshold, or to be proportional to the ratio of solvent vs. slurry. The oil-poor Garden Banks sample basically showed such a threshold; with up to 200 μL of *n*-hexane addition cell abundances were in the same range as the standard extraction, then drop sharply at higher solvent additions. This would be an indication that cell lysis starts even at very low solvent concentrations. The positive effect of hydrocarbon dissolution dominates over the negative effect of cell lysis at low solvent concentrations. This is confirmed by the fact, that the optimal amount of solvent (i.e., 200 μL of *n*-hexane or MeOH) lyses 20% of the cells of a formalin-fixed pure culture, whereas at higher solvent concentrations up to 90% of the cells were lysed (data not shown). The recovery of only 55% of *E. coli* cells added to a crude oil sand sample indicates that lysis by the solvent treatment is not the only factor that reduces cell recovery. The most likely other reason is that cells become stuck on oil-coated mineral grains and thereby end up in the sediment pellet and not in the supernatant.

The *n*-hexane extraction of the oil-free Lake Van sample also shows a similar trend, however, cell numbers decrease even by the smallest solvent addition. There does not seem to be a threshold but rather an immediate negative effect due to solvent addition. The MeOH extraction shows a rather surprising trend with one single sample reaching about 100% efficiency, whereas all other solvent to slurry ratios remain <50%. So far we have no satisfactory explanation for this observation. There is a good chance that this high result is an artifact, because all other results fall into a narrow range.

The recovery of about one third of cells after spiking an oil-free sample with a light (non-biodegraded) oil shows that it is not yet possible to retrieve all cells out of sediment that contains light oil.

It was possible to retrieve about half of the cells from a sample that was spiked with strongly biodegraded oil, using MeOH as a solvent. This is quite surprising because biodegraded oils are much more viscous and sticky and we assumed that these properties would cause more cells to remain stuck on sediment particles and therefore avoid cell extraction.

The fact that *n*-hexane produces better results in samples containing fresh oils, whereas MeOH works better for samples with heavy oils may be explained by the fact that fresh oils contain more alkanes, which dissolve preferentially in other alkanes like *n*-hexane. Heavy oils contain a higher fraction of alcohols and water-soluble compounds for which MeOH is a better solvent. Although solvent extraction improves cell extraction efficiency, it has to be kept in mind that cell abundances will always be underestimated.

For the solvent extraction of hydrocarbon-containing sediments, the maximum cell extraction efficiency is achieved with a ratio of primary slurry to pure solvent between 1:2 and 1:5. Outside of this optimum ratio, extraction efficiency is drastically reduced.

CONCLUSION

Based on the method of Kallmeyer et al. (2008) we developed a cell extraction procedure for hydrocarbon-containing sediments. The focus of this method lies on the removal of hydrocarbons, because they prevent cell enumerations by interacting with the DNA-binding stain causing high background fluorescence. For the dissolution of hydrocarbons, *n*-hexane turned out to be the most appropriate solvent for light (non-biodegraded) oils whereas MeOH is most appropriate for heavy (biodegraded) oils.

This method works well with sediments from a wide variety of environments containing either heavy or light oils. However, the extraction protocol needs to be tested and individually fine-tuned for every type of sediment and oil in order to find the best working solvent and the optimum solvent to sample ratio at which hydrocarbon extraction is maximized and the effect of cell lysis kept at a minimum. In hydrocarbon-free sediments, the method does not show any positive effects.

Although we developed this extraction technique primarily for cell enumeration, parts or all of it may also be useful for other microbiological and molecular techniques that require hydrocarbon-free samples.

ACKNOWLEDGMENTS

The marine sediment samples from the Gulf of Mexico were provided by Andreas P. Teske (UNC Chapel Hill). The oil sand and the extracted oil sand samples were provided by the University of Alberta as part of the HAI (Helmholtz Alberta Initiative) project. Clemens Glombitza provided the Lake Van sample. We would like to thank Mareike Noah and Heinz Wilkes from the GFZ (GeoForschungsZentrum) Potsdam for measuring the TOC content of the samples.

REFERENCES

Anderson, R. K., Scalan, R. S., Parker, P. L., and Behrens, E. W. (1983). Seep oil and gas in gulf of mexico slope sediment. *Science* 222, 619–621.

Bushnell, L. D., and Haas, H. F. (1941). The utilization of certain hydrocarbons by microorganisms. *J. Bacteriol.* 41, 653–673.

Cooper, A. K., and Hart, P. E. (2002). High-resolution seismic-reflection investigation of the northern Gulf of Mexico gas-hydrate-stability zone. *Mar. Petrol. Geol.* 19, 1275–1293.

Cragg, B. A., Parkes, R. J., Fry, J. C., Herbert, R. A., Wimpenny, J. W. T., and Getliff, J. M. (1990). Bacterial biomass and activity profiles within deep sediment layers. *Proc. Ocean Drill. Prog. Sci. Results* 112, 607–619.

Edgcomb, V. P., Kysela, D. T., Teske, A., Gomez, A. D., and Sogin, M. L. (2002). Benthic eukaryotic diversity in the Guaymas Basin hydrothermal vent environment. *Proc. Natl. Acad. Sci. U.S.A.* 99, 7658–7662.

Fry, J. C. (1988). "Determination of biomass," in *Methods in Aquatic Bacteriology*, ed. B. Austin (John Wiley & Sons Ltd.), 27–72.

Head, I. M., Jones, D. M., and Larter, S. R. (2003). Biological activity in the deep subsurface and the origin of heavy oil. *Nature* 426, 344–352.

Head, I. M., Larter, S. R., Gray, N. D., Sherry, A., Adams, J. J., Aitken, C. M., Jones, D. M., Rowan, A. K., Huang, H., and Röling, W. F. M. (2010). "Hydrocarbon degradation in petroleum reservoirs," in *Handbook of Hydrocarbon and Lipid Microbiology*, ed. K. N. Timmis (Berlin: Springer-Verlag), 3097–3109.

Holba, A. G., Dzou, L. I. P., Hickey, J. J., Franks, S. G., May, S. J., and Lenney, T. (1996). Reservoir geochemistry of South Pass 61 Field, Gulf of Mexico: compositional heterogeneities reflecting filling history and biodegradation. *Org. Geochem.* 24, 1179–1198.

Huang, H. P., Zhou, S. Q., and Liu, Y. M. (2008). Biodegradation and origin of oil sands in the Western Canada sedimentary basin. *Petrol. Sci.* 5, 87–94.

Jones, S. E., Ditner, S. A., Freeman, C., Whitaker, C. J., and Lock, M. A. (1989). Comparison of a new inorganic membrane-filter (anopore) with a Track-etched polycarbonate membrane-filter (nuclepore) for direct counting of bacteria. *Appl. Environ. Microbiol.* 55, 529–530.

Joynt, J., Bischoff, M., Turco, R., Konopka, A., and Nakatsu, C. H. (2006). Microbial community analysis of soils contaminaed with lead, chromium and petroleum hydrocarbons. *Microb. Ecol.* 51, 209–219.

Kadioglu, M., Sen, Z., and Batur, E. (1997). The greatest soda-water lake in the world and how it is influenced by climatic change. *Ann. Geophysicae* 15, 1489–1497.

Kallmeyer, J., Smith, D. C., Spivack, A. J., and D'hondt, S. (2008). New cell extraction procedure applied to deep subsurface sediments. *Limnol. Oceanogr. Methods* 6, 236–245.

Kessler, J. D., Valentine, D. L., Redmond, M. C., Du, M. R., Chan, E. W., Mendes, S. D., Quiroz, E. W., Villanueva, C. J., Shusta, S. S., Werra, L. M., Yvon-Lewis, S. A., and Weber, T. C. (2011). A persistent oxygen anomaly reveals the fate of spilled methane in the deep Gulf of Mexico. *Science* 331, 312–315.

Litt, T., Krastel, S., Sturm, M., Kipfer, R., Orcen, S., Heumann, G., Franz, S. O., Ulgen, U. B., and Niessen, F. (2009). 'PALEOVAN,' International Continental Scientific Drilling Program (ICDP): site survey results and perspectives. *Quat. Sci. Rev.* 28, 1555–1567.

Morono, Y., Terada, T., Masui, N., and Inagaki, F. (2009). Discriminative detection and enumeration of microbial life in marine subsurface sediments. *ISME J.* 3, 503–511.

Oil and Gas Journal. (2005). Worldwide look at reserves and production. *Oil Gas J.* 103, 24–25.

Paisse, S., Goni-Urriza, M., Coulon, F., and Duran, R. (2010). How a bacterial community originating from a contaminated coastal sediment responds to an oil input. *Microb. Ecol.* 60, 394–405.

Rezak, R., Bright, T. J., and Mcgrail, D. W. (1985). *Reefs and Banks of the Northern Gulf of Mexico: Their Geological, Biological and Physical Dynamics.* New York: John Wiley and Sons, 259.

Shokes, R. F., Trabant, P. K., Presley, B. J., and Reid, D. F. (1977). Anoxic, hypersaline basin in Northern Gulf of Mexico. *Science* 196, 1443–1446.

Stockner, J. G., Klut, M. E., and Cochlan, W. P. (1990). Leaky filters – a warning to aquatic ecologists. *Can. J. Fish. Aquat. Sci.* 47, 16–23.

Strausz, O. P., Morales-Izquierdo, A., Kazmi, N., Montgomery, D. S., Payzant, J. D., Safarik, I., and Murgich, J. (2010). Chemical composition of Athabasca bitumen: the saturate fraction. *Energy Fuels* 24, 5053–5072.

Teske, A., Hinrichs, K.-U., Edgcomb, V., De Vera Gomez, A., Kysela, D., Sylva, S. P., Sogin, M. L., and Jannasch, H. W. (2002). Microbial diversity of hydrothermal sediments in the guaymas basin: evidence for anaerobic methanotrophic communities. *Appl. Environ. Microbiol.* 68, 1994–2007.

Van Cappellen, P., Viollier, E., Roychoudhury, A., Clark, L., Ingall, E., Lowe, K., and Dichristina, T. (1998). Biogeochemical cycles of manganese and iron at the oxic-anoxic transition of a stratified marine basin (Orca Basin, Gulf of Mexico). *Environ. Sci. Technol.* 32, 2931–2939.

Wyndham, R. C., and Costerton, J. W. (1981). Heterotrophic potentials and hydrocarbon biodegradation potentials of sediment microorganisms within the Athabasca oil sands deposit. *Appl. Environ. Microbiol.* 41, 783–790.

Conflict of Interest Statement: The authors declare that the research was conducted in the absence of any commercial or financial relationships that could be construed as a potential conflict of interest.

Received: 11 July 2011; accepted: 04 November 2011; published online: 21 November 2011.

Citation: Lappé M and Kallmeyer J (2011) A cell extraction method for oily sediments. Front. Microbio. ***2****:233. doi: 10.3389/fmicb.2011.00233*

This article was submitted to Frontiers in Extreme Microbiology, a specialty of Frontiers in Microbiology.

frontiers in
MICROBIOLOGY

ORIGINAL RESEARCH ARTICLE
published: 22 December 2011
doi: 10.3389/fmicb.2011.00253

Real-time PCR quantification and diversity analysis of the functional genes *aprA* and *dsrA* of sulfate-reducing prokaryotes in marine sediments of the Peru continental margin and the Black Sea

***Anna Blazejak*[1†] *and Axel Schippers*[1,2*]**

[1] *Geomicrobiology, Federal Institute for Geosciences and Natural Resources (BGR), Hannover, Germany*
[2] *Faculty of Natural Sciences, Leibniz Universität Hannover, Hannover, Germany*

Edited by:
Andreas Teske, University of North Carolina at Chapel Hill, USA

Reviewed by:
Julie A. Huber, Marine Biological Laboratory, USA
Kasthuri Venkateswaran, NASA-Jet Propulsion Laboratory, USA

***Correspondence:**
Axel Schippers, Geomicrobiology, Federal Institute for Geosciences and Natural Resources (BGR), Stilleweg 2, 30655 Hannover, Germany.
e-mail: axel.schippers@bgr.de

[†]***Present address:***
Anna Blazejak, Max Planck Institute for Marine Microbiology, Bremen, Germany.

Sulfate-reducing prokaryotes (SRP) are ubiquitous and quantitatively important members in many ecosystems, especially in marine sediments. However their abundance and diversity in subsurface marine sediments is poorly understood. In this study, the abundance and diversity of the functional genes for the enzymes adenosine 5′-phosphosulfate reductase (*aprA*) and dissimilatory sulfite reductase (*dsrA*) of SRP in marine sediments of the Peru continental margin and the Black Sea were analyzed, including samples from the deep biosphere (ODP site 1227). For *aprA* quantification a Q-PCR assay was designed and evaluated. Depth profiles of the *aprA* and *dsrA* copy numbers were almost equal for all sites. Gene copy numbers decreased concomitantly with depth from around 10^8/g sediment close to the sediment surface to less than 10^5/g sediment at 5 mbsf. The 16S rRNA gene copy numbers of total bacteria were much higher than those of the functional genes at all sediment depths and used to calculate the proportion of SRP to the total *Bacteria*. The *aprA* and *dsrA* copy numbers comprised in average 0.5–1% of the 16S rRNA gene copy numbers of total bacteria in the sediments up to a depth of ca. 40 mbsf. In the zone without detectable sulfate in the pore water from about 40–121 mbsf (Peru margin ODP site 1227), only *dsrA* (but not *aprA*) was detected with copy numbers of less than 10^4/g sediment, comprising ca. 14% of the 16S rRNA gene copy numbers of total bacteria. In this zone, sulfate might be provided for SRP by anaerobic sulfide oxidation. Clone libraries of *aprA* showed that all isolated sequences originate from SRP showing a close relationship to *aprA* of characterized species or form a new cluster with only distant relation to *aprA* of isolated SRP. For *dsrA* a high diversity was detected, even up to 121 m sediment depth in the deep biosphere.

Keywords: deep biosphere, real-time PCR, subsurface, ODP, sulfate-reducing prokaryotes, *aprA*, *dsrA*

INTRODUCTION

Sulfate reduction plays a crucial role in the past and present global sulfur cycle, and may be regarded as one of the oldest metabolic pathways on Earth (Castresana and Moreira, 1999; Schen et al., 2001). Therefore, sulfate-reducing prokaryotes (SRP) are biogeochemically important organisms in the environment, especially for the degradation of organic matter in coastal but also in deeply buried marine sediments in the open ocean (Jørgensen, 1982; Ferdelman et al., 1997; Knoblauch et al., 1999; Sahm et al., 1999; Thamdrup et al., 2000; Jørgensen et al., 2001; D'Hondt et al., 2004; Parkes et al., 2005; Schippers et al., 2005, 2010). Despite their importance in subsurface marine sediments the abundance and diversity of SRP in this environment is poorly understood. Global surveys of SRP cell numbers and gene sequencing data are missing and thus, more primary data for particular sediment sites are necessary. This includes the development of new methods for the detection of SRP in environmental samples.

The abundance of SRP in marine sediments has been determined by a variety of methods including MPN-cultivation (Knoblauch et al., 1999), 16S rRNA slot-blot hybridization (Sahm et al., 1999), or FISH and CARD-FISH with 16S rRNA gene probes (Ravenschlag et al., 2000; Gittel et al., 2008). Since SRP are phylogenetically diverse (Stahl et al., 2002), 16S rRNA approaches require a comprehensive set of 16S rRNA probes for a full, quantitative coverage of all SRP in an environmental sample (Ravenschlag et al., 2000). The functional gene encoding for dissimilatory sulfite reductase (*dsrA*) of SRP shows a high similarity in different SRP (Wagner et al., 1998), thus a *dsrA* specific PCR primer set targeting both, Gram-positive and Gram-negative SRP species, was developed for competitive PCR quantification (Kondo et al., 2004). These primers were also used to design a quantitative, real-time PCR (Q-PCR) assay for *dsrA* for SRP quantification in subsurface marine sediments (Schippers and Neretin, 2006; Leloup et al., 2007, 2009; Nunoura et al., 2009; Webster et al., 2009; Schippers et al., 2010) and the Black Sea water column (Neretin et al., 2007).

Other Q-PCR assays for *dsrA* based on other primers (Wagner et al., 1998; Dhillon et al., 2003; Geets et al., 2006) were also applied to marine sediments (Wilms et al., 2007; Engelen et al., 2008), oil (Agrawal and Lal, 2009), and wastewater (Ben-Dov et al., 2007). Furthermore, RT-Q-PCR was applied to quantify mRNA of *dsrA* (Neretin et al., 2003).

Due to PCR bias or mismatches of the *dsrA* of not yet discovered SRP with the available *dsrA* primers, important SRP might have been overlooked in environmental samples. This might have happened in studies of deeply buried marine sediments (e.g., Peru continental margin, ODP Leg 201) in which sulfate reduction was identified as an important biogeochemical process, but *dsrA* or 16S rRNA genes of SRP were scarcely detected (D'Hondt et al., 2004; Parkes et al., 2005; Schippers et al., 2005; Inagaki et al., 2006; Schippers and Neretin, 2006; Teske, 2006; Webster et al., 2006, 2009; Fry et al., 2008; Nunoura et al., 2009). For this reason, another independent SRP quantification method is useful to reveal *dsrA* data and to confirm the full quantitative coverage of SRP in environmental sample analyses, especially for the deep biosphere.

A second functional gene of SRP is the adenosine 5′-phosphosulfate reductase gene *aprA*. In sulfate reducers, APS reductase catalyzes the two-electron reduction of APS to sulfite and AMP. APS reductase consists of an alpha and beta subunit, encoded by the genes *aprA* and *aprB*, respectively. The *aprA* gene has been thoroughly studied in SRP, and specific PCR and Q-PCR amplification of *aprA* was shown (Friedrich, 2002; Blazejak et al., 2005; Ben-Dov et al., 2007; Meyer and Kuever, 2007).

The objective of this study was a better understanding of the abundance and diversity of SRP in subsurface marine sediments. A Q-PCR assay specific for *aprA* of SRP was designed and applied to samples from different marine sediments together with the published Q-PCR assay for *dsrA* quantification (Schippers and Neretin, 2006). The diversity of SRP was analyzed based on cloning and sequencing of their functional genes *aprA* and *dsrA*. Marine sediments of the Peru continental margin, including samples from the deep biosphere (ODP site 1227), and the Black Sea were chosen because previous studies indicate that sulfate reduction is an important biogeochemical process in these sediments (Jørgensen et al., 2001; D'Hondt et al., 2004; Schippers et al., 2005). In addition, the abundance of sulfate reducers and other microorganisms was already determined using different assays, allowing comparisons with our newly developed method (Schippers et al., 2005; Inagaki et al., 2006; Schippers and Neretin, 2006; Leloup et al., 2007; Blazejak and Schippers, 2010).

MATERIALS AND METHODS

SAMPLE COLLECTION

Samples were collected from different sediment depths at three marine sites during three research vessel expeditions. Site 1227 (8°59.5′S, 79°57.4′W) at a water depth of 427 m on the Peru margin was sampled with advanced piston coring up to 121 mbsf during Ocean Drilling Program (ODP) Leg 201 in March 2002 (D'Hondt et al., 2003; Jørgensen et al., 2005). Site 2MC (11°35.0′S, 77°33.1′W) at a water depth of 86 m on the Peru continental margin was sampled with a multicorer up to 0.34 mbsf during the cruise SO147 of R/V Sonne in June 2000. Site 20 (43°57.25′N, 35°38.46′E) at a water depth of 2048 m in the Black Sea was sampled with a gravity corer up to 5.8 mbsf during cruise M72-5 of R/V Meteor in May 2007.

Samples for molecular analysis were taken aseptically from the center of the cores at all stations and were stored at −20°C until further processing in the laboratory. For the recovery of deeply buried sediments from site 1227 on the Peru margin seawater based drilling fluid was used. Thus a potential contamination with seawater microorganisms was routinely checked by application of fluorescent beads of prokaryotic cell size and a chemical tracer (D'Hondt et al., 2003). Only uncontaminated samples were used for further analysis.

DNA EXTRACTION

DNA was isolated from 0.5–4 g sediment of various depths using a FastDNA®Spin for Soil Kit (MP Biomedicals, Solon, OH, USA) with the following modification: to increase the yield of isolated DNA from clayish sediments 200 µg polyadenylic acid (Roche Diagnostics GmbH, Mannheim, Germany) dissolved in sterile water was added to the sample at the first step of the extraction procedure (Webster et al., 2003). DNA extracts from blank tubes (no sediment added) were used as procedural contamination control in later PCR analyses. Isolated DNA was stored in aliquots to avoid multiple defrosting and freezing and was thawed for Q-PCR measurements not more than twice.

Q-PCR MEASUREMENTS

Quantitative PCR measurements were run in triplicate on an ABI Prism 7000 detection system (Applied Biosystems, Foster City, CA, USA). Quantification of *Bacteria* in total was performed using a Q-PCR assay based on the detection of the 16S rRNA gene (Nadkarni et al., 2002). The dissimilatory sulfite reductase gene *dsrA* of SRP was quantified using a published protocol (Schippers and Neretin, 2006) and primers (Kondo et al., 2004). The size of the amplified fragments was 219 bp. To quantify the adenosine 5′-phosphosulfate reductase gene *aprA* of SRP, a novel Q-PCR assay was designed. For specific amplification of this gene the primers APS1F (5-TGGCAGATCATGATYMAYGG-3) and APS4R (5-GCGCCAACYGGRCCRTA-3) were used (Blazejak et al., 2005; Meyer and Kuever, 2007). The size of the amplified fragments was 384–396 bp. The Q-PCR assay was performed with Platinum® SYBR® Green Q-PCR SuperMix-UDG with ROX (Invitrogen, Carlsberg, CA, USA), a primer concentration of 300 nM, and the following amplification conditions: 95°C for 10 min and 40 cycles of 95°C for 15 s and 60°C for 1 min. Two microliters sample DNA were added to a PCR reaction assay with a total volume of 25 µL. Melting curve analyses were run after each assay to check PCR specificity. For amplification of standards, DNA was extracted, amplified, and purified from minipreps of cloned *aprA* gene sequences from sulfate-reducing endosymbiotic bacteria with the accession numbers AM234052 and AM234053.

Q-PCR DATA ANALYSIS

Relative standards were prepared by serial dilution (1:10) of the PCR product. For each standard, the concentration was plotted against the cycle number at which the fluorescence signal increased above the background or cycle threshold (C_t value). The

slope of each calibration curve was included into the following equation to determine the efficiency of the PCR reaction: efficiency $= 10^{(-1/\text{slope})} - 1$. According to this formula, an efficiency of 100% means a doubling of the product in each cycle. Data evaluation was performed with the software StepOne™ v2.0 (Applied Biosystems, Foster City, CA, USA).

PCR AMPLIFICATION, CLONING, AND SEQUENCING OF THE *dsrA* AND *aprA* GENES

DNA was isolated from sediment samples of the Peru margin from three depths, 3.6, 65.3, and 121.4 mbsf (site 1227, ODP Leg 201) and in the Black Sea from four depths, 0.15, 2.7, 4.5, and 5.8 mbsf (site 20 GC, M72-5). Except for the number of cycles, amplification of the *dsrA* and *aprA* genes was carried out at the same conditions as for the Q-PCR assays (see above). For amplification of the *dsrA* gene, 30 cycles of PCR were required for the sediment sample from 3.6 mbsf depth of the Peru margin, and 35 cycles for the other samples. To amplify the *aprA* gene, 25 cycles of PCR were applied to the sediment samples from 0.15 and 2.7 mbsf depth in the Black Sea, and up to 35 cycles for the remaining samples. Three parallel PCR products obtained from each depth were combined, purified using a QIAquick PCR purification kit (Qiagen, Hilden, Germany), and subsequently cloned using the pGEM®-T Easy vector system (Promega, Madison, WI, USA) and TOP10 chemically competent cells (Invitrogen, Carlsbad, CA, USA) according to the manufacturer's protocol. Because of the high number of PCR cycles also the yield of the negative controls, although no visible amplification was observed, was purified, and cloned. Clones were randomly picked, suspended in PCR grade water and selected for the correct insert size by PCR with vector primers. Approximately 50 positive clones per depth were sequenced with the vector primer M13 Forward. Sequencing reactions were run using ABI BigDye on an ABI Prism 3100 genetic analyzer (Applied Biosystems, Foster City, CA, USA).

PHYLOGENETIC ANALYSIS

For sequence alignment and phylogenetic tree reconstruction sequences were analyzed with the BioEdit program[1] and the software ARB[2]. Briefly, after removal of the vector sequence, sequences were aligned and clustered. Phylogenetic calculations for the partial *aprA* genes were generated from 128–132 deduced amino acids sequences using maximum-likelihood analyses with a 25% positional conservation filter. For the phylogenetic analysis of the partial *dsrA* sequences first a maximum-likelihood tree was generated from *dsrAB* sequences of full length (approximately 650 amino acids), than successively single partial *dsrA* sequences (73 amino acids) were added to the tree using a 25% positional conservation filter.

NUCLEOTIDE ACCESSION NUMBERS

The *dsrA* and *aprA* gene sequences obtained in this study were submitted to the DDBJ/EMBL/GenBank nucleotide databases under the accession numbers HE575209–HE575212 and HE575674–HE575681 for *aprA* sequences and HE575682–HE575732 for *dsrA* sequences.

[1] www.mbio.ncsu.edu/BioEdit/bioedit.html
[2] www.arb-home.de

RESULTS AND DISCUSSION

In this study the abundance and diversity of the functional genes for adenosine 5′-phosphosulfate reductase (*aprA*) and dissimilatory sulfite reductase (*dsrA*) of SRP were analyzed in marine sediments from the Black Sea, and the Peru continental margin, including deep biosphere sediments (ODP site 1227). For *aprA* quantification a Q-PCR assay was designed. The evaluation results for this assay are followed by data on the abundance and diversity of *aprA* and *dsrA* in sediments. For comparison and interpretation, 16S rRNA gene copy numbers of total bacteria from a previous study (Blazejak and Schippers, 2010) have been included here.

EVALUATION OF THE Q-PCR ASSAY FOR *aprA*

Amplification quantities of the standard ranged from 1.0×10^1 to 1.0×10^7 molecules with a correlation coefficient of 0.996. The efficiency of the PCR reactions was 96%. Detection of contaminant DNA in the negative control was not observed. In our experiments the detection limit was set to 1.0×10^2 molecules. This could be lowered to 1.0×10^1 still ensuring reliable detection values since no contaminant DNA in the negative controls was identified. Detection limits for gene quantification by PCR for functional genes can range up to 10 copies per reaction (Vaerman et al., 2004; Bustin et al., 2009). However one critical limitation of PCR-based methods is their sensitivity to compounds that are co-extracted with the DNA from environmental samples, in particular from sediments and soils, that may influence and inhibit the real-time PCR-process. For example humic acids can hamper the PCR reaction and impair fluorescence, and metal ions can inhibit DNA polymerases (Lindberg et al., 2007) whereby the detection limit is lowered. The maximum fluorescence signal of the melting curve occurred at a temperature of 87°C. Melting curves were analyzed after each assay and always showed a single peak, verifying the specificity of the PCR amplification.

QUANTIFICATION OF THE FUNCTIONAL GENES *aprA* AND *dsrA* OF SRP AND 16S rRNA OF TOTAL BACTERIA IN MARINE SEDIMENT SAMPLES

Depth profiles of DNA copy numbers of the functional genes *aprA* and *dsrA* as marker for sulfate-reducing prokaryotes (SRP) and the 16S rRNA gene of total *Bacteria* are shown in **Figure 1** for three sediment sites, surface (site 2MC, 0–0.35 mbsf) and deep (site 1227, 0–121.4 mbsf) sediments on the Peru margin, and in the Black Sea (site 20, 0–5.8 mbsf). The copy numbers of all genes decreased with sediment depth in different depth gradients. An important finding of this study was that the depth profiles of copy numbers of both functional genes, *aprA* and *dsrA*, were almost equal for all sediment sites expect for the ODP site 1227 below 40 mbsf. Congruent SRP quantification profiles based on independent Q-PCR analysis of two functional genes imply that no SRP have been overlooked, and that the results are close to the actual SRP gene density in the subsurface. Two independent Q-PCR assays with different primers are very unlikely to generate identical PCR biases and quantification profiles by chance.

In the Black Sea at site 20, all gene copy numbers decreased rapidly within 65 cm from the sediment surface. The *dsrA* and *aprA* copy numbers decreased from 10^7–10^8 copies/g at the sediment surface to less than 10^5 copies/g below 0.6 mbsf. They decreased

further to less than 10^4 copies/g below 3 mbsf. The *dsrA* copy numbers close to the sediment surface were similar to those for another sediment site of the Black Sea (Leloup et al., 2007). Downcore, the numbers in our study decreased toward lower counts than those in the previous study. Similar differences between these two sites were also found for the 16S rRNA gene copy numbers of total *Bacteria*. While site 20 was located in the central basin of the Black Sea southeast of the peninsula Crimea at 2048 m water depth, the site of the previous study was located west of the peninsula Crimea on the slope at 1024 m water depth. Thus, different organic matter availability may explain the different gene copy numbers in the two studies.

In the Peru continental margin near-surface sediments (site 2MC) the *dsrA* and *aprA* copy numbers were very close to each other and exhibited a more pronounced depth gradient than the 16S rRNA gene copy numbers of total *Bacteria* (**Figure 1**). The *dsrA* and *aprA* copy numbers decreased from more than 10^8 copies/g at the sediment surface to 10^6–10^7 copies/g between 0.18 and 0.34 mbsf. In a previous Q-PCR study of the same site (Schippers and Neretin, 2006), the *dsrA* and 16S rRNA gene copy numbers of total *Bacteria* copy numbers were similar to those of this new study.

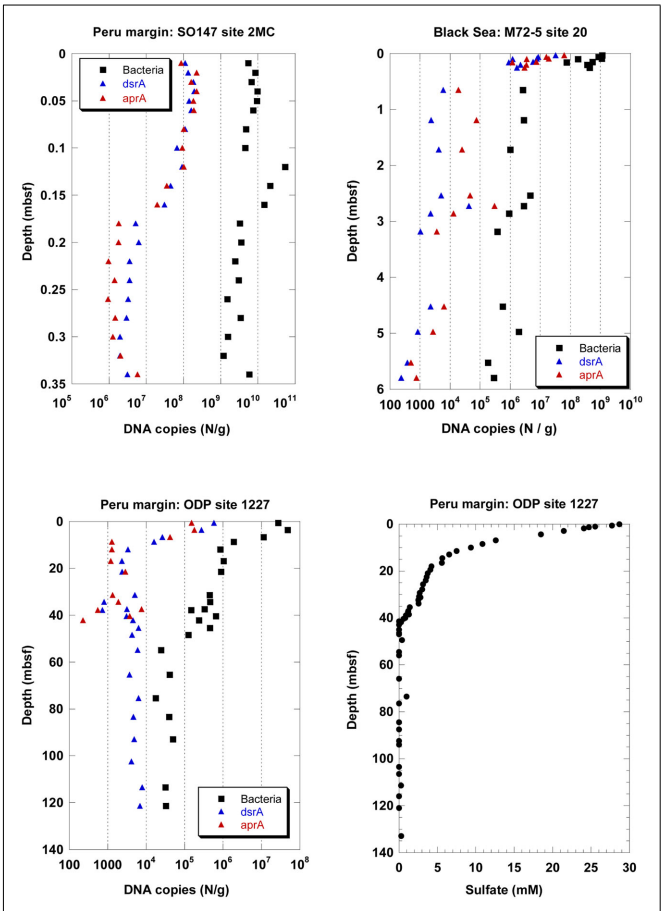

FIGURE 1 | Depth profiles of DNA copy numbers of the functional genes *aprA* and *dsrA* as marker for sulfate-reducing prokaryotes (SRP) and the 16S rRNA gene of total *Bacteria* at three sediment sites, surface (site 2MC, 0–0.35 mbsf) and deep (site 1227, 0–121.4 mbsf) sediments on the Peru margin, and in the Black Sea (site 20, 0–5.8 mbsf), and depth profile of pore water sulfate concentrations at site 1227 (0–135 mbsf, D'Hondt et al., 2004) on the Peru margin. ■, *Bacteria*; ▲, *dsrA*; ▲, *aprA*.

In the deeply buried Peru margin sediment (site 1227) the *dsrA* and *aprA* copy numbers decreased from 10^5–10^6/g sediment at the top of the core at 0.6 mbsf to less than 10^4/g sediment at 10 mbsf. These numbers for both genes stay steady up to 35 mbsf. Below 35 mbsf the run of the curves are different. After a slight increase of the *aprA* gene copy numbers between 37–40 mbsf they drop to less than 10^3/g sediment at 42 mbsf and are not more detectable underneath this depth. In contrast, *dsrA* copy numbers below 10^4 copies/g sediment are still observed up to the depth of 121 mbsf. For all samples between 10–121 mbsf, *dsrA* copy numbers remained consistent in this range. In contrast, *dsrA* was only patchily detected (5 out of 19 samples) in the previous study (Schippers and Neretin, 2006). The *dsrA* values in the deeper sediment are close to the detection limit of the Q-PCR method. Thus, slight differences in the efficiency of DNA extraction from the sediment or differences in the total amount of sediment used for DNA extraction may explain this discrepancy.

The 16S rRNA gene copy numbers of total *Bacteria* exceeded those of the functional genes at all sediment depths, and allowed to calculate the proportion of SRP to total *Bacteria*. The *aprA* and *dsrA* copy numbers comprised in average 0.5–1% of the 16S rRNA gene copy numbers of total *Bacteria* in the sediments of the Black Sea and those from the Peru continental margin up to a depth of ca. 40 mbsf. Below, only *dsrA* (but not *aprA*) was detected with copy numbers of less than 10^4/g sediment, comprising ca. 14% of the 16S rRNA gene copy numbers of total *Bacteria*. In other marine sediments sulfate reducers contributed to <1–30% to the prokaryotic community based on Q-PCR, FISH, or rRNA slot blot hybridization analyses (Sahm et al., 1999; Ravenschlag et al., 2000; Knittel et al., 2003; Schippers and Neretin, 2006; Leloup et al., 2007, 2009; Wilms et al., 2007; Gittel et al., 2008; Julies et al., 2010; Schippers et al., 2010). Overall our Q-PCR analysis of the functional genes revealed that SRP are a minor part of the prokaryotic community in the Peru margin sediments, in agreement with clone library data (Parkes et al., 2005; Inagaki et al., 2006; Webster et al., 2006). Based on Q-PCR analysis of the same sediment samples especially the bacterial groups *Chloroflexi* and/or candidate division JS-1 were shown to be dominant (Blazejak and Schippers, 2010), while *Archaea*, *Eukarya*, and the Fe(III)- and Mn(IV)-reducing bacteria of the family *Geobacteraceae* (Inagaki et al., 2006; Schippers and Neretin, 2006) were of minor abundance.

Active sulfate reduction for the two Peru margin sites up to a depth of ca. 40 mbsf was confirmed by pore water sulfate profiles and sulfate reduction rate measurements (Böning et al., 2004; D'Hondt et al., 2004; Schippers et al., 2005). At ca. 40 mbsf sulfate is reduced by methane oxidation (sulfate–methane transition zone) and a slight maximum of 16S rRNA genes was detected (Schippers et al., 2005; Schippers and Neretin, 2006; Sørensen and Teske, 2006; Teske and Sørensen, 2008). This maximum is not reflected by higher copy numbers of the functional genes *dsrA* or *aprA* of SRP indicating that sulfate-dependent anaerobic methane oxidation is not linked to a SRP population peak.

The detection of *dsrA* of SRP below ca. 40 mbsf was surprising because sulfate as the electron acceptor for active SRP was not detectable in the pore water from ca. 40–121 mbsf of site 1227 (**Figure 1**). There are three possibilities to explain this finding: 1. The detected *dsrA* was not extracted from living cells but is part of fossil DNA, persisting adsorbed to sediment particles over geological time scales as previously discussed (Inagaki et al., 2005; Schippers and Neretin, 2006; Schippers et al., 2010); 2. The *dsrA* originated from living SRP which use another electron acceptor than sulfate, e.g., Fe(III) as shown for several genera of SRP (Vandieken et al., 2006); 3. Low amounts of sulfate might be provided by anoxic oxidation of sulfides. The sulfate formed by this process is constantly consumed by SRP, thus it remained undetectable in the pore water.

We believe that the third possibility is most relevant. On the one hand very low rates of sulfate reduction have been measured with sulfate radiotracer for site 1227 even below 40 mbsf (Schippers et al., 2005). On the other hand, stable isotope data of oxygen and sulfate for sediment and experimental studies support a deep anoxic sulfur cycle. Sulfide oxidation occurs with reactive iron or manganese oxides as oxidant in deeply buried sediments (Bottrell et al., 2000, 2008; Schippers and Jørgensen, 2001; Riedinger et al., 2010; Holmkvist et al., 2011a,b).

DIVERSITY OF THE FUNCTIONAL GENES *aprA* AND *dsrA* IN SEDIMENT SAMPLES

To analyze not only the abundance but also the diversity of SRP, their metabolic key genes, *aprA* and *dsrA* genes, were cloned. Sediment samples of three depths at the Peru margin (site 1227), 3.6, 65.3, and 121.4 mbsf, and four depths in the Black Sea (site 20), 0.15, 2.7, 4.5, and 5.8 mbsf were selected for the study. Sequence analysis of the isolated *aprA* and *dsrA* sequences showed their relationship to *aprA* or *dsrA* genes from characterized SRP indicating that they also originate from SRP. Although high numbers of PCR cycles were required (up to 35 cycles for *dsrA* amplification), no visible amplification was observed in the negative controls. Sequences of a few clones obtained from the negative controls showed that only primer sequences were inserted into the cloning vectors. Thus, despite the high PCR cycle number no contamination was noted.

For *aprA* analysis, 50 clones from a Peru margin sediment at 3.6 mbsf, and 24–45 clones from each Black Sea sediment depth were sequenced. Sequences were grouped into distinct clone families based on their sequence similarities and their allocation within the phylogenetic tree after algorithmic calculations. Sequence similarities within a clone family as well as the similarity to the next relative sequence of a cultivated bacterium are shown in **Table 1**. For phylogenetic tree reconstruction all sequences were used; however only one representative sequence of each clone family is presented (**Figure 2**).

The *aprA* sequences isolated from 3.6 mbsf depth on the Peru margin were classified into four distinct clone families showing a close relationship to the sulfate-reducing bacteria (SRB) *Desulfococcus multivorans*, *Desulfomonile tiedjei*, *Desulfovibrio baarsii*, and a cluster including the genera *Desulfacinum*, *Desulforhabdus,* and *Syntrophobacter* (**Figure 2**; **Table 1**). In deeper sediment layers, at 65.3 and 121.4 mbsf, the *aprA* gene was not amplified although a high number of cycles (up to 35) was applied. This result corresponds to the absence of quantitative data of the *aprA* using the newly designed Q-PCR assay (**Figure 1**).

In the Black Sea sediment a slight decline of diversity with depth could be observed. Near-surface (0.15 mbsf) *aprA* sequences were assigned into four distinct clone families: *D. multivorans*, *D. tiedjei*, *Desulfobacterium anilini,* and a cluster including the genera *Desulfacinum*, *Desulforhabdus,* and *Syntrophobacter*. In contrast, sequences from 2.7 and 5.8 mbsf formed only two clone groups each, related to *Desulfonema magnum* and *Desulfobulbus elongatus,* and *Desulfomonile tiedjei* and *Desulfobacterium anilini,* respectively (**Figure 2**; **Table 1**).

Almost all isolated *aprA* sequences showed a close relationship to *aprA* sequences of cultivated, well characterized SRB of the *Deltaproteobacteria* indicating that they also originate from bacteria with a same metabolism. For two sequences (accession

Table 1 | Gene *aprA* clone library data for three sediment samples of the Peru margin and the Black Sea each.

Sampling site	No. of clones analyzed	Sequences classified as relatives to:						
		Desulfonema magnum	***Desulfococcus multivorans***	***Desulfobulbus elongatus***	***Desulfomonile tiedjei***	***Desulfovibrio baarsii***	***Desulfobacterium anilini***	***Desulfacinum, Desulforhabdus, Syntrophobacter***
		No. of clones (%)/sequence similarity within the group in %/sequence similarity to the next relative in %						
PERU MARGIN (SITE 1227)								
3.6 mbsf	50		22 (44)/100/90		5 (10)/81/74–77	6 (12)/100/85		17 (34)/100/66–69
65.3 mbsf	0							
121.4 mbsf	0							
BLACK SEA (SITE 20)								
0.15 mbsf	31		2 (6)/100/90		20 (65)/72–90/75–84		4 (13)/78/79–81	5 (16)/87/68–72
2.7 mbsf	45	1 (2)/100/91		44 (98)/97/87				
5.8 mbsf	24				20 (83)/98/83		4 (17)/83/81–84	

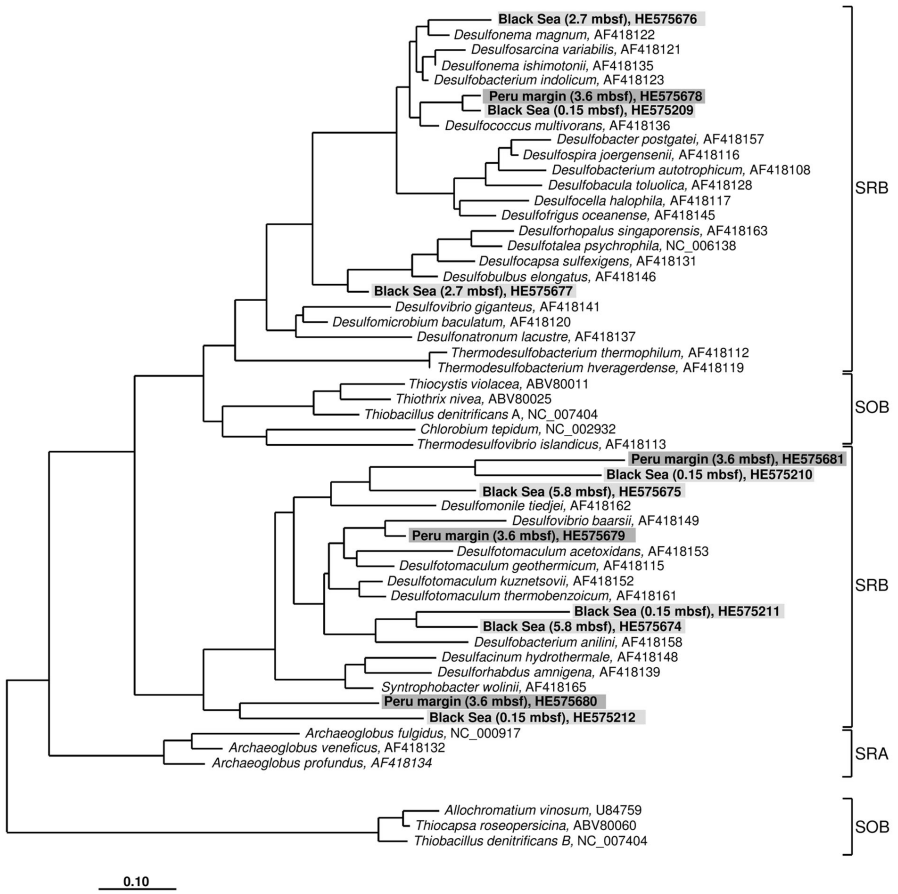

FIGURE 2 | Gene *aprA* phylogeny based on deduced amino acid sequences of the *aprA* gene coding for the alpha subunit of the adenosine 5′-phosphosulfate reductase. Sequences from this study are highlighted in light gray (Black Sea sediments) and dark gray (Peru margin sediments). Scale bar = 0.10 estimated substitutions per site. SOB, sulfide-oxidizing bacteria; SRB, sulfate-reducing bacteria; SRA, sulfate-reducing archaea.

numbers HE575680 and HE575212), their relationship to known organisms is difficult to predict because they form a separate branch and are only distantly related to *aprA* sequences of characterized SRB of the *Deltaproteobacteria* and Gram-positive SRB of the genus *Desulfotomaculum* (**Figure 2**; **Table 1**).

The *dsrA* sequences could be amplified from sediment samples of all analyzed depths from the Peru margin and the Black Sea (**Table 2**). Up to 51 clone sequences per depth were included in the phylogenetic analysis. Because of the high PCR cycle number of up to 35 cycles, the negative controls was also cloned although no PCR bands were observed. Sequences obtained from these negative controls showed that only primer sequences were inserted into the cloning vector, thus despite the high PCR cycle number no contamination was found. Phylogenetic analysis showed that all isolated *dsrA* sequences were closely related to the metabolic gene *dsrA*. The *dsrA* sequences isolated from the Peru margin and the Black Sea sediments were classified into eight clone families, showing overall a higher diversity than the isolated *aprA* sequences. Sequence similarities within a clone family as well as the similarity to the next relative sequence of cultivated prokaryote are shown in **Table 2**. For phylogenetic tree reconstruction all sequences were used however only one representative sequence of each clone family is presented in **Figure 3**. Except for three clone families, sequences belonging to all other groups are closely related to *dsrA* sequences isolated from SRP of *Deltaproteobacteria* showing for some sequences habitat specificity. For example: *dsrA* sequences related to *Desulfovibrio acrylicus*, *Desulfohalobium utahense*, and to the genera *Desulfobulbus*, *Desulfacinum*, and *Syntrophobacter* were only found in sediments from the Peru margin, whereas sequences related to the genus *Desulfomicrobium* and to *Desulfoarculus baarsii* were found exclusively in sediments from the Black Sea. A comparatively high proportion of *dsrA* sequences (20%) related to *D. acrylicus* were found in Peru margin deeply buried sediments at 121 mbsf. A specific feature of this anoxic, sulfate-reducing bacterium is the ability to switch from sulfate to acrylate reduction once this is energetically more favorable (van der Maarel et al., 1996). In contrast to *dsrA* sequences showing habitat specificity, sequences related to *Desulfococcus oleovorans*, *Desulfobacterium autotrophicum*, and *Desulfotalea psychrophila* were detected in sediments at both sites. Members of the genera *Desulfococcus* and *Desulfobacterium* belong

Table 2 | Gene *dsrA* clone library data for three sediment samples of the Peru margin and four sediment samples of the Black Sea.

Sampling site	No. of clones analyzed	Sequences classified as relatives to:						
		Desulfovibrio acrylicus	***Desulfo-microbium***	***Desulfohalo-bium utahense***	***Desufococcus oleovorans***	***Desulfobacterium autotrophicum***	***Desulfo-bulbus***	***Desulfotalea psychrophila***
		No. of clones (%)/sequence similarity within the group in %/sequence similarity to the next relative in %						
PERU MARGIN								
3.6 mbsf	32			1 (3)/100/87	5 (16)/100/77			1 (3)/100/76
65.3 mbsf	24				2 (8)/100/84	2 (8)/100/99		
121.4 mbsf	50	10 (20)/100/99		2 (4)/100/84		18 (36)/100/99	1 (2)/100/87	
BLACK SEA								
0.15 mbsf	31		1 (3)/100/84–87		15 (48)/78–96/84–85			
2.7 mbsf	51							51 (100)/100/69
4.5 mbsf	18				13 (72)/100/81	1 (6)/100/100		
5.8 mbsf	23		1 (4)/100/82		2 (9)/100/86	4 (18)/97/97–100		

Sampling site	***Desulfacinum/ Syntrophobacter***	***Desulfoarculus baarsii***	***Archaeoglobus fulgidus***	**Cluster A (see Fig. 3)**	**Cluster B (see Fig. 3)**
	No. of clones (%)/sequence similarity within the group in %/sequence similarity to the next relative in %				
PERU MARGIN					
3.6 mbsf	6 (19)/100/79				19 (59)/74–76
65.3 mbsf	2 (8)/100/79–80				18 (75)/71–87
121.4 mbsf	1 (2)/100/82–83				18 (36)/74–93
BLACK SEA					
0.15 mbsf		2 (7)/100/72	2 (7)/100/71	5 (16)/91	6 (19)/79
2.7 mbsf					
4.5 mbsf					4 (22)/68–70
5.8 mbsf		1 (4)/100/91		1 (4)/100	14 (61)/72–78

to the family of *Desulfobacteraceae* that are known to be able to oxidize a great variety of different electron donors completely to CO_2. Thus, they successfully inhabit anoxic marine environments such as Black Sea and Peru margin sediments (Ravenschlag et al., 2000; Liu et al., 2003; Mußmann et al., 2005; Kondo et al., 2007; Leloup et al., 2007, 2009) or the anoxic water column of the Black Sea (Vetriani et al., 2003; Neretin et al., 2007) and other marine habitats (Kondo et al., 2007). Besides *dsrA* sequences affiliated to *Desulfobacteraceae*, also numerous *aprA* sequences belonging to this family were detected in samples from the Black Sea and Peru margin sediments indicating that bacteria of this community play an important role in sulfate reduction in these sediments.

Only two *dsrA* sequences, isolated from sediment of the Black Sea, showed a distant relationship (71% amino acid similarity) to the sulfate-reducing archaeon (SRA) *Archaeoglobus fulgidus*. Primarily SRA of the genus *Archaeoglobus* were isolated from marine hydrothermal systems, North Sea oil fields, and from petroleum hydrocarbon-rich Guaymas Basin sediments off the coast of Mexico (Hartzell and Reed, 2006). A few *dsrA* sequences, allocated within the same cluster, could be isolated from other habitats as from the Nankai Trough deep-sea and Black Sea sediments (Kaneko et al., 2007; Leloup et al., 2007), and showed however also only a distant relationship to *dsrA* sequences of the genus *Archaeoglobus*. Because of this distant relationship and the fact that Black Sea sediments are not a typical habitat for SRA, the affiliation of these sequences to the genus *Archaeoglobus* is questionable. SRA may play only a minor role in these sediments because of the low numbers of detected *dsrA* sequences, and the lack of *aprA* clones related to SRA.

The affiliation of *dsrA* sequences of two clone families, named cluster A and B, could not be clearly identified. Sequences within the cluster A form a clearly separated branch based on their unique sequence signature and showed only distant similarities to *aprA* of *A. fulgidus* (70–71% amino acid similarity). The cluster B was generated by 24 different *dsrA* sequences isolated from sediments of both habitats from each depth. Within this cluster numerous *dsrA* clone sequences isolated from different marine sediments as from deep-sea sediments from the Nankai Trough (Kaneko et al., 2007) and the Guaymas Basin (Dhillon et al., 2003), but also from salt marsh sediments (Bahr et al., 2005), and fen soil (Loy et al., 2004) are represented (data not showed). The closest described relatives based on amino acid similarity searches are *dsrA* sequences from the archaeon *A. fulgidus* (65–76% amino acid sequence similarity), the SRB of the genus *Thermodesulfovibrio* of the class *Nitrospira* (63–76% amino acid sequence similarity), and gram-positive SRB of the genus *Desulfotomaculum* (61–73%

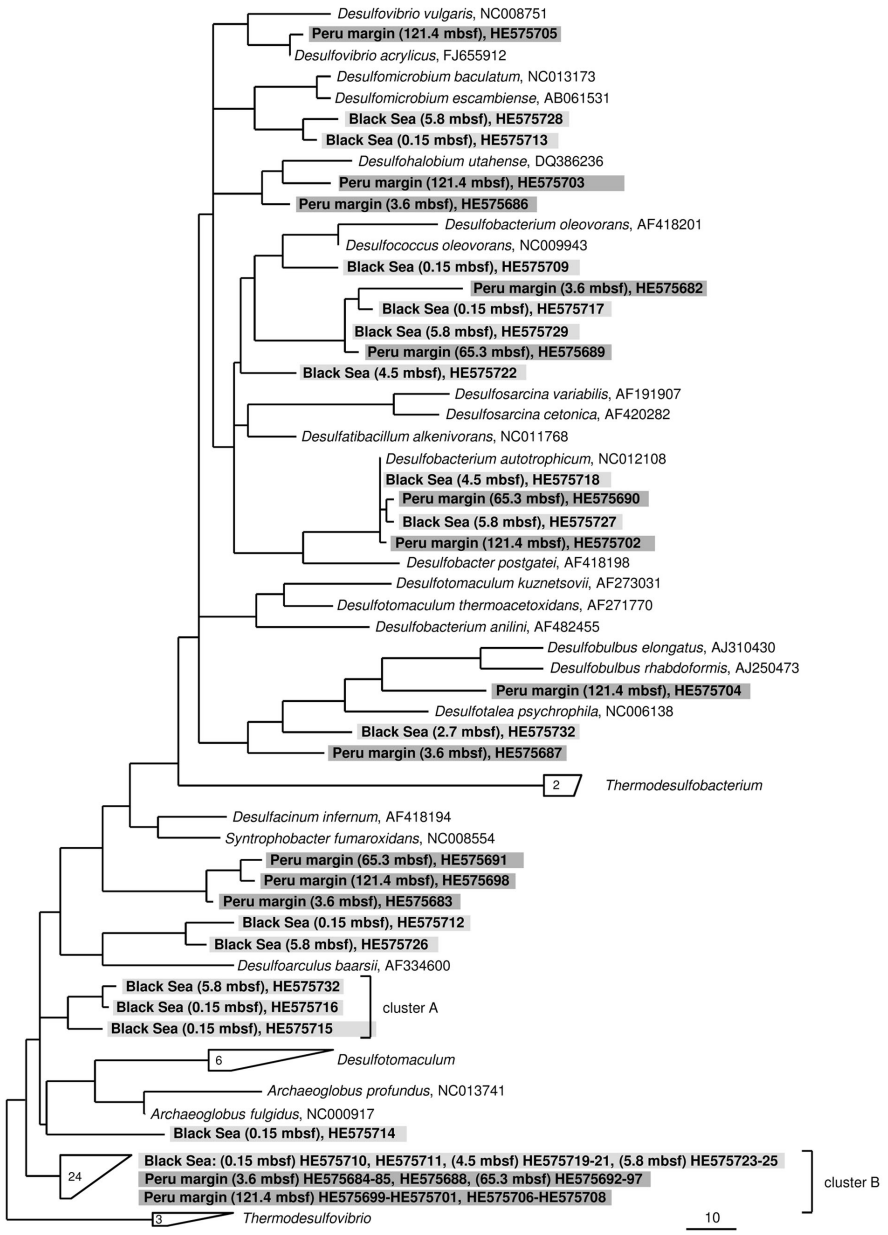

FIGURE 3 | Gene *dsrA* phylogeny based on deduced amino acid sequences of the *dsrA* gene coding for the alpha subunit of dissimilatory (bi)sulfite reductase. Sequences from this study are highlighted in light gray (Black Sea sediments) and dark gray (Peru margin sediments). Scale bar = 0.10 estimated substitutions per site.

amino acid sequence similarity). Because of the distant relationship to *dsrA* sequences from characterized microorganisms, the conclusion about the affiliation of the *dsrA* sequences of the cluster B to either SRA or SRB remains speculative. The common distribution of these *dsrA* sequences along the depth profiles of the two habitats and their high proportion within the clone libraries, up to 75%, argue for a significant role in sulfate/sulfite reduction of these microorganisms in marine sediments. They seem to be generalists and can adapt to a wide range of sulfate concentrations and electron donors, and it is tempting to suppose that they are a dominant group within the community of sulfate reducers in the anoxic sediments from the Black Sea and the Peru margin. Another unlike possibility could be that these *dsrA* sequences originate from microorganisms, which still contain this gene but have lost their ancestral ability of dissimilatory sulfate/sulfite reduction as shown for some members of *Desulfotomaculum* subcluster Ih (Imachi et al., 2006). This scenario would explain the unsuccessful cultivation of sulfate reducers related to the cluster B so far, because of incorrect selection of electron acceptors.

In summary of the *dsrA* diversity study, it can be concluded that this metabolic gene for the sulfate/sulfite reduction could

be detected in all analyzed sediment layers demonstrating a high diversity. Even in deeply buried sediments from the Peru margin in depths of 65 and 121 mbsf *dsrA* sequences were identified. Surprisingly, also in such an extreme habitat these sequences showed a high diversity belonging to well characterized genera as *Desulfobacterium* and *Desulfococcus* of the family *Desulfobacteraceae*, and *Desulfovibrio*, but also to novel deep-branching clusters A and B which phylogenetic affiliation and thus metabolism remain hidden. The presence of *aprA* and *dsrA* sequences affiliated to the same phylogenetic clusters, for example genera of the family *Desulfobacteraceae* or the genera *Syntrophobacter* and *Desulfacinum*, showed that sulfate reducers of equal phylogenesis were detected. This is particularly demonstrative for *aprA* and *dsrA* clone libraries from the Black Sea sediment of 2.7 mbsf depth showing that almost all *aprA* sequences (98%) and all *dsrA* sequences (100%) are affiliated either to *D. elongatus* or to *D. psychrophila*, respectively. The *aprA* and *dsrA* phylogeny of these two SRP of the family *Desulfobulbaceae* showed a close relationship to each other indicating that *aprA* and *dsrA* sequences detected in the Black Sea sediments could originate from the same bacterium.

Conclusively, although SRP do not belong to the most abundant prokaryotic groups, this study shows that they represent an inherent, diverse part of the microbial community in Black Sea sediments and the deep biosphere of Peru margin.

ACKNOWLEDGMENTS

We thank the ODP Leg 201, RV Meteor M72-5 personnel, and especially Gerrit Köweker for sediment sampling. Special thanks to Rudolf Amann for providing laboratory space at MPI Bremen for cloning. This research used samples and data provided by the ODP which is sponsored by the US National Science Foundation (NSF) and participating countries under management of Joint Oceanographic Institutions (JOI), Inc. This work was supported by the German Research Foundation (DFG) priority program IODP/ODP grant SCHI 535/5 to Axel Schippers.

REFERENCES

Agrawal, A., and Lal, B. (2009). Rapid detection and quantification of bisulfite reductase genes in oil field samples using real-time PCR. *FEMS Microbiol. Ecol.* 69, 301–312.

Bahr, M., Crump, B. C., Klepac-Ceraj, V., Teske, A., Sogin, M. L., and Hobbie, J. E. (2005). Molecular characterization of sulfate-reducing bacteria in a New England salt marsh. *Environ. Microbiol.* 7, 1175–1185.

Ben-Dov, E., Brenner, A., and Kushmaro, A. (2007). Quantification of sulfate-reducing bacteria in industrial wastewater, by real-time polymerase chain reaction (PCR) using dsrA and apsA genes. *Microbiol. Ecol.* 54, 439–451.

Blazejak, A., Erseus, C., Amann, R., and Dubilier, N. (2005). Coexistence of bacterial sulfide oxidizers, sulfate reducers, and spirochetes in a gutless worm (Oligochaeta) from the Peru margin. *Appl. Environ. Microbiol.* 71, 1553–1561.

Blazejak, A., and Schippers, A. (2010). High abundance of JS-1- and *Chloroflexi*-related *Bacteria* in deeply buried marine sediments revealed by quantitative, real-time PCR. *FEMS Microbiol. Ecol.* 72, 198–207.

Böning, P., Brumsack, H.-J., Böttcher, M. E., Schnetger, B., Kriete, C., Kallmeyer, J., and Borchers, S. L. (2004). Geochemistry of Peruvian near-surface sediments. *Geochim Cosmochim Acta* 68, 4429–4451.

Bottrell, S. H., Böttcher, M. E., Schippers, A., Parkes, R. J., Jørgensen, B. B, Raiswell, R., Telling, J., and Gehre, M. (2008). Abiotic sulfide oxidation via manganese fuels the deep biosphere. Goldschmidt Conference Abstracts. *Geochim. Cosmochim. Acta* 72(Suppl. 1), A102.

Bottrell, S. H., Parkes, R. J., Cragg, B. A., and Raiswell, R. (2000). Isotopic evidence for anoxic pyrite oxidation and stimulation of bacterial sulphate reduction in marine sediments. *J. Geol. Soc. London* 157, 711–714.

Bustin, S. A., Benes, V., Garson, J. A., Hellemans, J., Huggett, J., Kubista, M., Mueller, R., Nolan, T., Pfaffl, M. W., Shipley, G. L., Vandesompele, J., and Wittwer, C. T. (2009). The MIQE guidelines: minimum information for publication of quantitative real-time PCR experiments. *Clin. Chem.* 55, 611–622.

Castresana, J., and Moreira, D. (1999). Respiratory chains in the last common ancestor of living organisms. *J. Mol. Evol.* 49, 453–460.

Dhillon, A., Teske, A., Dillon, J., Stahl, D. A., and Sogin, M. L. (2003). Molecular characterization of sulfate-reducing bacteria in the Guaymas Basin. *Appl. Environ. Microbiol.* 69, 2765–2772.

D'Hondt, S. L., Jørgensen, B. B., Miller, D. J., Batzke, A., Blake, R., Cragg, B. A., Cypionka, H., Dickens, G. R., Ferdelman, T. G., Hinrichs, K. U., Holm, N. G., Mitterer, R., Spivack, A., Wang, G., Bekins, B., Engelen, B., Ford, K., Gettemy, G., Rutherford, S. D., Sass, H., Skilbeck, C. G., Aiello, I. W., Guèrin, G., House, C. H., Inagaki, F., Meister, P., Naehr, T., Niitsuma, S., Parkes, R. J., Schippers, A., Smith, D. C., Teske, A., Wiegel, J., Padilla, C. N., and Solis Acosta, J. L. (2004). Distributions of microbial activities in deep subseafloor sediments. *Science* 306, 2216–2221.

D'Hondt, S. L., Jørgensen, B, B., Miller, D. J., and Shipboard Scientific Party. (2003). Leg 201 Initial report – controls on microbial communities in deeply buried sediments, Eastern Equatorial Pacific and Peru margin. *Proc. ODP, Init. Repts.,* 201: College Station, TX (Ocean 131 Drilling Program). doi: 10.2973/odp.proc.ir.201.2003.

Engelen, B., Ziegelmüller, K., Wolf, L., Köpke, B., Gittel, A., Cypionka, H., Treude, T., Nakagawa, S., Inagaki, F., Lever, M. A., and Steinsbu, B. O. (2008). Fluids from the oceanic crust support microbial activities within the deep biosphere. *Geomicrobiol. J.* 25, 56–66.

Ferdelman, T. G., Lee, C., Pantoja, S., Harder, J., Bebout, B. M., and Fossing, H. (1997). Sulfate reduction and methanogenesis in a Thioploca-dominated sediment off the coast of Chile. *Geochim. Cosmochim. Acta* 61, 3065–3079.

Friedrich, M. W. (2002). Phylogenetic analysis reveals multiple lateral transfers of adenosine-5′-phosphosulfate reductase genes among sulfate-reducing microorganisms. *J. Bacteriol.* 184, 278–289.

Fry, J. C., Parkes, J. R., Cragg, B. A., Weightman, A. J., and Webster, G. (2008). Prokaryotic biodiversity and activity in the deep subseafloor biosphere. *FEMS Microbiol. Ecol.* 66, 181–196.

Geets, J., Borremans, B., Diels, L., Springael, D., Vangronsveld, J., van der Lelie, D., and Vanbroekhoven, K. (2006). DsrB gene-based DGGE for community and diversity surveys of sulfate-reducing bacteria. *J. Microbiol. Methods* 66, 194–205.

Gittel, A., Mußmann, M., Sass, H., Cypionka, H., and Könneke, M. (2008). Identity and abundance of active sulfate-reducing bacteria in deep tidal flat sediments determined by directed cultivation and CARD-FISH analysis. *Environ. Microbiol.* 10, 2645–2658.

Hartzell, P., and Reed, D. W. (2006). The genus *Archaeoglobus*. *Prokaryotes* 3, 82–100.

Holmkvist, L., Kamyshny, A. Jr., Vogt, C., Vamvakopoulos, K., Ferdelman, T. G., and Jørgensen, B. B. (2011a). Sulfate reduction below the sulfate–methane transition in Black Sea sediments. *Deep Sea Res. Part I Oceanogr. Res. Pap.* 58, 493–504.

Holmkvist, L., Ferdelman, T. G., and Jørgensen, B. B. (2011b). A cryptic sulfur cycle driven by iron in the methane zone of marine sediment (Aarhus Bay, Denmark). *Geochim. Cosmochim. Acta* 75, 3581–3599.

Imachi, H., Sekiguchi, Y., Kamagata, Y., Loy, A., Qiu, Y. L., Hugenholtz, P., Kimura, N., Wagner, M., Ohashi, A., and Harada, H. (2006). Non-sulfate-reducing, syntrophic bacteria affiliated with *Desulfotomaculum* cluster I are widely distributed in methanogenic environments. *Appl. Environ. Microbiol.* 72, 2080–2091.

Inagaki, F., Nunoura, T., Nakagawa, S., Teske, A., Lever, M., Lauer, A., Suzuki, M., Takai, K., Delwiche, M., Colwell, F. S., Nealson, K. H., Horikoshi, K., D'Hondt, S., and Jørgensen, B. B. (2006). Biogeographical distribution and diversity of microbes in methane hydrate-bearing deep marine sediments on the Pacific ocean margin. *Proc. Natl. Acad. Sci. U.S.A.* 103, 2815–2820.

Inagaki, F., Okada, H., Tsapin, A. I., and Nealson, K. H. (2005). The paleome: a sedimentary genetic record of past microbial communities. *Astrobiology* 5, 141–153.

Jørgensen, B. B. (1982). Mineralization of organic matter in the sea bed; the role of sulphate reduction. *Nature* 296, 643–645.

Jørgensen, B. B., D'Hondt, S., and Miller, D. J. (eds). (2005). *Proc. ODP, Sci. Results, 201*. Available at: http://www-odp.tamu.edu/publications/201_SR/synth/synth.htm

Jørgensen, B. B., Weber, A., and Zopfi, J. (2001). Sulfate reduction and anaerobic methane oxidation in Black Sea sediments. *Deep Sea Res. Part 1 Oceanogr. Res. Pap.* 48, 2097–2120.

Julies, E. M., Fuchs, B. M., Arnosti, C., and Brüchert, V. (2010). Organic carbon degradation in anoxic organic-rich shelf sediments: biogeochemical rates and microbial abundance. *Geomicrobiol. J.* 27, 303–314.

Kaneko, R., Hayashi, T., Tanahashi, M., and Naganuma, T. (2007). Phylogenetic diversity and distribution of dissimila- tory sulfite reductase genes from deep-sea sediment cores. *Mar. Biotechnol.* 9, 429–436.

Knittel, K., Boetius, A., Eilers, H., Lochte, K., Pfannkuche, O., Linke, P., and Amann, R. (2003). Activity, distribution, and diversity of sulfate reducers and other bacteria in sediments above gas hydrate (Cascadia margin, Oregon). *Geomicrobiol. J.* 20, 269–294.

Knoblauch, C., Jørgensen, B. B., and Harder, J. (1999). Community size and metabolic rates of psychrophilic sulfate-reducing bacteria in Arctic marine sediments. *Appl. Environ. Microbiol.* 65, 4230–4233.

Kondo, R., Purdy, K. J., Silva, S. Q., and Nedwell, D. B. (2007). Spatial dynamics of sulphate-reducing bacterial compositions in sediment along a salinity gradient in a UK estuary. *Microbes Environ.* 22, 11–19.

Kondo, R., Shigematsu, K., and Butani, J. (2004). Rapid enumeration of sulphate-reducing bacteria from aquatic environments using real-time PCR. *Plankton Benthos Res.* 3, 180–183.

Leloup, J., Fossing, H., Kohls, K., Holmkvist, L., Borowski, C., and Jørgensen, B. B. (2009). Sulfate-reducing bacteria in marine sediment (Aarhus Bay, Denmark): abundance and diversity related to geochemical zonation. *Environ. Microbiol.* 11, 1278–1291.

Leloup, J., Loy, A., Knab, N. J., Borowski, C., Wagner, M., and Jorgensen, B. B. (2007). Diversity and abundance of sulfate-reducing microorganisms in the sulfate and methane zones of a marine sediment, Black Sea. *Environ. Microbiol.* 9, 131–142.

Lindberg, E., Albrechtsen, H. J., and Jacobsen, C. S. (2007). Inhibition of real-time PCR in DNA extracts from aquifer sediment. *Geomicrobiol. J.* 24, 343–352.

Liu, X., Bagwell, C. E., Wu, L., Devol, A. H., and Zhou, J. (2003). Molecular diversity of sulfate-reducing bacteria from two different continental margin habitats. *Appl. Environ. Microbiol.* 69, 6073–6081.

Loy, A., Kusel, K., Lehner, A., Drake, H. L., and Wagner, M. (2004). Microarray and functional gene analyses of sulfate-reducing prokaryotes in low-sulfate, acidic fens reveal cooccurrence of recognized genera and novel lineages. *Appl. Environ. Microbiol.* 70, 6998–7009.

Meyer, B., and Kuever, J. (2007). Phylogeny of the alpha and beta subunits of the dissimilatory adenosine-5′-phosphosulfate (APS) reductase from sulfate-reducing prokaryotes – origin and evolution of the dissimilatory sulfate-reduction pathway. *Microbiology* 153, 2026–2044.

Mußmann, M., Ishii, K, Rabus, R., and Amann, R. (2005). Diversity and vertical distribution of cultured and uncultured deltaproteobacteria in an intertidal mud flat of the Wadden Sea. *Environ. Microbiol.* 7, 405–418.

Nadkarni, M. A., Martin, F. E., Jacques, N. A., and Hunter, N. (2002). Determination of bacterial load by real-time PCR using a broad-range (universal) probe and primers set. *Microbiology* 148, 257–266.

Neretin, L. N., Abed, R. M. M., Schippers, A., Schubert, C. J., Kohls, K., and Kuypers, M. M. M. (2007). Inorganic carbon fixation by sulfate-reducing bacteria in the Black Sea water column. *Environ. Microbiol.* 9, 3019–3024.

Neretin, L. N., Schippers, A., Pernthaler, A., Hamann, K., Amann, R., and Jørgensen, B. B. (2003). Quantification of dissimilatory (bi)sulphite reductase gene expression in *Desulfobacterium autotrophicum* using real-time RT-PCR. *Environ. Microbiol.* 5, 660–671.

Nunoura, T., Soffientino, B., Blazejak, A., Kakuta, J., Oida, H., Schippers, A., and Takai, K. (2009). Subseafloor microbial communities associated with rapid turbidite deposition in the Gulf of Mexico continental slope (IODP Expedition 308). *FEMS Microbiol. Ecol.* 69, 410–424.

Parkes, R. J., Webster, G., Cragg, B. A., Weightman, A. J., Newberry, C. J., Ferdelman, T. G., Kallmeyer, J., Jørgensen, B. B., Aiello, I. W., and Fry, J. C(2005). Deep sub-seafloor prokaryotes stimulated at interfaces over geological time. *Nature* 436, 390–394.

Ravenschlag, K., Sahm, K., Knoblauch, C., Jørgensen, B. B., and Amann, R. (2000). Community structure, cellular rRNA content and activity of sulfate-reducing bacteria in marine Arctic sediments. *Appl. Environ. Microbiol.* 66, 3592–3602.

Riedinger, N., Brunner, B., Formolo, M. J., Solomon, E., Kasten, S., Strasser, M., and Ferdelman, T. G. (2010). Oxidative sulfur cycling in the deep biosphere of the Nankai trough, Japan. *Geology* 38, 851–854.

Sahm, K., Knoblauch, C., and Amann, R. (1999). Phylogenetic affiliation and quantification of psychrophilic sulfate-reducing isolates in marine Arctic sediments. *Appl. Environ. Microbiol.* 65, 3976–3981.

Schen, Y., Buick, R., and Canfield, D. E. (2001). Isotopic evidence for microbial sulphate reduction in the early Archaean era. *Nature* 410, 77–81.

Schippers, A., and Jørgensen, B. B. (2001). Oxidation of pyrite and iron sulfide by manganese dioxide in marine sediments. *Geochim. Cosmochim. Acta* 65, 915–922.

Schippers, A., Köweker, G., Höft, C., and Teichert, B. (2010). Quantification of microbial communities in three forearc sediment basins off Sumatra. *Geomicrobiol. J.* 27, 170–182.

Schippers, A., and Neretin, L. N. (2006). Quantification of microbial communities in near-surface and deeply buried marine sediments on the Peru continental margin using real-time PCR. *Environ. Microbiol.* 8, 1251–1260.

Schippers, A., Neretin, L. N., Kallmeyer, J., Ferdelman, T. G., Cragg, B. A., Parkes, R. J., and Jørgensen, B. B. (2005). Prokaryotic cells of the deep sub-seafloor biosphere identified as living bacteria. *Nature* 433, 861–864.

Sørensen, K. B., and Teske, A. (2006). Stratified communities of active archaea in deep marine subsurface sediments. *Appl. Environ. Microbiol.* 72, 4596–4603.

Stahl, D. A., Fishbain, S., Klein, M., Baker, B. J., and Wagner, M. (2002). Origins and diversification of sulfate-respiring microorganisms. *Antonie Van Leeuwenhoek* 81, 189–195.

Teske, A. P. (2006). Microbial community composition in deep marine subsurface sediments of ODP Leg 201: sequencing surveys and cultivations. *Proc. Ocean Drill. Prog. Sci. Results* 201, Available at: http://www-odp.tamu.edu/publications/201_SR/120/120.htm

Teske, A. P., and Sørensen, K. B. (2008). Uncultured archaea in deep marine marine subsurface sediments: have we caught them all? *The ISME J.* 2, 3–18.

Thamdrup, B., Rosselló-Mora, R., and Amann, R. (2000). Microbial manganese and sulfate reduction in Black Sea shelf sediments. *Appl. Environ. Microbiol.* 66, 2888–2897.

Vaerman, J. L., Saussoy, P., and Ingargiola, I. (2004). Evaluation of real-time PCR data. *J. Biol. Regul. Homeost. Agents* 18, 212–214.

van der Maarel, M. J. E. C., van Bergeijk, S., van Werkhoven, A. F., Laverman, A. M., Meijer, W. G., Stam, W. T., and Hansen, T. A. (1996). Cleavage of dimethylsulfoniopropionate and reduction of acrylate by *Desulfovibrio acrylicus* sp. nov. *Arch. Microbiol.* 166, 109–115.

Vandieken, V., Finke, N., and Jørgensen, B. B. (2006). Pathways of carbon oxidation in an Arctic fjord sediment (Svalbard) and isolation of psychrophilic and psychrotolerant Fe(III)-reducing bacteria. *Mar. Ecol. Prog. Ser.* 322, 29–41.

Vetriani, C., Tran, H. V., and Kerkhof, L. J. (2003). Fingerprinting microbial assemblages from the oxic/anoxic chemocline of the Black Sea. *Appl. Environ. Microbiol.* 69, 6481–6488.

Wagner, M., Roger, A. J., Flax, J. L., Brusseau, G. A., and Stahl, D. A. (1998). Phylogeny of dissimilatory sulfite reductases supports an early origin of sulfate respiration. *J. Bacteriol.* 180, 2975–2982.

Webster, G., Blazejak, A., Cragg, B. A., Schippers, A., Sass, H., Rinna, J., Tang, X., Mathes, F., Ferdelman, T., Fry, J. C., Weightman, A. J., and Parkes, R. J. (2009). Subsurface microbiology and biogeochemistry of a deep, cold-water carbonate mound from the Porcupine Seabight (IODP Expedition 307). *Environ. Microbiol.* 11, 239–257.

Webster, G., Newberry, C. J., Fry, J. C., and Weightman, A. J. (2003). Assessment of bacterial community

structure in the deep sub-seafloor biosphere by 16S rDNA-based techniques: a cautionary tale. *J. Microbiol. Methods* 55, 155–164.

Webster, G., Watt, L. C., Rinna, J., Fry, J. C., Evershed, R. P., Parkes, J., and Weightman, A, J. (2006). A comparison of stable-isotope probing of DNA and phospholipid fatty acids to study prokaryotic functional diversity in sulfate-reducing marine sediment enrichment slurries. *Environ. Microbiol.* 8, 1575–1589.

Wilms, R., Sass, H., Köpke, B., Cypionka, H., and Engelen, B. (2007). Methane and sulfate profiles within the subsurface of a tidal flat are reflected by the distribution of sulfate-reducing bacteria and methanogenic archaea. *FEMS Microbiol. Ecol.* 59, 611–621.

Conflict of Interest Statement: The authors declare that the research was conducted in the absence of any commercial or financial relationships that could be construed as a potential conflict of interest.

Received: 11 August 2011; accepted: 29 November 2011; published online: 22 December 2011.

Citation: Blazejak A and Schippers A (2011) Real-time PCR quantification and diversity analysis of the functional genes aprA and dsrA of sulfate-reducing prokaryotes in marine sediments of the Peru continental margin and the Black Sea. Front. Microbio. ***2****:253. doi: 10.3389/fmicb.2011.00253*

This article was submitted to Frontiers in Extreme Microbiology, a specialty of Frontiers in Microbiology.

frontiers in
MICROBIOLOGY

ORIGINAL RESEARCH ARTICLE
published: 26 December 2011
doi: 10.3389/fmicb.2011.00255

Expression and partial characterization of an ice-binding protein from a bacterium isolated at a depth of 3,519 m in the Vostok ice core, Antarctica

***Amanda Marie Achberger*[1], *Timothy Ian Brox*[2], *Mark Leslie Skidmore*[2] *and Brent Craig Christner*[1]*

[1] Department of Biological Sciences, Louisiana State University, Baton Rouge, LA, USA
[2] Department of Earth Sciences, Montana State University, Bozeman, MT, USA

Edited by:
Andreas Teske, University of North Carolina at Chapel Hill, USA

Reviewed by:
Tim Magnuson, Idaho State University, USA
Kesen Ma, University of Waterloo, Canada

***Correspondence:**
Brent Craig Christner, Department of Biological Sciences, Louisiana State University, 282 Life Sciences Building, Baton Rouge, LA 70803, USA.
e-mail: xner@lsu.edu

Cryopreservation of microorganisms in ancient glacial ice is possible if lethal levels of macromolecular damage are not incurred and cellular integrity is not compromised via intracellular ice formation or recrystallization. Previously, a bacterium (isolate 3519-10) recovered from a depth of 3,519 m below the surface in the Vostok ice core was shown to secrete an ice-binding protein (IBP) that inhibits the recrystallization of ice. To explore the advantage that IBPs confer to ice-entrapped cells, experiments were designed to examine the expression of 3519-10's IBP gene and protein at different temperatures, assess the effect of the IBP on bacterial viability in ice, and determine how the IBP influences the physical structure of the ice. Total RNA isolated from cultures grown between 4 and 25°C and analyzed by reverse transcription-PCR indicated constitutive expression of the IBP gene. Sodium dodecyl sulfate-polyacrylamide gel electrophoretic analysis of 3519-10's extracellular proteins revealed a polypeptide of the predicted size of the 54-kDa IBP at all temperatures tested. In the presence of 100 μg mL^{-1} of extracellular protein from 3519-10, the survival of *Escherichia coli* was increased by greater than 100-fold after 5 freeze-thaw cycles. Microscopic analysis of ice formed in the presence of the IBP indicated that per square millimeter field of view, there were ~5 times as many crystals as in ice formed in the presence of washed 3519-10 cells and non-IBP producing bacteria, and ~10 times as many crystals as in filtered deionized water. Presumably, the effect that the IBP has on bacterial viability and ice crystal structure is due to its activity as an inhibitor of ice recrystallization. A myriad of molecular adaptations are likely to play a role in bacterial persistence under frozen conditions, but the ability of 3519-10's IBP to control ice crystal structure, and thus the liquid vein network within the ice, may provide one explanation for its successful survival deep within the Antarctic ice sheet for thousands of years.

Keywords: ice-binding protein, recrystallization inhibition, polycrystalline ice, freeze tolerance

INTRODUCTION

Research on the survival and distribution of microorganisms beneath the planet's ice sheets (total surface area of ~1.5×10^7 km^2) has indicated that a diverse range of habitable environments exist in the cryospheric subsurface (e.g., Skidmore, 2011). Extrapolations based on the few data which exist suggest that the ice sheets and subsurface environments of Greenland and Antarctica may contain a globally relevant, yet virtually ignored pool of microorganisms (~10^{29} cells) and carbon (~15 Pg of cell and dissolved organic carbon; Priscu et al., 2008; Lanoil et al., 2009). Subglacial locations harboring liquid water (e.g., subglacial lakes) have been identified as prime targets to search for viable microbial ecosystems (Fricker et al., 2011; Lukin and Bulat, 2011; Ross et al., 2011; Skidmore, 2011). There is also evidence that the physicochemical characteristics and structure of polycrystalline glacial and basal ice provide a tenable microbial habitat where cells reside either in liquid filled veins or the liquid films on the surface of entrained mineral grains (Price, 2000; Mader et al., 2006; Tung et al., 2006; Bakermans and Skidmore, 2011a). Viable bacteria and fungi have been recovered from ancient glacial ice originating from a number of geographical locations (Miteva, 2008); however, little is known about the molecular adaptations which aid these species in tolerating low water availability, osmotic stress, high hydrostatic pressure, and prolonged survival within the ice crystal matrix.

Some cold-adapted organisms mitigate the stress associated with freezing by producing ice-binding proteins (IBPs) which selectively bind to the prism facet of ice, prevent water molecules from joining along the *a*-axis, and influence ice structure. IBPs have been documented in a variety of cold-adapted organisms including plants (Smallwood et al., 1999), diatoms (Raymond and Knight, 2003), and fish (e.g., white flounder; Carpenter and Hansen, 1992), as well as alga and moss from cyanobacterial mats (Raymond and Fritsen, 2001). Although few bacterial IBPs have been characterized, the phenotype has been reported in isolates from Antarctic sea ice, ice-covered lakes, and glacial ice (Gilbert et al., 2005; Raymond et al., 2007, 2008), as well as cold soils (Walker

et al., 2006). Analysis of the IBPs from fish (Sicheri and Yang, 1995; Davies et al., 2002), insects (Graether et al., 2000), and the Antarctic bacterium *Marinomonas primoryensis* (Garnham et al., 2011) have provided structural information to elucidate the mechanism by which the protein binds to the ice crystal matrix. IBPs may have thermal hysteresis activity (i.e., depression of the freezing point without a change in the melting point; also known as antifreeze activity) and/or recrystallization inhibition (RI) activity. An activity toward the inhibition of recrystallization would have particular significance to microorganisms present within an ice matrix, as the growth of large membrane-damaging ice crystals is a process known to reduce cell viability during freezing and thawing (Miller and Mazur, 1976; Gage et al., 1985; Dumont et al., 2004).

Geomicrobiological investigations of the Vostok 5G ice core have provided data on the characteristics of cells entrapped in ice for as long as 420,000 years and limnological conditions in surface waters of the largest subglacial lake in Antarctica, Subglacial Lake Vostok (Karl et al., 1999; Priscu et al., 1999; Christner et al., 2006). Ice core samples from the deepest portions of the glacial ice in the 5G bore hole (from 3,450 to 3,537 m) contain particles too large to be of aeolian origin (>30 μm) and this portion of the core is interpreted to contain entrained bedrock material (Simoes et al., 2002). During the characterization of microbes cultured from melted samples of an ice core from a depth of 3,519 m in 5G, a bacterial isolate (3519-10; Flavobacteriaceae family) was identified that possesses a 54-kDa IBP homologous to those found in some cold-adapted marine bacteria, molds, and diatoms (Raymond et al., 2008). The IBP was found to cause ice pitting and had RI activity. Further, 3519-10 was shown to have the physiological potential to maintain metabolic activity in an ice matrix at temperatures as low as −33°C (Bakermans and Skidmore, 2011b).

To investigate the phenotypic advantage that an IBP with RI activity confers to an ice-entrapped cell population, we examined the expression of 3519-10's IBP as a function of growth temperature and its effect on cell viability during repeated freezing and thawing. Although the specific mechanism by which the IBP of 3519-10 interacts with ice crystal surfaces and protects the cells is still unclear, our results show that the presence of the IBP influences the ice crystal structure. The significance of our findings for microbial survival in polycrystalline ice is discussed.

MATERIALS AND METHODS

BACTERIAL STRAINS AND CULTURE CONDITIONS

Isolate 3519-10 (family Flavobacteriaceae) was previously isolated from a Vostok 5G ice core sample recovered approximately 3,519 m below the surface (actual sampling depth of 3518.03–3518.44 m in the 5G core; Christner et al., 2006; Raymond et al., 2008; **Figure 1**). 3519-10 was cultured aerobically in R2 (Difco Laboratories, Inc.) liquid media and incubated with shaking at 4, 10, 15, and 25°C. Cultures were grown until the mid-logarithmic phase of growth for the isolation of RNA and early stationary phase for extracellular protein recovery. B5 was isolated from basal ice of the Taylor Glacier, Antarctica (Skidmore et al., 2009), and based on 16S rRNA identity, is a member of the genus *Paenisporosarcina* (Phylum Firmicutes). *Paenisporosarcina* isolate B5 was cultured aerobically at 15°C in liquid R2 media until the late stationary phase of growth. *Escherichia coli* ATCC 11775 was cultured aerobically in tryptic soy broth (TSB; Difco Laboratories, Inc.) at 37°C until the mid-logarithmic phase of growth. For crystal imaging, cells cultured at 15°C were diluted in deionized water to an approximate cell concentration of 10^6 colony forming units (CFU) mL^{-1}.

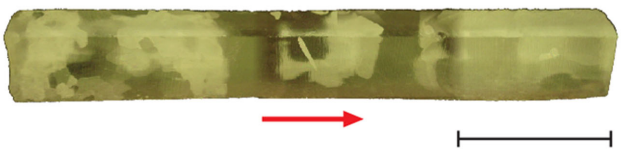

FIGURE 1 | Composite image of ice core section 3,519 viewed under cross-polarized illumination. The arrow is "up" and indicates the ice core orientation relative to the surface. The scale bar is 10 cm.

RNA EXTRACTION, PURIFICATION, AND ANALYSIS

Aliquots (500 μL) of 3519-10 cell suspensions that were grown at 4, 10, 15, and 25°C were removed from culture tubes, immediately preserved in 2 volumes of RNAprotect (Qiagen), and stored at −20°C. The preserved samples were subsequently thawed on ice and lysed by the addition of 15 mg mL^{-1} lysozyme in 200 μL of TE buffer (10 mM Tris–Cl, 1 mM EDTA, pH 8.0), followed by incubation for 10 min at 25°C. The bulk RNA in the lysate was purified with the RNeasy Mini Kit (Qiagen) and eluted into 50 μL of RNase-free water. Genomic DNA was digested with DNase using the TURBO DNA-free kit (Ambion); its removal was confirmed with PCR (**Figure 2B**).

Specific mRNA and small subunit rRNA sequences were reverse transcribed (RT) to cDNA and subsequently amplified using a OneStep reverse transcription-PCR (RT-PCR) kit (Qiagen). Primers were designed to target a 420-bp fragment of 3519-10's IBP gene (EU694412; IBP 421 bp F 5′-TACAAACGGCGCACTGGCCT-3′; IBP 421 bp R 5′-CAAAGCAGCTGCGCGGTTG-3′) and a 100-bp fragment of the *cspA* homolog (ACU07993; CspA1 F 5′-ATCCTTTGTTACCTTGCTGAACTTCGT-3′; CspA1 R 5′-AACGGAGGAGAAGACATCTTTGTTCA-3′) using sequence data available through GenBank (CP001673.1). The primers used to RT-PCR a ∼900 bp region of the 16S rRNA molecule (515F 5′-GTGCCAGCAGCCGCGGTAA-3′; 1391R 5′-GACGGGCGGTGTGTRCA-3′) were those described by Reysenbach and Pace (1995). RT-PCR amplification was performed with an initial RT step at 50°C for 30 min, followed by heating at 95°C for 15 min to inactivate the reverse transcriptase. The cDNA products were subsequently amplified for 30 cycles using the following conditions: 94°C for 1 min, 50.8°C (16S rRNA primers) or 60°C (IBP and *cspA* primers) for 1 min, and 72°C for 1.5 min, with a terminal elongation at 72°C for 10 min. The amplified DNA products were examined after electrophoresis though a 2% (w/v) agarose gel that was stained with 1 μg mL^{-1} ethidium bromide.

HARVESTING AND PREPARATION OF EXTRACELLULAR PROTEIN

Extracellular proteins were captured and washed using YP-30 Microcon (Millipore) or Ultra 15 centrifugal filter devices

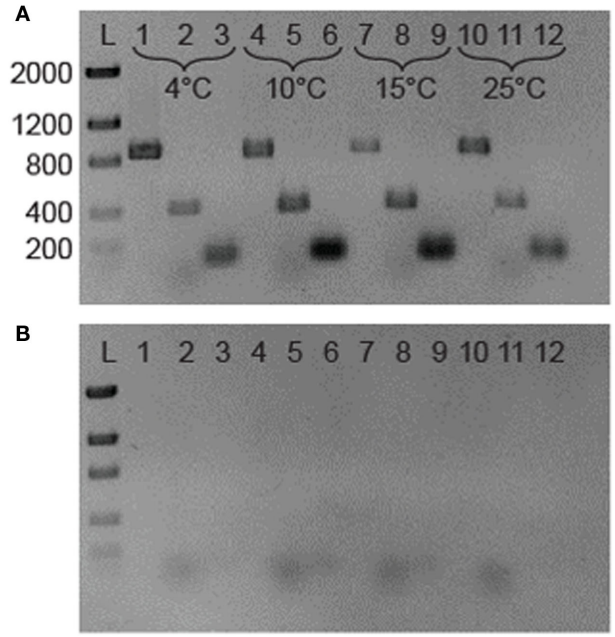

FIGURE 2 | (A) Reverse transcription-PCR analysis of gene expression in 3519-10. The 876-bp bands in lanes 1, 4, 7, and 10 represents the presence of 16S rRNA; the 421 and 100 bp bands are fragments of RT-PCR IBP and *cspA* transcripts, respectively. The template for lanes 1–3 was RNA from a 4°C grown culture of 3519-10, 4–6 from 10°C, 7–9 from 15°C, and 10–12 from 25°C cultures. **(B)**. Identical samples lacking a RT step. Lane assignments are the same as for **(A)**. L is a low DNA mass ladder (Invitrogen).

(Amicon), both of which have reported nominal molecular weight cutoffs of 30 kDa. Cultures of 3519-10 were centrifuged at 17,000 × *g* for 10 min to pellet the cells, and either 1.5 or 12 mL of the supernatant was filtered through the YP-30 or Ultra 15, respectively. After centrifugation at 13,500 × *g* for 12 min or 4,500 × *g* for 20 min. (YP-30 or Ultra 15, respectively), the filters were washed in deionized H_2O. The concentrated protein was recovered by inverting and centrifuging at 1,000 × *g* for 3 min (YP-30) or by using a pipette (Ultra 15) and was stored at 4°C until use. Samples containing deionized water were prepared in parallel to serve as controls.

The protein concentration was determined with the Coomassie (Bradford) Protein Assay kit (Pierce) and bovine serum albumin (BSA) as a standard. Absorbance at 595 nm was measured with a NanoDrop ND-1000 spectrophotometer. The extracellular proteins of 3519-10 were separated using sodium dodecyl sulfate-polyacrylamide gel electrophoresis (SDS-PAGE). The gel was buffered with tris–glycine (25 mM Tris Base, 250 mM glycine, 0.1% SDS, pH 8.3) and consisted of a 5% stacking and 12% running gel (w/v of polyacrylamide). SDS-PAGE was conducted at 70 V for 30 min and increased to 100 V for ∼3 h. The separated polypeptides were visualized by staining with Coomassie stain (Weber and Osborn, 1969). The size of polypeptides was estimated by comparison to the electrophoretic migration distance of a 10- to 250-kDa molecular weight standard (New England Biolabs).

FREEZE-THAW CYCLING VIABILITY ASSAY

Cultures of *E. coli* in the logarithmic phase of growth were harvested by centrifugation at 17,000 × *g* for 10 min., the supernatant was removed, and cells were washed twice with an equal volume of phosphate buffered saline (PBS; 137 mM NaCl, 2.7 mM KCl, 10 mM Na_2HPO_4, 2 mM KH_2PO_4; pH 7.4). The *E. coli* cell suspensions (∼10^8 CFU mL^{-1}) were amended with the extracellular protein fraction from 3519-10 at final concentrations of 1, 10, and 100 μg mL^{-1}. Frozen cell suspensions containing 1, 10, and 100 μg mL^{-1} BSA were prepared identically and served as controls. Additional controls consisted of frozen cell suspensions without amended protein and samples that remained at 25°C for the duration of the freeze-thaw cycling experiment. Each experimental data point represented a measurement from triplicate samples.

The cell suspensions were frozen rapidly by incubation at −80°C for ∼45 min., and then samples were transferred to −5°C for approximately 12 h. Samples were thawed rapidly in a 25°C water bath, an aliquot was removed from each sample for serial dilution plating, and the samples were refrozen as described above. This procedure was repeated up to six times. After incubation at 37°C for 18 h, the number of *E. coli* colonies formed on the dilution plate series was counted to determine the number of CFU per milliliter.

CRYSTAL STRUCTURE IMAGING

Samples of deionized water passed though a 0.2-μm pore size filter, washed 3519-10 and *Paenisporosarcina* isolate B5 cells, and the extracellular proteins harvested from 3519-10 were frozen at −10°C. Samples were frozen within modified 50 mL polypropylene centrifuge tubes. The bottom of each tube was removed and the tubes were attached to a 30.5-cm^2 and ∼1 cm thick aluminum plate using O.C.T. embedding compound (Tissue Tek, Sakura). Twenty milliliters of liquid sample was placed in the tubes affixed to the plate and the tubes were capped. The samples were insulated on the sides and top by 2″ of extruded polystyrene foam board to minimize air space around these portions of the sample to encourage prominent crystal growth in the vertical direction (i.e., away from the aluminum plate). A thermistor connected to a HOBO® data logger (Onset Corporation) was suspended in each tube 2 cm above the aluminum plate to record the temperature of the sample during supercooling, freezing, and equilibration with the ambient temperature.

Approximately 20 h after freezing, thin sections (∼1 mm) from ice in the lowest 5 mm of the ice column were prepared and imaged at −10°C under cross-polarized light using an Olympus BX51-TRF epifluorescence microscope equipped with a Linkam large area thermal stage. Eight to 15 images were collected via transect from the outside edge of the sample to the center of the sample (**Figure 3A**) depending on the amount of overlap between the images. The number of crystals per image was counted to calculate the average number of ice crystals per square millimeter. The field of view was calibrated using a 1-mm SPI PS8 micrometer.

RESULTS

EXPRESSION OF THE IBP

Reverse transcription-PCR amplification detected mRNA of the IBP gene at all growth temperatures tested between 4 and 25°C

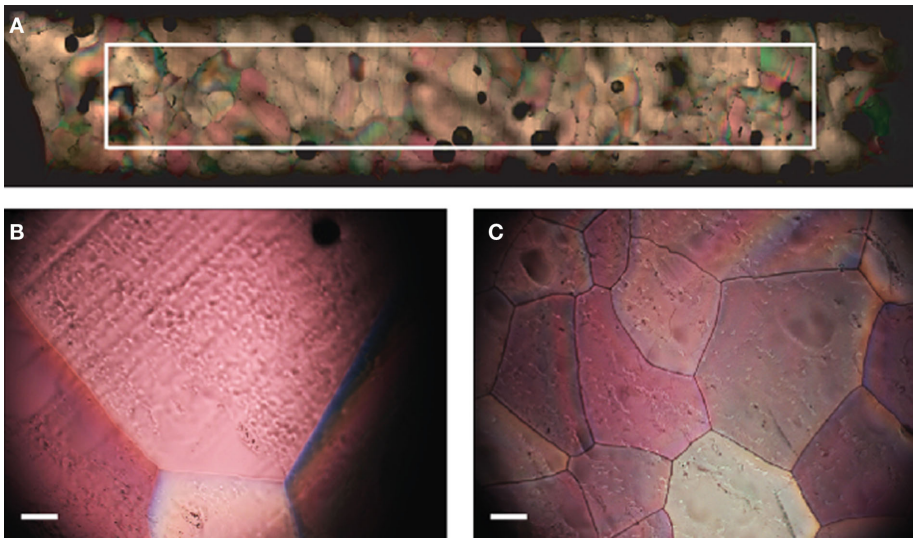

FIGURE 3 | (A) Image transect showing ice structure from the outside edge of the sample to center (left to right in image). The superimposed rectangle delineates a 1.5-mm by 10 mm area. **(B)** Ice structure formed from filtered deionized water. **(C)** Ice structure formed in the presence of extracellular proteins from 3519-10. Scale bars in **(B)** and **(C)** are 0.1 mm.

(**Figure 2A**), implying that the IBP gene is constitutively expressed during logarithmic growth. Expression of the major bacterial cold shock protein gene (*cspA*) and 16S rRNA were also detected under all conditions tested (**Figure 2A**). Amplicons were not produced in identical samples that omitted the RT step (**Figure 2B**), indicating that genomic DNA contamination was undetectable via PCR in the purified RNA samples. To assess if the IBP gene transcripts were translated and secreted from the cell under these conditions, preparations of the extracellular protein fraction from cultures incubated at intervals between 4 and 25˚C were analyzed by SDS-PAGE (**Figure 4**). At all temperatures examined, there were at least 25 discernable polypeptide bands that ranged in molecular weight between 15 and 150 kDa. Denatured polypeptides smaller in size than the 30-kDa nominal molecular weight cutoff of the filtration devices are likely to represent components of multi-subunit proteins and/or hydrolyzed peptide fragments. A polypeptide that corresponded to the size of the 54-kDa IBP (Raymond et al., 2008) was observed at all growth temperatures examined (**Figure 4**).

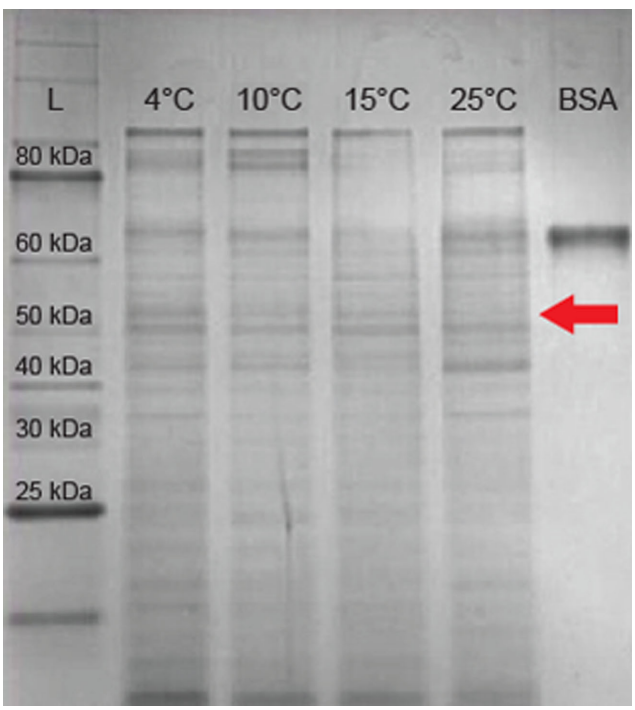

FIGURE 4 | Sodium dodecyl sulfate-polyacrylamide gel electrophoresis of extracellular proteins from 3519-10. Lane 1 contains a 10- to 250-kDa protein ladder. Lanes 2–5 contain 10 μg total extracellular protein harvested from cultures grown at 4, 10, 15, and 25˚C respectively. Lane 6 contains 10 μg of BSA (66 kDa). The arrow indicates the expected migration of the IBP based on the predicted size of 54 kDa.

BACTERIAL VIABILITY DURING FREEZING AND THAWING

To examine the effect of the IBP on bacterial viability during the phase transition occuring between frozen incubation at −5˚C and thawing, extracellular proteins harvested from 3519-10 were added to populations of *E. coli* at concentrations of 1, 10, and 100 μg mL^{-1}, and the suspensions were frozen. After 4 freeze-thaw cycles, a biphasic trend was observed in the reduction of viability for all treatments (**Figure 5**). The first two cycles resulted in a 4–5 log reduction in the number of culturable *E. coli* cells, whereas only a reduction of 1–2 log was observed during cycles 2–4. However, the survival of *E. coli* in samples containing 100 μg mL^{-1} of extracellular protein from 3519-10 cultured at 4˚C was significantly increased over that of the frozen control (cycles 1–4; $p < 0.03$; **Figure 5**) and had 34 and >100-fold higher recovery than frozen controls after 2 and 5 cycles, respectively. In comparison, proteins harvested from 3519-10 cultured at 25˚C only significantly increased the survival of *E. coli* after cycles 1 and 4 (cycles 2, 3, and 5 were not statistically different from the controls $p < 0.05$), and in general, appeared to be less effective than

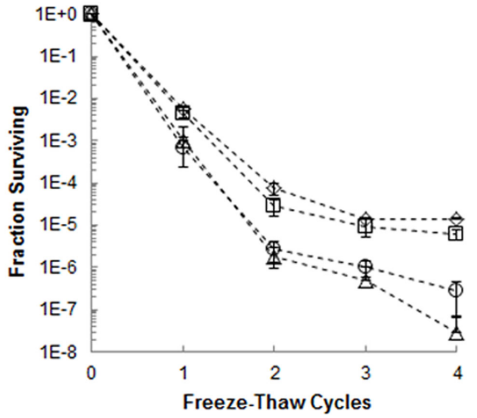

FIGURE 5 | Fraction of *E. coli* surviving four freeze-thaw cycles in the presence of 100 μg mL⁻¹ of extracellular proteins harvested from a culture of 3519-10 grown at 4°C (◇) and 25°C (□), as well as 100 μg mL⁻¹ BSA(Δ). The bars represent the SE of triplicate samples; the frozen control (○) is the average of six replicates from two experiments.

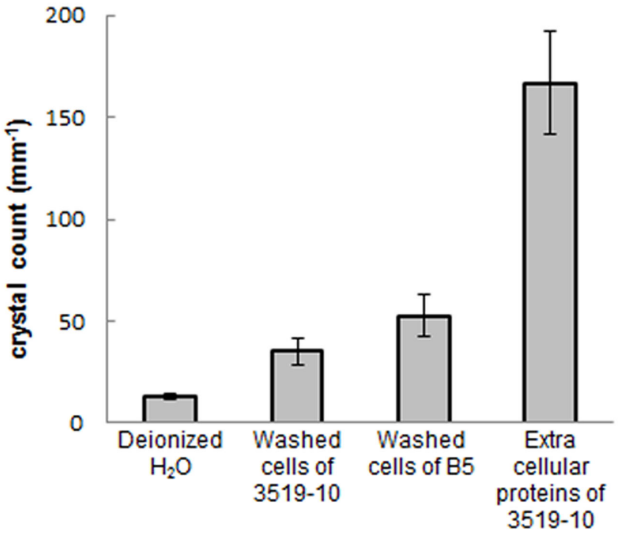

FIGURE 6 | Number of crystals per square millimeter for each ice sample (error bars are 1 σ). From left to right: ices made with filtered deionized water, washed 3519-10 cells, washed *Paenisporosarcina* isolate B5 cells, and 3519-10's extracellular proteins.

proteins from the 4°C cultures in increasing the survival of *E. coli* under these conditions. The data from viability experiments with 1 and 10 μg mL^{-1} of extracellular proteins (data not shown) or 100 μg mL^{-1} of BSA (**Figure 5**) were statistically indistinguishable from the controls. After 6 freeze-thaw cycles, only samples amended with 100 μg mL^{-1} of extracellular protein from 3519-10 contained viable population sizes of *E. coli* that were detectable after dilution plating and incubation.

ICE CRYSTAL STRUCTURE IMAGING

Temperature data from the probe suspended in each sample during freezing indicated that the samples supercooled and froze within ∼45 min., but remained at the melting point for the subsequent ∼2 h and were equilibrated with the ambient temperature (−10°C) by 3 h. Microtome-prepared thin sections of the ice were imaged approximately 20 h after freezing (**Figure 3A**.). Representative fields of view from the filtered deionized water sample (**Figure 3B**) and 3519-10 extracellular protein sample (**Figure 3C**) demonstrated an obvious difference in bulk ice structure. Ice samples frozen in the presence of a non-IBP producing bacteria (*Paenisporosarcina* isolate B5) and washed suspensions of 3519-10 contained 4.1 and 2.7-fold, respectively, more crystals per square millimeter than the ice formed from the filtered deionized water (**Figure 6**). Ice samples frozen in the presence of extracellular proteins from 3519-10 had 13-fold more crystals per square millimeter than filtered deionized water (**Figure 6**). The number of ice crystals in samples frozen in the presence of bacteria ($p < 0.00001$) and the extracellular proteins from 3519-10 ($p < 0.00001$) were statistically different from the control.

DISCUSSION

MICROBIAL SURVIVAL IN THE DEEP ICY BIOSPHERE

The upper 3,309 m of the Vostok 5G ice core provides one of the oldest paleoclimatic ice core records examined to date (Petit et al., 1999), whereas the deepest portion of the ice core (below 3,539 m) is accreted lake water from Subglacial Lake Vostok. The latter represents the only material available to date for assessing limnological conditions in a subglacial Antarctic lake (Karl et al., 1999; Priscu et al., 1999; Christner et al., 2006). Although the surface temperature at Vostok is commonly below −55°C, the temperature of the ice at a depth of 3,519 m is approximately −8°C (Salamatin et al., 2004), and the base of the ice sheet is close to or at the pressure melting point (−2.5°C; Wüest and Carmack, 2000; Siegert et al., 2003). Analysis of ice core depths between 3,450 and 3,539 m have reported significant ice crystal deformation, evidence for basal shearing, and large particles >30 μm; characteristics which are evidence that ice in this portion of the core has interacted with the bed (Simoes et al., 2002). The large irregular crystals observed at 3,519 m (**Figure 1**) are consistent with these prior observations and are indicative of ice that has experienced significant shear and deformation, both of which are factors known to increase the rate of recrystallization (Paterson, 1994). Since recrystallization is damaging to biological cells and tissues (e.g., Miller and Mazur, 1976), we hypothesized that microorganisms surviving within the basal ice horizon have adaptations to mitigate cellular damage and/or influence the structure of the ice matrix they inhabit.

Basal ice in ice sheets and glaciers form when liquid water and debris at the ice-bed interface becomes entrained via freeze-on or regelation processes (Knight, 1997). Therefore, studies of basal ice can provide information on the physical, chemical, and microbiological characteristics of the subglacial environment. In some locations in East Antarctica, it has been reported that the freezing of subglacial water has formed a 1.1-km layer of basal ice, representing about half of the total ice sheet thickness in this region (Bell et al., 2011). Thus, the basal ice of glaciers and ice sheets likely represents an important transient phase for microorganisms in the subglacial environment (e.g., transport via freeze-on at the

glacier bed) and may be a valuable source of microbial inocula and nutrients in downstream regions where basal melting and liquid water is widespread (Skidmore, 2011). Here we report an analysis of a bacterium isolated from basal ice from deep within the East Antarctic Ice Sheet that produces extracellular proteins, including a known IBP, that is capable of inhibiting recrystallization, conserving the ice crystal structure, and increasing the viability of bacteria entrapped within the ice matrix.

EXPRESSION OF THE IBP AND INCREASED TOLERANCE TO FREEZING AND THAWING

Ice-binding proteins have only been documented in cold tolerant organisms, and in bacteria, the phenotype has been observed in isolates from sea ice (Raymond and Knight, 2003; Raymond et al., 2007), glacial ice (Raymond et al., 2008), polar lakes (Raymond and Fritsen, 2000, 2001), and cold soils (Walker et al., 2006). Increased tolerance to freezing and thawing occurs when recrystallization is prevented. IBPs from a sea ice diatom (*Navicula*) have been shown to protect other diatoms (Raymond and Knight, 2003) and human red blood cells (Kang and Raymond, 2004) during freeze-thaw. Similarly, Walker et al. (2006) demonstrated that soil isolate "*Chryseobacterium* sp. strain C14" produced an ice-active substance that increased the survival of an *Enterococcus* sp. during freeze-thaw cycling. Consistent with prior observations, the presence of 3519-10's IBP increased cell viability during repeated freezing and thawing (**Figure 5**). Since our experiments were not conducted with purified preparations of 3519-10's IBP, it is not possible to determine the absolute concentration effect of the IBP on bacterial survival or ice crystal structure, nor are we able to discount the affect, positive or negative, that other proteins present may have had. However, in light of results from controls using BSA, our results are consistent with the activities reported for purified preparations of 3519-10's IBP (Raymond et al., 2008). Based on the total number of extracellular polypeptides observed by SDS-PAGE (∼25; **Figure 4**) and assuming equal weight distribution for each of the polypeptides, a crude estimate for the IBP concentration that significantly influenced bacterial viability is $\sim 4\,\mu g\,mL^{-1}$ (i.e., $100\,\mu g\,mL^{-1}/25$ polypeptides $= 4\,\mu g\,mL^{-1}$). A concentration of $0.01–1.4\,\mu g$ IBP mL^{-1} has been shown to inhibit ice recrystallization by microbial IBPs from Antarctic cyanobacterial mats, moss, and algae (Raymond and Fritsen, 2001), suggesting that 3519-10's IBP has a comparable RI activity. The IBP of 3519-10 is a soluble protein that is secreted by the cell and appears capable of protecting any cell in the ice matrix (e.g., *E. coli*). In the habitat of polycrystalline ice, species like 3519-10 might passively protect freeze-sensitive cells or form consortial relationships with such species, providing protection from ice crystal damage in exchange for substrates or other resources.

Much of what is known about the regulation of IBP expression is restricted to studies of polar fish that seasonally experience temperatures below 0°C and induce their IBPs accordingly (Fletcher et al., 2001). In Newfoundland winter flounder, IBP mRNA is detectable in the liver at temperatures below 8°C, and the IBP accumulates to detectable levels in the blood plasma after several weeks under these conditions (Fletcher et al., 2001). In contrast, adult cod only express their IBPs at temperatures ≤1°C (Fletcher et al., 1987), while the Newfoundland ocean pout produces IBP continually independent of temperature (Fletcher et al., 1985). Based on quantitative PCR analysis, the multiple IBP isoforms of the diatom *Fragilariopsis cylindrus* are differentially expressed in response to osmotic shock and low temperature (−4°C; Bayer-Giraldi et al., 2010). Polypeptides and mRNA corresponding to 3519-10's IBP were detected at all the growth temperatures tested (up to 25°C), indicating that low temperature was not required for active expression. Considering the energetic cost of protein synthesis and export, this apparent lack of regulation may hint at the importance of the IBP for ensuring survival of this bacterium in its environment. Based on the data in **Figure 5**, extracellular proteins containing the IBP produced by 3519-10 at 25°C did not protect *E. coli* viability to the same degree as those produced by cultures of 3519-10 grown at 4°C. Although the bulk protein concentration was identical between the treatments, there may have been fewer IBP molecules in the extracellular protein fraction of 25°C cultures compared to that in the 4°C cultures. Alternatively, the IBP may have a decreased activity and/or stability at warmer temperatures, providing a working hypothesis for future structural studies of this protein.

EFFECT OF IBPS AND CELLS ON THE ICE CRYSTAL STRUCTURE

During the phase transition to ice, particles the size of bacterial cells are rejected together with other soluble impurities into the solute-rich environment that exists at the grain boundaries (Mader et al., 2006). Under laboratory conditions, 3519-10 has been shown to be metabolically active in ice to temperatures as low as −33°C (Bakermans and Skidmore, 2011b). Price (2007) estimated that the concentration of nutrients and dissolved organic carbon in the aqueous fraction of the ice in deep portions of the Vostok core are sufficient to maintain the ambient concentration of cells in the ice for at least several hundred thousand years. In this study, the presence of 3519-10's IBP and $\sim 10^6$ bacterial cells per milliliter were found to affect the ice structure (**Figures 6** and **3C**). Since the 3519-10 cells were washed thoroughly to remove the secreted IBP and the *Paenisporosarcina* isolate B5 does not produce ice-active substances, the implication is that particles the size and composition of bacterial cells influence the ice structure. Though the mechanism by which this occurs is not decipherable with the data available, it may be due to the bacteria serving as nucleation sites. These results are interesting considering that similar concentrations of cells, up to $\sim 10^8\,mL^{-1}$ of which at least $10^6\,mL^{-1}$ are inferred to be viable, have been reported in basal ices (3,042–3,052 m) from the GISP2 Greenland ice core (Miteva et al., 2009). This suggests that the presence of microbial cells and their ice-interacting substances may influence the ice crystal structure of basal ices. In particular, recrystallization of ice grains via physical processes has been shown to significantly influence local strain rate (Paterson, 1994; Samyn et al., 2008). The magnitude by which microbes and their activities in a localized region of an ice mass, e.g., in the basal ice layer, could impact ice rheology is unknown and requires further investigation.

CONCLUSION

An IBP is a molecular adaptation that would be expected to enhance the survival and persistence of species in a diverse array of icy environments in the biosphere. Findings from the current

study demonstrate that IBPs with RI activity can offer a distinct survival advantage to cell populations immured in the polycrystalline habitat of ice. IBPs are not possessed by all microorganisms inhabiting frozen environments and microorganisms like 3519-10 may use this phenotype as a basis for mutualistic interactions, similar to those mediated by diffusible compounds in other bacteria (e.g., Sher et al., 2011). A number of bacteria, including 3519-10, have demonstrated the ability to be metabolically active within the matrix of ice crystals (e.g., Amato et al., 2010; Bakermans and Skidmore, 2011b). Although expression of 3519-10's IBP was documented at low temperature (4°C) under liquid conditions, determining if active expression of the IBP occurs in ice is territory for further study.

Proteins that affect ice crystal structure and inhibit recrystallization can be exploited to improve the texture of ice cream (Regand and Goff, 2006), cold tolerance in plants (Wen-li et al., 2005), and the cryopreservation of mammalian tissues (Bagis et al., 2006). Currently, protein structural data for bacterial IBPs are restricted to a single genetic form (Garnham et al., 2011). Unveiling the structure of 3519-10's IBP would provide important comparative data to aid in elucidating the molecular characteristics unique to IBPs and may reveal novel properties relevant to applications in the industrial and biomedical sciences (e.g., improved cryopreservation of cell lines and tissues).

In summary, expression of 3519-10's IBP was independent of growth temperature, affected the structure of ice crystals formed in its presence, and protected bacteria under conditions favorable to the process of recrystallization. Although the full range of molecular adaptations which play a role in bacterial persistence under frozen conditions has yet to be constrained, the ability to control ice crystal structure and preserve cellular integrity provides one possible explanation for how 3519-10 has successfully survived in deep Antarctic ice for thousands of years.

ACKNOWLEDGMENTS

This research was partially supported by grants EAR-0525567, ANT-0636828, and ANT-0636770 from the National Science Foundation. Amanda Marie Achberger was also supported by funding from the NSF award ANT-0838941 and the Howard Hughes Medical Institute Biomedical Education Program. Timothy Ian Brox was also supported by scholarships from Montana Space Grant Consortium (MSGC) as part of the Montana NASA EPSCoR Program and the Montana State University (MSU) Undergraduate Scholars Program and an award to Mark Leslie Skidmore from MSGC. Mark Leslie Skidmore and Timothy Ian Brox are grateful for use of the Subzero Science and Engineering Research Facility at MSU.

REFERENCES

Amato, P., Doyle, S. M., Battista, J. R., and Christner, B. C. (2010). Implications of subzero metabolic activity on long-term microbial survival in terrestrial and extraterrestrial permafrost. *Astrobiology* 10, 789–798.

Bagis, H., Aktoprakligil, D., Mercan, H. O., Yurdusev, N., Turgut, G., Sekmen, S., Arat, S., and Cetin, S. (2006). Stable transmission and transcription of newfoundland ocean pout type III fish antifreeze protein (AFP) gene in transgenic mice and hypothermic storage of transgenic ovary and testis. *Mol. Reprod. Dev.* 73, 1404–1411.

Bakermans, C., and Skidmore, M. L. (2011a). Microbial metabolism in ice and brine at −5°C. *Environ. Microbiol.* 13, 2269–2278.

Bakermans, C., and Skidmore, M. (2011b). Microbial respiration in ice at subzero temperatures (−4 to −33°C). *Environ. Microbiol. Rep.* 3, 774–782.

Bayer-Giraldi, M., Uhlig, C., John, U., Mock, T., and Valentin, K. (2010). Antifreeze proteins in polar sea ice diatoms: diversity and gene expression in the genus *Fragilariopsis*. *Environ. Microbiol.* 12, 1041–1052.

Bell, R. E., Ferraccioli, F., Creyts, T. T., Braaten, D., Corr, H., Das, I., Damaske, D., Frearson, N., Jordan, T., Rose, K., Studinger, M., and Wolovick, M. (2011). Widespread persistent thickening of the East Antarctic ice sheet by freezing from the base. *Science* 331, 1592–1595.

Carpenter, J. F., and Hansen, T. N. (1992). Antifreeze protein modulates cell survival during cryopreservation: mediation through influence on ice crystal growth. *Proc. Natl. Acad. Sci. U.S.A.* 89, 8953–8957.

Christner, B. C., Royston-Bishop, G., Foreman, C. M., Arnold, B. R., Tranter, M., Welch, K. A., Lyons, W. B., Tsapin, A. I., Studinger, M., and Priscu, J. C. (2006). Limnological conditions in Subglacial Lake Vostok, Antarctica. *Limnol. Oceanogr.* 51, 2485–2501.

Davies, P. L., Baardsnes, J., Kuiper, M. J., and Walker, V. K. (2002). Structure and function of antifreeze proteins. *Phil. Trans. R. Soc. Lond. B Biol. Sci.* 357, 927–935.

Dumont, F., Marechal, P. A., and Gervais, P. (2004). Cell size and water permeability as determining factors for cell viability after freezing at different cooling rates. *Appl. Environ. Microbiol.* 70, 268–272.

Fletcher, G. L., Hew, C. L., and Davies, P. L. (2001). Antifreeze proteins of teleost fishes. *Annu. Rev. Physiol.* 63, 359–390.

Fletcher, G. L., Hew, C. L., Li, X., Haya, K., and Kao, M. H. (1985). Year-round presence of high levels of plasma antifreeze peptides in a temperate fish, ocean pout (*Macrozoarces americanus*). *Can. J. Zool.* 63, 488–493.

Fletcher, G. L., King, M. J., and Kao, M. H. (1987). Low temperature regulation of antifreeze glycopeptide levels in Atlantic cod (*Gadus morhua*). *Can. J. Zool.* 65, 227–233.

Fricker, H. A., Powell, R., Priscu, J., Tulaczyk, S., Anandakrishnan, S., Christner, B. C., Fisher, A. T., Holland, D., Horgan, H., Jacobel, R., Mikucki, J., Mitchell, A., Scherer, R., and Severinghaus, J. (2011). "Siple Coast subglacial aquatic environments: the Whillans Ice Stream Subglacial Access Research Drilling (WISSARD) project," in *Antarctic Subglacial Aquatic Environments*, eds M. Siegert, M. Kennicutt, and R. Bindschadler, Geophysical Monograph 192 (Washington, DC: American Geophysical Union Press), 199–219.

Gage, A. A., Guest, K., Montes, M., Caruana, J. A., and Whalen, D. A. Jr. (1985). The effect of varying freezing and thawing rates in experimental cryosurgery. *Cryobiology* 22, 175–182.

Garnham, C. P., Campbell, R. L., and Davies, P. L. (2011). Anchored clathrate waters bind antifreeze proteins to ice. *Proc. Natl. Acad. Sci. U.S.A.* 108, 7363–7367.

Gilbert, J. A., Davies, P. L., and Laybourn-Parry, J. (2005). A hyperactive, Ca 2+-dependent antifreeze protein in an Antarctic bacterium. *FEMS Microbiol. Lett.* 245, 67–72.

Graether, S. P., Kuiper, M. J., Gagné, S. M., Walker, V. K., Jia, Z., Sykes, B. D., and Davies, P. L. (2000). β-Helix structure and ice-binding properties of a hyperactive antifreeze protein from an insect. *Nature* 406, 325–328.

Kang, J. S., and Raymond, J. A. (2004). Reduction of freeze-thaw-induced hemolysis of red blood cells by an algal ice-binding protein. *Cryo Lett.* 25, 307–310.

Karl, D. M., Bird, D. F., Björkman, K., Houlihan, T., Shackelford, R., and Tupas, L. (1999). Microorganisms in the accreted ice of Lake Vostok, Antarctica. *Science* 286, 2144–2147.

Knight, P. G. (1997). The basal ice layer of glaciers and ice sheets. *Quat. Sci. Rev.* 16, 975–993.

Lanoil, B., Skidmore, M., Priscu, J. C., Han, S., Foo, W., Vogel, S. W., Tulaczyk, S., and Engelhardt, H. (2009). Bacteria beneath the West Antarctic ice sheet. *Environ. Microbiol.* 11, 609–615.

Lukin, V., and Bulat, S. (2011). "Vostok subglacial lake: details of Russian plans/activities for drilling and aampling," in *Antarctic Subglacial Aquatic Environments*, eds M. Siegert, M. Kennicutt, and R. Bindschadler, Geophysical Monograph 192 (Washington, DC: American Geophysical Union Press), 187–197.

Mader, H. M., Pettitt, M. E., Wadham, J. L., Wolff, E. W., and Parkes, R. J. (2006). Subsurface ice as a microbial habitat. *Geology* 34, 169–172.

Miller, R. H., and Mazur, P. (1976). Survival of frozen-thawed human red cells a function of cooling and warming velocities. *Cryobiology* 13, 404–414.

Miteva, V. (2008). "Bacteria in snow and glacier ice," in *Psychrophiles: From Biodiversity to Biotechnology*, eds R. Margesin, F. Schinner, J.-C. Marx, and C. Gerday (Berlin: Springer), 31–50.

Miteva, V., Teacher, C., Sowers, T., and Brenchley, J. (2009). Comparison of the microbial diversity at different depths of the GISP2 Greenland ice core in relationship to deposition climates. *Environ. Microbiol.* 11, 640–656.

Paterson, W. S. B. (1994). *The Physics of Glaciers.* Oxford: Butterworth-Heinemann.

Petit, J. R., Jouzel, J., Raynaud, D., Barkov, N. I., Barnola, J. M., Basile, I., Bender, M., Chappellaz, J., Davis, M., Delaygue, G., Delmotte, M., Kotlyakov, V. M., Legrand, M., Lipenkov, V. Y., Lorius, C., Pe´pin, L., Ritz, C., Saltzman, E., and Stievenard, M. (1999). Climate and atmospheric history of the past 420,000 years from the Vostok ice core, Antarctica. *Nature* 399, 429–436.

Price, P. B. (2000). A habitat for psychrophiles in deep Antarctic ice. *Proc. Natl. Acad. Sci. U.S.A.* 97, 1247–1251.

Price, P. B. (2007). Microbial life in glacial ice and implications for a cold origin of life. *FEMS Microbiol. Ecol.* 59, 217–231.

Priscu, J. C., Adams, E. E., Lyons, W. B., Voytek, M. A., Mogk, D. W., Brown, R. L., McKay, C. P., Takacs, C. D., Welch, K. A., Wolf, C. F., Kirshtein, J. D., and Avci, R. (1999). Geomicrobiology of subglacial ice above Lake Vostok, Antarctica. *Science* 286, 2142–2144.

Priscu, J. C., Tulaczyk, S., Studinger, M., Kennicutt, M. C. II, Christner, B. C., and Foreman, C. M. (2008). "Antarctic subglacial water: origin, evolution and microbial ecology," in *Polar Lakes and Rivers*, eds W. Vincent and J. Laybourn-Parry (Oxford: Oxford University Press), 119–135.

Raymond, J. A., Christner, B. C., and Schuster, S. C. (2008). A bacterial ice-binding protein from the Vostok ice core. *Extremophiles* 12, 713–717.

Raymond, J. A., and Fritsen, C. H. (2000). Ice-active substances associated with Antarctic freshwater and terrestrial photosynthetic organisms. *Antarct. Sci.* 12, 418–424.

Raymond, J. A., and Fritsen, C. H. (2001). Semipurification and ice recrystallization inhibition activity of ice-active substances associated with Antarctic photosynthetic organisms. *Cryobiology* 43, 63–70.

Raymond, J. A., Fritsen, C. H., and Shen, K. (2007). An ice-binding protein from an Antarctic sea ice bacterium. *FEMS Microbiol. Ecol.* 61, 214–221.

Raymond, J. A., and Knight, C. A. (2003). Ice binding, recrystallization inhibition, and cryoprotective properties of ice-active substances associated with Antarctic sea ice diatoms. *Cryobiology* 46, 174–181.

Regand, A., and Goff, H. D. (2006). Ice recrystallization inhibition in ice cream as affected by ice structuring proteins from winter wheat grass. *J. Dairy Sci.* 89, 49–57.

Reysenbach, A.-L., and Pace, N. R. (1995). "Reliable amplification of hyperthermophilic archaeal 16s rRNA genes by the polymerase chain reaction," in *Archaea: A Laboratory Manual: Thermophiles*, eds F. T. Robb and A. R. Place (New York: Cold Springs Harbor Laboratory Press), 101–105.

Ross, N., Siegert, M. J., Rivera, A., Bentley, M. J., Blake, D., Capper, L., Clarke, R., Cockell, C. S., Corr, H. F. J., Harris, W., Hill, C., Hindmarsh, R. C. A., Hodgson, D. A., King, E. C., Lamb, H., Maher, B., Makinson, K., Mowlem, M., Parnell, J., Pearce, D. A., Priscu, J., Smith, A. M., Tait, A., Tranter, M., Wadham, J. L., Whalley, W. B., and Woodward, J. (2011). "Ellsworth Subglacial Lake, West Antarctica: a review of its history and recent field campagins," in *Antarctic Subglacial Aquatic Environments*, eds M. Siegert, M. Kennicutt, and R. Bindschadler, Geophysical Monograph 192 (Washington, DC: American Geophysical Union Press), 221–233.

Salamatin, A. N., Tsyganova, E. A., Lipenkov, V. Y., and Petit, J. R. (2004). Vostok (Antarctica) ice-core timescale from dating of different origins. *Ann. Glaciol.* 39, 283–292.

Samyn, D., Svensson, A., and Fitzsimons, S. J. (2008). Dynamic implications of discontinuous recrystallization in cold basal ice: Taylor Glacier, Antarctica. *J. Geophys. Res.* 113, F03S90.

Sher, D., Thompson, J. W., Kashtan, N., Croal, L., and Chisholm, S. W. (2011). Response of *Prochlorococcus* ecotypes to co-culture with diverse marine bacteria. *ISME J.* 5, 1125–1132.

Sicheri, F., and Yang, D. S. C. (1995). Ice-binding structure and mechanism of an antifreeze protein from winter flounder. *Nature* 375, 427–431.

Siegert, M. J., Tranter, M., Ellis-Evans, J. C., Priscu, J. C., and Lyons, W. B. (2003). The hydrochemistry of Lake Vostok and the potential for life in Antarctic subglacial lakes. *Hydrol. Process.* 17, 795–814.

Simões, J. C., Petit, J. R., Souchez, R., Lipenkov, V. Y., de Angelis, M., Leibao, L., Jouzel, J., and Duval, P. (2002). Evidence of glacial flour in the deepest 89 m of the Vostok ice core. *Ann. Glaciol.* 35, 340–346.

Skidmore, M. (2011). "Microbial communities in Antarctic subglacial aquatic environments," in *Antarctic Subglacial Aquatic Environments*, eds M. Siegert, M. Kennicutt, and R. Bindschadler, Geophysical Monograph 192 (Washington, DC: American Geophysical Union Press), 61–81.

Skidmore, M., Bakermans, C., Brox, T., Christner, B. C., and Montross, S. (2009). Microbial respiration at sub-zero temperatures in laboratory ices. *Geochim. Cosmochim. Acta* 73, A1234.

Smallwood, M., Worrall, D., Byass, L., Elias, L., Ashford, D., Doucet, C. J., Holt, C., Telford, J., Lillford, P., and Bowles, D. J. (1999). Isolation and characterization of a novel antifreeze protein from carrot (*Daucus carota*). *Biochem. J.* 340, 385–391.

Tung, H. C., Price, P. B., Bramall, N. E., and Vrdoljak, G. (2006). Microorganisms metabolizing on clay grains in 3-km-deep Greenland basal ice. *Astrobiology* 6, 69–86.

Walker, V. K., Palmer, G. R., and Voordouw, G. (2006). Freeze-thaw tolerance and clues to the winter survival of a soil community. *Appl. Environ. Microbiol.* 72, 1784–1792.

Weber, K., and Osborn, M. (1969). The reliability of molecular weight determinations by dodecyl sulfate-polyacrylamide gel electrophoresis. *J. Biol. Chem.* 244, 4406–4412.

Wen-li, X., Mei-qin, L., Xin, S., and Cun-fu, L. (2005). Expression of a carrot 36 kD antifreeze protein gene improves cold stress in transgenic tobacco. *For. Stud. China* 7, 11–15.

Wüest, A., and Carmack, E. (2000). A priori estimates of mixing and circulation in the hard-to-reach water body of Lake Vostok. *Ocean Model.* 2, 29–43.

Conflict of Interest Statement: The authors declare that the research was conducted in the absence of any commercial or financial relationships that could be construed as a potential conflict of interest.

Received: 30 September 2011; accepted: 01 December 2011; published online: 26 December 2011.

Citation: Achberger AM, Brox TI, Skidmore ML and Christner BC (2011) Expression and partial characterization of an ice-binding protein from a bacterium isolated at a depth of 3,519 m in the Vostok ice core, Antarctica. Front. Microbio. ***2****:255. doi: 10.3389/fmicb.2011.00255*

This article was submitted to Frontiers in Extreme Microbiology, a specialty of Frontiers in Microbiology.

frontiers in
MICROBIOLOGY

ORIGINAL RESEARCH ARTICLE
published: 27 December 2011
doi: 10.3389/fmicb.2011.00263

Linking microbial heterotrophic activity and sediment lithology in oxic, oligotrophic sub-seafloor sediments of the North Atlantic Ocean

***Aude Picard*[1,2]* *and Timothy G. Ferdelman*[1,2]**

[1] *Department of Biogeochemistry, Max Planck Institute for Marine Microbiology, Bremen, Germany*
[2] *MARUM – Center for Marine Environmental Sciences, Bremen, Germany*

Edited by:
Axel Schippers, Federal Institute for Geosciences and Natural Resources (BGR), Germany

Reviewed by:
Jens Kallmeyer, University of Potsdam, Germany
Gordon Webster, Cardiff University, UK

***Correspondence:**
Aude Picard, Geomicrobiology, Center for Applied Geoscience, Eberhard Karls University Tübingen, Sigwartstrasse 10, 72076 Tübingen, Germany.
e-mail: aude.picard@uni-tuebingen.de

Microbial heterotrophic activity was investigated in oxic sub-seafloor sediments at North Pond, a sediment pond situated at 23°N on the western flank of the Mid-Atlantic Ridge. The North Pond sediments underlie the oligotrophic North Atlantic Gyre at 4580-m water depth and cover a 7–8 million-year-old basaltic crust aquifer through which seawater flows. Discrete samples for experimentation were obtained from up to ∼9 m-long gravity cores taken at 14 stations in the North Pond area. Potential respiration rates were determined in sediment slurries incubated under aerobic conditions with ^{14}C-acetate. Microbial heterotrophic activity, as defined by oxidation of acetate to CO_2 (with O_2 as electron acceptor), was detected in all 14 stations and all depths sampled. Potential respiration rates were generally low (<0.2 nmol of respired acetate cm^{-3} d^{-1}) in the sediment, but indicate that microbial heterotrophic activity occurs in deep-sea, oxic, sub-seafloor sediments. Furthermore, discernable differences in activity existed between sites and within given depth profiles. At seven stations, activity was increased by several orders of magnitude at depth (up to ∼12 nmol of acetate respired cm^{-3} d^{-1}). We attempted to correlate the measures of activity with high-resolution color and element stratigraphy. Increased activities at certain depths may be correlated to variations in the sediment geology, i.e., to the presence of dark clay-rich layers, of sandy layers, or within clay-rich horizons presumably overlying basalts. This would suggest that the distribution of microbial heterotrophic activity in deeply buried sediments may be linked to specific lithologies. Nevertheless, high-resolution microbial examination at the level currently enjoyed by sedimentologists will be required to fully explore this link.

Keywords: microbial activity, heterotrophy, deep biosphere, oxic, marine sediment

INTRODUCTION

The mineralization of organic matter in marine sediments is governed by microbial metabolism. In the deep subsurface (>1.5 mbsf) of marine sediments, sulfate reduction, methanogenesis, and fermentation are considered to be the main metabolic activities responsible for the degradation of organic matter to small organic acids and CO_2 (e.g., Parkes et al., 2000; D'hondt et al., 2002). However, since most sub-seafloor sediments considered in previous studies underlie productive coastal or upwelling areas, the microbial processes reflect the consequences of a high organic carbon flux to the seafloor, in which oxygen is rapidly depleted (D'hondt et al., 2009). Oligotrophic regions occur in the subtropical ocean gyres that represent a major part of the world's ocean where the organic matter flux to the sediments is low, leading to deep oxygen penetration depths of tens of centimeters or more (Murray and Grundmanis, 1980). At the extreme, penetration depths of dissolved oxygen in the South Pacific Gyre sediments reached up to 9 m (D'hondt et al., 2009; Fischer et al., 2009).

Deep penetration of oxygen in sediments of the Atlantic Ocean to ∼9 meters have also been shown in sediments contained in ponded basins on the flanks of the North Mid-Atlantic Ridge (MAR), in the so-named North Pond (Cruise report MSM 11/1). North Pond is an isolated region of ponded sediment situated at ∼100 km west of the rift valley of the MAR and∼110 km south of the Kane fracture zone (22°46′N and 46°06′W; e.g., Hussong et al., 1979; Purdy et al., 1979). It is a large pond (∼13 km N–S and ∼7 km E–W) and lies below a low-productivity 4580-m water column. The sediment at North Pond can reach up to 300 m thickness and overlies a young basaltic active crust (7–8 Ma) through which vigorous lateral flow of cold seawater has been proposed to take place (Langseth et al., 1984).

We investigated microbial heterotrophic activity in sediment cores recovered at North Pond. Studies of microbial life in deep-oxic sediments are rare (D'hondt et al., 2009), and no measurements of experimentally determined, potential respiration rates have been reported yet in sub-seafloor sediment in which oxygen is penetrating several meters deep. We used ^{14}C-acetate in the deep-oxic sediments from North Pond for this purpose as acetate has been proven to be well-suited to estimate potential respiration and uptake rates of organic molecules in subsurface environments

(e.g., Wirsen and Jannasch, 1974; Phelps et al., 1989; Fredrickson et al., 1997). In the case of anoxic sediments the changes in pore water chemistry usually help to target the zones where specific types of microbial activity can be expected (i.e., sulfate–methane transition zones). At North Pond, the sampled sediments were oxic throughout, thus the sampling strategy was different. To gain an overview of the potential respiration rates, which were expected to be low and decreasing with depth at all stations, we sampled the oxic sediment with a regular spacing along the length of gravity cores obtained from North Pond. Occasionally, distinct layers, such as sandy, clay-rich, dark layers, were also sampled.

The goal of the microbial heterotrophic activity measurements was to compare potential respiration rates at different stations over a small area and investigate correlations between activity profiles and geological features. We present profiles of potential microbial heterotrophic activity in deep-sea, deep-oxic sub-seafloor sediments, and examine these rates in conjunction with respect to variations in sediment lithology.

MATERIALS AND METHODS

SEDIMENT COLLECTION

The North Pond area was visited during cruise MSM 11/1 on R/V Maria S. Merian in February–March 2009. Sediment cores were taken at 14 stations using a gravity corer (**Table 1**, **Figure 1**). Cores were split in two halves and labeled following the GeoB system of the University of Bremen. One half was kept intact for scanning analyses (archive half) while the other half was sampled for multiple purposes (work half). Sediment for activity measurements was sampled aerobically every meter. Additional samples were taken in specific cores when the sediment showed obvious lithological samples or color changes. Sediment was stored and transported at 4°C. Pore water samples for acetate measurements were taken within hours after core retrieval using Rhizone soil moisture samplers (Rhizosphere Research Products, Wageningen, The Netherlands). The Rhizone consists of an inert porous polymertube with a length of 10 cm and a pore size of 0.1 mm. Pore fluid is extracted by vacuum created with disposable 10 ml syringes connected to the Rhizone, frozen and kept at −20°C until analysis.

PROKARYOTIC ACTIVITY MEASUREMENTS

Sediment slurries were prepared with 1 volume of sediment for 4 volumes of oxic artificial seawater (ASW; Süß et al., 2004) and distributed into Eppendorf tubes for incubation (1 ml slurry per tube). The potential respiration rates were estimated by measuring the production of $^{14}CO_2$ from the oxidation of ^{14}C-acetate (sodium ^{14}C-acetate, 5.8 µl, 43 kBq, 20 nmol, GE Healthcare Life Sciences, UK or sodium ^{14}C-acetate, 1.16 µl, 43 kBq, 20 nmol, American RadioChemicals, Saint-Louis, MO, USA). Two living samples and one formaldehyde-treated sample (2% v/v final concentration, dead control) were prepared for each of three incubation periods (3, 8, and 15 days) and amended with the radiotracer. Samples were incubated at 4°C (close to the *in situ* temperature of 2.5°C). Incubation was terminated by pouring the 1 ml slurry into 9 ml of 2.5% NaOH. Measurement of $^{14}CO_2$ (diffusion method) was performed as described in Treude et al. (2003) with slight modifications. Samples in NaOH (5 ml) were transferred to 100-ml glass vials with 5 ml of 2.5% NaOH. A 6-ml scintillation vial containing 1 ml of beta-phenylethylamine and 1 ml of NaOH 0.5 M was fixed to the rubber stopper that closed the glass vial, hanging well above the sample to trap the $^{14}CO_2$ in the headspace. Samples were then acidified with 6 ml of HCl 6 N to release the CO_2 in the headspace and gently shaken (88 rpm) for at least 4 h at room temperature. A scintillation cocktail (ScintiGold, Perkin Elmer, USA) was added to the samples. Activity (in DPM) of the trapped $^{14}CO_2$ was measured using a liquid scintillation counter (Tri-Carb 2500TR or 2900TR, Packard, now Perkin Elmer, USA). Rates of acetate respiration were calculated using the following equation:

$$R = \frac{^{14}CO_2 \times \left[^{14}C \cdot \text{acetate}\right]}{^{14}C \cdot \text{acetate} \times v \times t} \quad (1)$$

where R is the rate of acetate respiration in the sediment (in nanomole cm^{-3} d^{-1}), $^{14}CO_2$ is the activity of the produced carbon

Table 1 | Stations of the MSM 11/1 cruise: sampling positions, water depth, sediment depth recovered, depths of samples for activity experiments.

Station (GeoB)	Latitude (N)	Longitude (W)	Water depth (m)	Total sediment depth (cm)	Number of samples for activity
13501	22°46,62′	46°6,42′	4480	844	9
13502	22°49,41′	46°3,23′	4250	847	10
13503	22°49,20′	46°3,50′	4365	689	5
13504	22°49,89′	46°2,78′	4096	72	4
13505	22°47,55′	46°7,40′	4402	76	2
13506	22°48,36′	46°7,51′	4143	574	6
13507	22°48,04′	46°6,30′	4395	865	11
13508	22°46,89′	46°6,59′	4475	344	4
13509	22°47,47′	46°6,45′	4438	267	3
13510	22°47,35′	46°6,44′	4448	515	6
13511	22°47,12′	46°6,49′	4445	468	5
13512	22°49,33′	46°6,45′	4200	516	5
13513	22°49,00′	46°2,64′	4262	504	5
13514	22°49,15′	46°2,39′	4040	237	3

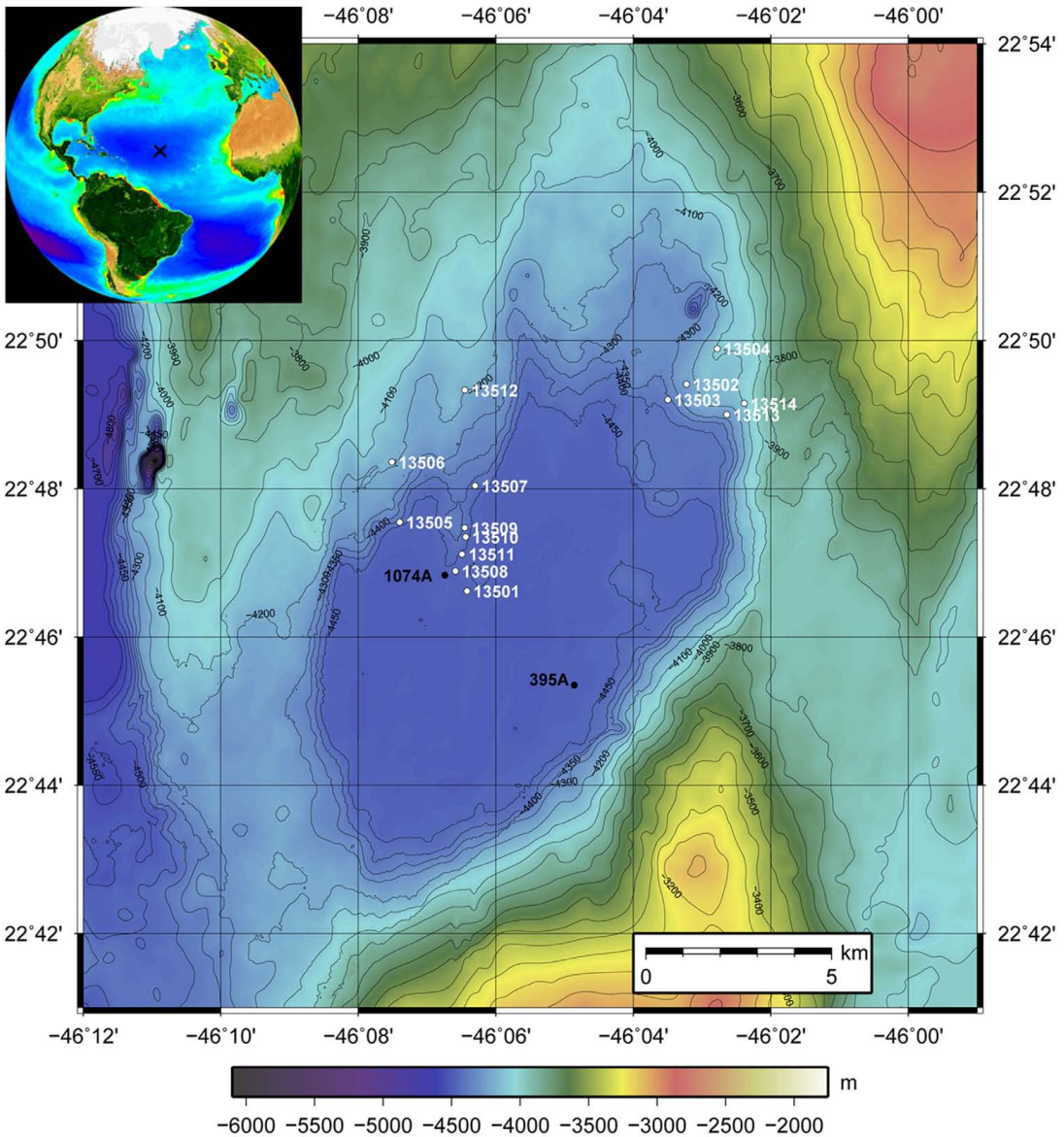

FIGURE 1 | Bathymetric map of North Pond. Stations are indicated with the white numbers (GeoB 13501–GeoB 13514). GeoB 13501 is the reference station situated near the center of the pond in the flat, deep center of the sediment pond. All others cores have been taken at shallower depths on the edges of the pond where sediment thicknesses are reduced. The inset shows the situation of North Pond in the Atlantic Ocean (generated on oceancolor.gsfc.nasa.gov/SeaWiFS).

dioxide in the living samples (in DPM) corrected by the activity (in DPM) in the dead samples, [^{14}C-acetate] is the concentration of acetate added as a tracer (in nmol), ^{14}C-acetate is the activity of the tracer added (in DPM), v is the volume of sediment (in cm^3), and t is the time of incubation (in d).

MONITORING OF OXYGEN CONCENTRATION DURING SLURRY INCUBATION

Oxygen concentration was monitored in one sediment sample to evaluate if the conditions remained oxic throughout the experiment. The sample was selected from core GeoB 13506 (131.5 cm below the seafloor) and slurry was prepared as described above and transferred to a borosilicate glass vial without headspace. Incubation was performed at 4°C. Non-labeled acetate was added at the same concentration than in the experiment with labeled acetate. Oxygen was measured during the incubation with a needle-type optical oxygen microsensor (PreSens Precision Sensing GmbH, Germany). It consisted of a fiber optic cable mounted in a needle at the end of a 1-ml syringe. The needle was inserted into the borosilicate vial through a silicon septum. The sensor was extended for measurement into the sediment phase of the slurry. The microsensor readout was made using a Microx TX3 (PreSens

Precision Sensing GmBH) micro-fiber optic oxygen transmitter. A two-point calibration using anoxic and air-saturated ASW at 4°C was used.

ACETATE MEASUREMENTS

Concentrations of acetate (and other volatile fatty acids) were determined in pore water samples by high-performance liquid chromatography (HPLC) using the method of Albert and Martens (1997), as adapted by Finke and Jorgensen (2008). Pore water samples (1 ml) were transferred into borosilicate glass vials (previously combusted at 480°C for 4 h). Acids were derivatized with *p*-nitrophenyl hydrazine, eluted with ion-pairing solvents and separated by HPLC using a LiChrosphere 80/100 column (Knauer, Berlin, Germany) at 25°C. The presence of acids was determined by UV absorption at 400 nm with a UV/VIS detector (Linear). The chromatograms were analyzed using the commercially available software Chromstar (Bechenheim, Germany). Standard solutions containing known concentrations of lactate, acetate, formate, propionate, isobutyrate, and butyrate were used. The detection limit for acetate was at 3 μM.

CORE ANALYSES

Undisturbed, archive halves of the gravity core sections were stored at 4°C at the core repository of the University of Bremen (Germany) until analyzed in 2011. Nine sediment cores chosen for detailed core analysis were prepared for non-destructive high-resolution digital, light, and x-ray fluorescence scanning using stainless steel or glass blades to provide a smooth and regular surface.

Digital imaging

High-resolution digital images of the split cores were taken using the GEOTEK Geoscan-III color line scan camera (3 CCD device using 3 × 1024 pixel CCD arrays, RGB detectors) mounted on the rack of the GEOTEK Multi-Sensor Core Logger (MSCL) at the University of Bremen.

Light reflectance

The light reflectance (L*) was measured at the surface of the split cores (covered with a thin film) using a Konica Minolta portable color spectrophotometer CM-2600d with diffuse illumination and 8° viewing angle (University of Bremen). Measurements were done every 2 cm on an 8-mm diameter area. The wavelength range of the instrument was 360–740 nm. The instrument was calibrated using a white-calibration plate and a zero-calibration box.

X-ray Fluorescence scanning

X-ray fluorescence (XRF) core scanner data were collected every 2 cm down-core (except for core 13504, every 1 cm down-core) over a 120 mm^2 area and with a sampling time of 20 s directly at the split core surface of the archive half with the Avaatech XRF Core Scanner II at MARUM-University of Bremen. The split core surface was covered with a 4 μm thin SPEX CertiPrepUltralene® foil to avoid contamination of the XRF measurement and desiccation of the sediment. The X-ray generator was an Oxford Instruments XTF5011 Rhodium X-ray tube 93057 set at an energy of 10 keV and at a current of 0.2 mA. The XRF data were acquired by a Canberra X-PIPS Silicon Drift Detector (SDD, model SXD 15C-150-500) with 150 eV X-ray resolution with a Canberra digital spectrum analyzer DAS 1000 as interface. Raw XRF spectra were processed using the WIN AXIL (Analysis of X-ray spectra by Iterative Least square) package from Canberra Eurisys.

RESULTS

SITE DESCRIPTION AND SEDIMENT CHARACTERISTICS

Fourteen gravity cores were taken during MSM 11/1 in water depths between 4040 and 4480 m (**Table 1**; **Figure 1**). Station 13501 is near the center of the pond at a water depth of 4480 m and served as a reference since it is in the deep, flat part of the pond with the greatest sediment thickness. Other stations were sampled where sediment thicknesses are reduced, at the N–E edge of the pond (GeoB13502, 13503, 13504, 13513, and 13514), at the N–W edge of the pond (GeoB13505, 13506, 13507, and 13512), and on a crest directed toward the center of the pond (GeoB13508, 13509, 13510, and 13511). Slumps of sediments occur on the slopes, thus the sedimentary pile is reduced. We targeted the sediment–basalt interface at these stations.

The principal lithology at North Pond is yellowish-brown to brownish-yellow pelagic sediment, ranging from nannofossil ooze with variable amounts of clay and foraminifers to foraminifer rich sand to clay (Timofeev et al., 1979; Cruise report MSM 11/1). The presence of sharp, irregular bottom contacts, and normal graded bedding indicates that the sandy coarse-grained intervals are the result of gravity flows supplied from the surrounding slopes (e.g., in GeoB 13501, **Figure 2**). Sand layers are found only in cores retrieved from depths >4300 m below sea level. At two sites, GeoB13504 (**Figure 3**) and GeoB13505, dense yellow to ochre clay was recovered. This clay ostensibly overlies basalt (Timofeev et al., 1979). The lower clay layer at GeoB13504 contained micrometer-sized fragments of basalt and glass. Mn micronodules within the nannofossil ooze, ranging from <1 to 3 mm in diameter, were identified in many cores.

Visible-light reflectance was measured at the surface of the archive core halves of nine selected stations and correlates well with the carbonate content of the sediment as established previously (Giosan et al., 2002; Rogerson et al., 2006). XRF provided semi-quantitative measurements of light elements (Al, Si, K, Ca, Ti, Mn, and Fe) that can be used to evaluate their relative abundance along the cores. Ca is used to record carbonate content; Ca/Al is used as an indicator of fine-grained sediments vs. coarse-grained sediments, thus the higher the ratio the coarser the grain size (Richter et al., 2006). GeoB13501 (**Figure 2**) and 13504 (**Figure 3**) contain the principal lithological features observed at North Pond during MSM 11/1 cruise and are therefore described here in details. Values of L* ranged from 40.27 to 64.25 in Core GeoB13501 (**Figure 2**); foraminifer sand layers at 257–261, 264–271, 538–546, 644–653, 702–713, 742–764, and 777–781 cm (yellow lines in **Figure 2**) correspond to L* maxima and are further highlighted by peaks in the Ca/Al ratio. The high L* values are generally correlated with high Ca counts, which, in turn, correspond to a high carbonate content. The lowest L* values at 444 and 518 cm in GeoB13501 occur at dark layers richer in clay than the surrounding nannofossil ooze and correspond to low Ca/Al ratios (gray lines in **Figure 2**). The presence of Mn micronodules at ∼440, ∼580, ∼675, and ∼800 cm is

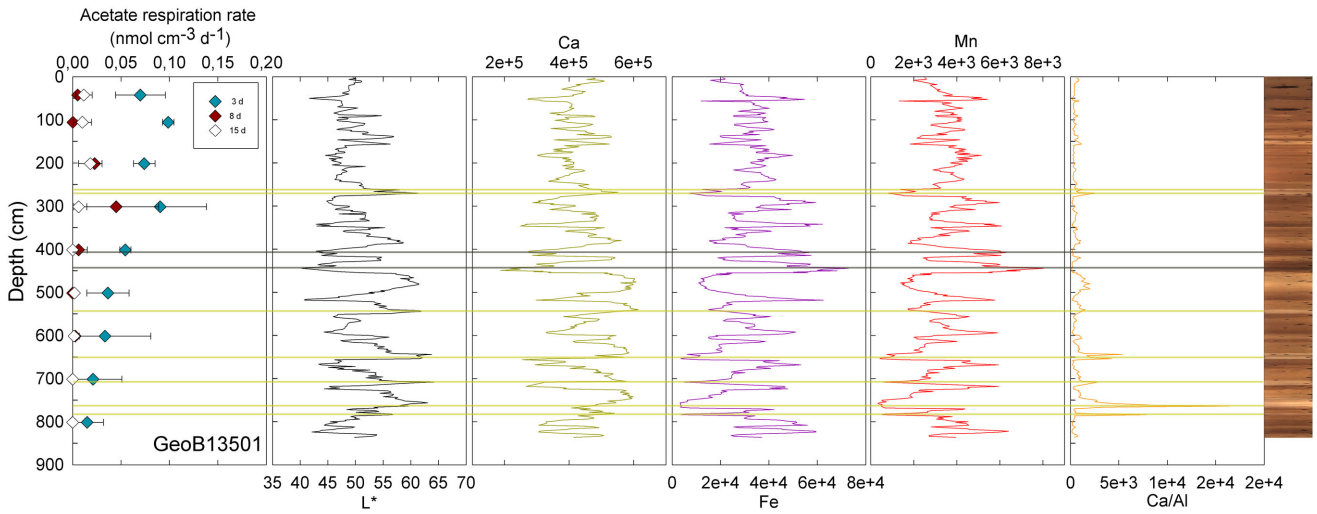

FIGURE 2 | GeoB 13501 activity rates (at 42.5, 105.5, 201.5, 301.5, 401.5, 501.5, 601.5, 701.5, 801.5 cm) and detailed lithological features (L*, Ca, Fe, Mn, and Ca/Al). GeoB 13501 presents several sand layers (yellow lines) and two clay-rich layers (gray lines). Mn micronodules occur at the Mn peaks.

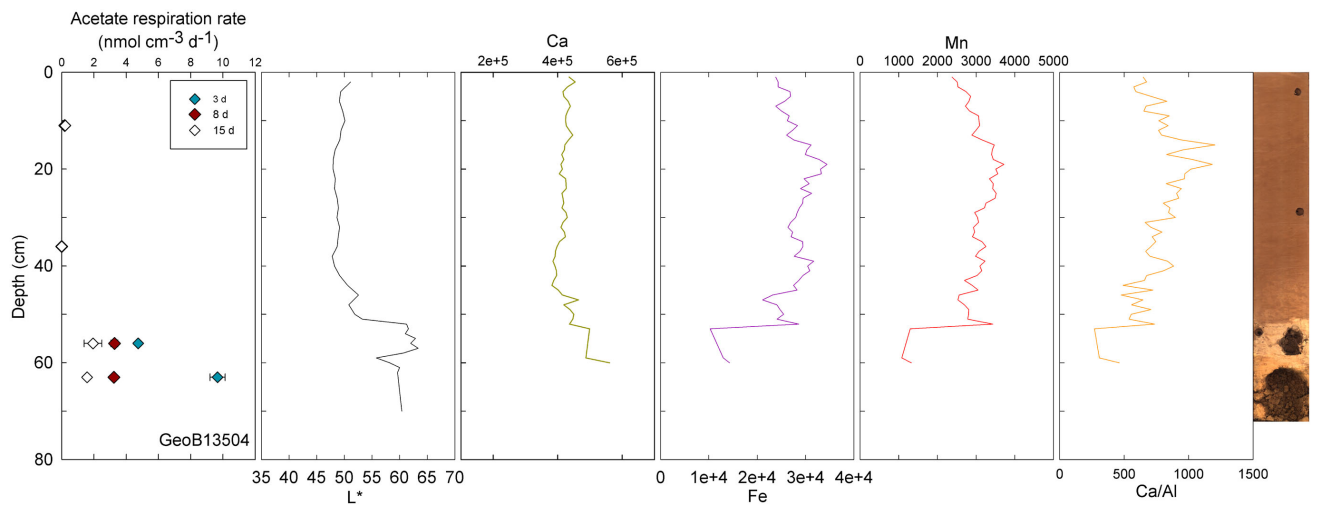

FIGURE 3 | GeoB 13504 activity rates (at 11, 36, 56, and 63 cm) and detailed lithological features (L*, Ca, Fe, Mn, and Ca/Al). GeoB 13504 is characteristic of the sediment–basalt transition beginning at ~52 cm. Micro-fragments of basalt are present in the lower clay-rich layer.

confirmed by Mn and Fe maxima. In GeoB13504, L* ranged from 47.86 to 63.41 (**Figure 3**). L* increased abruptly at the transition (~55 cm) between the nannofossil ooze and the putative dense clay layer. Ca and thus carbonate content increased while Fe and Mn decreased. However the Ca/Al ratio decreased significantly at the transition, confirming the presence of very fine-grained sediment which may overlie basalt.

POTENTIAL RESPIRATION RATES IN DEEP-OXIC SUB-SEAFLOOR SEDIMENTS

Acetate concentrations were below the detection limit (3 μM). However, potential microbial heterotrophic activity (as measured by the oxidation of ^{14}C-acetate to $^{14}CO_2$) was detected in sediment samples recovered from all 14 stations. In all of the samples, the highest rate was measured after the shortest incubation time (3 days) except in samples from GeoB13502 and 13510. A sample from core GeoB 13506 was selected to monitor the oxygen concentration in the slurry as a function of time. In this sample, in which the maximal rate was at 0.41 nmol cm^{-3} d^{-1}, oxygen was completely depleted only after 20 days. We therefore assumed that most of the slurries remained oxic throughout the experiment. Thus, a switchover to anaerobic respiration after 3 days can be excluded. Overall, most of the experiments yielded low rates of potential activity (<0.2 nmol cm^{-3} d^{-1}), consistent with the expected low fluxes of organic matter to the sediments at North Pond.

At three stations, rates of activity were greatest in the samples taken in the upper 80 cm: 0.21 nmol cm^{-3} d^{-1} at 57.5 cm in GeoB13511, up to 1.46 nmol cm^{-3} d^{-1} at 6 cm in GeoB13510,

and 10.62 nmol cm^{-3} d^{-1} at 75.5 cm in GeoB 13512. In contrast, enhanced rates of potential acetate turnover were not restricted to just near the surface at the other seven stations. At GeoB13506 (131.5 cm), rates reached 0.41 nmol cm^{-3} d^{-1} in a layer that presented subtle color mottling (presumably associated with preserved bioturbation structures). At GeoB13508, peaks in activity were present at depth with rates of up to 0.17 (281.5 cm) and 0.21 nmol cm^{-3} d^{-1} (331.5 cm). Higher rates of potential acetate turnover were located just below and near sandy layers, which are present at 264–265 cm and 326–344 cm. Another example of increased activity in sandy layer is present in GeoB13507 (**Figure 4**), where in the sample taken at 718 cm in the middle of a sand layer (713–722 cm) activity was up to 7.52 nmol cm^{-3} d^{-1}. The increase in activity is even more remarkable in the sample taken at 723.5 cm just below the sandy layer (up to 12.10 nmol cm^{-3} d^{-1}). The deepest sample investigated in GeoB 13507 (822.5 cm), which is also situated below a sand layer at 812–814 cm, also showed high rates of potential activity (up to 4.63 nmol cm^{-3} d^{-1}). At GeoB 13513, the highest rate (up to 1.01 nmol cm^{-3} d^{-1}) occurred in the sample taken at 159.5 cm, which, as shown in **Figure 5**, correlated with a relatively distinct peaks in L*, Ca counts and Ca/Al. In GeoB 13502, the peaks in potential acetate turnover occurred at three layers at depth: 104.5, 604.5, and 804.5 cm (**Figure 6**).

Conversely, enhanced rates of acetate turnover at 104.5 cm correspond to low L*, and low Ca/Al values. Likewise, a slight increase of activity in GeoB13507 (up to 0.99 nmol cm^{-3} d^{-1}) at 300.5 cm, occurs in one of the darkest layers of the core (L* at 302 cm is at 41.31). This layer is also associated with the lowest intensity of Ca and a low Ca/Al ratio. This dark layer is also characterized by the presence of Mn micronodules, as confirmed by high Mn contents (data not shown). Finally, at GeoB 13504 (**Figure 3**) and GeoB13514 (**Figure 7**), activity peaks occurred in the deepest layers recovered, 56 and 63 cm and 205.5 cm, respectively. The presence of clay and basalt micro-fragments at the bottom of core 13504 suggests proximity to the basalt. The clay was very light in color and thus the L* value is the highest zone. The high L* matches a high Ca content up to 60 cm.

Samples taken at 604.5 in GeoB 13514 and at 804.5 cm in GeoB 13502, high L* (as well as high Ca/Fe ratio) was coincident with enhanced rates of acetate turnover. In the lower parts of cores 13502 and 13514, the sediment became dense and light-colored. Cores 13504, 13514, and 13502 have in common their location at the top of the north–east edge of the pond, the two first being at a water depth of 4096 and 4040 m, respectively, while the latter is at 4250 m water depth.

DISCUSSION

North Pond sediments are oligotrophic, nonetheless, our experiments indicate that microbial heterotrophic communities continue to be active in these deeply buried sediments. The communities react immediately to the supply of acetate as substrate, as no lag phase was observed before the oxidation of acetate to carbon dioxide. In our experiments, we added labeled acetate to concentrations of 20 μmol l^{-1}. Growth of a specific aerobic acetotrophic (acetate-oxidizing) community can be excluded with a reasonable probability. More likely, heterotrophic communities are present and potentially active at all depths of the sediments sampled. Moreover, the range of potential activities is highly variable on both depth and lateral scales.

Such heterogeneity in potential activity rates over a small area is remarkable in such an oligotrophic environment, where one would expect low activity rates throughout the cores without much variation. Conversely, nitrate and oxygen fluxes at the surface sediment – water interface appear to be similar across all sites (Cruise report MSM 11/1). Some of this variability in potential activity may be linked to the location and water depth of the sites sampled. In three cores, the activity maxima occurred near the surface, where organic matter is younger and expectedly more accessible toward microbial degradation. The location in the pond might thus influence the magnitude of the increase in activity. For example, the three stations with greater near-surface acetate turnover rates follow a crest directed toward the center of the pond. GeoB13511 is at the bottom of the slope at 4445 m water depth; GeoB13510 is a bit further north on the slope at 4448 m water depth and GeoB13512 is northern at 4200 m water depth at the top of the edge. However, these three stations were the only ones where potential activity was greatest near the surface observed in the upper core; otherwise, peaks in potential acetate turnover could be observed at various depths.

While microbial cell counts and activities tend to decrease with increasing depth in the deep anaerobic sub-seafloor (Parkes et al., 1994, 2000), occurrences of enhanced activity in deep anoxic subseafloor layers have been attributed to geochemical reaction zones, e.g., at sulfate–methane transition zones; at fluid or gas-venting sites; or due to thermally driven alteration of organic matter to form acetate or methane (Cragg et al., 1992, 1995; Wellsbury et al., 1997; Parkes et al., 2005). Remarkable case of increases in subseafloor microbial population abundances and activities have also been observed in gas hydrate associated sediments (Cragg et al., 1995, 1996; Wellsbury et al., 2000).

On the other hand, down-core variability in microbial populations and enhanced microbial activities may be more closely related to changes in the lithology. At an open-ocean site of the Equatorial Pacific (site 1226, ODP Leg 201), prokaryotic activity was stimulated within Miocene age diatomaceous-rich layers (Parkes et al., 2005). At this same site, fluctuations in microbial populations have been related to depositional cycles of high organic carbon content linked to Milankovitch cycles (Aiello and Bekins, 2010). The stimulation of microbial activity at interfaces has also been studied in subsurface consolidated sedimentary structures. For example, increased microbial activity was observed in permeable sandstone layers adjacent to low-permeability organic-rich shales (Fredrickson et al., 1997; Krumholz et al., 1997) and was fueled by excess organic acids produced in the shales which diffused into the adjacent sandstone sediments (McMahon and Chapelle, 1991; McMahon et al., 1992; Fredrickson et al., 1997; Krumholz et al., 1997; Fry et al., 2009).

The North Pond sedimentary ecosystem is, at first glance, different from the systems described above. Specifically geochemical measurements indicate the presence of only one electron acceptor, i.e., oxygen (Cruise report MSM 11/1). In such an oligotrophic environment one would assume low rates of activity that decrease with increasing depth. Nevertheless, lithologic variability on a

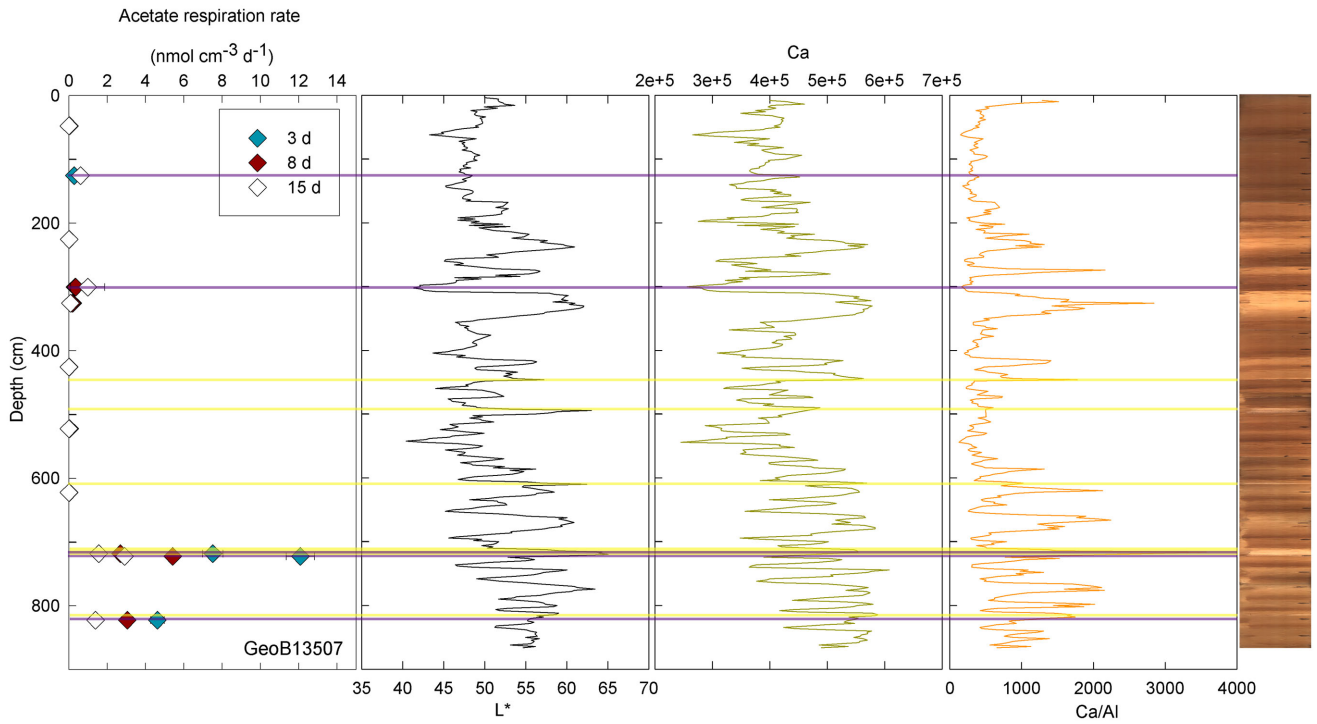

FIGURE 4 | GeoB 13507 linked activities and lithological features. Yellow lines denote sandy layers; purple lines denote depths of greater potential acetate turnover. Samples were taken at 47.5, 125.5, 225.5, 300.5, 325.5, 425.5, 522.5, 622.5, 718, 722.5, and 822.5 cm.

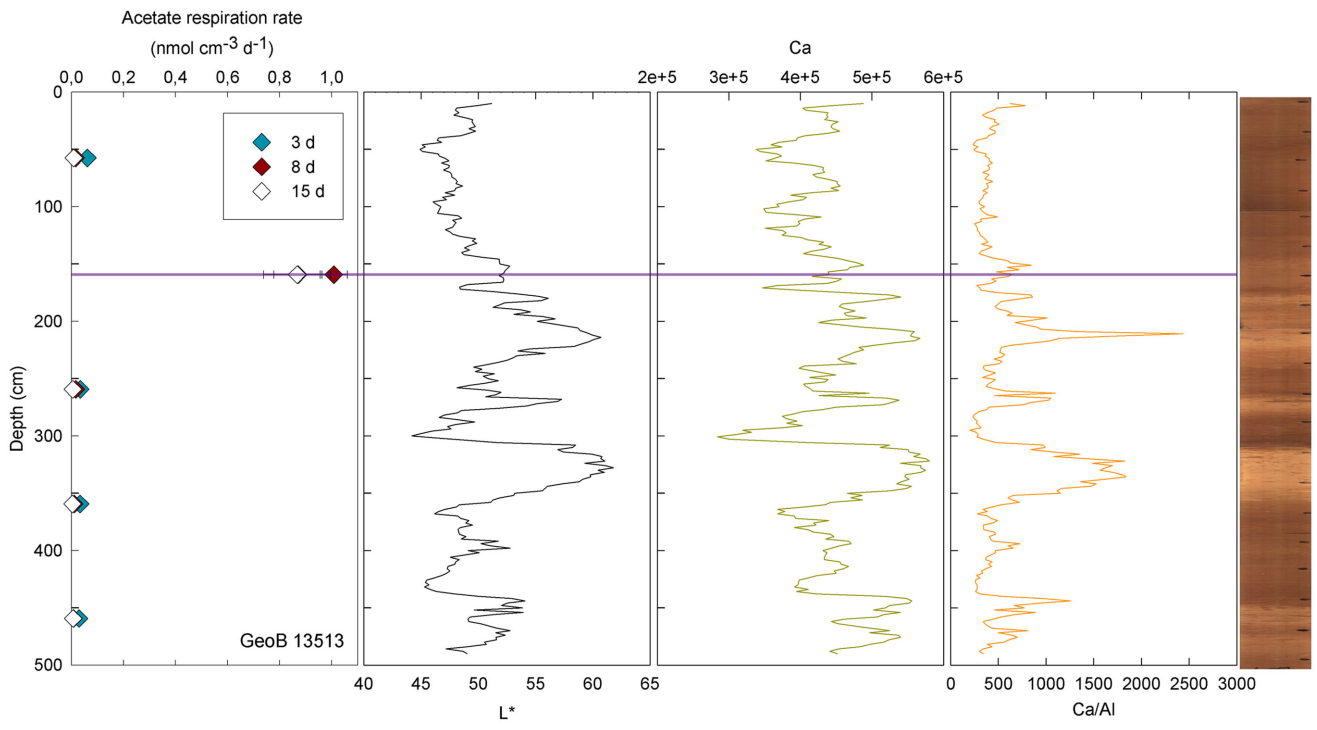

FIGURE 5 | GeoB 13513 linked activities and lithological features. Purple line denotes depth of greater potential acetate turnover. Samples were taken at depths 57.5, 159.5, 259.5, 359.5, and 459.5 cm.

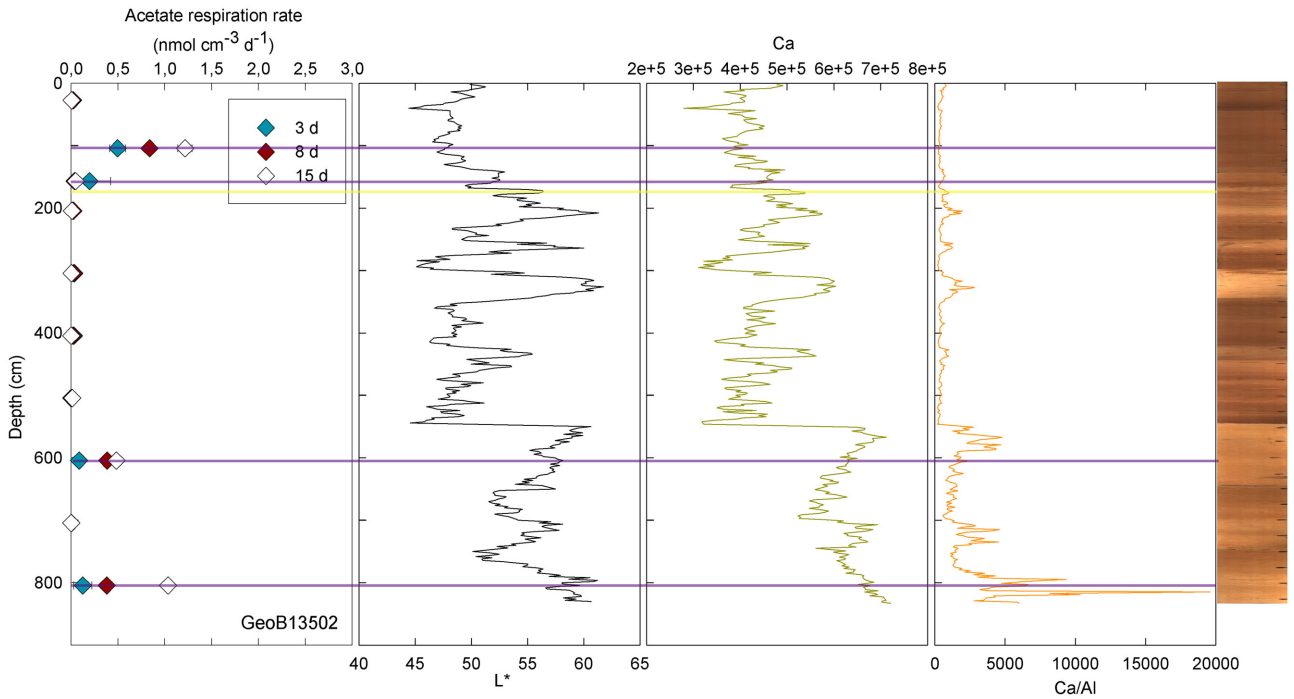

FIGURE 6 | GeoB 13502 linked activities (at 27.5, 104.5, 157, 204.5, 304.5, 404.5, 504.5, 604.5, 704.5, and 804.5 cm) and lithological features (L*, Ca, and Ca/Al). Yellow lines denote sandy layers; purple lines denote depths of greater potential acetate turnover.

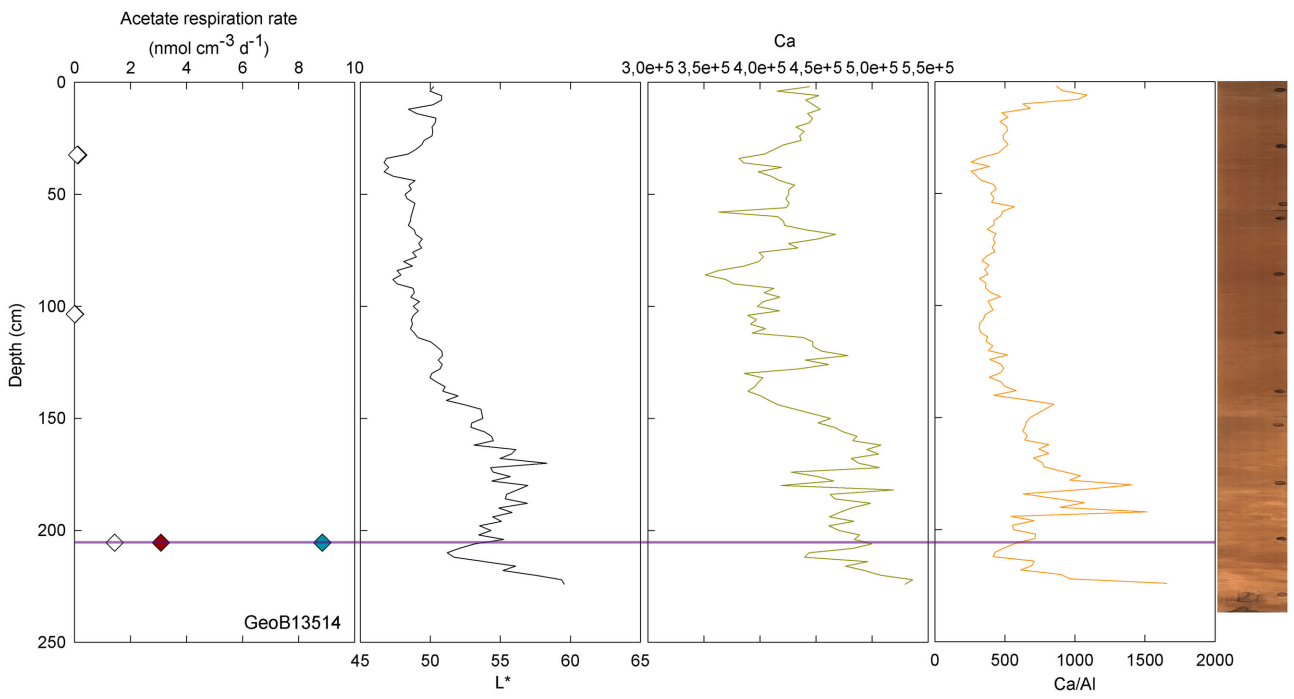

FIGURE 7 | GeoB 13514 linked activities (at 32.5, 103.5, and 205.5 cm) and lithological features (L*, Ca, and Ca/Al). Purple line denotes depths of greater potential acetate turnover.

centimeter- to decimeter-scale can be seen throughout all of the examined cores (e.g., color scan figures in **Figures 2–7**). A link between sediment lithology and potential activity might therefore dictate the variability in the observed rates of potential activity.

We can associate the peaks in potential acetate turnover with three different types of lithology, but no one single lithological type appears to dominate. (1) In cores GeoB13507 and GeoB13508 increased microbial heterotrophic activity can be observed near sandy layers, which are characterized by a high L* value, a high Ca content and a high Ca/Al ratio. Due to a different permeability, sand layers may be a source of dissolved organic matter that diffuses into the adjacent clay layers, for example as described by Fredrickson et al. (1997) and Krumholz et al. (1997). (2) Other carbonate-rich layers also seem to influence microbial heterotrophic activity in several of the sites cores. In GeoB13506, 13513, 13502, 13514, and 13504, increases in activity are also related to relatively high L* value, Ca content and Ca/Al ratio. At GeoB 13504 the presence of clay indicates the proximity to the basaltic basement. Based on increases with depth of dissolved oxygen (Cruise report MSM 11/1), it is inferred that the basalt is in near proximity at GeoB13514, GeoB 13504, and GeoB13502. Even without the presence of clay at GeoB 13514 and GeoB 13502, it is probable that the basal part of the retrieved sediment section represents the transition to the clay overlying the basaltic basement. (3) Finally there are occurrences of increased activity in cores 13502 and 13507 at dark layers, presumably containing more clay than the surrounding nannofossil ooze.

The experiments show that heterotrophic microbial communities are active in deeply buried sediments, even in oligotrophic, low-organic carbon flux conditions. Most of the highest rates could be partially correlated with the presence of basalt nearby or directly associated with the presence of sandy layers. This suggests that microbial populations are stimulated near/at geological layers where lateral transport of fluids can occur and potential substrates can be provided to the microbes residing in the sediments. Nevertheless, we also detected potential rates of acetate turnover in other distinctly different lithological layers.

Thus, while we can not link increased microbial heterotrophic activity to a single, distinct lithological type, this study highlights the importance of a sampling strategy following the basic characteristics of the sediment, such as the color or the light reflectance, in the absence of strong pore water chemical gradients. A high-resolution study of the interfaces foraminifer sand/nannofossil ooze and basalt/clay would be of great interest. In the case of deep-oxic sediments, in which exposure to the atmosphere is not as critical, the sampling procedure could be dictated by non-destructive core analysis such as those employed in this study.

ACKNOWLEDGMENTS

The authors would like to thank the captain Klaus Bergmann and the crew of the R/V Maria S. Merian; chief scientist HeinerVillinger, and all participants of the MSM 11/1 cruise. We are particularly thankful to Wolfgang Bach for providing the sediment description, as well as insightful comments; to Verena Heuer for providing the pore water samples for acetate measurements; to Friederike Schmidt-Horn for providing the bathymetry map; and to Wiebke Ziebis for discussion. We thank Gabi Schüßler for the assistance in the lab with the $^{14}CO_2$ diffusion method. This research used data acquired at the XRF Core Scanner Lab at MARUM – Center for Marine Environmental Sciences, University of Bremen, Germany. We are thankful to Vera Lukes for help with digital picture and XRF data acquisition. XRF and light reflectance data are available on www.pangaea.de. Aude Picard was funded through DFG-Research Center/Excellence Cluster "The Ocean in the Earth System" and the Max Planck Society. Cruise MSM 11/1 was funded by the German Science Foundation (DFG).

REFERENCES

Aiello, I. W., and Bekins, B. A. (2010). Milankovitch-scale correlations between deeply buried microbial populations and biogenic ooze lithology. *Geology* 38, 79–82.

Albert, D. B., and Martens, C. S. (1997). Determination of low-molecular-weight organic acid concentrations in seawater and pore-water samples via HPLC. *Mar. Chem.* 56, 27–37.

Cragg, B. A., Harvey, S. M., Fry, J. C., Herbert, R. A., and Parkes, R. J. (1992). Bacterial biomass and activity in the deep sediment layers of the JapanSea, hole 798B. *Proc. Ocean Drill. Prog. Sci. Results* 127/128, 761–776.

Cragg, B. A., Parkes, R. J., Fry, J. C., Weightman, A. J., Rochelle, P. A., and Maxwell, J. R. (1996). Bacterial populations and processes in sediments containing gas hydrates (ODP Leg 146: Cascadia Margin). *Earth Planet. Sci. Lett.* 139, 497–507.

Cragg, B. A., Parkes, R. J., Weightman, A. J., Rochelle, P. A., Maxwell, J. R., Kastner, M., Hovland, M., Whiticar, M. J., and Sample, J. C. (1995). The impact of fluid and gas venting on bacterial populations and processes in sediments from the Cascadia Margin accretionary system (sites 888–892) and the geochemical consequences. *Proc. Ocean Drill. Prog. Sci. Results* 146, 399–411.

D'hondt, S., Rutherford, S., and Spivack, A. J. (2002). Metabolic activity of subsurface life in deep-sea sediments. *Science* 295, 2067–2070.

D'hondt, S., Spivack, A. J., Pockalny, R., Ferdelman, T. G., Fischer, J. P., Kallmeyer, J., Abrams, L. J., Smith, D. C., Graham, D., Hasiuk, F., Schrum, H., and Stancin, A. M. (2009). Subseafloor sedimentary life in the South Pacific Gyre. *Proc. Natl. Acad. Sci. U.S.A.* 106, 11651–11656.

Finke, N., and Jorgensen, B. B. (2008). Response of fermentation and sulfate reduction to experimental temperature changes in temperate and Arctic marine sediments. *ISME J.* 2, 815–829.

Fischer, J. P., Ferdelman, T. G., D'hondt, S., Roy, H., and Wenzhofer, F. (2009). Oxygen penetration deep into the sediment of the South Pacific gyre. *Biogeosci. Discuss.* 6, 3159–3186.

Fredrickson, J. K., Mckinley, J. P., Bjornstad, B. N., Long, P. E., Ringelberg, D. B., White, D. C., Krumholz, L. R., Suflita, J. M., Colwell, F. S., Lehman, R. M., and Phelps, T. J. (1997). Pore-size constraints on the activity and survival of subsurface bacteria in a Late Cretaceous shale-sandstone sequence, northwestern New Mexico. *Geomicrobiol. J.* 14, 183–202.

Fry, J. C., Horsfield, B., Sykes, R., Cragg, B. A., Heywood, C., Kim, G. T., Mangelsdorf, K., Mildenhall, D. C., Rinna, J., Vieth, A., Zink, K.-G., Sass, H., Weightman, A. J., and Parkes, R. J. (2009). Prokaryotic populations and activities in an interbedded coal deposit, including a previously deeply buried section (1.6–2.3 km) above (150 Ma basement rock. *Geomicrobiol. J.* 26, 163–178.

Giosan, L., Flood, R. D., and Aller, R. C. (2002). Paleoceanographic significance of sediment color on western North Atlantic drifts: I. Origin of color. *Mar. Geol.* 189, 25–41.

Hussong, D. M., Fryer, P. B., Tuthill, J. D., and Wipperman, L. K. (1979). The geological and geophysical setting near DSDP site 395, North Atlantic Ocean. *Init. Repts. DSDP* 45, 23–37.

Krumholz, L. R., Mckinley, J. P., Ulrich, G. A., and Suflita, J. M. (1997). Confined subsurface microbial communities in Cretaceous rock. *Nature* 386, 64–66.

Langseth, M. G., Hyndman, R. D., Becker, K., Hickman, S., and Salisbury, M. H. (1984). The hydrogeological regime of isolated sediment ponds in mid-ocean ridges. *Init. Repts. DSDP* 78B, 825–837.

McMahon, P. B., and Chapelle, F. H. (1991). Microbial production of organic acids in aquitard sediments and its role in aquifer geochemistry. *Nature* 349, 233–235.

McMahon, P. B., Chapelle, F. H., Falls, W. F., and Bradley, P. M. (1992). Role of microbial processes in linking sandstone diagenesis with organic rich clays. *J. Sediment. Petrol.* 62, 1–10.

Murray, J. W., and Grundmanis, V. (1980). Oxygen consumption in pelagic marine sediments. *Science* 209, 1527–1530.

Parkes, R. J., Cragg, B. A., Bale, S. J., Getliff, J. M., Goodman, K., Rochelle, P. A., Fry, J. C., Weightman, A. J., and Harvey, S. M. (1994). Deep bacterial biosphere in Pacific ocean sediments. *Nature* 371, 410–413.

Parkes, R. J., Cragg, B. A., and Wellsbury, P. (2000). Recent studies on bacterial populations and processes in subseafloor sediments: a review. *Hydrogeol. J.* 8, 11–28.

Parkes, R. J., Webster, G., Cragg, B. A., Weightman, A. J., Newberry, C. J., Ferdelman, T. G., Kallmeyer, J., Jorgensen, B. B., Aiello, I. W., and Fry, J. C. (2005). Deep sub-seafloor prokaryotes stimulated at interfaces over geological time. *Nature* 436, 390–394.

Phelps, T. J., Hedrick, D. B., Ringelberg, D., Fliermans, C. B., and White, D. C. (1989). Utility of radiotracer measurements for subsurface microbiology studies. *J. Microbiol. Methods* 9, 15–27.

Purdy, G. M., Rabinowitz, P. D., and Schouten, H. (1979). The mid-Atlantic ridge at 23°N. Bathymetry and magnetics. *Init. Repts. DSDP* 45, 119–128.

Richter, T. O., Van Der Gaast, S., Koster, B., Vaars, A., Gieles, R., De Stigter, H. C., De Haas, H., and Van Weering, T. C. E. (2006). "The Avaatech XRF core scanner: technical description and applications to NE Atlantic sediments," in *New Techniques in Sediment Core Analysis*, ed. R. G. Rothwell (London: Geological Society), 39–50.

Rogerson, M., Weaver, P. P. E., Rohling, E. J., Lourens, L. J., Murray, J. W., and Hayes, A. (2006). "Colour logging as a tool in high-resolution palaeoceanography," in *New Techniques in Sediment Core Analysis*, ed. R. G. Rothwell. (London: Geological Society), 99–112.

Süß, J., Engelen, B., Cypionka, H., and andSass, H. (2004). Quantitative analysis of bacterial communities from Mediterranean sapropels based on cultivation-dependent methods. *FEMS Microbiol. Ecol.* 51, 109–121.

Timofeev, P. P., Varentsov, I. M., Rateev, M. A., and Renngarten, N. V. (1979). Lithology, mineralogy, and geochemistry of upper cenozoic sediments at 23°N near the Mid-Atlantic Ridge, drilled on Leg 45. *Init. Repts. DSDP* 45, 323–347.

Treude, T., Boetius, A., Knittel, K., Wallmann, K., and Jorgensen, B. B. (2003). Anaerobic oxidation of methane above gas hydrates at Hydrate Ridge, NE Pacific Ocean. *Mar. Ecol. Prog. Ser.* 264, 1–14.

Wellsbury, P., Goodman, K., Barth, T., Cragg, B. A., Barnes, S. P., and Parkes, R. J. (1997). Deep marine biosphere fuelled by increasing organic matter availability during burial and heating. *Nature* 388, 573–576.

Wellsbury, P., Goodman, K., Cragg, B. A., and Parkes, R. J. (2000). The geomicrobiology of deep marine sediments from BlakeRidge containing methane hydrate (sites 994, 995, and 997). *Proc. Ocean Drill. Prog. Sci. Results* 164, 379–391.

Wirsen, C. O., and Jannasch, H. W. (1974). Microbial transformations of some 14C-labeled substrates in coastal water and sediment. *Microb. Ecol.* 1, 25–37.

Conflict of Interest Statement: The authors declare that the research was conducted in the absence of any commercial or financial relationships that could be construed as a potential conflict of interest.

Received: 02 October 2011; paper pending published: 20 October 2011; accepted: 08 December 2011; published online: 27 December 2011.

*Citation: Picard A and Ferdelman TG (2011) Linking microbial heterotrophic activity and sediment lithology in oxic, oligotrophic sub-seafloor sediments of the North Atlantic Ocean. Front. Microbio. **2**:263. doi: 10.3389/fmicb.2011.00263*

This article was submitted to Frontiers in Extreme Microbiology, a specialty of Frontiers in Microbiology.

frontiers in
MICROBIOLOGY

ORIGINAL RESEARCH ARTICLE
published: 06 January 2012
doi: 10.3389/fmicb.2011.00268

Metagenomic evidence for H_2 oxidation and H_2 production by serpentinite-hosted subsurface microbial communities

William J. Brazelton[1,2]*, Bridget Nelson[1] and Matthew O. Schrenk[1]

[1] *Department of Biology, East Carolina University, Greenville, NC, USA*
[2] *School of Oceanography, University of Washington, Seattle, WA, USA*

Edited by:
Jennifer F. Biddle, University of Delaware, USA

Reviewed by:
Barbara J. Campbell, University of Delaware, USA
Brent Craig Christner, Louisiana State University, USA

****Correspondence:***
William J. Brazelton, School of Oceanography, University of Washington, Box 357940, Seattle, WA 98195, USA.
e-mail: wbrazelton@gmail.com

Ultramafic rocks in the Earth's mantle represent a tremendous reservoir of carbon and reducing power. Upon tectonic uplift and exposure to fluid flow, serpentinization of these materials generates copious energy, sustains abiogenic synthesis of organic molecules, and releases hydrogen gas (H_2). In order to assess the potential for microbial H_2 utilization fueled by serpentinization, we conducted metagenomic surveys of a marine serpentinite-hosted hydrothermal chimney (at the Lost City hydrothermal field) and two continental serpentinite-hosted alkaline seeps (at the Tablelands Ophiolite, Newfoundland). Novel [NiFe]-hydrogenase sequences were identified at both the marine and continental sites, and in both cases, phylogenetic analyses indicated aerobic, potentially autotrophic Betaproteobacteria belonging to order Burkholderiales as the most likely H_2-oxidizers. Both sites also yielded metagenomic evidence for microbial H_2 production catalyzed by [FeFe]-hydrogenases in anaerobic Gram-positive bacteria belonging to order Clostridiales. In addition, we present metagenomic evidence at both sites for aerobic carbon monoxide utilization and anaerobic carbon fixation via the Wood–Ljungdahl pathway. In general, our results point to H_2-oxidizing Betaproteobacteria thriving in shallow, oxic–anoxic transition zones and the anaerobic Clostridia thriving in anoxic, deep subsurface habitats. These data demonstrate the feasibility of metagenomic investigations into novel subsurface habitats via surface-exposed seeps and indicate the potential for H_2-powered primary production in serpentinite-hosted subsurface habitats.

Keywords: hydrogenase, serpentinization, alkaline spring, metagenome, subsurface

INTRODUCTION

The potentially vast microbial diversity and biomass of the subsurface biosphere (Whitman et al., 1998) has been frequently noted (Biddle et al., 2006; Huber et al., 2007; Santelli et al., 2008; Schrenk et al., 2010), but there is very little evidence to indicate how much of it is supported by new primary production or by recycling of buried organic carbon. Earth's mantle is primarily composed of ultramafic rocks that undergo a geochemical process known as serpentinization when they are tectonically uplifted into the crust and exposed to water. Serpentinization is highly exothermic and can release large quantities of hydrogen gas (H_2) and variable amounts of methane and low-molecular weight organic compounds (McCollom and Seewald, 2007; Proskurowski et al., 2008). Therefore, serpentinization is a potential source of reducing power and organic carbon for organisms inhabiting the ultramafic subsurface. Actively serpentinizing rocks are present on all of the world's continents and comprise significant portions of the deep seafloor, and yet they are some of the most poorly understood portions of the biosphere.

The most dramatic example of an ecosystem supported by serpentinization is the Lost City hydrothermal field, which is situated on a serpentinite-rich massif 15 km from the Mid-Atlantic Ridge. Carbonate chimneys at Lost City vent warm (up to 90°C), pH 9–11 fluids rich in calcium, H_2 (up to 14 mmol/kg), and methane (1–2 mmol/kg; Kelley et al., 2005). Methane and larger hydrocarbon chains with up to four carbon atoms in Lost City fluids show evidence of an abiogenic origin in the deep subsurface (Proskurowski et al., 2008), but the amount of microbial activity supported by this abiotic source of organics has not been quantified. The anoxic interiors of Lost City carbonate chimneys are dominated by Methanosarcinales-related archaea potentially involved in methane production and oxidation (Schrenk et al., 2004; Brazelton et al., 2011). The oxic chimney exteriors are dominated by aerobic methane- and sulfur-oxidizing bacteria (Brazelton et al., 2006, 2010). The role of H_2-metabolizing bacteria in Lost City chimneys, though, has not been explicitly investigated.

In addition to marine hydrothermal systems such as Lost City, Ophiolites abducted onto continents also provide a potential window into subsurface habitats supported by serpentinization. The Tablelands Ophiolite in western Newfoundland, Canada features extensive ultramafic exposures including serpentinites associated with the seepage of highly reducing, pH 12 fluids, and extensive calcium carbonate (travertine) deposits. The Tablelands fluids are enriched in calcium, H_2 (up to ~500 μM), and methane (Szponar et al., submitted). The geochemical similarities between the alkaline springs at the Tablelands and the vent fluids at Lost City strongly suggest that they are the surface expressions of ongoing serpentinization-associated reactions occurring in the underlying ultramafic subsurface.

In order to identify potential inhabitants of the ultramafic subsurface in both marine and continental settings, we conducted a metagenomic survey of two Tablelands alkaline springs as a comparison to a previously published metagenome from a Lost City chimney (Brazelton and Baross, 2009, 2010). In this report, we focus on the potential for H_2-fueled microbial activity by investigating the incidence and diversity of sequences encoding hydrogenase enzymes. Hydrogenases catalyze the reversible conversion between molecular hydrogen and its component protons and electrons: $H_2 \leftrightarrow 2H^+ + 2e^-$. This reaction is catalyzed by two main classes of hydrogenase: [NiFe]-hydrogenases are required for uptake and oxidation of H_2, while [FeFe]-hydrogenases are typically involved in microbial H_2 production. Although the two classes share some sequence similarity, they do not appear to be monophyletic (Vignais et al., 2001; Vignais and Billoud, 2007). Therefore, phylogenetic analyses of possible hydrogenase-encoding sequences should reliably indicate a genetic potential for H_2 oxidation or H_2 production. The results presented here indicate that both types of hydrogenase are abundant in the Tablelands and Lost City metagenomes and that the identity of the H_2-metabolizing organisms at both sites are intriguingly similar. Additional metagenomic evidence also indicates the potential for carbon fixation pathways involving carbon monoxide utilization or acetogenesis by H_2-metabolizing organisms. In general, this initial metagenomic survey highlights the potential for H_2-fueled primary production in the ultramafic subsurface.

MATERIALS AND METHODS

LOST CITY METAGENOME

The Lost City metagenomic dataset included in this analysis was previously described in Brazelton and Baross (2009, 2010). In summary, a ∼1 kg carbonate chimney sample (H03_072705_R0424) was collected from the central "Poseidon" edifice (**Figure 1A**) of the Lost City hydrothermal field on 27 July 2005 by the DSV *Hercules* during the 2005 Lost City expedition aboard the R/V Ronald H. Brown. The fluids venting from this chimney can reach 88°C, pH 10.7, and are highly enriched in H_2 (13 mmol/kg) and methane (1.5 mmol/kg; Proskurowski et al., 2008). DNA extraction and purification is described in Brazelton and Baross (2010). Shotgun library construction and Sanger end-sequencing of pUC18 inserts were conducted according to standard protocols at the DOE Joint Genome Institute in 2007. Two libraries were constructed from two subsamples of the same carbonate chimney sample. Reads from both libraries were combined for assembly and for analyses described here. Mean read length for the 46,360 reads from both libraries was 755 bp, and the mean length of all 6324 contigs was 1583 bp, with a maximum of 24 kb. All sequencing reads and assembled contigs are publicly available on the MG-RAST (Meyer et al., 2008) server under project name "Lost City hydrothermal field" and MG-RAST IDs 4461585.3 (reads) and 4470602.3 (contigs).

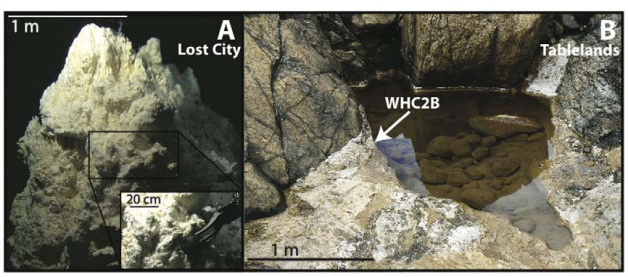

FIGURE 1 | Photographs of the Lost City (A) and Tablelands (B) sites where metagenome samples were collected. The Lost City metagenome sample was grabbed by the manipulator on the ROV Hercules, comprising approximately 1 kg of carbonate minerals and associated biofilm material (A inset) from the Poseidon pinnacle **(A)** at the Lost City hydrothermal field. The WHC2b metagenome sample was collected by filtering 10 L of fluid from a pH 12 pool approximately 2.5 m long, 1 m wide, and less than 1 m deep **(B)**. Fluid was collected by gentle suction from a depression in the bottom of the pool underneath a ledge [arrow in **(B)**], which appeared to be a source of the spring fluid. Travertine (carbonate) deposits are visible around the edge of the pool. Lost City photo credit: Deborah Kelley, U. of Washington, IFE, URI–IAO, NOAA.

COLLECTION OF TABLELANDS SAMPLES

Two springs ∼2 km apart were sampled for this study. A fluid sample from the WHC2b spring was collected from the bottom of a pH 12 pool (∼1 m deep) surrounded by travertine (carbonate) deposits in Winter House Canyon on 25 August 2010. The sampling tubing inlet was placed at the highest pH (12.06) and lowest E_h (−733 mV) location detected at the time of sampling, which was a depression at the bottom edge of the pool (**Figure 1B**). The pool depth is less than 1 m, so the pool represents a very strong redox gradient from the surface (which is in contact with the atmosphere) to the anoxic bottom. At the time of sampling, the measured H_2 concentration was ∼0.24 mmol/kg, and a maximum of 0.52 mmol/kg was measured at the same location one year later (Szponar et al., submitted). These concentrations are much lower than that of the astonishingly H_2-rich Lost City fluids, but are nevertheless indicative of significant H_2 enrichment over background surface waters. The surface temperature of the pool is determined by the air temperature, and the bottom of the pool is typically 1–4°C cooler than the surface. The pH and E_h of fluid flowing through the tube was monitored during sampling to verify that ambient fluid with more neutral pH or more oxidizing E_h did not dilute the sample. Approximately 10 L of fluid was collected from WHC2b by repeated pulls with a 60 mL sterile syringe and stored in sterile bottles until filtration through four replicate 0.2 μm Sterivex (Millipore) filter cartridges. Sterivex filters were immediately frozen in liquid N_2, transported on dry ice, and stored at –80°C until DNA extraction.

A fluid sample was collected from a spring (called TLE) associated with a large travertine deposit on the northeastern face of Table Mountain on 17 June 2010. The spring fluid was visibly mixing with surface runoff, as evidenced by the lower pH and higher E_h compared to WHC2b: pH 10.5 and $E_h + 25$ mV. No H_2 was detected at the time of sampling, but concentrations of 65 and 180 μM have been measured at this location by prior sampling efforts (Szponar et al., submitted). The temperature of the spring was not measured at the time of sampling, but subsequent measurements have shown that it is typically much cooler than air temperature (∼9°C with air temperature of ∼20°C) due to its subsurface source and/or its mixing with runoff from snowmelt. The spring was sampled by repeated pulls with a 60 mL sterile syringe

for a total of 1.2 L stored in sterile bottles. Filtration, transportation, and storage of the TLE sample was conducted as described above for the WHC2b sample.

DNA EXTRACTION AND SEQUENCING OF TABLELANDS SAMPLES

DNA extraction from Sterivex filters was conducted according to the protocol described by Huber et al. (2002) and Sogin et al. (2006). The DNA yield from the TLE sample was insufficient for metagenomic sequencing, so a minimal amount of whole genome amplification (WGA) was conducted according to the following protocol. RepliG (Qiagen) WGA reactions were incubated for only 3 h according to the manufacturer's instructions, followed by inactivation of the enzyme at 65°C for 3 min. Four replicate RepliG WGA reactions were pooled, and amplification products were purified with QiAamp (Qiagen) columns, treated with S1 Nuclease at 37°C for 1hr, purified with phenol/chloroform/isoamyl alcohol, and finally precipitated with ethanol and sodium acetate. TRFLP profiles of 16S rRNA amplicons from TLE pre- and post-WGA were nearly identical (86% Sorensen similarity; 75% Jaccard similarity, calculated with EstimateS[1] after clustering peaks according to the method of (Abdo et al., 2006). Differences between pre- and post-WGA TRFLP profiles involved the loss of a few minor peaks and moderate increase in the size of major peaks in the post-WGA profiles. Therefore, WGA may have limited the diversity of rare sequences in the TLE metagenomic dataset, but we do not expect any taxonomic bias in the most abundant sequences. Approximately 1 μg of DNA from each sample was submitted to the Engencore facility (University of South Carolina) for shotgun metagenomic pyrosequencing on a Roche Titanium sequencer.

METAGENOMIC ANALYSIS AND ASSEMBLY

Low-quality ends of sequencing reads were trimmed in Geneious (Biomatters Ltd.) with default parameters, and reads were dereplicated with the server[2] described by Gomez-Alvarez et al. (2009). Dereplicated reads (80,830 reads from 118,348 original reads for WHC2b; 56,965 reads from 135,538 original reads for TLE) were used for *de novo* metagenomic assembly in Geneious with default parameters for "medium sensitivity." Taxonomic classification of WHC2b contigs > 2 kb was conducted with the TaxSom server (Weber et al., 2010) with a pre-calculated model for all Archaea and Bacteria. Automated annotation of open reading frames in contig WHC2b.C1 was performed by the RAST server (Aziz et al., 2008). All sequencing reads and assembled contigs for both samples are available on the MG-RAST (Meyer et al., 2008) server under project name "Serpentinite springs" and MG-RAST IDs 4460689.3, 4460690.3, 4461618.3, and 4461619.3. Furthermore, MIMS-compliant metadata are provided in **Table A1** in Appendix.

PHYLOGENETIC ANALYSES

Hydrogenase sequences were detected in metagenomic datasets by TBLASTN (Altschul et al., 1997) using as query a file of PFAM (Finn et al., 2008) seed sequences for the large subunits of [FeFe]-hydrogenase (PF02906) or [NiFe]-hydrogenase (PF00374). For comparative purposes, we included in this tblastn search additional metagenomic datasets that are publicly available in the MG-RAST (Meyer et al., 2008) and DOE Joint Genome Institute IMG/M (Markowitz et al., 2006) databases. For metagenomic reads with tblastn *E*-values better than 10^{-5}, the aligned regions were translated and included in further phylogenetic analyses. All phylogenetic trees involving metagenomic sequences (**Figures 3** and **5–7**; **Figures A1** and **A2** in Appendix) were constructed with a multi-step approach utilizing reference alignments and trees in order to minimize errors and biases introduced by the fragmentary and non-overlapping nature of the metagenomic sequences. For each tree, a multiple sequence alignment was constructed with ClustalX (Larkin et al., 2007) using sequences from the studies by (Vignais et al., 2001; Boyd et al., 2009, 2010) and additional close relatives found in GenBank by blastx. Unaligned metagenomic fragments were added to the reference alignment profile with ClustalX in order to avoid alteration of the relative positions of residues in the reference alignment. Next, a bootstrapped maximum-likelihood tree was constructed from the reference-only alignment using the "-f a" algorithm in RAxML version 7.0.3 (Stamatakis, 2006). The reference-only tree with the highest-likelihood was used as a constraint tree ("-r" flag in RAxML) for 100 inferences from the full alignment (including metagenomic fragments) by RAxML, and bootstrap support values were drawn on the highest-likelihood tree. CODH and ACS trees were constructed using the same method; CODH reference sequences were obtained from (Cunliffe et al., 2008), and ACS reference sequences were obtained from (Gagen et al., 2010). The closest relatives to the 16S rRNA sequences were identified with the aid of the SILVA aligner and database (Pruesse et al., 2007) visualized in ARB (Ludwig et al., 2004). The alignment was exported from ARB, re-aligned with MUSCLE version 3.6 (Edgar, 2004), manually corrected, and built into a bootstrapped maximum-likelihood tree with RaxML.

RESULTS

TAXONOMIC ANALYSIS OF METAGENOMIC ASSEMBLIES

A previous study (Brazelton and Baross, 2010) demonstrated that almost all of the large contigs assembled from Lost City chimney shotgun metagenomic sequences contain open reading frames with significant sequence similarity to at least one protein encoded by the genome of *Thiomicrospira crunogena* XCL-2, indicating that *Thiomicrospira*-related organisms dominated the metagenomic assembly.

Figure 2 displays the %GC and length of the 907 contigs with length > 2 kb obtained from the assembly of WHC2b shotgun metagenomic sequencing reads. Despite relatively low sequencing effort, *de novo* assembly yielded moderately large contigs and revealed a few dominant populations, highlighting the low diversity of the spring fluid. Most of the largest contigs were taxonomically classified by the TaxSOM server (Weber et al., 2010) as members of the Comamonadaceae family within order Burkholderiales (**Figure 2**). A secondary assemblage of low %GC Firmicutes contigs (orders Bacillales and Clostridiales) is also evident in WHC2b (**Figure 2**).

The *de novo* metagenomic assembly from TLE yielded only 118 contigs > 2 kb, and the longest was just 8.5 kb (data not shown). Most of the same taxonomic groups in WHC2b are also present in

[1] http://viceroy.eeb.uconn.edu/estimates
[2] http://microbiomes.msu.edu/replicates

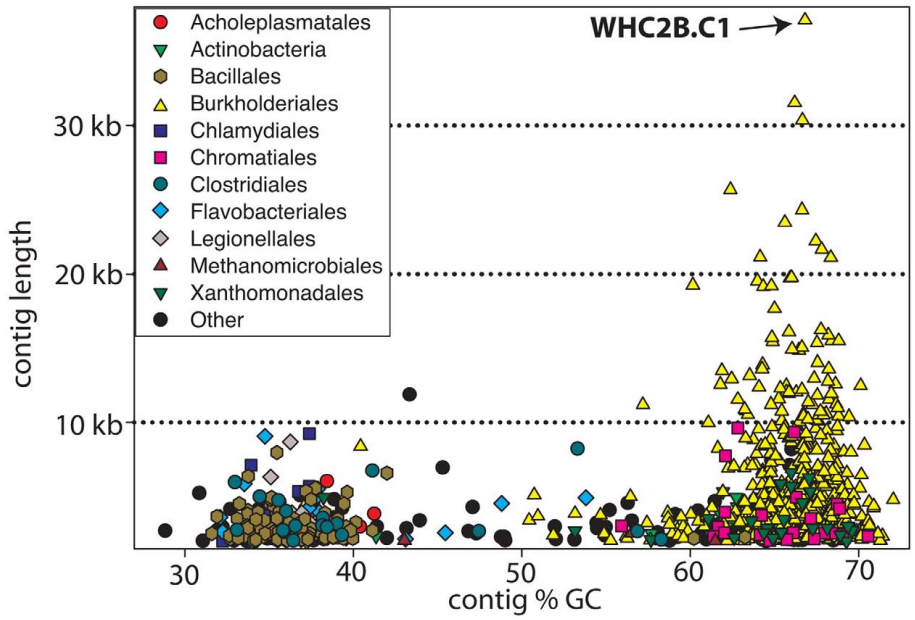

FIGURE 2 | Taxonomic assignment of contigs (plotted with respect to length and %GC) assembled from WHC2b metagenomic sequences. Large Burkholderiales contigs with high %GC (yellow triangles) dominate the assembly. Most of the smaller contigs have low %GC, and many of these are assigned to Gram-positive bacteria including Bacillales and Clostridiales. Only contigs > 2 kb are shown.

TLE, including Burkholderiales, Bacillales, and Clostridiales, but the Burkholderiales do not dominate the assembly as they do in WHC2b.

A partial 16S rRNA sequence was identified in one of the Burkholderiales contigs in each Tablelands fluid sample (WHC2b.C991: 1.6 kb, 56% GC, 3.6 mean coverage; TLE.C712: 1.5 kb, 54% GC, 1.3 mean coverage). Maximum-likelihood phylogenetic analysis placed both sequences in genus *Hydrogenophaga* (**Figure 3**), which is consistent with the phylogeny of the hydrogenases discussed below. Two Burkholderiales-related 16S rRNA gene clones were also recovered from the same Lost City carbonate structure that is the source of the metagenome discussed here; these clones were previously described in Brazelton et al. (2006). They are 99% similar over 1471 bp (calculated with MatGat; Campanella et al., 2003) to the 16S rRNA sequence of *Ralstonia pickettii*, an oligotroph known to grow in moist biofilms (Stelzmueller et al., 2006). The 16S rRNA sequence of *R. eutropha* (the hydrogenases of which are discussed below) is 96% similar to the Lost City clones (**Figure 3**).

The largest WHC2b contig (WHC2b.C1: 37 kb, 67% GC, comprising 615 shotgun reads at 6.6 mean coverage) contains putative operons for a [NiFe]-hydrogenase, carbon monoxide dehydrogenase (CODH), and Rubisco (**Figure 4**). The Rubisco cluster includes RAST annotations for the small and large subunits of Rubisco, six carboxysome shell proteins, and two Rubisco activation proteins. The hydrogenase cluster includes RAST annotations for the small and large subunits of uptake [NiFe]-hydrogenase, a signal transduction histidine kinase (HoxJ), and a transcriptional regulatory protein (HoxA). The CODH cluster is at the edge of the contig and is most likely incomplete. It includes RAST annotations for the three subunits of CODH (CoxMSL) with an upstream CoxC and a downstream CoxD. This arrangement is consistent

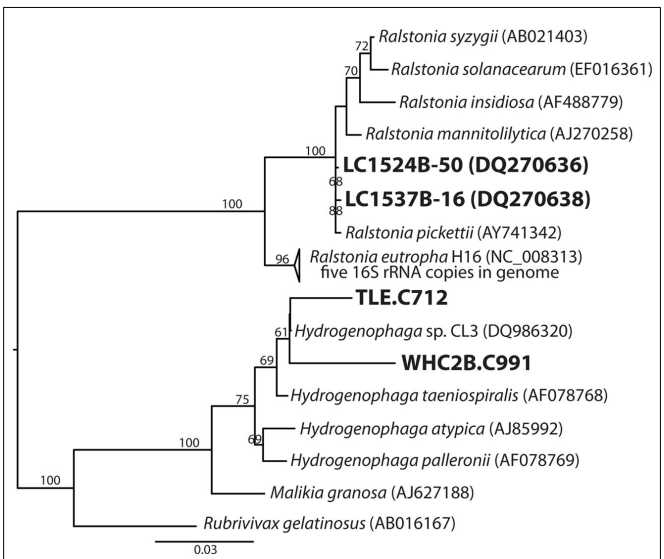

FIGURE 3 | Phylogenetic tree of Burkholderiales 16S rRNA sequences including two 16S rDNA clones from Lost City carbonate chimneys and a partial 16S rRNA coding sequence identified in a metagenomic contig from the Tablelands fluid sample WHC2b.

with that found in type I CODH clusters in Marine *Roseobacter* Clades (Cunliffe, 2011). The phylogenetic relationships of the [NiFe]-hydrogenase large subunit and CODH large subunit from this contig are described below.

The relatively high coverage and presence of a plasmid partitioning protein in WHC2b.C1 (**Figure 4**) suggests the possibility

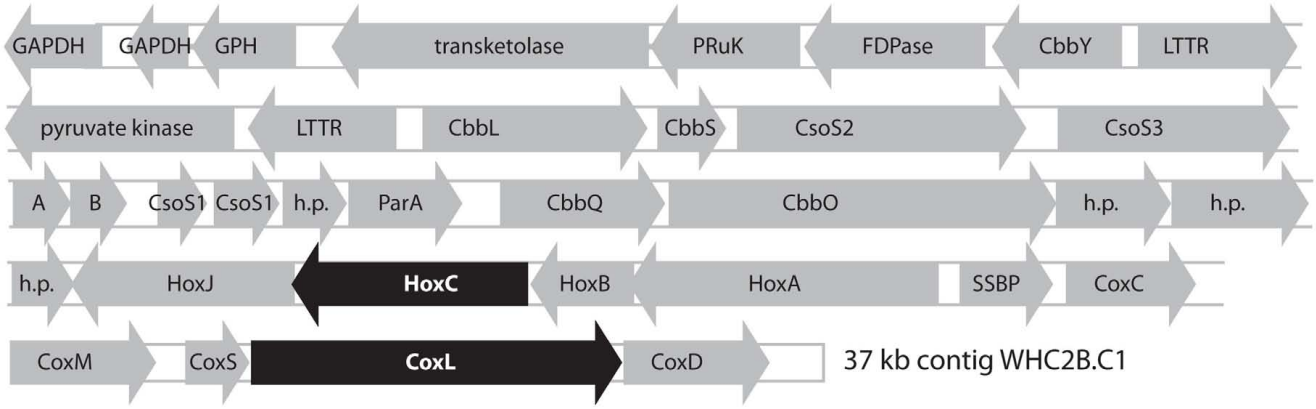

FIGURE 4 | Predicted products of open reading frames identified in the longest contig from Tablelands fluid sample WHC2b (37 kb, 67% GC, comprising 615 shotgun reads at 6.6 mean coverage). The putative large subunits of [NiFe]-hydrogenase (HoxC) and carbon monoxide dehydrogenase (CoxL) are highlighted in black to indicate that their phylogenetic relationships are shown in **Figures 5** and **Figure A1** in Appendix. GAPDH: NAD-dependent glyceraldehyde-3-phosphate dehydrogenase. GPH, phosphoglycolate phosphatase; PRuK, phosphoribulokinase; FDPase, type I fructose-1,6-bisphosphatase; CbbY, rubisco-associated hydrolase; LTTR, LysR-type transcriptional regulator; CbbL, CbbS, ribulose bisphosphate carboxylase, large and small chains; CbbS, ribulose bisphosphate carboxylase small chain; CsoS2, CsoS3, CsoS1, carboxysome shell proteins; A, B, putative carboxysome peptides; h. p., hypothetical protein; ParA, chromosome (plasmid) partitioning protein; CbbQ, CbbO, rubisco activation proteins; HoxJ, HoxA, hydrogenase regulation proteins; HoxC, HoxB, uptake [NiFe]-hydrogenase, large and small subunits; SSBP, single-stranded DNA binding protein; CoxC, carbon monoxide dehydrogenase signaling protein; CoxM, CoxS, CoxL, carbon monoxide dehydrogenase, medium, small, and large subunits; CoxD, carbon monoxide dehydrogenase accessory protein.

that this contig represents a plasmid. Indeed, the H_2 oxidation and carbon fixation capabilities of *Ralstonia eutropha* are encoded in a "megaplasmid," and loss of this plasmid would result in a strictly heterotrophic lifestyle (Schwartz et al., 2009). The plasmid partitioning protein in WHC2b.C1 does not contain any homologs in the *R. eutropha* megaplasmid, however, and the contig is not a complete plasmid sequence, so we cannot conclude with certainty whether it is a plasmid. Nevertheless, all sequenced members of the Burkholderiaceae family contain multiple replicons; the additional genetic molecules other than the main chromosome are sometimes called "chromosomes" and sometimes "megaplasmids" (Fricke et al., 2009). No genomes from *Hydrogenophaga* species (Comamonadaceae family) have been sequenced yet, and we are not aware of any data pertaining to whether their hydrogenases are plasmid-encoded.

ABUNDANCE OF SEQUENCES ENCODING HYDROGENASES

We investigated the genetic potential for communities in these samples to metabolize H_2 by conducting a tblastn search for potential homologs of the catalytic (large) subunits of [FeFe]-hydrogenase and [NiFe]-hydrogenase. For each metagenome, the number of unique sequencing reads that match at least one hydrogenase is reported in **Table 1**. For comparative purposes, only unassembled sequences were included in the quantification of hydrogenase abundance because quantitative comparisons of gene abundance among assembled metagenomes is problematic due to their varying assembly strategies and sequencing coverages.

The Lost City chimney metagenome and the Tablelands metagenome WHC2b both contained a similar proportion of putative hydrogenase sequences as those found in other metagenomes from environments where H_2 metabolism is expected to occur (**Table 1**). These environments (including methanotrophic sediments, hot springs, marine hydrothermal vents, organic degradation bioreactors, acid mine drainage, and a hypersaline microbial mat) contained >10× greater density of hydrogenases than the combined dataset from the Global Ocean Sampling expedition. Remarkably, zero hydrogenase sequences were detected in the metagenomic data from the TLE spring, which exhibited more moderate pH and E_h values compared to WHC2b.

The Lost City metagenome was exceptionally rich in sequences matching [NiFe]-hydrogenases; only two metagenomes in the MG-RAST and IMG/M databases contained a higher proportion (**Table 1**). The WHC2b metagenome, in contrast, was exceptionally rich in sequences matching [FeFe]-hydrogenases, which are typically involved in H_2 production during fermentation. Indeed, the only metagenomes with a higher proportion of [FeFe]-hydrogenases than WHC2b are derived from cellulose-degrading fermentation bioreactors.

Inferring the abundance of H_2-oxidizing or H_2-producing organisms from the abundance of hydrogenases genes is problematic because multiple hydrogenases are frequently present in a given genome (Vignais and Billoud, 2007). Furthermore, our tblastn search could have detected hydrogenases found in all three domains of life. Phylogenetic analyses, however, can constrain the taxonomic possibilities for each hydrogenase sequence and therefore enable one to test hypotheses about which hydrogenases are encoded by which organisms. The phylogenetic analyses described below indicate that both the Tablelands and Lost City springs feature [NiFe]-hydrogenases primarily encoded by Betaproteobacteria related to known H_2-oxidizers and [FeFe]-hydrogenases encoded by Clostridia-related to known H_2-producers. No archaeal or eukaryotic hydrogenases were detected in this study.

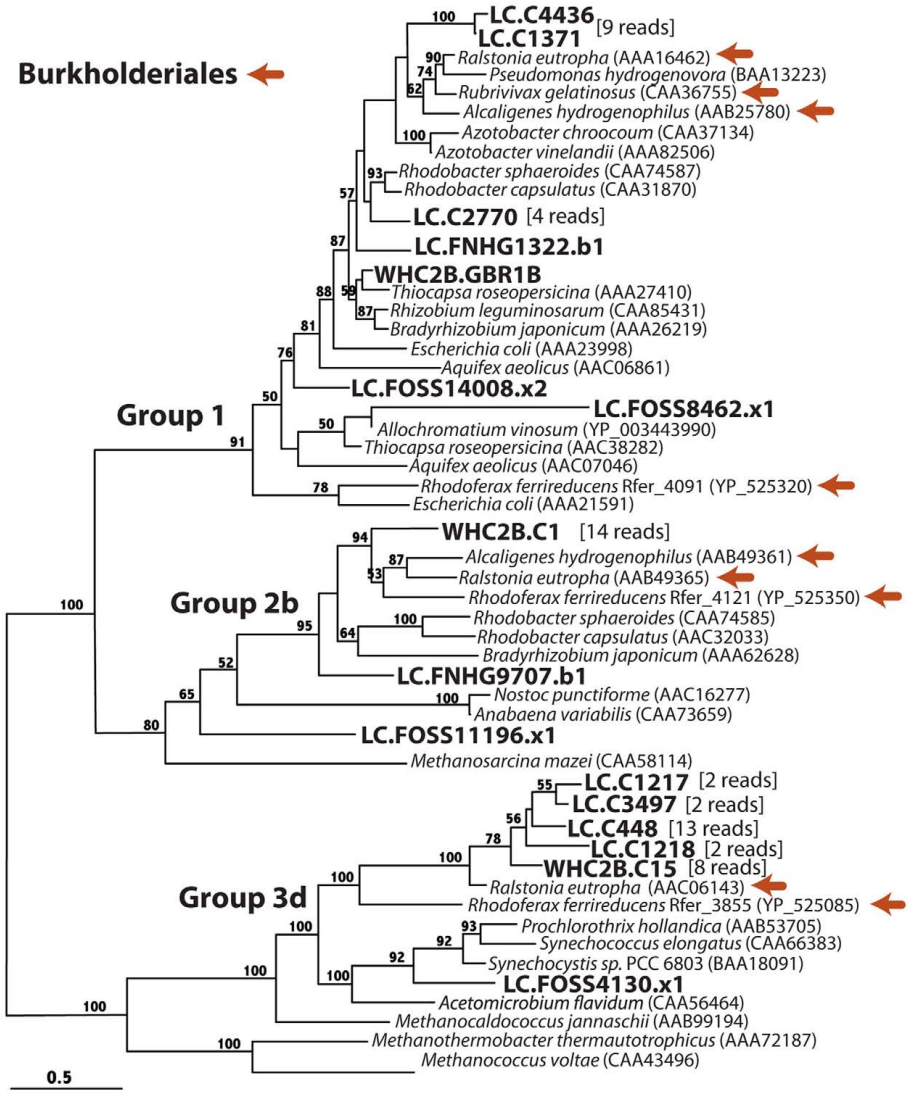

FIGURE 5 | Phylogenetic diversity of putative [NiFe]-hydrogenase detected in metagenomes from a Lost City chimney and Tablelands spring fluid. Burkholderiales references sequences are indicated with orange arrows, and Lost City (LC), and Tablelands (WHC2b) sequences are in large, bold font. If additional metagenomic sequencing reads are associated with the representative on the tree, the number of sequencing reads is indicated in brackets. Group numbers are consistent with the phylogeny reported by Vignais et al. (2001) and Vignais and Billoud (2007). Maximum-likelihood bootstrap support values > 50 are shown.

[NiFe]-HYDROGENASE DIVERSITY

In order to further characterize the putative hydrogenase sequences identified in the tblastn search, we constructed maximum-likelihood phylogenetic trees (**Figures 5–7**) in which the putative hydrogenase sequences were incorporated into a constraint tree comprised of previously characterized hydrogenases. The resulting [NiFe]-hydrogenase phylogeny (**Figure 5**) is congruent with that reported by Vignais et al. (2001) and Vignais and Billoud (2007), who identified four monophyletic groups consistent with the original classification by Wu and Mandrand (1993). Each of the four groups includes archaeal and bacterial representatives. None of the sequences in this study, however, exhibited significant phylogenetic affinity with archaeal hydrogenases. The phylogenetic relationships of the putative bacterial hydrogenases are described in detail below.

Group 1 includes the membrane-bound respiratory uptake hydrogenases, which couple H_2 oxidation to a cytochrome, resulting in proton pumping across the membrane. Nitrogen-fixing organisms also use Group 1 [NiFe]-hydrogenases to recapture H_2 produced by nitrogenase. The [NiFe]-hydrogenase phylogeny (**Figure 5**) shows that many Lost City sequences and a single WHC2b shotgun sequencing read belong to Group 1. Two Lost City contigs representing nine reads are most similar to hydrogenases from Burkholderiales members *Ralstonia eutropha*, *Rubrivivax gelatinosus*, and *Alcaligenes hydrogenophilus*. A third Lost City contig contained a hydrogenase closely related

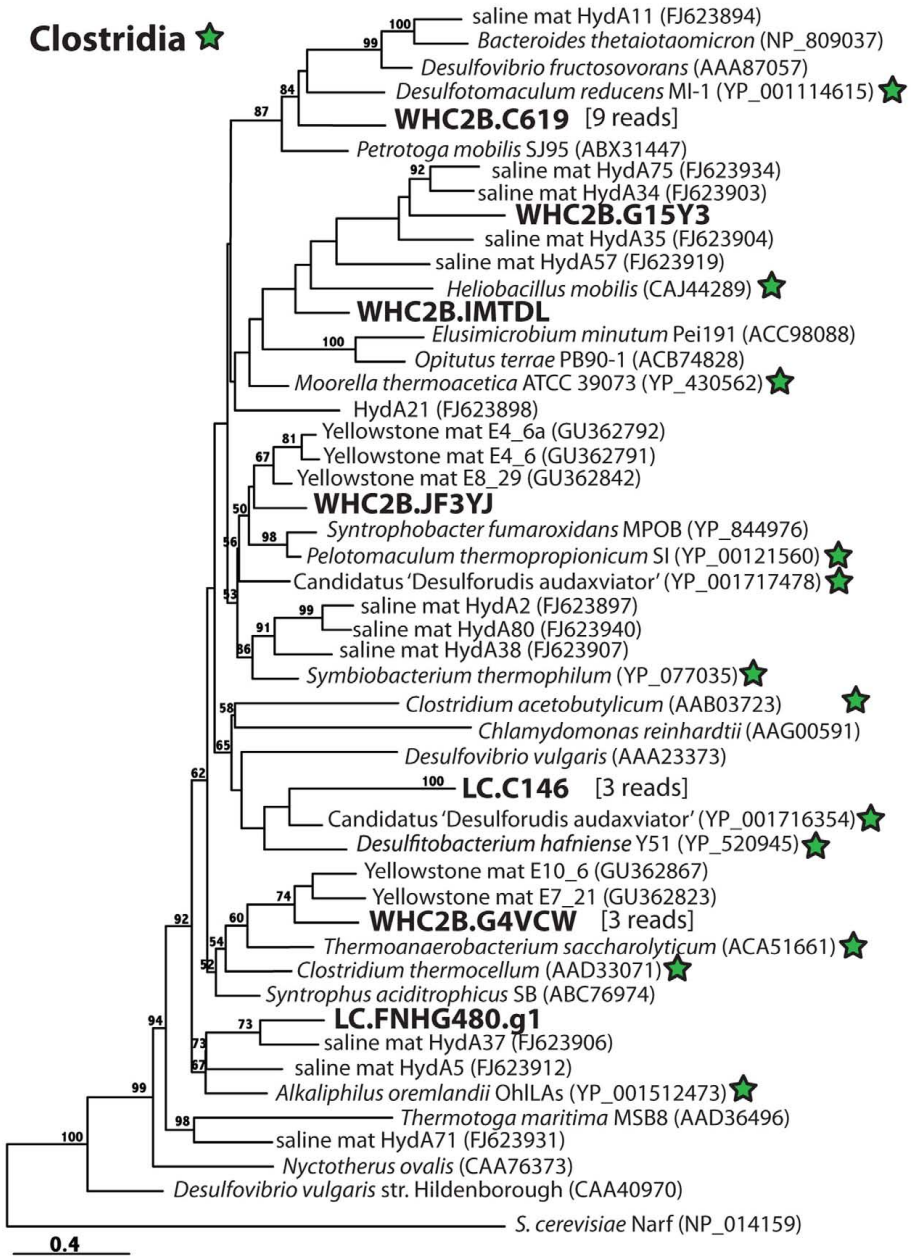

FIGURE 6 | Phylogenetic diversity of putative [FeFe]-hydrogenases detected in metagenomes from a Lost City chimney and Tablelands spring fluid. Clostridia reference sequences are indicated with green stars, and Lost City (LC), and Tablelands (WHC2b) sequences are in large, bold font. The number of metagenomic shotgun sequencing reads associated with each representative on the tree is indicated in brackets. Maximum-likelihood bootstrap support values > 50 are shown.

to that from two *Rhodobacter* species. Three additional Lost City reads belong to Group 1, but their phylogenetic affiliations are unresolved. Only one read from WHC2b contained a Group 1 [NiFe]-hydrogenase, and its closest relative was from *Thiocapsa roseopersicina*, a nitrogen-fixing member of order *Chromatiales*.

Group 2b includes H_2-sensing proteins that are involved in H_2-regulated gene expression and do not directly provide energy from H_2 to the cell (Vignais et al., 2001). They include Alpha- and Beta-proteobacteria. A cluster of 14 reads representing the contig WHC2b.C1 are most similar to Burkholderiales Group 2b hydrogenases. Two Lost City reads with unresolved phylogenetic affiliations are also in the Group 2b clade. Group 2a (not show) is specific to cyanobacterial hydrogenases; none of these were detected by this study.

Group 3 includes cytoplasmic hydrogenases capable of reversible H_2 oxidation with a soluble cofactor. Groups 3a and 3c are specific to archaea, and a Group 3c representative (from

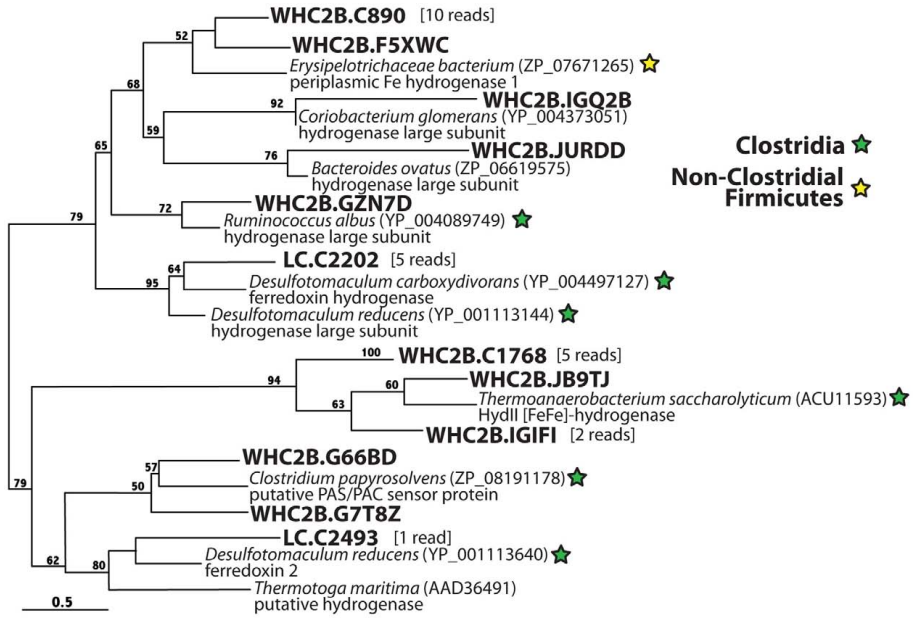

FIGURE 7 | Phylogenetic diversity of hypothetical [FeFe]-hydrogenases detected in metagenomes from a Lost City chimney and Tablelands spring fluid. These sequences show weak similarity to the characterized hydrogenases in **Figure 6** but are highly similar to hypothetical hydrogenases.

Methanocaldococcus jannaschii) is shown in **Figure 5** as an outgroup to Group 3d, which is specific to bacteria. The contig WHC2b.C15 (21 kb, 64% GC) representing eight shotgun reads clustered with four Lost City contigs and two Burkholderiales Group 3d hydrogenases. An additional Lost City read is most similar to cyanobacterial Group 3d hydrogenases. No sequences in this study shared significant similarity with archaeal hydrogenases.

Group 4 includes H_2-producing [NiFe]-hydrogenases that are typically involved in the disposal of excess reducing equivalents in archaea (Vignais and Billoud, 2007). No Group 4 homologs were identified in this study.

[FeFe]-HYDROGENASE DIVERSITY

Whereas [NiFe]-hydrogenases are typically involved in H_2 uptake and oxidation, almost all [FeFe]-hydrogenases catalyze the production of H_2 (Vignais and Billoud, 2007). (The one known exception does not have any phylogenetic affiliation with any sequences in this study.) The enzyme can be monomeric, dimeric, trimeric, or tetrameric in different species, and the variable number and diversity of paralogs in closely related species obscures phylogenetic relationships (Vignais et al., 2001). Therefore, [FeFe]-hydrogenase phylogeny has limited utility for inferring taxonomic affiliations of metagenomic sequences. Nevertheless, the phylogeny illustrated in **Figure 6**, which is consistent with that reported by Boyd et al. (2009), shows that all of the putative [FeFe]-hydrogenase sequences detected in Lost City and Tablelands samples have close phylogenetic relationships with Clostridia. The largest cluster of putative [FeFe]-hydrogenase sequences represents nine shotgun sequencing reads from WHC2b and shares high sequence similarity with *Desulfotomaculum reducens* (60% identity, 76% similarity over 140 amino acid residues). Members of genus *Desulfotomaculum* are typically sulfate-reducers; some species oxidize H_2, and others require organic carbon compounds as electron donors. Some species are incapable of sulfate reduction, however, and produce H_2 during fermentation as part of a syntrophic relationship with methanogens (Imachi et al., 2006).

A 1.9 kb contig from Lost City (LC.C146) contains a predicted [FeFe]-hydrogenase that is most closely related to that of Candidatus "*Desulforudis audaxviator*" (**Figure 6**), a deep subsurface organism that is very closely related to the *Desulfotomaculum*. Its genome sequence encodes multiple hydrogenases, including uptake [NiFe]-hydrogenases that indicate the potential for uptake and oxidation of H_2 (Chivian et al., 2008). Only [FeFe]-hydrogenases (**Figure 6**) and no [NiFe]-hydrogenases related to Clostridia, however, were detected in the Lost City or Tablelands metagenomes.

Figure 7 illustrates phylogenetic relationships among proteins predicted to be [FeFe]-hydrogenases by homology but are clearly divergent from and may not be monophyletic with the well-characterized [FeFe]-hydrogenases in **Figure 6**. Almost all of these hypothetical [FeFe]-hydrogenases show high similarity to predicted proteins in Clostridia genomes, the one exception being a cluster of 11 reads from WHC2b that is most similar to a predicted protein from the genome of an unidentified Erysipelotrichaceae bacterium. To our knowledge, the only sequence in this tree for which there is any published experimental characterization is the HydII of *Thermoanaerobacterium saccharolyticum*, which groups with a cluster of eight WHC2b reads. This sequence forms a gene cluster required for H_2 production during fermentation by *T. saccharolyticum*, but deletion of the *hyd*II gene alone had no effect on H_2 production (Shaw et al., 2009). Therefore, the sequences in this tree are potentially associated with H_2 production but are not likely to encode the catalytic subunits of H_2-evolving hydrogenases.

Table 1 | [FeFe]-hydrogenase and [NiFe]-hydrogenase abundance in selected metagenomes, as measured by the number of unique shotgun sequencing reads with tblastn matches to Pfam families PF02906 and PF00374, respectively, with *E*-values better than 10^{-5}.

	MG-RAST or GOLD ID	Total reads	Total Mb	[FeFe]-hydrogenase			[NiFe]-hydrogenase		
				# Reads	% Reads	Per 100 Mb	# Reads	% Reads	Per 100 Mb
ANME sediment 9-12 cm	Gs0000778	628,644	250.2	92	0.015	36.8	378	0.060	151.1
Hulk Marine Vent Virome	4448187.3	231,246	77.2	1	0.000	1.3	85	0.037	110.1
Lost City chimney	4461585.3	46,360	34.6	12	0.026	34.7	37	0.080	107.0
Alvinella worm symbionts	4441102.3	293,065	290.4	3	0.001	1.0	285	0.097	98.2
Anammox bioreactor	Gs0000439	319,509	122.8	8	0.003	6.5	112	0.035	91.2
Great boiling spring 77˚C cellulolytic enrichment	Gs0000682	421,849	98.9	210	0.050	212.3	80	0.019	80.9
Great boiling spring 85˚C cellulolytic enrichment	Gs0000683	1,447,430	455.1	466	0.032	102.4	336	0.023	73.8
ANME sediment 6–9 cm	Gs0000775	585,529	153.4	62	0.011	40.4	113	0.019	73.7
ANME sediment 0–3 cm	Gs0000776	587,961	213.8	35	0.006	16.4	151	0.026	70.6
Guerrero Negro hypersaline mat	4440963.3–4440972.3	129,147	84.2	44	0.034	52.2	47	0.036	55.8
Black soudan mine drainage	4440282.3	388,627	38.5	5	0.001	13.0	20	0.005	51.9
WHC2b spring	4460690.3	118,348	58.5	44	0.037	75.2	23	0.019	39.3
Mixed alcohol bioreactor 40˚C	Gs0000872	2,261,434	491.5	527	0.023	107.2	136	0.006	27.7
Fungus-growing termite	Gs0000760	1,736,328	634.9	138	0.008	21.7	149	0.009	23.5
Great boiling spring surface sediment	Gs0000680	1,203,155	451.8	0	0.000	0.0	89	0.007	19.7
Mixed alcohol bioreactor 55˚C	Gs0000871	2,129,475	693.8	1004	0.047	144.7	125	0.006	18.0
ANME sediment 3–6 cm	Gs0000777	496,041	151.5	6	0.001	4.0	19	0.004	12.5
Beowulf spring (Yellowstone)	Gs0000972	1,141,299	356.7	0	0.000	0.0	27	0.002	7.6
UBA acid mine drainage	4441138.3	138,453	144.2	0	0.000	0.0	10	0.007	6.9
One hundred springs plain B (Yellowstone)	Gs0000781	581,599	215	0	0.000	0.0	12	0.002	5.6
One hundred springs plain C (Yellowstone)	Gs0000782	507,891	180.5	0	0.000	0.0	10	0.002	5.5
Global ocean sampling expedition	4441121.3–4442709.3	11,798,293	12,357.9	60	0.001	0.5	335	0.003	2.7
Red soudan mine drainage	4440281.3	334,386	35.4	0	0.000	0.0	0	0.000	0.0
Octopus spring virome (Yellowstone)	4441096.3	22,272	22.6	0	0.000	0.0	0	0.000	0.0
TLE chimney	4460689.3	135,538	69.4	0	0.000	0.0	0	0.000	0.0

It is important to note that these hypothetical hydrogenases are included in the tblastn results for [FeFe]-hydrogenases reported in **Table 1**, and our phylogenetic analyses were required to distinguish them from homologs of characterized H_2-evolving hydrogenases (**Figure 6**).

CARBON MONOXIDE DEHYDROGENASE DIVERSITY

The oxidation of carbon monoxide by aerobic carboxydotrophs (organisms that use CO as their sole electron donor and carbon source) is catalyzed by carbon monoxide dehydrogenase (CODH; Ragsdale, 2004; King and Weber, 2007). (Note that this enzyme is distinct from the CODH/ACS enzyme complex that is required for carbon fixation in the Wood–Ljungdahl pathway discussed below.) CODH is encoded by the *cox*, also called *cut*, genes, which can be used as marker genes for aerobic carboxydotrophs (King, 2003; Cunliffe et al., 2008; Cunliffe, 2011). The largest WHC2b contig in our dataset (WHC2b.C1, 37 kb) contains putative homologs for the three structural subunits of CODH, CoxMSL. The CoxL homolog shows a close phylogenetic affinity to other Betaproteobacteria CoxL genes (**Figure A1** in Appendix) including that of *Hydrogenophaga pseudoflava*, a facultative anaerobe that can grow autotrophically on H_2 or CO (Willems et al., 1989). The only other potential CoxL homolog detected in our datasets by tblastn search was a Lost City shotgun read (**Figure A1** in Appendix) that is most similar to *Labrenzia aggregata* (formerly *Stappia aggregata*), a marine aerobic carboxydotroph belonging to the alphaproteobacterial order Rhodobacterales (Weber and King, 2007).

ACETYL-CoA SYNTHASE DIVERSITY

Many Clostridia use H_2 to generate acetate, so we explored the metagenomic data to test whether the clostridial hydrogenases (**Figure 6**) are potentially encoded by acetogens. Acetogens and methanogens utilize the Wood–Ljungdahl (also known as reductive acetyl-CoA) pathway for carbon fixation, and the key enzyme acetyl-CoA synthase (ACS) is unique to that pathway (Ragsdale and Pierce, 2008). To investigate the potential for anaerobic carbon fixation via the Wood–Ljungdahl pathway in the Tablelands springs and Lost City chimneys, we conducted a tblastn search for ACS sequences in our metagenomes. The phylogenetic relationships among the three WHC2b shotgun sequencing reads and two Lost City shotgun sequencing reads with potential ACS homologs are displayed in **Figure A2** in Appendix. All three WHC2b sequences cluster with the ACS of *Dethiobacter alkaliphilus*, a H_2-oxidizing autotrophic Clostridia that can use acetate as a carbon source but not as an energy source (Sorokin et al., 2008). To our knowledge, there is no published evidence that *D. alkaliphilus* can carry out acetogenesis. The KEGG annotation of its genome available at the DOE Joint Genome Institute's IMG database (Markowitz et al., 2008) indicates the presence of at least three additional homologs required for the Wood–Ljungdahl pathway, but it is unclear whether a complete pathway for acetogenesis is present. The ACS of *Moorella thermoacetica*, a known thermophilic acetogen (Pierce et al., 2008), has 60% identity and 78% similarity over 161 amino acid residues with shotgun read WHC2b.JXG7G. The Lost City sequences, by contrast, group with methanogen ACS sequences (**Figure A2** in Appendix). *Methanosarcinales*-related archaea are known to dominate the anoxic interiors of Lost City chimney biofilm communities (Schrenk et al., 2004), but methanogen sequences are rare in this Lost City metagenomic dataset, presumably because it is derived from more oxidized, exterior portions of the chimney (Brazelton et al., 2006; Brazelton and Baross, 2010).

DISCUSSION

POTENTIAL FOR H_2-FUELED CARBON FIXATION BY BURKHOLDERIALES

The metagenomic and phylogenetic data presented above indicate that Betaproteobacteria belonging to order Burkholderiales are potentially important primary producers adapted to the extreme conditions of the Tablelands springs. Their potential for H_2 oxidation is indicated by the diversity of uptake [NiFe]-hydrogenase sequences (**Figure 5**) in the WHC2b spring, which are absent in the TLE spring. Their potential for carbon fixation is indicated by the presence of gene clusters encoding carbon monoxide dehydrogenase (CODH) and Rubisco in the largest WHC2b contig (WHC2b.C1; **Figure 4**). The phylogenies of the [NiFe]-hydrogenases, CODH, and 16S rRNA sequences in WHC2b contigs indicate close relationships with *Hydrogenophaga* species and *Ralstonia eutropha* (now *Cupriavidus necator*). These organisms are facultatively autotrophic; i.e., they only utilize H_2 or fix carbon when organic carbon is unavailable (Willems et al., 1989; Schwartz et al., 2009). Therefore, further characterization of the physiology of these organisms and their access to organic matter in the Tablelands springs is required to estimate their contribution to primary production. Furthermore, all *Hydrogenophaga* and *Ralstonia* species are aerobic or facultatively anaerobic, so the corresponding organisms at the Tablelands and Lost City are likely to inhabit oxic–anoxic transition zones where they have access to both H_2 and oxygen. Both of these systems feature strong oxygen gradients between the atmosphere and spring water (at the Tablelands) and between oxygenated seawater and hydrothermal fluid (at Lost City), so there is potential in each system for organisms to utilize both H_2 and oxygen.

It is unclear whether the TLE spring also hosts H_2-fueled carbon fixation. Although a Burkholderiales 16S rRNA sequence was identified in a metagenomic contig from TLE and automated taxonomy classifiers identify many Burkholderiales-related sequences in the TLE metagenome (MG-RAST and TaxSOM, data not shown), no hydrogenases were detected in TLE. The absence of hydrogenases could be due to a combination of lower abundance of Burkholderiales in TLE and lower sequencing depth of the TLE metagenome compared to WHC2b. It is also possible that the Burkholderiales species in TLE have lost their hydrogenase genes, which may have resulted from the loss of the plasmid potentially represented by contig WHC2b.C1, as discussed above in the description of **Figure 4**.

Most H_2-oxidizing autotrophs utilize both membrane-bound (Group 1) and cytoplasmic (Group 3) [NiFe]-hydrogenases. The [NiFe]-hydrogenase in the WHC2b.C1 contig belongs to the Group 2 H_2 sensor proteins, which are involved in the regulation of carbon fixation by H_2 but do not directly couple H_2 oxidation with energy conservation (Vignais et al., 2001). Therefore, the evidence from this one contig indicates only that carbon fixation in the corresponding organism is regulated by the presence of H_2 and not necessarily fueled by H_2 oxidation. The phylogeny of the Group 2 [NiFe]-hydrogenase in WHC2b.C1, however, is congruent with the phylogeny of the Group 3 [NiFe]-hydrogenase in a 21 kb contig (WHC2b.C15; **Figure 5**). It seems highly likely that both contigs are derived from the same species, and both hydrogenases are highly similar to putative homologs in *Ralstonia eutropha*. The Group 1, 2, and 3 hydrogenases in *R. eutropha* are all encoded in a 452 kb megaplasmid, and it is possible that contigs WHC2b.C1 and WHC2b.C15 are partial sequences of the same plasmid (as described above).

The lack of a *Ralstonia*-related Group 1 [NiFe]-hydrogenase in the WHC2b metagenome is puzzling, however (**Figure 5**). *Nitrosospira multiformis* is one of the few examples listed in the exhaustive survey by Vignais and Billoud (2007) of an organism that has only a Group 3d [NiFe]-hydrogenase and no representative from Group 1. The function of the *N. multiformis* Group 3d [NiFe]-hydrogenase is unknown but suspected to be the catalysis of NAD reduction by H_2 in order to "increase the overall energetic yield from ammonia oxidation" (Norton et al., 2008). Therefore, it is possible that the *Ralstonia*-like organisms in the Tablelands only utilize H_2 to supplementary their primary electron donor (e.g., organic carbon). The current metagenomic dataset from WHC2b is relatively low coverage, however, and additional sequencing at higher coverage may eventually recover a Group 1 homolog.

Both Group 1 and Group 3 [NiFe]-hydrogenases related to *R. eutropha* are present in several Lost City contigs (**Figure 5**), indicating that a *Ralstonia*-related organism with the genetic potential for H_2 oxidation also inhabits Lost City chimneys. The Lost City metagenomic dataset is dominated by sequences with high

similarity to that of *Thiomicrospira crunogena*, a cosmopolitan sulfur-oxidizing autotroph in marine hydrothermal vents. Previous studies have noted the inability of *T. crunogena* to utilize H_2 as a sole electron donor despite the presence of a Group 1 [NiFe]-hydrogenase in its genome (Scott et al., 2006). None of the hydrogenases detected in this study have high sequence similarity to the *T. crunogena* hydrogenase, nor do any of the large Lost City contigs expected to correspond to *Thiomicrospira*-like organisms contain predicted hydrogenases. Therefore, H_2-oxidizing organisms in young, hot Lost City chimneys are most likely aerobic or facultatively anaerobic Betaproteobacteria belonging to order Burkholderiales and appear to be less abundant than the dominant sulfur-oxidizing *Thiomicrospira*-like population.

POTENTIAL FOR CO UTILIZATION BY BURKHOLDERIALES

Carbon dioxide is extremely scarce in the highly reducing, high pH fluids of the Tablelands and Lost City, so alternative carbon species may be more favorable substrates for carbon fixation. The largest Tablelands contig (WHC2b.C1; **Figure 4**) includes the CoxMSL gene cluster which encodes all three subunits of the carbon monoxide dehydrogenase (CODH) used by aerobic carboxydotrophs (Ragsdale, 2004; King and Weber, 2007). This enzyme is frequently plasmid-encoded (Hugendieek and Meyer, 1992), providing additional but not conclusive evidence that the WHC2b.C1 contig represents a plasmid. The phylogeny of the large subunit of CODH from WHC2b.C1 indicates a close phylogenetic relationship with *Hydrogenophaga pseudoflava*, an aerobic autotrophic member of Burkholderiales that can grow on either H_2 or CO (Willems et al., 1989; Kang and Kim, 1999). Therefore, the phylogeny of the CODH in the WHC2b.C1 contig is consistent with that of the [NiFe]-hydrogenases discussed above. CODH is typically involved in aerobic oxidation of CO, but some studies indicate that oxidation of low levels of CO can be coupled to nitrate rather than oxygen (King, 2006). Therefore, CO utilization could be advantageous in Tablelands springs when concentrations of H_2, oxygen, and organic compounds are too low to support growth, but any conclusions about the importance of CO in these systems will require further investigations. At Lost City, CO utilization seems unlikely because of the abundance and ubiquity of H_2 and because CODH appears to be very rare (identified in only a single shotgun sequencing read).

POTENTIAL FOR H_2 PRODUCTION BY CLOSTRIDIA

Nearly all of the [FeFe]-hydrogenases detected in the WHC2b spring at the Tablelands and in the Lost City chimney have close phylogenetic relationships with putative homologs in Clostridia. [FeFe]-hydrogenases catalyze H_2 production by anaerobic bacteria, typically during fermentation, so one would expect them to be prevalent in anoxic environments where H_2 production is favorable. Potential subsurface sources of fermentable organic material are indicated by elevated levels of dissolved organic carbon in Lost City fluids (Lang et al., 2010) and the presence of low molecular weight hydrocarbons with potentially abiogenic origins in both Lost City and Tablelands fluids (Proskurowski et al., 2008; Szponar et al., submitted). No hydrogenases were detected in the Tablelands spring (TLE) that was collected from a more dilute and oxidizing seep (pH 10.5, $E_h + 25$ mV) only ~2 km from WHC2b (pH 12.06, $E_h - 733$ mV). Therefore, the presence of [FeFe]-hydrogenases in the WHC2b metagenome supports the notion that the spring is supplied by fluid from an anoxic environment. Their presence in the Lost City chimney could be indicative of anoxic niches within chimney biofilms and/or the contribution of subsurface fluid to the chimney sample. The greater abundance of Clostridia-related 16S rRNA gene sequences in younger, hotter Lost City chimneys is consistent with both of these possibilities (Brazelton et al., 2010).

The community structure of Tablelands springs and Lost City chimneys, as described here, resembles that of deep boreholes in South Africa (Moser et al., 2005; Lin et al., 2006). The subsurface fluids sampled by these boreholes are also basic (pH ~9) and enriched in H_2 (up to 3.7 mM). The shallow fluids described by Moser et al. (2005) are dominated by Betaproteobacteria belonging to the Comamonadaceae family, and deeper fluids are comprised almost exclusively of Clostridia affiliated with genus *Desulfotomaculum*. The deep subsurface *Desulfotomaculum*-related organisms are predicted to be sulfate-reducers in these environments, which is consistent with metagenomic data representing the dominant organism, Candidatus "*Desulforudis audaxviator*" (Chivian et al., 2008). Some closely related species, however, are known to lack the genes required for sulfate reduction and instead subsist on fermentation, producing H_2 as part of a syntrophic relationship with methanogens (Imachi et al., 2006). Indeed, no sequences encoding dissimilatory sulfite reductase were identified in the Tablelands metagenomes, a striking result compared to the abundance of hydrogenases. The Lost City metagenome encodes a dissimilatory sulfite reductase with high sequence similarity to multiple *Desulfotomaculum* species (Brazelton, 2010), but it was detected in only a single sequencing read, indicating that it is far less abundant than the hydrogenases. Therefore, the Clostridia in Tablelands springs and Lost City chimneys are potential sulfate-reducers, but the abundance of [FeFe]-hydrogenases in metagenomic data from both environments indicates that they are more likely to be involved in H_2-generating fermentation. It is unclear whether this putative fermentation is syntrophic with H_2-utilizing methanogens. Automated annotation predicted very few methanogen sequences in the Tablelands and Lost City metagenomes (data available on the MG-RAST server), but they were present and may be more abundant in deeper habitats that were not well-represented in the samples described in this study.

It is also possible that the Clostridia detected in this study are acetogens that are adapted to the elevated H_2 concentrations in the Tablelands and Lost City fluids. No sequences encoding acetyl-CoA synthase were detected at Lost City, but the phylogeny of ACS sequences from WHC2b is consistent with the presence of clostridial acetogens in very low abundance. Acetogens are known to be capable of producing H_2 and harboring a wide diversity of [FeFe]-hydrogenases (Kellum and Drake, 1984; Schmidt et al., 2010, 2011), so determining the role of these Clostridia in the H_2 budget of these systems will require physiological and biogeochemical investigations. Only three ACS sequences were recovered from WHC2b, however, and none of these were assembled into contigs. Therefore, the current dataset indicates that acetogenesis may occur but does not appear to be prevalent in the Tablelands springs. It is possible that a more representative sample of the

subsurface habitat underlying the spring could reveal more abundant evidence of acetogenesis, as well as other anaerobic metabolic pathways.

CONCLUSION

Both the marine and continental serpentinite springs investigated in this study show evidence of aerobic organisms capable of H_2-fueled (or at least H_2-regulated) primary production (i.e., Burkholderiales) and anaerobic organisms capable of H_2 production from fermentation of organic carbon (i.e., Clostridia). This community structure resembles that of the deep subsurface habitat sampled by a ∼3 km deep borehole in South Africa (Moser et al., 2005), indicating that the surface-exposed springs described in this study provide access to organisms flushed from the subsurface. Furthermore, the remarkably high density of hydrogenases in both the marine and continental springs (Lost City and WHC2b) in this study and their complete absence in a spring showing evidence of extensive mixture with surface runoff (TLE) indicate that the H_2-associated metabolic activities discussed here are specific to subsurface processes.

The predicted metabolic characteristics of the dominant organisms in the Tablelands springs are consistent with the known abiogenic products of subsurface serpentinization-associated processes: H_2 and low molecular-weight organic compounds. A major unanswered question, however, is whether the H_2-oxidizing Burkholderiales subsist on abiogenic H_2 generated by serpentinization in the subsurface or if they depend on biogenic H_2 produced by Clostridia. In either case, it seems likely that the Burkholderiales in the Tablelands springs and Lost City chimneys inhabit oxic–anoxic interfaces where they have access to both H_2 and oxygen. Our metagenomic evidence also suggests that these organisms may be able to survive on carbon monoxide if H_2 is unavailable. The Clostridia are likely inhabitants of anoxic, subsurface habitats where they ferment organic compounds into H_2, but the source of these organic compounds is unknown. If they are ultimately derived from reduction of carbon by serpentinization-associated reactions (as evidenced in (Proskurowski et al., 2008) and predicted by experiments reviewed in (McCollom and Seewald, 2007), then fermentation of these compounds could be considered a kind of primary production as it would be the generation of new biomass from non-biological carbon and energy.

Therefore, both the H_2-oxidizing Burkholderiales and H_2-producing Clostridia may be important mediators of carbon and energy exchange between the deep Earth and the surface biosphere. Further research should investigate whether these organisms are *bona fide* denizens of the anoxic subsurface by probing deeper to obtain more representative samples of deep subsurface habitats.

In particular, the Clostridia and methanogens should be better represented in deeper samples. Nevertheless, the datasets presented here represent a proof-of-concept metagenomic study that demonstrates the potential of surface-exposed springs to yield insights into the microbial diversity of the subsurface biosphere.

ACKNOWLEDGMENTS

We gratefully acknowledge logistical support and scientific inspiration from P. Morrill, N. Szponar, and many other faculty, staff, and students at Memorial University of Newfoundland. This work was supported by ECU startup funds to MOS and a NASA Astrobiology Institute grant through Cooperative Agreement NNA04CC09A to the Geophysical Laboratory at the Carnegie Institution for Science. William J. Brazelton was supported by a NASA Astrobiology Institute postdoctoral fellowship.

REFERENCES

Abdo, Z., Schüette, U. M., Bent, S. J., Williams, C. J., Forney, L. J., and Joyce, P. (2006). Brief report statistical methods for characterizing diversity of microbial communities by analysis of terminal restriction fragment length polymorphisms of 16S rRNA genes. *Environ. Microbiol.* 8, 929–938.

Altschul, S. F., Madden, T. L., Schaffer, A. A., Zhang, J. H., Zhang, Z., Miller, W., and Lipman, D. J. (1997). Gapped BLAST and PSI-BLAST: a new generation of protein database search programs. *Nucleic Acids Res.* 25, 3389–3402.

Aziz, R. K., Bartels, D., Best, A. A, DeJongh, M., Disz, T., Edwards, R. A, Formsma, K., Gerdes, S., Glass, E. M., Kubal, M., Meyer, F., Olsen, G. J., Olson, R., Osterman, A. L., Overbeek, R., McNeil, L. K., Paarmann, D., Paczian, T., Parrello, B., Pusch, G. D., Reich, C., Stevens, R., Vassieva, O., Vonstein, V., Wilke, A., and Zagnitko, O. (2008). The RAST Server: rapid annotations using subsystems technology. *BMC Genomics* 9, 75. doi:10.1186/1471-2164-9-75

Biddle, J. F., Lipp, J. S., Lever, M. A., Lloyd, K. G., Sørensen, K. B., Anderson, R., Fredricks, H. F., Elvert, M., Kelly, T. J., Schrag, D. P., Sogin, M. L., Brenchley, J. E., Teske, A., House, C. H., and Hinrichs, K. (2006). Heterotrophic Archaea dominate sedimentary subsurface ecosystems off Peru. *Proc. Natl. Acad. Sci. U.S.A.* 103, 3846–3851.

Boyd, E. S., Hamilton, T. L., Spear, J. R., Lavin, M., and Peters, J. W. (2010). [FeFe]-Hydrogenase in Yellowstone National Park: evidence for dispersal limitation and phylogenetic niche conservatism. *ISME J.* 4, 1485–1495.

Boyd, E. S., Spear, J. R., and Peters, J. W. (2009). [FeFe] Hydrogenase genetic diversity provides insight into molecular adaptation in a saline microbial mat community. *Appl. Environ. Microbiol.* 75, 4620–4623.

Brazelton, W. J. (2010). *Ecology of Archaeal and Bacterial Biofilm Communities at the Lost City Hydrothermal Field.* Ph.D. dissertation, University of Washington, Seattle, WA.

Brazelton, W. J., and Baross, J. A. (2009). Abundant transposases encoded by the metagenome of a hydrothermal chimney biofilm. *ISME J.* 3, 1420–1424.

Brazelton, W. J., and Baross, J. A. (2010). Metagenomic comparison of two thiomicrospira lineages inhabiting contrasting deep-sea hydrothermal environments. *PLoS ONE* 5, e13530. doi:10.1371/journal.pone.0013530

Brazelton, W. J., Ludwig, K. A., Sogin, M. L., Andreishcheva, E. N., Kelley, D. S., Shen, C.-C., Edwards, R. L., and Baross, J. A. (2010). Archaea and bacteria with surprising microdiversity show shifts in dominance over 1000-year time scales in hydrothermal chimneys. *Proc. Natl. Acad. Sci. U.S.A.* 107, 1612–1617.

Brazelton, W. J., Mehta, M. P., Kelley, D. S., and Baross, J. A. (2011). Physiological differentiation within a single-species biofilm fueled by serpentinization. *MBio.* 2, e00127–11.

Brazelton, W. J., Schrenk, M. O., Kelley, D. S., and Baross, J. A. (2006). Methane- and sulfur-metabolizing microbial communities dominate the Lost City hydrothermal field ecosystem. *Appl. Environ. Microbiol.* 72, 6257–6270.

Campanella, J. J., Bitincka, L., and Smalley, J. (2003). MatGAT: an application that generates similarity/identity matrices using protein or DNA sequences. *BMC Bioinformatics* 4, 29. doi:10.1186/1471-2105-4-29

Chivian, D., Brodie, E. L., Alm, E. J., Culley, D. E., Dehal, P. S., DeSantis, T. Z., Gihring, T. M., Lapidus, A., Lin, L.-H., Lowry, S. R., Moser, D. P., Richardson, P. M., Southam, G., Wanger, G., Pratt, L. M., Andersen, G. L., Hazen, T. C., Brockman, F. J., Arkin, A. P., and Onstott, T. C. (2008). Environmental genomics reveals a single-species ecosystem deep within Earth. *Science* 322, 275–278.

Cunliffe, M. (2011). Correlating carbon monoxide oxidation with cox genes in the abundant Marine Roseobacter Clade. *ISME J.* 5, 685–691.

Cunliffe, M., Schäfer, H., Harrison, E., Cleave, S., Upstill-Goddard, R., and Murrell, J. C. (2008). Phylogenetic and functional gene analysis of the bacterial and archaeal communities associated with the surface microlayer of an estuary. *ISME J.* 2, 776–789.

Edgar, R. C. (2004). MUSCLE: multiple sequence alignment with high accuracy and high throughput. *Nucleic Acids Res.* 32, 1792–1797.

Finn, R. D., Tate, J., Mistry, J., Coggill, P. C., Sammut, S. J., Hotz, H.-R., Ceric, G., Forslund, K., Eddy, S. R., Sonnhammer, E. L, and Bateman, A. (2008). The Pfam protein families database. *Nucleic Acids Res.* 36, D281–D288.

Fricke, W. F., Kusian, B., and Bowien, B. (2009). The genome organization of *Ralstonia eutropha* strain H16 and related species of the Burkholderiaceae. *J. Mol. Microbiol. Biotechnol.* 16, 124–135.

Gagen, E. J., Denman, S. E., Padmanabha, J., Zadbuke, S., Al Jassim, R., Morrison, M., and McSweeney, C. S. (2010). Functional gene analysis suggests different acetogen populations in the bovine rumen and tammar wallaby forestomach. *Appl. Environ. Microbiol.* 76, 7785–7795.

Gomez-Alvarez, V., Teal, T. K., and Schmidt, T. M. (2009). Systematic artifacts in metagenomes from complex microbial communities. *ISME J.* 3, 1314–1317.

Huber, J. A., Butterfield, D. A., and Baross, J. A. (2002). Temporal changes in archaeal diversity and chemistry in a mid-ocean ridge subseafloor habitat. *Appl. Environ. Microbiol.* 68, 1585–1594.

Huber, J. A, Mark Welch, D. B., Morrison, H. G., Huse, S. M., Neal, P. R., Butterfield, D. A., and Sogin, M. L. (2007). Microbial population structures in the deep marine biosphere. *Science* 318, 97–100.

Hugendieek, I., and Meyer, O. (1992). The structural genes encoding CO dehydrogenase subunits (cox L, M and S) in *Pseudomonas carboxydovorans* OM5 reside on plasmid pHCG3 and are, with the exception of *Streptomyces thermoautotrophicus*, conserved in carboxydotrophic bacteria. *Arch. Microbiol.* 157, 301–304.

Imachi, H., Sekiguchi, Y., Kamagata, Y., Loy, A., Qiu, Y.-L., Hugenholtz, P., Kimura, N., Wagner, M., Ohashi, A., and Harada, H. (2006). Non-sulfate-reducing, syntrophic bacteria affiliated with *Desulfotomaculum* cluster I are widely distributed in methanogenic environments. *Appl. Environ. Microbiol.* 72, 2080–2091.

Kang, B. S., and Kim, Y. M. (1999). Cloning and molecular characterization of the genes for carbon monoxide dehydrogenase and localization of molybdopterin, flavin adenine dinucleotide, and iron-sulfur centers in the enzyme of *Hydrogenophaga pseudoflava*. *J. Bacteriol.* 181, 5581–5590.

Kelley, D. S., Karson, J. A., Fruh-Green, G. L., Yoerger, D. R., Shank, T. M., Butterfield, D. A., Hayes, J. M., Schrenk, M. O., Olson, E. J., Proskurowski, G., Jakuba, M., Bradley, A., Larson, B., Ludwig, K., Glickson, D., Buckman, K., Bradley, A. S., Brazelton, W. J., Roe, K., Elend, M. J., Delacour, A., Bernasconi, S. M., Lilley, M. D., Baross, J. A., Summons, R. E., and Sylva, S. P. (2005). A serpentinite-hosted ecosystem: the Lost City hydrothermal field. *Science* 307, 1428–1434.

Kellum, R., and Drake, H. L. (1984). Effects of cultivation gas phase on hydrogenase of the acetogen *Clostridium thermoaceticum*. *J. Bacteriol.* 160, 466–469.

King, G. M. (2003). Molecular and culture-based analyses of aerobic carbon monoxide oxidizer diversity. *Appl. Environ. Microbiol.* 69, 7257–7265.

King, G. M. (2006). Nitrate-dependent anaerobic carbon monoxide oxidation by aerobic CO-oxidizing bacteria. *FEMS Microbiol. Ecol.* 56, 1–7.

King, G. M., and Weber, C. F. (2007). Distribution, diversity and ecology of aerobic CO-oxidizing bacteria. *Nat. Rev. Microbiol.* 5, 107–118.

Lang, S. Q., Butterfield, D. A., Schulte, M., Kelley, D. S., and Lilley, M. D. (2010). Elevated concentrations of formate, acetate and dissolved organic carbon found at the Lost City hydrothermal field. *Geochim. Cosmochim. Acta* 74, 941–952.

Larkin, M. A., Blackshields, G., Brown, N. P., Chenna, R., McGettigan, P. A., McWilliam, H., Valentin, F., Wallace, I. M., Wilm, A., Lopez, R., Thompson, J. D., Gibson, T. J., and Higgins, D. G. (2007). Clustal W and Clustal X version 2.0. *Bioinformatics* 23, 2947–2948.

Lin, L.-H., Wang, P.-L., Rumble, D., Lippmann-Pipke, J., Boice, E., Pratt, L. M., Sherwood Lollar, B., Brodie, E. L., Hazen, T. C., Andersen, G. L., DeSantis, T. Z., Moser, D. P., Kershaw, D., and Onstott, T. C. (2006). Long-term sustainability of a high-energy, low-diversity crustal biome. *Science* 314, 479–482.

Ludwig, W., Strunk, O., Westram, R., Richter, L., Meier, H., Yadhukumar, Buchner, A., Lai, T., Steppi, S., Jobb, G., Förster, W., Brettske, I., Gerber, S., Ginhart, A. W., Gross, O., Grumann, S., Hermann, S., Jost, R., König, A., Liss, T., Lüssmann, R., May, M., Nonhoff, B., Reichel, B., Strehlow, R., Stamatakis, A., Stuckmann, N., Vilbig, A., Lenke, M., Ludwig, T., Bode, A., and Schleifer, K.-H. (2004). ARB: a software environment for sequence data. *Nucleic Acids Res.* 32, 1363–1371.

Markowitz, V. M., Ivanova, N., Palaniappan, K., Szeto, E., Korzeniewski, F., Lykidis, A., Anderson, I., Mavromatis, K., Mavrommatis, K., Kunin, V., Garcia Martin, H., Dubchak, I., Hugenholtz, P., and Kyrpides, N. C. (2006). An experimental metagenome data management and analysis system. *Bioinformatics* 22, e359–e367.

Markowitz, V. M., Szeto, E., Palaniappan, K., Grechkin, Y., Chu, K., Chen, I.-M., Dubchak, I., Anderson, I., Lykidis, A., Mavromatis, K., Ivanova, N. N., and Kyrpides, N. C. (2008). The integrated microbial genomes (IMG) system in 2007: data content and analysis tool extensions. *Nucleic Acids Res.* 36, D528–D533.

McCollom, T. M., and Seewald, J. S. (2007). Abiotic synthesis of organic compounds in deep-sea hydrothermal environments. *Chem. Rev.* 107, 382–401.

Meyer, F., Paarmann, D., D'Souza, M., Olson, R., Glass, E. M., Kubal, M., Paczian, T., Rodriguez, A., Stevens, R., Wilke, A., Wilkening, J., and Edwards, R. A. (2008). The metagenomics RAST server – a public resource for the automatic phylogenetic and functional analysis of metagenomes. *BMC Bioinformatics* 9, 386. doi:10.1186/1471-2105-9-386

Moser, D. P., Gihring, T. M., Brockman, F. J., Fredrickson, J. K., Balkwill, D. L., Dollhopf, M. E., Lollar, B. S., Pratt, L. M., Boice, E., Southam, G., Wanger, G., Baker, B. J., Pfiffner, S. M., Lin, L.-H., and Onstott, T. C. (2005). *Desulfotomaculum* and *Methanobacterium* spp. Dominate 4- to 5-kilometer-deep fault. *Appl. Environ. Microbiol.* 71, 8773–8783.

Norton, J. M., Klotz, M. G., Stein, L. Y., Arp, D. J., Bottomley, P. J., Chain, P. S., Hauser, L. J., Land, M. L., Larimer, F. W., Shin, M. W., and Starkenburg, S. R. (2008). Complete genome sequence of *Nitrosospira multiformis*, an ammonia-oxidizing bacterium from the soil environment. *Appl. Environ. Microbiol.* 74, 3559–3572.

Pierce, E., Xie, G., Barabote, R. D., Saunders, E., Han, C. S., Detter, J. C., Richardson, P., Brettin, T. S., Das, A., Ljungdahl, L. G., and Ragsdale, S. W. (2008). The complete genome sequence of *Moorella thermoacetica* (f. *Clostridium thermoaceticum*). *Environ. Microbiol.* 10, 2550–2573.

Proskurowski, G., Lilley, M. D., Seewald, J. S., Fruh-Green, G. L., Olson, E. J., Lupton, J. E., Sylva, S. P., and Kelley, D. S. (2008). Abiogenic hydrocarbon production at lost city hydrothermal field. *Science* 319, 604–607.

Pruesse, E., Quast, C., Knittel, K., Fuchs, B. M., Ludwig, W., Peplies, J., and Glöckner, F. O. (2007). SILVA: a comprehensive online resource for quality checked and aligned ribosomal RNA sequence data compatible with ARB. *Nucleic Acids Res.* 35, 7188–7196.

Ragsdale, S. W. (2004). Life with carbon monoxide. *Crit. Rev. Biochem. Mol. Biol.* 39, 165–195.

Ragsdale, S. W., and Pierce, E. (2008). Acetogenesis and the Wood-Ljungdahl pathway of CO2 fixation. *Biochim. Biophys. Acta* 1784, 1873–1898.

Santelli, C. M., Orcutt, B. N., Banning, E., Bach, W., Moyer, C. L., Sogin, M. L., Staudigel, H., and Edwards, K. J. (2008). Abundance and diversity of microbial life in ocean crust. *Nature* 453, 653–656.

Schmidt, O., Drake, H. L., and Horn, M. A. (2010). Hitherto unknown [Fe-Fe]-hydrogenase gene diversity in anaerobes and anoxic enrichments from a moderately acidic fen. *Appl. Environ. Microbiol.* 76, 2027–2031.

Schmidt, O., Wüst, P. K., Hellmuth, S., Borst, K., Horn, M. A., and Drake, H. L. (2011). Novel [NiFe]- and [FeFe]-hydrogenase gene transcripts indicative of active facultative aerobes and obligate anaerobes in earthworm gut contents. *Appl. Environ. Microbiol.* 77, 5842–5850.

Schrenk, M. O., Huber, J. A., and Edwards, K. J. (2010). Microbial provinces in the subseafloor. *Annu. Rev. Mar. Sci.* 2, 279–306.

Schrenk, M. O., Kelley, D. S., Bolton, S. A., and Baross, J. A. (2004). Low archaeal diversity linked to subseafloor geochemical processes at the Lost City Hydrothermal Field, Mid-Atlantic Ridge. *Environ. Microbiol.* 6, 1086–1095.

Schwartz, E., Voigt, B., Zühlke, D., Pohlmann, A., Lenz, O., Albrecht, D., Schwarze, A., Kohlmann, Y., Krause, C., Hecker, M., and Friedrich, B. (2009). A proteomic view of the facultatively chemolithoautotrophic

lifestyle of *Ralstonia eutropha* H16. *Proteomics* 9, 5132–5142.

Scott, K. M., Sievert, S. M., Abril, F. N., Ball, L. A., Barrett, C. J., Blake, R. A., Boller, A. J., Chain, P. S., Clark, J. A., Davis, C. R., Detter, C., Do, K. F., Dobrinski, K. P., Faza, B. I., Fitzpatrick, K. A., Freyermuth, S. K., Harmer, T. L., Hauser, L. J., Hugler, M., Kerfeld, C. A., Klotz, M. G., Kong, W. W., Land, M., Lapidus, A., Larimer, F. W., Longo, D. L., Lucas, S., Malfatti, S. A., Massey, S. E., Martin, D. D., McCuddin, Z., Meyer, F., Moore, J. L., Ocampo, L. H. Jr., Paul, J. H., Paulsen, I. T., Reep, D. K., Ren, Q., Ross, R. L., Sato, P. Y., Thomas, P., Tinkham, L. E., and Zeruth, G. T. (2006). The genome of deep-sea vent chemolithoautotroph *Thiomicrospira crunogena* XCL-2. *PLoS Biol.* 4, e383. doi:10.1371/journal.pbio.0040383

Shaw, A. J., Hogsett, D. A., and Lynd, L. R. (2009). Identification of the [FeFe]-hydrogenase responsible for hydrogen generation in *Thermoanaerobacterium saccharolyticum* and demonstration of increased ethanol yield via hydrogenase knockout. *J. Bacteriol.* 191, 6457–6464.

Sogin, M. L., Morrison, H. G., Huber, J. A., Mark Welch, D., Huse, S. M., Neal, P. R., Arrieta, J. M., and Herndl, G. J. (2006). Microbial diversity in the deep sea and the underexplored "rare biosphere." *Proc. Natl. Acad. Sci. U.S.A.* 103, 12115–12120.

Sorokin, D. Y., Tourova, T. P., Mussmann, M., and Muyzer, G. (2008). *Dethiobacter alkaliphilus* gen. nov. sp. nov., and *Desulfurivibrio alkaliphilus* gen. nov. sp. nov.: two novel representatives of reductive sulfur cycle from soda lakes. *Extremophiles* 12, 431–439.

Stamatakis, A. (2006). RAxML-VI-HPC: maximum likelihood-based phylogenetic analyses with thousands of taxa and mixed models. *Bioinformatics* 22, 2688–2690.

Stelzmueller, I., Biebl, M., Wiesmayr, S., Eller, M., Hoeller, E., Fille, M., Weiss, G., Lass-Floerl, C., and Bonatti, H. (2006). *Ralstonia pickettii*-innocent bystander or a potential threat? *Clin. Microbiol. Infect.* 12, 99–101.

Vignais, P. M., and Billoud, B. (2007). Occurrence, classification, and biological function of hydrogenases: an overview. *Chem. Rev.* 107, 4206–4272.

Vignais, P. M., Billoud, B., and Meyer, J. (2001). Classification and phylogeny of hydrogenases. *FEMS Microbiol. Rev.* 25, 455–501.

Weber, C. F., and King, G. M. (2007). Physiological, ecological, and phylogenetic characterization of Stappia, a marine CO-oxidizing bacterial genus. *Appl. Environ. Microbiol.* 73, 1266–1276.

Weber, M., Teeling, H., Huang, S., Waldmann, J., Kassabgy, M., Fuchs, B. M., Klindworth, A., Klockow, C., Wichels, A., Gerdts, G., Amann, R., and Glöckner, F. O. (2010). Practical application of self-organizing maps to interrelate biodiversity and functional data in NGS-based metagenomics. *ISME J.* 918–928.

Whitman, W. B., Coleman, D. C., and Wiebe, W. J. (1998). Prokaryotes: the unseen majority. *Proc. Natl. Acad. Sci. U.S.A.* 95, 6578–6583.

Willems, A., Busse, J., Goor, M., Pot, B., Falsen, E., Jantzen, E., Hoste, B., Gillis, M., Kersters, K., Auling, G., and De Ley, J. (1989). Hydrogenophaga, a new genus of hydrogen-oxidizing bacteria that includes *Hydrogenophaga flava* comb. nov. (Formerly *Pseudomonas flava*), *Hydrogenophaga palleronii* (Formerly *Pseudomonas palleronii*), *Hydrogenophaga pseudoflava* (Formerly *Pseudomonas pseudoflava* and "*Pseudomonas carboxydoflava*"), and *Hydrogenophaga taeniospiralis* (Formerly *Pseudomonas taeniospiralis*). *Int. J. Syst. Bacteriol.* 39, 319–333.

Wu, L. F., and Mandrand, M. A. (1993). Microbial hydrogenases: primary structure, classification, signatures and phylogeny. *FEMS Microbiol. Rev.* 10, 243–269.

Conflict of Interest Statement: The authors declare that the research was conducted in the absence of any commercial or financial relationships that could be construed as a potential conflict of interest.

Received: 13 September 2011; accepted: 16 December 2011; published online: 06 January 2012.

Citation: Brazelton WJ, Nelson B and Schrenk MO (2012) Metagenomic evidence for H_2 oxidation and H_2 production by serpentinite-hosted subsurface microbial communities. Front. Microbio. ***2****:268. doi: 10.3389/fmicb.2011.00268*

This article was submitted to Frontiers in Extreme Microbiology, a specialty of Frontiers in Microbiology.

APPENDIX

Table A1 | MIMS-compliant metadata for lost city and tablelands metagenomes.

MIMARKS fields	Description	Units	Lost_City_ biofilm_LC0443	Tablelands_spring_ WHC2B	Tablelands_spring_TLE
submitted_to_insdc	Submitted to insdc		MG-RAST	MG-RAST	MG-RAST
investigation_type	Investigation type		Metagenome	Metagenome	Metagenome
project_name	Project name		Serpentinite springs	Serpentinite springs	Serpentinite springs
lat_lon	Geographic location (latitude and longitude)		30.12, −42.12	49.4653, −57.9576	49.4730, −57.9813
geo_loc_name	Geographic location (country and/or sea region)		Atlantic ocean	Canada	Canada
collection_date	Collection date		2005-07-27	2010-08-25	2010-06-17
biome	Environment (biome)		Extreme habitat	Extreme habitat	Extreme habitat
feature	Environment (feature)		–	–	–
material	Environment (material)		–	–	–
env_package	Environmental package		Microbial mat/biofilm	Water	water
samp_collect_device	Sample collection device or method		ROV grab	Suction through tubing and syringe, collection in Nalgene bottles	Suction through tubing and syringe, collection in Nalgene bottles
samp_mat_process	Sample material processing		None	0.2 μm Sterivex filtering	0.2 μm Sterivex filtering
samp_size	amount or size of sample collected	kg or L	1	10	1.2
nucl_acid_ext	Nucleic acid extraction		doi: 10.1371/journal.pone.0013530	This study	This study
nucl_acid_amp	Nucleic acid amplification		None	None	This study
lib_reads_seqd	Library reads sequenced		46,360	118,348	135,538
lib_vector	Library vector		pUC18	NA	NA
seq_meth	Sequencing method		JGI Sanger end-sequencing	EnGenCore 454 Titanium	EnGenCore 454 Titanium
assembly	Assembly		JGI standard	Geneious medium sensitivity	Geneious medium sensitivity
ENVIRONMENTAL FIELDS					
diss_hydrogen	Dissolved hydrogen	mmol/kg	13	0.235	0.065–0.18
ph	pH		10.7	12.06	10.5
redox_potential	Redox potential	mV	NA	−733	+25
ADDITIONAL FIELDS					
MG_RAST ID	MG_RAST ID		4461585.3, 4470602.3	4460690.3, 4461619.3	4460689.3, 4461618.3
sample_id	Brazelton/Schrenk internal sample ID		H03_072705_R0424	TL10_57	TL10_40

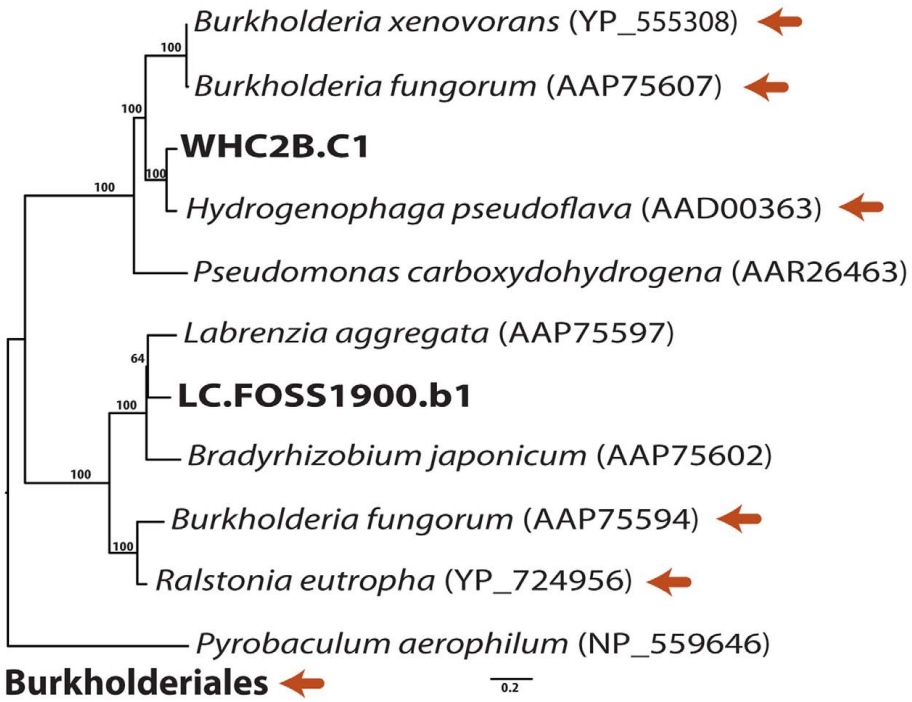

FIGURE A1 | Phylogenetic relationships of putative carbon monoxide dehydrogenase (CODH) sequences in the longest WHC2b contig and in a Lost City shotgun sequencing read. Burkholderiales reference sequences are indicated with orange arrows. Maximum-likelihood bootstrap support values > 50 are shown.

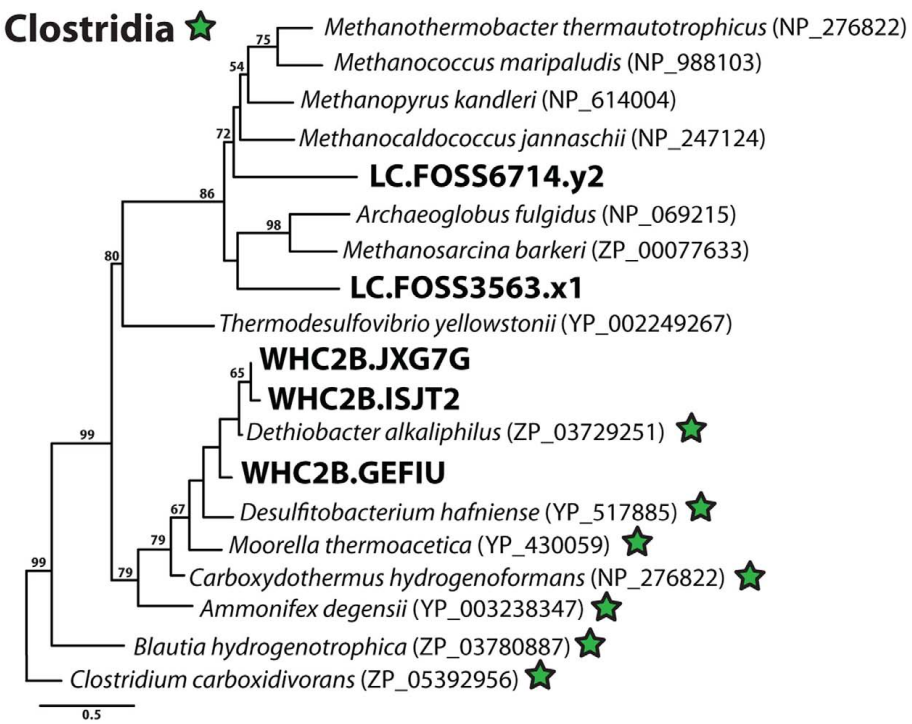

FIGURE A2 | Phylogenetic diversity of putative acetyl-CoA synthase (ACS) sequences in Lost City and Tablelands metagenomic shotgun sequencing reads. Clostridia reference sequences are indicated with green stars, and Lost City (LC), and Tablelands (WHC2b) sequences are in large, bold font. Maximum-likelihood bootstrap support values > 50 are shown.

frontiers in MICROBIOLOGY

HYPOTHESIS AND THEORY ARTICLE
published: 13 January 2012
doi: 10.3389/fmicb.2011.00284

Acetogenesis in the energy-starved deep biosphere – a paradox?

Mark Alexander Lever*

Department of Bioscience, Center for Geomicrobiology, Aarhus University, Aarhus, Denmark

Edited by:
Andreas Teske, University of North Carolina at Chapel Hill, USA

Reviewed by:
Matthew Schrenk, East Carolina University, USA
Aharon Oren, The Hebrew University of Jerusalem, Israel

****Correspondence:***
Mark Alexander Lever, Department of Bioscience, Center for Geomicrobiology, Aarhus University, Ny Munkegade 114, bng 1535-1540, DK-8000 Århus C, Denmark.
e-mail: mark.lever@biology.au.dk

Under anoxic conditions in sediments, acetogens are often thought to be outcompeted by microorganisms performing energetically more favorable metabolic pathways, such as sulfate reduction or methanogenesis. Recent evidence from deep subseafloor sediments suggesting acetogenesis in the presence of sulfate reduction and methanogenesis has called this notion into question, however. Here I argue that acetogens can successfully coexist with sulfate reducers and methanogens for multiple reasons. These include (1) substantial energy yields from most acetogenesis reactions across the wide range of conditions encountered in the subseafloor, (2) wide substrate spectra that enable niche differentiation by use of different substrates and/or pooling of energy from a broad range of energy substrates, (3) reduced energetic cost of biosynthesis among acetogens due to use of the reductive acetyl CoA pathway for both energy production and biosynthesis coupled with the ability to use many organic precursors to produce the key intermediate acetyl CoA. This leads to the general conclusion that, beside Gibbs free energy yields, variables such as metabolic strategy and energetic cost of biosynthesis need to be taken into account to understand microbial survival in the energy-depleted deep biosphere.

Keywords: acetogenesis, deep biosphere, subsurface, marine, energy, sediment, carbon cycling, starvation survival

INTRODUCTION

Past studies on anoxic sediments have demonstrated a redox zonation among terminal organic matter remineralizing microbes in relation to electron acceptor availability (e.g., Froelich et al., 1979; Canfield et al., 1993). Organisms using the electron acceptor with the highest Gibbs free energy yields dominate over groups using energetically less favorable electron acceptors (e.g., Cappenberg, 1974; Lovley and Goodwin, 1988; Hoehler et al., 1998). Higher energy yields support faster growth rates and result in competitive exclusion of groups using less favorable electron acceptors (Cord-Ruwisch et al., 1988). Energy substrates with high turnover rates, e.g., hydrogen (H_2) and acetate, can even be drawn down to thermodynamic threshold concentrations, at which only the most energetically favorable electron acceptor present provides sufficient energy for proton translocation across the cell membrane, ATP formation, and growth (Hoehler et al., 2001; Hoehler, 2004). Evidence supporting the notion of biological redox zonation comes from freshwater and coastal marine sediments, as well as laboratory-based chemostat and coculture experiments.

Consistent with the notion of redox zonation, the processes of denitrification, manganese and iron reduction, and sulfate reduction should exclude energetically less favorable reactions involving CO_2 reduction or disproportionation, wherever the available nitrate, manganese (IV), iron (III), and sulfate pools are not rate-limiting (e.g., Froelich et al., 1979; Canfield et al., 1993). In freshwater and coastal marine sediments depletion of the most favorable oxidants often occurs shallowly owing to an excess of electron donors produced by fermentation and hydrolysis reactions (Capone and Kiene, 1988). This creates a niche for methane-producing Archaea (methanogens) and acetate-synthesizing microbes (acetogens), groups that are able to harvest energy from CO_2 reduction in underlying layers (e.g., Phelps and Zeikus, 1984; Avery et al., 2002; Ferry and Lessner, 2008; Liu and Conrad, 2011). Contrastingly, in more oligotrophic offshore marine sediments, which cover most of the Earth's surface, organic matter and hence electron donor availability are typically limiting. Depletion of nitrate, oxidized metals, sulfate, and/or even dioxygen (O_2) does not occur until tens of meters below the seafloor – if at all (e.g., D'Hondt et al., 2004; D'Hondt et al., 2009). Accordingly methanogens and acetogens should be absent or at best lead fringe existences – dormant, or surviving in small numbers on non-competitive energy substrates not used by the other groups, such as methylated C1 compounds or methoxylated aromatic compounds (Franklin et al., 1988; Lever et al., 2010). Hence, recent evidence from deeply buried marine sediments indicating significant accumulation of biogenic methane in the presence of sulfate and metal reducing populations seems surprising (Wang et al., 2008). Moreover, even though sulfate reducers and methanogens gain more energy than acetogens from shared energy substrates, there is increasing evidence that acetogens play a quantitatively important role in organic carbon cycling in the marine and terrestrial deep biosphere (Heuer et al., 2006, 2009; Griebler and Lueders, 2008; Pedersen et al., 2008; Lever et al., 2010).

In the following sections I will examine possible reasons for the coexistence of acetogenesis with other pathways that are considered to be energetically more favorable in the deep subsurface. In my analyses, I will (1) conservatively calculate the energy yields of widespread acetogenesis reactions in the subsurface, (2) examine

the potential for substrate generalism as a successful strategy under extreme energy limitation, and (3) examine the cost of biosynthesis and potential ways by which acetogens may reduce energy expended on biosynthesis.

MATERIALS AND METHODS

Potential energy yields were calculated for a total of 14 acetogenic substrates and 20 acetogenesis reactions (**Table 1**). Criteria for the choice of these substrates were (1) widespread use by acetogens, (2) previously shown quantitative importance of these or related substrates as metabolic intermediates in anaerobic sediments, (3) representation of a wide range of substrate types used by acetogens, and (4) previously published thermodynamic properties (**Table 2**). The reactions included inorganic substrates (H_2–CO_2, CO), monocarboxylic acids (formate, lactate), dicarboxylic acids (glycolate, oxalate), alcohols (methanol, ethanol), ketones (pyruvate), carbohydrates (glucose, cellobiose), methyl halides (methyl chloride, CH_3Cl; also known as chloromethane), and methoxylated aromatic compounds (syringate, vanillate).

Given the scarcity/absence of concentration data for most of these compounds from the deep subseafloor, I used conservative concentration estimates. This means that educt concentrations used in calculations were in the lower end of the spectrum previously determined for these or similar substrates in the sedimentary or marine setting, whereas product concentrations were near the upper end of the previously measured concentration spectrum (Meyer-Reil, 1978; Ansbaek and Blackburn, 1979; Sørensen et al., 1981; Kaiser and Hanselmann, 1982; King et al., 1982, 1983; Smith and Oremland, 1983; Smith et al., 1985; Edenborn and Litchfield, 1987; King, 1988, 2007; Lovley and Goodwin, 1988; Martens, 1990; Liu and Suflita, 1993; Hoehler et al., 1998; Chidhaisong et al., 1999; Ballschmiter, 2003; Dhillon et al., 2005; Finke et al., 2006; Chapelle and Bradley, 2007; Heuer et al., 2009; Lever et al., 2010). Accordingly, a concentration of 0.1 nM was used for dissolved gaseous energy substrates (CO, CH_3Cl; H_2 see next sentence), while 100 nM were assumed for all other energy substrates. To compensate for the high uncertainty regarding the accuracy of existing H_2 concentration data from below the seafloor, due to the importance of hydrogen as a (co-)substrate in several acetogenesis reactions (**Table 1**), and due to previously published evidence suggesting acetogenesis via CO_2 reduction with H_2 in the deep subsurface (Heuer et al., 2009), two hydrogen concentrations were used, 0.1 nM and 1 μM. These concentrations include the range measured across a wide range of organic-rich to ultra-oligotrophic subsurface sites during ocean drilling program (ODP) Legs 201 and 204, IODP Expedition 329, and Meteor Expedition M76 to the Benguela Upwelling Regime (Shipboard Scientific Party, 2003; Lorenson et al., 2006; Expedition 329 Scientists, 2011; Lin et al., 2011). For acetogenesis reactions involving H_2 as a co-substrate, 1 μM H_2 should be non-limiting. For metabolic products, I assumed a 1-mM concentration of acetate, 100 nM gallate and protocatechuate, and typical seawater concentrations of protons (10^{-8} M) and chloride (0.56 M; Pilson, 1998). Bicarbonate concentrations of 2 mM (typical seawater concentration) were used when bicarbonate was an educt, and 200 mM when bicarbonate was a product. For sulfate reduction reactions, I used sulfate concentrations of 10 mM, and sulfide concentrations of 1 mM. For methanogenesis reactions, I assumed methane concentrations of 1 mM. The pH used in all calculations was 8.0.

For calculations of the *in situ* energy yields of acetogenesis reactions from H_2–CO_2, formate–H_2, and formate, I used published data generated during ODP Leg 201 to the Equatorial Pacific and Peru Margin (Shipboard Scientific Party, 2003). Measured H_2, dissolved inorganic carbon (DIC), formate, and

Table 1 | Overview of acetogenesis reactions examined in this study (from Drake et al., 2006).

Type	Compound name	Reaction
Inorganic	H_2–CO_2	$2\,HCO_3^- + 4\,H_2 + H^+ \rightarrow\ CH_3COO^- + 4\,H_2O$
	Carbon monoxide	$4\,CO + 4\,H_2O \rightarrow CH_3COO^- + 2\,HCO_3^- + 3\,H^+$
	Carbon monoxide + H_2	$2\,CO + 2\,H_2 \rightarrow CH_3COO^- + H^+$
Monocarboxylic acids	Formate	$4\,HCOO^- + H^+ \rightarrow CH_3COO^- + 2\,HCO_3^-$
	Formate–H_2	$2\,HCOO^- + 2\,H_2 + H^+ \rightarrow CH_3COO^- + 2\,H_2O$
	Lactate	$2\,CH_3CHOHCOO^- \rightarrow 3\,CH_3COO^- + H^+$
	Lactate + H_2–CO_2	$CH_3CHOHCOO^- + 6\,H_2 + 3\,HCO_3^- + H^+ \rightarrow 3\,CH_3COO^- + 6\,H_2O$
Dicarboxylic acids	Glycolate	$4\,CH_2OCOO^{2-} + 3\,H^+ \rightarrow 3\,CH_3COO^- + 2\,HCO_3^-$
	Oxalate	$4\,OOCCOO^{2-} + 4\,H_2O + H^+ \rightarrow CH_3COO^- + 6\,HCO_3^-$
Alcohols	Methanol	$4\,CH_3OH + 2\,HCO_3^- \rightarrow 3\,CH_3COO^- + 4\,H_2O + H^+$
	Methanol + H_2–CO_2	$CH_3OH + H_2 + HCO_3^- \rightarrow CH_3COO^- + 2\,H_2O$
	Methanol + formate	$CH_3OH + HCOO^- \rightarrow CH_3COO^- + H_2O$
	Ethanol	$2\,CH_3CH_2OH + 2\,HCO_3^- \rightarrow 3\,CH_3COO- + 2\,H_2O + H^+$
Ketones	Pyruvate	$4\,CH_3COCOO^- + 4\,H_2O \rightarrow 5\,CH_3COO^- + 2\,HCO_3- + 3\,H^+$
Carbohydrates	Glucose	$C_6H_{12}O_6 \rightarrow 3\,CH_3COO^- + 3\,H^+$
	Cellobiose	$C_{12}H_{22}O_{11} + H_2O \rightarrow 6\,CH_3COO^- + 6\,H^+$
Methyl halides	Methyl chloride	$4\,CH_3Cl + 2\,HCO_3- \rightarrow 3\,CH_3COO^- + 4\,Cl^- + 5\,H^+$
Methoxylated aromatic compounds	Syringate	$2\,Syringate[-OCH_3]_2 + 2\,HCO_3^- \rightarrow 2\,gallate[-OH]_2 + 3\,CH_3COO^- + H^+$
	Syringate + H_2–CO_2	$Syringate[-OCH_3]_2 + 2\,HCO_3^- + 2\,H_2 \rightarrow gallate[-OH]_2 + 2\,CH_3COO^- + 2\,H_2O$
	Vanillate	$4\,Vanillate[-OCH_3] + 2\,HCO_3^- \rightarrow 4\,protocatechuate[-OH] + 3\,CH_3COO^- + H^+$

Table 2 | Thermodynamic data of aqueous educts and products under standard conditions (N/A = no available published values).

Compound	ΔG_f° (kJ mol^{-1})	ΔH_f° (kJ mol^{-1})	ΔV_f° (cm^3 mol^{-1})	Reference
Proton (H^+)	0.0	0.0	0.0	Shock et al. (1997)
Hydrogen (H_2)	17.6	−4.2	25.2	Wagman et al. (1982), Shock and Helgeson (1990)
Water	−237.2	−285.8	18.0	Amend and Shock (2001)
Bicarbonate	−586.9	−692.0	24.6	Wagman et al. (1982), Shock et al. (1997)
Carbon monoxide	−120.1	N/A	N/A	Oelkers et al. (1995)
Chloride	−131.4	−167.2	0.1	Shock et al. (1997)
Formate	−351.0	−425.7	26.2	Shock and Helgeson (1990)
Acetate	−369.4	−486.4	40.5	Shock and Helgeson (1990)
Lactate	−513.0	−686.9	56.3	Shock (1995)
Glycolate	−507.3	−647.7	39.9	Shock (1995)
Oxalate	−674.5	−825.6	30.3	Shock (1995)
Methanol	−175.4	−246.5	38.2	Shock and Helgeson (1990)
Ethanol	−181.8	−287.4	55.1	Shock and Helgeson (1990)
Pyruvate	−474.9	−586.9	41.5	Dalla-Betta and Schulte (2009)
Glucose	−915.9	−1262.2	112.2	Amend and Plyasunov (2001)
d-cellobiose	−1578.6	−2236.1	N/A	Tewari et al. (2008)
Methyl chloride	−51.4	−101.7	N/A	Wagman et al. (1982)
Syringate	−564.0	N/A	N/A	Kaiser and Hanselmann (1982)
Gallate	−706.0	N/A	N/A	Kaiser and Hanselmann (1982)
Vanillate	−480.0	N/A	N/A	Kaiser and Hanselmann (1982)
Protocatechuate	−551.0	N/A	N/A	Kaiser and Hanselmann (1982)
Ammonium (NH_4^+)	−79.45	−133.26	18.13	Shock and Helgeson (1988)
Aspartate	−699.91	−940.10	73.83	Amend and Helgeson (1997)
Glutamate	−700.07	−980.34	89.36	Amend and Helgeson (1997)
Glycine	−380.79	−522.43	43.19	Amend and Helgeson (1997)
Serine	−518.83	−721.89	60.57	Amend and Helgeson (1997)
Sulfate (SO_4^{2-})	−744.96	−910.21	13.88	Shock et al. (1997)
Sulfide (HS^-)	11.97	−16.12	20.65	Shock et al. (1997)
l-α-aspartate (asp^{2-})	−699.91	−940.10	73.83	Amend and Helgeson (1997)
l-α-glutamate (glu^{2-})	−700.07	−980.34	89.36	Amend and Helgeson (1997)
l-α-glycine	−380.79	−522.43	43.19	Amend and Helgeson (1997)
l-α-serine	−518.83	−721.89	60.57	Amend and Helgeson (1997)

acetate concentrations were used, in addition to pH. *In situ* temperature was calculated from the measured thermal gradient at each site. *In situ* pressure was calculated from the water and sediment depth, assuming an average water density of 1.029 g cm^{-3} and using average sediment bulk density values for site-specific sedimentary subunits (Shipboard Scientific Party, 2003). Measured amino acid concentrations (glutamate, aspartate, serine, glycine) in ODP Leg 201 sediment cores were obtained from Mitterer (2006).

Gibbs free energies per reaction were calculated for standard conditions (25°C, 1 atm), as well as temperature and pressure extremes inclusive of most subsurface sediments on Earth (Stumm and Morgan, 1981). −1.9°C, the freezing temperature of most seawater, represents the lower temperature boundary likely to be encountered in the deep biosphere, while 122°C marks the upper temperature boundary tolerated by known life (Takai et al., 2008). The pressure range of 1–1000 atm applies from shallow coastal sediments to the vast majority of subsurface sediments in the open ocean. Activities were approximated from concentrations by using the measured activity coefficient, γ, of bicarbonate (0.532) for anionic acetogenesis substrates/products (formate, acetate, lactate, oxalate, glycolate, syringate, vanillate), as well as the measured activity coefficient of methane (1.24) for gases (H_2, CO) and alcohols (methanol, ethanol; both from Millero and Schreiber, 1982). The activity coefficients of water, carbohydrates (glucose, cellobiose), and amino acids (aspartate, glutamate, glycine, serine) were set to 1.0. Published activity coefficients were used for sulfate (0.104) and sulfide (0.410; Millero and Schreiber, 1982).

Gibbs energies per substrate were calculated from Gibbs energies per reaction by dividing the latter by the number of substrates per reaction. Thermodynamic threshold concentrations of each substrate were calculated by setting $\Delta G_r'$ to a an estimated biological energy quantum (BEQ) of −10 kJ mol^{-1} and solving the equation for the substrate concentration, all other educt, and product, concentrations remaining the same and as outlined above.

RESULTS AND DISCUSSION

THE THERMODYNAMIC ARGUMENT

To assess the energetic feasibility of microbial metabolic reactions (**Table 1**) in deep subseafloor sediments, it is helpful to

conservatively calculate their energy yields under conditions that resemble those found *in situ*. In this section, I examine the energetic potential of various acetogenesis reactions to occur in deep subseafloor sediments by examining (1) Gibbs free energy yields per reaction ($\Delta G_r'$), (2) Gibbs free energy yields per substrate ($\Delta G_s'$), (3) thermodynamic threshold concentrations of substrates for acetogenesis reactions to be thermodynamically favorable, (4) *in situ* energy yields of the reactions for which educt and product concentrations have been quantified in subseafloor sediments, and (5) energy yields per hydrogen molecule (H_2) of the various litho- and organotrophic acetogenesis reactions involving H_2 compared to competing hydrogenotrophic sulfate reduction and methanogenesis reactions.

Which acetogenesis reactions are thermodynamically favorable?

Calculated Gibbs free energies indicate that most acetogenesis reactions are thermodynamically favorable in deep subseafloor sediments – with energy yields exceeding the BEQ ($\Delta G_r' = -10\ kJ\ mol^{-1}$) under a wide range of temperatures, pressures, and hydrogen concentrations (**Table 3**). The highest energy values with $\Delta G_r' < -100\ kJ\ mol^{-1}$ are in carbohydrates, pyruvate, methyl chloride, methoxylated aromatic compounds, and lactate. Other substrates, such as glycolate, oxalate, methanol, and ethanol also produce energy yields exceeding the BEQ. By contrast, the classic autotrophic ("homoacetogenic") reaction from H_2–CO_2 and reactions from formate are endergonic at 0.1 nM H_2 concentrations (**Table 3A**), and only yield energy at 1 μM H_2 concentrations and low to intermediate temperatures (**Table 3B**). For energy-yielding substrates that can be used with or without H_2, i.e., carbon monoxide, lactate, methanol, and syringate, reactions not involving H_2 yield more energy at $[H_2] = 0.1$ nM than reactions involving H_2; in the case of carbon monoxide and lactate, this difference is crucial, since reactions without hydrogen produce high-energy yields, whereas reactions with H_2 are endergonic (**Table 3A**). At $[H_2] = 1$ μM this changes, i.e., energy yields of some of the reactions with hydrogen are exergonic, yielding more energy than the BEQ (**Table 3B**); in one case (lactate, −1.9°C) free energy yields even exceed those of acetogenesis from lactate alone at low to

Table 3 | Gibbs free energy yields of the various acetogenesis reactions at a wide range of temperatures, pressures, and H_2 concentrations.

Temperature	−1.9°C		+25°C		+122°C	
Pressure	**1 atm**	**1000 atm**	**1 atm**	**1000 atm**	**1 atm**	**1000 atm**
A						
H_2–CO_2	45.2	41.4	72.4	68.6	170	167
Carbon monoxide	ND	ND	**−54.7**	ND	ND	ND
Carbon monoxide + H_2	ND	ND	−2.57	ND	ND	ND
Formate	24.0	22.5	43.0	41.5	111	110
Formate + H_2	24.2	21.6	46.3	43.6	126	123
Lactate	**−99.5**	**−98.6**	**−101**	**−100**	**−106**	**−105**
Lactate + H_2	18.0	12.8	58.1	52.9	203	198
Glycolate	**−38.0**	**−36.9**	**−16.8**	**−15.6**	59.9	61.0
Oxalate	**−93.9**	**−94.4**	**−84.1**	**−84.6**	**−48.8**	**−49.4**
Methanol	**−104**	**−105**	**−91.8**	**−92.6**	**−45.9**	**−46.8**
Methanol + H_2	**−14.8**	**−13.7**	−4.84	−3.68	31.1	32.3
Methanol + formate	**−25.3**	**−25.9**	**−17.9**	**−18.5**	8.82	8.23
Ethanol	**−37.7**	**−37.9**	**−34.3**	**−34.5**	**−22.0**	**−22.2**
Pyruvate	**−172**	**−170**	**−157**	**−155**	**−102**	**−100**
Glucose	**−332**	**−331**	**−345**	**−344**	**−394**	**−393**
Cellobiose	**−715**	ND	**−747**	ND	**−861**	ND
Methyl chloride	**−210**	ND	**−198**	ND	**−152**	ND
Syringate	ND	ND	**−275**	ND	ND	ND
Syringate + H_2	ND	ND	**−101**	ND	ND	ND
Vanillate	ND	ND	**−263**	ND	ND	ND
B						
H_2–CO_2	**−37.9**	**−41.7**	**−18.9**	**−22.7**	49.4	45.7
Carbon monoxide + H_2	ND	ND	**−48.2**	ND	ND	ND
Formate + H_2	**−17.3**	**−20.0**	0.610	−2.04	65.3	62.7
Lactate + H_2	**−107**	**−112**	**−78.9**	**−84.1**	21.2	16.0
Methanol + H_2	**−35.6**	**−34.4**	**−27.7**	**−26.5**	0.891	2.05
syringate + H_2	ND	ND	**−130**	ND	ND	ND

For reactions that yield more energy than a BEQ of $\Delta G_r' = -10\ kJ\ mol^{-1}$ these values are indicated in bold. (A) $[H_2] = 0.1$ nM in reactions with H_2; (B) $[H_2] = 100$ nM. ND = not determined, due to absence of published ΔH_f° and ΔV_f° values.

Table 4 | Gibbs free energy yields per substrate for the various acetogenesis reactions at a wide range of temperatures (°C), pressures (atm), and H_2 concentrations.

	Substrates reaction^{-1}	−1.9°C		+25°C		+122°C	
		1 atm	1000 atm	1 atm	1000 atm	1 atm	1000 atm
A							
H_2–CO_2	4	11.3	10.3	18.1	17.1	42.6	41.7
CO	4	ND	ND	**−13.7**	ND	ND	ND
CO + H_2	2	ND	ND	−1.28	ND	ND	ND
Formate	4	6.00	5.62	10.7	10.4	27.9	27.5
Formate + H_2	2	12.1	10.8	23.1	21.8	62.9	61.6
Lactate	2	**−49.8**	**−49.3**	**−50.5**	**−50.0**	**−53.0**	**−52.5**
Lactate + H_2	1	18.0	12.8	58.1	52.9	203	198
Glycolate	4	**−9.51**	**−9.23**	**−4.20**	**−3.91**	15.0	15.3
Oxalate	4	**−23.5**	**−23.6**	**−21.0**	**−21.2**	**−12.2**	**−12.3**
Methanol	4	**−26.1**	**−26.3**	**−22.9**	**−23.2**	**−11.5**	**−11.7**
Methanol + H_2	1	**−14.8**	**−13.7**	−4.84	−3.68	31.1	32.3
Methanol + formate	1	**−25.3**	**−25.9**	**−17.9**	**−18.5**	8.82	8.23
Ethanol	2	**−18.9**	**−19.0**	**−17.2**	**−17.3**	**−11.0**	**−11.1**
Pyruvate	4	**−43.0**	**−42.6**	**−39.1**	**−38.8**	**−25.4**	**−25.1**
Glucose	1	**−332**	**−331**	**−345**	**−344**	**−394**	**−393**
Cellobiose	1	**−715**	ND	**−747**	ND	**−861**	ND
Methyl chloride	4	**−52.6**	ND	**−49.5**	ND	**−38.1**	ND
Syringate	2	ND	ND	**−137**	ND	ND	ND
Syringate + H_2	1	ND	ND	**−101**	ND	ND	ND
Vanillate	4	ND	ND	**−65.9**	ND	ND	ND
B							
$H_2 - CO_2$	4	**−9.48**	**−10.4**	**−4.73**	**−5.68**	12.4	11.4
CO + H_2	2	ND	ND	**−24.1**	ND	ND	ND
Formate + H_2	2	**−8.67**	**−9.99**	0.305	−1.02	32.7	31.3
Lactate + H_2	1	**−107**	**−112**	**−78.9**	**−84.1**	21.2	16.0
Methanol + H_2	1	**−35.6**	**−34.4**	**−27.7**	**−26.5**	0.89	2.05
Syringate + H_2	1	ND	ND	**−130**	ND	ND	ND

Reactions yielding energy in excess of a BEQ of $\Delta G_r' = -10$ kJ mol^{-1} are indicated in bold. (A) [H_2]= 0.1 nM in reactions with H_2; (B) [H_2]= 100 nM.

intermediate temperatures (also see Results and Discussion on **Table 4** in next section).

Within the calculated ranges, temperature has a much greater impact on free energy yields of acetogenesis reactions than pressure. For pressure changes from 1 to 1000 atm, the largest effect is in reactions that include H_2, with lactate + H_2 having the greatest change (5.2 kJ mol^{-1}); for all reactions without H_2, the difference in $\Delta G_r'$ between 1 and 1000 atm pressure is $\leq$2 kJ mol^{-1}. By comparison, the difference in $\Delta G_r'$ due to a temperature change from −1.9 to +122°C is always greater than the difference in $\Delta G_r'$ caused by a pressure change from 1 to 1000 atm. For reactions from H_2–CO_2, formate–H_2, lactate–H_2, and cellobiose, the change in $\Delta G_r'$ values going from −1.9 to +122°C even exceeds 100 kJ mol^{-1} of the reaction.

The magnitude of temperature effects seems to follow trends. First of all, of the six reactions involving H_2 or formate for which temperature effects could be calculated, none are thermodynamically favorable at 122°C. This, and the vast overall decrease in free energy yields for acetogenesis reactions involving H_2 or formate in response to temperature, suggests a strong selection against these reactions at temperatures approaching the known upper limit of life – unless H_2 or formate concentrations at high temperatures are much higher than assumed here. Secondly, there appears to be a systematic difference in how temperature affects energy yields. For all C_1–C_3 substrates except reactions from lactate alone, free energy yields decrease with temperature; for reactions from lactate alone, there is a slight increase with temperature. By contrast, the free energy yields of acetogenesis reactions from the carbohydrates glucose (C_6) and cellobiose (C_{12}) show strong increases in response to temperature. Based on the small number of substrates included in these calculations and that the only two large substrates included are carbohydrates, it is premature to argue that larger carbon substrates should be consumed preferably at high temperatures. Yet, the fact that certain substrates or acetogenesis reactions increase, while others decrease in energy yield in response to temperature, suggests that temperature exerts an important control over which substrates are consumed and energy-yielding reactions performed by acetogens in the deep biosphere.

Which acetogenesis reactions are most likely under the conditions examined?

The Gibbs free energy yield of a metabolic reaction indicates whether this reaction can be used as a source of energy in a given environment. Under substrate-limiting conditions, as are likely in the deep biosphere, one might, however, expect microbial consumer choices – assuming they follow optimum foraging behavior – to be driven by energy yields per mole of substrate – as long as the overall reaction produces more energy than the BEQ. For substrates that can be metabolized via multiple reactions that each yield more energy than the BEQ, e.g., methanol at −1.9°C (**Table 3**), one might expect consumers to show a preference toward the reactions with the highest energy yield per substrate. Additionally, it is possible that organisms, despite being energy-starved, show a preference toward certain substrates over others based on energy content per substrate molecule. To examine possible consequences of an optimum foraging behavior that is driven by energy yields per substrate, the latter were calculated (**Table 4**).

Comparing different substrates on a per-substrate-level, Gibbs free energy yields remain high ($\Delta G'_s < -100\ kJ\ mol^{-1}$) for cellobiose, glucose (all T and P), lactate + H_2 (only at $[H_2] = 1\ \mu M$, −1.9 and 25°C; all unchanged compared to **Table 3**), as well as syringate (**Table 4**). Provided their availability in the deep biosphere, and that acetogens make choices based on energy per substrate molecule, these substrates should be consumed preferentially over the others examined. Other good substrates may include – in order of descenting energy yields – vanillate, methyl chloride, lactate, pyruvate, methanol, and oxalate. The classic lithoautotrophic reaction from H_2–CO_2, and reactions from formate and glycolate, are the least energy-yielding on a per-substrate-level, and therefore the least likely to be consumed, should energy content on a substrate-level determine acetogenic substrate choice.

When comparing energy yields of acetogenesis substrates for which multiple reaction pathways are known, i.e., CO, formate, lactate, methanol, and syringate, the same overall trends seen on a per-reaction-level still hold for formate and syringate – independent of H_2 concentrations (**Tables 3** and **4**). For carbon monoxide, lactate, and methanol, the same trends occur at $[H_2] = 1$ nM, but not at $[H_2] = 1\ \mu M$. In spite of the overall reaction from carbon monoxide yielding more energy than the reaction from carbon monoxide + H_2 at high $[H_2]$ (**Table 4**), acetogenesis from carbon monoxide + H_2 yields more energy on a per-substrate-level (**Table 4**). For lactate, reactions from lactate + H_2 at high H_2 yield more energy per lactate than reactions from lactate alone – not only, as previously, at −1.9°C (**Table 3**), but also at +25°C (**Table 4**). And for methanol – unlike before (**Table 3**) – reactions with H_2 yield more energy per methanol at high H_2 and low temperature (−1.9 to 25°C) than reactions with methanol alone (**Table 4**). These results confirm the importance of calculating energy yields on a per-substrate-level. Moreover, they underscore the likely importance of temperature in regulating which acetogenesis reactions are occurring *in situ* – even when these reactions involve the same carbon substrate.

The extent to which microbes can detect and respond to (minor) differences in energy yields of different reactions involving the same substrates, thereby optimizing their foraging behavior with respect to energy yields per substrate, is poorly understood. The potential advantages for survival in energy-starved environments are apparent. Yet, it is not known whether microbes express any form of substrate selectivity in the energy-starved deep biosphere, or rather indiscriminately consume any metabolizable substrate that enters their reach. The strategy employed by an individual cell may not solely depend on the energy yield per substrate. Other factors, such as substrate turnover rate, energetic cost of substrate/metabolite transport across the cell membrane, and energy return on investment for each enzyme that needs to be synthesized to catabolize an additional energy substrate will most likely also affect which substrates are consumed.

Which acetogenesis reactions are likely to occur in situ?

The calculated free energy yields presented so far are based on limited published information on concentrations of acetogenic substrates. Only H_2, formate, and acetate concentration data have been published for the deep subseafloor biosphere (Shipboard Scientific Party, 2003; Lorenson et al., 2006; Heuer et al., 2009; Lever et al., 2010; Expedition 329 Scientists, 2011); concentrations of the other substrates had to be approximated using data from surficial marine sediments (Meyer-Reil, 1978; Sørensen et al., 1981; King et al., 1983; Smith and Oremland, 1983; Parkes et al., 1989; Martens, 1990; Hoehler et al., 2001; Dhillon et al., 2005; Finke et al., 2006; King, 2007), freshwater sediments (King et al., 1982; Lovley and Goodwin, 1988; Chidhaisong et al., 1999; Keppler et al., 2000), marine water columns (Edenborn and Litchfield, 1987; Ballschmiter, 2003), and the terrestrial deep biosphere (Chapelle and Bradley, 2007). Since concentrations of H_2, formate, and acetate in the deep biosphere overlap with the concentrations of these species in other sedimentary environments, it seems realistic to conservatively approximate subseafloor concentrations of other substrates, such as glucose or oxalate, with the lowest values measured in other sedimentary environments. This cannot hide the fact that actual concentrations have not been measured, however. An alternative to calculating energy yields at assumed substrate concentrations is therefore to calculate the threshold concentrations required for acetogens to meet the BEQ from a substrate. This can be done conservatively, since the concentrations of most other reaction educts and products, i.e., H^+, H_2O, HCO_3^-, acetate, H_2, Cl^-, are well-constrained for the deep biosphere and/or set to conservative values (see Materials and Methods). Thermodynamic threshold concentrations were, as previously, calculated for $[H_2] = 0.1$ nM and $1\ \mu M$ (**Table 5**).

At first glance it is clear that the concept of threshold concentrations is only relevant for a subset of acetogenic substrates. For glucose, cellobiose, syringate, as well as syringate + H_2 at $1\ \mu M$ $[H_2]$, threshold concentrations are lower than a single molecule of the substrate per liter. In fact, thermodynamic threshold concentrations for glucose and cellobiose are even orders of magnitude lower than one molecule per Earth's entire ocean volume (**Table 5**)! For carbon monoxide, lactate, pyruvate, methyl chloride, syringate + H_2 at low $[H_2]$, or lactate + H_2 at high $[H_2]$ it also seems unlikely that meeting the BEQ is a realistic obstacle. For these reactions, threshold concentrations are at most in the low picomolar range – and with that ∼2–3 orders of magnitude lower than microbes are known to draw limiting metabolite concentrations down to (e.g.,

Table 5 | Thermodynamic threshold concentrations of widespread acetogenesis reactions at a wide range of temperatures and pressures, assuming a biological energy quantum of $\Delta G_f' = -10\,kJ\,mol^{-1}$.

Temperature	−1.9°C		+25°C		+122°C	
Pressure	**1**	**1000**	**1**	**1000**	**1**	**1000**
A						
H_2–CO_2	4.5E − 08	3.0E − 08	4.1E − 07	2.8E − 07	9.2E − 05	6.9E − 05
CO	ND	ND	1.1E − 12	ND	ND	ND
CO + H_2	ND	ND	4.5E − 10	ND	ND	ND
Formate	4.3E − 06	3.7E − 06	2.1E − 05	1.8E − 05	1.0E − 03	9.2E − 04
Formate–H_2	2.0E − 04	1.1E − 04	8.5E − 03	5.0E − 03	9.5E + 01	6.4E + 01
Lactate	2.4E − 16	2.9E − 16	1.1E − 15	1.3E − 15	4.6E − 14	5.2E − 14
Lactate + H_2	2.5E − 02	2.5E − 03	8.6E + 04	1.0E + 04	1.3E + 21	2.7E + 20
Glycolate	4.5E − 09	5.1E − 09	5.0E − 08	5.7E − 08	2.0E − 05	2.2E − 05
Oxalate	9.2E − 12	8.6E − 12	5.7E − 11	5.4E − 11	5.2E − 09	5.0E − 09
Methanol	2.8E − 12	2.6E − 12	2.6E − 11	2.4E − 11	6.5E − 09	6.1E − 09
Methanol + H_2	1.2E − 08	2.0E − 08	8.0E − 07	1.3E − 06	2.8E − 02	3.9E − 02
Methanol + formate	1.1E − 10	8.6E − 11	4.1E − 09	3.2E − 09	3.1E − 05	2.6E − 05
Ethanol	2.1E − 10	2.0E − 10	7.4E − 10	7.1E − 10	1.6E − 08	1.6E − 08
Pyruvate	1.6E − 19	1.9E − 19	3.8E − 18	4.4E − 18	9.4E − 15	1.0E − 14
Glucose	2.7E − 96	4.1E − 96	4.8E − 93	7.1E − 93	5.4E − 85	7.2E − 85
Cellobiose	6.5E − 204	ND	3.4E − 197	ND	1.4E − 180	ND
Methyl chloride	5.1E − 24	ND	5.9E − 23	ND	2.5E − 20	ND
Syringate	ND	ND	6.6E − 34	ND	ND	ND
Syringate + H_2	ND	ND	1.0E − 23	ND	ND	ND
Vanillate	ND	ND	7.9E − 19	ND	ND	ND
B						
H_2–CO_2	4.5E − 08	3.0E − 08	4.1E − 07	2.8E − 07	9.2E − 05	6.9E − 05
CO + H_2	ND	ND	4.5E − 14	ND	ND	ND
Formate + H_2	2.0E − 08	1.1E − 08	8.5E − 07	5.0E − 07	9.5E − 03	6.4E − 03
Lactate + H_2	2.5E − 26	2.5E − 27	8.6E − 20	1.0E − 20	1.3E − 03	2.7E − 04
Methanol + H_2	1.2E − 12	2.0E − 12	8.0E − 11	1.3E − 10	2.8E − 06	3.9E − 06
Syringate + H_2	ND	ND	1.0E − 31	ND	ND	ND

Concentrations are for the first substrate listed, e.g., H_2 for H_2–CO_2. ***(A)*** *[H_2] = 0.1 nM in reactions with H_2;* ***(B)*** *[H_2] = 100 nM.*

Fuhrman and Ferguson, 1986; Hoehler et al., 2001; Stolper et al., 2010). If previously measured concentrations of organic substrates in deep subsurface sediments, which have for the most part been (0.1 μM (e.g., Shipboard Scientific Party, 2003; Mitterer, 2006; Heuer et al., 2009; Lever et al., 2010), are a good reference, then we are left with the same conclusions as before (**Table 4**), i.e., that most acetogenesis reactions produce energy yields in excess of the BEQ, even at substrate concentrations that are low for the deep biosphere.

More interestingly, perhaps, examining those substrates that were previously considered less likely to be used by acetogens (based on **Tables 3** and **4**), suggests that even formate and H_2–CO_2 are potential acetogen substrates in some subsurface environments. Formate concentrations from low micromolar to tens of micromolar (**Table 5**) have been documented for sites ranging from organic-rich (ODP Site 1230) to highly oligotrophic (ODP Site 1231; Shipboard Scientific Party, 2003). Thermodynamic calculations based on measured formate concentrations suggest that formate could be a substrate of acetogenesis at certain depths in subsurface sediments on the Juan de Fuca Ridge Flank (Lever et al., 2010). Accurate quantifications of hydrogen concentrations in the deep biosphere are fraught with uncertainty, with two different methods yielding results differing by up to two orders of magnitude (Lin et al., 2011). Yet, independent of the method used, measured concentrations exceeding 10 nM are not uncommon (Shipboard Scientific Party, 2003; Lorenson et al., 2006; Expedition 329 Scientists, 2011; Lin et al., 2011), and suggest that even acetogenesis from H_2–CO_2 is possible in some places, if not widespread.

In situ energy yields of acetogenesis reactions based on measured concentrations

To the best of my knowledge, the only subseafloor sediment samples for which all educt and product concentrations of acetogenesis reactions have been quantified are from ODP Leg 201 (Shipboard Scientific Party, 2003). The seven sites sampled during this expedition vary from organic-rich to oligotrophic and cover a range of energy conditions that is likely to include most anoxic subseafloor sediments on Earth. For these samples, the concentrations of formate and hydrogen (and no other acetogenic substrates) were measured in parallel with concentrations of acetate, DIC (proxy

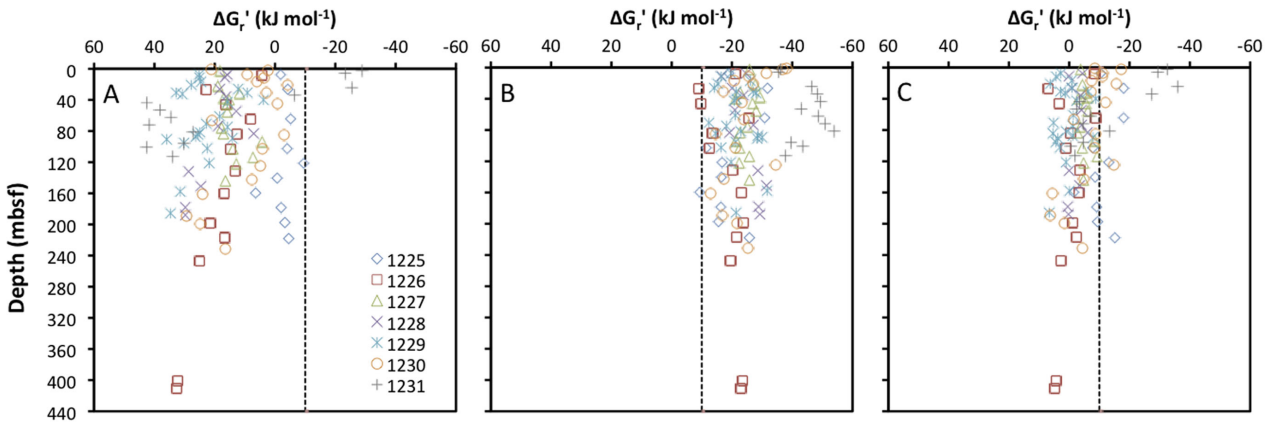

FIGURE 1 | Depth profiles of energy yields associated with acetogenesis reactions from (A) H_2–CO_2, (B) formate, and (C) formate–H_2 for ODP sites 1225-31. All calculations are based on measurements from sediment cores collected during ODP Leg 201 (Shipboard Scientific Party, 2003).

for bicarbonate), and pH, allowing for the calculation of *in situ* energy yields of acetogenesis reactions from H_2–CO_2, formate, and formate + H_2 (**Figure 1**).

Calculated free energy yields for the three reactions show clear trends: reactions from H_2–CO_2 are mostly endergonic, and only yield energy in excess of the BEQ value at a few shallow depths at ODP Site 1231 (**Figure 1A**). Reactions from formate are exergonic with energy yields around or exceeding the BEQ across all sites and depths sampled (**Figure 1B**). Reactions from formate + H_2, are for the most part slightly exergonic, but only exceed the BEQ at a few depths at ODP Sites 1225, 1230, and 1231 (**Figure 1C**).

Based on these results, one might suppose that acetogenesis from formate is possible across a wide range of subseafloor habitats, whereas acetogenesis reactions involving H_2–CO_2 or formate + H_2 are unlikely. Yet, the high uncertainty associated with the quantification of porewater H_2 concentrations needs to be taken into account. H_2 concentrations measured during ODP Leg 201 were obtained via an incubation method, which assumes headspace hydrogen to be in equilibrium with dissolved hydrogen in pore fluids after an incubation period (Lovley and Goodwin, 1988; Hoehler et al., 1998). When compared to a new, extraction-based method on the same samples, the incubation method yields concentration measurements that are consistently lower by one to two orders of magnitude (Lin et al., 2011). If *in situ* concentrations of H_2 in sediments sampled during Leg 201 are one order of magnitude higher than measured previously, this would lower the $\Delta G_r'$ for acetogenesis from H_2–CO_2 by ~22 kJ mol^{-1}. In this case, close to half of the samples would have energy values exceeding the BEQ (**Figure 1A**). If *in situ* concentrations are two orders of magnitude higher, this will lower the $\Delta G_r'$ for acetogenesis from H_2–CO_2 by an additional ~22 kJ mol^{-1} – by a total of ~44 kJ mol^{-1} of the reaction compared to the measured H_2 data. In this case, energy yields of acetogenesis from H_2–CO_2 would exceed the BEQ in the overwhelming majority of samples collected during Leg 201.

Energy yields of acetogenesis reactions involving H_2 compared to competing sulfate reduction and methanogenesis reactions

The main empirical support for the concept of redox zonation comes from isotopic tracer studies and measurements of hydrogen concentrations in sulfate-reducing and methanogenic freshwater and coastal surface sediments (e.g., Cappenberg, 1974; Capone and Kiene, 1988; Lovley and Goodwin, 1988; Hoehler et al., 1998; Heimann et al., 2010). Acetogenesis has received less attention in sediments due to the difficulty of detecting the process; after all the end product acetate is also a key substrate to sulfate reducers and methanogens, and rapid turnover results in acetate typically not accumulating to high concentrations – unlike the end products of sulfate reduction and methanogenesis, sulfide, and methane. Moreover, acetogenesis is often equated with the "homoacetogenic" reaction from H_2–CO_2, which is thermodynamically unfavorable under thermodynamic control of H_2 concentrations in sulfate-reducing or methanogenic sediments. Only rarely have energy yields of organotrophic acetogenesis reactions that include H_2 been taken into account (Liu and Suflita, 1993; Lever et al., 2010). Here I compare the energy yields of various acetogenesis reactions involving H_2 to those of the widespread hydrogenotrophic sulfate reduction and methanogenesis reactions at a wide range of H_2 concentrations (**Figure 2**).

At first glance it is apparent that acetogenesis from H_2–CO_2 is thermodynamically less favorable than sulfate or methanogenesis reactions from H_2–CO_2, independent of H_2 concentrations (**Figure 2A**). Under the conditions used in calculations, sulfate reducers can meet the BEQ down to H_2 concentrations of ~0.6 nM, methanogens down to 11 nM, whereas acetogens require 410 nM H_2 concentrations. Acetogenesis from formate + H_2 is also unlikely, as its energy yields are below the BEQ unless H_2 concentrations are in the micromolar range. More energetically favorable than sulfate reduction or methanogenesis is, however, the acetogenic reaction from syringate + H_2, which even at H_2 concentrations as low as 0.01 nM produces high-energy yields (~−90 kJ mol^{-1}) – concentrations at which both sulfate reduction and methanogenesis are endergonic. Moreover, while sulfate reduction from H_2–CO_2 is the overall second most energy-yielding reaction, acetogenesis reactions from CO, methanol, and lactate produce more energy than hydrogenotrophic methanogenesis at H_2 concentrations within the typical range measured in deep subseafloor sediments.

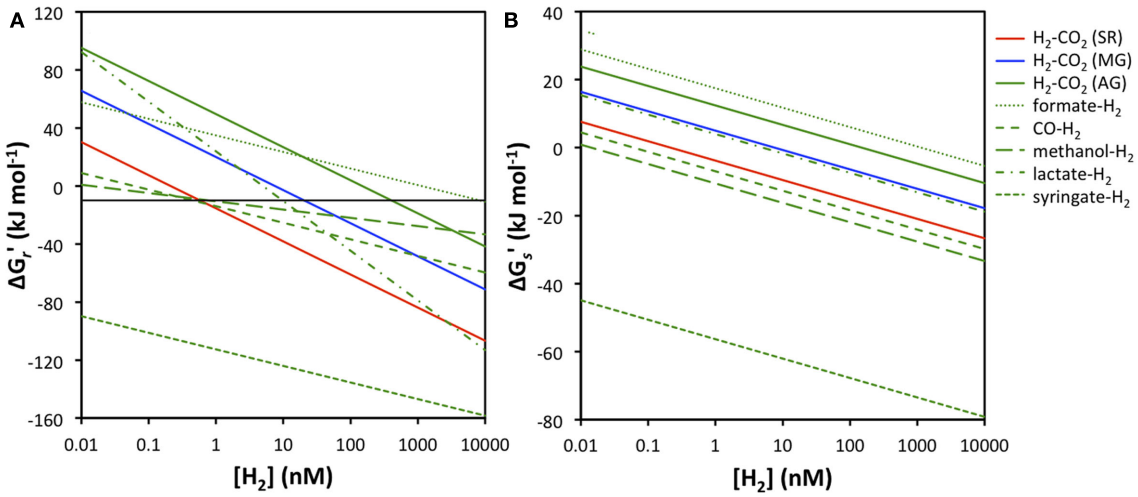

FIGURE 2 | Relationship between H_2 concentrations and energy yields for sulfate reduction, methanogenesis, and acetogenesis from H_2–CO_2, as well as acetogenesis from formate–H_2, CO–H_2, methanol–H_2, lactate–H_2, and syringate–H_2. (A) energy yields per reaction ($\Delta G_r'$), the black line indicates the BEQ, (B) energy yields per substrate ($\Delta G_s'$). All calculations were done assuming standard temperature and pressure, and using educt and product concentrations as outlined in the Materials and Methods, except for [H_2].

When energy yields are considered on a per hydrogen molecule level, the results are even more striking. Acetogenesis reactions from syringate + H_2, methanol + H_2, and CO + H_2 all provide more energy per H_2 molecule than sulfate reduction from H_2–CO_2 (**Figure 2B**). The reaction from lactate + H_2 yields less energy than hydrogenotrophic sulfate reduction, but slightly more than hydrogenotrophic methanogenesis, while acetogenesis reactions from formate + H_2 and H_2–CO_2 produce the least amount of energy per H_2 molecule and are endergonic except at micromolar H_2 concentrations (**Figure 2B**).

One might argue that carboxydo- and organotrophic acetogenesis reactions involving H_2 are unlikely in marine sediments. After all, reactions involving the same carbon substrate without H_2 yield more energy except when high H_2 concentrations coincide with low temperature (**Tables 3** and **4**) – a condition that has traditionally only been observed during season-induced temporary disequilibria in shallow sediments (Hoehler et al., 1999) and is perhaps unlikely in seasonally stable subsurface sediments. Yet, the method-dependent discrepancies in measured H_2 concentrations in deep subsurface sediments (Lin et al., 2011) leave room for high uncertainty; if the higher [H_2] measurements obtained with a new extraction-based method (Lin et al., 2011) turn out to be accurate, then carboxydo- and organotrophic acetogenesis reactions with H_2 may be competitive, if not energetically favorable, over carboxydo- and organotrophic reactions without H_2 in the predominantly cold, deep biosphere. Evidence supporting the importance of organotrophic reactions with H_2 comes from subsurface sediments of the Atlantic Coastal Plain (Liu and Suflita, 1993). An acetogenic isolate from these sediments only showed growth through *O*-demethoxylation of syringate under an H_2–CO_2 atmosphere, while no growth on syringate was observed under an N_2–CO_2 or N_2 atmosphere. And by metabolizing syringate with H_2, this organism was able to outcompete hydrogenotrophic methanogens for H_2 in the initial sediment enrichment.

The ability to gain energy from the demethoxylation of syringate or other lignin monomers is widespread among acetogens, but not among sulfate reducers or methanogens, suggesting that methoxy-groups on aromatic rings might represent non-competitive substrates (Lever et al., 2010). The same is not true for the other substrates, lactate, CO, and methanol (**Figure 2**). Lactate serves as a growth substrate not only to many acetogens (Lever et al., 2010), but also to many sulfate reducers (Rabus et al., 2006), which can be expected to have higher energy yields from competing sulfate reduction reactions. Similarly, despite being less widely used as growth substrates than among acetogens (Lever et al., 2010), CO, and methanol can also serve as energy substrates to certain sulfate reducers (reviewed in Mörsdorf et al., 1992), as well as several methanogens (reviewed in Whitman et al., 2006, and in Ferry, 2010). Both sulfate reducers and methanogens can be expected to gain more energy from reactions involving CO or methanol than acetogens. Hence, evidence suggesting an important role for acetogenesis in the cycling of CO and methanol in marine and freshwater sediments might be surprising (King, 2007; Jiang et al., 2010). In the following section, I will argue that the ability of acetogens to use a wide range of substrates is a viable survival strategy under conditions of energy limitation – despite lower energy yields per substrate.

METABOLIC STRATEGIES OF ACETOGENS

A striking feature of acetogens as a metabolic guild is the widespread ability to use a large number and wide diversity of carbon compounds as energy substrates. Over half of all cultured strains test positively for growth on H_2/CO_2, carbon monoxide, formate, methanol, ethanol, other aliphatic compounds such as lactate, and methoxylated aromatic compounds (Lever et al., 2010). Further widely used growth substrates include carbohydrates, other short-chain fatty acids and alcohols, methoxylated aliphatic compounds, betaines, amino acids, and aldehydes (Drake et al., 2006). Even

complex organic polymers, such as cellulose or carboxymethylcellulose, are used by some strains (Wolin and Miller, 1994; Karita et al., 2003; Wolin et al., 2003). Due to the limited number of energy substrates on which growth is typically tested, substrate ranges of acetogens may significantly exceed the currently known spectrum. Any methyl or methoxyl groups of compounds found in the environment represent potential energy substrates, that, given thermodynamically favorable conditions, might be combined with CO_2 to form acetate.

Considering the striking metabolic versatility of acetogens, it seems plausible that the resulting plasticity with respect to substrate use is part of the strategy that enables acetogens to coexist with sulfate reducers and methanogens. In the following sections, I will examine two hypotheses that seek to explain the benefits of a wide metabolic spectrum. The first hypothesis is that acetogens can coexist with sulfate reducers and methanogens due to niche differentiation with respect to substrate use. In other words, acetogens may avoid competition by consuming substrates not used by sulfate reducers or methanogens. The second hypothesis is that the ability to pool energy from a wide range of metabolic reactions enables coexistence despite lower energy from shared substrates. These two hypotheses are not incompatible, but should rather be regarded as two complementary advantages of a generalist metabolic strategy.

Niche differentiation based on substrate use

When viewed collectively, sulfate reducers, though not to the same extent as acetogens, can also exploit a large variety of substrates. When examined more closely, however, it appears that only the ability to use H_2, short-chain fatty acids, and ethanol is truly widespread across the various genera (Rabus et al., 2006). Common acetogenic substrates such as methanol, glucose, fructose, carbon monoxide, and methoxylated lignin monomers are not substrates to the vast majority of sulfate reducers (Mörsdorf et al., 1992; Rabus et al., 2006). The thermodynamic advantage of higher energy yields of sulfate reduction compared to acetogenesis thus only plays out for a subset of acetogenic substrates that are also utilized by sulfate reducers. Tracer experiments indicating H_2 and short-chain fatty acids as the main electron donors used by sulfate reducers in estuarine and marine sediments support this conclusion (Sørensen et al., 1981; Parkes et al., 1989). Similarly, experimental evidence indicating acetogens as key consumers of CO and methoxyl groups in sulfate-reducing marine sediments (Küsel et al., 1999; King, 2007) suggests that, despite overlaps in substrates, acetogens, and sulfate reducers practice a form of niche differentiation in which each group favors different energy substrates where they coexist.

Vastly less metabolically versatile than acetogens or sulfate reducers, the substrate range of methanogens is limited to (1) CO_2 reduction (H_2/CO_2, formate, a few use carbon monoxide or alcohols), (2) acetate disproportionation, and (3) demethylation of C1 compounds (methanol, methyl sulfides, and methylamines). With the exception of one genus (*Methanosarcina*), most methanogens are substrate specialists and only capable of growth on one of these three substrate groups (Whitman et al., 2006). Hence, potential competition between acetogens and methanogens for substrates is limited to a small subset of acetogenic substrates.

Niche differentiation, resulting in use of different energy substrates where the groups coexist, may thus explain why sulfate reducers and methanogens do not competitively exclude acetogens in anoxic sediments. Why have sulfate reducers not adapted to use the full spectrum of substrates used by acetogens? And, given that both acetogens and methanogens utilize the reductive acetyl CoA pathway for energy production and/or C fixation and overlap in substrate use (Drake et al., 2006; Whitman et al., 2006), why might these two groups differ so drastically with respect to their metabolic versatility? The ultimate evolutionary explanations remain subject to speculation. On a more proximal level, differences in energy yields and turnover rates of energy substrates may have played a role in driving differences in metabolic strategies.

The most common substrates used by sulfate reducers and methanogens, i.e., H_2 and acetate, so called central intermediates of organic carbon degradation (e.g., Valentine, 2001; Dolfing et al., 2008), are presumably the electron donors with the highest turnover rates in anoxic sediments. Other short-chain fatty acids, which represent important energy substrates to sulfate reducers are also known to have high turnover rates (Sørensen et al., 1981; Parkes et al., 1989); even methylated compounds used by methanogens, i.e., methanol, methylamines, and methyl sulfides, are known to have high turnover rates in certain environments (e.g., Zhilina and Zavarzin, 1990; Mitterer et al., 2001; Jiang et al., 2010; Lin et al., 2010). Substrates with high turnover rates are typically small, as they derive from a variety of individually less abundant, larger source molecules; they also often harbor less energy than larger organic molecules with lower turnover rates (**Tables 3** and **4**). Why might certain groups utilize substrates with high turnover rates but low-energy yields, while others use substrates with low turnover rates but high-energy yields? Part of the answer may lie in the universal requirement of cells to meet maintenance energy requirements.

Meeting maintenance energy requirements is especially challenging in deep subsurface sediments, as these have typically been cut off from fresh organic matter supplies for thousands to millions of years. Here the vast majority of cells is likely to be in a permanent state of starvation (D'Hondt et al., 2004; Jørgensen et al., 2006) and starvation may even represent the primary source of mortality. Based on chemostat experiments, the following relationship between maintenance energy and temperature has been established (Tijhuis et al., 1993; Harder, 1997):

$$\mathrm{ME} = A * \mathrm{e}^{-E_\mathrm{a}/RT} \quad (1)$$

where ME is the maintenance energy (kJ (g dry mass)$^{-1}$ d^{-1}), A a constant [4.99×10^{12} kJ (g dry mass)$^{-1}$ d^{-1}], E_a the activation energy (69.4 kJ mol^{-1} K^{-1}), R the universal gas constant (0.008314 kJ mol^{-1} K^{-1}), and T the temperature (K). The value of the constant A was calculated from the energy supply rate at which microbial cell growth and replication stops in chemostat experiments (Tijhuis et al., 1993). It has since been estimated that the actual threshold energy required for cell maintenance is three orders of magnitude lower than the threshold for growth/replication (Price and Sowers, 2004; Biddle et al., 2006). Therefore, I will use a value of 4.99×10^9 kJ (g dry mass)$^{-1}$ d^{-1} for A in all calculations of ME. Based on this value of A, a maintenance

energy of 1.26 kJ (g dry mass)$^{-1}$ year^{-1} can be calculated at standard temperature. Tijhuis et al. (1993) propose that 26 g of cell dry mass on average contain 12 g cell carbon. Combined with the published estimate of 10 fg C per cell for sediment-inhabiting microbes (Whitman et al., 1998), one can then calculate a cell-specific maintenance energy, ME_{cell}, of 2.74×10^{-14} kJ cell^{-1} year^{-1} at standard temperature.

The relationship between ME_{cell}, the Gibbs free energy yield per substrate, $\Delta G'_s$ (kJ mol^{-1}), and the cell-specific substrate turnover rate, k_{cell} (mol cell^{-1} year^{-1}) that is required for a cell to meet maintenance energy requirements, can be expressed as follows:

$$ME_{cell} = \sum \left[\left(\Delta G'_{s,A} \times k_{cell,A} \right) + \left(\Delta G'_{s,B} \times k_{cell,B} \right) + \ldots \right] \quad (2)$$

where A and B indicate substrates A and B, respectively. If cells are only consuming one substrate, this expression simplifies, so the equation can be solved for k_{cell}, if ME_{cell} and $\Delta G'_s$ are known:

$$k_{cell} = ME_{cell} / \Delta G'_s \quad (3)$$

The relationship between k_{cell} and $\Delta G'_s$ is hyperbolic (**Figure 3A**). This has implications for metabolic strategies among microbes: for instance, microbes can meet maintenance energy requirements by consuming substrates with low-energy yields as long as turnover rates are high and the BEQ is met (ME_A); alternatively, microbes can meet ME requirements at low turnover rates, as long as energy yields per substrate are high (ME_B).

A further implication is that small changes in $\Delta G'_s$ greatly influence the turnover rate required to meet ME_{cell} if energy yields per substrate are small (here <50 kJ mol^{-1}), but not if they are high (here ≥ 100 kJ mol^{-1}; **Figure 3B**). If $\Delta G'_s$ changes from -10 to -20 kJ mol^{-1}, the turnover rate required to meet maintenance energy requirements drops by 50%. By comparison, if $\Delta G'_{s,B}$ changes from -100 to -110 kJ mol^{-1}, the decrease in required turnover rate is only ~9%.

What does this mean regarding the substrates used by sulfate reducers and methanogens compared to the substrates used by acetogens? In **Figure 3C**, maintenance turnover rates are illustrated for the same metabolic reactions, A and B, as in **Figure 3A** (plus 0), as well as for three hypothetical pathways that produce higher energy yields per substrate (plus 10, plus 20, plus 30); "plus 0" exemplifies acetogenesis reactions from a high turnover, low-energy substrate (ME_A), and a low turnover, high-energy substrate (ME_B), respectively; the pathways behind "plus 10," "plus 20," and "plus 30" are energetically more favorable methanogenesis and sulfate-reducing reactions involving the same two substrates. The differences in $\Delta G'_s$ of -10, -20, and -30 kJ mol^{-1} relative to acetogenic reactions are based on typical differences in $\Delta G'_s$ calculated for methanogenesis/sulfate reduction vs. acetogenesis reactions involving the substrates formate, methanol, and lactate across a wide range of temperatures (275–337 K) and sulfate concentrations (0–28 mM) in subsurface sediments (Lever et al., 2010). The comparison illustrates that acetogenesis reactions operating near the thermodynamic threshold (ME_A, $\Delta G'_s = -10\ kJ\ mol^{-1}$; **Figure 3C**) have a tremendous disadvantage in meeting ME_{cell} compared to competing methanogenic or sulfate-reducing reactions, which can operate at one-half, one-third, or one-fourth the substrate turnover (**Table 6**). The advantage of vastly lower turnover rates required to meet ME_{cell} diminishes with increasing energy yields per substrate (ME_B, **Figure 3C**). It follows that the minimum turnover rates of the three competing methanogenesis and sulfate reduction reactions are only lower by 9, 17, and 23%, when the energy yield per substrate is -100 kJ mol^{-1} for the acetogenesis reaction (**Table 6**).

Returning to the question raised earlier in this section, i.e., whether methanogens/sulfate reducers and acetogens may practice a form of niche differentiation, in which each group uses different substrates where they co-occur, the model presented here provides clear answers. Feeding on high-energy, low turnover substrates is a viable survival strategy for microbes, as is feeding on low-energy, high turnover substrates. The two strategies may, at least in part, explain the coexistence of acetogenic with sulfate-reducing and/or methanogenic microbial populations. A reason

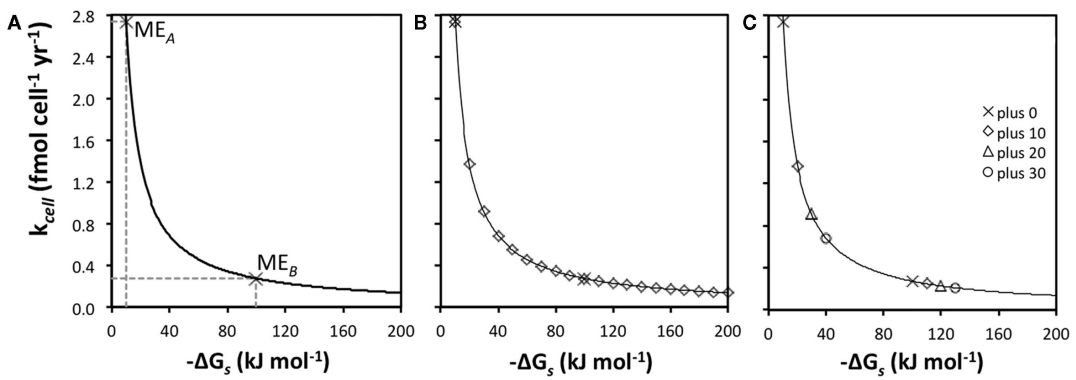

FIGURE 3 | Relationships between energy yields per substrate ($\Delta G'_s$) and turnover rate (k_{cell}). (A) Hyperbolic relationship between $\Delta G'_s$ and k_{cell} assuming $ME_{cell} = 2.74 \times 10^{-14}$ kJ cell^{-1} year^{-1}. ME_A and ME_B indicate two different strategies to meet ME_{cell}, ME_A for a substrate with low-energy yields ($\Delta G'_s = -10\ kJ\ mol^{-1}$) and a high k_{cell}, and ME_B for a substrate with high-energy yields ($\Delta G'_s = -100\ kJ\ mol^{-1}$) and a low k_{cell}. **(B)** Illustration of the effect of 10 kJ mol^{-1} increments in energy yields per substrate on the turnover rate required to meet ME_{cell}. **(C)** Turnover rates for ME_A and ME_B ("plus 0") compared to competing reactions "plus 10," "plus 20," and "plus 30" with 10, 20, and 30 kJ mol^{-1} higher energy yields per substrate, respectively.

Table 6 | Overview of cell-specific substrate turnover rates (k_{cell}; fmol cell^{-1} year^{-1}) required to meet the theoretical maintenance energy requirement of 2.74 × 10^{-14} kJ cell^{-1} year^{-1} at different free energy yields per substrate ($\Delta G'_s$; kJ mol^{-1}).

Plus 0		Plus 10		Plus 20		Plus 30		Ratios of turnover rates		
$\Delta G'_s$	k_{cell}	$\Delta G'_s$	k_{cell}	$\Delta G'_s$	k_{cell}	$\Delta G'_s$	k_{cell}	$k_{cell, plus\ 0}$: $k_{cell, plus\ 10}$	$k_{cell, plus\ 0}$: $k_{cell, plus\ 20}$	$k_{cell, plus\ 0}$: $k_{cell, plus\ 30}$
A										
10	2.74	20	1.37	30	0.91	40	0.68	0.50	0.33	0.25
20	1.37	30	0.91	40	0.68	50	0.55	0.67	0.50	0.40
50	0.55	60	0.46	70	0.39	80	0.34	0.83	0.71	0.63
75	0.36	85	0.32	95	0.29	105	0.26	0.88	0.79	0.71
100	0.27	110	0.25	120	0.23	130	0.21	0.91	0.83	0.77
200	0.14	210	0.13	220	0.12	230	0.12	0.95	0.91	0.87
500	0.05	510	0.05	520	0.05	530	0.05	0.98	0.96	0.94
Plus 0 (A + B)		**Plus 10**		**Plus 20**		**Plus 30**		**Ratios of turnover rates**		
$\Sigma\Delta G'_s$	k_{cell}	$\Delta G'_s$	k_{cell}	$\Delta G'_s$	k_{cell}	$\Delta G'_s$	k_{cell}	$k_{cell, plus\ 10}$: $k_{cell, plus\ 0}$	$k_{cell, plus\ 20}$: $k_{cell, plus\ 0}$	$k_{cell, plus\ 30}$: $k_{cell, plus\ 0}$
B										
20	1.4	20	1.4	30	0.91	40	0.68	1.00	0.67	0.50
40	0.69	30	0.91	40	0.68	50	0.55	1.33	1.00	0.80
100	0.27	60	0.46	70	0.39	80	0.34	1.66	1.43	1.25
150	0.18	85	0.32	95	0.29	105	0.26	1.76	1.58	1.43
200	0.14	110	0.25	120	0.23	130	0.21	1.82	1.66	1.54
400	0.07	210	0.13	220	0.12	230	0.12	1.90	1.82	1.74
1000	0.03	510	0.05	520	0.05	530	0.05	1.96	1.92	1.88

Calculations are shown for four different "pathways"; "plus 0" is the pathway with the lowest Gibbs free energies, and an analog for acetogenesis; "plus 10," "plus 20," and "plus 30" are energetically more favorable pathways that produce 10, 20, and 30 kJ more energy per mole of substrate. These energetically more favorable pathways are analogs for methanogenesis and sulfate reduction reactions. The ratios in required substrate turnover rates for the plus 0 pathway vs. the other three pathways to match the above maintenance energy requirement are shown on the far right. ***(A)*** *all four pathways only use one substrate, A;* ***(B)*** *plus 0 pathway uses two substrates, A and B, that are equal in $\Delta G'_s$ and k_{cell}, while plus 10, plus 20, and plus 30 pathways still only use substrate A.*

why sulfate reducers/methanogens may mainly use low-energy, high turnover substrates is their vast energetic advantage over acetogens in metabolizing these substrates. At high $\Delta G'_s$, the energetic advantage of sulfate reducers/methanogens over acetogens decreases, and other guild-specific traits may increase in importance. One of these will be discussed in the following section.

Specialist vs. generalist arguments

The potential advantages of a specialist vs. a generalist life style have been the subject of discussions among ecologists for over five decades. A traditional view is that selectivity (specialization) pays off under non-limiting energy conditions, while less discrimination toward food sources (generalism) is the more effective survival strategy under energy limitation (e.g., Emlen, 1966; Dykhuizen and Davies, 1980; for reviews see Pianka, 1994; Egli, 1995). With respect to microbial ecology, this argumentation has been called into question by certain microbial growth experiments, in which long starvation periods appeared to favor specialists (e.g., Kuenen, 1983).

A fundamental difference between microbes and macrobiota under energy limitation is that microbes not only struggle to meet maintenance energy requirements, but also to acquire a minimum free energy (BEQ) from a metabolic reaction to even be able to produce ATP. Hence, substrate specialists are often equipped with high substrate affinities down to very low concentrations that enable them to outcompete not only other metabolic guilds, but also other members of their own metabolic guild. A classic example among methanogens is the obligately aceticlastic *Methanosaeta* genus which can grow on acetate concentrations below 10 μM (Jetten et al., 1992). By comparison, the (by methanogen standards) "generalistic" *Methanosarcina* genus, members of which can grow via CO_2 reduction, acetate disproportionation, and demethylation of C1 compounds, requires acetate concentration of at least 200 μM for growth (Jetten et al., 1992). High substrate affinity appears to be a strategy among specialists by which they can more efficiently take up substrates and drive substrate concentrations below the threshold concentrations required by generalists. This form of energetic (i.e., thermodynamic) exclusion, which only occurs in microbes, provides a gateway for substrate specialists, provided they can meet maintenance energy requirements. The costs of substrate specialization are a smaller accessible energy pool due to utilization of fewer energy substrates and lower energy yields per substrate.

In energy-starved environments, such as deep subsurface sediments, a specialist metabolic strategy may work effectively for

substrates with high turnover rates. High turnover rates and relatively high cell densities are necessary to maintain the low substrate concentrations that enable specialists to thermodynamically exclude less efficient consumers of the same substrate. As shown earlier (**Tables 1–3**), thermodynamic exclusion of acetogens is only likely for the low-energy substrates H_2 and formate, however. Other, less common, but more energy-rich substrates occur at concentrations exceeding the thermodynamic threshold, and provide little incentive for specialization due to the impossibility of thermodynamically excluding other groups, such as acetogens, from consuming them. Hence, a more generalist metabolic strategy may be more effective among consumers of these more rare, energy-rich substrates.

As discussed in a previous section, substrate generalism is a widespread trait among acetogens. With respect to meeting maintenance energy requirements, there are clear advantages to using more than one substrate (**Figure 4**); for instance, at high turnover rates and low ΔG_s (-10 kJ mol^{-1} substrate) combining the energy yields of two substrates, A and B, with the same $\Delta G'_s$ and k_{cell} may enable acetogens to lower their required substrate turnover by 50% and successfully compete with methanogens/sulfate reducers that gain 10 kJ more energy per mole of substrate A (ME_A; **Figure 4**; **Table 6B**). While this is an improvement of competitiveness, pooling the energy from two substrates is still insufficient to compete with methanogens/sulfate reducers gaining 20 or 30 kJ more per mole of substrate, which still can meet ME_{cell} on turnover rates that are 33 and 50% lower, respectively (**Table 6B**). To match energy yields of the latter, energy from three or four substrates with the properties of substrate A would need to be pooled – a considerable disadvantage in terms of energy efficiency as one might argue. This changes for substrates with high-energy yields (e.g., -100 kJ mol^{-1} substrate) and resultingly low required turnover rates (ME_B; **Figure 4**). For these, pooling the energy from two substrates would enable an acetogen to grow at a significantly lower turnover rate than any of the competing methanogens/sulfate reducers utilizing only one substrate – a significant advantage (**Figure 4**; **Table 6B**). It follows from this that pooling the energy from multiple substrates would increase acetogenic competitiveness with sulfate reducers and methanogens overall – and in particular for energy-rich substrates.

The same principle as in comparing the benefits of using two vs. one substrates applies in comparing the benefits of using more, e.g., 3 vs. 2, 5 vs. 4, 10 vs. 5, etc., substrates. The main point is that acetogens typically have wider substrate spectra than sulfate reducers or methanogens, and that pooling energy from a larger number of substrates may enable acetogens to in some cases survive on lower substrate turnover rates than the other groups, despite lower energy yields per substrate. Experimental evidence that confirms pooling of energy sources as the explanation for the coexistence of acetogenic with sulfate-reducing and/or methanogenic populations in the deep biosphere is still missing. However, the same principle has been demonstrated in continuous-flow cultures involving other groups of microorganisms that were grown under carbon-limiting conditions: here several studies have shown substrate generalists to grow at lower substrate concentrations than substrate specialists when incubations included multiple substrates (Gottschal et al., 1979; Dykhuizen and Davies, 1980; reviewed in Egli et al., 1993; Egli, 1995).

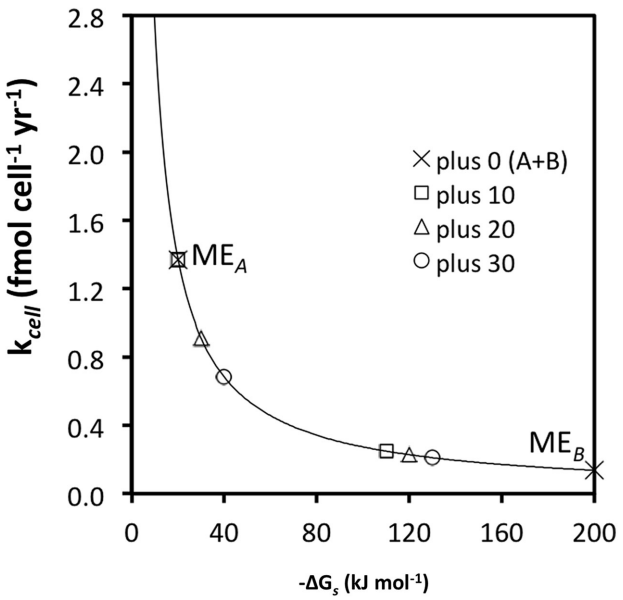

FIGURE 4 | The same relationship as in Figure 3C, except that turnover rates required for ME_A and ME_B ("plus 0") are now calculated for the sum of two substrates, A and B ["plus 0 (A + B)"]. All other values are the same as before.

Based on the calculations presented (**Figure 4**; **Table 6B**), one might conclude that pooling energy is only an effective strategy for subseafloor acetogens to meet ME_{cell} if it involves high-energy substrates. For low-energy substrates, more specialized organisms with higher energy yields per substrate, i.e., sulfate reducers and methanogens, should have a vast advantage (**Figure 4**), provided that energy yields of acetogenesis reactions even exceed the BEQ. Even the most efficient specialist will reach a limit when substrate turnover rates drop below the threshold required to meet ME_{cell}, however; at this point the specialist is either forced to consume additional substrates, or to allow substrate concentrations above the thermodynamic threshold. Evidence potentially supporting the latter comes from oligotrophic sediments of the South Pacific Gyre and Equatorial Pacific, where H_2 concentration peaks in the tens of nanomolar range have been reported for subsurface horizons with exceedingly low microbial activities (Shipboard Scientific Party, 2003; Expedition 329 Scientists, 2011). If substrate specialists are forced to allow substrate concentrations above the thermodynamic threshold, they become vulnerable to less efficient, more generalistic organisms competing for their preferred substrate. Ultimately, because of the larger accessible substrate and hence energy pool, one might therefore expect substrate generalists to dominate under the most energy-depleted conditions.

The results presented thus far suggest that it is very difficult to predict the outcome of the complex competition between acetogens and other groups for substrates in the deep biosphere. Beside physical variables, such as temperature and pressure, it may

be necessary to measure concentrations of all educts and products of relevance – a very challenging task with acetogens, due to their wide substrate spectra – as well as measure substrate-specific turnover rates – a seemingly impossible undertaking given the very low turnover rates in the deep biosphere. Even with complete knowledge on concentrations and turnover rates, predicting competitive outcomes on a substrate-level would be compromised by our still limited knowledge on the metabolic capabilities of microbes inhabiting anoxic (subseafloor) sediments, as well as other important life history traits. One of the latter is the energetic cost of biosynthesis – a variable that is likely to vary widely across microbes and microbial metabolic guilds.

THE ENERGETIC COST OF BIOSYNTHESIS AMONG ACETOGENS

Of the currently known six pathways of autotrophic carbon fixation, the reductive acetyl CoA pathway is the simplest and energetically most favorable due to the absence of complex biochemical intermediates (Russell and Martin, 2004; Berg et al., 2010). This strictly anaerobic pathway only consists of a carbonyl branch, in which CO_2 is reduced to an enzyme-bound carbonyl group, and a methyl branch, in which CO_2 is reduced to a cofactor-bound methyl group. The bifunctional enzyme CO dehydrogenase/acetyl CoA synthase (CODH/ACS) carries out both the reduction of CO_2 to CO, as well as the synthesis of the end product, acetyl CoA, by joining the carbonyl and methyl groups (e.g., Hügler and Sievert, 2011). The reductive acetyl CoA pathway is unique among C fixation pathways in that it is linear; given geochemically favorable conditions, e.g., in alkaline hydrothermal vent environments, each step is exergonic, meaning that CO_2 fixation can occur spontaneously (Martin and Russell, 2007). It has therefore been suggested that this pathway started as a geochemical pathway (Russell and Martin, 2004). Moreover, due to it being the only known C fixation pathway that occurs in both Bacteria and Archaea, it has been conjectured that the reductive acetyl CoA pathway is the most ancient C fixation pathway (Fuchs and Stupperich, 1985), or even the very first biochemical pathway to have evolved on Earth (Peretó et al., 2004). The great simplicity and low energetic cost suggest that anaerobic organisms using this pathway have an energetic advantage over organisms using other C fixation pathways, such as the reverse tricarboxylic acid cycle.

The reductive acetyl CoA pathway is found in all known acetogens and methanogens, as well as several autotrophic sulfate reducers and anammox bacteria (Schauder et al., 1989; Drake et al., 2006; Strous et al., 2006; Whitman et al., 2006). Certain methanogens and autotrophic sulfate reducers use the pathway exclusively for biosynthesis, while others, including acetate-oxidizing sulfate reducers, aceticlastic methanogens, and syntrophic acetate oxidizers, can produce energy by reversing the pathway so it becomes oxidative (e.g., Spormann and Thauer, 1988; Hattori et al., 2005; Liu and Whitman, 2008). Acetogens, and among these I include facultative acetogens, such as certain sulfate reducers, methanogens, and anaerobic acetate oxidizers (e.g., Jansen et al., 1984; Rother and Metcalf, 2004; Hattori et al., 2005; Lessner et al., 2006; Henstra et al., 2007), are the only group known to perform this pathway both for biosynthesis and energy production. A possible advantage of using the same pathway for energy production and biomass assimilation is that smaller genomes and fewer enzymes need to be produced and maintained. Since starvation mode is likely to be the rule rather than the exception among microbes in energy-deprived subseafloor sediments (Jørgensen et al., 2006), reducing the energetic cost of genome maintenance and enzyme synthesis may confer a significant advantage to microbes that are able to carry out energy production and biosynthesis via the same pathway.

It has, in fact, been postulated that the synthesis and maintenance of enzymes to repair DNA from depurination reactions and proteins from racemization reactions are the main energy expenditures among microorganisms in survival mode (Price and Sowers, 2004). While too little is known about cell-specific enzyme concentrations and turnover rates in the deep subseafloor to calculate the energetic cost of synthesizing and maintaining these enzymes, concentrations of protein building blocks, i.e., certain amino acids (aspartate, glutamate, serine, glycine), have been measured in subsurface sediments of the Peru Margin and Equatorial Pacific (Mitterer, 2006). I use these here to calculate the energetic cost of their lithoautotrophic synthesis. Irrespective of the site, a high energetic cost can be expected for the synthesis of all four amino acids (**Figure 5**). Assuming that this is a general trend across amino acids, the lithoautotrophic synthesis of proteins, and hence enzymes, can be expected to be an energetically costly process in subseafloor sediments. A key intermediate during amino acid synthesis under anaerobic conditions is the energy-rich acetyl CoA molecule, which is also a crucial intermediate during acetogenesis. Assuming that acetogenesis from H_2–CO_2 is associated with an energetic cost (**Figure 1A**), then obligate lithoautotrophs, including many methanogens and sulfate reducers, which synthesize amino acids from H_2 and CO_2, will spend significant amounts of energy on the reductive synthesis of acetyl CoA alone. By contrast, the majority of organotrophic acetogenesis reactions are exergonic (**Table 3**). Most acetogens may therefore be able to cut back energy expenditures during enzyme synthesis, compared to obligately autotrophic organisms, by using organic substrates to synthesize the amino acid precursor acetyl CoA.

CONCLUSION

If energy yields per substrate are the only important variable controlling microbial metabolism in energy-starved subsurface sediments, then acetogenic microbes should be outcompeted by other anaerobic microbes that perform energetically more favorable pathways, such as sulfate reduction and methanogenesis. While this may be the case in some places, recent δ^{13}C-isotopic analyses that indicate a significant acetogenic contribution to total acetate turnover have suggested otherwise (Heuer et al., 2009; Lever et al., 2010). In this study, I discuss several potentially advantageous traits of acetogenic microbes that may enable them to coexist with sulfate reducers and methanogens in spite of lower energy yields per substrate.

Using conservative calculations, I show that most acetogenic substrates are likely to occur at concentrations that vastly exceed the thermodynamic threshold concentration for acetogenesis and are thus potential energy substrates to acetogens in the deep biosphere. Due to their ability to metabolize certain substrates via multiple different reactions, e.g., methanol alone, methanol + H_2,

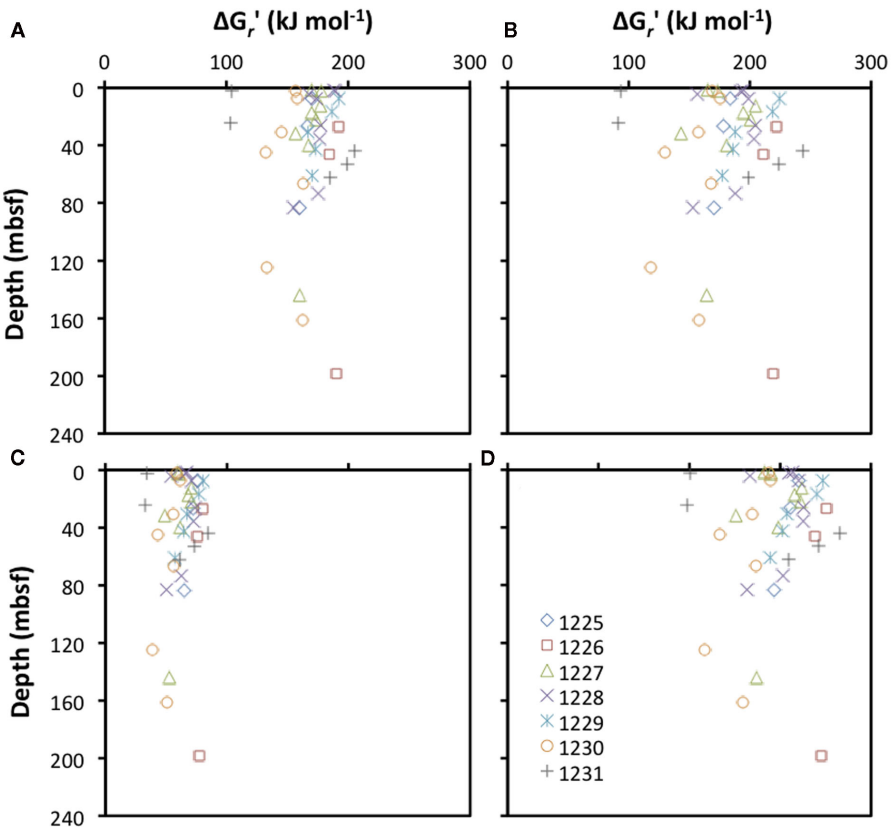

FIGURE 5 | Depth profiles of energetic cost of the lithoautotrophic synthesis of the amino acids (A) aspartic acid [asp^{2-}; 4 $HCO_3^- + NH_4^+ + 6\ H_2 + H^+ \rightarrow {}^-OOCCH(NH_2)CH_2COO^- + 8\ H_2O$], (B) glutamic acid [$glu^{2-}$; 5 $HCO_3^- + NH_4^+ + 9\ H_2 + 2\ H^+ \rightarrow {}^-OOC(CH_2)_2CH(NH_2)COO^- + 11\ H_2O$], (C) serine [3 $HCO_3^- + NH_4^+ + 5\ H_2 + 2\ H^+ \rightarrow CH_2OHCH(NH_3^+)COO^- + 6\ H_2O$], and (D) glycine (2 $HCO_3^- + NH_4^+ + 3\ H_2 + H^+ \rightarrow NH_3^+CH_2COO^- + 4\ H_2O$) at ODP sites 1225-31. All calculations are based on measurements obtained from sediment cores collected during ODP Leg 201 (Shipboard Scientific Party, 2003; Mitterer, 2006).

or methanol + formate, acetogens have a remarkable metabolic flexibility compared to sulfate reducers and methanogens, which in some cases may enable them to gain higher energy yields per substrate than these two groups. Acetogens also have a greater metabolic versatility with respect to the number and breadth of substrates utilized than sulfate reducers and methanogens. As a result, they may avoid competition via niche differentiation, i.e., by feeding on substrates not utilized by most sulfate reducers or methanogens. The greater substrate breadth furthermore means that acetogens are able to access energy from a greater overall number of substrates. Rather than evolving to become highly efficient and specialized consumers of abundant single substrates, acetogens are therefore likely to be substrate generalists with the capacity to draw on a large pool of less abundant (rare) substrates.

A further advantage of the acetogenic lifestyle may lie in the ability of acetogens to curb energy spent on biosynthesis. Acetogens use the reductive acetyl CoA pathway, the energetically least costly of all C fixation pathways. By using this pathway for both energy production and biosynthesis, they may cut back on energy that other groups spend on the maintenance of additional genes and enzymes. Use of organic compounds rather than H_2/CO_2 as starting blocks of biomass synthesis may moreover enable acetogens to circumvent energetically costly lithoautotrophic C fixation. Given the high energetic cost of amino acid synthesis in deep subsurface sediments, and the fact that synthesis and maintenance of enzymes for DNA and protein repair are likely to be the main energy expenditures of microbes in starvation mode, acetogens may be able to save crucial energy for survival by virtue of the simplicity and versatility of their biochemical pathway.

Given that the vast majority of cells in deep subsurface sediments are probably in starvation mode with generation times of hundreds to thousands of years (Biddle et al., 2006; Jørgensen et al., 2006), basic questions regarding the ecology of these organisms remain unanswered. Are the cells found highly recalcitrant survivors from surface environments, or have they adapted to the conditions of extreme energy limitation? Have microbes actively colonized sediments long after their accumulation, or have they been present since their initial deposition? Irregardless of the answers to these questions, it is likely that the ability of acetogens to use wide substrate ranges and perform biosynthesis at low energetic cost represent valuable survival traits in the deep biosphere – even if they did not originally evolve as adaptations to this environment.

ACKNOWLEDGMENTS

I would like to thank Bo Barker Jørgensen and other members of the Center for Geomicrobiology for constructive discussions on the potential importance of acetogenesis in the subseafloor, and Bente Aa. Lomstein for helpful feedback regarding the chemistry of amino acids. This study was supported by the Danish National Research Foundation and the Max Planck Society (grants to Bo Barker Jørgensen), as well as a Marie Curie Intra-European Fellowship awarded to the author (# 255135).

REFERENCES

Amend, J. P., and Helgeson, H. C. (1997). Calculation of the standard molal thermodynamic properties of aqueous biomolecules at elevated temperatures and pressures. Part 1 L-α-amino acids. *J. Chem. Soc. Faraday Trans.* 93, 1927–1941.

Amend, J. P., and Plyasunov, A. V. (2001). Carbohydrates in thermophile metabolism: calculation of the standard molar thermodynamic properties of aqueous pentoses and hexoses at elevated temperatures and pressures. *Geochim. Cosmochim. Acta* 65, 3901–3917.

Amend, J. P., and Shock, E. L. (2001). Energetics of overall metabolic reactions of thermophilic and hyperthermophilic archaea and bacteria. *FEMS Microbiol. Rev.* 25, 175–243.

Ansbaek, J., and Blackburn, T. H. (1979). A method for the analysis of acetate turnover in a coastal marine sediment. *Microb. Ecol.* 5, 253–264.

Avery, G. B., Shannon, R. D., White, J. R., Martens, C. S., and Alperin, M. J. (2002). Controls on methane production in a tidal freshwater estuary and a peatland: methane production via acetate fermentation and CO_2 reduction. *Biogeochemistry* 62, 19–37.

Ballschmiter, K. (2003). Pattern and sources of naturally produced organohalogens in the marine environment: biogenic formation of organohalogens. *Chemosphere* 52, 313–324.

Berg, I., Kockelkorn, D., Ramos-Vera, H. G., Say, R. F., Zarzycki, J., Hügler, M., Alber, B. E., and Fuchs, G. (2010). Autotrophic carbon fixation in archaea. *Nat. Rev. Microbiol.* 10, 1–14.

Biddle, J. F., Lipp, J. S., Lever, M. A., Lloyd, K. G., Sørensen, K. B., Anderson, R., Fredricks, H. F., Elvert, M., Kelly, T. J., Schrag, D. P., Sogin, M. L., Brenchley, J. E., Teske, A., House, C. H., and Hinrichs, K.-U. (2006). Heterotrophic archaea dominate sedimentary subsurface ecosystems off Peru. *Proc. Natl. Acad. Sci. U.S.A.* 103, 3846–3851.

Canfield, D. E., Jørgensen, B. B., Fossing, H., Glud, R., Gundersen, J., Ramsing, N. B., Thamdrup, B., Hansen, J. W., Nielsen, L. P., and Hall, P. O. J. (1993). Pathways of organic carbon oxidation in three continental margin sediments. *Mar. Geol.* 113, 27–40.

Capone, D. G., and Kiene, R. P. (1988). Comparison of microbial dynamics in marine and freshwater sediments: contrasts in anaerobic carbon catabolism. *Limnol. Oceanogr.* 33, 725–749.

Cappenberg, T. E. (1974). Interrelations between sulfate-reducing and methane-producing bacteria in bottom deposits of a freshwater lake. 2. Inhibition experiments. *Antonie Van Leeuwenhoek* 56, 1247–1258.

Chapelle, F. H., and Bradley, P. M. (2007). Hydrologic significance of carbon monoxide concentrations in ground water. *Ground Water* 45, 272–280.

Chidhaisong, A., Rosenstock, B., and Conrad, R. (1999). Measurement of monosaccharides and conversion of glucose to acetate in anoxic rice field soil. *Appl. Environ. Microbiol.* 65, 2350–2355.

Cord-Ruwisch, R., Seitz, H.-J., and Conrad, R. (1988). The capacity of hydrogenotrophic anaerobic bacteria to compete for traces of hydrogen depends on the redox potential of the terminal electron acceptor. *Arch. Microbiol.* 149, 350–357.

Dalla-Betta, P., and Schulte, M. (2009). Calculation of the aqueous thermodynamic properties of citric acid cycle intermediates and precursors and the estimation of high temperature and pressure equation of state parameters. *Int. J. Mol. Sci.* 10, 2809–2837.

Dhillon, A., Lever, M., Lloyd, K. G., Albert, D. B., Sogin, M. L., and Teske, A. (2005). Methanogen diversity evidenced by molecular characterization of methyl coenzyme M reductase (mcrA) genes in hydrothermal sediments of the Guaymas Basin. *Appl. Environ. Microbiol.* 71, 4592–4601.

D'Hondt, S., Jørgensen, B. B., Miller, D. J., Batzke, A., Blake, R., Cragg, B. A., Cypionka, H., Dickens, G. R., Ferdelman, T., Hinrichs, K.-U., Holm, N. G., Mitterer, R., Spivack, A., Wang, G., Bekins, B., Engelen, B., Ford, K., Gettemy, G., Rutherford, S. D., Sass, H., Skilbeck, C. G., Aiello, I. W., Guèrin, G., House, C. H., Inagaki, F., Meister, P., Naehr, T., Niitsuma, S., Parkes, R. J., Schippers, A., Smith, D. C., Teske, A., Wiegel, J., Padilla, C. N., and Acosta, J. L. S. (2004). Distributions of microbial activities in deep subseafloor sediments. *Science* 306, 2216–2221.

D'Hondt, S., Spivack, A. J., Pockalny, R., Ferdelman, T. G., Fischer, J. P., Kallmeyer, J., Abrams, L. J., Smith, D. C., Graham, D., Hasiuk, F., Schrum, H., and Stancin, A. M. (2009). Subseafloor sedimentary life in the South Pacific Gyre. *Proc. Nat. Acad. Sci. U.S.A.* 106, 11651–11656.

Dolfing, J., Larter, S. R., and Head, I. M. (2008). Thermodynamic constraints on methanogenic crude oil biodegradation. *ISME J.* 2, 442–452.

Drake, H. L., Küsel, K., Matthies, C. (2006). "Acetogenic prokaryotes," in *The Prokaryotes: An Evolving Electronic Resource for the Microbiological Community*, eds M. Dworkin, S. Falkow, E. Rosenberg, K.-H. Schleifer, and E. Stackebrandt (New York: Springer), 354–420.

Dykhuizen, D., and Davies, M. (1980). An experimental model: bacterial specialists and generalists competing in chemostats. *Ecology* 61, 1213–1227.

Edenborn, H. M., and Litchfield, C. D. (1987). Glycolate turnover in the water column of the New York Bight apex. *Mar. Biol.* 95, 459–467.

Egli, T. (1995). The ecological and physiological significance of the growth of heterotrophic microorganisms with mixtures of substrates. *Adv. Microb. Ecol.* 14, 305–386.

Egli, T., Lendenmann, U., and Snozzi, M. (1993). Kinetics of microbial growth with mixtures of carbon sources. *Antonie Van Leeuwenhoek* 63, 289–298.

Emlen, J. M. (1966). The role of time and energy in food preference. *Am. Nat.* 100, 611–617.

Expedition 329 Scientists. (2011). "South Pacific Gyre subseafloor life," in *Proceedings of Integrated Ocean Drilling Program,* (College Station, TX: IODP), 1–108.

Ferry, J. G. (2010). CO in methanogenesis. *Ann. Microbiol.* 60, 1–12.

Ferry, J. G., and Lessner, D. J. (2008). Methanogenesis in marine sediments. *Ann. N. Y. Acad. Sci.* 1125, 147–157.

Finke, N., Vandieken, V., and Jørgensen, B. B. (2006). Acetate, lactate, propionate, and isobutyrate as electron donors for iron and sulfate reduction in Arctic marine sediments, Svalbard. *FEMS Microbiol. Ecol.* 59, 10–22.

Franklin, M. J., Wiebe, W. J., and Whitman, W. B. (1988). Populations of methanogenic bacteria in a Georgia salt marsh. *Appl. Environ. Microbiol.* 54, 1151–1157.

Froelich, P. N., Klinkhammer, G. P., Bender, M. L., Luedtke, N. A., Heath, G. R., Cullen, D., Dauphin, P., Hammond, D., Hartman, B., and Maynard, V. (1979). Early oxidation of organic matter in pelagic sediments of the eastern equatorial Atlantic: suboxic diagenesis. *Geochim. Cosmochim. Acta* 43, 1075–1090.

Fuchs, G., and Stupperich, E. (1985). "Evolution of autotrophic CO_2 fixation," in *Evolution of Prokaryotes*, eds K. H. Schleifer and E. Stackebrandt (London: Academic Press), 235–251. [FEMS Symposium No. 29].

Fuhrman, J. A., and Ferguson, R. L. (1986). Nanomolar concentrations and rapid turnover of dissolved free amino acids in seawater: agreement between chemical and microbiological measurements. *Mar. Ecol. Prog. Ser.* 33, 237–242.

Gottschal, J. S., de Vries, S., and Kuenen, J. G. (1979). Competition between the facultatively chemolithotrophic *Thiobacillus* A2, and obligately chemolithotrophic *Thiobacillus* and a heterotrophic *Spirillum* for inorganic and organic substrates. *Arch. Microbiol.* 121, 241–249.

Griebler, C., and Lueders, T. (2008). Microbial diversity in groundwater ecosystems. *Freshw. Biol.* 54, 649–677.

Harder, J. (1997). Species-independent maintenance energy and natural population sizes. *FEMS Microbiol. Ecol.* 23, 39–44.

Hattori, S., Galushko, A. S., Kamagata, Y., and Schink, B. (2005). Operation of the CO dehydrogenase/acetyl coenzyme A pathway in both acetate oxidation and acetate formation by the syntrophically acetate-oxidizing bacterium *Thermoacetogenium phaeum*. *J. Bacteriol.* 187, 3471–3476.

Heimann, A., Jakobsen, R., and Blodau, C. (2010). Energetic constraints on H_2-dependent terminal electron accepting processes in anoxic environments: a review of observations and model approaches. *Environ. Sci. Technol.* 44, 24–33.

Henstra, A. M., Dijkema, C., and Stams, A. J. M. (2007). *Archaeoglobus fulgidus* couples CO oxidation to sulfate reduction and acetogenesis with transient formate accumulation. *Environ. Microbiol.* 9, 1836–1841.

Heuer, V., Elvert, M., Tille, S., Krummen, M., Prieto Mollar, X., Hmelo, L. R., and Hinrichs, K.-U. (2006). Online δ13C analysis of volatile fatty acids in sediment/porewater systems by liquid chromatography-isotope ratio-mass spectrometry. *Limnol. Oceanogr. Methods* 4, 346–357.

Heuer, V. B., Pohlman, J. W., Torres, M. E., Elvert, M., and Hinrichs, K.-U. (2009). The stable carbon isotope biogeochemistry of acetate and other dissolved carbon species in deep subseafloor sediments at the northern Cascadia margin. *Geochim. Cosmochim. Acta* 73, 3323–3336.

Hoehler, T. M. (2004). Biological energy requirements as quantitative boundary conditions for life in the subsurface. *Geobiology* 2, 205–215.

Hoehler, T. M., Albert, D. B., Alperin, M. J., and Martens, C. S. (1999). Acetogenesis from CO_2 in an anoxic marine sediment. *Limnol. Oceanogr.* 44, 662–667.

Hoehler, T. M., Alperin, M. J., Albert, D. B., and Martens, C. S. (1998). Thermodynamic control on hydrogen concentrations in anoxic sediments. *Geochim. Cosmochim. Acta* 62, 1745–1756.

Hoehler, T. M., Alperin, M. J., Albert, D. B., and Martens, C. S. (2001). Apparent minimum free energy requirements for methanogenic archaea and sulfate-reducing bacteria in an anoxic marine sediment. *FEMS Microbiol. Ecol.* 38, 33–41.

Hügler, M., and Sievert, S. M. (2011). Beyond the Calvin Cycle: autotrophic carbon fixation in the ocean. *Ann. Rev. Mar. Sci.* 3, 261–289.

Jansen, K., Thauer, R. K., Widdel, F., and Fuchs, G. (1984). Carbon assimilation pathways in sulfate reducing bacteria. Formate, carbon dioxide, carbon monoxide, and acetate assimilation by *Desulfovibrio baarsii*. *Arch. Microbiol.* 138, 257–262.

Jetten, M. S. M., Stams, A. J. M., and Zehnder, A. J. B. (1992). Methanogenesis from acetate: a comparison of the acetate metabolism in *Methanothrix soehngenii* and *Methanosarcina* spp. *FEMS Microbiol. Rev.* 88, 181–198.

Jiang, N., Wang, Y., and Dong, X. (2010). Methanol as the primary methanogenic and acetogenic precursor in the cold Zoige wetland at Tibetan plateau. *Microb. Ecol.* 60, 206–213.

Jørgensen, B. B., D'Hondt, S. L., and Miller, D. J. (2006). "Leg 201 synthesis: controls on microbial communities in deeply buried sediments," in *Proceedings Ocean Drilling Program Science Results*, eds B. B. Jørgensen, S. L. D'Hondt, and D. J. Miller (College Station, TX: ODP), 201, 1–45.

Kaiser, J.-P., and Hanselmann, K. W. (1982). Fermentative metabolism of substituted monoaromatic compounds by a bacterial community from anaerobic sediments. *Arch. Microbiol.* 133, 185–194.

Karita, S., Nakayama, K., Goto, M., Sakka, K., Kim, W.-J., and Ogawa, S. (2003). A novel cellulolytic, anaerobic, and thermophilic bacterium, *Moorella* sp. strain F21. *Biosci. Biotechnol. Biochem.* 67, 183–185.

Keppler, F., Eiden, R., Niedan, V., Pracht, J., and Schöler, H. F. (2000). Halocarbons produced by natural oxidation processes during degradation of organic matter. *Nature* 203, 298–301.

King, G. M. (1988). Dehalogenation in marine sediments containing natural sources of halophenols. *Appl. Environ. Microbiol.* 54, 3079–3085.

King, G. M. (2007). Carbon monoxide consumption in salt marsh sediments. *FEMS Microbiol. Ecol.* 59, 2–9.

King, G. M., Klug, M. J., and Lovley, D. R. (1982). Glucose metabolism in sediments of a eutrophic lake: tracer analysis of uptake and product formation. *Appl. Environ. Microbiol.* 44, 1308–1317.

King, G. M., Klug, M. J., and Lovley, D. R. (1983). Metabolism of acetate, methanol, and methylated amines in intertidal sediments of Lowes Cove, Maine. *Appl. Environ. Microbiol.* 45, 1848–1853.

Kuenen, J. G. (1983). "The role of specialists and generalists in microbial population interactions," chapter 10 in *Foundations of Biochemical Engineering*, eds H. W. Blanch, E. T. Papoutsakis, and G. Stephanopoulos (Washington, DC: ACS Publications), 229–251.

Küsel, K., Pinkart, H. C., Drake, H., and Devereux, R. (1999). Acetogenic and sulfate-reducing bacteria inhabiting the rhizoplane and deep cortex cells of the sea grass *Halodule wrightii*. *Appl. Environ. Microbiol.* 65, 5117–5123.

Lessner, D. J., Li, L., Li, Q., Rejtar, T., Andreev, V. P., Reichlen, M., Hill, K., Moran, J. J., Karger, B. L., and Ferry, J. G. (2006). An unconventional pathway for reduction of CO_2 to methane in CO-grown *Methanosarcina acetivorans* revealed by proteomics. *Proc. Natl. Acad. Sci. U.S.A.* 103, 17921–17926.

Lever, M. A., Heuer, V. B., Morono, Y., Masui, N., Schmidt, F., Alperin, M. J., Inagaki, F., Hinrichs, K.-U., and Teske, A. (2010). Acetogenesis in deep subseafloor sediments of the Juan de Fuca Ridge Flank: a synthesis of geochemical, thermodynamic, and gene-based evidence. *Geomicrobiol. J.* 27, 183–211.

Lin, Y. S., Heuer, V. B., Ferdelman, T. G., and Hinrichs, K.-U. (2010). Microbial conversion of inorganic carbon to dimethylsulfide in anoxic lake sediment (Plußsee, Germany). *Biogeosciences* 7, 2433–2444.

Lin, Y. S., Heuer, V. B., Goldhammer, T., Kellermann, M. Y., Zabel, M., and Hinrichs, K.-U. (2011). Towards constraining H_2 concentration in subseafloor sediment: a proposal for combined analysis by two distinct approaches. *Geochim. Cosmochim. Acta* 77, 186–201.

Liu, F., and Conrad, R. (2011). Chemolithotrophic acetogenic H_2/CO_2 utilization in Italian rice field soil. *ISME J.* 5, 1526–1539.

Liu, S., and Suflita, J. M. (1993). H_2-CO_2-dependent anaerobic *O*-demethylation activity in subsurface sediments and by an isolated bacterium. *Appl. Environ. Microbiol.* 59, 1325–1331.

Liu, Y., and Whitman, W. B. (2008). Metabolic, phylogenetic, and ecological diversity of the methanogenic archaea. *Ann. N. Y. Acad. Sci.* 1125, 171–189.

Lorenson, T. D., Colwell, F. S., Delwiche, M., and Dougherty, J. A. (2006). "17. Data report: acetate and hydrogen concentrations in pore fluids associated with a large gas hydrate reservoir, southern hydrate ridge, offshore Oregon, USA," in *Proceedings of Ocean Drilling Program Scientific Results 204*, eds A. M. Tréhu, G. Bohrmann, M. E. Torres, and F. S. Colwell (College Station, TX: IODP), 1–20.

Lovley, D. R., and Goodwin, S. (1988). Hydrogen concentrations as an indicator of the terminal electron-accepting reactions in aquatic sediments. *Geochim. Cosmochim. Acta* 52, 2993–3003.

Martens, C. S. (1990). Generation of short chain organic acid anions in hydrothermally altered sediments of the Guaymas Basin, Gulf of California. *Appl. Geochem.* 5, 71–76.

Martin, W., and Russell, M. J. (2007). On the origin of biochemistry at an alkaline hydrothermal vent. *Philos. Trans. R. Soc. Lond. B Biol. Sci.* 362, 1887–1925.

Meyer-Reil, L.-A. (1978). Uptake of glucose by bacteria in the sediment. *Mar. Biol.* 44, 293–298.

Millero, F. J., and Schreiber, D. R. (1982). Use of the ion pairing model to estimate activity coefficients of the ionic components of natural waters. *Am. J. Sci.* 282, 1508–1540.

Mitterer, R. M. (2006). "12. Data report: D/L ratios and concentrations of selected amino acids in interstitial waters, Equatorial Pacific and Peru Margin, ODP Leg 201," in *Controls on Microbial Communities in Deeply Buried Sediments, Eastern Equatorial Pacific and Peru Margin Sites*, eds B. B. Jørgensen, S. L. D'Hondt, and D. J. Miller (College Station, TX: ODP), 1–7.

Mitterer, R. M., Malone, M. J., Goodfriend, G. A., Swart, P. K., Wortmann, U. G., Logan, G. A., Feary, D. A., and Hine, A. C. (2001). Co-generation of hydrogen sulfide and methane in marine carbonate sediments. *Geophys. Res. Lett.* 28, 3931–3934.

Mörsdorf, G., Frunzke, K., Gadkari, D., and Meyer, O. (1992). Microbial growth on carbon monoxide. *Biodegradation* 3, 61–82.

Oelkers, E. H., Helgeson, H. C., Shock, E. L., Sverjensky, D. A., Johnson, J. W., and Pokrovskii, V. A. (1995). Summary of the apparent standard molal Gibbs free energies of formation of aqeous species, minerals, and gases at pressures 1 to 5000 bars and temperatures 5 to 1000°C. *J. Phys. Chem. Ref. Data* 24, 1401–1560.

Parkes, R. J., Gibson, G. R., Mueller-Harvey, I., Buckingham, W. J., and Herbert, R. A. (1989). Determination of the substrates for sulphate-reducing bacteria within marine and estuarine sediments with different rates of sulphate reduction. *J. Gen. Microbiol.* 135, 175–187.

Pedersen, K., Arlinger, J., Eriksson, S., Hallbeck, A., Hallbeck, L., and Johansson, J. (2008). Numbers, biomass and cultivable diversity of microbial populations related to depth and borehole-specific conditions in groundwater from depths of 4-450 m in Olkiluoto, Finland. *ISME J.* 2, 760–775.

Peretó, J., Lopez-Garcia, P., and Moreira, D. (2004). Ancestral lipid biosynthesis and early membrane evolution. *Trends Biochem. Sci.* 29, 469–477.

Phelps, T. J., and Zeikus, J. G. (1984). Influence of pH on terminal carbon metabolism in anoxic sediments from a mildly acidic lake. *Appl. Environ. Microbiol.* 48, 1088–1095.

Pianka, E. R. (1994). *Evolutionary Ecology,* 5th Edn. New York: Harper-Collins College Publishers, 486.

Pilson, M. E. Q. (1998). *An introduction to the Chemistry of the Sea*. Upper Saddle River, NJ: Prentice-Hall, Inc.

Price, P. B., and Sowers, T. (2004). Temperature dependence of metabolic rates for microbial growth, maintenance, and survival. *Proc. Natl. Acad. Sci. U.S.A.* 101, 4631–4636.

Rabus, R., Hansen, T. A., and Widdel, F. (2006). "Dissimilatory sulfate- and sulfur- reducing prokaryotes", in *The Prokaryotes: An Evolving Electronic Resource for the Microbiological Community*, eds M. Dworkin, S. Falkow, E. Rosenberg, K.-H. Schleifer, and E. Stackebrandt (New York: Springer), 659–768.

Rother, M., and Metcalf, W. W. (2004). Anaerobic growth of *Methanosarcina acetivorans* C2A on carbon monoxide: an unusual way of life for a methanogenic archaeon. *Proc. Natl. Acad. Sci. U.S.A.* 101, 16929–16934.

Russell, M. J., and Martin, W. (2004). The rocky roots of the acetyl-CoA pathway. *Trends Biochem. Sci.* 29, 358–363.

Schauder, R., Preuß, A., Jetten, M., and Fuchs, G. (1989). Oxidative and reductive acetyl CoA/ carbon monoxide dehydrogenase pathway in *Desulfobacterium autotrophicum*. *Arch. Microbiol.* 151, 84–89.

Shipboard Scientific Party. (2003). "Controls on microbial communities in deeply buried sediments, Eastern Equatorial Pacific and Peru Margin sites 1225–1231," in *Proceedings Of Ocean Drilling Program Initial Reports. 201*, eds S. L. D'Hondt, B. B. Jørgensen, D. J. Miller, and et al. (College Station, TX: ODP). Available at: http://www-odp.tamu.edu/publications/201_IR/201ir.htm

Shock, E. L. (1995). Organic acids in hydrothermal solutions: standard molal thermodynamic properties of carboxylic acids, and estimates of dissociation constants at high temperatures and pressures. *Am. J. Sci.* 295, 496–580.

Shock, E. L., and Helgeson, H. C. (1988). Calculation of the thermodynamic and transport-properties of aqueous species at high-pressures and temperatures–correlation algorithms for ionic species and equation of state predictions to 5-kb and 1000°C. *Geochim. Cosmochim. Acta* 52, 2009–2036.

Shock, E. L., and Helgeson, H. C. (1990). Calculation of the thermodynamic and transport properties of aqueous species at high pressures and temperatures: standard partial molal properties of organic species. *Geochim. Cosmochim. Acta* 54, 915–945.

Shock, E. L., Sassani, D. C., Willis, M., and Sverjensky, D. A. (1997). Inorganic species in geologic fluids: correlations among standard molal thermodynamic properties of aqueous ions and hydroxide complexes. *Geochim. Cosmochim. Acta* 61, 907–950.

Smith, R. L., and Oremland, R. S. (1983). Anaerobic oxalate degradation: widespread natural occurrence in aquatic sediments. *Appl. Environ. Microbiol.* 46, 106–113.

Smith, R. L., Strohmaier, F. E., and Oremland, R. S. (1985). Isolation of anaerobic oxalate-degrading bacteria from freshwater lake sediments. *Arch. Microbiol.* 141, 8–13.

Sørensen, J., Christensen, D., and Jørgensen, B. B. (1981). Volatile fatty acids and hydro-gen as substrates for sulfate-reducing bacteria in anaerobic marine sediment. *Appl. Environ. Microbiol.* 42, 5–90.

Spormann, A. M., and Thauer, R. K. (1988). Anaerobic acetate oxidation to CO_2 by *Desulfotomaculum acetoxidans*. *Arch. Microbiol.* 150, 374–380.

Stolper, D. A., Revsbech, N. P., and Canfield, D. E. (2010). Aerobic growth at nanomolar oxygen concentrations. *Proc. Nat. Acad. Sci. U.S.A.* 107, 18755–18760.

Strous, M., Pelletier, E., Mangenot, S., Rattei, T., Lehner, A., Taylor, M. W., Horn, M., Daims, H., Bartol-Mavel, D., Wincker, P., Barbe, V., Fonknechten, N., Vallenet, D., Segurens, B., Schenowitz-Truong, C., Médigue, C., Collingro, A., Snel, B., Dutilh, B. E., Op den Camp, H. J. M., van der Drift, C., Cirpus, I., van de Pas- Schoonen, K. T., Harhangi, H. R., van Niftrik, L., Schmid, M., Keltjens, J., van de Vossenberg, J., Kartal, B., Meier, H., Frishman, D., Huynen, M. A., Mewes, H.-W., Weissenbach, J., Jetten, M. S. M., Wagner, M., and Le Paslier, D. (2006). Deciphering the evolution and metabolism of an anammox bacterium from a community genome. *Nature* 440, 790–794.

Stumm, W., and Morgan, J. J. (1981). *Aquatic Chemistry. An Introduction Emphasizing Chemical Equilibria in Natural Waters,* 3rd Edn. New York: John Wiley & Sons, 1022.

Takai, K., Nakamura, K., Toki, T., Tsunogai, U., Miyazaki, M., Miyazaki, J., Hirayama, H., Nakagawa, S., Nunoura, T., and Horikoshi, K. (2008). Cell proliferation at 122°C and isotopically heavy CH_4 production by a hyperthermophilic methanogen under high-pressure cultivation. *Proc. Natl. Acad. Sci. U.S.A.* 105, 10949–10954.

Tewari, Y. B., Lang, B. E., Decker, S. R., and Goldberg, R. N. (2008). Thermodynamics of the hydrolysis reactions of 1,4-β-D-xylobiose, 1,4-β-D-xylotriose, D-cellobiose, and D-maltose. *J. Chem. Thermodyn.* 40, 1517–1526.

Tijhuis, L., van Loosdrecht, M. C. M., and Heijnen, J. J. (1993). A thermodynamically based correlation for maintenance Gibbs energy requirements in aerobic and anaerobic microbial growth. *Biotechnol. Bioeng.* 42, 509–519.

Valentine, D. L. (2001). "Thermodynamic ecology of hydrogen-based syntrophy," in *Cellular Origin, Life in Extreme Habitats and Astrobiology*, Chap. 192. NewYork: Springer.

Wagman, D. D., Evans, W. H., Parker, V. B., Schumm, R. H., Halow, I., Bailey, S. M., Churney, K. L., and Nuttall, R. L. (1982). The NBS tables of chemical thermodynamic properties: selected values for inorganic and C1 and C2 organic substances in SI units. *J. Phys. Chem. Ref. Data* 11, 392.

Wang, G. Z., Spivack, A. J., Rutherford, S., Manor, U., and D'Hondt, S. (2008). Quantification of co-occurring reaction rates in deep subseafloor sediments. *Geochim. Cosmochim. Acta* 72, 3479–3488.

Whitman, W. B., Bowen, T. L., and Boone, D. R. (2006). "The methanogenic bacteria," in *The Prokaryotes: An Evolving Electronic Resource for the Microbiological Community*, eds M. Dworkin, S. Falkow, E. Rosenberg, K. H. Schleifer, and E. Stackebrandt (New York: Springer), 165–207.

Whitman, W. B., Coleman, D. C., and Wiebe, W. J. (1998). Prokaryotes: the unseen majority. *Proc. Nat. Acad. Sci. U.S.A.* 95, 6578–6583.

Wolin, M. J., and Miller, T. L. (1994). "Acetogenesis from CO_2 in the human colonic ecosystem," in *Acetogenesis*, ed. H. L. Drake (New York: Chapman and Hall), 365–385.

Wolin, M. J., Miller, T. L., Collins, M. D., and Lawson, P. A. (2003). Formate-dependent growth and homoacetogenic fermentation by a bacterium from human feces: description of *Bryantella formatexigens* gen. nov., sp. nov. *Appl. Environ. Microbiol.* 69, 6321–6326.

Zhilina, T. N., and Zavarzin, G. A. (1990). Extremely halophilic, methylotrophic, anaerobic bacteria. *FEMS Microbiol. Lett.* 87, 315–321.

Conflict of Interest Statement: The author declares that the research was conducted in the absence of any commercial or financial relationships that could be construed as a potential conflict of interest.

Received: 15 November 2011; paper pending published: 19 December 2011; accepted: 31 December 2011; published online: 13 January 2012.

*Citation: Lever MA (2012) Acetogenesis in the energy-starved deep biosphere – a paradox? Front. Microbio. **2**:284. doi: 10.3389/fmicb.2011.00284*

This article was submitted to Frontiers in Extreme Microbiology, a specialty of Frontiers in Microbiology.

frontiers in
MICROBIOLOGY

PERSPECTIVE ARTICLE
published: 24 January 2012
doi: 10.3389/fmicb.2011.00285

Prospects for the study of evolution in the deep biosphere

Jennifer F. Biddle[1]*, Jason B. Sylvan[2], William J. Brazelton[3], Benjamin J. Tully[2], Katrina J. Edwards[2], Craig L. Moyer[4], John F. Heidelberg[2] and William C. Nelson[2]

[1] College of Earth, Ocean and the Environment, University of Delaware, Lewes, DE, USA
[2] Department of Biological Sciences, University of Southern California, Los Angeles, CA, USA
[3] Department of Biology, East Carolina University, Greenville, NC, USA
[4] Biology Department, Western Washington University, Bellingham, WA, USA

Edited by:
Andreas Teske, University of North Carolina at Chapel Hill, USA

Reviewed by:
Patricia Lynne Siering, Humboldt State University, USA
Casey R. J. Hubert, Newcastle University, UK

****Correspondence:***
Jennifer F. Biddle, College of Earth, Ocean and the Environment, University of Delaware, Lewes, DE 19958, USA.
e-mail: jfbiddle@udel.edu

Since the days of Darwin, scientists have used the framework of the theory of evolution to explore the interconnectedness of life on Earth and adaptation of organisms to the ever-changing environment. The advent of molecular biology has advanced and accelerated the study of evolution by allowing direct examination of the genetic material that ultimately determines the phenotypes upon which selection acts. The study of evolution has been furthered through examination of microbial evolution, with large population numbers, short generation times, and easily extractable DNA. Such work has spawned the study of microbial biogeography, with the realization that concepts developed in population genetics may be applicable to microbial genomes (Martiny et al., 2006; Manhes and Velicer, 2011). Microbial biogeography and adaptation has been examined in many different environments. Here we argue that the deep biosphere is a unique environment for the study of evolution and list specific factors that can be considered and where the studies may be performed. This publication is the result of the NSF-funded Center for Dark Energy Biosphere Investigations (C-DEBI) theme team on Evolution (www.darkenergybiosphere.org).

Keywords: deep biosphere, subsurface, evolution, C-DEBI, adaptation

WHAT IS THE DEEP BIOSPHERE?

The deep biosphere is often operationally defined as described in Teske and Sørensen (2008). For this paper, we consider the marine deep biosphere, starting on average at 1 mbsf (meters below seafloor). Sediments above 10 cm have an average cell density of 10^9 cells/ml, versus sediments below 10 m averaging 10^7 cells/ml (Whitman et al., 1998). Studies suggest that despite the low apparent biomass in this environment, the large total volume of the deep biosphere could allow it to harbor the majority of biomass on the planet (Gold, 1992; Whitman et al., 1998). Using this definition of deep biosphere, we also include all potential reserviors in the igneous crust. Recent projects have begun to delineate the abundance and diversity of organisms present in the subseafloor biosphere and their global geochemical importance (D'Hondt et al., 2004, 2009). Genetic studies tracking the locations of microorganisms (Inagaki et al., 2006) and observations of their genomes (Biddle et al., 2008, 2011) have shown that subsurface habitats, even those with low biomass, are tractable for genomic studies.

WHAT MAKES THE DEEP BIOSPHERE A UNIQUE PLACE TO STUDY EVOLUTION?

It is our opinion that the deep biosphere offers a unique opportunity to examine microbial evolution in action. Often, microbial evolution is studied in an environment where numerous factors are controlling the rate of diversification and adaptation, in areas of abundant resources, undetermined connectedness and unknown species interactions. In contrast, the deep biosphere offers an environment where many of the standard forces in ecology are either not in play or much reduced. As examples, we will focus on dispersal, activity, metabolic flexibility, and thermodynamic extremes.

DISPERSAL

The deep biosphere in the marine realm is an environment existing in a physical matrix of sediments or igneous basalt. Unlike pelagic environments, where transport is influenced by many factors including temperature, currents, wind, and attachment to larger surfaces, dispersal is constrained in the deep biosphere. The study of subsurface hydrology in igneous crustal habitats has shown us that fluid exchange between crustal and oceanic reservoirs spans the range between advection and diffusion, and may be quite dynamic. In contrast, fluid exchange in deep sedimentary biomes is dictated almost entirely by diffusion. This range of constraints on the exchange between reservoirs of microbial diversity can facilitate the study of the evolution of individual populations by specifically addressing how adaptation in isolation influences evolution. For example as seen in the study of *Sulfolobus* species in hot spring environments in the continental realm (Whitaker et al., 2003). The study of local adaptation as an evolutionary force has been widespread throughout isolated populations (Kawecki and Ebert, 2004) however, the extreme time scales over which populations in the subsurface are isolated from the rest of the planet are likely to have profound evolutionary consequences, perhaps the drastic slowing or speeding of molecular clocks, that should be experimentally testable, and provide a unique place to study local adaptation.

ACTIVITY

The deep biosphere, where it has been examined so far (i.e., principally in sedimentary habitats) is generally considered to be a

nutrient poor environment, despite some "hot spots" of high nutrients, such as those seen below active upwelling regions on continental margins (D'Hondt et al., 2004). Consequently, subsurface microbes are considered to have low activity and extremely long doubling times, potentially as long as 200–2,000 years (Biddle et al., 2006). This decrease in activity may result in mostly isolated cells, whose individual cellular responses may have more control over metabolism than signals given through ecological interactions among the community. Additionally, the role of viruses is relatively unknown in the deep biosphere (see Anderson et al., 2011, for a theoretical examination of their role and Engelhardt et al., 2011 for empirical discussion). The deep biosphere is therefore a unique place to study the evolution of organisms living at the lower limits of metabolic activity.

METABOLIC FLEXIBILITY/INVENTION

Due to nutrient limitation and interaction with geologic features within the deep biosphere, novel metabolisms may exist in its microbial inhabitants that are not seen elsewhere. Already geochemical evidence points to the microbial production of ethane and propane, although a defined pathway has not been determined (Hinrichs et al., 2006). Many physiological processes may behave in surprising ways under the pressure and temperature extremes encountered in deep life, such as the formation of isotopically heavy methane (Takai et al., 2008). A comparison between metagenomes from the marine water column and subsurface sediments reveals that subsurface metagenomes exist in their own genetic "space," as seen by the subsurface sample's separation from the other samples, based on PCA plots of KEGG categories (**Figure 1**; Biddle et al., 2006, 2011), indicating unique genomic innovation may have evolved in this biome.

EXTREME HABITATS

The deep biosphere is one of the few places on Earth where a similar physical environment, for example: sediment, is in contact with multiple geochemical and geothermal regimes. For example, sediments within one drilled hole can range in temperatures from 2 to 50°C (Parkes et al., 2000). Sediments cored during the

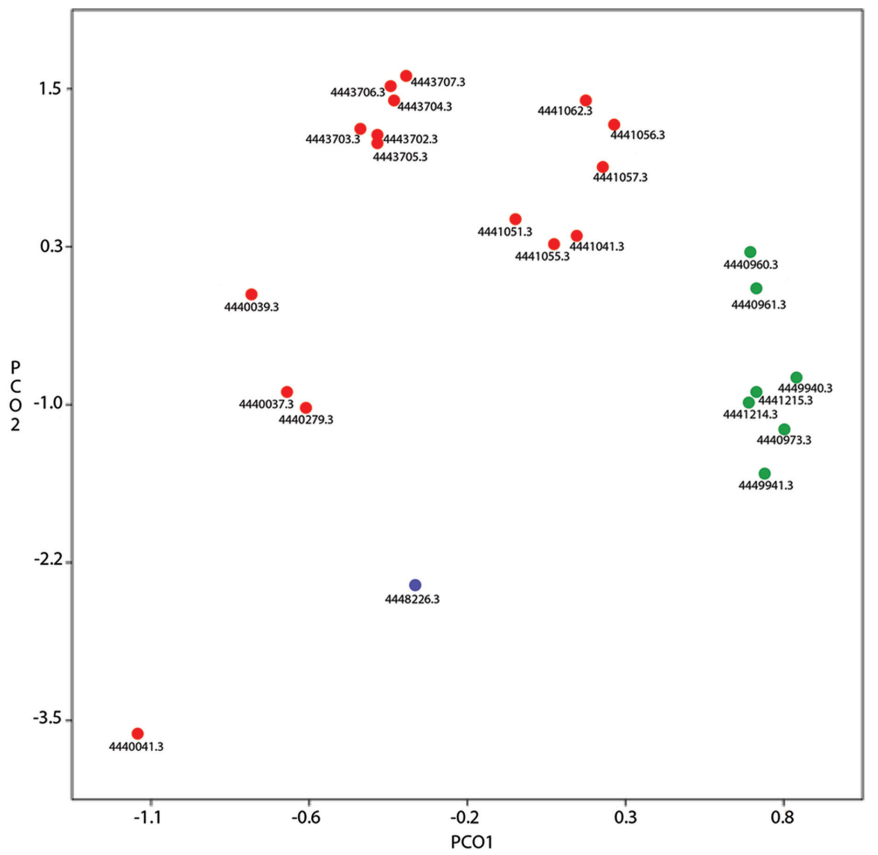

FIGURE 1 | Principle component analysis of KEGG categories from pyrosequenced marine metagenomes available in MG-RAST. A filter for alignments over 25 bp was used. Metagenome IDs in MG-RAST are listed. Green symbols are from sediment metagenomes [ODP (Ocean Drilling Program) Site 1229, IODP (Integrated Ocean Drilling Program) Site 1320], blue symbols are from hydrothermal vent fluid (Mariana Trough Hydrothermal Fluid), red symbols are other marine water pyrosequenced metagenomes (Northern Line Islands, HOT/ALOHA series, Coastal Plymouth Marine). PCO1 explains 59% of the data, PCO2 explains 10%. The blue symbol groups toward the subsurface samples, an example of how hydrothermal systems are viewed as windows to the deep biosphere. The separation between the red and green symbols indicates the distinctiveness between the sediment and pelagic biomes.

expedition to the Newfoundland Margin ranged from seafloor temperature of 4°C up to 100°C, where microbial signatures were still detected (Roussel et al., 2008). The ability to analyze taxonomically similar microbial populations across multiple temperatures, as detected in this environment, is a unique opportunity, considering that in most environments with hydrothermal activity (Yellowstone hot springs, hydrothermal vents) microbial communities rapidly change across the heat gradient (Rothschild and Mancinelli, 2001). Thermal gradients are often more gradual in the subsurface biome, compared to vent environments, where extreme gradients exist across a mere few centimeters. This allows for more careful experimentation with the effects of thermal gradients on evolution within microbial populations that may take place slowly over millennia.

WHAT ARE WAYS TO STUDY EVOLUTION IN THE DEEP BIOSPHERE?

Many major questions can affect the ability to study evolution in the deep biosphere. Factors governing dispersal need to be constrained in order to assess the amount of gene flow and isolation that may occur in the subsurface. As suggested above, there may be limited dispersal of microorganisms in this mostly solid environment, but areas of high fluid exchange through subsurface basalt where fast advective flow may allow gene flow among microbes (e.g., Wheat and Fisher, 2008). The doubling times of subsurface organisms is not well constrained, and may need to be examined in detail in order to estimate a proper sampling distance for evolutionary studies. Additionally, habitat size and quality will influence local adaptation, so geochemical and geophysical parameters should also be considered during sampling schemes (Kawecki and Ebert, 2004). Due to the difficulty of sampling and detection in the deep biosphere, coupled with the prediction that the majority of its inhabitants are microbial, we anticipate the evolutionary studies will predominantly be genome-based, observed by the genomes of model organisms, metagenomic, and PCR-generated sequences.

USE OF MODEL ORGANISMS/GENOMES

Considering the challenges in the assessment of biogeography and evolution of microbial populations, a focus on a particular group of microorganisms may be warranted in order to detect evolutionary events of local adaptation. Microbial groups such as the Zetaproteobacteria, Epsilonproteobacteria, Chloroflexi, and Miscellaneous Crenarchaeotal Group (MCG; **Figure 2**) serve as a few of the interesting candidates for the study of evolution due to the following reasons:

ZETAPROTEOBACTERIA

The Zetaproteobacteria contain iron-oxidizing bacteria, or FeOB, including the cultured isolate *Mariprofundus ferrooxydans* (Emerson et al., 2007). Recently the Zetaproteobacteria, now recognized as ubiquitous microorganisms that often dominate specific deep-sea habitats such as seamounts and borehole fluid, were shown to exhibit biogeographic separation based on habitat (McAllister et al., 2011). Some groups of Zetaproteobacteria appear ubiquitous throughout the Pacific Ocean, while others show more endemism toward their local habitats. Due to the widespread distribution and unique biogeochemistry of the Zetaproteobacteria, this group is an intriguing one to examine, particularly since analysis of the Zetaproteobacterial sequences originating from borehole fluids of the Southern Mariana Trough suggests that there may be a unique group of these organisms endemic to the deep subsurface (McAllister et al., 2011). In addition, Zetaproteobacteria have been detected (IODP Expedition 331) using enrichment culture and by qPCR from distinct subsurface habitats (Moyer and McAllister, 2011). A genome sequence is available for *M. ferrooxydans*, allowing for more intricate examination of FeOB endemism, beyond the small subunit ribosomal RNA gene (Singer et al., 2011).

EPSILONPROTEOBACTERIA

The Epsilonproteobacteria (**Figure 2A**) are abundant and ubiquitous inhabitants of many hydrothermal vent environments including chimneys, fluids, sediments, and animal hosts (Campbell et al., 2006). Most species are supported by hydrogen or sulfur oxidation, but the group is extraordinarily diverse. One hydrothermal chimney can harbor many different metabolic guilds of Epsilonproteobacteria in distinct ecological niches (Campbell et al., 2006), and a single fluid sample can contain thousands of Epsilonproteobacterial 16S rRNA sequence clusters (Huber et al., 2007). Furthermore, there are indications of biogeographic patterns in the Epsilonproteobacterial populations within and among vent fields (Huber et al., 2010). Because the fluid samples collected from the chimneys are exiting from the subsurface, these results indicate local and global dispersal limitations in the subsurface biosphere. The Epsilonproteobacteria are amenable to laboratory cultivation (Takai et al., 2005; Campbell et al., 2006), making them ideal representatives of the subsurface for experimental research.

CHLOROFLEXI

Chloroflexi (**Figure 2A**) are highly abundant in deeply buried marine sediments, but unlike their representatives in surface environments, they have resisted classic cultivation techniques (**Figure 2A**; Blazejak and Schippers, 2010). The phylum Chloroflexi is frequently divided into at least six classes: Chloroflexi, Thermomicrobia, Anaerolineae, Caldilineae, Dehalococcoidetes, and subphylum IV (SAR202 cluster; Rappe and Giovannoni, 2003; Hugenholtz and Stackebrandt, 2004; Morris et al., 2004). The most common Chloroflexi sequences in marine margin sediments fall within the classes Anaerolineae, Caldilineae, and Dehalococcoidetes (Parkes et al., 2005; Biddle et al., 2006; Inagaki et al., 2006). Members of Dehalococcoidetes derive energy through the reduction of organohalide compounds and the oxidation of H_2 (Seshadri et al., 2005). The wide distribution of Dehalococcoidetes sequences in deep anoxic sediments may indicate a common niche for organisms that grow on organohalides that is globally exploited, and the presence of reductive dehalogenase homologous (rdhA) genes globally distributed in subsurface sediments (Futagami et al., 2009) supports this hypothesis. Members of the Dehalococcoidetes have also shown a high potential for horizontal gene transfer, moving ecologically relevant, content-variable genomic islands between members of the same species (McMurdie et al., 2011), further increasing their potential as a model group of interest allowing for the study of horizontal gene transfer within the deep marine sediment environment.

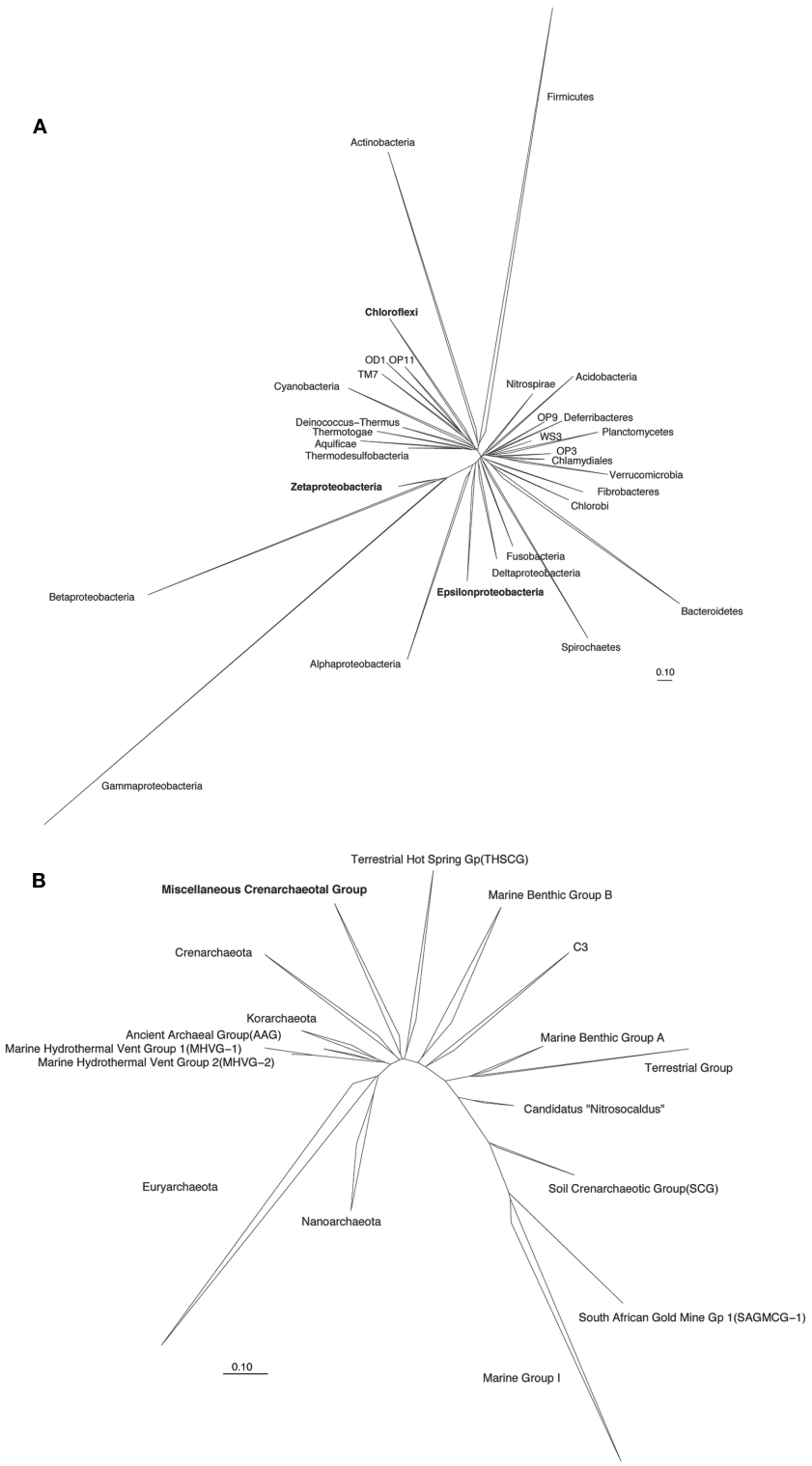

FIGURE 2 | Overview of the phylogenetic relationship of 16S rRNA genes sequences for **(A)** Bacteria and **(B)** Archaea. For the Archaea phylogenetic tree, the groups of the phylum Thaumarchaeota are shown in detail to highlight the relationship of the Miscellaneous Crenarchaeotal Group (MCG) within the phylum. Trees were exported (pre-aligned) from the SILVA comprehensive ribosomal RNA database (SSU database, Release 108) and visualized in ARB. Bar, 10 nucleotide substitutions per 100 nucleotides.

MCG ARCHAEA

The MCG was first labeled in 2003 and since then the group's molecular signatures have been found in a wide array of subsurface habitats (**Figure 2B**; Inagaki et al., 2003). This archaeal group remains uncultivated and its metabolism is currently unknown. The group's wide distribution in sediments indicates that it may be a useful group to examine for the transition into a "deep" lifestyle, since phylogenetically similar clones are seen in shallow estuaries and deep ocean sediments (Biddle et al., 2006; Meng et al., 2009). This group could also be used for biogeography studies in the deep biosphere since it appears to have a global distribution in anoxic sediments (Inagaki et al., 2003; Biddle et al., 2006).

WHERE TO STUDY EVOLUTION IN THE DEEP BIOSPHERE?

The ability to compare different physical conditions, geographically distinct settings, or settings that are geographically distinct but have similar physical conditions would benefit the study of deep biosphere evolution greatly. Proposals for future drilling expeditions can be submitted and those that are planned can be viewed through the IODP web resources (www.iodp.org/expeditions). Here we make the case for the study of evolution in model systems that have been suggested for future exploration based on prior research:

AREAS OF SIMILAR GEOCHEMISTRY

Expeditions have often focused on areas of sediment that contain high concentrations of methane, including methane hydrates, to investigate the biological and physical formations of this gas. Those cruises include: Cascadia Margin (IODP Expeditions 311, 328, and ODP Leg 146), Costa Rica (IODP expeditions 344, 334, and ODP Legs 137, 140, 148), Peru Margin (ODP Legs 112, 201, 202), and other margin areas. The examination of similarly aged sediments with similar geochemical regimes (for example, the sulfate/methane transition zone) would allow for the specific investigation of how geographic separation may affect microorganisms undergoing potential divergent evolutionary processes. If possible, finding areas of similar sediment composition (typically seen on margin sites), sediment age, and similar geochemistry (such as an SMTZ), it may be possible to limit variables to interpret the effect of geographic location. Similar surface studies have yielded interesting results (Whitaker et al., 2003), suggesting that geographic separation alone can yield evolutionary shifts in microbes when populations are subjected to similar chemical forces. A potential similar experiment focusing on subsurface rocks could ask similar questions in a massive sulfide setting. This ubiquitous subseafloor substrate was drilled during ODP Legs 158 (Humphris et al., 1995) and 169 (Zierenberg et al., 1998).

REACTIVATION AFTER STASIS

The idea that some microbial groups may be dormant in deep sediments due to a lack of nutrient and energy fluxes may play a role in the evolution of subsurface microbes. A microbial response to an increase in nutrients made available by geothermal activity was examined on the Newfoundland Margin on ODP Leg 210 (Roussel et al., 2008). This type of investigation is in its infancy, but due to the success of the initial experiments, this type of system could be investigated more thoroughly in the future. The evolution occurring in these "reactivated" microbes may parallel the models of bursts in positive selection seen after stasis in influenza A viral populations (Wolf et al., 2006). Additionally, it may provide insight into microbial succession.

RIDGE FLANKS

The Juan de Fuca ridge flank in the Pacific Ocean has recently become a site of intense scientific focus for understanding the deep biosphere in igneous ocean crust. Pioneering work using observatories has enabled scientists for the first time to study microbial populations *in situ* within the crust (see Edwards et al., 2012). The first long-term observatory study conducted at Juan de Fuca revealed succession of microbial communities over time which correlated with geochemical and mineralogical conditions within the borehole (Orcutt et al., 2011). Current work at a contrasting geochemical/geological setting in the Atlantic (North Pond, IODP Expedition 336) will allow for important comparisons to be made about ridge flank microbial communities as a function of these conditions (Edwards et al., 2012). The porous and permeable upper oceanic aquifer system at Juan de Fuca, North Pond, and other ridge flank settings allow for questions regarding the interconnectedness and evolutionary forces that shape these subseafloor microbial communities.

FUTURE POTENTIAL SUBSURFACE EXPERIMENTS, ALL OF WHICH REQUIRING THE USE OF DRILLING PLATFORMS, WHICH HAVE NOT BEEN PREVIOUSLY INVESTIGATED BY DRILLING: LOST CITY

A major uncertainty in subsurface ecosystems is the availability of energy and carbon to drive microbial activity. Hydration of the ultramafic rocks of the Atlantis Massif underlying the Lost City hydrothermal field (Kelley et al., 2005) results in a set of geochemical reactions known as serpentinization, which is highly exothermic and can release large quantities of hydrogen gas and variable levels of methane and other low molecular weight organic compounds. These chemicals support dense microbial communities in the carbonate chimneys of the Lost City hydrothermal field, but the extent and activity of organisms in the underlying subsurface awaits exploration and initial examination of unroofed gabbros has begun (Mason et al., 2011). The apparent longevity of serpentinization-associated processes (Fruh-Green et al., 2003) indicates that the microbial denizens of the Atlantis Massif subsurface have had access to copious energy and organic carbon for possibly millions of years. The nature of fluid circulation between the massif and adjacent regions of the seafloor is currently unknown, but would have profound consequences on the dispersal of microorganisms within the subsurface biosphere. It is possible that some organisms could be reactivated during their transit through the massif and then return to a dormant state after they have been transported out of it. Clearly, this habitat provides exciting opportunities for studying the evolution of potentially isolated but energy-rich ecosystems and their influence on other regions of the subsurface biosphere.

MARINE AND FRESHWATER HYDROTHERMAL SYSTEMS

One of the great surprises in subsurface microbiology is that some of the dominant organisms detected in terrestrial subsurface habitats, such as gold mines, are very similar to those detected in the marine subsurface basement (Takai et al., 2001; Moser et al.,

2005). With this in mind, much can be learned by studying similar environments in terrestrial and marine settings, with the specific goal of determining degrees of connectedness between these biomes and testing hypotheses about convergent evolution. Freshwater hydrothermal systems are common in rift lakes such as Lake Baikal in Russia (Crane et al., 1991) and Lake Tanganyika in Africa (Tiercelin et al., 1993), and these systems harbor microbial fauna similar to those in deep-sea hydrothermal vents. Similarly, freshwater alkaline springs harbor microbial communities that bear resemblances to those in seafloor alkaline springs (Brazelton et al., 2011). Subsurface studies of a series of hydrothermal systems from freshwater and marine systems are likely fertile areas for exciting discoveries in biogeography and geographical isolation, and may also have similarities to well studied thermal systems such as Yellowstone National Park. Additionally, the study of several systems for one project would require international cooperation and many researchers, thereby fostering collaboration within the international research community.

SUMMARY AND OUTLOOK

Although the deep subsurface biosphere is difficult to access and most often can be studied as only a snapshot of an environment, many experiments to assess the unique forces acting on evolution in this vast habitat are possible. Through the study of specific groups of microorganisms that are common inhabitants of the subseafloor, biogeography, and local adaptation questions may be posed. Understanding of hydrogeology and geophysical parameters are needed, making any evolutionary questions posed in this environment inherently multidisciplinary in nature, even if they are approached with a genomics-oriented investigation. Past expeditions have allowed the generation of hypotheses or situational investigations and future expeditions, including long-term CORK observatories, will allow for further investigation into this unique biosphere on our planet.

ACKNOWLEDGMENTS

This paper is a product of the Center for Dark Energy Biosphere Investigations (C-DEBI) Science and Technology Center Evolution theme team, which met on Catalina Island in 2011. Team member Jonathan Eisen contributed to discussions that led to this paper. Funding for the meeting was provided by the Center for Dark Energy Biosphere Investigations, NSF OCE-0939564. This is C-DEBI publication 112.

REFERENCES

Anderson, R. E., Brazelton, W. J., and Baross, J. A. (2011). Is the genetic landscape of the deep subsurface biosphere affected by viruses? *Front. Microbio.* 2:219. doi: 10.3389/fmicb.2011.00219

Biddle, J. F., Fitz-Gibbon, S., Schuster, S. C., Brenchley, J. E., and House, C. H. (2008). Metagenomic signatures of the Peru Margin subseafloor biopshere show a genetically distinct environment. *Proc. Natl. Acad. Sci. U.S.A.* 105, 10583–10588.

Biddle, J. F., Lipp, J. S., Lever, M. A., Lloyd, K. G., Sørensen, K. B., Anderson, R., Fredricks, H. F., Elvert, M., Kelly, T. J., Schrag, D. P., Sogin, M. L., Brenchley, J. E., Teske, A., House, C. H., and Hinrichs, K. U. (2006). Heterotrophic archaea dominate sedimentary subsurface ecosystems off Peru. *Proc. Natl. Acad. Sci. U.S.A.* 103, 3846–3851.

Biddle, J. F., White, J. R., Teske, A. P., and House, C. H. (2011). Metagenomics of the subsurface Brazos-Trinity Basin (IODP site 1320): comparison with other sediment and pyrosequenced metagenomes. *ISME J.* 5, 1038–1047.

Blazejak, A., and Schippers, A. (2010). High abundance of JS-1 and Chloroflexi-related bacteria in deeply buried marine sediments revealed by quantitative, real-time PCR. *FEMS Microbiol. Ecol.* 72, 198–207.

Brazelton, W. J., Nelson, B., and Schrenk, M. O. (2011). Metagenomic evidence for H2 oxidation and H2 production by serpentinite-hosted subsurface microbial communities. *Front. Microbio.* 2:268. doi: 10.3389/fmicb.2011.00268

Campbell, B. J., Engel, A. S., Porter, M. L., and Takai, K. (2006). The versatile Epsilonproteobacteria: key players in sulphidic habitats. *Nat. Rev. Microbiol.* 4, 458–468.

Crane, K., Hecker, B., and Golubev, V. (1991). Hydrothermal vents in Lake Baikal. *Nature* 350, 281.

D'Hondt, S., Jørgensen, B. B., Miller, D. J., Batzke, A., Blake, R., Cragg, B. A., Cypionka, H., Dickens, G. R., Ferdelman, T., Hinrichs, K. U., Holm, N. G., Mitterer, R., Spivack, A., Wang, G., Bekins, B., Engelen, B., Ford, K., Gettemy, G., Rutherford, S. D., Sass, H., Skilbeck, C. G., Aiello, I. W., Guèrin, G., House, C. H., Inagaki, F., Meister, P., Naehr, T., Niitsuma, S., Parkes, R. J., Schippers, A., Smith, D. C., Teske, A., Wiegel, J., Padilla, C. N., and Acosta, J. L. (2004). Distributions of microbial activities in deep subseafloor sediments. *Science* 306, 2216–2221.

D'Hondt, S., Spivack, A. J., Pockalny, R., Ferdelman, T. G., Fischer, J. P., Kallmeyer, J., Abrams, L. J., Smith, D. C., Graham, D., Hasiuk, F., Schrum, H., and Stancin, A. M. (2009). Subseafloor sedimentary life in the South Pacific Gyre. *Proc. Natl. Acad. Sci. U.S.A.* 106, 11651–11656.

Edwards, K., Fisher, A., and Wheat, C. (2012). The deep subsurface biosphere in igneous ocean crust: frontier habitats for microbiological exploration. *Front. Microbio.* 3:8. doi: 10.3389/fmicb.2012.00008

Emerson, D., Rentz, J. A., Lilburn, T. G., Davis, R. E., Aldrich, H., Chan, C., and Moyer, C. L. (2007). A novel lineage of proteobacteria involved in formation of marine Fe oxidizing microbial mat communities. *PLoS ONE* 2, e667. doi:10.1371/journal.pone.0000667

Engelhardt, T., Sahlberg, M., Cypionka, H., and Engelen, B. (2011). Induction of prophages from deep-subseafloor bacteria. *Environ. Microbiol. Rep.* 4, 459–465.

Fruh-Green, G. L., Kelley, D. S., Bernasconi, S. M., Karson, J. A., Ludwig, K. A., Butterfield, D. A., Boschi, C., and Proskurowski, G. (2003). 30,000 years of hydrothermal activity at the lost city vent field. *Science* 301, 495–498.

Futagami, T., Morono, Y., Terada, T., Kaksonen, A. H., and Inagaki, F. (2009). Dehalogenation activities and distribution of reductive dehalogenase homologous genes in marine subsurface sediments. *Appl. Environ. Microbiol.* 75, 6905–6909.

Gold, T. (1992). The deep, hot biosphere. *Proc. Natl. Acad. Sci. U.S.A.* 89, 6045–6049.

Hinrichs, K.-U., Hayes, J. M., Bach, W., Spivack, A. J., Hmelo, L. R., Holm, N. G., Johnson, C. G., and Sylva, S. P. (2006). Biological formation of ethane and propane in the deep marine subsurface. *Proc. Natl. Acad. Sci. U.S.A.* 103, 14684–14689.

Huber, J. A., Cantin, H. V., Huse, S. M., Mark Welch, D. B., Sogin, M. L., and Butterfield, D. A. (2010). Isolated communities of epsilonproteobacteria in hydrothermal vent fluids of the Mariana Arc seamounts. *FEMS Microbiol. Ecol.* 73, 538–549.

Huber, J. A., Welch, D. B., Morrison, H. M., Huse, S. M., Neal, P. R., Butterfield, D. A., and Sogin, M. L. (2007). Microbial population structures in the deep marine biosphere. *Science* 318, 97–100.

Hugenholtz, P., and Stackebrandt, E. (2004). Reclassification of *Sphaerobacter thermophilus* from the subclass Sphaerobacteridae in the phylum Actinobacteria to the class Thermomicrobia (emended description) in the phylum Chloroflexi (emended description). *Int. J. Syst. Evol. Microbiol.* 54, 2049–2051.

Humphris, S. E., Herzig, P. M., Miller, D. J., Alt, J. C., Becker, K., Brown, D., Brugmann, G., Chiba, H., Fouquet, Y., Gemmell, J. B., Guerin, G., Hannington, M. D., Holm, N. G., Honnorez, J. J., Iturrino, G. J., Knott, R., Ludwig, R., Nakamura, K., Petersen, S., Reysenbach, A. L., Rona, P. A., Smith, S., Sturz, A. A., Tivey, M. K., and Zhao, X. (1995). The internal structure of an active sea-floor massive sulfide deposit. *Nature* 377, 713–716.

Inagaki, F., Nunoura, T., Nakagawa, S., Teske, A., Lever, M., Lauer, A., Suzuki, M., Takai, K., Delwiche, M., Colwell, F. S., Nealson, K. H., Horikoshi, K., D'Hondt, S., and Jørgensen, B. B. (2006). Biogeographical distribution and diversity of microbes in methane hydrate-bearing deep marine sediments on the Pacific Ocean Margin. *Proc. Natl. Acad. Sci. U.S.A.* 103, 2815–2820.

Inagaki, F., Suzuki, M., Takai, K., Oida, H., Sakamoto, T., Aoki, K., Nealson, K. H., and Horikoshi, K. (2003). Microbial communities associated with geological horizons in coastal subseafloor sediments from the sea of Okhotsk. *Appl. Environ. Microbiol.* 69, 7224–7235.

Kawecki, T. J., and Ebert, D. (2004). Conceptual issues in local adaptation. *Ecol. Lett.* 7, 1225–1241.

Kelley, D. S., Karson, J. A., Fruh-Green, G. L., Yoerger, D. R., Shank, T. M., Butterfield, D. A., Hayes, J. M., Schrenk, M. O., Olson, E. J., Proskurowski, G., Jakuba, M., Bradley, A., Larson, B., Ludwig, K., Glickson, D., Buckman, K., Bradley, A. S., Brazelton, W. J., Roe, K., Elend, M. J., Delacour, A., Bernasconi, S. M., Lilley, M. D., Baross, J. A., Summons, R. E., and Sylva, S. P. (2005). Aserpentinite-hosted ecosystem: the Lost City hydrothermal field. *Science* 307, 1428–1434.

Manhes, P., and Velicer, G. J. (2011). Experimental evolution of selfish policing in social bacteria. *Proc. Natl. Acad. Sci. U.S.A.* 108, 8357–8362.

Martiny, J. B., Bohannan, B. J., Brown, J. H., Colwell, R. K., Furhman, J. A., Green, J. L., Horner-Devine, M. C., Kane, M., Krumins, J. A., Kuske, C. R., Morin, P. J., Naeem, S., Ovreås, L., Reysenbach, A. L., Smith, V. H., and Staley, J. T. (2006). Microbial biogeography: putting microorganisms on the map. *Nat. Rev. Microbiol.* 4, 102–112.

Mason, O. U., Nakagawa, T., Rosner, M., Van Nostrand, J. D., Zhou, J., Maruyama, A., Fisk, M., and Giovannoni, S. J. (2011). First investigation of the microbiology of the deepest layer of ocean crust. *PLoS ONE* 5, e15399. doi:10.1371/journal.pone.0015399

McAllister, S. M., Davis, R. E., McBeth, J. M., Tebo, B. M., Emerson, D., and Moyer, C. L. (2011). Biodiversity and emerging biogeography of the neutrophilic iron-oxidizing Zetaproteobacteria. *Appl. Environ. Microbiol.* 77, 5445–5457.

McMurdie, P. J., Hug, L. A., Edwards, E. A., Holmes, S., and Spormann, A. M. (2011). Site-specific mobilization of vinyl chloride respiration islands by a mechanism common in dehalococcoides. *BMC Genomics* 12, 287. doi:10.1186/1471-2164-12-287

Meng, J., Wang, F., Wang, F., Zheng, Y., Peng, X., Zhou, H., and Xiao, X. (2009). An uncultivated 478 crenarchaeota contains functional bacteriochlorophyll a synthase. *ISME J.* 3, 106–116.

Morris, R. M., Rappe, M. S., Urbach, E., Connon, S. A., and Giovannoni, S. J. (2004). Prevalence of the Chloroflexi-related SAR202 bacterioplankton cluster throughout the mesopelagic zone and deep ocean. *Appl. Environ. Microbiol.* 70, 2836–2842.

Moser, D. P., Gihring, T. M., Brockman, F. J., Fredrickson, J. K., Balkwill, D. L., Dollhopf, M. E., Lollar, B. S., Pratt, L. M., Boice, E., Southam, G., Wanger, G., Baker, B. J., Pfiffner, S. M., Lin, L. H., and Onstott, T. C. (2005). *Desulfotomaculum* and *Methanobacterium* spp. dominate a 4-to 5-kilometer-deep fault. *Appl. Environ. Microbiol.* 71, 8773–8783.

Moyer, C. L., and McAllister, S. M. (2011). IODP Exp 331: Iron-oxidizing bacteria from the Okinawa trough deep subsurface biosphere. *AGU Fall Meeting.* abstr. B51K-0556.

Orcutt, B. N., Sylvan, J. B., Knab, N. J., and Edwards, K. J. (2011). Microbial ecology of the dark ocean above, at, and below the seafloor. *Microbiol. Mol. Biol. Rev.* 75, 361–422.

Parkes, R. J., Cragg, B. A., and Wellsbury, P. (2000). Recent studies on bacterial populations and processes in subseafloor sediments: a review. *Hydrogeol. J.* 8, 11–28.

Parkes, R. J., Webster, G., Cragg, B. A., Weightman, A. J., Newberry, C. J., Ferdelman, T. G., Kallmeyer, J., Jørgensen, B. B., Aiello, I. W., and Fry, J. C. (2005). Deep sub-seafloor prokaryotes stimulated at interfaces over geological time. *Nature* 436, 390–394.

Rappe, M. S., and Giovannoni, S. J. (2003). The uncultured microbial majority. *Annu. Rev. Microbiol.* 57, 369–394.

Rothschild, L., and Mancinelli, R. L. (2001). Life in extreme environments. *Nature* 409, 1092–1100.

Roussel, E. G., Bonavita, M. C., Querellou, J., Cragg, B. A., Webster, G., Prieur, D., and Parkes, R. J. (2008). Extending the sub-seafloor biosphere. *Science* 320, 1046.

Seshadri, R., Adrian, L., Fouts, D. E., Eisen, J. A., Phillippy, A. M., Methe, B. A., Ward, N. L., Nelson, W. C., Deboy, R. T., Khouri, H. M., Kolonay, J. F., Dodson, R. J., Daugherty, S. C., Brinkac, L. M., Sullivan, S. A., Madupu, R., Nelson, K. E., Kang, K. H., Impraim, M., Tran, K., Robinson, J. M., Forberger, H. A., Fraser, C. M., Zinder, S. H., and Heidelberg, J. F. (2005). Genome sequence of the PCE-dechlorinating bacterium *Dehalococcoides ethenogenes*. *Science* 307, 105–108.

Singer, E., Emerson, D., Webb, E. A., Barco, R. A., Kuenen, J. G., Nelson, W. C., Chan, C. S., Comolli, L. R., Ferriera, S., Johnson, J., Heidelberg, J. F., and Edwards, K. J. (2011). *Mariprofundus ferroosydans* PV-1 the first genome of a marine Fe(II) oxidizing Zetaproteobacterium. *PLoS ONE* 6, e25386. doi:10.1371/journal.pone.0025386

Takai, K., Campbell, B. J., Cary, S. C., Suzuki, M., Oida, H., Nunoura, T., Hirayama, H., Nakagawa, S., Suzuki, Y., Inagaki, F., and Horikoshi, K. (2005). Enzymatic and genetic characterization of carbon and energy metabolisms by deep-sea hydrothermal chemolithoautotrophic isolates of Epsilonproteobacteria. *Appl. Environ. Microbiol.* 71, 7310–7320.

Takai, K., Moser, D. P., Deflaun, M., Onstott, T. C., and Fredrickson, J. K. (2001). Archaeal diversity in waters from deep South African gold mines. *Appl. Environ. Microbiol.* 67, 5750–5760.

Takai, K., Nakamur, K., Toki, T., Tsunogai, U., Miyazaki, M., Miyazaki, J., Hirayama, H., Nakagawa, S., Nunoura, T., and Horikoshi, K. (2008). Cell proliferation at 122C and isotopically heavy CH4 production by a hyperthermophilic methanogen under high-pressure cultivation. *Proc. Natl. Acad. Sci. U.S.A.* 105, 10949–10954.

Teske, A., and Sørensen, K. (2008). Uncultured archaea in deep marine sediments: have we caught them all? *ISME J.* 2, 3–18.

Tiercelin, J. J., Pflumio, C., Castrec, M., Boulegue, J., Gente, P., Rolet, J., Coussement, C., Stetter, K. O., Huber, R., Buku, S., and Mifundu, W. (1993). Hydrothermal vents in Lake Tanganyika, East African rift system. *Geology* 21, 499–502.

Wheat, C. G., and Fisher, A. T. (2008). Massive, low-temperature hydrothermal flow from a basaltic outcrop on 23 Ma seafloor of the Cocos Plate: chemical constraints and implications. *Geochem. Geophys. Geosyst.* 9, Q12O14.

Whitaker, R. J., Grogan, D. W., and Taylor, J. W. (2003). Geographic barriers isolate endemic populations of hyperthermophilic archaea. *Science* 301, 976–978.

Whitman, W. B., Coleman, D. C., and Wiebe, W. J. (1998). Prokaryotes: the unseen majority. *Proc. Natl. Acad. Sci. U.S.A.* 95, 6578–6583.

Wolf, Y. I., Viboud, C., Holmes, E. C., Koonin, E. V., and Lipman, D. J. (2006). Long intervals of stasis punctuated by bursts of positive selection in the seasonal evolution of influenza A virus. *Biol. Direct* 1. doi:10.1186/1745-6150-1-34

Zierenberg, R. A., Fouquet, Y., Miller, D. J., Bahr, J. M., Baker, P. A., Bjerkgard, T., Brunner, C. A., Duckworth, R. C., Gable, R., Gieskes, J., Goodfellow, W. D., Groschel-Becker, H. M., Guerin, G., Ishibashi, J., Iturrino, G., James, R. H., Lackschewitz, K. S., Marquez, L. L., Nehlig, P., Peter, J. M., Rigsby, C. A., Schultheiss, P., Shanks, W. C., Simoneit, B. R. T., Summit, M., Teagle, D. A. H., Urbat, M., and Zuffa, G. G. (1998). The deep structure of a sea-floor hydrothermal deposit. *Nature* 392, 485–488.

Conflict of Interest Statement: The authors declare that the research was conducted in the absence of any commercial or financial relationships that could be construed as a potential conflict of interest.

Received: 14 October 2011; accepted: 31 December 2011; published online: 24 January 2012.

Citation: Biddle JF, Sylvan JB, Brazelton WJ, Tully BJ, Edwards KJ, Moyer CL, Heidelberg JF and Nelson WC (2012) Prospects for the study of evolution in the deep biosphere. Front. Microbio. ***2****:285. doi: 10.3389/fmicb.2011.00285*

This article was submitted to Frontiers in Extreme Microbiology, a specialty of Frontiers in Microbiology.

frontiers in
MICROBIOLOGY

HYPOTHESIS AND THEORY ARTICLE
published: 03 February 2012
doi: 10.3389/fmicb.2012.00008

The deep subsurface biosphere in igneous ocean crust: frontier habitats for microbiological exploration

Katrina J. Edwards[1]*, Andrew T. Fisher[2] and C. Geoffrey Wheat[3]

[1] *Department of Biological Sciences, University of Southern California, Los Angeles, CA, USA*
[2] *Department of Earth and Planetary Sciences, University of California Santa Cruz, Santa Cruz, CA, USA*
[3] *Global Undersea Research Unit, University of Alaska Fairbanks, Fairbanks, CA, USA*

Edited by:
Andreas Teske, University of North Carolina at Chapel Hill, USA

Reviewed by:
John Stolz, Duquesne University, USA
Jens Kallmeyer, University of Potsdam, Germany

****Correspondence:***
Katrina J. Edwards, Department of Biological Sciences, Division of Marine Environmental Biology, 3616 Trousdale Blvd 91030, AHF 203, Los Angeles, CA, USA.
e-mail: kje@usc.edu

We discuss ridge flank environments in the ocean crust as habitats for subseafloor microbial life. Oceanic ridge flanks, areas far from the magmatic and tectonic influence of seafloor spreading, comprise one of the largest and least explored microbial habitats on the planet. We describe the nature of selected ridge flank crustal environments, and present a framework for delineating a continuum of conditions and processes that are likely to be important for defining subseafloor microbial "provinces." The basis for this framework is three governing conditions that help to determine the nature of subseafloor biomes: crustal age, extent of fluid flow, and thermal state. We present a brief overview of subseafloor conditions, within the context of these three characteristics, for five field sites where microbial studies have been done, are underway, or have been proposed. Technical challenges remain and likely will limit progress in studies of microbial ridge flank ecosystems, which is why it is vital to select and design future studies so as to leverage as much general understanding as possible from work focused at a small number of sites. A characterization framework such that as presented in this paper, perhaps including alternative or additional physical or chemical characteristics, is essential for achieving the greatest benefit from multidisciplinary microbial investigations of oceanic ridge flanks.

Keywords: microbiology, deep subsurface, ocean crust, basalt, ecology, provinces, marine

INTRODUCTION

Of all the potentially habitable deep subsurface environments on Earth, the igneous ocean crust is one most intriguing, being spatially extensive, voluminous, and (in many places) hospitable for development and maintenance of life. Yet, igneous crust remains among the least studied and most poorly understood of Earth's major biological habitats (Shrenk et al., 2009). Most studies on subseafloor crustal microbiology have focused on mid-ocean ridge (MOR) seafloor spreading areas. In contrast, much of the remaining 300,000 km^3 ($\sim 2.3 \times 10^{18}$ m^3 of pore fluid volume; Orcutt et al., 2011b) of potentially habitable igneous ocean crust is virtually unexplored for microbiology. This deep subseafloor biosphere, developed and maintained as part of ridge flank hydrothermal (RFH) systems, represents a relatively unexplored frontier for scientific discovery.

Researchers are pursuing fundamental questions concerning ridge flank crustal microbiology, including: what is the activity of life within ridge flanks? How are evolutionary forces expressed in these settings? What are the physical and chemical limits for survival and reproduction in the subseafloor? What is the biogeography of life in the subsurface and what are the most important dispersal mechanisms? What are the influences of subseafloor microbiology on global biogeochemical processes?

Ocean crust has existed through much of Earth's history, long before there were continents, and has been exposed to a range of chemical and thermal conditions that overlap with those found today. Therefore, the ocean crust is one of the oldest biomes on the planet; understanding how life developed to occupy and survive in this biome will help to answer fundamental questions about evolution and persistence of microbial communities on Earth. The ocean crust is large, and the flow of water, heat, and solutes between the crust and ocean rivals those from riverine sources (Mackenzie, 1992; Stein and Stein, 1994; Elderfield and Schultz, 1996; Wheat et al., 2003).

Elucidating the nature and function of ocean crustal microbial ecosystems is critical to understanding the global-scale storage and transfer of carbon, nutrients, and life-supporting metals over geological time. This understanding has implications for the early Earth, modern Earth, and perhaps other planetary bodies where there are mixing and reactions between rock, water, carbon, and heat (e.g., Cody et al., 2000; Chyba and Phillips, 2002).

Most geobiological research is conducted on continents, where environments and samples are readily accessible in the surface world. In the oceans, most studies occur in the water column, shallow sediments along continental margins, and near the surface of seafloor spreading centers. These are some of the easiest marine sites to locate and sample, although in general marine sites are more challenging to access than are sites on land. There are comparatively few studies of mineral–microbe interactions in RFH areas, even though hydrothermal systems in these areas represent an enormous fraction of the subseafloor microbial realm where mineral–microbe interactions are likely to play a critical role in biogeochemical processes and ecosystem function. Our understanding of the Earth as a geobiological system suffers if one

of the most voluminous parts of this biome remains so under sampled.

There is an opportunity to accelerate the pace of microbial exploration, discovery, and experimentation in the ocean crust, in association with scientific ocean drilling. The initial science plan for the Integrated Ocean Drilling Program (IODP; 2003–2013; IODP, 2003), includes a major emphasis on the microbial biosphere and related studies of crustal formation, marine hydrogeology, biogeochemistry, and rock alteration. Ocean drilling has been profoundly important in developing new technology, linking multidisciplinary research projects, and providing access to samples and data that cannot be recovered in any other way. The science plan for the successor to IODP, the International Ocean Discovery Program (2013–2023; IODP, 2011), also includes a prominent focus on subseafloor microbiology. Yet fielding a major drilling effort involves considerable planning, engineering development, and funding, a lengthy process often requiring 5 years or more. Without rapid action, few new expeditions focusing on subseafloor microbiology will be completed during the next phase of scientific ocean drilling.

Advances and research in the subsurface biome are not limited by scientific drilling operations; much can also be learned from sampling materials with submersibles and remotely operated vehicles (ROVs) at sites where crustal fluids seep from the seafloor. Nevertheless, it is highly unlikely that researchers will develop enough ridge flank drilling and submersible studies to provide a statistically robust global data set from RFH systems; the extent of ridge flank biomes is simply too vast, and the complexity and cost of fielding dozens of field programs is too great. Instead, strategies are needed to plan for ridge flank studies of subseafloor microbiology and related disciplines by identifying critical parameters and processes that occur across a wide range of natural conditions. Many of the key parameters are understood based on theoretical considerations, laboratory studies, and (limited) *in situ* work completed to date. The delineation of microbiological "provinces" in the igneous ocean crust, based on consideration of "geologically and geographically coherent regions of the subseafloor that may serve as potential microbial habitats" (Schrenk et al., 2009), provides an important framework for identifying targets and planning for efficient and successful sampling.

In the present study, we apply this process- and province-based approach to identifying conditions that define the scientifically compelling potential habitats in oceanic ridge flanks. Based on delineation of key parameters, one can select a modest number of field areas where rapid progress can be achieved. Sites and systems selected on the basis of their locations within a parameter space of ridge flank processes can subsequently be used to develop (and eventually test) fully coupled models of deep subsurface microbial life. Initial field studies can also help to determine where gaps in understanding may persist, and help with identification of essential needs for field surveys, tools, and experiments.

In the next section of this paper, we explore some of the key physical and chemical parameters that should have a significant influence on the development and maintenance of subseafloor microbiological systems, focusing on those parameters that are most readily measured on the basis of regional surveys. We use a subset of these parameters to delineate a range of physical and chemical conditions, and describe selected field sites that occupy relatively narrow ranges of these parameters. We also identify where there are remaining gaps in this representation of ridge flank microbial provinces. The present study focuses on volcanic-hosted ("hard rock") biomes within deep-sea ridge flanks, but similar approaches are readily developed for other settings (deep-sea sedimentary environments, very young seafloor near spreading centers, continental shelves, etc.) and sets of parameters (productivity in the overlying water, water depth, proximity to continents, etc.).

THERMAL, GEOCHEMICAL, HYDROLOGICAL, AND GEOLOGICAL REGIMES

Most new oceanic crust forms where tectonic plates separate at divergent boundaries, resulting in partial melting of ultramafic mantle rocks to form basaltic magma. This process occurs under a wide range of spreading rates and tectonic regimes, yet results (to a first order) in a remarkably consistent ocean crustal stratigraphy, as originally defined from study of ophiolites (Raitt, 1963; Moores and Vine, 1971; Shor et al., 1971; Cann, 1974). Extrusive volcanic rocks having a basaltic composition generally form the upper 500–1000 m of ocean crust, and are underlain by 5–6 km of intrusive mafic rocks (basalt, gabbro). There are common variations in this typical crustal structure, particularly where plates spread at slow rates ($\leq$3 cm/year). At very low spreading rates, plate divergence is diffuse, and the seafloor lacks a readily identifiable spreading center. In these and in other areas, the ocean crust is frequently faulted and delaminated almost as quickly as it is formed, exposing deeper crustal levels at the seafloor. This has important biogeochemical implications for associated microbial ecosystems. Additional deviations in crustal structure occur at fracture zones and around seamounts, where additional tectonic and volcanic processes are active.

The nature of processes and conditions at depth below seafloor spreading centers remain poorly known and is a subject of debate within the scientific community. For example, geophysical and geochemical studies from some sites have been interpreted to indicate that relatively cool conditions may extend completely through the crust close to seafloor spreading centers, with rapid circulation of cool seawater into the upper mantle, extracting a large fraction of crustal heat (e.g., Dunn et al., 2000; VanTongeren et al., 2008; Spinelli and Harris, 2011). In contrast, comprehensive water column plume studies along spreading centers suggest that the advective heat output from hydrothermal circulation can account for the cooling of only the upper 1–2 km of the crust (Baker, 2007), and crustal alteration studies on some settings reveal a lack of evidence for the penetration of cool fluids into gabbros of the lower crust (e.g., Dunn et al., 2000; Humphris and Cann, 2000; Coogan et al., 2007). Secondary fluid circulation near spreading centers, penetrating only a short distance below the seafloor, could result in sustained cool conditions in the upper crust, even where and when heat extraction by deeply circulating fluids is incomplete. In aggregate, there is compelling evidence from many sources that at least the upper 1–2 km of ocean crust is cooled efficiently by circulating fluids at and near many seafloor spreading centers, and cool temperatures may predominate in the crust in these regions,

except in the immediately vicinity of recently emplaced magma or at high-temperature hydrothermal upflow zones.

The thermal state of the upper crust as it moves away from seafloor spreading centers is highly variable, depending on factors such as the nature and rate of sedimentation, extent and frequency of faulting, and the occurrence of off axis volcanism. The latter is often not widely appreciated, but recent studies suggest that the seafloor is dotted with 10^6–10^7 seamounts having an elevation of 100 m or more above the surrounding basaltic crust (Hillier and Watts, 2007; Wessel et al., 2010). These features facilitate hydrogeologic exchange between the crust and ocean for millions of years (Fisher and Wheat, 2010).

Standard lithospheric (conductive) cooling models generally suggest that crustal heat output decreases as $1/\sqrt{\text{age}}$ (e.g., Parsons and Sclater, 1977), but in practice conditions differ considerably between sites having similar ages. On a global basis, the throughput of RFH fluid is similar to the discharge of the global river system into the ocean; thus a volume equivalent to that of the global ocean is passed through the crust about once every 10^5–10^6 years (e.g., Mottl and Wheat, 1994; Johnson and Pruis, 2003; Wheat et al., 2003). This is a very short residence time for the ocean in the crust when considered over the duration of Earth history. In addition, based on consideration of the volume of pore space available in the volcanic ocean crust, and the global rate of fluid throughput, the global residence time of fluids in the crust is relatively short, only 10^3–10^4 years, about the same as the residence time of deep water in the northern Pacific Ocean.

High-temperature hydrothermal sites at seafloor spreading centers and other areas of active volcanism provide some of the most dramatic visual, chemical, thermal, and biologic expressions of fluid flow from the volcanic ocean crust. High-temperature vent fluids differ in composition from seawater in numerous important ways. These fluids tend to be depleted in magnesium and sulfate, rich in dissolved metals and calcium, and contain reduced forms of nitrogen, carbon, sulfur, and hydrogen. During circulation, high-temperature fluids may reach temperatures in excess of 350–400°C, sterilizing the entrained seawater. However, when this fluid mixes with cool oxygenated bottom seawater, microbial growth can be rampant, for example producing "snow blower" events, where large amounts of flocculent biofilm materials are flushed from the seafloor (Haymond et al., 1993).

Another source for reduced chemical species in crustal fluids is sediment that overlies the volcanic crust. Microbial processes in sediment commonly lead to reducing pore fluids, which exchange diffusively with the underlying volcanic crustal reservoir (Elderfield et al., 1999; Wheat et al., 2000). Diffusive fluxes from the sediment can be the dominant control for the composition of some dissolved species in crustal fluids, resulting in a distinctly altered seawater composition.

However, in many cases the composition of fluids in many RFH systems may be only subtly different from that of bottom seawater. Within low temperature RFH systems, which are kept cool by the vigor of fluid exchange between the crust and ocean, crustal fluids will remain cool and oxic if the advective flux through the crust exceeds the aggregate of downward diffusive fluxes from overlying sediment and reaction with basement volcanic rocks. Relatively low temperatures in such systems minimize the amount and type of reduced nitrogen, carbon, sulfur, and hydrogen available in fluids for microbes within the basaltic crust, and tend to slow inorganic exchange. On average, the residence time of fluids within the crust on ridge flanks is orders of magnitude longer than that of MOR crustal fluids (Kadko and Moore, 1988; Fisher, 2003). In some cases, this can permit significant changes in the composition of ridge flank crustal fluids, even where reactions are kinetically slow.

Cool RFH systems have a profound influence on heat loss from the crust. And despite having a composition that is subtly different from bottom seawater, such systems can have a significant impact on the composition of the crust and seawater because the flows are so large. The magnitude of RFH flows is determined mainly by the efficiency of fluid circulation in removing crustal heat, relative to conduction. Lithospheric heat loss drives fluid flow on ridge flanks, leading to differences between pressures at the base of recharging and discharging columns of fluid within the crust. The flowing system effectively functions as a "hydrothermal siphon" (Fisher et al., 2003a; Hutnak et al., 2006; Fisher and Wheat, 2010; **Figure 1**). Circulating fluids are warmed (relative to bottom water) and expand, such that where discharge occurs, the column

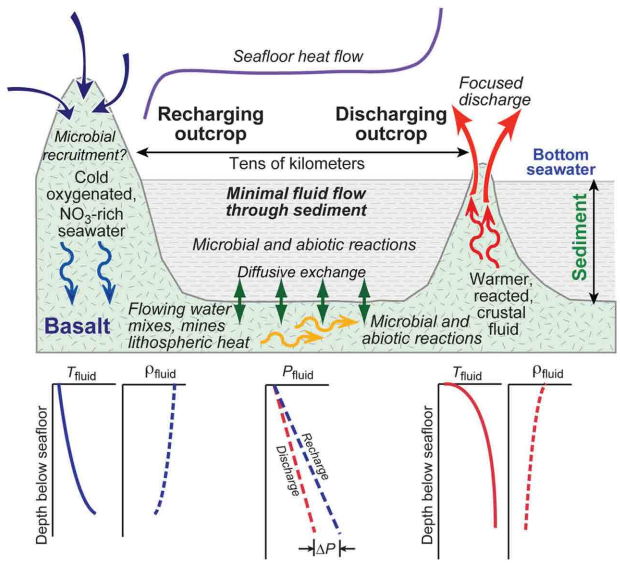

FIGURE 1 | Schematic illustrations of the causes and impacts of ridge flank hydrothermal circulation. In this example, seamounts or other basement outcrops play a key role in guiding fluid flow into and out of the crust, between areas that are blanketed with marine sediment. Within recharging and discharging volcanic rock outcrops, fluid temperatures (T_{fluid}) and densities (r_{fluid}) remain relatively constant so long as vertical transport (descent and ascent) is rapid. The difference between fluid pressures (P_{fluid}) at the base of recharging and discharging columns of fluid (C). ΔP, is the primary driving force for ridge flank hydrothermal circulation. This pressure difference is available to move fluid laterally within the reactive basement aquifer, mining heat, reacting with the crust, and providing nutrients and/or energy to microbial communities living in pore spaces. Seafloor heat flow is generally higher adjacent to discharging outcrops, and lower adjacent to recharging outcrops. Between outcrops, heat flow may be equal to or less than conductive plate cooling values, depending on the regional efficiency of lithospheric heat extraction.

of fluid rising through the crust has a density that is comparatively low. In contrast, the density of cold bottom seawater entering the crust is comparatively high. So long as there is a good hydrologic connection between recharging and discharging fluids, with the intervening crust having high permeability (ease of flow), fluids will continue to flow because of the density (and associated pressure) contrast. In addition, such systems will flow at a rate that is optimized to remove as much heat from the crust as possible, which often means circulating a large volume of slightly warmed (and slightly altered) fluid rather than a smaller volume of hotter (and more altered) fluid.

MODEL MICROBIAL PROVINCES

On the basis of the preceding discussion concerning thermal, chemical, hydrological, and geological regimes, we can delineate a modest number of end-member microbial provinces in the volcanic ocean crust (**Figure 2**) Description of key physical, thermal, and chemical conditions for these biomes is helpful in defining where attention could be placed in the coming decades so as to focus time and resources on locations that can have broad applicability and can influence our understanding of subseafloor microbial processes in general. This approach is different from trying to define a global "average" set of conditions. In a highly heterogeneous environment like the volcanic ocean crust, "average" conditions may actually be rare. Or, like many natural stream systems, it may be end-member conditions (high flow, low flow) that dominate system morphology and the nature of ecosystems.

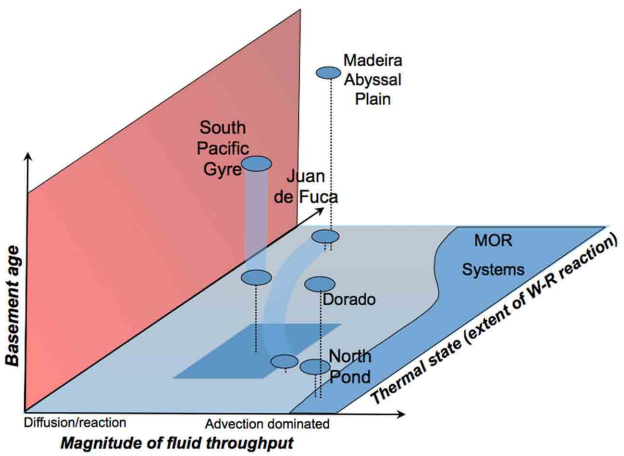

FIGURE 2 | Cartoon illustrating how ridge flank hydrothermal field areas discussed in this paper might vary in terms of three key physical and chemical parameters: age of basement rocks, magnitude of fluid flow through the crust, and then thermal state of the basement aquifer (which indicates the likely extent of water–rock interaction). Information used to construct this figure is listed in **Table 1**). The height of individual dots indicates basement age, whereas position on the horizontal space indicates fluid and thermal states. The South Pacific Gyre sites span a range of parameters (height of dots indicates range of basement ages, in addition to fluid and thermal state). There are two main parts of the eastern flank of the Juan de Fuca Ridge, indicated by the swath between two dots. Properties of many areas associated with mid-ocean ridges (MORs) are indicative of young basement age, a wide range of temperatures, and additional variability in fluid throughput, as shown.

We propose that three primary factors be considered in selection of characteristic biomes: volcanic crustal age, typical fluid temperature, and the throughput of water (extent of water–rock interaction; **Figure 2**). Numerous other factors might be selected that are equally illustrative (for example, concentrations of nutrients or dissolved ions, inorganic and organic carbon content in fluids, rock type, spreading rate of crustal formation, or fluid residence time). However, appropriate values for many of these parameters are poorly known on a regional basis, challenging to determine in practice, or may serve as proxies for more direct biological controls in specific field areas.

Plotted in this three-dimensional space are selected locations where subseafloor microbiological work has been completed to date, and where future studies are planned or have been proposed. Characteristics of these sites are summarized in **Table 1**. We are particularly interested in using this framework to define pairs or sets of sites that share some characteristics, but differ in one or more key aspects, as this will allow the strongest delineation of what factors control the development and maintenance of microbial communities. Once these factors are identified, results from work at a small number of carefully selected field sites can be extrapolated more broadly, both spatially and temporally. The latter is especially important when one considers that subseafloor biomes evolve with time (as the seafloor spreads and ages, lithospheric heat flow declines, and sediment accumulates on top of volcanic rocks), such that researchers working in some settings will be challenged to detangle multiple generations of legacy microbial processes.

EASTERN FLANK OF THE JUAN DE FUCA RIDGE

There is only one site on Earth where a complete hydrologic flow path through a seafloor hydrothermal system has been delineated with confidence: within 3.5–3.6 million years old crust on the eastern flank of the Juan de Fuca Ridge (JFR; Wheat et al., 2000; Fisher et al., 2003a; Hutnak et al., 2006). In this area, fluids enter Grizzly Bare outcrop, an inactive seamount, traverse more than 50 km to the northeast, then exit the seafloor through Baby Bare outcrop, with fluid travel time that is likely to be on the order of a few tens of years to a few hundred years. Fluids moving through this

Table 1 | Summary of selected characteristics for sites discussed in this paper.

Site	Basement age (million years)	Fluid throughput	Thermal state (W–R reaction)
Juan de Fuca flank	0.7–3.6	High to moderate	Cool (low) to warm (high)
North Pond	8	High	Cool (low)
Dorado outcrop	23	High	Cool (low)
South Pacific Gyre	15–100	High to low	Cool (low)
Madeira Abyssal plain	~100	Low?	Warm (high)

Site characteristics are based on studies cited in the next of the paper. Two hydrothermal regimes are discussed for the eastern flank of the Juan de Fuca Ridge, a younger (cooler) area closer to the active spreading center, and an older (warmer) region farther from the spreading center.

part of the RFH system undergo extensive alteration, and fluid temperatures in the crust reach ∼65°C before seeping from the seafloor. The only natural seeps that have been sampled from a RFH system were collected on Baby Bare outcrop (Mottl et al., 1998; Wheat and Mottl, 2000). Subsequently a lance was deployed to penetrate thin sediment and create an artificial vent, allowing collection of fluids for microbial characterization (Huber et al., 2006).

To the west of this area, on younger crust, sediment cover is discontinuous, there is greater basement exposure, and RFH systems are generally cooler (Davis et al., 1992; Wheat and Mottl, 1994; Elderfield et al., 1999). This cooler RFH system may be more characteristic of RFH systems on average, with lower temperatures and greater fluid throughput, but because there are more places where fluids could enter and exit the crust in this area, flow paths are poorly constrained.

A transect of eight sites was drilled across 0.9–3.6 Ma seafloor in 1996 (Ocean Drilling Program Leg 168), allowing sample collection and installation of first generation subseafloor borehole observatories (CORKs) within uppermost ocean crust (Davis et al., 1997). No microbial work was planned when these systems were designed or installed, but samples for microbial characterization were collected later from one of the CORKs installed near Baby Bare outcrop (in Hole 1026B), where fluids are warm and reducing (Cowen et al., 2003). IODP Expedition 301 returned to this area in 2004 to drill and sample deeper in basement, replace the Hole 1026B borehole observatory, and establish two new ones, each instrumented with novel downhole microbial colonization experiments (Orcutt et al., 2011a; Smith et al., 2011). A later generation of CORKs was installed during IODP Expedition 327 in 2010, including additional microbial samplers, enrichment experiments, and colonization substrate (Fisher et al., 2011).

CORKs installed in this area during ODP Leg 168 and IODP Expedition 301 have produced valuable fluid and microbial samples indicating the nature of linked geochemical and microbiological conditions in basement (e.g., Cowen et al., 2003; Wheat et al., 2004, 2010; Orcutt et al., 2011a; Smith et al., 2011). Fluids and microbial samples collected at depth in two holes have compositions resulting from reducing conditions in basement. CORKs deployed during IODP Expedition 327 should provide even better samples of endemic microbial communities from the crust, because the newer observatories were designed and constructed with materials so as to be more compatible with microbiological investigations. With respect to the continuum of physical and chemical conditions highlighted earlier, the JFR flank sites span a range of thermal states (cool to warm) and magnitude of fluid flow (diffusion to advection dominated), but all are within relatively young seafloor (**Figure 2**; **Table 1**).

NORTH POND

North Pond is located in the mid-Atlantic at 22°N on the western flank of the Mid-Atlantic Ridge. North Pond is an isolated northeast-trending sediment pond bounded by 1-km high basement ridges and a range of sediment thicknesses up to 300 m thick at the southernmost part of the basin. This was a drilling target during DSDP Leg 45 (Site 395) to examine crustal properties to characterize the geology of young oceanic crust. Here the crust is relatively young (8 million years) with vigorous crustal fluid circulation that allows warming of circulating fluids to only 10–15°C before they are discharged from the crust. There have been numerous return visits to this area since the initial deep-sea drilling, with the most recent work occurring on IODP Exp 336 to install borehole observatories and experiments and core sediment and volcanic rocks, with a focus on subseafloor microbial systems.

Samples and data collected during a heat flow and sediment coring expedition in 2009 suggest a crustal fluid having considerable dissolved oxygen and seawater-like concentrations for most major and trace ions and nutrients, indicating a short residence time for fluids within basaltic basement. Because temperatures are low, sluggish abiotic rates of reaction favor alteration by kinetically enhanced biotic reactions. These reactions could support microbial communities that alter the crust directly. North Pond was selected for new drilling and CORK installation during IODP Exp 336 in part because of the contrasts it provides with the eastern flank of the JFR (**Figure 2**; **Table 1**).

Hydrologically, North Pond is characteristic of areas where volcanic crustal rocks are exposed across large areas, and continuous cover by sediment is the exception rather than the rule (Langseth et al., 1984, 1992). Drilling, coring, logging, and limited borehole experiments suggest that the upper crust in this area is highly porous and permeable (Hickman et al., 1984; Becker, 1990; Gable et al., 1992; Bartetzko et al., 2001). There is extensive, vigorous fluid circulation in the crust of this area, likely more circulation per unit of basement rock than observed where fluids are hotter and more altered on the eastern flank of the JDF, but delineating fluid flow pathways from recharge to discharge around North Pond is challenging. The North Pond microbial province is indicative of low temperature and advection dominated conditions, within relatively young ocean crust (**Table 1**).

DORADO OUTCROP

Dorado outcrop is located on the eastern flank of the East Pacific Rise (EPR) spreading center on the Cocos Plate, off-shore of the Nicoya Peninsula of Costa Rica. Here the crust is about 23 million years old (Barckhausen et al., 2001). Surveys using swath-mapping, multi-channel seismic reflection data, and multi-penetration heat flow measurements identified basement outcrops and delineated thermal anomalies with respect to global lithospheric cooling models and regional heat loss (Fisher et al., 2003b; Hutnak et al., 2007). These surveys revealed that a large part of the Cocos Plate is anomalously cool, having upper basement temperatures of 5–30°C below thick sediments, consistent with rapid and extensive shallow fluid circulation through the crust. Comparison of regional seafloor heat flow data to lithospheric model predictions indicates that a seafloor area of 14,500 km^2 loses ∼1 GW of heat, requiring RFH fluid throughput of 4–80 m^3/s (Hutnak et al., 2008). This three to four orders of magnitude more fluid than flows from Baby Bare outcrop, and is at the extreme end of what occurs globally on ridge flanks. Most of this fluid enters and exits the crust through a small number of basement outcrops. Dorado outcrop was identified as a location of rapid hydrothermal discharge, and Tengosed Seamount, 20 km away, is the closest likely conduit for hydrothermal recharge (Fisher et al., 2003b; Hutnak et al., 2008; Wheat and Fisher, 2008).

Regional basement chemical and thermal conditions around Dorado outcrop are similar to those observed in North Pond, and probably are typical of a large fraction of the global RFH systems. In contrast to North Pond, potential fluid entry and exit points around Dorado outcrop are constrained by regionally thick sediments, which makes delineation of flow paths more feasible. Fluid circulation rates and residence times in the volcanic crust around Dorado outcrop are probably similar to those around North Pond, and at the western end of the JFR flank transect, but the age of basement is three to five times older at the Dorado outcrop (**Table 1**).

Studies around Dorado outcrop could allow for assessment of how large fluxes of seawater circulation through very permeable pathways alter crust over time. No microbial studies of basement samples have been completed to date near Dorado outcrop, presenting opportunity for low temperature RFH exploration and discovery. A sampling survey is currently planned for 2013, with the primary goal of recovering pristine hydrothermal fluid discharging from Dorado outcrop.

SOUTH PACIFIC GYRE

The South Pacific Gyre (SPG) is characterized by a region with low surface chlorophyll-a concentrations, a measure of plankton productivity. Low surface productivity results in low sediment organic matter compositions, low sedimentation, and low microbial activity. The region spans much of the Pacific Ocean from 20°S to 30°S and was sampled on IODP Exp 329 at seven sites having crustal ages of 15–100 million years in locations having 18–131 m of sediment above volcanic crustal rocks. Heat flow from SPG sites younger than 65 million years is generally less than values predicted by conductive lithospheric cooling models, consistent with global datasets, suggesting that a fraction of heat is extracted advectively from the crust (Expedition 329 Scientists, 2011). Heat flow data from older SPG sites are consistent with more sluggish fluid flow and little or no heat extraction by fluids. Throughout the region, temperatures in upper basaltic crust are close to 10°C.

The SPG region includes features that may be characteristic of several microbial provinces (**Figure 2**). On younger crust, where fluid flow is most vigorous, RFH systems will be similar to those of North Pond and Dorado outcrop; however, the low microbial activity at SPG sites should limit the sedimentary influence on basalt hosted microbial communities. On older SPC crust, where fluid flow within the crust is limited, thin sediment keeps the temperature in basement relatively low, providing an interesting contrast to both old sites and younger sites where basement temperatures are greater. Sedimentary influences on basaltic basement conditions (e.g., C, Fe, Mn, sulfate) should be minimal in the SPG region. Given the organic matter-starved region of the SPG, metabolic activity may be enhanced by water radiolysis and hydrogen may be the most significant electron donor for microbial respiration.

MADEIRA ABYSSAL PLAIN

The Madeira Abyssal plain (MAP) comprises a region of $\sim 10^5$ km^2 in the Canary Basin, west of the Canary Islands, north Atlantic Ocean (Searle, 1987). The MAP is the deepest part of the Canary Basin, with typical water depth of 5400 m, although the tops of large seamounts to the east (notably parts of the Meteor Seamount chain) extend to within 300 m of the sea surface. The crustal age in the MAP area is about 106 Ma, consistent with slow seafloor spreading at 1.5 cm/year (Noel, 1985; Searle, 1987). Sediment cover is regionally thick and extensive, both because of the age of the plate and because turbidites have poured into the Canary Basin from continental areas the east, but there are basement outcrops associated with abyssal hill topography, presumably from off axis volcanism.

There are two strong indicators of sustained hydrothermal circulation through old MAP seafloor: thermal and chemical. Variations in heat flow correlate with basement relief and are consistent with fluid circulation at rates of 0.3–3 m/year, requiring relatively high upper basement permeabilities (Fisher and Von Herzen, 2005). Geochemical data collected during sedimentological studies associated with ODP Leg 157 (Schmincke et al., 1995) show pore water gradients that are reversed at depth, as has been interpreted elsewhere to indicate the passage of relatively young and unreacted fluids through the upper crust (e.g., Baker et al., 1991; Wheat and Mottl, 1994; Elderfield et al., 1999).

No microbiological work has been completed in this area to date, but it is an intriguing site for such investigations for several reasons. This is one of the oldest seafloor locations where hydrothermal circulation is thought to occur (Von Herzen, 2004). Basement outcrops are relatively widely spaced, limiting the number of fluid entry and exit points from the crust. Although sediment in this area is comparatively thick, upper basement temperatures are projected to be only 10–30°C because lithospheric heat flow is so low in old crust. This range of temperatures overlaps with those inferred for the western end of the JFR flank area, North Pond, and Dorado outcrop, but MAP fluids pass through crust that is much older. The upper crustal volcanic rocks in the MAP area may have seen >100 million years of continued hydrothermal circulation.

The thick accumulations of volcanic and continentally derived sediment in this area are likely to be relatively rich in organic carbon. Diffusive exchange between sediment and upper basement fluids could provide an important source of carbon, or could be insignificant at present because circulation has continued for 100 million years, depleting basal sediment of microbially important substrates. Sample collection from the MAP area offers the intriguing possibility of recovering microbial material that has been physically (and perhaps genetically) isolated for tens of millions of years, but under physical and chemical conditions consistent with younger sites. Rock samples from the MAP area could similarly provide important information on the nature of long-term, integrated rock alteration patterns in association with both inorganic and microbial processes, linking physical, chemical, and microbial controls.

ADDITIONAL CONTROLS ON OCEAN CRUSTAL MICROBIOLOGY

The five field areas identified above span a range of crustal ages and magnitudes of fluid flow that should comprise and intriguing suite of field sites for comparative microbial studies in RFH systems (**Table 1**). However, even among these sites, a comparatively narrow array of basement temperatures is represented (~5–65°C; **Figure 2**). There are clear gaps in the representation

of end-member characteristics that we highlight with these sites, particularly those involving rapid fluid flow and high-temperature conditions, or sluggish to no fluid flow and cooler temperatures. The former is likely to be found at MORs (as marked in **Figure 2**) and in other settings where volcanism occurs (e.g., around volcanically active seamounts). Conditions of sluggish to no fluid flow and cooler temperatures in basement are likely to be rare in nature, occurring perhaps where long-term fluid circulation has clogged fluid pathways through the crust, but the sedimentation rate has remained low, limiting the extent of crustal burial and thermal insulation.

Many additional or alternative physical and chemical parameters could be used to define other characteristics that control RFH microbial environments. For example, some areas have an abundant source of organic carbon in overlying sediment (generally close to continental sources or in areas of sustained upwelling and associated primary productivity, for, e.g., Guaymas basin), whereas others are more carbon limited (e.g., North Pond). A similar approach could be taken with respect to limiting nutrients and microbial energy sources, for example, contrasting upwelling regimes with open ocean sites. There are also likely to be differences associated with sediment type (e.g., carbonate vs. clay content), thickness, and the related spacing of basement outcrops that enhance fluid entry and subsequent discharge from the crust. Other factors that could be considered include spreading rate and mechanisms of crustal construction. For example, there are significant differences in the relative importance of faulting between slow and fast spreading centers, the former being associated with extensive faulting and ridge flank dissection compared to the latter. One could similarly consider the spacing and amplitude of abyssal hill topography, or other aspects of crustal tectonic fabric. The selection of defining characteristics for end-member microbial provinces is, by necessity, somewhat arbitrary. That said, it makes sense to select parameters that can be mapped and delineated relatively easily using conventional (regional) survey techniques, so that a modest number of field sites can be selected for more intensive (expensive, difficult, time consuming) study. Whatever parameters are chosen for comparative purposes, the approach outlined in this study can be beneficial for understanding why crustal microbial systems occur as they do, and what strategies have been developed within these systems for survival across long periods of geological time.

TECHNOLOGY

The preceding discussion of RFH provinces suggests that there are a number of targets available for microbial studies. Yet locating positions of seawater input to, and fluid egress from, RFH systems remains challenging. At MORs, focused venting of hydrothermal fluids generates chemical, thermal, and microbial plumes that can be traced from the water column back to seafloor vents many kilometers away. In contrast, on ridge flanks such plumes may rise only meters to tens of meters, and will be difficult to distinguish from bottom water even under ideal survey conditions. Most RFH sites have been discovered using combined geophysical and geochemical methods (seismic data, heat flow measurements, and pore water composition from sediment gravity cores). Submersible or ROV operations are then required to identify and sample sites of focused fluid flow.

The research community needs to sample multiple sites that are representative of overlapping biomes, to quantify the physical, chemical, and hydrologic conditions that control microbial development. Given the vastness of the seafloor, and the need to nest detailed studies within coarser surveys, technical advances in survey tools are required. For example, long-range, autonomous gliders with seismic sensors (chirp sonar) are needed to survey large expanses near basaltic outcrops. Such surveys coupled with systematic heat flow surveys are required to assess the vigor of local and regional fluid circulation in the crust. Autonomous vehicles are also needed that can acquire high-quality bathymetric maps and sample the water column to identify RFH plumes. The latter will require considerable improvement to sensor capabilities to allow detection of subtle chemical and microbial plume characteristics that are the most promising for remote plume detection. Although some, but certainly not all, of these sampling capabilities are present in existing AUVs; however, power consumption limits dive time to ∼12 h. Thus, to survey even a small portion of the ridge flanks would require a fleet of AUVs each conducting a portion of the overall mission (**Figure 3**).

Once sites of fluid seepage from basaltic crust are located, sampling for and *in situ* measurements of microbiological characterization can commence. There are additional technological

FIGURE 3 | Duane Thompson and Doug Conlin prepare a benthic imaging AUV. The two other AUVs are an upper water column vehicle and a mapping vehicle. Although the nose and tail cones are identical, the payload of each AUV is specifically designed for a particular mission. No AUV in existence has the combined components to tackle the initial mission of searching for RFH venting and detecting chemical and microbial characteristics of the venting fluid. Such a vehicle would require significant power for its sonars and must be able to rechargeable its batteries to explore the vastness of the ridge flanks where hundreds of thousands of small outcrops exist. Small outcrops tend to be sites where fluids seep from the crust and are not detected by satellite gravimetry measurements. Long-range vehicles (e.g., gliders) exist but are underpowered for such a mission. Vehicles and sonars with appropriate capabilities exist but are limited to an 12-h dive and lack the suite of sensors required for detecting chemical and microbial signatures of RFH venting. Copyright MBARI 2010. Photo by Todd Walsh.

challenges pertaining to sample contamination and preservation. *In situ* systems capable of pumping fluids into multiple sterile bags and filters have been established (Butterfield et al., 2004; Cowen et al., 2012), but remain developmental and require significant technical expertise to operate. Simpler syringe-style samplers have been deployed for single 50–100 ml discrete samples that can be used in concert with a filter or *in situ* preservation (Fisher et al., 2012). Presently, the only deep-sea *in situ* microbial measurements are those from the environmental processing system (ESP; Scholin et al., 2009) and deep ultra-violet fluorescent technologies such as the Deep Exploration Biosphere Investigative tool (DEBI-t; based on technology adapted from Bhartia et al., 2010), both presently impractical for wide-spread use.

Because of the limited number of known sites of focused fluid seepage from RFH systems, studies of microbial community and processes have looked toward analyzing materials from deep-ocean drilling. At present, molecular techniques are challenging to apply directly to recovered igneous materials, because of poor and biased recovery (10–30% overall in upper volcanic crust, generally favoring more massive rocks), contamination during drilling, and low cell counts and analytical interference with the crustal matrix. A few studies have been successful to date working with recovered volcanic materials (Mason et al., 2010; Santelli et al., 2010). Analytical advances in this area will greatly increase productivity on future deep-ocean drilling operations.

Because of these sampling recovery and analytical issues, an alternative approach to studying microbial processes in the ocean crust are through the development and use of borehole observatories (CORKs; Davis et al., 1997). On the basis of initial microbial studies harbored *in situ* within a borehole (Orcutt et al., 2011a; Smith et al., 2011), CORK observatories have been modified and deployed to enhance the return of microbial data while minimizing artifacts. For example, on IODP Exp 336 three new CORKs were deployed, some with multiple sampling horizons and each using materials that minimize additional carbon sources and potential REDOX reactions (coated steel, fiberglass, and high density plastic; Edwards et al., 2010). To examine reaction pathways *in situ*, transects of drill holes and CORK observatories are required in order to intersect hydrological units of interest within the volcanic crust.

Improvements and versatility are incorporated in each new CORK system. The first generation of CORK observatories were often successful on initial deployment, but were not designed to facilitate collection of high-quality borehole fluid and microbial samples nor house *in situ* experiments. Some of these CORK systems remain operational more than two decades after deployment, although others have failed over time. Later generations of CORKs, including those that isolate multiple depth intervals, contain redundant seal systems, and were designed for installation deep within unstable boreholes, are generally more difficult to deploy. Approximately half to two thirds of modern CORKs are successfully installed as intended. Technical challenges can be addressed, but this requires extensive planning, long lead times, attention, and considerable financial resources. Ultimately the number of CORK observatories that will be deployed in the next 10–20 years for microbial studies is going to be limited, perhaps 10–20 in total. This makes it essential to select sites in the context of the microbial province concept, so that results from each system can be used to leverage other studies.

Additional technical advances are needed for *in situ* samplers, sensors, and experiments. Presently systems for deployment within boreholes well below the seafloor have been limited to designs that use osmotic-powered pumps (Wheat et al., 2011). While such designs offer a variety of sampling and experimental possibilities, the borehole environment does not prelude electrically powered sensors. Several such sensors have been deployed for geophysical study (e.g., Kopf et al., 2011) and only a downhole dissolved oxygen sensor exists for microbial characterization. In contrast, seafloor samplers and sensors can tap into hydrologic horizons of interest through the use of an umbilical – stainless steel or hardened Teflon coated tubing with a valve at the wellhead and open to the formation at depth. The present technology includes a pump system that pulls fluid up the umbilical to the seafloor and pushes borehole fluids past a variety of sensors and into samplers (Cowen et al., 2012). Here, bringing the laboratory to the seafloor and conducting manipulative (e.g., rate and enrichment) experiments are critical next steps to further our understanding of RFH microbial environments. For example, near term technological advances for wellhead sampling and sensing operations include mass spectrometry and fast flow osmotic pumps for continuous sampling of borehole fluids via the umbilical. Other technological advances could include a flow cytometer or other visual-based (light or laser) systems for microbial detection or characterization (e.g., DEBI-t). As in the past, present studies in borehole observatories will evolve future instrumentation needs.

Unfortunately, opportunities to deploy CORK observatories are likely to remain limited because of ongoing fiscal, scheduling, and technical challenges. Hardware and downhole science materials for a single borehole observatory can cost as much as $1 million US, depending on complexity. Plans often need to be developed over a period of several years given long lead times for delivery of key components, and the need to facilitate multiple experimental and observational goals (geophysical, hydrologic, biogeochemical, microbial). Even with rigorous planning, deployment is frequently difficult. Following deployment, there remain ongoing technological, logistical, and fiscal challenges for maintaining CORKs, monitoring borehole conditions, and conducting experiments. Ship time and submersibles or ROVs are required for nearly all observatory work (the exception is a CORK that is tied to a cabled network, e.g., Neptune). Given the nature of microbiological analysis, which requires physical samples, all microbiological observatory work requires that researchers physically access the borehole.

There are ∼30 "legacy" boreholes from past deep-ocean scientific drilling expeditions that have been drilled into basement and cased through the sediment. Presumably these boreholes are open to basaltic crust and could be sampled with wire-line sensing and sampling systems that need to be developed or through a modified borehole observatory design (CORK). At the writing of this manuscript, IODP Hole U1383B is one such candidate borehole. It has a reentry cone and is cased through the sediment section with open borehole into basalt below the casing. In the spring of 2012, researchers will deploy a long-term observatory in this borehole. The ROV *Jason II* will deploy the new wellhead and downhole sampler–sensor–experiment string to monitor

the chemical composition of ocean crustal fluids and microbial communities and to conduct microbial enrichment experiments. Similar deployments are possible at other legacy boreholes, which would help to expend sampling and monitoring across a wider range of physical and chemical conditions.

CONCLUSION

We have described the overall nature of RFH systems, and discussed a means for characterizing these systems based on determination of fundamental physical and chemical characteristics. We illustrated this approach through presentation of example RFH systems that occupy specific regions on a plot of RFH parameter space (**Figure 2**; **Table 1**), helping to define a range of microbial provinces found below the ocean on a global basis. We also discussed some of the technological hurdles associated with studying these systems that must be overcome in the next few decades.

The framework we propose for understanding geological, geochemical, and hydrological links to ocean crustal microbial systems can be used to guide future site selection. We acknowledge that numerous additional factors may be important in determining the nature of crustal microbial ecosystems, including the availability of nutrients, carbon, and energy sources. While these and other factors certainly are important, they generally do not lend themselves well to evaluation based on regional surveys, and so have limited applicability in terms of identifying key locations for future studies. This may change with advances in technology and improved availability of established tools, and additional sites will be identified serendipitously during surveys planned for other purposes.

This is truly an "age of exploration" for microbiological study of RFH systems, and many more aspects of them and new sites will surely be identified in the future, hopefully guided by strategies that maximize return on knowledge that can be applied on a global basis, rather than understanding of individual sites in isolation. Big picture projects require large teams of researchers from multiple disciplines to come together to properly plan and coordinate complex programs, and this requires taking a long-term view. But worked completed and discoveries made to date show that patience, persistence, and vision can pay off over time.

ACKNOWLEDGMENTS

This research was supported by the US National Science Foundation grants OCE 0939564 (to Katrina J. Edwards with subawards to Andrew T. Fisher, C. Geoffrey Wheat), OCE-0727952 (Andrew T. Fisher), OCE-1031808 (Andrew T. Fisher), OCE-1130146 (C. Geoffrey Wheat), and 1030061 (C. Geoffrey Wheat), by US Science Support Program for IODP projects T327A7 and T327B7 (Andrew T. Fisher). This is C-DEBI contribution #1XX.

REFERENCES

Baker, E. T. (2007). Hydrothermal cooling of midocean ridge axes: do measured and modeled heat fluxes agree. *Earth Planet. Sci. Lett.* 263, 140–150.

Baker, P., Stout, P., Kastner, M., and Elderfield, H. (1991). Large-scale lateral advection of seawater through oceanic crust in the central equatorial Pacific. *Earth Planet. Sci. Lett.* 105, 522–533.

Barckhausen, U., Renaro, C., von Huene, R., Cande, S. C., and Roeser, H. A. (2001). Revised tectonic boundaries in the Cocos Plate off Costa Rica: implications for the segmentation of the convergent margin and for plate tectonic models. *J. Geophys. Res.* 106, 19,207–19,220.

Bartetzko, A., Pezard, P., Goldberg, D., Sun, Y.-F., and Becker, K. (2001). Volcanic stratigraphy of DSDP/ODP Hole 395A: an interpretation using well-logging data. *Mar. Geophys. Res.* 22, 111–127.

Becker, K. (1990). "Measurements of the permeability of the upper oceanic crust at Hole 395A, ODP Leg 109," in *Proceedings of Ocean Drilling Program, Scientific Results*, eds R. Detrick, J. Honnorez, W. B. Bryan, and T. Juteau (College Station, TX: Ocean Drilling Program), 213–222.

Bhartia, R., Salas, E. C., Hug, W. F., Reid, R. D., Lane, D. J., Edwards, K. J., and Nealson, K. H. (2010). Label-free bacterial imaging with deep UV laser induced native fluorescence. *Appl. Environ. Microbiol.* 76, 7231–7237.

Butterfield, D. A., Roe, K. K., Lilley, M. D., Huber, J., Baross, J. A., Embley, R. W., and Massoth, G. J. (2004). "Mixing reaction and microbial activity in sub-seafloor revealed by temporal and spatial variation in diffuse flow vents at axial volcano," in *The Subseafloor Biosphere at Mid-Ocean Ridges*, eds R. W. Wilcock, E. F. DeLong, D. P. Kelley, J. A. Baross, and C. Cary (Washington, DC: American Geophysical Union), 269–289.

Cann, J. R. (1974). A layered model for oceanic crust developed. *Geophys. J. R. Astron. Soc.* 39, 169–187.

Chyba, C. F., and Phillips, C. B. (2002). Europa as an abode for life. *Orig. Life Evol. Biosph.* 32, 47–67.

Cody, G. D., Boctor, N. Z., Filley, T. R., Hazen, R. M., Scott, J. H., Sharma, A., and Yoder, H. S. Jr. (2000). Primordial carbonylated iron-sulfur compounds and the synthesis of pyruvate. *Science* 289, 1377–1340.

Coogan, L. A., Jenkins, G. R., and Wison, R. N. (2007). Contrasting cooling rates in the lower oceanic crust at fast- and slow-spreading ridges revealed by geospeedometry. *J. Petrol.* 48, 3311–2231.

Cowen, J. P., Copson, D. A., Jolly, J., Hsieh, C.-C., Lin, H.-T., Glazer, B. T., and Wheat, C. G. (2012). Advanced instrument system for real-time and time-series microbial geochemical sampling of the deep (basaltic) crustal biosphere. *Deep Sea Res. Part I Oceanogr. Res. Pap.* 61, 43–56.

Cowen, J. P., Giovannoni, S. J., Kenig, F., Johnson, H. P., Butterfield, D., Rappé, M. S., Hutnak, M., and Lam, P. (2003). Fluids from ageing ocean crust that support microbial life. *Science* 299, 120–123.

Davis, E. E., Chapman, D. S., Mottl, M. J., Bentkowski, W. J., Dadey, K., Forster, C., Harris, R., Nagihara, S., Rohr, K., Wheat, G., and Whiticar, M. (1992). FlankFlux: an experiment to study the nature of hydrothermal circulation in young oceanic crust. *Can. J. Earth Sci.* 29, 925–952.

Davis, E. E., Fisher, A. T., and Firth, J. (1997). *Proceedings of Ocean Drilling Program Initial Reports,* Vol. 168 (College Station, TX: Ocean Drilling Program), 470.

Dunn, R. A., Toomey, D. R., and Solomon, S. C. (2000). Three-dimentional seismic structure and physical properties of the crust and shallow mantle beneath the East Pacific Rise at 9°30′N. *J. Geophys. Res.* 105, 23537–23555.

Edwards, K. J., Bach, W., and Klaus, A. (2010). *Integrated Ocean Drilling Program Prospectus, Expedition 336.* College Station: IODP.

Elderfield, H., and Schultz, A. (1996). Mid-ocean ridge hydrothermal fluxes and the chemical composition of the ocean. *Annu. Rev. Earth Planet. Sci.* 24, 191–224.

Elderfield, H., Wheat, C. G., Mottl, M. J., Monnin, C., and Spiro, B. (1999). Fluid and geochemical transport through oceanic crust: a transect across the eastern flank of the Juan de Fuca Ridge. *Earth Planet. Sci. Lett.* 172, 151–165.

Expedition 327 Scientists. (2010). The Hydrogeologic Architecture of Basaltic Oceanic Crust: Compartmentalization, Anisotropy, Microbiology, and Crustal-Scale Properties on the Eastern Flank of Juan de Fuca Ridge, Eastern Pacific Ocean. Integrated Ocean Drilling Program Expedition 327 Preliminary Report, College Station. doi:10.2204/iodp.pr.327.2010

Expedition 329 Scientists. (2011). *South Pacific Gyre Subseafloor Life.* Integrated Ocean Drilling Program Expedition 329 Preliminary Report, College Station. doi:10.2204/iodp.pr.329.2011

Fisher, A. T. (2003). "Geophysical constraints on hydrothermal circulation: observations and models," in *Energy and Mass Transfer in Submarine Hydrothermal Systems*, eds P. Halbach, V. Tunnicliffe, and J. Hein (Berlin: Dahlem University Press), 29–52.

Fisher, A. T., Davis, E. E., Hutnak, M., Spiess, V., Zühlsdorff, L., Cherkaoui, A., Christiansen, L., Edwards, K., Macdonald, R., Villinger, H., Mottl, M. J., Wheat, C. G., and Becker, K. (2003a). Hydrothermal recharge and discharge across 50 km guided by seamounts on a young ridge flank. *Nature* 421, 618–621.

Fisher, A. T., Stein, C. A., Harris, R. N., Wang, K., Silver, E. A., Pfender, M., Hutnak, M., Cherkaoui, A., Bodzin, R., and Villinger, H. (2003b). Abrupt thermal transition reveals hydrothermal boundary and role of seamounts within the Cocos Plate. *Geophys. Res. Lett.* 30, 1550.

Fisher, A. T., Tsuki, T., Petronotis, K., Wheat, C. G., Becker, K., Clark, J. F., Cowen, J., Edwards, K. J., and the IODP Expedition 327 and Atlantis Expedition AT18-07 Shipboard Parties. (2012). Installing and servicing borehole crustal observatories to run three-dimensional cross-hole perturbation and monitoring experiments on the eastern flank of the Juan de Fuca Ridge: IODP Expedition 327 and Atlantis Expedition AT18-07. *Sci. Drill.* 13 (in press).

Fisher, A. T., Wheat, C. G., Becker, K., Cowen, J., Orcutt, B., Hulme, S., Inderbitzen, K., Haddad, A., Pettigrew, T. L., Davis, E. E., Jannasch, H., Grigar, K., Aduddell, R., Meldrum, R., Macdonald, R., and Edwards, K. J. (2011). "Design, deployment, and status of borehole observatory systems used for single-hole and cross-hole experiments, IODP Expedition 327, eastern flank of the Juan de Fuca Ridge," in *Proceedings of Integrated Ocean Drilling Program 327*, eds A. T. Fisher, T. Tsuji, and K. Petronotis (Tokyo: IODP). doi:10.2204/iodp.proc.327.107.2011

Fisher, A. T., and Von Herzen, R. (2005). Models of hydrothermal circulation within 106 Ma seafloor: constraints on the vigor of fluid circualtion and crustal properties below the Madeira Abyssal Plain. *Geochem. Geophys. Geosyst.* 6. doi:10.1029/2005GC001013

Fisher, A. T., and Wheat, C. G. (2010). Seamounts as conduits for massive fluid, heat, and solute fluxes on ridge flanks. *Oceanography* 23, 74–87.

Gable, R., Morin, R. H., and Becker, K. (1992). Geothermal state of DSDP Holes 333A, 395A and 534A: results from the dianaut program. *Geophys. Res. Lett.* 19, 505–508.

Haymond, R. M., Fornari, D. J., Von Damm, K. L., Lilley, M. D., Perfit, M. R., Edmond, J. M., Shanks, W. C., Lutz, R. A., Grebmeier, J. M., Carbotte, S., Wright, D., McLaughlin, E., Smith, M., Beedle, N., and Olson, E. (1993). Volcanic eruption of the mid-ocean ridge along the East Pacific Rise crest at 9°45–52′N: direct submersible observations of seafloor phenomena associated with an eruption event in April 1991. *Earth Planet. Sci. Lett.* 119, 85–101.

Hickman, S. H., Langseth, M. G., and Svitek, J. F. (1984). "Initial reports," in *Deep Sea Drilling Project*, Vol. 78B, eds R. D. Hyndman and M. H. Salisbury (Washington, DC: U. S. Govt. Printing Office), 699–708.

Hillier, J. K., and Watts, A. B. (2007). Global distribution of seamounts from ship-track bathymetry data. *Geophys. Res. Lett.* 34. doi:10.1029/2007GL029874

Huber, J. A., Johnson, H. P., Butterfield, D. A., and Baross, J. A. (2006). Microbial life in ridge flank crustal fluids. *Environ. Microbiol.* 8, 88–99.

Humphris, S. E., and Cann, J. R. (2000). Constraints on the energy and chemical balances of the modern TAG and ancient Cyprus seafloor sulfide deposits. *J. Geophys. Res.* 105, 428477–428488.

Hutnak, M., Fisher, A. T., Harris, R., Stein, C., Wang, K., Spinelli, G., Schindler, M., Villinger, H., and Silver, E. (2008). Large heat and fluid fluxes driven through mid-plate outcrops on ocean crust. *Nat. Geosci.* 1, 611–614.

Hutnak, M., Fisher, A. T., Stein, C. A., Harris, R., Wang, K., Silver, E., Spinelli, G., Pfender, M., Villinger, H., Pisani, P. C., Deshon, H., and MacKnight, B. (2007). "The thermal state of 18-24 Ma upper lithosphere subducting below the Nicoya Peninsula, northern Costa Rica margin," in *MARGINS Theoretical Institute: SIEZE Volume*, eds T. Dixon, C. Moore, E. Silver, S. Stein, K. Furlong, and K. Brown (New York: Columbia University Press), 86–122.

Hutnak, M., Fisher, A. T., Zühlsdorff, L., Spiess, V., Stauffer, P., and Gable, C. W. (2006). Hydrothermal recharge and discharge guided by basement outcrops on 0.7–3.6 Ma seafloor east of the Juan de Fuca Ridge: observations and numerical models. *Geochem. Geophys. Geosyst.* 7. doi:10.1029/2006GC001242

IODP. (2003). *Earth, Oceans, and Life.* IODP.

IODP. (2011). *Discovering Earth's Hidden Frontiers Through Scientific Ocean Drilling.* MD: IODP.

Johnson, H. P., and Pruis, M. J. (2003). Fluxes of fluid and heat from the oceanic crustal reservoir. *Earth Planet. Sci. Lett.* 216, 565–574.

Kadko, D., and Moore, W. (1988). Radiochemical constraints on the crustal residence time of submarine hydrothermal fluids: endeavour ridge. *Geochim. Cosmochim. Acta* 52, 659–668.

Kopf, A., Saffer, D. M., Davis, E., Hammerschmidt, S., LaBonte, A., Meldrum, R., Toczko, S., Lauer, R., Heesemann, M., Macdonald, R., Wheat, C. G., Jannasch, H. W., Edwards, K., Orcutt, B., Haddad, A., Villinger, H., Araki, E., Kitada, K., Kimura, T., and Kido, Y. (2011). "The SmartPlug and GeniusPlug: simple retrievable observatory systems for NanTroSEIZE borehole monitoring," in *Proceedings of the Integrated Ocean Drilling Program*, Vol. 322, eds A. Kopf, E. Araki, S. Toczko (College Station: IODP). doi:10.2204/iodp.proc.332.105.2011

Langseth, M. G., Becker, K., Von Herzen, R. P., and Schultheiss, P. (1992). Heat and fluid flux through sediment on the western flank of the Mid-Atlantic Ridge: a hydrogeological study of North Pond. *Geophys. Res. Lett.* 19, 517–520.

Langseth, M. G., Hyndman, K., Becker, R. D., Hickman, S. H., and Salisbury, M. H. (1984). "The hydrogeological regime of isolated sediment ponds in mid-oceanic ridges," in *Initial Reports Deep Sea Drilling Projects*, eds R. H. Hyndman and M. H. Salisbury (Washington, DC: U.S. Government Printing Office), 825–837.

Mackenzie, F. T. (1992). *Chemical Mass Balance Between Rivers and Oceans. Encyclopedia of Earth System Science.* New York: Academic Press.

Mason, O. U., Di Meo-Savoie, C., Van Nostrand, J. D., Zhou, J., Fisk, M. R., and Giovannoni, S. J. (2010). First investigation of the microbiology of the deepest layer of ocean crust. *PLoS ONE* 5, e15399. doi:10.1371/journal.pone.0015399

Moores, E. M., and Vine, F. J. (1971). The Troodos massif, Cyprus, and other ophiolites as oceanic crust: evaluations and implications. *Proc. R. Soc. Lond. A Math. Phys. Sci.* 268, 443–466.

Mottl, M. J., and Wheat, C. G. (1994). Hydrothermal circulation through mid-ocean ridge flanks: fluxes of heat and magnesium. *Geochim. Cosmochim. Acta* 58, 2225–2237.

Mottl, M. J., Wheat, C. G., Baker, N., Davis, E. E., Feely, R. A., Grehan, A., Kadko, D., Lilley, M., Massoth, G., Moyer, C., and Sansone, F. (1998). Warm springs discovered on 3.5 Ma oceanic crust, eastern flank of the Juan de Fuca Ridge. *Geology* 26, 51–54.

Noel, M. (1985). Heat flow, sediment faulting and porewater advection in the Madeira Abyssal Plain. *Earth planet. Sci. Lett.* 73, 398–406.

Orcutt, B. N., Bach, W., Becker, K., Fisher, A. T., Hentscher, M., Toner, B. M., Wheat, C. G., and Edwards, K. J. (2011a). Colonization of subsurface microbial observatories deployed in young ocean crust. *ISME J.* 5, 692–703.

Orcutt, B. N., Sylvan, J. B., Knab, N. J., and Edwards, K. J. (2011b). Microbial ecology of the dark ocean above, at and below the seafloor. *Microbiol. Mol. Biol. Rev.* 75, 361–422.

Parsons, B., and Sclater, J. G. (1977). An analysis of the variation of ocean floor bathymetry and heat flow with age. *J. Geophys. Res.* 82, 803–829.

Raitt, R. W. (1963). "The crustal rocks," in *The Sea, Vol. 3, The Earth Beneath the Sea*, ed. M. N. Hill (New York: Wiley-Interscience), 85–102.

Santelli, C. M., Bach, W., Banerjee, N. R., and Edwards, K. J. (2010). Tapping the subsurface ocean crust biosphere: low biomass and drilling-related contamination calls for improved quality controls. *Geomicrobiol. J.* 27, 158–169.

Schmincke, H.-U., Weaver, P. P. E., Firth, J. V., and Shipboard Scientific Party. (1995). *Leg 157*, Vol. 157. College Station, TX: Ocean Drilling Program, 841.

Scholin, C. G., Doucette, S., Jensen, S., Roman, B., Pargett, D., Marin, R. I., Preston, C., Jones, W., Feldman, J., Everlove, C., Harris, A., Alvarado, N., Massion, E., Birch, J., Greenfield, D., Vrijenhoek, R., Mikulski, C., and Jones, K. (2009). Remote detection of marine microbes, small invertebrates, harmful algae and biotoxins using the environmental sample processor (ESP). *Oceanography* 22, 158–167.

Schrenk, M. O., Huber, J. A., and Edwards, K. J. (2009). Microbial provinces in the subseafloor. *Oceanography* 2, 85–110.

Searle, R. C. (1987). "Regional setting and geophysical characterization of the Great Meteor East area in the Maderia Abyssal Plain," in *Geology and Geochemistry of Abyssal Plains*, eds P. P. E. Weaver and J. Thomson (London: The Geological Society of London), 49–70.

Shor, G. G. Jr., Menard, W. H., and Raitt, R. W. (1971). "Structure of the Pacific basin," in *The Sea, Vol. 4, New Concepts of Sea Floor Evolution*, ed A. E. Maxwell (New York: Wiley-Interscience), 3–27.

Shrenk, M. O., Huber, J. A., and Edwards, K. J. (2009). Microbial provinces in the subseafloor. *Oceanography* 2, 279–304.

Smith, A., Popa, R., Fisk, M., Nielsen, M., Wheat, C. G., Jannasch, H.,

Fisher, A. T., Becker, K., Sievert, S. M., and Flores, G. (2011). In situ enrichment of ocean crust microbes on igneous minerals and glasses using an osmotic flow-through device. *Geochem. Geophys. Geosyst.* 12, Q06007.

Spinelli, G. A., and Harris, R. N. (2011). Effects of the legacy of axial cooling on partioning of hydrothermal heat extraction from oceanic lithosphere. *J. Geophys. Res.* 116. doi:10.1029/2011JB008248

Stein, C. A., and Stein, S. (1994). Constraints on hydrothermal heat flux through the oceanic lithosphere from global heat flow. *J. Geophys. Res.* 99, 3081–3095.

VanTongeren, J. A., Kelemen, P. B., and Hanghoi, K. (2008). Cooling rates in the lower crust of the Oman ophiolite: Ca in olivine, revisited. *Earth Planet. Sci. Lett.* 267, 69–82.

Von Herzen, R. P. (2004). "Geothermal evidence for continuing hydrothermal circulation in older (>60 Ma) ocean crust," in *Hydrogeology of the Oceanic Lithosphere,* eds. E. E. Davis, and H. Elderfield (Cambridge: Cambridge University Press), 414–450.

Wessel, P., Sandwell, D. T., and Kim, S.-S. (2010). The global seamount census. *Oceanography* 23, 24–33.

Wheat, C. G., Elderfield, H., Mottl, M. J., and Monnin, C. (2000). Chemical composition of basement fluids within an oceanic ridge flank: implications for along-strike and across-strike hydrothermal circulation. *J. Geophys. Res.* 105, 13437–13447.

Wheat, C. G., and Fisher, A. T. (2008). Massive, low-temperature hydrothermal flow from a basaltic outcrop on 23 Ma seafloor of the Cocos Plate: chemical constraints and implications. *Geochem. Geophys. Geosyst.* 9, Q12O14. doi:10.1029/2008GC002136

Wheat, C. G., Jannasch, H., Fisher, A. T., Becker, K., Sharkey, J., and Hulme, S. (2010). Subseafloor seawater-basalt-microbe reactions: continuous sampling of borehole fluids in a ridge flank environment. *Geochem. Geophys. Geosyst.* 11, Q07011. doi: 10.1029/2010GC003057.

Wheat, C. G., Jannasch, H. W., Kastner, M., Hulme, S., Cowen, J., Edwards, K., Orcutt, B. N., and Glazer, B. (2011). "Fluid sampling from oceanic borehole observatories: design and methods for CORK activities (1990–2010)," in *Proceedings of the IODP, Expedition 327,* eds A. T. Fisher, T. Tsuji, and K. Petronotis (Tokyo: Integrated Ocean Drilling Program Management International, Inc.), doi: 10.2204/iodp.proc.327.109.2011

Wheat, C. G., Jannasch, H. W., Kastner, M., Plant, J. N., DeCarlo, E., and Lebon, G. T. (2004). Venting formation fluids from deep-sea boreholes in a ridge flank setting: ODP Sites 1025 and 1026. *Geochem. Geophys. Geosyst.* 5, Q08007.

Wheat, C. G., McManus, J., Mottl, M. J., and Giambalvo, E. (2003). Oceanic phosphorous imbalence: the magnitude of the ridge-flank hydrothermal sink. *Geophys. Res. Lett.* 30, OCE5.1–OCE5.4.

Wheat, C. G., and Mottl, M. J. (1994). Hydrothermal circulation, Juan de Fuca Ridge eastern flank: factors controlling basement water composition. *J. Geophys. Res.* 99, 3067–3080.

Wheat, C. G., and Mottl, M. J. (2000). Composition of pore and spring waters from baby bare: global implications of geochemical fluxes from a ridge flank hydrothermal system. *Geochim. Cosmochim. Acta* 64, 629–642.

Conflict of Interest Statement: The authors declare that the research was conducted in the absence of any commercial or financial relationships that could be construed as a potential conflict of interest.

Received: 04 November 2011; paper pending published: 23 November 2011; accepted: 05 January 2012; published online: 03 February 2012.

Citation: Edwards KJ, Fisher AT and Wheat CG (2012) The deep subsurface biosphere in igneous ocean crust: frontier habitats for microbiological exploration. Front. Microbio. ***3****:8. doi: 10.3389/fmicb.2012.00008*

This article was submitted to Frontiers in Extreme Microbiology, a specialty of Frontiers in Microbiology.

frontiers in
MICROBIOLOGY

HYPOTHESIS AND THEORY ARTICLE
published: 31 May 2012
doi: 10.3389/fmicb.2012.00168

Archaea in organic-lean and organic-rich marine subsurface sediments: an environmental gradient reflected in distinct phylogenetic lineages

***Alan M. Durbin*[1] *and Andreas Teske*[2] ***

[1] *Department of Ecology and Evolutionary Biology, University of California Irvine, Irvine, CA, USA*
[2] *Department of Marine Sciences, University of North Carolina at Chapel Hill, Chapel Hill, NC, USA*

Edited by:
Virginia P. Edgcomb, Woods Hole Oceanographic Institution, USA

Reviewed by:
Peter D. Countway, Bigelow Laboratory for Ocean Sciences, USA
Julie A. Huber, Marine Biological Laboratory, USA

***Correspondence:**
Andreas Teske, Department of Marine Sciences, University of North Carolina at Chapel Hill, 3117B Venable Hall, CB 3300, Chapel Hill, NC 27599, USA.
e-mail: teske@email.unc.edu

Examining the patterns of archaeal diversity in little-explored organic-lean marine subsurface sediments presents an opportunity to study the association of phylogenetic affiliation and habitat preference in uncultured marine Archaea. Here we have compiled and re-analyzed published archaeal 16S rRNA clone library datasets across a spectrum of sediment trophic states characterized by a wide range of terminal electron-accepting processes. Our results show that organic-lean marine sediments in deep marine basins and oligotrophic open ocean locations are inhabited by distinct lineages of archaea that are not found in the more frequently studied, organic-rich continental margin sediments. We hypothesize that different combinations of electron donor and acceptor concentrations along the organic-rich/organic-lean spectrum result in distinct archaeal communities, and propose an integrated classification of habitat characteristics and archaeal community structure.

Keywords: archaea, marine sediments, oligotrophy, subsurface, phylogeny, uncultured archaea

INTRODUCTION

Marine sedimentary microbial communities are key mediators of global biogeochemical cycles (e.g., D'Hondt et al., 2002, 2004; Wellsbury et al., 2002). The Domain Archaea accounts for a large portion, perhaps the majority, of deep-subsurface prokaryotic cells and biomass (Biddle et al., 2006; Lipp et al., 2008), and by implication, global biomass (Parkes et al., 1994; Whitman et al., 1998). The majority of studies thus far have focused on relatively organic-rich deep-subsurface sediments (e.g., Parkes et al., 1994, 2005; Reed et al., 2002; Wellsbury et al., 2002; D'Hondt et al., 2004; Biddle et al., 2006; Inagaki et al., 2006; Sørensen and Teske, 2006; Kendall et al., 2007; Heijs et al., 2008; Nunoura et al., 2008). However, abyssal sediments >2000 m water depth cover a much larger extent of the ocean floor (∼89%; Dunne et al., 2007) and, in contrast to margin or coastal sediments, are generally oligotrophic, with low organic carbon content (<1%) and slow rates of deposition (Seiter et al., 2004; Dunne et al., 2007). Electron acceptors such as oxygen or nitrate penetrate these oligotrophic sediments on a scale of meters (D'Hondt et al., 2004) or tens of meters (Gieskes and Boulègue, 1986; D'Hondt et al., 2009), in contrast to organic-rich continental margin or shelf sediments where these strong electron acceptors are used up within centimeters. This expansion of the oxic and nitrate-reducing zone in oligotrophic sediments is a function of the slow rates of carbon deposition and microbial carbon remineralization. The combination of higher-energy electron acceptor type and slower flux of electron donor substrates likely imposes distinct constraints on life in oligotrophic marine sediments, which cover the majority of the surface of Earth.

Several phylum-level uncultured archaeal lineages have been identified as typical deep-subsurface sediment-associated groups (Inagaki et al., 2003, 2006; Parkes et al., 2005; Biddle et al., 2006, 2008; Sørensen and Teske, 2006; Teske and Sørensen, 2008; Fry et al., 2008). These include the Marine Benthic Group B (MBG-B, Vetriani et al., 1999), a deeply branching phylum-level lineage; the Miscellaneous Crenarchaeotal Group (MCG, Inagaki et al., 2003), a frequently detected crenarcheotal lineage with high intra-group diversity; the South African Gold Mine Euryarchaeotal Group (SAGMEG, Takai et al., 2001); and the Marine Benthic Group D (MBG-D, Vetriani et al., 1999), a euryarchaeotal group affiliated with the Thermoplasmatales. All of these are approximately phylum-level in divergence, with the exception of the MBG-D, which groups along with the MG-II archaea (DeLong, 1992; Fuhrman et al., 1992) and MG-III archaea (Fuhrman and Davis, 1997) in a well-supported clade affiliated with the Thermoplasmatales (Durbin and Teske, 2011). However, our current datasets on archaeal community composition in deep marine sediments are biased toward organic-rich continental margin sediments (Teske and Sørensen, 2008). Relatively few studies have surveyed the archaeal diversity of abyssal or ocean gyre sediments to date. A more or less comprehensive list includes: Vetriani et al., 1999; Inagaki et al., 2001; Sørensen et al., 2004; Wang et al., 2004; Nercessian et al., 2005; Wang et al., 2005; Xu et al., 2005; Gillan and Danis, 2007; Li et al., 2008; Tao et al., 2008; Roussel et al., 2009; Wang et al., 2010a, Liao et al., 2011; Durbin and Teske, 2010, 2011. Most of these studies are limited to shallow sediments (<1 m deep) or to few depth intervals. Thus, the available database for archaeal communities in oligotrophic marine subsurface sediments has not yet reached the same coverage as eutrophic sediments. Nonetheless, initial datasets from the South Pacific (Durbin et al., 2009; Durbin and Teske, 2010, 2011) and other datasets in the literature point to profoundly different archaeal communities, with little or no overlap at the phylum and subphylum level.

Examining the patterns of archaeal diversity in little-explored oligotrophic sediments presents an opportunity to study the association of phylogenetic affiliation and habitat preference in uncultured Archaea. We expect a linkage between sediment habitat type and phylogenetic identity, since the distinct physiological demands – sustaining metabolism and growth with low-energy electron acceptors in anaerobic, organic-rich sediments, in contrast to electron donor limitation in oxidized sediments – should select for distinct organisms in organic-lean, oxidized sediments that differ from those in organic-rich, reduced sediments. Specialization in terminal electron acceptors with higher redox potential for a given substrate may differentiate organisms adapted to oxic/suboxic organic-lean environments from those adapted to more organic-rich, typically anoxic environments.

However, an important caveat is that free-energy yield is highly contingent on *in situ* conditions, possibly subverting the expected hierarchy of electron acceptor energy yields based on standard conditions. Factors such as syntrophy (McInerney and Beaty, 1988), biotic (Wang et al., 2008, 2010b), or abiotic (König et al., 1997, 1999) release from feedback inhibition, pH (Postma and Jakobsen, 1996; Thamdrup, 2000), and substrate competitive release or substrate-pooling (e.g., Lever et al., 2010) may all impact *in situ* energetics of metabolisms. Additionally, redox niche adaptation likely extends beyond simply the ability to use a particular electron acceptor. *In situ* redox state (E_h) determines the thermodynamic favorability of a given biosynthetic pathway, as biosynthetic pathways feasible under highly reduced conditions are less favorable in more oxidized environments; fatty acid biosynthesis (palmitate) is a classic example (McCollom and Amend, 2005). Low substrate concentrations in organic-lean environments may be countered with high-substrate-affinity catabolic enzymes, as in the oligotrophic archaeon *Nitrosopumilus maritimus* (Martens-Habbena et al., 2009). Economical use of electron acceptors with a high redox potential, as shown for ammonia-oxidizing Thaumarchaeota (Schleper and Nicol, 2010), may allow organisms to take advantage of the expanded redox transition zones in organic-lean environments.

With the largely unexplored complexity of organismal redox adaptation noted, we hypothesize that different combinations of electron donor and acceptor concentrations along the organic-rich/organic-lean spectrum result in distinct archaeal communities that have optimized their energetic requirements for cell maintenance and growth. This hypothesis article examines published archaeal 16S rDNA clone library datasets across a wide spectrum of sediment trophic states and terminal electron-accepting processes.

SAMPLING SITES

This study analyses archaeal communities in organic-lean subsurface sediments from the South China Sea (Wang et al., 2010a), the Fairway Basin in the Western Tropical Pacific (Roussel et al., 2009), the Peru Basin offshore Peru (Sørensen et al., 2004), the equatorial upwelling zone west of the Galapagos (Teske, 2006; Teske and Sørensen, 2008), and the South Pacific Subtropical Front northeast of New Zealand (Durbin and Teske, 2011; **Table 1**; **Figure 1**). These sediments were contrasted with organic-rich sediments of ODP Leg 201 sites 1227 and 1229, located beneath the highly productive Peruvian upwelling zone, with the methane-clathrate-bearing deep-subsurface sediments of ODP site 1230 in the Peru Trench (Parkes et al., 2005; Biddle et al., 2006; Inagaki et al., 2006; Sørensen and Teske, 2006), and with sediments from the Cascadia Margin offshore Oregon recovered during ODP Leg 204 (Inagaki et al., 2006; Nunoura et al., 2008). ODP Leg 201 Site 1226 south of Galapagos was included as an example of a mesotrophic deep marine sediment, and IODP Expedition 308 sites U1319 and U1320 were included as examples of turbidite continental slope sediments (Nunoura et al., 2009). Methane seep sediments from the Mediterranean provided an example of a deepwater, yet highly reducing shallow sediment environment (Heijs et al., 2008). A phylogenetic and environmental outgroup is provided by sequences from two non-marine anoxic habitats, an anaerobic digestor (Chouari et al., 2005) and rumen (Sundset et al., 2009).

Although geochemical data were incomplete, two sites from the South China Sea (MD05-2896, MD05-2902; Wang et al., 2010a) and several sediment columns from the Coral Sea (ZoNéCo-12 sites; Roussel et al., 2009) were included as oligotrophic to mesotrophic sedimentary environments (**Table 1**; **Figure 1**) based on nearby ODP sites with complementary geochemistry data. Approx. 195 km separates ODP Leg 184 Site 1148 and MD05-2902, both are located at similar depths (Site 1148: ∼3700; MD05-2902: ∼3300 m) in the Pearl River Basin, Northern South China Sea. ODP Leg 184 Site 1143 and MD05-2896 are separated by ∼210 km within the Dangerous Grounds geologic province of the South China Sea. Although these sites are at significantly different depths (approx. 1650 m for MD05-2896 and ∼2770 m for Site 1143), they share a common sedimentary regime of pelagic drape amid broken carbonate platforms distant from the continental shelf (Hutchison, 2004). Analogs for the ZoNeCo-12 sites in the Fairway Basin south of New Caledonia come from a prior geochemical survey (ZoNéCo-5) of the same marine basin. The sites from these two surveys are ∼127 to 285 km distant, and are located at similar depths (ZoNeCo-5: 2700 m; ZoNeCo-12: ∼2500–2700 m), with presumably similar sedimentation regimes (Dickens et al., 2001).

Some oligotrophic sediments are problematic since their microbial community structure and geochemical characteristics overlap with those of hydrothermal sediments (Inagaki et al., 2001; Nercessian et al., 2005; Li et al., 2008) and the deep-water column. Several studies of oligotrophic abyssal sediments (Wang et al., 2004; Xu et al., 2005; Gillan and Danis, 2007) sampled only surficial sediments and recovered the same archaeal phylum, the Marine Group I Crenarchaeota, that is presumed dominant in the overlying water column (e.g., Karner et al., 2001; Church et al., 2003; Agogué et al., 2008; Durbin and Teske, 2010). Because of the high potential for cross-contamination and the phylogenetic similarity between oxic sediments and the overlying water column, to confidently label MG-I clones collected from oxic sediments as indigenous requires stringent contamination controls and/or investigations of the diversity of contamination sources (Durbin and Teske, 2010). Due to these difficulties, MG-I sequences were excluded from the current analysis.

THE SEDIMENTARY TROPHIC STATE SPECTRUM

In the following section, we summarize some of the most informative biogeochemical and microbiological parameters for

Table 1 | Overview of site characteristics and parameters relating to trophic state of organic-lean to organic-rich marine subsurface sediments.

Site	Marine Province, location	Water depth	Length of cored Sediment and total sediment thickness, mbsf	Log[10] range, and mbsf range of cell counts	Sedimentation rate, m/My [DSDP/ODP site]	TOC, % weight of sediment	Max. DIC, mM	Ammonia, μM	Oxygen depletion depth, mbsf	Nitrate depletion depth, mbsf	Sulfate concentration minima [mM] and depth [mbsf]	Sulfide/ reduced metals	Reference
SPG11	South Pacific Gyre 41°51.13S, 153°06.38W	5076	2.98 [67]	3.87–6.63 [2.96–0.1]	0.9 [averaged over entire sediment column]	0.51 (0.0–0.05 mbsf)	2.44 mEq (alkalinity)	Below detection	No depletion	No depletion	No depletion	–/–	D'Hondt et al. (2009), Durbin and Teske (2010)
SPG12	South Pacific Subtrop. Front 45°57.86S, 163°11.05W	5306	4.98 [130]	5.37–6.3 [4.9–0.25]	1.8 [averaged over entire sediment column]	0.34 (0.0–0.05 mbsf)	3.23 mEq (alkalinity)	Below detection	∼0.70	2.55	No depletion	–/+	D'Hondt et al. (2009), Durbin and Teske (2011)
ODP Leg 201, site 1231	Peru Basin 12°01.29 S, 81°54.24W	4813	119.1 [∼120]	5.14–8.24 [81.64–0.01]	Closest analog: Eocene-Quaternary, 4-10 [DSDP 321]*	0.07–0.7	3.64	7.64–32.72	No data	0.1–0.4	No depletion	–/+	Shipboard Scientific Party (2003f), D'Hondt et al. (2004), *Shipboard Scientific Party (1976)
ODP Leg 201, site 1225	Eastern Equat. Pacific 02°46.22 N, 110°34.30W	3760	315.6 [∼320]	5.26–6.87 [320–0.85]	Closest analog: Miocene-Quaternary, 15–65 [ODP 851]*	0.00–0.53	3.98	6.15–38.48	No data	∼1.5	No depletion	–/+	Shipboard Scientific Party (2003a), *Shipboard Scientific Party (1992a)

(Continued)

Table 1 | Continued

Site	Marine Province, location	Water depth	Length of cored Sediment and total sediment thickness, mbsf	Log[10] range, and mbsf range of cell counts	Sedimentation rate, m/My [DSDP/ODP site]	TOC, % weight of sediment	Max. DIC, mM	Ammonia, μM	Oxygen depletion depth, mbsf	Nitrate depletion depth, mbsf	Sulfate concentration minima [mM] and depth [mbsf]	Sulfide/ reduced metals	Reference
ODP Leg 201, site 1226	South Equat. Current near Galapagos 03°05.80 S, 90°49.07 W	3297	418.9 [421]	∼6–8.67 [420–0.01]	Closest analog: Miocene-Quaternary, ∼40 [ODP 846]*	0.25–3.49	7.03	51.7–641	No data	Not resolved	Partial depletion (18.9 mM at 246 m depth)	+/+	Shipboard Scientific Party (2003b), *Shipboard Scientific Party (1992b)
MD05-2902 North Core	South China Sea, Pearl River Basin 17°57.70 N, 114°57.33 E	3697	9.42 [>850]	No data	Closest analog: Miocene, 11–17 Pliocene to Pleistocene, 27–63 [ODP 1148]*	0.2–1.4	Closest analog: 9.14 [ODP 1148]*	Closest analog: 640-1390 [ODP 1148]*	No data	No data	Closest analog: 3 mM at 630–650 m [ODP 1148]*	+/+	Wang et al. (2010a), *ODP Leg 184: Shipboard Scientific Party (2000b)
MD05-2896 South Core	Southern, South China Sea 08°49.59 N, 111°26.47 E	1657	11.03 [>500]	No data	Closest analog: Miocene to recent, 30–50 [ODP 1143]*	0.2–1.3	Closest analog: 11.18 [ODP 1143]*	Closest analog: 200–1900 [ODP 1143]*	No data	No data	Closest analog: 6.3 mM at 500 mbsf [ODP 1143]*	+/+	Wang et al. (2010a), *ODP Leg 184: Shipboard Scientific Party (2000a)
ZoNeCo-12: MD06-3022, MD063026, MD063027, MD063028	Fairway Basin, Coral Sea 24°S, 163°E	2294 (MD06-3022), ∼2700 others	9.4 [>>560]	6.2–8.3 [9.4–0.2]	Closest analog: Neogene, 10 [ZoNeCo-5 sites in Fairway Basin]*	No data	No data	No data	No data	No data	18 mM at 7.5 mbsf Extrapolated depletion depth at 3022: ∼60 m	+/+	Roussel et al. (2009), *Dickens et al. (2001)
IODP leg 308, site U1320	Brazos Basin 27°18.08 N, 94°23.25 W	1480	299.6	<4–6.08 [284.8–7.5]	1810 [Holocene to 80 ky]	0.03–1.99	15.99 [alkalinity]	132–3816	No data	No data	Depletion to 0.6 mM at 22 mbsf	+/+	Expedition 308 Scientists (2006b)

IODP leg 308, site U1319	Brazos Basin 27°15.96 N, 94°24.19 W	1440	157.5	<4–6.08 [157.5–4.4]	150 [Holocene} 2310 [>90–150 ky]	0.16–1.9	19.45 [alkalinity]	291 – 4411	No data	No data	Depletion to 0.5 mM at 15 mbsf	+/+	Expedition 308 Scientists (2006a)
ODP Leg 201, site 1227	Peru Margin 08°59.45 N, 79°57.35 W	427	151 (> >)	6.25–7.70 [151-0.15]	Miocene-Quaternary: 20-50 [ODP 684]*	1.16–10.57	25.78	3168.2–8875.5	No data	Not resolved	Depletion at ∼41 mbsf	+/+	Shipboard Scientific Party (2003c) *Shipboard Scientific Party (1988a)
ODP Leg 201, site 1229	Peru Margin 10°58.57 S, 77°57.46 W	151	192.9 (>>)	6.43–9.97 [185.7–90.45]	Quaternary∼80 [ODP 681]*	0.83–3.97	21.14	5335.69–6746.53	No data	Not resolved	Depletion at ∼32 mbsf	+/+	Shipboard Scientific Party (2003d) *Shipboard Scientific Party (1988b)
ODP Leg 201, site 1230	Peru Trench 09°06.78 S, 80°35.01 W	5086	277.3 (>>)	6.1–8.62 [257.7–0.01]	Miocene-Quaternary: 100–250 [ODP 685]*	1.27–3.98	162.95	1920–40170	No data	Not resolved	Depletion at ∼9 mbsf	+/+	Shipboard Scientific Party (2003e) *Shipboard Scientific Party (1988c)
ODP Leg 204, site 1244	Cascadia Margin 44°35.18 N, 125°07.19 W	890	380 (>>)	∼6–7, qPCR [123–2.0]*	60–270	0.87–1.75	68.9 [alkalinity]	Max. 22700	No data	No data	Depletion to ∼0.5–1 mM at ∼11 mbsf	+/+	Shipboard Scientific Party (2003g) *Nunoura et al. (2008)

(Continued)

Table 1 | Continued

Site	Marine Province, location	Water depth	Length of cored Sediment and total sediment thickness, mbsf	Log[10] range, and mbsf range of cell counts	Sedimentation rate, m/My [DSDP/ODP site]	TOC, % weight of sediment	Max. DIC, mM	Ammonia, μM	Oxygen depletion depth, mbsf	Nitrate depletion depth, mbsf	Sulfate concentration minima [mM] and depth [mbsf]	Sulfide/ reduced metals	Reference
ODP Leg 204, site 1245	Cascadia Margin 44°35.16 N, 125°08.95 W	870	540 (>>)	Not detected in qPCR*	100–620	0.71–1.46	73.31 [alkalinity]	Max. 21800	No data	No data	Depletion to ∼0.5–1 mM at ∼8 mbsf	+/+	Shipboard Scientific Party (2003h) *Nunoura et al. (2008)
ODP Leg 204, site 1251	Cascadia Margin 44°34.21 N, 125°04.44 W	1216	445 (>>)	∼6–8, qPCR [204.2–4.5]*	600–1600	0.58–3.06	122.37 [alkalinity]	Max. 14800	No data	No data	Depletion to ∼0.5 - 1 mM at ∼3 mbsf	+/+	Shipboard Scientific Party (2003i) *Nunoura et al. (2008)
Napoli cold seep	Eastern Mediterranean 33°43.47 N, 24°42.09 E	1947	0.28 (>>)	No data	Not applicable	1.22–3.95	No data	217.2–40.6	No data	0 cmbsf	Not resolved	+/no data	Heijs et al. (2008)
Kazan mud volcano	Eastern Mediterranean 35°26.00 N, 30°33.50 E	1720	0.34 (>>)	No data	Not applicable	2.59–17.4	No data	30.0–158.5	No data	∼6 cmbsf	Depletion at 0.35–0.40 mbsf [0.25 mbsf]*	+/no data	Heijs et al. (2008) *Kormas et al. (2008)
Amsterdam mud volcano	Eastern Mediterranean 35°19.85 N, 30°16.85 E	2050	0.31 (>>)	No data	Not applicable	3.9–4.31	No data	50.6–152.5	No data	0 cmbsf	Not resolved	+/no data	Heijs et al. (2008)

From top to bottom: ultraoligotrophic site without depletion of oxygen or nitrate (SPG11); oligotrophic sites with nitrate depletion within meters (SPG12, ODP 1225 and 1231); mesotrophic sites (ODP 1226, South China Sea, Coral Sea); and eutrophic sites (IODP 308 sites U1319, U1320 with caveats; ODP Leg 201 sites 1227, 1229, 1230; ODP Leg 204 sites 1244, 1245, 1251) characterized by high DIC and NH_4 porewater concentration maxima, and high sedimentation rates. Outgroup, Mediterranean seep sediments.

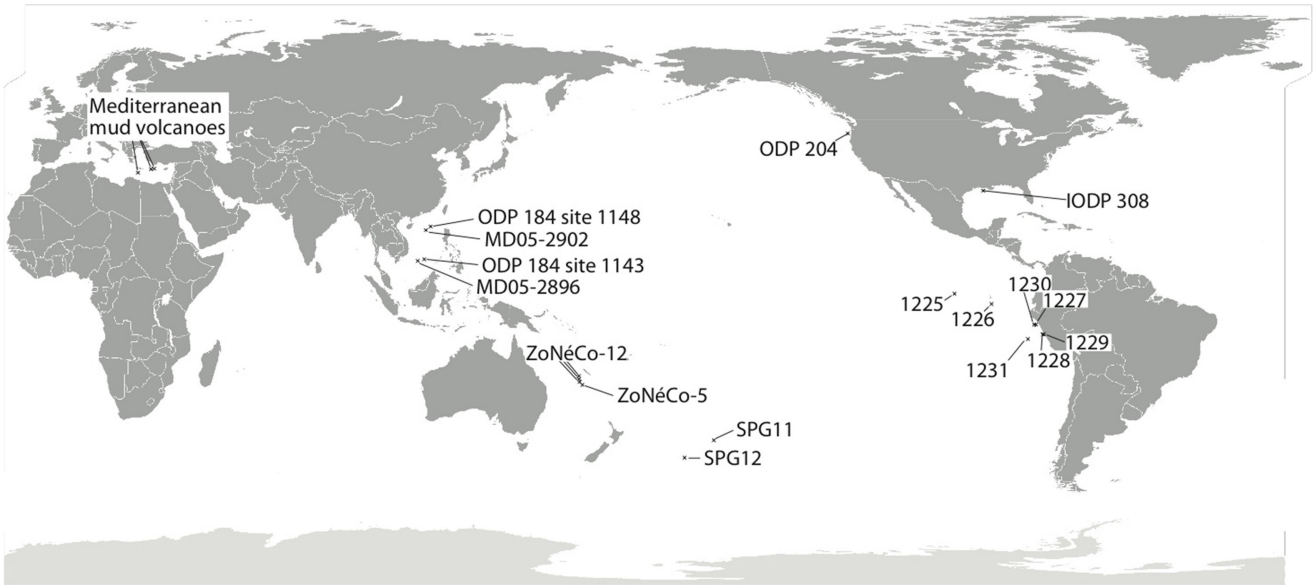

FIGURE 1 | Map depicting approximate location of marine sediment cores discussed in the current review. SPG11 occurs just inside the southern South Pacific Gyre, while SPG12 lies on the subtropical front separating the gyre from the Southern Ocean (D'Hondt et al., 2009). Sites MD05-2896 and MD05-2902 (Wang et al., 2010a) are from the South China Sea, with additional geochemical data on these sites sourced from nearby ODP Leg 184 Sites 1143 and 1148 (Shipboard Scientific Party, 2000a,b). The ZoNéCo-12 sites lie in the Fairway Basin in the Coral Sea (Roussel et al., 2009), with additional information from ZoNéCo-5 sites (Dickens et al., 2001). The IODP 308 sites (U1319, U1320) are located in the turbidite depositional Brazos-Trinity Basin on the continental slope of the northern Gulf of Mexico (Nunoura et al., 2009). The ODP Leg 201 Sites (Shipboard Scientific Party, 2003a–f; D'Hondt et al., 2004) include sites from the eastern equatorial upwelling region (1225), South Equatorial Current (1226), Peru Margin (1227, 1229), Peru Trench (1230), and the Peru Basin (1231). The ODP Leg 204 Cascadia Margin sites include sites 1244, 1245, and 1251 (Nunoura et al., 2008). Mud volcano/cold seep sites are represented by three examples from the eastern Mediterranean (Heijs et al., 2008).

oligotrophic marine subsurface sediments (**Table 1**) and show that these sites appear to fall into several natural groups.

SEDIMENTATION RATES

Sedimentation rates can approximate sediment trophic states, albeit with some exceptions for high-carbonate or turbidite-associated sedimentation and changing oceanographic conditions in the surface ocean, which can all enrich or impoverish deep marine sediments relative to the expected trophic state based on surface ocean productivity, or if a significant fraction of sedimentation is inorganic carbonate or silicate. Sedimentation rates at SPG Sites 11 and 12, are near 0.9 and 1.8 m/My, averaged over the entire depth and age of the sediment column (D'Hondt et al., 2009). For reference, averaged ocean sedimentation rates for the Atlantic, Pacific, and Indian Ocean based on DSDP cores ranged from 30 to 50 m/my for quaternary sediments, and decreased to 2–5 m/my for paleocene sediments (Whitman and Davis, 1979). Among ODP Leg 201 sites, Site 1231 is the slowest-accumulating site, but still 4 to 10 times or 2 to 5 times faster than the South Pacific sites SPG11 or SPG12 (**Table 1**). The Peru Margin, Peru Trench, and Cascadia Margin sites form a cohort with increasingly high sedimentation rates, up to 1600 m/my at Cascadia Margin site 1251 (**Table 1**), three orders of magnitude higher than at the South Pacific sites (**Table 1**), dramatically illustrating the different constraints shaping eutrophic margin environments and ultraoligotrophic gyre sediments. An extreme outlier are the Gulf of Mexico slope turbidite sediments sampled on IODP Expedition 308 (**Table 1**).

POREWATER DIC

Concentrations of porewater DIC above or below the mean seawater concentration are an indicator of the magnitude and direction of net metabolism. Net heterotrophy due to remineralization of organic matter to CO_2 increases DIC concentrations, at least at the more oligotrophic end of the scale; in highly organic-rich sediments, a large fraction of organic carbon may be remineralized not to CO_2 but to methane. Nevertheless, because DIC directly reflects metabolic rates, it integrates over unknowns inherent in interpreting sedimentation rates or electron acceptor depletion profiles. Comparisons of maximum DIC for Leg 201 sites suggest a spectrum from highly DIC-enriched Cascadia Margin sites 1244, 1245, and 1251 and Peru Trench Site 1230, to Peru Margin sites 1229 and 1227, the Gulf of Mexico Expedition 308 sites, the South China Sea sites, to ODP sites 1226, 1225, and 1231; the SPG sites 12 and 11 mark the DIC-poor end of the spectrum (**Table 1**). Here, alkalinity (∼96% of which is DIC, at seawater pH) remains at seawater values throughout the sampled sediment column at SPG11, while SPG12 displays a downcore alkalinity increase concomitant with oxygen drawdown, and stabilizing thereafter (**Table 1**). Maximal porewater NH_4 concentrations show the same trend and sort the

sites into the same sequence as porewater DIC (**Table 1**), reflecting the origin of NH_4 from remineralization of buried biomass.

ORGANIC CARBON AVAILABILITY

Organic carbon concentration is not a directly proportional measure of sediment trophic state, as substrate lability and organic carbon residence time can vary between sediments with similar organic carbon contents. Therefore, trophic state of the sediment can change without necessarily affecting the sediment organic carbon percent weight, and organic carbon content between sites of possibly different trophic state can overlap. Among the South Pacific Gyre sites, organic carbon content values for SPG11 ranged from 0.59 to 0.45 dry weight% over the upper 9 cmbsf (centimeter below surface), with little change after the upper 2 cmbsf; surface sediments (0–5 cmbsf) from SPG12 contained 0.34% (D'Hondt et al., 2009). A global TOC analysis in marine sediments showed that abyssal sediments contain less than or at most 1 weight% TOC, close to the global mean for marine sediments (Seiter et al., 2004); this is consistent with the oligotrophic sites in this survey. Higher TOC values in the range of up 1–2% are shared by the South China Sea sites and the Gulf of Mexico turbidite sediments (**Table 1**). The eutrophic Leg 201 sites varied between ∼1 and 10% TOC for different horizons, with ∼4% most typical for the majority of the sediment column, and typically decreasing with depth (**Table 1**). Interestingly, the Cascadia Margin Leg 204 sites showed lower TOC concentrations (maxima ca. 1.5–3%) than the Leg 201 Peru Margin and Peru Trench sediments, and resembled in this regard the Gulf of Mexico turbidites (**Table 1**).

CELL DENSITIES

Total prokaryotic cell densities at the SPG sites are the lowest yet recorded for any equivalent depth horizon (D'Hondt et al., 2009). For all sites, cell counts declined with sediment depth, with the lowest value typically being the deepest. Cell counts ranged from $10^{3.9}$ to $10^{6.6}$ per ml over the upper 2.8 m at SPG11, and $10^{5.4}$ to $10^{6.3}$ per ml over the upper ∼5 m at SPG12, again setting SPG11 apart. These cell counts were lower than those of deepwater ODP sites 1231 and 1225 at comparable depth; the deepwater ODP sites had similar or higher cell counts over a much broader depth range, and declined to their lowest levels of $\sim 10^5$ at greater depths, 81.6 mbsf for 1231 and 320 mbsf for 1225. Given their location on continental margins, the Gulf of Mexico turbidite sediments of Expedition 308 had unusually low cell densities; the maxima in the range of $10^{5.3}$ to $10^{6.08}$ cells per ml were found near the sediment surface, and cell densities decreased rapidly with depth (Nunoura et al., 2009). Cell counts of the mesotrophic ODP 1226 and the eutrophic Peru Margin and Trench sites ranged from 10^6 to 10^{10} cells per cm^3 throughout the sediment column (**Table 1**). No direct cell counts are available from the ODP 204 sites; the qPCR data for 16S rRNA gene copy numbers have to be viewed with caution, given occasionally complete PCR inhibition (Nunoura et al., 2008).

OXYGEN, NITRATE, AND SULFATE GRADIENTS

Typically, electron acceptors for microbial metabolism are depleted downcore in order of declining energy yield; depletion depth increases with organic substrate scarcity. Thus, organic-carbon limited sediments are expected to be deeply permeated by high-energy electron acceptors. Within increasingly organic-rich sediments, oxidants retreat toward the seawater/sediment interface, leading to a shrinking zone of oxidant availability. The porewater gradients of the strongest oxidants (oxygen, nitrate) are therefore strongly compressed toward the sediment surface, whereas the porewater profiles of weaker oxidants (oxidized metals, sulfate) extend deeply into the sediment column (D'Hondt et al., 2002, 2004).

At the ultraoligotrophic SPG11 site, oxygen drawdown is minimal and nitrate drawdown is not evident; porewater oxygen remains at ∼160 μM at 280 cmbsf and is unlikely to be depleted downcore, unless there are deep biotic or abiotic sediment oxygen sinks (D'Hondt et al., 2009). At site SPG12, oxygen becomes depleted near 70 cmbsf, and nitrate is depleted at 253–258 cmbsf (D'Hondt et al., 2009). Oxygen data are not available for ODP sediment cores; sediment cores from ODP sites 1225 and 1231 show nitrate depletion on the scale of 10–40 cmbsf for 1231, and ∼150 cmbsf for site 1225 (**Table 1**). The surficial 1–2 m sediment horizons,and the nitrate and oxygen porewater profiles therein, are generally lost or disturbed during ODP coring. Nitrate and oxygen profiles in centimeter resolution can be obtained from sediment cores with undamaged surface layers, sampled by submersible or ROV. For example, downcore nitrate depletion occurred between 6 and 22 cmbsf for the Kazan mud volcano, and indirect evidence points to oxygen penetration within the upper 6 cm. Nitrate remained near 1–2 μM in the other two mud volcano sites (Amsterdam and Napoli), and no oxygen penetration could be inferred (Heijs et al., 2008).

Sulfate was not measurably drawn down at the SPG12 site, nor at the oligotrophic ODP sites 1231 and 1225. Mesotrophic ODP site 1226 displayed sulfate drawdown but not depletion over the entire sampled sediment column, along with apparent metal redox cycling to at least ∼70 mbsf and methanogenesis throughout nearly the entire sediment column. Likewise, the ODP proxy sites from the South China Sea revealed sulfate drawdown but not depletion over several hundred meters of sediment. Sulfate profiles for the shallow Coral Sea cores are incomplete; however, extrapolating from the upper 9 m sulfate profile of Core MD06-3022 (Roussel et al., 2009) suggests a minimum depletion depth of 60 m or greater. The Gulf of Mexico and Peru Margin sites displayed sulfate depletion within tens of meters (D'Hondt et al., 2004), the Peru Trench and Cascadia Margin sites showed sulfate depletion within a few meters (**Table 1**). Often, porewater sulfate concentrations below depletion depth do not decrease to zero, but fluctuate in the range of 0.5 or 1 mM, reflecting sulfide reoxidation after exposure of sulfidic cores to oxygen. In Mediterranean mud volcano sediments, sulfate was depleted within the ∼40 cm measured for the Amsterdam and Napoli mud volcanoes, while the Kazan seep displayed little to no drawdown of sulfate (Heijs et al., 2008). Geochemical and microbial variability within each mud volcano site is evident from another recent survey of the Kazan mud volcano, where sulfate was drawn down within 25 cm sediment depth (Kormas et al., 2008).

METAL REDOX CYCLING

Metal reduction represents a key avenue for anaerobic terminal electron-accepting processes (Thamdrup, 2000). Manganese and iron reduction are both typical suboxic processes (Berner, 1981), with manganese reduction comparable to nitrate reduction,

and reduction of amorphous iron oxyhydroxides closer to sulfate reduction in energy yield (Lovley and Goodwin, 1988). However, the fact that iron reduction involves both soluble and solid reactants and products, and the different bioavailability of different iron oxide phases, complicate iron geochemistry by introducing additional contingent factors. These include chemical surface inactivation (Fredrickson et al., 1998; Urrutia et al., 1998; Urrutia et al., 1999); retention of reduced iron in clay lattices, which counteracts product inhibition of iron reduction (König et al., 1997, 1999) and favors increased *in situ* free-energy yields for iron reduction; and the pH and phase dependence of free-energy yields (Postma and Jakobsen, 1996; Fredrickson et al., 1998), which may result in higher *in situ* energy yields for sulfate reduction. In particular, precipitation of the reduced byproducts of sulfate and iron reduction results in a mutualistic positive feedback that equalizes energy yields for both (Wang et al., 2008, 2010b). Together, these factors allow recalcitrant metal oxides to persist deep in anoxic zones (D'Hondt et al., 2004; Wang et al., 2008, 2010b), while Mn and reactive Fe(III) are mostly reduced nearer to the sediment-water interface (König et al., 1997; Thamdrup, 2000; Wang et al., 2008).

Sediment redox state can be characterized by considering iron and sulfate reduction together. Ultraoligotrophic, oxic site SPG11 shows no evidence of either iron or sulfate reduction (**Table 1**). The anaerobic, oligotrophic sites SPG12, 1225, and 1231 display net iron reduction but no sulfide production. In mesotrophic and eutrophic sites from the South China Sea, Coral Sea, the Gulf of Mexico, the Peru Margin, Peru Trench, and Cascadia Margin, the precipitation of metal sulfides indicates co-occurring sulfate and iron reduction. **Table 1** presents presence/absence patterns for sulfide and reduced metals for different sites, using both direct measurement of sulfide (Leg 201 and Mediterranean sites), dissolved porewater iron and manganese (Leg 201, Leg 204, and IODP 308 sediments), as well as indirect indicators for the presence or absence of reduced sulfur and metal species, such as a measured lack of net sulfate reduction (SPG12, SPG11), the presence of authigenic sulfide minerals (Leg 184, Leg 204), or brown–green color transitions (König et al., 1997; Thamdrup, 2000) that are an indicator of sedimentary Fe(III)/Fe(II) redox fronts (SPG12, Leg 184 sites, ZoNéCo sites, IODP308 sites).

SEDIMENT TROPHIC STATE HIERARCHY

In terms of electron acceptor gradients, oxygen and nitrate penetration over tens of centimeters to meters, and the absence of sulfate depletion, characterize the oligotrophic sites SPG12, ODP 1231, and ODP 1225; the lack of oxygen depletion at SPG11 sets this ultraoligotrophic site apart. Based on cell densities, nitrate and oxygen penetration depth, sedimentation rate, and possibly maximum DIC value, SPG12 is the most organic-lean among the oligotrophic sites, which would also include ODP deepwater sites 1231 and 1225. ODP Site 1226 and the South China Sea sites displayed sulfate drawdown but not depletion several hundred meters deep into the sediment, with the Coral Sea and the Fairway Basin also possibly in that category, suggesting a "mesotrophic" label for these sites. By contrast, eutrophic sites have oxygen and nitrate penetration depths of mere centimeters to millimeters, and sulfate depletion depths of tens of meters or less. The Gulf of Mexico Expedition 308 sites show a curious mixture of eutrophic characteristics (high DIC and NH_4 porewater concentration maxima, very high sedimentation rates) combined with mesotrophic (low TOC content) or even oligotrophic characteristics (very low cell numbers). The fully eutrophic sediments are represented by the Peru Margin, Peru Trench, and Cascadia Margin sites. Where available, DIC and NH_4 porewater concentrations are perhaps the most reliable trophic state indicators, as they directly reflect the rate and amount of biomass recycled by microbial communities. Maximum DIC values range from seawater concentrations for ultraoligotrophic SPG11, to >10 mM for mesotrophic sites, and significantly more for eutrophic sites (**Table 1**). Maximum NH_4 values range from below detection for the ultraoligotrophic SPG sites, to ca. 0.5–2 mM for mesotrophic sites, and to >3 mM for eutrophic sites (**Table 1**).

PHYLOGENY OF OLIGOTROPHIC ARCHAEA

A key problem in surveying the archaeal diversity of marine sediments is reliably defining phylogenetically meaningful groups. Long branch attraction, hyperthermophile high-GC convergence (Boussau and Gouy, 2006; Brochier-Armanet et al., 2008), and chimeric sequences in public databases (Hugenholtz and Huber, 2003; Ashelford et al., 2005) result in statistically poorly supported clades – often para- or polyphyletic on closer inspection – that are highly dependent on details of species selection, and have little use in a phylogenetic context, but that are nevertheless reported in the literature. A related complication is the proliferation of different names for equivalent groups or nearly equivalent groups, which hampers comparability of results. As an attempt to address some of these difficulties, we constructed phylogenies of the major archaeal lineages (**Figure 2**), of the Euryarchaeota (**Figures 3–5**) and Crenarchaeota (**Figure 6**), which reflect the nomenclature introduced by a range of studies (**Tables 2** and **3**). Although these phylogenies do not address the deep relationships between archaeal phyla, such as the placement of *Micrarchaeum* and *Parvarchaeum*, and the grouping of Archaeoglobi, Methanomicrobia, and Halobacteria, these phylogenies are similar to well-supported clades reported in previous studies (e.g., Brochier-Armanet et al., 2008; Baker et al., 2010). Particular attention was given to the Thermoplasmata (**Figure 5**), in an effort to distinguish phylogenetically valid clades, alongside the organic-rich-associated MBG-D clade, that occur in oligotrophic sediments. The phylogenetic structure of the uncultured Thermoplasmata, and other highly diversified groups, such as the MCG archaea, remains a work in progress.

ARCHAEAL OCCURRENCE TRENDS ACROSS SITES

Relative abundances of deeply branching Archaeal lineages in 16S rRNA gene clone libraries from oligotrophic and organic-rich sediments are compiled in **Figure 7**. These 16S rRNA gene clone library data should not be understood as accurate proportional representation of archaeal lineages in the environment; diverging methodologies, clone library size limitations and the resulting detection thresholds qualify what is subsequently called "abundance." High-throughput sequencing approaches are very likely to modify these initial clone library-based surveys (Biddle et al., 2008, 2011). Yet, the clone library data provide a window into distinctly different detection patterns of archaeal clades within

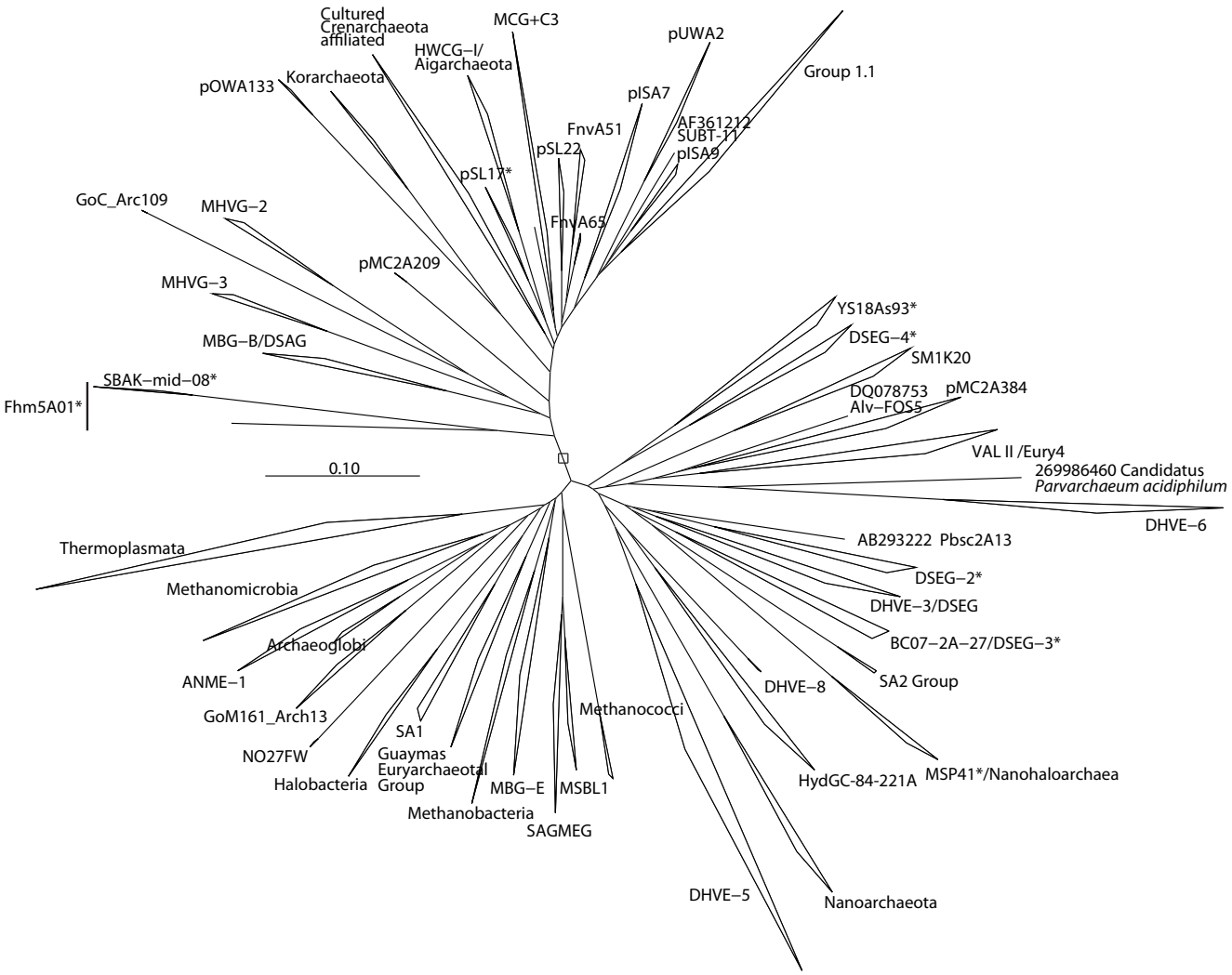

FIGURE 2 | Phylogenetic context of major phylum or class-level lineages of cultured and uncultured Archaea, as estimated by the ARB neighbor-joining algorithm. Sites with nucleotides at least 60% conserved within all Euryarchaeota included in the tree were used in the analysis for Euryarchaeota and Crenarchaeota together. Certain lineages, such as *Methanopyrus kandleri,* were excluded due to their tendency to attract hyperthermophiles to the base of the tree.

organic-lean and organic-rich sediments. All clades absent from eutrophic sites, or which occur at less than 1.5% relative abundance in any eutrophic site, are colored blue (numbers 1-16 in **Figure 7**). Those clades found only in the eutrophic end-member sites, or which occur in these sites at more than 1.5% frequency, are colored red. Overall, archaeal phyla that predominate either in the oligotrophic or in the eutrophic endmember sites are declining in relative abundance along environmental gradients of redox state, organic carbon content and biomass remineralization (**Figure 7**; **Table 1**). Dominant benthic archaeal groups of organic-rich sediments disappear in the most oxidized sediment environments, and vice versa.

A specific archaeal assemblage of MBG-B, MCG, SAGMEG and MBG-D archaea is found repeatedly in the eutrophic subsurface sediments of the Peru Margin (ODP sites 1227,1229), Peru Trench (ODP site 1230), Cascadia Margin (ODP sites 1244, 1245, 1251), and the highly reducing Mediterranean methane seeps, and also in the Gulf of Mexico 308 sites with mixed eutrophic/mesotrophic/oligotrophic characteristics. These uncultured archaeal lineages that are commonly detected in clone libraries (**Table 2**) should be congruent with the cren- and euryarcheotal proportion (15–45%) of phylogenetically informative pyrosequencing fragments in the Peru Margin and Brazos Basin metagenomes (Biddle et al., 2008, 2011). The archaeal groups that are typically found in eutrophic sediments also persist to a considerable extent into organic-leaner sediments. For example, MCG is found in all mesotrophic sites in the South China Sea, Fairway Basin, and ODP site 1226; MBG-B persists in the same sites in the mesotrophic spectrum, and also in ODP sites 1225 and 1231 (**Figure 7**). Some members of these and other archaeal clades that are typically found in anaerobic, eutrophic marine sediments also occur in reducing, non-marine habitats. For example, the MCG

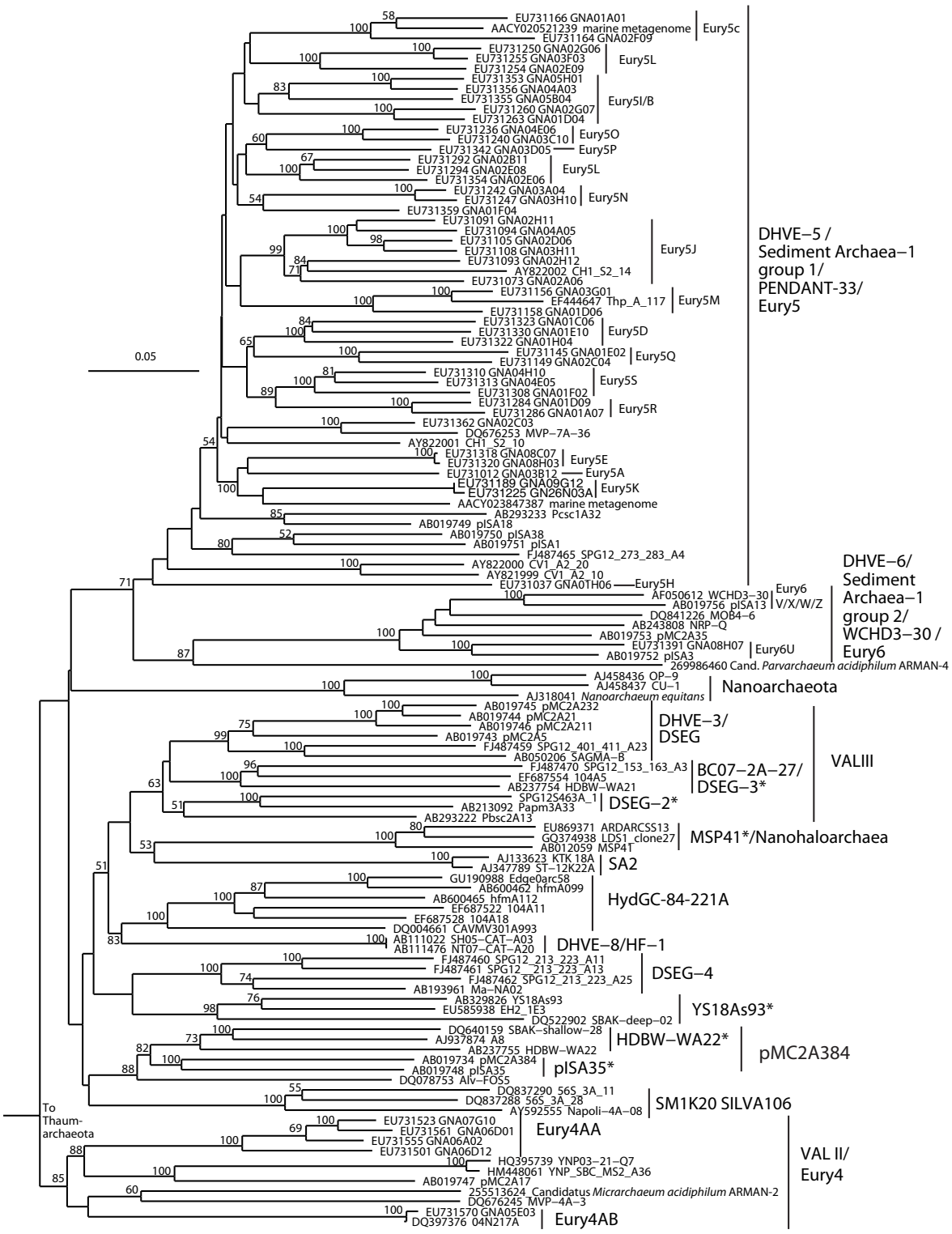

FIGURE 3 | Neighbor-joining 16S rRNA gene phylogeny of apparently deeply branching Euryarchaeota, designated DHVEG-II after Takai and Horikoshi (1999). Alignment size, filtered using the arch_ssuref mask available in ARB, is 1090 sites. Statistical support was estimated using 500 maximum likelihood bootstrap replications in TreeFinder (Jobb et al., 2004). Branches are annotated with names and acronyms that are used in the literature (**Table 3**). The archaeal taxa marked with asterisks are novel designations introduced either in Durbin and Teske, 2011 or in this study (**Table 3**).

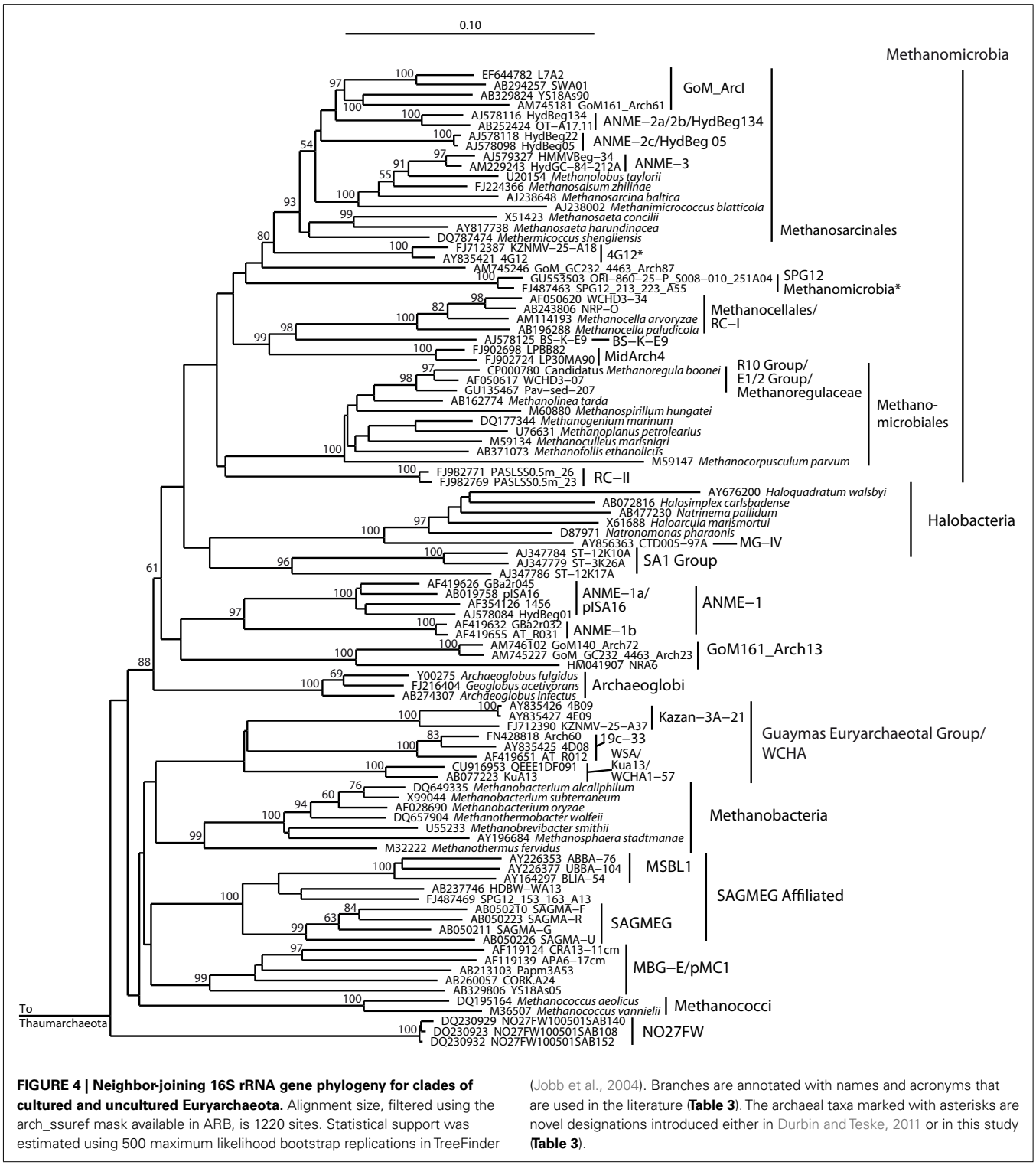

FIGURE 4 | Neighbor-joining 16S rRNA gene phylogeny for clades of cultured and uncultured Euryarchaeota. Alignment size, filtered using the arch_ssuref mask available in ARB, is 1220 sites. Statistical support was estimated using 500 maximum likelihood bootstrap replications in TreeFinder (Jobb et al., 2004). Branches are annotated with names and acronyms that are used in the literature (**Table 3**). The archaeal taxa marked with asterisks are novel designations introduced either in Durbin and Teske, 2011 or in this study (**Table 3**).

occurred in the anaerobic digestor and in several marine samples; the Guaymas Euryarchaeotal Group (Dhillon et al., 2005) was also found in the anaerobic digestor (Chouari et al., 2005) and in the Mediterranean methane seeps (Heijs et al., 2008); and methanogens were recovered in the rumen library and among the Peru Margin/Trench sequences.

The oligotrophic end of the sediment spectrum starts with an entirely different archaeal community. The most oligotrophic site featured in **Table 1** is SPG11, where oxygen is present throughout the measured sediment column and DIC (alkalinity) does not vary from seawater values (D'Hondt et al., 2009). All archaeal sequences recovered for this site were members of MG-I, and formed

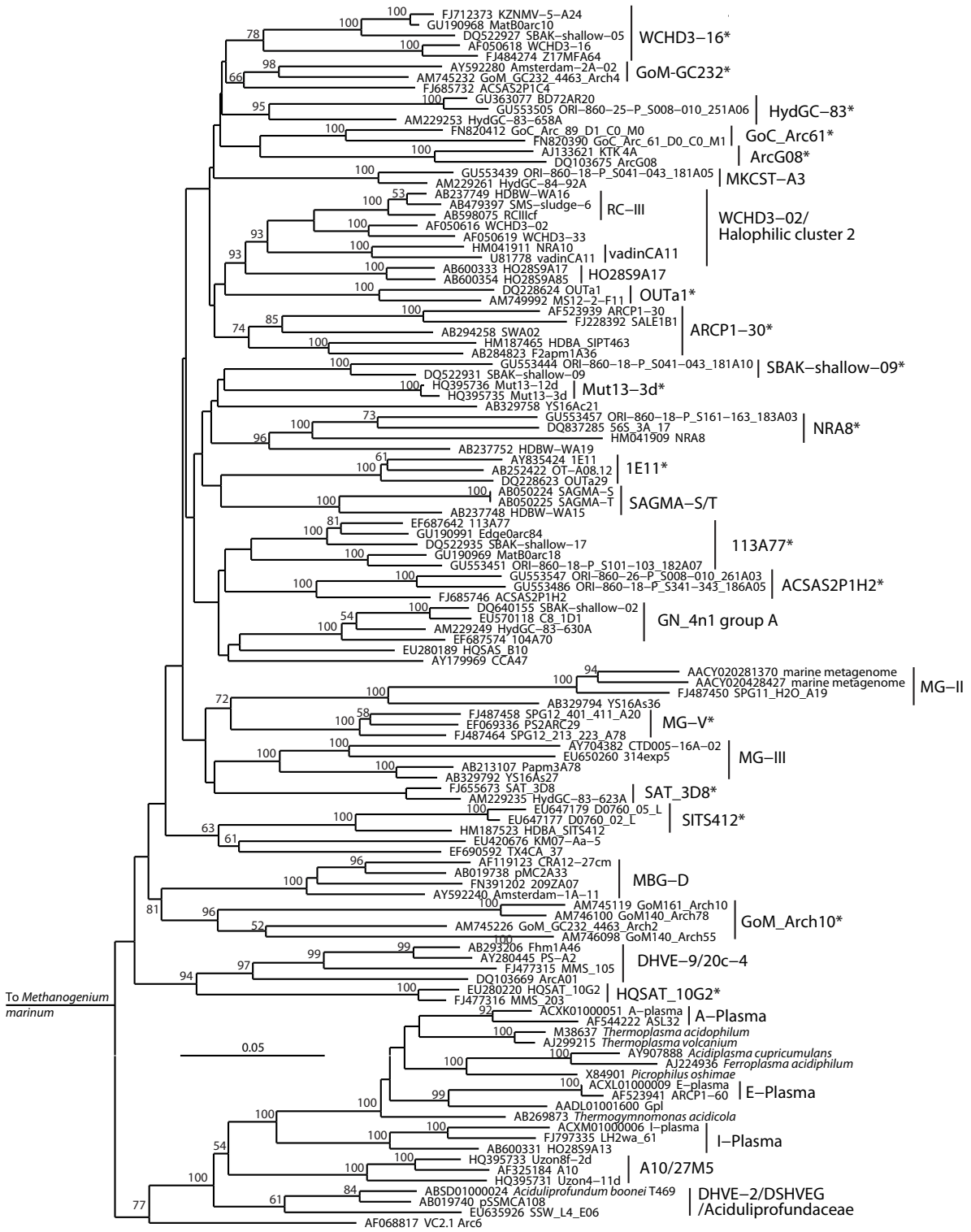

FIGURE 5 | Neighbor-joining 16S rRNA gene phylogeny of Thermoplasmata-affiliated monophyletic lineages in the Euryarchaeota. Alignment size, filtered using the arch_ssuref mask available in ARB, is 1145 sites. Statistical support was estimated using 500 maximum likelihood bootstrap replications in TreeFinder (Jobb et al., 2004). Branches are annotated with names and acronyms that are used in the literature (**Table 3**). The archaeal taxa marked with asterisks are novel designations introduced either in Durbin and Teske, 2011 or in this study (**Table 3**).

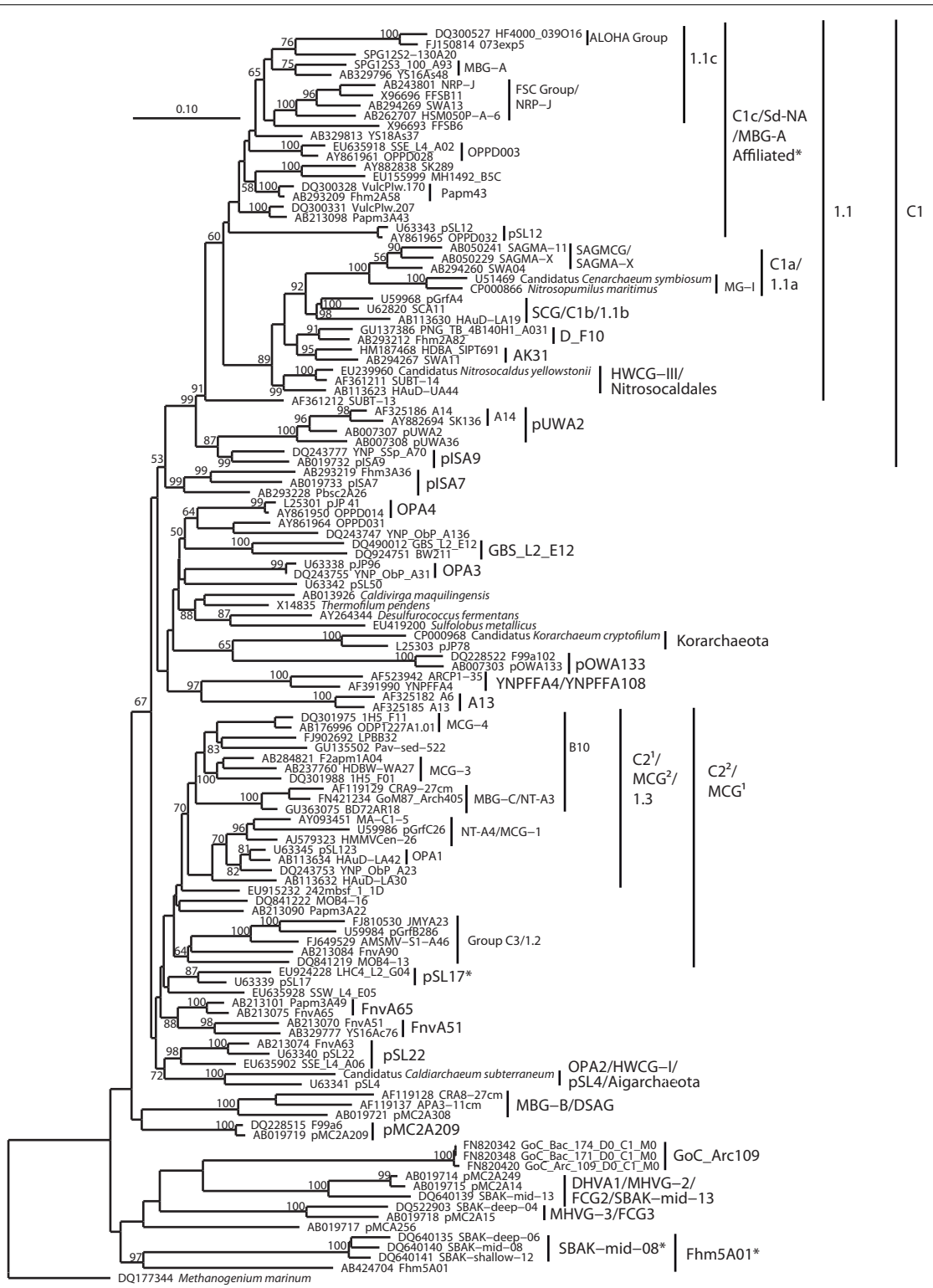

FIGURE 6 | Neighbor-joining 16S rRNA gene phylogeny of Crenarchaeota/Thaumarchaeota and associated deeply branching lineages. Alignment size, filtered using the arch_ssuref mask available in ARB, is 1177 sites. Bootstrap support was estimated using 500 maximum likelihood bootstrap replications in TreeFinder (Jobb et al., 2004). Branches are annotated with names and acronyms that are used in the literature (**Table 3**). The archaeal taxa marked with asterisks are novel designations introduced either in Durbin and Teske, 2011 or in this study (**Table 3**). Note that further MBG-B groups are defined in Robertson et al. (2009).

Table 2 | Relevant methodological features for the archaeal clone library studies compared in this review.

Study site	Extraction depths, mbsf	Extraction protocol	DNA or RNA?	Forward Primer	Reverse Primer	Primer annealing temp.˚C	Pre-screening	No. of clones, MG-I excluded	Reference
SPG12	0.60–4.11	S, BB, PC	DNA	8f	1492r	55	No	320	Durbin and Teske (2011)
ODP 201: Site 1231	1–43	S, BB, PC; S, EL, PC	DNA	8f ▶ 344f	1492r ▶ 915r	58	No	124	Sørensen et al. (2004)
ODP 201: Site 1225	1.5, 7.8	S, EL, PC	DNA	8f ▶ 8f	1492r ▶ 915r	58	No	18	Teske (2006)
ODP 201: Site 1226	1.3–45.2	S, BB	DNA	21f	915r	58	No	32	Biddle et al. (unpublished)
ZoNéCo-12	0.2–9.4	S, BB	DNA	8f ▶ 344f	1492r ▶ 915r	51 ▶ 57	No	280	Roussel et al. (2009)
MD05-2902	0.0–9.42	S, HT, HS, EL, PC	DNA	21f	958r	55	T-RFLP	1078	Wang et al. (2010a)
MD05-2896	0.05–11.03	S, HT, HS, EL, PC	DNA	21f	958r	55	T-RFLP	1212	Wang et al. (2010a)
IODP 308:									
Site 1319	4.3–76.9,	S, BB	DNA	21f	958r	50	No	287	Nunoura et al. (2009)
Site 1320	2.9–256.9		DNA						
ODP 201:	6.55–45.35,	S, BB, PC	RNA	8f	915r	58	No		Sørensen and Teske (2006)
Site 1227	1–50		DNA	21f	958r	50	No		Inagaki et al. (2006)
	37.8		RNA	8f	915r	58	No		Biddle et al. (2006)
ODP 201:	29.4, 86.8;	S, BB, PC	RNA	8f	915r	58	No		Biddle et al. (2006)
Site 1229	6.7–86.7		DNA	109f	958r	45-42	No		Parkes et al. (2005)
ODP 201:	11	S, BB, PC	RNA	8f	915r	58	No	1347	Biddle et al. (2006)
Site 1230	1–278		DNA	21f	958r	50	No		Inagaki et al. (2006)
ODP 204:									
Site 1244	0.45–129.2	S, BB	DNA	349f	806r	50	No	470	Nunoura et al. (2008)
Site 1245	157.9–194.7								
Site 1251	4.5–330.6								
Cold seeps:									
Napoli	0.0–0.28	S, BB, EL,	DNA	21f	1406r	57.5	No	237	Heijs et al. (2008)
Kazan	0.0–0.34	PC		21f ▶ 21f	1406 ▶ 958r				
Amsterdam	0.0–0.31			21f	1406r				
Outgroups:									
Anoxic digestor		HT, EL, PC	DNA	21f	1390r	59	No	271	Chouari et al. (2005)
Reindeer rumen		S, BB	DNA	Met86F	Met1340R	53	No	97	Sundset et al. (2009)

Extraction protocol column lists key features of nucleic acid extractions: S, use of sodium dodecyl sulfate as a membrane disruption agent; HT, high temperature (membrane disruptor); HS, high salt (membrane disruptor); BB, using of bead beating as means of cell lysis; EL, enzymatic cell lysis; PC, phenol–chloroform extraction and purification. If nested amplification was used, nested primer set is indicated by carrot; multiple primer sets used in parallel separated by comma. Pre-screening indicates whether entire clone libraries were sequenced, or phylotype abundances in clone libraries were extrapolated based on T-RFLP screening and sequencing of unique T-RFLP profiles. Primer references: 8f, 1492r, Teske et al. (2002); 21f, 915r, 958r, DeLong (1992); 1406r, Lane (1991); 1390r, Zheng et al. (1996); Met96F, Met1340R, Wright and Pimm (2003); 344f, Sørensen et al. (2004); 109f, Großkopf et al. (1998a); 349f, Takai and Horikoshi (2000).

sediment-specific clades within this lineage (Durbin and Teske, 2010). However, MG-I archaea also appear occasionally in very deep sediment samples (such as ODP1230; Inagaki et al., 2006) where they almost certainly represent seawater or drilling fluid contamination; for this reason, MG-I archaea are not included in **Figure 7**. The oligotrophic site SPG12 resembles SPG11 in the dominance of MG-1 archaea (subsurface clusters) in the upper sediment layers and lacks the typical archaea of eutrophic sites (MCG, MBG-B, MBG-D); only a single SAGMEG-related clone and two divergent Methanogen-affiliated clones were recovered from SPG12. The dominant archaea at SPG12, including MG-V, DSEG-2, DSEG-4, and the MBG-A-related lineages, were not recovered from any of the organic-rich sediments (**Figure 7**). ODP sites 1225 and 1231 resemble SPG12 geochemically and microbiologically. Their clone libraries include a significant proportion of groups found in organic-lean sites (DSEG-4, MBG-A), but also include some groups abundant at eutrophic sites (MBG-B).

Table 3 | Reference key to archaeal clade nomenclature in Figures 3–6.

Figure 3		Figure 4		Figure 5		Figure 6	
BC07-2A-27	DeSantis et al. (2006)	19c-33	SILVA 106	1E11	*Novel	1.1	Ochsenreiter et al. (2003)
DHVE-3	Takai and Horikoshi (1999)	4G12	*Novel	113A77	*Novel	1.2	Ochsenreiter et al. (2003)
DHVE-5	Takai and Horikoshi (1999)	ANME-1	Hinrichs et al. (1999)	20c-4	SILVA 106	1.3	Ochsenreiter et al. (2003)
DHVE-6	Takai and Horikoshi (1999)	ANME-1a	Teske et al. (2002)	27M5	DeSantis et al. (2006)	1.1a	Ochsenreiter et al. (2003)
DHVE-8	Nercessian et al. (2003)	ANME-1b	Teske et al. (2002)	A-Plasma	Dick et al. (2009)	1.1b	Ochsenreiter et al. (2003)
DSEG	Takai et al. (2001)	ANME-2C	Orphan et al. (2001)	A10	SILVA 106	1.1c	Ochsenreiter et al. (2003)
DSEG-2	*Durbin and Teske (2011)	ANME-3	Knittel et al. (2005)	ACSAS2P1C4	*Novel	A13	DeSantis et al. (2006)
DSEG-3	*Durbin and Teske (2011)	ANME-2a/2b	Orphan et al. (2001)	ACSAs2P1H2	*Novel	A14	DeSantis et al. (2006)
DSEG-4	*Durbin and Teske (2011)	BS-K-E9	SILVA 106	ArcG08	*Novel	AK31	SILVA 106
Eury4	Robertson et al. (2009)	E1/2 Group	Cadillo-Quiroz et al. (2006)	ARCp1-30	*Novel	Aloha Group	Pester et al. (2011)
Eury4AA	Robertson et al. (2009)	GoM_ArcI	SILVA 106	DHVE-2	Takai and Horikoshi (1999)	B10	McDonald et al. (2011)
Eury4AB	Robertson et al. (2009)	GoM161_Arch13	DeSantis et al. (2006)	DHVE-9	Pagé et al. (2004)	C1	Hugenholtz (2002)
Eury5	Robertson et al. (2009)	HA1-57	SILVA 106	DSHVEG	Takai et al. (2001)	C1a	Hugenholtz (2002)
Eury5c	Robertson et al. (2009)	HydBeg134	DeSantis et al. (2006)	E-Plasma	Dick et al. (2009)	C1b	Hugenholtz (2002)
Eury5D	Robertson et al. (2009)	Kazan-3A-21	SILVA 106	GN_4n1 group A	Jahnke et al. (2008)	C1c	Hugenholtz (2002)
Eury5E	Robertson et al. (2009)	Kua13	DeSantis et al. (2006)	GoC_Arc61*	*Novel	C21	Hugenholtz (2002)
Eury5H	Robertson et al. (2009)	MBG-E	Vetriani et al. (1999)	GoM_Arch10	*Novel	C22	DeSantis et al. (2006)
Eury5I/B	Robertson et al. (2009)	MG-IV	López-Garcia et al. (2001)	Halophilic cluster 2	Jahnke et al. (2008)	C3	Hales et al. (1996)
Eury5J	Robertson et al. (2009)	MidArch4	SILVA 106	HO28S9A17	SILVA 106	C3	Hugenholtz (2002)
Eury5K	Robertson et al. (2009)	MSBL1	Van der Wielen et al. (2005)	HQSAT_10G2	*Novel	D_F10	SILVA 106
Eury5L	Robertson et al. (2009)	NO27FW	DeSantis et al. (2006)	HydGC-83	*Novel	DHVA1	Takai and Horikoshi (1999)
Eury5L	Robertson et al. (2009)	pISA16	DeSantis et al. (2006)	I-Plasma	Dick et al. (2009)	DSAG	Takai et al. (2001)
Eury5M	Robertson et al. (2009)	pMC1	Hugenholtz (2002)	KM07	*Novel	FCG2	Hugenholtz (2002)
Eury5N	Robertson et al. (2009)	pMC1	DeSantis et al. (2006)	MBG-D	Vetriani et al. (1999)	FCG3	Hugenholtz (2002)
Eury5O	Robertson et al. (2009)	R10 Group	Hales et al. (1996)	MG-II	Fuhrman et al. (1992)	Fhm5A01	*Novel
Eury5P	Robertson et al. (2009)	RC-I	Groβkopf et al. (1998b)	MG-III	Fuhrman and Davis (1997)	FnvA51	DeSantis et al. (2006)
Eury5Q	Robertson et al. (2009)	RC-II	Groβkopf et al. (1998b)	MG-V	*Durbin and Teske (2011)	FnvA65	DeSantis et al. (2006)
Eury5R	Robertson et al. (2009)	SAGMEG	Takai et al. (2001)	MKCST-A3	SILVA 106	FSC Group	Takai et al. (2001)
Eury5S	Robertson et al. (2009)	SAGMEG-Affiliated	*Novel	Mut13-3d	*Novel	GBS_L2_E12	DeSantis et al. (2006)
Eury6	Robertson et al. (2009)	Methanomicrobia	*Durbin and Teske (2011)	NRA8	*Novel	GoC_Arc109	SILVA 106
Eury6U	Robertson et al. (2009)	WSA	Hugenholtz (2002)	OUTa1	*Novel	HWCG-I	Nunoura et al. (2005)
Eury6V/X/W/Z	Robertson et al. (2009)			SAGMA-S/T	Schleper et al. (2005)	HWCG-III	Nunoura et al. (2005)
HDBW-WA22	*Novel			SAT_3D8	*Novel	MBG-A	Vetriani et al. (1999)
HF-1	DeSantis et al. (2006)			SBAK-shallow-09	*Novel	MBG-A Affiliated	*Novel
HydGC-84-221A	McDonald et al. (2011)			SITS412	*Novel	MBG-B	Vetriani et al. (1999)
MSP41	*Novel			vadinCA11	DeSantis et al. (2006)	MBG-C	Vetriani et al. (1999)
Nanohaloarchaea	Narasingarao et al. (2012)						

PENDANT-33	Schleper et al. (2005)
pISA35	*Novel
pMC2A384	McDonald et al. (2011)
SA2	Eder et al. (2002)
Sediment Archaea-1 group 1	Hugenholtz (2002)
Sediment Archaea-1 group 2	Hugenholtz (2002)
SM1K20	SILVA 106
VAL II	Jurgens et al., 2000
VALIII	Jurgens et al., 2000
WCHD3-30	DeSantis et al. (2006)
YS18As93	*Novel
vadinCA11	SILVA 106
WCHD3-02	DeSantis et al. (2006)
WCHD3-16	*Novel
MCG-1	Inagaki et al. (2003)
MCG2	Inagaki et al. (2006)
MCG-1	Teske and Sørensen (2008)
MCG-3	Teske and Sørensen (2008)
MCG-4	Teske and Sørensen (2008)
MG-I	DeLong (1992)
MG-I	Fuhrman et al. (1992)
MHVG-2	Takai et al. (2001)
MHVG-3	Takai et al. (2001)
NRP-J	DeSantis et al. (2006)
NT-A3	Reed et al. (2002)
NT-A4	Reed et al. (2002)
OPA1	Hugenholtz (2002)
OPA2	Hugenholtz (2002)
OPA3	Hugenholtz (2002)
OPA4	Hugenholtz (2002)
OPPD003	SILVA 106
Papm43	SILVA 106
pISA7	DeSantis et al. (2006)
pISA9	DeSantis et al. (2006)
pMC2A209	SILVA 106
pOWA133	DeSantis et al. (2006)
pSL12	SILVA 106
pSL17	*Novel
pSL22	DeSantis et al. (2006)
pSL4	DeSantis et al. (2006)
pUWA2	DeSantis et al. (2006)
SAGMA-X	DeSantis et al. (2006)
SAGMCG	Takai et al. (2001)
SBAK-mid-08	*Novel
SBAK-mid-13	DeSantis et al. (2006)
SCG	Takai et al. (2001)
Sd-NA	DeSantis et al. (2006)
YNPFFA4/ YNPFFA108	DeSantis et al. (2006)

The GreenGene nomenclature (DeSantis et al., 2006) is derived from the November 2008 GreenGenes version (see Methods); some clades are based on the 2011 version (McDonald et al., 2011).

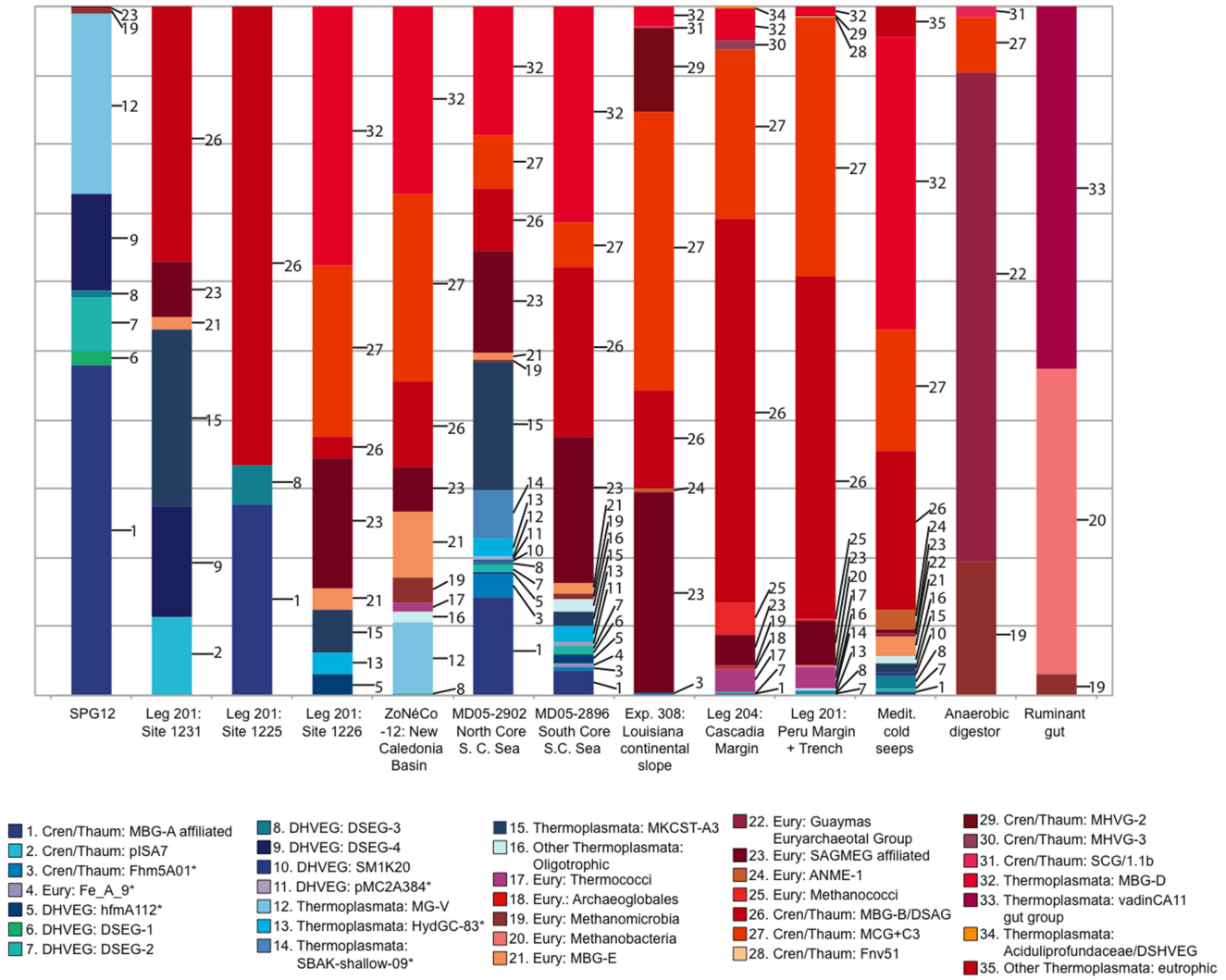

FIGURE 7 | Representation of archaeal lineages in 16S rRNA gene clone libraries across a spectrum of oligotrophic to eutrophic marine subsurface sediments. The sites are arranged from oligotrophic (left) to eutrophic (right). Clades 1–16, colored blue, were either entirely absent from eutrophic sites, or comprised less than 1.5% of total clones in any eutrophic site. Some archaeal datasets were pooled from multiple sites of a geographic region (Brazos Basin, Peru Margin/Trench, Cascadia Margin, Mediterranean seeps). For Peru Margin/Trench sites, sequences labeled "Thermococci" (Inagaki et al., 2006) also include an unspecified number of Methanococci. As outgroup examples of anaerobic, extremely organic-rich environments, an anaerobic wastewater digestor (Chouari et al., 2005) and a ruminant foregut (Sundset et al., 2009) are included.

The intermediate, mesophilic spectrum includes ODP site 1226, and the South China and Coral Sea sites. In comparison to oligotrophic sites, these sites yielded a smaller proportion of lineages typical for organic-lean sites, congruent with more organic-rich habitat characteristics. As a caveat, the South China and Coral Sea cores are relatively shallow; deeper coring and sampling in these locations might impact the archaeal diversity results. The impact of shallow sampling can be seen in the detection of organic-lean archaeal lineages in the Mediterranean cold seep dataset, attributable to the shallow horizons sampled as well as the geochemically heterogeneous nature of cold seeps that are surrounded by organic-lean deep-sea sediments (**Figure 7**).

Despite these complications, the proportion of lineages common in organic-lean sediments decreases as measures of sediment organic richness increase. Certain archaeal clades occur – in changing configuration – in oligotrophic sediments, but do not occur or occur only rarely in eutrophic sediments. There are three likely drivers of such a changes in community composition:

(1) Refractory organic matter. Organic matter changes significantly in composition and quantity during sinking, and is expected to become more refractory overall after passage through the deep-sea water column (Wakeham et al., 1997). Microbes that can metabolize the highly refractory substrates in oligotrophic sediments where competition for electron donors is strong would have an advantage over microbes not able to use these substrates.

(2) Low sedimentation rates. Oligotrophic sediments are primarily characterized by slow sedimentation rates, leading to a low substrate flux for microbes and hence energy limitation. As the incoming carbon substrates are microbially degraded, increasingly recalcitrant compounds become enriched.
(3) Deep permeation of high-energy electron acceptors. Since decreasing sedimentation and carbon flux leads to slower depletion of electron acceptors, energy-rich electron acceptors (oxygen, nitrate) permeate a larger depth range of the sediment column in oligotrophic sediments, in contrast to the surficial sediments to which they are confined otherwise. Thus, some subsurface Archaea may specialize in the electron acceptor that maximizes the energy yield for a given substrate, and this leads to the predominance of specific archaeal lineages in oligotrophic sediments.

These variables are expected to be congruent to some degree. It also seems likely that some combination of these three factors determines community composition: while electron acceptor specialization may be a determinative factor for one group, another group may thrive since it uses a particularly recalcitrant carbon substrate.

This discussion of low-energy adaptations of microbial cells in oxidized, oligotrophic sediments should not distract from the fact that low-energy adaptations should also apply to microorganisms in organic-rich subsurface sediments where the lack of high-energy electron acceptors and of fresh carbon substrates impose very low free-energy fluxes at or near maintenance-energy requirements (Lever et al., 2010), such that microbial activity persists in sediment horizons over geological time scales (Parkes et al., 2005) and sustains very slow biomass turnover on time frames ranging from years to millennia (Jørgensen, 2011). The different archaeal communities in oligotrophic and eutrophic sediments should not be viewed in terms of simplistic "low-energy vs. high energy" habitat characteristics; instead, the distinct reduction potentials, substrate spectra, electron donors, and acceptors in oligotrophic and eutrophic sediment environments determine which catabolic, carbon-fixing, and biosynthetic pathways are feasible (McCollom and Amend, 2005).

ASSOCIATION OF ARCHAEAL LINEAGES WITH HIGH-ENERGY ELECTRON ACCEPTORS

The link between redox specialization and specific benthic archaeal lineages is not limited to sedimentary habitats: archaeal clades typical for oligotrophic sediments appear frequently in other oxic or suboxic environments, and less often in anoxic environments. In other words, mutually independent clone library surveys demonstrate that a given archaeal lineage is preferentially found in a particular redox environment. **Figure 8** shows the number of different studies that have recovered a given lineage from a particular redox

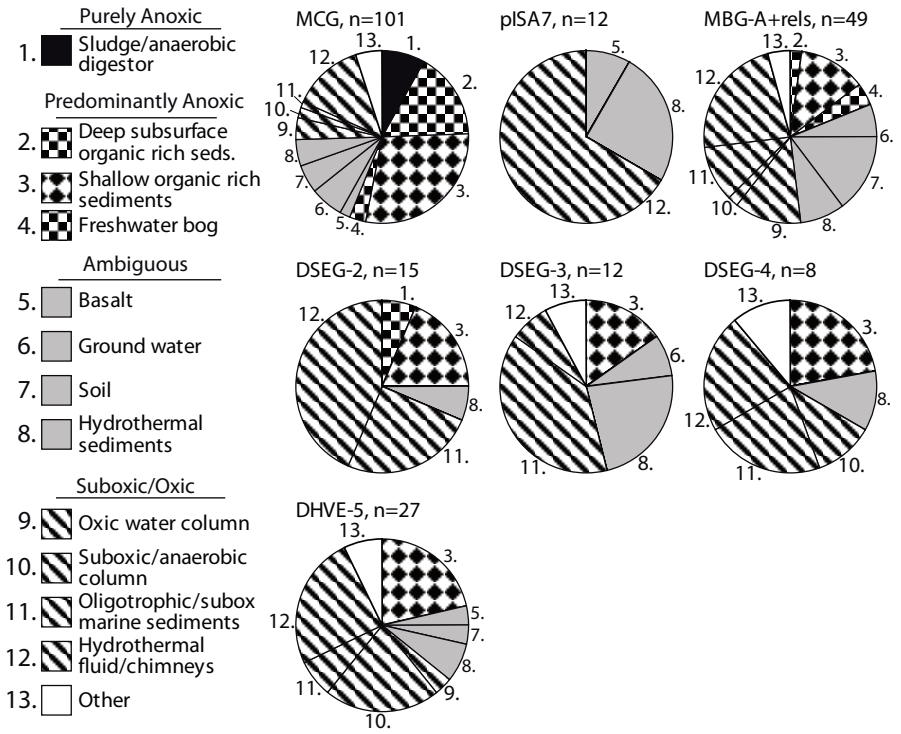

FIGURE 8 | Habitat–lineage association showing the number of different studies that have recovered oligotrophic lineages that are rarely or not found in eutrophic sediments from a particular redox environment. All sequences belonging to the relevant clades in SILVA SSU Ref V.95 (Pruesse et al., 2007) were examined by counting each instance of a clade being recovered within a specific study and habitat; the habitats were then cataloged and categorized as anoxic, oxic/suboxic, or ambiguous in cases of uncertain or heterogeneous redox status. See text for explanation of habitat redox categorization.

environment, for all relevant sequences in the SILVA SSU Ref v.95 database (Pruesse et al., 2007). Based on geochemical metadata for each sequence data set, the redox status of the environments considered was conservatively identified as purely anoxic, predominantly anoxic, ambiguous, and suboxic/oxic (**Figure 8**). Methodological biases inherent in DNA extraction method, PCR primer selection and cloning methodology rule out a strict proportionality of geochemical regime to clone library membership and relative abundance (Teske and Sørensen, 2008). Therefore, these cumulative presence/absence data can be thought of as "averaging" of experimental variability associated with PCR surveys of microbial diversity.

Notably, lineages from oxidized, organic-lean sediments have not been recovered from purely anoxic environments such as anaerobic digestors, indicating basic physiological incompatibility (**Figure 8**). However, some predominantly anoxic sites, mostly shallow organic-rich sediments, harbor lineages that are commonly found in oxidized sediments (**Figure 8**). These organic-rich sediment environments can be distinguished from the purely anoxic environments (such as anoxic bioreactors) because they often have oxidized niches or micro-environments that co-occur with anoxic niches (e.g., Jørgensen, 1977; Mäkelä and Tuominen, 2003; Jørgensen et al., 2005; Glud, 2008), particularly for near-shore marine sediments where weathering mineral input may introduce significant quantities of metal oxides (Poulton and Raiswell, 2002). These permeable boundaries between sediment habitat types might also work the other way around. For example, a key component of organic-rich, reduced marine subsurface sediments, the MCG archaea, also occur in freshwater bogs and in surficial, partially oxidized sediments (Kubo et al., 2012).

Hydrothermal fluids are often highly reduced and anoxic at their source, but turn more oxidized within the thermally habitable mixing gradient between an anoxic, hydrothermal source fluid, and an oxic endmember such as seawater, oxygenated groundwater, or atmosphere-exposed surface water (e.g., Amend and Shock, 1998; Teske et al., 2002; Spear et al., 2005; Dias and Barriga, 2006; Rogers and Amend, 2006). As a consequence of hydrothermal convection and seawater admixture, archaeal lineages that are associated with oxidized, organic-lean sediments could thrive in the shallow, partially mixed and partially oxidized vent subsurface, and are then frequently recovered from hydrothermal fluids (**Figure 8**). The second largest group of source habitats for these archaeal lineages that tolerate partially oxidized conditions are environments with heterogeneous or variable redox states, such as soil (Conrad, 1996), ground water (Jakobsen, 2007), and surficial hydrothermally influenced sediments and mineral deposits permeated by hydrothermal fluid (Teske et al., 2002; Nercessian et al., 2005; Dias and Barriga, 2006; Severmann et al., 2006). These habitats provide access to high-energy electron acceptor niches.

Thus, partially oxidized environments, including oxic/suboxic sediments or water column, and the redox-oscillating environments of hydrothermal fluids and chimney surfaces, account for a majority or plurality of detection of organic-lean archaeal lineages, such as the pISA7 Crenarchaeotal and the DHVEG-II Euryarchaeotal lineages (**Figure 8**). As a caveat, these trends are suggestive but require consistency checks over increasingly fine-grained phylogenetic scales; minority clades within lineages may have metabolisms that are atypical for that lineage. The observed patterns also reflect uncertainty in identifying the exact redox state of the environment from which the clone was recovered, particularly problematic for datasets with sketchy or unspecific sequence-source descriptions. With these limitations, these results are again compatible with a metabolism requiring high-energy electron acceptors and oxidized redox conditions for the archaeal lineages from organic-lean habitats.

PROBLEMS AND PROSPECTS FOR FUTURE RESEARCH

Considerable uncertainty remains regarding the phylogeographic trends described and their putative link to environmental redox state. Principally, these uncertainties revolve around the familiar problems of primer and PCR bias, the significant variation in availability of key geochemical measurements, and the meager database especially at the oligotrophic end of the spectrum. Improving the cross-comparability of 16S rRNA survey data would require consistent molecular methodology as well as unified geochemical metadata across a wide range of marine sediment environments; this problem is acute in large-scale molecular surveys of the marine microbial world (Zinger et al., 2011). New sampling sites with good metadata, for example the oligotrophic sediments of North Pond underlying the North Atlantic subtropical gyre, are being explored (Ziebis et al., 2012) and will enlarge the molecular database as well. Additional evidence from cultivations, genome sequencing, and environmental genomics, is needed to further query the functional repertoire of archaeal 16S rRNA lineages. For example, genome analysis, enrichments, and cultivations of Thaumarchaeota (MGI archaea) suggest an ammonia-oxidizing metabolism for this archaeal lineage (Pester et al., 2011), a conclusion at least partially consistent with the largely suboxic/microoxic habitat preferences of the MG-I-related lineages discussed here.

Detailed environmental 16S rRNA surveys and geochemical measurements are complementary to genomic and cultivation approaches, given that neither genomics nor cultivations currently are capable of delivering the phylogenetic resolution or coverage of 16S rRNA surveys. Using such surveys and comprehensive geochemical datasets as hypothesis-generating and -refining tools, one can better constrain the putative redox adaptation of different microbial clades, and thus the role redox adaptation may play as an evolutionary force that shapes the biogeography of deep 16S rRNA clades. One approach would be to examine the hierarchical level at which phylogenetic lineages assort between sediments where the same electron acceptors persist in different environmental contexts, e.g., the spatially expanded suboxic/oxic strata of abyssal sediments and the spatially compressed suboxic/oxic strata perched on top of deep anoxic sediments, or even metal oxides persisting into euxinic sediments. This would allow examination whether factors such as reductant/oxidant concentration or sediment redox potential, as distinct from electron acceptor availability, play key roles in redox adaptation, possibly in determining the type of biosynthetic pathways utilized.

Big-picture studies examining the deep phylogeography of microbes have established that deeply rooted clades indeed assort according to habitat (von Mering et al., 2007), and have additionally revealed several factors that may explain some of the variance observed in archaeal biogeography, with the most

important habitat-defining distinctions being salinity and terrestrial vs. aquatic (Auguet et al., 2010). Microbial biogeography has also been explored by focusing on a specific subset of environmental parameters that are hypothesized to determine habitat specialization, revealing, for example, that carbon lability differences between soils correlate with the relative abundance of different bacterial phyla, observations which are in line with hypotheses about the physiology of "copiotroph" or "oligotroph" organisms (Fierer et al., 2007). In a similar fashion, the current review proceeds from the hypothesis that marine sediments of different redox state represent different habitat niches for microbes, and examines the patterns of community membership and abundance across these putative distinct habitats. The definition of distinct redox habitats implies specific microbial activities and physiologies in each habitat; thus, working hypotheses on microbial function emerge from the analysis of diversity patterns across these habitats. However, when comparing different environments defined operationally by one or a few variables, it should be kept in mind that other parameters may co-vary. For example, the freshwater–saltwater biogeographic divide which appears to be rarely crossed in evolution (Logares et al., 2009; Auguet et al., 2010) could be maintained due to differences in exterior osmotic pressure, sulfur compound availability, carbonate speciation, pH, or biosynthetic requirements. Caution in overinterpreting the functional significance of biogeographic patterns is warranted.

CONCLUSION

Archaeal communities undergo a marked shift along gradients of sediment trophic state. Archaeal lineages found in oligotrophic, oxidized sediments significantly expand the higher-order taxonomic diversity within the Archaea. These lineages have most often been found in other environments that are suboxic or oxic, with some proportion occupying habitats of ambiguous redox state, or primarily anoxic habitats that contains partially oxidized microniches (organic-rich surficial sediments). Such a lineage distribution is consistent with redox specialization determining in large part the distribution of archaeal lineages in the marine subsurface. Since the phylogenetic groups associated with this diversity shift were deeply branching (possibly class or phylum level), redox specialization could represent a fundamental correlate with deep phylogenetic diversification within the archaeal domain. Further studies are needed to resolve the phylogenetic placement of these novel lineages, as well as to explore the how the defining characteristics of oligotrophic sediments – nutrient limitation, oxidized environmental redox state, and availability of high-energy electron acceptors – have shaped archaeal evolution.

METHODS FOR SAMPLING, NUCLEIC ACID EXTRACTION, AND DIVERSITY ANALYSIS

This study reanalyzes archaeal 16S rRNA sequences from gravity cores at site SPG12, sampled during Cruise Knox02RR to the South Pacific Gyre (D'Hondt et al., 2009; Durbin and Teske, 2010, 2011). Additional published sequences from different marine sediments were used for this study (**Table 2**); the published sampling procedures are briefly summarized here. Archaeal 16S rRNA gene sequences for the Mediterranean cold seeps were derived from the upper 20–30 cm sediments, which were subsampled from a box core using aluminum cores and divided into two or three subsections before freezing (Heijs et al., 2008). Samples from the South China Sea were retrieved via gravity coring and subsampling from the center of the split cores (Wang et al., 2010a), while sediments from the Coral Sea were sampled via piston core and aseptically subsampled (Roussel et al., 2009). Archaeal 16S rRNA gene sequences from SPG12 were extracted and amplified from sediments subsampled from gravity core sections using a sterilized cut-off syringe, at a sampling resolution of 10 cm. Archaeal 16S rRNA gene sequences for the Gulf of Mexico IODP 308 samples were obtained from advanced piston-cored and XCB-cored sediments at depth horizons 4.45, 12.0, and 77 m of the Brazos Basin core U1319A; and at four depths (2.9, 7.4, 13.9, and ca. 28m) within the sulfate-reducing zone, and 92.4, 226.9, and 256.0 m of Brazos Basin core U1320A (Nunoura et al., 2009). Archaeal 16S sequences for the Peru Margin ODP sites were derived from the upper sulfate-methane transition zone (SMTZ) at site 1227 (37.8 mbsf, Biddle et al., 2006; 35.35, 34.25, 37.75, and 40.35 mbsf, Sørensen and Teske, 2006), as well as intervals above and below the SMTZ (6.55, 7.35, 21.35, 45.35 mbsf; Sørensen and Teske, 2006). Sequences from site 1229 were obtained from the upper and lower SMTZs at 29.4/30.2 and 86.8/86.67, mbsf respectively (Parkes et al., 2005; Biddle et al., 2006), as well as from 6.7 and 42.03 mbsf (Parkes et al., 2005). Site 1230 was sampled at 11.0 mbsf near the SMTZ (Biddle et al., 2006). ODP site 1226 was sampled from approximately 1.3, 7.2, 26.2, and 45.2 mbsf; methane and sulfate coexist throughout the sediment column and suggest that both methanogenesis and sulfate reduction occur. Finally, ODP sites 1244, 1245, and 1251 were sampled mostly below the SMTZ, from 0.45, 6.7, 16.2, 31.2, and 129.2 mbsf (1244), 157.9 and 194.7 mbsf (1245), and 4.5, 22.7, 43.2, 64.2, 82.7, 104.5, 123.1, 142.2, 169.9, 179.9, 204.2, 228.2, and 330.6 mbsf (Nunoura et al., 2008).

DIVERSITY SURVEY METHODS

While all studies used slightly different nucleic acid extraction protocols (**Table 2**), most involved chemical cell-membrane disruption with sodium dodecyl sulfate (SDS), mechanical membrane disruption with bead beating, and phenol–chloroform extraction (e.g., Zhou et al., 1996). The sites with the largest sample size and most extensive geochemical data, i.e., SPG12, the Peru Margin and Peru Basin sites, and the Mediterranean cold seeps, all used some variation of a SDS/bead beating/phenol–chloroform based extraction protocol, although some sequences from 1231 were only amplified using an enzymatic-lysis + SDS based extraction (Sørensen et al., 2004). Primers used for 16S rRNA gene amplification differed within and between oligotrophic, mesotrophic, and eutrophic sediments. Primer and PCR bias undoubtedly plays an important, but unknown role in the between-library differences observed for all libraries. Finally, although amplicon size has been shown to influence clone library composition, all amplicons considered here fell into a size range from 850 or 900 nucleotides to 1500 nucleotides (**Table 2**) in which variation in amplicon size minimally impacts clone library composition (Huber et al., 2009).

DATABASE SEARCHES AND PHYLOGENETIC IDENTIFICATION

A search for all available Archaeal 16S sequences from oligotrophic marine sediment sites was conducted first by identifying closest relatives to SPG12 Archaeal sequences via BLAST searches and searches within the ARB v.95 REF 16S/18S database (Pruesse

et al., 2007). If a sequence was derived from an oligotrophic sediment environment, defined as any marine benthic environment not situated on a continental slope or shelf, all sequences from the associated publication were imported and aligned in ARB (Ludwig et al., 2004). Any closest relatives presented in the associated publication were also imported and aligned. Further internet searches using keywords yielded no additional publications. Studies with archived sequence reads or published abundances of representative phylotypes were then used for comparative analysis. The archaeal ARB file is available from the authors on request (amdurbin@gmail.com; teske@email.unc.edu) or online at http://jmartiny.bio.uci.edu/lab/Data.html.

For all earlier clades subsumed by a later taxonomy, the original definition is depicted, unless the later, subsuming taxonomy significantly expanded or changed the original definition, in which case both are depicted; however, only phylogenetically valid clades were depicted. For example, the GreenGene 2006/2008 taxonomy (DeSantis et al., 2006) subsumed some identical taxonomic designations of Hugenholtz (2002); when valid clades shared the same name but phylogenetically differed between these two taxonomies, both definitions are given. We used the GreenGenes taxonomy according to the November 2008 GreenGenes version (greengenes236469.arb.gz, downloadable from http://greengenes.lbl.gov/Download/Sequence_Data/Arb_databases/), which differed from the original GreenGenes release (DeSantis et al., 2006) by adding a few novel designations. The GreenGenes 2011 release differed substantially from the 2008 release in that it removed many GreenGenes 2008 designations, and added, modified, or kept unmodified relatively few. In this case, only the 2011 additions or modifications were noted according to their 2011 definitions (McDonald et al., 2011), while those designations common to both versions were noted according to the GreenGenes 2008 release (**Table 3**).

For the Thermoplasmata-affiliated sequences (**Figure 5**), a lack of monophyletic clades defined for this group was addressed via an extensive analysis including all diversity represented by 16S rRNA gene sequences >1000 bp available in SILVA v.106. In constructing this tree, the primary goal was to create the deepest stable clades achievable using an alignment ~1000 bp and minimal chimera screening beyond that already performed by SILVA's Pintail screening, by removing sequences that appear to destabilize clades, avoiding clades with shallow internal branch lengths relative to terminal branch lengths. After amending monophyletic clades with new sequences, the newly populated and expanded clade should be as consistent as its earlier version, with stable bootstrap support and with the same intergroup distance to the neighbor clades. Statistical support was estimated with 500 maximum likelihood bootstrap replications using TreeFinder (Jobb et al., 2004).

ACKNOWLEDGMENTS

This study was supported by the NASA Astrobiology Institutes "Environmental genomes" (NCC 2-1054), "Subsurface biospheres" (NCC 2-1275), and by NSF (NSF-Ocean Drilling Program 0527167). Andreas Teske was further supported by a Hanse Institute Fellowship, and by the Center for Dark Energy Biosphere Investigations (C-DEBI). We thank Jennifer Biddle, Amanda Martino, and Chris House for the summary on the archaeal communities in ODP site 1226 (**Figure 4**), and Marc Alperin for a thoughtful reading of the manuscript.

REFERENCES

Agogué, H., Brink, M., Dinasquet, J., and Herndl, G. J. (2008). Major gradients in putatively nitrifying and non-nitrifying Archaea in the deep North Atlantic. *Nature* 456, 788–792.

Amend, J. P., and Shock, E. L. (1998). Energetics of amino acid synthesis in hydrothermal ecosystems. *Science* 281, 1659–1662.

Ashelford, K. E., Chuzhanova, N. A., Fry, J. C., Jones, A. J., and Weightman, A. J. (2005). At least 1 in 20, 16S rRNA sequence records currently held in public repositories is estimated to contain substantial anomalies. *Appl. Environ. Microbiol.* 71, 7724–7736.

Auguet, J.-C., Barberan, A., and Casamayor, E. O. (2010). Global ecological patterns in uncultured Archaea. *ISME J.* 4, 182–190.

Baker, B. J., Comolli, L. R., Dick, G. J., Hauser, L. J., Hyatt, D., Dill, B. D., Land, M. L., VerBerkmoes, N. C., Hettich, R. L., and Banfield, J. F. (2010). Enigmatic, ultrasmall, uncultivated archaea. *Proc. Natl. Acad. Sci. U.S.A.* 107, 8806–8811.

Berner, R. A. (1981). A new geochemical classification of sedimentary environments. *J. Sed. Petrol.* 51, 359–365.

Biddle, J. F., Fitz-Gibbon, S., Schuster, S. C., Brenchley, J. E., and House, C. H. (2008). Metagenomic signatures of the Peru Margin subseafloor biosphere show a genetically distinct environment. *Proc. Natl. Acad. Sci. U.S.A.* 105, 10583–10588.

Biddle, J. F., Lipp, J. S., Lever, M. A., Lloyd, K. G., Sørensen, K. B., Anderson, R., Fredricks, H. F., Elvert, M., Kelly, T. J., Schrag, D. P., Sogin, M. L., Brenchley, J. E., Teske, A., House, C. H., and Hinrichs, K.-U. (2006). Heterotrophic Archaea dominate sedimentary subsurface ecosystems off Peru. *Proc. Natl. Acad. Sci. U.S.A.* 103, 3846–3851.

Biddle, J. F., White, J. R., Teske, A. P., and House, C. H. (2011). Metagenomics of the subsurface Brazos-Trinity Basin (IODP site 1320): comparison with other sediment and pyrosequenced metagenomes. *ISME J* 5, 108–1047.

Boussau, B., and Gouy, M. (2006). Efficient likelihood computations with nonreversible models of evolution. *Syst. Biol.* 55, 756–768.

Brochier-Armanet, C., Boussau, B., Gribaldo, S., and Forterre, P. (2008). Mesophilic Crenarchaeota: proposal for a third archaeal phylum, the Thaumarchaeota. *Nat. Rev. Microbiol.* 6, 245–252.

Cadillo-Quiroz, H., Brauer, S., Yashiro, E., Sun, Christine, Yavitt, J., and Zinder, S. (2006). Vertical profiles of methanogenesis and methanogens in two contrasting acidic peatlands in central New York State, USA. *Environ. Microbiol.* 8, 1428–1440.

Chouari, R., Le Paslier, D., Dauga, C., Daegelen, P., Weissenbach, J., and Sghir, A. (2005). Novel major bacterial candidate division within a municipal anaerobic sludge digester. *Appl. Environ. Microbiol.* 71, 2145–2153.

Church, M. J., DeLong, E. F., Ducklow, H. W., Karner, M. B., Preston, C. M., and Karl, D. M. (2003). Abundance and distribution of planktonic Archaea and Bacteria in the waters west of the Antarctic Peninsula. *Limnol. Oceanogr.* 48, 1893–1902.

Conrad, R. (1996). Soil microorganisms as controllers of atmospheric trace gases (H_2, CO, CH_4, OCS, N_2O, and NO). *Microbiol. Rev.* 60, 609–640.

DeLong, E. F. (1992). Archaea in coastal marine environments. *Proc. Natl. Acad. Sci. U.S.A.* 89, 5685–5689.

DeSantis, T. Z., Hugenholtz, P., Larsen, N., Rojas, M., Brodie, E. L., Keller, K., Huber, T., Dalevi, D., Hu, P., and Andersen, G. L. (2006). Greengenes, a chimera-checked 16S rRNA gene database and workbench compatible with ARB. *Appl. Environ. Microbiol.* 72, 5069–5072.

Dhillon, A., Lever, M., Lloyd, K., Albert, D. B., Sogin, M. L., and Teske, A. (2005). Methanogen diversity evidenced by molecular characterization of methyl coenzyme M reductase A (mcrA) genes (mcrA) in hydrothermal sediments of the guaymas basin. *Appl. Environ. Microbiol.* 71, 4592–4601.

D'Hondt, S., Jørgensen, B. B., Miller, D. J., Batzke, A., Blake, R., Cragg, B. A., Cypionka, H., Dickens, G. R., Ferdelman, T., Hinrichs, K.-U., Holm, N. G., Mitterer, R., Spivack, A., Wang, G., Bekins, B., Engelen, B., Ford, K., Gettemy, G., Rutherford, S. D., Sass, H., Skilbeck, C. G., Aiello, I. W., Gurin, G., House, C. H., Inagaki, F., Meister, P., Naehr, T., Niitsuma, S., Parkes, R. J., Schippers, A., Smith, D. C., Teske, A., Wiegel, J., Padilla, C. N., and Acosta, J. L. S. (2004). Distribution of microbial activities in deep subseafloor sediments. *Science* 306, 2216–2221.

D'Hondt, S., Rutherford, S., and Spivack, A. J. (2002). Metabolic activity of subsurface life in deep-sea sediments. *Science* 295, 2067–2070.

D'Hondt, S., Spivack, A. J., Pockalny, R., Ferdelman, T. G., Fischer, J. P., Kallmeyer, J., Abrams, L. J., Smith, D. C., Graham, D., Hasiuk, F., Schrum, H., and Stancin, A. M. (2009). Subseafloor sedimentary life in the South Pacific Gyre. *Proc. Natl. Acad. Sci. U.S.A.* 106, 11651–11656.

Dias, A. S., and Barriga, F. J. A. S. (2006). Mineralogy and geochemistry of hydrothermal sediments from the serpentinite-hosted Saldanha hydrothermal field (36°34′N; 33°26′W) at MAR. *Mar. Geol.* 225, 157–175.

Dick, G. J., Andersson, A. F., Baker, B. J., Simmons, S. S., Thomas, B. C., Yelton, A. P., and Banfield, J. F. (2009). Community-wide analysis of microbial genome sequence signatures. *Genome Biol.* 10, R85.

Dickens, G., Exon, N., Holdway, D., Lafoy, Y., Auzende, J. M., Dunbar, G., and Summons, R. (2001). *Quaternary Sediment Cores from the Southern Fairway Basin on the Northern Lord Howe Rise (Tasman Sea)*, AGSO–Geoscience Australia, Record 2001/31. Canberra, Australia.

Dunne, J. P., Sarmiento, J. L., and Gnanadesikan, A. (2007). A synthesis of global particle export from the surface ocean and cycling through the ocean interior and on the seafloor. *Global Biogeochem. Cycles* 21, GB4006.

Durbin, A. M., Biddle, J. F., Martino, A., House, C., Fischer, J., Spivack, A., Schrum, H., D'Hondt, S., and Teske, A. (2009). Microbial community stratification in TOC-depleted marine subsurface sediments of the Pacific Ocean. *Geochem. Cosmochim. Acta* 73 (Suppl.), A316.

Durbin, A. M., and Teske, A. (2010). Sediment-associated microdiversity within the Marine Group I Crenarchaeota. *Environ. Microbiol. Rep.* 2, 693–703.

Durbin, A. M., and Teske, A. (2011). Microbial diversity and stratification of oligotrophic abyssal South Pacific sediments. *Environ. Microbiol.* 13, 3219–3234.

Eder, W., Schmidt, M., Koch, M., Garbe-Schönberg, D., and Huber, R. (2002). Prokaryotic phylogenetic diversity and corresponding geochemical data of the brine–seawater interface of the Shaban Deep, Red Sea. *Environ. Microbiol.* 4, 758–763.

Expedition 308 Scientists. (2006a). "Site U1319," in *Proceedings of the Integrated Ocean Drilling Program 308*, eds P. B. Flemings, J. H. Behrmann, C. M. John, and the Expedition 308 Scientists (College Station, TX: Integrated Ocean Drilling Program Management International, Inc.).

Expedition 308 Scientists. (2006b). "Site U1320," in *Proceedings of the Integrated Ocean Drilling Program 308*, eds P. B. Flemings, J. H. Behrmann, C. M. John, and the Expedition 308 Scientists (College Station, TX: Integrated Ocean Drilling Program Management International, Inc.).

Fierer, N., Bradford, M. A., and Jackson, R. B. (2007). Toward an ecological classification of soil bacteria. *Ecology* 88, 1354–1364.

Fredrickson, J. K., Zachara, J. M., Kennedy, D. W., Dong, H., Onstott, T., Hinman, N. W., and Li, S.-M. (1998). Biogenic iron mineralization accompanying the dissimilatory reduction of hydrous ferric oxide by a groundwater bacterium. *Geochim. Cosmochim. Acta* 62, 3239–3257.

Fry, J. C., Parkes, R. J., Cragg, B. A., Weightman, A. J., and Webster, G. (2008). Prokaryotic biodiversity and activity in the deep subseafloor biosphere. *FEMS Microbiol. Ecol.* 66, 181–196.

Fuhrman, J. A., and Davis, A. A. (1997). Widespread Archaea and novel Bacteria from the deep sea as shown by 16S rRNA gene sequences. *Mar. Ecol. Prog. Ser.* 150, 275–285.

Fuhrman, J. A., McCallum, K., and Davis, A. A. (1992). Novel major archaebacterial group from marine plankton. *Nature* 356, 148–149.

Gieskes, J. M., and Boulègue, J. (1986). "Interstitial water studies, Leg 92," in *Initial Reports Deep Sea Drilling Project 92*, eds M. Leinen, D. K. Rea, R. N. Anderson, K. Becker, J. J. Boulègue, J. Erzinger, J. M. Gieskes, D. Goldberg, M. Goldfarb, R. Goldsborough, M. A. Hobart, M. Kastner, S. Knuettel, M. W. Lyle, D. Moos, R. Newmark, T. Nishatani, R. M. Owen, J. A. Pearce, K. Romine, and R. A. Stephan (Washington: US Government Printing Office), 423–429.

Gillan, D. C., and Danis, B. (2007). The archaebacterial communities in Antarctic bathypelagic sediments. *Deep Sea Res. II* 54, 1682–1690.

Glud, R. N. (2008). Oxygen dynamics of marine sediments. *Mar. Biol. Res.* 4, 243–289.

Groβkopf, R., Janssen P. H., and Liesack, W. (1998a). Diversity and structure of the methanogenic community in anoxic rice paddy soil microcosms as examined by cultivation and direct 16S rRNA gene sequence retrieval. *Appl. Environ. Microbiol.* 64, 960–969.

Groβkopf, R., Stubner, S., and Liesack, W. (1998b). Novel euryarchaeotal lineages detected on rice roots and in the anoxic bulk soil of flooded rice microcosms. *Appl. Environ. Microbiol.* 64, 4983–4989.

Hales, B. A., Edwards, C., Ritchie, D. A., Hall, G., Pickup, R. W., and Saunders, J. R. (1996). Isolation and identification of methanogen-specific DNA from blanket bog peat by PCR amplification and sequence analysis. *Appl. Environ. Microbiol.* 62, 668–675.

Heijs, S. K., Laverman, A. M., Forney, L. J., Hardoim, P. R., and Van Elsas, J. D. (2008). Comparison of deep-sea sediment microbial communities in the Eastern Mediterranean. *FEMS Microbiol. Ecol.* 64, 362–377.

Hinrichs, K.-U., and Hayes, J. M., Sylva, S. P., Brewer, P. G., and DeLong, E. F. (1999). Methane-consuming archaebacteria in marine sediments. *Nature* 398, 802–805.

Huber, J. A., Morrison, S. M., Neal, P. R., Sogin, M. L., and Welch, M. D. B. (2009). Effect of PCR amplicon size on assessments of clone library microbial diversity and community structure. *Environ. Microbiol.* 11, 1292–1302.

Hugenholtz, P. (2002). Exploring prokaryotic diversity in the genomic era. *Genome Biol.* 3, reviews0003–reviews0003.8.

Hugenholtz, P., and Huber, T. (2003). Chimeric 16S rDNA sequences of diverse origin are accumulating in the public databases. *Int. J. Syst. Evol. Microbiol.* 53, 289–293.

Hutchison, C. S. (2004). Marginal basin evolution: the southern South China Sea. *Mar. Pet. Geol.* 21, 1129–1148.

Inagaki, F., Nunoura, T., Nakagawa, S., Teske, A., Lever, M., Lauer, A., Suzuki, M., Takai, K., Delwiche, M., Colwell, F. S., Nealson, K. H., Horikoshi, K., D'Hondt, S., and Jorgensen, B. B. (2006). Biogeographical distribution and diversity of microbes in methane hydrate-bearing deep marine sediments on the Pacific Ocean Margin. *Proc. Natl. Acad. Sci. U.S.A.* 103, 2815–2820.

Inagaki, F., Suzuki, M., Takai, K., Oida, H., Sakamoto, T., Aoki, K., Nealson, K. H., and Horikoshi, K. (2003). Microbial communities associated with geological horizons in coastal subseafloor sediments from the Sea of Okhotsk. *Appl. Environ. Microbiol.* 69, 7224–7235.

Inagaki, F., Takai, K., Komatsu, T., Kanamatsu, T., Fujiioka, K., and Horikoshi, K. (2001). Archaeology of Archaea: geomicrobiological record of Pleistocene thermal events concealed in a deep-sea subseafloor environment. *Extremophiles* 5, 385–392.

Jahnke, L. L., Orphan, V. J., Embaye, T., Turk, K. A., Kubo, M. D., Summons, R. E., and DesMarais, D. J. (2008). Lipid biomarker and phylogenetic analyses to reveal archaeal biodiversity and distribution in hypersaline microbial mat and underlying sediment. *Geobiology* 6, 394–410.

Jakobsen, R. (2007). Redox microniches in groundwater: a model study on the geometric and kinetic conditions required for concomitant Fe oxide reduction, sulfate reduction, and methanogenesis. *Water Resour. Res.* 43, W12S12.

Jobb, G., von Haeseler, A., and Strimmer, K. (2004). TREEFINDER: a powerful graphical analysis environment for molecular phylogenetics. *BMC Evol. Biol.* 4, 18. doi:10.1186/1471-2148-4-18

Jørgensen, B. B. (1977). Bacterial sulfate reduction within reduced microniches of oxidized marine sediments. *Mar. Biol.* 4, 7–17.

Jørgensen, B. B. (2011). Deep subseafloor microbial cells on physiological standby. *Proc. Natl. Acad. Sci. U.S.A.* 108, 18193–18194.

Jørgensen, B. B., Glud, R. N., and Holby, O. (2005). Oxygen distribution and bioirrigation in Arctic fjord sediments (Svalbard, Barents Sea). *Mar. Ecol. Prog. Ser.* 292, 89–95.

Jurgens, G., Glöckner, F.-O., Amann, R., Saano, A., Montonen, L., Likolammi, M., and Münster, U. (2000). Identification of novel Archaea in bacterioplankton of a boreal forest lake by phylogenetic analysis and fluorescent in situ hybridization. *FEMS Microbiol. Ecol.* 34, 45–56.

Karner, M. B., DeLong, E. F., and Karl, D. M. (2001). Archaeal dominance in the mesopelagic zone of the Pacific Ocean. *Nature* 409, 507–510.

Kendall, M. M., Wardlaw, G. D., Tang, C. F., Bonin, A. S., Liu, Y., and Valentine, D. L. (2007). Diversity of Archaea in marine sediments from Skan Bay, Alaska, including cultivated methanogens, and description of *Methanogenium boonei* sp. nov. *Appl. Environ. Microbiol.* 73, 407–414.

Knittel, K., Lösekann, T., Boetius, A., Kort, R., and Amann, R. (2005). Diversity and distribution of methanotrophic archaea at Cold Seeps. *Appl. Environ. Microbiol.* 71, 467–479.

König, I., Drodt, M., Suess, E., and Trautwein, A. X. (1997). Iron reduction through the tan-green

color transition in deep-sea sediments. *Geochim. Cosmochim. Acta* 61, 1679–1683.

König, I., Haeckel, M., Drodt, M., Suess, E., and Trautwein, A. X. (1999). Reactive Fe(II) layers in deep-sea sediments. *Geochim. Cosmochim. Acta* 63, 1517–1526.

Kormas, K. A., Meziti, A., Dählmann, A., De Lange, G. J., and Lykousis, V. (2008). Characterization of methanogenic and prokaryotic assemblages based on mcrA and 16S rRNA gene diversity in sediments of the Kazan mud volcano (Mediterranean Sea). *Geobiology* 6, 450–460.

Kubo, K., Lloyd, K., Biddle, J. F., Amann, R., Teske, A., and Knittel, K. (2012). Archaea of the Miscellaneous Crenarchaeotal Group (MCG) are abundant, diverse and widespread in marine sediments. *ISME J.* doi: 10.1038/ismej.2012.37

Lane, D. J. (1991). "16S/23S rRNA sequencing," in *Nucleic Acid Techniques in Bacterial Systematics*, eds E. Stackebrandt and M. Goodfellow (New York: John Wiley & Sons), 115–148.

Lever, M. A., Heuer, V. B., Morono, Y., Masui, N., Schmidt, F., Alperin, M. J., Inagaki, F., Hinrichs, K.-U., and Teske, A. (2010). Acetogenesis in deep subseafloor sediments of the Juan de Fuca ridge flank: a synthesis of geochemical, thermodynamic, and gene-based evidence. *Geomicrobiol. J.* 27, 183–211.

Li, Y., Li, F., Zhang, X., Qin, S., Zeng, Z., Dang, H., and Qin, Y. (2008). Vertical distribution of bacterial and archaeal communities along discrete layers of a deep-sea cold sediment sample at the East Pacific Rise (13°N). *Extremophiles* 12, 575–585.

Liao, L., Xu, X-W., Jiang, X. W., Wang, C. S., Zhang, D. S., Ni, J. Y., and Wu, M. (2011). Microbial diversity in deep-sea sediment from the cobalt-rich crust deposit region in the Pacific Ocean. *FEMS Microbiol. Ecol.* 78, 565–585.

Lipp, J. S., Morono, Y., Inagaki, F., and Hinrichs, K.-U. (2008). Significant contribution of Archaea to extant biomass in marine subsurface sediments. *Nature* 454, 991–994.

Logares, R., Bråte, J., Bertilsson, S., Clasen, J. L., Shalchian-Tabrizi, K., and Rengefors, K. (2009). Infrequent marine-freshwater transitions in the microbial world. *Trends Microbiol.* 17, 414–422.

López-Garcia, P., Rodriguez-Valera, F., Pedrós-Aliós, C., and Moreira, D. (2001). Unexpected diversity of small eukaryotes in deep-sea Antarctic plankton. *Nature* 409, 603–607.

Lovley, D. R., and Goodwin, S. (1988). Hydrogen concentrations as an indicator of the predominant terminal electron-accepting reactions in aquatic sediments. *Geochim. Cosmochim. Acta* 52, 2993–3003.

Ludwig, W., Strunk, O., Westram, R., Richter, L., Meier, H., Yadhukumar, K., Buchner, A., Lai, T., Steppi, S., Jobb, G., Förster, W., Brettske, I., Gerber, S., Ginhart, A. W., Gross, O., Grumann, S., Hermann, S., Jost, R., König, A., Liss, T., Lüßmann, R., May, M., Nonhoff, B., Reichel, B., Strehlow, R., Stamatakis, A., Stuckmann, N., Vilbig, A., Lenke, M., Ludwig, T., Bode, A., and Schleifer, K.-H. (2004). ARB: a software environment for sequence data. *Nucleic Acids Res.* 32, 1363–1371.

Mäkelä, K., and Tuominen, L. (2003). Pore water nutrient profiles and dynamics in soft bottoms of the northern Baltic Sea. *Hydrobiologia* 492, 43–53.

Martens-Habbena, W., Berube, P. M., Urakawa, H., de la Torre, J. R., and Stahl, D. A. (2009). Ammonia oxidation kinetics determine niche separation of nitrifying Archaea and Bacteria. *Nature* 461, 976–981.

McCollom, T. M., and Amend, J. P. (2005). A thermodynamic assessment of energy requirements for biomass synthesis by chemolithoautotrophic microorganisms in oxic and anoxic environments. *Geobiology* 3, 135–144.

McDonald, D., Price, M. N., Goodrich, J., Nawrocki, E. P., DeSantis, T. Z., Probst, A., Andersen, G. L., Knight, R., and Hugenholtz, P. (2011). An improved Greengenes taxonomy with explicit ranks for ecological and evolutionary analyses of bacteria and archaea. *ISME J.* 6, 610–618.

McInerney, M. J., and Beaty, P. S. (1988). Anaerobic community structure from a nonequilibrium thermodynamic perspective. *Can. J. Microbiol.* 34, 487–493.

Narasingarao, P., Podell, S., Ugalde, J. A., Brochier-Armanet, C., Emerson, J. B., Brocks, J. J., Heidelberg, K. B., Banfield, J. F., and Allen, E. E. (2012). De novo metagenomic assembly reveals abundant novel major lineage of Archaea in hypersaline microbial communities. *ISME J.* 6, 81–93.

Nercessian, O., Fouquet, Y., Pierre, C., Prieur, D., and Jeanthon, C. (2005). Diversity of Bacteria and Archaea associated with carbonate-rich metalliferous sediment sample from the Rainbow vent field on the Mid-Atlantic Ridge. *Environ. Microbiol.* 7, 698–714.

Nercessian, O., Reysenbach, A.-L., Prieur, D., and Jeanthon, C. (2003). Archaeal diversity associated with in situ samplers deployed on hydrothermal vents on the East Pacific Rise (13°N). *Environ. Microbiol.* 5, 492–502.

Nunoura, T., Hirayama, H., Takami, H., Oida, H., Nishi, S., Shimamura, S., Suzuki, Y., Inagaki, F., Takai, K., Nealson, K. H., and Horikoshi, K. (2005). Genetic and functional properties of uncultivated thermophilic crenarchaeotes from a subsurface gold mine as revealed by analysis of genome fragments. *Environ. Microbiol.* 7, 1967–1984.

Nunoura, T., Inagaki, F., Delwiche, M. E., Colwell, F. S., and Takai, K. (2008). Subseafloor microbial communities in methane hydrate-bearing sediment at two distinct locations (ODP Leg 204) in the Cascadia Margin. *Microbes Environ.* 23, 317–325.

Nunoura, T., Soffientino, B., Blazejak, A., Kakuta, J., Oida, H., Schippers, A., and Takai, K. (2009). Subseafloor microbial communities associated with rapid turbidite deposition in the Gulf of Mexico continental slope (IODP Expedition 308). *FEMS Microbiol. Ecol.* 69, 410–424.

Ochsenreiter, T., Selezi, D., Quaiser, A., Bonch-Osmolovskaya, L., and Schleper, C. (2003). Diversity and abundance of Crenarchaeota in terrestrial habitats studied by 16S RNA surveys and real time PCR. *Environ. Microbiol.* 5, 787–797.

Orphan, V. J., Hinrichs, K.-U., Paull, C. K., Taylor, L. T., Sylva, S., and DeLong, E. F. (2001). Comparative analysis of methane-oxidizing archaea and sulfate-reducing bacteria in anoxic marine sediments. *Appl. Environ. Microbiol.* 67, 1922–1934.

Pagé, A., Juniper, S. K., Olagnon, M., Alain, K., Desrosiers, G., Quérellou, J., and Cambon-Bonavita, M.-A. (2004). Microbial diversity associated with a Paralvinella sulfincola tube and the adjacent substratum on an active deep-sea vent chimney. *Geobiology* 2, 225–238.

Parkes, R. J., Cragg, B. A., Bale, S. J., Getliff, J. M., Goodman, K., Rochelle, P. A., Fry, J. C., Weightman, A. J., and Harvey, S. M. (1994). Deep bacterial biosphere in Pacific Ocean sediments. *Nature* 371, 410–413.

Parkes, R. J., Webster, G., Cragg, B. A., Weightman, A. J., Newberry, C. J., Ferdelman, T. G., Kallmeyer, J., Jørgensen, B. B., Aiello, I. W., and Fry, J. C. (2005). Deep subseafloor prokaryotes stimulated at interfaces over geologic time. *Nature* 436, 390–394.

Pester, M., Schleper, C., and Wagner, M. (2011). The Thaumarchaeota: an emerging view of their phylogeny and ecophysiology. *Curr. Opin. Microbiol.* 14, 300–306.

Postma, D., and Jakobsen, R. (1996). Redox zonation: equilibrium constraints on the Fe(III)/SO4-reduction interface. *Geochim. Cosmochim. Acta* 17, 3169–3175.

Poulton, S. W., and Raiswell, R. (2002). The low-temperature geochemical cycle of iron: from continental fluxes to marine sediment deposition. *Am. J. Sci.* 302, 774–805.

Pruesse, E., Quast, C., Knittel, K., Fuchs, B. M., Ludwig, W., Peplies, J., and Glöckner, F. O. (2007). SILVA: a comprehensive online resource for quality checked and aligned ribosomal RNA sequence data compatible with ARB. *Nucleic Acids Res.* 35, 7188–7196.

Reed, D., Fujita, Y., Delwiche, M. E., Blackwelder, D. B., Sheridan, P. P., and Uchida, T. Colwell, F. S. (2002). Microbial communities from methane hydrate-bearing deep marine sediments in a forearc basin. *Appl. Environ. Microbiol.* 68, 3759–3770.

Robertson, C. E., Spear, J. R., Harris, J. K., and Pace, N. R. (2009). Diversity and stratification of archaea in a hypersaline microbial mat. *Appl. Environ. Microbiol.* 75, 1801–1810.

Rogers, K. L., and Amend, J. P. (2006). Archaeal diversity and geochemical energy yields in a geothermal well on Vulcano Island, Italy. *Geobiology* 3, 319–322.

Roussel, E. G., Sauvadet, A.-L., Chaduteau, C., Fouquet, Y., Charlou, J.-L., Prieur, D., and Bonavita, M.-A. C. (2009). Archaeal communities associated with shallow to deep subseaflorr sediments of the New Caledonia Basin. *Environ. Microbiol.* 11, 2446–2462.

Schleper, C., Jurgens, G., and Jonuscheit, M. (2005). Genomic studies of uncultivated archaea. *Nat. Rev. Microbiol.* 3, 479–488.

Schleper, C., and Nicol, G. W. (2010). Ammonia-oxidizing archaea – physiology, ecology and evolution. *Adv. Microb. Physiol.* 57, 1–41.

Seiter, K., Hensen, C., Schroter, J., and Zabel, M. (2004). Organic carbon content in surface sediments-defining regional provinces. *Deep Sea Res. I* 51, 2001–2026.

Severmann, S., Mills, R. A., Palmer, M. R., Telling, J. P., Cragg, B., and Parkes, R. J. (2006). The role of prokaryotes in subsurface weathering of hydrothermal sediments: a combined geochemical and microbiological investigation. *Geochim. Cosmochim. Acta* 70, 1677–1694.

Shipboard Scientific Party. (1976). "Site 321," in *Initial Reports Deep Sea Drilling Project 34*, eds R. S. Yeats, S. R., Hart, J. M. Ade-Hall, M. N. Bass, W. E. Benson, R. A. Hart, P. G. Quilty, H. M. Sachs, M. H. Salisbury, and T. L. Valier (Washington: Government Printing Office), 111–153.

Shipboard Scientific Party. (1988a). "Site 684," in *Proceedings of the Ocean Drilling Program, Initial Reports 112*, eds E. Suess, R. von Huene, K.-C. Emeis, J. Bourgois, J. d. C. Cruzado-Castañeda, P. De Wever, G. Eglinton, R. Garrison, M. Greenberg, E. H. Paz, P. Hill, M. Ibaraki, M. Kastner, A. E. S. Kemp, K. Kvenvolden, R. Langridge, N. Lindsley-Griffin, J. Marsters, E. Martini, R. McCabe, L. Ocola, J. Resig, A. Q. Sanchez-Fernandez, H.-J. Schrader, T. Thornburg, G. Wefer and M. Yamano (College Station: Ocean Drilling Program), 525–596.

Shipboard Scientific Party. (1988b). "Site 681," in *Proceedings of the Ocean Drilling Program, Initial Reports 112*, eds E. Suess, R. von Huene, K.-C. Emeis, J. Bourgois, J. d. C. Cruzado-Castañeda, P. De Wever, G. Eglinton, R. Garrison, M. Greenberg, E. H. Paz, P. Hill, M. Ibaraki, M. Kastner, A. E. S. Kemp, K. Kvenvolden, R. Langridge, N. Lindsley-Griffin, J. Marsters, E. Martini, R. McCabe, L. Ocola, J. Resig, A. Q. Sanchez-Fernandez, H.-J. Schrader, T. Thornburg, G. Wefer and M. Yamano (College Station: Ocean Drilling Program), 305–362.

Shipboard Scientific Party. (1988c). "Site 685," in *Proceedings of the Ocean Drilling Program, Initial Reports 112*, eds E. Suess, R. von Huene, K.-C. Emeis, J. Bourgois, J. d. C. Cruzado-Castañeda, P. De Wever, G. Eglinton, R. Garrison, M. Greenberg, E. H. Paz, P. Hill, M. Ibaraki, M. Kastner, A. E. S. Kemp, K. Kvenvolden, R. Langridge, N. Lindsley-Griffin, J. Marsters, E. Martini, R. McCabe, L. Ocola, J. Resig, A. Q. Sanchez-Fernandez, H.-J. Schrader, T. Thornburg, G. Wefer and M. Yamano (College Station: Ocean Drilling Program), 597–704.

Shipboard Scientific Party. (1992a). "Site 851b," in *Proceedings of the Ocean Drilling Program, Initial Reports 138 (Pt. 2)*, eds L. Mayer, N. G. Pisias, T. R. Janecek, J. G. Baldauf, S. F. Bloomer, K. A. Dadey, K.-C. Emeis, J. Farrell, J. A. Flores, E. M. Galimov, T. K. Hagelberg, P. Holler, S. A. Hovan, M. Iwai, A. E. S. Kemp, D. C. Kim, G. Klinkhammer, M. Leinen, S. Levi, M. A. Levitan, M. W. Lyle, A. K. MacKillop, L. M. Meynadier, A. C. Mix, T. C. Moore, I. Raffi, C. Ravelo, D. Schneider, N. J. Shackleton, J.-P. Valet and E. Vincent (College Station: Ocean Drilling Program), 891–965.

Shipboard Scientific Party. (1992b). "Site 846," in *Proceedings of the Ocean Drilling Program, Initial Reports 138 (Pt. 1)* eds L. Mayer, N. G. Pisias, T. R. Janecek, J. G. Baldauf, S. F. Bloomer, K. A. Dadey, K.-C. Emeis, J. Farrell, J. A. Flores, E. M. Galimov, T. K. Hagelberg, P. Holler, S. A. Hovan, M. Iwai, A. E. S. Kemp, D. C. Kim, G. Klinkhammer, M. Leinen, S. Levi, M. A. Levitan, M. W. Lyle, A. K. MacKillop, L. M. Meynadier, A. C. Mix, T. C. Moore, I. Raffi, C. Ravelo, D. Schneider, N. J. Shackleton, J.-P. Valet and E. Vincent (College Station: Ocean Drilling Program), 265–333.

Shipboard Scientific Party. (2000a). "Site 1143," in *Proceedings of the Ocean Drilling Program, Initial Reports 184*, eds P. Wang, W. L. Prell, P. Blum, E. M. Arnold, C. J. Bühring, M.-P. Chen, S. C. Clemens, P. D. Clift, C. J. G. Colin, J. W. Farrell, M. J. Higginson, Z. Jian, W. Kuhnt, C. E. Laj, C. Lauer-Leredde, J. S. Leventhal, A. Li, Q. Li, J. Lin, K. McIntyre, C. R. Miranda, S. A. Nathan, J.-P. Shyu, P. A. Solheid, X. Su, F. Tamburini, A. Trentsaux and L. Wang (College Station: Ocean Drilling Program), 1–103.

Shipboard Scientific Party. (2000b). "Site 1148," in *Proceedings of the Ocean Drilling Program, Initial Reports 184*, eds P. Wang, W. L. Prell, P. Blum, E. M. Arnold, C. J. Bühring, M.-P. Chen, S. C. Clemens, P. D. Clift, C. J. G. Colin, J. W. Farrell, M. J. Higginson, Z. Jian, W. Kuhnt, C. E. Laj, C. Lauer-Leredde, J. S. Leventhal, A. Li, Q. Li, J. Lin, K. McIntyre, C. R. Miranda, S. A. Nathan, J.-P. Shyu, P. A. Solheid, X. Su, F. Tamburini, A. Trentsaux, and L. Wang (College Station: Ocean Drilling Program), 1–121.

Shipboard Scientific Party. (2003a). "Site 1225," in *Proceedings of the Ocean Drilling Program, Initial Reports 201*, eds S. D'Hondt, B. B. Jørgensen, D. J. Miller, I. W. Aiello, B. Bekins, R. Blake, B. A. Cragg, H. Cypionka, G. R. Dickens, T. Ferdelman, K. Ford, G. L. Gettemy, G. Guerin, K.-U. Hinrichs, N. Holm, C. House, F. Inagaki, P. Meister, R. M. Mitterer, T. Naehr, S. Niitsuma, J. R. Parkes, A. Schippers, C. G. Skilbeck, D. C. Smith, A. J. Spivack, A. Teske and J. Wiegel (College Station: Ocean Drilling Program), 1–86.

Shipboard Scientific Party. (2003b). "Site 1226," in *Proceedings of the Ocean Drilling Program, Initial Reports 201*, eds S. D'Hondt, B. B. Jørgensen, D. J. Miller, I. W. Aiello, B. Bekins, R. Blake, B. A. Cragg, H. Cypionka, G. R. Dickens, T. Ferdelman, K. Ford, G. L. Gettemy, G. Guerin, K.-U. Hinrichs, N. Holm, C. House, F. Inagaki, P. Meister, R. M. Mitterer, T. Naehr, S. Niitsuma, J. R. Parkes, A. Schippers, C. G. Skilbeck, D. C. Smith, A. J. Spivack, A. Teske, and J. Wiegel (College Station: Ocean Drilling Program), 1–96.

Shipboard Scientific Party. (2003c). "Site 1227," in *Proceedings of the Ocean Drilling Program, Initial Reports 201*, eds S. D'Hondt, B. B. Jørgensen, D. J. Miller, I. W. Aiello, B. Bekins, R. Blake, B. A. Cragg, H. Cypionka, G. R. Dickens, T. Ferdelman, K. Ford, G. L. Gettemy, G. Guerin, K.-U. Hinrichs, N. Holm, C. House, F. Inagaki, P. Meister, R. M. Mitterer, T. Naehr, S. Niitsuma, J. R. Parkes, A. Schippers, C. G. Skilbeck, D. C. Smith, A. J. Spivack, A. Teske, and J. Wiegel (College Station: Ocean Drilling Program), 1–66.

Shipboard Scientific Party. (2003d). "Site 1229," in *Proceedings of the Ocean Drilling Program, Initial Reports 201*, eds S. D'Hondt, B. B. Jørgensen, D. J. Miller, I. W. Aiello, B. Bekins, R. Blake, B. A. Cragg, H. Cypionka, G. R. Dickens, T. Ferdelman, K. Ford, G. L. Gettemy, G. Guerin, K.-U. Hinrichs, N. Holm, C. House, F. Inagaki, P. Meister, R. M. Mitterer, T. Naehr, S. Niitsuma, J. R. Parkes, A. Schippers, C. G. Skilbeck, D. C. Smith, A. J. Spivack, A. Teske, and J. Wiegel, (College Station: Ocean Drilling Program), 1–78.

Shipboard Scientific Party. (2003e). "Site 1230," in *Proceedings of the Ocean Drilling Program, Initial Reports 201*, eds S. D'Hondt, B. B. Jørgensen, D. J. Miller, I. W. Aiello, B. Bekins, R. Blake, B. A. Cragg, H. Cypionka, G. R. Dickens, T. Ferdelman, K. Ford, G. L. Gettemy, G. Guerin, K.-U. Hinrichs, N. Holm, C. House, F. Inagaki, P. Meister, R. M. Mitterer, T. Naehr, S. Niitsuma, J. R. Parkes, A. Schippers, C. G. Skilbeck, D. C. Smith, A. J. Spivack, A. Teske, and J. Wiegel (College Station: Ocean Drilling Program), 1–107.

Shipboard Scientific Party. (2003f). "Site 1231," in *Proceedings of the Ocean Drilling Program, Initial Reports 201*, eds S. D'Hondt, B. B. Jørgensen, D. J. Miller, I. W. Aiello, B. Bekins, R. Blake, B. A. Cragg, H. Cypionka, G. R. Dickens, T. Ferdelman, K. Ford, G. L. Gettemy, G. Gierin, K.-U. Hinrichs, N. Holm, C. House, F. Inagaki, P. Meister, R. M. Mitterer, T. Naehr, S. Niitsuma, J. R. Parkes, A. Schippers, C. G. Skilbeck, D. C. Smith, A. J. Spivack, A. Teske, and J. Wiegel (College Station: Ocean Drilling Program), 1–64.

Shipboard Scientific Party. (2003g). "Site 1244," in *Proceedings of the Ocean Drilling Program, Initial Reports 204*, eds A. M. Tréhu, G. Bohrmann, F. R. Rack, M. E. Torres, N. L. Bangs, S. R. Barr, W. S. Borowski, G. E. Claypool, T. S. Collett, M. E. Delwiche, G. R. Dickens, D. S. Goldberg, E. Gràcia, G. Guérin, M. Holland, J. E. Johnson, Y.-J. Lee, C.-S. Liu, P. E. Long, A. V. Milkov, M. Riedel, P. Schultheiss, X. Su, B. Teichert, H. Tomaru, M. Vanneste, M. Watanabe and J. L. Weinberger (College Station: Ocean Drilling Program), 1–132.

Shipboard Scientific Party. (2003h). "Site 1245," in *Proceedings of the Ocean Drilling Program, Initial Reports 204*, eds A. M. Tréhu, G. Bohrmann, F. R. Rack, M. E. Torres, N. L. Bangs, S. R. Barr, W. S. Borowski, G. E. Claypool, T. S. Collett, M. E. Delwiche, G. R. Dickens, D. S. Goldberg, E. Grácia, G. Guérin, M. Holland, J. E. Johnson, Y.-J. Lee, C.-S. Liu, P. E. Long, A. V. Milkov, M. Riedel, P. Schultheiss, X. Su, B. Teichert, H. Tomaru, M. Vanneste, M. Watanabe and J. L. Weinberger (College Station: Ocean Drilling Program), 1–131.

Shipboard Scientific Party. (2003i). "Site 1251," in *Proceedings of the Ocean Drilling Program, Initial Reports 204*, eds A. M. Tréhu, G. Bohrmann, F. R. Rack, M. E. Torres, N. L. Bangs, S. R. Barr, W. S. Borowski, G. E. Claypool, T. S. Collett, M. E. Delwiche, G. R. Dickens, D. S. Goldberg, E. Gràcia, G. Guérin, M. Holland, J. E. Johnson, Y.-J. Lee, C.-S. Liu, P. E. Long, A. V. Milkov, M. Riedel, P. Schultheiss, X. Su, B. Teichert, H. Tomaru, M. Vanneste, M. Watanabe and J. L. Weinberger (College Station: Ocean Drilling Program), 1–119.

Sørensen, K. B., Lauer, A., and Teske, A. (2004). Archaeal phylotypes in a metal-rich and low-activity deep subsurface sediment of the Peru Basin, ODP Leg 201, Site 1231. *Geobiology* 2, 151–161.

Sørensen, K. B., and Teske, A. (2006). Stratified communities of active

Archaea in deep marine subsurface sediments. *Appl. Environ. Microbiol.* 72, 4596–4603.

Spear, J. R., Walker, J. J., McCollom, T. M., and Pace, N. R. (2005). Hydrogen and bioenergetics in the Yellowstone geothermal ecosystem. *Proc. Natl. Acad. Sci. U.S.A.* 102, 2555–2560.

Sundset, M. A., Edwards, J. E., Cheng, Y. F., Senosiain, R. S., Fraile, M. N., Northwood, K. S., Praesteng, K. E., Glad, T., Mathiesen, S. D., and Wright, A.-D. G. (2009). Rumen microbial diversity in Svalbard reindeer, with particular emphasis on methanogenic archaea. *FEMS Microbiol. Ecol.* 70, 553–562.

Takai, K., and Horikoshi, K. (1999). Genetic diversity of Archaea in deep-sea hydrothermal vent environments. *Genetics* 152, 1285–1297.

Takai, K., and Horikoshi, K. (2000). Rapid detection and quantification of members of the archaeal community by quantitative PCR using fluorogenic probes. *Appl. Environ. Microb.* 66, 5066–5072.

Takai, K., Moser, D. P., DeFlaun, M., Onstott, T. C., and Fredrickson, J. K. (2001). Archaeal diversity in waters from deep South African gold mines. *Appl. Environ. Microbiol.* 67, 5750–5760.

Tao, L., Peng, W., and Pinxian, W. (2008). Microbial diversity in surface sediments of the Xisha Trough, the South China Sea. *Acta Ecol. Sin.* 28, 1166–1173.

Teske, A. (2006). Microbial communities of deep marine subsurface sediments: molecular and cultivation surveys. *Geomicrobiol. J.* 23, 357–368.

Teske, A., Hinrichs, K.-U., Edgcomb, V., de Vera Gomez, A., Kysela, D., Sylva, S. P., Sogin, M. L., and Jannasch, H. W. (2002). Microbial diversity of hydrothermal sediments in the Guaymas Basin: evidence for anaerobic methanotrophic communities. *Appl. Environ. Microbiol.* 68, 1994–2007.

Teske, A., and Sørensen, K. B. (2008). Uncultured archaea in deep marine subsurface sediments: have we caught them all? *ISME J.* 2, 3–18.

Thamdrup, B. (2000). "Bacterial manganese and iron reduction in aquatic sediments," in *Advances in Microbial Ecology*, Vol. 16, ed. B. Schink (New York: Kluwer Academic), 41–81.

Urrutia, M. M., Roden, E. E., Fredrickson, J. K., and Zachara, J. M. (1998). Microbial and surface chemistry controls on reduction of synthetic Fe(III) oxide minerals by the dissimilatory iron-reducing bacterium Shewanella alga. *Geomicrobiol. J.* 15, 269–291.

Urrutia, M. M., Roden, E. E., and Zachara, J. M. (1999). Influence of aqueous and solid-phase Fe(II) complexants on microbial reduction of crystalline iron(III) oxides. *Environ. Sci. Technol.* 33, 4022–4028.

Van der Wielen, P. W., Bolhuis, H., Borin, S., Daffonchio, D., Corselli, C., Giuliano, L., D'Auria, G., de Lange, G. J., Huebner, A., Varnavas, S. P., Thomson, J., Tamburini, C., Marty, D., McGenity, T. J., Timmis, K. N., and BioDeep Scientific Party. (2005). The enigma of prokaryotic life in deep hypersaline anoxic basins. *Science* 307, 121–123.

Vetriani, C., Jannasch, H. W., MacGregor, B. J., Stahl, D. A., and Reysenbach, A.-L. (1999). Population structure and phylogenetic characterization of marine benthic archaea in deep-sea sediments. *Appl. Environ. Microbiol.* 65, 4375–4384.

von Mering, C., Hugenholtz, P., Tringe, S. G., Doerks, T., Jensen, L. J., Ward, N., and Bork, P. (2007). Quantitative phylogenetic assessment of microbial communities in diverse environments. *Science* 315, 1126–1130.

Wakeham, S. G., Lee, C., Hedges, J. I., Hernes, P. J., and Peterson, M. L. (1997). Molecular indicators of diagenetic status in marine organic matter. *Geochim. Cosmochim. Acta* 61, 5363–5369.

Wang, G., Spivack, A. J., Rutherford, S., Manor, U., and D'Hondt, S. (2008). Quantification of co-occurring reaction rates in deep subseafloor sediments. *Geochim. Cosmochim. Acta* 72, 3479–3488.

Wang, P., Li, T., Hu, A., Wei, Y., Guo, W., Jiao, N., and Zhang, C. (2010a). Community structure of archaea from deep-sea sediments of the South China Sea. *Microb. Ecol.* 60, 796–806.

Wang, G., Spivack, A. J., and D'Hondt, S. (2010b). Gibbs energies of reaction and microbial mutualism in anaerobic deep subseafloor sediments of ODP Site 1226. *Geochim. Cosmochim. Acta* 74, 3938–3947.

Wang, P., Wang, F., Xu, M., and Xiao, X. (2004). Molecular phylogeny of methylotrophs in a deep-sea sediment from a tropical west Pacific Warm Pool. *FEMS Microbiol. Ecol.* 47, 77–84.

Wang, P., Xiao, X., and Wang, F. (2005). Phylogenetic analysis of Archaea in the deep-sea sediments of west Pacific Warm Pool. *Extremophiles* 9, 209–217.

Wellsbury, P., Mather, I., and Parkes, R. J. (2002). Geomicrobiology of deep, low organic carbon sediments in the Woodlark Basin, Pacific Ocean. *FEMS Microbiol. Ecol.* 42, 59–70.

Whitman, J. M., and Davis, T. A. (1979). Cenozoic oceanic sedimentation rates: how good are the data? *Mar. Geol.* 30, 296–284.

Whitman, W. B., Coleman, D. C., and Wiebe, W. J. (1998). Prokaryotes: the unseen majority. *Proc. Natl. Acad. Sci. U.S.A.* 95, 6578–6583.

Wright, A.-D. G., and Pimm, C. (2003). Improved strategy for presumptive identification of methanogens using 16S riboprinting. *J. Microbiol. Methods* 55, 337–349.

Xu, M., Wang, P., Wang, F., and Xiao, X. (2005). Microbial diversity at a deep-sea station of the Pacific nodule province. *Biodivers. Conserv.* 14, 3363–3380.

Zheng, D., Alm, E. W., Stahl, D. A., and Raskin, L. (1996). Characterization of universal small-subunit rRNA hybridization probes for quantitative molecular microbial ecology studies. *Appl. Environ. Microbiol.* 62, 4504–4513.

Zhou, J., Bruns, M. A., and Tiedje, J. M. (1996). DNA recovery from soils of diverse composition. *Appl. Environ. Microbiol.* 62, 316–322.

Ziebis, W., McManus, J., Ferdelman, T. G., Schmidt-Schierhorn, F., Bach, W., Muratli, J., Edwards, K. J., and Villinger, H. (2012). Interstitial fluid chemistry of sediments underlying the North Pond Atlantic Gyre and the influence of subsurface fluid flow. *Earth Planet. Sci. Lett.* 323–324, 79–91.

Zinger, L, Amaral-Zettler, L. A., Fuhrman, J. A., Horner-Devine, M. C., Huse, S. M., Mark Welch, D. B., Martiny, J. B. H., Sogin, M., Boetius, A., and Ramette, A. (2011). Global patterns of bacterial beta-diversity in seafloor and seawater ecosystems. *PLoS ONE* 6, e24570. doi:10.1371/journal.pone.0024570

Conflict of Interest Statement: The authors declare that the research was conducted in the absence of any commercial or financial relationships that could be construed as a potential conflict of interest.

Received: 30 January 2012; accepted: 16 April 2012; published online: 31 May 2012.

Citation: Durbin AM and Teske A (2012) Archaea in organic-lean and organic-rich marine subsurface sediments: an environmental gradient reflected in distinct phylogenetic lineages. Front. Microbio. ***3****:168. doi: 10.3389/fmicb.2012.00168*

This article was submitted to Frontiers in Extreme Microbiology, a specialty of Frontiers in Microbiology.

frontiers in
MICROBIOLOGY

ORIGINAL RESEARCH ARTICLE
published: 20 February 2012
doi: 10.3389/fmicb.2012.00065

Isolation of sulfate-reducing bacteria from sediments above the deep-subseafloor aquifer

Katja Fichtel, Falko Mathes†, Martin Könneke†, Heribert Cypionka and Bert Engelen*

Paleomicrobiology, Institute for Chemistry and Biology of the Marine Environment, University of Oldenburg, Oldenburg, Germany

Edited by:
Andreas Teske, University of North Carolina at Chapel, USA

Reviewed by:
Alexander Loy, University of Vienna, Austria
Julia Maresca, University of Delaware, USA

***Correspondence:**
Bert Engelen, Paleomicrobiology, Institute for Chemistry and Biology of the Marine Environment, Carl-von-Ossietzky-Straße 9-11, 26129 Oldenburg, Germany.
e-mail: engelen@icbm.de

†Present address:
Falko Mathes, School of Earth and Ocean Sciences, Cardiff University, Cardiff, UK.;
Martin Könneke, Max Planck Institute for Marine Microbiology, Bremen, Germany.

On a global scale, crustal fluids fuel a large part of the deep-subseafloor biosphere by providing electron acceptors for microbial respiration. In this study, we examined bacterial cultures from sediments of the Juan de Fuca Ridge, Northeast Pacific (IODP Site U1301). The sediments comprise three distinctive compartments: an upper sulfate-containing zone, formed by bottom-seawater diffusion, a sulfate-depleted zone, and a second (~140 m thick) sulfate-containing zone influenced by fluid diffusion from the basaltic aquifer. In order to identify and characterize sulfate-reducing bacteria, enrichment cultures from different sediment layers were set up, analyzed by molecular screening, and used for isolating pure cultures. The initial enrichments harbored specific communities of heterotrophic microorganisms. Strains affiliated to *Desulfosporosinus lacus*, *Desulfotomaculum* sp., and *Desulfovibrio aespoeensis* were isolated only from the top layers (1.3–9.1 meters below seafloor, mbsf), while several strains of *Desulfovibrio indonesiensis* and a relative of *Desulfotignum balticum* were obtained from near-basement sediments (240–262 mbsf). Physiological tests on three selected strains affiliated to *Dv. aespoeensis*, *Dv. indonesiensis*, and *Desulfotignum balticum* indicated that all reduce sulfate with a limited number of short-chain *n*-alcohols or fatty acids and were able to ferment either ethanol, pyruvate, or betaine. All three isolates shared the capacity of growing chemolithotrophically with H_2 as sole electron donor. Strain P23, affiliating with *Dv. indonesiensis*, even grew autotrophically in the absence of any organic compounds. Thus, H_2 might be an essential electron donor in the deep-subseafloor where the availability of organic substrates is limited. The isolation of non-sporeforming sulfate reducers from fluid-influenced layers indicates that they have survived the long-term burial as active populations even after the separation from the seafloor hundreds of meters above.

Keywords: *Desulfovibrio, Desulfotignum*, diversity, deep biosphere, Juan de Fuca Ridge, hydrogen, chemolithoautotrophy, IODP

INTRODUCTION

The subseafloor biosphere is probably the largest reservoir for prokaryotic life on Earth (Whitman et al., 1998; Heberling et al., 2010). It extends several hundred meters into deeply buried sediments (Parkes et al., 1994; Roussel et al., 2008) and even further down into the upper layers of the oceanic crust (Thorseth et al., 1995; Furnes and Staudigel, 1999; Ehrhardt et al., 2007). Recently, it was estimated that the ocean crust contains a similar amount of microorganisms as the entire volume of the world's oceans (Heberling et al., 2010). The continuous circulation of seawater within the upper crust turns these voluminous, porous, and permeable basalts into the largest globally connected aquifer (Johnson and Pruis, 2003; Johnson et al., 2006).

Intense fluid circulation is a consequence of specific geological settings evolved during crust formation at ocean-spreading centers. It is especially pronounced at ocean ridges such as the Juan de Fuca Ridge in the Northeast Pacific (Johnson et al., 2006). This area is one of the most intensively studied locations in terms of heat-driven fluid flow (Fisher et al., 2003; Hutnak et al., 2006). While cold bottom-seawater is recharged at seamounts, it warms up within the oceanic crust beneath the sediments before being discharged again at other rocky outcrops exposed at the seafloor. The chemical composition of these low-temperature hydrothermal fluids [<150°C (Cowen, 2004)] is altered during long-term circulation through the basalt due to continuous abiotic water–rock interaction (Edwards et al., 2003) especially with increasing basement temperature (Wheat and Mottl, 1994; Wheat et al., 2000), or as a response to volcanic eruption (Butterfield et al., 1997). Additionally, microbial activity of crust-hosted communities contributes to changes in fluid composition by removing seawater constituents such as sulfate as indicated by sulfur-isotope measurements (Rouxel et al., 2008). However, due to a limitation in electron donors, crustal fluids are not fully reduced and still contain suitable electron acceptors, such as sulfate, for anaerobic respiration (Wheat and Mottl, 1994; Wheat et al., 2000; Cowen et al., 2003; Edwards et al., 2005).

It was postulated that basement fluids not only supply electron donors and acceptors to microbial life within the crust, but also to the microbial communities in the overlying sediments by diffusion from below (Cowen et al., 2003; DeLong, 2004; D'Hondt

et al., 2004). We tested this hypothesis during an expedition to the eastern flank of the Juan de Fuca Ridge (IODP Exp. 301) by analyzing a 265-m-long sediment column of IODP site U1301. Sampling included material taken only two meters above the sediment–basement interface (Expedition 301 Scientists, 2005). At this site, sulfate diffuses into the sediments from both the seafloor (∼27 mM) and the underlying basement (∼16 mM). As a precondition for a sound microbiological and geochemical analysis, contamination controls were performed directly onboard the drillship JOIDES Resolution and proved the pristine character of the sediment samples (Lever et al., 2006).

Our previous work has shown that fluids from the oceanic crust do support microbial life in the overlying sediments (Engelen et al., 2008). Exoenzyme activities and sulfate reduction rates were not only elevated near the seafloor but also at the bottom of the sediment column which correlated well with the overall geochemical settings. We detected enhanced microbial abundance in sediment layers above the basement by direct counting and the cultivation-based most probable number (MPN) technique. Microbial growth in anoxic MPN dilution series from sediment layers near the oceanic crust indicated considerable amounts of viable microbial populations. Thus, the detection of a deep sulfate reduction zone and the successful enrichment of anaerobic microorganisms was the motivation for isolating sulfate-reducing bacteria (SRB) especially from fluid-influenced sediment layers. Identifying defined physiological adaptations of indigenous microorganisms to environmental conditions can be achieved best when pure cultures are available.

Even though sulfate reduction is supposed to be an important process in deeply buried sediments, only few isolates are available in strain collections. The type strain of *Desulfovibrio profundus* was isolated from 500 m depth in sediments of the Japan Sea (Parkes et al., 1995; Bale et al., 1997). Other piezophilic isolates closely related to *Dv. profundus* were cultivated from 222 m deep sediments of the Cascadia margin of the Pacific Ocean (Barnes et al., 1998). However, cultivation-based studies on the marine deep biosphere are still limited to a few sampling sites representing pinpricks in the ocean floor. So far, isolates from the marine subsurface were obtained from sediment samples retrieved from Mediterranean sediments (Süss et al., 2004) and from various sites in the Pacific Ocean: The Sea of Okhotsk, north of Japan (Inagaki et al., 2003), the Nankai Trough south–east of Japan (Mikucki et al., 2003; Toffin et al., 2004a,b, 2005; Kendall et al., 2006), the Equatorial Pacific, and the Peru Margin (D'Hondt et al., 2004; Biddle et al., 2005; Lee et al., 2005; Batzke et al., 2007). Recently, several heterotrophic bacteria and methanogenic Archaea were isolated from up to 106 mbsf deep sediments off Shimokita Peninsula, Japan using a continuous-flow bioreactor (Imachi et al., 2011).

In this study, we extended our previous investigations on IODP Site U1301 to determine the microbial diversity within different sediment layers of the deep subsurface. We hypothesize, that zones with different sulfate concentrations harbor different populations of SRB due to varying substrate availabilities. A cultivation-based approach in combination with molecular screening tools was chosen to isolate and compare SRB from fluid-influenced sediments and near-surface layers. The metabolic properties of the isolates might provide new insights on the impact of crustal fluids on microbial metabolism in the deep-subseafloor biosphere where substrates are recalcitrant but electron acceptors are still available.

MATERIALS AND METHODS

SAMPLE MATERIAL

Sediment samples were recovered from the eastern flank of the Juan de Fuca Ridge by the drill ship "JOIDES Resolution" during IODP Expedition 301 in 2004. Characteristics of IODP Site U1301 were described in the expedition report (Expedition 301 Scientists, 2005). Sediment sampling, contamination tests, and subsampling for further analyses were described in detail by Engelen et al. (2008). All samples proved to be free of contamination as previously described by Lever et al. (2006).

INITIAL ENRICHMENTS OF DEEP-BIOSPHERE BACTERIA

To elucidate the diversity of cultured bacteria, a total of 736 initial enrichment cultures were set up directly onboard. Sediment slurries from 17 representative depth intervals (Engelen et al., 2008) were prepared immediately after sample recovery with anoxic artificial seawater medium (Süss et al., 2004). MPN series for anoxic and oxic microorganisms from these slurries were performed in 10-fold steps within 96-deep-well microtiter plates as previously described (Engelen et al., 2008). In addition, liquid dilution series in 20 ml-glass tubes were inoculated, flushed with N_2 and sealed with butyl rubber stoppers. Anoxic substrate gradient tubes were prepared with undisturbed 1-cm^3-sediment subcores from hole U1301C, only by embedding them within agar-solidified artificial seawater media (Köpke et al., 2005). In general, a mixture of the following substrates were supplied to stimulate microbial growth: glycerol, glucose, lactate, fumarate, malate, succinate, methanol, ethanol, 1-propanol, 1-butanol, formate, acetate, propionate, butyrate, valerate, caproate, and all the 20 L-amino acids (final concentration of each compound: 0.1 mM). For a better comparison of all enrichments, incubation was performed at 20°C.

Anoxic and oxic MPN viable counts were determined after 14 weeks of incubation to quantify the cultured part of the microbial communities within the sampled sediment layers. Procedure and results have already been published by Engelen et al. (2008). For the present cultivation study, all dilution cultures showing growth were transferred into 20 ml-glass tubes containing freshly prepared media and further incubated for at least five months at 20°C. Since cell densities were generally low, growth was determined several times during incubation by epifluorescence microscopy using Sybr® GreenI as a fluorescent dye. Growth of sulfate reducers was monitored by measuring the formation of sulfide (Cord-Ruwisch, 1985). Gradient cultures were incubated for approximately one year without interruption. Stimulation of growth within the sediment subcore was analyzed by microscopy and molecular methods. Finally, a total of 116 positive cultures were analyzed by means of molecular biological methods as described below to identify the cultivated microorganisms and to select enrichments for further isolation processes.

ISOLATION OF PURE CULTURES

Pure cultures from SRB and other anaerobes were isolated and maintained in a slightly different artificial seawater media. One liter of this basal medium contained 24.32 g NaCl, 10.0 g

$MgCl_2 \cdot 6H_2O$, 1.5 g $CaCl_2 \cdot 2H_2O$, 4.0 g Na_2SO_4, 0.66 g KCl, and 0.09 g KBr. Resazurin (1 mg/l) was added as redox-indicator. The media was autoclaved, cooled under a nitrogen atmosphere, and supplemented with the following sterile solutions: NH_4Cl (2 mM), KH_2PO_4 (1 mM), CO_2-saturated sodium bicarbonate (30 mM), and from sterile stocks: 1 ml/l of trace element solution SL10 (Widdel and Bak, 1992) 0.2 ml/l of selenite-tungsten solution (Widdel and Bak, 1992) and 2 ml/l of a solution of 10 vitamins (Balch et al., 1979). The anoxic medium was reduced by addition of Na_2S (final concentration: ∼1 mM) and few crystals of sodium dithionite. The pH was adjusted to 7.2–7.5 with 4 M NaOH. To increase cell density of all subcultures, a 10-fold higher concentrated substrate mix was provided (i.e., final concentration of each compound: 1 mM).

Repeated application of the deep-agar dilution method (Widdel and Bak, 1992) or dilution-to-extinction was performed to isolate deep-biosphere bacteria from liquid enrichments. Sediment subcores from gradient cultures were homogenized and slurried with 4 ml anoxic artificial seawater to further establish subcultures as gradient dilution series (up to 10^{-6}). Aerobic microorganisms were subcultured for isolation by the liquid dilution-to-extinction method with subsequent purification on agar plates using a HEPES/bicarbonate-buffered oxic seawater medium. The purity of all isolates was checked by microscopy and molecular analysis as described below. Furthermore, the cultures were transferred to a complex HEPES-buffered oxic seawater medium containing yeast extract (0.03 g/l), glucose (1 mM), lactate (5 mM), and peptone (0.06 g/l) as substrates to check for contamination.

MOLECULAR SCREENING OF ENRICHMENT CULTURES

The above described enrichment and isolation procedure was monitored and directed by molecular screening to identify unique phylotypes. Positive dilutions or growing colonies were analyzed by using polymerase chain reaction (PCR) of 16S rRNA gene-fragments, denaturing gradient gel electrophoresis (DGGE), and subsequent sequencing of re-amplified DGGE bands. DNA from liquid cultures was extracted using a protocol combining bead-beating with phenol/chloroform/isoamyl alcohol treatment and isopropanol/sodium acetate precipitation (Stevens et al., 2005). Nucleic acid extraction from substrate gradient cultures was performed by using the UltraClean™Soil DNA Isolation Kit (MoBio Laboratories, Inc., Carlsbad, CA, USA) according to the manufacturers' instructions.

Polymerase chain reaction-amplification of bacterial 16S rRNA genes was conducted in 50-μl volumes containing the following components: 1–2 μl of DNA-template, 10 pmol of each primer, 0.2 mM of each dNTP, 0.5–2 μl of bovine serum albumin (BSA, 10 mg/ml), 5 μl of 10×-ThermoPol reaction buffer and 1 U/μl of Taq Polymerase (New England Biolabs, Inc., Ipswich, MA, USA) and nuclease-free water. For DGGE analysis, the almost complete 16S rRNA genes were amplified with the primer set 8f/1492r (Overmann and Tuschak, 1997). The samples were incubated in a thermal cycler (Mastercycler, Eppendorf, Hamburg, Germany) under the following conditions: initial denaturation at 95°C for 5 min, 28 cycles of amplification by denaturation at 95°C for 30 s, annealing at 40°C for 60 s, and elongation at 72°C for 3 min. Terminal elongation was performed at 72°C for 10 min. The resulting amplicons were used as templates for a nested PCR. Shorter 16S rRNA gene-fragments were amplified (Wilms et al., 2006a) using the universal bacterial primer set GC-341f and 907r (Overmann and Tuschak, 1997). All PCR products were always visualized by agarose-gel electrophoresis (Wilms et al., 2006a). DGGE was performed with a gradient from 40 to 70% (Süss et al., 2004). PCR products were mixed with loading buffer before loading onto the gel (Wilms et al., 2006a).

SEQUENCING OF DGGE BANDS AND PURE CULTURES

For sequence analysis of DGGE bands, distinctive bands were excised, eluted in 50 μl nuclease-free water, re-amplified in a 25-μl-PCR (primers 341f/907r, Wilms et al., 2006b), and purified (Wilms et al., 2006a) using the QIAquick PCR purification Kit (Qiagen GmbH, Hilden, Germany) or the PCR-Purifying-Kit (SeqLab, Göttingen, Germany) and sequenced with a IRDyeTM800 labeled 907r-primer (Süss et al., 2004). For phylogenetic identification of pure cultures, genomic DNA was extracted from the isolated strains using a freeze and thaw procedure. From picked colonies or 2 ml of liquid cultures, 1 μl of a cell pellet was resuspended with 100 μl of filter-sterilized Tris-buffer (50 mM, pH 7.4). The suspension was frozen at −80°C for 3 min and heated at 85°C for 3 min. This procedure was repeated five times, and 2 μl of the final extract were added to 48 μl of PCR mixture. Partial or nearly full-length bacterial 16S rRNA gene sequences were amplified using the bacteria-specific primer set 341f/907r and 8f/1492r, respectively, and sequenced as described above. In case of sulfate-reducing strains, DNA was sequenced in both directions using the respective PCR primers and the service of GATC Biotech AG (Konstanz, Germany). Consensus sequences were constructed after alignment by using the BioEdit software tool version 7.0.9[1]. All 16S rRNA gene sequences obtained in this study were compared for their affiliation to the closest relatives using the BLASTN program 2.2.26+ (Altschul et al., 1990; Morgulis et al., 2008)[2]. The partial 16S rRNA gene sequences of all 40 isolates are deposited in GenBank database under the accession numbers JQ411257–JQ411296.

PHYSIOLOGICAL CHARACTERIZATION OF SULFATE-REDUCING ISOLATES

Physiological tests were generally performed in sealed glass tubes containing 10 ml of artificial seawater medium. Sulfidogenic growth was tested with 18 different substrates at final concentrations between 1 and 5 mM in the presence of sulfate. Fermentative growth with betaine, ethanol, malate, or pyruvate (2–5 mM, each) was tested in medium without additional electron acceptors. The cultures were incubated for at least 4 weeks at 20°C in the dark. Chemolithotrophic growth with H_2 as electron donor was tested with a headspace (2/3 of the culture volume) filled with a mixture of H_2/CO_2 (80/20 v/v, 1 kPa). Those cultures were incubated horizontally at 20°C. Growth was checked by visual inspection of turbidity, by phase contrast microscopy, and by sulfide formation (Cord-Ruwisch, 1985). Substrate utilization was defined to be positive after the third successful transfer into fresh media.

[1] http://www.mbio.ncsu.edu/BioEdit/bioedit.html
[2] http://blast.ncbi.nlm.nih.gov/Blast.cgi

The capability of anaerobic respiration was tested in sulfate-free medium with ethanol or lactate (5 mM, each) as electron donor in combination with six different electron acceptors. Reduction of Fe(III) was indicated by the formation of black precipitates under the expense of the reddish ferric hydroxide. Mn(IV) utilization was shown by the disappearance of brown manganese carbonates and the occurrence of white precipitates. The production of sulfide as a result of the reduction of thiosulfate or sulfite was measured at 480 nm using a Shimadzu UV-1202 photometer (Cord-Ruwisch, 1985). In addition, cultures were checked microscopically for the presence of bacterial cells.

Growth experiments for autotrophic growth were performed at 35˚C, the optimum temperature for growth of our test strain P23. Growth rates were calculated from linear regression of produced sulfide (Cord-Ruwisch, 1985) and formed cell protein (Bradford, 1976) as function of time.

The temperature range for growth of SRB was tested from 4 to 55˚C with lactate (10 mM) as electron donor. Growth was followed at OD_{436} via sulfide production and by photometrical determination of protein concentrations (Bradford, 1976).

For phase contrast microscopy, agarose-coated slides were used. To prepare those, slides were thoroughly cleaned and preheated by infrared light in order to get a smooth agarose film. Then, 1 ml of the hot agarose solution (2% w/v) was dispensed on the warm slides. Before usage, the agarose slides were air dried. Upon placing a drop of a bacterial culture to a coated slide, the liquid diffuses into the dry agarose, while the cells are gently squeezed under the cover slip and get fixed in the same plane. Cell dimensions were determined using a Leitz DMRB microscope (Wetzlar, Germany).

Transmission-electron microscopy was performed as follows: a 400-mesh Formvar copper grid (Plano) was placed on a drop of cell suspension for 10 min. Cells adsorbed to the grid were stained with 0.5% aqueous uranyl acetate for 1 min, washed twice in a drop of water for a few seconds and examined with a transmission-electron microscope (EM 902A, Zeiss). A Proscan High Speed SSCCD camera system with iTEMfive software was used for images acquisition.

RESULTS

GEOCHEMICAL PROFILES DIVIDE THE SEDIMENT COLUMN INTO THREE DISTINCTIVE ZONES

The geomorphological structure of the eastern flank of the Juan de Fuca Ridge leads to a hydrological situation where sulfate-containing fluids from the oceanic crust diffuse ∼140 m into overlying sediment layers. The effect of this heat-driven fluid circulation was reflected by the temperature gradient within the sediments of 2˚C at the seafloor to approximately 62˚C above the basement (Expedition 301 Scientists, 2005). Using the porewater profile of sulfate, the sediment column can be separated into three zones (**Figure 1**). The upper sulfate-containing zone was formed by bottom-seawater diffusion showing decreasing concentrations from 27 mM at the top to 3 mM in 35 mbsf. Below, a sulfate-depleted zone was located between 47 and 121 mbsf (<1 mM). The lower sulfate-containing zone was characterized by increasing sulfate concentrations from 2 to 16 mM toward the basement at ∼265 mbsf due to sulfate diffusion from crustal fluid flow into the overlying sediments.

SHIFTS IN MICROBIAL DIVERSITY BETWEEN THE INITIAL ENRICHMENT CULTURES FROM THE DIFFERENT ZONES

Anoxic and oxic MPN series, liquid dilution series in tubes and the substrate gradient technique were used to enrich and further isolate deep-biosphere bacteria. The cultivation progress was monitored by microscopy and PCR–DGGE. Unique DGGE bands were subsequently sequenced to identify the community composition within the enrichments. A total of 135 partial 16S rRNA gene sequences were obtained after DGGE analysis of growing cultures. The technique was not only chosen to prevent multiple isolation of one strain and to check the purity of cultures, but also to identify community members that could not be isolated. This molecular-directed cultivation indicated the presence of diverse viable microbial populations within the different zones of the investigated sediment column.

The phylogenetic screening of the initial enrichments identified different bacterial populations among the growing cultures obtained from the three sediment zones (**Figure 1**). A typical decrease in cultivation success with respect to the conditions set in our growth media was observed for the two upper zones, which correlates with the general depletion of electron donors and acceptors. Within the top 30 m of the sediment column, 35 different operational taxonomic units (OTUs, defined at 97% sequence similarity) were detected via PCR–DGGE in enrichments from the respective sediment layers. From the sulfate-depleted zone, 21 OTUs were retrieved. For samples from the deep, fluid-influenced sediment zone, the cultivation success increased again with 48 identified OTUs.

In general, the number of OTUs belonging to the *Firmicutes* decreased with sediment depth from 60% in enrichments from the upper sulfate-containing zone to 21% in the lower sulfate zone. In addition, *Gammaproteobacteria* accounted for 40% of all OTUs retrieved from enrichments of the lower sulfate zone. Bacteria belonging to the phylum *Acidobacteria, Bacteroidetes,* and the classes *Beta-* and *Epsilonproteobacteria* were enriched as identified by molecular methods but could not be isolated or were lost during purification procedures. The majority of the enriched but not isolated organisms were phylogenetically affiliated to uncultured bacteria from different terrestrial and marine environments (data not shown in detail).

DIVERSITY OF ISOLATED PURE CULTURES

From the 116 initial enrichments that were tested positively for growth, 40 strains could be isolated (14 from the upper sulfate-containing zone, 8 from the sulfate-depleted zone, and 18 from the lower sulfate-containing zone). Based on 16S rRNA gene sequences, the 40 pure cultures could be affiliated to the phyla *Actinobacteria, Firmicutes,* and *Tenericutes* or the classes *Alphaproteobacteria, Gammaproteobacteria, Deltaproteobacteria* (**Table 1**). The majority of isolates (32 of 40) were obtained from liquid dilution series that were initially inoculated with hundred to million fold diluted sediment (10^{-2} to 10^{-6}), indicating a significant number of cells *in situ*. Nearly all isolates were closely related to cultivated species from sediments or soils, fluids, or other aquatic environments. Among them, 13 were strict anaerobes. With exception of the sporeforming *Firmicutes* all other pure cultures including those obtained from oxic media were

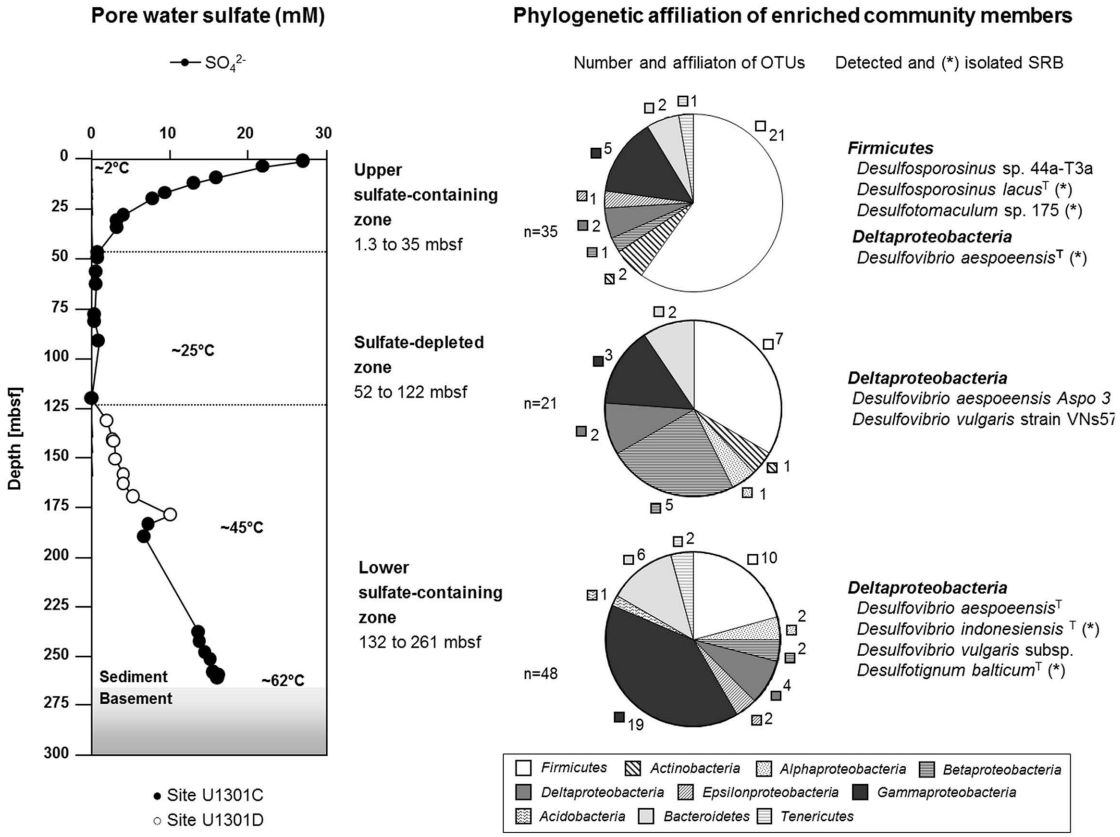

FIGURE 1 | Zonation of the 265-m-long sediment column of the eastern flank of the Juan de Fuca Ridge, Northeast Pacific (IODP Site U1301), and phylogenetic affiliation of enriched and isolated marine subsurface bacteria with special emphasis on sulfate-reducing bacteria. Operational taxonomic units (OTUs) detected via PCR–DGGE are defined at 97% sequence similarity.

considered to be facultatively anaerobic, since they originated from anoxic sediment horizons. While some isolates seem to be ubiquitous within the sediment column [e.g., *Shewanella frigidimarina*, 98–99% sequence similarity or *Bacillus* spp. (96–100%)], others were retrieved from single sediment layers, only (e.g., *Anaerovirgula multivorans* or *Marinobacter flavimaris*, both 99% sequence similarity).

SULFATE-REDUCING BACTERIA WERE ISOLATED FROM BOTH SULFATE-CONTAINING ZONES

The sulfate reducers isolated from the upper 10 m predominantly belonged to the *Firmicutes* (**Figures 1** and **2**; **Table 1**). Three strains were identified as members of the genera *Desulfotomaculum* and *Desulfosporosinus*. The latter shared 97% sequence similarity with its closest described relative *Desulfosporosinus lacus*, firstly isolated from freshwater lake sediments (Ramamoorthy et al., 2006). The *Desulfotomaculum* strains were phylogenetically related to isolates originally obtained from a terrestric aquifer system (Detmers et al., 2001). Another isolate from a near-surface layer (strain P20) was closely affiliated to *Desulfovibrio aespoeensis*. This *Deltaproteobacterium* was also enriched in co-culture with strains related to *Desulfovibrio indonesiensis* (culture P34 and P19) from 240 and 260 mbsf, respectively, as identified by DGGE and subsequent sequencing of the bands. Two sequences affiliated to sulfate reducers were also detected in enrichment cultures from sediments of the sulfate-depleted zone (**Figure 1**). However, no isolates could be retrieved. SRB isolated from the deepest sediments above the basement solely belonged to the *Deltaproteobacteria*, namely *Desulfotignum balticum* (strain P18; 260 mbsf) and *Dv. indonesiensis* (strains P12, P19-1, P23, P33, and P34). The latter phylotype was highly abundant in the lower sulfate-containing zone as it was frequently retrieved from different fluid-influenced layers (240, 252, 260 mbsf). Furthermore, strains P18, P23, and P34 were isolated from million fold diluted MPN-cultures, allowing the assumption, that they must be present in higher numbers within the respective sediment layer, where they probably play an active role.

MORPHOLOGICAL AND PHYSIOLOGICAL CHARACTERISTICS OF THREE REPRESENTATIVE SULFATE-REDUCING ISOLATES

Strains affiliated to *Dv. aespoeensis* (strain P20), *Dv. indonesiensis* (strain P23), and *Desulfotignum balticum* (strain P18) were morphologically and physiologically investigated in more detail (**Figure 2**; **Table 2**). Strain P20 was used for further analysis since it was the only available pure culture related to *Dv. aespoeensis* that was obtained in this study. Other relatives of this species were

Table 1 | Origin and phylogenetic affiliation of isolated strains from IODP Site U1301, a 265-m-long sediment column of the eastern flank of the Juan de Fuca Ridge, Northeast Pacific.

Phylogenetic group, closest relative* in GenBank (accession no.)	Similarity (%)	Sediment depth (mbsf)	No. of isolates	Habitat of closest relatives***
ACTINOBACTERIA				
Bacterium Ellin5115 (AY234532)	99	112	1	Soil, Australia
[*Actinomycetospora chibensis*^{T} (AB514517)]	99			Paddy soil, Japan
Iron-reducing enrichment clone Cl-A3 (DQ676995)	99	31	1**	Estuary sediment, Europe
[*Propionicimonas paludicola*^{T} (FR733712)]	99			Rice-field soil, Japan
FIRMICUTES				
Anaerovirgula multivorans^T (NR_041291)	99	1.3	1**	Owens Lake, USA
Bacillus siralis^T (NR_028709)	98, 96	112, 132	2	General study
Bacillus sp. AS7 HS-2008 (AM950301)	98, 99	99, 112	2	Brine Lake Sediment, Mediterranean
Bacillus sp. Hs56 (JF803865)	99	1.3, 169	2	Marine sponge, Bay in Ireland
Desulfosporosinus lacus^T (NR_042202)	97	1.3	1**	Sediments of Lake Stechlin, Germany
Desulfotomaculum sp. 175 (AF295656)	98, 99	1.3, 9.1	2**	Aquifer/lignite seam, Germany
Marinilactibacillus sp. A5 (DQ344853)	98, 99	75, 99	2**	Deep-sea sediment, Pacific
Paenibacillus sp. UXO5-11 (DQ522106)	99	31	1	Marine sediments, Hawaii
Bacillus circulans USC24 (HQ441221)	99	9.1	1	Fish tank sediment, Spain
Uncult. bacterium clone LCKS880B24 (EF201766)	98	9.1	1**	Lake Chaka, China
[*Desulfonispora thiosulfatigenes*^{T} (NR_026497)]	90			Sewage plant, Germany
ALPHAPROTEOBACTERIA				
Pelagibacterium halotolerans^T (EU709017)	99	132	1	Ocean water, China
GAMMAPROTEOBACTERIA				
Alteromonas sp. USC168 (HQ441215)	99	31, 52	2	Mediterranean surface water, Spain
Halomonas sp. 1B.4 (HQ427421)	99	141	1	Ocean crust, JdF Ridge. Pacific
Halomonas axialensis^T (NR_027219)	100	163	1	Hydrothermal fluid, JdF Ridge, Pacific
Halomonas sp. PEB09 (GU213166)	99	163	1	Estuarine microbial mat, Spain
Marinobacter flavimaris^T (NR_025799)	99	141	1	Sea water, Yellow Sea in Korea
Pseudoalteromonas sp. D20 (AY582936)	99	150	1	Deep-sea sediment, Pacific
Pseudomonas sp. G12a-1 (FN397994)	99	141, 150	2	Deep-sea sediment, Indian Ocean
Shewanella frigidimarina ACAM 584 (U85902)	98–99	1.3, 31, 52, 260	4	Southern Ocean waters
Vibrio diazotrophicus^T (NR_026123)	98	150	1	General study
Vibrio pelagius^T (X74722)	98	31, 150	2	General study
DELTAPROTEOBACTERIA				
Desulfotignum balticum^T (NR_041852)	99	260	1**	Marine mud, Denmark
Desulfovibrio aespoeensis^T (NR_029307)	98	1.3	1**	Aespoe hard rock borehole, Sweden
Desulfovibrio indonesiensis^T (NR_044916)	99	240, 252, 260	3**	Corroding ship, Indonesia
TENERICUTES				
Anaerobic bacterium MO-XQ (AB598274)	99	260	1	Subseafloor sediments, Japan
[*Acholeplasma palmae*^{T} (NR_029152)]	93			Plant surface

**In case of environmental clones the next cultivated organism is indicated in square brackets.*

***Strictly anaerobic isolates.*

****Based upon the results of the megaBLAST search (NCBI).*

enriched from near-basement layers, but only in co-culture with strains affiliated to *Dv. indonesiensis*. Various efforts to separate the two species failed. Strain P23, obtained from the deepest sediment layer (260 mbsf), was chosen as a representative for strains related to *Dv. indonesiensis*, since the other closely related isolates showed nearly identical characteristics under the growth conditions tested.

For all investigated strains, colonies formed in deep-agar dilution series exhibited yellowish to brownish colors. The *Desulfovibrio* affiliated strains showed curved, motile cells (**Figures 2A,C**) with single polar flagella as identified by electron microscopy of negatively stained cells (**Figures 2B,D**). The relative of the non-motile *Desulfotignum balticum* formed ∼2–3 μm short thick rods with rounded ends (**Figures 2E,F**).

Desulfovibrio aespoeensis strain P20 grew within a temperature range of 20–35°C with an optimum at 25°C. *Desulfotignum* strain P18 and *Dv. indonesiensis* strain P23 instead exhibited growth within a broad temperature range from 4 to 48°C and 10 to 48°C,

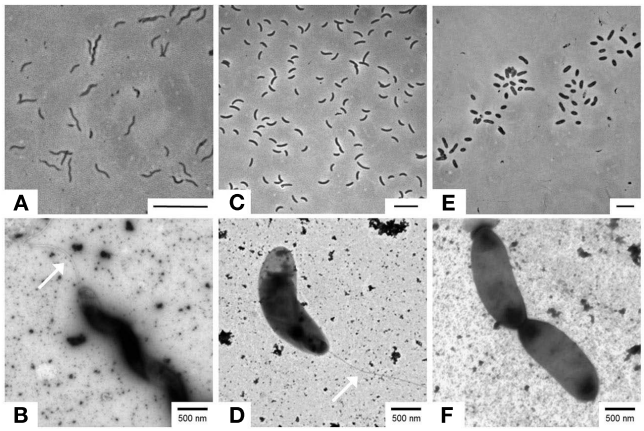

FIGURE 2 | Microscopic images from three sulfate-reducing isolates obtained from sediments of IODP Site U1301. (A,B) *Desulfovibrio aespoeensis* strain P20 (1.3 mbsf); **(C,D)** *Desulfovibrio indonesiensis* strain P23 (260.4 mbsf); **(E,F)** *Desulfotignum balticum* strain P18 (260.4 mbsf). Upper images: phase contrast (bar = 5 μm); lower images: transmission-electron microscopy, TEM (bar = 500 nm). Arrows in **(B,D)** indicate flagella.

respectively, with the optimal growth temperature lying between 25 and 35°C.

All strains were capable of using sulfite or thiosulfate as alternative electron acceptor other than sulfate. Slow growth by iron or manganese reduction on lactate was observed for *Desulfotignum balticum* strain P18 and *Dv. indonesiensis* strain P23. Growth was not as fast as with sulfate as electron acceptor and high cell densities were not achieved. However, growth on metal oxides occurred even after the third transfer. None of the strains used nitrate as electron acceptor for anaerobic respiration.

Of all substrates provided, *Dv. aespoeensis* strain P20 only utilized lactate and formate for growth in the presence of sulfate. In contrast, the type strain of *Dv. aespoeensis* only grew on lactate as sole substrate (Motamedi and Pedersen, 1998). The two other strains tested (P18 and P23) showed a slightly broader substrate spectrum. Strain P23, for instance, grew on different *n*-alcohols (C2–C4), formate, fumarate, lactate, and pyruvate. Only *Desulfotignum* strain P18 grew on acetate, benzoate, betaine, butyrate, and succinate, whereas fast growth and high cell densities were achieved with betaine, which was also fermented. Fermentative growth with pyruvate occurred in *Desulfovibrio* strains, only. All strains used hydrogen as electron donor. *Desulfotignum balticum* strain P18 grew autotrophically but only in the presence of vitamins. This was already known for the type strain of *Desulfotignum balticum*, which was described to grow on H_2 and CO_2 (Kuever et al., 2001). Surprisingly, autotrophic growth for *Dv. indonesiensis* strain P23 was observed in media that did not contain any organic additives such as vitamins, resazurin, or yeast extract and after at least 10 transfers to eliminate carbon sources from initial cultures (**Figure 3**). Growth rates (based on protein production) for strain P23 were 0.12 d^{-1} under autotrophic conditions, and approximately three times higher (0.30 d^{-1}) when 1 mM of acetate was added.

DISCUSSION

ORGANIC MATTER AND SULFATE AVAILABILITY GENERATE THE THREE DIFFERENT ZONES OF THE SEDIMENT COLUMN

The stratification of the different sediment compartments has an imprint on the life conditions. In both, the seawater- and fluid-influenced layers, the availability of electron acceptors stimulates microbial growth and activity of indigenous microorganisms (Engelen et al., 2008). In terms of electron donors, bacteria that thrive in the upper 30 m of the sediments are supported by burial of relatively young organic carbon (Fisher et al., 2003; Johnson et al., 2006). Therefore, they are used to a higher supply of electron donors and adapt much better to the given cultivation conditions. In deeper sediment horizons, indigenous bacteria have to survive long-term burial by adapting to a minimum supply of substrates and electron acceptors. Their limited availability strongly influences the metabolic activities in the deep marine subsurface. Indeed, based on geochemical porewater profiles, it has been concluded that the metabolic activities of subseafloor prokaryotes are very low (D'Hondt et al., 2002, 2004). They probably have developed different life strategies such as slow growth or survival as spores. The latter were presumably stimulated to germinate during our cultivation experiments since a major part of 16S rRNA gene sequences detected in all enrichment cultures affiliated to spore-forming *Firmicutes* (**Figure 1**). However, the decreasing number of *Firmicutes* with depth indicates that not all of them survive the long-term burial as spores as they might have germinated stochastically over geological time scales (Epstein, 2009).

Other subsurface organisms that are adapted to low organic carbon concentrations might not be able to grow under the given laboratory conditions. Even though the composition of our culture media was designed to provide organic substrates in submillimolar concentrations, a substrate shock (Straskrabová, 1983) might not have been circumvented. For instance, we were not able to grow any *Archaea* (data not shown) even though they are proposed to represent a substantial part of the deep biosphere as indicated by intact-lipid analysis (Lipp et al., 2008).

The supply of electron acceptors into the sediment column by crustal fluid diffusion dramatically changes the situation for microbial life within these deeply buried layers. The large numbers of non-sporeforming *Gammaproteobacteria* that were enriched from near-basement layers indicate the presence of viable cells. Many *Gammaproteobacteria* are adapted to elevated substrate concentrations (Lauro et al., 2009) and are therefore readily cultivated using our media. Some of them might even be typical for oceanic ridge systems. *Halomonas* and *Marinobacter* species were found to be present in hydrothermal fluids collected at the Juan de Fuca Ridge (Kaye et al., 2011). They were enriched during *in situ* colonization experiments on basaltic crust (Smith et al., 2011) and have also been detected in basaltic seafloor lavas and overlying seawater at the East Pacific Rise (Santelli et al., 2008).

THE UPPER AND LOWER SULFATE-CONTAINING ZONES HARBOR DIFFERENT SULFATE-REDUCING BACTERIA

The majority of sequences obtained from upper sediment horizons that were affiliated to SRB have *Desulfosporosinus* and *Desulfotomaculum* species as closest relatives, both sporeforming *Firmicutes*. However, it is unclear if they contribute to the high sulfate

Table 2 | Comparison of characteristics of sulfate-reducing isolates from IODP Site U1301: temperature range of growth, morphology, substrate utilization, and alternative electron acceptors.

Isolated strain	P20	P23	P18
Closest relative in GenBank	***Desulfovibrio aespoeensis*^{T}**	***Desulfovibrio indonesiensis*^{T}**	***Desulfotignum balticum*^{T}**
Sediment depth (mbsf)	1.30	260.43	260.43
T_{range}	20–35°C	10–48°C	4–48°C
T_{opt}	25°C	25–35°C	25–35°C
Morphology	Highly motile, thin, *vibrio* like, spirilloid cells, 3.8 μm (±0.9 μm) long, 0.4 μm (±0.1 μm) thick	Motile, *vibrio* shaped cells, 2.7 μm (±0.4 μm) long, 0.7 μm (±0.1 μm) thick	Non-motile, short thick rods with rounded ends, 2.3 μm (±0.4 μm) long, 1.0 μm (±0.1 μm) thick
ELECTRON DONORS AND SUBSTRATES IN THE PRESENCE OF SULFATE			
H_2, CO_2 + acetate (1 mM)	+	+	+**
H_2, CO_2 (excess)	−	+*	+**
Acetate (5 mM)	−	−	(+)
Benzoate (2.5 mM)	−	−	+
Betaine (2 mM)	n.t.	−	+
Butanol (5 mM)	−	+	+ (No H_2S)
Butyrate (5 mM)	−	−	(+)
Ethanol (5 mM)	−	+	−
Formate (5 mM)	+	+	(+) Slow
Fumarate (5 mM)	−	+	+
Lactate (5 mM)	+	+	+
Propanol (5 mM)	−	(+)	−
Pyruvate (5 mM)	−	+	+
Succinate (5 mM)	−	−	(+) Slow
FERMENTATION			
Ethanol (5 mM)	−	(+) Slow	(+) Slow
Betaine (2 mM)	n.t.	n.t.	+
Pyruvate (5 mM)	(+)	+	−
ELECTRON ACCEPTORS* **			
Sulfate (28 mM)	+	+	+
Sulfite (10 mM)	+	+	+
Thiosulfate (10 mM)	+	+	+
Fe(III) hydroxide (∼40 mM)	−	(+)	(+)
Mn(IV) (20 mM)	−	(+)	(+)

+, Substrate used for growth as indicated by turbidity increase and production of H_2S in the presence of sulfate, sulfite, or thiosulfate; (+), poor growth, no turbidity increase, but significant production of H_2S, in the presence of sulfate; −, no growth; n.t., not tested.

**Even in absence of vitamins and resazurin as redox-indicator; **In presence of vitamins only.*

****In presence of N_2/CO_2 or H_2/CO_2 and lactate or ethanol.*

The culture medium contained 28 mM sulfate as electron acceptor. For fermentation tests and utilization of alternative electron acceptors, a sulfate-free culture medium was used. No strain grew on amino acid mix (1 mM), glucose (5 mM), malate (5 mM), methanol (5 mM), propionate (2 mM), or yeast extract (0.005% v/v). None of the strains fermented malate (5 mM) or used nitrate (10 mM) as alternative electron acceptor.

reduction rates of up to 8 nmol cm^{-3} d^{-1} determined for the upper sulfate-containing zone of IODP Site U1301 (Engelen et al., 2008). This would only be the case if these SRB are present as viable cells. It cannot be specified if they are metabolically active or if they only survive as spores within these layers.

In contrast, fluid-influenced sediments exclusively harbor sulfate reducers that are members of the *Deltaproteobacteria*, which are not known to form any resting stages. These viable populations contribute to sulfate reduction rates of up to 3 pmol cm^{-3} d^{-1} within the lower sulfate reduction zone (Engelen et al., 2008). Due to their high abundance, this activity might derive from sulfate reducers affiliated to *Dv. indonesiensis*. This is quite surprising since the *in situ* temperature is around 60°C and most *Desulfovibrio* species are not active above 40°C (Widdel and Bak, 1992). However, a broad temperature range of growth was not only found for our isolates, but also for the Japan Sea isolates of *Dv. profundus* (Bale et al., 1997) and might represent an adaptation to the conditions in the deep biosphere.

Thus, one reason for the divergence in the SRB communities detected in both sulfate-containing zones might be the different temperature and pressure regimes present at the top and bottom of the sediment column. Surprisingly, the isolates from the

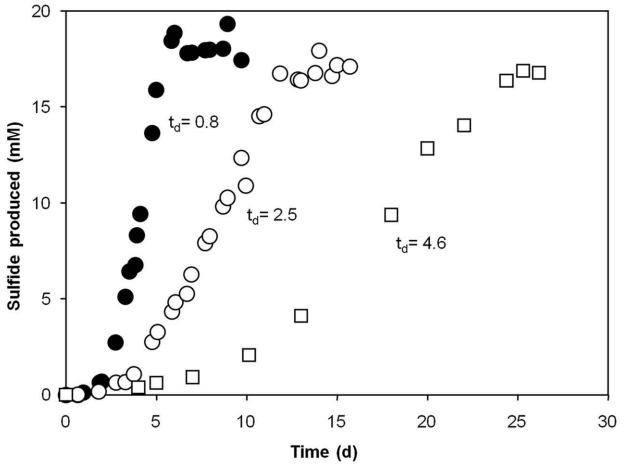

FIGURE 3 | Comparison of heterotrophic and autotrophic growth of *Desulfovibrio indonesiensis* strain P23 at 35°C (○) under autotrophic conditions using hydrogen, CO_2 and sulfate (28 mM); (●) after addition of 1 mM acetate, both in the presence of resazurin and vitamins; (□) under autotrophic conditions in media without vitamins and resazurin. Doubling times (t_d) in days are indicated.

deepest fluid-influenced layers did not grow at *in situ* temperatures of approximately 60°C. This might be due to the chosen initial incubation conditions at 20°C and ambient hydrostatic pressure instead of the *in situ* pressure of ∼30 MPa. As temperature and pressure counteract on the cell membrane composition (Mangelsdorf et al., 2005), an insufficient combination of both parameters might result in membrane disintegration. This assumption is supported by the fact that no isolates were obtained from enrichment cultures that were incubated under *in situ* temperatures (data not shown). In future experiments, pressure incubations might help to overcome such problems in cultivation efficiencies.

SULFATE-REDUCING BACTERIA FROM THE LOWER ZONE HAVE RELATIVES IN DEEP TERRESTRIAL AQUIFERS

Previous microbiological investigations on crustal fluids from the Juan de Fuca Ridge have identified several isolates (Nakagawa et al., 2006) and 16S rRNA clones (Cowen et al., 2003; Huber et al., 2006) that were affiliated to SRB. In general, the overlap between these studies compared with our culture collection from fluid-influenced sediments is quite low. Only relatives of *Desulfotomaculum* and *Desulfonatronovibrio* species were detected in two studies on the adjacent ODP Site 1026. One 16S rRNA gene sequence that is affiliated to *Desulfobacterium* species was found in fluids that discharge at "Baby bare seamount." A possible explanation for this discrepancy might be that most of our isolates represent typical sediment inhabitants, which do not necessarily occur in the upper oceanic crust. However, our *Deltaproteobacteria* that were isolated from the lower sulfate-containing zone are facing similar physico-chemical conditions in the highly compacted sediments above the basement as in the crustal aquifer.

A close relation of deep marine with terrestrial aquifers is indicated by the cultivation of *Dv. aespoeensis* strains from the fluid-influenced layers. *Dv. aespoeensis* is the most abundant sulfate reducer within formation waters of deep terrestrial boreholes at the Aespoe hard rock laboratory in Sweden (Motamedi and Pedersen, 1998). Those aquifers are also inhabited by complex microbial communities that are comparable to those thriving within the ocean crust (Pedersen, 2000). The energetical constrains are similar and select for, e.g., iron-reducing bacteria, acetogens, methanogens, and sulfate reducers (Pedersen, 1997).

Our most frequently isolated strains from up to 260 m deep fluid-influenced sediments that are affiliated to *Dv. indonesiensis* also have close relatives within the deep terrestrial biosphere. Even though the type strain was originally isolated from a biofilm on a corroded ship off the Indonesian coast (Feio et al., 1998, 2000), relatives were obtained from porewater brines of a deep terrestrial gas-reservoir (Sass and Cypionka, 2004). Furthermore, these organisms are supposedly involved in iron corrosion as determined during a study on hydrogen-consuming microorganisms in oil facilities from Japan (Mori et al., 2010). Biocorrosive capabilities (Feio et al., 1998) of *Dv. indonesiensis* might be an indication for a crustal origin of this species as this process plays an important role in the weathering of basalts (Edwards et al., 2005). Under anoxic conditions, SRB, and especially *Desulfovibrio* species are responsible for the corrosion of metal surfaces in consuming cathodic hydrogen (Pankhania, 1988; Dinh et al., 2004). This process might occur in the habitat as well as in our metabolic tests. As all isolates deriving from the fluid-influenced zone were capable of using hydrogen as electron donor, they might even exhibit a chemolithoautotrophic life-mode *in situ*.

CHEMOLITHOAUTOTROPHY WITHIN THE DEEP BIOSPHERE

Autotrophic, hydrogen-consuming microorganisms were repeatedly detected in deep continental aquifers and can even outnumber heterotrophs (Stevens and McKinley, 1995). The assumption that autotrophy is also a common metabolic attribute within the crust at IODP Site U1301, is supported by the isolation of a novel member of the genus *Archaeoglobus* from a fluid-influenced sample of ODP Site 1226 (Steinsbu et al., 2010). *Archaeoglobus sulfaticallidus* sp. nov., is a thermophilic and facultatively lithoautotrophic sulfate reducer and was isolated from black rust formations on top of a leaking borehole seal.

Although there is no clear evidence available for lithoautotrophy within the subseafloor (Stevens, 1997), there are numerous studies that deal with hydrogen as suitable source for deep subsurface life. In these habitats, hydrogen can originate from many sources (Nealson et al., 2005) such as the fermentation of organic matter or mechanochemical processes due to the tectonic action of the Earth (Parkes et al., 2011), degassing from the Earth's mantle during serpentinization of ultramafic rocks (McCollom and Bach, 2009), or even by radiolysis of water (Blair et al., 2007; D'Hondt et al., 2009). Furthermore, in the presence of sulfate, the oxidation of hydrogen is thermodynamically favored at high temperatures (Orcutt et al., 2010).

Thus, in many deep subsurface habitats, hydrogen might become apparently the biochemically most important electron donor and carbon dioxide is a ubiquitous carbon source. For example, both gases were found in micro-molar concentrations in deep igneous-rock aquifers (Pedersen, 1997) and deep aquifers of the Columbia river basalt which is located close to our investigated

site (Stevens and McKinley, 1995). For both sites, the authors have proposed a model for a hydrogen-driven biosphere. They assume autotrophic acetogens to form acetate from hydrogen and carbon dioxide. Acetoclastic methanogens can utilize acetate to produce methane or hydrogenotrophic methanogens might directly use hydrogen and CO_2. At relatively young ridge-flank systems, hydrogen-utilizing sulfate reducers will outcompete methanogens as sulfate is still available within the fluids.

CONCLUSION

Even though cultivation might not cover the whole microbial diversity of a given habitat, we were able to isolate and physiologically characterize indigenous microorganisms that are numerically and metabolically important for the marine deep subsurface. Thus, cultivation-based studies offer the opportunity to complement molecular techniques. In our study, the isolation of SRB from deep sediment layers was the precondition to answer questions concerning specific metabolic adaptations to the conditions at the sediment–basement interface.

The isolation of facultatively autotrophic sulfate reducers from near-basement layers strongly suggests that these organisms survive due to their capability of consuming hydrogen after organic compounds have been depleted or become too recalcitrant for microbial degradation. The continuous supply of sulfate from the aquifer below supports their viability within their respective sediment layers even after the separation from organic matter input at the seafloor due to sediment accumulation. When organic substrate availability from the ocean becomes a limiting factor, hydrogen becomes the most important electron donor.

ACKNOWLEDGMENTS

Katharina Schmidt, Heiner Hartwich, Dewi Nasima, and Martin Mierzejewski assisted in molecular analyses and cultivation studies. Andrea Schlingloff is thanked for her help in DNA sequencing and Erhard Rhiel is acknowledged for preparing TEM photos. This study used samples and data provided by the Integrated Ocean Drilling Program from IODP Exp. 301. The work was financially supported by the German Research Foundation (DFG).

REFERENCES

Altschul, S. F., Gish, W., Miller, W., Myers, E. W., and Lipman, D. J. (1990). Basic local alignment search tool. *J. Mol. Biol.* 215, 403–410.

Balch, W. E., Fox, G. E., Magrum, L. J., Woese, C. R., and Wolfe, R. S. (1979). Methanogens: reevaluation of a unique biological group. *Microbiol. Rev.* 43, 260–296.

Bale, S. J., Goodman, K., Rochelle, P. A., Marchesi, J. R., Fry, J. C., Weightman, A. J., and Parkes, R. J. (1997). *Desulfovibrio profundus* sp. nov., a novel barophilic sulfate-reducing bacterium from deep sediment layers in the Japan Sea. *Int. J. Syst. Bacteriol.* 47, 515–521.

Barnes, S. P., Bradbrook, S. D., Cragg, B. A., Marchesi, J. R., Weightman, A. J., Fry, J. C., and Parkes, R. J. (1998). Isolation of sulfate-reducing bacteria from deep sediment layers of the Pacific Ocean. *Geomicrobiol. J.* 15, 67–83.

Batzke, A., Engelen, B., Sass, H., and Cypionka, H. (2007). Phylogenetic and physiological diversity of cultured deep-biosphere bacteria from equatorial Pacific Ocean and Peru Margin sediments. *Geomicrobiol. J.* 24, 261–273.

Biddle, J. F., House, C. H., and Brenchley, J. E. (2005). "Enrichment and cultivation of microorganisms from sediment from the slope of the Peru Trench (ODP Site 1230)," in *Proceedings of Ocean Drilling Program, Scientific Results, 201*, eds B. B. Jørgensen, S. L. D'Hondt, and D. J. Miller (College Station, TX: Ocean Drilling Program), Available at: http://www-odp.tamu.edu/publications/201_SR/107/107.htm

Blair, C., D'Hondt, S., Spivack, A., and Kingsley, R. (2007). Radiolytic hydrogen and microbial respiration in subsurface sediments. *Astrobiology* 7, 951–970.

Bradford, M. M. (1976). A rapid and sensitive method for the quantitation of microgram quantities of protein utilizing the principle of protein-dye binding. *Anal. Biochem.* 72, 248–254.

Butterfield, D. A., Jonasson, I. R., Massoth, G. J., Feely, R. A., Roe, K. K., Embley, R. E., Holden, J. F., McDuff, R. E., Lilley, M. D., and Delaney, J. R. (1997). Seafloor eruptions and evolution of hydrothermal fluid chemistry. *Philos. Trans. R. Soc. Lond. A* 355, 369–386.

Cord-Ruwisch, R. (1985). A quick method for the determination of dissolved and precipitated sulfides in cultures of sulfate-reducing bacteria. *J. Microbiol. Methods* 4, 33–36.

Cowen, J. P. (2004). The microbial biosphere of sediment-buried oceanic basement. *Res. Microbiol.* 155, 497–506.

Cowen, J. P., Giovannoni, S. J., Kenig, F., Johnson, H. P., Butterfield, D., Rappe, M. S., Hutnak, M., and Lam, P. (2003). Fluids from aging ocean crust that support microbial life. *Science* 299, 120–123.

DeLong, E. F. (2004). Microbial life breathes deep. *Science* 306, 2198–2200.

Detmers, J., Schulte, U., Strauss, H., and Kuever, J. (2001). Sulfate reduction at a lignite seam: microbial abundance and activity. *Microb. Ecol.* 42, 238–247.

D'Hondt, S., Jørgensen, B. B., Miller, D. J., Batzke, A., Blake, R., Cragg, B. A., Cypionka, H., Dickens, G. R., Ferdelman, T., Hinrichs, K. U., Holm, N. G., Mitterer, R., Spivack, A., Wang, G. Z., Bekins, B., Engelen, B., Ford, K., Gettemy, G., Rutherford, S. D., Sass, H., Skilbeck, C. G., Aiello, I. W., Guèrin, G., House, C. H., Inagaki, F., Meister, P., Naehr, T., Niitsuma, S., Parkes, R. J., Schippers, A., Smith, D. C., Teske, A., Wiegel, J., Padilla, C. N., and Acosta, J. L. S. (2004). Distributions of microbial activities in deep subseafloor sediments. *Science* 306, 2216–2221.

D'Hondt, S., Rutherford, S., and Spivack, A. J. (2002). Metabolic activity of subsurface life in deep-sea sediments. *Science* 295, 2067–2070.

D'Hondt, S., Spivack, A., Pockalny, R., Ferdelman, T., Fischer, J., Kallmeyer, J., Abrams, L., Smith, D., Graham, D., Hasiuk, F., Schrum, H., and Stancin, A. (2009). Subseafloor sedimentary life in the South Pacific Gyre. *Proc. Natl. Acad. Sci. U.S.A.* 106, 11651–11656.

Dinh, H. T., Kuever, J., Mussmann, M., Hassel, A. W., Stratmann, M., and Widdel, F. (2004). Iron corrosion by novel anaerobic microorganisms. *Nature* 427, 829–832.

Edwards, K. J., Bach, W., and McCollom, T. M. (2005). Geomicrobiology in oceanography: mineral-microbe interactions at and below the seafloor. *Trends Microbiol.* 13, 449–459.

Edwards, K. J., Bach, W., and Rogers, D. R. (2003). Geomicrobiology of the ocean crust: a role for chemoautotrophic Fe-bacteria. *Biol. Bull.* 204, 180–185.

Ehrhardt, C. J., Haymon, R. M., Lamontagne, M. G., and Holden, P. A. (2007). Evidence for hydrothermal Archaea within the basaltic flanks of the East Pacific Rise. *Environ. Microbiol.* 9, 900–912.

Engelen, B., Ziegelmüller, K., Wolf, L., Köpke, B., Gittel, A., Cypionka, H., Treude, T., Nakagawa, S., Inagaki, F., Lever, M. A., and Steinsbu, B. O. (2008). Fluids from the oceanic crust support microbial activities within the deep biosphere. *Geomicrobiol. J.* 25, 56–66.

Epstein, S. S. (2009). Microbial awakenings. *Nature* 457, 1083.

Expedition 301 Scientists. (2005). "Site U1301," in *Proceedings of Integrated Ocean Drilling Program, 301*, eds A. T. Fisher, T. Urabe, A. Klaus, and Expedition 301 Scientists (College Station, TX: Integrated Ocean Drilling Program Management International, Inc.), doi:10.2204/iodp.proc.301.106.2005

Feio, M. J., Beech, I. B., Carepo, M., Lopes, J. M., Cheung, C. W. S., Franco, R., Guezennec, J., Smith, J. R., Mitchell, J. I., Moura, J. J. G., and Lino, A. R. (1998). Isolation and characterisation of a novel sulphate-reducing bacterium of the *Desulfovibrio* genus. *Anaerobe* 4, 117–130.

Feio, M. J., Beech, I. B., Carepo, M., Lopes, J. M., Cheung, C. W. S., Franco, R., Guezennec, J., Smith, J. R., Mitchell, J. I., Moura, J. J. G., and Lino, A. R. (2000). "*Desulfovibrio indonesiensis corrig.* sp. nov.," in validation of publication of new names and new combinations previously effectively published outside the IJSEM. List no. 75. *Int. J. Syst. Evol. Microbiol.* 50, 1415–1417.

Fisher, A. T., Davis, E. E., Hutnak, M., Spiess, V., Zühlsdorff, L., Cherkaoui, A., Christiansen, L., Edwards, K., Macdonald, R., Villinger, H., Mottl,

M. J., Wheat, C. G., and Becker, K. (2003). Hydrothermal recharge and discharge across 50 km guided by seamounts on a young ridge flank. *Nature* 421, 618–621.

Furnes, H., and Staudigel, H. (1999). Biological mediation in ocean crust alteration: how deep is the deep biosphere? *Earth Planet. Sci. Lett.* 166, 97–103.

Heberling, C., Lowell, R. P., Liu, L., and Fisk, M. R. (2010). Extent of the microbial biosphere in the oceanic crust. *Geochem. Geophys. Geosyst.* 11, 1–15.

Huber, J. A., Johnson, H. P., Butterfield, D. A., and Baross, J. A. (2006). Microbial life in ridge flank crustal fluids. *Environ. Microbiol.* 8, 88–99.

Hutnak, M., Fisher, A. T., Zühlsdorff, L., Spiess, V., Stauffer, P. H., and Gable, C. W. (2006). Hydrothermal recharge and discharge guided by basement outcrops on 0.7–3.6 Ma seafloor east of the Juan de Fuca Ridge: observations and numerical models. *Geochem. Geophys. Geosyst.* 7, 1–36.

Imachi, H., Aoi, K., Tasumi, E., Saito, Y., Yamanaka, Y., Saito, Y., Yamaguchi, T., Tomaru, H., Takeuchi, R., Morono, Y., Inagaki, F., and Takai, K. (2011). Cultivation of methanogenic community from subseafloor sediments using a continuous-flow bioreactor. *ISME J.* 5, 1913–1925.

Inagaki, F., Suzuki, M., Takai, K., Oida, H., Sakamoto, T., Aoki, K., Nealson, K. H., and Horikoshi, K. (2003). Microbial communities associated with geological horizons in coastal subseafloor sediments from the sea of Okhotsk. *Appl. Environ. Microbiol.* 69, 7224–7235.

Johnson, H. P., Baross, J. A., and Bjorklund, T. A. (2006). On sampling the upper crustal reservoir of the NE Pacific Ocean. *Geofluids* 6, 251–271.

Johnson, H. P., and Pruis, M. J. (2003). Fluxes of fluid and heat from the oceanic crustal reservoir. *Earth Planet. Sci. Lett.* 216, 565.

Kaye, J. Z., Sylvan, J. B., Edwards, K. J., and Baross, J. A. (2011). *Halomonas* and *Marinobacter* ecotypes from hydrothermal vent, subseafloor and deep-sea environments. *FEMS Microbiol. Ecol.* 75, 123–133.

Kendall, M. M., Liu, Y., Sieprawska-Lupa, M., Stetter, K. O., Whitman, W. B., and Boone, D. R. (2006). *Methanococcus aeolicus* sp. nov., a mesophilic, methanogenic archaeon from shallow and deep marine sediments. *Int. J. Syst. Evol. Microbiol.* 56, 1525–1529.

Köpke, B., Wilms, R., Engelen, B., Cypionka, H., and Sass, H. (2005). Microbial diversity in coastal subsurface sediments: a cultivation approach using various electron acceptors and substrate gradients. *Appl. Environ. Microbiol.* 71, 7819–7830.

Kuever, J., Könneke, M., Galushko, A., and Drzyzga, O. (2001). Reclassification of Desulfobacterium *phenolicum* as *Desulfobacula phenolica* comb. nov. and description of strain SaxT as *Desulfotignum balticum* gen. nov., sp. nov. *Int. J. Syst. Evol. Microbiol.* 51, 171–177.

Lauro, F. M., McDougald, D., Thomas, T., Williams, T. J., Egan, S., Rice, S., DeMaere, M. Z., Ting, L., Ertan, H., Johnson, J., Ferriera, S., Lapidus, A., Anderson, I., Kyrpides, N., Munk, A. C., Detter, C., Han, C. S., Brown, M. V., Robb, F. T., Kjelleberg, S., and Cavicchioli, R. (2009). The genomic basis of trophic strategy in marine bacteria. *Proc. Natl. Acad. Sci. U.S.A.* 106, 15527–15533.

Lee, Y.-J., Wagner, I., Brice, M., Kevbrin, V., Mills, G., Romanek, C., and Wiegel, J. (2005). *Thermosediminibacter oceani* gen. nov., sp. nov. and *Thermosediminibacter litoriperuensis* sp. nov., new anaerobic thermophilic bacteria isolated from Peru Margin. *Extremophiles* 9, 375–383.

Lever, M. A., Alperin, M., Engelen, B., Inagaki, F., Nakagawa, S., Steinsbu, B. O., Teske, A., and IODP Expedition 301 Scientists. (2006). Trends in basalt and sediment core contamination during IODP Expedition 301. *Geomicrobiol. J.* 23, 517–530.

Lipp, J. S., Morono, Y., Inagaki, F., and Hinrichs, K. U. (2008). Significant contribution of Archaea to extant biomass in marine subsurface sediments. *Nature* 454, 991–994.

Mangelsdorf, K., Zink, K. G., Birrien, J. L., and Toffin, L. (2005). A quantitative assessment of pressure dependent adaptive changes in the membrane lipids of piezosensitive deep sub-seafloor bacterium. *Org. Geochem.* 36, 1459–1479.

McCollom, T. M., and Bach, W. (2009). Thermodynamic constraints on hydrogen generation during serpentinization of ultramafic rocks. *Geochim. Cosmochim. Acta* 73, 856–875.

Mikucki, J. A., Liu, Y., Delwiche, M., Colwell, F. S., and Boone, D. R. (2003). Isolation of a methanogen from deep marine sediments that contain methane hydrates, and description of *Methanoculleus submarinus* sp. nov. *Appl. Environ. Microbiol.* 69, 3311–3316.

Morgulis, A., Coulouris, G., Raytselis, Y., Madden, T. L., Agarwala, R., and Schäffer, A. A. (2008). Database indexing for production MegaBLAST searches. *Bioinformatics* 15, 1757–1764.

Mori, K., Tsurumaru, H., and Harayama, S. (2010). Iron corrosion activity of anaerobic hydrogen-consuming microorganisms isolated from oil facilities. *J. Biosci. Bioeng.* 110, 426–430.

Motamedi, M., and Pedersen, K. (1998). *Desulfovibrio aespoeensis* sp. nov., a mesophilic sulfate-reducing bacterium from deep groundwater at Äspö hard rock laboratory, Sweden. *Int. J. Syst. Bacteriol.* 48, 311–315.

Nakagawa, S., Inagaki, F., Suzuki, Y., Steinsbu, B. O., Lever, M. A., Takai, K., Engelen, B., Sako, Y., Wheat, C. G., Horikoshi, K., and IODP Expedition(301)Scientists. (2006). Microbial community in black rust exposed to hot ridge flank crustal fluids. *Appl. Environ. Microbiol.* 72, 6789–6799.

Nealson, K. H., Inagaki, F., and Takai, K. (2005). Hydrogen-driven subsurface lithoautotrophic microbial ecosystems (SLiMEs): do they exist and why should we care? *Trends Microbiol.* 13, 405–410.

Orcutt, B. N., Bach, W., Becker, K., Fisher, A. T., Hentscher, M., Toner, B. M., Wheat, C. G., and Edwards, K. J. (2010). Colonization of subsurface microbial observatories deployed in young ocean crust. *ISME J.* 5, 692–703.

Overmann, J., and Tuschak, C. (1997). Phylogeny and molecular fingerprinting of green sulfur bacteria. *Arch. Microbiol.* 167, 302–309.

Pankhania, I. P. (1988). Hydrogen metabolism in sulphate-reducing bacteria and its role in anaerobic corrosion. *Biofouling* 1, 27–47.

Parkes, R. J., Cragg, B. A., Bale, S. J., Getliff, J. M., Goodman, K., Rochelle, P. A., Fry, J. C., Weightman, A. J., and Harvey, S. M. (1994). Deep bacterial biosphere in Pacific Ocean sediments. *Nature* 371, 410–413.

Parkes, R. J., Cragg, B. A., Bale, S. J., Goodman, K., and Fry, J. C. (1995). A combined ecological and physiological approach to studying sulfate reduction within deep marine sediment layers. *J. Microbiol. Methods* 23, 235–249.

Parkes, R. J., Linnane, C. D., Webster, G., Sass, H., Weightman, A. J., Hornibrook, E. R. C., and Horsfield, B. (2011). Prokaryotes stimulate mineral H_2 formation for the deep biosphere and subsequent thermogenic activity. *Geology* 39, 219–222.

Pedersen, K. (1997). Microbial life in deep granitic rock. *FEMS Microbiol. Rev.* 20, 399–414.

Pedersen, K. (2000). Exploration of deep intraterrestrial microbial life: current perspectives. *FEMS Microbiol. Lett.* 185, 9–16.

Ramamoorthy, S., Sass, H., Langner, H., Schumann, P., Kroppenstedt, R. M., Spring, S., Overmann, J., and Rosenzweig, R. F. (2006). *Desulfosporosinus lacus* sp nov., a sulfate-reducing bacterium isolated from pristine freshwater lake sediments. *Int. J. Syst. Evol. Microbiol.* 56, 2729–2736.

Roussel, E. G., Bonavita, M. A. C., Querellou, J., Cragg, B. A., Webster, G., Prieur, D., and Parkes, R. J. (2008). Extending the sub-sea-floor biosphere. *Science* 320, 1046–1046.

Rouxel, O., Ono, S., Alt, J., Rumble, D., and Ludden, J. (2008). Sulfur isotope evidence for microbial sulfate reduction in altered oceanic basalts at ODP Site 801. *Earth Planet. Sci. Lett.* 268, 110–123.

Santelli, C. M., Orcutt, B. N., Banning, E., Bach, W., Moyer, C. L., Sogin, M. L., Staudigel, H., and Edwards, K. J. (2008). Abundance and diversity of microbial life in ocean crust. *Nature* 453, 653–656.

Sass, H., and Cypionka, H. (2004). Isolation of sulfate-reducing bacteria from the terrestrial deep subsurface and description of *Desulfovibrio cavernae* sp. nov. *Syst. Appl. Microbiol.* 27, 541–548.

Smith, A., Popa, R., Fisk, M., Nielsen, M., Wheat, C. G., Jannasch, H. W., Fisher, A. T., Becker, K., Sievert, S. M., and Flores, G. (2011). In situ enrichment of ocean crust microbes on igneous minerals and glasses using an osmotic flow-through device. *Geochem. Geophys. Geosyst.* 12, 1–19.

Steinsbu, B. O., Thorseth, I. H., Nakagawa, S., Inagaki, F., Lever, M. A., Engelen, B., Øvreås, L., and Pedersen, R. B. (2010). *Archaeoglobus sulfaticallidus* sp. nov., a novel thermophilic and facultatively lithoautotrophic sulfate-reducer isolated from black rust exposed to hot ridge flank crustal fluids. *Int. J. Syst. Evol. Microbiol.* 60, 2745–2752.

Stevens, H., Brinkhoff, T., and Simon, M. (2005). Composition of free-living, aggregate-associated and sediment surface-associated bacterial communities in the German Wadden Sea. *Aquat. Microb. Ecol.* 38, 15–30.

Stevens, T. (1997). Lithoautotrophy in the subsurface. *FEMS Microbiol. Rev.* 20, 327–337.

Stevens, T. O., and McKinley, J. P. (1995). Lithoautotrophic microbial

ecosystems in deep basalt aquifers. *Science* 270, 450–455.

Straskrabová, V. (1983). The effect of substrate shock on populations of starving aquatic bacteria. *J. Appl. Bacteriol.* 54, 217–224.

Süss, J., Engelen, B., Cypionka, H., and Sass, H. (2004). Quantitative analysis of bacterial communities from Mediterranean sapropels based on cultivation-dependent methods. *FEMS Microbiol. Ecol.* 51, 109–121.

Thorseth, I. H., Torsvik, T., Furnes, H., and Muehlenbachs, K. (1995). Microbes play an important role in the alteration of oceanic crust. *Chem. Geol.* 126, 137–146.

Toffin, L., Bidault, A., Pignet, P., Tindall, B. J., Slobodkin, A., Kato, C., and Prieur, D. (2004a). *Shewanella profunda* sp. nov., isolated from deep marine sediment of the Nankai trough. *Int. J. Syst. Evol. Microbiol.* 54, 1943–1949.

Toffin, L., Webster, G., Weightman, A. J., Fry, J. C., and Prieur, D. (2004b). Molecular monitoring of culturable bacteria from deep-sea sediment of the Nankai trough, Leg 190 Ocean Drilling Program. *FEMS Microbiol. Ecol.* 48, 357–367.

Toffin, L., Zink, K., Kato, C., Pignet, P., Bidault, A., Bienvenu, N., Birrien, J. L., and Prieur, D. (2005). *Marinilactibacillus piezotolerans* sp. nov., a novel marine lactic acid bacterium isolated from deep sub-seafloor sediment of the Nankai trough. *Int. J. Syst. Evol. Microbiol.* 55, 345–351.

Wheat, C. G., Elderfield, H., Mottl, M. J., and Monnin, C. (2000). Chemical composition of basement fluids within an oceanic ridge flank: implications for along-strike and across-strike hydrothermal circulation. *J. Geophys. Res.* 105, 13437–13447.

Wheat, C. G., and Mottl, M. J. (1994). Hydrothermal circulation, Juan de Fuca Ridge eastern flank: factors controlling basement water composition. *J. Geophys. Res.* 99, 3067–3080.

Whitman, W. B., Coleman, D. C., and Wiebe, W. J. (1998). Prokaryotes: the unseen majority. *Proc. Natl. Acad. Sci. U.S.A.* 95, 6578–6583.

Widdel, F., and Bak, F. (1992). "Gram-negative mesophilic sulfate-reducing bacteria," in *The Prokaryotes*, eds A. Balows, H. G. Trüper, M. Dworkin, W. Harder, and K. H. Schleifer (New York: Springer-Verlag), 3352–3378.

Wilms, R., Köpke, B., Sass, H., Chang, T. S., Cypionka, H., and Engelen, B. (2006a). Deep biosphere-related bacteria within the subsurface of tidal flat sediments. *Environ. Microbiol.* 8, 709–719.

Wilms, R., Sass, H., Köpke, B., Köster, J., Cypionka, H., and Engelen, B. (2006b). Specific bacterial, archaeal, and eukaryotic communities in tidal-flat sediments along a vertical profile of several meters. *Appl. Environ. Microbiol.* 72, 2756–2764.

Conflict of Interest Statement: The authors declare that the research was conducted in the absence of any commercial or financial relationships that could be construed as a potential conflict of interest.

Received: 15 November 2011; paper pending published: 16 December 2011; accepted: 06 February 2012; published online: 20 February 2012.

*Citation: Fichtel K, Mathes F, Könneke M, Cypionka H and Engelen B (2012) Isolation of sulfate-reducing bacteria from sediments above the deep-subseafloor aquifer. Front. Microbio. **3**:65. doi: 10.3389/fmicb.2012.00065*

This article was submitted to Frontiers in Extreme Microbiology, a specialty of Frontiers in Microbiology.

frontiers in
MICROBIOLOGY

ORIGINAL RESEARCH ARTICLE
published: 17 November 2011
doi: 10.3389/fmicb.2011.00231

Comparative study of subseafloor microbial community structures in deeply buried coral fossils and sediment matrices from the Challenger Mound in the Porcupine Seabight

Tatsuhiko Hoshino[1], Yuki Morono[1], Takeshi Terada[2], Hiroyuki Imachi[3], Timothy G. Ferdelman[4] and Fumio Inagaki[1]*

[1] *Geomicrobiology Group, Kochi Institute for Core Sample Research, Japan Agency for Marine-Earth Science and Technology, Nankoku, Kochi, Japan*
[2] *Marine Works Japan Ltd., Yokohama, Japan*
[3] *Extremobiosphere Research Program, Institute of Biogeosciences, Japan Agency for Marine-Earth Science and Technology, Yokosuka, Japan*
[4] *Biogeochemistry Group, Max Planck Institute for Marine Microbiology, Bremen, Germany*

Edited by:
Andreas Teske, University of North Carolina at Chapel Hill, USA

Reviewed by:
Doug Bartlett, Scripps Institution of Oceanography, USA
Karine Alain, Centre National de la Recherche Scientifique, France

***Correspondence:**
Fumio Inagaki, Geomicrobiology Group, Kochi Institute for Core Sample Research, Japan Agency for Marine-Earth Science and Technology, Nankoku, Kochi 783-8502, Japan.
e-mail: inagaki@jamstec.go.jp

Subseafloor sedimentary environments harbor remarkably diverse microbial communities. However, it remains unknown if the deeply buried fossils in these sediments play ecological roles in deep microbial habitats, or whether the microbial communities inhabiting such fossils differ from those in the surrounding sediment matrix. Here we compare the community structures of subseafloor microbes in cold-water coral carbonates (*Madrepora oculata* and *Lophelia pertusa*) and the clay matrix. Samples were obtained from the Challenger Mound in the Porcupine Seabight at Site U1317 Hole A during the Integrated Ocean Drilling Program Expedition 307. DNA was extracted from coral fossils and the surrounding sedimentary matrix at 4, 20, and 105 m below the seafloor. 16S rRNA genes of Bacteria and Archaea were amplified by PCR, and a total of 213,792 16S rRNA gene-tagged sequences were analyzed. At the phylum level, dominant microbial components in both habitats consisted of *Proteobacteria*, *Firmicutes*, *Nitrospirae*, *Chloroflexi*, and Miscellaneous Crenarchaeota Group (MCG) at all three of the depths examined. However, at the genus and/or species level (similarity threshold 97.0%), the community compositions were found to be very different, with 69–75 and 46–57% of bacterial and archaeal phylotypes not overlapping in coral fossils and the clay matrix, respectively. Species richness analysis revealed that bacterial communities were generally more diverse than archaea, and that the diversity scores of coral fossils were lower than those in sediment matrix. However, the evenness of microbial communities was not significantly different in all the samples examined. No eukaryotic DNA sequences, such as 18S rRNA genes, were obtained from the corals. The findings suggested that, even at the same or similar depths, the sedimentological characteristics of a habitat are important factors affecting microbial diversity and community structure in deep subseafloor sedimentary habitats.

Keywords: 16S rRNA gene, tag sequence, deep subseafloor biosphere, community structure, coral fossils

INTRODUCTION

During the past decade, numerous studies to infer microbial diversity using 16S rRNA gene-clone libraries have been undertaken in subseafloor sedimentary habitats that have been explored by scientific ocean drilling. These molecular ecological surveys have demonstrated that phylogenetically diverse bacteria and archaea are present, even in deep and old subseafloor sediments, and that these taxa are generally physiologically distinct from known isolates obtained at the surface (e.g., Inagaki et al., 2006; Teske, 2006; Webster et al., 2006). In most cases, core samples used for molecular analysis are 10-cm (or less) whole-round cores (i.e., without half-splitting), which are immediately frozen onboard. Since this sampling scheme minimizes potential microbiological contamination of the innermost core region, microbiologists are able to extract bulk nucleic acids from indigenous microbial cells for molecular ecological studies. However, although 10 cm whole-round core samples may represent a certain period of sedimentological history, little is known about how the concealed sedimentological characteristics and physical properties affect microbial diversity and community structure in such a fine-scaled habitat. For example, a previous study revealed that microbial diversity in hemipelagic clay and volcanic ash layers of a core from the Sea of Okhotsk supported very different bacterial and archaeal subseafloor microbial communities (Inagaki et al., 2003). In addition, differences in paleoenvironmental settings, such as depositional rates, affect the hydrological regimes of sediments resulting in stratification of different microbial communities at different depths (Beck et al., 2011).

During the Integrated Ocean Drilling Program (IODP) Expedition 307, cold-water coral reefs buried in Pleistocene sediments were recovered from Site U1317 on the Challenger Mound in the Porcupine Seabight located in the southwest of Ireland (Ferdelman et al., 2006). The cored samples provided an unprecedented opportunity to study how buried fossil corals (i.e., carbonate skeletons), which constitute sedimentologically distinct habitat compared to the surrounding matrix, affect subseafloor microbial communities. The upper sedimentary unit at Site U1317 was primarily composed of dead, deep-sea cold-water coral matter derived from species such as *Madrepora oculata* and *Lophelia pertusa*, that had been embedded in a clay-type matrix (De Mol et al., 2007). Previous microbiological studies of living *Lophelia* corals on the seafloor showed that microbial communities associated with *Lophelia* are distinct from those in the surrounding sediment and seawater, and that this was likely because the living corals provided the microbes with specific nutrients and niches (Schöttner et al., 2009). However, it is not currently known how the burial of coral reefs and its diagenetic processes (e.g., carbonate dissolution) affect the microbial diversity or community structure of microbes in subseafloor sediments.

Microscopic and quantitative molecular analyses of the Pleistocene sediment matrix at Site U1317 revealed that the site harbors relatively low numbers of microbial cells ($\sim 10^6$ cell/cm^3; Webster et al., 2009). The composition of bacterial communities was previously examined at three different depths by denaturing gradient gel electrophoresis (DGGE). The few resulting DGGE-fragments were subjected to nested-PCR analysis, which revealed the presence of members of *Beta-*, *Gamma-*, *Deltaproteobacteria, Chloroflexi*, and *Actinobacteria* (Webster et al., 2009). Tracer incubation experiments (e.g., methanogenesis and thymidine incorporation) indicated the presence of metabolically active microbial components that mediate biogeochemical cycles in the carbonate mound (Webster et al., 2009), albeit at very low rates for continental margin setting.

In this study, we extracted DNA from the coral carbonate structure and the surrounding clay matrix at three different depths at Site U1317, and examined the community structures of the associated bacterial and archaeal communities by statistically analyzing 454-pyrosequenced 16S rRNA gene fragments. We also attempted PCR amplification of 18S rRNA genes to determine whether the coral DNA fragments buried in the ancient sedimentary layers had been preserved or not. Based on the molecular results obtained from two distinct sedimentary habitats at almost the same depth and age, the potential impacts of sedimentological characteristics on subseafloor microbial communities were also discussed.

MATERIALS AND METHODS

SITE DESCRIPTION

We examined the coral fossils contained in deep-frozen, whole-round cores obtained 4, 20, and 105 meters below the seafloor (mbsf; sample codes: 1H-3, 3H-3, and 12H-3, respectively). Core samples were obtained as 10 cm whole-round cores from Site U1317 (51°22.8′N, 11°43.1′W) at the Challenger Mound in the Porcupine Seabight during IODP Expedition 307 (Ferdelman et al., 2006). Total organic carbon content in the clay matrix of 1H-3, 3H-3, and 12H-3 were 0.06, 0.21, and 0.31%, respectively. Microbial cell counts, as well as some other biogeochemical and paleontological characteristics, such as sulfate and methane concentrations and sedimentation ages, have been reported elsewhere (Ferdelman et al., 2006; Kano et al., 2007; Webster et al., 2009). After core recovery on the drilling vessel *JOIDES Resolution*, the whole-round cores were immediately placed in a deep freezer and kept at −80°C until laboratory use. X-ray computed tomography (CT) showed that the cores contained intact carbonate skeletons of deep-sea cold-water corals, such as *L. pertusa* and *M. oculata* (De Mol et al., 2007; **Figures 1A,B**); the seafloor sediments of the Challenger Mound have few to no modern living corals (Foubert et al., 2005).

X-RAY COMPUTED TOMOGRAPHY

X-ray CT scanning was performed using PRATICO X-ray CT Scanner (Hitachi Medical Corporation, Tokyo, Japan) with a resolution of 0.5 mm in the scanned cross-section. Obtained images from half-round cores were reconstructed to 3D transmission images using the OsiriX software[1].

SUB-SAMPLING PROCEDURE AND DNA EXTRACTION

The frozen whole-round cores were first aseptically cut without sample melt using an electric band saw system in a clean booth equipped with two HEPA-filter units (Masui et al., 2009). To avoid potential contamination, the surface of the core was carefully removed with sterile spatulas in a laminar-flow clean bench. Approximately 10 g of dead coral material (referred to hereafter as "coral fossils") were carefully removed from the clayish sedimentary matrix of each core sample using sterile tweezers, placed in 30 ml phosphate buffered saline (pH 8.0), and then washed at least three times with shaking (**Figure 1**). Samples of the sediment matrix were also collected from the same sample using sterile spatulas. Subsequently, 2 g (wet weight) of the coral fossils or sediment matrix were separately placed in a sterile plastic tube containing several autoclaved metal beads before being mechanically crushed by shaking (Shake Master, Bio Medical Science, Tokyo, Japan).

[1]http://www.osirix-viewer.com/

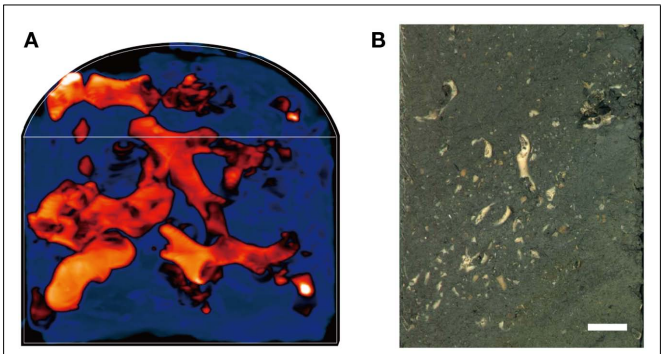

FIGURE 1 | An example of core samples that contain coral fossils. (A) A 3D X-ray CT scan image of a half-round core sample from 20 mbsf (Sample code: 3H-3). Orange-red color indicates the buried coral fossils, while dark blue indicate the sediment matrix. **(B)** A photo image of half-round core surface (3H-3). Scale bar: 1 cm.

Whole DNA was then extracted using a Power Max Soil DNA Isolation Kit (MoBIO Lab. Inc., CA, USA) according to the manufacturer's instructions. The concentration of the extracted DNA was measured using a Quanti-iT DNA assay kit (Invitrogen, CA, USA), and the DNA samples were stored at −20°C until further use.

PCR AMPLIFICATION AND PYROSEQUENCING

PCR amplification of 16S RNA gene fragments was conducted with the primers EUB27F (Frank et al., 2008) and EUB338Rmix (I: 5′-ACTCCTACGGGAGGCAGC-3′, II: 5′-ACACCTACGGGTGGoCTGC-3′, III: 5′-ACACCTACGGGTGGC AGC-3′; Amann et al., 1990) for bacteria, and ARC21F (5′-TTCCGGTTGATCCYGCCGGA-5′; DeLong, 1992) and ARC912R (I: 5′-CCCCCGCCAATTCCTTTAA-3′, II: 5′-CCCCCGTCAATTC CTTCAA-3′, III: 5′-CCCCCGCCAATTTCTTTAA-3′; Miyashita et al., 2009) for archaea. To amplify the archaeal sequences belonged to SAGMEG-1 and *Korarchaeota*, which sequences are potentially biased by the previously used primer set (i.e., ARC21F and ARC912R-I), we mixed two new primers (i.e., ARC912R-II and III) for the PCR reaction used in this study. The used PCR conditions were initial denaturation at 98°C for 30 s followed by 35–38 cycles of 98°C for 10 s, 50°C for 15 s, and 68°C for 30 s for bacterial 16S rRNA genes; 31–34 cycles of 98°C for 10 s, 50°C for 15s, and 68°C for 60s for archaeal 16S rRNA genes. The number of PCR cycles was determined by real-time PCR, for which the amplification curve did not reach a plateau at the cycle number used in this study. For sequencing using a GS FLX pyrosequencer (454 Life Sciences, Branford, CT, USA), another amplification (six cycles) was performed using primers [EUB27F and EUB338Rmix for bacteria, and UNIV530F (I: 5′-GTGCCAGCMGCCGCGG-3′, II: 5′-GTGTCAGCCGCCGCGG-3′) and ARC912R for archaea] with 454 FLX Titanium adapters A, B, and a six-base sample identifier tag. Purification of the amplified product, quality checks, and sequencing with the GS FLX pyrosequencer were conducted by TaKaRa Bio Inc. (Shiga, Japan). All the sequences obtained in this study have been deposited in the DDBJ Sequence Read Archive (accession numbers DRS001093 through DRS001103).

SEQUENCES ANALYSES

All of the reads, including sample identifier tags and primer sequences, were first processed with the Pipeline Initial Process[2], which is part of the Ribosomal Database Project (Cole et al., 2009). Parameters for the Pipeline Initial Process are; forward primer max edit distance: 2, max number of N's: 0, minimum average exp. quality score: 20, reverse primer max edit distance: 0, min sequence length: 150. Reads that did not match the tags and primer sequences were also eliminated through this process. Taxonomic classification of each processed read was then assigned by BLAST analysis with a customized computer script using the ARB SILVA sequence package (Pruesse et al., 2007) as the database.

STATISTICAL ANALYSIS OF MICROBIAL COMMUNITY STRUCTURE

Statistical analysis of the 16S rRNA gene-primer-tagged sequence data was performed using the Mothur Utility package (Schloss et al., 2009). Operational taxonomic units (OTU) were calculated using a 97% sequence similarity cutoff, and the Chao-1 estimator (Chao, 1987) and Shannon diversity index (Krebs, 1989) were also calculated. To evaluate the evenness of community structure, we calculated Pielou's evenness index (J') using the equation (Pielou, 1966)

$$J' = \frac{H'}{\ln S}$$

where, H' is the number derived from the Shannon diversity index and S is the total number of OTUs. The difference in bacterial and archaeal community composition was assessed by the P-test (Martin, 2002). To evaluate similarity between microbial communities, Sørensen's similarity coefficient (Sørensen, 1957) was calculated as follows:

$$\mathrm{QS} = \frac{2AB}{A+B}$$

where, A and B are the number of OTUs observed in communities A and B, respectively, and AB is the number of OTUs occurring in both of the communities. Consequently, QS corresponds to the ratio of the number of shared OTUs between communities A and B to the sum of the total number of OTUs in each community.

RESULTS AND DISCUSSION

PHYLUM-LEVEL MICROBIAL COMMUNITY COMPOSITIONS

Whole DNA was extracted from the coral fossil and sediment matrix samples collected from three different depths (4, 20, and 105 mbsf). Using a commercial DNA extraction kit, we obtained PCR-amplifiable DNA from 1 g of coral fossil material at yields of 143, 80, and 78 ng from of the fossils from the 1H-3C, 3H-3C, and 12H-3C samples, respectively. Markedly higher DNA yields were obtained concentrations of at 980 and 348 ng from the 1H-3M and 3H-3M samples, respectively. However, we did not obtain any measurable or PCR-amplifiable DNA from the clay matrix sample from 12H-3M at 105 mbsf, which is not expected from the cell count result that all of the depths contained the order of 10^6 cells and did not show significant difference (Webster et al., 2009). It is not apparent why, but possibly because of inefficient lysis of the microbes in the sample or fragmentation of extracted DNA, which are often the problem in DNA extraction from the environmental sample. Primer-tagged PCR of bacterial and archaeal 16S rRNA genes resulted in successful amplification of the target gene sequences. No amplification was observed in the negative control samples (i.e., DNA extracts performed without substrate samples). Approximately 20,000 reads from each sample were obtained by 454-sequencing (i.e., 213,792 fragment reads in total) and then used for the comparative statistical analysis of microbial community structure of the different subseafloor habitats.

Phylogenetic clustering analysis of primer-tagged bacterial 16S rRNA gene fragments showed that the dominant bacterial taxa belonged to *Proteobacteria, Actinobacteria*, Candidate division OD1, candidate division OP1, Candidate division OP11, *Chloroflexi*, *Firmicutes*, and *Nitrosopirae* (**Figure 2A**. Sequences related to *Chloroflexi* were identified as the dominant bacterial components in all the samples examined, accounting for 20–46% of

[2]http://pyro.cme.msu.edu/init/form.spr

all the bacterial 16S rRNA gene-tagged sequences (**Figure 2A**). These bacterial sequences have frequently been detected in the organic-rich sediments at the continental margins (e.g., off Peru, Nankai Trough), suggesting that the Challenger Mound may support an heterotrophic microbial ecosystem, even though the microbial populations and activities, as well as total organic matter concentrations, are all relatively low (Ferdelman et al., 2006; Webster et al., 2009). Interestingly, the sequences of Candidate division JS1 and the *Planctomycetes*, both of which are generally widespread in organic-rich subseafloor sediments (Inagaki et al., 2003, 2006; Webster et al., 2004), were rarely detected in the collected samples. Members of gamma *Proteobacteria* which were reported to be a major component of microbial community associated with living *L. pertusa* (Neulinger et al., 2008; Kellogg et al., 2009) and highly dominant in metabolically active portion of a microbial community colonizing dead *L. pertusa* (Yakimov et al., 2006) did not constitute large fraction in this study.

At the phylum level, archaeal community compositions were generally simpler than that observed in the bacterial communities. The members of the Miscellaneous Crenarchaeotic Group (MCG; Inagaki et al., 2003) were the most commonly detected archaeal phylotypes in all of the samples, representing 80% of the 16S rRNA gene-tagged-archaeal sequences obtained (**Figure 2B**). Some of the sequences were affiliated to the South African Gold Mine Euryarchaeotic Group (SAGMEG) and the Deep-Sea Archaeal Group [DSAG; alternatively classified as Marine Benthic Group D (MBG-D)]. Marine Group I archaea were only detected from the sediment matrix of 1H-3. The sequences of potential methanogens within the *Methanomicrobia* were detected from 1H-3 and 3H-3 as relatively minor archaeal components.

SIMILARITIES BETWEEN COMMUNITIES IN DIFFERENT HABITATS

Classifications generated using the 16S rRNA gene-tagged sequences revealed that the community compositions of the coral fossil and the clay matrix samples were generally similar at the

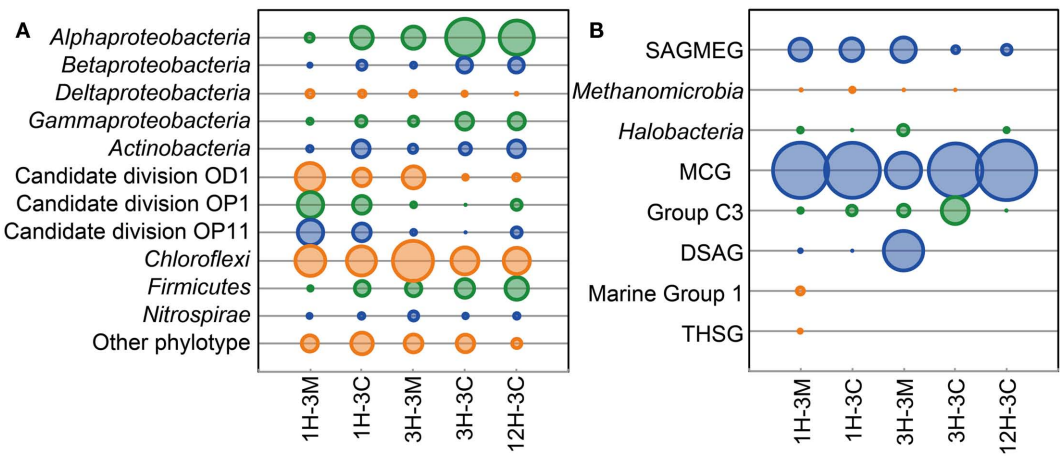

FIGURE 2 | Microbial community compositions in the buried coral fossil carbonates and the clay matrices. Phylogenetic clustering analysis of **(A)** bacterial and **(B)** archaeal communities is based on the 16S rRNA gene-tagged sequences. The area of each bubble represents the phylotype frequency in the sample examined.

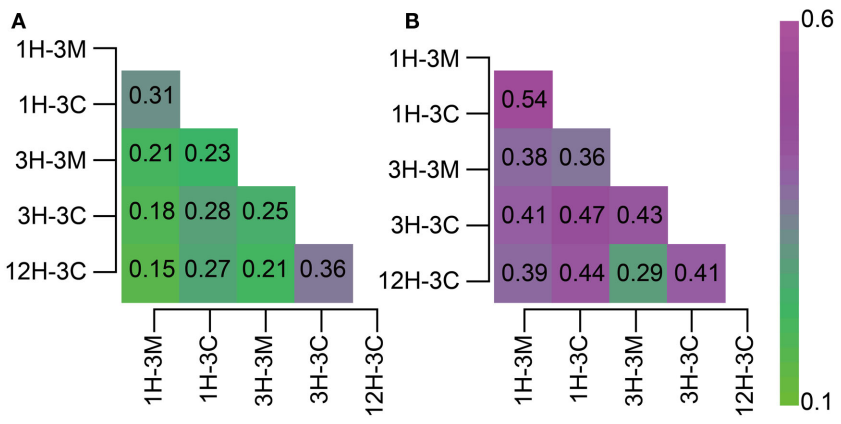

FIGURE 3 | Heat map matrix of Sørenson index values among 16S rRNA gene-tagged sequence libraries. The index score indicates the similarity between two **(A)** bacterial or **(B)** archaeal communities.

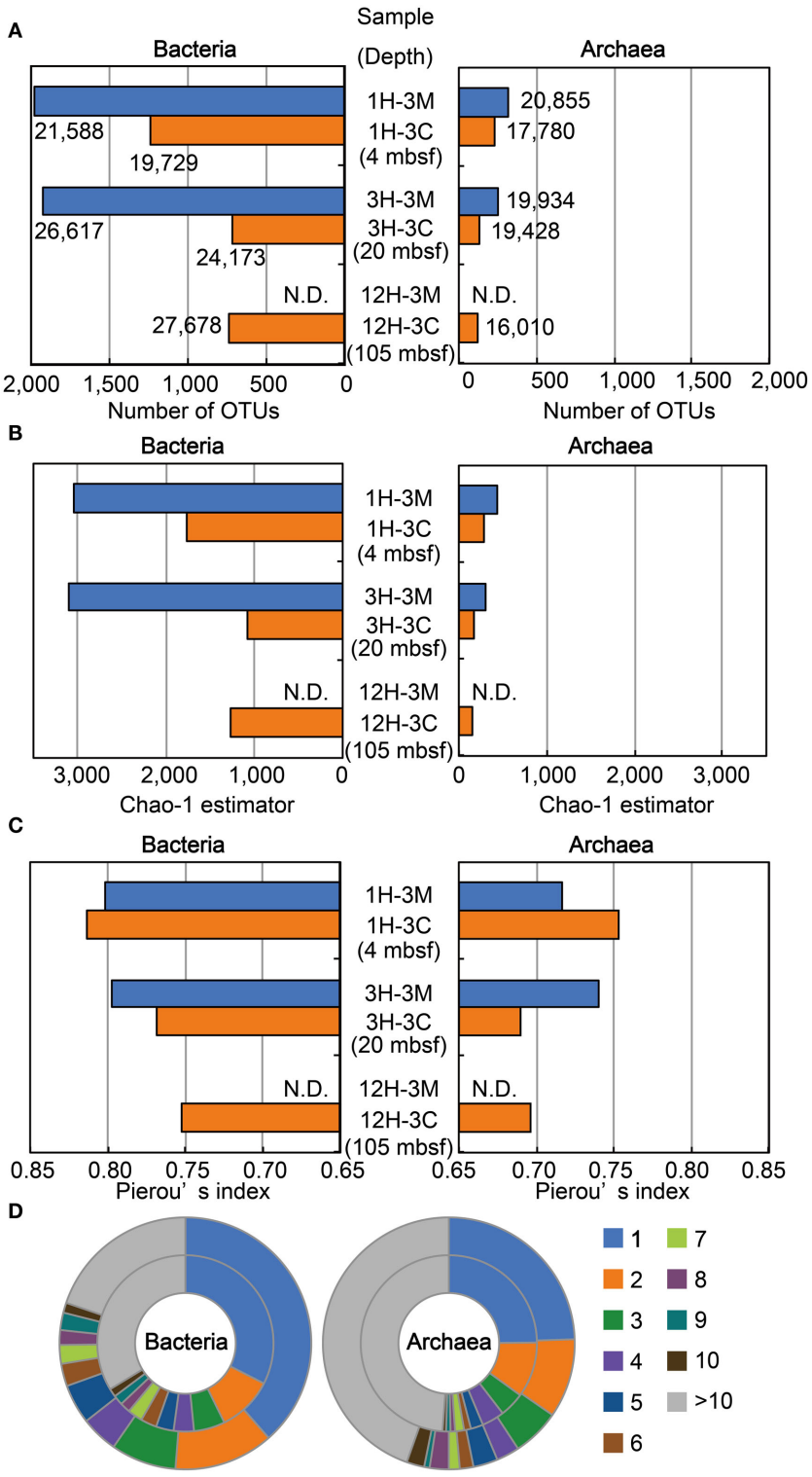

FIGURE 4 | Microbial diversity and community structure estimated by OTU-based analysis of 16S rRNA gene-tagged sequences. (A) The number of OTUs defined as a group of sequences with less than 3% sequence divergence. The number of tag sequences obtained by 454-pyrosequencing is shown adjacent to the bars. **(B)** Chao-1 estimator for estimating community richness. **(C)** Pierou's index for assessing evenness of the community. **(D)** Phylotype frequency for total bacterial (left) and archaeal (right) communities. The outer and inner circles indicate the community from clay matrices and coral fossils, respectively. The number of tag sequences classified as the same phylotype (OTU) is indicated by color as shown in the right legend. Blue and orange bars in **(A–C)** indicate sediment matrix and coral fossil, respectively. N.D., Not determined.

phylum- and class-levels (**Figure 2**). We therefore analyzed the data further using the *P*-test (Martin, 2002) and Sørensen's similarity coefficient. Interestingly, all of the *P*-values obtained were less than 0.01, implying that microbial communities from any different habitats and depths were distinct from each other; except for samples 1H-3M and 3H-3C for which the difference was not significant ($P > 0.1$). Sørencen's index values (QS) among bacterial communities ranged from 0.15 to 0.36, indicating that even though bacterial communities were similar at the phylum level, the bacterial community compositions are very different at the genus- or species level (**Figure 3A**). Similarly, QS values among archaeal communities ranged from 0.29 to 0.54, which were slightly higher than those obtained for bacteria (**Figure 3B**). Even when the community compositions of the coral fossils and matrices from the same depth were compared, the QS values are unexpectedly low: e.g., QS values among bacterial communities in coral fossils and matrices from 4 to 20 mbsf were 0.31 and 0.25, respectively. The highest QS value for bacteria was obtained from 3H-3C (4 mbsf) and 12H-3C (105 mbsf), which were derived from the spatially distinct subseafloor habitat. This finding suggests that the carbonate coral fossils harbor microbial communities that are more similar to each other than the communities in the matrix from the same depth (i.e., QS = 0.25 for 3H-3M and 3H-3C, 0.31 for 1H-3M and 1H-3C). The coral fossils also harbor more shared archaeal components than the clay matrix (i.e., QS = 0.47 for 1H-3C and 3H-3C, 0.44 for 1H-3C and 12H-3C, and 0.41 for 3H-3C and 12H-3C). These finding provide conclusive statistical evidence of microbial diversity differences in sedimentologically distinct microbial habitats, and that deeply buried carbonate fossils constitute an ecologically significant habitat for unique microbial components.

COMPARISON OF COMMUNITY RICHNESS AND EVENNESS

We examined the structure of bacterial and archaeal communities using a total of 213,792 16S rRNA gene-tagged sequences (119,785 and 94,007 for bacteria and archaea, respectively: **Figure 4A**). The number of OTUs determined by 3% sequence divergence (**Figure 4A**), as well as the Chao-1 estimator (**Figure 4B**), clearly showed that bacterial communities were generally more diverse than archaeal communities. The results showed that Chao-1 estimates of the bacterial communities in matrix samples (i.e., 1H-3M and 3H3-M) had over 3,000 OTUs, whereas the Chao estimates of coral fossils (i.e., 1H-3C, 3H-3C, and 12H-3C) were approximately 50% of the diversity richness (**Figure 4B**). A similar trend was also observed in the community structure of the archaea. Taken together, these findings indicate that microbial communities inhabiting the buried coral carbonate fossils were less diverse than those in the clay matrix. Interestingly, the diversity of the microbial communities in the Porcupine Mound subseafloor habitat was very similar between different depth, and no decrease of the diversity along the depths was observed (**Figure 4B**).

Results obtained for Pielou's evenness index (J') and the phylotype frequency are shown in **Figures 4C,D**, respectively. The evenness scores of bacterial and archaeal communities ranged from 0.75 to 0.81 and 0.69 to 0.75, respectively (**Figure 4C**). These data indicate that the relatively high evenness of microbial communities are observed in all of the samples examined, and that the phylotypes of bacterial communities are more evenly distributed than those of archaeal communities. The Pielou's index data were highly consistent with the ratios obtained for phylotype frequency (**Figure 4D**). For example, the ratios of singletons in the bacterial 16S rRNA gene-tagged sequence data were higher than those obtained for archaeal tag sequences, even though the frequency patterns of the obtained OTUs in coral fossils and clay matrices were relatively similar to each other. These analyses of community structure using measures of diversity and evenness consistently suggest that habitability of the detected microbial components might be relatively evenly supported by geochemical and/or geophysical constraints.

EUKARYOTIC DNA AMPLIFICATION

In order to determine whether coral DNA could be preserved in sediments over a geological timescale, we attempted to amplify eukaryotic 18S rRNA genes from fossil coral and clays. Although no eukaryotic DNA fragments were obtained, several archaeal 16S rRNA genes were amplified (data not shown), most likely due to the mismatched primer annealing. These results suggested that the buried eukaryotic DNA had been almost completely degraded and utilized by indigenous microbes in the sediments. The data also indicate that the presence of eukaryotes living below the seafloor is unlikely in the environment examined, or if any eukaryotes were present, the populations are either below detectable limits or not detected with the used primers.

CONCLUSION AND PROSPECTS

In this study, we characterized the structure of microbial communities in different sedimentary habitats of the Porcupine Mound. We found that the buried coral carbonate fossils harbor microbial communities that differ from those in the sediment matrices. Bacterial communities were generally more diverse than archaeal communities in all substrate types and depths. The species richness of microbial communities in the sediment matrix was higher than that in the coral fossil substrates, while evenness was relatively high for all of the samples examined. These results suggested that the Pleistocene coral sediments in the Porcupine Mound represent unique subseafloor microbial habitat and, even at the same or similar depths, the characteristics of the sediments were shown to affect microbial diversity and community structure. However, it remains to be determined whether fossil coral-associated microbial components play an ecological role in carbonate diagenesis. Similarly, since the role of geochemical factors and/or geophysical constraints on niche preference by subseafloor microbial communities remains unknown. These factors should be clarified through scientific ocean drilling in the future.

ACKNOWLEDGMENTS

The authors thank Ms. Sayo Hashimoto for technical assistance and Dr. Takayuki Tomiyama for X-CT imaging of core samples. Samples and photo images used in this study were provided by the Integrated Ocean Drilling Program (IODP) Expedition 307. This work is supported in part by the JSPS Strategic Fund for Strengthening Leading-Edge Research and Development (to JAMSTEC), and the JSPS Funding Program for Next Generation World-Leading Researchers (NEXT Program; to Fumio Inagaki).

REFERENCES

Amann, R. I., Binder, B. J., Olson, R. J., Chisholm, S. W., Devereux, R., and Stahl, D. A. (1990). Combination of 16S rRNA-targeted oligonucleotide probes with flow cytometry for analyzing mixed microbial populations. *Appl. Environ. Microbiol.* 56, 1919–1925.

Beck, M., Riedel, T., Graue, J., Köster, J., Kowalski, N., Wu, C. S., Wegener, G., Lipsewers, Y., Freund, H., Böttcher, M. E., Brumsack, H.-J., Cypionka, H., Rullkötter, J., and Engelen, B. (2011). Imprint of past and present environmental conditions on microbiology and biogeochemistry of coastal quaternary sediments. *Biogeosciences* 8, 55–68.

Chao, A. (1987). Estimating the population size for capture-recapture data with unequal catchability. *Biometrics* 43, 783–791.

Cole, J. R., Wang, Q., Cardenas, E., Fish, J., Chai, B., Farris, R. J., Kulam-Syed-Mohideen, A. S., McGarrell, D. M., Marsh, T., Garrity, G. M., and Tiedje, J. M. (2009). The Ribosomal Database Project: improved alignments and new tools for rRNA analysis. *Nucleic Acids Res.* 37, D141–D145.

De Mol, B., Kozachenko, M., Wheeler, A., Alvares, H., Henriet, J. P., and Olu-Le Roy, K. (2007). Thérèse Mound: a case study of coral bank development in the Belgica Mound Province, Porcupine Seabight. *Int. J. Earth Sci.* 96, 103–120.

DeLong, E. F. (1992). Archaea in coastal marine environments. *Proc. Natl. Acad. Sci. U.S.A.* 89, 685–689.

Ferdelman, T. G., Kano, A., Williams, T., Henriet, J. P., and the Expedition 307 Scientists. (2006). "Modern carbonate mounds: Porcupine drilling," in *Proceedings of the Integrated Ocean Drilling Program, Volume 307 Expedition Reports.* Washington, DC: IODP Management International. doi:10.2204/iodp.proc.307.102.2006

Foubert, A., Beck, T., Wheeler, A. J., Opderbecke, J., Grehan, A., Klages, M., Thiede, J., Henriet, J.-P., and the Polar-stern ARK-XIX/3A Shipboard Party. (2005). "New view of the Belgica Mounds, Porcupine Seabight, NE Atlantic: preliminary results from the Polarstern ARK-XIX/3a ROV cruise," in *Cold Water Corals and Ecosystems*, eds A. Freiwald and J. M. Roberts (Heidelberg: Springer-Verlag), 403–415.

Frank, J. A., Reich, C. I., Sharma, S., Weisbaum, J. S., Wilson, B. A., and Olsen, G. J. (2008). Critical evaluation of two primers commonly used for amplification of bacterial 16S rRNA genes. *Appl. Environ. Microbiol.* 74, 2461–2470.

Inagaki, F., Nunoura, T., Nakagawa, S., Teske, A, Lever, M., Lauer, A., Suzuki, M., Takai, K., Delwiche, M., Colwell, F. S., Nealson, K. H., Horikoshi, K., D'Hondt, S., and Jørgensen, B. B. (2006). Biogeographical distribution and diversity of microbes in methane hydrate-bearing deep marine sediments on the Pacific Ocean Margin. *Proc. Natl. Acad. Sci. U.S.A.* 103, 2815–2820.

Inagaki, F., Suzuki, M., Takai, K., Oida, H., Sakamoto, T., Aoki, K., Nealson, K. H., and Horikoshi, K. (2003). Microbial communities associated with geological horizons in coastal subseafloor sediments from the Sea of Okhotsk. *Appl. Environ. Microbiol.* 69, 7224-7235

Kano, A., Ferdelman, T. G., Williams, T., Henriet, J. P., Ishikawa, T., Kawagoe, N., Takashima, C., Kakizaki, Y., Abe, K., Sakai, S., Browning, E. L., Li, X., and Integrated Ocean Drilling Program Expedition 307 Scientists. (2007). Age constraints on the origin and growth history of a deep-water coral mound in the northeast Atlantic drilled during Integrated Ocean Drilling Program Expedition 307. *Geology* 35, 1051–1054.

Kellogg, C. A., Lisle, J. T., and Galkiewicz, J. P. (2009). Culture-independent characterization of bacterial communities associated with the cold-water coral *Lophelia pertusa* in the northeastern Gulf of Mexico. *Appl. Environ. Microbiol.* 75, 2294–2303.

Krebs, C. J. (1989). *Ecological Methodology*, 2nd Edn. Menlo Park, CA: Benjamin/Cummings.

Martin, A. P. (2002). Phylogenetic approaches for describing and comparing the diversity of microbial communities. *Appl. Environ. Microbiol.* 68, 3673–3682.

Masui, N., Morono, Y., and Inagaki, F. (2009). Bio-archive core storage and subsampling procedure for subseafloor molecular biological research. *Sci. Drill.* 8, 35–37.

Miyashita, A., Mochimaru, H., Kazama, H., Ohashi, A., Yamaguchi, T., Nunoura, T., Horikoshi, K., Takai, K., and Imachi, H. (2009). Development of 16S rRNA gene-targeted primers for detection of archaeal anaerobic methanotrophs (ANMEs). *FEMS Microbiol. Lett.* 297, 31–37.

Neulinger, S. C., Jarnegren, J., Ludvigsen, M., Lochte, K., and Dullo, W. C. (2008). Phenotype-specific bacterial communities in the cold-water coral *Lophelia pertusa* (Scleractinia) and their implications for the coral's nutrition, health, and distribution. *Appl. Environ. Microbiol.* 74, 7272–7285.

Pielou, E. C. (1966). Species-diversity and pattern-diversity in the study of ecological succession. *J. Theor. Biol.* 10, 370–383.

Pruesse, E., Quast, C., Knittel, K., Fuchs, B. M., Ludwig, W., Peplies, J., and Glockner, F. O. (2007). SILVA: a comprehensive online resource for quality checked and aligned ribosomal RNA sequence data compatible with ARB. *Nucleic Acids Res.* 35, 7188–7196.

Schloss, P. D., Westcott, S. L., Ryabin, T., Hall, J. R., Hartmann, M., Hollister, E. B., Lesniewski, R. A., Oakley, B. B., Parks, D. H., Robinson, C. J., Sahl, J. W., Stres, B., Thallinger, G. G., Van Horn, D. J., and Weber, C. F. (2009). Introducing mothur: open-source, platform-independent, community-supported software for describing and comparing microbial communities. *Appl. Environ. Microbiol.* 75, 7537–7541.

Schöttner, S., Hoffmann, F., Wild, C., Rapp, H. T., Boetius, A., and Ramette, A. (2009). Inter- and intra-habitat bacterial diversity associated with cold-water corals. *ISME J.* 3, 756-759

Sørensen, T. (1957). A method of establishing groups of equal amplitude in plant sociology based on similarity of species and its application to analyses of the vegetation on Danish commons. *Biologiske Skrifter/Kongelige Danske Videnskabernes Selskab* 5, 1–34

Teske, A. P. (2006). Microbial communities of deep marine subsurface sediments: molecular and cultivation surveys. *Geomicrobiol. J.* 23, 357–368.

Webster, G., Blazejak, A., Cragg, B. A., Schippers, A., Sass, H., Rinna, J., Tang, X., Mathes, F., Ferdelman, T. G., Fry, J. C., Weightman, A. J., and Parkes, R. J. (2009). Subsurface microbiology and biogeochemistry of a deep, cold-water carbonate mound from the Porcupine Seabight (IODP Expedition 307). *Environ. Microbiol.* 11, 239–257.

Webster, G., Parkes, R. J., Cragg, B. A., Newberry, C. J., Weightman, A. J., and Fry, J. C. (2006). Prokaryotic community composition and biogeochemical processes in deep subseafloor sediments from the Peru Margin. *FEMS Microbiol. Ecol.* 58, 65–85.

Webster, G., Parkes, R. J., and Weightman, A. (2004). Widespread occurrence of a novel division of bacteria identified by 16S rRNA gene sequences originally found in deep marine sediments. *Appl. Environ. Microbiol.* 70, 5708–5713.

Yakimov, M. M., Cappello, S., Crisafi, E., Tursi, A., Savini, A., Corselli, C., Scarfi, S., and Giuliano, L. (2006). Phylogenetic survey of metabolically active microbial communities associated with the deep-sea coral *Lophelia pertusa* from Apulian plateau, Central Mediterranean Sea. *Deep Sea Res. Part I.* 53, 62–75.

Conflict of Interest Statement: The authors declare that the research was conducted in the absence of any commercial or financial relationships that could be construed as a potential conflict of interest.

Received: 19 August 2011; paper pending published: 06 September 2011; accepted: 01 November 2011; published online: 17 November 2011.

*Citation: Hoshino T, Morono Y, Terada T, Imachi H, Ferdelman TG and Inagaki F (2011) Comparative study of subseafloor microbial community structures in deeply buried coral fossils and sediment matrices from the Challenger Mound in the Porcupine Seabight. Front. Microbio. **2**:231. doi: 10.3389/fmicb.2011.00231*

This article was submitted to Frontiers in Extreme Microbiology, a specialty of Frontiers in Microbiology.

frontiers in
MICROBIOLOGY

ORIGINAL RESEARCH ARTICLE
published: 21 December 2011
doi: 10.3389/fmicb.2011.00249

Anaerobic oxidation of methane at a marine methane seep in a forearc sediment basin off Sumatra, Indian Ocean

***Michael Siegert*[1,2], *Martin Krüger*[1]*, *Barbara Teichert*[1†], *Michael Wiedicke*[1] and *Axel Schippers*[1,2]**

[1] *Federal Institute for Geosciences and Natural Resources, Hannover, Germany*
[2] *Faculty of Natural Sciences, Leibniz Universität Hannover, Hannover, Germany*

Edited by:
Andreas Teske, University of North Carolina at Chapel Hill, USA

Reviewed by:
Nils Risgaard-Petersen, Aarhus University, Denmark
Heide N. Schulz-Vogt, Max-Planck-Institute for Marine Microbiology, Germany

***Correspondence:**
Martin Krüger, Federal Institute for Geosciences and Natural Resources, Stilleweg 2, 30655 Hannover, Germany.
e-mail: martin.krueger@bgr.de

[†]***Present address:***
Barbara Teichert, Institut für Geologie und Paläontologie, Universität Münster, 48149 Münster, Germany.

A cold methane seep was discovered in a forearc sediment basin off the island Sumatra, exhibiting a methane-seep adapted microbial community. A defined seep center of activity, like in mud volcanoes, was not discovered. The seep area was rather characterized by a patchy distribution of active spots. The relevance of anaerobic oxidation of methane (AOM) was reflected by ^{13}C-depleted isotopic signatures of dissolved inorganic carbon. The anaerobic conversion of methane to CO_2 was confirmed in a ^{13}C-labeling experiment. Methane fueled a vital microbial community with cell numbers of up to 4×10^9 cells cm^{-3} sediment. The microbial community was analyzed by total cell counting, catalyzed reporter deposition–fluorescence in situ hybridization (CARD–FISH), quantitative real-time PCR (qPCR), and denaturing gradient gel electrophoresis (DGGE). CARD–FISH cell counts and qPCR measurements showed the presence of *Bacteria* and *Archaea*, but only small numbers of *Eukarya*. The archaeal community comprised largely members of ANME-1 and ANME-2. Furthermore, members of the *Crenarchaeota* were frequently detected in the DGGE analysis. Three major bacterial phylogenetic groups (δ-*Proteobacteria,* candidate division OP9, and *Anaerolineaceae*) were abundant across the study area. Several of these sequences were closely related to the genus *Desulfococcus* of the family *Desulfobacteraceae,* which is in good agreement with previously described AOM sites. In conclusion, the majority of the microbial community at the seep consisted of AOM-related microorganisms, while the relevance of higher hydrocarbons as microbial substrates was negligible.

Keywords: DGGE, quantitative PCR, CARD–FISH, methane seep, stable isotopes, AOM, hydrocarbon-dependent methanogenesis

INTRODUCTION

Anaerobic oxidation of methane (AOM) has been described for decades, but became accepted as a key process in anaerobic carbon cycling only during the last 15 years (Davis and Yarbrough, 1966; Barnes and Goldberg, 1976; Reeburgh, 1976, 2007; Knittel and Boetius, 2009). So far, it has been observed in many marine environments contributing significantly to carbon cycling in the sediments and the reduction of methane emissions. Continental margins and their forelands were examined in numerous biogeochemical studies (e.g., Bohrmann et al., 1998; Reed et al., 2002; Inagaki et al., 2006) and AOM was associated mainly to gas seeps and mud volcanoes (Aloisi et al., 2000; Joye et al., 2004; Valentine et al., 2005; Niemann et al., 2006b; Lösekann et al., 2007). Such cold seep ecosystems, especially in the Eel River Basin (Orphan et al., 2002), the Hydrate Ridge (Bohrmann et al., 1998), the Black Sea (Michaelis et al., 2002), and the Gulf of Mexico (Roberts and Aharon, 1994), have been intensively studied regarding the geochemistry and microbiology of AOM. Within these AOM ecosystems, ANaerobic MEthanotrophs (ANME) populations are often the prevailing constituents and drive the biogeochemical processes.

In sediment systems with diffusive methane fluxes, the distribution of ANME is restricted to the sulfate–methane transition zone (SMTZ), the only place where both methane and sulfate are available. The ANME populations and their sulfate-reducing partner bacteria are principally the same as those at cold seeps. However, cell numbers and activities of AOM-related populations are significantly lower (Knittel and Boetius, 2009).

Although the importance of AOM in a global context has been widely recognized, the process is on a mechanistical and physiological level still not very well understood (Thauer, 2011). In the initial AOM reports, methanogenesis and sulfate reduction were believed to be mutually exclusive processes (Martens and Berner, 1974). However, AOM coincides with methanogenesis (Krüger et al., 2005; Niemann et al., 2006b), and was therefore proposed to be reverse methanogenesis (Krüger et al., 2003; Scheller et al., 2010). So far, it was demonstrated that sulfate and nitrite reduction couple to AOM as a joint process of specialized methane oxidizers and sulfate- or nitrite-reducing microorganisms (Boetius et al., 2000; Raghoebarsing et al., 2006; Ettwig et al., 2010). Metal reduction coupled to AOM was also suggested (Beal et al., 2009). Phylogenetic analysis of AOM-sediments identified three novel groups of so-called ANME-*Archaea*, ANME-1, ANME-2, and ANME-3. These ANME are distantly related to cultivated methanogenic members from the orders *Methanosarcinales* and *Methanomicrobiales* (Orphan et al.,

2002; Knittel et al., 2005; Niemann et al., 2006b). FISH techniques showed that ANME occur in aggregates (Boetius et al., 2000; Michaelis et al., 2002; Knittel et al., 2005) with bacteria related to *Desulfosarcina–Desulfococcus* or *Desulfobulbus*. These findings suggest that AOM coupled to sulfate reduction is a syntrophic process, in which ANME convert methane to a metabolite which is used as electron donor by the sulfate-reducing bacterial partner.

The Sumatra forearc is spatially remote from previous study sites. Therefore, our main objective on the R/V Sonne cruise SO189-2 into the Sumatra forearc basins was to detect and investigate methane seeps on the seafloor, and to describe the related geochemical and microbiological features in comparison to background sediments of nearby sites. After the successful first-time discovery of a methane-driven cold seep in this geographical region, we analyzed different biogeochemical proxies for AOM to determine related microbial activities. This was combined with molecular biological methods to study the involved microbial populations, to allow a comparison of the present results with those already published on other seep sites worldwide.

MATERIALS AND METHODS

SITE DESCRIPTION AND SAMPLING

General features of the Simeulue and the Nias Basin in the Sumatra forearc are described in Sieh and Natawitjaja (2000) and Schippers et al. (2010). Focus of this study is an area without seismic reflections ("seismic blanking") discovered SE of the Simeulue basin, indicating free gases in the sediment (**Figures 1** and **2**). Measurements of dissolved gas of samples taken from the water column indicated elevated methane concentrations in the water column in this area (Wiedicke-Hombach et al., 2006). Additionally, pictures and samples from the seafloor revealed a typical seep fauna comprising mainly bivalves and white crabs (Martin and Haney, 2005), colonizing outcropping carbonate precipitations, and the surrounding sediments.

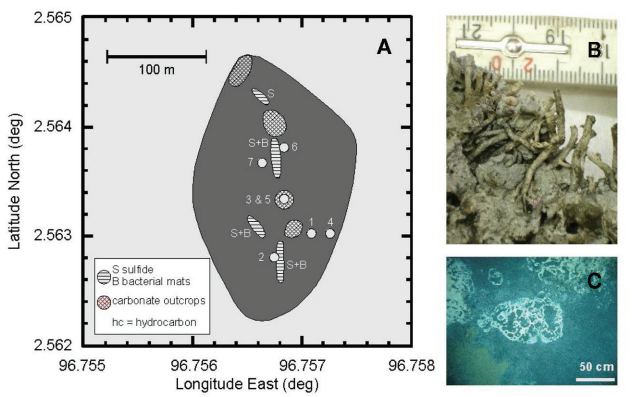

FIGURE 1 | (A) Map of the methane seep in the Simeulue basin off Sumatra. The area without seismic reflections in the sediment is shaded in dark gray. Circles indicate sampling stations according to the ship's position. Wire mesh areas depict carbonate outcrops and horizontal lines sulfide-rich surfaces "S" with microbial mats "B." **(B)** Unclassified tubeworms found at the carbonate outcrops. **(C)** White bacterial mats near the sediment surface of the station 2.

During the R/V *Sonne* cruise SO189-2 in 2006, nine sediment stations were sampled at the suspected seep area in the Simeulue basin, a reference site, and also in the Nias basin as summarized in **Table 1**. The sediment was sampled using a 6-m long gravity corer (SL), a 0.5 m long multicorer (MC), and a TV camera guided 0.9 m × 0.9 m grab (TV). The sediment in the TV-grab was further sampled using hand-held small pushcores.

BIOLOGICAL SAMPLES

Immediately after porewater sampling (see Geochemical Analyses), approx. 300–400 ml sediment samples of multicorer or 20–100 ml sediment of gravity cores were collected in glass bottles. Bottles were sealed with butyl rubber stoppers and plastic screw caps. The headspace was flushed with nitrogen gas. These "live" samples for sediment microcosm were stored and transported at 4°C until further on-shore processing. For quantitative real-time PCR (qPCR) and denaturing gradient gel electrophoresis (DGGE) community analysis, parallel samples were frozen onboard at −20°C. For fluorescence microscopic methods, samples were treated as described below.

INCUBATION EXPERIMENTS TO DETERMINE MICROBIAL ACTIVITY IN SEDIMENT MICROCOSMS

An overview over the experimental setup of the microcosms is displayed in **Table 2**.

General slurry preparation and microcosm inoculation

To prepare slurries for inoculation, sediment samples were mixed 1:1 with artificial seawater medium (Widdel and Bak, 1992). Subsequently, 10 ml of sediment slurry were added to 20 ml of medium, resulting in 5 ml sediment per bottle. Serum bottles of 60 ml volume were used. All manipulations were carried out under dinitrogen atmosphere in an anoxic glove box at room temperature. The headspace of the incubation tubes consisted of either methane (100%) or N_2/CO_2 (90%/10%$_{v/v}$). These microcosms were incubated horizontally in the dark without shaking at *in situ* temperature which was either 6 or 23°C (**Table 1**).

Monitoring of AOM microcosms and determination of sulfate reduction rates

Anaerobic oxidation of methane was measured *in vitro* by methane-dependent sulfate reduction unless stated otherwise (Nauhaus et al., 2002; Krüger et al., 2005; Treude et al., 2005). Sulfide concentrations were determined spectrophotometrically by the formation of copper sulfide (Cord-Ruwisch, 1985). Sulfide concentrations of methane amended microcosms were subtracted from sulfide concentrations of controls without methane before rates were calculated. Rates are given in μmol cm^{-3} day^{-1} wet sediment and deviations are expressed as 95% confidence intervals unless stated otherwise.

AOM labeling experiment with ^{13}C-methane

For further verification of AOM activity, ^{13}C-labeled methane (17%$_{v/v}$) was added to two first transfer microcosms (stations 1 and 2). After 14 months of incubation of the transfers, a 10-ml headspace sample was precipitated in 1 ml concentrated BaOH solution. The obtained $BaCO_3$ suspension was transferred to a

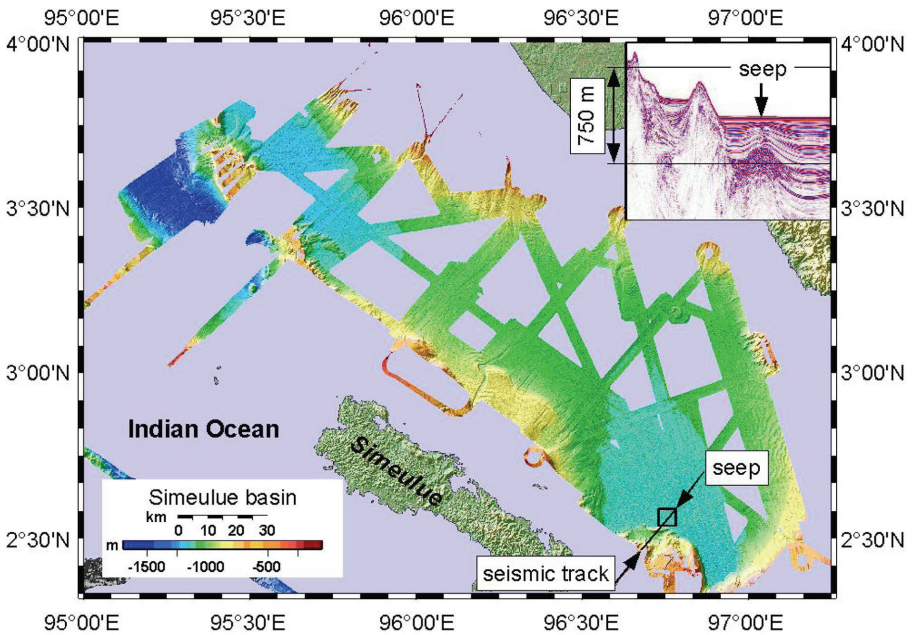

FIGURE 2 | Bathymetric map of the Simeulue basin with the seep area in the SE. The insert (covering the island Sumatra) shows a seismic profile of the track drawn in the SE. 750 m is an approximate value.

Table 1 | Sampled stations in forearc sediment basins off Sumatra.

Station	Ship position		Water depth (m)	Sampling depth (cmbsf)	Temperature (°C)	Basin	Referred as
	Latitude	Longitude					
SEEP STATIONS							
128TV	2°33.780N	96°45.424E	1130	16	6	Simeulue	Station 1
137TV	2°33.770N	96°45.404E	1134	6	6	Simeulue	Station 2
98MC	2°33.800N	96°45.410E	1135	28	6	Simeulue	Station 3
131SL	2°33.781N	96°45.429E	1134	367	6	Simeulue	Station 4
127TV	2°33.800N	96°45.410E	1135	Surface	6	Simeulue	Station 5
70SL	2°33.830N	96°45.410E	1134	133	6	Simeulue	Station 6
134TV	2°33.818N	96°45.397E	1134	Surface	6	Simeulue	Station 7
OTHER							
52MC	0°59.610N	98°02.415E	90	40	22	Nias	Station 8
64MC	0°59.571N	97°47.426E	70	40	23	Nias	Station 9

cmbsf, centimeters below seafloor.

helium flushed vial and acidified with 100 µl concentrated HCl. To determine the $\delta^{13}C$ value, a nearly methane-free headspace sample was injected into a MAT 252 GC-IRMS. Mean $\delta^{13}C$ values were obtained from three individual batch cultures.

Determination of methanogenesis from TMA, methanol, and different hydrocarbons

Potential rates of methane production were determined in microcosms without substrates, with addition of typical marine substrates trimethylamine (TMA) and methanol, or selected hydrocarbons. Final concentrations in the microcosms for TMA and methanol were 1 and 2.4 mM. To demonstrate hydrocarbon-dependent methanogenesis, anaerobic microcosms with butane, hexadecane, and ethylbenzene were prepared. Butane was added by replacing the microcosm headspace completely by gaseous butane. Hexadecane or ethylbenzene were added directly to the medium in concentrations of $0.1\%_{v/v}$. Methane was measured using a GC–FID equipped with a silica gel column (SRI 8610 C, SRI Instruments, USA). Rates are given in $\mu mol\ cm^{-3}\ day^{-1}$. To simulate marine *in situ* conditions, all initial setups contained sulfate (28 mM) as electron acceptor. Alternatively applied electron acceptors to sulfate were nitrate (1 mM), ferrihydrite ($2.5\ mmol^{-1}$), or manganese dioxide ($1.2\ mmol^{-1}$). Stock solutions of the metal oxides were prepared as follows: ferrihydrite

Table 2 | Incubation scheme of initial microcosm setups and of subsequent transfers.

Station	Substrate	Electron acceptors tested	Incubation times (months)	
			Initial setup	First transfer
SEEP				
Station 1	Methane	None, SO_4^{2-}, NO_3^-, Fe(III), Mn(IV)	17	14
Station 2	Methane	None, SO_4^{2-}, NO_3^-, Fe(III), Mn(IV)	17	14
Station 1	Butane, hexadecane, or ethylbenzene	None, SO_4^{2-}, NO_3^-, Fe(III), Mn(IV)	7	14
Station 2	Butane, hexadecane, or ethylbenzene	None, SO_4^{2-}, NO_3^-, Fe(III), Mn(IV)	6	31
Station 1	TMA or methanol	None	2	31
Station 2	TMA or methanol	None	2	n/a
Station 6	Butane, hexadecane, or ethylbenzene	None, SO_4^{2-}, NO_3^-, Fe(III), Mn(IV)	7	31
Station 7	Butane, hexadecane, or ethylbenzene	None, SO_4^{2-}, NO_3^-, Fe(III), Mn(IV)	7	31
NIAS BASIN				
Station 8	Butane, hexadecane, or ethylbenzene	None, SO_4^{2-}, NO_3^-, Fe(III), Mn(IV)	7	31
Station 9	Butane, hexadecane, or ethylbenzene	None, SO_4^{2-}, NO_3^-, Fe(III), Mn(IV)	7	31
Station 8	TMA or methanol	None	2	n/a
Station 9	TMA or methanol	None	2	n/a

Trimethylamine (TMA) or methanol were not used as substrates at station 6 and 7. n/a, not analyzed.

was precipitated by neutralization of a $FeCl_3$ solution (Lovley and Phillips, 1986). Manganese dioxide was prepared by oxidation of a $MnCl_2$ solution with $KMnO_4$ (Lovley and Phillips, 1988). Hydrocarbon degradation was not measured directly. Methanogenesis served as proxy for anaerobic hydrocarbon degradation (Zengler et al., 1999; Siegert et al., 2011). Methane concentrations were measured after 2 months (TMA and methanol) or 7 months (hydrocarbons).

DETERMINATION OF CELL NUMBERS BY SYBR GREEN® AND CARD–FISH

For SYBR Green® total cell counts and catalyzed reporter deposition–fluorescence in situ hybridization (CARD–FISH), fixations were carried out immediately after sampling. Two fixatives, either formaldehyde (FA) or ethanol, were applied each. A volume of 1 cm^3 wet sediment was treated for 10–15 h at 4°C with 1 ml fixative solution [4%$_{w/v}$ FA in phosphate buffered saline (PBS)], removed in two centrifugation steps by washing with 1 ml PBS and stored at −20°C in 50%$_{v/v}$ ethanol/PBS. Samples were transported to the home laboratory on dry ice. For total cell counts, in each sample 800–1000 cells were counted after SYBR Green® staining according to Weinbauer et al. (1998). CARD–FISH counts were conducted as described in Pernthaler et al. (2002) and Schippers et al. (2005).

GENE QUANTIFICATION BY qPCR

DNA extraction was carried out using a Fast DNA for Soil Kit (BIO 101, MP Biomedicals, Germany). To block sedimentary nucleic acid binding capacities, 10 µl of a 1% polyadenylic acid solution were added in the initial step (Webster et al., 2003). Directly before PCR, 125 µl of 0.3% bovine serum albumine (BSA) in ultra pure water were added as blocking agent to the Taqman master mix (Applied Biosystems, Germany) or the SYBR green® master mix (Eurogenetec, Germany). A real-time PCR instrument (ABI Prism 7000, Applied Biosystems) was employed to determine the 16S rRNA gene copy numbers of *Archaea* (Takai and Horikoshi, 2000) and *Bacteria* (Nadkarni et al., 2002). Eukaryotic 18S rRNA genes were quantified according to the manual's instructions of the kit and cited literature therein (Applied Biosystems, 2002). The functional genes *dsrA* and *mcrA* were investigated according to Schippers and Nerretin (2006) and Nunoura et al. (2006) respectively. Specific functional *mcrA* genes from anaerobic methanotrophic *Archaea* ANME-1 and ANME-2 were quantified using assays of Nunoura et al. (2006). Values are expressed in copy numbers per cm^3 wet sediment.

DENATURING GRADIENT GEL ELECTROPHORESIS

For DGGE, 16S rRNA genes of *Bacteria* were amplified using the primer set 533F (5′-TTACCGCGGCTGCTGGCAC-3′)/907R (5′-AATTCCTTTGAGTTT-3′) with a GC-clamp (5′-CGCCCGCCGCGCCCCGCGCCCGGCCCGCCGCCCCCGCC CC-3′) attached to the reverse primer 907R at the 5′-end (Weisburg et al., 1991; Muyzer et al., 1995). A thermocycler was programmed for a hot start PCR and 35 repetitions of each cycle: 94°C for 1 min, 63°C for 0.75 min, and 72°C for 1.5 min. Archaeal 16S rRNA genes were amplified with the primer set 340F (5′-CCCTACGGGGYGCASCAG-3′) and 915R (5′-GTGCTCCCCCGCCAATTCCT-3′; Øvreås et al., 1997; Coolen et al., 2002), a GC-clamped (as for 907R) 340F forward primer and a cycler program with 35 cycles each: 94°C for 1 min, 60°C for 1 min, 72°C for 1.5 min. A total of 2 µg of amplified and purified DNA (QIA quick PCR Purification Kit, Qiagen, Germany) was applied to each pocket of the gel and separated in a DCode System (BioRad, Germany) for 20 h at 60°C. Denaturing gradients of urea/formamide were 30–70%$_{w/v}$ (20–80%$_{w/v}$ for *Archaea*) and the acrylamide concentration was 6.5%$_{w/v}$. Dominant bands were excised and stored at −20°C, vacuum-dried at 60°C for 3 h (Eppendorf Concentrator 5301, Eppendorf, Germany), extracted with 30 µl PCR grade water (4°C, over night), re-amplified without GC-clamps, and purified as described above. Sequencing

reactions were conducted at Seqlab GmbH (Göttingen, Germany). Primers were 533F, 550F (5′-CGGAATTATTGGGCGTAAAG-3′), and 906R (5′-CCCCAATTCCTTTGAGTTTC-3′) for bacterial 16S rRNA genes and 340F and 915R for archaeal 16S rRNA genes. The obtained DNA sequences were aligned online by ARB-SILVA[1] and assembled in an existing Parsimony tree of a recent reference database (SSURef 102, February 2010) according to (Ludwig et al., 2004; Pruesse et al., 2007). All sequence data were submitted to the GenBank database[2] under accession numbers HQ231693 (see text footnote 2) to HQ231746 (see text footnote 2).

BATHYMETRY AND PARASOUND

A Kongsberg SMRAD EM 120 multibeam echosounder was operated continuously 24 h day^{-1} during the cruise. The device enabled mapping to full ocean depth with a sonar frequency of 12 kHz, an angular coverage of 150° and 191 beams per ping. The parasound device vessel integrate (Krupp Atlas Electronics, Germany) was used as a low frequency sediment echosounder at 18.0 and 21.5 kHz to map seismic profiles of basin sediments. The transparent character of the seafloor (seismic blanking) was found to be indicative for defining the extent of sediments affected by methane seepage and authigenic carbonate precipitation (**Figure 2**). However, seismic blanking may as well be indicative for high density gas hydrates overlaying low density free gas, unveiled by a bottom simulating reflector (BSR; Hyndman and Spence, 1992; Berndt et al., 2004). Nevertheless, seismic blanking does not always indicate free gas in the sediment (Zühlsdorff et al., 1999).

GEOCHEMICAL ANALYSES

Duplicate sediment core samples were taken for microbiological and geochemical analyses. TOC was measured with the instrument LECO CS 200 (LECO Corporation, USA). Porewater was squeezed from sediment slices of up to 125 cm^3 using a porewater press at atmospheric pressure. Between 20 and 40 ml of porewater were obtained and filtered through a 0.45 μm cellulose nitrate filter (Sartorius, Germany) and directly collected in polypropylene-vials. Polypropylene-vials were acid prewashed and dried to remove possible traces of carbonate from the vial surface. To remove particles and microorganisms, the collected porewater was filtered again through 0.2 μm polyethersulfone filters (Sartorius, Germany). For metal ion and sulfate concentrations, 5 ml porewater were acidified with 50 μl HNO_3 and measured using an ICP-MS instrument (Perkin Elmer Sciex Elan 5000, USA) as published by Dekov et al. (2006). After preservation of the sediment samples with $ZnCl_2$, porewater sulfide was determined spectrophotometrically as described by Cline (1969).

To determine carbon stable isotopes of dissolved inorganic carbon (DIC), 2 ml of porewater, treated with 10 μl saturated $HgCl_2$ solution on board, were analyzed in a Finnigan MAT 252 (Thermo Electron, USA) connected to a Finnigan Kiel III (Thermo Electron) carbonate preparation device (Wachter and Hayes, 1985). Free gases were measured using 5 ml fresh sediment from the center of the core which was immediately transferred into 10 ml 2 M NaOH in a 56 ml serum bottle. The bottle was sealed quickly with a butyl rubber stopper and the sediment was suspended by shaking the flask. Immediately, 5 ml headspace were removed and stored upside down in 20 ml injection vials over saturated NaCl solution for on-shore measurement. This procedure allowed a separation of free from adsorbed gases but some adsorbed gas may have evaporated as well (Faber and Stahl, 1983). $\delta^{13}C$ values for free gases were obtained by direct injection into a Finnigan MAT 253 (Thermo Electron, USA) connected to a gas chromatograph (GC 6890, Agilent, USA).

To determine the carbon stable isotopic composition of the macro fauna, the soft tissues of bivalves and crabs were freeze dried, milled, weighed into tin capsules, and stored in a desiccator until measurement. Samples were taken from one individual bivalve and two individual crabs. One crab was sampled twice and the other one was sampled once. For TOC carbon isotope ratios, dried sediment was treated with 10% HCl in acid washed tin capsules and stored in a desiccator until measurement. Isotope ratios were determined by a coupled system of an elemental analyzer and a MAT 252 isotope ratio mass spectrometer (Thermo Electron, USA) via a Finnigan ConFlo III open split interface. Concentrations and isotopic data are given as the arithmetic mean of at least two measurements. Isotopic carbon values are expressed in ‰ relative to Vienna PeeDeeBelemnite (VPDB). Concentrations are relative to 1 cm^3 of fresh (wet) sediment.

RESULTS

SEAFLOOR OBSERVATIONS

Areas covered with white-colored microbial mats were discovered and sampled in the Simeulue seep area using a TV-guided grab (**Table 1**; **Figure 1**). In the seep area, parts of the sediment were characterized by a black color and a strong sulfidic odor. The higher seafloor biota comprised tubeworms, bivalves, and crabs. The latter colonized carbonate outcrops and could be identified as members of the species *Shinkaia crosnieri* (Enrique Macpherson, personal communication). Their soft tissue stable carbon isotopic signature ranged from −31 to −45‰. Soft tissue of one mytilid bivalve individual had a $\delta^{13}C$ of −31‰.

FREE GASES AND THEIR ISOTOPIC COMPOSITION

Free methane concentrations in the water column ranged from 10 to 200 nmol l^{-1} at the seep location as shown in **Figure 1**. In the southeast boundary of the seep, methane concentration never reached values above 5 nmol l^{-1}. At the sediment surface of the station 1 and 2, methane accounted for a total of >99.9% of all hydrocarbon gases. Isotopic data of gases sampled at the methane seep are listed in **Table 3**.

POREWATER COMPOSITION AND STABLE CARBON ISOTOPES

All geochemical porewater data of the Simeulue seep are summarized in **Figure 3**. At stations 1 and 2, $\delta^{13}C_{DIC}$ values were mainly below −40‰. At the station 3, $\delta^{13}C_{DIC}$ values were always above −8‰. At station 4, $\delta^{13}C_{DIC}$ values ranged from −2‰ at 6 cmbsf to −24‰ at 293 cmbsf. However, a clearly decreasing trend was observed with depth down to 392 cmbsf (**Figure 3**). Clear trends were missing in case of the solid phase $\delta^{13}C_{TOC}$ values. However, there was a slight decrease from −22.3‰ at 6 cmbsf to −27.6‰ at 153 cmbsf of the station 4. The values remained stable below

[1] http://www.arb-silva.de
[2] http://www.ncbi.nlm.nih.gov

Table 3 | Analyses of *in situ* gas and microbial AOM activity in sediments of the Simeulue seep.

Station	Depth	Methane			Ethane			SRR methane	*t*-Test
	(cmbsf)	(pmol cm^{-3}) ± error	Repl	$\delta^{13}C$ (‰ VPDB) ± error	($\%_{v/v}$) ± error	Ratio C1/C2	Repl	($\mu mol\ cm^{-3}\ day^{-1}$) ± error	*p*-Value
Station 1	Surface	8.5 ± 0.4	2	−70.9 ± 5.3	0.048 ± 0.030	2889	3	0.57 ± 0.10	0.016
Station 2	Surface	10.1 ± 0.5	2	−74.8 ± 2.0	0.019 ± 0.003	5406	6	0.35 ± 0.09	0.013
Station 4	11	<1		n/a	n/a	n/a	n/a	n/a	
	67	<1		n/a	n/a	n/a	n/a	n/a	
	167	1.4	1	−39.6	0	n/a	1	n/a	
	267	1.4	1	−43.6	0	n/a	1	n/a	
	367	<1		n/a	n/a	n/a	n/a	n/a	

Errors are SD from the mean of the given number of replicates (repl). Methane concentrations and carbon isotopic ratios of methane ($\delta^{13}C_{CH_4}$) were determined in separate measurements and the number of replicates differs. All gas concentrations are approximate values because TV grabs and gravity cores were not pressure locked and therefore affected by outgassing. Ethane concentrations were determined in the same measurement as carbon isotopic ratios of methane, and the number of replicates is therefore identical. Sulfate reduction rates (SRR) of microcosms with methane in their headspaces were determined in five replicate microcosms of which the mean and errors are given within 95% confidence limits. SRR were calculated using sulfide concentrations that were subtracted from incubation without methane. The Student's t-test was conducted using paired samples (e.g., manganese with methane and manganese without methane) in a one tailed calculation of the full five sample population. n/a, not applicable; cmbsf, centimeters below seafloor; repl., number of replicate measurements.

−27.0‰ up to a depth of 293 cmbsf (**Figure 3**). At the stations 1 and 2, sulfate concentrations decreased with depth while sulfide concentrations increased. At the stations 3 and 4, neither such a decline of porewater sulfate concentrations was found, nor was sulfide detected. Elevated concentrations of reduced manganese were found at the station 2 as well as at the surface of the station 4 (**Figure 3**). Except for the station 1, no higher amounts of reduced iron in the porewater were observed (**Figure 3**).

ANAEROBIC OXIDATION OF METHANE

Results obtained from microcosm experiments do not necessarily reflect the *in situ* situation but provide an estimate of microbial activity (Krüger et al., 2005; Treude et al., 2005). Sulfate reduction rates (SRR) in Simeulue seep sediment microcosms were higher with methane as electron donor than in controls without methane and the difference is shown in **Table 3**. The observed differences can be explained by AOM. However, sulfate reduction at station 1 and 2 without methane was 0.13 and 0.11 $\mu mol\ cm^{-3}\ day^{-1}$, respectively. To confirm this, the conversion of methane into carbon dioxide was tested in 1:10 diluted subcultures of the initial microcosms incubated with 17%$_{v/v}$ ^{13}C-methane. The label was recovered as ^{13}C-enriched carbon dioxide. The detected $\delta^{13}C_{CO_2}$ values were +503 ± 331‰ (station 1) and +319 ± 279‰ (station 2) for microcosms prepared from sulfidic sediments of the Simeulue methane seep. This provides evidence for the oxidation of ^{13}C-methane to $^{13}CO_2$ at both stations. In controls with unlabeled methane, $\delta^{13}C_{CO_2}$ values were −15.7 and −17.4‰ respectively. The corresponding $\delta^{1}3C_{CH_4}$ values of unlabeled methane were −36.6 and −34.9‰ respectively.

In 1:10 diluted subcultures of the initial microcosms, containing sulfate, nitrate, FeOOH, or MnO_2, methanotrophy was observed after 14 months incubation as well. The methanotrophic rates, measured by headspace analysis of methane, were similar and ranged from 0.8 $\mu mol\ cm^{-3}\ day^{-1}$ (with MnO_2) at the station 1 to 1.8 $\mu mol\ cm^{-3}\ day^{-1}$ (with sulfate) at station 2.

METHANOGENESIS FROM TRIMETHYLAMINE (TMA), METHANOL, HYDROCARBONS

Except station 5, methanogenesis in microcosms without added methanogenic substrates (TMA, methanol, or hydrocarbons) was less than 1.8 nmol methane $cm^{-3}\ day^{-1}$ (**Table 4**). However, when TMA or methanol were added to microcosms of the seep stations (1, 2, 5, and 7), methanogenesis increased by two orders of magnitude. The other seep stations (3, 4, and 6) were not tested for TMA or methanol methanogenesis. In microcosms prepared from sediments of the Nias basin, where no methane seepage was observed (stations 8 and 9), TMA or methanol did not stimulate methanogenesis. For the hydrocarbon substrates butane, hexadecane, and ethylbenzene, little methanogenesis was observed after 7 months incubation in 27 microcosms out of 280 initial microcosms (**Table 4**). To exclude false positive signals by means of stimulation of methanogenic TOC digesting microorganisms the hydrocarbon microcosms were compared with microcosms without hydrocarbons. For this, first 1:10 transfers of the methanogenic microcosms were prepared. In first transfers, the hydrocarbon-dependent methanogenesis rate at the seep station 2 was 6.5 nmol $cm^{-3}\ day^{-1}$ (hexadecane and manganese dioxide) and 14.5 nmol $cm^{-3}\ day^{-1}$ at station 6 (ethylbenzene and ferrihydrite). In the Nias basin, it was 17.5 nmol $cm^{-3}\ day^{-1}$ at station 8 (hexadecane and sulfate) and 18.0 nmol $cm^{-3}\ day^{-1}$ at station 9 (hexadecane and manganese dioxide).

CELL NUMBERS AND QUANTIFICATION OF FUNCTIONAL GENES

Results of CARD–FISH and total cell counts for the stations 1, 3, and 4 are shown in **Figure 4**. At station 2, only the top and bottom layer were investigated and data for this station are therefore not depicted in **Figure 4** but described in the following. At this station, total cell numbers of 1×10^9 cells cm^{-3} at the top (0 cmbsf) and 4×10^9 cells cm^{-3} at the bottom (8 cmbsf) were counted. CARD–FISH cell counts of active cells revealed cell numbers of

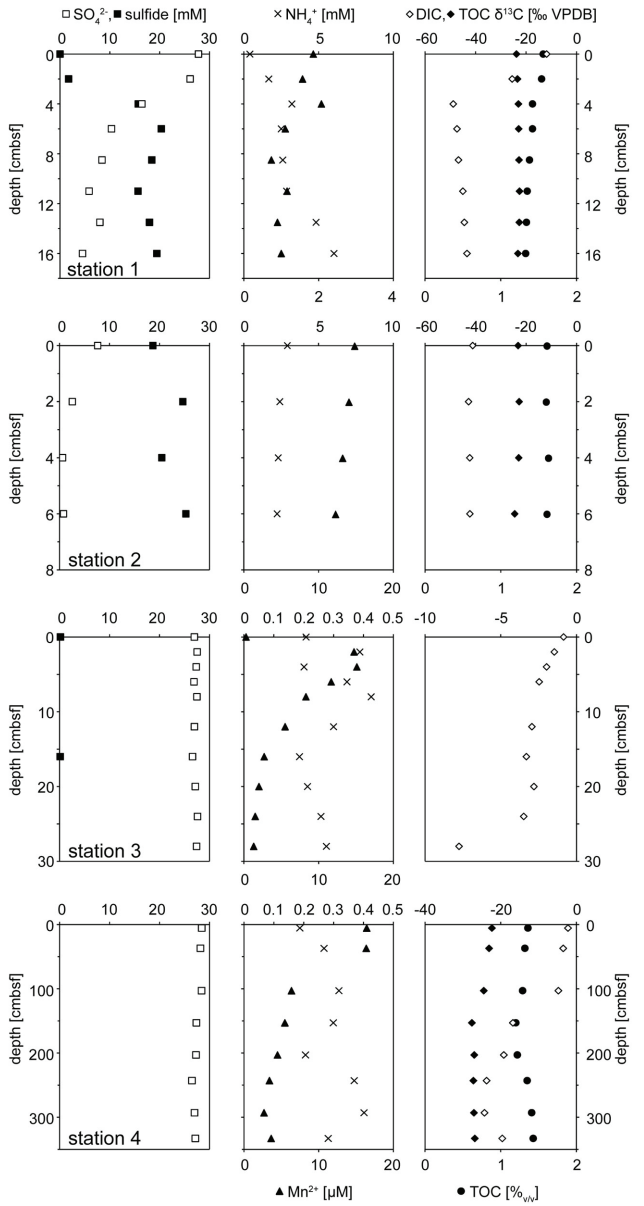

FIGURE 3 | Geochemical profiles of stations 1 – 4. Stations 1 and 2 comprised ANME rich sediments actively performing AOM. The left panel shows sulfate (□) and sulfide (■) profiles. When sulfide concentrations were below the detection limit of 0.1 they are not sown. The central panel depicts dissolved manganese (▲) and ammonium (×). $\delta^{13}C$ isotopic compositions of DIC (◇) and TOC (◆) are displayed on the right. The concentration of TOC (●) in the dry mass is given in (%).

2×10^8 cells cm^{-3} for *Bacteria* and 4×10^7 cm^{-3} for *Archaea* at the station 2. At the stations 3 and 4, CARD–FISH indicated no living archaeal cells (**Figure 4**).

Domain specific 16S rRNA gene copies, obtained from qPCR measurements, and selected functional genes at three different stations are displayed in **Figure 4**. In general, a clear trend was observed only for *Eukarya* and only at the station 4 (**Figure 4**). The copy numbers increased with depth (**Figure 4**).

For functional genes, a trend with depth was observed only at the deeper sampled station 4. Its most prominent feature was the increase of all *mcrA* gene copy numbers, beginning at 103 cmbsf down to 267 cmbsf, and dropping again to the values at the surface further below. An opposite tendency was observed for *dsrA* gene copy numbers showing a clear decrease with depth. At station 2, ANME-2 *mcrA* gene copies increased from 6×10^6 copies cm^{-3} in the top layer to 2×10^8 copies cm^{-3} at the bottom (8 cmbsf). An opposite trend appeared for the ANME-1 *mcrA* gene with copy numbers of 2×10^8 copies cm^{-3} at the surface layer and 7×10^7 copies cm^{-3} at the bottom. No change with depth was observed for the *Methanosarcina mcrA* group where copy numbers of 5×10^8 copies cm^{-3} were detected. The *dsrA* gene measurement resulted in copy numbers of 3×10^6 copies cm^{-3} at the top and 6×10^7 copies cm^{-3} at the bottom of this core.

MICROBIAL DIVERSITY

Parsimony trees of 16S rRNA gene sequences obtained from DGGE separation of extracted DNA from Simeulue sediment stations are depicted in **Figures 5** and **6**. PCR products of the station 3 were run on a separate gel without reference to the stations 1 and 2. Therefore, band patterns were not comparable and a DGGE gel photograph is not shown. Stations 1, 2, and 4 are shown in **Figure 5**.

Three major bacterial phylogenetic groups (δ-*Proteobacteria*, candidate division OP9, and *Anaerolineaceae*) were abundant across the study area. According to their band thickness in the DGGE gel, OP9 bacteria, and relatives of *Desulfobacteraceae* seemed to become increasingly important with depth at the station 4 (**Figures 4** and **5**). Nonetheless, since band thickness is an imprecise measure for abundance, this result indicates only a trend, despite the fact that when the total amount of amplified DNA products was equal for each layer. Besides δ-*Proteobacteria*, other *Proteobacteria* sequences were not recovered from the DGGE gels. Sequences affiliated to the clusters *Desulfobacteraceae, Desulfarculaceae,* and Sh765B-TzT-29 dominated the δ-*Proteobacteria* (**Figure 5**). One deeply branching sequence of the station 2 was more closely related to sequences obtained from municipal wastewater sludge (Rivière et al., 2009) than to the genus *Leptolinea* (**Figure 6**). Another deeply branching sequence of the station 3 was closely related to the genus *Rhodococcus* (**Figure 6**). Two bands found at stations 2, 3, and 4 were relatively close relatives of the genus *Spirochaeta*.

Simeulue seep sequences of all stations were related to three prominent archaeal groups (ANME-1, ANME-2, and Crenarchaeota; **Figure 7**). One sequence of the station 3 was assigned into the Deep Hydrothermal Vent Euryarchaeotal Group 6 (DHVEG6). The remaining sequences (stations 3 and 4) belonged to not further specified *Crenarchaeota*. Except for the *Crenarchaeota,* members of all other clusters were identified in stations 1–4. In summary, the bacterial diversity was greater than the archaeal one, with most sequences related to organisms typically found at methane and hydrocarbon seeps or mud volcanoes.

DISCUSSION

For the first time, an active methane seep was discovered in the Indian Ocean. The discovered seep comprised highly active

Table 4 | Rates of methane release when TMA, methanol, or hydrocarbons were fed to the microcosms.

Station	Electron acceptor	Substrate	Methane release		
			Initial setup		First transfer + substrate
			+Substrate (μmol cm^{-3} day^{-1})	−Substrate (nmol cm^{-3} day^{-1})	(nmol cm^{-3} day^{-1})
SEEP					
Station 1	n/a	TMA	0.28	1.5	n/a
	n/a	Methanol	0.50	1.5	n/a
Station 2	n/a	TMA	0.30	0.1	n/a
	n/a	Methanol	0.72	0.1	n/a
Station 5	n/a	TMA	0.31	55.4	n/a
	n/a	Methanol	0.70	55.4	n/a
Station 7	n/a	TMA	0.26	1.8	n/a
	n/a	Methanol	0.74	1.8	n/a
			(nmol cm^{-3} day^{-1})	(nmol cm^{-3} day^{-1})	(nmol cm^{-3} day^{-1})
Station 2	Sulfate	Ethylbenzene	8.2	0.1	3.8
	Mn(IV)	Hexadecane	6.4	0.5	6.5
Station 6	Sulfate	Ethylbenzene	12.4	0.0	10.5
	Fe(III)	Ethylbenzene	20.6	0.3	**14.5**
Station 7	Sulfate	Hexadecane	4.1	0.0	5.1
	Mn(IV)	Ethylbenzene	12.1	0.4	9.1
NIAS BASIN					
Station 8	Sulfate	Hexadecane	36.1	0.6	**17.5**
	Sulfate	Ethylbenzene	38.5	0.8	6.2
	Mn(IV)	Ethylbenzene	29.7	0.0	6.5
Station 9	Sulfate	Ethylbenzene	37.7	0.0	9.8
	Nitrate	Ethylbenzene	37.8	0.0	1.1
	Fe(III)	Hexadecane	34.1	1.1	5.8
	Mn(IV)	Hexadecane	32.5	0.0	**18.0**

b.d.l., below detection limit; n/a, not applicable, bold numbers indicate significantly (95% confidence intervals) elevated methanogenic hydrocarbon degradation rates.

(stations 1 and 2) and less active or inactive (stations 3 and 4) AOM-influenced areas (**Table 1**; **Figure 4**). The highly active stations 1 and 2 were characterized by black sulfidic surface sediments, depleted sulfate, and high sulfide concentrations and light $\delta^{13}C_{DIC}$ values of the porewater, the presence of ANME-1 and ANME-2 representatives, as well as high cell and high copy numbers of 16S rRNA and functional genes related to AOM, methanogenesis, and sulfate reduction. A defined seep center of activity, like in mud volcanoes, was not discovered, the seep area was rather characterized by a patchy distribution of active spots. Carbonate- or sulfide-rich spots were distributed randomly over the surface. A reason for the patchiness might be tectonic activity. While some gas conduits might have been shut, other could have opened over time. An apparent feature of the active parts at the seep was the strong depletion of ^{13}C in DIC, which was also observed for TOC of the guts of the seep's macro fauna. This confirms the importance of methane as carbon source for the benthos at this location. In addition, methanogenic activity was confirmed in sediment microcosms of the Simeulue seep area as well as in the Nias basin, where AOM activity was absent.

METHANOTROPHY AND SULFATE REDUCTION ACTIVITIES AT THE SEEP STATIONS

Methane is an indirect electron source for dissimilatory microbial sulfate reducers in the syntrophic process of AOM (Knittel and Boetius, 2009). The terminal reaction products are carbonate and sulfide. The produced sulfide in turn may be oxidized at the oxic/anoxic interface near the sediment surface. White, sometimes filamentous sulfide-oxidizing bacteria are typical indicators for this interface (Niemann et al., 2006b). Areas covered with such white-colored microbial mats were discovered in the Simeulue basin and sampled in their proximity using a TV-guided grab (station 2, **Figure 1**). In contrast, microbial mats were absent near the station 1. Most likely, the white color of such mats is a result of intracellular sulfur inclusions as observed in *Thioploca, Beggiatoa,* or *Thiomargarita* aggregates, regularly found on the surface of sulfide-rich marine sediments (Gallardo, 1977; Jannasch et al., 1989; Schulz et al., 1999).

At the Simeulue seep, methane was probably a carbon source for higher biota, as indicated by their ^{13}C-depleted carbon signatures. However, the $\delta^{13}C$ (−31 to −45‰) values of the sampled crab guts indicate a mixed carbon source originating from AOM and

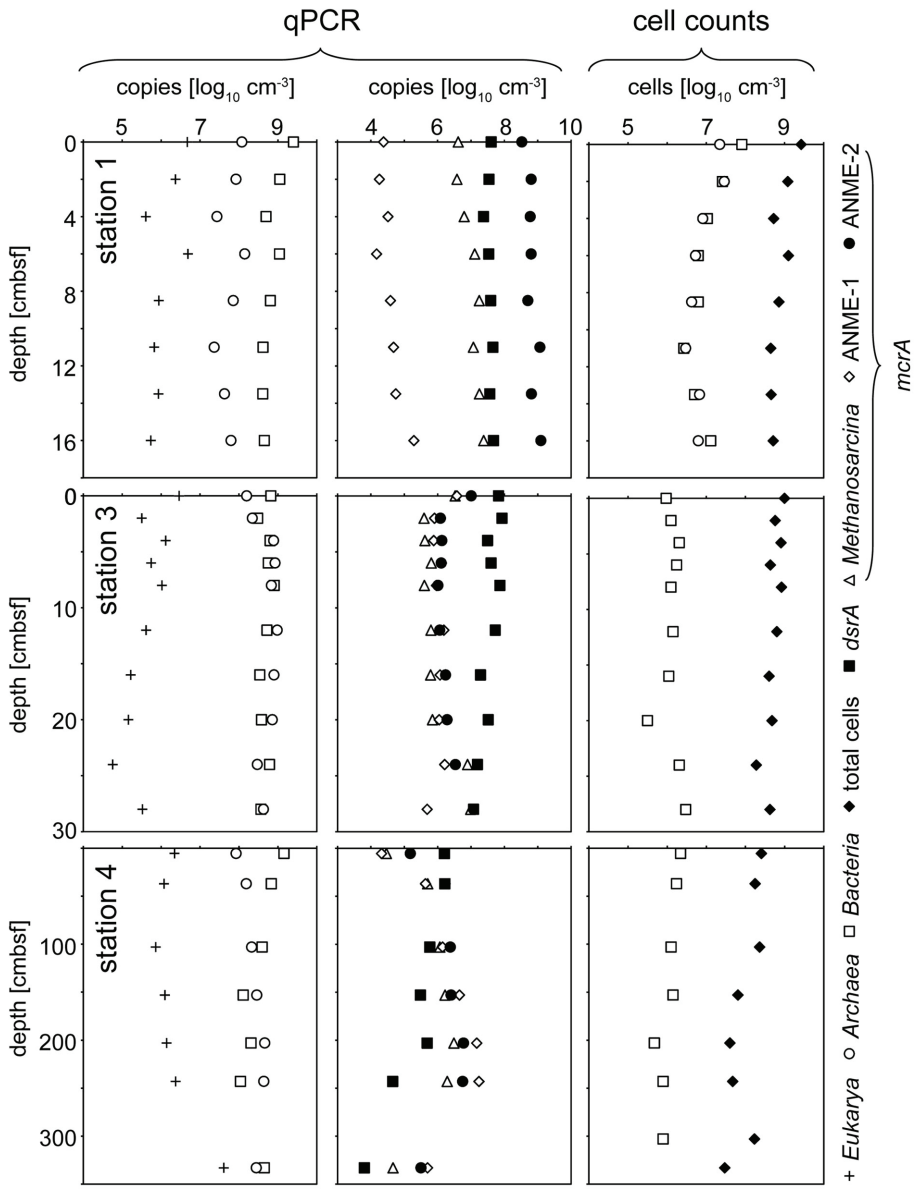

FIGURE 4 | Depth trend of quantitative community composition of three different stations from the Simeulue seep. The left panel illustrates the composition of the three domains *Bacteria, Archaea* and *Eukarya* according to qPCR quantification of 16S or 18S rRNA genes, respectively. The middle panel gives an overview over the distribution of the functional gene numbers. In the right panel, total cell counts are compared to CARD–FISH cell counts for *Bacteria* and *Archaea* detecting active cells.

water column carbon ($\delta^{13}CCH_4$ −70.9 to 74.8‰, $\delta^{13}C_{DIC}$ −0.8 to −48.8‰, $\delta^{13}C_{TOC}$ −22.3 to 27.6‰). Heterotrophic processes as well as symbiosis between methanotrophic microorganisms and macrofauna are well described for several hot and cold deep marine vents (Childress et al., 1986; Duperron et al., 2005; Petersen and Dubilier, 2009). AOM was clearly a carbon donating process. It has been previously demonstrated that more than 99% of the methane in AOM systems is used for energy metabolism (Wegener et al., 2008). The oxidized carbon is than excreted as carbonate and probably reassimilated into biomass. The same seems likely for the Simeulue invertebrate community as previously shown for symbiotic CO_2-fixing microorganisms and the gutless worm *Olavius* (Blazejak et al., 2005). Symbiosis of higher benthos and methanotrophic microorganisms is also often associated with aerobic methanotrophy (Childress et al., 1986; Duperron et al., 2005; Niemann et al., 2006b; Petersen and Dubilier, 2009). However, the DGGE 16S rRNA gene analyses, focusing on dominant bands, did not reveal aerobic methane oxidizers in the seep sediments (**Figures 5** and **6**).

The anoxic nature of the sediment was confirmed by porewater data, showing in particular high sulfide concentrations, reduced iron, and manganese as well as ammonium to be present

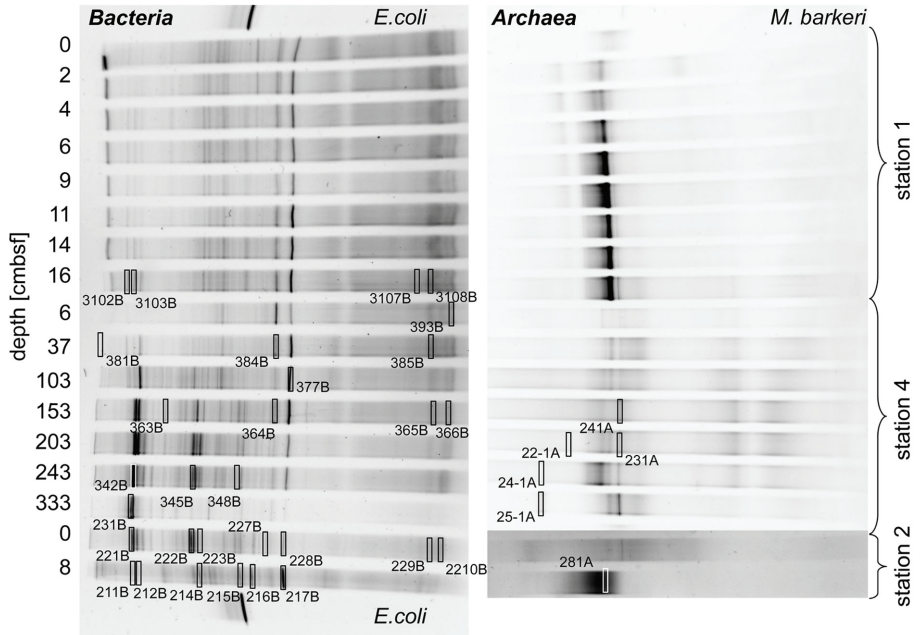

FIGURE 5 | Denaturing gradient gel electrophoresis photographs showing the 16S rRNA gene sequence diversity of *Bacteria* (left) and *Archaea* (right) of the stations 1, 2, and 4 of the Simeulue seep. *Escherichia coli* and *Methanosarcina barkeri* served as positive controls. Excised bands used for 16S rRNA gene sequencing are highlighted by open rectangles. The numbers enumerate gels, lanes, and bands and refer to the phylogenetic trees in this figure and **Figure 6**. Multiple gels were prepared and bands excised from different gels could be relocated in the shown photographs. Bands resulting in unsuccessful PCR re-amplifications or sequencing reactions are not shown.

(**Figure 3**). While sulfide concentrations increased downward into the sediment, sulfate decreased to micromolar concentrations. However, a clear SMTZ was not observed.

Large amounts of dissolved gas with strong sulfidic odor evaporated from the sediment during sampling of the stations 1 and 2. Indicators for ongoing AOM at stations 1 and 2 were the low $\delta^{13}C_{DIC}$ values in the porewater apparently derived from ^{13}C-depleted methane (**Tables 2** and **3**). These values were comparable to other methane influenced seeps, as in the Gulf of Mexico (Coffin et al., 2008) or at the Hydrate Ridge (Valentine et al., 2005). Since ocean water $\delta^{13}C_{DIC}$ values are usually between 0 and −10‰ (Deuser et al., 1968), DIC at the Simeulue seep was obviously derived from the anaerobic oxidation of upward migrating methane (**Figure 3**). $\delta^{13}CCH_4$ values were below −70‰ at the stations 1 and 2 (**Table 3**). It is commonly agreed that biogenic methane exhibits $\delta^{13}CCH_4$ values below −70‰ (Whiticar et al., 1986). Hence, the observed methane at the Simeulue seep was likely biogenic methane as well.

The AOM rates observed for the Simeulue seep area were slightly lower than maximum rates reported for other methane seeps, but higher than rates observed for mud volcanoes or sediments from various marine SMTZ (Knittel and Boetius, 2009).

That methane rather than TOC was the carbon source for microorganisms is supported by low $\delta^{13}C_{TOC}$ values at station 1 and 2. These values were in a narrow range between −22.7 and −24.5‰ which are typical for marine cellular carbon (Deuser et al., 1968; Rice, 1993). These values contrast $\delta^{13}C_{DIC}$ values between −11.8 and −48.8‰ at the stations 1 and 2, most of them below −40.0‰ (**Figure 3**). Since the carbon isotopic composition of methane at both sites was below −70.0‰ (**Table 3**), it is obvious that AOM contributed to the DIC budget at these active AOM sites. The calculated SRR in the equilibrium zone, i.e., the zone of sulfur input from sulfate does not exceed the SRR, and was between 0.43 μmol cm^{-1} day^{-1} at 4 cmbsf and 0.56 μmol cm^{-1} day^{-1} at 8 cmbsf. The fluid flux was assumed to be 10 cm $year^{-1}$ (Girguis et al., 2003) and the equilibrium was reached when the sum of sulfide and sulfate concentrations did not exceed the bottom water concentration of sulfate any more (27.79 mM, **Figure 3**). Moreover, the seep sediments were highly methane laden, as indicated by intensive gas emission during sampling. Huge discrepancies between sulfate reduction and AOM rates are usually observed only when methane plays a minor role in the investigated system (Niemann et al., 2006a), which is not the case here.

However, one may expect that there would have been a greater contribution of AOM derived carbon to TOC as observed, as methane was apparently a carbon source for the AOM performing microorganisms. Wegener et al. (2008) reported the assimilation of methane derived carbon into AOM performing microbial consortia of various geographic origins via CO_2 fixation. Furthermore, they could show that methane mostly serves microbial catabolism and to little extent microbial anabolism. This is also reflected in carbon stable isotopic signatures of DIC and TOC of the Simeulue seep, where stronger methane signals were detected in DIC and low $\delta^{13}C_{TOC}$ values do not support a significant impact of methane derived carbon to TOC (**Table 3**; **Figure 3**). On the other hand, ammonium concentrations decrease between 6 and

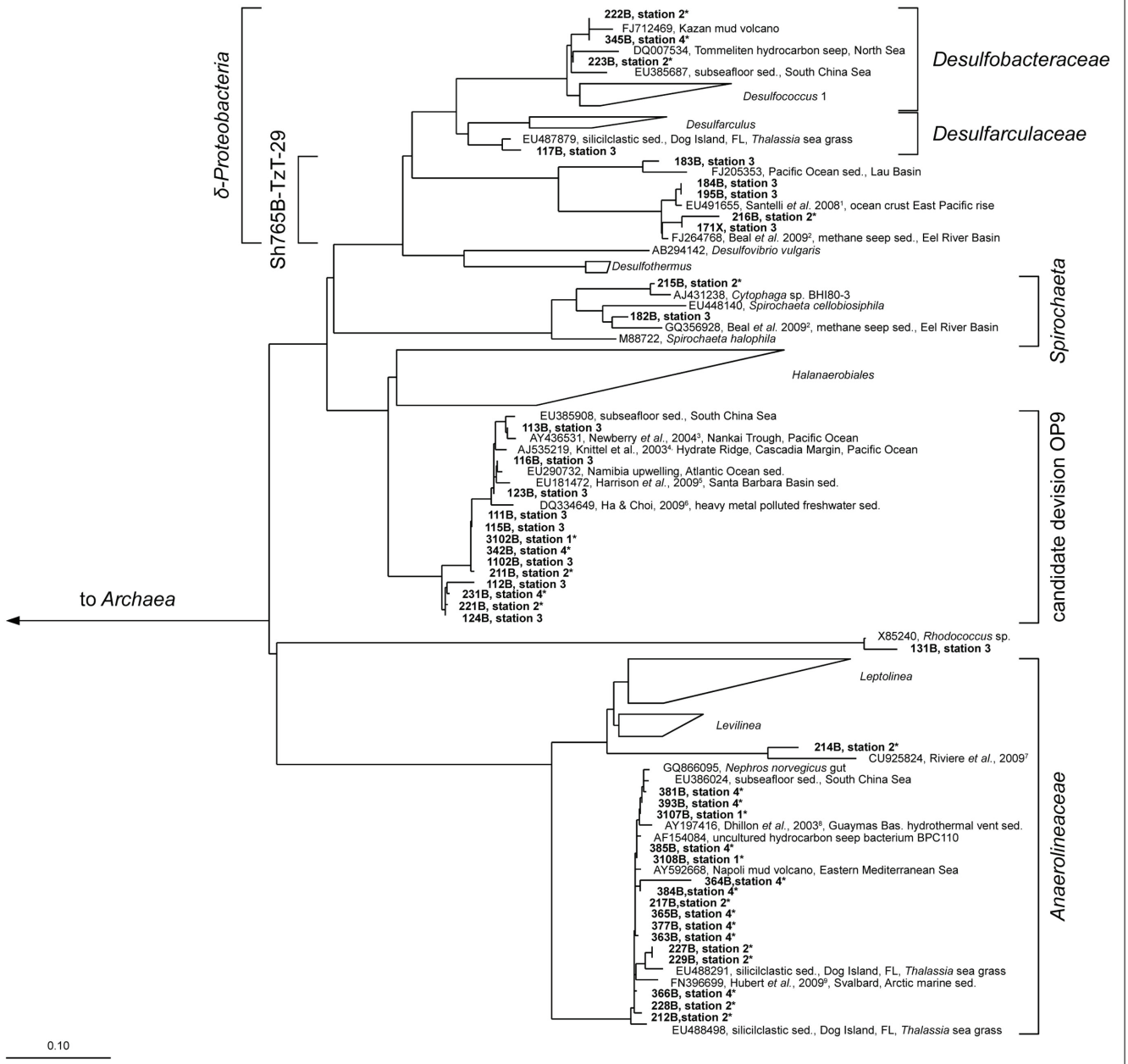

FIGURE 6 | Parsimony tree of bacterial 16S rRNA gene sequences with all sampled stations. The tree is based on the SILVA tree version 102 (Pruesse et al., 2007). Sequences obtained from the Simeulue seep are in bold letters. Bold numbers describe bands excised and used for 16S rRNA gene sequencing from three different DGGE gels. On the right, the deepest branching affiliations are shown. References are indicated in upper case: [1]Santelli et al. (2008), [2]Beal et al. (2009), [3]Newberry et al. (2004), [4]Knittel et al. (2003), [5]Harrison et al. (2009), [6]Ha and Choi (2009), [7]Rivière et al. (2009), [8]Dhillon et al. (2003), [9]Hubert et al. (2009). Asterisks (∗) indicate bands from DGGE gels in **Figure 5**. sed., Sediment.

11 cmbsf at station 1. This could either be due to (i) heterotrophic TOC degradation for energy metabolism, (ii) hypothetical anaerobic ammonium oxidation with sulfate (Schrum et al., 2009), or (iii) ammonium uptake due to the increase of biomass upon AOM. TOC degradation would liberate ammonium and can be excluded (e.g., Wehrmann et al., 2011). Anaerobic ammonium oxidation with sulfate was suggested based on geochemical sediment profiles (Schrum et al., 2009; Wehrmann et al., 2011) but has not been convincingly demonstrated *in vitro* yet. However, it would have a stoichiometry of 1 mol sulfate reduced to 2.67 mol ammonium oxidized. From 4 to 6 cmbsf, the stoichiometry is 1–6.47 mol (**Figure 3**). That would indicate either an inefficient ammonium oxidation or a contribution of AOM to the ammonium decline. Given a one to one stoichiometry of sulfate driven AOM, the

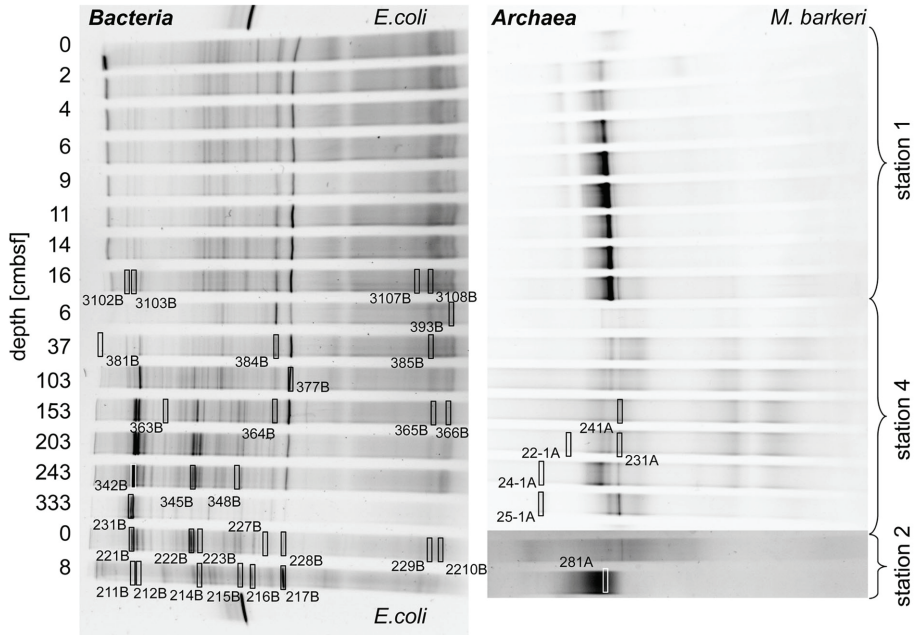

FIGURE 5 | Denaturing gradient gel electrophoresis photographs showing the 16S rRNA gene sequence diversity of *Bacteria* (left) and *Archaea* (right) of the stations 1, 2, and 4 of the Simeulue seep. *Escherichia coli* and *Methanosarcina barkeri* served as positive controls. Excised bands used for 16S rRNA gene sequencing are highlighted by open rectangles. The numbers enumerate gels, lanes, and bands and refer to the phylogenetic trees in this figure and **Figure 6**. Multiple gels were prepared and bands excised from different gels could be relocated in the shown photographs. Bands resulting in unsuccessful PCR re-amplifications or sequencing reactions are not shown.

(**Figure 3**). While sulfide concentrations increased downward into the sediment, sulfate decreased to micromolar concentrations. However, a clear SMTZ was not observed.

Large amounts of dissolved gas with strong sulfidic odor evaporated from the sediment during sampling of the stations 1 and 2. Indicators for ongoing AOM at stations 1 and 2 were the low $\delta^{13}C_{DIC}$ values in the porewater apparently derived from ^{13}C-depleted methane (**Tables 2** and **3**). These values were comparable to other methane influenced seeps, as in the Gulf of Mexico (Coffin et al., 2008) or at the Hydrate Ridge (Valentine et al., 2005). Since ocean water $\delta^{13}C_{DIC}$ values are usually between 0 and −10‰ (Deuser et al., 1968), DIC at the Simeulue seep was obviously derived from the anaerobic oxidation of upward migrating methane (**Figure 3**). $\delta^{13}CCH_4$ values were below −70‰ at the stations 1 and 2 (**Table 3**). It is commonly agreed that biogenic methane exhibits $\delta^{13}CCH_4$ values below −70‰ (Whiticar et al., 1986). Hence, the observed methane at the Simeulue seep was likely biogenic methane as well.

The AOM rates observed for the Simeulue seep area were slightly lower than maximum rates reported for other methane seeps, but higher than rates observed for mud volcanoes or sediments from various marine SMTZ (Knittel and Boetius, 2009).

That methane rather than TOC was the carbon source for microorganisms is supported by low $\delta^{13}C_{TOC}$ values at station 1 and 2. These values were in a narrow range between −22.7 and −24.5‰ which are typical for marine cellular carbon (Deuser et al., 1968; Rice, 1993). These values contrast $\delta^{13}C_{DIC}$ values between −11.8 and −48.8‰ at the stations 1 and 2, most of them below −40.0‰ (**Figure 3**). Since the carbon isotopic composition of methane at both sites was below −70.0‰ (**Table 3**), it is obvious that AOM contributed to the DIC budget at these active AOM sites. The calculated SRR in the equilibrium zone, i.e., the zone of sulfur input from sulfate does not exceed the SRR, and was between 0.43 μmol cm^{-1} day^{-1} at 4 cmbsf and 0.56 μmol cm^{-1} day^{-1} at 8 cmbsf. The fluid flux was assumed to be 10 cm $year^{-1}$ (Girguis et al., 2003) and the equilibrium was reached when the sum of sulfide and sulfate concentrations did not exceed the bottom water concentration of sulfate any more (27.79 mM, **Figure 3**). Moreover, the seep sediments were highly methane laden, as indicated by intensive gas emission during sampling. Huge discrepancies between sulfate reduction and AOM rates are usually observed only when methane plays a minor role in the investigated system (Niemann et al., 2006a), which is not the case here.

However, one may expect that there would have been a greater contribution of AOM derived carbon to TOC as observed, as methane was apparently a carbon source for the AOM performing microorganisms. Wegener et al. (2008) reported the assimilation of methane derived carbon into AOM performing microbial consortia of various geographic origins via CO_2 fixation. Furthermore, they could show that methane mostly serves microbial catabolism and to little extent microbial anabolism. This is also reflected in carbon stable isotopic signatures of DIC and TOC of the Simeulue seep, where stronger methane signals were detected in DIC and low $\delta^{13}C_{TOC}$ values do not support a significant impact of methane derived carbon to TOC (**Table 3**; **Figure 3**). On the other hand, ammonium concentrations decrease between 6 and

with the presence of reduced iron and manganese in the porewater (**Figure 3**), it seems possible that metal reduction played a role as electron acceptor, besides sulfate, for AOM.

MICROBIAL COMMUNITY COMPOSITION AT THE SEEP STATIONS

Anaerobic oxidation of methane supported a vital microbial community as demonstrated by ^{13}C-methane labeling experiments, rate measurements *in vitro*, rate estimations *in situ*, the presence of ANME-related *mcrA* genes, and an active archaeal and bacterial community at stations 1 and 2 (**Figure 4**). Many archaeal sequences obtained from the Simeulue seep stations 1 to 4, were distributed over the ANME-1 and -2 clusters (**Figure 7**). *OTUs* from the stations 1 and 2 were assigned to ANME-1b and ANME-2b clusters. Also at the station 3, ANME-2a/c members were identified. Furthermore, members of the *Crenarchaeota* were frequently detected in the DGGE analysis at both AOM-stations and the station 3. The occurrence of *Crenarchaeota* at a methane seep is not unusual and has been reported for other sites (Knittel et al., 2005; Knittel and Boetius, 2009).

Most bacterial groups belonged to the family *Anaerolineaceae* (phylum *Chloroflexi*), the candidate division OP9 (Webster et al., 2004) and the class δ-*Proteobacteria.* These groups have been described to be dominant in marine sediments (Teske, 2006; Blazejak and Schippers, 2010). Sequences affiliated to the family Anaerolineaceae were derived from stations 1 to 4. The nearest cultured genus *Leptolinea* (distance matrix: 84.5% identity with the nearest *Leptolinea* member) has been described as saccharolytic, including pectin and cellulose degrading species (Yamada et al., 2006; Ishii et al., 2008). In these studies, members of the genus *Leptolinea* were not able to reduce sulfate or other sulfur species (Yamada et al., 2006). *Leptolinea* and *Levilinea* species largely comprise taxa discovered in anaerobic waste water sludge (Rivière et al., 2009), indicating the possibility of active heterotrophic processes at the AOM seep. However, sequences from the Simeulue seep were closer related to sequences which could not be assigned to these genera (**Figure 6**). Three sequences of the stations 1 and 2 were closely related to the genus *Desulfococcus* of the family *Desulfobacteraceae,* which is in good agreement with previously described AOM sites (Knittel and Boetius, 2009).

At the stations 1 and 2 (only data for station 1 are shown in **Figure 4**), *mcrA* genes encoding for the enzyme methyl-CoM-reductase of the anaerobic methanotrophic ANME-2 group dominated over ANME-1. ANME-1 *mcrA* genes prevailed only at the surface of the station 2. The *Methanosarcina* ("methanogenic") type of the *mcrA* gene was detected throughout the whole seep area, while it was completely absent in other sediments of the Sumatra forearc (Schippers et al., 2010). The simultaneous occurrence of both, methane production and oxidation in the seep area, underscores the important role of the methane cycle for this system. The *dsrA* gene, an indicator for the presence of sulfate reducers, was found in slightly higher gene copy numbers at the station 1–3 (**Figure 4**).

Catalyzed reporter deposition–fluorescence in situ hybridization cell counts, assessing the active community, indicated that living *Bacteria* were present with at least two orders of magnitude more cells than *Archaea* at the station 2. At the station 1, active bacterial and archaeal cells were distributed equally. In contrast, results obtained by qPCR, targeting also inactive microorganisms, indicate a dominance of *Bacteria* over *Archaea* by one order of magnitude.

The total cell numbers of 10^7 to 10^9 cells cm^{-3} at the Simeulue seep were quite similar to those at sites of the Sumatra forearc basins not influenced by methane seepage (Schippers et al., 2010). These are also comparable to cell numbers reported for the arctic, methane emitting, Haakon Mosby mud volcano, hosting mainly aerobic methylotrophs (Niemann et al., 2006b). Also the decrease of cell numbers with sediment depth was similar compared to this mud volcano. CARD–FISH cell counts, and qPCR measurements showed the presence of *Bacteria* and *Archaea*, but only small numbers of *Eukarya.* This observation is in agreement with previous marine sediment studies (Schippers and Nerretin, 2006; Schippers et al., 2010).

METHANOGENESIS AS A CONCOMITANT PROCESS

Another goal of this research was to demonstrate methanogenic hydrocarbon degradation (Zengler et al., 1999; Head et al., 2003). From a geological point of view, the Sumatra forearc seems a promising location for hydrocarbon generation in the deep subsurface, a potential source for upward migrating of complex hydrocarbons. Hence, all stations were screened for such processes. Hydrocarbon-dependent methanogenesis was observed in microcosms of the Simeulue seep and the Nias basin. After a first transfer of sediment microcosms of five stations (**Table 2**), three stations showed sustained methanogenesis in the presence of higher hydrocarbons. Only one of these stations was located in the seep area (station 6), the other two in the Nias basin. The rates estimated in the initial setups as well as in the first transfers, were in the same range compared to a hydrocarbon adapted community of contaminated harbor mud in the North Sea (Siegert et al., 2011).

Methanogenesis was absent in microcosms without added substrates. Possibly, the presence of 28 mM sulfate and other electron acceptors inhibited methanogenesis from TOC, but not from higher hydrocarbons. In contrast, it seems likely that the addition of higher hydrocarbons stimulated activity of TOC and hydrocarbon utilizing microorganisms. Positive controls containing the substrates TMA or methanol with 28 mM sulfate confirmed that methanogenic activity in spite of present sulfate. Methanogenesis from these substrates evolved rapidly within the first weeks of incubation and was in the same order with the AOM rates.

Desulfobacteraceae species may be indicative for AOM consortia (Knittel and Boetius, 2009), but one member of this family is the hexadecane degrader *Desulfococcus oleovorans* strain Hxd3 (Aeckersberg et al., 1991; So et al., 2003). Hence, the occurrence of this family suggests the presence of consortia capable of anaerobic degradation of higher hydrocarbons. The finding of other closely related hydrocarbon seep associated sequences, e.g., from mud volcanoes or contaminated sites, confirmed this (**Figure 6**). However, hydrocarbons are abundant substances in nature and our culturing experiments show that the presence of hydrocarbon degraders does not necessarily depend on the presence of hydrocarbons in higher concentrations. In summary, hydrocarbon utilizing methanogenic communities were present in the Sumatra forearc sediments irrespective of methane seepage, and their presence does not infer that higher hydrocarbons played a significant

role in the carbon cycle. Nonetheless, this is the first report of stable microcosms of hydrocarbon-dependent methanogenic microbial communities from the deep ocean.

CONCLUSION

The first-time discovery of an AOM-influenced methane seep in the Indian Ocean was confirmed by the presence of dissolved methane as well as methane-dependent pro- and eukaryotic communities. Methane $\delta^{13}C$ signatures indicate a microbial origin of methane. The released methane was oxidized by an active microbial community, sharing features with other seep communities. Albeit negligible *in situ*, it was also observed that higher hydrocarbons were converted to methane *in vitro*.

ACKNOWLEDGMENTS

We thank G. Mengel-Jung, D. Zoch, U. Günther, H.-E. Gäbler, T. M. Segl, C. Ostertag-Henning, S. Schlömer, and H. Probst for technical support and fruitful discussions. We thank the officers, crew and shipboard scientific party of R/V SONNE especially A. Lückge for excellent support during expedition SO189-2. This work was funded by the BMBF research grant 03G0189A and the DFG grants KR 3311/5-1 and 5-2.

REFERENCES

Aeckersberg, F., Bak, F., and Widdel, F. (1991). Anaerobic oxidation of saturated hydrocarbons to CO2 by a new type of sulfate-reducing bacterium. *Arch. Microbiol.* 156, 5–14.

Aloisi, G., Pierre, C., Rouchy, J.-M., Foucher, J.-P., Woodside, J., and Party, M. S. (2000). Methane-related authigenic carbonates of eastern Mediterranean Sea mud volcanoes and their relation to gas hydrate destabilisation. *Earth Planet. Sci. Lett.* 184, 321–338.

Barnes, R. O., and Goldberg, E. D. (1976). Methane production and consumption in anoxic marine sediments. *Geology* 4, 297–300.

Beal, E. J., House, C. H., and Orphan, V. J. (2009). Manganese- and iron-dependent marine methane oxidation. *Science* 325, 184–187.

Berndt, C., Bünz, S., Clayton, T., Mienert, J., and Saunders, M. (2004). Seismic character of bottom simulating reflectors: examples from the mid-Norwegian margin. *Mar. Petrol. Geol.* 21, 723–733.

Blazejak, A., Erséus, C., Amann, R., and Dubilier, N. (2005). Coexistence of bacterial sulfide oxidizers, sulfate reducers, and spirochetes in a gutless worm (Oligochaeta) from the Peru margin. *Appl. Environ. Microbiol.* 71, 1553–1561.

Blazejak, A., and Schippers, A. (2010). High abundance of JS-1- and Chloroflexi-related bacteria in deeply buried marine sediments revealed by quantitative, real-time PCR. *FEMS Microbiol. Ecol.* 72, 198–207.

Boetius, A., Ravenschlag, K., Schubert, C. J., Rickert, D., Widdel, F., Gieseke, A., Amann, R., Jørgensen, B. B., Witte, U., and Pfannkuche, O. (2000). A marine microbial consortium apparently mediating anaerobic oxidation of methane. *Nature* 407, 423–426.

Bohrmann, G., Greinert, J., Suess, E., and Torres, M. (1998). Authigenic carbonates from the Cascadia subduction zone and their relation to gas hydrate stability. *Geology* 26, 647–650.

Childress, J. J., Fisher, C. R., Brooks, J. M., Kennicutt, M. C., Bidigare, R., and Anderson, A. E. (1986). A methanotrophic marine molluscan (Bivalvia, Mytilidae) symbiosis: mussels fueled by gas. *Science* 233, 1306–1308.

Cline, J. D. (1969). Spectrophotometric determination of hydrogen sulfide in natural waters. *Limnol. Oceanogr.* 14, 454–458.

Coffin, R., Hamdan, L., Plummer, R., Smith, J., Gardner, J., Hagen, R., and Wood, W. (2008). Analysis of methane and sulfate flux in methane-charged sediments from the Mississippi Canyon, Gulf of Mexico. *Mar. Petrol. Geol.* 25, 977–987.

Coolen, M. J. L., Cypionka, H., Sass, A. M., Sass, H., and Overmann, J. (2002). Ongoing modification of mediterranean pleistocene sapropels mediated by prokaryotes; online supplementary material. *Science* 296, 2407–2410.

Cord-Ruwisch, R. (1985). A quick method for the determination of dissolved and precipitated sulfides in cultures of sulfate-reducing bacteria. *J. Microbiol. Methods* 4, 33–36.

Davis, J. B., and Yarbrough, H. F. (1966). Anaerobic oxidation of hydrocarbons by *Desulfovibrio desulfuricans*. *Chem. Geol.* 1, 137–144.

Dekov, V. M., Kamenov, G. D., Savelli, C., Stummeyer, J., and Marchig, V. (2006). Origin of basal dolomitic claystone in the Marsili Basin, Tyrrhenian Sea. *Mar. Geol.* 236, 121–141.

Deuser, W. G., Degens, E. T., and Guillard, R. R. L. (1968). Carbon isotope relationships between plankton and sea water. *Geochim. Cosmochim. Acta* 32, 657–660.

Dhillon, A., Teske, A., Dillon, J., Stahl, D. A., and Sogin, M. L. (2003). Molecular characterization of sulfate-reducing bacteria in the Guaymas basin. *Appl. Environ. Microbiol.* 69, 2765–2772.

Duperron, S., Nadalig, T., Caprais, J.-C., Sibuet, M., Fiala-Médioni, A., Amann, R., and Dubilier, N. (2005). Dual symbiosis in a *Bathymodiolus* sp. mussel from a methane seep on the Gabon continental margin (Southeast Atlantic): 16S rRNA phylogeny and distribution of the symbionts in gills. *Appl. Environ. Microbiol.* 71, 1694–1700.

Ettwig, K. F., Butler, M. K., Le Paslier, D., Pelletier, E., Mangenot, S., Kuypers, M. M. M., Schreiber, F., Dutilh, B. E., Zedelius, J., De Beer, D., Gloerich, J., Wessels, H. J. C. T., Van Alen, T., Luesken, F., Wu, M. L., Van De Pas-Schoonen, K. T., Op Den Camp, H. J. M., Janssen-Megens, E. M., Francoijs, K.-J., Stunnenberg, H., Weissenbach, J., Jetten, M. S. M., and Strous, M. (2010). Nitrite-driven anaerobic methane oxidation by oxygenic bacteria. *Nature* 464, 543–548.

Faber, E., and Stahl, W. (1983). Analytic procedure and results of an isotope geochemical surface survey in an Area of the British North Sea. *Geol. Soc. Lond. Spec. Publ.* 12, 51–63.

Gallardo, V. A. (1977). Large benthic microbial communities in sulphide biota under Peru-Chile subsurface countercurrent. *Nature* 268, 331–332.

Geißler, A. (2003). *Molekulare Analyse der bakteriellen Diversität in Uranabraumhalden*. Freiberg: Technische Universität Bergakademie Freiberg.

Girguis, P. R., Orphan, V. J., Hallam, S. J., and Delong, E. F. (2003). Growth and methane oxidation rates of anaerobic methanotrophic archaea in a continuous-flow bioreactor. *Appl. Environ. Microbiol.* 69, 5472–5482.

Ha, M.-H., and Choi, J. (2009). Effects of environmental contaminants on hemoglobin gene expression in *Daphnia magna*: a potential biomarker for freshwater quality monitoring. *Arch. Environ. Contam. Toxicol.* 57, 330–337.

Harrison, B. K., Zhang, H., Berelson, W., and Orphan, V. J. (2009). Variations in archaeal and bacterial diversity associated with the sulfate-methane transition zone in continental margin sediments (Santa Barbara, California). *Appl. Environ. Microbiol.* 75, 1487–1499.

Head, I. M., Jones, D. M., and Larter, S. R. (2003). Biological activity in the deep subsurface and the origin of heavy oil. *Nature* 426, 344–352.

Heijs, S. K., Haese, R. R., Van Der Wielen, P. W. J. J., Forney, L. J., and Van Elsas, J. D. (2007). Use of 16S rRNA gene based clone libraries to assess microbial communities potentially involved in anaerobic methane oxidation in a mediterranean cold seep. *Microb. Ecol.* 53, 384–398.

Holler, T., Wegener, G., Knittel, K., Boetius, A., Brunner, B., Kuypers, M. M. M., and Widdel, F. (2009). Substantial 13C/12C and D/H fractionation during anaerobic oxidation of methane by marine consortia enriched in vitro. *Environ. Microbiol. Rep.* 1, 370–376.

Hubert, C., Loy, A., Nickel, M., Arnosti, C., Baranyi, C., Bruchert, V., Ferdelman, T., Finster, K., Christensen, F. M., Rosa De Rezende, J., Vandieken, V., and Jorgensen, B. B. (2009). A constant flux of diverse thermophilic bacteria into the cold arctic seabed. *Science* 325, 1541–1544.

Hyndman, R. D., and Spence, G. D. (1992). A seismic study of methane hydrate marine bottom simulating reflectors. *J. Geophys. Res.* 97, 6683–6698.

Inagaki, F., Nunoura, T., Nakagawa, S., Teske, A., Lever, M., Lauer, A., Suzuki, M., Takai, K., Delwiche, M., Colwell, F. S., Nealson, K. H., Horikoshi, K., D'Hondt, S., and Jørgensen, B. B. (2006). Biogeographical distribution and diversity of microbes in methane hydrate-bearing deep marine sediments on the Pacific Ocean Margin. *Proc. Natl. Acad. Sci. U.S.A.* 104, 2815–2820.

Ishii, S., Shimoyama, T., Hotta, Y., and Watanabe, K. (2008). Characterization of a filamentous biofilm community established in a cellulose-fed microbial fuel cell. *BMC Microbiol.* 8, 6. doi:10.1186/1471-2180-8-6

Jannasch, H. W., Nelson, D. C., and Wirsen, C. O. (1989). Massive natural occurrence of unusually large bacteria (*Beggiatoa* sp.) at a hydrothermal deep-sea vent site. *Nature* 342, 834–836.

Joye, S. B., Boetius, A., Orcutt, B. N., Montoya, J. P., Schulz, H. N., Erickson, M. J., and Lugo, S. K. (2004). The anaerobic oxidation of methane and sulfate reduction in sediments from Gulf of Mexico cold seeps. *Chem. Geol.* 205, 219–238.

Knittel, K., and Boetius, A. (2009). Anaerobic oxidation of methane: progress with an unknown process. *Annu. Rev. Microbiol.* 63, 311–334.

Knittel, K., Boetius, A., Eilers, H., Lochte, K., Pfannkuche, O., Linke, P., and Amann, R. (2003). Activity, distribution, and diversity of sulfate reducers and other bacteria in sediments above gas hydrate (Cascadia Margin, Oregon). *Geomicrobiol. J.* 20, 269–294.

Knittel, K., Lösekann, T., Boetius, A., Kort, R., and Amann, R. (2005). Diversity and distribution of methanotrophic archaea at cold seeps. *Appl. Environ. Microbiol.* 71, 467–479.

Kormas, K. A., Tamaki, H., Hanada, S., and Kamagata, Y. (2009). Apparent richness and community composition of bacteria and archaea in geothermal springs. *Aquat. Microb. Ecol.* 57, 113–122.

Krüger, M., Meyerdierks, A., Glöckner, F. O., Amann, R., Widdel, F., Kube, M., Reinhardt, R., Kahnt, J., Böcher, R., Thauer, R. K., and Shima, S. (2003). A conspicuous nickel protein in microbial mats that oxidize methane anaerobically. *Nature* 426, 878–818.

Krüger, M., Treude, T., Wolters, H., Nauhaus, K., and Boetius, A. (2005). Microbial methane turnover in different marine habitats. *Palaeogeogr. Palaeoclimatol. Palaeoecol.* 227, 6–17.

Lösekann, T., Knittel, K., Nadalig, T., Fuchs, B., Niemann, H., Boetius, A., and Amann, R. (2007). Diversity and abundance of aerobic and anaerobic methane oxidizers at the Haakon Mosby Mud Volcano, Barents Sea. *Appl. Environ. Microbiol.* 73, 3348–3362.

Lovley, D. R., and Phillips, E. J. P. (1986). Organic matter mineralization with reduction of ferric iron in anaerobic sediments. *Appl. Environ. Microbiol.* 51, 683–689.

Lovley, D. R., and Phillips, E. J. P. (1988). Novel mode of microbial energy metabolism: organic carbon oxidation coupled to dissimilatory reduction of iron or manganese. *Appl. Environ. Microbiol.* 54, 1472–1480.

Ludwig, W., Strunk, O., Westram, R., Richter, L., Meier, H., Yadhukumar, Buchner, A., Lai, T., Steppi, S., Jobb, G., Förster, W., Brettske, I., Gerber, S., Ginhart, A. W., Gross, O., Grumann, S., Hermann, S., Jost, R., König, A., Liss, T., Lüßmann, R., May, M., Nonhoff, B., Reichel, B., Strehlow, R., Stamatakis, A., Stuckmann, N., Vilbig, A., Lenke, M., Ludwig, T., Bode, A., and Schleifer, K.-H. (2004). ARB: a software environment for sequence data. *Nucleic Acids Res.* 32, 1363–1371.

Martens, C. S., and Berner, R. A. (1974). Methane production in the interstitial waters of sulfate-depleted marine sediments. *Science* 185, 1167–1169.

Martin, J. W., and Haney, T. A. (2005). Decapod crustaceans from hydrothermal vents and cold seeps: a review through 2005. *Zool. J. Linn. Soc.* 145, 445–522.

Michaelis, W., Seifert, R., Nauhaus, K., Treude, T., Thiel, V., Blumenberg, M., Knittel, K., Gieseke, A., Peterknecht, K., Pape, T., Boetius, A., Amann, R., Jørgensen, B. B., Widdel, F., Peckmann, J., Pimenov, N. V., and Gulin, M. B. (2002). Microbial reefs in the black sea fueled by anaerobic oxidation of methane. *Science* 297, 1013–1015.

Muyzer, G., Teske, A., Wirsen, C. O., and Jannasch, H. W. (1995). Phylogenetic relationships of *Thiomicrospira* species and their identification in deep-sea hydrothermal vent samples by denaturing gradient gel electrophoresis of 16S rDNA fragments. *Arch. Microbiol.* 164, 165–172.

Nadkarni, M. A., Martin, F. E., Jacques, N. A., and Hunter, N. (2002). Determination of bacterial load by real-time PCR using a broad-range (universal) probe and primers set. *Microbiology* 148, 257–266.

Nauhaus, K., Boetius, A., Krüger, M., and Widdel, F. (2002). In vitro demonstration of anaerobic oxidation of methane coupled to sulphate reduction in sediments from a marine gas hydrate area. *Environ. Microbiol.* 4, 296–305.

Newberry, C. J., Webster, G., Cragg, B. A., Parkes, R. J., Weightman, A. J., and Fry, J. C. (2004). Diversity of prokaryotes and methanogenesis in deep subsurface sediments from the Nankai Trough, ocean drilling program leg 190. *Environ. Microbiol.* 6, 274–287.

Niemann, H., Duarte, J., Hensen, C., Omoregie, E., Magalhães, V. H., Elvert, M., Pinheiro, L. M., Kopf, A., and Boetius, A. (2006a). Microbial methane turnover at mud volcanoes of the Gulf of Cadiz. *Geochim. Cosmochim. Acta* 70, 5336–5355.

Niemann, H., Lösekann, T., De Beer, D., Elvert, M., Nadalig, T., Knittel, K., Amann, R., Sauter, E. J., Schluter, M., Klages, M., Foucher, J. P., and Boetius, A. (2006b). Novel microbial communities of the Haakon Mosby mud volcano and their role as a methane sink. *Nature* 443, 854–858.

Nunoura, T., Oida, H., Toki, T., Ashi, J., Takai, K., and Horikoshi, K. (2006). Quantification of mcrA by quantitative fluorescent PCR in sediments from methane seep of the Nankai Trough. *FEMS Microbiol. Ecol.* 57, 149–157.

Orphan, V. J., House, C. H., Hinrichs, K.-H., Mckeegan, K. D., and Delong, E. F. (2002). Multiple archaeal groups mediate methane oxidation in anoxic cold seep sediments. *Proc. Natl. Acad. Sci. U.S.A.* 99, 7663–7668.

Øvreås, L., Forney, L., Daae, F. L., and Torsvik, V. (1997). Distribution of bacterioplankton in meromictic lake saelenvannet, as determined by denaturing gradient gel electrophoresis of PCR-amplified gene fragments coding for 16S rRNA. *Appl. Environ. Microbiol.* 63, 3367–3373.

Pernthaler, A., Pernthaler, J., and Amann, R. (2002). Fluorescence in situ hybridization and catalyzed reporter deposition for the identification of marine bacteria. *Appl. Environ. Microbiol.* 68, 3094–3101.

Petersen, J. M., and Dubilier, N. (2009). Methanotrophic symbioses in marine invertebrates. *Environ. Microbiol. Rep.* 1, 319–335.

Pruesse, E., Quast, C., Knittel, K., Fuchs, B., Ludwig, W., Peplies, J., and Glöckner, F. O. (2007). SILVA: a comprehensive online resource for quality checked and aligned ribosomal RNA sequence data compatible with ARB. *Nucleic Acids Res.* 35, 7188–7196.

Raghoebarsing, A. A., Arjan Pol, A., Van De Pas-Schoonen, K. T., Smolders, A. J. O., Ettwig, K. F., Rijpstra, W. I. C., Schouten, S., Damste, J. S. S., Op Den Camp, H. J. M., Jetten, M. S. M., and Strous, M. (2006). A microbial consortium couples anaerobic methane oxidation to denitrification. *Nature* 440, 918–921.

Reeburgh, W. S. (1976). Methane consumption in Cariaco Trench waters and sediments. *Earth Planet. Sci. Lett.* 28, 337–344.

Reeburgh, W. S. (2007). Oceanic methane biogeochemistry. *Chem. Rev.* 107, 486–513.

Reed, D. W., Fujita, Y., Delwiche, M. E., Blackwelder, D. B., Sheridan, P. P., Uchida, T., and Colwell, F. S. (2002). Microbial communities from methane hydrate-bearing deep marine sediments in a forearc basin. *Appl. Environ. Microbiol.* 68, 3759–3770.

Rice, D. D. (1993). "Composition and origins of coalbed gas," in *AAPG Studies in Geology, Hydrocarbons from Coal,* eds B. E. Law and D. D. Rice (Tulsa: American Association of Petroleum Geologists), 159–184.

Rivière, D., Desvignes, V., Pelletier, E., Chaussonnerie, S., Guermazi, S., Weissenbach, J., Li, T., Camacho, P., and Sghir, A. (2009). Towards the definition of a core of microorganisms involved in anaerobic digestion of sludge. *ISME J* 3, 700–714.

Roberts, H. H., and Aharon, P. (1994). Hydrocarbon-derived carbonate buildups of the northern Gulf of Mexico continental slope: a review of submersible investigations. *Geol. Mar. Lett.* 14, 135–148.

Robertson, C. E., Spear, J. R., Harris, J. K., and Pace, N. R. (2009). Diversity and stratification of archaea in a hypersaline microbial mat. *Appl. Environ. Microbiol.* 75, 1801–1810.

Santelli, C. M., Orcutt, B. N., Banning, E., Bach, W., Moyer, C. L., Sogin, M. L., Staudigel, H., and Edwards, K. J. (2008). Abundance and diversity of microbial life in ocean crust. *Nature* 253, 653–656.

Scheller, S., Goenrich, M., Boecher, R., Thauer, R. K., and Jaun, B. (2010). The key nickel enzyme of methanogenesis catalyses the anaerobic oxidation of methane. *Nature* 465, 606–608.

Schippers, A., Köweker, G., Höft, C., and Teichert, B. M. A. (2010). Quantification of microbial communities in three forearc sediment basins off Sumatra. *Geomicrobiol. J.,* 1–13.

Schippers, A., Neretin, L. N., Kallmeyer, J., Ferdelman, T. G., Cragg, B. A., Parkes, J. R., and Jørgensen, B. B. (2005). Prokaryotic cells of the deep sub-seafloor biosphere identified as living bacteria. *Nature* 433, 861–864.

Schippers, A., and Nerretin, L. N. (2006). Quantification of microbial communities in near-surface and deeply buried marine sediments on the Peru continental margin using real-time PCR. *Environ. Microbiol.* 8, 1251–1260.

Schrum, H. N., Spivack, A. J., Kastner, M., and D'Hondt, S. (2009). Sulfate-reducing ammonium oxidation: a thermodynamically feasible metabolic pathway in subseafloor sediment. *Geology* 37, 939–942.

Schulz, H. N., Brinkhoff, T., Ferdelman, T. G., Mariné, M. H., Teske, A., and Jørgensen, B. B. (1999). Dense populations of a giant sulfur bacterium in Namibian shelf sediments. *Science* 284, 493–495.

Siegert, M., Cichocka, D., Herrmann, S., Gründger, F., Feisthauer, S., Richnow, H.-H., Springael, D., and Krüger, M. (2011). Accelerated methanogenesis from aliphatic and aromatic hydrocarbons under iron and sulfate reducing conditions. *FEMS Microbiol. Lett.* 315, 6–16.

Sieh, K., and Natawitjaja, D. (2000). Neotectonics of the Sumatran fault, Indonesia. *J. Geophys. Res.* 105, 28295–28326.

So, C. M., Phelps, C. D., and Young, L. Y. (2003). Anaerobic transformation of alkanes to fatty acids by a sulfate-reducing bacterium, Hxd3. *Appl. Environ. Microbiol.* 69, 3892–3900.

Takai, K., and Horikoshi, K. (2000). Rapid detection and quantification of members of the archaeal community by quantitative PCR using fluorogenic probes. *Appl. Environ. Microbiol.* 6, 5066–5072.

Teske, A. (2006). "Microbial community composition in deep marine subsurface sediments of ODP Leg 201: sequencing surveys and cultivations," in *Proc. ODP, Sci. Results 201*, ed. B. B. Jørgensen, College Station, Texas, 1–20.

Thauer, R. K. (2011). Anaerobic oxidation of methane with sulfate: on the reversibility of the reactions that are catalyzed by enzymes also involved in methanogenesis from CO_2. *Curr. Opin. Microbiol.* 14, 292–299.

Treude, T., Krüger, M., Boetius, A., and Jørgensen, B. B. (2005). Environmental control on anaerobic oxidation of methane in the gassy sediments of Eckernförde Bay (German Baltic). *Limnol. Oceanogr.* 50, 1771–1786.

Valentine, D. L., Solem, R. C., Kastner, M., Wardlaw, G. D., Boone, D. R., Kendall, M., Wang, X., Hill, T. M., Purdy, A., and Bartlett, D. H. (2005). Biogeochemical investigations of marine methane seeps, Hydrate Ridge, Oregon. *J. Geophys. Res.* 110, 1–17.

Wachter, E. A., and Hayes, J. M. (1985). Exchange of oxygen in carbon dioxide-phosphoric acid systems. *Chem. Geol.* 52, 365–374.

Webster, G., Newberry, C. J., Fry, J. C., and Weightman, A. J. (2003). Assessment of bacterial community structure in the deep sub-seafloor biosphere by 16S rDNA-based techniques: a cautionary tale. *J. Microbiol. Methods* 55, 155–164.

Webster, G., Parkes, R. J., Fry, J. C., and Weightman, A. J. (2004). Widespread occurrence of a novel division of bacteria identified by 16S rRNA gene sequences originally found in deep marine sediments. *Appl. Environ. Microbiol.* 70, 5708–5713.

Wegener, G., Niemann, H., Elvert, M., Hinrichs, K.-U., and Boetius, A. (2008). Assimilation of methane and inorganic carbon by microbial communities mediating the anaerobic oxidation of methane. *Environ. Microbiol.* 10, 2287–2298.

Wehrmann, L. M., Risgaard-Petersen, N., Schrum, H. N., Walsh, E. A., Huh, Y., Ikehara, M., Pierre, C., D'Hondt, S., Ferdelman, T. G., Ravelo, A. C., Takahashi, K., and Zarikian, C. A. (2011). Coupled organic and inorganic carbon cycling in the deep subseafloor sediment of the northeastern bering sea slope (IODP Exp. 323). *Chem. Geol.* 284, 251–261.

Weinbauer, M. G., Beckmann, C., and Höfle, M. G. (1998). Utility of green fluorescent nucleic acid dyes and aluminum oxide membrane filters for rapid epifluorescence enumeration of soil and sediment bacteria. *Appl. Environ. Microbiol.* 64, 5000–5003.

Weisburg, W. G., Barns, S. M., Pelletier, D. A., and Lane, D. J. (1991). 16S ribosomal DNA amplification for phylogenetic study. *J. Bacteriol.* 173, 697–703.

Whiticar, M. J., Faber, E., and Schoell, M. (1986). Biogenic methane formation in marine and freshwater environments: CO_2 reduction vs. acetate fermentation –isotope evidence. *Geochim. Cosmochim. Acta* 50, 693–709.

Widdel, F., and Bak, F. (1992). "Gram-negative mesophilic sulfate-reducing bacteria," in *The Prokaryotes,* ed. M. Dworkin (New York: Springer), 3352–3372.

Wiedicke-Hombach, M., Ardhayastuti, S., Bruns, A., Delisle, G., Goergens, R., Hermawan, T., Kanamatsu, T., Lückge, A., Mohtadi, M., Mühr, P., Rahadyan, T., Riyadi, A., Rühlemann, C., Schippers, A., Schlömer, S., Taufik, M., Teichert, B., Vink, A., Weiss, W., Wijaya, H., Wöhrl, C., Zeibig, M., and Zoch, D. (2006). *SUMATRA – The Hydrocarbon System of the Sumatra Forearc – SO189-2 Cruise Report.* Hannover: Bundesanstalt für Geowissenschaften und Rohstoffe.

Yamada, T., Sekiguchi, Y., Hanada, S., Imachi, H., Ohashi, A., Harada, H., and Kamagata, Y. (2006). *Anaerolinea thermolimosa* sp. nov., *Levilinea saccharolytica* gen. nov., sp. nov. and *Leptolinea tardivitalis* gen. nov., sp. nov., novel filamentous anaerobes, and description of the new classes *Anaerolineae* classis nov. and *Caldilineae* classis nov. in the bacterial phylum Chloroflexi. *Int. J. Syst. Evol. Microbiol.* 56, 1331–1340.

Zengler, K., Richnow, H. H., Rossello-Mora, R., Michaelis, W., and Widdel, F. (1999). Methane formation from long-chain alkanes by anaerobic microorganisms. *Nature* 401, 266–269.

Zühlsdorff, L., Spieß, V., Hübscher, C., and Breitzke, M. (1999). Seismic reflectivity anomalies in sediments at the eastern flank of the Juan de Fuca Ridge: evidence for fluid migration? *J. Geophys. Res.* 104, 15351–15364.

Conflict of Interest Statement: The authors declare that the research was conducted in the absence of any commercial or financial relationships that could be construed as a potential conflict of interest.

Received: 09 August 2011; accepted: 23 November 2011; published online: 21 December 2011.

Citation: Siegert M, Krüger M, Teichert B, Wiedicke M and Schippers A (2011) Anaerobic oxidation of methane at a marine methane seep in a forearc sediment basin off Sumatra, Indian Ocean. Front. Microbio. ***2****:249. doi: 10.3389/fmicb.2011.00249*

This article was submitted to Frontiers in Extreme Microbiology, a specialty of Frontiers in Microbiology.

frontiers in
MICROBIOLOGY

ORIGINAL RESEARCH ARTICLE
published: 20 December 2011
doi: 10.3389/fmicb.2011.00254

Potential for nitrogen fixation and nitrification in the granite-hosted subsurface at Henderson Mine, CO

Elizabeth D. Swanner*†* and *Alexis S. Templeton

Department of Geological Sciences, University of Colorado, Boulder, CO, USA

Edited by:
Andreas Teske, University of North Carolina at Chapel Hill, USA

Reviewed by:
Barbara J. Campbell, University of Delaware, USA
Tim Magnuson, Idaho State University, USA
Christine M. Foreman, Montana State University, USA

***Correspondence:**
Elizabeth D. Swanner, Department of Geological Sciences, University of Colorado, Campus Box 399, Boulder, CO 80309, USA.
e-mail: swanner@colorado.edu

†***Present address:***
Elizabeth D. Swanner, Center for Applied Geoscience (ZAG), EberhardKarls University Tübingen, Sigwartstrasse 10, 72076 Tübingen, Germany.

The existence of life in the deep terrestrial subsurface is established, yet few studies have investigated the origin of nitrogen that supports deep life. Previously, 16S rRNA gene surveys cataloged a diverse microbial community in subsurface fluids draining from boreholes 3000 feet deep at Henderson Mine, CO, USA (Sahl et al., 2008). The prior characterization of the fluid chemistry and microbial community forms the basis for the further investigation here of the source of NH_4^+. The reported fluid chemistry included N_2, NH_4^+ (5–112 μM), NO_2^- (27–48 μM), and NO_3^- (17–72 μM). In this study, the correlation between low NH_4^+ concentrations in dominantly meteoric fluids and higher NH_4^+ in rock-reacted fluids is used to hypothesize that NH_4^+ is sourced from NH_4^+-bearing biotite. However, biotite samples from the host rocks and ore-body minerals were analyzed by Fourier transform infrared (FTIR) microscopy and none-contained NH_4^+. However, the nitrogenase-encoding gene *nifH* was successfully amplified from DNA of the fluid sample with high NH_4^+, suggesting that subsurface microbes have the capability to fix N_2. If so, unregulated nitrogen fixation may account for the relatively high NH_4^+ concentrations in the fluids. Additionally, the *amoA* and *nxrB* genes for archaeal ammonium monooxygenase and nitrite oxidoreductase, respectively, were amplified from the high NH_4^+ fluid DNA, while bacterial *amoA* genes were not. Putative nitrifying organisms are closely related to ammonium-oxidizing *Crenarchaeota* and nitrite-oxidizing *Nitrospira* detected in other subsurface sites based upon 16S rRNA sequence analysis. Thermodynamic calculations underscore the importance of NH_4^+ as an energy source in a subsurface nitrification pathway. These results suggest that the subsurface microbial community at Henderson is adapted to the low nutrient and energy environment by their capability of fixing nitrogen, and that fixed nitrogen may support subsurface biomass via nitrification.

Keywords: subsurface, nitrogen fixation, archaeal ammonia oxidation, nitrite oxidation, *Crenarchaeota, Nitrospira*

INTRODUCTION

At depths of at least 3.2 km, an abundant and diverse microbial biosphere in habits terrestrial hard rock settings (Pedersen, 1997; Moser et al., 2003; Kovacik et al., 2006; Sahl et al., 2008), but the rock type is likely to exert tremendous control over the geochemically available nutrients and energy sources. In the basaltic-hosted subsurface settings, organisms may be sustained by H_2 generated from reactions between water and Fe-rich mafic minerals (Stevens and Mckinley, 1995; Lin et al., 2006b). Organisms living in metamorphosed Precambrian sediments likely utilize H_2 and SO_4^{2-} derived from the reaction of decaying radionuclides with water and sulfide minerals in a process known as radiolysis (Lin et al., 2005, 2006b; Lefticariu et al., 2010). In sedimentary rock, organisms may be energetically supported by organic carbon associated with the deposits (Fredrickson et al., 1997; Kovacik et al., 2006). While most studies have focused on determining the energy sources supporting life in the terrestrial subsurface (see Lovley and Chapelle, 1995; Pedersen, 2000; Amend and Teske, 2005; Fredrickson and Balkwill, 2006 for reviews), the origins of nutrients to subsurface microbial communities have been insufficiently investigated. While field and laboratory experiments have implicated microbes in the release of species such as Ca, Si, P, and Fe from minerals (Rogers et al., 1998; Edwards et al., 2003; Rogers and Bennett, 2004; Wu et al., 2008, 2009; Shelbolina et al., 2010), whether or not geologically sourced nitrogen (i.e., as ammonium substituted into potassic rocks) supports subsurface life is a question that has not yet been posed.

Many forms of nitrogen can be utilized biologically both for biosynthesis and energy metabolism. In subsurface settings, N_2 may be sourced from the mantle (i.e., Crossey et al., 2009). Where oxidized nitrogen is absent, ammonium formed in the subsurface may be the most important form of nitrogen sustaining subsurface communities, but the origin of subsurface ammonium supporting microbial communities is unknown. However, at least two processes are possible. Although few nitrogen-bearing minerals are known, the substitution of NH_4^+ for K^+ in silicate minerals is a widespread process (Holloway and Dahlgren, 2002). Granites, for instance, contain on average ~45 ppm ammonium (Hall, 1999). Another source of ammonium to subsurface environments is biological fixation of subsurface N_2. However, the reduction of N_2 to NH_4^+ by the nitrogenase enzyme requires input of ATP at a high energetic cost (Broda and Paschek, 1980) that may inhibit this

process under oligotrophic and anoxic conditions vs. photosynthetically supported surface environments (Lovley and Chapelle, 1995). Despite this, ammonium has been detected in numerous subsurface settings (Lin et al., 2006a; Onstott et al., 2006; Sahl et al., 2008).

Where ammonium is present in the subsurface, it may play a critical role not just as a nutrient, but as an energy source that sustains nitrifying subsurface microbial organisms. Functional gene studies have been used in characterizing nitrification in other subsurface sites where ammonia-oxidizing bacteria (AOB) and/or ammonia-oxidizing archaea (AOA) and nitrite-oxidizing bacteria (NOB; *Proteobacteria* or *Nitrospira*) are present (Hirayama et al., 2005; Spear et al., 2007; Weidler et al., 2007). Both archaeal *amoA* genes and AOA have been detected and commonly exceed the AOB and bacterial *amoA* genes in a number of oligotrophic settings, indicating that AOA may be adapted to low substrate niches (Martens-Habbena et al., 2009). Nitrite oxidation has also been recognized as a potentially important microbially mediated process in the deep subsurface (Hirayama et al., 2005; Gihring et al., 2006), specifically by the *Nitrospira* genus of bacteria. *Nitrospira* appear to be the most diverse and abundant NOB in nitrifying environments, thriving in nitrite and oxygen concentrations are too low to support proteobacterial NOB (Daims et al., 2001, 2006).

This study evaluates the origin of ammonium in fluids circulating through a granite-hosted molybdenum ore-body at >3000 foot depth. The fluids contain N_2, N_2O, NO_3^-, NO_2^-, and ammonium and an estimated 10^3–10^4 cells ml (Sahl et al., 2008), and thermodynamically favorable nitrification reactions may be important in supporting the biomass detected in the fluids (Swanner, 2011). To evaluate possible geologic sources of ammonium, subsurface biotites, and muscovites were screened with Fourier transform infrared (FTIR) microscopy for the presence of NH_4^+. Concurrently, the potential for the microbial community to fix N_2 into NH_4^+ was assessed based on the presence of genes for nitrogen fixation in DNA from NH_4^+-bearing borehole fluids. The DNA was also used to evaluate whether genes for ammonium- and nitrite-oxidation were present. The current work builds on the prior study of Sahl et al. (2008), which reported the presence of archaea and *Nitrospira* in 16S rRNA clone libraries of the borehole fluids. The new mineralogical, functional gene, and phylogenetic analyses yield insight into the source of ammonium to the subsurface, and how the ecology of the subsurface microbial community may be influenced by the presence of ammonium as an energy source in the oligotrophic granite-hosted environment.

MATERIALS AND METHODS

SAMPLE COLLECTION AND PROCESSING

Fluid samples were collected for geochemistry and molecular biology from boreholes draining at the 7025-foot level (elevation above sea level) within Henderson Mine during sampling trips in March 2006. The collection and processing of these samples has already been reported in Sahl et al. (2008). Samples were taken both before and after expandable packers were inserted to exclude O_2 present in the mine tunnel air from equilibrating with draining fluids. Samples of the borehole fluids are named according to the level within the mine they were collected (e.g., 7025), whether they were collected from boreholes before or after insertion of packing devices ("D" for drain, "P" for packer) and the assigned number of each borehole on that level (1, 2, 3, etc.). Additional geochemical data for borehole 7025-D3 reported here was analyzed according to the methodology described in Sahl et al. (2008).

Mineral samples for NH_4^+ analysis (biotites and muscovites) in this study were collected from surface sites surrounding the mine, and from a drill core (**Table 1**). The surface samples were collected from outcrops of Proterozoic biotite gneiss and migmatite (metasediments) intruded by the 1.4 Ga Silver Plume granite within a 10-mile radius of Henderson Mine (Theobald, 1965). Subsurface samples from the ore-bearing stocks, the intruding

Table 1 | Potassic minerals for FTIR analysis.

Sample name	Sample type	Location	Mineral	[NH_4^+] ppm	Reference
STANDARD					
MS-14	Pelitic and banded schists	Moine succession, Scotland	Biotite	845	Boyd and Philippot (1998)
SAMPLE					
SP1009	Biotite gneiss and migmatite[a]	Vasquez Creek Road, CO	Biotite	ND	This study
HS-82-14	Henderson Urad porphyry	Henderson underground	Biotite	ND	Stein (1985)
HS-82-42	Henderson Urad porphyry	Henderson underground	Biotite	ND	Stein (1985)
HS-82-43	Henderson porphyry	Henderson underground	Biotite	ND	Stein (1985)
HS-82-59	Henderson Urad porphyry	Henderson drill core	Biotite	ND	Stein (1985)
HS-82-60	Henderson primos interior	Henderson drill core	Biotite	ND	Stein (1985)
HS-82-61	Henderson seriate granite	Henderson drill core	Biotite	ND	Stein (1985)
HS-82-62	Henderson Dailey stock	Henderson drill core	Biotite	ND	Stein (1985)
HS-82-15	Henderson, silver plume granite	Henderson underground	Biotite	ND	Stein (1985)
HS-82-53	Silver plume granite, type locality	Silver plume, CO quarry	Biotite	ND	Stein (1985)
1225 m	Henderson granite	DUSEL drill core	Muscovite	ND	Jung et al. (2007)
1900 m	Henderson granite	DUSEL drill core	Muscovite	ND	Jung et al. (2007)

[a]*Theobald (1965); ND = not detected.*

Henderson, Seriate, and Urad granite and the Silver Plume granite were acquired from Holly Stein at Colorado State University (Stein, 1985). Hydrothermally altered Henderson Granite was also acquired from a drill core, and named according to the depth of drilling in feet (Sahl et al., 2008). Samples were crushed, sieved between 100 and 400 μm and biotites were concentrated with a Frantz magnetic separator. Minerals were washed in distilled H_2O and dried at 50°C prior to analysis.

FTIR MICROSCOPY

Analysis for NH_4^+ in biotites and muscovites was made by FTIR microscopy as previously described (Busigny et al., 2003, 2004; Papineau et al., 2005; Papineau, 2006). Briefly, individual grains were analyzed using a Thermo Nicolet Continuum microscope linked to a Nexus 670 FTIR spectrometer at the University of Colorado on NaCl plates under CO_2-purged air. The infrared beam was collimated to a 100 μm × 100 μm window and focused normal to the *c*-axis of mica grains. Two hundred transmission IR (4000–650 cm) spectra were collected per grain using an MCT/A detector cooled by liquid nitrogen to minimize electronic noise and absorption of water.

AMPLIFICATION OF FUNCTIONAL GENES

The DNA used in this study was originally acquired through DNA extraction and amplification procedures reported in Sahl et al. (2008). The DNA was tested here for the presence of functional genes of the nitrogen cycle by PCR amplification, cloning, and sequencing. To evaluate the potential for ammonium to be biologically fixed in the boreholes, the *nifH* gene that encodes for part of the nitrogenase enzyme was amplified from DNA of the 7025-P4 borehole using a nested PCR approach with primer sets nifA/nifRev and nifB/nifRev, respectively (Reed et al., 2010). The *nifH* products were extracted and cleaned from a gel using the EZNA gel extraction kit (Omega Bio-Tek, Inc.). The products were then cloned using a TOPO 1-shot cloning kit (Invitrogen) and sequenced commercially with M13F by SeqWright (Houston, TX, USA).

In addition to the N-fixation genes, two marker genes for nitrification were also assessed by PCR amplification. The primers 301F/302R (Norton et al., 2002) were used to amplify the bacterial ammonium-oxidation gene (*amoA*) that encodes for part of the ammonium monooxygenase enzyme under previously described cycling conditions (Hirayama et al., 2005). The potential presence of archaeal *amoA* genes was also assessed with previously described primers (Francis et al., 2005; Spear et al., 2007). Finally, the presence of nitrite oxidation genes from the *Nitrospira* genus was interrogated with the nxrBF916 and nxrBR1237 primers designed to target a 321 bp fragment of the *nxrB* gene that encodes for the β subunit of the nitrite oxidoreductase enzyme (Lücker et al., 2010). This gene was previously called *norB*, which is also the notation for nitric oxide reductase, and so was recently changed to *nxrB* to eliminate confusion (Starkenburg et al., 2006). As the *nxrB* gene is related to genes from the *nar* family that encodes for nitrate reductase in phylogenetically diverse organisms, it was necessary to use primers specific to the nitrite oxidoreductase-encoding genes from the *Nitrospira* genus. Only one definitive *Nitrospira nxrB* gene sequence exists in the public database from the metagenome of Ca. *Nitrospira defluvii* (Lücker et al., 2010), and so the primers for that organism were used here. Successfully amplified genes were cloned and sequenced as described above for *nifH*. Representative functional gene sequences from this study have been submitted to GenBank under accession numbers JN560700–JN560714.

PHYLOGENETIC ANALYSIS OF FUNCTIONAL GENES

Nucleotide sequences were edited with Sequencher 4.7. Nucleotide sequences of the functional genes *nifH* and *nxrB* were translated to protein (amino acid) sequences using the transAlign script (Bininda-Emonds, 2005). Both nucleotide and amino acid sequences of functional genes were aligned using ClustalW. Similar sequences were identified from a blastn or blastx search of the NCBI database, and reference sequences were subsequently downloaded from this database. Phylogenetic trees were assembled using the RAxMLBlackBox with the JTT model of substitution (Stamatakis et al., 2008). The maximum-likelihood search was used to find the best-scoring tree, which was selected and edited in FigTree (http://tree.bio.ed.ac.uk/software/figtree/). Additionally, 16S rRNA sequences of *Nitrospira* from borehole 7025-P4 reported in Sahl et al. (2008) were reanalyzed in order to resolve the genus-level groupings of these organisms. The sequences were aligned using the Greengenes database (Desantis et al., 2006) and RAxMLBlackBox was used for tree construction.

RESULTS

GEOCHEMISTRY OF THE FLUIDS

The aqueous geochemistry of fluids from boreholes 7025-D1/P1, 7025-D4/P4, 7150-D1, and 7150-D3 were previously reported (Sahl et al., 2008). Geochemistry from an additional borehole, 7025-D3, are reported here to establish that NH_4^+ increases corresponding to Mn along at least three boreholes (**Figure 1**). Borehole 7025-D3 had a pH of 6.14 and contained 0.52 mM Mn, 4.2 mM SO_4^{2-}, 0.68 mM F, and 3 μM NH_4^+.

NH_4^+ CONTENT OF MICAS

Biotite samples analyzed for NH_4^+ content (**Table 1**) were collected from surface outcrops of biotite gneiss and migmatite (sample SP1009) surrounding Henderson Mine. Biotites were also analyzed from subsurface samples of the Henderson and Seriate granite, the mineralized stocks of the Henderson and Urad ore-bodies, and the Silver Plume granite (sample names beginning with HS-82). Muscovite grains from hydrothermally altered Henderson granite obtained from drill core were also analyzed (samples 1225 and 1900 m). Although reference biotites from the Moine metasediment (MS-14; Boyd and Philippot, 1998) were successfully analyzed as NH_4^+-bearing standards with a characteristic and quantitative peak for NH_4^+ bending at 1429 cm under FTIR (data not shown), none of the Henderson subsurface biotite or muscovite samples displayed a peak corresponding to NH_4^+ bending.

AMPLIFICATION AND PHYLOGENETIC ANALYSIS OF FUNCTIONAL GENES OF THE NITROGEN CYCLE

Genomic DNA samples from boreholes for which 16S rRNA clone libraries had been assembled (7025-D1/P1 and 7025-P4; Sahl et al., 2008) were screened for the presence of functional genes of the nitrogen cycle. The *nifH* gene was successfully amplified only from

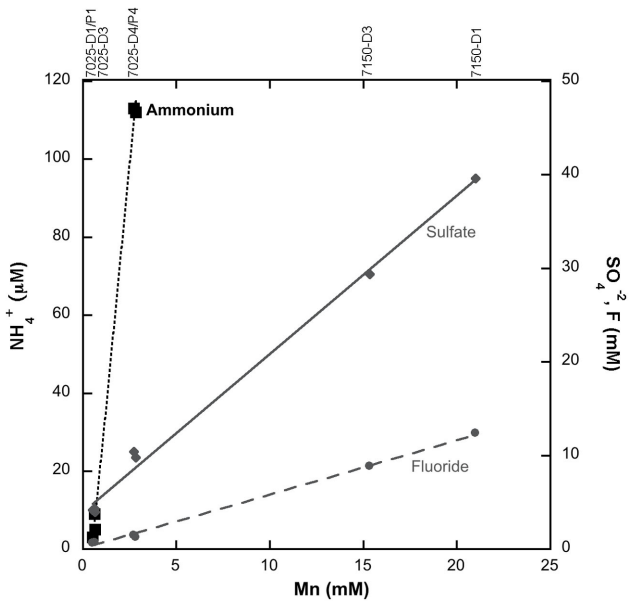

FIGURE 1 | The fluid chemistry of five boreholes from two levels within Henderson Mine demonstrate linear correlations between Mn and F^- or SO_4^{2-} as recognized by Sahl et al. (2008), which is interpreted as mixing between a rock-reacted fluid and meteoric water. NH_4^+ concentrations for the boreholes 7025-D1/P1 and 7025-D1/P4 as reported by Sahl et al. (2008) and additional data from borehole 7025-D3 reported here suggest that ammonium may also source from water-rock reaction.

borehole 7025-P4 DNA. Cloning and sequencing of this product resulted in retrieval of 39 *nifH* sequences of ∼370 bp. The two unique *nifH* phylotypes (defined by >90% amino acid identity) are shown in the phylogenetic tree in **Figure 2**, along with *nifH* from other environments, all of which are longer than 300 bp. One phylotype ($n = 2$) groups with *Verrucomicrobia nifH* sequences that encode the C-type nitrogenases characteristic of *Clostridium,* Gram positive bacteria, and δ-*Proteobacteria* (Mehta et al., 2003; Young, 2005). However, there were no *Verrucomicrobial* 16S rRNA gene sequences detected in this sample. The Gram positive group includes the *Paenibacillus* that are known to fix nitrogen (Canfield et al., 2005), and *Paenibacillus* were isolated previously from Henderson Mine (Mayhew et al., 2008). No *nifH* sequences were amplified from the DNA of the *Paenibacillus* isolates with the *nifH* primers used in this study (data not shown), suggesting *nifH* may not be present in Henderson Mine *Paenibacillus.* The second phylotype ($n = 37$) clusters separately, near to *nifH* sequences from the *Nitrospira* phylum and encodes B-type nitrogenases (characteristic of *Proteobacteria, Cyanobacteria,* and *Firmicutes*; Young, 2005). The only members of the *Nitrospirae* phylum detected in 7025-P4 DNA sample were from the genus *Nitrospira*, and none of these organisms are known to contain *nifH* (Lücker et al., 2010).

The *amoA* gene for bacterial ammonia oxidation could not be amplified from either of the borehole samples. DNA from a Japanese Gold Mine that contained AOB (Hirayama et al., 2005) was used as a positive control to ensure that this was indeed a negative result and not due to a problem with the amplification protocol. In contrast, 43 archaeal ammonium-oxidation *amoA* gene sequences of ∼700 bp were amplified from 7025-P4 DNA. Four unique phylotypes (>90% nucleotide identity) were recovered. The relationship of 7025-P4 *amoA* and other environmental and pure culture *amoA* are shown in **Figure 3**, where all of the sequences included in the analysis are longer than 500 bp. One phylotype groups together with sequences from a mine adit in Colorado and hot springs clones in China (Spear et al., 2007; Zhang et al., 2008; Jiang et al., 2010), while two other phylotypes fall into a previously described cluster of *amoA* (Beman and Francis, 2006), determined by a common node with high bootstrap values.

The *nxrB* primers amplified several differently sized products, and as such are non-specific and should not be used in future amplification of *nxrB* from environmental DNA. For this reason, and because none of the proteobaterial nitrifying organisms (i.e., *Nitrobacter*, *Nitrococcus,* and *Nitrospina*) were detected in 7025-P1 DNA (Sahl et al., 2008), the *nxrB* primers were only used on 7025-P4 DNA. Amplification of the *nxrB* gene with *Nitrospira*-specific primers was successful for the *Nitrospira*-containing DNA from borehole 7025-P4, retrieving two sequences of ∼339 bp that are 93% identical in amino acid to the *nxrB* of Ca. *Nitrospira defluvii* (FP929003; Lücker et al., 2010). The 7025-P4 *nxrB* amino acid sequences were aligned with the *nxrB* from nitrite-oxidizing *Proteobacteria*, as well as with sequences of the related *nar* genes (encoding the nitrate reductase enzyme). All of the sequences included in the analysis were longer than 250 bp. The 7025-P4 *nxrB* cluster closely with the Ca. *Nitrospira defluvii nxrB*, a relationship that is supported by high bootstrap values (**Figure 4**). This cluster is separated from the *nar* sequences and the *nxrB* sequences of *Proteobacteria.*

DISCUSSION

GEOLOGICAL CONTRIBUTIONS TO THE SUBSURFACE NITROGEN CYCLE

The aqueous geochemistry of two of the borehole fluids at the 7025 level addressed in this study have been previously reported (Sahl et al., 2008). The ammonium concentrations of boreholes P1 and P4 were 5 and 112 µM, respectively 2 weeks after being fitted with packing devices, and the concentrations are very similar to those reported before packer insertion (9 and 113 µM, respectively). Sahl et al. (2008) noted geochemical trends from this dataset signifying the mixing of different fluids, a rock-reacted brine, and meteoric water, via the covariance in F or SO_4^{2-} and the dissolved Mn concentration across fluids sampled from five boreholes at two levels within Henderson Mine. In this study we note that the fluid NH_4^+ concentration also appears to increase corresponding with the greater degree of water-rock interaction across boreholes of the 7025 level, when data from a third borehole, 7025-D3 (reported here) is included (**Figure 1**). This trend suggests that NH_4^+ is sourced from the breakdown of NH_4^+-bearing minerals at depth. From the mineral assemblage present at Henderson (Theobald, 1965; Stein, 1985), the phases most likely to contain NH_4^+ are biotite and muscovite, where NH_4^+ can be substituted for K^+ (Honma and Itihara, 1981; Hall, 1987).

Geological nitrogen as NH_4^+ substituted for K^+ could not be detected in biotite collected from Precambrian metasedimentary rocks surrounding Henderson Mine. Thus it is unlikely that the Henderson granite or stocks would have taken up NH_4^+ directly

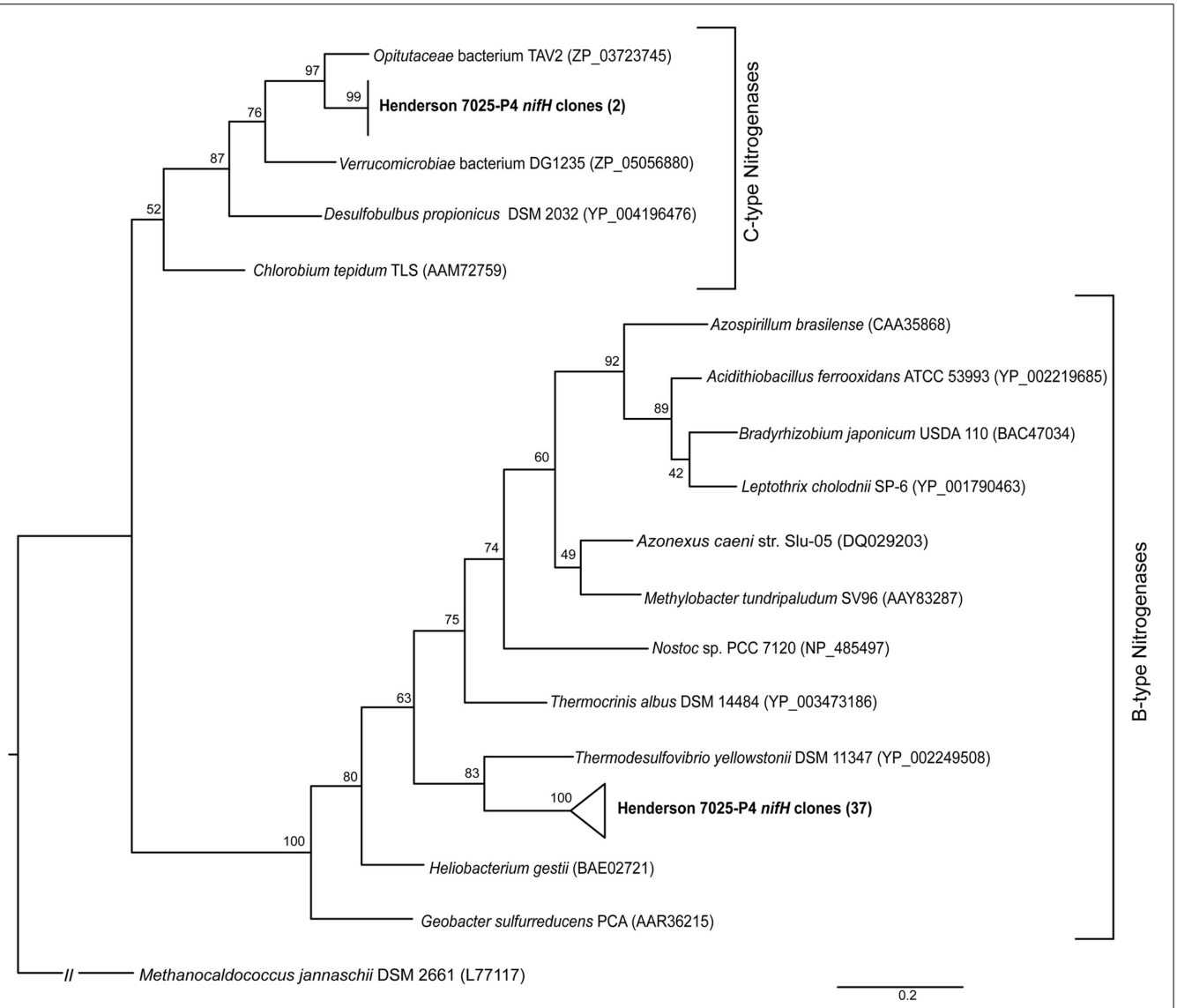

FIGURE 2 | Maximum-likelihood phylogenetic tree constructed of all translated *nifH* sequences retrieved from borehole 7025-P4 DNA (bold) and sequences of *nifH* retrieved from the public databases for organisms that are closely related to those detected in boreholes 7025-P4 by 16S rRNA sequence. Two phylotypes were detected in 7025-P4, and they group with either the B- or C-type nitrogenases. Bootstrap values are shown, and the scale bar represents 0.2 substitutions per site. The tree was constructed using an archaeal *nifH* sequence as an outgroup.

from the metasediments when they were emplaced (i.e., Hall et al., 1991). However, the Tertiary Henderson granite and ore-bearing stocks (e.g., variably containing molybdenite, quartz, K-feldspar, biotite, fluorite, pyrite, or magnetite) are not directly hosted by the metasediments, but rather by the Precambrian Silver Plume granite. For this reason, biotites from the Silver Plume granite were also screened for the presence of ammonium. The Silver Plume granite biotites also do not show evidence of NH_4^+ incorporation. Even if Silver Plume granite did contain ammonium, it is unlikely to have been transferred to the Henderson granite and ore-bearing stocks, because previous isotopic studies indicate little chemical interaction between the Henderson ore-body and surrounding wall rocks (Stein and Hannah, 1985).

Another possible mechanism that could supply ammonium to biotites of the Tertiary Henderson granite and the ore-bearing stocks would be from interaction with the Proterozoic basement, if it contains NH_4^+ (Honma and Itihara, 1981; Hall, 1988). This type of transfer is possible based on the ε_{Nd} and ε_{Sr} values of Henderson granite, which sources its Mo from the mid- to lower crust (Farmer and Depaolo, 1984). Although an appropriate mid- or lower-crust sample was not available for FTIR analysis to screen for NH_4^+-content, none of the biotites of the Henderson granite and stocks contained NH_4^+. While other potassic phases were not analyzed (i.e., muscovite and potassium feldspar), biotites generally have the highest NH_4^+ contents of silicate minerals (Honma and Itihara, 1981; Hall, 1987). However, muscovites that formed

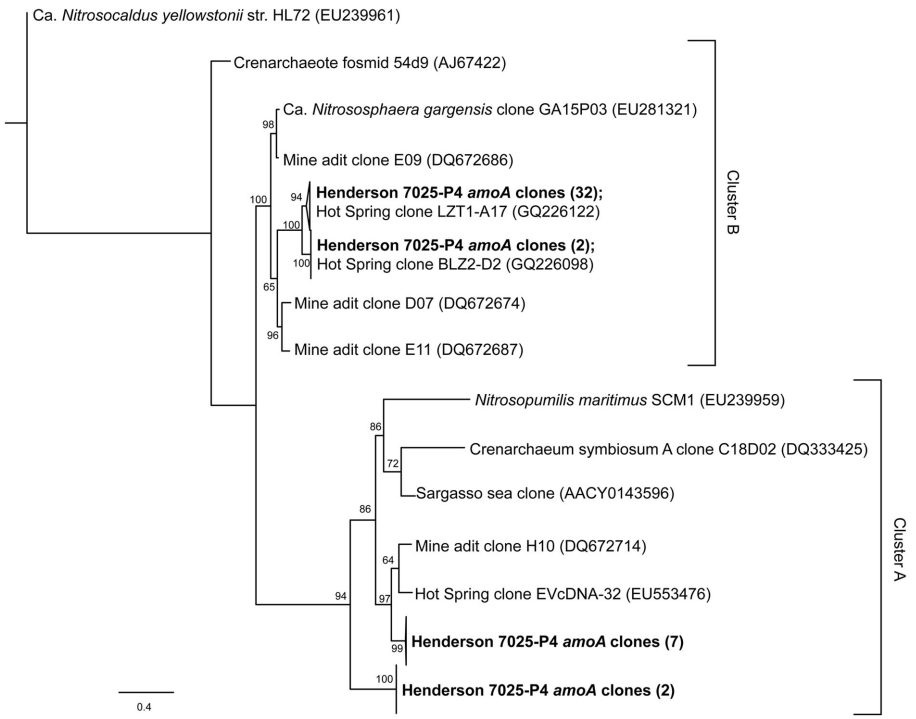

FIGURE 3 | Schematic representation of the best-scoring maximum-likelihood tree generated by an alignment of nucleotide sequences corresponding to the archaeal *amoA* genes amplified from this study (bold) and other environments and pure cultures. The phylotypes from this study fall into four distinct sub-clusters within the previously defined A and B clusters (Beman and Francis, 2006; Zhang et al., 2008). The bacterial *amoA* outgroup has been removed for visual clarity. The scale represents 0.4 substitutions per site.

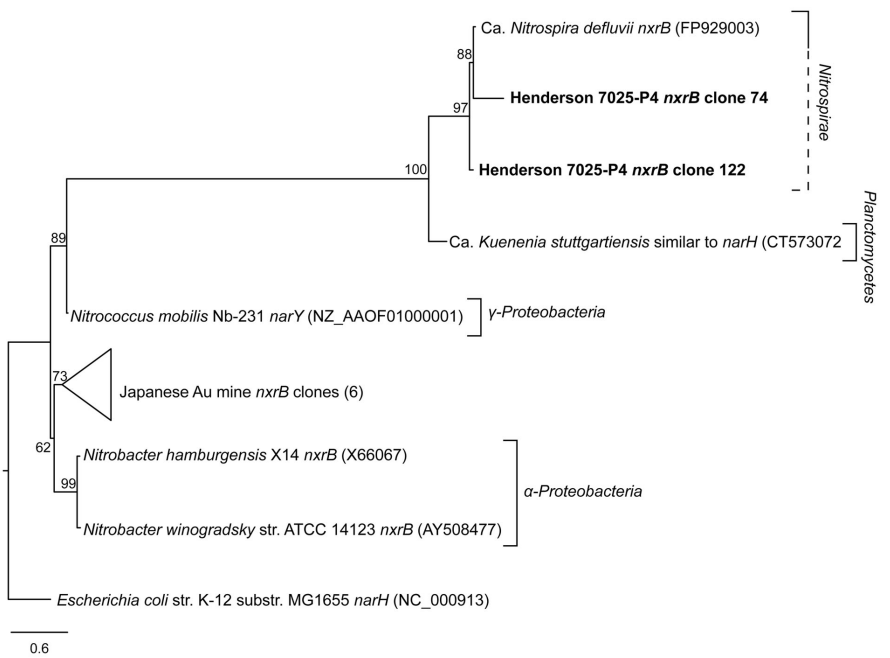

FIGURE 4 | Best-scoring maximum-likelihood phylogenetic analysis of amino acid sequences for *nxrB* and related *nar* genes. The Henderson *nxrB* amino acid sequences retrieved in this study, clones 74 and 122 (bold) are highly similar to the sequence of *nxrB* in Ca. *Nitrospira defluvii*, and this relationship is supported by high bootstrap values. The other *nxrB* sequences belong to organisms of the *Proteobacteria*, except for the Japanese Au mine clones (Hirayama et al., 2005), whose phylogenetic affiliation is unknown. Scale bar represents 0.6 substitutions per site.

after hydrothermal alteration of the Henderson granite were analyzed for NH_4^+ because hydrothermal alteration of granites with fluids that have interacted with NH_4^+-bearing crustal rocks has been observed for intrusive granites in Italy (Hall et al., 1991). The hydrothermal muscovites did not contain NH_4^+, which is consistent with the geological interpretation that the suite of hydrothermally altered minerals at Henderson formed due to the introduction of juvenile, magmatic fluids that that did not interact with the surrounding metasediments, granite, or groundwater (Seedorff and Einaudi, 2004).

There are other potential sources of non-biological NH_4^+ that could not be evaluated for several reasons. For example, nitrogen compounds could have been introduced to subsurface fluids through ammonium nitrate fuel oil (ANFO) that was used as a blasting agent at Henderson (Jensen et al., 1983). However, the boreholes had flushed for almost a year prior to sampling and only the rock-reacted fluids being dewatered from the mine contained high NH_4^+ (i.e., borehole 7025-P4; 112 μM). A meteoric source was unlikely as well, as the most dilute, meteoric-dominated waters contained the lowest levels of N (as NH_4^+, NO_2^-, and NO_3^-; **Figure 1**). Modern precipitation in Colorado can exhibit high levels of nitrate (up to ∼20 μM) in the mountains from industrial activities (Faure and Mensing, 2005) that could be transported to the subsurface in meteoric water. However, the dilute borehole waters at Henderson have an average residence time of 13,000 years based on ^{14}C dating, and is dominantly pre-1950s based on tritium content (Sahl et al., 2008), further underscoring that this modern meteoric water is not likely to be the nitrogen source to subsurface fluids.

BIOLOGICAL FIXATION AS A SOURCE OF SUBSURFACE AMMONIUM

The presence of *nifH* genes in DNA in borehole 7025-P4 (**Figure 2**; 112 μM NH_4^+), and the lack of detectable *nifH* genes in boreholes 7025-D1/P1 (5–9 μM NH_4^+) suggests that microbes inhabiting 7025-P4 fluids are capable of fixing N_2 gas to NH_4^+. This finding of a biological source of nitrogen specific to 7025-P4 is consistent with the lack of evidence for a general subsurface nitrogen source from the breakdown of NH_4^+-bearing potassic minerals (**Table 1**). However, the presence of functional genes does not necessarily signify expression or activity of the encoded enzymes, and so further experiments are needed to evaluate whether nitrogen fixation is occurring. Fresh samples would be needed to measure ^{15}N uptake or acetylene reduction as evidence for nitrogen fixation, and we have been unable to access Henderson Mine for further sampling of these boreholes, and so the further geochemical assays could not be undertaken to augment the dataset in the current study.

If organisms in 7025-P4 fluids do fix nitrogen, they would need to be utilizing a metabolic reaction capable of generating enough ATP and electrons to fuel nitrogen fixation. Although specific N_2-fixing organisms cannot be identified in 7025-P4 based solely on the detected 16S rRNA and *nifH* genes, the geochemical dataset of Sahl et al. (2008) can be used to infer which chemolithoautotrophic metabolisms could support the subsurface community thermodynamically. The reaction of H_2S oxidation with electron acceptors such as O_2, NO_3^-, $Fe(OH)_3$ and MnO_2, or S^0 and Fe^{2+} oxidation with NO_2^-, are more thermodynamically favorable in borehole 7025-P4 relative to 7025-P1(Swanner, 2011). There is a greater than -10 kJ mol^{-1} of electrons transferred increase between 7025-P1 and 7025–P4 for all of these reactions, and all yield at least -20 kJ mol^{-1} of electrons transferred in borehole 7025-P4. Thus nitrogen fixation may be fueled preferentially in the more rock-reacted borehole fluid by any of these reactions. Given the fact that the borehole fluid microbial community compositions are modulated by the degree of mixing between meteoric and rock-reacted fluids (Sahl et al., 2008), we suggest that the potential for nitrogen fixation is strongly tied to the aqueous geochemistry. Furthermore, despite this energetic strain of nitrogen fixation, it has been documented for deep-sea sulfate-reducing methanotroph consortia, whose syntrophic metabolisms provides one of the lowest energetic yields known to sustain microbial life (∼40 kJ mol^{-1} electron transferred to support two organisms; Dekas et al., 2009), suggesting that the energetic yields of reactions possible in 7025-P4 fluids could support nitrogen fixation.

The inference that ammonium is biologically fixed in Henderson fluids raises another question about why nitrogen-fixing organisms would fix nitrogen to levels as high as 112 μM NH_4^+ in an environment where total numbers of microbes are only 10^3–10^4 cells ml, and only half of the nitrogen is converted into organic forms (Sahl et al., 2008). Intriguingly, nitrogen fixation occurs in deep-sea methane-oxidizing archaeal/bacteria consortia in sediments that already contain ammonium (Dekas et al., 2009), suggesting either that localized depletions of ammonium within the consortium drive fixation, or that nitrogenase activity is not well regulated by NH_4^+ concentrations. A lack of regulation on N_2-fixation by NH_4^+ concentrations up to 94 mM has been recently documented for the verrucomicrobial methanotroph *Methylacidiphilum fumairiolicum* strain SolV (Khadem et al., 2010), and some proteobacterial nitrogenases also appear to be unregulated by NH_4^+ (Rudnick et al., 1997). One other reason for nitrogen fixation in the presence of abundant ammonium may be that the transfer of ammonium between nitrogen-fixing and ammonium-utilizing microbes may not be very efficient. Nitrogen-fixing cyanobacteria from the Baltic Sea have been observed to lose up to 30% of their fixed nitrogen to bulk surroundings (Ploug et al., 2010). Further culture and assay-based studies are needed to determine if and why excess nitrogen is being fixed in 7025-P4, but such experiments were not undertaken in the current work due to the sampling limitations discussed above.

It is well established that *nifH* tree topology often mirrors topology of the 16S rRNA gene tree (with some variation due to lateral gene transfer; Hennecke et al., 1985; Normand and Bouquet, 1989; Young, 2005). Although not definitive evidence of phylogenetic affiliation, the *nifH* sequences detected in borehole 7025-P4 DNA may be useful in informing the classes of potential nitrogen-fixing organisms. In **Figure 2** the C-type *nifH* phylotype ($n = 2$) groups with *Verrucomicrobia nifH*, but no 16S rRNA from *Verrucomicrobia* were detected in the DNA of 7025-P4. This phylotype of *nifH* may source from the *Chlorobi* in 7025-P4 DNA, which are phylogenetically close to *Verrucomicrobia* by 16S rRNA and *nifH* measures. *Chlorobi* 16S rRNA genes were detected in this sample (Sahl et al., 2008), although the Henderson *nifH* and *Chlorobi nifH* protein sequences were only 91% similar. A more likely possibility is that this *nif* operon was horizontally transferred (Hirsch et al., 1995) and may not reflect the true phylogeny of organisms.

The B-type *nifH* phylotype ($n = 37$) was much more abundant than the C-type phylotype in 7025-P4 DNA, implying the organisms from which these sequences came from must be much more abundant in the sample. In fact, the most dominant organism in this sample by the measure of 16S rRNA gene sequences (37%) are the novel phylum Henderson candidate division that were first detected in the Henderson environment (Sahl et al., 2008), and subsequently detected in seafloor basalt (Omoregie et al., 2008; Santelli et al., 2008). The phylogenetic analysis of Sahl et al. (2008) demonstrate that the closest related phyla to Henderson candidate division are the *Acidobacteria* and the *Nitrospirae*. In **Figure 2**, the B-type *nifH* phylotype is similarly related to the *Nitrospirae* sequence from *T. yellowstonii*. There were *Nitrospirae* 16S rRNA sequences detected in this sample (Sahl et al., 2008), but they belong specifically to the *Nitrospira* genus, whose only representative sequenced genome does not contain any homologs to the *nifH* gene, suggesting this genus is unlikely to fix nitrogen (Lücker et al., 2010). There were also *Acidobacteria* 16S rRNA sequences detected in the 7025-P4 DNA sample, but of the three sequenced *Acidobacteria* genomes, none possess any *nif* genes (Ward et al., 2009). The B-type *nifH* phylotype may source from Henderson candidate division bacteria, but this phylotype of *nifH* was not amplified from the DNA of borehole 7025-P1, which contained 56% Henderson candidate division 16S rRNA sequences. Without further investigation of the genome of Henderson candidate division or other organisms in borehole 7025-P4, it is unclear which organisms the B-type or C-type *nifH* phylotype source from.

HENDERSON FLUIDS SUPPORT NITRIFICATION

The presence of high NH_4^+, NO_2^-, and $NO_3^-$and low levels of O_2 (1.25 μM) in borehole 7025-P4 suggest that ammonium and nitrite oxidation may be occurring. In fact, both of the reactions of nitrification, summarized by Eq. 1 and 2 below, are thermodynamically favorable in borehole 7025-P4 (Swanner, 2011).

$$NH_4^+ + 1.5O_2 \rightarrow NO_2^- + H_2O + 2H^+ \quad (1)$$

$$NO_2^- + 0.5O_2 \rightarrow NO_3^- \quad (2)$$

Reactions 1 and 2 yield −40 and −35 kJ mol electron transferred, respectively. In addition, micromolar quantities of gaseous N_2O were detected in 7025-P4. N_2O is an intermediate in both microbial nitrification/denitrification, and as such is a hallmark of biological nitrogen cycling. One abiotic mechanism for N_2O production involves reaction of NO_2^- or NO_3^- with (ultra)mafic rocks and minerals (dolerite, augite, and olivine; Samarkin et al., 2010), but none of these phases are present at Henderson and so this mechanism is unlikely. N_2O can also be produced from NO_2^- in the presence of Fe^{2+} and Cu^{2+} (both observed in the borehole fluids) within 24 h at pH 6 (Moraghan and Buresh, 1977). Therefore, even if N_2O is abiotically produced, the additional presence of NO_2^- strongly implicates either nitrification or denitrification in 7025-P4 fluids as a mechanism for continued NO_2^- production. Because of the presence of N_2O, it is also worth noting that nitrate reduction coupled to inorganic electron donors is thermodynamically favorable; in contrast, microbially mediated reactions such as anammox, the anaerobic oxidation of ammonium with nitrite is less likely in Henderson, due to predicted unfavorable thermodynamics under *insitu* conditions (Swanner, 2011). In addition, no organisms belonging to the phylum *Planctomycetes* were detected at Henderson, and only these organisms are currently known to carry out anammox (Kuenen, 2008). A final consideration on the favorability of nitrification in the borehole fluids is that the *C*:*N* is near unity, which should drive the consumption of ammonium by nitrification relative to the assimilation of ammonium by heterotrophs, because *C*:*N* values generally need to be > 20 for heterotrophic ammonium uptake to predominate (Strauss and Lambert, 2000). Additionally, inorganic phosphate levels were was below detection (Sahl et al., 2008), further suggesting that the borehole fluids are oligotrophic.

The organisms most likely to be carrying out ammonium-oxidation in borehole 7025-P4 are AOA, as no AOB were detected in 7025-P4 DNA by 16S rRNA (Sahl et al., 2008). The archaeal organisms previously detected in borehole 7025-P4 belong to the phylum *Crenarchaeota* (Brochier-Armanet et al., 2008; Spang et al., 2010) as reported in Figure 6 of Sahl et al. (2008). Our re-alignment of these previously retrieved 16S rRNA sequences with sequences from other subsurface mines (data not shown) reveal that they are closely related to other subsurface *Crenarchaeota*, some of which have been implicated in archaeal ammonium oxidation (Takai et al., 2001; Nunoura et al., 2005; Spear et al., 2007; Rastogi et al., 2010). Four of the six archaeal sequences retrieved from 7025-P4 are 97% identical to *Ca. Nitrososphaera gargensis*, an ammonium-oxidizing (AOA) isolate (Hatzenpichler et al., 2008), and *amoA* genes have been detected and implicated in ammonium oxidation for other closely related organisms within the *Crenarchaeota* (Treusch et al., 2004). Our finding of *amoA* in DNA of the 7025-P4 borehole that contains high NH_4^+ and organisms closely related to AOA suggests, in conjunction with the geochemical evidence for nitrification, that AOA may be active in subsurface fluids at Henderson Mine. Furthermore, this study is at least the third to amplify archaeal *amoA* from a terrestrial subsurface setting (Spear et al., 2007; Weidler et al., 2007), and our phylogenetic analysis in **Figure 3** suggests that there may be sub-clusters of *amoA* defined by subsurface and hot spring clones (Beman and Francis, 2006; Zhang et al., 2008). Future subsurface studies may reveal further AOA and *amoA* diversity, and will establish the contribution of these processes at depth to the global nitrogen cycle.

The presence of archaeal *amoA* in the 7025-P4 DNA sample and absence of the bacterial version of this gene may be explained by the geochemical conditions. The sub-millimolar concentration of NH_4^+ in borehole 7025-P4 is ideal for AOA who are inhibited by higher concentrations of NH_4^+ (i.e., 2–3 mM). One cultivated AOA, *Nitrosopumilus maritimus* has an ammonia monooxygenase enzyme that reaches maximal activity at NH_4^+ concentrations that are 100-fold less than those observed for AOB enzymes (Martens-Habbena et al., 2009). The low-O_2 concentrations in 7025-P4 may favor AOA who thrive when dissolved O_2 is 3–20 μM (Ergruder et al., 2009). The archaea were only detected after packer insertion, further supporting their adaptation to thrive in low-O_2 niches. The presence of sulfide in wastewater reactors and estuary sediments has an inhibitory effect on the activity of AOB relative to AOA (Sears et al., 2004; Caffrey et al., 2007), and a similar phenomenon has been observed in cultivated AOB (Hooper and Terry,

1973). Dissolved sulfide was not measured in Henderson fluids, but is likely present due to the extensive sulfide mineralization at Henderson, and the formation of elemental sulfur where borehole fluids are released into oxic mine tunnels (Templeton and Swanner, unpublished data).

While the *Crenarchaeota* have only recently been characterized as AOA (Könnecke et al., 2005), the ensuing widespread detection of AOA in soils, estuaries and marine environments and their abundance worldwide relative to AOB signifies that these organisms likely do account for a large portion of both terrestrial and marine nitrogen cycling (Francis et al., 2007). AOA are also preferentially found in low-nutrient environments (Ergruder et al., 2009), and they seem to be adapted to higher salinity (Bernhard et al., 2010), although AOB appear to outnumber AOA in estuarine environments regardless of varying nutrient fluxes (Wankel et al., 2011). AOA are also predominant in environments above 40°C (Zhao et al., 2011), which is the temperature of Henderson fluids. Furthermore, AOA are phylogenetically diverse, and this diversity may underscore their adaptation to diverse environmental conditions relative to the phylogenetically restricted AOB (Francis et al., 2005).

AOB and AOA are not the only organisms capable of oxidizing ammonia. Methanotrophs can also oxidize ammonia due to the broad substrate specificity of the enzyme methane monooxygenase. However, methanotrophs cannot grow using ammonia as a substrate, nor can ammonia oxidizers grow using methane as a substrate (Bédard and Knowles, 1989; Hanson and Hanson, 1996). Bacterial methanotrophs reside within the α- and γ-*Proteobacteria*. Both of these Proteobacterial divisions were detected in borehole 7025-P4 DNA via 16S rRNA, and the fluids from this sample contained submicromolar levels of methane (Sahl et al., 2008). However, the closest isolated methanotrophs were only 92% related to the 7025-P4 α-*Proteobacteria* sequence, and only 86% identical to the γ-*Proteobacteria* sequences. Although ammonium-oxidation by methanotrophs may not be significant in Henderson borehole fluids, it could be an important process in other sites were ammonium and methanotrophs are both abundant, such as a Japanese gold mine (Hirayama et al., 2005). Methanotrophs could contribute to subsurface nitrogen cycling by fixing nitrogen as well (Hanson and Hanson, 1996; Auman et al., 2001). The ability to fix nitrogen may confer a selective advantage for methanotrophs inhabiting low-nutrient subsurface habitats, as is hypothesized for a Japanese uranium mine (Mills et al., 2010).

The nitrification pathway may be carried to completion by the nitrite-oxidizing *Nitrospira* genus (Daims et al., 2001). 16S rRNA sequences belonging to the *Nitrospira* genus were detected in borehole 7025-P4 DNA (1% of the microbial community; Sahl et al., 2008). As was the case with AOA, *Nitrospira* were not detected in the DNA of borehole 7025-D1/P1. The *Nitrospira* sequences from 7025-P4 are distinct at the phylum level from the Henderson candidate division proposed for unique sequences detected in DNA from both boreholes at the Henderson 7025 level (D1/P1 and P4; Sahl et al., 2008). In the current analysis in **Figure 5**, the *Nitrospira* sequences detected from 7025-P4 DNA group closely with a clone from a deep gold mine (Gihring et al., 2006), but apart from other identified clusters of *Nitrospira* (Daims et al., 2001; Lebedeva et al., 2011). The bootstrap values that support this topology are all >90%, suggesting that Henderson sequences may define a novel cluster of subsurface *Nitrospira*. All sequences included in this analysis were longer than 800 bp.

Despite the limited sequence data available for the *Nitrospira nxrB* gene, which encodes the nitrite oxidoreductase, the primers of Lücker et al. (2010) did successfully amplify *nxrB* from the DNA sample of 7025-P4. As 7025-P4 DNA did not contain any 16S rRNA sequences corresponding to *Proteobacterial* nitrite-oxidizers (i.e., *Nitrobacter, Nitrococcus,* and *Nitrospina*), it is possible the *nxrB* sequences we amplified are from *Nitrospira* spp. Because of the high similarity of the amino acid sequence of the amplified genes to that of the Ca. *Nitrospira defluvii nxrB* and the high bootstrap values supporting this relationship, it is likely 7025-P4 *nxrB* clones 74 and 122 are actual *Nitrospira nxrB* sequences (**Figure 4**). Alternatively, this sequence could encode a related *nar* gene or a *nxrB* gene from *Proteobacteria*, but this is unlikely as no nitrifying *Proteobacteria* were detected in this sample. However, without direct evidence from longer sequences of the *Nitrospira* genome in borehole 7025-P4 DNA, it cannot be established that the *nxrB* genes from this study belong to *Nitrospira* genus, and the sample limitations discussed above prohibit further genetic analysis. The *nxrB* sequences retrieved in this study may be useful in future primer design and acquisition of quality environmental sequence data for *Nitrospira*, which will aid in understanding the evolutionary history of the enzymes involved in nitrite/nitrate oxidation and reduction and the organisms that possess them.

The presence of *Nitrospira* in borehole 7025-P4 offers insight into the ecology of these organisms. Three pure cultures consist of obligately lithotrophic nitrite-oxidizers from the genus *Nitrospira* (Watson et al., 1986; Ehrich et al., 1995; Lebedeva et al., 2008, 2011). The cultures were isolated out of both freshwater and marine habitats (Koops and Pommerening-Röser, 2001), as well as hot springs (Lebedeva et al., 2011), suggesting the ecology of this genus is not limited to one type of geochemical environment. The abundance of *Nitrospira* in nitrite-oxidizing environments in comparison to nitrite-oxidizers of the *Proteobacterial* nitrite-oxidizers (i.e., *Nitrobacter*) is evidence for their contribution to nitrite oxidation in a number of environments (Daims et al., 2001). The *Nitrospira* genus seems to be inhibited by higher concentrations of nitrite (i.e., >5–15 mM; Ehrich et al., 1995; Lebedeva et al., 2011) and O_2 (Altmann et al., 2003) than are preferred by *Nitrobacter* species (Ehrich et al., 1995; Daims et al., 2006), suggesting *Nitrospira* may be preferentially adapted to oligotrophic conditions such as are experienced in borehole 7025-P4. *Nitrospira* have now been detected in three subsurface settings where O_2 was <10 μM and NO_2^- did not exceed 120 μM (i.e., borehole 7025-P4; Hirayama et al., 2005; Weidler et al., 2007), although they have also been detected in subsurface fluids with millimolar concentrations of NO_2^- but low-O_2 (Gihring et al., 2006). *Nitrospira* may well be quite common in subsurface settings that contain NO_2^-, and future investigations may uncover more phylogenetic and physiological knowledge about this important genus.

CONCLUSION

This study demonstrates that the deep subsurface microbial communities in the borehole fluids of Henderson Mine have the

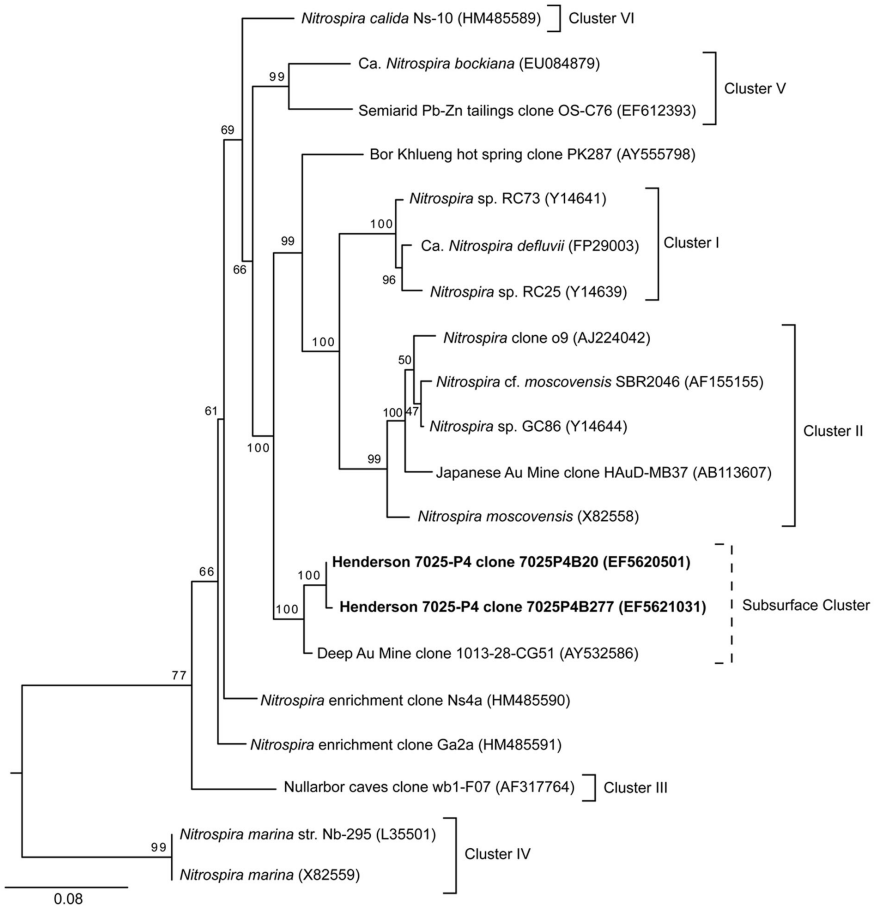

FIGURE 5 | Phylogenetic relationship of NOB in the *Nitrospira* genus as determined by an alignment of the 16S rRNA nucleotide sequences from borehole 7025-P4 (bold) reported in Sahl et al. (2008) and those from the literature. While the phylogenetic affiliation of these sequences in the *Nitrospira* phylum was established by Sahl et al. (2008), further analysis was undertaken here to resolve the position of these sequences within the *Nitrospira* genus. The relationships are represented by a best-scoring maximum-likelihood tree in which clusters I–VI are marked (after Daims et al., 2001; Lebedeva et al., 2011). The two sequences retrieved from Henderson Mine do not group in a known cluster, but bootstrap values support their association with a South African Au Mine clone, which may represent a new subsurface *Nitrospira* cluster. Bootstrap values are shown, and the scale bar represents 0.1 substitutions per site. The proteobacterial outgroup has been removed for clarity.

genetic capacity to fix nitrogen. This fixed nitrogen, as ammonium, is likely to be the primary nitrogen source for organisms living in the subsurface, as no evidence was found that ammonium was sourced geologically from NH_4^+-bearing potassic minerals such as biotites. Although the presence of *nifH* genes in borehole 7025-P4 is only indirect evidence that nitrogen fixation is occurring, it is also correlates to elevated NH_4^+ concentrations and the lack of *nifH* in boreholes with lower NH_4^+ concentrations. If nitrogen fixation is occurring at Henderson it highlights the phenomenon of excess nitrogen fixation under energy–poor conditions. The availability of ammonium, regardless of the ultimate source, also has important consequences for the subsurface microbial community not only as an essential nutrient but because it can also be used as an energy source. There is evidence for ammonium and nitrite oxidation in borehole 7025-P4 where ammonium concentrations are highest based on the detection of archaeal ammonia monooxygenase (*amoA*) and nitrite oxidoreductase (*nxrB*) functional genes. While other subsurface studies have detected genes encoding for both steps of nitrification (Hirayama et al., 2005; Weidler et al., 2007), neither study addressed the source of ammonium fueling this process. Moreover, the *nxrB* sequences detected from borehole 7025-P4 are the first amplified from the *Nitrospira* genus in environmental samples. The presence of nitrifiers 3000 feet below the surface at Henderson also reinforces the idea that *Crenarchaea* and *Nitrospira* may be adapted to low nutrient and substrate environments and could be key players in nitrogen cycling in similar settings. Thus this also work highlights the potential that biological nitrogen fixation and nitrification may be ubiquitous biogeochemical processes in the deep subsurface and maybe important to consider in accounts of global nitrogen cycling.

ACKNOWLEDGMENTS

This work was supported by grants from the David and Lucille Packard Foundation and the National Science Foundation (NSF-BIO 0623815) to Alexis S. Templeton. The investigation was also

made possible by a Geological Society of America Graduate Student Research Grant to Elizabeth D. Swanner. We thank Henderson Mine and Robert Callaghan for previous access to borehole fluids, Jason Sahl, and John Spear for providing DNA samples for analysis, Hisako Hirayama for contributing a positive control for PCR, and Holly Stein for sharing subsurface mineral samples described in Stein (1985). Katherine Wright engaged in helpful discussions, Terry Legg, Diana Nemergut, and Chuck Robertson provided assistance with phylogenetic analyses, and Steve Mojzsis and Nicole Cates assisted with sample collection.

REFERENCES

Altmann, D., Stief, P., Amann, R., De Beer, D., and Schramm, A. (2003). In situ distribution and activity of nitrifying bacteria in freshwater sediment. *Environ. Microbiol.* 5, 798–803.

Amend, J. P., and Teske, A. (2005). Expanding frontiers in deep subsurface microbiology. *Palaeogeogr. Palaeoclimatol. Palaeoecol.* 219, 131–155.

Auman, A. J., Speake, C. C., and Lidstrom, M. E. (2001). nifH Sequences and nitrogen fixation in type I and type II methanotrophs. *Appl. Environ. Microbiol.* 67, 4009–4016.

Bédard, C., and Knowles, R. (1989). Physiology, biochemistry and specific inhibitors of CH_4, NH_4^+, and CO oxidation by methanotrophs and nitrifiers. *Microbiol. Rev.* 53, 68–84.

Beman, J. M., and Francis, C. A. (2006). Diversity of ammonia-oxidizing archaea and bacteria in the sediments of a hypernutrified subtropical estuary: Bahia del Tobari, Mexico. *Appl. Environ. Microbiol.* 72, 7767–7777.

Bernhard, A. E., Landry, Z. C., Blevins, A., De La Torre, J. R., Giblin, A. E., and Stahl, D. A. (2010). Abundance of ammonia-oxidizing archaea and bacteria along an estuarine salinity gradient in relation to potential nitrification rates. *Appl. Environ. Microbiol.* 76, 1285–1289.

Bininda-Emonds, O. R. P. (2005). TransAlign: using amino acids to facilitate the multiple alignment of protein-coding DNA sequences. *BMC Bioinformatics* 6, 156. doi:10.1186/1471-2105-6-156

Boyd, S. R., and Philippot, P. (1998). Precambrian ammonium biogeochemistry: a study of the Moine metasediments, Scotland. *Chem. Geol.* 144, 257–268.

Brochier-Armanet, C., Boussau, B., Gribaldo, S., and Forterre, P. (2008). Mesophilic crenarchaeota: proposal for a third archaeal phylum, the Thaumarchaeota. *Nat. Rev. Microbiol.* 6, 245–252.

Broda, E., and Paschek, G. A. (1980). Evolutionary considerations on the thermodyamics of nitrogen fixation. *BioSystems* 13, 47–56.

Busigny, V., Cartigny, P., Philippot, P., and Javoy, M. (2003). Ammonium quantification in muscovite by infrared spectroscopy. *Chem. Geol.* 198, 21–31.

Busigny, V., Cartigny, P., Philippot, P., and Javoy, M. (2004). Quantitative analysis of ammonium in biotite using infrared spectroscopy. *Am. Mineral.* 89, 1625–1630.

Caffrey, J. M., Bano, N., Kalanetra, K., and Hollibaugh, J. T. (2007). Ammonia oxidation and ammonia-oxidizing bacteria and archaea from estuaries with differing histories of hypoxia. *ISME J.* 1, 660–662.

Canfield, D. E., Thamdrup, B., and Kristensen, E. (2005). *Aquatic Geomicrobiology*. San Diego, CA: Elsevier Academic Press.

Crossey, L. J., Karlstrom, K. E., Springer, A. E., Newell, D., Hilton, D. R., and Fischer, T. (2009). Degassing of mantle-derived CO_2 and He from springs in the southern Colorado Plateau region – Neotectonic connections and implications for groundwater systems. *Geol. Soc. Am. Bull.* 121, 1034–1053.

Daims, H., Maixner, F., Lücker, S., Stoecker, K., Hace, K., and Wagner, M. (2006). Ecophysiology and niche differentiation of Nitrospira-like bacteria, the key nitrite oxidizers in wastewater treatment plants. *Water Sci. Technol.* 54, 21–27.

Daims, H., Nielsen, J. L., Nielsen, P. H., Schleifer, K.-H., and Wagner, M. (2001). In situ characterization of nitrospira-like nitrite-oxidizing bacteria active in wastewater treatment plants. *Appl. Environ. Microbiol.* 67, 5273–5284.

Dekas, A. E., Poretsky, R. S., and Orphan, V. J. (2009). Deep-sea archaea fix and share nitrogen in methane-consuming microbial consortia. *Science* 326, 422–426.

Desantis, T. Z. Jr., Hugenholtz, P., Keller, K., Brodie, E. L., Larsen, N., Piceno, Y. M., Phan, R., and Andersen, G. L. (2006). NAST: a multiple sequence alignment server for comparative analysis of 16S rRNA genes. *Nucleic Acids Res.* 34, W394–W399.

Edwards, K. J., Mccollom, T. M., Konishi, H., and Buseck, P. R. (2003). Seafloor bioalteration of sulfide minerals: results from in situ incubation studies. *Geochim. Cosmochim. Acta* 67, 2843–2856.

Ehrich, S., Behrens, D., Lebedeva, E., Ludwig, W., and Bock, E. (1995). A new obligately chemolithoautotrophic, nitrite-oxidizing bacterium, *Nitrospira moscoviensis* sp. nov. and its phylogenetic relationship. *Arch. Microbiol.* 164, 16–23.

Ergruder, T. H., Boon, N., Wittebolle, L., Marzorati, M., and Verstraete, W. (2009). Environmental factors shaping the ecological niches of ammonia-oxidizing archaea. *FEMS Microbiol. Rev.* 33, 855–869.

Farmer, G. L., and Depaolo, D. J. (1984). Origin of mesozoic and tertiary granite in the Western United States and implications for pre-mesozoic crustal structure 2. Nd and Sr isotopic studies of unmineralized and Cu- and Mo-mineralized granite in the precambrian craton. *J. Geophys. Res.* 89, 10141–10160.

Faure, G., and Mensing, T. M. (2005). *Isotopes: Principles and Application*. Hoboken, NJ: John Wiley and Sons, Inc.

Francis, C. A., Beman, J. M., and Kuypers, M. M. M. (2007). New processes and players in the nitrogen cycle: the microbial ecology of anaerobic and archaeal ammonia oxidation. *ISME J.* 1, 19–27.

Francis, C. A., Roberts, K. J., Beman, J. M., Santoro, A. E., and Oakley, B. B. (2005). Ubiquity and diversity of ammonia-oxidizing archaea in water columns and sediments of the ocean. *Proc. Natl. Acad. Sci. U.S.A.* 102, 14683–14688.

Fredrickson, J. K., and Balkwill, D. L. (2006). Geomicrobial processes and biodiversity in the deep terrestrial subsurface. *Geomicrobiol. J.* 23, 345–356.

Fredrickson, J. K., Mckinley, J. P., Bjornstad, B. N., Long, P. E., Ringelberg, D. B., White, D. C., Krumholz, L. R., Suflita, J. M., Colwell, F. S., Lehman, R. M., Phelps, T. J., and Onstott, T. C. (1997). Pore-size constraints on the activity and survival of subsurface bacteria in a late cretaceous shale-sandstone sequence, northwestern New Mexico. *Geomicrobiol. J.* 14, 183–202.

Gihring, T. M., Moser, D. P., Lin, L.-H., Davidson, M., Onstott, T. C., Morgan, L., Milleson, M., Kieft, T. L., Trimarco, E., Balkwill, D. L., and Dollhopf, M. E. (2006). The distribution of microbial taxa in the subsurface water of the Kalahari Shield, South Africa. *Geomicrobiol. J.* 23, 415–430.

Hall, A. (1987). The ammonium content of Caledonian granites. *J. Geol. Soc. London* 144, 671–674.

Hall, A. (1988). Crustal contamination of minette magmas: evidence from their ammonium contents. *Neues Jb. Miner. Monat.* 3, 137–143.

Hall, A. (1999). Ammonium in granites and its petrogenetic significance. *Earth Sci. Rev.* 45, 145–165.

Hall, A., Bencini, A., and Poli, G. (1991). Magmatic and hydrothermal ammonium in granites of the Tuscan magmatic province, Italy. *Geochim. Cosmochim. Acta* 55, 3657–3664.

Hanson, R. S., and Hanson, T. E. (1996). Methanotrophic bacteria. *Microbiol. Rev.* 60, 439–471.

Hatzenpichler, R., Lebedeva, E., Spieck, E., Stoecker, K., Richter, A., Daims, H., and Wagner, M. (2008). A moderately thermophilic ammonia-oxidizing crenarchaeote from a hot spring. *Proc. Natl. Acad. Sci. U.S.A.* 105, 2134–2139.

Hennecke, H., Kaluza, K., Thöny, B., Fuhrmann, M., Ludwig, W., and Stackenbrandt, E. (1985). Concurrent evolution of nitrogenase gens and 16S rRNA in Rhizobium species and other nitrogen fixing bacteria. *Arch. Microbiol.* 142, 342–348.

Hirayama, H., Takai, K., Inagaki, F., Yamato, Y., Suzuki, M., Nealson, K. H., and Horikoshi, K. (2005). Bacterial community shift along a subsurface geothermal water stream in a Japanese gold mine. *Extremophiles* 9, 169–184.

Hirsch, A. M., Mckhann, H. I., Reddy, A., Liao, J., Fang, Y., and Marshall, C. R. (1995). Assessing horizontal transfer of nifHDK genes in eubacteria: nucleotide sequence of nifK from Frankia strain HFPCcI3. *Mol. Biol. Evol.* 12, 16–27.

Holloway, J. M., and Dahlgren, R. A. (2002). Nitrogen in rock: occurrences and biogeochemical implications. *Global Biogeochem. Cycles* 16, 1118.

Honma, H., and Itihara, Y. (1981). Distribution of ammonium in minerals of metamorphic and granitic rocks. *Geochim. Cosmochim. Acta* 45, 983–988.

Hooper, A. B., and Terry, K. R. (1973). Specific inhibitors of ammonia oxidation in Nitrosomonas. *J. Bacteriol.* 115, 480–485.

Jensen, E. B., Doane, C. E., and Pirozzoli, J. F. (1983). Nonelectric explosives detonation at the Henderson mine. *Min. Eng.* 35, 1560–1563.

Jiang, H., Huang, Q., Dong, H., Wang, P., Wang, F., Li, W., and Zhang, C. (2010). RNA-based investigation of ammonia-oxidizing archaea in hot springs of Yunnan Province, China. *Appl. Environ. Microbiol.* 76, 4538–4541.

Jung, C. K., Claes, D. R., Kuchta, M., Wilson, R. J., and Zimmerman, E. D. (2007). *Proposal for DUSEL at Henderson Mine.* Henderson Mine, CO: National Science Foundation.

Khadem, A. F., Pol, A., Jetten, M. S. M., and Op Den Camp, H. J. M. (2010). Nitrogen fixation by the verrucomicrobial methanotroph 'Methylacidiphilum fumariolicum' SolV. *Microbiology* 156, 1052–1059.

Könnecke, M., Bernhard, A. E., De La Torre, J. R., Walker, C. B., Waterbury, J. B., and Stahl, D. A. (2005). Isolation of an autotrophic ammonia-oxidizing marine archaeon. *Nature* 437, 543–546.

Koops, H.-P., and Pommerening-Röser, A. (2001). Distribution and ecophysiology of the nitrifying bacteria emphasizing cultured species. *FEMS Microbiol. Ecol.* 37, 1–9.

Kovacik, Jr. W. P., Takai, K., Mormile, M. R., Mckinley, J. P., Brockman, F. J., Fredrickson, J. K., and Holben, W. E. (2006). Molecular analysis of deep subsurface Cretaceous rock indicates abundant Fe(III)- and S(-reducing bacteria in a sulfate-rich environment. *Environ. Microbiol.* 8, 141–155.

Kuenen, J. G. (2008). Anammox bacteria: from discovery to application. *Nat. Rev. Microbiol.* 6, 320–326.

Lebedeva, E. V., Alawi, M., Maixner, F., Jozsa, P.-G., Daims, H., and Spieck, E. (2008). Physiological and phylogenetic characterization of a novel lithoautotrophic nitrite-oxidizing bacterium, 'Candidatus Nitrospira bockiana.' *Int. J. Syst. Evol. Microbiol.* 58, 242–250.

Lebedeva, E. V., Off, S., Zumbrägel, S., Kruse, M., Shagzhina, A., Lücker, S., Maixner, F., Lipski, A., Daims, H., and Spieck, E. (2011). Isolation and characterization of a moderately thermophilic nitrite-oxidizing bacterium from a geothermal spring. *FEMS Microbiol. Ecol.* 75, 195–204.

Lefticariu, L., Pratt, L. A., Laverne, J. A., and Schimmelmann, A. (2010). Anoxic pyrite oxidation by water radiolysis products – a potential source of biosustaining energy. *Earth Planet. Sci. Lett.* 292, 57–67.

Lin, L.-H., James, H., Onstott, T. C., Gihring, T., Lollar, B. S., Boice, E., Pratt, L., Lippmann-Pipke, J., and Bellamy, R. E. S. (2006a). Planktonic microbial communities associated with fracture-derived groundwater in a deep gold mine of South Africa. *Geomicrobiol. J.* 23, 475–497.

Lin, L.-H., Wang, P.-L., Rumble, D., Lippmann-Pipke, J., Boice, E., Pratt, L. M., Lollar, B. S., Brodie, E. L., Hazen, T. C., Andersen, G. L., Desantis, T. Z., Moser, D. P., Kershaw, D., and Onstott, T. C. (2006b). Long-term sustainability of a high-energy, low-diversity crustal biome. *Science* 314, 479–482.

Lin, L.-H., Slater, G. F., Sherwood Lollar, B., Lacrampe-Couloume, G., and Onstott, T. C. (2005). The yield and isotopic composition of radiolytic H_2, a potential energy source for the deep subsurface biosphere. *Geochim. Cosmochim. Acta* 69, 893–903.

Lovley, D. R., and Chapelle, F. H. (1995). Deep subsurface microbial processes. *Rev. Geophys.* 33, 365–381.

Lücker, S., Wagner, M., Roger, A. J., Flax, J. L., Brusseau, G. A., Stahl, D. A., Maixner, F., Pelletier, E., Koch, H., Vacherie, B., Rattei, T., Sinninghe Damsté, J. S., Spieck, E., Le Paslier, D., and Daims, H. (2010). A Nitrospira metagenome illuminates the physiology and evolution of globally important nitrite-oxidizing bacteria. *Proc. Natl. Acad. Sci. U.S.A.* 107, 13479–13484.

Martens-Habbena, W., Berube, P. M., Urakawa, H., De La Torre, J. R., and Stahl, D. A. (2009). Ammonia oxidation kinetics determine niche separation of nitrifying Archaea and Bacteria. *Nature* 461, 976–979.

Mayhew, L. E., Swanner, E. D., Martin, A. P., and Templeton, A. S. (2008). Phylogenetic relationships and functional genes: distribution of a gene (mnxG) encoding a putative manganese-oxidizing enzyme in *Bacillus* species. *Appl. Environ. Microbiol.* 74, 7265–7271.

Mehta, M. P., Butterfield, D. A., and Baross, J. A. (2003). Phylogenetic diversity of nitrogenase (nifH) genes in deep-sea and hydrothermal vent environments of the Juan de Fuca Ridge. *Appl. Environ. Microbiol.* 69, 960–970.

Mills, C. T., Amano, Y., Slater, G. F., Dias, R. F., Iwatsuki, T., and Mandernack, K. W. (2010). Microbial carbon cycling in oligotrophic regional aquifers near the Tono Uranium Mine, Japan as inferred from (14 C values of in situ phospholipid fatty acids and carbon sources. *Geochim. Cosmochim. Acta* 74, 3785–3805.

Moraghan, J. T., and Buresh, R. J. (1977). Chemical reduction of nitrite and nitrous-oxide by ferrous iron. *Soil Sci. Soc. Am. J.* 41, 47–50.

Moser, D. P., Onstott, T. C., Fredrickson, J. K., Brockman, F. J., Balkwill, D. L., Drake, G. R., Pfiffner, S. M., White, D. C., Takai, K., Pratt, L. M., Fong, J., Lollar, B. S., Slater, G., Phelps, T. J., Spoelstra, N., Deflaun, M., Southam, G., Welty, A. T., Baker, B. J., and Hoek, J. (2003). Temporal shifts in the geochemistry and microbial community structure of an ultradeep mine borehole following isolation. *Geomicrobiol. J.* 20, 517–548.

Normand, P., and Bouquet, J. (1989). Phylogeny of nitrogenase sequences in Frankia and other nitrogen-fixing microorganisms. *J. Mol. Evol.* 29, 436–447.

Norton, J. M., Alzerreca, J. J., Suwa, Y., and Klotz, M. G. (2002). Diversity of ammonia monooxygenase operon in autotrophic ammonia-oxidizing bacteria. *Arch. Microbiol.* 177, 139–149.

Nunoura, T., Hirayama, H., Takami, H., Oida, H., Nishi, S., Shimamura, S., Suzuki, Y., Inagaki, F., Takai, K., Nealson, K. H., and Horikoshi, K. (2005). Genetic and functional properties of uncultivated thermophilic crenarchaeotes from a subsurface gold mine as revealed by analysis of genome fragments. *Environ. Microbiol.* 7, 1967–1984.

Omoregie, E. O., Mastalerz, V., De Lange, G., Straub, K. L., Kappler, A., Roy, H., Stadnitskaia, A., Foucher, J. -P., and Boetius, A. (2008). Biogeochemistry and community composition of iron- and sulfur-precipitating microbial mats at the Chefren Mud Volcano (Nile Deep Sea Fan, Eastern Mediterranean). *Appl. Environ. Microbiol.* 74, 3198–3215.

Onstott, T., Lin, L.-H., Davidson, M., Mislowack, B., Borcsik, M., Hall, J., Slater, G., Ward, J., Lollar, B., Lippmann-Pipke, J., Boice, E., Pratt, L., Pfiffner, S., Moser, D., Gihring, T., Kieft, T., Phelps, T., Vanheerden, E., Litthaur, D., Deflaun, M., Rothmel, R., Wanger, G., and Southam, G. (2006). The origin and age of biogeochemical trends in deep fracture water of the Witwatersrand Basin, South Africa. *Geomicrobiol. J.* 23, 369–414.

Papineau, D. (2006). *The Rise of Atmospheric Oxygen and the Evolution of the Sulfur and Nitrogen Cycles on the Archaean and Proterozoic Earth.* Ph. D., University of Colorado, Boulder, CO.

Papineau, D., Mojzsis, S. J., Karhu, J. A., and Marty, B. (2005). Nitrogen isotopic composition of ammoniated phyllosilicates: case studies from Precambrian metamorphosed sedimentary rocks. *Chem. Geol.* 216, 37–58.

Pedersen, K. (1997). Microbial life in deep granitic rock. *FEMS Microbiol. Rev.* 20, 399–414.

Pedersen, K. (2000). Exploration of deep intraterrestrial microbial life: current perspectives. *FEMS Microbiol. Lett.* 185, 9–16.

Ploug, H., Musat, N., Adam, B., Moraru, C. L., Lavik, G., Vagner, T., Bergman, B., and Kuypers, M. M. M. (2010). Carbon and nitrogen fluxes associated with the cyanobacterium Aphanizomenon sp. in the Baltic Sea. *ISME J.* 4, 1215–1223.

Rastogi, G., Osman, S. M., Kukkadapu, R., Englehard, M., Vaishampayan, P. A., Andersen, G. L., and Sani, R. K. (2010). Microbial and mineralogical characterizations of soils collected from the deep biosphere of the former Homestake Gold Mine, South Dakota. *Microb. Ecol.* 60, 539–550.

Reed, S. C., Townsend, A. R., Cleveland, C. C., and Nemergut, D. R. (2010). Microbial community shifts influence patterns in tropical forest nitrogen fixation. *Oecologia* 164, 521–531.

Rogers, J. R., and Bennett, P. C. (2004). Mineral stimulation of subsurface microorganisms: release of limiting nutrients from silicates. *Chem. Geol.* 203, 91–108.

Rogers, J. R., Bennett, P. C., and Choi, W. J. (1998). Feldspars as a source of nutrients for microorganisms. *Am. Mineral.* 83, 1532–1540.

Rudnick, P., Meletzus, D., Green, A., He, L., and Kennedy, C. (1997). Regulation of nitrogen fixation by ammonium in diazotrophic species of proteobacteria. *Soil Biol. Biochem.* 29, 831–841.

Sahl, J. W., Schmidt, R., Swanner, E. D., Mandernack, K. W., Templeton, A. S., Kieft, T. L., Smith, R. L., Sanford, W. E., Callaghan, R. L., Mitton, J. B., and Spear, J. R. (2008). Subsurface microbial diversity in deep-granitic-fracture water in Colorado. *Appl. Environ. Microbiol.* 74, 143–152.

Samarkin, V. A., Madigan, M. T., Bowles, M. W., Casciotti, K. L., Priscu, J. C., Mckay, C. P., and Joye, S. B. (2010). Abiotic nitrous oxide emission from the hypersaline Don Juan Pond in Antarctica. *Nat. Geosci* 3, 341–344.

Santelli, C. M., Orcutt, B. N., Banning, E., Bach, W., Moyer, C. L., Sogin, M. L., Staudigel, H., and Edwards, K. J. (2008). Abundance and diversity of microbial life in ocean crust. *Nature* 453, 653–656.

Sears, K., Alleman, J. E., Barnard, J. L., and Oleszkiewicz, J. A. (2004). Impacts of reduced sulfur components on active and resting ammonia oxidizers. *J. Ind. Microbiol. Biotechnol.* 31, 369–378.

Seedorff, E., and Einaudi, M. T. (2004). Henderson porphyry molybdenum system, Colorado: II. Decoupling of introduction and deposition of metals during geochemical evolution of hydrothermal fluids. *Econ. Geol.* 99, 39–72.

Shelbolina, E., Xu, H., Konishi, H., Kukkadapu, R., Wu, T., and Roden, E. (2010). Microbial oxidation and mineralogical alteration of biotite. *Geochim. Cosmochim. Acta* 74, A944.

Spang, A., Hatzenpichler, R., Brochier-Armanet, C., Rattei, T., Tischler, P., Spieck, E., Streit, W., Stahl, D., Wagner, W., and Schleper, C. (2010). Distinct gene set in two different lineages of ammonia-oxidizing archaea supports the phylum Thaumarchaeota. *Trends Microbiol.* 18, 331–340.

Spear, J. R., Barton, H. A., Robertson, C. E., Francis, C. A., and Pace, N. R. (2007). Microbial community biofabrics in a geothermal mine adit. *Appl. Environ. Microbiol.* 73, 6172–6180.

Stamatakis, A., Hoover, P., and Rougemont, J. (2008). A rapid bootstrap algorithm for the RAxML web servers. *Syst. Biol.* 57, 758–771.

Starkenburg, S. R., Chain, P. S. G., Sayavedra-Soto, L. A., Hauser, L., Land, M. L., Larimer, F. W., Malfatti, S. A., Klotz, M. G., Bottomley, P. J., Arp, D. J., and Hickey, W. J. (2006). Genome sequence of the chemolithoautotrophic nitrite-oxidizing bacterium *Nitrobacter winogradskyi* Nb-255. *Appl. Environ. Microbiol.* 72, 2050–2063.

Stein, H. J. (1985). *A Lead, Strontium and Sulfur Isotope Study of Laramide-Tertiary Intrusions and Mineralization in the Colorado Mineral Belt with Emphasis on Climax-Type Porphyry Molybdenum Systems Plus a Summary of Other Newly Acquired Isotopic and Rare Earth Element Data.* Ph. D., The University of North Carolina, Chapel Hill, NC.

Stein, H. J., and Hannah, J. L. (1985). Movement and origin of ore fluids in climax-type systems. *Geology* 13, 469–474.

Stevens, T. O., and Mckinley, J. P. (1995). Lithoautotrophic microbial ecosystems in deep basalt aquifers. *Science* 270, 450–455.

Strauss, E. A., and Lambert, G. A. (2000). Regulation of nitrification in aquatic sediments by organic carbon. *Limnol. Oceanogr.* 45, 1854–1859.

Swanner, E. D. (2011). *Microbially-Mediated Geochemical Cycling of Iron and Nitrogen within the Granite-Hosted Subsurface of Henderson Mine CO.* Ph. D., University of Colorado, Boulder, CO.

Takai, K., Moser, D. P., Deflaun, M., Onstott, T. C., and Fredrickson, J. K. (2001). Archaeal diversity in waters from deep South African Gold Mines. *Appl. Environ. Microbiol.* 67, 5750–5760.

Theobald, P. K. (1965). *Preliminary Geologic Map of the Berthoud Pass Quadrangle, Clear Creek and Grand Counties, Colorado*. Washington, DC: US Geological Survey.

Treusch, A. H., Kletzin, A., Raddatz, G., Ochsenreiter, T., Quaiser, A., Meurer, G., Schuster, S. C., and Schleper, C. (2004). Characterization of large-insert DNA libraries from soil for environmental genomic studies of Archaea. *Environ. Microbiol.* 6, 970–980.

Wankel, S. D., Moisier, A. C., Hansel, C. M., Paytan, A., and Francis, C. A. (2011). Spatial variability in nitrification rates and ammonia-oxidizing microbial communities in the agriculturally impacted Elkhorn Slough Estuary, California. *Appl. Environ. Microbiol.* 77, 269–280.

Ward, N. L., Challacombe, J. F., Janssen, P. H., Henrissat, B., Coutinho, P. M., Wu, M., Xie, G., Haft, D. H., Sait, M., Badger, J., Barabote, R. D., Bradley, B., Brettin, T. S., Brinkac, L. M., Bruce, D., Creasy, T., Daugherty, S. C., Davidsen, T. M., Deboy, R. T., Detter, J. C., Dodson, R. J., Durkin, A. S., Ganapathy, A., Gwinn-Giglio, M., Han, C. S., Khouri, H., Kiss, H., Kothari, S. P., Madupu, R., Nelson, K. E., Nelson, W. C., Paulsen, I., Penn, K., Ren, Q., Rosovitz, M. J., Selengut, J. D., Shrivastava, S., Sullivan, S. A., Tapia, R., Thompson, L. S., Watkins, K. L., Yang, Q., Yu, C., Zafar, N., Zhou, L., and Kuske, C. R. (2009). Three genomes from the phylum Acidobacteria provide insight into the lifestyles of these microorganisms in soils. *Appl. Environ. Microbiol.* 75, 2046–2056.

Watson, S. W., Bock, E., Valois, F. W., Waterbury, J. B., and Schlosser, U. (1986). *Nitrospira marina* gen. nov. sp. nov.: a chemolithotrophic nitrite-oxidizing bacterium. *Arch. Microbiol.* 144, 1–7.

Weidler, G. W., Dornmayr-Pfaffenhuemer, M., Gerbl, F. W., Heinen, W., and Stan-Lotter, H. (2007). Communitites of Archaea and Bacteria in a subsurface radioactive thermal spring in the Austrian Central Alps, and evidence of ammonia-oxidizing Crenarchaeota. *Appl. Environ. Microbiol.* 73, 259–270.

Wu, L., Beard, B. L., Roden, E. E., and Johnson, C. M. (2009). Influence of pH and dissolved Si on Fe isotope fractionation during dissimilatory microbial reduction of hematite. *Geochim. Cosmochim. Acta* 73, 5584–5599.

Wu, L., Jacobson, A. D., and Hausner, M. (2008). Characterization of elemental release during microbe-granite interactions at T = 28°C. *Geochim. Cosmochim. Acta* 72, 1076–1095.

Young, J. P. W. (2005). "The phylogeny and evolution of nitrogenases," in *Genomes and Genomics of Nitrogen-fixing organisms*, eds R. Palacios and W. E. Newton (Dordrecht: Springer), 221–241.

Zhang, C. L., Ye, Q., Huang, Z., Li, W., Chen, J., Song, Z., Zhao, W., Bagwell, C., Inskeep, W. P., Ross, C., Gao, L., Wiegel, J., Romanek, C. S., Shock, E. L., and Hedlund, B. P. (2008). Global occurrence of archaeal amoA genes in terrestrial hot springs. *Appl. Environ. Microbiol.* 74, 6417–6426.

Zhao, W., Song, Z., Jiang, H., Li, W., Mou, X., Romanek, C. S., Wiegel, J., Dong, H., and Zhang, C. L. (2011). Ammonia-oxidizing Archaea in Kamchatka Hot Springs. *Geomicrobiol. J.* 28, 149–159.

Conflict of Interest Statement: The authors declare that the research was conducted in the absence of any commercial or financial relationships that could be construed as a potential conflict of interest.

Received: 29 August 2011; accepted: 01 December 2011; published online: 20 December 2011.

Citation: Swanner ED and Templeton AS (2011) Potential for nitrogen fixation and nitrification in the granite-hosted subsurface at Henderson Mine, CO. Front. Microbio. ***2****:254. doi: 10.3389/fmicb.2011.00254*

This article was submitted to Frontiers in Extreme Microbiology, a specialty of Frontiers in Microbiology.

frontiers in
MICROBIOLOGY

METHODS ARTICLE
published: 23 January 2012
doi: 10.3389/fmicb.2012.00017

Novel degenerate PCR method for whole-genome amplification applied to Peru Margin (ODP Leg 201) subsurface samples

Amanda J. Martino[1], Matthew E. Rhodes[1], Jennifer F. Biddle[2], Leah D. Brandt[1], Lynn P. Tomsho[3] and Christopher H. House[1]*

[1] Department of Geosciences, Penn State Astrobiology Research Center, Pennsylvania State University, University Park, PA, USA
[2] School of Marine Science and Policy, College of Earth Ocean and Environment, University of Delaware, Lewes, DE, USA
[3] Department of Biochemistry and Molecular Biology, Pennsylvania State University, University Park, PA, USA

Edited by:
Andreas Teske, University of North Carolina at Chapel Hill, USA

Reviewed by:
Julie A. Huber, Marine Biological Laboratory, USA
John R. Spear, Colorado School of Mines, USA

***Correspondence:**
Christopher H. House, Department of Geosciences, Penn State Astrobiology Research Center, Pennsylvania State University, 220 Deike Building, University Park, PA 16802, USA.
e-mail: chrishouse@psu.edu

A degenerate polymerase chain reaction (PCR)-based method of whole-genome amplification, designed to work fluidly with 454 sequencing technology, was developed and tested for use on deep marine subsurface DNA samples. While optimized here for use with Roche 454 technology, the general framework presented may be applicable to other next generation sequencing systems as well (e.g., Illumina, Ion Torrent). The method, which we have called random amplification metagenomic PCR (RAMP), involves the use of specific primers from Roche 454 amplicon sequencing, modified by the addition of a degenerate region at the 3′ end. It utilizes a PCR reaction, which resulted in no amplification from blanks, even after 50 cycles of PCR. After efforts to optimize experimental conditions, the method was tested with DNA extracted from cultured *E. coli* cells, and genome coverage was estimated after sequencing on three different occasions. Coverage did not vary greatly with the different experimental conditions tested, and was around 62% with a sequencing effort equivalent to a theoretical genome coverage of 14.10×. The GC content of the sequenced amplification product was within 2% of the predicted values for this strain of *E. coli*. The method was also applied to DNA extracted from marine subsurface samples from ODP Leg 201 site 1229 (Peru Margin), and results of a taxonomic analysis revealed microbial communities dominated by Proteobacteria, Chloroflexi, Firmicutes, Euryarchaeota, and Crenarchaeota, among others. These results were similar to those obtained previously for those samples; however, variations in the proportions of taxa identified illustrates well the generally accepted view that community analysis is sensitive to both the amplification technique used and the method of assigning sequences to taxonomic groups. Overall, we find that RAMP represents a valid methodology for amplifying metagenomes from low-biomass samples.

Keywords: whole-genome amplification, metagenomics, deep biosphere, low biomass, bacteria, archaea, next-gen sequencing

INTRODUCTION

The deep subseafloor biosphere represents a frontier for the discovery of new microbial life, and for investigations of the extent, versatility, and perseverance of life on earth. However, there are many challenges in studying this community of microorganisms, and the past 20 years of study have only begun to produce an understanding of this vast and complex ecosystem. Marine subsurface microorganisms are isolated from the direct energy of sunlight, receive limited nutrients, and sometimes experience extreme pressures and challenging temperatures. Investigations to date suggest that many of these microbes appear to be only distantly related to those we know from the study of surface environments (Sørensen et al., 2004; Inagaki et al., 2006; Lipp et al., 2008). Cultivation studies have produced some useful results (Bale et al., 1997; Mikucki et al., 2003; Toffin et al., 2004), but the majority of microbes in this environment (as well as most microbes on Earth) still evade cultivation efforts. Cultivation-independent methods such as polymerase chain reaction (PCR) amplification and subsequent sequencing directly from environmental DNA hold great promise, and have provided the majority of the information obtained to date (Jørgensen and Boetius, 2007; Orcutt et al., 2011); however, there are still many challenges to overcome in utilizing these methods to their full potential.

Among the available cultivation-independent methods, automated metagenomic sequencing via platforms such as Roche 454, is one of the most promising tools for probing the depths of diversity and exploring metabolic capabilities of subsurface microbes. However, even with recent advances in technology, this type of high-throughput sequencing requires, ideally, at least 500 ng of sample DNA (as per Roche 454 protocol). The relatively low concentrations of cells in the marine subsurface coupled with the difficulties of extracting DNA from marine sediment (Webster et al., 2003) results in quantities of extracted DNA which are often too low for direct, unamplified, metagenomic sequencing.

Over the past couple of decades, researchers have been experimenting with different methods of amplifying genomic DNA. Some of the resulting whole-genome amplification (WGA) methods are modifications to the standard PCR, which reduce its specificity, allowing for a general amplification of DNA. These methods include interspersed repetitive sequence PCR (IRS-PCR; Nelson et al., 1989), primer-extension-preamplification PCR (PEP-PCR; Zhang et al., 1992), improved primer-extension-preamplification PCR (I-PEP-PCR; Dietmaier et al., 1999), degenerate oligonucleotide-primed PCR (DOP-PCR; Telenius et al., 1992), and long products from low DNA quantities DOP-PCR (LL-DOP-PCR; Kittler et al., 2002). In addition to the PCR-based methods, a non-PCR method called multiple displacement amplification (MDA) was developed in attempt to overcome problems with the PCR methods, which included incomplete coverage, amplification artifacts, and DNA too short for some applications (Dean et al., 2002). MDA is an isothermal, strand-displacing reaction employing the phi29 DNA polymerase and random hexamer primers. Several commercial versions of MDA now exist, including the REPLI-g Whole-Genome Amplification Kit (Qiagen) and the GenomiPhi DNA Amplification Kit (GE Healthcare). Two commercial MDA kits, along with PEP-PCR and DOP-PCR, were analyzed for genome coverage bias in a 454 metagenomic sequencing study and all were found to induce significant bias (Pinard et al., 2006). For both microbial genomes utilized in that study, the MDA reactions resulted in the least bias, followed by PEP-PCR, and lastly, DOP-PCR. These results were consistent with those obtained through a *TaqMan* quantitative PCR analysis of eight genes after amplification of human genomic DNA using MDA, DOP-PCR, and PEP-PCR (Dean et al., 2002).

As a result, MDA-based techniques are most often the method of choice in applications where bias and coverage are significant concerns. For metagenomic sequencing of subseafloor environmental DNA samples, however, the use of MDA as an amplification technique is often problematic. In particular, the tendency of MDA to synthesize a DNA product even in the absence of added cells, means that a reliable negative control for the amplification reaction is very difficult to achieve (Raghunathan et al., 2005). These products that form in the negative controls can be as large as 15 kb and greater (Biddle, 2006). While they have not been sequenced, failure of attempts to PCR amplify specific genes from the products suggests that they are more likely primer-dimer type formations rather than microbial contamination (Biddle, 2006). This may be a consequence of the competitive nature of the reaction, whereby in the absence of anything else of which to anneal, the random hexamers anneal to each other. If this were the case, the problem would be of greatest significance when sample DNA template is very low, and unable to compete with the hexamers for annealing and amplification. It has been shown that the DNA product formed in negative controls can be avoided if the reaction is monitored closely with a qPCR protocol and stopped before amplification in the negative control begins (Biddle et al., 2011). However, in many cases, this occurs after less than 2 h reaction time, and stopping the reaction at this length of time may hinder the amplification of sample DNA as well, particularly when the sample had very small amounts of DNA to begin with (Biddle et al., 2011), as is the case with most deep subseafloor samples.

Due to the difficulties with using available WGA methods for amplifying subseafloor DNA samples, we undertook efforts to develop an alternative method of WGA that may be of use when sequencing low-biomass environmental samples. We hypothesized that the production of DNA in reaction negatives of MDA was a result of the high level of degeneracy of the primers. We recognized, however, that this high level of degeneracy was critical in obtaining amplified DNA with the least amount of bias, which appears to be the reason that the PEP-PCR and MDA methods produce less bias than the PCR methods with more specific primers. Consequently, our strategy was to design a PCR method with primers that would be more degenerate than IRS-PCR and DOP-PCR – and thus applicable to environmental DNA samples, but less degenerate than PEP-PCR and MDA. In addition, with the rapidly increasing use of next generation metagenomic sequencing technology, we aimed to have our new method aid in streamlining the process of preparing samples for metagenomic sequencing using these new technologies. The result was a PCR-based method of WGA utilizing 454 amplicon primers with an attached degenerate region at the 3′ end. We refer to this method as random amplification metagenomic PCR (RAMP). While optimized here for use with Roche 454 sequencing, the developed method may be viewed as a general framework for using PCR for WGA of low-biomass environmental DNA samples in preparation for metagenomic sequencing using next generation sequencing technologies.

MATERIALS AND METHODS

DNA EXTRACTION

E. coli DNA was extracted from a culture of *E. coli* Mach1™-T1R cells from a TOPO TA Cloning® Kit (Invitrogen, Inc.). The parental strain of Mach1™-T1R *E. coli* is the non-K-12, wild-type W strain (ATCC #9637, S. A. Waksman), and the cells contain slight modifications to the genome necessary for the cloning process. The cells were grown overnight in Luria–Bertani (LB) broth at 37°C. Cells for DNA extraction were pelleted using a centrifuge from 5 mL of the liquid culture. Cell pellets were added to bead tubes of a Mo Bio UltraClean DNA Isolation kit (MO BIO Laboratories). The kit protocol was followed except for the substitution of 30 s of vortexing in place of bead beating.

The environmental DNA samples used in this study were aliquots remaining from a previous study (Biddle et al., 2008), frozen at −80°C after the original extraction. The method of DNA extraction is described therein and summarized as follows: Frozen sediment cores from ODP Leg 201 Site 1229 were processed by removal of the top ∼1 cm of potentially contaminated sediment. Aliquots of the remaining sediment were homogenized and DNA was extracted using the Mo Bio UltraClean Microbial DNA kit (MO BIO Laboratories) with some modifications, including the addition of a 65°C water bath incubation step and a decrease in the recommended amount of bead beating time to 1 min (Biddle et al., 2008).

PRIMER DESIGN

The non-degenerate 5′ ends of the RAMP primers were chosen from the primers utilized in Roche 454 sequencing technology. These included a set of primers used for amplicon sequencing,

and a set of adaptors used for metagenomic sequencing. Both the amplicon primers and metagenomic adaptors were updated with the switch to "Titanium" sequencing reagents, providing a total of four sets of available primers to be tested. These sequencing primers were then altered by the addition of degenerate bases to the 3′ ends, with the goal of maximizing degeneracy while limiting the possibility of primer-dimers and DNA hairpins. A total of 12 unique primers were tested on culture DNA as well as environmental DNA for use in the RAMP protocol (**Table 1**). Success of the primers was evaluated by visualization of the amplified products after electrophoretic separation on 1% agarose gels. All primers were ordered from Integrated DNA Technologies, Inc. "B" primers included a 5′ biotin tag (for sequencing preparations) and HPLC purification, while "A" primers were ordered with standard desalting purification.

PCR OPTIMIZATION

The following PCR conditions were chosen for RAMP reactions of samples sequenced in this study: Reagents (Per 25 μL reaction): 1.6 μM each FLXampA + 5N and FLXampB + 5N primers (**Table 1**), 1.25 units SpeedSTAR™HS DNA Polymerase (Takara Bio, Inc.) with 2.5 μL accompanying FB1 buffer containing 30 mM $MgCl_2$, and 2.0 μL accompanying dNTP mixture containing 2.5 mM each dNTP. Cycling conditions: 5 min at 94°C, followed by 25 cycles of 10 s at 94°C, 15 s at 47 (or 25)°C, 20 s at 72°C, followed by a final extension of 10 min at 72°C. The amount of DNA template used per reaction varied by sample, but the sensitivity of the RAMP reaction to concentration of DNA template was tested using a dilution series of *E. coli* DNA ranging from about 10 ng/μL down to about 0.0625 ng/μL. Multiple ranges of other PCR parameters were tested as well during protocol optimization. For primers, concentrations tested included 1–7 μM in increments of 1, plus lower concentrations of 0.0016–1.6 μM by powers of 10, and higher concentrations of 8 and 36.5 μM (data not shown). Annealing temperature tested ranged from 25 to 70°C, and number of cycles ranged from 25 to 60. Another DNA Taq polymerase was tested, TaKaRa Ex Taq™(Takara Bio, Inc.), as well as a Pfu DNA polymerase, Stratagene PfuUltra™High-Fidelity DNA Polymerase (Agilent Technologies, Inc.), with PCR reagents and conditions as recommended by those manufacturers. Optimal values for each parameter were assessed, prior to sequencing, by visualization of product after electrophoretic separation on 1% agarose gels. All amplifications were performed in either an MJ Research PTC-100 Thermal Cycler or an Eppendorf Mastercycler Gradient Thermal Cycler. Only products amplified with SpeedSTAR polymerase were used for sequencing.

Table 1 | All primer designs tested during method development.

Name	Sequence (5′ → 3′)	Amplification
FLXampA + 4ND	GCCTCCCTCGCGCCATCAGNNNND	Yes
FLXampA + 5N	GCCTCCCTCGCGCCATCAGNNNNN	Yes
FLXampB + 5N	GCCTTGCCAGCCCGCTCAGNNNNN	Yes
FLXadpA + B4NTY	CCATCTCATCCCTGCGTGTCCCATC TGTTCCCTCCCTGTCTCAGBNNNNTY	No
FLXadpB + B4NTY	CCTATCCCCTGTGTGCCTTGCCTAT CCCCTGTTGCGTGTCTCAGBNNNNTY	No
FLXampA + 6N	GCCTCCCTCGCGCCATCAGNNNNNN	No
TIadpA + 5N	CCATCTCATCCCTGCGTGTCTC CGACTCAGNNNNN	No
TIadpB + 5N	CCTATCCCCTGTGTGCCTTGGC AGTCTCAGNNNNN	No
TIadpA + 5N (cut)	CTGCGTGTCTCCGACTCAGNNNNN	No
TIadpB + 5N (cut)	TGTGCCTTGGCAGTCTCAGNNNNN	No
TIampA + 5N	CGTATCGCCTCCCTCGCGCCAT CAGNNNNN	Yes
TIampB + 5N	CTATGCGCCTTGCCAGCCCGCT CAGNNNNN	Yes

In primer names, "FLX" refers to the use of sequence from 454 FLX reagents, while "TI" refers to use of sequence from the 454 Titanium reagents. Further, "amp" denotes amplicon sequencing primers, while "adp" denotes metagenome adaptors, and "A" and "B" are the two primers or adaptors utilized as a set during 454 sequencing. Primers were tested in pairs except in two cases (FLXampA + 4ND and FLXampA + 6N), where only the forward primer was tested. In primer sequences, N = ACGT, D = AGT, B = CGT, and Y = CT.

454 SEQUENCING

Amplified DNA products were purified via a gel extraction, to remove excess primer and to select for a size range of DNA fragments that worked well with the current 454 sequencing technology. Products were subject to electrophoretic separation on a 1% agarose gel, along with DNA markers to estimate the size of the fragments. The portion of the gel containing amplified products ranging in size from about 650 to 850 base pairs (bp) long for *E. coli* and environmental DNA samples sequenced with "Titanium" reagents (or 250–500 bp long for *E. coli* samples sequenced with FLX reagents) was excised, and the DNA was purified using a QIAEX II Gel Extraction Kit (Qiagen). After gel purification, DNA was quantified using PicoGreen, on a handheld fluorometer (Turner Biosystems, TBS-380). Because the RAMP primers incorporated the 454 sequencing primers, the library preparation step usually needed to ligate the sequencing primers to the DNA fragments was unnecessary. Isolation of only those DNA fragments with both "A" and "B" primers was accomplished using a biotin–streptavidin selection protocol, employing the biotin label incorporated onto the RAMP "B" primers. Sequencing was carried out by the Schuster Lab at the Pennsylvania State University on a Roche 454 Genome Sequencer FLX sequencing system (454 Life Sciences) as described (Poinar et al., 2006). For *E. coli* coverage tests, ¼ of a picotiter plate was sequenced on each of three separate occasions using FLX chemistry for tests 1 and 2, and the newer Titanium chemistry for test 3 due to upgrades in 454 technology. For sequencing of RAMP-amplified environmental samples, ¼ of a picotiter plate was sequenced for each sample using the Titanium chemistry. The two new RAMP-amplified environmental metagenomes were uploaded to MG-RAST (metagenomics.anl.gov) as job numbers 37975 and 37977.

PROCESSING OF SEQUENCE DATA

Raw metagenomic sequence datasets from three samples sequenced in 2008 (Biddle et al., 2008) were downloaded from the

National Center for Biotechnology Information (NCBI) GenBank archive (SRA001015) and converted into FASTA format using the online resource, Galaxy (Giardine et al., 2005; Blankenberg et al., 2010; Goecks et al., 2010). These three metagenomes, along with all metagenomes generated in the present study, were screened to remove replicate sequences and sequences containing ambiguous bases.

Random amplification metagenomic PCR-amplified metagenomes from *E. coli* genomic DNA were compared to the reference *E. coli W* genome (downloaded from the NCBI genome database) in order to estimate genome coverage. Comparisons were carried out via a BLASTN search with an *e*-value of 10^{-15}. Genomic locations of the respective top BLAST results were recorded, and the total number of matched base pairs was tabulated using a 98% identity cut-off value. This approach may have overlooked some highly repetitive regions and thus should serve as a slight underestimate. Genome coverage for test 3 of *E. coli* sequencing (carried out with newer sequencing technology) was estimated both for the whole dataset and for a random sub-sampling of the dataset, equivalent in size to those available from *E. coli* tests 1 and 2. The GC content of the metagenomic datasets was assessed via simple mathematical calculations performed with a home written Python script.

Environmental metagenomes from the 2008 study as well as the present study were further processed to include only those sequence reads greater than 150 bp in length. The environmental metagenomes were compared to the NCBI database of non-redundant (nr) protein sequences (downloaded August 2010) via BLASTX with an *e*-value of 10^{-2}, to the Silva database of 16S rRNA nucleotide sequences (downloaded July 2010) via BLASTN with an *e*-value of 10^{-9}, and to a compiled database containing all available sequences of the RNA polymerase beta-subunit encoding gene (rpoB; downloaded September 2011, DOE Joint Genome Institute) via BLASTX with an *e*-value of 10^{-2}. For matches to the nr and rpoB databases detected by BLASTX, the software program MEGAN v.4.60.2 (Huson et al., 2007) was used to assign the sequences to phylogenetic groups, using the following parameter settings: minscore: 35.0, toppercent: 10.0, minsupport: 5, and winscore: 0.0. In short, MEGAN assigns BLAST-hit sequences to phylogenetic groups using bit-score to retain only significant hits, based on the parameters chosen. 16S matches detected by BLASTN were assigned to phylogenetic groups based on the most similar sequence found via the BLAST algorithm.

RESULTS

METHOD ASSESSMENT

Of the 12 primers tested in the development of the RAMP protocol (some as pairs and some singly), two sets and one single primer resulted in some amplification of DNA (**Table 1**). Only one set, however, amplified environmental DNA consistently and robustly. That set was the FLXampA + 5N/FLXampB + 5N combination. These primers worked best at concentrations from 1 to 3 μM, although amplification of template DNA was observed for all concentrations up to 7 μM (**Figure 1A**). Lower and higher concentrations of primers did not result in amplification of DNA template (data not shown). Further, amplification of DNA was observed over a wide range of annealing temperatures (25–70°C). The most concentrated amplified product occurred in the reaction

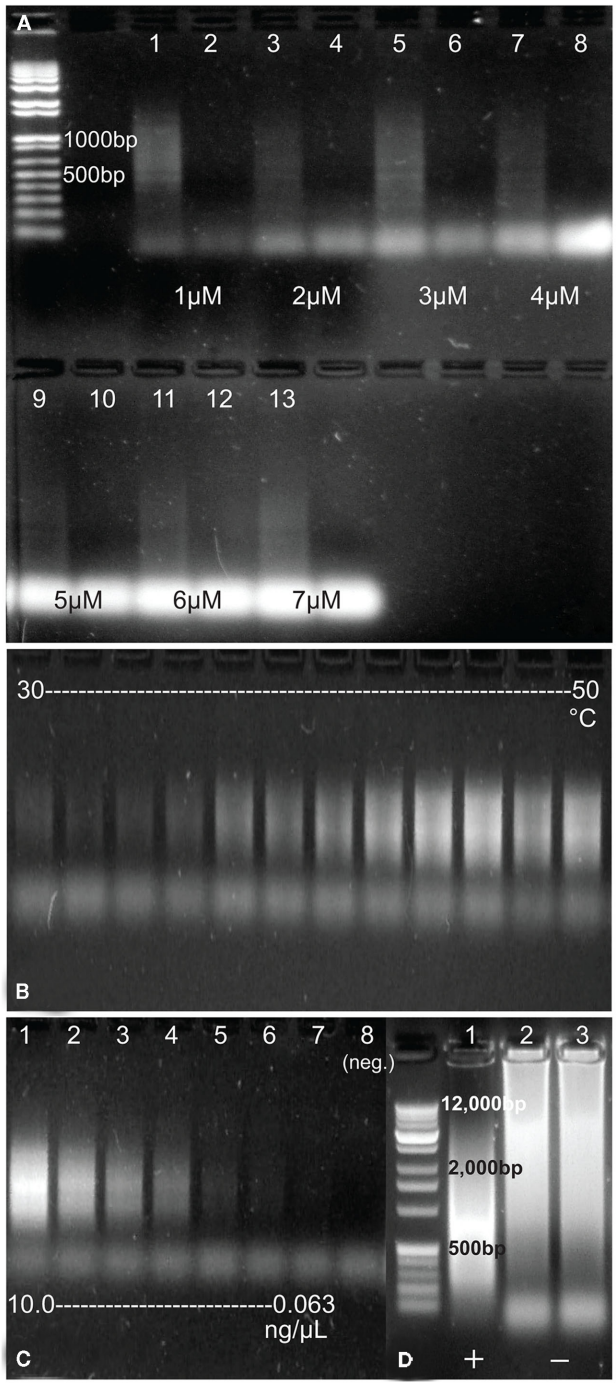

FIGURE 1 | (A) Products of RAMP-amplified *E. coli* DNA using a range of primer concentrations from 1 to 7 μM and their corresponding negative controls (no DNA added). Sizes of two of the DNA marker bands (far left) are included on the image. **(B)** Products of RAMP-amplified *E. coli* DNA using a range of annealing temperatures, from 30 to 50°C. **(C)** Products of RAMP-amplified *E. coli* DNA of a series of concentrations [∼10, 2, 1, 0.5, 0.25, 0.125, 0.0625, and 0 (negative control) ng/μL]. **(D)** Products of amplification of environmental DNA (lane 1) and two negative controls (lanes 2 and 3) after 60 cycles of RAMP. Sizes of a few DNA marker bands (far left) are included on the image.

at 47˚C, and concentrations appeared to decline at both lower and higher annealing temperatures (**Figure 1B**). Amplification was more consistent when using the SpeedSTAR DNA polymerase than when using the Ex Taq DNA polymerase, and the Pfu DNA polymerase failed to produce amplification at all. Using a primer concentration of 1.6 μM, an annealing temperature of 47˚C, and SpeedSTAR DNA polymerase, the sensitivity of the method to initial concentration of DNA in a sample was tested using a dilution series of *E. coli* DNA ranging from 10 to 0.0625 ng/μL. Amplification, as viewed on an agarose gel, was seen for all but the lowest concentration and the negative control (**Figure 1C**). Therefore, the threshold starting DNA concentration for visible amplification by RAMP under these reaction conditions is somewhere between 0.125 and 0.0625 ng/μL. However, when testing the method on environmental DNA, it was observed that increasing the number of PCR cycles and/or increasing the volume of sample added to the reaction resulted in greater amplification in some samples, which suggests that the method's sensitivity could be improved in some cases. Experimentation revealed that the number of PCR cycles for RAMP could be increased to as much as 50, but increasing to 60 cycles resulted in high molecular weight amplification products in the negative controls (**Figure 1D**). Attempts to use qPCR to better quantify a minimum threshold of DNA needed for RAMP amplification and to monitor possible formation of products in negative controls were unsuccessful. Further experimentation with the qPCR reaction suggested that the PicoGreen added to the qPCR reaction for quantification of the product may have been interfering in some way with the RAMP reaction. As an alternative means of quantification of amplified samples and negatives, future applications of RAMP could be coupled with other highly precise DNA quantification methods such as the use of a bioanalyzer or fluorometer.

The method was further tested by sequencing amplified DNA products extracted from *E. coli,* chosen because its complete sequenced genome was available for reference in estimating coverage bias. The first sequencing test was carried out on *E. coli* DNA amplified with the chosen primer set, with an annealing temperature of 47˚C, and 25 cycles of RAMP. Based on the amount of sequence data received, a theoretical genome coverage of 3.64× was calculated, while the actual genome coverage for this sequencing test was estimated at 0.30×, or 30% of the genome (**Table 2**). The GC content of the sequenced metagenome was calculated as 50.9%. For the second sequencing test, all PCR conditions remained the same; however, 15 separate amplification reactions were carried out on the same DNA sample and pooled together prior to sequencing. The results were nearly the same as those from the first test – perhaps slightly poorer, with a theoretical coverage of 3.86× and again, actual coverage of 30%. GC content was 52.15% for this metagenome. For test three, only one reaction was carried out, but the annealing temperature during PCR cycling was lowered from 47 to 25˚C. Because this third test was sequenced with newer technology, the amount of data was far greater than the first two, but after accounting for that difference by randomly analyzing only a portion of the metagenome equivalent in size to the first two tests, the results showed a slight increase in genome coverage with sequencing effort, with 37% actual coverage resulting from a 3.51× sequencing effort.

Table 2 | Results of sequencing tests of RAMP-amplified *E. coli* DNA.

	Test 1	Test 2	Test 3
Annealing temperature (˚C)	47	47	25
No. of pooled reactions	1	15	1
No. of reads	69,965	80,009	197,496 (40,000)
Theoretical genome coverage	3.64×	3.86×	14.10× (3.51×)
Actual genome coverage	0.30×	0.30×	0.62× (0.37×)
GC content (compare to 50%)	50.90%	52.15%	51.76%

For test 3, numbers shown in parentheses are values pertaining to only a randomly sub-sampled portion of the larger dataset, included to make comparison even with the previous two tests, sequenced with earlier 454 technology. In addition to having more reads, test 3 had reads that were substantially longer than those in Tests 1 and 2, so fewer reads were needed for the same theoretical coverage.

When analyzing the entire third metagenome, theoretical genome coverage was 14.10×, and actual genome coverage was about 62%. Given this significant increase, an estimate of genome coverage in relation to sequencing effort was performed, by analyzing sequentially larger and larger portions of this third metagenome (**Figure 2**). Using a logarithmic fit relationship as an estimate [$y = 16.33\mathrm{Ln}(x) - 9.4203$], complete coverage would be achieved with 813 million base pairs of sequence data, or about two whole plates of 454 sequencing with current Titanium chemistry.

In all sequencing tests, the initial concentration of *E. coli* DNA prior to amplification with RAMP was ∼10 ng/μL. The concentration of DNA after amplification was not measured until after gel purification, which consumes a large portion of sample DNA, so absolute values are not available for the amount of DNA produced by the various RAMP conditions. However, by examining the values obtained for concentration after gel purification, we can still make relative comparisons. The concentrations for *E. coli* tests 1, 2, and 3 after gel purification were 8.2 ng/μL, 5.5 ng/μL, and 51 pg/μL, respectively. The concentrations of the 1- and 32-m below seafloor (mbsf) environmental samples after gel purification were 54 and 12.5 pg/μL, respectively. From this data, we see that DNA concentrations are orders of magnitude higher after RAMP at 47˚C annealing (*E. coli* tests 1 and 2) than after RAMP at 25˚C annealing (*E. coli* test 3 and both environmental samples).

ENVIRONMENTAL APPLICATION

The RAMP method utilized for "test 3" of sequencing in method development was also applied to two environmental DNA samples extracted from marine subsurface sediment. The marine sediment was from two depths – 1 and 32 mbsf – of a Peru Margin subsurface location (ODP Leg 201 site 1229). Aliquots of the DNA extracted from these two samples for an earlier study (Biddle et al., 2008) were available for re-analysis using the new method. In this way, RAMP could be compared to the WGA method used in the earlier study without concerns of DNA extraction bias influencing results. In the Biddle et al. study, the 1-mbsf sample was sequenced with no prior WGA, as well as with WGA via the REPLI-g kit (Qiagen) using the available 454 GS 20 technology. The 32-mbsf sample was sequenced only after WGA using REPLI-g as concentration of DNA was too low for unamplified sequencing. In the

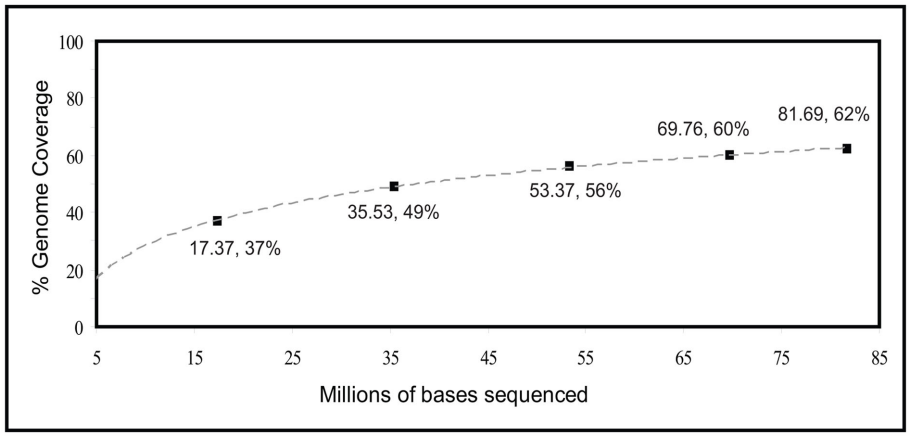

FIGURE 2 | Estimated percentage of genome coverage in relation to sequencing effort of RAMP-amplified *E. coli* genomic DNA.

present study, both the 1- and 32-mbsf samples were sequenced after amplification with RAMP.

In all, five metagenomes were analyzed, three old and two new: 1 mbsf, unamplified; 1 mbsf amplified with REPLI-g; 32 mbsf amplified with REPLI-g; 1 mbsf amplified with RAMP; and 32 mbsf amplified with RAMP. After comparing all five metagenomes to the nr, 16S rRNA, and rpoB databases, RAMP metagenomes were found to have higher percentages of sequences with identifiable homologs in all cases (**Table 1**). Further, within each amplification method, matches to the databases decreased with increasing depth of the sample.

Matches to the nr, 16S rRNA, and rpoB databases were used to analyze community composition of the sample metagenomes and to compare the results obtained via the different amplification methods (**Figure 3**). Examining first the results from phylogeny assigned via the nr dataset, the different amplification methods appear to give very similar results to each other as well as to the unamplified control, with a few notable differences. Most apparent is the over-representation of the Chloroflexi sequences in the RAMP 1 mbsf metagenome (17.9% higher for RAMP than unamplified). In the REPLI-g 1 mbsf metagenome, the Euryarchaeota appear to be over-represented, although to a lesser degree (6.4% higher for REPLI-g than unamplified). Though there is no unamplified control for the 32-mbsf sample, comparison of the REPLI-g and RAMP samples to each other, appears to confirm these two patterns of over-representation, with the RAMP 32 mbsf metagenome displaying a higher percentage of Chloroflexi sequences by 17.2%, and the REPLI-g metagenome having more Euryarchaeota sequences by 10.1%. An additional trend is the under-representation of the Bacteroidetes/Chlorobi group in the RAMP samples, as compared with the unamplified and REPLI-g metagenomes, at both depths.

In comparing the community composition of the 1-mbsf sample to the 32-mbsf sample using the nr results, both REPLI-g and RAMP samples reveal the same trends of increasing or decreasing of certain taxa with depth, with only the degree of these changes differing slightly between the methods. According to both REPLI-g and RAMP datasets, the Chloroflexi, Crenarchaeota, and Euryarchaeota all show a notable increase with depth (6.9 and 5.7% higher at depth, respectively), while the Proteobacteria show a notable decrease with depth (15.3 and 13.5% lower at depth, respectively). Most other taxa also decrease with depth, perhaps only as a result of the increased dominance of the Chloroflexi and archaeal sequences. The exceptions are the Firmicutes, which increase slightly in the REPLI-g dataset only, and the minor taxa Thermotogae, which increases slightly in both datasets. These conclusions are consistent with those in the Biddle et al. (2008) study.

As another perspective of community composition, the metagenomes were also compared against the Silva 16S rRNA database. Using classification of organisms based on the most significant hit in these BLAST results, the community composition between metagenomes is not as consistent for either sample as it was when viewed via the nr results. In the 1-mbsf sample, the REPLI-g metagenome has several stark differences from the unamplified metagenome, including the complete absence of the Crenarchaeota and Proteobacteria, which make up 16.7 and 24.1% of the unamplified metagenome, respectively. Instead the REPLI-g sample is almost entirely dominated by Chloroflexi, at 71.4% of the 16S hits compared with 22.2% in the unamplified metagenome. The REPLI-g metagenome, however, had only 21 16S hits, compared with 54 in the unamplified metagenome, so the absence of some groups may be a result of under-sampling.

In contrast to the REPLI-g metagenome for the 1-mbsf sample, the RAMP metagenome for this sample had sequences from all of the major taxonomic groups represented in the unamplified metagenome, differing only in their relative proportions. In this case, the most apparent differences are the over-representation of the Firmicutes (8.6% higher) and the under-representation of the Euryarchaeota (9.5% lower) in the RAMP 1 mbsf metagenome as compared with the unamplified.

For the 32-mbsf sample, the RAMP metagenome shows a much larger proportion of Proteobacteria and Firmicutes than the REPLI-g sample (28.7 and 21.1% higher), which is consistent with the comparisons in the 1-mbsf sample. However, there is a discrepancy between the 1- and 32-mbsf samples concerning the

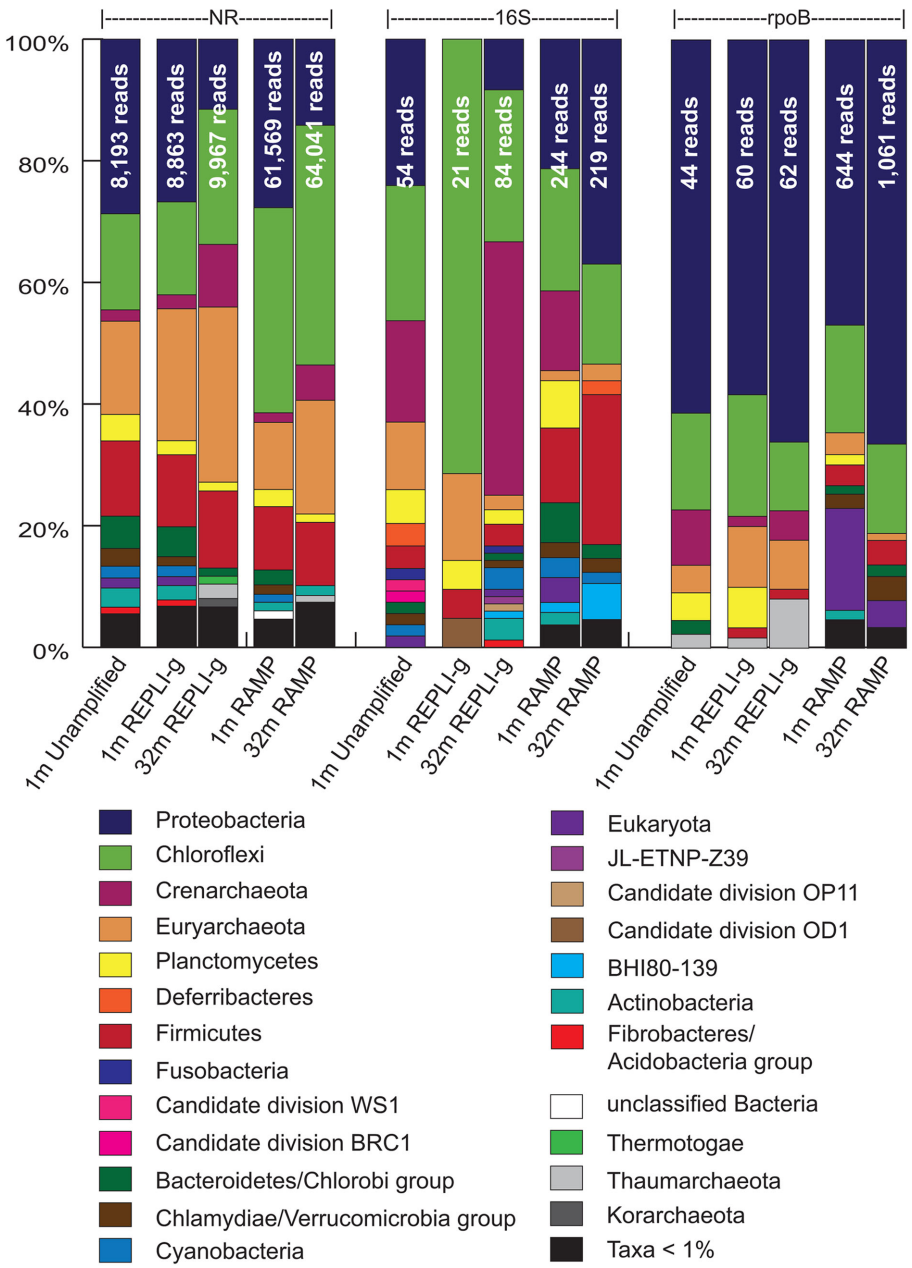

FIGURE 3 | Phylogenetic identities of sequences in all five metagenomes as revealed through comparison to the nr, 16S, and rpoB databases. Shown are the percentages of total identifiable hits. Total number of identifiable hits for each condition is listed at the top of the bars.

Crenarchaeota. In the 1-mbsf sample, the RAMP metagenome contained 13.1% Crenarchaeota sequences while the REPLI-g metagenome contained less than 1%. However, for the 32-mbsf sample, the REPLI-g metagenome contains 41.7% Crenarchaeota sequences while the RAMP metagenome contains less than 1%, essentially opposite trends.

Due to the inconsistent finding of the nr and 16S methods, the metagenomes were also compared against a dataset of rpoB gene sequences. In the rpoB classification, Proteobacteria heavily dominated all metagenomes, followed by Chloroflexi. In contrast to the nr classifications, and consistent with results of the 16S classification, the Proteobacteria increase with depth for both the REPLI-g and RAMP metagenomes (7.8 and 19.6% higher), while Chloroflexi decrease (8.7 and 3.0% lower). Also in contrast to the nr classification results, the Euryarchaeota decrease with depth in both the REPLI-g and RAMP metagenomes (1.9 and 2.4% lower). This is consistent with the 16S classification results for the REPLI-g metagenomes only. Finally, in this rpoB classification, the Crenarchaeota make up a significant percent of the classified sequences of the unamplified sample (9.1%), and while present

to a lesser degree in the REPLI-g dataset, still reveal an increase with depth (1.7–4.8%), consistent with the nr classification data and the 16S data for this amplification method. In the RAMP metagenomes however, the Crenarchaeota make up less than 1% of the rpoB-classified sequences.

In an attempt to clear up the trends associated with the archaea at the two depths in the different metagenomes, a classification of sequences at the domain level was performed, again using comparisons to the nr, 16S, and rpoB databases (**Figure 4**). In this interpretation, archaea increase in relative proportion with depth while bacteria decrease in relative proportion with depth in all cases except in the 16S classification of the RAMP metagenomes, where the opposite trend exists. Specifically, in the REPLI-g metagenomes, the proportion of archaeal sequences increases with depth by 11.9, 29.8, and 8.9% in the nr, 16S, and rpoB analyses, respectively. In the RAMP metagenomes, the proportion of archaeal sequences increases with depth by 12.2 and 12.3% in the nr and rpoB analyses, respectively, but decreases by 10.3% in the 16S analysis.

DISCUSSION

METHOD ASSESSMENT

General amplification of environmental DNA via the developed RAMP protocol is a means of producing DNA fragments suitable for immediate use in 454 metagenomic sequencing. The utilization of the PCR reaction with primers possessing a degenerate 3′ end results in general amplification of the genetic material without the creation of products in amplification reaction negative controls, allowing for confident amplification of low-biomass samples compared to MDA methods. Bias in coverage of starting genetic material is suggested by the estimated levels of coverage of the *E. coli* genome after sequencing of amplified products (**Table 2**). An increase in coverage levels with relation to sequencing effort (**Figure 2**), however, suggests that even with no improvements to the method, full coverage could be achieved with high enough levels of sequencing (estimated at 813 million base pairs or about two full plates of 454 sequencing). We had several hypotheses about the cause of bias in coverage. The first was that the bias was occurring due to the initial locations of primer annealing in the first cycle of PCR. After the first round of PCR, those regions amplified would be present in higher number than other regions and hence, more likely to amplify in subsequent rounds of PCR. This hypothesis was tested by combining the amplification products of 15 separate reactions, in theory allowing for 15 different sets of initial primer annealing locations due to random chance (test 2, **Table 2**). Analysis of sequenced products, however, revealed no significant reduction in bias. A second hypothesis was that the annealing temperature of the PCR reaction was favoring amplification of GC-rich regions of the genome, and that a lower annealing temperature may permit annealing at less GC-rich regions to be competitive. Sequencing after the use of a lower annealing temperature revealed a small reduction in bias, however, analysis of

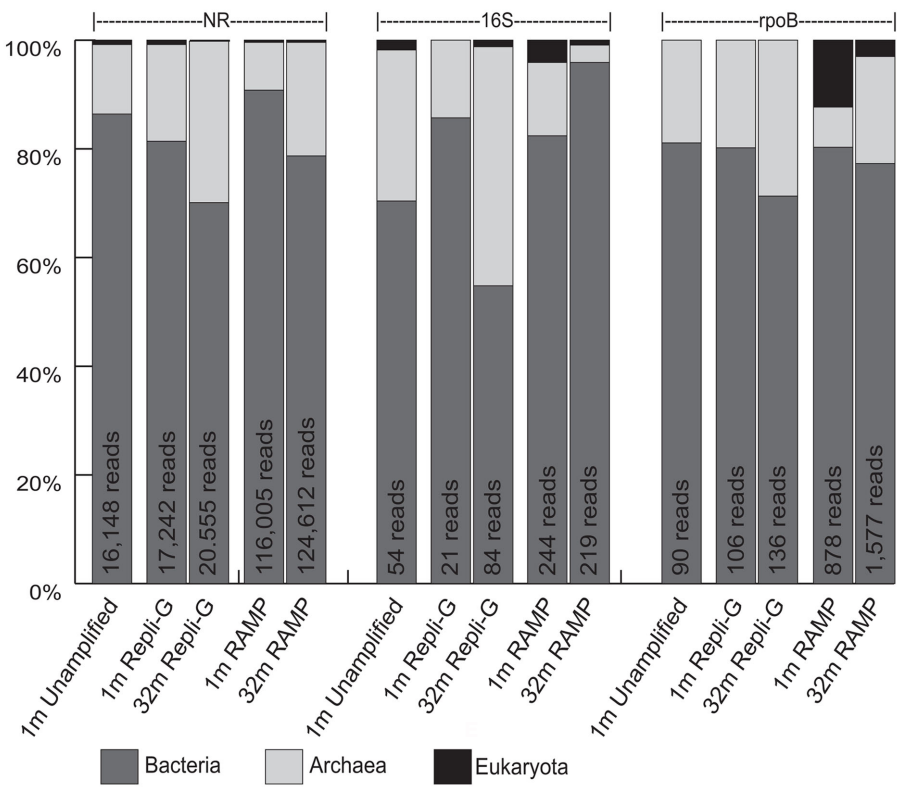

FIGURE 4 | Domain classification of sequences in all five metagenomes, as revealed through comparison to the nr, 16S, and rpoB databases. Shown are percentages of total identifiable hits. Total number of identifiable hits for each condition is listed at the top of the bars.

the GC content of sequenced products suggested no change in the proportion of GC-rich to GC-poor regions (test 3, **Table 2**). One observed problem with lowering the annealing temperature was a decrease in the yield of amplified DNA by a couple orders of magnitude.

Our current hypothesis on the cause of the bias is that it is related to the specific DNA sequence of the primer, particularly, the region closest to the degenerate 3′ end of the primer. Portions of the genome that match not only the five base pairs at the end of a primer, but also the next base or bases, would have a higher likelihood of primer annealing. This could explain the slight improvement in coverage resulting from a reduced annealing temperature, as less stringent PCR conditions allow for more non-specific annealing. One of the goals of primer development had been to maximize degeneracy while limiting the creation of DNA artifacts such as primer-dimers. In this effort, we attempted to increase the number of degenerate base pairs at the 3′ end of the primer. With six degenerate bases at the 3′ end of the primer, however, amplification failed for all PCR conditions attempted. This was more likely a result of hairpin formation of the primers than rampant primer-dimer formation, as primer-dimers viewed on the gel were less bright than those for the five degenerate base primer, ran as a control. One possible way to increase degeneracy of the primers without causing an increase in hairpin formation or primer-dimers, might be to create multiple primers, each with a different base preceding the 5-nucleotide degenerate 3′ end, carry out separate reactions with each primer, and combine the products at the end. In this way, the same effect of adding a sixth degenerate base might be achieved, without the problems of hairpin formation resulting from too many degenerate bases at the end of any one primer. However, this idea has not yet been tested.

Another possible limitation of the method is the sensitivity of the reaction to the concentration of starting DNA template. The *E. coli* dilution series test indicated that below a certain starting concentration of DNA, no significant amplification would occur (**Figure 1C**). In this test, amplification occurred with a starting concentration of 0.125 ng/μL but not for a starting concentration of 0.0625 ng/μL. As experimentation with environmental samples showed, increasing the number of cycles is one way to increase the sensitivity of the method, but this has not been quantified. Also, testing RAMP at 60 cycles revealed that there is a limit to how many cycles can be run before DNA artifacts appear in negative controls. Even so, there is likely much to be gained in terms of sensitivity between 25 and 50 cycles, and this is something we would like to test further in the future.

APPLICATION TO ENVIRONMENT

When applied to environmental samples from the Peru Margin subsurface, at 1 and 32 mbsf, RAMP again produced amplified DNA product suitable for use with 454 metagenomic sequencing. In order to make a qualitative assessment of coverage bias, the community composition of these environmental samples was analyzed, and compared to that obtained using REPLI-g amplification for both samples, as well as to that obtained by sequencing the unamplified 1 mbsf sample, using data from Biddle et al. (2008).

In terms of the quality of data obtained (length of sequence, genuine sequence versus amplification artifact, etc.), it is difficult to compare the sequenced RAMP products to the unamplified and REPLI-g amplified samples, as sequencing technology was greatly improved in the length of time between studies. However, we can say that both methods resulted in sequenced products of a length which was typical for the sequencing technology of the time [∼100 bp (2008) and ∼400 bp (2010)]. When the sequenced products were compared to the nr, rpoB, and 16S rRNA databases, RAMP products had much higher percentages of sequences with identifiable homologs in all cases except the 16S database, where they were still higher, but to a lesser degree (**Table 3**). This might be contributable entirely to the increase in read length capable with the newer sequencing technology, as longer reads would increase the likelihood of a match in the protein databases, but may make less of a difference in the nucleic acid-based 16S rRNA database, where shorter reads lead to identification almost as often as longer ones (Biddle et al., 2008). The fact that both of the 2008 amplified samples have similar values to the unamplified sample for percent of the metagenome with identifiable homologs in the three databases, suggests that the cause of the low identification rates is likely not due to the production of amplification artifacts by MDA, a question we had wanted to explore. These results are slightly different than those obtained by analysis of the data in 2008, where the amplified 32 mbsf sample did have a significantly lower percentage of identified sequences than the 1-mbsf unamplified sample (5.83% to nr as compared with 13.39%). The current analysis was done using more recent databases, and the identifiable percentage of all three 2008 metagenomes was higher than in the 2008 analysis, but it may be that the 32-mbsf sample benefited most from the addition of new sequences to the available databases.

Comparing the amplification methods using assessments of community composition via matches to the nr, rpoB, and 16S rRNA databases proved problematic, largely as a result of conflicting data between databases. When examining the community composition of all five metagenomes using results from the nr

Table 3 | Analysis of environmental sequence data.

Metagenome	No. of reads/Mb	Percentage of Metagenome			
		BLASTX (nr)	MEGAN (nr)	MEGAN (rpoB)	BLASTN (16S)
1 m Unamplified (Biddle et al., 2008)	94,332/7.14	22.54	8.69	0.05	0.06
1 m REPLI-g (Biddle et al., 2008)	111,964/8.00	20.51	7.92	0.05	0.02
32 m REPLI-g (Biddle et al., 2008)	148,041/17.24	19.08	6.73	0.04	0.06
1 m RAMP	219,909/80.89	65.83	27.99	0.29	0.11
32 m RAMP	246,979/84.74	65.21	25.93	0.43	0.09

database, both methods appear successful in paralleling the unamplified 1 mbsf sample in terms of major taxonomic groups. In addition, RAMP and REPLI-g appear to give similar results to each other for the deeper 32 mbsf, which had no unamplified control. Further, patterns of increasing and decreasing of the proportions of taxa are consistent between RAMP and REPLI-g. In this analysis, both methods imply that the Chloroflexi and the archaeal groups increase with depth, while the Proteobacteria decrease with depth. These trends are consistent with results from the Biddle et al. (2008) study.

The nr database, however, suffers from bias toward groups of organisms with many sequenced representatives; hence, the relative proportions of taxa may be misleading. The Silva 16S rRNA database, on the other hand, has a far greater diversity of organisms represented, including many environmental sequences from organisms not yet cultivated or sequenced. We chose to compare our metagenomes to this database, as another perspective of community composition. The results of this method of community analysis were much less consistent between amplification techniques and between the amplified and unamplified samples. Several factors may be contributing to these results. First, unlike the analysis using the nr database, the 16S rRNA database is only of a single gene. Therefore, there is the possibility of missing that one gene in any given organism due to under-sampling, whereas, one would have a higher chance of hitting at least one gene in the organism's genome that would provide a match to the nr database. This may be the issue with the 1-mbsf REPLI-g sample, as only 21 16S rRNA genes were identified (as contrasted with 84 in the 32-mbsf sample, of a similar dataset size). In the 2008 study, where more depths were examined, this 1 mbsf sample was a sort of outlier in the 16S analysis, where trends across the other depths were much more consistent (Biddle et al., 2008).

Other possibilities for the inconsistencies in this analysis could be related to WGA-induced bias as a result of DNA quantity or quality. It has been noted before for MDA that bias increases when less DNA template is used (Binga et al., 2008). In addition, the quality of the extracted DNA may result in differences in the success of amplification, favoring some DNA sequences over others. Perhaps such a bias in amplification could explain why the Crenarchaeota 16S rRNA genes are nearly completely absent from the 32-mbsf RAMP metagenome (matches were found, but constituted less than 1% of the identified reads). Alternatively, it is possible that REPLI-g has a strong bias toward the 16S rRNA of Crenarchaeota when starting DNA template is low or poor. As we do not have an unamplified metagenome for this deeper sample, it is very difficult to determine whether or not the trends we see are a result of WGA-induced bias of either or both of the amplification methods employed.

Attempting to use another marker gene, rpoB, did little to answer any questions about bias induced by WGA at depth, and added more confusion to the issue of what happens to the archaeal groups with depth, in some cases agreeing with the nr analysis, and in some cases with the 16S analysis. Hypothesizing that many of the archaeal sequences at depth were not being classified at the phylum level in the nr or rpoB analyses, we decided to carry out an analysis at the domain level, to get a better idea of archaeal trends in the subsurface, an ongoing question in deep biosphere research. This analysis, at least, revealed more consistency among the nr, 16S, and rpoB analysis, and showed that in nearly all cases, the proportion of archaea increased with depth (**Figure 4**). This is most consistent with the phylum level nr analysis, where both Crenarchaeota and Euryarchaeota increased with depth.

This study has introduced a new method of WGA, termed RAMP, which is a viable option for increasing DNA concentration for use with metagenomic sequencing. The method was designed specifically for the pyrosequencing platform of Roche 454, and helps to reduce preparation steps, as the 454 sequencing primers are attached to each fragment of DNA as it is amplified. With modifications to the primers and further optimization, this method may also be an option for use with other sequencing technologies, such as the Illumina or Ion Torrent sequencing systems, which utilize similar preparations as the 454 system. The method may have particular utility in very low-biomass samples, where the production of DNA artifacts produced by other methods of WGA may inhibit the amplification of sample DNA altogether. The method has room and flexibility for improvement, such as through further optimization of the primer design and cycling conditions, which may reduce some of the problems with potential biases. Based on the results of this study, however, it is clear that using any method of WGA may have a significant impact in community composition and diversity analyses. In addition, the results displayed herein should reinforce the caution that must be employed when analyzing community composition using any one method of analysis.

ACKNOWLEDGMENTS

We thank the ODP shipboard scientific party, and D. Jones and Z. Zhang for technical assistance. Samples for this research were provided by the Integrated Ocean Drilling Program [sponsored by the National Science Foundation (NSF) and participating countries]. This work was supported by NSF Grant OCE 05-50601, by the National Aeronautics and Space Administration (NASA) Astrobiology Institute (NAI) under NASA–Ames Cooperative Agreement NNA09DA76A, and through support from the Gordon and Betty Moore Foundation. The Roche 454 facility at the Pennsylvania State University Center for Comparative Genomics and Bioinformatics was funded, in part, by a grant from the Pennsylvania Department of Health using Tobacco Settlement Funds appropriated by the legislature. Jennifer F. Biddle was also supported by a NASA Postdoctoral Program Fellowship administered by Oak Ridge Associated Universities (ORAU).

REFERENCES

Bale, S. J., Goodman, K., Rochelle, P. A., Marchesi, J. R., Fry, J. C, Weightman, A. J., and Parkes, R. J. (1997). *Desulfovibrio profundus* sp. nov., a novel barophilic sulfate-reducing bacterium from deep sediment layers in the Japan Sea. *Int. J. Syst. Bacteriol.* 47, 515–521.

Biddle, J. F. (2006). *Microbial Populations and Processes in Subseafloor Marine Environments*. ProQuest Dissertations and Theses, The Pennsylvania State University, University Park, PA, 179.

Biddle, J. F., Fitz-Gibbon, S., Schuster, S. C., Brenchley, J. E., and House, C. H. (2008). Metagenomic signatures of the Peru Margin subseafloor biosphere show a genetically distinct environment. *Proc. Natl. Acad. Sci. U.S.A.* 105, 10583–10588.

Biddle, J. F., White, J. R., Teske, A. P., and House, C. H. (2011). Metagenomics of the subsurface Brazos-Trinity Basin (IODP site 1320): comparison with other sediment and pyrosequenced metagenomes. *ISME J.* 5, 1038–1047.

Binga, E. K., Lasken, R. S., and Neufeld, J. D. (2008). Something from (almost) nothing: the impact of multiple displacement amplification on microbial ecology. *ISME J.* 2, 233–241.

Blankenberg, D., Von Kuster, G., Coraor, N., Ananda, G., Lazarus, R., Mangan, M., Nekrutenko, A., and Taylor, J. (2010). Galaxy: a web-based genome analysis tool for experimentalists. *Curr. Protoc. Mol. Biol.* 19, 1–21.

Dean, F. B., Hosono, S., Fang, L., Wu, X., Faruqi, A. F., Bray-Ward, P., Sun, Z., Zong, Q., Du, Y., Du, J., Driscoll, M., Song, W., Kingsmore, S. F., Egholm, M., and Lasken, R. S. (2002). Comprehensive human genome amplification using multiple displacement amplification. *Proc. Natl. Acad. Sci. U.S.A.* 99, 5261–5266.

Dietmaier, W., Hartmann, A., Wallinger, S., Heinmöller, E., Kerner, T., Endl, E., Jauch, K. W., Hofstädter, F., and Rüshoff, J. (1999). Multiple mutation analysis in single tumor cells with improved whole genome amplification. *Am. J. Pathol.* 154, 83–95.

Giardine, B., Riemer, C., Hardison, R. C., Burhans, R., Elnitski, L., Shah, P., Zhang, Y., Blankenberg, D., Albert, I., Taylor, J., Miller, W., Kent, W. J., and Nekrutenko, A. (2005). Galaxy: a platform for interactive large-scale genome analysis. *Genome Res.* 15, 1451, 1455.

Goecks, J., Nekrutenko, A., Taylor, J., and The Galaxy Team. (2010). Galaxy: a comprehensive approach for supporting accessible, reproducible, and transparent computational research in the life sciences. *Genome Biol.* 11, R86.

Huson, D. H., Auch, A. F., Qi, J., and Schuster, S. C. (2007). MEGAN analysis of metagenomic data. *Genome Res.* 17, 377–386.

Inagaki, F., Nunoura, T., Nakagawa, S., Teske, A., Lever, M., Lauer, A., Suzuki, M., Takai, K., Delwiche, M., Colwell, F. S., Nealson, K. H., Horikoshi, K., D'Hondt, S., and Jørgensen, B. B. (2006). Biogeographical distribution and diversity of microbes in methane hydrate-bearing deep marine sediments on the Pacific Ocean Margin. *Proc. Natl. Acad. Sci. U.S.A.* 103, 2815–2820.

Jørgensen, B. B., and Boetius, A. (2007). Feast and famine – microbial life in the deep-sea bed. *Nature* 5, 770–781.

Kittler, R., Stoneking, M., and Kayser, M. (2002). A whole genome amplification method to generate long fragments from low quantities of genomic DNA. *Anal. Biochem.* 300, 237–244.

Lipp, J. S., Morono, Y., Inagaki, F., and Hinrichs, K.-U. (2008). Significant contribution of Archaea to extant biomass in marine subsurface sediments. *Nature* 454, 991–994.

Mikucki, J. A., Liu, Y., Delwiche, M., Colwell, F. S., and Boone, D. R. (2003). Isolation of a methanogen from deep marine sediments that contain methane hydrates, and description of *Methanoculleus submarinus* sp. nov. *Appl. Environ. Microbiol.* 69, 3311–3316.

Nelson, D. L., Ledbetter, S. A., Corbo, L., Victoria, M. F., Ramirez-Solis, R., Webster, T. D., Ledbetter, D. H., and Caskey, C. T. (1989). Alu polymerase chain reaction: a method for rapid isolation of human-specific sequences from complex DNA sources. *Proc. Natl. Acad. Sci. U.S.A.* 86, 6686–6690.

Orcutt, B. N., Sylvan, J. B., Knab, N. J., and Edwards, K. J. (2011). Microbial ecology of the dark ocean above, at, and below the seafloor. *Microbiol. Mol. Biol. Rev.* 75, 361–422.

Pinard, R., de Winter, A., Sarkis, G. J., Gerstein, M. B., Tartaro, K. R., Plant, R. N., Egholm, M., Rothberg, J. M., and Leamon, J. H. (2006). Assessment of whole genome amplification-induced bias through high-throughput, massively parallel whole genome sequencing. *BMC Genomics* 7, 216–236. doi:10.1186/1471-2164-7-216

Poinar, H. N., Schwarz, C., Qi, J., Shapiro, B., Macphee, R. D., Buigues, B., Tikhonov, A., Huson, D. H., Tomsho, L. P., Auch, A., Rampp, M., Miller, W., and Schuster, S. C. (2006). Metagenomics to paleogenomics: large-scale sequencing of mammoth DNA. *Science* 311, 392–394.

Raghunathan, A., Ferguson, H. R. Jr, Bornarth, C. J., Song, W., Driscoll, M., and Lasken, R. S. (2005). Genomic DNA amplification from a single bacterium. *Appl. Environ. Microbiol.* 71, 3342–3347.

Sørensen, K. B., Lauer, A., and Teske, A. (2004). Archaeal phylotypes in a metal-rich and low-activity deep subsurface sediment of the Peru Basin, ODP Leg 202, Site 1231. *Geobiology* 2, 151–161.

Telenius, H., Carter, N. P., Bebb, C. E., Nordenskjöld, M., Ponder, B. A. J., and Tunnacliffe, A. (1992). Degenerate oligonucleotide-primed PCR: general amplification of target DNA by a single degenerate primer. *Genomics* 13, 718–725.

Toffin, L., Webster, G., Weightman, A. J, Fry, J. C., and Prieur, D. (2004). Molecular monitoring of culturable bacteria from deep-sea sediment of the Nankai Trough, Leg 190 Ocean Drilling Program. *FEMS Microbiol. Ecol.* 48, 357–367.

Webster, G., Newberry, C. J., Fry, J. C., and Weightman, A. J. (2003). Assessment of bacterial community structure in the deep sub-seafloor biosphere by 16S rDNA-based techniques: a cautionary tale. *J. Microbiol. Methods* 55, 155–164.

Zhang, L., Cui, X., Schnitt, K., Hubert, R., Navidi, W., and Arnheim, N. (1992). Whole genome amplification from a single cell: implications for genetic analysis. *Proc. Natl. Acad. Sci. U.S.A.* 89, 5847–5851.

Conflict of Interest Statement: The authors declare that the research was conducted in the absence of any commercial or financial relationships that could be construed as a potential conflict of interest.

Received: 14 October 2011; paper pending published: 03 November 2011; accepted: 09 January 2012; published online: 23 January 2012.

Citation: Martino AJ, Rhodes ME, Biddle JF, Brandt LD, Tomsho LP and House CH (2012) Novel degenerate PCR method for whole-genome amplification applied to Peru Margin (ODP Leg 201) subsurface samples. Front. Microbio. ***3****:17. doi: 10.3389/fmicb.2012.00017*

This article was submitted to Frontiers in Extreme Microbiology, a specialty of Frontiers in Microbiology.

frontiers in
MICROBIOLOGY

ORIGINAL RESEARCH ARTICLE
published: 30 January 2012
doi: 10.3389/fmicb.2012.00016

Quantification of microbial communities in subsurface marine sediments of the Black Sea and off Namibia

Axel Schippers [1,2] ****, Dagmar Kock*** [1,2] ***, Carmen Höft*** [1,2] ***, Gerrit Köweker*** [1,2] ***and Michael Siegert*** [1,2]

[1] *Geomicrobiology, Federal Institute for Geosciences and Natural Resources, Hannover, Germany*
[2] *Faculty of Natural Sciences, Leibniz Universität Hannover, Hannover, Germany*

Edited by:
Andreas Teske, University of North Carolina at Chapel Hill, USA

Reviewed by:
Aharon Oren, The Hebrew University of Jerusalem, Israel
Timothy Ferdelman, Max Planck Institute for Marine Microbiology, Germany

****Correspondence:***
Axel Schippers, Bundesanstalt für Geowissenschaften und Rohstoffe, Stilleweg 2, 30655 Hannover, Germany.
e-mail: axel.schippers@bgr.de

Organic-rich subsurface marine sediments were taken by gravity coring up to a depth of 10 m below seafloor at six stations from the anoxic Black Sea and the Benguela upwelling system off Namibia during the research cruises Meteor 72-5 and 76-1, respectively. The quantitative microbial community composition at various sediment depths was analyzed using total cell counting, catalyzed reporter deposition – fluorescence *in situ* hybridization (CARD–FISH) and quantitative real-time PCR (Q-PCR). Total cell counts decreased with depths from 10^9 to 10^{10} cells/mL at the sediment surface to 10^7–10^9 cells/mL below one meter depth. Based on CARD–FISH and Q-PCR analyses overall similar proportions of *Bacteria* and *Archaea* were found. The down-core distribution of prokaryotic and eukaryotic small subunit ribosomal RNA genes (16S and 18S rRNA) as well as functional genes involved in different biogeochemical processes was quantified using Q-PCR. *Crenarchaeota* and the bacterial candidate division JS-1 as well as the classes *Anaerolineae* and *Caldilineae* of the phylum *Chloroflexi* were highly abundant. Less abundant but detectable in most of the samples were *Eukarya* as well as the metal and sulfate-reducing *Geobacteraceae* (only in the Benguela upwelling influenced sediments). The functional genes *cbbL,* encoding for the large subunit of RuBisCO, the genes *dsrA* and *aprA,* indicative of sulfate-reducers as well as the *mcrA* gene of methanogens were detected in the Benguela upwelling and Black Sea sediments. Overall, the high organic carbon content of the sediments goes along with high cell counts and high gene copy numbers, as well as an equal abundance of *Bacteria* and *Archaea*.

Keywords: Benguela upwelling, Black Sea, CARD–FISH, deep biosphere, real-time PCR, sediments, subsurface

INTRODUCTION

The Black Sea and the Benguela upwelling system off the Atlantic coast of Namibia are both represent organic carbon-rich marine environments. Nevertheless, there are fundamental differences in the biogeochemistry and of these two settings. The Black Sea is the largest anoxic seawater basin on earth. It is characterized by high biological productivity in the oxygenated surface waters (Yilmaz et al., 2006). This and a deep anoxic water body below the chemocline at 100–150 m water depth (Neretin et al., 2007) provide suitable conditions for anaerobic microbial life and biogeochemical cycling in organic carbon-rich sediments. The sediments at water depths of 2000 m are under permanent anoxic and sulfidic conditions. Conversely, the Namibian continental margin underlies one of the most productive upwelling systems in the world. Periods of low oxygen, nitrate-rich, and sometimes sulfidic water, also leads to enhanced accumulation of organic carbon in the diatom-rich mud belt on the shelf. On the continental slope and rise the organic carbon flux to the underlying sediments is also relatively high. The sediments of these two marine areas have been well-studied for their biogeochemical processes (Niewöhner et al., 1998; Ferdelman et al., 1999; Brüchert et al., 2000, 2003, 2006; Fossing et al., 2000; Jørgensen et al., 2001, 2004; Emeis et al., 2004; Neretin et al., 2004; Knab et al., 2008; Dale et al., 2009; Goldhammer et al., 2010, 2011; Riedinger et al., 2010; Holmkvist et al., 2011) but microbiological data are available for surface sediments mainly (Schulz et al., 1999; Thamdrup et al., 2000; Schulz and Schulz, 2005; Coolen et al., 2006a; Neretin et al., 2007; Coolen and Shtereva, 2009; Schubotz et al., 2009; Julies et al., 2010). Only few microbiological data are published for subsurface sediments of the Black Sea and the Benguela upwelling system (Leloup et al., 2007; Schäfer et al., 2007; Blazejak and Schippers, 2010, 2011).

Subsurface marine sediments are populated by numerous prokaryotes mainly belonging to uncultivated phylogenetic lineages (Parkes et al., 2000; Teske, 2006; Biddle et al., 2008; Fry et al., 2008; Teske and Sørensen, 2008). The abundance of particular phylogenetic and physiological prokaryotic groups, i.e., *Archaea* and *Bacteria,* methanogens or sulfate-reducers, in subsurface sediments at various sites has been quantified based on 16S rRNA and functional gene analysis by quantitative, real-time PCR (Q-PCR), FISH, and catalyzed reporter deposition–fluorescence *in situ* hybridization (CARD–FISH; Schippers et al., 2005, 2010; Biddle et al., 2006; Inagaki et al., 2006; Schippers and Neretin, 2006; Engelen et al., 2008; Nunoura et al., 2009; Webster et al., 2009; Breuker et al., 2011). While the detection of 16S rRNA genes may not be a good indicator for an active

microbial community, FISH and CARD–FISH analyses, targeting intact ribosomal RNA, suggest that an active microbial community is present. Eukaryotic DNA comprising, e.g., fungi (Edgcomb et al., 2011) has been quantified in marine sediments at few sites in much lower concentration than prokaryotic DNA (Schippers and Neretin, 2006; Schippers et al., 2010). However, eukaryotic DNA may be preserved as fossil DNA from any buried biota and might be indicative for former biological communities (Coolen et al., 2006a,b; Inagaki and Nealson, 2006; Boere et al., 2011).

Sulfate-reducing microorganisms which are frequently found in near-surface sediments (Knoblauch et al., 1999; Sahm et al., 1999; Ravenschlag et al., 2000; Schippers et al., 2010), or methanogenic Archaea, were rarely detected in deep sediments (Parkes et al., 2005; Biddle et al., 2006; Inagaki et al., 2006; Teske, 2006; Teske and Sørensen, 2008; Webster et al., 2009). In addition to 16S rRNA gene analyses, sulfate-reducers and methanogenic lineages of *Archaea* have been detected and quantified detecting their functional genes. Such genes encode for the dissimilatory sulfite reductase (*dsrA*), adenosine 5′-phosphosulfate reductase subunit A (*aprA*), and methyl coenzyme M reductase (*mcrA*, Parkes et al., 2005; Schippers and Neretin, 2006; Leloup et al., 2007; Wilms et al., 2007; Colwell et al., 2008; Engelen et al., 2008; Nunoura et al., 2009; Webster et al., 2009; Schippers et al., 2010; Blazejak and Schippers, 2011). The frequent occurrence of genes involved in sulfate reduction and methanogenesis indicates that microbial communities actively perform carbon and sulfur cycling under reduced redox conditions.

Despite heterotrophy seems to be dominant in subsurface sediments (D'Hondt et al., 2004; Biddle et al., 2006), autotrophy may play a role and has scarcely been investigated. There are different pathways of CO_2 fixation, of which the Calvin–Benson–Bassham (CBB) cycle is the best described. The *cbbL* gene encoding for the large subunit of the form I "red-like" enzyme ribulose-1.5-bisphosphate carboxylase/oxygenase (RuBisCO) occurs in autotrophic *Proteobacteria* that fix CO_2 via the CBB cycle (Selesi et al., 2007; Badger and Bek, 2008). This gene was so far only quantified in terrestrial (Breuker et al., 2011), but not in subsurface marine sediments.

In this study, the quantitative microbial community composition at six marine sediment stations from the Black Sea and in the Benguela upwelling area off Namibia at various sediment depths up to 10 m below seafloor (mbsf) was analyzed using total cell counting, CARD–FISH for the quantification of living *Bacteria* and *Archaea*, and 12 different Q-PCR assays for the quantification of particular phylogenetic or functional groups.

MATERIALS AND METHODS

SEDIMENT DESCRIPTION

Samples were collected at six marine stations during two research vessel expeditions (**Table 1**). The M72-5 R/V Meteor cruise to the Black Sea took place in May/June 2007 (**Figure 1**). The sampled Black Sea sediments were permanently anoxic due to the overlaying anoxic water column. Sulfate reduction and methanogenesis are generally the predominant terminal biogeochemical processes for organic matter degradation (Jørgensen et al., 2004; Leloup et al., 2007). The sediments underlying the anoxic water column had an upper layer composed of laminated coccolith ooze with high organic carbon content, while an underlying sapropel is characterized by even higher organic content (Brumsack, 1989). At station 22 a sapropel layer occurred at a depth of 8 mbsf. This sapropel deposited 130 ka ago after the Eem glacial.

The M76-1 R/V Meteor cruise to the Benguela upwelling area off Namibia took place in April/May 2008 (**Figure 2**). In the coastal upwelling area off Namibia, sediments were sampled along a transect course. This transect commenced at the deep subseafloor at the lower continental margin at 3795 m water depth (station 8, GeoB 12808). This first core consisted of carbonate-rich deep sea clay, was oxic or suboxic with signs of bioturbation. The second station was situated at the upper continental margin at 1940 m water depth (station 3, GeoB 12803) was oxic and characterized by foraminifera and bioturbation. The third station was held at the shallow shelf in a mudbelt beneath a zone of high productivity (station 10, GeoB 12810) where foraminifera and dark olive colored mud characterized the sediment. A high abundance of *Thioploca* and *Beggiatoa*-like filaments from the surface down to 10–12 cm was found.

SEDIMENT SAMPLING

Sediment samples were taken from the near-surface sediment down to a depth of up to ca. 0.5 mbsf employing a multicorer (MUC). Deeper sediments down to 10 mbsf were sampled using a gravity corer (GC). The GC cores were quickly cut into 1 m sections onboard and immediately stored at 4°C. For further section-wise processing within several hours, each 1 m section was subsequently split lengthwise into half-core sections. During sampling, the outer surface of the core was carefully removed to avoid contamination with seawater.

Table 1 | Sampled sediment stations and total organic carbon [TOC, data from S. Eckert and B. Schnetger (Black Sea), Y. Lin and K.-U. Hinrichs (Namibia)].

Cruise	Area	Station	Sampling tool	Position	Water depth (m)	Sampling depth (mbsf)	Number of analyzed samples	TOC (%)
Black Sea		6	MUC and GC	43°25.91′N 32°16.48′E	2027	8.8	19	nd
M72-5		20	MUC and GC	43°57.25′N 35°38.46′E	2048	5.8	19	nd
		22	GC	42°13.53′N 36°29.55′E	840	9.7	19	0.3–4.4
Benguela	Mudbelt	10	MUC and GC	24°03.19′S 14°15.69′E	120	3.4	16	4.1–13.4
Upwelling	Upper slope	3	MUC and GC	25°45.60′S 13°04.20′E	1940	5.4	15	3.8–8.7
M76-1	Lower slope	8	MUC and GC	26°22.18′S 11°53.49′E	3795	5.4	19	1–1.8

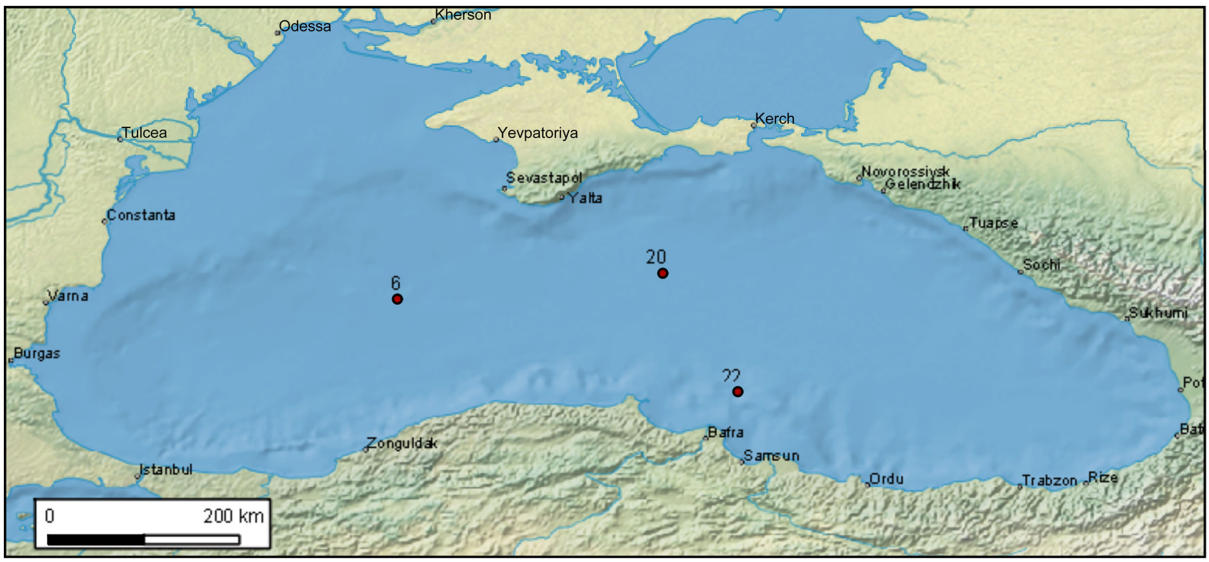

FIGURE 1 | Black Sea sediment stations of the cruise M72-5 analyzed in this study.

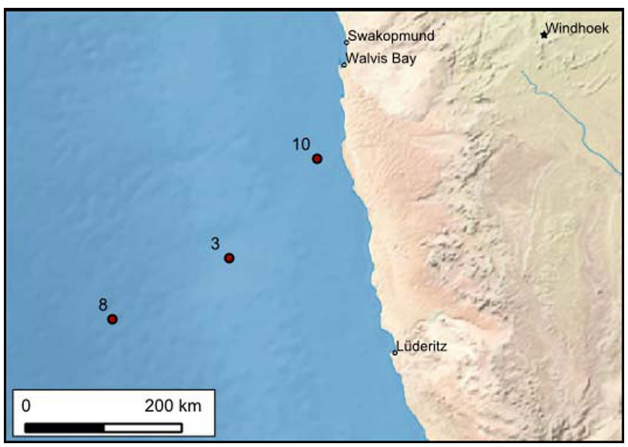

FIGURE 2 | Benguela upwelling transect sediment stations off Namibia of the cruise M76-1 analyzed in this study.

Microbiological samples for the quantification of microorganisms were taken with a sterilized 5 mL syringe of which the Leur head was cut off before. The uncontaminated center of the sediment core was sampled. For total cell counts, 0.5 mL sediment was fixed in 1 mL of a cold 4% formaldehyde–PBS [phosphate buffered saline (ultra), 150 mM sodium phosphate, 150 mM NaCl, pH 7.2] for 4–15 h at 4–10°C, washed twice with cold PBS using a mini-centrifuge (Eppendorf) at 13000 rpm for 10 min each, and finally stored at −20°C in 1 mL PBS–ethanol (1:1) in 2 mL vials (Eppendorf), transported to BGR frozen with dry ice as air-freight, and stored in BGR at −20°C. For DNA extraction and quantification with Q-PCR, several grams of fresh sediment were frozen immediately after sampling at −20°C in screw capped vials.

TOTAL CELL COUNTS AND CARD–FISH

Total cell numbers were determined in formaldehyde fixed samples by staining with SYBR Green® II following two different protocols. In analogy to acridine direct counts (AODC) we use the term SYBR Green® direct counts (SGDC). While cells were counted in the sediment matrix as described by Weinbauer et al., 1998, SGDC1), cells were detached from sediment particles before counting using the protocol of Kallmeyer et al., 2008, SGDC2). CARD–FISH analysis was carried out as described previously (Pernthaler et al., 2002; Schippers et al., 2005) and filters were hybridized for *Archaea* and *Bacteria* using probes ARCH915 or EUB338 I–III as a mixture. As a negative hybridization control the probe NON338 was applied.

QUANTITATIVE, REAL-TIME PCR ANALYSIS

The quantitative composition of the total (active and inactive) microbial community was analyzed using Q-PCR of extracted DNA. High-molecular-weight DNA was extracted from 0.5 g of a frozen sediment sample employing a modified Fast DNA Spin Kit for Soil (Bio101) protocol (Webster et al., 2003). Sterilized quartz sand treated in a muffle furnace for organic carbon removal was used as negative control in the extraction procedure. Extracted DNA was amplified by Q-PCR using the device ABI Prism 7000 (Applied Biosystems) and different master mixes from the companies Applied Biosystems, Eurogentec or Invitrogen. Each DNA extract was measured in triplicate. After each Q-PCR, melting curves were measured for SYBR Green® I assays. The copy numbers of the 16S rRNA gene were quantified for prokaryotes, *Archaea* (Takai and Horikoshi, 2000), *Bacteria* (Nadkarni et al., 2002), *Crenarchaeota* (Ochsenreiter et al., 2003), the JS-1- and *Chloroflexi*-related bacteria (Blazejak and Schippers, 2010), and the metal and sulfate-reducing *Geobacteraceae* (Holmes et al., 2002). The 18S rRNA gene of *Eukarya* was determined as previously described (Schippers and Neretin, 2006). Functional genes were quantified as described elsewhere: *mcrA* (*mcrA* assay 1, Wilms

et al., 2007; *mcrA* assay 2, Steinberg and Regan, 2009), *dsrA* (Schippers and Neretin, 2006); *aprA* (Blazejak and Schippers, 2011), and *cbbL* for (RuBisCO; Selesi et al., 2007).

RESULTS

Results of the quantitative microbial community composition in subsurface marine sediments of the Black Sea and the Benguela upwelling area off Namibia are shown in **Figures 3** and **4**, respectively.

BLACK SEA

Total cell counts and CARD–FISH

Total cells stained with SYBR Green® were counted following two different protocols. Depth profiles of total cell counts are shown in **Figure 3** (left). For both protocols, the maximal cell counts were detected near the sediment surface at all three Black Sea stations. The total cell counts sharply declined within the first meter sediment depth, and slightly decreased further below. The method comparison showed that the highest cell counts for all depths were obtained using the protocol without detaching cells from sediment particles (SGDC1, Weinbauer et al., 1998). For this protocol, maximum cell counts declined from 10^9 to 10^{10} cells/mL at the sediment surface to 10^7–10^8 cells/mL below 1 mbsf. In comparison, the cell counts obtained from the cell detachment protocol (SGDC2, Kallmeyer et al., 2008) were about one order of magnitude lower within the first 1 mbsf but showed similar values than SGDC1 below one meter depth. An increase of cell counts could be observed at 8–9 mbsf at station 22 where the layer of the organic carbon rich sapropel was discovered.

Catalyzed reporter deposition – fluorescence *in situ* hybridization cell counts above the detection limit of 10^5 cells/mL were obtained from the sediment surface down to 2.5 mbsf for the stations 6 and 20, and in the whole sampling depth of more than 8 mbsf for station 22. *Bacteria* and *Archaea* occurred in overall equal numbers.

Quantitative microbial community analysis by Q-PCR

Q-PCR results for 16S and 18S rRNA and functional genes at the three Black Sea stations are shown in **Figure 3** (middle and right, respectively). The Q-PCR data on archaeal and bacterial 16S rRNA gene copy numbers matched well with the total cell counts (SGDC1). In overall agreement with the CARD–FISH data, *Archaea* were found in similar copy numbers compared with *Bacteria* at all three sites. At station 22 between 2 and 8 mbsf, *Bacteria* could not be detected although the bacterial candidate division JS-1 and the classes *Anaerolineae* and *Caldilineae* of the phylum *Chloroflexi* were detectable in this depth range. At the other depths at all three stations these specific bacterial groups occurred in similar gene copy numbers than the *Bacteria* (data for station 20 from Blazejak and Schippers, 2010). Likewise, the *Crenarchaeota* frequently occurred in high gene copy numbers compared with *Archaea.* In some samples, the copy numbers of *Crenarchaeota* were even higher than those of *Archaea. Eukarya* were only detectable down to 1 mbsf at stations 6 and 22. However, they were detected throughout the whole core of station 20. Their 18S rRNA gene copy numbers were always lower than the prokaryotic 16S rRNA gene copy numbers.

Similar depth profiles were obtained for the functional genes (**Figure 3**, right). However the investigated genes were not detectable between 1 and 7 mbsf of station 22. Below, in the sapropel layer between 8 and 9 mbsf, they were again present. This was in good agreement with increased 16S rRNA gene copy numbers and increased SGDC1. Genes encoding for enzymes of sulfate-reducers (*dsrA* and *aprA*) were the most abundant (data for station 20 from Blazejak and Schippers, 2011). The *mcrA* gene of methanogens was detected at the surface of all three stations and on the bottom of the stations 20 and 22. The *cbbL* gene was found only in the near-surface sediment and in two deeper layers of the station 20.

BENGUELA UPWELLING AREA OFF NAMIBIA

The quantitative distribution of the microorganisms at the three stations along the transect course of the Benguela upwelling area (**Figure 4**) was more heterogeneous than for the three Black Sea stations. At the Benguela upwelling sediment station 10 (**Figure 4** bottom) a high abundance of *Thioploca* and *Beggiatoa*-like filaments was found at the near-surface sulfidic sediment of the shallow shelf. The other two stations on the continental slope at about 2000 m water depth (station 3, **Figure 4** top) and at about 4000 m water depth (station 8, **Figure 4** middle) were oxic or suboxic and bioturbated. The transect course followed a trend of decreasing organic carbon content (TOC, **Table 1**). However the TOC values were always above 1%, thus the sediments at all stations can be characterized as organic-rich and eutrophic.

Total cell counts and CARD–FISH

Depth profiles of total cell counts are shown in **Figure 4** (left). For both, SGDC1 and SGDC2, the maximal cell counts were found near the sediment surface at all three Benguela upwelling stations. Like for the Black Sea stations, the total cell counts sharply declined within the first 1 mbsf, and slightly decreased further below at the stations 3 and 8. At the station 10, no further decline of cell numbers was observed between 0.5 and 3.5 mbsf, the maximum sampling depth of this station. The maximum cell counts in the near-surface sediment were highest for the shelf station 10 with 10^{10} cells/mL and between 10^9 and 10^{10} cells/mL for the two continental slope stations. While SGDC1 remained above 10^9 cells/mL at 3.5 mbsf at station 10, the numbers were about an order of magnitude lower at the same depth for the two slope stations. The method comparison shows that SGDC1 was always slightly higher than SGDC2 for all three stations at all depths.

Catalyzed reporter deposition – fluorescence *in situ* hybridization signals were observed at almost all stations and depths. However, *Archaea* were detectable in equal numbers compared with *Bacteria* only in the near-surface sediment. In the deeper layers only *Bacteria* (besides two samples with *Archaea*) were detected in significantly lower numbers than the corresponding SGDC1.

Quantitative microbial community analysis by Q-PCR

For the Benguela upwelling sediments, Q-PCR analyses of the 16S and 18S rRNA and the functional genes are depicted in **Figure 4** (middle and right, respectively). The Q-PCR results for archaeal and bacterial 16S rRNA gene copy numbers were in good agreement with the total cell counts (SGDC1). In contrast to the CARD–FISH data, *Archaea* were found in similar copy numbers compared with the *Bacteria* at all three stations (as for the Black Sea results).

The archaeal copy numbers were higher than the bacterial ones in the deeper layers of station 10.

As found in the Black Sea sediments, the 16S rRNA gene copy numbers of the bacterial candidate division JS-1 and the classes

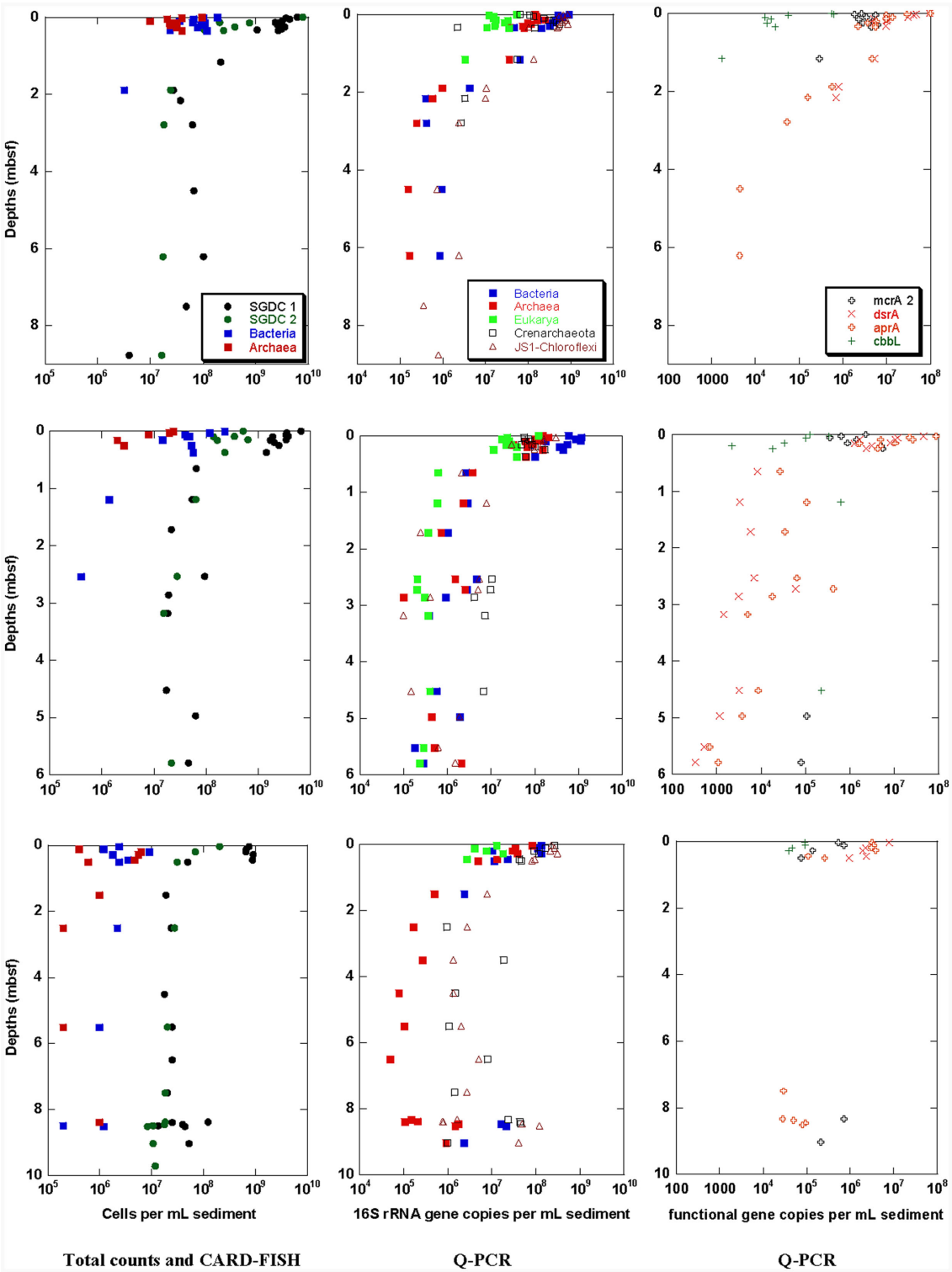

FIGURE 3 | Black Sea sediment samples of stations 6 (top), 20 (middle), and 22 (bottom). Total cell counts obtained with two different methods (SGDC1 after Weinbauer et al., 1998, SGDC2 after Kallmeyer et al., 2008) and CARD–FISH numbers for *Bacteria* and *Archaea* (left), and Q-PCR quantification of 16S or 18S rRNA genes of *Bacteria, Archaea, Eukarya, Crenarchaeota,* and JS-1–*Chloroflexi* (middle) and the functional genes *mcrA*, *dsrA*, *aprA*, and *cbbL* (right).

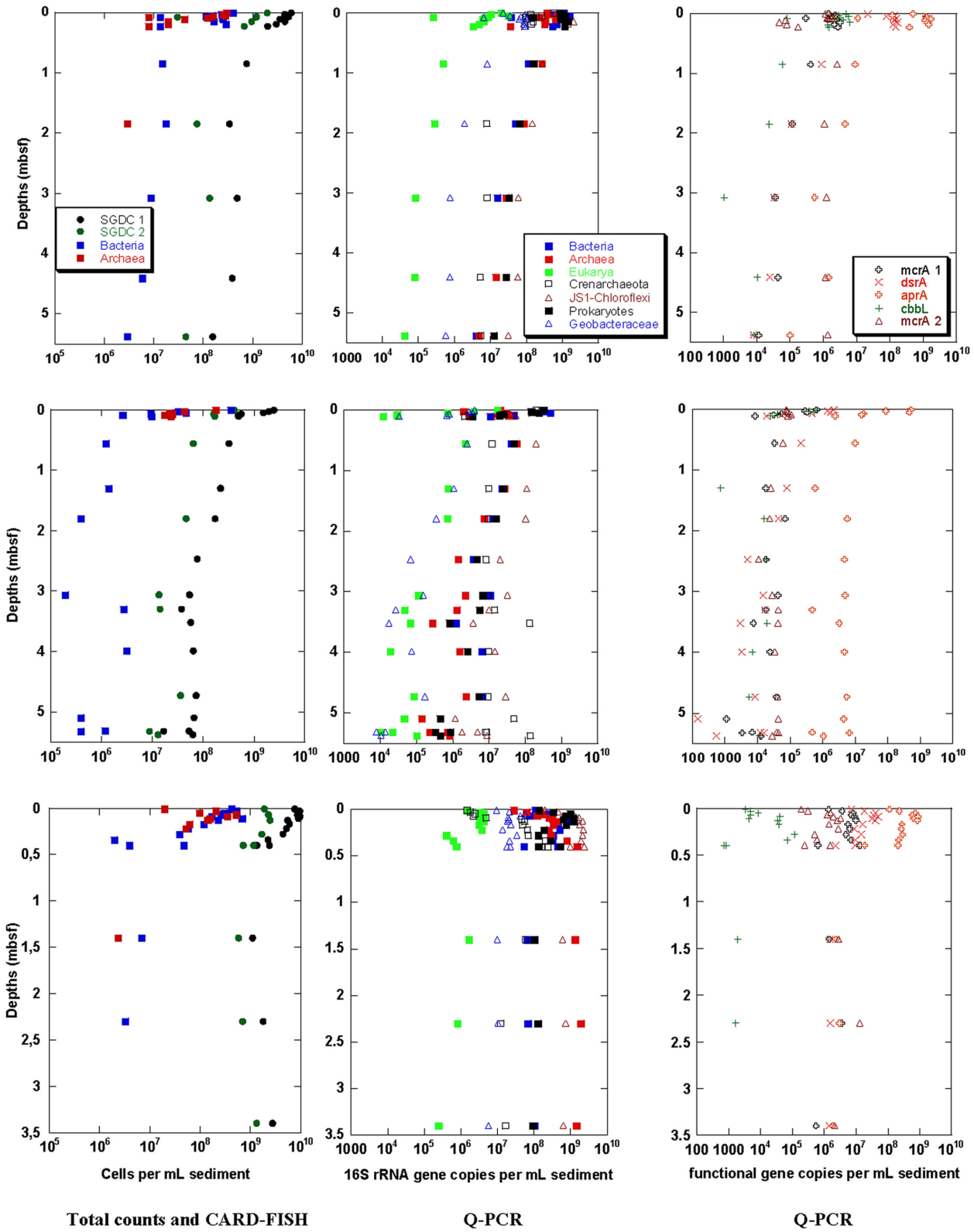

FIGURE 4 | Benguela upwelling sediment samples of stations 3 (top), 8 (middle), and 10 (bottom). Total cell counts obtained with two different methods (SGDC1 after Weinbauer et al., 1998, SGDC2 after Kallmeyer et al., 2008) and CARD–FISH numbers for *Bacteria* and *Archaea* (left), Q-PCR quantification of 16S rRNA genes of *Prokaryotes, Bacteria, Archaea, Eukarya, Crenarchaeota,* and JS-1–*Chloroflexi* (middle) and the functional genes *mcrA* 1 and 2, *dsrA*, *aprA*, and *cbbL* (right).

Anaerolineae and *Caldilineae* of the phylum *Chloroflexi* as well as those of the *Crenarchaeota* occurred in similar numbers of 10^6 to 10^9 copies/mL than the 16S rRNA gene copy numbers of *Prokaryotes, Bacteria,* and *Archaea.* The metal and sulfate-reducing family *Geobacteraceae* occurred at all three stations at all sediment depths in lower 16S rRNA gene copy numbers. The least abundant phylogenetic group was the *Eukarya* which nevertheless occurred in all analyzed samples.

Similar depth profiles like for the phylogenetic groups (and SGDC1) were obtained for the functional genes. All functional genes were detected in almost all analyzed samples. Among the functional groups, sulfate-reducers were most abundant, especially their functional gene *aprA* occurred with maximum numbers of 10^9 copies/mL sediment. In contrast to the Black Sea sediments, both *mcrA* assays 1 and 2 of methanogens provided successful gene amplification, and *mcrA* and *cbbL* occurred not only in the near-surface sediment but also in the deeper subsurface sediment.

DISCUSSION

Microbial communities in the subsurface marine sediments of the Black Sea and the Benguela upwelling area off Namibia have been analyzed. Total cell counts, CARD–FISH data as well as Q-PCR analysis exhibited a high abundance of prokaryotes in the eutrophic, organic carbon-rich sediments at all six stations. A similar high abundance of prokaryotes analyzed by the same methods has been detected in organic carbon-rich sediments of the Peru margin (ODP Leg 201, D'Hondt et al., 2004; Schippers et al., 2005; Inagaki et al., 2006), gas-hydrate bearing sediments from the Cascadia margin (ODP Leg 204; Inagaki et al., 2006), northeast Pacific ridge-flank sediments (IODP Exp. 301; Engelen et al., 2008), tidal flat sediments of the North Sea (Wilms et al., 2007), and sediments off Sumatra (Schippers et al., 2010). Less organic carbon-rich marine sediments exhibited, as expected, a lower abundance of prokaryotes as shown for the equatorial Pacific (ODP Leg 201; D'Hondt et al., 2004; Schippers et al., 2005), the Porcupine Seabight (IODP Exp. 307; Webster et al., 2009), and the Gulf of Mexico (IODP Exp. 308; Nunoura et al., 2009). Oligotrophic, organic carbon-poor marine sediments contain generally very low cell numbers as shown for the South Pacific Gyre (D'Hondt et al., 2009), and the Western flank of the Mid-Atlantic Ridge at 23°N (North Pond; A. Breuker and A. Schippers, unpublished). A compilation of mean cell numbers determined by total cell counting, Q-PCR, and CARD–FISH in subsurface marine sediments of various sites is given in **Table 2**.

In this study, a decrease of cell numbers with sediment depth was observed for all stations as described for subsurface marine sediments (Parkes et al., 1994, 2000; D'Hondt et al., 2004). However, in the sapropel layer at 8–9 mbsf of the Black Sea station 22, the cell as well as the gene copy numbers again increased by more than an order of magnitude, explainable by the increased organic carbon content of the sapropel serving as substrate for the microorganisms. Such an increase in biomass at distinct geologically different sediment layers has been described for other sediments as well (Inagaki et al., 2003; Parkes et al., 2005), and in particular for sapropels (Coolen et al., 2002).

In the sediments of this study, total cell counts were determined after staining with SYBR Green® following two different protocols. Cell numbers directly counted in the sediment matrix (SGDC1) were verified by comparing the counts with those of the SGDC2 protocol in which the cells were detached from sediment particles before counting. The general depth trends of SGDC1 could be confirmed with SGDC2. However, the cell detachment method revealed somehow lower cell numbers as previously shown for subsurface marine sediments off Sumatra (Schippers et al., 2010) and terrestrial sediments in the Chesapeake area (Breuker et al., 2011). The difference in cell numbers between these two protocols was never higher than one order of magnitude in our study. A comparison of the total cell counts with the 16S rRNA gene copy numbers of the *Bacteria* and *Archaea* obtained by Q-PCR gives a good match for SGDC1 as well as for SGDC2, indicting a high reliability of the data for these quantification methods. CARD–FISH cell numbers were always considerably lower than SGDC 1. This indicates that either the majority of the cells was inactive, which seems to be unlikely in the organic-rich sediments, or more likely, insufficient cell wall permeabilization in the CARD–FISH protocol and mismatches of the archaeal CARD–FISH probe ARCH915 with predominant environmental gene sequences (Teske and Sørensen, 2008) prevented the detection of many living cells, especially *Archaea.*

The proportions of *Bacteria* and *Archaea* in marine sediments have shown to be highly variable in different sediments and sediment layers. Based on CARD–FISH and Q-PCR analyses overall similar proportions of *Bacteria* and *Archaea* have been determined for sediments studied here. An almost equal abundance of *Bacteria* and *Archaea* has also been found for the Porcupine Seabight (IODP Exp. 307; Webster et al., 2009), the northeast Pacific ridge-flank (IODP Exp. 301; Engelen et al., 2008), and Sumatra forearc basins (Schippers et al., 2010). By contrast, using Q-PCR it has been discovered that *Bacteria* dominated other sediments such as the Sea of Okhotsk (Inagaki et al., 2003), the Gulf of Mexico (IODP Exp. 308; Nunoura et al., 2009), the Peru continental margin, and the equatorial Pacific sediments (ODP Leg 201; Schippers et al., 2005; Inagaki et al., 2006; Schippers and Neretin, 2006), as well as gas-hydrate bearing sediments from the Cascadia margin (ODP Leg 204; Inagaki et al., 2006). The dominance of *Bacteria* for the Peru continental margin was confirmed by CARD–FISH (Schippers et al., 2005). Unlike nucleic acid based methods (CARD–FISH and Q-PCR), the analysis of intact polar lipids (IPL) of prokaryotic cell membranes unveiled *Archaea* as prevailing prokaryotes in deeply buried sediments (Biddle et al., 2006; Lipp et al., 2008). These conflicting results may be explained by insufficient quantitative extraction protocols, or primer mismatches (Teske and Sørensen, 2008) and/or a different preservation of DNA and IPL in deeply buried sediments (e.g., stabilized on clay surfaces or organic matter; Coolen et al., 2006a,b; Inagaki and Nealson, 2006; Schippers and Neretin, 2006; Boere et al., 2011). Recently, Schouten et al. (2010) as well as Logemann et al. (2011) reported the preservation of archaeal IPL biomarkers in marine sediments indicating that IPL biomarkers do not necessarily detect living *Archaea* and putting their proposed dominance in the deep biosphere into question. Obviously, it is not yet understood which factors control the proportions of *Bacteria* and *Archaea* in marine sediments.

Particular phylogenetic and physiological groups, inhabiting Black Sea and Benguela upwelling sediments, were revealed by Q-PCR in this study. The sediments were clearly dominated by prokaryotes since the abundance of eukaryotic 18S rRNA genes

Table 2 | Compilation of mean cell numbers (N/mL) in the depth range of 1–10 and 10–200 mbsf in subsurface marine sediments; nd, not determined.

Expedition	Total counts	Q-PCR	CARD–FISH	Total counts	Q-PCR	CARD–FISH	Reference
	1–10 mbsf			10–200 mbsf			
~20 ODP and other sites	10^7–10^9	nd	nd	10^6–10^8	nd	nd	Parkes et al. (1994, 2000), Bird et al. (2001), Wellsbury et al. (2002), Inagaki et al. (2003), Kallmeyer et al. (2008), Morono et al. (2009), Roussel et al. (2009)
ODP Leg 201 Equatorial Pacific	10^7	nd	10^6	10^6–10^7	nd	10^6	D'Hondt et al. (2004), Schippers et al. (2005)
ODP Leg 201 Peru margin	10^7–10^8	10^7	10^6	10^7	10^6	10^6	D'Hondt et al. (2004), Schippers et al. (2005), Inagaki et al. (2006)
ODP Leg 204 Cascadia margin	10^7	10^7	nd	10^6	10^6	nd	Inagaki et al. (2006), Nunoura et al. (2008)
IODP 301 Juan de Fuca	10^8–10^9	10^6–10^8	nd	10^8	10^6	nd	Engelen et al. (2008)
IODP 307 Porcupine Seamount				10^6–10^7	10^5–10^6	10^5–10^6	Webster et al. (2009)
IODP 308 Gulf of Mexico	10^5–10^6	10^5–10^6	nd	10^4–10^5	10^4–10^5	nd	Nunoura et al. (2009)
IODP 313 New Jersey Shallow Shelf	10^6	10^5–10^6	nd	10^5–10^6	10^5–10^6	nd	A. Breuker, S. Stadler, and A. Schippers (unpublished)
North Sea tidal flat	10^7–10^8	10^7	nd				Wilms et al. (2007)
SO 189 Forearc off Sumatra	10^7–10^8	10^7–10^8	nd				Schippers et al. (2010)
South Pacific Gyre	10^3–10^4	nd	nd				D'Hondt et al. (2009)
MSM 11-1 "North Pond"	10^5–10^6	10^4–10^6	nd				A. Breuker and A. Schippers (unpublished)
M 72-5 Black Sea	10^7–10^8	10^5–10^6	10^5–10^6				This study
M 76-1 Benguela Upwelling	10^7–10^9	10^6–10^8	10^6–10^7				This study
ICDP Chesapeake Bay terrestrial sediments	10^6–10^7	10^6–10^7	10^6	10^6	10^6	nd	Breuker et al. (2011)

comprised only 3% and <1% of the number of prokaryotic 16S rRNA genes for the Black Sea and Namibia sediments, respectively. This can be attributed to the small pore space in subsurface sediments which impedes growth of large eukaryotic cells. Similar Q-PCR results were obtained for the organic carbon-rich sediments off Sumatra (Schippers et al., 2010) and for Peru margin sediments (Schippers and Neretin, 2006). In the latter sediments, mainly fungi have been identified as dominant *Eukarya* (Edgcomb et al., 2011). In the near-surface anoxic and sulfidic sediments of the Black Sea the following eukaryotic groups were detected via DGGE and 18S rRNA gene sequencing: copepods, rotifers, haptophytes, dinoflagellates, and ciliates (Coolen and Shtereva, 2009). Data on the composition of *Eukarya* in the deeper, subsurface sediment are not available.

As previously shown for the sediments off Sumatra, the Peru margin and the Black Sea station 20 (Blazejak and Schippers, 2010), the bacterial candidate division JS-1 and the classes *Anaerolineae* and *Caldilineae* of the phylum *Chloroflexi* were at least as highly abundant as the *Bacteria* for the other five stations of this study as well. This confirms their dominant role in subsurface marine sediments (Webster et al., 2004; Teske, 2006; Fry et al., 2008). *Crenarchaeota* were previously identified as dominant members in the archaeal 16S rRNA gene clone libraries (Teske, 2006; Fry et al., 2008; Teske and Sørensen, 2008). This is consistent with our finding that this group could be quantified by Q-PCR in comparable (or higher) copy numbers than the *Archaea* in subsurface marine sediments of the Black Sea and the Benguela upwelling sediments. Moreover, uncultured *Crenarchaeota* as well as *Chloroflexi* have also been identified in one subsurface sediment core (station GeoB 3703) from the Benguela upwelling area (Schäfer et al., 2007). In many samples of our study more *Crenarchaeota* than *Archaea,* and more JS-1 and *Chloroflexi* than *Bacteria* were detected. This discrepancy may be explained by PCR bias due to different PCR efficiencies for the particular Q-PCR assays, primer mismatches of the general 16S rRNA gene primers with predominant environmental gene sequences (Teske and Sørensen, 2008), and probably different 16S rRNA gene copy numbers per cell which are unknown for the particular specific archaeal and bacterial groups analyzed in this study.

Functional genes were quantified by Q-PCR to demonstrate the importance of particular physiological prokaryotic groups. The functional genes *dsrA* and *aprA* of sulfate-reducers and the gene *mcrA* of methanogens were highly abundant in the Black Sea as well as in the Namibia sediments. This finding is not surprising because sulfate reduction, methanogenesis, and anaerobic methane oxidation were shown to be important biogeochemical processes in these sediments (Niewöhner et al., 1998; Ferdelman et al., 1999; Fossing et al., 2000; Jørgensen et al., 2001, 2004; Brüchert et al., 2003, 2006; Knab et al., 2008; Riedinger et al., 2010; Holmkvist et al., 2011). Q-PCR based *dsrA* quantification in another Black Sea subsurface sediment core also revealed that sulfate-reducers were highly abundant throughout the whole sampling depth of 4.6 mbsf (Leloup et al., 2007). A *dsrA* clone library

in the same study showed mostly sequences affiliated with the *Desulfobacteraceae*.

The detection of the functional gene *cbbL* coding for the large subunit of the form I "red-like" RuBisCO was different for the Black Sea and the Benguela upwelling samples. While in the latter the gene was detected in lower copy numbers in most samples and all depth, *cbbL* was mainly detectable only in near-surface sediments of the Black Sea. Overall, autotrophy via the RuBisCO pathway seems to play some role in these samples, despite its high organic carbon content supporting heterotrophy as shown for the organic carbon-rich sediments of the Peru margin (D'Hondt et al., 2004; Biddle et al., 2006). A higher abundance of the same *cbbL* gene than in this study was recently detected in the organic carbon-poor terrestrial subsurface sediments in the Chesapeake Bay area, VA, USA (Breuker et al., 2011). There, in agreement with the lower organic carbon content, autotrophy seems to be more important than in the marine sediments of this study.

CONCLUSION

The microbial communities in the subsurface marine sediments of the Black Sea and the Benguela upwelling area off Namibia have been quantitatively analyzed at six stations using total cell counts, CARD–FISH and 12 different Q-PCR assays. A high abundance of *Prokaryotes* and overall similar proportions of *Bacteria* and *Archaea* were discovered in the eutrophic, organic carbon-rich sediments. *Crenarchaeota* and the bacterial candidate division JS-1 and the classes *Anaerolineae* and *Caldilineae* of the phylum *Chloroflexi* were as highly abundant. In agreement with the reported ongoing sulfate reduction and methanogenesis, the functional genes *dsrA* and *aprA* of sulfate-reducers and the gene *mcrA* of methanogens were highly abundant as well, suggesting a vital microbial community performing these processes. The detection of the *cbbL* gene shows the occurrence of autotrophic microorganisms.

ACKNOWLEDGMENTS

We thank the RV Meteor M72-5 and M76-1 chiefs C. Borowski, T. G. Ferdelman and M. Zabel, and especially B. Engelen for helpful suggestions and advice. Special thanks also go to G. Mengel-Jung and C. Struckmeyer for laboratory analyses, and S. Eckert, B. Schnettger, Y. Lin, and K.-U. Hinrichs for providing TOC data. This work was supported by the German Research Foundation (DFG) priority program IODP/ODP grant SCHI 535/7 to Axel Schippers.

REFERENCES

Badger, M. R., and Bek, E. J. (2008). Multiple Rubisco forms in proteobacteria: their functional significance in relation to CO_2 acquisition by the CBB cycle. *J. Exp. Bot.* 59, 1525–1541.

Biddle, J. F., Fitz-Gibbon, S., Schuster, S. C., Brenchley, J. E., and House, C. H. (2008). Metagenomic signatures of the Peru Margin subseafloor biosphere show a genetically distinct environment. *Proc. Natl. Acad. Sci. U.S.A.* 105, 10583–10588.

Biddle, J. F., Lipp, J. S., Lever, M., Lloyd, K. G., Sørensen, K. B., Anderson, R., Fredricks, H. F., Elvert, M., Kelly, T. J., Schrag, D. P., Sogin, M. L., Brenchley, J. E., Teske, A., House, C. H., and Hinrichs, K. U. (2006). Heterotrophic archaea dominate sedimentary subsurface ecosystems off Peru. *Proc. Natl. Acad. Sci. U.S.A.* 103, 3846–3851.

Bird, D. F., Juniper, S. K., Ricciardi-Rigault, M., Martineu, P., Prairie, Y. T., and Calvert, S. E. (2001). Subsurface viruses and bacteria in Holocene/Late Pleistocene sediments of Saanich Inlet, BC: ODP Holes 1033B and 1034B, Leg 169S. *Mar. Geol.* 174, 227–239.

Blazejak, A., and Schippers, A. (2010). High abundance of JS-1- and *Chloroflexi*-related bacteria in deeply buried marine sediments revealed by quantitative, real-time PCR. *FEMS Microbiol. Ecol.* 72, 198–207.

Blazejak, A., and Schippers, A. (2011). Real-time PCR quantification and diversity analysis of the functional genes *aprA* and *dsrA* of sulfate-reducing bacteria in marine sediments of the Peru continental margin and the Black Sea. *Front. Microbiol.* 2:253. doi:10.3389/fmicb.2011.00253

Boere, A. C., Rijpstra, W. I. C., DeLange, G. J., Sinninghe Damsté, J. S., and Coolen, M. J. L. (2011). Preservation potential of ancient plankton DNA in Pleistocene marine sediments. *Geobiology* 9, 377–393.

Breuker, A., Köweker, G., Blazejak, A., and Schippers, A. (2011). The deep biosphere in terrestrial sediments of the Chesapeake Bay impact structure, Virginia, USA. *Front. Microbiol.* 2:156. doi:10.3389/fmicb.2011.00156

Brüchert, V., Currie, B., Peard, K. R., Lass, U., Endler, R., Dübecke, A., Julies, E., Leipe, T., and Zitzmann, S. (2006). "Biogeochemical and physical control on shelf anoxia and water column hydrogen sulphide in the Benguela coastal upwelling system off Namibia," in *Past and Present Water Column Anoxia, NATO Science Series, IV. Earth and Environmental Sciences*, Vol. 64, ed. L. N. Neretin (Heidelberg: Springer), 161–193.

Brüchert, V., Jørgensen, B., Neumann, K., Riechmann, D., Schlösser, M., and Schulz, H. N. (2003). Regulation of bacterial sulfate reduction and hydrogen sulfide fluxes in the central Namibian coastal upwelling zone. *Geochim. Cosmochim. Acta* 67, 4505–4518.

Brüchert, V., Perez, M. E., and Lange, C. B. (2000). Coupled primary production, benthic foraminiferal assemblage, and sulfur diagenesis in organic-rich sediments of the Benguela upwelling system. *Mar. Geol.* 163, 27–40.

Brumsack, H.-J. (1989). Geochemistry of recent TOC-rich sediments from the Gulf of California and the Black Sea. *Geol. Rundsch.* 78, 851–882.

Colwell, F. S., Boyd, S., Delwiche, M. E., Reed, D. W., Phelps, T. J., and Newby, D. T. (2008). Estimates of biogenic methane production rates in deep marine sediments at Hydrate Ridge, Cascadia Margin. *Appl. Environ. Microbiol.* 74, 3444–3452.

Coolen, M. J. L., Boere, A., Abbas, B., Baas, M., Wakeham, S. G., and Sinninghe Damsté, J. S. (2006a). Fossil DNA derived from alkenone-biosynthesizing haptophytes and other algae in Holocene sediment from the Black Sea. *Paleoceanography* 21, 1–17.

Coolen, M. J. L, Muyzer, G., Schouten, S., Volkman, J. K., and Sinninghe Damsté, J. S. (2006b). "Sulfur and methane cycling during the Holocene in Ace Lake (Antarctica) revealed by lipid and DNA stratigraphy," in *Past and Present Water Column Anoxia, NATO Science Series, IV. Earth and Environmental Sciences*, Vol. 64, ed. L. N. Neretin (Heidelberg: Springer), 41–65.

Coolen, M. J. L., Cypionka, H., Sass, A. M., Sass, H., and Overmann, J. (2002). Ongoing modification of Mediterranean Pleistocene sapropels mediated by prokaryotes. *Science* 296, 2407–2410.

Coolen, M. J. L., and Shtereva, G. (2009). Vertical distribution of metabolically active eukaryotes in the water column and sediments of the Black Sea. *FEMS Microbiol. Ecol.* 70, 525–539.

Dale, A. W., Brüchert, V., Alperin, M., and Regnier, P. (2009). An integrated sulfur isotope model for Namibian shelf sediments. *Geochim. Cosmochim. Acta* 73, 1924–1944.

D'Hondt, S., Spivack, A. J., Pockalny, R., Ferdelman, T. G., Fischer, J. P., Kallmeyer, J., Abrams, L. J., Smith, D. C., Graham, D., Hasiuk, F., Schrum, H., and Stancin, A. M. (2009). Subseafloor sedimentary life in the South Pacific Gyre. *Proc. Natl. Acad. Sci. U.S.A.* 106, 11651–11656.

D'Hondt, S. L., Jørgensen, B. B., Miller, D. J., Batzke, A., Blake, R., Cragg, B. A., Cypionka, H., Dickens, G. R., Ferdelman, T. G., Hinrichs, K. U., Holm, N. G., Mitterer, R., Spivack, A., Wang, G., Bekins, B., Engelen, B., Ford, K., Gettemy, G., Rutherford, S. D., Sass, H., Skilbeck, C. G., Aiello, I. W., Guèrin, G., House, C. H., Inagaki, F., Meister, P., Naehr, T., Niitsuma, S., Parkes, R. J., Schippers, A., Smith, D. C., Teske, A., Wiegel, J., Padilla, C. N., and Solis Acosta, J. L. (2004). Distributions of microbial activities in deep subseafloor sediments. *Science* 306, 2216–2221.

Edgcomb, V. P., Beaudoin, D., Gast, R., Biddle, J. F., and Teske, A. (2011). Marine subsurface eukaryotes: the fungal majority. *Environ. Microbiol.* 13, 172–183.

Emeis, K., Brüchert, V., Currie, B., Endler, R., Ferdelman, T., Kiessling, A., Leipe, T., Noli-Peard, K., Struck, U., and Vogt, T. (2004). Shallow gas in shelf sediments of the Namibian coastal upwelling ecosystem. *Cont. Shelf Res.* 24, 627–642.

Engelen, B., Ziegelmüller, K., Wolf, L., Köpke, B., Gittel, A., Cypionka, H., Treude, T., Nakagawa, S., Inagaki, F., Lever, M. A., and Steinsbu, B. O. (2008). Fluids from the oceanic crust support microbial activities within the deep biosphere. *Geomicrobiol. J.* 25, 55–66.

Ferdelman, T. G., Fossing, H., Neumann, K., and Schulz, H. D. (1999). Sulfate reduction in surface sediments of the southeast Atlantic continental margin between 15°38'S and 27°57'S (Angola and Namibia). *Limnol. Oceanogr.* 44, 650–661.

Fossing, H., Ferdelman, T. G., and Berg, P. (2000). Sulfate reduction and methane oxidation in continental margin sediments influenced by irrigation (South–East Atlantic off Namibia). *Geochim. Cosmochim. Acta* 64, 897–910.

Fry, J. C., Parkes, R. J., Cragg, B. A., Weightman, A. J., and Webster, G. (2008). Prokaryotic diversity and activity in the deep subseafloor biosphere. *FEMS Microbiol. Ecol.* 66, 181–196.

Goldhammer, T., Brüchert, V., Ferdelman, T. G., and Zabel, M. (2010). Microbial sequestration of phosphorus in anoxic upwelling sediments. *Nat. Geosci.* 3, 557–561.

Goldhammer, T., Brunner, B., Bernasconi, S. M., Ferdelman, T. G., and Zabel, M. (2011). Phosphate oxygen isotopes: insights into sedimentary phosphorus cycling from the Benguela upwelling system. *Geochim. Cosmochim. Acta* 75, 3741–3756.

Holmes, D. E., Finneran, K. T., O'Neil, R. A., and Lovley, D. R. (2002). Enrichment of members of the family *Geobacteraceae* associated with stimulation of dissimilatory metal reduction in uranium-contaminated aquifer sediments. *Appl. Environ. Microbiol.* 68, 2300–2306.

Holmkvist, L., Kamyshny, A. Jr., Vogt, C., Vamvakopoulos, K., Ferdelman, T. G., and Jørgensen, B. B. (2011). Sulfate reduction below the sulfate–methane transition in Black Sea sediments. *Deep Sea Res. Part I Oceanogr. Res. Pap.* 58, 493–504.

Inagaki, F., and Nealson, K. H. (2006). "The paleome: letters from ancient earth", in *Past and Present Water Column Anoxia, NATO Science Series, IV. Earth and Environmental Sciences,* Vol. 64, ed. L. N. Neretin (Heidelberg: Springer), 21–39.

Inagaki, F., Nunoura, T., Nakagawa, S., Teske, A., Lever, M., Lauer, A., Suzuki, M., Takai, K., Delwiche, M., Colwell, F. S., Nealson, K. H., Horikoshi, K., D'Hondt, S., and Jørgensen, B. B. (2006). Biogeographical distribution and diversity of microbes in methane hydrate-bearing deep marine sediments on the Pacific ocean margin. *Proc. Natl. Acad. Sci. U.S.A.* 103, 2815–2820.

Inagaki, F., Suzuki, M., Takai, K., Oida, H., Sakamoto, T., Aoki, K., Nealson, K. H., and Horikoshi, K. (2003). Microbial communities associated with geological horizons in coastal subseafloor sediments from the Sea of Okhotsk. *Appl. Environ. Microbiol.* 69, 7224–7235.

Jørgensen, B. B., Böttcher, M. E., Holger, L., Neretin, L. N., and Volkov, I. I. (2004). Anaerobic methane oxidation and a deep H_2S sink generate isotopically heavy sulfides in Black Sea sediments. *Geochim. Cosmochim. Acta* 68, 2095–2118.

Jørgensen, B. B., Weber, A., and Zopfi, J. (2001). Sulfate reduction and anaerobic methane oxidation in Black Sea sediments. *Deep Sea Res. Part I Oceanogr. Res. Pap.* 48, 2097–2120.

Julies, E. M., Fuchs, B. M., Arnosti, C., and Brüchert, V. (2010). Organic carbon degradation in anoxic organic-rich shelf sediments: biogeochemical rates and microbial abundance. *Geomicrobiol. J.* 27, 303–314.

Kallmeyer, J., Smith, D. C., Spivack, A. J., and D'Hondt, S. L. (2008). New cell extraction procedure applied to deep subsurface sediments. *Limnol. Oceanogr. Methods* 6, 236–245.

Knab, N. J., Cragg, B. A., Hornibrook, E. R. C., Holmkvist, L., Borowski, C., Parkes, R. J., and Jørgensen, B. B. (2008). Regulation of anaerobic methane oxidation in sediments of the Black Sea. *Biogeosci. Discuss.* 5, 2305–2341.

Knoblauch, C., Jørgensen, B. B., and Harder, J. (1999). Community size and metabolic rates of psychrophilic sulfate-reducing bacteria in Arctic marine sediments. *Appl. Environ. Microbiol.* 65, 4230–4233.

Leloup, J., Loy, A., Knab, N. J., Borowski, C., Wagner, M., and Jørgensen, B. B. (2007). Diversity and abundance of sulfate-reducing microorganisms in the sulfate and methane zones of a marine sediment, Black Sea. *Environ. Microbiol.* 9, 131–142.

Lipp, J. S., Morono, Y., Inagaki, F., and Hinrichs, K. U. (2008). Significant contribution of *Archaea* to extent biomass in marine subsurface sediments. *Nature* 454, 991–994.

Logemann, J., Graue, J., Köster, J., Engelen, B., Rullkötter, J., and Cypionka, H. (2011). A laboratory experiment of intact polar lipid degradation in sandy sediments. *Biogeosci. Discuss.* 8, 3289–3321.

Morono, Y., Terada, T., Masui, N., and Inagaki, F. (2009). Discriminative detection and enumeration of microbial life in marine subsurface sediments. *ISME J.* 3, 503–511.

Nadkarni, M., Martin, F. E., Jacques, N. A., and Hunter, N. (2002). Determination of bacterial load by real-time PCR using a broad range (universal) probe and primer set. *Microbiology* 148, 257–266.

Neretin, L. N., Abed, R. M. M., Schippers, A., Schubert, C. J., Kohls, K., and Kuypers, M. M. M. (2007). Inorganic carbon fixation by sulfate-reducing bacteria in the Black Sea water column. *Environ. Microbiol.* 9, 3019–3024.

Neretin, L. N., Böttcher, M. E., Jørgensen, B. B., Volkov, I. I., Lüschen, H., and Hilgenfeldt, K. (2004). Pyritization processes and greigite formation in the advancing sulfidization front in the upper Pleistocene sediments of the Black Sea. *Geochim. Cosmochim. Acta* 68, 2081–2093.

Niewöhner, C., Hensen, C., Kasten, S., Zabel, M., and Schulz, H. D. (1998). Sulfate reduction completely mediated by anaerobic methane oxidation in sediments of the upwelling area off Namibia. *Geochim. Cosmochim. Acta* 62, 455–464.

Nunoura, T., Inagaki, F., Delwiche, M. E., Colwell, F. S., and Takai, K. (2008). Subseafloor microbial communities in methane hydrate-bearing sediments of two distinct locations (ODP Leg 204) in the Cascadia margin. *Microbes Environ.* 23, 317–325.

Nunoura, T., Soffientino, B., Blazejak, A., Kakuta, J., Oida, H., Schippers, A., and Takai, K. (2009). Subseafloor microbial communities associated with rapid turbidite deposition in the Gulf of Mexico continental slope (IODP Expedition 308). *FEMS Microbiol. Ecol.* 69, 410–424.

Ochsenreiter, T., Selezi, D., Quaiser, A., Bonch-Osmolovskaya, L., and Schleper, C. (2003). Diversity and abundance of *Crenarchaeota* in terrestrial habitats studied by 16S RNA surveys and real time PCR. *Environ. Microbiol.* 5, 787–797.

Parkes, R. J., Cragg, B. A., Bale, S. J., Getliff, J. M., Goodman, K., Rochelle, P. A., Fry, J. C., Weightman, A. J., and Harvey, S. M. (1994). Deep bacterial biosphere in Pacific Ocean sediments. *Nature* 371, 410–413.

Parkes, R. J., Cragg, B. A., and Wellsbury, P. (2000). Recent studies on bacterial populations and processes in subseafloor sediments: a review. *Hydrogeol. J.* 8, 11–28.

Parkes, R. J., Webster, G., Cragg, B. A., Weightman, A. J., Newberry, C. J., Ferdelman, T. G., Kallmeyer, J., Jørgensen, B. B., Aiello, I. W., and Fry, J. C. (2005). Deep sub-seafloor prokaryotes stimulated at interfaces over geological time. *Nature* 436, 390–394.

Pernthaler, A., Pernthaler, J., and Amann, R. (2002). Fluorescence in situ hybridization and catalyzed reporter deposition for the identification of marine bacteria. *Appl. Environ. Microbiol.* 68, 3094–3101.

Ravenschlag, K., Sahm, K., Knoblauch, C., Jørgensen, B. B., and Amann, R. (2000). Community structure, cellular rRNA content and activity of sulfate-reducing bacteria in marine Arctic sediments. *Appl. Environ. Microbiol.* 66, 3592–3602.

Riedinger, N., Brunner, B., Lin, Y.-S., Voßmeyer, A., Ferdelman, T. G., and Jørgensen, B. B. (2010). Methane at the sediment-water transition in the Black Sea sediments. *Chem. Geol.* 274, 29–37.

Roussel, E. G., Sauvadet, A.-L., Chaduteau, C., Fouquet, Y., Charlou, J.-L., Prieur, D., and Cambon Bonavita, M.-A. (2009). Archaeal communities associated with shallow to deep subseafloor sediments of the New Caledonia Basin. *Environ. Microbiol.* 11. 2446–2462.

Sahm, K., Knoblauch, C., and Amann, R. (1999). Phylogenetic affiliation and quantification of psychrophilic sulfate-reducing isolates in marine Arctic sediments. *Appl. Environ. Microbiol.* 65, 3976–3981.

Schäfer, H., Ferdelman, T. G., Fossing, H., and Muyzer, G. (2007). Microbial diversity in deep sediments of the Benguela Upwelling System. *Aquat. Microb. Ecol.* 50, 1–9.

Schippers, A., Köweker, G., Höft, C., and Teichert, B. (2010). Quantification

of microbial communities in three forearc sediment basins off Sumatra. *Geomicrobiol. J.* 27, 170–182.

Schippers, A., and Neretin, L. N. (2006). Quantification of microbial communities in near-surface and deeply buried marine sediments on the Peru continental margin using real-time PCR. *Environ. Microbiol.* 8, 1251–1260.

Schippers, A., Neretin, L. N., Kallmeyer, J., Ferdelman, T. G., Cragg, B. A., Parkes, R. J., and Jørgensen, B. B. (2005). Prokaryotic cells of the deep sub-seafloor biosphere identified as living bacteria. *Nature* 433, 861–864.

Schouten, S., Middelburg, J. J., Hopmans, E. C., and Sinninghe Damsté, J. S. (2010). Fossilization and degradation of intact polar lipids in deep subsurface sediments: a theoretical approach. *Geochim. Cosmochim. Acta* 74, 3806–3814.

Schubotz, F., Wakeham, S. G., Lipp, J. S., Fredricks, H. F., and Hinrichs, K.-U. (2009). Detection of microbial biomass by intact membrane lipid analysis in the water column and surface sediments of the Black Sea. *Environ. Microbiol.* 11, 2720–2734.

Schulz, H. N., Brinkhoff, T., Ferdelman, T. G., Mariné, M. H., Teske, A., and Jørgensen, B. B. (1999). Dense populations of a giant sulfur bacterium in Namibian shelf sediments. *Science* 284, 493–495.

Schulz, H. N., and Schulz, H. D. (2005). Large sulfur bacteria and the formation of phosphorite. *Science* 307, 416–418.

Selesi, D., Pattis, I., Schmid, M., Kandeler, E., and Hartmann, A. (2007). Quantification of bacterial RubisCO genes in soils by cbbL targeted real-time PCR. *J. Microbiol. Methods* 69, 497–503.

Steinberg, L. M., and Regan, J. M. (2009). *mcrA*-targeted real-time quantitative PCR method to examine methanogen communities. *Appl. Environ. Microbiol.* 75, 4435–4442.

Takai, K., and Horikoshi, K. (2000). Rapid detection and quantification of members of the archaeal community by quantitative PCR using fluorogenic probes. *Appl. Environ. Microbiol.* 66, 5066–5072.

Teske, A. P. (2006). Microbial communities of deep marine subsurface sediments: molecular and cultivation surveys. *Geomicrobiol. J.* 23, 357–368.

Teske, A. P., and Sørensen, K. B. (2008). Uncultured archaea in deep marine subsurface sediments: have we caught them all? *ISME J.* 2, 3–18.

Thamdrup, B., Rosselló-Mora, R., and Amann, R. (2000). Microbial manganese and sulfate reduction in Black Sea shelf sediments. *Appl. Environ. Microbiol.* 66, 2888–2897.

Webster, G., Blazejak, A., Cragg, B. A., Schippers, A., Sass, H., Rinna, J., Tang, X., Mathes, F., Ferdelman, T. G., Fry, J. C., Weightman, A. J., and Parkes, R. J. (2009). Subsurface microbiology and biogeochemistry of a deep, cold-water carbonate mound from the Porcupine Seabight (IODP Expedition 307). *Environ. Microbiol.* 11, 239–257.

Webster, G., Newberry, C. J., Fry, J. C., and Weightman, A. J. (2003). Assessment of bacterial community structure in the deep sub-seafloor biosphere by 16S rDNA-based techniques: a cautionary tale. *J. Microbiol. Methods* 55, 155–164.

Webster, G., Parkes, R. J., Fry, J. C., and Weightman, A. J. (2004). Widespread occurrence of a novel division of bacteria identified by 16S rDNA gene sequences originally found in deep marine sediments. *Appl. Environ. Microbiol.* 70, 5708–5713.

Weinbauer, M. G., Beckmann, C., and Höfle, M. G. (1998). Utility of green fluorescent nucleic acid dyes and aluminium oxide membrane filters for rapid epifluorescence enumeration of soil and sediment bacteria. *Appl. Environ. Microbiol.* 64, 5000–5003.

Wellsbury, P., Mather, I., and Parkes, R. J. (2002). Geomicrobiology of deep, low organic-carbon sediments in the Woodlark Basin, Pacific Ocean. *FEMS Microbiol. Ecol.* 42, 59–70.

Wilms, R., Sass, H., Köpke, B., Cypionka, H., and Engelen, B. (2007). Methane and sulfate profiles within the subsurface of a tidal flat are reflected by the distribution of sulfate-reducing bacteria and methanogenic archaea. *FEMS Microbiol. Ecol.* 59, 611–621.

Yilmaz, A., Çoban-Yildiz, Y., Telli-Karakoç, F., and Bologa, A. (2006). Surface and mid-water sources of organic carbon by photoautotrophic and chemoautotrophic production in the Black Sea. *Deep Sea Res. Part II Top. Stud. Oceanogr.* 53, 1988–2004.

Conflict of Interest Statement: The authors declare that the research was conducted in the absence of any commercial or financial relationships that could be construed as a potential conflict of interest.

Received: 07 September 2011; paper pending published: 06 October 2011; accepted: 09 January 2012; published online: 30 January 2012.

*Citation: Schippers A, Kock D, Höft C, Köweker G and Siegert M (2012) Quantification of microbial communities in subsurface marine sediments of the Black Sea and off Namibia. Front. Microbio. **3**:16. doi: 10.3389/fmicb.2012.00016*

This article was submitted to Frontiers in Extreme Microbiology, a specialty of Frontiers in Microbiology.

frontiers in
MICROBIOLOGY

GENERAL COMMENTARY
published: 31 January 2012
doi: 10.3389/fmicb.2012.00022

There must be an acetogen somewhere

Aharon Oren*

Department of Plant and Environmental Sciences, The Alexander Silberman Institute of Life Sciences, The Hebrew University of Jerusalem, Jerusalem, Israel
**Correspondence: orena@cc.huji.ac.il*

A commentary on

Acetogenesis in the energy-starved deep biosphere – a paradox?
by Mark Alexander Lever (2012). Front. Microbiol. 2:284. doi: 10.3389/fmicb.2011.00284

In the beginning of 1983, when I was a post-doctoral student at the University of Illinois, Ralph Wolfe handed me an offprint of a long article and said: "Read this!" That paper was the review by Thauer et al. (1977) on "Energy conservation in chemotrophic anaerobic bacteria." I have read it many times. I remember that the first and second time I understood very little. During the third and fourth reading I started to grasp the ideas expressed and to appreciate them. And after having read the paper for the fifth and sixth time I had become convinced that microbial metabolism and metabolic diversity can only be properly understood using the kind of thermodynamic analyses on which Thauer and his colleagues based their review. Until this day I use this thermodynamic approach to explain the functioning of the microbial world in the basic and more advanced microbiology courses I teach.

At the same time Ralph Wolfe also introduced me to the world of the acetogens. I still remember how excited he was that the culture of *Clostridium aceticum*, isolated in the 1930s (Wieringa, 1936) but subsequently considered as lost, had been revived from a preparation of endospores of the original strain and thus became again available for study (Braun et al., 1981). The place of the acetogens in nature, and especially those species that live as autotrophs on hydrogen as their energy source, has always been enigmatic. The reason becomes immediately obvious when calculating the thermodynamics of the process, comparing the Gibbs free energy change under standard conditions of three competing processes: sulfate reduction, methanogenesis, and homoacetogenic metabolism:

$$4H_2 + SO_4^{2-} + H^+ \rightarrow HS^- + 4H_2O$$
$$\Delta G_o' = -152.2 \text{ kJ}$$

$$4H_2 + HCO_3^- + H^+ \rightarrow CH_4 + 3H_2O$$
$$\Delta G_o' = -135.6 \text{ kJ}$$

$$4H_2 + 2HCO_3^- + H^+ \rightarrow CH_3COO^- + 4H_2O$$
$$\Delta G_o' = -104.6 \text{ kJ}$$

As long as sulfate is available, sulfate reducers will consume most of the hydrogen. They obtain more energy from hydrogen oxidation, and their affinity for hydrogen is much higher than that of the methanogenic Archaea, explaining why the methanogens are out-competed when the energy source is limiting (Kristjansson et al., 1982). When sulfate is limiting, methanogens will take over. No similar competition studies between methanogens and acetogens were ever reported, but based on the lower energy yield of the acetogenic reaction it is highly probably that the acetogens will lose the competition. Recent calculations confirm this: assuming a "biological energy quantum" (the minimum amount of free energy change of a reaction that can drive the formation of ATP) of −10 kJ, the thermodynamic threshold concentrations of H_2 calculated for chemolithoautotrophic sulfate reducers, methanogens, and acetogens are ~0.6, 11, and 410 nM, respectively (Lever, 2011). These numbers clearly show that the "homoacetogenic" reaction from H_2–CO_2 is thermodynamically unfavorable. The advantage of the methanogens over the acetogens is also demonstrated in the following calculation: at partial pressures for hydrogen and for methane of 10^{-4} and 0.5 atm, respectively, and bicarbonate, and acetate concentrations of 100 and 10 mM, the Gibbs free energy is −40 kJ per reaction for the formation of methane from bicarbonate and hydrogen, but only −13 kJ for the formation of acetate. Dolfing (1988) wrote: "A meaningful evaluation of the energy conservation and the selection mechanism that govern the outcome of competition between methanogens and acetogens has to wait until more data are available on (growth parameters) μ, K_s, K_m, Y, and q of these organisms, preferably obtained in chemostat experiments." To my knowledge no such experiments have yet been performed.

The question therefore remains where in nature the acetogens can out-compete the methanogens. In recent years evidence is accumulating that, unexpectedly, acetogens may represent a quantitatively important component of the microbial ecosystem in the oligotrophic marine and terrestrial deep biosphere. The paper by Lever provides an in-depth analysis of the possible factors that give the acetogens advantages in this vast, but largely unexplored niche. Lever argues that under conditions encountered in the subseafloor, the energy yields of most acetogenesis reactions are sufficient to support growth. Furthermore, acetogens have a remarkable metabolic flexibility compared to methanogens and sulfate reducers, and can use more substrates or substrate combinations as energy source. Moreover, the fact that they use the energy-efficient reductive acetyl-CoA pathway (also known as the Wood–Ljungdahl pathway) both for autotrophic carbon fixation and for energy production makes their metabolism highly efficient, enabling them to save precious energy for survival when stressed (Lever, 2011).

The title of this commentary – "There must be an acetogen somewhere" paraphrases Woese's (1994) "There must be a prokaryote somewhere." Nobody can have any doubt that prokaryotes play a central function in nature, but the role of the acetogens was never really clear. Therefore Lever's paper contributes much toward a proper assessment of the place of this intriguing group of prokaryotes in anaerobic ecosystems worldwide.

REFERENCES

Braun, M., Mayer, F., and Gottschalk, G. (1981). *Clostridium aceticum* (Wieringa), a microorganism producing acetic acid from molecular hydrogen and carbon dioxide. *Arch. Microbiol.* 128, 188–293.

Dolfing, J. (1988). "Acetogenesis," in *Environmental Microbiology of Anaerobes*, ed. A. J. B. Zehnder (New York: John Wiley & Sons), 417–468.

Kristjansson, J. K., Schönheit, P., and Thauer, R. K. (1982). Different Ks values for hydrogen of methanogenic bacteria and sulfate reducing bacteria: an explanation for the apparent inhibition of methanogenesis by sulfate. *Arch. Microbiol.* 131, 278–283.

Lever, M. A. (2011). Acetogenesis in the energy-starved deep biosphere – a paradox? *Front. Microbiol.* 2, 284. doi: 10.3389/fmicb.2011.00284

Thauer, R. K., Jungermann, K., and Decker, K. (1977). Energy conservation in chemotrophic anaerobic bacteria. *Bacteriol. Rev.* 41, 100–180.

Wieringa, K. T. (1936). Over het verdwijnen van waterstof en koolzuur onder anaerobe voorwaarden. *Antonie van Leeuwenhoek* 3, 263–273.

Woese, C. R. (1994). There must be a prokaryote somewhere: microbiology's search for itself. *Microbiol. Rev.* 58, 1–9.

Received: 12 January 2012; accepted: 13 January 2012; published online: 31 January 2012.

*Citation: Oren A (2012) There must be an acetogen somewhere. Front. Microbiol. **3**:22. doi: 10.3389/fmicb.2012.00022*

This article was submitted to Frontiers in Extreme Microbiology, a specialty of Frontiers in Microbiology.

frontiers in
MICROBIOLOGY

METHODS ARTICLE
published: 03 February 2012
doi: 10.3389/fmicb.2012.00025

A system for incubations at high gas partial pressure

Patrick Sauer*, Clemens Glombitza and Jens Kallmeyer

Geomicrobiology Group, Institute for Earth and Environmental Sciences, University of Potsdam, Potsdam, Germany

Edited by:
Andreas Teske, University of North Carolina at Chapel Hill, USA

Reviewed by:
Doug Bartlett, Scripps Institution of Oceanography, USA
Gordon Webster, Cardiff University, UK

****Correspondence:***
Patrick Sauer, Geomicrobiology Group, Institute for Earth- and Environmental Sciences, University of Potsdam, Karl-Liebknecht-Straße 24-25, 14476 Potsdam, Germany.
e-mail: sauer@geo.uni-potsdam.de

High-pressure is a key feature of deep subsurface environments. High partial pressure of dissolved gasses plays an important role in microbial metabolism, because thermodynamic feasibility of many reactions depends on the concentration of reactants. For gases, this is controlled by their partial pressure, which can exceed 1 MPa at *in situ* conditions. Therefore, high hydrostatic pressure alone is not sufficient to recreate true deep subsurface *in situ* conditions, but the partial pressure of dissolved gasses has to be controlled as well. We developed an incubation system that allows for incubations at hydrostatic pressure up to 60 MPa, temperatures up to 120˚C, and at high gas partial pressure. The composition and partial pressure of gasses can be manipulated during the experiment. To keep costs low, the system is mainly made from off-the-shelf components with only very few custom-made parts. A flexible and inert PVDF (polyvinylidene fluoride) incubator sleeve, which is almost impermeable for gases, holds the sample and separates it from the pressure fluid. The flexibility of the incubator sleeve allows for sub-sampling of the medium without loss of pressure. Experiments can be run in both static and flow-through mode. The incubation system described here is usable for versatile purposes, not only the incubation of microorganisms and determination of growth rates, but also for chemical degradation or extraction experiments under high gas saturation, e.g., fluid–gas–rock-interactions in relation to carbon dioxide sequestration. As an application of the system we extracted organic compounds from sub-bituminous coal using H_2O as well as a H_2O–CO_2 mixture at elevated temperature (90˚C) and pressure (5 MPa). Subsamples were taken at different time points during the incubation and analyzed by ion chromatography. Furthermore we demonstrated the applicability of the system for studies of microbial activity, using samples from the Isis mud volcano. We could detect an increase in sulfate reduction rate upon the addition of methane to the sample.

Keywords: high-pressure incubation system, gas partial pressure, sub-sampling, carbon dioxide, low molecular weight organic acids

INTRODUCTION

The incubation of deep subsurface microorganisms under high-pressure conditions is necessary because under non-*in situ* conditions (especially low pressure) metabolic processes and survival of microorganisms adapted to high hydrostatic pressure are negatively impacted (Yayanos and Dietz, 1983; Fang et al., 2010). Since the first isolation of a pressure-adapted bacterium by Yayanos et al. (1979) numerous studies on the effect of elevated pressure on genetic, metabolic, and physiological aspects of microorganisms were carried out. Multiple biological effects of pressure on organisms were observed: shifts in metabolic activity (Abe et al., 1999; Bothun et al., 2004), transcription profiles (e.g., Boonyaratanakornkit et al., 2007), and the dissociation of ribosomes (e.g., Schulz et al., 1976), changes in growth rates (Yayanos, 1986; Boonyaratanakornkit et al., 2006; Takai et al., 2009), gene regulation (Bartlett et al., 1989), stabilization of proteins (Hei and Clark, 1994; Sun and Clark, 2001), and the composition of membrane lipids (Delong and Yayanos, 1985; Kaneshiro and Clark, 1995). For reviews of pressure effects on biological processes see Jaenicke (1983) and Bartlett (2002). Biochemical processes are also influenced by physical implications of high hydrostatic pressure, because the thermal expansion coefficient (Frank, 1970) as well as viscosity and fluidity of water (Horne and Courant, 1965) affect chemical reactions and cellular processes.

The idea of constructing and using a high-pressure vessel for studying deep-sea life is quite old. Zobell and Oppenheimer (1950) described a simple pressure vessel for the application of high hydrostatic pressure on microorganisms. Pressure was applied to a culture tube with a neoprene stopper working as piston for transmitting pressure to the sample. This type of pressure application is still being used today (Orcutt et al., 2008). Yayanos (1969) and later Taylor and Jannasch (1976) presented techniques for sub-sampling of media and bacteria and the determination of reaction rates without decompression, thereby eliminating the repetitive and time-consuming decompression. The use of glass syringes or a flexible Teflon container instead of a sealed culture tube (Schmid et al., 1978) had the benefit of an inert reaction chamber. However, the leakage of gases from the media into the pressure liquid or vice versa required a gas-tight incubation chamber. Bernhardt et al. (1987) used flexible nickel tubes for incubations of methanogenic microorganisms with hydrogen. Also flexible cells made of gold (Seyfried, 1979) or titanium (Seyfried and Janecky, 1985) were

used as high-pressure reaction chamber. However, such devices were designed for studies of hydrothermal alteration of basalt and therefore made for much higher temperatures than what is necessary for biological incubations. All described techniques are still in use. Recently Parkes et al. (2009) presented a high-pressure system that can accept drill cores, taken with a high-pressure corer without decompression. The system also allows for sub-sampling without decompression.

Temperature also has an effect on growth rates and other physiological characteristics of all microorganisms. Thermophilic and thermotolerant microorganisms can be found at hydrothermal vents, terrestrial hot springs, and intraterrestrial habitats (Pedersen, 2000) like salt mines (Vreeland et al., 1998), groundwater deep within Earth (Lin et al., 2006; Chivian et al., 2008), or oil reservoirs (e.g., L'Haridon et al., 1995).

Several techniques for the incubation of these thermophilic microorganisms are used: thermistors (e.g., Bernhardt et al., 1987), drying ovens (Miller et al., 1988; Takai et al., 2008), and water baths (e.g., Jannasch et al., 1996). Incubators and water baths became the most commonly used techniques for keeping pressure vessels at the desired temperature.

The application of elevated gas concentration in high-pressure incubations started about 25 years ago. Gases were applied to high-pressure vessels to maintain anaerobic conditions in incubations of hyperthermophilic archaea (e.g., Raven et al., 1992), to obtain higher cell densities during incubation (e.g., Mukhopadhyay et al., 1999) or as substrate for methanogenic microorganisms (Bernhardt et al., 1987; Takai et al., 2008). Nauhaus et al. (2002) incubated sediment samples from a methane hydrate field at different partial pressures of methane and showed a strong correlation between microbial activity and methane partial pressure. None of these incubation systems allowed manipulation of the gas partial pressure during the incubation or sub-sampling without decompression.

Here, we present an inexpensive high-pressure high-temperature incubation system that allows the incubation of a sample at high hydrostatic pressure as well as the manipulation of the composition and concentration of the dissolved gasses in the medium during incubation. It is designed for both static and flow-through experiments and allows for sub-sampling the liquid phase including the dissolved gases without decompression. The key objective was to build a moderately priced incubation system that can easily be constructed and operated. To keep costs low we used standardized off-the-shelf items and only a few custom-made parts.

With this system not only microbiological experiments under high hydrostatic and gas partial pressure can be performed. Geochemical experiments, for example the extraction of organic and inorganic compounds from rock samples under specific pressure and temperature conditions or mineral alteration studies are also possible.

Initial tests of the system included applications for geochemical and microbiological experiments. The effect of high concentrations of CO_2 dissolved in water on the release of low molecular weight organic acids from sub-bituminous coal from the Waikato Basin (NZ) was studied, as well as the effect of high methane partial pressure on microbial activity in samples from the Isis mud volcano (IMV), off the Mediterranean coast of Egypt.

MATERIALS AND METHODS

The high-pressure incubation system (**Figure 1**) is composed of a reservoir vessel and a reaction vessel for the application of

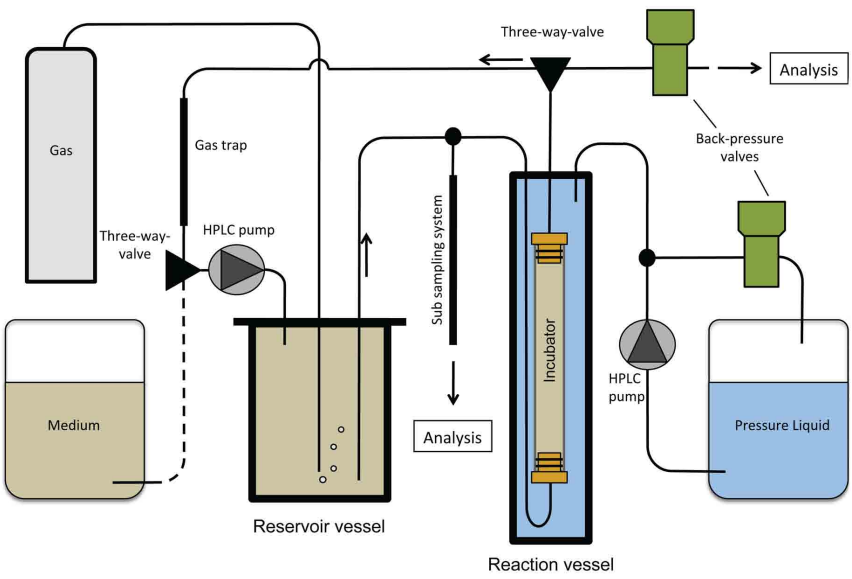

FIGURE 1 | Schematic drawing of the high-pressure incubation system. The medium is pressurized and enriched with gas in the reservoir vessel prior to flowing through the incubator sleeve that hangs inside the reaction vessel. Pressure in the reaction vessel is set and kept constant by a HPLC pump and a backpressure valve.

hydrostatic pressure on an incubator sleeve, which hangs inside the pressure vessel and holds the sample. A sub-sampling system allows the retrieval of liquid subsamples during the experiment without decompression. Temperature is maintained by a heating/cooling bath (Julabo Labortechnik GmbH, Seelbach, Germany) that pumps the liquid through heating jackets around the reservoir and the reaction vessel. Medium is circulated in a closed loop and HPLC pumps maintain hydrostatic pressure. A photograph of the entire unit is shown in **Figure 2**.

For microbiological experiments all parts of the high-pressure incubation system can be sterilized by autoclaving.

RESERVOIR VESSEL

The task of the temperature-controlled reservoir vessel is to saturate the medium with gas to the desired level and to hold a reservoir of medium that is pumped through the system.

The reservoir vessel is stainless steel cylinder (Dunze GmbH, Hamburg, Germany), with a volume of 255 cm^3 (inner dimensions: 3.4 cm diameter, 28.15 cm high; **Figure 3A**). Top and bottom are closed with plugs with bores for 1/16″ HPLC lines to allow for transfer of gas and medium in and out of the vessel.

REACTION VESSEL

The reaction vessel (**Figure 3B**) is a stainless steel cylinder (Dunze GmbH, Hamburg, Germany). The cylinder has an inner diameter of 3.5 and 27.0 cm in length (volume of 259.7 cm^3). Top and bottom are closed with plugs, each with bores for four 1/16″ HPLC lines each. The vessel is sealed with banjo screws that push the plugs into their seals.

INCUBATOR SLEEVE

The incubator (**Figure 3C**) is a sleeve of polyvinylidene fluoride (PVDF, Novoplast, Halberstadt, Germany), a polymer that is inert to almost all chemicals. Although this material is not as flexible as polytetrafluoroethylene (PTFE) or fluorinated ethylene propylene (FEP), it was chosen due to its very low permeability for gases (**Table 1**). The sleeve is closed with two gold-coated stainless steel plugs (3 μm gold thickness; Schempp and Decker, Berlin, Germany) with two gutters, each holding a perfluoro-elastomer O-ring (FFKM, Parker Hannifin, Pleidelsheim, Germany). FFKM was used for its chemical resistance. Both stoppers have a central threaded bore for the connection with a 1/16″ HPLC line: one for inflow of medium at the bottom of the incubator and one for outflow at the top of the incubator. The incubator was designed to avoid corrosion, therefore only inert materials (PVDF, FFKM, and gold) were used. The sleeve has a diameter of 25 mm and can have a maximum length of 22 cm, which leads to a maximum volume of 68 cm^3. Inside the incubator the medium first has to pass through a 1.5 cm thick layer of 2 mm diameter glass beads, followed by a 1.5 cm thick layer of quartz wool (organic free by annealing in a muffle furnace) so that the stream of medium passes evenly through the sample material over the entire cross section of the incubator sleeve. On top of the sample, the described layers follow in opposite order; first quartz wool for holding back most of the fine particles that could clog the lines and valves, followed by glass beads until the incubator is full and the sample well packed.

Additional to the chemical resistance and the almost complete impermeability for gases, further advantages of using a PVDF sleeve is its relatively low price, allowing for the possibility of using it as a disposable article. Thereby, cross contamination between samples can be excluded. Furthermore, mechanical stress leading to a weakening of the material and, therefore, a possible leakage of medium or inflow of pressure fluid will be prevented. The incubator sleeve hangs inside the reaction vessel and is connected to the top plug of the incubation vessel via the 1/16″ HPLC lines.

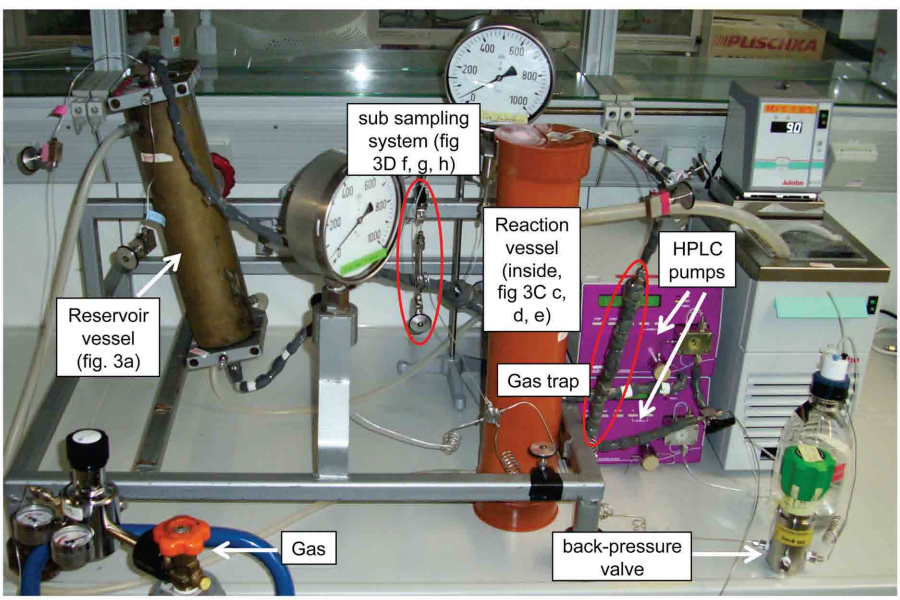

FIGURE 2 | Photograph of the high-pressure incubation system as seen in Figure 1. Reservoir vessel, reaction vessel, incubator, and sub-sampling device are shown in detail in **Figure 3**.

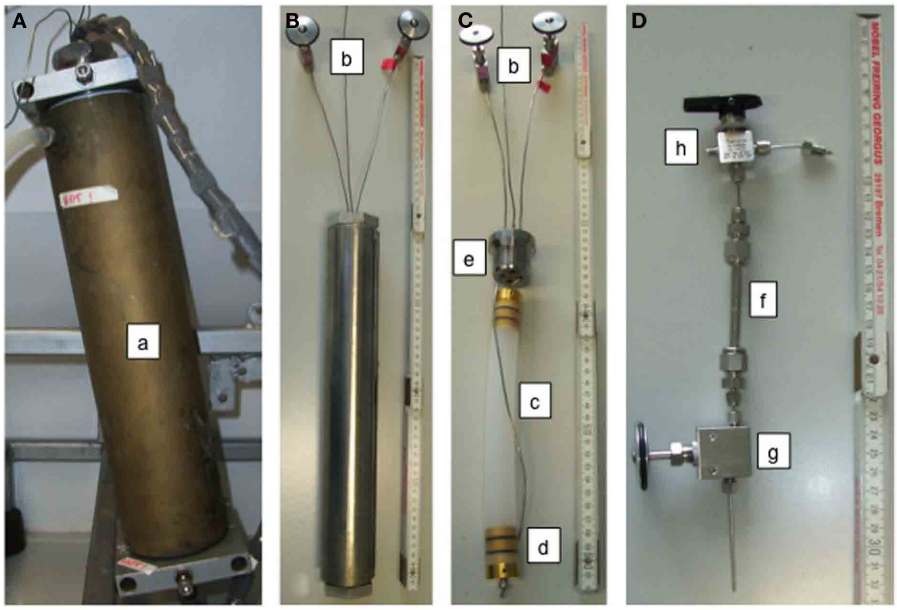

FIGURE 3 | (A) Reservoir vessel with a total volume of 255 cm^3; (a) pressure cylinder (invisible) with heating/cooling jacket; **(B)** high-pressure reaction vessel including connections with (b) valves for in- and out-flow of medium via the incubator; the third line (without a valve) is for the application of pressure to the reaction vessel; **(C)** PVDF-incubator with (b) valves, (c) PVDF incubation sleeve; maximum volume 60 cm^3, connected to in- and out-flow lines via the plug of the pressure vessel (e), (d) gold-coated stainless steel plugs with FFKM O-rings; **(D)** sub-sampling device; (f) 1/4″ high-pressure line, three-way-valve (h), shut-off valve (g).

SUB-SAMPLING SYSTEM

A sub-sampling device allows taking fluid samples during the experiment without decompression (**Figure 3D**). It is attached to the high-pressure line between the reservoir vessel and the reaction vessel. The sub-sampler is made from 1/4″ stainless steel tubing (7.9 cm in length, inner diameter 0.225 cm, total volume 0.513 cm^3) and has a three-way-valve (Swagelok Limited, Tromode, UK) at the top and a shut-off valve (Supelco) at the bottom. The three-way-valve connects the sub-sampler to the incubation system. The third connection of the valve is used to either apply vacuum to the sub-sampler prior to sampling to avoid oxidation of the sample or to apply overpressure (nitrogen gas) to push out the remainder of the sample. After the sub-sampler is evacuated, the three-way-valve is turned and the sample enters the sub-sampler. Then the three-way-valve is closed and the shut-off valve at the bottom of the system is opened and the sample transferred into a sampling vial. Nitrogen Gas is added through the three-way-valve to push out the remaining sample.

GAGES AND PUMPS, OTHER HARDWARE

Pressure is generated by a modified HPLC pressure pump (SYKAM S 1122, Sykam GmbH, Fuerstenfeldbruck, Germany, modifications according to Kallmeyer et al., 2003). A second identical pump is used to circulate the medium through the reservoir vessel and the incubator sleeve. Pressure is kept constant through a backpressure valve (pressure regulator series KHB, Swagelok Limited, Tromode, UK).

All pressure vessels (reservoir and reaction vessel) are connected to 100 MPa pressure gages (WIKA Alexander Wiegand SE and Co. KG, Klingenberg, Germany). All pumps and vessels are connected with 1/16″ HPLC lines (CS Chromatographie, Langerwehe, Germany). If not mentioned otherwise all valves were obtained from Supelco, Bellefonte, PA, USA.

Table 1 | Comparison of mechanical parameters and gas permeability of PTFE, FEP, and PVDF.

Mechanical parameters	Units	PTFE	FEP	PVDF
Shore durometer D	Durometer	55–72	55–60	73–85
Flexural strength	N/mm^2	600–800	660–680	1200–1400
Gas permeability in cm^3/m^2 or d/bar		**PTFE**	**FEP**	**PVDF**
Nitrogen		0.7	3.8	0.06
Oxygen		2.05	30	0.05
Carbon dioxide		5.7	60	0.2

Data supplied by Bohlender GmbH, Grünsfeld, Germany.

GAS TRAP

To avoid the possible entry of gas bubbles into the pump, an empty HPLC column (25.1 cm in length, inner diameter 0.45 cm, total volume 4 cm^3; Sykam GmbH, Fuerstenfeldbruck, Germany) is used as a gas trap, mounted vertically between the reaction vessel and the pump to collect any gas bubbles that may form. The medium flows from top to bottom, so the gas bubbles are trapped at the top.

APPLICATION OF THE SYSTEM

We used the system for the extraction of low molecular weight organic acids, which are a potential microbial energy source, from a coal sample using water and water–carbon dioxide mixture at 90°C and 5 MPa. In a second application we incubated sediment from a mud volcano that is known to exhibit high rates of anaerobic methane oxidation at 23°C and 10 MPa total pressure and 4 MPa methane partial pressure (96 mmol/l) and measured an increase in sulfide concentration.

COAL SAMPLE

We selected a sub-bituminous coal sample [vitrinite reflectance (R_0): 0.29%] from the Whangamarino formation (latest Miocene to late Pliocene), which is part of the Tauranga group. The sample was from a depth of 64.69 m below surface, taken from the DEBITS-1 well, which was drilled in 2004 within the scope of the deep biosphere in terrestrial systems (DEBITS) project at Ohinewai in the Waikare Coal Field of the Waikato Basin on the North Island of New Zealand.

The well had a total depth of 148 m and penetrated interbedded layers of organic-rich carbon (lignites and sub-bituminous coals) as well as mudstones, siltstones, and sandstones. The total organic carbon (TOC) content in the sample is approximately 30%. For further information about the sample material and the geology of the Waikato Basin see Glombitza et al. (2009).

Low molecular weight organic acids (LMWOAs) such as formate, acetate, and oxalate are known to be the main organic compounds obtained from aqueous extractions of lignites and coals (Vieth et al., 2008). The LMWOAs are also components of the macromolecular organic material of the coal (Glombitza et al., 2009) and are released from the coal matrix during ongoing maturation into the surrounding pore water.

MUD VOLCANO SEDIMENT

Isis mud volcano lies on the Egyptian continental margin in the Nile deep-sea fan (NDSF) in a water depth of ∼991 m and covers an area of approximately 10 km^2. The NDSF is a sedimentary wedge that is deposited since the late Miocene by the Nile river (Loncke et al., 2004) with an assumed thickness of up to 10 km. Deeper sediments become strongly overpressured by the thick sedimentary overburden, resulting in an upward migration of fluids and gases (Loncke et al., 2004). Among other mud volcanoes in the area, IMV is emitting large volumes of gas (Dupré et al., 2008), including methane, ethane, and propane (Mastalerz et al., 2009). These gases are probably a mixture from different sources, because their isotopic composition is rather inconclusive with regards to a thermogenic or microbial origin (Mastalerz et al., 2007).

The emitted gases – mostly methane – are substrates for microorganisms. In sediment samples of the IMV Omoregie et al. (2009) found several genera of sulfate-reducing bacteria (*Desulfosarcina, Desulfococcus, Desulfocapsa, Desulfobulbus*) as well as *Methanococcoides*, a methanogenic *Archea*, and the anaerobic methane oxidizers ANME-1, ANME-2, and ANME-3.

The sample was taken during the NAUTINIL expedition in 2003 at 32°22′N; 31°23′E in 1020 m water depth and stored in a glass bottle at 4°C with a nitrogen headspace. About a week prior to the experiments, the headspace was flushed with methane. Immediately prior to the incubation experiments, concentration of hydrogen sulfide and methane in the pore water was around 6 and 4.8 mmol/l, respectively.

EXPERIMENTAL PROCEDURE

We extracted the coal sample at elevated temperature (90°C) and pressure (5 MPa) using deionized water in the first experiment and a water–carbon dioxide mixture in the second. Five grams (approx. 9.4 cm^3) of the freeze-dried and powdered coal sample were placed in the incubator sleeve. For the water extraction, the experiment was started after reservoir and reaction vessel had reached 5 MPa and 90°C. In the second experiment with the H_2O–CO_2 mixture, gas was added to the reservoir vessel after heating to 90°C and left overnight for equilibration. The experiment and the circulation of the gas-saturated medium started after equilibration. Pressure was generated by adding CO_2 until 5 MPa were reached and pressure had stabilized as maximum gas saturation had been reached (approximately 106 g/l or 2.4 mol/l of dissolved CO_2).

Extractions were carried out for a total of 48 h. Subsamples (0.513 cm^3) of the medium were taken after 6, 22, 30, and 48 h and flushed into 513 µl of a 3.6/3.4 mmol/l solution of Na_2CO_3/$NaHCO_3$ containing 2% isopropanol to reduce the volatility of the LMWOAs thereby avoiding a loss of these compounds. The subsamples were immediately frozen until analysis (within 1 week). Sample analysis was performed by ion chromatography (IC) without further dilution.

The incubation of sediment samples from IMV was performed at a pressure of 10 MPa and a temperature of 23°C, using an artificial seawater medium (Widdel and Bak, 1992) with a sulfate concentration of 27 mmol/l.

In the first experiment the medium contains just 0.1 mmol/l of methane (from the dilution of the sediment sample pore water methane), whereas in the second experiment the medium contained 96 mmol/l methane. In order to be able to detect even small amounts of hydrogen sulfide, the volume of the reservoir vessel was reduced to 145 ml by adding glass beads (5 mm diameter). Inside an anaerobic glove box 10 cm^3 of IMV sediment were loaded into the incubator sleeve. The experiment with only artificial anoxic seawater medium was started after reservoir and reaction vessel were equilibrated to 10 MPa and 23°C. In the second experiment the medium was first pressurized with methane to 4 MPa, leading to a methane concentration of approximately 1.6 g/l or 96 mmol/l of dissolved methane and left overnight for equilibration. After methane saturation was complete, pressure was increased hydrostatically to 10 MPa with anoxic artificial seawater medium. The sample was loaded into the incubation vessel and pressurized prior to the experiment; circulation of the gas-saturated medium started after equilibration.

Incubations were carried out for a total of 432 h (9 days). Subsamples (0.513 cm^3) of the medium were taken every 2 days. The subsamples were mixed with equal volumes of a 5% (w/v) zinc acetate solution to fix the volatile sulfide as zinc sulfide. The fixed subsamples were immediately frozen until photometric analysis.

SAMPLE ANALYSIS BY ION CHROMATOGRAPHY

The samples were analyzed in replicates using IC. The IC system (Sykam GmbH, Fuerstenfeldbruck, Germany) was equipped

with an LCA A 20 column, a suppressor (SAMS, SeQuant, Sweden) and a SYKAM S3115 conductivity detector. The mobile phase was a 1.8/1.7 mmol/l Na_2CO_3/$NaHCO_3$ mixture. Elution was performed at isocratic conditions. The eluent flow was set to 0.8 ml/min. A blank sample (deionized water) and a multi-compound standard containing each 50 mg/l formate, acetate, and oxalate (for the extraction of coal) were measured prior to each sample. Standard deviation of sample and standard quantification was below 10% (determined from replicate analysis).

HYDROGEN SULFIDE QUANTIFICATION

Hydrogen sulfide concentration was quantified according to Cline (1969). In brief, 5 ml of deionized water and 400 µl of Cline-reagent (1.6 g of *N*,*N*-dimethyl-*p*-phenylenediamine sulfate plus 2.4 g of $FeCl_3 \cdot 6H_2O$ in 100 ml 50% HCl) are added to the sample. Adsorption is measured in a photometer at 680 nm after 20 min. The minimum detection limit with a 1 cm cell is around 50 µmol/l.

RESULTS

The main organic compounds extracted with water at 5 MPa and 90°C are formate, acetate, and oxalate. Vieth et al. (2008) reported comparable results from aqueous Soxhlet extraction of similar sample material from the DEBITS-1 well. The amounts of extracted LMWOAs increase over the course of the experiment (**Figure 4**, blue circles). The strongest increase in concentration of LMWOAs was observed during the first 22 h of extraction. In the following 26 h a slow but steady increase of extracted LMWOA was observed, suggesting that the experiment did not run to completion after 48 h. Nevertheless, the yields of the extracted LMWOAs are approaching steady state. Total amounts of extracted LMWOAs after 48 h were 2.3 mg/g_{TOC} formate, 3.8 mg/g_{TOC} acetate, and 5.2 mg/g_{TOC} oxalate.

In the second coal extraction experiment we used an H_2O–CO_2 mixture under the same pressure and temperature conditions (90°C, 5 MPa) but with 2.4 mol/l CO_2. Under these conditions, the same organic compounds (formate, acetate, and oxalate) were extracted (**Figure 4**, green circles). Like in the experiment with deionized water, the amounts of extracted LMWOAs increase with increasing extraction time, with the main increase during the first 20 h. The total amounts of extracted LMWOAs after 48 h were 2.4 mg/gTOC for formate, 2.7 mg/gTOC for acetate, and 4.5 mg/gTOC for oxalate. These numbers are somewhat lower than in the pure water extraction experiment (**Figure 4**).

During the first 48 h of both IMV sediment incubation experiment, hydrogen sulfide concentration increased to about 0.3 mmol/l due to the mixing of the sediment's pore water hydrogen sulfide with the medium. Over the course of the first experiment the concentration remained around 0.3 mmol/l for the remainder of the experiment (**Figure 5**, red circles).

In the second experiment with the added methane (4 MPa, 96 mmol/l), sulfide concentration remained around 0.3 mmol/l until ca. 144 h, before increasing almost exponentially (**Figure 5**, blue circles). The experiment was stopped after 432 h at a hydrogen sulfide concentration of 0.93 mmol/l.

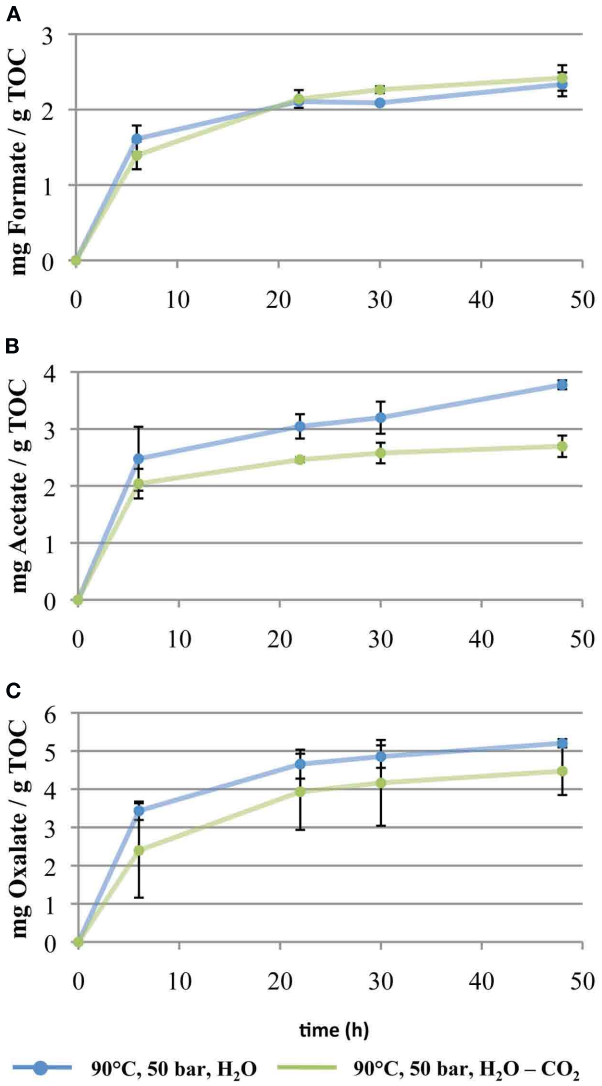

FIGURE 4 | Extraction of (A) formate, (B) acetate, and (C) oxalate from sub-bituminous coal sample taken from the DEBITS-1 well at Waikato Coal Area, North Island, New Zealand. Five grams of coal (approximately 30% TOC) were extracted for 48 h at 5 MPa and 90°C. Extractions were performed with water (blue circles) and water–carbon dioxide mixture (green triangles). Sample analysis was performed by ion chromatography.

DISCUSSION

The extracted LMWOAs (formate, acetate, and oxalate) have also been found to be the main organic acids obtained from water extraction of other low mature coals (Bou-Raad et al., 2000; Vieth et al., 2008; Glombitza, 2011).

High-pressure (5 MPa) extraction with pure water in our system resulted in significantly higher yields (2.4–4.5 mg organic acids/g_{TOC}) than what was reported from Soxhlet extraction of coal samples from a similar depth interval of the DEBITS-1 well, which yielded between 0.7 and 1.4 mg organic acid/g_{TOC} for individual LMWOAs (Vieth et al., 2008). The extraction of LMWOAs resulted in a decrease of pH in the extraction medium. The pH in

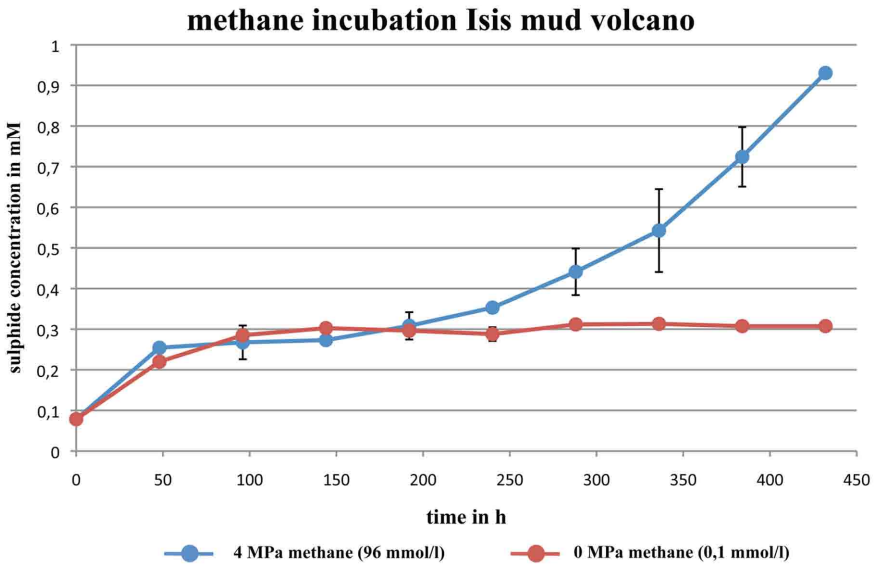

FIGURE 5 | Incubation of sediment samples from Isis mud volcano (IMV). Ten cubic centimeter of sediment were incubated for 432 h at 10 MPa and 23°C. Incubations were performed with 4 MPa methane (blue circles) and without addition of methane (red circles).

the reservoir of a Soxhlet apparatus decreases to approximately pH 4 after 48 h of extraction with deionized water (data not shown). However, the sample only gets into contact with freshly distilled water (pH 7) that drips over the sample. In the high-pressure system the extraction medium containing the extracted organic acids circulates through the system, thereby extracting the coal with a low-pH medium. The lower pH is supposed to enhance the release of LMWOAs from macromolecular organic matter in the coal by hydrolysis (Glombitza, 2011). This might explain the higher extraction yields of LMWOAs in our reactor system as compared to Soxhlet extraction.

Under *in situ* conditions, the extracted LMWOAs will remain in the pore water and thereby cause a drop in pH before they are eventually removed by diffusion or fluid flow. As Fry et al. (2009) reported from samples from the DEBITS-1 well, the majority of microbial activity and abundance is not found in the coals but rather in the surrounding and more porous sandstones. So the consumption of the produced LMWOA does not take place inside the coal seams but above or below them and removal of these substances from the coals is controlled by diffusion or fluid flow, not by microbial activity. It is therefore reasonable to assume that our high-pressure system provides reaction conditions that are much more realistic than Soxhlet extraction because the extracted compounds are not removed from the reaction.

When comparing the results of the first extraction with deionized water and the second extraction with an H_2O–CO_2 mixture, it becomes obvious that CO_2 reduces the amount of extracted acetate by a factor of 1.39 and oxalate by a factor of 1.16. For formate no clear influence of CO_2 on the extraction efficiency could be observed. At first sight, this result is surprising because carbon dioxide dissolved in water lowers the pH due to formation of carbonic acid (Meyassami et al., 1992). The lower pH was expected to enhance hydrolysis and, therefore, increase the yield of extractable LMWOAs. However, we observed a suppressing effect of CO_2.

The LMWOAs found in the extraction fluid may not just result from the actual extraction of the coal but also from different secondary reactions. It was suggested that oxalate in aqueous extracts of coals is a result of the decomposition of 1,2-dihydroxycarboxylic acids (Bou-Raad et al., 2000). Therefore it has to be assumed that at least for oxalate (and maybe for other LMWOAs as well) the extraction yield is not only affected by hydrolysis but also by secondary reactions, which may be inhibited or suppressed in the presence of CO_2 in the extraction medium.

The incubation experiment with sediment samples from the Isis mud volcano clearly showed the positive effect of elevated methane concentration on the rate of sulfide production, which is a direct result of sulfate reduction. Omoregie et al. (2009) conducted whole core $^{35}SO_4^{2-}$ radiotracer incubations of samples from the same mud volcano at atmospheric pressure (0.1 MPa) and with a maximum methane concentration of >10 μmol l^{-1}. They measured sulfate reduction rates of 7–240 nmol cm^{-3} day^{-1}. We conducted our experiment at much higher methane concentration (96 mmol l^{-1}) and *in situ* pressure (10 MPa), and measured a significantly higher sulfate reduction rate of ca. 2000 nmol cm^{-3} day^{-1}, which we attribute to the elevated methane concentration, as already shown by Nauhaus et al. (2002).

The aim of this paper is to present a new high-pressure incubation system and experiments to demonstrate the application of elevated temperature and pressure as well the use of elevated gas saturation and their effects on geochemical and microbiological processes. Therefore, we can only speculate about the reasons for the observed suppressing effect of the CO_2. This effect still remains puzzling and will be the topic of future investigations.

CONCLUSION

The high-pressure high-temperature incubation system is a moderately priced alternative to existing systems. Furthermore, it is easy to construct and to handle. Initial experiments demonstrate that the system is suitable for a wide range of applications in geo- and bio-sciences. The system allows the incubations at elevated pressure and temperature conditions (up to 120°C and 60 MPa) as well as manipulating the dissolved gases throughout the experiment. The system also allows subsampling of the fluid phase during the course of the experiment without decompression. Extraction of a sub-bituminous coal samples under high-pressure and temperature conditions showed a higher yield in LMWOAs from macromolecular organic matter as compared to an extraction with a Soxhlet apparatus. The high-pressure extraction of the coal sample with CO_2-saturated water revealed a suppressing effect of the CO_2 on the extraction yield or secondary formations of LMWOAs. Possible reasons for this effect are not identified yet and will be in the focus of future investigations. The incubation of sediment samples from a mud volcano harboring sulfate-reducing methanotrophs showed a clear positive response of methane addition on the sulfate reduction rate. Our high-pressure high-temperature incubation system has proven its suitability for a broad range of scientific applications.

ACKNOWLEDGMENTS

We would like to thank Harald Huber from the University of Regensburg for providing high-pressure equipment. The Helmholtz Centre Potsdam is gratefully acknowledged for providing the sample material for the test experiment. We thank Ann-Kathrin Scherf from the German Research Centre for Geosciences (GFZ) for the Soxhlet extraction of coal samples and pH measurement as well as Dr. Gunter Wegener from the Max Planck Institute fro Marine Microbiology for the sediment samples from Isis mud volcano. Furthermore we thank the Federal Ministry of Education and Research (BMBF) for funding this work within the "Forschungsverbund Geoenergien" (GeoEn, research network geoenergy).

REFERENCES

Abe, F., Kato, C., and Horikoshi, K. (1999). Pressure-regulated metabolism in microorganisms. *Trends Microbiol.* 7, 447–453.

Bartlett, D. H. (2002). Pressure effects on in vivo microbial processes. *Biochim. Biophys. Acta* 1595, 367–381.

Bartlett, D. H., Wright, M., Yayanos, A. A., and Silverman, M. (1989). Isolation of a gene regulated by hydrostatic pressure in a deep-sea bacterium. *Nature* 342, 572–574.

Bernhardt, G., Jaenicke, R., and Lüdemann, H. D. (1987). High-pressure equipment for growing methanogenic microorganisms on gaseous substrates at high temperature. *Appl. Environ. Microbiol.* 53, 1876–1879.

Boonyaratanakornkit, B. B., Cordova, J., Park, C. B., and Clark, D. S. (2006). Pressure affects transcription profiled of *Methanocaldococcus jannaschii* despite the absence of barophilic growth under gas-transfer limitation. *Environ. Microbiol.* 8, 2031–2035.

Boonyaratanakornkit, B. B., Miao, L. Y., and Clark, D. S. (2007). Transcriptional response of the deep-sea hyperthermophile *Methanocaldococcus jannaschii* under shifting extremes of temperature and pressure. *Extremophiles* 11, 495–503.

Bothun, G. D., Knutson, B. L., Berberich, J. A., Strobel, H. J., and Nokes, S. E. (2004). Metabolic selectivity and growth of *Clostridium thermocellum* in continuous culture under elevated hydrostatic pressure. *Appl. Microbiol. Biotechnol.* 65, 149–157.

Bou-Raad, M., Hobday, M. D., and Rix, C. J. (2000). Aqueous extraction of oxalate and other anions from coal. *Fuel* 79, 1185–1193.

Chivian, D., Brodie, E. L., Alm, E. J., Culley, D. E., Dehal, P. S., Desantis, T. Z., Gihring, T. M., Lapidus, A., Lin, L.-H., Lowry, S. R., Moser, D. P., Richardson, P. M., Southam, G., Wanger, G., Pratt, L. M., Anderson, G. L., Hazen, T. C., Brockman, F. J., Arkin, A. P., and Onstott, T. C. (2008). Environmental genomics reveals a single-species ecosystem deep within earth. *Science* 322, 275–278.

Cline, J. D. (1969). Spectrophotometric determination of hydrogen sulfide in natural waters. *Limnol. Oceanogr.* 14, 454–458.

Delong, E. F., and Yayanos, A. A. (1985). Adaptation of the membrane lipids of a deep-sea bacterium to changes in hydrostatic pressure. *Science* 228, 1101–1103.

Dupré, S., Buffet, G., Mascle, J., Foucher, J. P., Gauger, S., Boetius, A., Marfia, C., The AsterX AUV Team, The Quest ROV Team, and The BIONIL scientific party. (2008). High-resolution mapping of large gas emitting mud volcanoes on the Egyptian continental margin (Nile deep sea fan) by AUV surveys. *Mar. Geophys. Res.* 29, 275–290.

Fang, J., Zhang, L., and Bazylinski, D. A. (2010). Deep-sea piezosphere and piezophiles: geomicrobiology and biogeochemistry. *Trends Microbiol.* 18, 413–422.

Frank, H. S. (1970). The structure of ordinary water. *Science* 169, 635–641.

Fry, J. C., Horsfield, B., Sykes, R., Cragg, B. A., Heywood, C., Kim, G. T., Mangelsdorf, K., Mildenhall, D. C., Rinna, J., Vieth, A., Zink, K.-G., Sass, H., Weightman, A. J., and Parkes, R. J. (2009). Prokaryotic populations and activities in an interbedded coal deposit, including a previously deeply buried section (1.6-2.3 km) above (~150 Ma basement rock. *Geomicrobiol. J.* 26, 163–178.

Glombitza, C. (2011). *New Zealand Coals – A Potential Feedstock for Deep Microbial Life*. Thesis, Technical University Berlin, Berlin.

Glombitza, C., Mangelsdorf, K., and Horsfield, B. (2009). A novel procedure to detect low molecular weight compounds released by alkaline ester cleavage from low maturity coals to assess its feedstock potential for deep microbial life. *Org. Geochem.* 40, 175–183.

Hei, D. J., and Clark, D. S. (1994). Pressure stabilization of proteins from extreme thermophiles. *Appl. Environ. Microbiol.* 60, 932–939.

Horne, R. A., and Courant, R. A. (1965). Protonic conduction in the water I region. *J. Phys. Chem.* 69, 2224–2230.

Jaenicke, R. (1983). Biochemical processes under high hydrostatic pressure. *Naturwissenschaften* 70, 332–341.

Jannasch, H. W., Wirsen, C. O., and Doherty, K. W. (1996). A pressurized chemostat for the study of marine barophilic and oligotrophic bacteria. *Appl. Environ. Microbiol.* 62, 1593–1596.

Kallmeyer, J., Ferdelman, T. G., Jansen, K.-H., and Jorgensen, B. B. (2003). A high-pressure thermal gradient block for investigating microbial activity in multiple deep-sea samples. *J. Microbiol. Methods* 55, 165–172.

Kaneshiro, S. M., and Clark, D. S. (1995). Pressure effects on the composition and thermal behavior of lipids from the deep-sea thermophile. *J. Bacteriol.* 177, 3668–3672.

L'Haridon, S., Reysenbach, A.-L., Glénat, P., Prieur, D., and Jeanthon, C. (1995). Hot subterranean biosphere in a continental oil reservoir. *Nature* 377, 223–224.

Lin, L.-H., Wang, P.-W., Rumble, D., Lippmann-Pipke, J., Boice, E., Pratt, L. M., Sherwood-Lollar, B., Brodie, E. L., Hazen, T. C., Anderson, G. L., Desantis, T. Z., Moser, D. P., Kershaw, D., and Onstott, T. C. (2006). Long-term sustainability of a high-energy, low-diversity crustal biome. *Science* 314, 479–482.

Loncke, L., Mascle, J., and Fanil Scientific Parties. (2004). Mud volcanoes, gas chimneys, pockmarks and mounds in the Nile deep-sea fan (Eastern Mediterranean): geophysical evidences. *Mar. Petrol. Geol.* 21, 669–689.

Mastalerz, V., de Lange, G. J., and Dählmann, A. (2009). Differential aerobic and anaerobic oxidation of hydrocarbon gases discharged at mud volcanoes in the Nile deep-sea fan. *Geochim. Cosmochim. Acta* 73, 3849–3863.

Mastalerz, V., de Lange, G. J., Dählmann, A., and Feseker, T. (2007). Active venting at the Isis mud volcano, offshore Egypt: origin and migration of hydrocarbons. *Chem. Geol.* 246, 87–106.

Meyassami, B., Balaban, M. O., and Teixera, A. A. (1992). Prediction of pH in model systems pressurized with carbon dioxide. *Biotechnol. Prog.* 8, 149–154.

Miller, J. F., Almond, E. L., Shah, N. N., Ludlow, J. M., Zollweg, J. A., Streett, W. B., Zinder, S. H., and Clark, D. S. (1988). High-pressure-temperature bioreactor for studying pressure-temperature relationships in bacterial growth and productivity. *Biotechnol. Bioeng.* 31, 407–413.

Mukhopadhyay, B., Johnson, E. F., and Wolfe, R. S. (1999). Reactor-scale cultivation of the hyperthermophilic methanarchaeon *Methanococcus jannaschii* to high cell densities. *Appl. Environ. Microbiol.* 65, 5059–5065.

Nauhaus, K., Boetius, A., Kruger, M., and Widdel, F. (2002). In vitro demonstration of anaerobic oxidation of methane coupled to sulphate reduction in sediment from a marine gas hydrate area. *Environ. Microbiol.* 4, 296–305.

Omoregie, E. O., Niemann, H., Mastalerz, V., de Lange, G. J., Stadnitskaia, A., Mascle, J., Foucher, J.-P., and Boetius, A. (2009). Microbial methane oxidation and sulfate reduction at cold seeps of the deep Eastern Mediterranean Sea. *Mar. Geol.* 261, 114–127.

Orcutt, B., Samarkin, V., Boetius, A., and Joye, S. (2008). On the relationship between methane production and oxidation by anaerobic methanotrophic communities from cold seeps of the Gulf of Mexico. *Environ. Microbiol.* 10, 1108–1117.

Parkes, R. J., Sellek, G., Webster, G., Martin, D., Anders, E., Weightman, A. J., and Sass, H. (2009). Culturable prokaryotic diversity of deep, gas hydrate sediments: first use of a continuous high-pressure, anaerobic, enrichment and isolation system for subseafloor sediments (DeepIsoBUG). *Environ. Microbiol.* 11, 3140–3153.

Pedersen, K. (2000). Exploration of deep intraterrestrial microbial life: current perspectives. *FEMS Microbiol. Lett.* 185, 9–16.

Raven, N., Ladwa, N., Cossar, D., and Sharp, R. (1992). Continuous culture of the hyperthermophilic archaeon *Pyrococcus furiosus*. *Appl. Microbiol. Biotechnol.* 38, 263–267.

Schmid, G., Lüdemann, H.-D., and Jaenicke, R. (1978). Oxidation of sulfhydryl groups in lactate dehydrogenase under high hydrostatic pressure. *Eur. J. Biochem.* 86, 219–224.

Schulz, E., Lüdemann, H.-D., and Jaenicke, R. (1976). High pressure equilibrium studies on the dissociation – association of *E. coli* ribosomes. *FEBS Lett.* 64, 40–43.

Seyfried, W. E. Jr. (1979). A new reaction cell for hydrothermal solution equipment. *Am. Mineral.* 64, 646–649.

Seyfried, W. E. Jr., and Janecky, D. R. (1985). Heavy metal and sulfur transport during subcritical and supercritical hydrothermal alteration of basalt: influence of fluid pressure and basalt composition and crystallinity. *Geochim. Cosmochim. Acta* 49, 2545–2560.

Sun, M. M. C., and Clark, D. S. (2001). Pressure effects on activity and stability of hyperthermophilic enzymes. *Meth. Enzymol.* 334, 316–327.

Takai, K., Miyazaki, M., Hirayama, H., Nakagawa, S., Querellou, J., and Godfroy, A. (2009). Isolation and physiological characterization of two novel, piezophilic, thermophilic chemolithoautotrophs from a deep-sea hydrothermal vent chimney. *Environ. Microbiol.* 11, 1983–1997.

Takai, K., Nakamura, K., Toki, T., Tsunogai, U., Miyazaki, M., Miyazaki, J., Hirayama, H., Nakagawa, S., Nunoura, T., and Horikoshi, K. (2008). Cell proliferation at 122°C and isotopically heavy CH_4 production by a hyperthermophilic methanogen under high-pressure cultivation. *Proc. Natl. Acad. Sci. U.S.A.* 105, 10949–10954.

Taylor, C. D., and Jannasch, H. W. (1976). Subsampling techniques for measuring growth of bacterial cultures under high hydrostatic pressure. *Appl. Environ. Microbiol.* 32, 355–359.

Vieth, A., Mangelsdorf, K., Sykes, R., and Horsfield, B. (2008). Water extraction of coals – potential for estimating low molecular weight organic acids as carbon feedstock for the deep terrestrial biosphere. *Org. Geochem.* 39, 985–991.

Vreeland, R. H., Piselli, A. F. Jr., Mcdonnough, S., and Meyers, S. S. (1998). Distribution and diversity of halophilic bacteria in a subsurface salt formation. *Extremophiles* 2, 321–331.

Widdel, F., and Bak, F. (1992). "Gram negative mesophilic sulphate-reducing bacteria," in *The Prokaryotes,* eds A. Balows, H. G. Trüper, M. Dworkin, W. Harder, and K.-H. Schleifer (New York: Springer), 3352–3378.

Yayanos, A. A. (1969). A technique for studying biological reaction rates at high pressure. *Rev. Sci. Instrum.* 40, 961–963.

Yayanos, A. A. (1986). Evolutional and ecological implications of the properties of deep-sea barophilic bacteria. *Proc. Natl. Acad. Sci. U.S.A.* 83, 9542–9546.

Yayanos, A. A., and Dietz, A. S. (1983). Death of a Hadal deep-sea bacterium after decompression. *Science* 220, 497–498.

Yayanos, A. A., Dietz, A. S., and Van Boxtel, R. (1979). Isolation of a deep-sea barophilic bacterium and some of its growth characteristics. *Science* 205, 808–810.

Zobell, C. E., and Oppenheimer, C. H. (1950). Some effects of hydrostatic pressure on the multiplication and morphology of marine bacteria. *J. Bacteriol.* 60, 771–781.

Conflict of Interest Statement: The authors declare that the research was conducted in the absence of any commercial or financial relationships that could be construed as a potential conflict of interest.

Received: 09 September 2011; accepted: 15 January 2012; published online: 03 February 2012.

Citation: Sauer P, Glombitza C and Kallmeyer J (2012) A system for incubations at high gas partial pressure. Front. Microbio. ***3****:25. doi: 10.3389/fmicb.2012.00025*

This article was submitted to Frontiers in Extreme Microbiology, a specialty of Frontiers in Microbiology.

frontiers in
MICROBIOLOGY

ORIGINAL RESEARCH ARTICLE
published: 17 February 2012
doi: 10.3389/fmicb.2012.00049

Characterization of microbial population shifts during sample storage

Heath J. Mills[1]*, Brandi Kiel Reese[1,2] and Cruz St. Peter[1]

[1] *Department of Oceanography, Texas A&M University, College Station, TX, USA*
[2] *Department of Biological Science, University of Southern California, Los Angeles, CA, USA*

Edited by:
Andreas Teske, University of North Carolina at Chapel Hill, USA

Reviewed by:
Rebecca Gast, Woods Hole Oceanographic Institution, USA
Kesen Ma, University of Waterloo, Canada

****Correspondence:***
Heath J. Mills, Department of Oceanography, Texas A&M University, 716A Eller O&M Building, College Station, TX 77843-3146, USA.
e-mail: hmills@ocean.tamu.edu

The objective of this study was to determine shifts in the microbial community structure and potential function based on standard Integrated Ocean Drilling Program (IODP) storage procedures for sediment cores. Standard long-term storage protocols maintain sediment temperature at 4˚C for mineralogy, geochemical, and/or geotechnical analysis whereas standard microbiological sampling immediately preserves sediments at −80˚C. Storage at 4˚C does not take into account populations may remain active over geologic time scales at temperatures similar to storage conditions. Identification of active populations within the stored core would suggest geochemical and geophysical conditions within the core change over time. To test this potential, the metabolically active fraction of the total microbial community was characterized from IODP Expedition 325 Great Barrier Reef sediment cores prior to and following a 3-month storage period. Total RNA was extracted from complementary 2, 20, and 40 m below sea floor sediment samples, reverse transcribed to complementary DNA and then sequenced using 454 FLX sequencing technology, yielding over 14,800 sequences from the six samples. Interestingly, 97.3% of the sequences detected were associated with lineages that changed in detection frequency during the storage period including key biogeochemically relevant lineages associated with nitrogen, iron, and sulfur cycling. These lineages have the potential to permanently alter the physical and chemical characteristics of the sediment promoting misleading conclusions about the *in situ* biogeochemical environment. In addition, the detection of new lineages after storage increases the potential for a wider range of viable lineages within the subsurface that may be underestimated during standard community characterizations.

Keywords: sediment microbial ecology, pyrosequencing, geobiology, sediment core storage

INTRODUCTION

The Integrated Ocean Drilling Program (IODP) and its predecessor programs Deep Sea Drilling Program and Ocean Drilling Program have led scientific drilling of the marine subsurface for over 40 years. Three main repositories [Gulf Coast Repository, Bremen Core Repository (BCR), and Kochi Core Repository] collect and store drill material from around the world, providing a resource to land based scientists in an effort to expand the research potential of the Program. The main focus of subsurface research has been chemical and physical characterizations. However, recent initiatives have emphasized the importance of understanding the subseafloor biosphere (Bickle et al., 2011). With this new direction has come new technology and awareness to determine the biological effects on subsurface. Previous studies have described some aspects of the physical, chemical, and biological effects of long-term storage on core integrity (König et al., 2000; Lin et al., 2010), however a detailed analysis of changes in the active microbial community during core material storage has not been presented.

Advancements in drilling technology and expeditions dedicated to microbiology have provided an increase in the number of samples suitable for enhanced microbial community characterization. Resulting studies have produced a better understanding of *in situ* community structure and further described natural diagenetic processes deep beneath the seafloor. Multiple biological processes catalyzed by subsurface microbial populations have been shown to alter the physical and chemical structure of subsurface sediment and rock (reviewed in Fry et al., 2008). With minimal geochemical alteration in subsurface environmental conditions over short time scales (Jørgensen, 2011) the community structure would remain stable in composition and expressed metabolic processes. Therefore, disruptions to *in situ* fluid flow, temperature, or pressure, such as those created during the drilling process and subsequent core storage would be hypothesized to create shifts in both community structure and overall function. This newly structured population would utilize different chemical compounds at different rates compared to the undisturbed population and thus would change the physical and chemical composition of the stored material. Key to this assumption is the availability of a dormant fraction of the population, or a minor fraction that becomes more metabolically active following a disruption event. Dormancy is a valuable and common trait to microbial populations (Jones and Lennon, 2010) but has been more frequently associated with environments that experience periodic perturbations or shifts in environmental conditions (Fuhrman et al., 2006; Jones and McMahon, 2009). Lin

et al. (2010) suggested the presence of potential dormant populations in subsurface sediments by describing a shift in microbial community structure within stored IODP sediment samples. The next step is to determine a shift in metabolically active populations during storage to better describe both the microbial community and associated functional processes threatening core integrity.

This study provides a detailed examination and comparison of the metabolically active fraction of the microbial population at the time of sample recovery, representing near *in situ* conditions, and active microbial populations detected after 3 months of standard core storage. Total community 16S ribosomal RNA (rRNA) transcripts were sequenced from multiple sediment depths collected during IODP Expedition 325 on the Great Barrier Reef. High throughput sequencing using 454 FLX provided the sequencing capacity to statistically determine shifts in the population over time. This work supports and advances a previous study by Lin et al. (2010) by providing unique insight into the metabolically active microbial populations that would be contributing to alterations in physical and chemical properties of sediment cores during storage. These alterations should be considered during post-expedition sediment analysis. This study also demonstrates that minor and/or dormant lineages can be revived when environmental conditions change, providing evidence for a viable fraction of the community. A viable fraction would represent a sink for genetic material and metabolic processes potentially underestimated in current biosphere characterizations.

MATERIALS AND METHODS

SAMPLING ACQUISITION AND STORAGE

Sediment samples were collected during the IODP Expedition 325 aboard the mission specific platform *Greatship Maya*. Drilling occurred April 5th, 2010, at Noggin Pass (17°6.3461′S, 146°33.7526′E) drill hole M0058A using the advance piston coring (APC) drilling system. Immediately following recovery, whole round core sections were cut from the drill core liner at three depths below surface at 2, 20, and 40 m below sea floor (mbsf). For the purposes of this manuscript, the samples collected onboard the *Greatship Maya* are identified as "offshore samples" within this manuscript. These samples were transferred to −80°C freezer and shipped on dry ice to the Mills Laboratory after the completion of the expedition. The remaining core material was then maintained at 4°C during transit, shipping, and storage at the BCR in Bremen, Germany. During expedition onshore activities at the BCR, sediment was collected July 13, 2010 from the same core sections sampled offshore, at locations directly adjacent to the whole round core sections. A 2-cm wide sediment section was collected from the center of the core, homogenized, and frozen at −80°C prior to being shipped on dry ice to the Mills Laboratory. The samples stored at 4°C prior to sub-sampling at the BCR are identified as "onshore samples" within this manuscript.

GEOCHEMICAL ANALYSES

Sediment interstitial water was collected shipboard using Rhizon syringes for geochemical analysis. Samples designated for onshore analysis at BCR were preserved immediately upon collection by refrigerated acidified (cations) or by frozen unacidified (anions) and transported on ice. Ammonium (NH_4^+) was analyzed shipboard using a gas stripping technique described in Hall and Aller (1992). Porewater anions (e.g., SO_4^{2-} and Cl^-,) were measured onshore using ion chromatography at BCR and cations (e.g., Fe, Mn, Ca, S) were measured onshore using inductively coupled plasma–optical emission spectrometry (ICP–OES) at BCR. Total carbon (TC) and total organic carbon (TOC) was analyzed on 50 mg dried sediment taken every 50 cm using a LECO CC-125 carbon–sulfur analyzer onshore at BCR.

NUCLEIC ACID EXTRACTION AND RNA PURIFICATION

Nucleic acids were extracted from both offshore and onshore sampled sediments using a method modified from Mills et al. (2008). The description below provides details not previously published and represents the most updated version of this versatile extraction method. Key to the method was reducing time spent during the extraction process with extraction yields being inversely proportional to duration of extraction procedure. All chemicals were molecular biology grade (MBG) where available. All water for solutions was autoclaved and treated with diethylpyrocarbonate (DEPC) to remove nucleases. A 0.5-g sample was quickly chipped from frozen sediment under sterile conditions and placed into a 2-ml screw top tube with rubber gasket in lid. All samples remained frozen prior to extraction. Between 100 and 250 μl of extraction buffer [250 μl of 1 M Tris–HCl (MP Biomedicals; Solon, OH, USA; pH 8.0), 200 μl of 500 mM ethylenediamine tetraacetic acid (EDTA; EMD Chemicals; Gibbstown, NJ, USA; pH 8.0), and 230 μl of 40% glucose (Calbiochem; La Jolla, CA, USA) raised to a total 10 ml volume with sterile deionized water] was added to each sample tube. The final concentration of the extraction buffer is as follows: 25 mM Tris–HCl, 10 mM EDTA, and 0.92% glucose. Volume added of the extraction buffer was determined by the amount of porewater in sample and should be adjusted accordingly. Sufficient volume of buffer added is achieved when the sample can be adequately vortexed; forming a soft, well-mixed mud. Samples were cycled five times through a 45-s vortex, frozen in liquid nitrogen, and thawed for 1 min at 55°C. Samples were rapidly and completely thawed during 55°C incubation, but temperatures remained low to avoid increasing activity of DNases and RNases. After five cycles were completed, the following solutions were added: 0–150 μl extraction buffer (total volume of extraction buffer added equaled 250 μl between this and the previous addition steps), 100 μl lysozyme solution [extraction buffer with 4 mg ml^{-1} lysozyme (Rockland, Inc.; Gilbertsville, PA, USA) added], and 50 μl of 500 mM EDTA (pH 8.0). Samples were incubated for 10 min at 30°C while shaking at 150 rpm. A solution of phenol (EMD Chemicals; Gibbstown, NJ, USA):chloroform (BDH; West Chester, PA, USA):isoamyl alcohol (MP Biomedicals; Solon, OH, USA, 25:24:1) was added at 800 μl along with 50 μl of 10% sodium dodecyl sulfate (SDS; EMD Chemicals; Gibbstown, NJ, USA). Phenol was not buffered with Tris hydrochloric acid so that the pH remained acidic. Acidic phenol is optimal for RNA extraction. Samples were vortexed for 1 min to create an emulsion prior to centrifugation at 15,000 rpm (21,100 × *g*) for 3 min at room temperature. The top aqueous layer was transferred to a new 2 ml screw top tube containing 800 μl phenol:chloroform:isoamyl alcohol. Samples were again vortexed for 1 min and centrifuged for 3 min at 15,000 rpm (21,100 × *g*) at room temperature. The

aqueous layer was transferred to a new 1.5 ml microcentrifuge tube avoiding any traces of the phenol solution. A total of 50 µl of 3 M sodium acetate (J. T. Baker; Phillipsburg, NJ, USA; pH 6.4) and 1 ml 200 proof MPG ethanol was added to each sample prior to a 15-min centrifuge step at 15,000 rpm (21,100 × *g*) at 4°C. The supernatant was slowly removed and the pellet dried for 10 min. Pellets were resuspended in 50 µl of sodium citrate (pH 6.4) to optimize for RNA preservation. If DNA is desired, resuspend in autoclaved, deionized water (pH 8.0), and buffer the phenol to raise the pH to 8. For RNA sample preparation, extractions were treated with Turbo DNA Free (Ambion, Inc.; Austin, TX, USA) according to manufacturer's instructions to remove residual DNA co-extracted with the RNA.

RNA REVERSE TRANSCRIPTION

Small subunit (SSU) rRNA was reverse transcribed according to Reese et al. (2012). In brief, complementary DNA (cDNA) was produced using moloney murine leukemia virus (MMLV) reverse transcriptase (Promega, Madison, WI, USA) and 518R (5′-CGT ATT ACC GCG GCT GCT GG-3′; Nogales et al., 1999). Aliquots of RNA extract were screened for the presence of residual DNA using the Bacteria domain-specific SSU rRNA gene primers 27F (5′-AGR GTT TGA TCM TGG CTC AG-3′; Giovannoni et al., 1991) and 518R. Thermocycling conditions are described in Reese et al. (2012). All RNA extracts were determined free of residual DNA (data not shown).

PYROSEQUENCING

Primers 28F (5′-GAG TTT GAT CNT GGC TCA G-3′) and 519R (5′-GTN TTA CNG CGG CKG CTG-3′) produced amplicons from cDNA that spanned three hyper-variable regions (V1 through V3; Handl et al., 2011). cDNA amplicons from each of the sediment samples were sequenced at the Research and Testing Laboratory (Lubbock, TX, USA). Amplicons from each sample were first labeled with a 10 base unique multiplex identifier (MID) sequence to allow all samples to be sequenced on a single run of a Roche 454 FLX (454 Life Sciences; Branford, CT, USA). Downstream sequence analysis parsed the individual sequences into sample specific libraries. Resulting libraries were screened for reads less than 200 bases, reads lacking a Roche-designed four base key sequence, and non-bacterial reads lacking specific 28F primer recognition site. Sequences were checked for chimeras using the black box chimera check software (B2C2; Gontcharova et al., 2010). All sequences passing quality control were denoized prior to phylogenetic and statistical analysis. Sequences were then deposited to the National Center for Biotechnology Information database using Sequence Read Archive (SRA) under accession number SRA049351.

PHYLOGENETIC AND STATISTICAL ANALYSIS

All sequences passing quality control were taxonomically classified (percent of total sequence length that aligned with a given database sequence) using the NCBI Basic Local Alignment Search Tool (BLASTn) .NET algorithm (accessed January 2011; Dowd et al., 2005). Sequences with identity scores greater than 97% identity (<3% divergence) to known or well characterized 16S rRNA sequences were resolved at the species level, between 95 and 97% at the genus level, between 90 and 95% at the family, and between 85 and 90% at the order level, 80 and 85% at the class and 77–80% at phyla (Stackebrandt and Goebel, 1994). Only sequences meeting the genus taxonomic classification were incorporated into statistical analyses. Predictions of functional diversity were derived from genus level taxonomic characterization using previous studies for reference. Lineages with multiple metabolic functions identified were assigned to multiple groups to reduce effects of limited geochemical data. The percentage of sequences identified to individual lineages was determined for each sample providing relative abundance information within and among the samples based upon reads per sample. Sequences were further clustered into operational taxonomic units (OTU) using the Ribosome Database Project (RDP; University of Michigan; Lansing, MI, USA) using a 95% sequence similarity cutoff (corresponding to a genus level classification). The sequences were not trimmed prior to clustering to avoid potential biases for or against indel regions common to 16S rRNA. The authors recognize potential problems with this decision; however, using a lower sequence similarity cutoff (95% compared to a typical 97%) produced a reproducible calculation of OTUs with multiple clustering runs. Chao1, Shannon Wiener, and Evenness were calculated from the OTU clustering using RDP.

RESULTS

GEOCHEMICAL CHARACTERIZATION

Cations, anions, and TOC were measured onshore at BCR whereas ammonia and alkalinity were measured shipboard. Alkalinity, pH, and chloride concentrations were unchanged with depth into the sediment. Concentrations of ammonia increased from 0.1 mM near the sediment surface to 2.2 mM at 40 m depth (**Figure 1**). Conversely, sulfate concentrations decreased from 29 mM at the surface to 18 mM at depth. Iron concentrations were low in the top 5 m (1 µM) and increased sharply at 9 m (14 µM) followed by a decrease in concentration until 25 m (0.7 µM). Another sharp increase in iron concentration was observed at 29 m (11.7 µM) and at 36 m (10.9 µM). Manganese followed the same general trend as iron with spikes in concentration at the same depths. Manganese was highest in the surface (0.6 µM) and lowest at 34 m (0.1 µM).

Total carbon was 8.7 wt% on average in hole M0058A. Within the TC, TOC comprised 3% and total inorganic carbon (TIC; carbonates) was 97%. The TOC in M0058A averaged 0.3 wt% throughout the sediment column.

PHYLOGENETIC DISTRIBUTION OF BACTERIAL LINEAGES

All samples collect onboard the *Greatship Maya* and immediately stored at −80°C are referred to as "offshore" samples. This sampling strategy is commonly considered indicative of an *in situ* population characterization. Samples collected at the BCR following 3 months of storage at 4°C prior to being cryogenically frozen are referred to as "onshore" samples.

A total of 14,897 16S rRNA cDNA sequences passed quality control from the two sets of 2, 20, and 40 mbsf sediment samples. Twelve phyla representing 71 families were identified. Sequences derived from offshore samples contained a total of 38 families, while the onshore samples had 54 families. This increased diversity following 3 months storage was also observed in Chao1 and Shannon Wiener calculations (**Table 1**). With the exception of

the 20-mbsf sample collected during post-cruise operations, the evenness increased during storage. Changes in trends in sequence abundance per lineage were observed between the offshore and onshore samples (**Figure 2**). A majority of the samples had more than 99% of the total sequences represented by lineages that shifted in frequency of detection between sampling time points. Twenty families represented less than 1.0% of the total sequences and were omitted from this analysis. These 20 families accounted for 4.0% of the total sequences from the 2-m sample collected after storage, whereas they incorporated less than 0.8% of the total sequences for four of the other five samples.

MICROBIAL COMMUNITY STRUCTURE – OFFSHORE SAMPLES

A total of 40 families were detected from samples immediately frozen shipboard at −80°C. A subset of 19 families (83.4% of the offshore sequences) was more frequently detected at all depths compared to the samples collected during the onshore portion of Expedition 325 (**Table 2**). These families represented 94.5% at 2 mbsf, 87.5% at 20 mbsf, and 68.2% at 40 mbsf of the *in situ* sequences detected. In contrast, these families represented only 4.3, 14.8, and 23.8%, respectively, of the total sequences obtained from the corresponding depths in the onshore sediment samples.

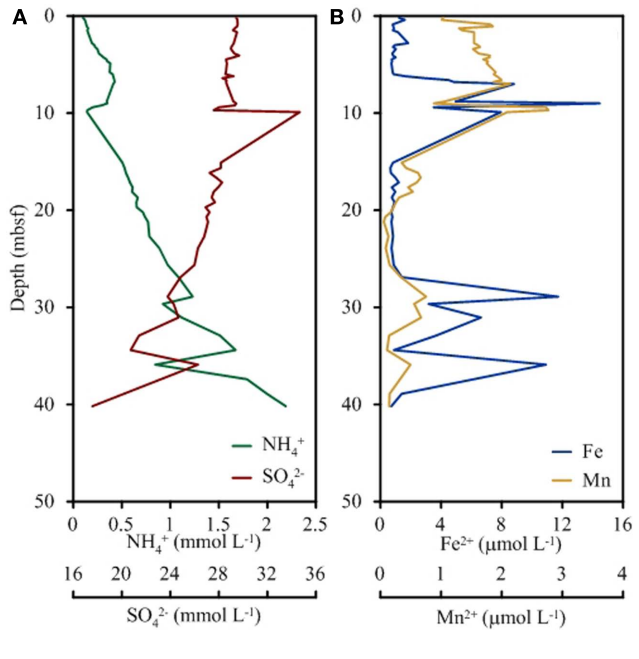

FIGURE 1 | Depth profile of key geochemical species significant to microbial respiration including ammonium and sulfate (A) and total iron and total manganese (B).

Of the 19 families detected in the 2-mbsf offshore sediment samples, Lachnospiraceae (24.5%), Ruminococcaceae (17.0%), Clostridiaceae (10.1%), Lactobacillaceae (9.3%), Enterococcaceae (8.1%), and Xanthomonadaceae (7.8%) were detected the most frequently (**Table 2**). These lineages collectively only represented 2.8% of the sequences obtained from the 2-mbsf sediments collected during on shore sampling. Functional classification suggest over 66% of these sequences were associated with lineages capable of fermentative processes (**Figure 3**). Aerobic lineages comprised 5.2% of the sequences while groups capable of carbonate dissolution represented 17.0%.

A total of 19 families were detected at 20 mbsf depth. Although the number of families detected was similar to the 19 families at 2 mbsf sample, a population shift was observed at 20 mbsf with no Lachnospiraceae, Clostridiaceae, Enterococcaceae, and Xanthomonadaceae detected (**Table 2**). Lactobacillaceae and Ruminococcaceae increased in abundance to represent 35.2 and 27.2% of the sequences obtained from this depth, respectively. Ruminococcaceae was not detected in the sediments after the storage period at 4°C. Similarly, Pseudomonadaceae represented 10.9% of the total sequences at this depth, but only 0.7% after the 3-month storage. Lactobacillaceae was detected at 13.6% of the total sequences obtained from the 20-mbsf sediment stored at 4°C. Rhizobiaceae (6.1%) and Enterobacteriaceae (5.5%) were also detected at greater than 5% abundance of total sequences (**Table 2**). Similar to the 2-mbsf sample, fermentative lineages were the most frequently detected (68.5% of total sequences; **Figure 3**). Aerobic lineages were again 5.0% of the sequences however groups capable of carbonate dissolution represented 27.2% of the total sequences. Nitrate reducing lineages increased in frequency detected (16.1% of the total sequences).

At 40 mbsf, 19 families were identified. Both Lactobacillaceae and Ruminococcaceae decreased in abundance (20.1 and 13.6%, respectively) compared to the 20-mbsf sample (**Table 2**). Other lineages detected at 40 mbsf included Microbacteriaceae (10.6%), Comamonadaceae (9.3%), Enterobacteriaceae (8.9%), Sphingomonadaceae (7.1%), and Corynebacteriaceae (7.0%). A

Table 1 | Sequence and classification abundances and statistical indices of each sample.

Sampling location	Depth (mbsf)	Number of Sequences	OTU[a]	Phyla	Family	Genus	Chao1[b]	Shannon	Evenness
Offshore	2	3161	79	7	17	17	133 (100–220)	3.01	0.689
	20	873	46	4	18	19	52 (48–71)	2.70	0.704
	40	2316	58	7	19	25	73 (62–109)	2.97	0.732
Onshore	2	2165	104	7	33	41	148 (121–214)	3.46	0.745
	20	3408	72	4	18	25	116 (89–182)	2.80	0.655
	40	3498	92	5	25	30	123 (103–176)	3.44	0.762

[a] *Operational taxonomic units defined by 95% sequence similarity.*

[b] *Numbers in parenthesis indicate 95% confidence interval.*

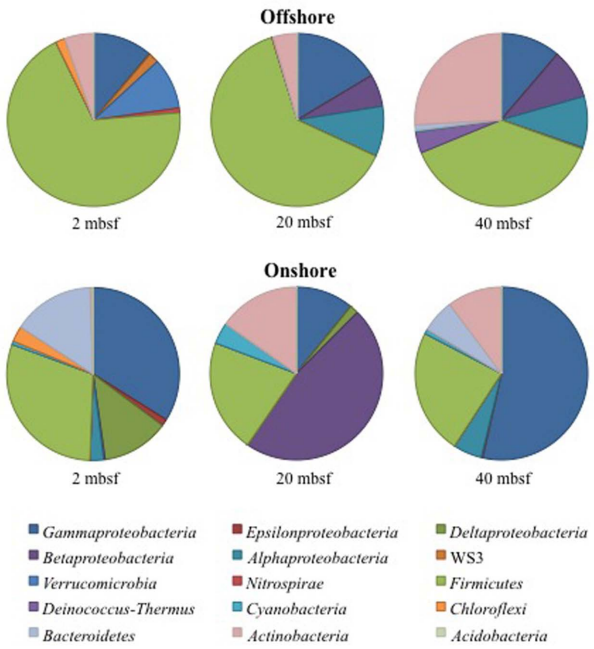

FIGURE 2 | Phyla and class level distribution of bacterial lineages. Sequences were annotated using RDP Classifier. Identification was determined with a confidence interval of 70%. Sequence data supports a high taxonomic level alteration of the community composition during 4˚C storage.

general trend of increasing abundance with depth was noted with all of these lineages. In addition, these lineages were detected over three times more frequently in the offshore samples compared to the onshore samples. A similar distribution of functional process was observed compared to the 20-m sample with the exception of no aerobic lineages detected (**Figure 3**).

MICROBIAL COMMUNITY STRUCTURE – ONSHORE SAMPLES

A total of 57 families were detected in the three samples collected during the onshore portion of Expedition 325 following 3 months of storage at 4˚C (**Table 2**). There were 24 families with a higher sequence abundance (62.1% of the total sequences) at all three depths following the 3-month storage at 4˚C (**??** in Appendix) compared to the samples collected and preserved at −80˚C on the ship. These families accounted for 91.4% at 2 mbsf, 23.3% at 20 mbsf, and 71.6% mbsf of the total classified sequences from sediments collected during the onshore portion of Expedition 325. In contrast, the same 24 families represented only 0.2, 1.4, and 2.3% of the sequences obtained from 2, 20, and 40 mbsf, respectively, from sediments stored immediately at −80˚C.

At 2 mbsf, a total of 33 families were detected with 20 families representing 90.3% of the sequences (**Table 2**). The most frequently detected lineages included Halomonadaceae (24.2%), Clostridia (19.7%), Flavobacteriaceae (12.2%), Geobacteraceae (8.9%), Carnobactericeae (3.4%), Oceanospirillales (3.3%), and Desulfobulbaceae (3.3%). No other family represented more than 3.0% of the total sequences. Aerobic lineages were the most frequently detected with 45.7% of the sequences attributed to this group (**Figure 3**). While fermentative lineages were also detected after the 3-months, the frequency decreased over 50% compared to the offshore samples. Nitrate, iron, and sulfate-reducing lineages represented 4.1, 10.2, and 6.4%, respectively. In contrast to the offshore 2 mbsf sample, carbonate reducing lineages accounted for only 1.1% of the sequences.

A total of 20 families were detected in the 20 mbsf sediment samples collected during the onshore portion of the Expedition (**Table 2**). Within this set, 23.3% of the total sequences were represented by 10 families that were more abundant in the stored sediments at all depths compared to the offshore samples. An additional 62.5% of the sequences from this sample were related to Comamonadaceae (44.3%), Microbacteriaceae (8.6%), and Enterobacteriaceae (8.6%; **Table 2**). Sequences related to Comamonadaceae increased in abundance by an order of magnitude between the offshore sampling (4.5%) and the post-cruise sampling period at 20 mbsf (44.3%). However, this lineage was not included in the initial percent calculations due to the abundance decreasing at 40 mbsf from 9.3 to 0.3% after 3 months at 4˚C. A similar trend was determined for Microbacteriaceae with an increase at 20 mbsf from 0.2 to 8.6% during the 3-month period at 4˚C, whereas in samples at 40 mbsf the abundance decreased from 10.6 to 0.0%. The 20 mbsf sample was the only depth where Enterobacteriaceae was more frequently detected in onshore sampled sediment (8.6%) compared to the offshore sampled sediment (4.3%). Collectively, the 10 families plus Comamonadaceae, Microbacteriaceae, and Enterobacteriaceae equal 84.9% of the sequences from the 20-m sample collected onshore, compared to 11.6% of the sequences from the corresponding offshore sample. Additional families detected frequently at 20 mbsf included Clostridia (7.3%), Oscillatoriales (3.7%), and Propionibacteriaceae (3.6%). In contrast to the 2-mbsf sediments, Halomonadaceae, Clostridia, Flavobacteriaceae, Geobacteraceae, Carnobactericeae, Oceanospirillales, and Desulfobulbaceae were not detected as this depth. Nitrate reducing lineages incorporated 45.0% of the total sequences while fermenters remained constant with depth (**Figure 3**).

At 40 mbsf, sequence annotation identified 29 total families within the sediments. A subset of 14 families represented 71.6% of the total sequences at this depth (**Table 2**). These families included Halomonadaceae (27.9%), Altermonadaceae (11.2%), Piscirickettsiaceae (7.7%), Flavobacteriaceae (6.2%), Streptococcaceae (4.6%), and Solirubrobacteraceae (4.3%). Only Streptococcaceae was also detected (1.8%) in the offshore samples. Although Lactobacillaceae (10.3%) and Enterobacteriaceae (4.6%) were detected frequently in the onshore samples, they were two times less that the number of sequences detected in sediments preserved on the ship. Aerobic lineages represented 44.6% of the sequences detected while fermenters accounted for 21.4% (**Figure 3**). Lineages associated with methylotrophs incorporated 7.8% of the total sequences while carbonate dissolution groups represented 3.4% of the sequences, the most at any depth in the onshore samples.

DISCUSSION

This study describes a shift in population structure within sediment core material obtained from borehole M00058A during

Table 2 | Phylogenetic classification of bacterial sequences obtained from Expedition 325.

Phylum	Class	Family	2 m		20 m		40 m	
			4˚C	−80˚C	4˚C	−80˚C	4˚C	−80˚C
Acidobacteria			0.1	0.0	0.0	0.0	0.0	0.0
		Acidobacteriaceae	0.1	0.0	0.0	0.0	0.0	0.0
Actinobacteria			0.4	5.4	15.3	4.5	10.3	25.9
		Corynebacteriaceae	0.0	0.0	0.0	0.3	2.4	7.0
		Geodermatophilaceae	0.0	0.0	0.0	0.0	0.5	8.1
		Intrasporangiaceae	0.0	0.1	1.7	0.0	0.1	0.0
		Microbacteriaceae	0.0	0.0	8.6	0.2	0.0	10.6
		Micrococcaceae	0.0	0.0	0.8	0.0	0.2	0.0
		Nocardiaceae	0.0	2.8	0.1	0.0	0.0	0.0
		Nocardioidaceae	0.0	2.4	0.4	3.5	0.0	0.0
		Propionibacteriaceae	0.3	0.1	3.6	0.5	2.7	0.2
		Solirubrobacteraceae	0.0	0.0	0.0	0.0	4.3	0.0
Bacteroidetes			15.3	0.0	0.0	0.0	6.2	1.1
		Marinilabiaceae	0.0	0.0	0.0	0.0	0.0	1.1
		Cytophagaceae	2.7	0.0	0.0	0.0	0.1	0.0
		Flavobacteriaceae	12.2	0.0	0.0	0.0	6.2	0.0
		Sphingobacteriales (family)	0.4	0.0	0.0	0.0	0.0	0.0
Chloroflexi			2.9	1.8	0.0	0.2	0.0	0.0
		Anaerolineaceae	2.1	1.8	0.0	0.0	0.0	0.0
		Caldilineaceae	0.0	0.0	0.0	0.2	0.0	0.0
		Chloroflexaceae	0.9	0.0	0.0	0.0	0.0	0.0
Cyanobacteria			0.6	0.0	4.0	0.0	0.9	0.3
		Microchaetaceae	0.0	0.0	0.1	0.0	0.0	0.0
		Nostocaceae	0.0	0.0	0.0	0.0	0.9	0.0
		Oscillatoriales (family)	0.1	0.0	3.7	0.0	0.0	0.0
		Pleurocapsales (family)	0.5	0.0	0.1	0.0	0.0	0.3
Deinococcus–Thermus			0.0	0.0	0.0	0.0	0.0	3.9
		Deinococcaceae	0.0	0.0	0.0	0.0	0.0	3.9
Firmicutes			30.0	69.1	21.2	63.3	23.5	38.3
		Bacillaceae	1.1	0.0	0.0	0.0	0.0	0.0
		Bacillales (family)	0.0	0.0	0.1	0.6	1.7	0.0
		Planococcaceae	2.1	0.0	0.0	0.0	0.0	0.0
		Carnobacteriaceae	3.4	0.0	0.0	0.0	0.0	0.0
		Lactobacillaceae	0.0	9.3	13.6	35.2	10.3	20.9
		Clostridia (family)	19.7	0.0	0.0	0.0	0.0	0.0
		Clostridiaceae	1.7	10.1	0.0	0.0	0.0	1.5
		Clostridiales (family)	0.0	0.0	7.3	0.3	0.0	0.0
		Eubacteriaceae	0.2	0.0	0.0	0.0	0.0	0.5
		Lachnospiraceae	0.0	24.5	0.0	0.0	3.5	0.0
		Ruminococcaceae	1.1	17.0	0.0	27.2	3.4	13.6
		Bacillales (family)	0.0	0.0	0.1	0.6	1.7	0.0
		Enterococcaceae	0.0	8.1	0.0	0.0	0.0	0.0
		Lactobacillaceae	0.0	9.3	13.6	35.2	10.3	20.9
		Streptococcaceae	0.8	0.0	0.0	0.0	4.6	1.8
Nitrospirae			0.0	0.9	0.0	0.0	0.0	0.0
		Nitrospiraceae	0.0	0.9	0.0	0.0	0.0	0.0
Proteobacteria			50.6	11.3	59.6	31.9	59.2	30.2
	Alphaproteobacteria		2.5	0.0	0.0	9.4	5.4	9.6
		Kopriimonadaceae	0.0	0.0	0.0	0.0	0.1	0.0
		Bradyrhizobiaceae	0.0	0.0	0.0	0.3	0.0	0.0

(Continued)

Table 2 | Continued

Phylum	Class	Family	2 m		20 m		40 m	
			4˚C	−80˚C	4˚C	−80˚C	4˚C	−80˚C
		Hyphomicrobiaceae	0.0	0.0	0.0	0.0	0.1	0.0
		Methylobacteriaceae	0.0	0.0	0.0	0.3	0.0	2.5
		Rhizobiaceae	0.1	0.0	0.0	6.2	0.0	0.0
		Rhodobacteraceae	1.1	0.0	0.0	0.0	0.0	0.0
		Acetobacteraceae	0.0	0.0	0.0	0.2	0.0	0.0
		Rhodospirillaceae	1.4	0.0	0.0	0.0	2.9	0.0
		Sphingomonadaceae	0.0	0.0	0.0	2.3	2.3	7.1
	Betaproteobacteria		0.3	0.1	47.1	6.1	0.3	9.3
		Alcaligenaceae	0.0	0.1	0.0	0.0	0.0	0.0
		Comamonadaceae	0.3	0.0	44.3	4.5	0.3	9.3
		Oxalobacteraceae	0.0	0.0	0.0	1.5	0.0	0.0
		Neisseriaceae	0.0	0.0	2.8	0.0	0.0	0.0
	Deltaproteobacteria		12.6	0.0	1.6	0.0	0.0	0.0
		Desulfobulbaceae	3.3	0.0	0.0	0.0	0.0	0.0
		Desulfuromonadaceae	0.4	0.0	0.0	0.0	0.0	0.0
		Geobacteraceae	8.9	0.0	0.0	0.0	0.0	0.0
		Cystobacteraceae	0.0	0.0	1.6	0.0	0.0	0.0
	Epsilonproteobacteria		1.3	0.0	0.0	0.0	0.0	0.0
		Campylobacteraceae	1.3	0.0	0.0	0.0	0.0	0.0
	Gammaproteobacteria		33.9	11.2	10.9	16.4	53.5	11.3
		Alteromonadaceae	0.6	0.0	0.0	0.0	11.2	0.0
		Colwelliaceae	0.3	0.0	0.0	0.0	0.0	0.0
		Moritellaceae	0.4	0.0	0.0	0.0	0.0	0.0
		Enterobacteriaceae	0.0	3.2	8.6	5.5	4.3	8.9
		Halomonadaceae	24.2	0.0	1.5	0.0	27.9	0.0
		Oceanospirillales (family)	3.3	0.0	0.0	0.0	0.0	0.0
		Moraxellaceae	2.2	0.0	0.0	0.0	1.1	0.0
		Pseudomonadaceae	1.4	0.2	0.7	10.9	0.1	0.0
		Piscirickettsiaceae	1.4	0.0	0.0	0.0	7.8	0.0
		Vibrionaceae	0.0	0.0	0.0	0.0	1.2	2.4
		Xanthomonadaceae	0.0	7.8	0.0	0.0	0.1	0.0
Verrucomicrobia			0.0	9.6	0.0	0.0	0.0	0.3
		Opitutaceae	0.0	0.0	0.0	0.0	0.0	0.3
		Spartobacteria (family)	0.0	0.2	0.0	0.0	0.0	0.0
		Verrucomicrobiaceae	0.0	9.4	0.0	0.0	0.0	0.0
WS3			0.0	1.9	0.0	0.0	0.0	0.0
		WS3 (family)	0.0	1.9	0.0	0.0	0.0	0.0

IODP Expedition 325 to the Great Barrier Reef following 3 months storage at 4˚C. These data indicate subsurface microbial populations remain metabolically active under these conditions and are thus capable of altering sediment geochemistry during storage. Unique to this analysis is the use of RNA-based targets to determine the metabolically active fraction of the total population. The concentration of ribosomes, and thus copies of SSU rRNA within a cell, is linearly correlated to cellular metabolic activity (Delong et al., 1989; Kerkhof and Ward, 1993; Lee and Kemp, 1994), with dormant and dead cells having few to no ribosomes present (Fegatella et al., 1998). The active population both responds to and changes the geochemistry in the environment. Therefore, characterizing this population provided a proxy for identifying potential shifts in the geochemistry and assessment of the integrity of the core. In addition, a change in this population determined a fraction of the population that was below detection limits or dormant during *in situ* geochemical conditions, but active during storage conditions. This viable fraction of the community represented a source for different metabolic processes available to the community when the environment changed and highlighted a potentially underestimated portion of the community. Further enrichment-based culturing has the potential to define a larger amount of diversity and function within this and other communities.

A shift at the family taxonomic level following 3 months of storage between the offshore and onshore sampling time points incorporated as much as 90% of the sequence data set from the

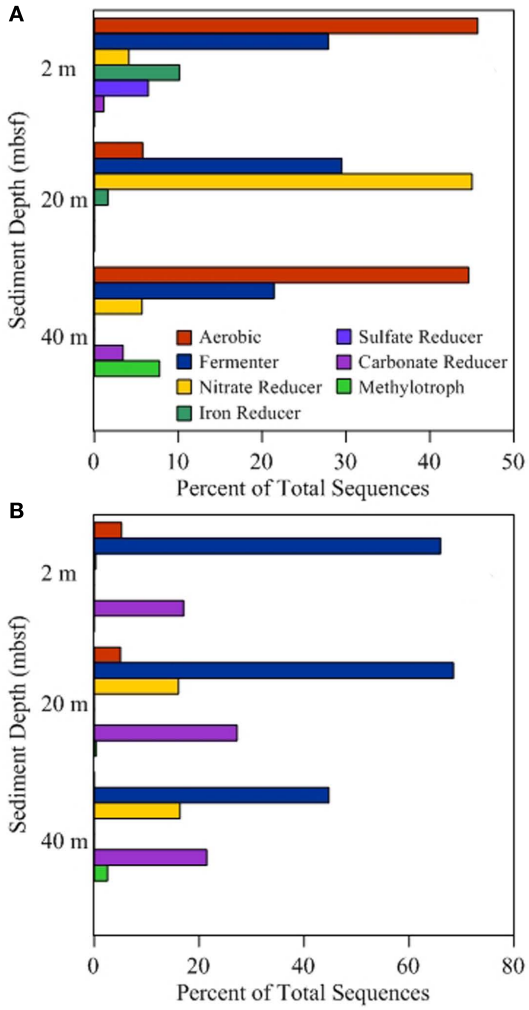

FIGURE 3 | Functional group distribution. Sequence annotation at the genus level was used to identify functional groups associated with different metabolic processes. Lineages associated with multiple processes were placed in multiple categories to avoid assumptions of activity. Percentages presented for onshore samples **(A)** and offshore samples **(B)** are based on the total number of sequences obtained and are independent of percentages reported for other categories.

active fraction of the population. Active microbial processes alter both the chemical and physical composition of subsurface sediments. These diagenetic processes are common and have been well studied *in situ*, however the potential for alteration has been less understood when the sediments were removed from the environment and placed in cold storage conditions. The integrity of core material is critical for post-expedition research and sediment curation efforts for programs like IODP. This manuscript serves to better understand the microbial populations that are metabolically active during sediment core storage and provide descriptions of potential processes acting on those sediments. In addition, increased diversity in the stored sediments compared to *in situ* analysis suggests that species diversity in the subsurface may be underestimated. Although sediments selected here are from an IODP expedition, results describing microbial activity at 4°C should be considered when storing any non-sterilized samples for subsequent analysis.

SHIFTS IN COMMUNITY STRUCTURE

Metabolically active microbial populations alter their surrounding environments through the consumption and production of chemical compounds. As populations shift, the consumption and production rates change and are no longer representative of *in situ* conditions. During initial characterization of the *in situ* metabolically active community structure, lineages associated with fermentation, including Lactobacillaceae, Clostridiaceae, and Ruminococcaceae, were detected at highest frequency compared to other lineages (**Figure 3**). In total, lineages associated with fermentation processes accounted for nearly 70% of the 2 and 20 mbsf samples and over 40% for the 40-mbsf sample. The prevalence of fermentative lineages in the shallow subsurface has been previously noted (Toffin et al., 2005), providing support for the annotation presented. These lineages may play a significant role in the conversion of organic matter present in the shallow sediments (Toffin et al., 2005).

Following storage for 3 months, the number of groups associated with fermentative sequences decreased over two times. This discrepancy may be attributed to a reduction of substrate due to disrupted *in situ* fluid flow. As the geochemical conditions changed, the niche advantage decreased allowing other lineages to become more abundant. In the 2- and 40-mbsf samples, fermentation capable lineages were in part replaced by an increase in aerobic lineages (**Figure 3**). While this group was detected in the offshore samples at 2 mbsf, no aerobic lineages were detected at the 40-mbsf sample. After the 3-months at 4°C, 44.6% of the sequences obtained related to aerobic organisms compared to 0.0% in the offshore sample at the same depth. This suggests oxygen intrusion into the core. Oxygen can affect both the biology as well as the chemistry of the sediments and should be avoided where possible. Lin et al. (2010) observed sulfide oxidation to sulfate when sediment cores experienced oxygen penetration. Additionally, the increase in sulfate was predicted to promote a community shift favoring sulfate-dependent methane oxidizers. While the Lin et al. (2010) study was DNA based, this current RNA-based study supports their conclusion as methylotrophs were detected in the metabolically active fraction of the total populations. The depletion of sulfate by these lineages may inhibit geochemical detection of the sulfide oxidation process, stressing the importance of molecular analyses coupled to geochemical measurements to better environmental characterizations. In contrast to the 40-mbsf sample, it is hypothesized that oxygen remained limiting in the sample collected at 20 mbsf as a rise in nitrate reducers were observed. An increase in nitrogen cycling populations, including Comamonadaceae, Rhodospirillaceae, and Rhodobacteraceae, would affect ammonia, nitrate, and nitrite analysis to levels not reflective of the *in situ* conditions. Differences between the 20- and 40-mbsf biogeochemical profiles suggest variable storage affects between core sections, adding to the unpredictability of geochemical and microbiological results from stored sediments.

A large percentage of offshore sequence data sets were associated with lineages capable of carbonate dissolution (**Figure 3**).

This was expected given the location of the sediments being in close proximity to the Great Barrier Reef. However, following incubation, the frequency of detection for these groups dropped an order of magnitude on average with the 20-mbsf sample populations shifting from 27.2% of the total sequences to undetectable. This shift suggests a major alteration of the geochemical environment, requiring specific analysis to determine the cause and implications. Due to shipboard limitations, this analysis could not be preformed and thus was beyond the capacity of this study. These data represent the first step to being able to identify metabolic processes within stored sediments and provide a more clear prediction of sediment alteration capacity.

A significant rise in the number of sequences related to iron and sulfate-reducing lineages was observed in the sediments obtained onshore compared to the offshore samples. Both iron and sulfate-reducing functional groups were only detected after sediment storage and accounted for over 10 and 6% of the total sequences. These populations becoming metabolically active would affect any post-expedition analysis of sulfur and iron chemistry. They have the potential to reduce sulfate and Fe(III) concentrations in marine systems to below detection limits while forming multiple iron sulfur mineral compounds. Secondary effects would change the pH of the sediment and alter organic matter content and concentration. In addition, the paleomagnetic record within the sediments, or other material would be altered by both iron reducing and oxidizing populations (Kostka and Nealson, 1995; Zachara et al., 1998 reviewed in Kopp and Kirschvink, 2008). An active microbial population would alter multiple characterization efforts within the sediment profile. Understanding these processes and how to better reducing them is required.

VIABLE FRACTION OF THE POPULATION – METABOLIC SINK

A community shift within a closed system implies that a portion of the population was either metabolically active but below detection limits, or dormant *in situ*. The implications of these shifts are critical for the core preservation strategies and down stream analysis reliability, as well as, for understanding the overall viable fraction of the subsurface biosphere. To verify a closed system, sediments collected were examined for contamination resulting from the drilling process. Results suggest that the contamination potential was very low, but the authors recognize that this possibility cannot be fully ruled out. A general contamination during drilling or storage would have resulted in a homogenization of the detected community structure. Variations in the detection frequency of multiple lineages suggest a general contamination did not occur. Aerobic populations were detected in the 40-mbsf onshore sample. These two lineages, Alteromonadaceae and Flavobacteriaceae were detected in the 2-mbsf sample as well, but not in the 20-mbsf sample. The increase in abundance of related sequences suggests oxygen intrusion into the sediment may have occurred, however these populations can be facultatively anaerobic as well. These two populations were not detected at 20 mbsf, reducing the potential for this to be a drilling contamination or air borne contamination during storage. Additional testing beyond the scope of this paper would be required to determine the true origin of this population.

These results support a fraction of the population remaining viable but dormant within the subsurface. The lower amount of diversity reported in the metabolically active *in situ* population (offshore sample) compared to the higher level of diversity observed on shore supports niche diversification during storage and the revival of dormant populations. The coring process disrupted multiple environmental factors, including resource availability, pressure, and temperature. These stressors have contributed to shifts in community composition in other environments (Hunter et al., 2006; Lewis, 2007). Within these samples, the environmental changes revived microbial populations in sediments dated to over 50 kyr cal before present (Yusuke et al., 2011). The subsurface is considered geochemically stable with slow change over time; a characteristic that has the potential to limit diversity (Orcutt et al., 2011) and the effectiveness of dormancy as a strategy to maintain a viable population (Jones and Lennon, 2010). However, the population characterized in these samples potentially provided a source of functional diversity for community activity over geologic timescales. This expands the potential range of such survival strategies beyond environments with periodic shifts in geochemical and geotechnical conditions (Cohen, 1970; Fuhrman et al., 2006; Jones and Lennon, 2010), and should be considered in estimates of community functional capacity. Future studies will quantify the depth of the functional sink available to respond to changing environments. In addition, the length of time these dormant populations remain viable will be determined to better understand the effect of temporal isolation.

ACKNOWLEDGMENTS

The authors would like to thank the science party of IODP Expedition 325 and the crew aboard the *Greatship Maya*. Additionally, we thank Scot Dowd, Alicia Shepard, and Laura Zinke with data processing. The Consortium of Ocean Leadership provided funding for this project. This paper is contribution number 126 to the Center for Dark Energy Biosphere Investigations (CDEBI).

REFERENCES

Bickle, M., Arculus, R., Barrett, P., Decanto, R., Camoin, G., Edwards, K., Fisher, A., Inagaki, F., Ravelo, C., Saffer, D., and Teagle, D. (2011). *Illuminating Earth's Past, Present, and Future: International Ocean Discovery Program Science Plan 2013–2023.* Washington DC: Integrated Ocean Drilling Program Management International.

Cohen, D. (1970). A theoretical model for the optimal timing of diapause. *Am. Nat.* 104, 389–400.

Delong, E. F., Wickham, G. S., and Pace, N. R. (1989). Phylogenetic stains – ribosomal RNA-based probes for the identification of single cells. *Science* 243, 1360–1363.

Dowd, S. E., Zaragoza, J., Rodriguez, J. R., Oliver, M. J., and Payton, P. R. (2005). Windows.NET network distributed Basic Local Alignment Search Toolkit (W.ND-BLAST). *BMC Bioinformatics* 6, 93. doi:10.1186/1471-2105-6-93

Fegatella, F., Lim, J., Kjelleberg, S., and Cavicchioli, R. (1998). Implications of rRNA operon copy number and ribosome content in the marine oligotrophic ultramicrobacterium *Sphingomonas* sp. strain RB2256. *Appl. Environ. Microbiol.* 64, 4433–4438.

Fry, J. C., Parkes, R. J., Cragg, B. A., Weightman, A. J., and Webster, G. (2008). Prokaryotic biodiversity and activity in the deep subseafloor biosphere. *FEMS Microbiol. Ecol.* 66, 181–196.

Fuhrman, J. A., Hewson, I., Schwalbach, M. S., Steele, J. A., Brown, M. V., and Naeem, S. (2006). Annually

reoccurring bacterial communities are predictable from ocean conditions. *Proc. Natl. Acad. Sci. U.S.A.* 103, 13104–13109.

Giovannoni, J. J., Wing, R. A., Ganal, M. W., and Tanksley, S. D. (1991). Isolation of molecular markers from specific chromosomal intervals using DNA pools from existing mapping populations. *Nucleic Acids Res.* 19, 6553–6558.

Gontcharova, V., Youn, E., Wolcott, R. D., Hollister, E. B., Gentry, T. J., and Dowd, S. E. (2010). Black box chimera check (B2C2): a windows-based software for batch depletion of chimeras from bacterial 16S rRNA gene datasets. *Open Microbiol. J.* 4, 47–52.

Hall, P. O., and Aller, R. C. (1992). Rapid, small-volume, flow-injection analysis for sigma CO2 and $NH4^+$ in marine and fresh waters. *Limnol. Oceanogr.* 37, 1113–1119.

Handl, S., Dowd, S. E., Garcia-Mazcorro, J. F., Steiner, J. M., and Suchodolski, J. S. (2011). Massive parallel 16S rRNA gene pyrosequencing reveals highly diverse fecal bacterial and fungal communities in healthy dogs and cats. *FEMS Microbiol. Ecol.* 76, 1–10.

Hunter, E. M., Mills, H. J., and Kostka, J. E. (2006). Microbial community diversity associated with carbon and nitrogen cycling in permeable marine sediments. *Appl. Environ. Microbiol.* 72, 5689–5701.

Jones, S. E., and Lennon, J. T. (2010). Dormancy contributes to the maintenance of microbial diversity. *Proc. Natl. Acad. Sci. U.S.A.* 107, 5881–5886.

Jones, S. E., and McMahon, K. D. (2009). Species-sorting may explain an apparent minimal effect of immigration on freshwater bacterial community dynamics. *Environ. Microbiol.* 11, 905–913.

Jørgensen, B. B. (2011). Deep subseafloor microbial cells on physiological standby. *Proc. Natl. Acad. Sci. U.S.A.* 108, 18193–18194.

Kerkhof, L. J., and Ward, B. B. (1993). Comparison of nucleic acid hybridization and fluorometry for measurement of RNA/DNA relationship with growth rate in a marine bacterium. *Appl. Environ. Microbiol.* 59, 1303–1307.

König, I., Lougear, A., Bruns, P., Gru¨tzner, J., Trautwein, A. X., and Dullo, W.-C. (2000). "Iron oxidation in sediment cores (site 1062) during six months of storage in the Ocean Drilling Program archive," in *Proceedings of the Ocean Drilling Program, Scientific Results*, eds L. D. Keigwin, D. Rio, G. D. Acton, and E. Arnold (College Station: Ocean Drilling Program).

Kopp, R. E., and Kirschvink, J. L. (2008). The identification and biogeochemical interpretation of fossil magnetotactic bacteria. *Earth Sci. Rev.* 86, 42–61.

Kostka, J. E., and Nealson, K. H. (1995). Dissolution and reduction of magnetite by bacteria. *Environ. Sci. Technol.* 29, 2535–2540.

Lee, S. H., and Kemp, P. F. (1994). Single cell RNA content of natural marine planktonic bacteria measured by hybridization with multiple 16S ribosomal RNA targeted fluorescent probes. *Limnol. Oceanogr.* 39, 869–879.

Lewis, K. (2007). Persister cells, dormancy and infectious disease. *Nat. Rev. Microbiol.* 5, 48–56.

Lin, Y. S., Biddle, J. F., Lipp, J. S., Orcutt, B. N., Holler, T., Teske, A., and Hinrichs, K. U. (2010). Effect of storage conditions on archaeal and bacterial communities in subsurface marine sediments. *Geomicrobiol. J.* 27, 261–272.

Mills, H. J., Hunter, E., Humphrys, M., Kerkhof, L., Mcguinness, L. M., Huettel, M., and Kostka, J. E. (2008). Characterization of nitrifying, denitrifying, and overall bacterial communities in permeable marine sediments of the northeastern Gulf of Mexico. *Appl. Environ. Microbiol.* 74, 4440–4453.

Nogales, B., Moore, E. R. B., Abraham, W. R., and Timmis, K. N. (1999). Identification of the metabolically active members of a bacterial community in a polychlorinated biphenyl-polluted moorland soil. *Environ. Microbiol.* 1, 199–212.

Orcutt, B. N., Sylvan, J. B., Knab, N. J., and Edwards, K. J. (2011). Microbial ecology of the dark ocean above, at, and below the seafloor. *Microbiol. Mol. Biol. Rev.* 75, 361–422.

Reese, B. K., Mills, H. J., Dowd, S., and Morse, J. W. (2012). Benthic biogeochemistry of microbial iron and sulfate reduction in the Gulf of Mexico hypoxic zone. *Geomicrobiology* (in press).

Stackebrandt, E., and Goebel, B. M. (1994). A place for DNA-DNA reassociation and 16S ribosomal RNA sequence analysis in the present species definition in bacteriology. *Int. J. Syst. Bacteriol.* 44, 846–849.

Toffin, L., Zink, K., Kato, C., Pignet, P., Bidault, A., Bienvenu, N., Birrien, J. L., and Prieur, D. (2005). *Marinilactibacillus piezotolerans* sp nov., a novel marine lactic acid bacterium isolated from deep sub-seafloor sediment of the Nankai Trough. *Int. J. Syst. Evol. Microbiol.* 55, 345–351.

Yusuke, Y., Webster, J. M., Cotterill, C., Braga, J. C., Jovane, J., Mills, H. J., Morgan, S., Suzuki, A., and Scientists, T. I. E. (2011). IODP Expedition 325: Great Barrier Reefs reveals past sea-level, climate and environmental changes since the last ice age. *Sci. Drilling* 12, 32–45.

Zachara, J. M., Fredrickson, J. K., Li, S. M., Kennedy, D. W., Smith, S. C., and Gassman, P. L. (1998). Bacterial reduction of crystalline Fe3+ oxides in single phase suspensions and subsurface materials. *Am. Mineral.* 83, 1426–1443.

Conflict of Interest Statement: The authors declare that the research was conducted in the absence of any commercial or financial relationships that could be construed as a potential conflict of interest.

Received: 23 November 2011; paper pending published: 16 December 2011; accepted: 30 January 2012; published online: 17 February 2012.

Citation: Mills HJ, Reese BK and Peter CS (2012) Characterization of microbial population shifts during sample storage. Front. Microbio. ***3****:49. doi: 10.3389/fmicb.2012.00049*

This article was submitted to Frontiers in Extreme Microbiology, a specialty of Frontiers in Microbiology.

APPENDIX

Table A1 | Taxonomic identification of the Great Barrier Reef subsurface sequence data set.

Phylum	Class	Order	Family	Genus	2 m		20 m		40 m	
					4°C	−80°C	4°C	−80°C	4°C	−80°C
Acido bacteria					0.1	0.0	0.0	0.0	0.0	0.0
	Acidobacteria (class)				0.1	0.0	0.0	0.0	0.0	0.0
		Acidobacteriales			0.1	0.0	0.0	0.0	0.0	0.0
			Acidobacteriaceae		0.1	0.0	0.0	0.0	0.0	0.0
				Acidobacterium	0.1	0.0	0.0	0.0	0.0	0.0
Actino bacteria					0.4	5.4	15.3	4.5	10.3	25.9
	Actinobacteria (class)				0.4	5.4	15.3	4.5	10.3	25.9
		Acidimicrobiales			0.0	0.0	0.1	0.0	0.0	0.0
			Acidimicrobiaceae		0.0	0.0	0.1	0.0	0.0	0.0
				Acidimicrobiaceae (genus)	0.0	0.0	0.1	0.0	0.0	0.0
		Actinomycetales			0.4	5.4	15.2	4.5	5.9	25.9
			Actinomycetaceae		0.1	0.0	0.0	0.0	0.0	0.0
				Actinomyces	0.1	0.0	0.0	0.0	0.0	0.0
			Corynebacteriaceae		0.0	0.0	0.0	0.3	2.4	7.0
				Corynebacterium	0.0	0.0	0.0	0.3	2.4	7.0
			Geodermatophilaceae		0.0	0.0	0.0	0.0	0.5	8.1
				Geodermatophilaceae (genus)	0.0	0.0	0.0	0.0	0.0	8.1
				Geodermatophilus	0.0	0.0	0.0	0.0	0.5	0.0
			Intrasporangiaceae		0.0	0.1	1.7	0.0	0.1	0.0
				Intrasporangium	0.0	0.0	0.0	0.0	0.1	0.0
				Ornithinimicrobium	0.0	0.1	0.0	0.0	0.0	0.0
				Phycicoccus	0.0	0.0	0.2	0.0	0.0	0.0
				Terrabacter	0.0	0.0	1.5	0.0	0.0	0.0
			Microbacteriaceae		0.0	0.0	8.6	0.2	0.0	10.6
				Frondihabitans	0.0	0.0	0.0	0.0	0.0	2.7
				Labedella	0.0	0.0	8.6	0.0	0.0	0.0
				Leifsonia	0.0	0.0	0.0	0.0	0.0	0.1
				Microbacteriaceae (genus)	0.0	0.0	0.0	0.0	0.0	0.1
				Microbacterium	0.0	0.0	0.0	0.2	0.0	2.4
				Schumannella	0.0	0.0	0.0	0.0	0.0	5.3
			Micrococcaceae		0.0	0.0	0.8	0.0	0.2	0.0
				Arthrobacter	0.0	0.0	0.8	0.0	0.0	0.0
				Kocuria	0.0	0.0	0.0	0.0	0.2	0.0
			Nocardiaceae		0.0	2.8	0.1	0.0	0.0	0.0
				Rhodococcus	0.0	2.8	0.1	0.0	0.0	0.0
			Nocardioidaceae		0.0	2.4	0.4	3.5	0.0	0.0
				Nocardioides	0.0	2.4	0.4	3.5	0.0	0.0
			Propionibacteriaceae		0.3	0.1	3.6	0.5	2.7	0.2
				Propionibacterium	0.3	0.1	3.6	0.5	2.7	0.2
		Solirubrobacterales			0.0	0.0	0.0	0.0	4.3	0.0

(Continued)

Table A1 | Continued

Phylum	Class	Order	Family	Genus	2 m		20 m		40 m	
					4°C	−80°C	4°C	−80°C	4°C	−80°C
			Solirubrobacteraceae		0.0	0.0	0.0	0.0	4.3	0.0
				Solirubrobacter	0.0	0.0	0.0	0.0	4.3	0.0
Bacteroidetes					15.3	0.0	0.0	0.0	6.2	1.1
	Bacteroidia				0.0	0.0	0.0	0.0	0.0	1.1
		Bacteroidales			0.0	0.0	0.0	0.0	0.0	1.1
			Marinilabiaceae		0.0	0.0	0.0	0.0	0.0	1.1
				Alkaliflexus	0.0	0.0	0.0	0.0	0.0	1.1
	Cytophagia				2.7	0.0	0.0	0.0	0.1	0.0
		Cytophagales			2.7	0.0	0.0	0.0	0.1	0.0
			Cytophagaceae		2.7	0.0	0.0	0.0	0.1	0.0
				Cytophaga	2.7	0.0	0.0	0.0	0.0	0.0
				Meniscus	0.0	0.0	0.0	0.0	0.1	0.0
	Flavobacteria				12.2	0.0	0.0	0.0	6.2	0.0
		Flavobacteriales			12.2	0.0	0.0	0.0	6.2	0.0
			Flavobacteriaceae		12.2	0.0	0.0	0.0	6.2	0.0
				Flavobacterium	0.0	0.0	0.0	0.0	0.1	0.0
				Oceanistipes	0.1	0.0	0.0	0.0	0.0	0.0
				Psychroserpens	0.2	0.0	0.0	0.0	0.0	0.0
				Tenacibaculum	0.0	0.0	0.0	0.0	6.1	0.0
				Xanthobacillum	11.8	0.0	0.0	0.0	0.0	0.0
	Sphingobacteria				0.4	0.0	0.0	0.0	0.0	0.0
		Sphingobacteriales			0.4	0.0	0.0	0.0	0.0	0.0
			Sphingobacteriales (family)		0.4	0.0	0.0	0.0	0.0	0.0
				Sphingobacteriales (genus)	0.4	0.0	0.0	0.0	0.0	0.0
					2.9	1.8	0.0	0.2	0.0	0.0
	Anaerolineae				2.1	1.8	0.0	0.0	0.0	0.0
		Anaerolineales			2.1	1.8	0.0	0.0	0.0	0.0
			Anaerolineaceae		2.1	1.8	0.0	0.0	0.0	0.0
				Anaerolinea	0.0	1.8	0.0	0.0	0.0	0.0
				Levilinea	2.1	0.0	0.0	0.0	0.0	0.0
	Caldilineae				0.0	0.0	0.0	0.2	0.0	0.0
		Caldilineales			0.0	0.0	0.0	0.2	0.0	0.0
			Caldilineaceae		0.0	0.0	0.0	0.2	0.0	0.0
				Caldilinea	0.0	0.0	0.0	0.2	0.0	0.0
	Chloroflexi (class)				0.9	0.0	0.0	0.0	0.0	0.0
		Chloroflexales			0.9	0.0	0.0	0.0	0.0	0.0
			Chloroflexaceae		0.9	0.0	0.0	0.0	0.0	0.0
				Chloroflexus	0.9	0.0	0.0	0.0	0.0	0.0
					0.6	0.0	4.0	0.0	0.9	0.3
	Cyanobacteria (class)				0.6	0.0	4.0	0.0	0.9	0.3
		Nostocales			0.0	0.0	0.1	0.0	0.9	0.0
			Microchaetaceae		0.0	0.0	0.1	0.0	0.0	0.0
				Tolypothrix	0.0	0.0	0.1	0.0	0.0	0.0
			Nostocaceae		0.0	0.0	0.0	0.0	0.9	0.0
				Nostoc	0.0	0.0	0.0	0.0	0.9	0.0

(Continued)

Table A1 | Continued

Phylum	Class	Order	Family	Genus	2 m		20 m		40 m	
					4°C	−80°C	4°C	−80°C	4°C	−80°C
		Oscillatoriales			0.1	0.0	3.7	0.0	0.0	0.0
			Oscillatoriales (family)		0.1	0.0	3.7	0.0	0.0	0.0
				Leptolyngbya	0.1	0.0	3.7	0.0	0.0	0.0
		Pleurocapsales			0.5	0.0	0.1	0.0	0.0	0.3
			Pleurocapsales (family)		0.5	0.0	0.1	0.0	0.0	0.3
				Chroococcidiopsis	0.5	0.0	0.1	0.0	0.0	0.3
		Stigonematales			0.0	0.0	0.1	0.0	0.0	0.0
			Stigonematales (family)		0.0	0.0	0.1	0.0	0.0	0.0
				Stigonematales (genus)	0.0	0.0	0.1	0.0	0.0	0.0
					0.0	0.0	0.0	0.0	0.0	3.9
	Deinococci				0.0	0.0	0.0	0.0	0.0	3.9
		Deinococcales			0.0	0.0	0.0	0.0	0.0	3.9
			Deinococcaceae		0.0	0.0	0.0	0.0	0.0	3.9
				Deinococcus	0.0	0.0	0.0	0.0	0.0	3.9
					30.0	69.1	21.2	63.3	23.5	38.3
	Bacilli				6.5	9.2	1.4	1.3	0.1	18.8
		Bacillales			3.1	0.0	0.1	0.6	1.7	0.0
			Bacillaceae		1.1	0.0	0.0	0.0	0.0	0.0
				Bacillaceae (genus)	1.1	0.0	0.0	0.0	0.0	0.0
			Bacillales (family)		0.0	0.0	0.1	0.6	1.7	0.0
				Exiguobacterium	0.0	0.0	0.1	0.0	0.0	0.0
			Planococcaceae		2.1	0.0	0.0	0.0	0.0	0.0
				Planococcus	2.1	0.0	0.0	0.0	0.0	0.0
		Lactobacillales			4.2	17.4	13.6	35.2	14.9	22.7
			Carnobacteriaceae		3.4	0.0	0.0	0.0	0.0	0.0
				Marinilactibacillus	3.4	0.0	0.0	0.0	0.0	0.0
			Lactobacillaceae		0.0	9.3	13.6	35.2	10.3	20.9
				Lactobacillus	0.0	9.3	13.6	35.2	10.3	20.9
	Clostridia				22.6	51.7	7.5	27.6	6.9	15.7
		Clostridia (order)			19.7	0.0	0.0	0.0	0.0	0.0
			Clostridia (family)		19.7	0.0	0.0	0.0	0.0	0.0
				Clostridia (genus)	19.7	0.0	0.0	0.0	0.0	0.0
		Clostridiales			3.0	51.7	7.5	27.6	6.9	15.7
			Clostridiaceae		1.7	10.1	0.0	0.0	0.0	1.5
				Clostridiisalibacter	1.6	0.0	0.0	0.0	0.0	0.0
				Clostridium	0.1	0.0	0.0	0.0	0.0	1.5
				Sarcina	0.0	10.1	0.0	0.0	0.0	0.0
			Clostridiales (family)		0.0	0.0	7.3	0.3	0.0	0.0
				Anaerococcus	0.0	0.0	7.3	0.0	0.0	0.0
				Clostridiales (genus)	0.0	0.0	0.0	0.3	0.0	0.0
			Eubacteriaceae		0.2	0.0	0.0	0.0	0.0	0.5
				Eubacterium	0.2	0.0	0.0	0.0	0.0	0.5
			Lachnospiraceae		0.0	24.5	0.0	0.0	3.5	0.0
				Roseburia	0.0	24.5	0.0	0.0	3.5	0.0
			Peptostreptococcaceae		0.0	0.0	0.2	0.0	0.0	0.0
				Peptostreptococcus	0.0	0.0	0.2	0.0	0.0	0.0

(Continued)

Table A1 | Continued

Phylum	Class	Order	Family	Genus	2 m		20 m		40 m	
					4°C	−80°C	4°C	−80°C	4°C	−80°C
			Ruminococcaceae		1.1	17.0	0.0	27.2	3.4	13.6
				Ethanoligenens	0.0	0.0	0.0	0.0	0.0	0.2
				Faecalibacterium	0.0	17.0	0.0	0.0	0.0	0.0
				Ruminococcus	1.1	0.0	0.0	27.2	3.4	13.4
	Firmicutes (class)				0.8	8.2	12.3	34.5	16.5	3.8
		Bacillales			3.1	0.0	0.1	0.6	1.7	0.0
			Bacillales (family)		0.0	0.0	0.1	0.6	1.7	0.0
				Staphylococcus	0.0	0.0	0.1	0.6	1.7	0.0
		Lactobacillales			4.2	17.4	13.6	35.2	14.9	22.7
			Enterococcaceae		0.0	8.1	0.0	0.0	0.0	0.0
				Enterococcus	0.0	8.1	0.0	0.0	0.0	0.0
			Lactobacillaceae		0.0	9.3	13.6	35.2	10.3	20.9
				Lactobacillus	0.0	9.3	13.6	35.2	10.3	20.9
			Streptococcaceae		0.8	0.0	0.0	0.0	4.6	1.8
				Streptococcus	0.8	0.0	0.0	0.0	4.6	1.8
					0.0	0.9	0.0	0.0	0.0	0.0
	Nitrospirae (class)				0.0	0.9	0.0	0.0	0.0	0.0
		Nitrospirales			0.0	0.9	0.0	0.0	0.0	0.0
			Nitrospiraceae		0.0	0.9	0.0	0.0	0.0	0.0
				Nitrospira	0.0	0.9	0.0	0.0	0.0	0.0
					50.6	11.3	59.6	31.9	59.2	30.2
	Alphaproteobacteria				2.5	0.0	0.0	9.4	5.4	9.6
		Kopriimonadales			0.0	0.0	0.0	0.0	0.1	0.0
			Kopriimonadaceae		0.0	0.0	0.0	0.0	0.1	0.0
				Kopriimonas	0.0	0.0	0.0	0.0	0.1	0.0
		Rhizobiales			0.1	0.0	0.0	6.9	0.1	2.5
			Bradyrhizobiaceae		0.0	0.0	0.0	0.3	0.0	0.0
				Bradyrhizobium	0.0	0.0	0.0	0.3	0.0	0.0
			Hyphomicrobiaceae		0.0	0.0	0.0	0.0	0.1	0.0
				Zhangella	0.0	0.0	0.0	0.0	0.1	0.0
			Methylobacteriaceae		0.0	0.0	0.0	0.3	0.0	2.5
				Methylobacterium	0.0	0.0	0.0	0.3	0.0	2.5
			Rhizobiaceae		0.1	0.0	0.0	6.2	0.0	0.0
				Rhizobium	0.1	0.0	0.0	6.2	0.0	0.0
		Rhodobacterales			1.1	0.0	0.0	0.0	0.0	0.0
			Rhodobacteraceae		1.1	0.0	0.0	0.0	0.0	0.0
				Citreicella	0.9	0.0	0.0	0.0	0.0	0.0
				Rhodobacter	0.1	0.0	0.0	0.0	0.0	0.0
				Roseobacter	0.1	0.0	0.0	0.0	0.0	0.0
		Rhodospirillales			1.4	0.0	0.0	0.2	2.9	0.0
			Acetobacteraceae		0.0	0.0	0.0	0.2	0.0	0.0
				Acetobacteraceae (genus)	0.0	0.0	0.0	0.2	0.0	0.0
			Rhodospirillaceae		1.4	0.0	0.0	0.0	2.9	0.0
				Roseospira	1.4	0.0	0.0	0.0	2.9	0.0
		Sphingomonadales			0.0	0.0	0.0	2.3	2.3	7.1
			Sphingomonadaceae		0.0	0.0	0.0	2.3	2.3	7.1
				Sphingomonadaceae (genus)	0.0	0.0	0.0	2.3	0.0	0.0

(Continued)

Table A1 | Continued

Phylum	Class	Order	Family	Genus	2 m		20 m		40 m	
					4°C	−80°C	4°C	−80°C	4°C	−80°C
				Sphingomonas	0.0	0.0	0.0	0.0	2.3	7.1
	Betaproteobacteria				0.3	0.1	47.1	6.1	0.3	9.3
		Burkholderiales			0.3	0.1	44.3	6.1	0.3	9.3
			Alcaligenaceae		0.0	0.1	0.0	0.0	0.0	0.0
				Achromobacter	0.0	0.1	0.0	0.0	0.0	0.0
			Comamonadaceae		0.3	0.0	44.3	4.5	0.3	9.3
				Delftia	0.3	0.0	44.3	4.5	0.0	9.3
				Macromonas	0.0	0.0	0.0	0.0	0.3	0.0
			Oxalobacteraceae		0.0	0.0	0.0	1.5	0.0	0.0
				Duganella	0.0	0.0	0.0	1.5	0.0	0.0
		Neisseriales			0.0	0.0	2.8	0.0	0.0	0.0
			Neisseriaceae		0.0	0.0	2.8	0.0	0.0	0.0
				Neisseria	0.0	0.0	2.8	0.0	0.0	0.0
	Deltaproteobacteria				12.6	0.0	1.6	0.0	0.0	0.0
		Desulfobacterales			3.3	0.0	0.0	0.0	0.0	0.0
			Desulfobulbaceae		3.3	0.0	0.0	0.0	0.0	0.0
				Desulforhopalus	0.2	0.0	0.0	0.0	0.0	0.0
				Desulfotalea	3.0	0.0	0.0	0.0	0.0	0.0
		Desulfuromonadales			9.3	0.0	0.0	0.0	0.0	0.0
			Desulfuromonadaceae		0.4	0.0	0.0	0.0	0.0	0.0
				Desulfuromonas	0.4	0.0	0.0	0.0	0.0	0.0
			Geobacteraceae		8.9	0.0	0.0	0.0	0.0	0.0
				Geopsychrobacter	8.9	0.0	0.0	0.0	0.0	0.0
		Myxococcales			0.0	0.0	1.6	0.0	0.0	0.0
			Cystobacteraceae		0.0	0.0	1.6	0.0	0.0	0.0
				Melittangium	0.0	0.0	1.6	0.0	0.0	0.0
	Epsilonproteobacteria				1.3	0.0	0.0	0.0	0.0	0.0
		Campylobacterales			1.3	0.0	0.0	0.0	0.0	0.0
			Campylobacteraceae		1.3	0.0	0.0	0.0	0.0	0.0
				Arcobacter	1.3	0.0	0.0	0.0	0.0	0.0
	Gammaproteobacteria				33.9	11.2	10.9	16.4	53.5	11.3
		Alteromonadales			1.3	0.0	0.0	0.0	11.2	0.0
			Alteromonadaceae		0.6	0.0	0.0	0.0	11.2	0.0
				Marinobacter	0.3	0.0	0.0	0.0	5.3	0.0
				Marinobacterium	0.0	0.0	0.0	0.0	5.9	0.0
				Saccharophagus	0.3	0.0	0.0	0.0	0.0	0.0
			Colwelliaceae		0.3	0.0	0.0	0.0	0.0	0.0
				Colwellia	0.3	0.0	0.0	0.0	0.0	0.0
			Moritellaceae		0.4	0.0	0.0	0.0	0.0	0.0
				Moritella	0.4	0.0	0.0	0.0	0.0	0.0
		Enterobacteriales			0.0	3.2	8.6	5.5	4.3	8.9
			Enterobacteriaceae		0.0	3.2	8.6	5.5	4.3	8.9
				Escherichia	0.0	3.2	8.4	0.7	0.0	7.9
				Proteus	0.0	0.0	0.0	0.0	4.3	0.0
				Shigella	0.0	0.0	0.2	4.8	0.0	0.9
		Oceanospirillales			27.5	0.0	1.5	0.0	27.9	0.0
			Halomonadaceae		24.2	0.0	1.5	0.0	27.9	0.0
				Halomonas	24.2	0.0	1.5	0.0	27.9	0.0
			Oceanospirillales (family)		3.3	0.0	0.0	0.0	0.0	0.0

(Continued)

Table A1 | Continued

Phylum	Class	Order	Family	Genus	2 m		20 m		40 m	
					4°C	−80°C	4°C	−80°C	4°C	−80°C
				Neptuniibacter	1.2	0.0	0.0	0.0	0.0	0.0
				Oceanospirillales (genus)	2.2	0.0	0.0	0.0	0.0	0.0
		Pseudomonadales			3.6	0.2	0.7	10.9	1.1	0.0
			Moraxellaceae		2.2	0.0	0.0	0.0	1.1	0.0
				Psychrobacter	2.2	0.0	0.0	0.0	1.1	0.0
			Pseudomonadaceae		1.4	0.2	0.7	10.9	0.1	0.0
				Pseudomonas	1.4	0.2	0.7	10.9	0.1	0.0
		Thiotrichales			1.4	0.0	0.0	0.0	7.8	0.0
			Piscirickettsiaceae		1.4	0.0	0.0	0.0	7.8	0.0
				Methylophaga	0.0	0.0	0.0	0.0	7.8	0.0
				Thiomicrospira	1.4	0.0	0.0	0.0	0.0	0.0
		Vibrionales			0.0	0.0	0.0	0.0	1.2	2.4
			Vibrionaceae		0.0	0.0	0.0	0.0	1.2	2.4
				Vibrio	0.0	0.0	0.0	0.0	1.2	2.4
		Xanthomonadales			0.0	7.8	0.0	0.0	0.1	0.0
			Xanthomonadaceae		0.0	7.8	0.0	0.0	0.1	0.0
				Lysobacter	0.0	0.0	0.0	0.0	0.1	0.0
				Stenotrophomonas	0.0	7.8	0.0	0.0	0.0	0.0
Verruco microbia					0.0	9.6	0.0	0.0	0.0	0.3
	Opitutae				0.0	0.0	0.0	0.0	0.0	0.3
		Opitutales			0.0	0.0	0.0	0.0	0.0	0.3
			Opitutaceae		0.0	0.0	0.0	0.0	0.0	0.3
				Opitutus	0.0	0.0	0.0	0.0	0.0	0.3
	Spartobacteria				0.0	0.2	0.0	0.0	0.0	0.0
		Spartobacteria (order)			0.0	0.2	0.0	0.0	0.0	0.0
			Spartobacteria (family)		0.0	0.2	0.0	0.0	0.0	0.0
				Chthoniobacter	0.0	0.2	0.0	0.0	0.0	0.0
	Verrucomicrobia				0.0	9.4	0.0	0.0	0.0	0.0
		Verrucomicrobiales			0.0	9.4	0.0	0.0	0.0	0.0
			Verrucomicrobiaceae		0.0	9.4	0.0	0.0	0.0	0.0
				Verrucomicrobium	0.0	9.4	0.0	0.0	0.0	0.0
WS3					0.0	1.9	0.0	0.0	0.0	0.0
	WS3 (class)				0.0	1.9	0.0	0.0	0.0	0.0
		WS3 (order)			0.0	1.9	0.0	0.0	0.0	0.0
			WS3 (family)		0.0	1.9	0.0	0.0	0.0	0.0
				WS3 (genus)	0.0	1.9	0.0	0.0	0.0	0.0

frontiers in
MICROBIOLOGY

ORIGINAL RESEARCH ARTICLE
published: 03 April 2012
doi: 10.3389/fmicb.2012.00113

Characterization of metabolically active bacterial populations in subseafloor Nankai Trough sediments above, within, and below the sulfate–methane transition zone

Heath J. Mills[1]*, Brandi Kiel Reese[1,2], Alicia K. Shepard[3], Natascha Riedinger[4], Scot E. Dowd[5], Yuki Morono[6] and Fumio Inagaki[6]

[1] *Department of Oceanography, Texas A&M University, College Station, TX, USA*
[2] *Department of Biological Sciences, University of Southern California, Los Angeles, CA, USA*
[3] *Department of Marine Biology, Texas A&M University at Galveston, Galveston, TX, USA*
[4] *Department of Earth Sciences, University of California, Riverside, CA, USA*
[5] *Research and Testing Laboratory, Medical Biofilm Research Institute, Lubbock, TX, USA*
[6] *Geomicrobiology Group, Kochi Institute for Core Sample Research, Japan Agency for Marine-Earth Science and Technology, Kochi, Japan*

Edited by:
Andreas Teske, University of North Carolina at Chapel Hill, USA

Reviewed by:
William D. Orsi, Woods Hole Oceanographic Institution, USA
Aharon Oren, The Hebrew University of Jerusalem, Israel
Martin Krüger, Federal Institute for Geosciences and Natural Resources, Germany

****Correspondence:***
Heath J. Mills, Department of Oceanography, Texas A&M University, Mail Stop 3146, College Station, TX 77843, USA.
e-mail: hmills@ocean.tamu.edu

A remarkable number of microbial cells have been enumerated within subseafloor sediments, suggesting a biological impact on geochemical processes in the subseafloor habitat. However, the metabolically active fraction of these populations is largely uncharacterized. In this study, an RNA-based molecular approach was used to determine the diversity and community structure of metabolically active bacterial populations in the upper sedimentary formation of the Nankai Trough seismogenic zone. Samples used in this study were collected from the slope apron sediment overlying the accretionary prism at Site C0004 during the Integrated Ocean Drilling Program Expedition 316. The sediments represented microbial habitats above, within, and below the sulfate–methane transition zone (SMTZ), which was observed approximately 20 m below the seafloor (mbsf). Small subunit ribosomal RNA were extracted, quantified, amplified, and sequenced using high-throughput 454 pyrosequencing, indicating the occurrence of metabolically active bacterial populations to a depth of 57 mbsf. Transcript abundance and bacterial diversity decreased with increasing depth. The two communities below the SMTZ were similar at the phylum level, however only a 24% overlap was observed at the genus level. Active bacterial community composition was not confined to geochemically predicted redox stratification despite the deepest sample being more than 50 m below the oxic/anoxic interface. Genus-level classification suggested that the metabolically active subseafloor bacterial populations had similarities to previously cultured organisms. This allowed predictions of physiological potential, expanding understanding of the subseafloor microbial ecosystem. Unique community structures suggest very diverse active populations compared to previous DNA-based diversity estimates, providing more support for enhancing community characterizations using more advanced sequencing techniques.

Keywords: microbial ecology, sulfate–methane transition zone, Nankai Trough sediment, 454 pyrosequencing, SSU rRNA, metabolically active

INTRODUCTION

Microbial populations in subseafloor sediments on the global continental margins account for one tenth to one third of the total biomass on Earth (Whitman et al., 1998; Parkes et al., 2000; Lipp et al., 2008). Although microbial populations have been detected ubiquitously in the marine subseafloor environment, the diversity, activity, metabolic processes, and interactions with geochemistry are still largely unknown (D'Hondt et al., 2007; Bach et al., 2010). Microbial processes in the marine subsurface are potentially significant to global carbon and nutrient cycles (Whiticar, 1999; D'Hondt et al., 2002) and provide relevant analogs to the emerging astrobiology field (Gold, 1992; Chapelle et al., 2002). To better understand the subseafloor biosphere, the Integrated Ocean Drilling Program (IODP) has made microbiology and biogeochemistry a prominent initiative on recent drilling expeditions recognizing the broad scientific benefit (Bickle et al., 2011). Microbiological samples were collected during the IODP Nankai Trough Seismogenic Zone Experiment (NanTroSEIZE) Expedition 316. The expedition provided an opportunity to advance the understanding of the subseafloor biosphere in an active crustal seismogenic zone characterized by large-scale earthquake- and tsunami-genesis (Kimura et al., 2008).

The sulfate–methane transition zone (SMTZ) represents a distinct geochemical demarcation within the marine subseafloor (Iversen and Jørgensen, 1985; D'Hondt et al., 2002). Geochemistry predicts a thermodynamic driven stratification of the associated microbial community structure within this zone (D'Hondt et al., 2004; Parkes et al., 2005; Inagaki et al., 2006). While some microbial processes associated with the SMTZ have been previously examined (Parkes et al., 2005; Biddle et al., 2006), recent findings suggest that microbial activity may not be as restricted as predicted by redox potential (Orcutt et al., 2011). Geochemical descriptions of microbial activity rely on the consumption or production of measurable compounds. Transformations of such compounds may be undetectable using standard geochemical analysis if the end products of the reactions are consumed by a secondary reaction. For example, sulfur-related cryptic cycles have been previously noted in the oxygen minimum zone off the Chilean coast where sulfur is being reduced but rapidly re-oxidized leaving no geochemical marker of the reduction pathway (Canfield et al., 2010). The active reduction pathway was determined by molecular analysis active sulfate reducing bacteria. Therefore, molecular characterizations of metabolically active microbial populations is necessary to determine these geochemically cryptic cycles and provide a better understanding of the subsurface biosphere.

Previous analyses of subseafloor microbial populations have targeted ribosomal RNA genes (DNA-based) to describe the total microbial community, which includes metabolically active populations as well as potentially dormant and/or dead cells (e.g., Newberry et al., 2004; Inagaki et al., 2006; Polymenakou et al., 2009). DNA-based studies reported few shifts in microbial population structure associated with varying geochemical conditions (Parkes et al., 2005). Metagenomic analyses have observed shifts with depth in gene abundance associated with sulfur metabolism but lacked variability in genes associated with methanogenesis despite a pronounced SMTZ (Biddle et al., 2008). DNA-based analysis of microbial communities within the subseafloor, as in other environments, may detect dormant or extremely low metabolically active populations in the natural environment and thus may not correspond with observed geochemistry (Davis et al., 1986).

In contrast, the ribosomal RNA transcripts (RNA-based) can be used to describe the metabolically active community, providing a better link to the geochemistry. Detection of rRNA transcripts have been correlated to reproducing cells (Neidhardt and Magasanik, 1960) as they rapidly degrade upon cell dormancy or death (Davis et al., 1986). Two previous molecular studies analyzed metabolically active *Archaea* using cloning and Sanger sequencing of RNA targets (Biddle et al., 2006; Sørensen and Teske, 2006), however a detailed description of the active bacterial population using more robust techniques is lacking. Recent advances in pyrosequencing technologies have increased the accuracy and decreased the associated costs, providing access to the depth of sequencing required to more adequately sample environmental microbial diversity compared to previous methods, such as cloning (Edwards et al., 2006; Sogin et al., 2006; Liu et al., 2008). The authors recognize that this method does not eliminate PCR amplification biases common with cloning and Sanger based sequencing. This study is the first report to utilize high-throughput sequencing of RNA targets from the marine subseafloor providing a novel analysis of the metabolically active and ecologically relevant bacterial community structure and function.

This study advances current understanding of subseafloor microbial communities by characterizing the metabolically active bacterial populations surrounding and within the SMTZ in the Nankai Trough subseafloor sediments. Structural diversity of the active community was used to interpret potential metabolic function and was compared to measured geochemical concentrations. We hypothesized that the functional diversity of subseafloor microbial populations will exceed the observed geochemically predicted zones as some carbon and nutrient measured below detection limits. Therefore, RNA characterizations of microbial communities will provide a more informative description of environmental microbial ecology than DNA or geochemical-based methods alone.

MATERIALS AND METHODS

SITE AND SAMPLE DESCRIPTION

Sediment samples were obtained during IODP Expedition 316 from Site C0004 in the Nankai Trough, located approximately 63 nautical miles southeast from the city of Shingu off the Kii Peninsula of Japan (see Kinoshita et al., 2009 for IODP Expedition 316 Site Map). A detailed geological description of this area is available as part of the IODP site description report (Kimura et al., 2008). Site C0004 Hole C (33°13.0′N, 136°43.0′E) was drilled on December 20, 2008 using the hydraulic piston coring system. Core sediments were processed less than 1 h after core recovery (Kimura et al., 2008; Strasser et al., 2009, 2011). Whole round cores were sectioned, immediately stored at −80°C for preservation of both RNA and DNA, and were shipped to the Mills laboratory on dry ice. Samples from three different depths of 1, 19, and 57 m below sea floor (mbsf) were selected for RNA and geochemical analysis surrounding and within the SMTZ.

GEOCHEMICAL ANALYSES

Standard shipboard operations obtained concentrations of methane, sulfate, and iron (Fe^{2+}; Kimura et al., 2008). To assess the amount of iron sulfide minerals in these sediments, chromium reducible sulfur (CRS = FeS_2, S^0 and remaining part of Fe_3S_4) concentrations were determined by treating samples of approximately 0.5 g with the two-step acid Cr (II) method (Fossing and Jørgensen, 1989). Trapped sulfide was analyzed by the methylene blue method (Cline, 1969).

CELL COUNTS

Cells were stained with SYBR Green I and then enumerated by fluorescent image-based cell count technique (Morono et al., 2009) using an automated slide-loader system (Morono et al., 2009; Morono and Inagaki, 2010).

NUCLEIC ACID EXTRACTION AND REVERSE TRANSCRIPTION-PCR

Microbial SSU ribosomal RNA (rRNA) was extracted from approximately 0.5 g of sediment from the center of a whole round core using the Mills Extraction Method as described in Mills et al. (2008). Extraction controls containing no sediment were performed simultaneously with environmental samples to confirm lack of contamination during the extraction process.

All incubation steps during the reverse transcription (RT)-PCR were conducted on a Veriti 96-well Fast Thermal Cycling System (Applied Biosystems, Foster City, CA, USA). Ribosomal RNA was reverse transcribed to cDNA using the Moloney murine leukemia virus (M-MLV) reverse transcriptase and *Bacteria* domain specific Small subunit ribosomal RNA (SSU rRNA) reverse primer 518R (Nogales et al., 1999). RNA was incubated at 65˚C for 5 min followed by an incubation of both RNA extract and primer at 70˚C for 5 min. The total RT-PCR reaction mixture [1X M-MLV buffer containing 50 mM Tris–HCl, 3 mM $MgCl_2$, 75 mM KCl, and 10 mM DTT (Promega, USA), 10 mM deoxynucleotide triphosphate solution mix (New England Biolabs, USA), 1 U of M-MLV enzyme (Promega, USA), and molecular grade water] was incubated at 37˚C for 60 min. PCR amplification of cDNA used *Bacteria* domain specific SSU rRNA forward primer 27F (Giovannoni, 1991) and reverse primer 518R (Nogales et al., 1999). This fragment of the 16S rRNA gene includes the hypervariable V3 region. The reaction mixture was as follows: 1× buffer [10 mM KCl, 10 mM $(NH_4)_2$ SO_4, 20 mM Tris–HCl, 2 mM Mg SO_4, 0.1% Triton X-100; New England Biolabs, USA], 10 mM deoxynucleotide triphosphate solution mix (New England Biolabs, USA), 1 U of *Taq* DNA Polymerase (New England Biolabs, USA), and molecular grade water. Thermal cycling conditions were 95˚C for 5 min, 40 cycles of 95˚C for 30 s, 50˚C for 30 s, and 72˚C for 30 s with a final extension of 72˚C for 10 min. Amplicons were visualized by gel electrophoresis on 0.7% agarose gels, stained with ethidium bromide, and illuminated by UV exposure. DNA contamination of RNA extracts was determined by omitting the RT step. No amplifiable DNA remained in RNA extracts. Standard negative controls for the RT and PCR steps were also incorporated, both indicated no contamination of the reactions.

QUANTITATIVE RT-PCR

To quantify the bacterial SSU rRNA transcripts, a series of standards were amplified from purified pure culture bacterial SSU rRNA gene amplicons. The PCR product was obtained using primers 331F and 797R (Nadkarni et al., 2002). Amplicon size was confirmed by gel electrophoresis. PCR purification was completed using the QIAquick PCR purification kit (Qiagen, Valencia, CA, USA) according to the manufacturer's instructions. The concentration of standards was determined on a NanoDrop 1000 Spectrophotometer (Thermo Scientific, Waltham, MA, USA). Copy number was calculated assuming a molecular mass of 660 Da for a base pair of DNA and using the following formula: Copy Number $= [6.023 \times 10^{23}$ (bp mol^{-1} bp^{-1}) × concentration of standard (ng μL^{-1})]/[PCR Product Size (bp gene copy^{-1}) × 1×10^9 (ng g^{-1}) × 660 (g mol^{-1} bp^{-1})] (Mattes and Jin, 2010). Standard concentrations ranged over five orders of magnitude from 2.6 to 2.6×10^4 copies μL^{-1} and were amplified in triplicate during Q-PCR. Environmental samples and extract controls were reverse transcribed as described above using the 797R primer and was Q-PCR amplified from two dilutions, 1× and 1/100× of the reverse transcribed product, in duplicate. All samples were amplified using the primers 331F and 797R and *Taq*Man probe Bac*Taq* (Nadkarni et al., 2002). Manufacturers suggested Q-PCR reaction mixes were used with thermal cycling conditions as follows: initial warming step at 50˚C for 2 min, a denaturation step at 95˚C for 10 min followed by 40 cycles of 95˚C for 30 s, 52˚C for 1 min, 65˚C for 30 s, and a final extension step at 65˚C for 6 min. The quantification and data analysis was conducted using a StepOnePlus Real-Time PCR System (Applied Biosystems, Foster City, CA, USA[1]) and the StepOne Software 2.0 (Applied Biosystems, Foster City, CA, USA). Baseline and C_t values were automatically selected by the provided software and visually verified by the user.

PYROSEQUENCING AND SEQUENCE ANALYSIS

Sequences were obtained from two dilutions of cDNA reverse transcribed from a single RNA extract. The dilutions were sequenced as described below with the libraries combined after the sequences were quality checked. Pyrosequencing, including initial amplification of the cDNA with primers containing unique sequence identifiers, was conducted at the Medical Biofilm Research Institute (Research and Testing Laboratory, Lubbock, TX, USA) according to standard laboratory procedures using a 454 FLX Sequencer (454 Life Sciences, Branford, CT, USA). Pyrosequencing conditions are routinely optimized by the Research and Testing Laboratory to limit multiple strand attachment. Long homopolymer regions can be misread by 454 (Jones, 2010), however such misreads are less problematic for SSU rRNA analysis. Resulting sequences were first de-noised and then individual sequences were parsed the into sample specific libraries. Libraries were screened for reads less than 200 bases, reads lacking a Roche-designed four base key sequence, and non-bacterial reads lacking specific 28F primer recognition site. Chimera detection was completed using the Chimera Slayer system adapted for the Mothur Program (Schloss et al., 2009; Haas et al., 2011). Sequences were uploaded to the National Center for Biotechnology Information Sequence Read Archive (NCBI-SRA) under accession number SRA049352.

Phylogenetic analyses were conducted on the combined sequence data sets to reduce the potential for RT-PCR and pyrosequencing biases. Sequences were aligned using the Ribosomal Database Project (RDP) Pyrosequencing Aligner tool, which is based on Infernal aligner (Nawrocki and Eddy, 2007). Sequences were clustered at a 95% sequence similarity using farthest-neighbor method on the RDP Complete Linkage Clustering program available on the RDP pyrosequencing pipeline[2] (Cole et al., 2009) and verified using the Mothur Program[3] (Schloss et al., 2009). Taxonomic classification of the sequences was completed using the NET Network Distributed Basic Local Alignment Search Toolkit (W.ND-BLAST) program (Dowd et al., 2005) and randomly checked against the Basic Local Alignment Search Tool (BLAST) pipeline through National Center for Biotechnology Information (NCBI) database. The highest classification level with a confidence interval greater than 80% was used in downstream analysis. Genera identified by more then 1% of the sequence data set at a given depth were used in community functional group characterization.

Diversity indices including Shannon, Chao1, and rarefaction were calculated from the 95% similarity operational taxonomic units (OTU) defined by the RDP clustering at. Comparison of

[1] www.appliedbiosystems.com
[2] http://pyro.cme.msu.edu/
[3] http://www.mothur.org/wiki/Main_Page

OTUs that were absent or present between samples was completed using the shared OTU and Venn diagram systems in the mothur program (Schloss et al., 2009).

The authors acknowledge and have taken steps to limit potential for bias associated with extraction, amplification, and sequencing of SSU rRNA from marine sediments. The authors recognize that the use of one primer set may reduce the detection of overall diversity. Multiple sediment samples at each depth were combined to limit effects of community and sediment chemistry heterogeneity. PCR and Q-PCR cycling conditions were optimized for the specific reagents to reduce effects of mis-priming, primer–dimer formation, unequal amplification efficiency of template, and the potential formation of chimeric sequence formation. In addition, amplicons were obtained from two dilutions of cDNA and combined according to depth reduce the potential for RT-PCR biases. Despite the biases inherent with molecular studies, the steps taken to reduce the effect of these biases have produced a data set that is comparable to previous studies and is of sufficient quality for future comparisons.

STATISTICAL ANALYSIS

Geochemical data was correlated to phylogenetic profiles through Singular value decomposition (SVD) and principal component analysis (PCA) using Microsoft Excel Pop Tools. Geochemical and phylogenetic data was first transformed using either chi-square or arcsine statistical tests, where appropriate, and normalized prior to SVD and PCA analyses. Statistical significance ($p < 0.01$) was determined using the Monte Carlo significance test with 10,000 iterations.

RESULTS

SITE DESCRIPTION

Site C0004 Hole C was located on the slope of the accretionary prism in the Nankai Trough, over an active megasplay fault that has repeatedly caused episodic earthquakes and tsunamis (Strasser et al., 2009). Water depth at Site C0004 Hole C was 2,627 m. A total of 403 m of sediment core was retrieved during IODP Expedition 316. In this study, sediment samples were selected from above, within, and below the SMTZ (1, 19, and 57 mbsf, respectively) in the upper sedimentary unit of the slope apron overlying the accretionary prism (i.e., Lithologic Unit I, 0–78.08 mbsf). The sediment samples are mainly composed of nannofossil-rich hemi-pelagic mud (Strasser et al., 2009).

GEOCHEMICAL PROFILES

Pore water geochemical characteristics for sediments at Site C0004 were determined onboard during IODP Expedition 316 (Kimura et al., 2008). Sulfate and methane concentration profiles showed that the SMTZ was located between 18.5 and 22.9 mbsf (**Figure 1**). The sulfate concentration was 25.3 mM at 2.7 mbsf and decreased with increasing depth down to below detection limits at 22.9 mbsf (**Figure 1**). Methane concentrations increased three orders of magnitude from an initial 1.8×10^{-3} mM at 1.4 mbsf to 1.4 mM at 18.5 mbsf and continued to increase to a maximum concentration of 9.7 mM at 35.3 mbsf (**Figure 1**). The Fe (II) concentration was 2.5 μM at 1 mbsf but then remained less than 1.0 μM until approximately 48.6 mbsf where it began to increase to a concentration of

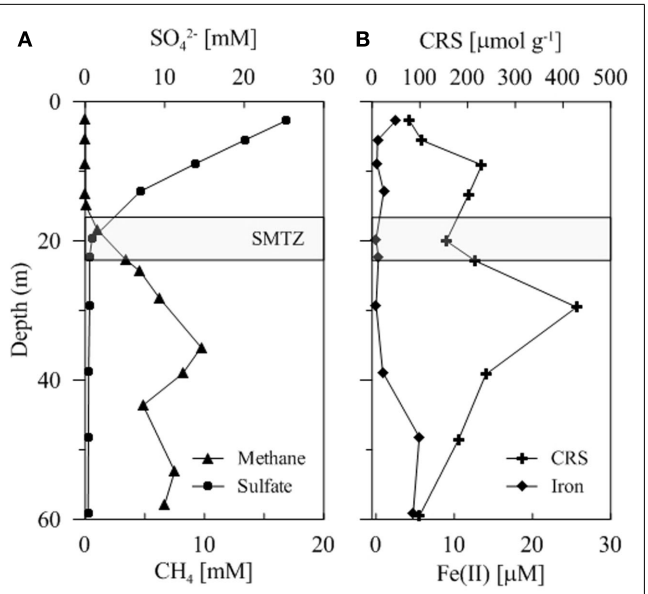

FIGURE 1 | (A) Concentration of SO_4^{2-} in millimolar and CH_4 in millimolar with depth to 60 mbsf. **(B)** Concentration of Fe^{2+} (μM) and iron sulfides, determined as chromium reducible sulfur (CRS; μmol g^{-1}), with depth to 60 mbsf.

4.7 μM at 59.5 mbsf (**Figure 1**). The amount of iron sulfide phases (determined by CRS) increased from 78.1 μmol g^{-1} at 2.8 mbsf and to a maximum of 428.4 μmol g^{-1} at 29.5 mbsf. Below this depth the concentration of iron sulfides decreases consistently down to 99.4 μmol g^{-1} at approximately 59.5 mbsf (**Figure 1**).

CELL ABUNDANCE AND QUANTIFICATION OF BACTERIAL SSU rRNA

Cell abundance in sediment at 1 mbsf was 3.4×10^7 cells cm^{-3} and decreased approximately two orders of magnitude to 1.3×10^5 cells cm^{-3} at both the 19- and 57-mbsf sampling depths. The trend of cell concentration matched the yield of SSU rRNA gene transcript. Quantitative real-time PCR analyses showed that the bacterial SSU cDNA reverse transcribed from Hole C0004C sediment RNA extracts were estimated to be 6.5×10^6 copies g^{-1} in the 1.0-mbsf sample and 3.3×10^3 copies g^{-1} at 19 mbsf and 9.0×10^4 copies g^{-1} at 57 mbsf. The ratio of transcripts per cell increases at the lowest depth from 0.19 at 1 mbsf to 0.03 at 19 mbsf to 0.69 at 57 mbsf.

BACTERIAL COMMUNITY STRUCTURE

Pyrosequencing of reverse transcribed bacterial SSU rRNA gene transcripts from the metabolically active fraction of the total microbial community resulted in a total of 12,020 sequences with an average length of 426 base pairs (**Table 1**). Two different species diversity indices were calculated from the pyrosequencing data. For sample depths 1, 19, and 57 mbsf, Shannon diversity index calculated values of 6.32, 3.02, and 3.13 and Chao1 index calculated values of 2,638, 67, 90, respectively (**Table 1**). The rarefaction curve generated for the 1-mbsf sample did not indicate exhaustive sampling of the sequence data set whereas the rarefaction curves generated from the 19- and 57-mbsf libraries indicated that

Table 1 | Summary of sequence analysis data Nankai Site C0004 Hole C.

Sample	Library size	Number of OTUs		Shannon (H')	Chao1
		RDP	Mothur		
All depths	12,020	1,624	1,531	$5.41 \pm 4.1 \times 10^{-4}$	$2{,}737 \pm 232$
1 mbsf	6,152	1,532	1,448	$6.32 \pm 4.3 \times 10^{-4}$	$2{,}638 \pm 234$
19 mbsf	2,012	54	59	$3.02 \pm 5.1 \times 10^{-4}$	67 ± 34
57 mbsf	3,856	81	80	$3.13 \pm 4.6 \times 10^{-4}$	90 ± 23

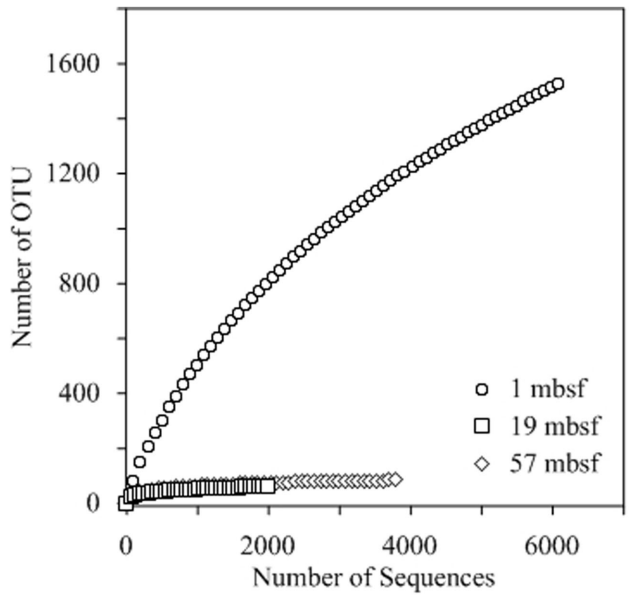

FIGURE 2 | Rarefaction analysis based on pyrosequencing of community bacterial SSU rRNA from 1, 20, and 57 mbsf. Sequences with 95% sequence similarity were combined as a single OTU. These data indicate that the sampling effort at 19 and 57 mbsf adequately represents the phylogenetic diversity of the population. Although additional sequencing would be required to fully annotate the entire diversity of the bacterial population at 1 mbsf, sufficient data have been collected to make conclusions regarding the more frequently detected lineages.

sequencing efforts sufficiently represented the detectable diversity of the community based on the methods used in this study (**Figure 2**). Comparison of OTUs observed between those depths showed that 1.3% of OTUs were shared between 1 and 19 mbsf, 1.2% of OTUs were shared between 1 and 57 mbsf, and 23.6% of OTUs were shared between 19 and 57 mbsf (**Figure 3**).

Phylogenetic analysis detected 18 unique phyla (**Figure 4**). At all depths sampled, Proteobacteria had the highest sequence abundance (68.4, 49.8, and 58.6% of total sequences obtained from 1, 19, and 57 mbsf, respectively). Additional lineages detected and their associated sequence detection frequency at 1 mbsf included Chloroflexi (10.3%), Cyanobacteria (5.3%), Bacteroidetes (3.8%), Deferribacteres (3.0%), Actinobacteria (2.0%), and Firmicutes (1.7%; **Figure 4**). A shift in community composition occurred between the 1 mbsf and the 19 and 57 mbsf depth ranges.

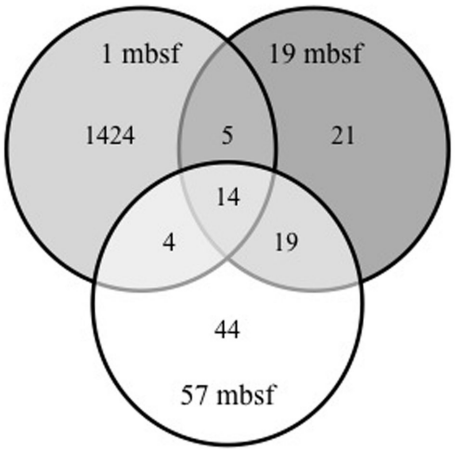

FIGURE 3 | Venn diagram comparing OTUs shared by and unique to the 1, 19, and 57 mbsf sampling depths. Sequences with 95% sequence similarity were combined as a single OTU. These data indicate that the bacterial diversity at 1 mbsf is greater than at 19 and 57 msbf. Although the abundance of OTUs at 19 and 57 mbsf is similar only 24% are shared between depths.

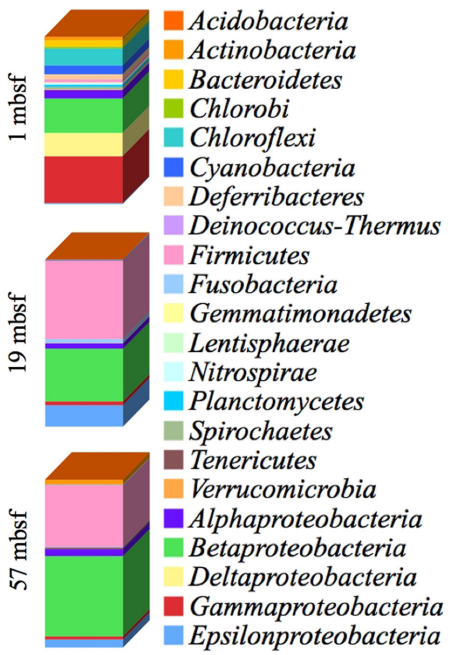

FIGURE 4 | Combined bacterial diversity at the phylum level based on small subunit ribosomal (SSU rRNA) at 1, 19, and 57 m below the seafloor (mbsf) from PCR amplicons at 1× and 1/10× dilutions. The phylum Proteobacteria is separated into the classes Alphaproteobacteria, Betaproteobacteria, Deltaproteobacteria, Epsilonproteobacteria, and Gammaproteobacteria. The presence and abundance of different phyla varied between depths and treatments. The majority of the sequences were contained within the Proteobacteria, Bacteroidetes, and Firmicutes phyla.

In the 19- and 57-mbsf depths the majority of non-Proteobacteria sequences were related to the Firmicutes (46.8,

37.0%) phyla while the phyla Chloroflexi, Cyanobacteria, Bacteroidetes, and Deferribacteres individually represented less than 0.5% of the sequences obtained in both samples or were not observed (**Figure 4**). However, the Fusobacteria, which were identified as 0.1% of the sequences at 1 mbsf and 0.0% at 57 mbsf, comprised 2.4% of the sequences at 19 mbsf (**Figure 4**). The Actinobacteria accounted for 1.0% at 1 mbsf and only 0.2% of the sequences at 19 mbsf but represented 2.9% of the sequences at 57 mbsf (**Figure 4**). The Tenericutes composed 1.0% of the sequences at 57 mbsf whereas they were not observed at the other depths.

POTENTIAL METABOLIC FUNCTION

The authors acknowledge the limitations of using SSU rRNA for functional characterization of microbial communities. The trends in potential metabolic function are presented recognizing that pyrosequencing technology is semi-quantitative. Lineages with known metabolic functions were described and the abundance of each genus was noted as a percentage of the total sequences obtained at 1, 19, and 57 mbsf. Forty-two genera were observed to compose greater than 1.0% of the sequences obtained within at least one of the sampling depths (Table S1 in Supplementary Material). In general, sequences representing lineages capable of sulfur cycling accounted for 15.5, 12.83, and 4.66% of the total sequences at 1, 19, and 57 mbsf, respectively. Genera previously linked with iron cycling composed 2.7, 2.7, and 1.4% of the total sequences from 1, 19, and 57 mbsf, respectively. Genera that are potentially associated with nitrogen cycling were associated with 29.5, 29.1, and 49.5% of the total sequences at 1, 19, and 57 mbsf respectively. Finally, 14.7, 43.3, and 27.9% of the sequences were observed to be associated with lineages capable of fermentative-based metabolism at 1, 19, and 57 mbsf, respectively.

Sulfur cycling

Metabolically active genera were identified having the potential to contribute to sulfur cycling in the marine subseafloor. A majority of these sequences were detected in the 1-mbsf sample (Table S1 in Supplementary Material). The genera *Desulfonema* (Kuever and Meyer, 2007), *Desulfobacterium* (Brysch et al., 1987), *Desulfosarcina* (Leloup et al., 2009), and *Desulfuromonas* have the capacity to use sulfate as a terminal electron acceptor, while a *Helicobacter*-related lineage within the Epsilonproteobacteria has been shown to reduce sulfur to hydrogen sulfide (Campbell et al., 2006). Previous studies have shown that the genera *Achromatium* (Head et al., 2000), *Thioalkalispira* (Sorokin et al., 2002), and *Thiothrix* (Macalady et al., 2008) have the capacity for full or partial oxidation of sulfur species. The number of sequences related to sulfate reducing and sulfur-oxidizing lineages detected in the database were negatively correlated with the amount of iron sulfide and depth ($p < 0.01$; i.e., as depth from surface increases, the number of sequences related to sulfate reducing and sulfur-oxidizing lineages detected decreases) but positively correlated ($p < 0.01$) with a loss of sulfate. The percentage of sequences associated with each lineage is presented in Table S1 in Supplementary Material.

Iron cycling

The potential for metabolically active iron cycling by bacteria was observed at all depths (Table S1 in Supplementary Material). In the 1-mbsf sample, the genera *Acidimicrobium* has the potential to oxidize iron (Clark and Norris, 1996). Genera capable of reducing iron for energy conservation detected in this study included *Anaeromyxobacter* (Sanford et al., 2002), *Dyella* (Lu et al., 2010), and *Ralstonia* (Roling et al., 2007). These lineages were detected at all depths with the highest percentage of sequences at the 19-mbsf depth. The frequency of detecting iron reducing lineage sequences were positively correlated ($p < 0.01$) with depth, whereas Fe(II) accumulation was negatively correlated ($p < 0.01$) with iron oxidizing lineage sequences, as observed through SVD.

Nitrogen cycling

Multiple genera capable of using nitrogen species as a terminal electron acceptor were throughout the sediment samples (Table S1 in Supplementary Material). The most frequently detected lineage with the sequence database was *Cupriavidus* (described in Van Damme and Coenye, 2004), representing 14.7, 21.9, and 36.3% of the total sequences at 1, 19, and 57 mbsf (Table S1 in Supplementary Material). Additional nitrogen-reducing lineages detected as being metabolically active included *Alcanivorax* (Nakano et al., 2008), *Burkholderia* (Igual et al., 2006), *Caldithrix* (Miroshnichenko et al., 2003), *Corynebacterium* (Renner and Becker, 1970), and *Stenotrophomonas*. The number of nitrate reducing lineage sequences detected did not significantly change with depth. Genera detected as metabolically active with the capacity for nitrogen fixation included *Herbaspirillum* (Rigo et al., 2007), *Alkalilimnicola* (Tourova et al., 2007), *Spirochaeta* (Rainey et al., 1991), and *Cyanothece* (Pakrasi et al., 2008) were identified in all samples (Table S1 in Supplementary Material), despite ammonia concentrations being positively correlated ($p < 0.01$) with depth.

Fermentation and methylotrophy metabolism

Genera with the capacity for fermentative metabolism were frequently detected at each depth, accounting for 14.7, 43.3, and 27.9% of the total sequences (Table S1 in Supplementary Material). These genera included *Anaerophaga* (Schink et al., 2002), *Byssovorax* (Kunze et al., 2006), *Caldilinea* (Ollivier et al., 2011), *Faecalibacterium* (Fidopiastis et al., 2006), *Lactobacillus* (Kandler et al., 1983), *Leptolinea* (Yamada et al., 2006), *Levillnea* (Yamada et al., 2006), *Staphylococcus* (Gregory et al., 2003), and *Turicibacter* (Bosshard et al., 2002). Group 1 methylotrophs, *Methylobacter* and *Methylomicrobium* (Bowman et al., 1993), were detected in the 1-mbsf sequence database but were absent from the deeper depths (Table S1 in Supplementary Material).

DISCUSSION

The community characterization data presented in this study represent one of the first RNA-based pyrosequencing and quantitative PCR analyses of microbial communities associated with the subseafloor sedimentary habitat. The highly resolved sequence dataset produced a novel structural view of the metabolically active fraction of subseafloor bacterial populations. Sequence data also revealed numerous genera that individually represented less than 1% of the sequence dataset highlighting the overall diversity of the community. Active microbial populations and their environmental factors were compared by combining geochemical analysis to robust molecular data to predict the local microbial ecology and metabolic processes. In addition, this study enhances

sequence databases produced by previous RNA-based community pyrosequencing efforts from marine water samples (Frias-Lopez et al., 2008; Gilbert et al., 2008) and from soil samples (Leininger et al., 2006; Urich et al., 2008) to improve understanding of the metabolically active fraction of the microbial communities.

METABOLICALLY ACTIVE COMMUNITY STRUCTURE

Quantification of cell and SSU rRNA transcript abundance indicated a decreasing population density and reduced overall metabolic activity from the top depth horizon to within and below the SMTZ. The reported cell abundance was in agreement with previously observed ranges within the subsurface and follows a similar decreasing trend with depth (Parkes et al., 1994, 2000). Similar trends were detected in Peru margin sediments where bacterial SSU rRNA gene abundance (DNA) decreased rapidly over the top 20 mbsf but remained unchanged to 50 mbsf (Biddle et al., 2008). A similar trend was observed with transcript abundance. It was interesting to note that the ratio of transcripts detected to cells counted increased over 3.5 fold from the 1-mbsf sample to the 57-mbsf sample. This does not imply higher activity at depth, as there are both more cells and more transcripts in the surfaces communities. However, it does suggest a higher proportion of the total population may be metabolically active at depth compared to the shallow communities. The concentration of ribosomes, and thus copies of SSU rRNA transcripts within a cell, is linearly correlated to cellular metabolic activity (DeLong et al., 1989; Kemp et al., 1993; Kerkhof and Ward, 1993; Lee and Kemp, 1994), with dormant and dead cells having few to no ribosomes present (Davis et al., 1986; Fegatella et al., 1998). The shallow sediments may have more dormant or dead cells, elevating the cell counts while not increasing the transcript abundance. The potential for geochemical flux in the shallow sediments may be the driver for this community composition, while geochemical conditions in the deeper sediments would remain more stable. These data suggest the deeper subsurface environments may select for fewer dormant populations and may effectively recycle dead cells. Previous results have made similar observations reporting predominantly metabolically active populations (Morono et al., 2011) and a limited of number of dead cells within biomass calculations (Takano et al., 2010). Further analysis specifically targeting dormant populations should be completed to test the role these communities play in the environment and diversity of the community.

Cell and transcript abundances in the SMTZ (19 mbsf) and the deeper horizon (57 mbsf) were similar, suggesting that abundance of active bacterial populations below the SMTZ decreases less rapidly than above the SMTZ in these sediments. The observation of a similar trend in transcript abundance indicates that the fraction of active microbial population is positively related to the total cell abundance. Therefore, the decrease of SSU rRNA gene abundance in subseafloor sediments may be attributed to decreasing cell abundance. The bacterial SSU rRNA transcript abundance in this study were four to seven orders of magnitude lower than that of marine estuarine sedimentary environments (Smith et al., 2006), which was expected given lower organic carbon concentrations. While the results of this study indicate that the metabolic activity levels within the subseafloor sedimentary habitats were substantially less than other shallow, higher organic carbon environments, it is important to note that a metabolically active population was detected at all depths selected.

Sequences were grouped into OTUs based on 95% sequence similarity to obtain a genus-level clustering of the metabolically active bacterial community. For the purpose of this study, the designation of genus will be used as a descriptor of relative taxonomic level but may not reflect a true genus-level classification despite the use of 95% sequence similarity in other studies (Zhang et al., 2010). The sequencing capacity required to reach the depth of phylogenetic analyses presented here is unique for the characterization of subseafloor microbial communities. In addition, the V1–V3 regions were selected based on the overall volume of sequences available for comparison and the widely accepted and used primer sets available. As deep subsurface sediments have not been well characterized for primer optimization (Teske and Sørensen, 2008), this initial study provides a resource for future primer development efforts.

The bacterial diversity observed in sediments at 1 mbsf was similar to that found in other marine sedimentary environments considered to host diverse active microbial communities, such as near-shore sediments (Reese et al., 2012). The level of diversity determined in this study indicated that this system was more complex than anticipated. It is important to note that a majority of the genera observed comprised less than 1% of the total population. This is supported by high Shannon index values indicating species richness. The identification of these populations was possible as a result of the high-throughput sequencing efforts and may still play important roles in the overall community function. However, many of these genera have not been physiologically characterized in marine systems. To enhance the descriptive nature of molecular datasets, additional effort is required in cultivation-based molecular ecological and biogeochemical studies.

A limited number of shared OTUs at each depth indicated that the observed metabolically active populations were unique from each other. Although the samples had similar phyla characterization and similar abundance of genera at both 19 and 57 mbsf, they only shared 24% of their OTUs. Statistical data including rarefaction and Chao1 estimates suggested that a majority of the active microbial community was likely characterized at 19 and 57 mbsf. While these communities are both deep in the subsurface, the different community structure can be in part attributed to local variations in geochemistry, such as proximity to the SMTZ. Previous studies have shown that geological variability can support differences in microbial population diversity in subseafloor sediments (Inagaki et al., 2006; Hoshino et al., 2011). A broad study describing the horizontal spatial variability of microbial populations in marine subseafloor has yet to be compiled.

The OTU abundance was significantly at 19 and 57 mbsf compared to the community at 1 mbsf. These data supported a reduction in diversity with increasing sediment depth in subseafloor microbial populations. A similar loss of diversity with increasing depth below surface was previously shown in subseafloor microbial communities using bacterial SSU rRNA gene targets (Parkes et al., 2005; Biddle et al., 2008). Increased sampling resolution should be performed in future studies to determine the level of heterogeneity within the subseafloor biosphere. It is interesting

to note that the diversity at the phylum level observed in this study was greater than previous subseafloor microbial characterizations despite using RNA to target the metabolically active fraction of the total population. Furthermore, the total diversity in these sediments are predicted to be higher than indicated by an RNA-based analysis, as only a fraction of the total diversity would be active. These results suggest that previous studies have underestimated the total diversity of the subseafloor microbial community and that more robust techniques should be routinely applied. The combination of extraction method and pyrosequencing techniques may have produced a higher nucleic acid yield and deeper sequencing effort, yielding the increased diversity observations. Therefore, the Nankai sediments may support increased diversity compared to other subsurface locations or these results represent an advancement of the procedures used to characterize microbial populations. Such uncertainty stresses the need for standardizing molecular methods between laboratories working on the subseafloor biosphere as well as expanding characterizations using RNA targets.

PREDICTED BIOGEOCHEMICAL INTERACTIONS

Combined biologic and geochemical comparisons provide a more complete understanding of the subseafloor biosphere. Geochemical profiles indicated that the SMTZ was at approximately 20 mbsf. Multiple microbial processes are predicted as being metabolically active within this zone including: sulfate reduction, methane oxidation, methanogenesis, and potentially metal reduction. These processes, along with fermentation are considered dominant metabolic processes throughout anaerobic subsurface sediments (D'Hondt et al., 2002, 2004), however geochemical analysis is used to predict stratification of the microbial process and thus populations. Presence and abundance of active genera were examined to determine potential changes in the overall metabolic function of the community corresponding to depth and local geochemical conditions. As previously noted, the authors acknowledge the limitation of using SSU rRNA for functional characterization of microbial communities.

Thermodynamically predicted processes

Thermodynamics predicts that microbial populations in the marine subseafloor will be stratified based on the potential energy gain available from the oxidation and reduction reactions of electron donors and acceptors (Froelich et al., 1979; Orcutt et al., 2011). Molecular data from this study support metabolically active subseafloor microbial populations can be linked to the predicted geochemical conditions, though anomalies do occur as discussed below. Previous studies have predicted that shallow subsurface sediments with high sulfate concentrations and low electron donor concentrations would support a wide zone of sulfate reduction and with a majority of the microbial population using sulfur metabolism (D'Hondt et al., 2002). Ship-based geochemical analysis indicated a gradual loss of sulfate from the surface to the top of the SMTZ followed by a more rapidly decrease in concentration through the SMTZ. These data support microbial sulfate reduction occurring above and within the SMTZ. Correspondingly, RNA-based molecular analysis identified metabolically active organisms capable of sulfate reduction in the 1- and 19-mbsf samples. Additionally, there were organisms capable of oxidizing sulfides generated in the 1-mbsf sample to completely cycle sulfur species at the surface. A shift to sulfur reduction was observed at 19 mbsf with over 12% of the sequences related to Helicobacteraceae. This lineage, also detected at 57 mbsf but not detected in the active fraction at 1 mbsf, has the potential to utilize the products of reduced sulfate to produce the hydrogen sulfide detected in geochemical analysis. The localization of this lineage within and below the SMTZ is supported by the inferred physiology and may provide a critical linkage to the complete reduction of sulfate to hydrogen sulfide. Members of this family have been noted as being understudied while frequently detected in marine systems (Campbell et al., 2006). Additional sequence analysis of the V1–V3 region will be completed to determine if detection of this lineage is biased in NCBI Blast results, and does not recognize the sequence similarity to other, sediment-associated Helicobacteraceae.

Processes other than sulfate reduction may contribute to the overall community metabolic function at 1 mbsf despite low organic carbon concentrations donors. Approximately 2.7% of the total population observed at the 1-mbsf was capable of iron oxidation and reduction, indicating that complete cycling of iron species is also possible in shallow subseafloor sediments. Additionally 30.9% of the total population observed in the sample at 1 mbsf is potentially associated with nitrogen cycling. Nitrogen cycling in these shallow sediments may play a substantial role in the overall microbial ecology despite previous predictions of a sulfate dominated environment (D'Hondt et al., 2002). However, recent reports suggest that sulfate reduction can be coupled to ammonium oxidation, providing a link between the two pathways in the shallow subsurface (Schrum et al., 2009). These results stress the need to couple geochemical analysis with molecular characterization of microbial populations. Studies limited to one of these procedures would result in inaccurate interpretations of the microbial ecology.

Lineages detected outside of thermodynamically predicted zones

Multiple lineages capable of nitrogen and iron reduction were detected as metabolically active outside of thermodynamically predicted zones, i.e., above the SMTZ (Froelich et al., 1979). Sequence data indicated lineages capable of iron reduction comprised 2.7 and 1.4% of the total sequences at 19 and 57 mbsf, respectively. A slight increase of dissolved iron [Fe(II)] concentration corresponding to a decrease of iron sulfides (CRS) potentially explains the observation of iron reducers below the SMTZ (**Figure 1**). It is important to note that since the increase of Fe(II) is small, it might be attributed to procedural biases associated with the determination of Fe(II) concentration. However, corresponding molecular evidence supports the geochemical result corroborating this as natural variability. As a result of the dissolution of the metal sulfide compounds, Fe(III) may be produced at depth through chemical reactions with fermentation products including hydrogen peroxide (Brooijmans et al., 2009). Iron reducers active at depth, as suggested by molecular results at 57 mbsf, would reduce the Fe(III) upon formation. Future research in this area would provide a more defined link between the products of fermentation and the oxidation of reduced substrates at depth.

Active iron and nitrogen cycling below the SMTZ may indicate the presence of geochemically cryptic cycles at depth. In addition

to iron reduction, nitrogen-reducing lineages were detected within (23.5% of the total sequences) and below (43.7% of the total sequences) the SMTZ. Oxidizing populations were metabolically active at depth although they were less than 1% of the total sequences obtained. For example, the genus *Dyella* was detected at 19 and 57 mbsf and has species capable of both iron oxidation and iron reduction (Lu et al., 2010). Lineages at 57 mbsf included sulfur-oxidizing *Thioalkalispira*, and the Mn(II) oxidation genus *Leptothrix* (Boogerd and Devrind, 1987). Detection of these lineages being metabolically active supports the presence of complex interactions between microbial communities within the marine subseafloor that may not be solely directed geochemically. The co-occurrence of populations with the capacity to conduct both oxidative and reductive processes recently described as cryptic biogeochemical cycling (Holmkvist et al., 2011; Orcutt et al., 2011). The nature of the redox pairs would result in a lack of detectable geochemical end products at the standard resolution of analysis, keeping one half of the process geochemically undetectable. However the low abundance of oxidizers and the presence of reduced compounds suggest oxidizing processes may be the limiting component.

Further investigations into the active metabolisms of the populations found at various depths using culture assays is essential to gain a better understanding of how these organisms survive in marine subseafloor environments. Cultivation-based characterizations of lineages isolated from the subsurface are currently ongoing in the Mills laboratory and will be used to support community characterizations. Future research will focus on combining molecular techniques including the isolation of functional gene targets, metatranscriptomic, and proteomic analyses. In addition, increasing sequence resolution in these environments will provide a better characterization of genera detected at low frequency. Description of the rare biosphere is important to understand the extent of total diversity in the subseafloor biosphere.

ACKNOWLEDGMENTS

The authors would like to thank the Integrated Ocean Drilling Program, the Science Party and Crew of the Chikyu during IODP Expedition 316, Tim Ferdelman, Raymond Cruz St. Peter, and Emily Hollister for their contributions to this research. Additionally, we would like to thank the Ocean Drilling and Sustainable Earth Sciences faculty and the Department of Oceanography at Texas A&M University for their contributions toward funding this research. This paper is contribution number 128 to the Center for Dark Energy Biosphere Investigations (CDEBI).

SUPPLEMENTARY MATERIAL

The Supplementary Material for this article can be found online at http://www.frontiersin.org/extreme_microbiology/10.3389/fmicb.2012.00113/abstract

Table S1 | Taxonomic identification of the Nankai subsurface sequence data set.

REFERENCES

Bach, W., Ravelo, C., Behrmann, J., Camoin, G., Duncan, R., Edwards, K., Gulick, S., Inagaki, F., Pälike, H., and Tada, R. (2010). IODP New Ventures in Exploring Scientific Targets (INVEST): defining the new goals of an international drilling program. *Sci. Drill.* 9, 54–64.

Bickle, M., Arculus, R., Barrett, P., DeConto, R., Camoin, G., Edwards, K., Fisher, A., Inagaki, F., Kodaira, S., Ohkouchi, N., Pälike, H., Ravelo, C., Saffer, D., and Teagle, D. (2011). *Illuminating Earth's Past, Present and Future: Science Plan for 2013–2023.* Washington: IODP Press, 92.

Biddle, J. F., Fitz-Gibbon, S., Schuster, S. C., Brenchley, J. E., and House, C. H. (2008). Metagenomic signatures of the Peru Margin subseafloor biosphere show a genetically distinct environment. *Proc. Natl. Acad. Sci. U.S.A.* 105, 10583–10588.

Biddle, J. F., Lipp, J. S., Lever, M. A., Lloyd, K. G., Sorensen, K. B., Anderson, R., Fredricks, H. F., Elvert, M., Kelly, T. J., Schrag, D. P., Sogin, M. L., Brenchley, J. E., Teske, A., House, C. H., and Hinrichs, K. U. (2006). Heterotrophic *Archaea* dominate sedimentary subsurface ecosystems off Peru. *Proc. Natl. Acad. Sci. U.S.A.* 103, 3846–3851.

Boogerd, F. C., and Devrind, J. P. M. (1987). Manganese oxidation by *Leptothrix discophora*. *J. Bacteriol.* 169, 489–494.

Bosshard, P. P., Zbinden, R., and Altwegg, M. (2002). *Turicibacter sanguinis* gen. nov., sp nov., a novel anaerobic, Gram-positive bacterium. *Int. J. Syst. Evol. Microbiol.* 52, 1263–1266.

Bowman, J. P., Sly, L. I., Nichols, P. D., and Hayward, A. C. (1993). Revised taxonomy of the methanotrophs – description of *Methylobacter* gen. nov, emendation of *Methylococcus*, validation of *Methylosinus* and *Methylocystis* species, and a proposal that the family Methylococcaceae includes only the Group I methanotrophs. *Int. J. Syst. Evol. Microbiol.* 43, 735–753.

Brooijmans, R. J. W., De Vos, W. M., and Hugenholtz, J. (2009). *Lactobacillus plantarum* WCFS1 electron transport chains. *Appl. Environ. Microbiol.* 75, 3580–3585.

Brysch, K., Schneider, C., Fuchs, G., and Widdel, F. (1987). Lithoautotrophic growth of sulfate-reducing bacteria, and description of *Desulfobacterium autotrophicum* gen nov, sp. nov. *Arch. Microbiol.* 148, 264–274.

Campbell, B. J., Engel, A. S., Porter, M. L., and Takai, K. (2006). The versatile ε-proteobacteria: key players in sulphidic habitats. *Nat. Rev. Microbiol.* 4, 458–468.

Canfield, D. E., Stewart, F. J., Thamdrup, B., De Brabandere, L., Dalsgaard, T., DeLong, E. F., Revsbech, N. P., and Ulloa, O. (2010). A cryptic sulfur cycle in oxygen-minimum-zone waters off the Chilean Coast. *Science* 330, 1375–1378.

Chapelle, F. H., O'Neil, K., Bradley, P. M., Methe, B. A., Cluto, S. A., Knobel, L. L., and Lovely, D. R. (2002). A hydrogen-based subsurface microbial community dominated by methanogens. *Nature* 415, 312–314.

Clark, D. A., and Norris, P. R. (1996). *Acidimicrobium ferrooxidans* gen nov, sp nov: mixed-culture ferrous iron oxidation with *Sulfobacillus* species. *Microbiology* 142, 785–790.

Cline, J. D. (1969). Spectrophotometric determination of hydrogen sulfide in natural waters. *Limnol. Oceanogr.* 14, 454–458.

Cole, J. R., Wang, Q., Cardenas, E., Fish, J., Chai, B., Farris, R. J., Kulam-Syed-Mohideen, A. S., McGarrell, D. M., Marsh, T., Garrity, G. M., and Tiedje, J. M. (2009). The Ribosomal Database Project: improved alignments and new tools for rRNA analysis. *Nucleic Acids Res.* 37, D141–D145.

Davis, B. D., Luger, S. M., and Tai, P. C. (1986). Role of ribosome degradation in the death of starved *Escherichia coli* cells. *J. Bacteriol.* 166, 439–445.

DeLong, E. F., Wickham, G. S., and Pace, N. R. (1989). Phylogenetic stains – ribosomal RNA-based probes for the identification of single cells. *Science* 243, 1360–1363.

D'Hondt, S., Inagaki, F., Ferdelman, T., Jørgensen, B. B., Kato, K., Kemp, P., Sobecky, P., Sogin, M., and Takai, K. (2007). Exploring subseafloor life with the Integrated Ocean Drilling Program. *Sci. Drill.* 5, 26–37.

D'Hondt, S., Jørgensen, B. B., Miller, D. J., Batzke, A., Blake, R., Cragg, B. A., Cypionka, H., Dickens, G. R., Ferdelman, T., Hinrichs, K. U., Holm, N. G., Mitterer, R., Spivack, A., Wang, G. Z., Bekins, B., Engelen, B., Ford, K., Gettemy, G., Rutherford, S. D., Sass, H., Skilbeck, C. G., Aiello, I. W., Guerin, G., House, C. H., Inagaki, F., Meister, P., Naehr, T., Niitsuma, S., Parkes, R. J., Schippers, A., Smith, D. C., Teske, A., Wiegel, J., Padilla, C. N., and Acosta, J. L. S. (2004). Distributions of microbial activities in deep subseafloor sediments. *Science* 306, 2216–2221.

D'Hondt, S., Rutherford, S., and Spivack, A. J. (2002). Metabolic activity of subsurface life in deep-sea sediments. *Science* 295, 2067–2070.

Dowd, S. E., Zaragoza, J., Rodriguez, J. R., Oliver, M. J., and Payton, P. R. (2005). Windows.NET network distributed basic local alignment search toolkit (W.ND-BLAST). *BMC Bioinformatics* 6, 93. doi:10.1186/1471-2105-6-93

Edwards, R. A., Rodriguez-Brito, B., Wegley, L., Haynes, M., Breitbart, M., Peterson, D. M., Saar, M. O., Alexander, S., Alexander, E. C. Jr., and Rohwer, F. (2006). Using pyrosequencing to shed light on deep mine microbial ecology. *BMC Genomics* 7, 57. doi:10.1186/1471-2164-7-57

Fegatella, F., Lim, J., Kjelleberg, S., and Cavicchioli, R. (1998). Implications of rRNA operon copy number and ribosome content in the marine oligotrophic ultramicrobacterium *Sphingomonas* sp. strain RB2256. *Appl. Environ. Microbiol.* 64, 4433–4438.

Fidopiastis, P. M., Bezdek, D. J., Horn, M. H., and Kandel, J. S. (2006). Characterizing the resident, fermentative microbial consortium in the hindgut of the temperate-zone herbivorous fish, *Hermosilla azurea* (Teleostei: Kyphosidae). *Mar. Biol.* 148, 631–642.

Fossing, H., and Jørgensen, B. B. (1989). Measurement of bacterial sulfate reduction in sediments. Evaluation of a single-step chromium reduction method. *Biogeochemistry* 8, 205–222.

Frias-Lopez, J., Shi, Y., Tyson, G. W., Coleman, M. L., Schuster, S. C., Chisholm, S. W., and DeLong, E. F. (2008). Microbial community gene expression in ocean surface waters. *Proc. Natl. Acad. Sci. U.S.A.* 105, 3805–3810.

Froelich, P. N., Klinkhammer, G. P., Bender, M. L., Luedtke, N. A., Heath, G. R., Cullen, D., Dauphin, P., Hammond, D., Hartman, B., and Maynard, V. (1979). Early oxidation of organic matter in pelagic sediments of the eastern equatorial Atlantic suboxic diagenesis. *Geochim. Cosmochim. Acta* 43, 1075–1090.

Gilbert, J., Field, D., Huang, Y., Edwards, R., Li, W., Gilna, P., and Joint, I. (2008). Detection of large numbers of novel sequences in the metatranscriptomes of complex marine microbial communities. *PLoS ONE* 3, e3042. doi:10.1371/journal.pone.0003042

Giovannoni, S. J. (1991). "The polymerase chain reaction," in *Nucleic Acid Techniques in Bacterial Systematics*, eds. E. Stackenbrandt and M. Goodfellow (Chichester: Wiley), 177–203.

Gold, T. (1992). The deep, hot biosphere. *Proc. Natl. Acad. Sci. U.S.A.* 89, 6045–6049.

Gregory, L. G., Bond, P. L., Richardson, D. J., and Spiro, S. (2003). Characterization of a nitrate-respiring bacterial community using the nitrate reductase gene (narG) as a functional marker. *Microbiology* 149, 229–237.

Haas, B. J., Gevers, D., Earl, A. M., Feldgarden, M., Ward, D. V., Giannoukos, G., Ciulla, D., Tabbaa, D., Highlander, S. K., Sodergren, E., Methe, B., Desantis, T. Z., Petrosino, J. F., Knight, R., Birren, B. W., and Consortium, H. M. (2011). Chimeric 16S rRNA sequence formation and detection in Sanger and 454-pyrosequenced PCR amplicons. *Genome Res.* 21, 494–504.

Head, I. M., Gray, N. D., Babenzien, H. D., and Glockner, F. O. (2000). Uncultured giant sulfur bacteria of the genus *Achromatium*. *FEMS Microbiol. Ecol.* 33, 171–180.

Holmkvist, L., Ferdelman, T. G., and Jørgensen, B. B. (2011). A cryptic sulfur cycle driven by iron in the methane zone of marine sediment (Aarhus Bay, Denmark). *Geochim. Cosmochim. Acta* 75, 3581–3599.

Hoshino, T., Morono, Y., Terada, T., Imachi, H., Ferdelman, T. F., and Inagaki, F. (2011). Comparative study of subseafloor microbial community structures in deeply buried coral fossils and sediment matrices from the Challenger Mound in the Porcupine Seabight. *Front. Microbiol.* 2:231. doi:10.3389/fmicb.2011.00231

Igual, J. M., Valverde, A., Delvasto, P., Peix, A., Velazquez, E., Santa-Regina, I., Ballester, A., Rodriguez-Barrueco, C., and Garcia-Balboa, C. (2006). *Burkholderia ferrariae* sp nov., isolated from an iron ore in Brazil. *Int. J. Syst. Evol. Microbiol.* 56, 2421–2425.

Inagaki, F., Nunoura, T., Nakagawa, S., Teske, A., Lever, M., Lauer, A., Suzuki, M., Takai, K., Delwiche, M., Colwell, F. S., Nealson, K. H., Horikoshi, K., D'Hondt, S., and Jørgensen, B. B. (2006). Biogeographical distribution and diversity of microbes in methane hydrate-bearing deep marine sediments, on the Pacific ocean margin. *Proc. Natl. Acad. Sci. U.S.A.* 103, 2815–2820.

Iversen, N., and Jørgensen, B. B. (1985). Anaerobic methane oxidation rates at the sulfate methane transition in marine sediments from Kattegat and Skagerrak (Denmark). *Limnol. Oceanogr.* 30, 944–955.

Jones, W. J. (2010). High-throughput sequencing and metagenomics. *Estuaries Coast* 33, 944–952.

Kandler, O., Schillinger, U., and Weiss, N. (1983). *Lactobacillus bifermentans* sp. nov, nom rev, an organism forming CO2 and H2 from lactic acid. *Syst. Appl. Microbiol.* 4, 408–412.

Kemp, P. F., Lee, S., and Laroche, J. (1993). Estimating the growth rate of slowly growing marine bacteria from RNA content. *Appl. Environ. Microbiol.* 59, 2594–2601.

Kerkhof, L. J., and Ward, B. B. (1993). Comparison of nucleic acid hybridization and fluorometry for measurement of RNA/DNA relationship with growth rate in a marine bacterium. *Appl. Environ. Microbiol.* 59, 1303–1307.

Kimura, G., Screaton, E. J., Curewitz, D., and Expedition 316 Scientists. (2008). *NanTroSEIZE Stage 1A: NanTroSEIZE Shallow Megasplay and Frontal Thrusts.* IODP Preliminary Report, College Station, 316.

Kinoshita, M., Tobin, H., Ashi, J., Kimura, G., Lallemant, S., Screaton, E. J., Curewitz, D., Masago, H., Moe, K. T., and the Expedition 314/315/316 Scientists. (2009). "NanTroSEIZE Stage 1: Investigations of seismogenesis Nankai Trough, Japan," in *Proceeding of the Integrated Ocean Drilling Program*, 314/315/316 Expedition Reports, College Station.

Kuever, J., and Meyer, B. (2007). Phylogeny of the alpha and beta subunits of the dissimilatory adenosine-5′-phosphosulfate (APS) reductase from sulfate-reducing prokaryotes – origin and evolution of the dissimilatory sulfate-reduction pathway. *Microbiology* 153, 2026–2044.

Kunze, B., Steinmetz, H., Hofle, G., Huss, M., Wieczorek, H., and Reichenbach, H. (2006). Cruentaren, a new antifungal salicylate-type macrolide from *Byssovorax cruenta* (*Myxobacteria*) with inhibitory effect on mitochondrial ATPase activity – fermentation and biological properties. *J. Antibiot.* 59, 664–668.

Lee, S. H., and Kemp, P. F. (1994). Single cell RNA content of natural marine planktonic bacteria measured by hybridization with multiple 16S ribosomal RNA targeted fluorescent probes. *Limnol. Oceanogr.* 39, 869–879.

Leininger, S., Urich, T., Schloter, M., Schwark, L., Qi, J., Nicol, G. W., Prosser, J. I., Schuster, S. C., and Schleper, C. (2006). Archaea predominate among ammonia-oxidizing prokaryotes in soils. *Nature* 442, 806–809.

Leloup, J., Fossing, H., Kohls, K., Holmkvist, L., Borowski, C., and Jørgensen, B. B. (2009). Sulfate-reducing bacteria in marine sediment (Aarhus Bay, Denmark): abundance and diversity related to geochemical zonation. *Environ. Microbiol.* 11, 1278–1291.

Lipp, J. S., Morono, Y., Inagaki, F., and Hinrichs, K. U. (2008). Significant contribution of Archea to extant biomass in marine subsurface sediments. *Nature* 454, 991–994.

Liu, Z., Desantis, T. Z., Andersen, G. L., and Knight, R. (2008). Accurate taxonomy assignments from 16S rRNA sequences produced by highly parallel pyrosequencers. *Nucleic Acids Res.* 36, e120.

Lu, S. P., Gischkat, S., Reiche, M., Akob, D. M., Hallberg, K. B., and Kusel, K. (2010). Ecophysiology of Fe-cycling bacteria in acidic sediments. *Appl. Environ. Microbiol.* 76, 8174–8183.

Macalady, J. L., Dattagupta, S., Schaperdoth, I., Jones, D. S., Druschel, G. K., and Eastman, D. (2008). Niche differentiation among sulfur-oxidizing bacterial populations in cave waters. *ISME J.* 2, 590–601.

Mattes, T. E., and Jin, Y. O. (2010). A quantitative PCR assay for aerobic, vinyl chloride- and ethene-assimilating microorganisms in groundwater. *Environ. Sci. Technol.* 44, 9036–9041.

Mills, H. J., Hunter, E., Humphrys, M., Kerkhof, L., McGuinness, L., Huettel, M., and Kostka, J. E. (2008). Determination of high resolution microbial community structure in permeable marine sediments of the northeastern Gulf of Mexico. *Appl. Environ. Microbiol.* 74, 4440–4453.

Miroshnichenko, M. L., Kostrikina, N. A., Chernyh, N. A., Pimenov, N. V., Tourova, T. P., Antipov, A. N., Spring, S., Stackebrandt, E., and Bonch-Osmolovskaya, E. A. (2003). *Caldithrix abyssi* gen. nov., sp nov., a nitrate-reducing, thermophilic, anaerobic bacterium isolated from a Mid-Atlantic Ridge hydrothermal vent, represents a novel bacterial lineage. *Int. J. Syst. Evol. Microbiol.* 53, 323–329.

Morono, Y., and Inagaki, F. (2010). Automatic slide-loader fluorescence microscope for discriminative enumeration of subseafloor life. *Sci. Drill.* 9, 32–36.

Morono, Y., Terada, T., Masui, N., and Inagaki, F. (2009). Discriminative detection and enumeration of microbial life in marine subsurface sediments. *ISME J.* 3, 503–511.

Morono, Y., Terada, T., Nishizawa, M., Ito, M., Hillion, F., Takahata, N., Sano, Y., and Inagaki, F. (2011). Carbon and nitrogen assimilation in deep subseafloor microbial cells. *Proc. Natl. Acad. Sci. U.S.A.* 108, 18295–18300.

Nadkarni, M. A., Martin, F. E., Jacques, N. A., and Hunter, N. (2002). Determination of bacterial load by real-time PCR using a broad-range (universal) probe and primers set. *Microbiology* 148, 257–266.

Nakano, M., Shimizu, Y., Okumura, H., Sugahara, I., and Maeda, H. (2008). Construction of a consortium comprising ammonia-oxidizing bacteria and denitrifying bacteria isolated from marine sediment. *Biocontrol Sci.* 13, 73–89.

Nawrocki, A. P., and Eddy, S. R. (2007). Query-dependant banding (QDB) for faster RNA similarity searches. *PLoS Comput. Biol.* 3, E56.

Neidhardt, F. C., and Magasanik, B. (1960). Studies on the role of ribonucleic acid in the growth of bacteria. *Biochim. Biophys. Acta* 42, 99–116.

Newberry, C. J., Webster, G., Cragg, B. A., Parkes, R. J., Weightman, A. J., and Fry, J. C. (2004). Diversity of prokaryotes and methanogenesis in deep subsurface sediments from the Nankai Trough, Ocean Drilling Program Leg 190. *Environ. Microbiol.* 6, 274–287.

Nogales, B., Moore, E. R. B., Abraham, W. R., and Timmis, K. N. (1999). Identification of the metabolically active members of a bacterial community in a polychlorinated biphenyl-polluted moorland soil. *Environ. Microbiol.* 1, 199–212.

Ollivier, B., Gregoire, P., Bohli, M., Cayol, J. L., Joseph, M., Guasco, S., Dubourg, K., Cambar, J., Michotey, V., Bonin, P., and Fardeau, M. L. (2011). *Caldilinea tarbellica* sp nov., a filamentous, thermophilic, anaerobic bacterium isolated from a deep hot aquifer in the Aquitaine Basin. *Int. J. Syst. Evol. Microbiol.* 61, 1436–1441.

Orcutt, B. N., Sylvan, J. B., Knab, N. J., and Edwards, K. J. (2011). Microbial ecology of the dark ocean above, at, and below the seafloor. *Microbiol. Mol. Biol. Rev.* 75, 361–422.

Pakrasi, H. B., Welsh, E. A., Liberton, M., Stoeckel, J., Loh, T., Elvitigala, T., Wang, C., Wollam, A., Fulton, R. S., Clifton, S. W., Jacobs, J. M., Aurora, R., Ghosh, B. K., Sherman, L. A., Smith, R. D., and Wilson, R. K. (2008). The genome of *Cyanothece* 51142, a unicellular diazotrophic cyanobacterium important in the marine nitrogen cycle. *Proc. Natl. Acad. Sci. U.S.A.* 105, 15094–15099.

Parkes, R. J., Cragg, B. A., Bale, S. J., Getliff, J. M., Goodman, K., Rochelle, P. A., Fry, J. C., Weightman, A. J., and Harvey, S. M. (1994). Deep bacterial biosphere in Pacific ocean sediments. *Nature* 371, 410–413.

Parkes, R. J., Cragg, B. A., and Wellsbury, P. (2000). Recent studies on bacterial populations and processes in subseafloor sediments: a review. *Hydrogeol. J.* 8, 11–28.

Parkes, R. J., Webster, G., Cragg, B. A., Weightman, A. J., Newberry, C. J., Ferdelman, T. G., Kallmeyer, J., Jørgensen, B. B., Aiello, I. W., and Fry, J. C. (2005). Deep sub-seafloor prokaryotes stimulated at interfaces over geological time. *Nature* 436, 390–394.

Polymenakou, P. N., Lampadariou, N., Mandalakis, M., and Tselepides, A. (2009). Phylogenetic diversity of sediment bacteria from the southern Cretan margin, Eastern Mediterranean Sea. *Syst. Appl. Microbiol.* 32, 17–26.

Rainey, F. A., Janssen, P. H., Wild, D. J. C., and Morgan, H. W. (1991). Isolation and characterization of an obligately anaerobic, polysaccharolytic, extremely thermophilic member of the genus *Spirochaeta*. *Arch. Microbiol.* 155, 396–401.

Reese, B. K., Mills, H. J., Dowd, S., and Morse, J. W. (2012). Benthic biogeochemistry of microbial iron and sulfate reduction in the Gulf of Mexico hypoxic zone. *Geomicrobiol. J.* (in press).

Renner, E. D., and Becker, G. E. (1970). Production of nitric oxide and nitrous oxide during denitrification by *Corynebacterium nephridii*. *J. Bacteriol.* 101, 821–826.

Rigo, L. U., Schwab, S., Ramos, H. J., Souza, E. M., Pedrosa, F. O., Yates, M. G., and Chubatsu, L. S. (2007). Identification of $NH4^+$-regulated genes of *Herbaspirillum seropedicae* by random insertional mutagenesis. *Arch. Microbiol.* 187, 379–386.

Roling, W. F. M., Lin, B., Hyacinthe, C., Bonneville, S., Braster, M., and Van Cappellen, P. (2007). Phylogenetic and physiological diversity of dissimilatory ferric iron reducers in sediments of the polluted Scheldt estuary, Northwest Europe. *Environ. Microbiol.* 9, 1956–1968.

Sanford, R. A., Cole, J. R., and Tiedje, J. M. (2002). Characterization and description of *Anaeromyxobacter dehalogenans* gen. nov., sp nov., an aryl-halorespiring facultative anaerobic myxobacterium. *Appl. Environ. Microbiol.* 68, 893–900.

Schink, B., Denger, K., Warthmann, R., and Ludwig, W. (2002). *Anaerophaga thermohalophila* gen. nov., sp nov., a moderately thermohalophilic, strictly anaerobic fermentative bacterium. *Int. J. Syst. Evol. Microbiol.* 52, 173–178.

Schloss, P. D., Westcott, S. L., Ryabin, T., Hall, J. R., Hartmann, M., Hollister, E. B., Lesniewski, R. A., Oakley, B. B., Parks, D. H., Robinson, C. J., Sahl, J. W., Stres, B., Thallinger, G. G., Van Horn, D. J., and Weber, C. F. (2009). Introducing mothur: open-source, platform-independent, community-supported software for describing and comparing microbial communities. *Appl. Environ. Microbiol.* 75, 7537–7541.

Schrum, H., Spivack, A. J., Kastner, M., and D'Hondt, S. (2009). Sulfate-reducing ammonium oxidation: a thermodynamically feasible metabolic pathway in subseafloor sediment. *Geology* 37, 939–942.

Smith, C. J., Nedwell, D. B., Dong, L. F., and Osborn, A. M. (2006). Evaluation of quantitative polymerase chain reaction-based approaches for determining gene copy and gene transcript numbers in environmental samples. *Environ. Microbiol.* 8, 804–815.

Sogin, M. L., Morrison, H. G., Huber, J. A., Welch, D. M., Huse, S. M., Neal, P. R., Arrieta, J. M., and Herndi, G. J. (2006). Microbial diversity in the deep sea and the underexplored "rare biosphere". *Proc. Natl. Acad. Sci. U.S.A.* 103, 12115–12120.

Sørensen, K. B., and Teske, A. (2006). Stratified communities of active archaea in deep marine subsurface sediments. *Appl. Environ. Microbiol.* 72, 4596–4603.

Sorokin, D. Y., Tourova, T. P., Kolganova, T. V., Sjollema, K. A., and Kuenen, J. G. (2002). *Thioalkalispira microaerophila* gen. nov., sp nov., a novel lithoautotrophic, sulfur-oxidizing bacterium from a soda lake. *Int. J. Syst. Evol. Microbiol.* 52, 2175–2182.

Strasser, M., Moore, G. F., Kimura, G., Kitamura, Y., Kopf, A. J., Lallemant, S., Park, J. O., Screaton, E. J., Su, X., Underwood, M. B., and Zhao, X. X. (2009). Origin and evolution of a splay fault in the Nankai accretionary wedge. *Nat. Geosci.* 2, 648–652.

Strasser, M., Moore, G. F., Kimura, G., Kopf, A. J., Underwood, M. B., Guo, J., and Screaton, E. J. (2011). Slumping and mass transport deposition in the Nankai fore arec: evidence from IODP drilling and 3-D reflection seismic data. *Geochem. Geophys. Geosyst.* 12, Q0AD13.

Takano, Y., Chikaraishi, Y., Ogawa, N. O., Nomaki, H., Morono, Y., Inagaki, F., Kitazato, H., Hinrichs, K.-U., and Ohkouchi, N. (2010). Sedimentary membrane lipids recycled by deep-sea benthic archaea. *Nat. Geosci.* 3, 858–861.

Teske, A., and Sørensen, K. (2008). Uncultured archaea in deep marine subsurface sediments: have we caught them all? *ISME J.* 2, 3–18.

Tourova, T. P., Spiridonova, E. M., Berg, I. A., Slobodova, N. V., Boulygina, E. S., and Sorokin, D. Y. (2007). Phylogeny and evolution of the family Ectothiorhodospiraceae based on comparison of 16S rRNA, *cbbL* and *nifH* gene sequences. *Int. J. Syst. Evol. Microbiol.* 57, 2387–2398.

Urich, T., Lanzen, A., Huson, D. H., Schleper, C., and Schuster, S. C. (2008). Simultaneous assessment of soil microbial community structure and function through analysis of the meta-transcriptome. *PLoS ONE* 3, e2527. doi:10.1371/journal.pone.0002527

Van Damme, P., and Coenye, T. (2004). Taxonomy of the genus *Cupriavidus*: a tale of lost and found. *Int. J. Syst. Evol. Microbiol.* 54, 2285–2289.

Whiticar, M. J. (1999). Carbon and hydrogen isotope systematics of bacterial formation and oxidation of methane. *Chem. Geol.* 161, 291–314.

Whitman, W. B., Coleman, D. C., and Wiebe, W. J. (1998). Prokaryotes: the unseen majority. *Proc. Natl. Acad. Sci. U.S.A.* 95, 6578–6583.

Yamada, T., Sekiguchi, Y., Hanada, S., Imachi, H., Ohashi, A., Harada, H., and Kamagata, Y. (2006). *Anaerolinea thermolimosa* sp nov., *Levilinea saccharolytica* gen. nov., sp nov and *Leptolinea tardivitalis* gen. nov., so. nov., novel filamentous anaerobes, and description of the new classes Anaerolineae classis nov and Caldilineae classis nov in the bacterial phylum Chloroflexi. *Int. J. Syst. Evol. Microbiol.* 56, 1331–1340.

Zhang, H. S., Ziv-El, M., Rittmann, B. E., and Krajmalnik-Brown, R. (2010). Effect of dechlorination and

sulfate reduction on the microbial community structure in denitrifying membrane-biofilm reactors. *Environ. Sci. Technol.* 44, 5159–5164.

Conflict of Interest Statement: The authors declare that the research was conducted in the absence of any commercial or financial relationships that could be construed as a potential conflict of interest.

Received: 02 October 2011; accepted: 12 March 2012; published online: 03 April 2012.
Citation: Mills HJ, Reese BK, Shepard AK, Riedinger N, Dowd SE, Morono Y and Inagaki F (2012) Characterization of metabolically active bacterial populations in subseafloor Nankai Trough sediments above, within, and below the sulfate–methane transition zone. Front. Microbio. ***3****:113. doi: 10.3389/fmicb.2012.00113*
This article was submitted to Frontiers in Extreme Microbiology, a specialty of Frontiers in Microbiology.

frontiers in
MICROBIOLOGY

ORIGINAL RESEARCH ARTICLE
published: 10 May 2012
doi: 10.3389/fmicb.2012.00175

Trace elements affect methanogenic activity and diversity in enrichments from subsurface coal bed produced water

Burcu Ünal[1], Verlin Ryan Perry[2†], Mili Sheth[2†], Vicente Gomez-Alvarez[1], Kuk-Jeong Chin[2] and Klaus Nüsslein[1]*

[1] *Department of Microbiology, University of Massachusetts, Amherst, MA, USA*
[2] *Department of Biology, Georgia State University, Atlanta, GA, USA*

Edited by:
Andreas Teske, University of North Carolina at Chapel Hill, USA

Reviewed by:
Martin Krüger, Federal Institute for Geosciences and Natural Resources, Germany
Craig Lee Moyer, Western Washington University, USA

****Correspondence:***
Klaus Nüsslein, Department of Microbiology, University of Massachusetts, 203 Morrill Science Center IVN, 639 North Pleasant Street, Amherst, MA 01003, USA.
e-mail: nusslein@microbio.umass.edu

[†]Verlin Ryan Perry and Mili Sheth have contributed equally to this work.

Microbial methane from coal beds accounts for a significant and growing percentage of natural gas worldwide. Our knowledge of physical and geochemical factors regulating methanogenesis is still in its infancy. We hypothesized that in these closed systems, trace elements (as micronutrients) are a limiting factor for methanogenic growth and activity. Trace elements are essential components of enzymes or cofactors of metabolic pathways associated with methanogenesis. This study examined the effects of eight trace elements (iron, nickel, cobalt, molybdenum, zinc, manganese, boron, and copper) on methane production, on *mcrA* transcript levels, and on methanogenic community structure in enrichment cultures obtained from coal bed methane (CBM) well produced water samples from the Powder River Basin, Wyoming. Methane production was shown to be limited both by a lack of additional trace elements as well as by the addition of an overly concentrated trace element mixture. Addition of trace elements at concentrations optimized for standard media enhanced methane production by 37%. After 7 days of incubation, the levels of *mcrA* transcripts in enrichment cultures with trace element amendment were much higher than in cultures without amendment. Transcript levels of *mcrA* correlated positively with elevated rates of methane production in supplemented enrichments ($R^2 = 0.95$). Metabolically active methanogens, identified by clone sequences of *mcrA* mRNA retrieved from enrichment cultures, were closely related to *Methanobacterium subterraneum* and *Methanobacterium formicicum*. Enrichment cultures were dominated by *M. subterraneum* and had slightly higher predicted methanogenic richness, but less diversity than enrichment cultures without amendments. These results suggest that varying concentrations of trace elements in produced water from different subsurface coal wells may cause changing levels of CBM production and alter the composition of the active methanogenic community.

Keywords: methanogens, trace elements, coal bed methane, *mcrA* transcript, enrichments

INTRODUCTION

Coal bed methane (CBM) is a form of natural gas that is trapped at large quantities in deep unmineable coal bed basins and produced from boreholes (Thielemann et al., 2004). CBM is held at coal internal surfaces by the combination of physical sorption and hydrostatic pressure of subsurface water. Gas extraction is accomplished by pumping water from subsurface coal bed basins to the surface through drilled access wells that end within the coal bed. As water is pumped to the surface, methane is no longer held by the hydrostatic pressure in micro pore structures of coal beds and migrates from the subsurface coal into the water stream flowing to the well. At the surface, methane is separated from produced water and extracted to be used as an energy source (Wheaton and Donato, 2004). Seventy percentage of the world's CBM production is supplied by the United States while the remainder is produced by Australia, India, Canada, China, United Kingdom, Columbia, Russia, Ukraine, and Austria primarily from shallow to deep subsurface coal beds (Flores et al., 2008).

The production of CBM has increased dramatically, and currently supplies about 10% of the total natural gas produced annually in the U.S. (Fletcher, 2005; Petzet, 2005). The most active methane producing coal seams found in the U.S. are located in Alabama/Mississippi, Southern Colorado/New Mexico, and Montana/Wyoming (Harris et al., 2008). CBM is produced either via microbial degradation of organic molecules (i.e., biogenic gas) or via transformation of organic matter by geochemical processes (i.e., thermogenic gas; Flores et al., 2008). Coal deposits of the Powder River Basin (PRB) in Wyoming have emerged as having some of the most active biogenic gas production, with methane as the main constituent (85–90%; Flores et al., 2008; Strąpoć et al., 2008). Coal beds in the PRB basin are entirely continental, and are deposited in fresh water systems with insignificant concentrations of chloride (Van Voast, 2003). The $\delta^{13}C_{CO_2}$ values and associated fractionation factors indicate microbial CO_2 reduction as the overwhelming pathway for methane generation in the PRB (Flores et al., 2008).

Current knowledge of the indigenous microbiota residing in coal bed basins, of the role they play in mediating coal biodegradation to methane, and of the biogeochemical and physical factors that may influence biological methanogenesis is limited. Jones

et al. (2010) recently reported variations in the rates of biogenic methane production among CBM wells in the Gulf Coast Basin, Texas. Possible factors causing this interwell variability remain unknown. Only recently have subsurface microbial communities been characterized that contribute to methane production from unmined or abandoned coal beds (Shimizu et al., 2007; Green et al., 2008; Klein et al., 2008; Li et al., 2008; Midgley et al., 2010; Penner et al., 2010; Beckmann et al., 2011; Guo et al., 2012). Other studies determined the potential of these microbes to generate methane (Green et al., 2008; Harris et al., 2008; Jones et al., 2008; Ulrich and Bower, 2008), as well as to characterize the metabolic pathways involved in generating methane in subsurface systems (Strąpoć et al., 2008; Jones et al., 2010).

Analyses of archaeal diversity based on 16S rRNA genes in subsurface coal bed basins have revealed the presence of diverse assemblages of acetoclastic, methylotrophic, and hydrogenotrophic methanogens. For example, the hydrogenotrophic genus *Methanoculleus* was found together with the methylotrophic genus *Methanolobus* in groundwater samples from Ishikari coal field, Hokkaido, Japan (Shimizu et al., 2007), and *Methanolobus* dominated production water in the Ordos Basin, China (Guo et al., 2012). Members of *Methanosarcina* spp., known to use a wide range of substrates (H_2/CO_2, acetate, methanol, and methylamines) were detected in a methanogenic enrichment from coal beds in Alberta, Canada (Penner et al., 2010). While hydrogenotrophic *Methanobacterium* ssp. were found in enrichment cultures from the Jharia coal field, India (Singh et al., 2012), and Methanosarcinales (Green et al., 2008), Methanobacteriales, and Methanococcales (Klein et al., 2008) were discovered in the PRB, Wyoming. Some studies questioned whether members of the methanogenic community could be enhanced for methane production by manipulating temperature, pH, coal particle surface, electron acceptors or donors, or rapid release of organic substrates (Green et al., 2008; Harris et al., 2008; Jones et al., 2010; Penner et al., 2010). However, these attempts involved addition of electron acceptors or donors that might limit methanogenesis by diverting electrons away from methanogens, or, in case of enhanced organic matter release might limit methanogens by the creation of toxic conditions for methane generation within coal beds (Jones et al., 2010).

Microbial communities in subsurface coal beds likely feed on organic and inorganic sources either deposited within the coal during coalification (coal formation process) or those that have migrated from the surface along groundwater flow paths (Krumholz et al., 1997; Ulrich and Bower, 2008). Furthermore, trace elements (e.g., iron, nickel, cobalt, molybdenum, copper, zinc, tungstate, selenium, and boron) are crucial along with macronutrients (C, N, P, etc.), for proper growth and metabolism of microorganisms (Goodwin et al., 1990; Takashima et al., 1990; Lengeler et al., 1999). Various trace element demands of microorganisms are determined by the enzymes and the proteins needed for their particular metabolisms such as CO_2 assimilation, catabolism of organic compounds, and respiration (Zhang and Gladyshev, 2009). Iron (Fe), nickel (Ni), cobalt (Co), zinc (Zn), copper (Cu), molybdenum (Mo), and tungstate (W) are known as crucial trace elements for enzymatic activity in the methanogenic system (Takashima et al., 1990; Zhang and Gladyshev, 2010; Glass and Orphan, 2012). Requirement and optimal concentrations of trace elements for diverse microbial metabolisms are commonly studied with pure cultures only, which are orders of magnitude higher than *in situ* concentrations in most natural environments (Glass and Orphan, 2012). Although, some studies tested the effects of trace elements on methanogenesis in different anaerobic environments such as peatlands, maize silage, food industrial waste, and activated waste water sludge (Burgess et al., 1999; Gonzalez-Gil et al., 1999; Basiliko and Yavitt, 2001; Feng et al., 2010; Pobeheim et al., 2010), no studies have investigated whether methanogenesis in coal bed basins is influenced by trace elements. Two geochemical investigations of trace element chemistry across the PRB in Wyoming did not find consistent trends of trace element concentrations in CBM production waters (McBeth et al., 2003; Jackson and Reddy, 2007).

The aim of this study was to investigate the effect of trace element amendments on methanogenic activity and diversity in an enrichment culture from subsurface produced CBM water. This study was designed in three phases to understand (i) the effect of varying concentrations of trace element mixtures on methane production, (ii) the effect of trace element addition on transcript levels of the gene *mcrA*, which encodes the α-subunit of methyl coenzyme M reductase, and (iii) the effect of trace element addition on the community structure of metabolically active methanogens.

MATERIALS AND METHODS

FIELD SAMPLING, ANALYTICAL CHEMISTRY, AND DNA EXTRACTION OF CBM PRODUCED WATER

Three separate samples of CBM produced water were collected from a CBM well that is located within the Wall coal seam formation at a depth of 376 m below surface in the southern PRB, Wyoming, USA. The water sample was filtered through a series of 0.45 and 0.22 μm filters into gas tight Nalgene sample bottles, and acidified to pH <2 with 1% nitric acid (Trace metal grade, Fisher Scientific, Pittsburgh, PA, USA). Trace element concentrations in filtered water samples were quantified by inductively coupled plasma mass spectrometry (ICP-MS).

For the extraction of DNA 200 ml of water sample were drawn into a sterile 0.22 μm cellulose acetate filter (Millipore, Billerica, MA, USA) inside a presterilized 25-mm Swinnex filter holder, fast frozen on dry ice, and transported to the laboratory for storage at −80°C until further processing. Total DNA was extracted from the filters with the PowerWater DNA isolation kit according to manufacturer's instructions (MoBio Laboratories, CA, USA).

MICROCOSMS

Microcosms were initiated immediately after sampling from an actively gas-producing well stream by inoculating CBM produced water with pea-sized sub-bituminous coal sampled from the PRB. Ten replicates were set up with 30 ml of produced water and 5 g of coal in 120 ml anoxic serum vials capped with butyl rubber stoppers under a headspace of N_2/CO_2 [80:20 (v/v)] and incubated at 37°C without agitation. Yeast extract was not added, as coal is the only organic matter to be used for microbial growth. A separate set of microcosms was initiated from the same well stream by inoculating only CBM produced water in basal salt medium. All microcosms were set up anaerobically (Balch and

Wolfe, 1976) in 160 ml of anoxic serum vials capped with butyl rubber stoppers. Upon arrival at the laboratory, various electron acceptors were tested and microbial growth and methane production were observed in microcosms incubated at 37°C without agitation. The electron donor H_2 (H_2/CO_2 (80/20 (v/v)) was replaced with 50 mM sodium acetate or 5 mM methanol with N_2/CO_2 as the headspace gas.

ENRICHMENTS

Long term methanogenic enrichment cultures were established from CBM produced water by transferring cultures grown on H_2/CO_2 [80/20 (v/v)] after 50–80 days of incubation during a period of 2.5 years. Enrichment cultures were established in 160 ml serum vials with H_2/CO_2 [80/20 (v/v)] and basal salt medium consisting of the following components; 15 ml of KH_2PO_4 (27.2 g/l), 15 ml $Na_2HPO_4{\cdot}2H_2O$ (35.6 g/l), 12.5 ml of a mixture of NH_4Cl (24 g/l), $MgCl_2{\cdot}6H_2O$ (8 g/l), and NaCl (24 g/l), and 40 ml of $NaHCO_3$ (100 g/l); 10 ml vitamin solution (Biotin 2.0 mg, Folic acid 2.0 mg, Pyridoxine-HCl 10.0 mg, Thiamine-HCl·2 H_2O 5.0 mg, Riboflavin 5.0 mg, Nicotinic acid 5.0 mg, D-Ca-pantothenate 5.0 mg, *p*-aminobenzoic acid 5.0 mg, Thioctic acid 5.0 mg/l). To this 1 ml of a well defined trace element solution (SL-10) was added, that contained (per liter) 1.5 g of $FeCl_2{\cdot}4H_2O$, 70 mg of $ZnCl_2$, 100 mg of $MnCl_2{\cdot}4H_2O$, 6 mg of H_3BO_3, 190 mg of $CoCl_2{\cdot}6H_2O$, 2 mg of $CuCl_2{\cdot}2H_2O$, 24 mg of $NiCl_2{\cdot}6H_2O$, 36 mg of $Na_2MoO_4{\cdot}2H_2O$, 15 mg of Na_2WO_4, 15 mg of $Na_2SeO_3{\cdot}5H_2O$, and 10 ml of 25% HCl (Widdel et al., 1983). Resazurin (2.0 g/l) was added as a reducing indicator. The medium pH was adjusted to 7.2 ± 0.2 with dilute HCl. Cysteine at 0.5 mg ml^{-1} HCl was added into medium as the sole reductant. The commonly used $Na_2S{\cdot}9H_2O$ was not preferred as a reductant to avoid a reaction with metals in the medium. It was observed that there is no significant effect on methane production without addition of $Na_2S{\cdot}9H_2O$ (data not shown).

TRACE ELEMENT-AMENDED ENRICHMENT CULTURES

In the first phase of this study, the effects of varying concentrations of trace elements on methane production were evaluated. Initially, 10% (v/v) actively growing log-phase enrichment was incubated in 160 ml of anoxic serum vials capped with butyl rubber stoppers with fresh medium described in the Section "Enrichments." Yeast extract was not added, since it is a source of trace elements and its element content is unknown. The headspace of serum bottles was aseptically flushed with H_2/CO_2 [80/20 (v/v)]. No external electron acceptors were supplied and CO_2 was the sole electron acceptor. Increasing concentrations of trace element mix solutions (1×-TES, 2.5×-TES, and 5×-TES) were added into enrichment cultures prepared in triplicates. 1×-TES is the concentration of the SL-10 trace element solution for a mixture of eight trace elements (iron, nickel, cobalt, molybdenum, zinc, manganese, boron, and copper), which is given in detail above. Enrichments and abiotic controls were incubated for 6 weeks under strict anaerobic condition in the dark at 37 ± 1°C without agitation. Glassware utilized in the study was pre-cleaned and treated with 10% nitric acid over night and baked at 550°C for 6 h.

For the second and third phases of this study, 10% (v/v) actively growing log-phase enrichment was incubated into fresh medium free of trace elements three times over a period of four and a half months. The last transfer culture was used as seed for 1×-TES amended and unamended enrichment cultures. Medium preparation and incubation conditions were the same as in phase one. Enrichments were set up in 10 replicates and incubated over 5 weeks. The medium pH was adjusted to 7.2 ± 0.2 with dilute HCl, and checked every week. Every week two duplicate incubations were sacrificed for RNA isolation and total cell counting.

TOTAL CELL ENUMERATION WITH DAPI STAINING

Total cell numbers were estimated with 4′, 6-diamidino-2-phenylindole (DAPI) nucleic acid staining (Becerra et al., 2009) in 1×-TES amended and unamended enrichment cultures and in CBM produced water samples. A sequence of 40 randomly chosen microscopic fields across each slide was examined under 1000× oil-immersion magnification using an epifluorescence microscope (Nikon Eclipse E400) equipped with a Hamamatsu digital camera to determine the average number of cells in the samples.

DETECTION OF METHANE PRODUCTION

Methane accumulation in the headspace was monitored and quantified for all microcosms and enrichments by gas chromatography using a GC-17A (Shimadzu, Co., Kyoto) equipped with an Equity-1 column (30 m × 0.53 mm ID, 3.0 μm, Supelco, St. Louis, MO, USA) and a flame ionization detector with helium as the carrier gas. The injector and column temperatures were adjusted to 100°C and the detector was held at 125°C. Certificated standard CH_4 (Fisher Scientific, Pittsburgh, PA, USA) was used for calibration. Methane concentration in the headspace was calculated by comparing peak areas of sample and standard.

EXTRACTION OF TOTAL RNA AND mRNA

Total RNA was extracted from 1×-TES amended and unamended enrichment cultures at 2, 7, 14, 21, and 28 days using the method described by Chin et al. (2008) with some modifications. The complete procedure was performed at 2°C or on ice. A volume of 2.0 ml of enrichment culture was anaerobically removed from a serum bottle and transferred to 2.0 ml RNase-free screw-cap tubes. Tubes were centrifuged for 5 min and supernatant was decanted. Approximately 0.6 g of 0.1 mm diameter glass beads, 0.6 ml TPM buffer (50 mM Tris–HCl, 1.7% polyvinylpyrrolidon, 20 mM $MgCl_2{\cdot}6H_2O$, in DEPC-treated water) and 2 μl yeast tRNA (mRNA carrier) were added to the cell pellet. The tubes were shaken upside down for 10 min, followed by ballistic cell destruction for 1 min at 4200 rpm using a mini-bead beater (BioSpec Products; Bartlesville, OK, USA). Cell debris and glass beads were concentrated by centrifugation for 3 min. The supernatant was transferred to a tube containing 1 μl RNase inhibitor (Ambion, Austin, TX, USA). The pellet was resuspended in 0.6 ml phenol-saturated lysis buffer [50 mM Tris/HCl (pH 7.0), 50 mM EDTA, 1% (w/v) sodium dodecyl sulfate (Ambion), and 6% water-saturated phenol. After an additional round of bead beating at the same conditions, the tubes were exposed to centrifugation for 5 min and the supernatant was pooled with the supernatant of the first

round of bead-beating. A volume of 0.6 ml phenol (pH 4.3) was added to the pooled supernatant, the tubes were vortexed for 40 s and exposed to centrifugation for 5 min. The supernatant was extracted with phenol–chloroform–isoamylalcohol [pH 7.8–8.2; 25:24:1 (v/v)] and chloroform–isoamylalcohol [24:1 (v/v)]. The aqueous phase was transferred to a fresh 2 ml tube containing 1/10th volume of 3 M NaAc (pH 5.2) and 2 μl of linear acrylamide (5 mg/ml; Ambion), and filled with 100% cold ethanol up to a final volume of 2 ml. The tubes were invert mixed and contents concentrated by centrifugation for 30 min. The pellets were washed with 0.5 ml 70% cold ethanol, invert mixed, and again centrifuged for 10 min. The pellet was dried in a desiccator for 5 min and resuspended in water. RNA was treated with RNase free-DNase (Ambion) to remove DNA contamination. DNase treated RNA was further purified by precipitating with 1/10th volume 3 M NaAc (pH 5.2), and 4 volumes of cold ethanol followed by centrifugation for 20 min. The pellet was washed twice with 0.5 ml 70% cold ethanol, dried, and resuspended in water. Enrichment of mRNA was performed with DNase treated and purified RNA using the MICROB Express purification system (Ambion). DNA contamination was checked with agarose gel electrophoresis following reverse transcription-polymerase chain reaction (RT-PCR) by performing control experiments in which no reverse transcriptase was added to the isolated RNA before the PCR step. RNA concentration was determined by absorption at 260 nm with a Biophotometer (Eppendorf, Hamburg, Germany). Purified RNA was stored at -80˚C.

REVERSE TRANSCRIPTION-POLYMERASE CHAIN REACTION

The cDNA of mRNA for the gene *mcrA* was generated with the primer mcrA-rev, (Steinberg and Regan, 2008) with 0.5 μg mRNA as the template. Multiscribe Reverse Transcriptase™ (250 U; Applied Biosystems) was used according to the manufacturer's instructions. The conditions used in the cDNA synthesis program were as follows: initial incubation at 25˚C for 10 min, incubation at 37˚C for 120 min, enzyme inactivation at 85˚C for 5 s, followed by rapid cooling to 4˚C. cDNA samples were stored at −20˚C until use. Methyl-coenzyme M reductase (MCR) is the essential and unique enzyme for methane production. It catalyzes the final step of methanogenesis, which reduces a methyl group linked to coenzyme M to methane (Ellerman et al., 1988). Because this enzyme is found in all known methanogens and is absent from non-methanogenic Archaea and Bacteria (Chistoserdova et al., 1998; Thauer, 1998; Bapteste et al., 2005), the *mcrA* gene is used as a specific functional marker to detect methanogens (Weil et al., 1988; Hallam et al., 2003). Previous studies have suggested that the phylogeny of *mcrA* follows the 16S rRNA phylogeny within various environments, and thus has been used as an alternative phylogenetic tool to detect and identify methanogens (Springer et al., 1995; Lueders et al., 2001; Luton et al., 2002; Friedrich, 2005). The MCR operons are found in two forms; MCRI (*mcrBDCGA*) which encodes *mcrA* and MCRII (*mrtBDGA* or *mrtBGA*) which encodes *mrtA*. Although, MCRI exists in all methanogens, MCRII is only found in members of the orders Methanobacteriales and Methanococcales (Lehmacher and Klenk, 1994; Bult et al., 1996; Reeve et al., 1997).

CLONING, SEQUENCING, AND PHYLOGENETIC ANALYSIS

Extracted genomic DNA was used as template for PCR amplification of 16S rRNA genes using archaea-specific primers ARC21F (DeLong, 1992) and 1492R (Lane, 1991). PCR cycles were as follows: 1 cycle at 94˚C for 5 min, 30 cycles at 94˚C for 1 min, 58˚C for 1.5 min and 72˚C for 2 min, and a final extension step at 72˚C for 10 min. In addition, three mRNAs clone libraries were generated from *mcrA*-specific RT-PCR amplicons (491 bp length amplified with primers mlas and mcrA-rev; Steinberg and Regan, 2008) obtained from trace element amended (TES-T1) and unamended enrichment cultures (NO-TES) after 7 days of incubation, and from startup enrichment cultures designated as time zero (T0). The purified RT-PCR amplicons from enrichment cultures and Archaeal 16S rRNA genes from produced water were ligated into the pGEM®-T Easy Vector (Promega) and transformed into *Escherichia coli* JM109. Positive clones were verified by PCR amplification with vector specific primers M13F and M13R according to the protocol supplied by manufacturer. Clones were randomly selected, and plasmid inserts were sequenced with the M13F primer by Sanger sequencing. Sequences were checked manually and edited for ambiguous bases using the software Chromas sequence viewer (Technelysium, Tewantin, Australia), and multiple sequence alignments were created using ClustalX v.1.83 (Thompson et al., 1997). Archaeal 16S rRNA gene sequences were assigned to an Operational Taxonomic Unit (OTU) using the software package DOTUR based on $\geq$97% similarity (Schloss and Handelsman, 2005). Phylogenetic and taxonomic analyses were conducted using a representative sequence from each OTU. Phylogenetic trees based on the *mcrA* amino acid sequence were constructed using the Neighbor-Joining method (Saitou and Nei, 1987) with the "percentage of acceptance mutations distance correction model (PAM)" provided by the software package MEGA4.1 (Kumar et al., 2008).

To estimate the confidence of tree topology, bootstrap resampling analysis for 1000 replicates was performed with the Neighbor-Joining method. After sequences were assigned to OTUs, the frequency data at species level were used to construct rarefaction curves and to calculate diversity and richness indices using DOTUR. Estimates of phylotype richness were calculated according to the Chao1 estimator that takes into account the number of different OTUs in a sample, and the abundance-based coverage estimate (ACE). Species richness and evenness were calculated using the Shannon diversity index (H_{SHANNON}) and the Simpson's index (H_{SIMPSON}), which takes into account the level of phylotype dominance.

REAL-TIME PCR QUANTIFICATION

Dilution series of purified *mcrA* RT-PCR amplicons were used as calibration standards for the real-time PCR quantification. The purified RT-PCR products were quantified and prepared for serial dilution as described previously (Chin et al., 2004b). The detection limits were determined from two independent measurements with dilution series of purified RT-PCR products (standards) in real-time PCR (108–101 target molecules per reaction). The copy numbers of unknown samples were calculated after real-time amplification from the linear regression of the standard curve. The cDNA generated with *mcrA* gene-specific

primers was quantified with real-time quantitative PCR using SYBR Green. The levels of *mcrA* transcripts (per μg mRNA) were determined in enrichment cultures for which methane production was measured in parallel. All reactions were carried out in 20 μl reaction volume containing 0.02 units of iProof High Fidelity polymerase (BioRad), buffer, 2.5 pmol of each dNTP, bovine serum albumin, and 20 pmol of each primer of the pair mlas-mcrArev (Steinberg and Regan, 2008). The temperature profile was composed of an initial incubation at 98°C for 1 min, followed by 35 cycles of 98°C for 10 s, 58°C annealing for 10 s, 65°C extension for 32 s, and a final extension at 65°C for 6 min. Dissociation curve analysis to detect the presence of primer dimers and non-specific amplification peaks was performed after the final extension. The size of the PCR products was checked with agarose gel electrophoresis, and the specificity of PCR products was verified by sequence analysis of the clone library. Quantitative analysis of the cDNA was carried out with the 7500 Real-Time PCR System (Applied Biosystem, Foster City, CA, USA) using 7500 Real-Time PCR System Sequence Detection software (v 1.3.1). The precision as well as the reproducibility of quantification were carefully optimized, and PCR products were checked for their correct lengths as described previously (Chin et al., 2004b).

NUCLEOTIDE SEQUENCE ACCESSION NUMBERS

The sequences for *mcrA* mRNA clones and for archaeal 16S rRNA gene clones generated in this study were deposited in the GenBank database under the following accession numbers: JQ917180 to JQ917194 for all mcrA sequences, and JQ917195 to JQ917203 for archaeal 16S rRNA sequences.

STATISTICAL ANALYSES

Statistical comparisons were performed using one-way ANOVA followed by the all pairwise multiple comparison procedures (Holm-Sidak method) on the probability level $P < 0.001$. Data analyses were performed using the software package SYSTAT 11 (Systat Software, 2004).

RESULTS

CBM PRODUCED WATER CHARACTERIZATION

In situ conditions at well depth indicated a pH value of 6.7 and a temperature of 29.6°C. Physicochemical analysis of the CBM produced water included: dissolved inorganic carbon (DIC) 13.161 mm/kg; F, 0.68 mM; Cl, 0.31 mM; SO_4, 0.07 mM; Na, 6.24 mM; Mg, 0.12 mM; K, 0.13 mM; Ca, 0.26 mM; Ba, 0.365 mM; total cations at 7.11 mM, and total anions at 6.65 mM. Trace element concentrations (μg/l) were B, 32.05; Al, 0.100; V, 0.49; Mn, 6.84; Fe, 14.92; Co, 0.03; Ni, 0.76; Cu, 0.48; Zn, 21.61; As, 0.07; Mo, 0.62; Ag, 0.07; Ba, 329.100; Tl, 0.01; Pb, 0.02; and U, 0.01. The concentrations of trace elements in 1×-TES, which was the concentration of trace elements in the SL-10 solution, was far greater than *in situ* concentrations except for boron, which was at a lower concentration in trace element enrichment cultures (21.3 μg/l). The calculated concentrations of elements in 1×-TES enrichment cultures were 785 times more in Fe, 132 times more in Ni, four orders magnitude more in Co, 476 times more Mo, 73 times more Mn, 28 times more Zn and 31 times more Cu than *in situ* concentrations.

METHANOGENIC POTENTIAL AND PHYLOGENETIC ANALYSIS OF METHANOGENS IN CBM PRODUCED WATER

Total cell number in the CBM produced water sample was determined at 3.2×10^5 by DAPI staining, which is within midrange of cell numbers observed in other deep aquifers (Pedersen, 1993). Significant amounts of methane were produced in microcosms inoculated with pie-size coals (9.2 ± 0.6 μmol/ml) after 6 months of incubation. This indicates that the methanogenic community had the ability to degrade coal into methane.

Since coal is potentially the source of trace elements (Jackson and Reddy, 2007), we did not use coal as a carbon source to test the effects of trace elements on methanogenesis. For controlled and reproducible conditions, the CBM produced water sample was supplemented with a methanogen specific medium and amended with electron acceptors such as acetate, methanol, or CO_2. After 5 months of incubation, methane production was detected only in microcosms with H_2/CO_2 (80/20 v/v) at the cumulative amount of 7.7 μmol/ml, and subsequent enrichments were continued based on this set of cultures.

An archaeal 16S RNA gene clone library was constructed to identify the methanogens in the CBM produced water sample. Nine OTUs were identified within the 67 clonal sequences based on a "cut-off" value of ≥97% nucleotide sequence identity. The archaeal community was dominated by the genus *Methanobacterium* sp. (60%) with 40% identified as uncultured archaea (**Table 1**). A total of 25 sequences were affiliated with *Methanobacterium* sp. GH (96–99% similarity) which was previously isolated from sediments of the Gahai Lake in China (Zhu et al., 2011). Fifteen sequences were affiliated with *Methanobacterium* sp. SA-12 (97%) found in a subsurface gold mine (unpublished data, GenBank accession number AY695843.1) and to an uncultured clone (97%) from a minerotrophic fen (Cadillo-Quiroz et al., 2008). Five clones were affiliated with an uncultured archaeon clone (93%) from a gas hydrate production research well, Canada (unpublished data); four clones were affiliated (92–97%) with clones obtained from the deep aquifer of gold mines, South Africa (Takai et al., 2001); 10 clones were affiliated (96%) with clones from deep subsurface sediments in the Pacific (Biddle et al., 2006; Zhang et al., 2010); and eight clones were affiliated with a clone (91%) from hydrothermal sediments in Japan (Nunoura et al., 2010).

EFFECT OF INCREASING CONCENTRATIONS OF TRACE ELEMENTS ON METHANE PRODUCTION

The effect of increasing concentrations of trace elements (1×-TES, 2.5×-TES, and 5×-TES) on methane production in CBM produced water enrichments was tested weekly for a total duration of 42 days. The differences in the average values of cumulative methane production among the enrichment cultures amended with 1× and 2.5× trace element concentrations were statistically significant ($P < 0.001$), when compared with unamended enrichment cultures. At the end of the incubation period, the level of methane production was significantly lower (8.52 μmol/ml) in enrichment cultures without addition of trace elements than in enrichment cultures with addition of trace elements (11.7 μmol/ml; **Figure 1A**). This suggests that methanogenic activity became diminished under trace element limitation. It was also observed that there was a significant negative effect on

Table 1 | Phylogenetic affiliations of archaeal phylotypes based on 16S rRNA gene sequences in the produced water from a CBM well in the PRB.

Sequence ID	No of Sequences	Closest cultured relative (% identity)	Maximum identity to GenBank (% identity)	Environmental source
OTU-1	22	*Methanobacterium* sp. GH, [EU333914], (99)	Uncultured archaeon clone DR9IPCA16SCT2, [AY604061], (99)	Deep dolomite aquifer, South Africa
OTU-10	3	*Methanobacterium* sp. GH, [EU333914], (96)	Uncultured archaeon clone DR9IPCA16SCT2, [AY604061], (96)	Deep dolomite aquifer, South Africa
OTU-7	15	*Methanobacterium* sp. SA-12, [AY695843], (97)	Uncultured archaeon clone MH1100_B4C [EU155989], (97)	Rich minerotrophic fen, New York State, USA
OTU-8	5		Uncultured archaeon clone:pMLA-5 [AB109882], (93)	Gas hydrate production research well, Canada
OTU-6	2		Uncultured archaeon clone MD3059N-45 [GQ927542], (92)	Deep aquifer from gold mines, South African
OTU-45	2		Uncultured archaeon SAGMA-E [AB050209], (97)	Deep aquifer from gold mines, South African
OTU-16	8		Uncultured archaeon clone MD3059S-72 [GQ927695], (96)	Deep-sea sediments from tropical western Pacific
OTU-30	2		Uncultured archaeon clone 4H3_ar33 [DQ302026], (96)	Pacific deep subsurface sediments
OTU-38	8		Uncultured archaeon clone MD3059P-24 16, [GQ927572], (91)	Hydrothermal sediments, Japan

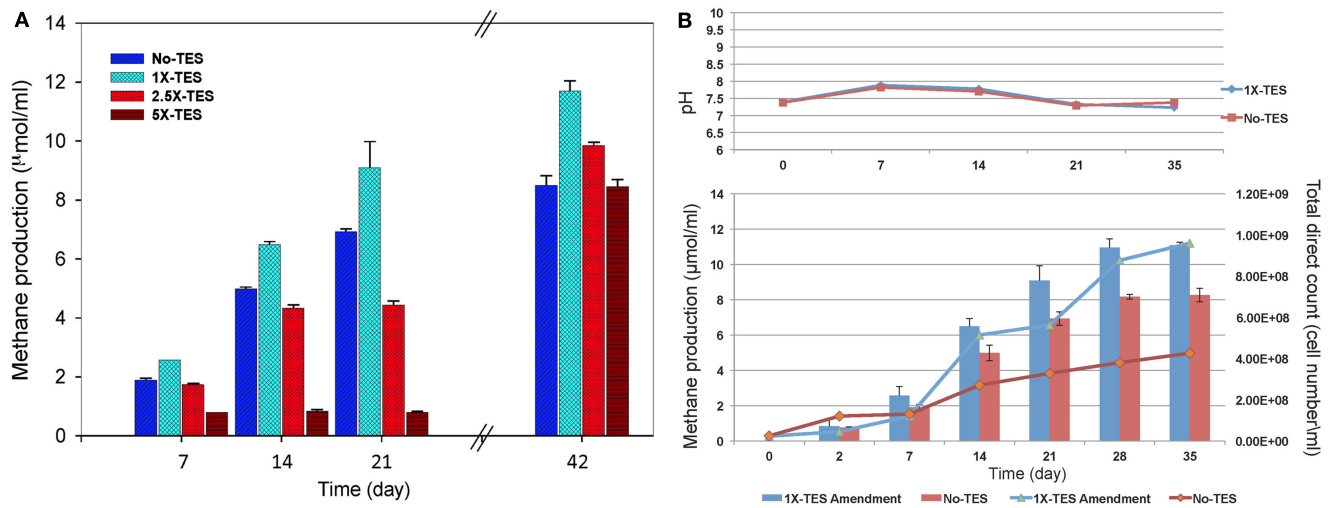

FIGURE 1 | (A) Effect of increasing concentration of trace elements on cumulative methane production over time. No-TES is the enrichment without addition of any trace elements, 1×-TES, 2.5×-TES, and 5×-TES are the enrichments amended with increasing concentrations of trace element mix solutions. 1×-TES is detailed in the Section "Materials and Methods." Error bars represent standard deviations ($n = 3$). Probability values were calculated for cumulative methane production at the end of 6 weeks. $P < 0.001$ for 1×-TES and 2.5×-TES; and $P = 0.822$ for 5×-TES. **(B)** Changes in pH value and total cell number (lines; DAPI total direct counts), and cumulative methane production (bars) over time in 1× -TES-amended and unamended cultures (No-TES) ($n = 3$).

methane production in enrichment cultures with higher concentration of trace elements (5×-TES) during 42 days of incubation ($P = 0.822$). Here we determined that the undiluted, 1×-TES concentration of trace element solution was the optimum concentration for methane production. Consequently, we used this concentration for further experiments to investigate the effect of trace element addition on *mcrA* transcript level and on the composition of methanogenic communities in the enrichment cultures.

Methane production rate during the first week in 1×-TES enrichment cultures, was the highest ($2.57\,\mu mol\,ml^{-1}\,week^{-1}$). While, methane production rate in unamended enrichment cultures reached its highest level at the end of the second week of incubation ($2.64\,\mu mol\,ml^{-1}\,week^{-1}$; **Table 2**). The cumulative methane production was significantly lower ($P < 0.001$) than 1×-TES enrichments over 6 weeks of incubation (**Figure 1A**). The methane production rate in 5×-TES enrichment cultures was low and remained stable during the first 3 weeks. However, after

6 weeks it reached the highest level (10.70 μmol ml^{-1} week^{-1}; **Table 2**), which might be the result of adaptation over time of the methanogenic community to higher amounts of trace element concentrations.

Direct cell counts were obtained over 35 days to document cell growth in 1×-TES amended and unamended cultures (**Figure 1B**). Amended and unamended studies were started with the addition of 2.3×10^7 and 2.5×10^7 cells/ml, respectively. At the end of the incubation time, cell densities had increased to 9.61×10^8 and to 4.26×10^8, respectively. Total cell numbers were ∼125% higher in trace element amended than in unamended enrichment cultures after 5 weeks of incubation. Since these are mixed cultures, growth trends were not well resolved for lag, log, and stationary phases (Meyer-Dombard et al., 2012). Calculated generation times were ∼70 h during the first 168 h (day 7) for amended and unamended cultures. After 7–14 days, the generation times for amended cultures were ∼80 h and two times longer (∼159 h) for unamended cultures. Total cell numbers increased steadily during incubation time for unamended cultures with increasing doubling times ∼622, ∼791, and ∼1019 h for 14–21, 21–28, and 28–35 days, respectively. However, in amended cultures cell numbers fluctuated. Generation times were increased to ∼1281 h between 14 and 21 days, dropped back to ∼264 h between 21 and 28 days and were calculated as ∼1273 h between 28 and 35 days. Changes in pH values were observed in all incubations, but there was no significant difference between enrichment cultures during the entire incubation time (**Figure 1B**).

Table 2 | Comparison of methane production rates between enrichments amended with increasing concentrations of trace elements (1×-TES, 2.5×-TES, 5×-TES) and enrichments without addition of trace elements over 6 weeks.

Time period week (day)	Methane production rate (μmol ml^{-1} week^{-1})			
	No-TES	1×-TES	2.5×-TES	5×-TES
0–1 (7)	1.89 ± 0.07	2.57 ± 0.12	1.73 ± 0.04	0.80 ± 0.05
1–2 (14)	2.64 ± 0.05	2.53 ± 0.10	2.50 ± 0.11	1.04 ± 0.01
2–3 (21)	1.39 ± 0.09	1.40 ± 0.89	1.02 ± 0.13	0.95 ± 0.04
3–6 (42)	1.23 ± 0.32	1.29 ± 0.33	2.22 ± 0.11	10.70 ± 0.24

Enrichment cultures were grown under a headspace of H_2/CO_2 (80/20 v/v).

QUANTIFYING *mcr*A TRANSCRIPTS

The levels of *mcrA* transcripts in 1×-TES amended and unamended enrichments were quantified in weekly time intervals using quantitative RT-PCR over 35 days of incubation. After 1 week, a quicker and stronger response was observed for *mcrA* transcript levels in amended enrichments compared to unamended enrichments. At this time point, the addition of trace elements enhanced *mcrA* transcript levels to its maximum (2.18×10^7 copy numbers/μg mRNA), while the level of *mcrA* transcripts remained much lower in enrichment cultures without addition of trace elements (7.03×10^6 copy numbers/μg mRNA). Unamended cultures reached their maximum levels at 14 days of incubation (1.3×10^7), but it was still lower than amended enrichment cultures after 7 days of incubation (**Figure 2**). After 35 days of incubation, *mcrA* transcript numbers were relatively low, with 3.05×10^4 and 1.05×10^4 for amended and unamended enrichment cultures, respectively.

The increased levels of *mcrA* transcripts in response to trace element addition correlated positively with elevated rates of methane production ($R^2 = 0.95$), while a very weak correlation was determined in unamended cultures ($R^2 = 0.69$; **Figure 3**). Additionally, the rate of methane production in unamended enrichments was lower than in amended enrichments, which correlates with *mcrA* transcript levels over the first 7 days of incubation (**Table 2**; **Figure 2**).

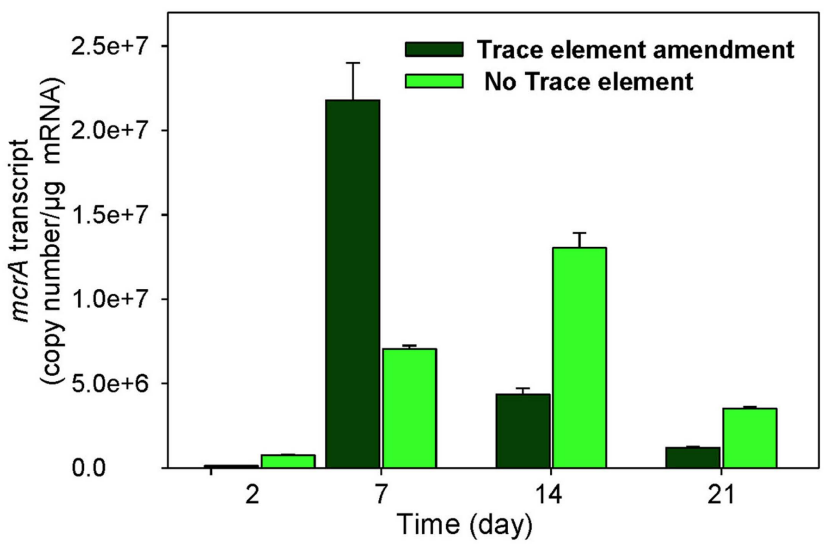

FIGURE 2 | Levels of *mcrA* transcripts in enrichment cultures with (trace element amendment) and without (no trace element) addition of trace elements over time.

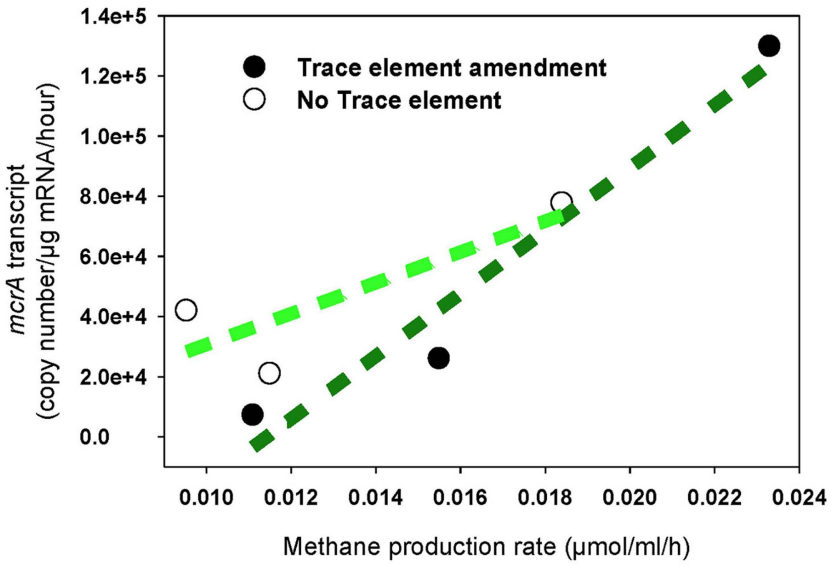

FIGURE 3 | Methane production rate correlated with *mcrA* transcription in enrichment cultures with addition of trace elements (regression coefficient $R^2 = 0.95$) and without addition of trace elements (regression coefficient $R^2 = 0.69$). Black circle: Enrichment cultures amended with trace element mix solution, white circle: enrichment cultures without addition of any trace elements.

Table 3 | Sequence identities of dominant members, clone library sizes, and richness and diversity indices of *mcrA* sequences based on 97% OTU clusters.

Samples	Sequence identity (%)				Richness estimators		Diversity estimators		% Coverage
	M. subterraneum	*M. formicicum*	Clones	S_{Obs}	S_{CHAO1}	S_{ACE}	$H_{SHANNON}$	$H_{SIMPSON}$	
T0	96	91	26	3	3.00	4.08	0.82	0.44	100
T1:TES	96–98	88–93	27	6	7.00	9.75	0.97	0.54	86
T1:NoTES	95–98	91–93	26	6	6.00	6.34	1.54	0.23	100

OUT, operational taxonomic unit; T0, startup enrichment cultures at time-zero; T1, TES, trace element amended enrichment cultures after 7 days of incubation; T1, No; TES, not trace element amended enrichment cultures after 7 days of incubation; S_{Obs}, observed richness; % Coverage, observed richness/chao1 estimate × 100.

TRACE ELEMENT EFFECT ON METHANOGENIC COMMUNITY STRUCTURE AND DIVERSITY

Enrichments incubated for 1 week were chosen to construct clone libraries based on their highest methane production rates (2.57 µmol ml^{-1} week^{-1}) and paralleled by highest *mcrA* transcript levels (2.18×10^7 copy numbers/µg mRNA) as a proxy of highest methanogenic activity over 6 weeks of incubation (**Table 2**; **Figure 2**). Three clone libraries of RT-PCR amplicons of *mcrA* mRNA were constructed to compare the metabolically active methanogenic taxa in 1×-TES amended (designated T1:TES) and unamended (T1:No TES) enrichment cultures after 1 week of incubation, and in startup enrichment cultures (designated T0). Eighty-one unique sequences were clustered into individual phylotypes (OTUs) to calculate rarefaction and nonparametric estimators (**Table 3**). *Methanobacterium formicicum*- and *Methanobacterium subterraneum*-like sequences were detected in startup, amended, and unamended enrichment cultures.

Both richness and diversity of the methanogenic community changed during 7 days of incubation. Enrichment cultures with addition of trace elements had a slightly higher predicted methanogen richness and diversity than enrichment cultures without the addition of trace elements (**Table 3**).

The effects of trace elements on the relative abundance and distribution of methanogens were monitored. Addition of trace elements contributed specifically to the enhancement of *M. subterraneum*-like sequences over *M. formicicum*-like sequences (**Figure 4**). Amended and unamended enrichments were dominated by clones that grouped closely with the *mcrA* genes of *M. subterraneum*-like sequences (81.5% in amended enrichments and 46.2% in unamended enrichments) and *M. formicicum*-like sequences (18.5% in amended enrichments and 53.8% in unamended enrichments). The methanogenic community composition in the starting enrichment culture (T0) appeared to be unchanged during 1 week of incubation, and *mcrA* genes from *M. subterraneum*-like sequences comprised 46.2% and *M. formicicum*-like sequences 53.8% of the clone library, representing similar ratios between both taxa in enrichment cultures without addition of trace elements (**Figure 4**).

Rarefaction analysis based on 97% sequence similarity showed adequate sampling for the startup enrichment, whereas

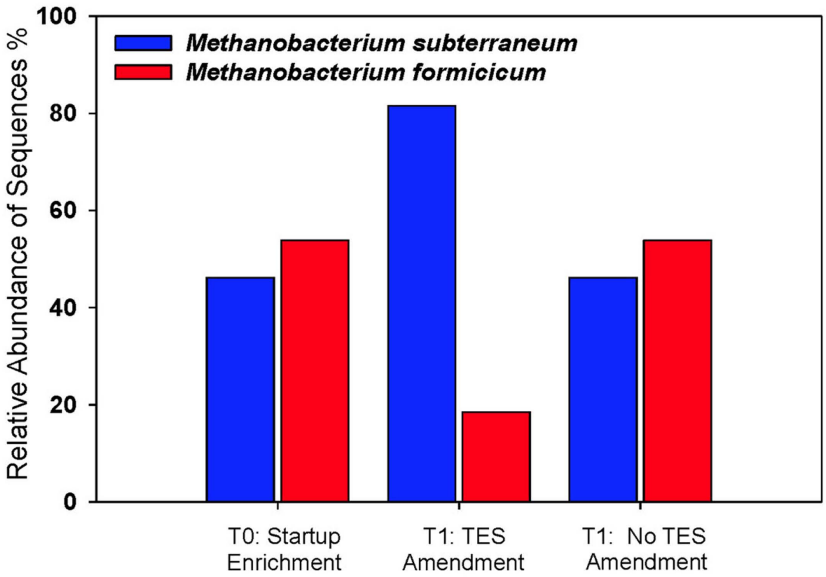

FIGURE 4 | Methanogenic community structure in trace element-amended and unamended enrichments. Startup enrichment culture (T0), trace element amended (T1:TES), and unamended (T1:No TES) enrichments. Blue bars: *Methanobacterium subterraneum*-like sequences; red bars: *Methanobacterium formicicum*-like sequences.

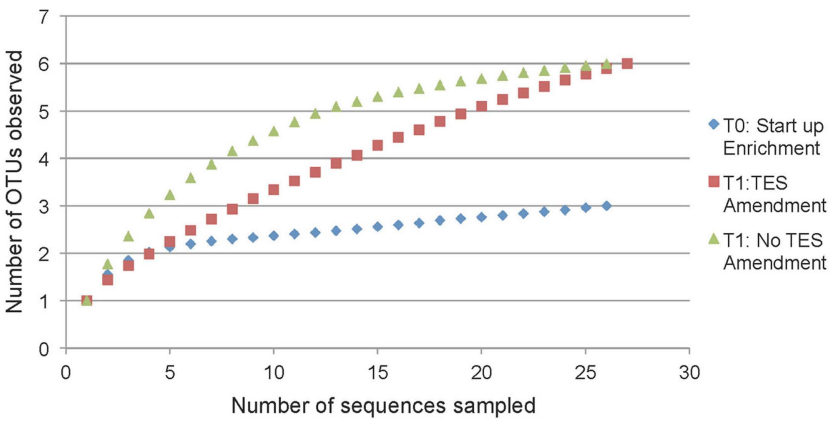

FIGURE 5 | Rarefaction curves indicating *mcrA* richness within clone libraries derived from the startup enrichment culture (T0), trace element amended (T1:TES), and trace element unamended (T1:No TES) enrichment cultures. Sequences were grouped into phylotypes based on 97% sequence similarity.

enrichments with and without addition of trace elements did not reach asymptotes (**Figure 5**). Non-parametric statistical analyses (**Table 3**) showed that the observed richness covered between 100, 86, and 100% of the estimated total methanogenic richness in startup enrichment, trace element amended and unamended enrichment cultures, respectively.

PHYLOGENETIC ANALYSES OF METHANOGENS

A phylogenetic tree based on amino acid sequences of the genes *mcrA* was constructed using a selection of sequences from cultured methanogens and environmental clones from the public database GenBank. Several clones from T1:TES, T1:No TES, and T0 clone libraries were found to be closely related (95–99%) with two sequences identified in subsurface shale environments (GenBank accession numbers EF117654, EF117630). Clone TES-3 was the most dominant clone in amended enrichments, representing 20 out of 27 clones. It exhibited 97% sequence identity with *M. subterraneum* which is the nearest isolated relative. Clone No-15 represented 11 of 26 clones and clustered most closely with *M. subterraneum* with 98% similarity. Only one clone from T1:TES and three clones from T1:No TES were closely related to unpublished clone rlm_673a (97%) which was identified in an anaerobic waste water digester (GenBank accession number JF460370.1). As many as 14 and 12 out of 26 clones in T0 clone libraries have 91 and

95–97% identities to the next closest pure culture, *M. formicicum and M. subterraneum,* respectively (**Figure 6**).

DISCUSSION

This study has enhanced our understanding of trace element effects on methane production, and on the activity and diversity of methanogens in enrichments of water produced from a CBM well. In the present study, we showed that addition of an optimized concentration of trace elements elevated methane production over 37% and increased total cell number by 125%. By comparing enrichment cultures with and without trace element amendments (Fe, Ni, Co, Mo, Co, Zn, B, Mn), we have found not only a correlation between increasing *mcrA* levels and elevated methane production, but have also demonstrated a shift in the metabolically active methanogenic community from a *M. formicicum*-like group to a *M. subterraneum*-like group.

TRACE ELEMENT AS A LIMITING FACTOR IN SUBSURFACE COAL BED METHANE WELLS

Microbial methane production in deep coal bed basins indicates the ability to sustain microbial life in these limiting environmental conditions (dark, anoxic, reduced, limited substrate replenishment, etc.). The associated physical, chemical, and biological restrictions may influence activity, function, and diversity of the microbial species in the anaerobic biodegradation of organic matter in coal. It is suggested that distribution and activity of the microbial communities are supported by water–coal interaction in subsurface environments (Green et al., 2008). The organic fraction (e.g., carbon, hydrogen, nitrogen, oxygen, and sulfur) and the inorganic constituents of coal (e.g., trace elements) support growth in this subsurface biosphere, and the geochemical potential determines the energy profile for microbial growth, maintenance, and survival under dormancy. Coal–water interactions are expected to provide trace elements for microorganisms (Finkelman, 1995). Yet, our water chemical analysis from the coal bed well in the PRB demonstrated that the amount of trace elements concentrations at this habitat was far lower than the concentrations required for optimum methanogenesis (**Figure 1A**).

Biodegradation of coal organic deposits into methane is limited to anoxic and reduced conditions, and by the interaction of at least four metabolically diverse groups of microorganisms, hydrolytic, fermentative, acetogenic, and methanogens (Wawrik et al., 2012). Although the rate-limiting step for coal biodegradation is the initial solubilization of a macromolecular, polycyclic, lignin-derived aromatic network into utilizable substrates by microorganisms (Fakoussa and Hofrichter, 1999), we argued that methanogenesis would be another limiting step in coal biodegradation to methane, if the amount of trace elements is limited. Methanogens are the

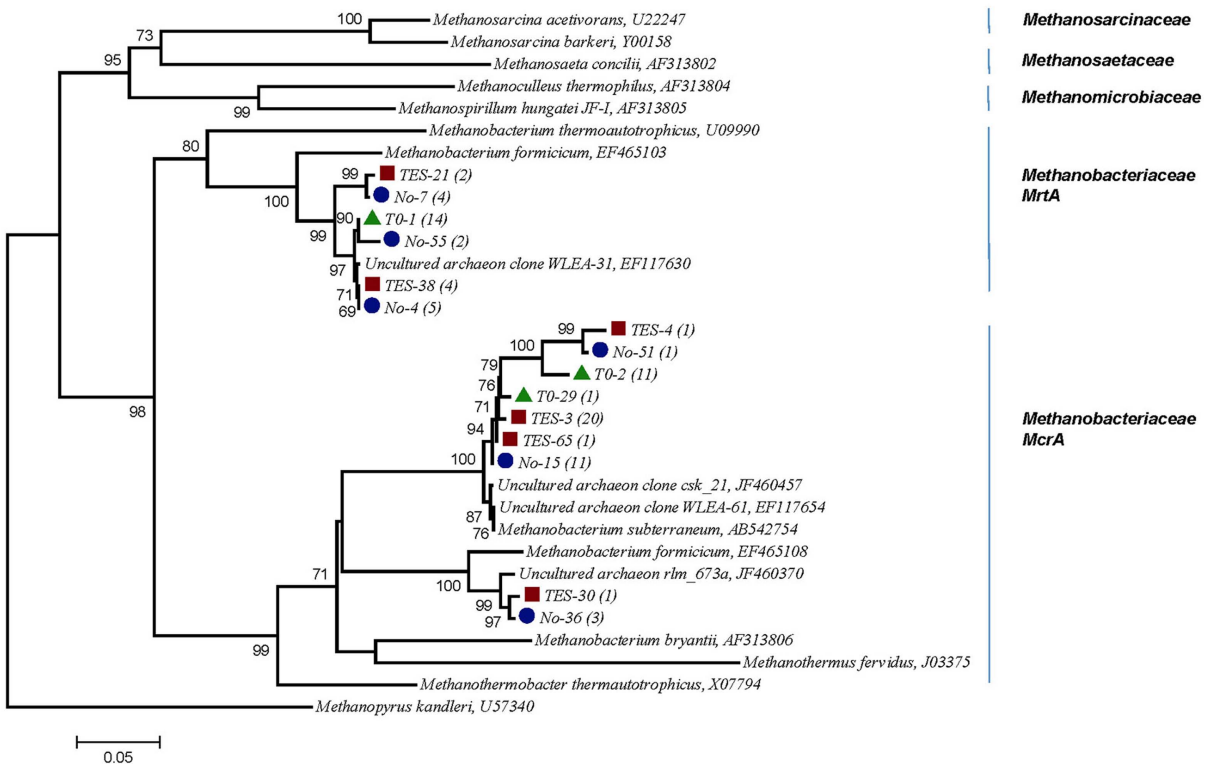

FIGURE 6 | Phylogenetic tree of 15 selected *mcrA* mRNA sequences retrieved from methanogenic enrichment cultures in this study and their relationship to reference sequences of cultivated methanogens and to other environmental clone sequences. Numbers in parentheses reflect the number of sequences in each OTU. Red square, trace element amended enrichment culture (TES); blue circle, non-amended enrichment culture (No); green triangle, startup enrichment culture (T0). Evolutionary history was inferred using the Neighbor-Joining method. Bootstrap values are shown for nodes in an analysis of 1000 replicates. Evolutionary distances were computed based on amino acid sequences, the scale bar represents 0.05 substitutions per amino acid position. *Methanopyrus kandleri*, the deepest branching methanogen, was chosen as out-group (Burggraf et al., 1991).

terminal oxidizers in anaerobic biodegradation of organic matter and they are vital for the resultant production of methane (Strąpoć et al., 2008). This study provides the novel consideration that the availability of optimized trace element concentrations might have an influence on methanogenic community structures and on methanogenesis.

Trace elements in coal bed basins may be concentrated in three different ways: (1) concentration during the life of plants prior to coalification; (2) concentration during the decay of organic substances; and (3) concentration by aqueous solution after burial of plant materials (Goldschmidt, 1935). Trace element concentration should be unique in each coal bed deposit, since the composition of plant material and the water source for each coal bed basin can vary with the geological formation, surrounding geochemical conditions, and adjacent overlying mudstones, siltstones, and sandstones. This geological material might be the source of trace elements, which leach with the groundwater into coal bed basins. Furthermore, the source of CBM produced waters might be water accumulated during coal formations or derived from meteoric waters (Flores et al., 2008). Since coal has trace elements embedded within its structure at varying concentrations, we avoided to add coal to incubations to prevent uncontrolled trace element effects.

METHANE PRODUCTION IN DIFFERENT CONCENTRATIONS OF ADDED TRACE ELEMENTS

Optimal concentrations of trace elements exist for cellular activity, and concentrations beyond this optimum can have a toxic effect on cells (Swaine and Goodarzi, 1995). The results of this study demonstrated that an optimized concentration of trace elements added to the enrichment cultures from coal bed produced water is beneficial for methanogenic growth and activity. Some recent studies suggested that the addition of high amounts of trace elements leads to a decrease in methanogenic activity in environmental applications (Chakraborty et al., 2010; Pobeheim et al., 2010). Our results indicate that the lack of added trace elements (No-TES) to enrichment cultures limited methane production in a way similar to adding high concentrations of trace elements (2.5×-TES, and 5×-TES; **Figure 1A**).

EFFECT OF METHANOGENIC COMMUNITY SHIFT ON METHANOGENIC ACTIVITY

In addition, the results from this study demonstrated that addition of trace elements to production water enrichments influenced methanogenic community structure (**Table 3**). This suggests that trace elements in coal bed basins may be an important factor influencing the methanogenic community structure in coal bed basins *in situ*. It also indicates that *M. subterraneum*-like group has a growth advantage over *M. formicicum*-like group in the applied concentration of trace elements after 7 days of incubation (**Figure 4**).

Trace elements, utilized by microorganisms, provide proteins with unique coordination, catalytic, and electron transfer properties. Shi et al. (2005) reported that almost one fourth of structurally characterized proteins required a coordinated metal atom. Cobalt (Co), nickel (Ni), iron (Fe), zinc (Zn), molybdenum (Mo), and/or tungsten (W) are known to be crucial for the activity of enzymes in methanogens (Takashima et al., 1990). The concentration and type of trace elements required for metabolism and growth may vary among different species of microorganisms (Basiliko and Yavitt, 2001). Burgess et al. (1999) reported that trace metals influence microbial waste degradation and species diversity within sewage sludge. Gough and Stahl (2010) have shown that individual microbial populations are selected by exposition to varying levels of metals in different regions of an anoxic freshwater lake. Chin et al. (2004) reported that structural changes in the methanogenic community lead to functional changes in methane production in rice fields.

The active microbial community can be represented by RNA rather than DNA analysis (Lloyd et al., 2010), and previous studies suggested a correlation between metabolic activity and the transcript level of key genes (Fleming et al., 1993; Nazaret et al., 1994; Chin et al., 2008). In fact, transcripts for *mcrA* can be employed to demonstrate that methanogens are metabolically active in the environment (Juottonen et al., 2008; Yuan et al., 2011). The results from this study suggest that addition of trace elements caused the methanogenic community shift in composition, and a range of *mcrA* transcript levels could be directly associated with a rate of methane production and thus with the activity of methanogens (**Figure 3**).

In this study, *mcrA* genes of *M. formicicum* and *M. subterraneum*, and the gene *mrtA* of *M. formicicum* were identified from both trace elements amended and unamended enrichment cultures (**Figure 6**). Since there is a high degree of DNA sequence conservation between *mcrA* and *mrtA* sequences (Luton et al., 2002), primers designed for detection of *mcrA* sequences also detect *mrtA* sequences. Since the gene *mrtA* has arisen by lateral transfer from the Methanococcales rather than gene duplication (Reeve et al., 1997), they form a distinct cluster on the phylogenetic tree closer to Methanococcales than Methanobacteriales *mcrA* sequences (Luton et al., 2002).

METHANOBACTERIUM SSP. IN SUBSURFACE COAL BEDS IN THE PRB

Molecular analyses and cultivation studies demonstrated that methanogens are one of the most abundant groups in subsurface environments such as petroleum reservoirs, faults, and marine sediments (Orphan et al., 2000; Shlimon et al., 2004; Moser et al., 2005). So far, very few methanogenic species were isolated from these environments (Kotelnikova et al., 1998; Lai and Wu, 2011). In this study, both results, the phylogenetic analysis of archaea and the methane production in microcosms with H_2/CO_2, supported that methane production dominantly occurs via the hydrogenotrophic pathway in the sampled coal bed well. Our result was supported Klein et al. (2008) who found *Methanobacterium* sp. in CBM produced water and also associated with coal samples from PRB, Wyoming. Furthermore, many other studies also reported findings of Methanobacteriales in a variety of deep subsurface coal basins such as the Jhari Gippsland basin, Australia (Midgley et al., 2010), Alberta coal beds of Canada (Penner et al., 2010), and coal fields located at Parbatpur in India (Singh et al., 2012). After ∼2.5 years of routine transfers of CBM produced water into methanogenic media, the enrichments were highly dominated by two species of *Methanobacterium* sp., which are *M. subterraneum and M. formicicum.* It is important to note that enrichment

cultures successfully represented the majority of methanogens in the CBM produced water sample (**Table 1**). *M. subterraneum* was isolated from deep subterranean granitic aquifers, and its phenotypic and phylogenetic characteristics were described previously (Kotelnikova et al., 1998). *M. formicicum* was isolated from a domestic sewage sludge digest (Bryant and Boone, 1987) and in a municipal land field sample as an endosymbiont of a ciliate (Finlay and Fenchel, 1991). H_2/CO_2 and formate are the growth substrates for these two species but they cannot grow on methylamines, acetate, pyruvate, dimethyl sulfide, methanol, or other alcohols plus carbon dioxide. Growth of *M. subterraneum* strain A08 is inhibited by yeast extract (Kotelnikova et al., 1998). In the present study, H_2/CO_2, acetate, and methanol were each tested as growth substrate for microcosms, and H_2/CO_2 was found to be main carbon and energy source. Additionally, yeast extract, which was used in the initial enrichment culture, was not added to the trace element amended enrichments due to the unknown quantities of trace elements in it. Optimum temperature conditions for *M. subterraneum* strain A08 and *M. formicicum* are described as 20–40˚C and 37–45˚C, respectively. Optimum pH values for *M. subterraneum* strain A08 and *M. formicicum* are between pH 6.6–6.8 and pH 7.8–8.8, respectively (Kotelnikova et al., 1998). In this study, the pH value in enrichments was adjusted to 7.2 ± 0.2 and no differences were observed during 7 days of incubation at 37˚C between trace element amended and non-amended enrichments. Among all growth factors in the enrichments such as temperature, pH, or added substrates, trace element addition was the only variable that could have an effect on methanogenesis.

There are still many unknowns regarding the effect of trace elements, due to their bioavailability and optimal concentration on facilitated methanogenesis, and their toxic concentrations for microbial growth and activity in coal bed basins *in situ*. Bioavailability and toxicity of trace elements in the environment is under the control of geochemical processes such as mineral dissolution, precipitation, and ion adsorption/desorption. In this study, highly enriched methanogenic cultures were used to investigate the effect of trace elements on methanogenesis. However, in the natural environment, abundance and concentration of trace elements might enhance the rate of carbon source degradation by methanogens either directly or in a more indirect way. For example, it might increase the specific metabolic activity of bacterial groups such as primary or secondary fermenters whose products are the substrates for methanogens. Further study should focus on effects of trace elements on bacterial activity in coal biodegradation pathways and their associated community compositions. Effects of individual trace elements on growth and activity of methanogens and on fermenters might provide further insights to enhance biogenic methane production in coal bed wells. Therefore, better understanding of trace elements as a limiting factor for methanogenic activity in a coal bed basin will have a broader impact on our knowledge about ecology and physiology of methanogens.

ACKNOWLEDGMENTS

We are grateful to Dr. K. Baek for intensive discussions and to Drs. M. Kirk and A. Martini for ICP-MS measurements of trace elements. We thank the Turkish Ministry of Education for a scholarship to Burcu Ünal. This project was supported in part by a Agriculture and Food Research Initiative Competitive Grant no. 2009-35319-05186 and Hatch funds no. MAS00945 from the USDA National Institute of Food and Agriculture to Klaus Nüsslein.

REFERENCES

Balch, W. E., and Wolfe, R. S. (1976). New approach to the cultivation of methanogenic bacteria: 2-mercaptoethanesulfonic acid (HS-CoM)-dependent growth of *Methanobacterium ruminatium* in a pressurized atmosphere. *Appl. Environ. Microbiol.* 32, 781–791.

Bapteste, E., Brochier, C., and Boucher, Y. (2005). Higher-level classification of the *Archaea*: evolution of methanogenesis and methanogens. *Archaea* 1, 353–363.

Basiliko, N., and Yavitt, J. B. (2001). Influence of Ni, Co, Fe, and Na additions on methane production in Sphagnum-dominated Northern American peatlands. *Biogeochemistry* 52, 133–153.

Becerra, C. A., and Lopez-Luna, E., Ergas, S. J., Nüsslein, K. (2009). Microcosm-based study of the attenuation of an acid mine drainage-impacted site through biological sulfate and iron reduction, *Geomicrobiol. J.* 26, 9–20.

Beckmann, S., Lueders, T., Krüger, M., von Netzer, F., Engelen, B., and Cypionka, H. (2011). *Appl. Environ. Microbiol.* 77, 3749–3756.

Biddle, J. F., Lipp, J. S., Lever, M. A., Lloyd, K. G., Sorensen, K. B., Anderson, R., Fredricks, H. F., Elvert, M., Kelly, T. J., Schrag, D. P., Sogin, M. L., Brenchley, J. E., Teske, A., House, C. H., and Hinrichs, K. U. (2006). Heterotrophic *Archaea* dominate sedimentary subsurface ecosystems off Peru. *Proc Natl. Acad. Sci. U.S.A.* 103, 3846–3851.

Bryant, M. P., and Boone, D. R. (1987). Isolation and characterization of *Methanobacterium formicicum* MF. *Int. Union Microbiol. Soc.* 37, 171.

Bult, C. J., White, O., Olsen, G. J., Zhou, L., Fleischmann, R. D., Sutton, G. G., Blake, J. A., FitzGerald, L. M., Clayton, R. A., Gocayne, J. D., Kerlavage, A. R., Dougherty, B. A., Tomb, J. F., Adams, M. D., Reich, C. I., Overbeek, R., Kirkness, E. F., Weinstock, K. G., Merrick, J. M., Glodek, A., Scott, J. L., Geoghagen, N. S., and Venter, J. C. (1996). Complete genome sequence of the methanogenic archaeon, *Methanococcus jannaschii*. *Science* 23, 1058–1073.

Burgess, J. E., Quarmby, J., and Stephenson, T. (1999). Role of micronutrients in activated sludge-based biotreatment of industrial effluents. *Biotechnol. Adv.* 17, 50–70.

Burggraf, S., Stetter, K. O., Rouvière, P., and Woese, C. R. (1991). *Methanopyrus kandleri*: an archaeal methanogen unrelated to all other known methanogens. *Syst. Appl. Microbiol.* 14, 346–351.

Cadillo-Quiroz, H., Yashiro, E., Yavitt, J. B., and Zinder, S. H. (2008). Characterization of the archaeal community in a minerotrophic fen and terminal restriction fragment length polymorphism-directed isolation of a novel hydrogenotrophic methanogen. *Appl. Environ. Microbiol.* 74, 2059–2068.

Chakraborty, N., Chatterjee, M., Sarkar, G. M., and Lahiri, S. C. (2010). Inhibitory effects of the divalent metal ions on biomethanation by isolated mesophilic methanogen in AC21 medium in presence or absence of juices from water hyacinth. *Bioenergy Res* 3, 314–320.

Chin, K.-J., Lueders, T., Friedrich, M. W., Klose, M., and Conrad, R. (2004a). Archaeal community structure and pathway of methane formation on rice roots. *Microb. Ecol.* 47, 59–67.

Chin, K.-J., Esteve-Nunez, A., Leang, C., and Lovley, D. R. (2004b). Direct correlation between rates of anaerobic respiration and levels of mRNA for key respiratory genes in *Geobacter sulfurreducens*. *Appl. Environ. Microbiol.* 70, 5183–5189.

Chin, K.-J., Sharma, M. L., Russell, L. A., O'Neill, K. R., and Lovley, D. R. (2008). Quantifying expression of a dissimilatory (bi)sulfite reductase gene in petroleum-contaminated marine harbor sediments. *Microb. Ecol.* 55, 489–499.

Chistoserdova, L., Vorholt, J. A., Thauer, R. K., and Lidstrom, M. E. (1998). C1 transfer enzymes and coenzymes linking methylotrophic bacteria and methanogenic *Archaea*. *Science* 281, 99–102.

DeLong, E. F. (1992). *Archaea* in coastal marine environments. *Proc. Natl. Acad. Sci. U.S.A.* 89, 5685–5689.

Ellerman, J., Hedderich, R., Bocher, R., and Thauer, R. K. (1988). The final step in methane formation. Investigations with highly purified methyl-CoM reductase (component C) from *Methanobacterium thermoautotrophicum* (strain Marburg). *Eur. J. Biochem.* 172, 669–677.

Fakoussa, R. M., and Hofrichter, M. (1999). Biotechnology and microbiology of coal degradation. *Appl. Environ. Microbiol.* 52, 25–40.

Feng, X. M., Karlsson, A., Svensson, B. H., and Bertilsson, S. (2010). Impact of trace element addition on biogas production from food industrial waste-linking process to microbial communities. *FEMS Microbiol. Ecol.*74, 226–240.

Finkelman, R. B. (1995). "Modes of occurrence of environmentally-sensitive trace elements in coal," in *Environmental Aspects of Trace Elements in Coal*, eds D. J. Swaine and F. Goodarzi (Dordrecht: Kluwer Academic Publishing), 24–50.

Finlay, B. J., and Fenchel, T. (1991). An anaerobic protozoon, with symbiotic methanogens, living in municipal landfill material. *FEMS Microbiol. Lett.* 85, 169–179.

Fleming, J. T., Sanseverino, J., and Sayler, G. S. (1993). Quantitative relationship between naphthalene catabolic gene frequency and expression in predicting PAH degradation in soils at town gas manufacturing sites. *Environ. Sci. Technol.* 27, 1068–1074.

Fletcher, S. (2005). Unconventional gas vital to, U.S. supply. *Oil Gas J.* 103, 20–25.

Flores, R. M., Rice, C. A., Stricker, G. D., Warden, A., and Ellis, M. S. (2008). Methanogenic pathways of coal-bed gas in the Powder River Basin, United States: the geologic factor. *Int. J. Coal Geol.* 76, 52–75.

Friedrich, M. W. (2005). Methyl-coenzyme M reductase genes: unique functional markers for methanogenic and anaerobic methane-oxidizing *Archaea. Meth. Enzymol.* 397, 428–442.

Glass, J. B., and Orphan, V. J. (2012). Trace metal requirements for microbial enzymes involved in the production and consumption of methane and nitrous oxide. *Front. Microbiol.* 61, 1–20. doi:10.3389/fmicb.2012.00061

Goldschmidt, V. M. (1935). Rare elements in coal ashes. *Ind. Eng. Chem.* 27, 1100–1102.

Gonzalez-Gil, G., Kleerebezem, R., and Lettinga, G. (1999). Effects of nickel and cobalt on kinetics of methanol conversion by methanogenic sludge as assessed by on-line ch4 monitoring. *Appl. Environ. Microbiol.* 65, 1789–1793.

Goodwin, J., Wase, D., and Forster, C. (1990). Effects of nutrient limitation on the anaerobic upflow sludge blanket reactor. *Enzyme Microb. Technol.* 12, 877–884.

Gough, H. L., and Stahl, D. A. (2010). Microbial community structures in anoxic freshwater lake sediment along a metal contamination gradient. *ISME J.* 5, 543–558.

Green, M. S., Flanegan, K. C., and Gilcrease, P. C. (2008). Characterization of a methanogenic consortium enriched from a coal bed methane well in the Powder River Basin, U.S.A. *Int. J. Coal Geol.* 76, 34–45.

Guo, H., Liu, R., Yu, Z., Zhang, H., Yun, J., Li, Y., Liu, X., and Pan, J. (2012). Pyrosequencing reveals the dominance of methylotrophic methanogenesis in a coal bed methane reservoir associated with Eastern Ordos Basin in China. *Int. J. Coal Geol.* 93, 56–61.

Hallam, S. J., Girguis, P. R., Preston, C. M., Richardson, P. M., and DeLong, E. F. (2003). Identification of methyl coenzyme M reductase A (mcrA) genes associated with methane-oxidizing *Archaea. Appl. Environ. Microbiol.* 69, 5483–5491.

Harris, S. H., Smith, R. L., and Barker, C. E. (2008). Microbial and chemical factors influencing methane production in laboratory incubations of low-rank subsurface coals. *Int. J. Coal Geol.* 76, 46–51.

Jackson, R. E., and Reddy, K. J. (2007). Trace element chemistry of coalbed natural gas produced water in the Powder River Basin, Wyoming. *Environ. Sci. Technol.* 1, 5953–5959.

Jones, E. J. P., Voytek, M. A., Corum, M. D., and Orem, W. H. (2010). Stimulation of methane generation from nonproductive coal by addition of nutrients or a microbial consortium. *Appl. Environ. Microbiol.* 76, 7013–7022.

Jones, E. J. P., Voytek, M. A., Warwick, P. D., Corum, M. D., Cohn, A., Bunnell, J. E., Clark, A. J., and Orem, W. H. (2008). Bioassay for estimating the biogenic methane-generating potential of coal samples. *Int. J. Coal Geol.* 76, 138–150.

Juottonen, H., Tuittila, E., Juutinen, S., Fritze, H., and Yrjälä, K. (2008). Seasonality of rDNA- and rRNAderived archaeal communities and methanogenic potential in a boreal mire. *ISME J.* 2, 1157–1168.

Klein, D. A., Flores, R. M., Venot, C., Gabbert, K., Schmidt, R., Stricker, G. D., Pruden, A., and Mandernack, K. (2008). Molecular sequences derived from Paleocene Fort Union Formation coals vs. associated produced waters: implications for CBM regeneration. *Int. J. Coal Geol.* 76, 3–13.

Kotelnikova, S., Macario, A. J. L., and Pedersen, A. (1998). *Methanobacterium subterraneurn* sp. nov., a new alkaliphilic, eurythermic and halotolerant methanogen isolated from deep granitic groundwater. *Int. J. Syst. Bacteriol.* 48, 357–367.

Krumholz, L. R., McKinley, J. P., Ulrich, G. A., and Suflita, J. M. (1997). Confined subsurface microbial communities in Cretaceous rock. *Nature* 386, 64–66.

Kumar, S., Nei, M., Dudley, J., and Tamura, K. (2008). MEGA: a biologist-centric software for evolutionary analysis of DNA and protein sequences. *Brief. Bioinform.* 9, 299–306.

Lai, M. C., and Wu, S. Y. (2011). Methanogenic *Archaea* isolated from Taiwan's Chelungpu fault. *Appl. Environ. Microbiol.* 77, 830–838.

Lane, D. J. (1991). Nucleic Acid Techniques in Bacterial Systematics. eds E. Stackebrandt and M. Goodfellow (New York: Wiley), 115–175.

Lehmacher, A., and Klenk, H.-P. (1994). Characterization and phylogeny of mcrII, a gene cluster encoding an isoenzyme of methyl coenzyme M reductase from hyperthermophilic *Methanothermus fervidus. Mol. Gen. Genet.* 243, 198–206.

Lengeler, L., Drews, G., and Schlegel, H. (1999). *Biology of the Prokaryotes.* Stuttgart: Blackwell Science.

Li, D., Hendry, P., and Faiz, M. (2008). A survey of the microbial populations in some Australian coalbed methane reservoirs. *Int. J. Coal Geol.* 76, 1–2.

Lloyd, K. G., Albert, D. B., Biddle, J. F., Chanton, J. P., Pizarro, O., and Teske, A. (2010). Spatial structure and activity of sedimentary microbial communities underlying a *Beggiatoa* spp. Mat in a Gulf of Mexico hydrocarbon seep. *PLoS ONE* 5, e8738. doi:10.1371/journal.pone.0008738

Lueders, T., Chin, K. J., Condrad, R., and Frederich, M. (2001). Molecular analyses of methyl-coenzyme M reductase alpha-subunit (mcrA) genes in rice field soil and enrichment cultures reveal the methanogenic phenotype of a novel archaeal lineage. *Environ. Microbiol.* 3, 194–204.

Luton, P. E., Wayne, J. M., Sharp, R. J., and Riley, P. W. (2002). The mcrA gene as an alternative to 16S rRNA in the phylogenetic analysis of methanogen populations in landfill. *Microbiology* 148, 3521–3530.

McBeth, I., Reddy, K. J., and Skinner, Q. D. (2003). Chemistry of trace elements in coalbed methane product water. *Water Res.* 37, 884–890.

Meyer-Dombard, D. R., Shock, E. L., and Amend, J. P. (2012). Effects of trace element concentrations on culturing thermophiles. *Extremophiles* 16, 317–331.

Midgley, D. J., Hendry, P., Pinetown, K. L., Fuentes, D., Gong, S., Mitchell, D. L., and Faiz, M. (2010). Characterization of a microbial community associated with a deep, coal seam methane reservoir in the Gippsland Basin, Australia. *Int. J. Coal Geol.* 8, 232–239.

Moser, D. P., Gihring, T. M., Brockman, F. J., Fredrickson, J. K., Balkwill, D. L., Dollhopf, M. E., Lollar, B. S., Pratt, L. M., Boice, E., Southam, G., Wanger, G., Baker, B. J., Pfiffner, S. M., Lin, L.-H., and Onstott, T. C. (2005). *Desulfotomaculum* and *Methanobacterium* spp. Dominate a 4- to 5-kilometer-deep fault. *Appl. Environ. Microbiol.* 71, 8773–8783.

Nazaret, S., Jeffrey, H. W., Saouter, E., Haven, R. V., and Barkay, T. (1994). merA gene expression in aquatic environments measured by mRNA production and Hg(II) volatilization. *Appl. Environ. Microbiol.* 60, 4059–4065.

Nunoura, T., Oida, H., Nakaseama, M., Kosaka, A., Ohkubo, S. B., Kikuchi, T., Kazama, H., Hosoi Tanabe, S., Nakamura, K., Kinoshita, M., Hirayama, H., Inagaki, F., Tsunogai, U., Ishibashi, J., and Takai, K. (2010). Archaeal diversity and distribution along thermal and geochemical gradients in hydrothermal sediments at the Yonaguni Knoll IV hydrothermal field in the Southern Okinawa trough. *Appl. Environ. Microbiol.* 76, 1198–1211.

Orphan, V. J., Taylor, L. T., Hafenbradl, D., and Delong, L. T. (2000). Culture-dependent and culture-independent characterization of microbial assemblages associated with high-temperature petroleum reservoirs. *Appl. Environ. Microbiol.* 66, 700–711.

Pedersen, K. (1993). The deep subterranean biosphere. *Earth Sci. Rev.* 34, 243–260.

Penner, T. J., Foght, J. M., and Budwill, K. (2010). Microbial diversity of western Canadian subsurface coal beds and methanogenic coal enrichment cultures. *Int. J. Coal Geol.* 82, 81–93.

Petzet, A. (2005). Resource plays, CBM to fuel drilling upturns in, U.S. Canada. *Oil Gas J.* 103, 32–34.

Pobeheim, H., Munk, B., Johansson, J., and Guebitz, G. M. (2010). Influence of trace elements on methane formation from a synthetic model substrate for maize silage. *Bioresour. Technol.* 101, 836–839.

Reeve, J. N., Nolling, J., Morgan, R. M., and Smith, D. R. (1997). Methanogenesis: genes, genomes, and who's on first? *J. Bacteriol.* 179, 5975–5986.

Saitou, N., and Nei, M. (1987). The neighbor-joining method-a new method for reconstructing phylogenetic trees. *Mol. Biol. Evol.* 4, 406–425.

Schloss, P. D., and Handelsman, J. (2005). Introducing DOTUR, a computer program for defining operational taxonomic units and estimating species richness. *Appl. Environ. Microbiol.* 71, 1501–1506.

Shi, W., Zhan, C., Ignatov, A., Manjasetty, B., Marinkovic, N., Sullivan, M., Huang, R., and Chance, M. R. (2005). Metalloproteomics: high-throughput structural and functional annotation of proteins in structural genomics. *Structure* 13, 1473–1486.

Shimizu, S., Akiyama, M., Naganuma, T., Fujioka, M., Nako, M., and Ishijima, Y. (2007). Molecular characterization of microbial communities in deep coal seam groundwater of northern Japan. *Geobiology* 5, 423–433.

Shlimon, A. G., Friedrich, M. W., Niemann, H., Ramsing, N. B., and Finster, K. (2004). *Methanobacterium aarhusense* sp. nov., a novel methanogen isolated from a marine sediment (Aarhus Bay, Denmark). *Int. J. Syst. Evol. Microbiol.* 54, 759–763.

Singh, D. N., Kumar, A., Sarbhai, M. P., and Tripathi, A. K. (2012). Cultivation-independent analysis of archaeal and bacterial communities of the formation water in an Indian coal bed to enhance biotransformation of coal into methane. *Appl. Microbiol. Biotechnol.* 93, 1337–1350.

Springer, E., Sachs, M. S., Woese, C. R., and Boone, D. R. (1995). Partial gene sequences for the A subunit of methyl-coenzyme M reductase (mcrI) as a phylogenetic tool for the family Methanosarcinaceae. *Int. J. Syst. Bacteriol.* 45, 554–559.

Steinberg, L. M., and Regan, J. M. (2008). Phylogenetic comparison of the methanogenic communities from an acidic, oligotrophic fen and an anaerobic digester treating municipal wastewater sludge. *Appl. Environ. Microbiol.* 73, 6663–6671.

Strąpoć, D., Picardal, F. W., Turich, C., Schaperdoth, I., Macalady, J. L., Lipp, J. S., Lin, Y., Ertefa, T. F., Schubotz, F., Hinrichs, K., Mastalerz, M., and Schimmelmann, A. (2008). Methane-producing microbial community in a coal bed of the Illinois Basin. *Environ. Microbiol.* 74, 2424–2432.

Swaine, D. J., and Goodarzi, F. (1995). *Environmental Aspects of Trace Elements in Coal*. Dordrecht, Boston: Kluwer Academic Publishers..

Systat Software, I. (2004). *SYSTAT for Windows, Version11*. San Jose, CA: Systat Software.

Takai, K., Moser, D. P., DeFlaun, M., Onstott, T. C., and Fredrickson, J. K. (2001). Archaeal diversity in waters from deep South African gold mines. *Appl. Environ. Microbiol.* 67, 5750–5760.

Takashima, M., Speece, R. E., and Parkin, G. F. (1990). Mineral requirements for methane fermentation. *Crit. Rev. Environ. Control* 19, 465–479.

Thauer, R. K. (1998). Biochemistry of methanogenesis: a tribute to Marjory Stephenson. *Microbiology* 144, 2377–2406.

Thielemann, T., Cramer, B., and Schippers, A. (2004). Coalbed methane in the Ruhr basin, Germany: a renewable energy resource? *Adv. Org. Geochem.* 35, 1537–1549.

Thompson, J. D., Gibson, T. J., Plewniak, F., Jeanmougin, F., and Higgins, D. G. (1997). The CLUSTAL_X windows interface: flexible strategies for multiple sequence alignment aided by quality analysis tools. *Nucleic Acids Res.* 15, 4876–4882.

Ulrich, G., and Bower, S. (2008). Active methanogenesis and acetate utilization in power river basin coals, United States. *Int. J. Coal Geol.* 76, 25–33.

Van Voast, W. A. (2003). Geochemical signature of formation waters associated with coalbed methane. *Am. Assoc. Pet. Geol. Bull.* 87, 667–676.

Wawrik, B., Mendivelso, M., Parisi, V. A., Suflita, J. M., Davidova, I. A., Marks, C. R., Van Nostrand, J. D., Liang, Y., Zhou, J., Huizinga, B. J., Strąpoć, D., and Callaghan, A. V. (2012). Field and laboratory studies on the bioconversion of coal to methane in the San Juan Basin. *FEMS Microbiol. Ecol.* 80. doi: 10.1111/j.1574-6941.2011.01272.x

Weil, C. F., Cram, D. S., Sherf, B. A., and Reeve, J. N. (1988). Structure and comparative analysis of the genes encoding component C of methyl coenzyme M reductase in the extremely thermophilic archaebacterium *Methanothermus fervidus*. *J. Bacteriol.* 170, 4718–4726.

Wheaton, J., and Donato, T. (2004). Coal bed methane basics: Powder River Basin, Montana. Montana Bureau of Mines and Geology, *Information Pam.* 5, 1–25.

Widdel, F., Kohring, G. W., and Mayer, F. (1983). Studies on dissimilatory sulfate-reducing bacteria that decompose fatty acids. 111. Characterization of the filamentous gliding *Desulfonema limicola*. *Microbiology* 134, 286–294.

Yuan, Y., Conrad, R., and Lu, Y. (2011). Transcriptional response of methanogen mcrA genes to oxygen exposure of rice field soil. *Environ Microbiol. Rep.* 3, 320–328.

Zhang, W., Saren, G., Li, T., Yu, X., and Zhang, L. (2010). Diversity and community structure of archaea in deep subsurface sediments from the tropical Western pacific. *Curr. Microbiol.* 60, 439–445.

Zhang, Y., and Gladyshev, V. D. (2009). Comparative genomics of trace elements: emerging dynamic view of trace element utilization and function. *Chem. Rev.* 4828, 4828–4861.

Zhang, Y., and Gladyshev, V. D. (2010). General trends in trace element utilization revealed by comparative genomic analyses of Co, Cu, Mo, Ni, and Se. *J. Biol. Chem.* 285, 3393–3405.

Zhu, J., Liu, X., and Dong, X. (2011). *Methanobacterium* movens sp. nov. and *Methanobacterium* flexile sp. nov., isolated from lake sediment. *Int. J. Syst. Evol. Microbiol.* 61, 2974–2978.

Conflict of Interest Statement: The authors declare that the research was conducted in the absence of any commercial or financial relationships that could be construed as a potential conflict of interest.

Received: 16 November 2011; accepted: 20 April 2012; published online: 10 May 2012.

Citation: Ünal B, Perry VR, Sheth M, Gomez-Alvarez V, Chin K-J and Nüsslein K (2012) Trace elements affect methanogenic activity and diversity in enrichments from subsurface coal bed produced water. Front. Microbio. ***3****:175. doi: 10.3389/fmicb.2012.00175*

This article was submitted to Frontiers in Extreme Microbiology, a specialty of Frontiers in Microbiology.

frontiers in
MICROBIOLOGY

ORIGINAL RESEARCH ARTICLE
published: 29 June 2012
doi: 10.3389/fmicb.2012.00232

Microbial communities at the borehole observatory on the Costa Rica Rift flank (Ocean Drilling Program Hole 896A)

Lisa M. Nigro[1], Kate Harris[1], Beth N. Orcutt[2,3], Andrew Hyde[1], Samuel Clayton-Luce[1], Keir Becker[4] and Andreas Teske[1]*

[1] Department of Marine Sciences, University of North Carolina at Chapel Hill, Chapel Hill, NC, USA
[2] Center for Geomicrobiology, Aarhus University, Aarhus, Denmark
[3] Bigelow Laboratory for Ocean Sciences, East Boothbay, ME, USA
[4] Rosenstiel School of Marine and Atmospheric Science, University of Miami, Miami, FL, USA

Edited by:
Axel Schippers, Federal Institute for Geosciences and Natural Resources, Germany

Reviewed by:
Julie A. Huber, Marine Biological Laboratory, USA
James Cowen, University of Hawaii, USA

***Correspondence:**
Andreas Teske, Department of Marine Sciences, University of North Carolina at Chapel Hill, 340 Chapman Hall, CB 3300, Chapel Hill, NC 27599, USA.
e-mail: teske@email.unc.edu

The microbiology of subsurface, hydrothermally influenced basaltic crust flanking mid-ocean ridges has remained understudied, due to the difficulty in accessing the subsurface environment. The instrumented boreholes resulting from scientific ocean drilling offer access to samples of the formation fluids circulating through oceanic crust. We analyzed the phylogenetic diversity of bacterial communities of fluid and microbial mat samples collected *in situ* from the observatory at Ocean Drilling Program Hole 896A, drilled into ~6.5 million-year-old basaltic crust on the flank of the Costa Rica Rift in the equatorial Pacific Ocean. Bacterial 16S rRNA gene sequences recovered from borehole fluid and from a microbial mat coating the outer surface of the fluid port revealed both unique and shared phylotypes. The dominant bacterial clones from both samples were related to the autotrophic, sulfur-oxidizing genus *Thiomicrospira*. Both samples yielded diverse gamma- and alphaproteobacterial phylotypes, as well as members of the Bacteroidetes, Planctomycetes, and Verrucomicrobia. Analysis of ribulose-1,5-bisphosphate carboxylase/oxygenase (RuBisCO) genes (*cbbL* and *cbbM*) from the sampling port mat and from the borehole fluid demonstrated autotrophic carbon assimilation potential for *in situ* microbial communities; most *cbbL* genes were related to those of the sulfur-oxidizing genera *Thioalkalivibrio* and *Thiomicrospira*, and *cbbM* genes were affiliated with uncultured phylotypes from hydrothermal vent plumes and marine sediments. Several 16S rRNA gene phylotypes from the 896A observatory grouped with phylotypes recovered from seawater-exposed basalts and sulfide deposits at inactive hydrothermal vents, but there is little overlap with hydrothermally influenced basaltic boreholes 1026B and U1301A on the Juan de Fuca Ridge flank, suggesting that site-specific characteristics of Hole 896A (i.e., seawater mixing into borehole fluids) affect the microbial community composition.

Keywords: basalt, chemolithoautotrophic bacteria, CORKs, Costa Rica rift, formation fluids, ocean drilling program, subsurface, thiomicrospira

INTRODUCTION

The deep-sea subsurface is characterized by relatively low organic carbon input, elevated pressures, geographically variable temperatures, and sparse nutrient availability. Together, these conditions create unique and challenging habitats for microorganisms. Subseafloor sediments are estimated to constitute a large proportion of Earth's biomass (Whitman et al., 1998; Parkes et al., 2000), although local cell densities and microbial activities are low compared to surficial sediments (D'Hondt et al., 2004, 2009; Jørgensen and Boetius, 2007). Less is known, however, about a biosphere potentially hosted in subsurface oceanic basalt crust, largely due to difficulties is accessing this environment. Chemical and microscopic evidence coupled with theoretical models of potential metabolic reactions (Bach and Edwards, 2003) suggest that microbial activity in oceanic crust occurs and may have a significant impact on global biogeochemical cycles. Specifically, gradual microbial oxidation of reduced metals and sulfur species within the basalt crusts results in increased oxidation state and biocatalyzed weathering of ocean crust, as it ages and moves from the center of a mid-ocean ridge to the outer flanks (Bach and Edwards, 2003). Microaerophilic, autotrophic iron-oxidizing, or nitrate-reducing bacteria from ridge flank surfaces have been isolated, and include alpha- and gammaproteobacteria (Edwards et al., 2003); seafloor basalts from the 9°N East Pacific Rise harbor mostly gamma- and alphaproteobacteria, and Planctomycetes (Santelli et al., 2008, 2009). The question is whether similar bacteria are active in the deep basaltic subsurface.

Scientific ocean drilling provides one potential mechanism for the collection of deep subsurface samples for microbiological analysis. Such drilling is often conducted within the framework of the

Integrated Ocean Drilling Program (IODP) and its precursor, the Ocean Drilling Program (ODP). Subsurface drilling can work well in sedimentary layers, since contamination monitoring protocols allow for stringent control of seawater and drilling fluid contamination (Lever et al., 2006). By contrast, collection of pristine hard rock crustal samples through drilling is often problematic (Santelli et al., 2010), and rock sample surfaces are generally prone to seawater and drilling fluid contamination (Lever et al., 2006). Installation of long-term observatories within the resulting borehole offers an alternative for exploring subsurface crustal environments. Such borehole observatories, known as Circulation Obviation Retrofit Kits or "CORKs" (Davis et al., 1992; Becker and Davis, 2005), have been used successfully in the past to study hydrogeologic properties of crustal aquifers (Fisher et al., 2008) and to examine the biogeochemical composition of fluids circulating within oceanic crust (Wheat et al., 2010).

More recently, the composition of microbial communities inhabiting deep basaltic crust has been investigated through the collection of observatory fluids (Cowen et al., 2003), mineral crusts formed on the surface on observatories (Nakagawa et al., 2006), and mineral chip colonization experiments conducted within the observatories (Orcutt et al., 2011). Those experiments have focused on a series of CORK observatories, mostly at ODP Hole 1026B and IODP Hole U1301A (Fisher et al., 2005), installed on the eastern flank of the Juan de Fuca Ridge in the northeastern Pacific Ocean. Here, reduced, anoxic, sulfate-rich hydrothermal (∼64°C) fluids flow within 3.5 million-year-old basaltic crust. Analysis of borehole fluids and mineral crusts from these sites revealed diverse microbial communities containing novel Firmicutes bacteria, some of which are distantly related to *Ammonifex degensii*, a chemolithoautotrophic, thermophilic bacterium that oxidizes hydrogen, formate or pyruvate with nitrate, sulfate or elemental sulfur (Cowen et al., 2003; Nakagawa et al., 2006; Orcutt et al., 2011). Furthermore, enrichment experiments conducted on mineral crusts from the Hole 1026B observatory yielded anaerobic thermophiles, including methanogens, fermenters, and sulfate reducers (Nakagawa et al., 2006; Steinsbu et al., 2010). Archaeal communities in these observatories appear to be less diverse and align more closely with cultivated members of thermophilic, hydrogenotrophic methanogens of the genus *Methanothermococcus* (Nakagawa et al., 2006). Similar microbial communities of deep basalt origin might permeate adjacent layers of the overlying sediment column, as indicated by elevated counts of bacteria and archaea in sediments just above the basalt/sediment interface at Juan de Fuca (Engelen et al., 2008). The microbial community composition of the Juan de Fuca Ridge flank crustal subsurface differs significantly from the composition of communities harbored in seafloor-exposed basalts (Santelli et al., 2008, 2009), near-surface hydrothermal fluids circulating within basaltic outcrops (Huber et al., 2006), and hydrothermal fluids collected from sulfide- and/or iron-rich hydrothermal vents (Suzuki et al., 2004; Perner et al., 2007; Takai et al., 2008; Rassa et al., 2009). This disparity suggests that, although the crustal subsurface shares similar mineralogical and geochemical characteristics with the other habitats, it nonetheless harbors a unique subsurface crustal biosphere (Orcutt et al., 2011). Investigations of other subsurface crustal habitats are necessary to evaluate this hypothesis.

Here, we report the results of culture-independent 16S rRNA and RuBisCO gene molecular surveys conducted on opportunistic borehole fluid and mineral crust samples collected from an observatory in ODP Hole 896A. Hole 896A is located on the southern flank of the Costa Rica Rift in the equatorial Pacific Ocean at a water depth of 3,440 m (Shipboard Scientific Party, 1993). The borehole was drilled in 1993 to a maximum depth of 469 meters below seafloor (mbsf), with the lowermost 290 m penetrating roughly 6.8 million-year-old altered basaltic basement. Many features of the Hole 896A crustal aquifer are similar to those observed at the Juan de Fuca Ridge flank sites mentioned earlier. For instance, both sites are characterized by pillow and sheet-flow plagioclase-olivine phyric basalts; and vein filling with saponite and celadonite alteration minerals indicates complex hydrothermal evolutions of the systems (Alt et al., 1996; Hunter et al., 1999). Furthermore, formation fluids at Hole 896A are roughly 58°C (Becker et al., 2004), which is similar to those observed in the Juan de Fuca boreholes. Chemically, the basement fluids at both sites are characterized by reduced, high sulfate, low alkalinity fluids with relatively high calcium and low magnesium contents, indicating hydrothermal fluid-rock interactions (**Table 1**). Finally, both sites are located on buried basement highs (Alt et al., 1996; Fisher et al., 2005) with inferred fluid flow on the order of hundreds of liters per hour (Becker et al., 2004). As at the Juan de Fuca Ridge flank sites, microbial alteration textures, elemental analyses, cell counts, extractable DNA, and carbon and oxygen isotope data from basalts of Hole 896A indicate microbial activity (Giovannoni et al., 1996; Fisk et al., 1998; Torsvik et al., 1998; Furnes et al., 2001).

In this study, samples were collected from an observatory placed at Hole 896A in 2001 and revisited in 2002 (Becker et al., 2004) to conduct comparative phylogenetic analysis for evaluating the *in situ* microbial communities.

MATERIALS AND METHODS

STUDY SITE

ODP Hole 896A on the Costa Rica Rift (1°13′ N, 83°43′ W; **Figure 1**) is 3,463 m below sea level and drilled to a depth of 469 mbsf (**Figure 1**). The lower 290 m of the hole consists of altered basaltic oceanic crust. During drilling in 1993, the upper 196 m section of Hole 896A was cased, thus sealing out sediment pore water and allowing the influx and accumulation of hydrothermal subsurface fluids from the basaltic crust. In 2001, roughly 8 years after the borehole was originally drilled, a wireline packer seal apparatus similar to a CORK observatory was deployed with the intent to plug the hole, record the pressure and temperature in the sealed zones, sample borehole formation fluids, and monitor the return to *in situ* hydrogeological conditions (Becker et al., 2004). The wireline CORK apparatus was constructed primarily from mild steel, and it included one packer in the cased section and a second packer intended to be set about 50 m into the open-hole section, as well as steel tubing umbilicals to bring formation fluids to sampling ports at the wellhead. However, on deployment, the lower packer became stuck in the hole about 20 m above the intended setting depth. In the attempts to deal with this, it is likely that the tubing umbilicals were damaged and the packers could not be inflated to seal the hole.

Table 1 | Comparative chemistry of fluids from Costa Rica Ridge flank Holes 896A and 504B with Juan de Fuca Ridge flank fluids, with seawater for comparison.

Component	Units	Hole 896A[a]	Hole 504B[b]	Hole U1301A[c]	Baby Bare[d]	Seawater[e]
Temperature	°C	~60	58	64	64	2
Cl^-	mmol/kg	547	546	553	554	541
SO_4^{2-}	mmol/kg	18.5	17	17.6	17.8	27.9
Alkalinity	meq/kg	0.6	0.1	0.4	0.43	2.44
Na^+	mmol/kg	460	456	463	473	463.5
K^+	mmol/kg	6.8	7	6.9	6.88	10.1
Ca^{2+}	mmol/kg	50.5	58	55.8	55.2	10.2
Mg^{2+}	mmol/kg	8.5	8	1.9	0.98	52.6

[a] *Data extrapolated from basal sediment pore water samples collected from ODP Holes 501, 504, 677, and 678 (Holes 678 became Hole 896A; Mottl, 1989).*
[b] *Data from Hole 504B borehole fluids collected in situ 1,233 days after drilling (Mottl and Gieskes, 1990; Wheat and Mottl, 2000).*
[c] *Near steady-state formation fluid from Hole U1301A CORK OsmoSamplers deployed in basement borehole for ~4 years (Wheat et al., 2010).*
[d] *Fluids sampled from the Baby Bare basalt outcrop of the Juan de Fuca Ridge flank (Wheat and Mottl, 2000).*
[e] *Bottom seawater from the Costa Rica Ridge flank (Mottl, 1989).*

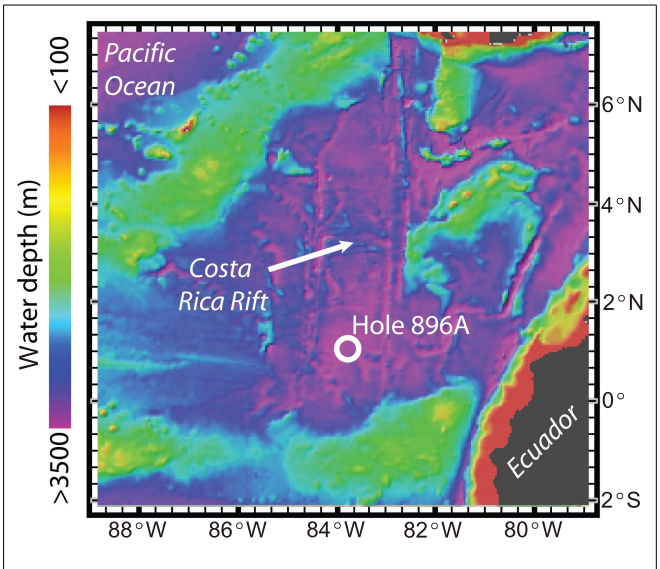

FIGURE 1 | Map of the Ocean Drilling Program Hole 896A study site in the Pacific Ocean in relation to the Costa Rica Rift. Color gradient scale provided for water depth in meters. Maps were created using the GeoMapApp software (www.geomapapp.org; Ryan et al., 2009).

Immediately prior to the attempt to deploy the wireline packer, a video and temperature log had been conducted to verify that the hole was open down to the intended setting depth of the lower packer about 50 m into open hole. The temperature log indicated that upper basement formation fluids were being produced up the hole, with an average temperature of 57.8°C and total fluid flow rate through the casing of 12 m/h, equivalent to a volume flux of 800 l/h (Becker et al., 2004). *In situ* video monitoring revealed the presence of thick whitish crusts resembling sulfur-oxidizing bacterial mats on both the cased and open-hole sections of Hole 896A, and flocculent material seems to be entering the borehole around 220 mbsf (Becker et al., 2004).

SAMPLE COLLECTION

Roughly 15 months after the installation of the observatory, fluid and microbial mat samples were collected on November 18, 2002 during submersible operations with DSV *Alvin* (Dive 3840; Woods Hole Oceanographic Institution). Because the wireline CORK packers had not been inflated, it is likely that the uphole flow of upper basement fluids revealed by the 2001 temperature log was continuing up around the wellhead. The microbial mat sample, referred to as *mat*, consisted of a flocculent grey crust growing on the seawater exposed exterior of Port L that was swabbed with a fresh green plastic sponge, which was exposed to seawater and therefore not sterile (**Figure 2A**). The sponge was stored on the submersible in a closed plastic biobox filled with site bottom water before return to the ship. The fluid sample, referred to as *bore*, consisted of fluids collected at a wellhead sampling port about 10 min after the valve (Port L; **Figure 2A**) was opened, into an ethanol-sterilized titanium bottle using a flexible sampling hose (**Figure 2B**). The sampling port was connected to the tubing leading from just below the lower packer. However, because of the possibility of damage to the umbilical and lack of packer seal, it is likely that a mix of bottom water and true formation fluids was being sampled. No warm water venting and efflux of borehole water was observed at Port L. After return to the ship, approximately 0.75 l of borehole fluid was filtered, using a handpump, through a 90-mm diameter 0.22 μm mesh nylon filter to collect particulate matter and microorganisms. Both samples were returned to the ship (RV *Atlantis*, Woods Hole Oceanographic Institution) within a few hours and immediately frozen at −80°C for preservation of DNA. Samples were then transported frozen to a shore-based laboratory.

DNA EXTRACTION, AMPLIFICATION, AND SEQUENCING

Environmental DNA was extracted from samples following a protocol modified from two published procedures for extracting DNA from deep subsurface sediments (Juniper et al., 2001; Kormas

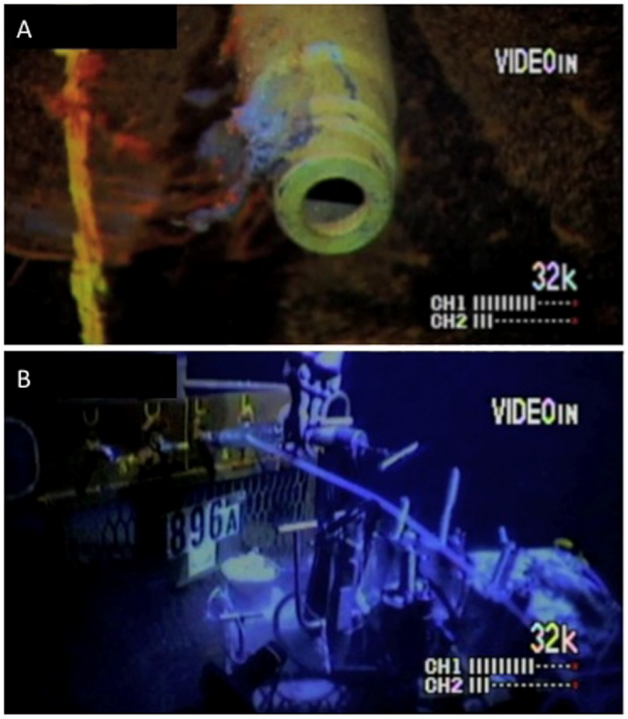

FIGURE 2 | Microbial mat and fluid sampling at ODP Hole 896A made from still images captured during *Alvin* operations. (A) The L port with attached biofilm, removed with the first scrubber and sequenced as "mat" sample; **(B)** water sampling (the material used here) by tube coupling to the L port.

et al., 2003). Using sterilized tools, the filter and sponge were cut into pieces and then transferred into replicate vials of 6 ml DNA extraction buffer (200 mM NaCl, 200 mM Tris, 2 mM sodium citrate, 10 mM $CaCl_2$, 50 mM EDTA, pH 8). The filter pieces were vortexed, and subjected to two freeze-thaw cycles (alternating −80°C and +65°C). Fifty microliters of Proteinase K (20 mg/ml) and 100 μl of 20% [w/v] sodium dodecyl sulfate (SDS) were added, and the samples were incubated for 30 min at 37°C. About 1.5 ml of 20% SDS was added and the samples were incubated at 55°C for 2 h in a shaking chamber. Then, the samples were centrifuged at 6,000×*g* for 10 min, the supernatant was harvested, an equal amount of 24:25:1 phenol/chloroform/isoamyl alcohol was added, and they were centrifuged again at 6,000×*g* for 10 min. The upper phase was harvested and 2.5× volume of ice-cold ethanol and 0.1× volume of ice-cold 5 M NaCl were added. The samples were placed in the −80°C freezer overnight to allow for DNA precipitation. The DNA was harvested by centrifuging at 10,000×*g* for 30 min, removing the supernatant, washing with 500 μl of 70% EtOH, and centrifuging again at 10,000×*g* for an additional 30 min. The remaining pellet was allowed to air dry before re-dissolving in 50 μl sterile water. To obtain more sequences, additional filter and mat samples were extracted with the Powersoil DNA Isolation Kit (Mobio) according to the manufacturer's instructions and final volume of 50 μl elution solution.

Near full-length 16S rRNA genes were amplified by polymerase chain reaction (PCR) using bacterial primers BAC-8F (5′-AGRGTTTGATCCTGGCTCAG-3′) and BAC-1492R (5′-CGGCTACCTTGTTACGACTT-3′; Lane, 1991). The PCR mixture for the phenol/chloroform/isoamyl alcohol extracted samples consisted of 1 μl of the environmental DNA, 2 μl of each primer (0.5 mM), 0.5 μl of enzyme included in the Failsafe™ PCR System kit (EpiCentre Biotechnologies), 25 μl of Failsafe™ Premix B and a balance of water for a total reaction volume of 50 μl. The PCR cycle conditions involved an initial denaturation at 95°C for 2 min, followed by 30 cycles of denaturation at 95°C for 1 min, annealing at 55°C for 1 min, and extension at 72°C for 3 min. These 30 cycles were followed by a final extension at 72°C for 10 min. Samples extracted with the Mobio Powersoil DNA Isolation Kit were amplified with Speedstar HS DNA Polymerase (Takara) using 2 μl of DNA sample and the manufacturer's recommendations concentrations of buffer, dNTPs, and polymerase in a final volume of 25 μl. Thermal cycling was performed as previously described above with the exception that cycling times were 95°C for 10 s, 52°C for 15 s, and 72°C for 20 s over 28 cycles.

To examine the potential for autotrophy using the Calvin cycle, *ccbL* and *ccbM* genes involved in the formation of ribulose-1,5-bisphosphate carboxylase/oxygenase (RuBisCO) from the *mat* sample environmental DNA were PCR amplified as described previously (Elsaied and Nagamuna, 2001). An initial round of PCR, cloning and sequencing yielded only one *cbbL* clone and three *cbbM* clones (mat clones A06, E03, H09, and F03). Additional DNA was amplified from the Powersoil Isolation Kit extractions with the GoTaq Flexi DNA Polymerase (Promega) using a final concentration of 3 mM $MgCl_2$, 1 μM of each primer, and the manufacturer's recommendation of dNTP, buffer, and polymerase concentration. Primers for the *cbbL* gene included cbbL1AF172 (5′-ACNTGGACNACNGTNTGG-3′) and cbbL1AR1382 (5′-TCR AAYTTGATYTCBTTCCA-3′). Primers for the *cbbM* gene included cbbM337F (5′-AACCARGYATGGGYGAY-3′) and cbbM1126R (5′-TCATRCCVCCVGADAT-3′). In the bore sample, non-specific priming was extensive in one *cbbL* PCR sample and an additional primer, cbbL1AR1142 (5′-GGCATRTGCCANACRT GRAT-3′), was used with primer cbbLAF172 in a nested PCR using 0.2 μl of the bore PCR sample and the same mixture and cycling conditions described above, with the exception that the number of cycles was reduced to 20. We note that the *cbbL* primers did not fully target the total diversity of the "red-like" IC form of RuBisCO (Badger and Bek, 2008) due to the need to limit the number of degeneracies; some diversity may have been missed.

The PCR products were subjected to 1.5% agarose gel electrophoresis, stained with 0.5 μg/ml of ethidium bromide or 1× GelRed (Biotium), and visualized by UV excitation for bands indicating successful DNA amplification. PCR products were either excised from the agarose gel or directly purified using the Wizard® PCR preparation kit (Promega) or the Qiagen Minelute Gel Extraction kit, and then cloned using TOPO XL PCR cloning kit (Invitrogen). From each clone library, clones were selected randomly for sequencing at the Josephine Bay Paul Center of the Marine Biological Laboratory in Woods Hole, MA, USA or Genewiz (Research Triangle Park, NC, USA).

PHYLOGENETIC ANALYSIS

Raw 16S rRNA gene and RuBisCO sequences were edited using Chromas or Sequencher (Genecodes) software to remove cloning vector sequences, and potential chimeric sequences were evaluated using Pintail[1]. Closely related sequences were identified using the Basic Local Alignment Search Tool (BLAST) program searches in GenBank[2] (Altschul et al., 1997). 16S rRNA gene sequences were aligned against a curated sequence database (using the NAST alignment tool available at greengenes.org; DeSantis et al., 2006a) and manually checked for alignment accuracy against reference sequences from the Greengenes database (DeSantis et al., 2006b) using the ARB software package (Ludwig et al., 2004). A phylogenetic tree of the nearly full-length 16S rRNA gene sequences of this study, plus key reference sequences, was calculated in ARB based on Jukes-Cantor distances via neighbor joining. The *cbbL* and *cbbM* gene sequences were translated to amino-acid sequences and aligned with Clustal W in MEGA 4.0 (Kumar et al., 2008) using a Gonnet protein weight matrix. The RuBisCO phylogeny was constructed in MEGA using a neighbor-joining method based on Poisson-corrected distances. Statistical support of tree topology was estimated by bootstrapping with 1,000 replicates in MEGA. The 16S rRNA gene sequences reported here are available in GenBank under the accession numbers GQ903340–GQ903342, GQ903344, GQ903346–GQ903350, and GQ903352–GQ903376. The RuBisCO genes have GenBank accession numbers HQ856238–HQ856241 and JQ795724–JQ795729.

The similarity of the *bore* and *mat* 16S rRNA gene clone libraries to previously published clone libraries was evaluated by comparing sequence similarity distance matrices with the programs DOTUR and SONS (Schloss and Handelsman, 2005, 2006) using methods described previously (Santelli et al., 2008). In particular, the nearly full-length Hole 896A 16S rRNA gene sequences were compared to sequence datasets generated from seafloor-exposed basalts from the East Pacific Rise and the Loihi Seamount (Santelli et al., 2008); from subsurface (3 m) hydrothermal basalt formation fluids from the Baby Bare outcrop on the Juan de Fuca Ridge flank (Huber et al., 2006); from fluids freely venting from the ODP Hole 1026B borehole (Huber et al., 2006); from bottom water samples collected above the Juan de Fuca Ridge flank (Huber et al., 2006); and from seafloor-exposed inactive massive sulfides from the East Pacific Rise (Sylvan et al., 2012). Sequence datasets were compared to identify the number and type of shared "species" between samples, with "species" operationally defined as operational taxonomic units (OTUs) with 97% or greater sequence similarity, as defined previously (Santelli et al., 2008). Sequence distance matrices were generated in ARB using the neighbor-joining method, the Jukes–Cantor correction, and application of an in-program filter for bacteria, of *E. coli* base pair positions 228–1420. Diversity estimators were calculated in DOTUR under standard settings at the 97% or greater sequence similarity definition level, and shared richness estimates were generated using standard settings in the SONS program.

[1]www.bioinformatics-toolkit.org/Web-Pintail/

[2]www.ncbi.nlm.nih.gov

RESULTS

16S rRNA GENE PHYLOGENY

A total of 66 and 60 nearly full-length 16S rRNA gene clones were successfully sequenced from the *bore* and *mat* sample clone libraries, respectively. Phylogenetic analysis of the clone libraries revealed 40 phylotypes from several bacterial phylum-level groups including Bacteroidetes, aerobic and anaerobic heterotrophs widespread in soil and water (Kirchman, 2002); Cyanobacteria; Actinobacteria (OM1 group; Rappé et al., 1997), oxygenic marine phototrophs; the phylum-level lineages Verrucomicrobia and Planctomycetes, often detected in oxygen-depleted marine habitats (Kirkpatrick et al., 2006) and with relatively few cultured chemoorganotrophic isolates (Wagner and Horn, 2006); and diverse Alpha-, Gamma-, and Epsilonproteobacteria (**Figures 3 and 4**). The seven most abundant phylotypes (highlighted in purple in **Figures 3 and 4**) were found in both the borehole fluids and the microbial mat.

Despite using bacteria-specific 16S rRNA gene primers, one archaeal clone was also recovered from the *mat* sample. This clone, *mat1*, was related to *Thermocladium modestius*, an extremely thermophilic crenarchaeote isolated from acidic hot spring areas in Japan (Itoh et al., 1998). The presence of an archaeal clone in a bacterial 16S rRNA gene clone library was unexpected, given that the bacterial and archaeal versions of the forward primers had five nucleotide mismatches and thus strong PCR bias against archaeal gene amplification.

A number of sequences grouped near known sulfur cycling microorganisms. Phylotype *mix2* was related to the free-living, autotrophic, oxygen- and nitrate-respiring, sulfur-oxidizing genus *Thiomicrospira* of the Gammaproteobacteria; this phylotype comprised nearly half of the sequences of both the *bore* and *mat* clone libraries (**Figure 3**). This phylotype has also been observed in clone libraries from seafloor-exposed massive sulfides (Sylvan et al., 2012) and in fluids sampled from the ODP Hole 1026B observatory on the Juan de Fuca Ridge flank (Huber et al., 2006). One *bore* phylotype affiliated with the sulfur-oxidizing chemolithoautotrophic Epsilonproteobacteria *Sulfurimonas denitrificans* and *S. autotrophica*. Generally, hydrogen- and sulfur-oxidizing, chemolithoautotrophic Epsilonproteobacteria have a wide environmental distribution at hydrothermal vents and in marine surficial sediments (Campbell et al., 2006; Nakagawa and Takai, 2008) and employ an alternative pathway of autotrophic CO_2 fixation, the reverse tricarboxylic acid (TCA) cycle (Hügler et al., 2005). The whitish mats deposited on the walls of the observatory and recorded in video logs of the Hole 896A borehole (Becker et al., 2004) bear a conspicuous resemblance to the sulfur precipitates and flocs produced by sulfur-oxidizing bacteria (Kuenen and Veldkamp, 1972; Taylor and Wirsen, 1997; Wirsen et al., 2002).

Several other *bore* and *mat* sequences also grouped most closely with uncultivated environmental sequences recovered from seawater-exposed basalts and inactive sulfides from the East Pacific Rise and Hawaii (Santelli et al., 2009; Sylvan et al., 2012), from hydrothermal fluids from a basaltic outcrop (Huber et al., 2006) and from cold seep and hydrothermally influenced deep marine sediments. These phylotypes are highlighted with colored circles in **Figures 3 and 4**. Nine of the forty observed bacterial

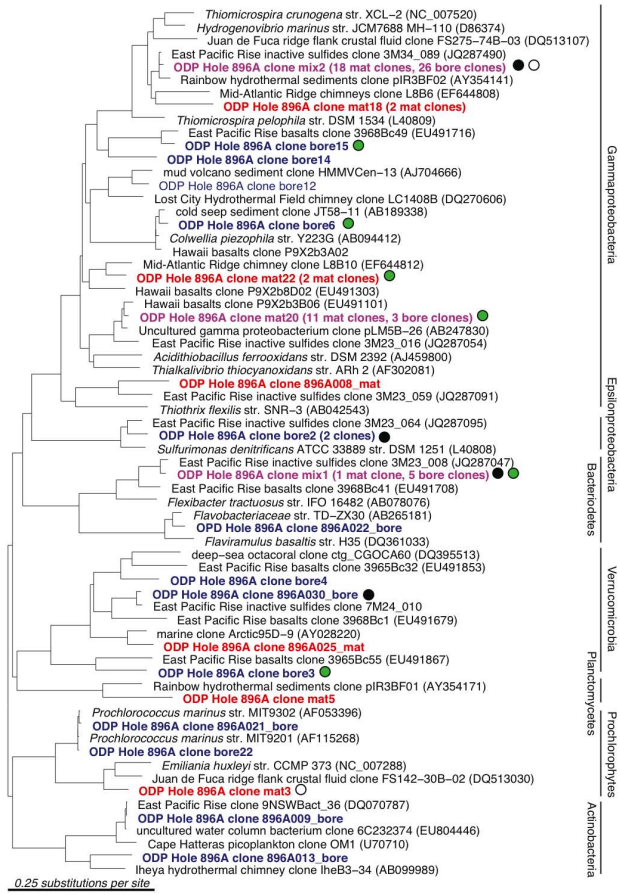

FIGURE 3 | 16S rRNA gene neighbor-joining phylogenetic tree for Hole 896A observatory *bore* and *mat* sample sequences in comparison to close relatives from the GenBank database, excluding the Alphaproteobacteria phylum. Clones from borehole fluids collected at the observatory spigot are labeled as *bore* in blue, and clones from the microbial *mat* on the exterior of the borehole are labeled as *mat* in red. Identical clones from both samples are labeled in purple. Short sequences are indicated with asterisks. Sequences that are shared with other clone libraries are indicated with colored dots: East Pacific Rise inactive massive sulfides (black); East Pacific Rise and Loihi Seamount basalts (green); Juan de Fuca Ridge flank crustal fluids (white); Juan de Fuca CORK Hole 1301A (yellow).

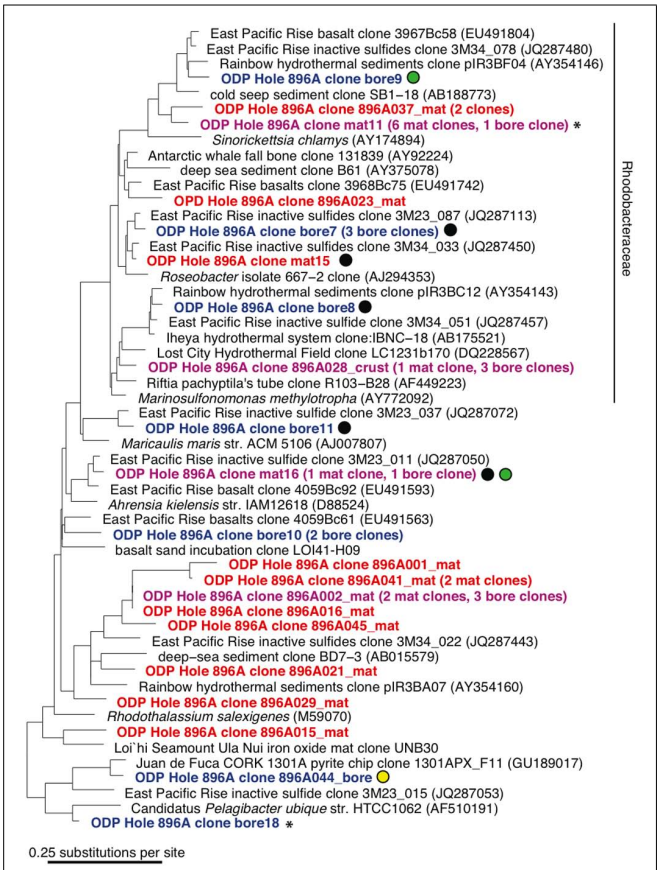

FIGURE 4 | 16S rRNA gene neighbor-joining phylogenetic tree for Hole 896A observatory *bore* and *mat* sample Alphaproteobacteria sequences in comparison to close relatives from the GenBank database. Same details as for **Figure 3**.

phylotypes, marked with black circles, grouped closely with phylotypes from inactive massive sulfide samples collected from the East Pacific Rise (Sylvan et al., 2012), whereas eight phylotypes, marked with green circles, were shared with clone libraries from seafloor-exposed basalts (Santelli et al., 2009). Three phylotypes, marked with white and yellow circles, were similar to clones from samples from other deep basalt observatories. Of these, one alphaproteobacterial sequence (**Figure 4**) grouped closely with a sequence from a biofilm formed on pyrite incubated in the subsurface for 4 years (Orcutt et al., 2011); the *Thiomicrospira*-related clone mix 2 and Prochlorophyte clone mat 3 are close to clones from venting basalts at Baby Bare on the Juan de Fuca ridge (Huber et al., 2006). No 16S rRNA clone library phylotypes were shared between the Hole 896A samples and background bottom water collected above basaltic lavas the Pacific Ocean (Santelli et al., 2008). While the identification of shared phylotypes is robust, shared diversity estimates between the sample sets were tested, but they were skewed due to the difference in clone library sizes between the Hole 896A samples and the comparison studies, and the possibility of seawater entrainment in the Hole 896A samples.

Several sequences grouped most closely to environmental sequences commonly found in seawater (**Figures 3 and 4**). For example, the *bore18* phylotype grouped near *Pelagibacter ubique* within the SAR 11 cluster, a cosmopolitan clade of marine oligotrophic bacteria (Rappé et al., 2002). Several alphaproteobacterial phylotypes from each sample grouped within the *Rhodobacteraceae* or marine Roseobacter group, a cosmopolitan group of marine bacteria that often metabolize and oxidize organosulfur compounds (Buchan et al., 2005; Brinkhoff et al., 2008). Two phylotypes were most closely related (99% identity) to sequences from the marine cyanobacterial genus *Prochlorococcus*, which is found at varying depths in the water column in oceans worldwide (West et al., 2001). The presence of these phylotypes is unexpected in samples of oceanic basement formation fluids, and indicates seawater entrainment and contamination during sampling of the *bore* and *mat* samples at the observatory platform, or seawater entrainment into the mixed borehole fluids itself. Moreover, the

occasional close phylogenetic association of some phylotypes with known aerobic chemoorganotrophic isolates, such as *Flaviramulus basaltis* and *Marivirga tractuosus* (**Figure 3**), suggests chronic oxic seawater mingling with basement fluids at the Hole 896A observatory.

RuBisCO PHYLOGENY

Amplification of the *cbbM* and *cbbL* genes of RuBisCO yielded sequences of sufficient length and quality for phylogenetic analysis from the mat sample and from the borehole fluid sample. BLAST search based on amino-acid sequence, and subsequent phylogenetic analysis (**Figure 5**) revealed that most *cbbL* sequences (*mix clone ODP3_4_1*) recovered from the mat (45 clones) as well as the borehole sample (16 clones) were most closely related to the obligately chemolithoautotrophic, sulfur-oxidizing gammaproteobacterial genera *Thioalkalivibrio*, isolated from Siberian and East African soda lakes (Sorokin et al., 2001; *Thioalkalivibrio thiocyanoxidans*, GenBank accession ZP_08930733, 93% identity), to sequences from hypersaline soda lake sediment in Kulunda Steppe (Russia; Kovaleva et al., 2011; GenBank ADN96557, 97% identity), and to the facultatively phototrophic sulfur oxidizer *Thiocapsa* (Guyoneaud et al., 1998), capable of chemolithoautotrophic growth with reduced sulfur compounds under microoxic conditions (Caumette, 1986). Other clones (*mix clone ODP 6_1_9*; five bore and one mat clone) were most closely related to *Thiomicrospira* (*Thiomicrospira crunogena*, GenBank YP_391108, 94% identity) isolated from marine sediments and hydrothermal vents (Jannasch et al., 1985; Scott et al., 2006) and the obligately autotrophic hydrogen oxidizer *Hydrogenovibrio marinus*, phylogenetically a lineage within the genus *Thiomicrospira* (GenBank BAD15312, 93% identity; Nishihara et al., 1998). Two other borehole sequences were most closely related to those from a pogonophoran bacterial endosymbiont from a cold methane seep in the Japan Trench (Nagamuna et al., 2007).

Only five *cbbM* sequences from the mat and bore sample were obtained in total despite attempts to amplify the gene with published (Elsaied and Nagamuna, 2001) and newly designed primers (this study). The *cbbM* sequences recovered from the Hole 896A samples were related to *cbbM* sequences of uncultivated bacteria from the hydrothermally active Suiyo Seamount, a submarine black smoker volcano in the Izu-Bonin trench off Japan (Clone Suiyo II-5, nucleotide accession number AB174751, protein ID BAD13304; Elsaied et al., 2007) and to *cbbM* sequences obtained from reducing sediments near the deepest known chemosynthetic microbial community, in deep-sea sediments of the Japan Trench at 7,434 m depth (Clone JT-Sed(II)-5, nucleotide accession number AB040517, protein ID BAD94441; Elsaied and Nagamuna, 2001; **Figure 5**).

DISCUSSION

The phylogenetic data presented here from Hole 896A on the Costa Rica Rift flank represents the second dataset from a basaltic crust borehole observatory, providing the first comparison to the available data from the Holes 1026B and U1301A CORK observatories

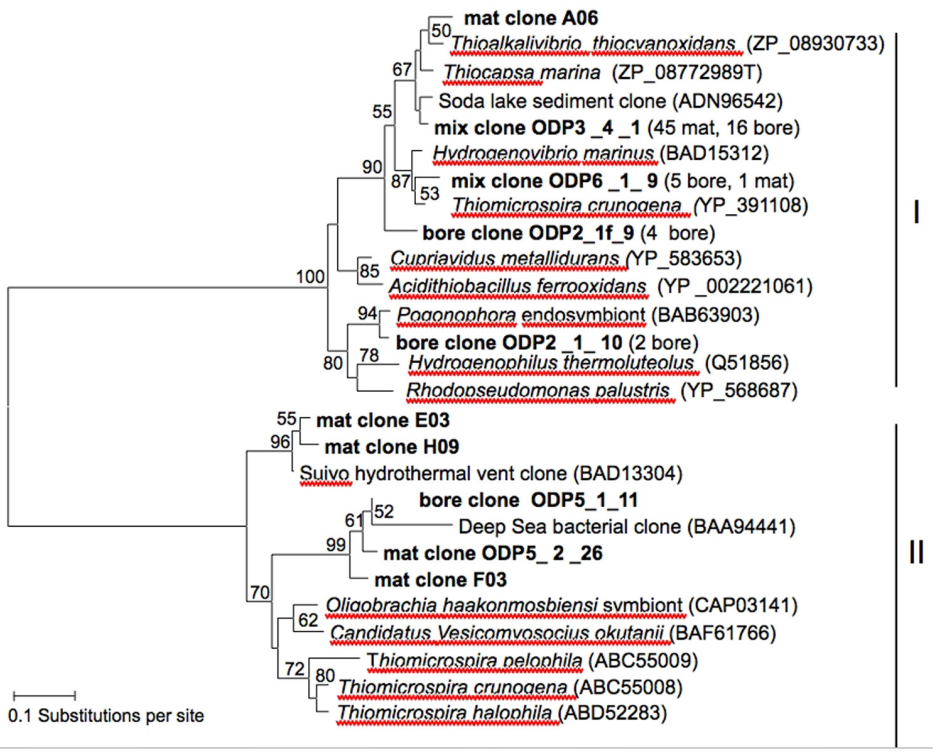

FIGURE 5 | Neighbor-joining tree based on amino-acid sequences translated from RuBisCO *cbbL* and *cbbM* large subunit gene sequences. Bootstrap values (1,000 replicates) above 50% are displayed beside the nodes. Clone sequences are indicated in bold.

on the Juan de Fuca Ridge flank (Cowen et al., 2003; Nakagawa et al., 2006; Orcutt et al., 2011). Such comparisons face important limitations; the two samples from the Hole 896A observatory were not pristine, and the sample type (formation fluids from the damaged observatory, and a scraping of a mat on the observatory exterior – both with likely seawater admixture) differs from previous samples, for example the enrichments on mineral surfaces in Hole U1301A (Orcutt et al., 2011), the CORK mineral crusts at Hole U1301A (Nakagawa et al., 2006), the vent fluids at Hole 1026B (Huber et al., 2006), or the biocolumn enrichments at 1026B (Cowen et al., 2003). However, we believe that the samples still allow broad comparisons toward a more complete picture of the biosphere hosted in subsurface oceanic crust. Our analysis also highlights operational issues that need to be addressed for future efforts to investigate the subsurface deep biosphere.

COMPARISON OF HOLE 896A MICROBIAL COMMUNITIES TO THOSE FROM OTHER HABITATS

Based on 16S rRNA gene clone libraries, the microbial communities observed in the Hole 896A samples (**Figures 3 and 4**) bore little resemblance to the communities described in formation fluids and mineral crusts from Holes 1026B and U1301A, despite the previously reported similarities in mineralogy, basement fluid chemistry, and temperature (**Table 1**). Holes 1026B and U1301A on the Juan de Fuca ridge flank reveal subsurface microbial communities characterized by an abundance of Firmicutes bacteria (Cowen et al., 2003; Nakagawa et al., 2006; Orcutt et al., 2011). The predominant bacterial phylotypes in the Hole 1026B clone libraries were distantly related to thermophilic, nitrate-, and sulfate-reducing bacteria, such as the hydrogen-oxidizing nitrate-reducing ammonia producer *Ammonifex degensii*, and the gram-positive, spore-forming sulfate reducing genus *Desulfotomaculum*. In contrast, the Hole 896A observatory samples were dominated by sequences grouping with Gammaproteobacteria related to the chemolithoautotrophic, sulfur-oxidizing genus *Thiomicrospira* that is predominantly isolated from sulfidic marine sediments and hydrothermal vents, and hydrothermal plumes; these bacteria were not detected in other borehole surveys (Cowen et al., 2003; Nakagawa et al., 2006; Orcutt et al., 2011).

One explanation for these differences in the dominant members of the microbial communities, with suspected metabolic differences as well, may be different redox regimes within the boreholes, despite the similarity in major ion concentrations of the formation fluids (**Table 1**). Namely, the extensive accumulation of white flocculent crusts in Hole 896A (Becker et al., 2004) suggests microoxic or nitrate-reducing conditions, while an anaerobic environment is known to prevail in Holes 1026B and U1301A (Wheat et al., 2010). The formation of extensive white flocs is also known from bioreactor experiments, where microaerobic sulfur-oxidizing bacteria produce extracellular sulfur in large amounts (Taylor and Wirsen, 1997); sulfur precipitation is also a characteristic by-product of aerobic, sulfur-oxidizing *Thiomicrospira* spp. growing in laboratory culture (for an instructive example, see Figure 2 in Kuenen and Veldkamp, 1972). The *in situ* observation of the flocculent mat-like material within the Hole 896A borehole (Becker et al., 2004) indicates *in situ* production of biomass and flocculent mats by sulfur-oxidizing bacteria within the borehole. Seawater influence at the Hole 896A CORK observatory is consistent with this interpretation. If seawater were entrained or mixed with the borehole fluids, which are presumably rich in reduced substrates such as sulfur and iron, this might create an ideal niche for the enrichment for the sulfide-oxidizing and biofilm-forming phylotypes observed. The sulfur-oxidizing bacteria that dominate the borehole could ultimately be derived from bottom water mixed with highly dilute hydrothermal plumes and microbial populations (Huber et al., 2006, 2007). The observation of seawater-related phylotypes such as SAR11, *Roseobacter*, Prochlorophytes, and OM1 Actinobacteria in the bore hole sample clone libraries also supports the argument for seawater entrainment. In consequence, the *in situ* enrichment of bacteria growing under likely conditions of seawater entrainment in the borehole and within the CORK distorts the assessment of potential indigenous microbial diversity in basaltic basement fluids (Cowen, 2004).

AUTOTROPHIC POTENTIAL

Based on theoretical models of the energy available from sulfur and iron oxidation in basaltic crust, significant levels of primary production should occur in the subsurface (Bach and Edwards, 2003), a prediction testable by RuBisCO genes analysis. RuBisCO catalyzes the assimilation of carbon dioxide to organic carbon via the Calvin–Benson–Bassham cycle. Of its currently four known forms, form I is oxygen tolerant and found predominantly in cyanobacteria, chloroplasts, and aerobic chemolithoautotrophic bacteria, while form II is adapted to high CO_2 conditions and found predominantly in microaerobic or anaerobic bacteria (Delwiche and Palmer, 1996; Badger and Bek, 2008). We observed both forms of RuBisCO in the Hole 896A mat and borehole samples (**Figure 5**). RuBisCO sequences were phylogenetically related to *Thiomicrospira*, the closest cultured relative of the most frequently recovered 16S rRNA sequences at the 896A CORK. The form I RuBisCO sequences obtained from the bore hole and from the mat sample were most closely related to the sulfur-oxidizing chemolithoautotrophic genera *Thioalkalivibrio*, *Thiocapsa*, and *Thiomicrospira*, within the form IA "green-type" clade that is associated with proteobacteria and cyanobacteria (Badger and Bek, 2008). This pattern is consistent with the 16S rRNA sequencing results, and with the interpretation that the borehole fluid and the mat sample contain autotrophic, sulfur-oxidizing bacteria related to these gammaproteobacterial genera. The presence of additional autotrophic bacteria (or of bacteria that contain form II in addition to one of the form I sequences found here) is indicated by the form II sequences in the mat; these sequences were related to RuBisCO of uncultured marine bacteria, not from the open water column but from methane seep sediments and hydrothermal plumes (**Figure 5**).

As a note of caution, RuBisCO has a high rate of horizontal gene transfer events (Delwiche and Palmer, 1996). The gammaproteobacterial form I types are also found in cyanobacteria, for example, the common marine cyanobacterium *Prochlorococcus* which most likely acquired its RuBisCO genes by horizontal gene transfer (Hess et al., 2001). Thus, the RuBisCO sequences do not rule out seawater contamination, as indicated by the two *Prochlorococcus* 16S rRNA gene sequences found in the borehole

fluid (**Figure 3**). A certain degree of seawater contamination is obvious, but it does not invalidate the abundance of phylotypes most closely related to sulfur-oxidizing bacteria (*Thiomicrospira*, *Sulfurimonas*) and to basalt-associated bacterial phylotypes. With this caveat, the 16S rRNA gene and RuBisCO sequence data are consistent with autotrophic, most likely sulfur-oxidizing bacterial populations growing within the borehole and on the sampling ports of the CORK; this interpretation is fully consistent with *in situ* borehole observations of microbial mat growth within the borehole (Becker et al., 2004).

RECOMMENDATIONS FOR FUTURE OBSERVATORY STUDIES

The Hole 896A observatory was installed for primarily geophysical experiments (Becker et al., 2004) and was not designed for high-quality sampling for microbiological analysis of the subsurface crustal biosphere. Nevertheless, samples were collected opportunistically and analyzed despite potential contamination pitfalls, as they represented a unique chance to evaluate the crustal biosphere. Our analysis indicates that fluids from the crustal subsurface mixed with seawater can support microbial communities that appear to form biofilms, and that some of these biofilm-forming species are related to known sulfide oxidizing microbial groups like *Thiomicrospira*. Given the stark differences in the microbial communities observed between subsurface observatories placed in similar crustal settings (i.e., between the Hole 896A observatory and the Juan de Fuca Ridge flank Holes 1026B and U1301A), enhanced sample characterization may shed light on the underlying environmental conditions that could explain these differences. For example, analysis of borehole fluid oxygen, nitrate and redox conditions may help resolve whether the presence of these electron acceptors may have influenced the Hole 896A community. A time series analysis of the Hole 896A observatory would provide background information on whether the observed community was representative of "steady state" formation fluids or if it instead represented a transitory evolution of the community post-observatory installation, as has been observed elsewhere for microbial communities in other boreholes (Orcutt et al., 2011). Most importantly, improvements in the Hole 896A observatory infrastructure to allow cleaner microbiological sampling would reduce the confounding influence of seawater contamination.

ACKNOWLEDGMENTS

We thank Steve D'Hondt and Eddie Roggenstein for obtaining samples from the ODP Hole 896A observatory during *DSV Alvin* dives in November 2002, and C. Geoff Wheat for helpful discussion regarding borehole fluid chemistry. Installation of the wireline CORK and the 2002 Alvin dives were supported by the National Science Foundation under grant OCE-9819316 to Keir Becker. Funding for this project was provided by the American Society for Microbiology Undergraduate Research Fellowship to Kate Harris, and by the NASA Astrobiology Institutes "Subsurface Biospheres" at the University of Rhode Island, and "Environmental Genomes" at the Marine Biological Laboratory. Andreas Teske was further supported through the Center for Dark Energy Biosphere Investigations. We thank the reviewers for their constructive comments that improved this manuscript significantly.

REFERENCES

Alt, J. C., Teagle, D. A. H., Laverne, C., Vanko, D., Bach, W., Honnorez, J., Becker, K., Ayadi, M., and Pezard, P. A. (1996). "Ridge flank alteration of upper ocean crust in the eastern Pacific: a synthesis of results for volcanic rocks of holes 504B and 896A," in *Proceedings of the ODP, Scientific Results*, Vol. 148, eds J. C. Alt, H. Kinoshita, L. B. Stokking, and P. J. Michael (College Station, TX: Ocean Drilling Program), 434–452.

Altschul, S. F., Madden, T. L., Schaffer, A. A., Zhang, J., Zhang, Z., Miller, W., and Lipman, D. J. (1997). Gapped BLAST and PSI-blast: a new generation of protein data-base search programs. *Nucleic Acids Res.* 25, 3389–3402.

Bach, W., and Edwards, K. J. (2003). Iron and sulfide oxidation within the basaltic ocean crust: implications for chemolithoautotrophic microbial mass production. *Geochim. Cosmochim. Acta* 67, 3871–3887.

Badger, M. R., and Bek, E. J. (2008). Multiple Rubisco forms in proteobacteria: their functional significance in relation to CO_2 acquisition by the CBB cycle. *J. Exp. Bot.* 59, 1525–1541.

Becker, K., and Davis, E. E. (2005). "A review of CORK designs and operations during the ocean drilling program," in *Proceedings of the IODP 301*, eds A. T. Fisher, T. Urabe, A. Klaus, and the Expedition 301 Scientists (College Station, TX: Integrated Ocean Drilling Program Management International, Inc.), 1–28.

Becker, K., Davis, E. E., Spiess, F. N., and de Moustier, C. (2004). Temperature and video logs from the upper oceanic crust, Holes 504B and 896A, Costa Rica Rift flank: implications for the permeability of the upper oceanic crust. *Earth Planet. Sci. Lett.* 222, 881–896.

Brinkhoff, T., Giebel, H.-A., and Simon, M. (2008). Diversity, ecology and genomics of the Roseobacter clade: a short overview. *Arch. Microbiol.* 189, 531–539.

Buchan, A., González, J. M., and Moran, A. M. (2005). Overview of the marine *Roseobacter* lineage. *Appl. Environ. Microbiol.* 71, 5665–5677.

Campbell, B. J., Engel, A. S., Porter, M. L., and Takai, K. (2006). The versatile ε-proteobacteria: key players in sulphidic habitats. *Nat. Rev. Microbiol.* 4, 458–468.

Caumette, P. (1986). Phototrophic sulphur bacteria and sulphate-reducing bacteria causing red waters in a shallow brackish coastal lagoon (Prévost Lagoon, France). *FEMS Microbiol. Ecol.* 38, 113–124.

Cowen, J. P. (2004). The microbial biosphere of sediment-buried oceanic basement. *Res. Microbiol.* 155, 497–506.

Cowen, J. P., Giovannoni, S. J., Kenig, F., Johnson, H. P., Butterfield, D., Rappe, M. S., Hutnak, M., and Lam, P. (2003). Fluids from aging ocean crust that support microbial life. *Science* 299, 120–123.

Davis, E. E., Becker, K., Pettigrew, T., Carson, B., and MacDonald, R. (1992). CORK: a hydrologic seal and downhole observatory for deep-ocean boreholes. *Proc. Ocean Drill. Prog. Init. Rep.* 139, 43–53.

Delwiche, C., and Palmer, J. (1996). Rampant horizontal gene transfer and duplication of RuBisCO genes in eubacteria and plastids. *Mol. Biol. Evol.* 13, 873–882.

DeSantis, T. Z., Hugenholtz, P., Keller, K., Brodie, E. L., Larsen, N., Piceno, Y. M., Phan, R., and Andersen, G. L. (2006a). NAST: a multiple sequence alignment server for comparative analysis of 16S rRNA genes. *Nucleic Acids Res.* 34, W394–W399.

DeSantis, T. Z., Hugenholtz, P., Larsen, N., Rojas, M., Brodie, E. L., Keller, K., Huber, T., Dalevi, D., Hu, P., and Andersen, G. L. (2006b). Greengenes, a chimera-checked 16S rRNA gene database and workbench compatible with ARB. *Appl. Environ. Microbiol.* 75, 5069–5072.

D'Hondt, S., Jørgensen, B. B., Miller, D. J., Batzka, A., Blake, R., Cragg, B. A., Cypionka, H., Dickens, G. R., Ferdelman, T., Hinrichs, K.-U., Holm, N. G., Mitterer, R., Spivack, A., Wang, G., Bekins, B., Engelen, B., Ford, K., Gettemy, G., Rutherford, S., Sass, H., Skilbeck, C. G., Aiello, I. W., Guèrin, G., House, C. H., Inagaki, F., Meister, P., Naher, T., Niitsuma, S., Parkes, R. J., Schippers, A., Smith, D. C., Teske, A., Wiegel, J., Padilla, C. N., and Acosta, J. L. S. (2004). Distributions of microbial activities in deep subseafloor sediments. *Science* 306, 2216–2221.

D'Hondt, S., Spivack, A. J., Pockalny, R., Ferdelman, T. G., Fischer, J. P., Kallmeyer, J., Abrams, L. J., Smith, D. C., Graham, D., Hasiuk, F., Schrum, H., and Stancin, A. M. (2009). Subseafloor sedimentary life in the South Pacific Gyre. *Proc. Nat. Acad. Sci. U.S.A.* 106, 11651–11656.

Edwards, K. J., Rogers, D. R., and Wirsen, C. O. (2003). Isolation and characterization of novel psychrophilic, neutrophilic, Fe-oxidizing chemolithoautotrophic alpha- and gamma-proteobacteria from the

deep-sea. *Appl. Environ. Microbiol.* 69, 2906–2913.

Elsaied, H., and Nagamuna, T. (2001). Phylogenetic diversity of ribulose-1,5-bisphosphate carboxylase/oxygenase large-subunit genes from deep-sea microorganisms. *Appl. Environ. Microbiol.* 67, 1751–1765.

Elsaied, H. E., Kimura, H., and Nagamuna, T. (2007). Composition of archaeal, bacterial, and eukaryal RuBisCO genes in three Western Pacific arc hydrothermal vent systems. *Extremophiles* 11, 191–202.

Engelen, B., Ziegelmüller, K., Wolf, L., Köpke, B., Gittel, A., Cypionka, H., Treude, T., Nakagawa, S., Inagaki, F., Lever, M. A., and Steinsbu, B. O. (2008). Fluids from the ocean crust support microbial activities within deep biosphere. *Geomicrobiol. J.* 25, 56–66.

Fisher, A. T., Davis, E. E., and Becker, K. (2008). Borehole-to-borehole hydrologic response across 2.4 km in the upper oceanic crust: implications for crustal-scale properties. *J. Geophys. Res.* 113, B07106.

Fisher, A. T., Wheat, C. G., Becker, K., Davis, E. E., Jannasch, H., Schroeder, D., Dixon, R., Pettigrew, T. L., Meldrum, R., McDonald, R., Nielsen, R., Fisk, M., Cowen, J., Bach, W., and Edwards, K. (2005). "Scientific and technical design and deployment of long-term, subseafloor observatories for hydrogeologic and related experiments, IODP Expedition 301, eastern flank of Juan de Fuca Ridge," in *Proceedings of the IODP 301*, eds A. T. Fisher, T. Urabe, A. Klaus, and the Expedition 301 Scientists (College Station, TX: Integrated Ocean Drilling Program Management International, Inc.), 1–39.

Fisk, M. R., Giovannoni, S. J., and Thorseth, I. H. (1998). Alteration of oceanic volcanic class: textural evidence of microbial activity. *Science* 281, 978–980.

Furnes, H., Muehlenbachs, K., Torsvik, T., Thorseth, I. H., and Tumyr, O. (2001). Microbial fractionation of carbon isotopes in altered basaltic glass from the Atlantic Ocean, Lau Basin, and Costa Rica Rift. *Chem. Geol.* 173, 313–330.

Giovannoni, S. J., Fisk, M. R., Mullins, T. D., and Furnes, H. (1996). "Microbial activity in the alteration of glass from pillow lavas from ODP Hole 896A," in *Proceedings of the ODP Science Results*, Vol. 148, eds J. C. Alt, H. Kinoshita, L. B. Stokking, and P. J. Michael (College Station, TX: Ocean Drilling Program), 191–206.

Guyoneaud, R., Süling, J., Petri, R., Matheron, R., Caumette, P., Pfennig, N., and Imhoff, J. F. (1998). Taxonomic rearrangements of the genera *Thiocapsa* and *Amoebobacter* on the basis of 16S rDNA sequence analyses, and description of *Thiolamprovum* gen. nov. *Int. J. Syst. Bacteriol.* 48, 957–964.

Hess, W. R., Rocap, G., Ting, C. S., Larimer, F., Stilwagen, S., Lamerdin, J., and Chrisholm, W. (2001). The photosynthetic apparatus of *Prochlorococcus*: insights through comparative genomics. *Photosynth. Res.* 70, 53–71.

Huber, J. A., Johnson, H. P., Butterfield, D. A., and Baross, J. A. (2006). Microbial life in ridge flank crustal fluids. *Environ. Microbiol.* 8, 88–99.

Huber, J. A., Welch, D. B. M., Morrison, H. G., Huse, S. M., Neal, P. R., Butterfield, D. A., and Sogin, M. L. (2007). Microbial population structure in the deep marine biosphere. *Science* 318, 97–100.

Hügler, M., Wirsen, C. O., Fuchs, G., Taylor, C. D., and Sievert, S. M. (2005). Evidence for autotrophic CO_2 fixation via the reductive tricarboxylic acid cycle by members of the epsilon subdivision of proteobacteria. *J. Bacteriol.* 187, 3020–3027.

Hunter, A. G., Kempton, P. D., and Greenwood, P. (1999). Low-temperature fluid-rock interaction – an isotopic and mineralogical perspective of upper crustal evolution, eastern flank of the Juan de Fuca Ridge (JdFR), ODP Leg 168. *Chem. Geol.* 155, 3–28.

Itoh, T., Suzuki, K., and Nakase, T. (1998). *Thermocladium modestius* gen. nov., sp. nov., a new genus of rod-shaped, extremely thermophilic crenarchaeote. *Int. J. Syst. Evol. Microbiol.* 48, 879–887.

Jannasch, H. W., Wirsen, C. O., Nelson, D. C., and Robertson, L. A. (1985). *Thiomicrospira crunogena*, sp. nov., a colorless, sulfur-oxidizing bacterium from a deep-sea hydrothermal vent. *Int. J. Syst. Bacteriol.* 35, 422–424.

Jørgensen, B. B., and Boetius, A. (2007). Feast and famine – microbial life in the deep-sea bed. *Nat. Rev. Microbiol.* 5, 770–781.

Juniper, S. K., Cambon, M.-A, Lesongeur, F., and Barbier, G. (2001). Extraction and purification of DNA from organic rich subsurface sediments (ODP Leg 169S). *Mar. Geol.* 174, 241–247.

Kirchman, D. L. (2002). The ecology of Cytophaga–Flavobacteria in aquatic environments. *FEMS Microbiol. Ecol.* 39, 91–100.

Kirkpatrick, J., Oakley, B., Fuchsman, C., Srinivasan, S., Staley, J. T., and Murray, J. W. (2006). Diversity and distribution of Planctomycetes and related bacteria in the suboxic zone of the Black Sea. *Appl. Environ. Microbiol.* 72, 3079–3083.

Kormas, K., Smith, D. C., Edgcomb, V., and Teske, A. (2003). Molecular analysis of deep subsurface microbial communities in Nankai Trough sediments (ODP Leg 190, Site 1176). *FEMS Microbiol. Ecol.* 45, 115–125.

Kovaleva, O. L., Tourova, T. P., Muyzer, G., Kolganova, T. V., and Sorokin, D. Y. (2011). Diversity of RuBisCO and ATP citrate lyase genes in soda lake sediments. *FEMS Microbiol. Ecol.* 75, 37–47.

Kuenen, J. G., and Veldkamp, H. (1972). *Thiomicrospira pelophila*, gen. nov., sp. nov., a new obligately chemolithotrophic colourless sulfur bacterium. *Antonie van Leeuwenhoek* 38, 241–256.

Kumar, S., Dudley, J., Nei, M., and Tamura, K. (2008). MEGA: a biologist-centric software for evolutionary analysis of DNA and protein sequences. *Brief. Bioinform.* 9, 299–306.

Lane, D. J. (1991). "16S/23S rRNA sequencing," in *Nucleic Acid Techniques in Bacterial Systematics*, eds E. Stackebrandt and M. Goodfellow (New York, NY: John Wiley & Sons), 115–175.

Lever, M. A., Alperin, M., Inagaki, F., Nakagawa, S., Steinsbu, B. O., Teske, A., and IODP Expedition 301 Scientists. (2006). Trends in basalt and sediment core contamination during IODP Expedition 301. *Geomicrobiol. J.* 23, 517–530.

Ludwig, W., Strunk, O., Westram, R., Richter, L., Meier, H., Yadhukumar, Buchner, A., Lai, T., Steppi, S., Jobb, G., Förster, W., Brettske, I., Gerber, S., Ginhart, A., Gross, O., Grumann, S., Hermann, S., Jost, R., König, A., Liss, T., Lüssmann, R., May, M., Nonhoff, B., Reichel, B., Strehlow, R., Stamatakis, A., Stuckmann, N., Vilbig, A., Lenke, M., Ludwig, T., Bode, A., and Schleifer, K.-H. (2004). ARB: a software environment for sequence data. *Nucleic Acids Res.* 32, 1363–1371.

Mottl, M. J. (1989). Hydrothermal convection, reaction, and diffusion in sediments on the Costa Rica Rift flank: pore-water evidence from ODP Sites 677 and 678. *Proc. ODP. Sci. Results* 111, 195–213.

Mottl, M. J., and Gieskes, J. M. (1990). Chemistry of waters sampled from oceanic basement boreholes, 1979–1988. *J. Geophys. Res.* 95, 9227–9242.

Nagamuna, T., Elsaied H. E., Hoshii, G., and Kimura, H. (2007). Bacterial endosymbioses of gutless tube-dwelling worms in nonhydrothermal vent habitats. *Mar. Biotechnol.* 6, 416–428.

Nakagawa, S., Inagaki, F., Suzuki, Y., Steinsbu, B. O., Lever, M. A., Takai, K., Engelen, B, Sako, Y., Wheat, C. G., Horikoshi, K., and Integrated Ocean Drilling Program Expedition 301 Scientists. (2006). Microbial community in black rust exposed to hot ridge flank crustal fluids. *Appl. Environ. Microbiol.* 72, 6789–6799.

Nakagawa, S., and Takai, K. (2008). Deep-sea vent chemoautotrophs: diversity, biochemistry and ecological significance. *FEMS Microbiol. Ecol.* 65, 1–14.

Nishihara, H., Yaguchi, T., Chung, S. Y., Suzuki, K.-I., Yanagi, M., Yamasato, K., Kodama, T., and Igarashi, Y. (1998). Phylogenetic position of an obligately chemoautotrophic, marine hydrogen-oxidizing bacterium, *Hydrogenovibrio marinus*, on the basis of 16S rRNA gene sequences and two form I RubisCO gene sequences. *Arch. Microbiol.* 169, 364–368.

Orcutt, B., Bach, W., Becker, K., Fisher, A. T., Hentscher, M., Toner, B. M., Wheat, C. G., and Edwards, K. J. (2011). Colonization of subsurface microbial observatories deployed in young ocean crust. *ISME J.* 5, 692–703.

Parkes, R. J., Cragg, B. A., and Wellsbury, P. (2000). Recent studies on bacterial populations and processes in subseafloor sediments: a review. *Hydrogeol. J.* 8, 160.

Perner, M., Kuever, J., Seifert, R., Pape, T., Koschinsky, A., Schmidt, K., Strauss, H., and Imhoff, J. F. (2007). The influence of ultramafic rocks on microbial communities at the Logatchev hydrothermal field, located 15°N on the Mid-Atlantic Ridge. *FEMS Microbiol. Ecol.* 61, 97–109.

Rappé, M. S., Connon, S. A., Vergin, K. L., and Giovannoni, S. J. (2002). Cultivation of the ubiquitous SAR11 marine bacterioplankton clade. *Nature* 418, 630–633.

Rappé, M. S., Kemp, P. F., and Giovannoni, S. J. (1997). Phylogenetic diversity of marine coastal picoplankton 16S rRNA genes cloned from the continental shelf off Cape Hatteras, North Carolina. *Limnol. Oceanogr.* 45, 811–826.

Rassa, A. C., McAllister, S. M., Safran, S. A., and Moyer, C. L. (2009). Zetaproteobacteria dominate the colonization and formation of microbial

mats in low-temperature hydrothermal vents at Loihi Seamount, Hawaii. *Geomicrobiol. J.* 26, 623–638.

Ryan, W. B. F., Carbotte, S. M., Coplan, J. O., O'Hara, S., Melkonian, A., Arko, R., Weissel, R. A., Ferrini, V., Goodwillie, A., Nitsche, F., Bonczkowski, J., and Zemsky, R. (2009). Global multi-resolution topography synthesis, *Geochem. Geophys. Geosyst.* 10, Q03014.

Santelli, C. M., Banarjee, N., Bach, W., and Edwards, K. J. (2010). Tapping into the subsurface ocean crust biosphere: low biomass and drilling-related contamination calls for improved quality controls. *Geomicrobiol. J.* 27, 158–169.

Santelli, C. M., Edgcomb, V. P., Bach, W., and Edwards, K. J. (2009). The diversity and abundance of bacteria in habiting seafloor laves positively correlate with rock alteration. *Environ. Microbiol.* 11, 86–98.

Santelli, C. M., Orcutt, B. N., Banning, E., Bach, W., Moyer, C. L., Sogin, M. L., Staudigel, H., and Edwards, K. J. (2008). Abundance and diversity of microbial life in ocean crust. *Nature* 453, 653–656.

Schloss, P. D., and Handelsman, J. (2005). Introducing DOTUR, a computer program for defining operational taxonomic units and estimating species richness. *Appl. Environ. Microbiol.* 71, 1501–1506.

Schloss, P. D., and Handelsman, J. (2006). Introducing SONS, a tool for operational taxonomic unit-based comparisons of microbial community memberships and structures. *Appl. Environ. Microbiol.* 72, 6773–6779.

Scott, K. M., Sievert S. M., Abril, F. N., Ball, L. A., Barrett, C. J., Blake, R. A., Boller, A. J., Chain, P. S., Clark, J. A., Davis, C. R., Detter, C., Do, K. F., Dobrinski, K. P., Faza, B. I., Fitzpatrick, K. A., Freyermuth, S. K., Harmer, T. L., Hauser, L. J., Hügler, M., Kerfeld, C. A., Klotz, M. G., Kong, W. W., Land, M., Lapidus, A., Larimer, F. W., Longo, D. L., Lucas, S., Malfatti, S. A., Massey, S. E., Martin, D. D., McCuddin, Z., Meyer, F., Moore, J. L., Ocampo, L. H. Jr., Paul, J. H., Paulsen, I. T., Reep, D. K., Ren, Q., Ross, R. L., Sato, P. Y., Thomas, P., Tinkham, L. E., and Zeruth, G. T. (2006). The genome of deep-sea vent chemolithoautotroph *Thiomicrospira crunogena* XCL-2. *PLoS Biol.* 4, 2196–2212. doi: 10.1371/journal.pbio.0040383

Shipboard Scientific Party. (1993). "Site 896," in *Proceedings of the ODP, Scientific Results,* eds J. C. Alt, H. Kinoshita, L. B. Stokking, and P. J. Michael (College Station, TX: Ocean Drilling Program), 123–192.

Sorokin, D. Y., Lysenko, A. M., Mityushina, L. L., Tourova, T. P., Jones, E., Rainey, F. A., Robertson, L. A., and Kuenen, J. G. (2001). *Thioalkalimicrobium aerophilum* gen. nov., sp. nov., and *Thioalkalimicrobium sibericum* sp. nov., and *Thioalkalivibrio versutus* gen. nov., sp. nov. *Thioalkalivibrio nitratis* sp. nov., and *Thioalkalivibrio denitrificans* sp. nov., novel obligately alkaliphilic and obligately chemolithoautotrophic sulfur-oxidizing bacteria from soda lakes. *Int. J. Syst. Evol. Microbiol.* 51, 565–580.

Steinsbu, B. O., Thorseth, I. H., Nakagawa, S., Inagaki, F., Lever, M. A., Engelen, B., Øvreas, L., and Pedersen, R. B. (2010). *Archaeoglobus sulfaticallidus* sp. nov., a novel thermophilic and facultative lithoautotrophic sulfate-reducer isolated from black rust exposed to hot ridge flank crustal fluids. *Int. J. Syst. Evol. Microbiol.* 60, 2745–2752.

Suzuki, Y., Inagaki, F., Takai, K., Nealson, K. H., and Horikoshi, K. (2004). Microbial diversity in inactive chimney structures from deep-sea hydrothermal systems. *Microb. Ecol.* 47, 186–196.

Sylvan, J. B., Toner, B. M., and Edwards, K. J. (2012). Life and death of deep-sea vents: bacterial diversity and ecosystem succession on inactive hydrothermal sulfides. *MBio* 3, e00279-11. doi: 10.1128/mBio.00279-11

Takai, K., Nunoura, T., Ishibashi, J., Lupton, J., Suzuki, R., Hamasaki, H., Ueno, Y., Kawagucci, S., Gamo, T., Suzuki, Y., Hirayama, H., and Horikoshi, K. (2008). Variability in the microbial communities and hydrothermal fluid chemistry at the newly discovered Mariner hydrothermal field, southern Lau Basin. *J. Geophys. Res.* 113, G02031.

Taylor, C. D., and Wirsen, C. O. (1997). Microbiology and ecology of filamentous sulfur formation. *Science* 277, 1483–1485.

Torsvik, T., Furnes, H., Muehlenbachs, K., Thorseth, T. H., and Tumyr, O. (1998). Evidence for microbial activity at the glass-alteration interface in oceanic basalts. *Earth Planet. Sci. Lett.* 162, 165–176.

Wagner, M., and Horn, M. (2006). The Planctomycetes, Verrucomicrobia, Chlamydiae and sister phyla comprise a superphylum with biotechnological and medical relevance. *Curr. Opin. Biotechnol.* 17, 241–249.

West, N. J., Schonhuber, W. A., Fuller, N. J., Amann, R. I., Rippka, R., Post, A. F., and Scanlan, D. J. (2001). Closely related *Prochlorococcus* genotypes show remarkably different depth distributions in two oceanic regions as revealed by in situ hybridization using 16S rRNA-targeted oligonucleotides. *Microbiology* 147, 1731–1744.

Wheat, C. G., Jannasch, H. W., Fisher, A. T., Becker, K., Sharkey, J., and Hulme, S. (2010). Subseafloor seawater-basalt-microbe reactions: continuous sampling of borehole fluids in a ridge flank environment. *Geochem. Geophys. Geosyst.* 11, Q07011.

Wheat, C. G., and Mottl, M. J. (2000). Composition of pore and spring waters from Baby Bare: global implications of geochemical fluxes from a ridge flank hydrothermal system. *Geochim. Cosmochim. Acta* 64, 629–642.

Whitman, W. B., Coleman, D. C., and Wiebe, W. J. (1998). Prokaryotes: the unseen majority. *Proc. Natl. Acad. Sci. U.S.A.* 95, 6578–6583.

Wirsen, C. O., Sievert, S. M., Cavanaugh, C. M., Molyneaux, S. J., Ahmad, A., Taylor, L. T., DeLong, E. F., and Taylor, C. D. (2002). Characterization of an autotrophic sulfide-oxidizing marine *Arcobacter* sp. that produces filamentous sulfur. *Appl. Environ. Microbiol.* 68, 316–325.

Conflict of Interest Statement: The authors declare that the research was conducted in the absence of any commercial or financial relationships that could be construed as a potential conflict of interest.

Received: 22 March 2011; accepted: 07 June 2012; published online: 29 June 2012.

Citation: Nigro LM, Harris K, Orcutt BN, Hyde A, Clayton-Luce S, Becker K and Teske A (2012) Microbial communities at the borehole observatory on the Costa Rica Rift flank (Ocean Drilling Program Hole 896A). Front. Microbio. ***3****:232. doi: 10.3389/fmicb.2012.00232*

This article was submitted to Frontiers in Extreme Microbiology, a specialty of Frontiers in Microbiology.

frontiers in
MICROBIOLOGY

ORIGINAL RESEARCH ARTICLE
published: 30 August 2012
doi: 10.3389/fmicb.2012.00311

Stratified active archaeal communities in the sediments of Jiulong River estuary, China

*Qianqian Li[1,2], Fengping Wang[1,2], Zhiwei Chen[3], Xijie Yin[4] and Xiang Xiao[1,2]**

[1] State Key Laboratory of Microbial Metabolism, School of Life Science and Biotechnology, Shanghai, P.R. China
[2] State Key Laboratory of Ocean Engineering, Shanghai Jiao Tong University, Shanghai, P.R. China
[3] School of Life Sciences, Xiamen University, Xiamen, China
[4] Third Institute of Oceanography, State Oceanic Administration, Xiamen, P.R. China

Edited by:
Andreas Teske, University of North Carolina at Chapel Hill, USA

Reviewed by:
Matthew Schrenk, East Carolina University, USA
Aharon Oren, The Hebrew University of Jerusalem, Israel
Runar Stokke, University of Bergen, Norway

****Correspondence:***
Xiang Xiao, Laboratory of Microbial Oceanography, Department of Life Science and Biotechnology, Shanghai Jiao Tong University, 800 Dongchuan Road, Shanghai 200240, China.
e-mail: xoxiang@sjtu.edu.cn

Here the composition of total and active archaeal communities in a sediment core of Jiulong River estuary at Fujian Province, Southern China was reported. Profiles of CH_4 and SO_4^{2-} concentrations from the sediment core indicated the existence of a sulfate-methane transition zone (SMTZ) in which sulfate reduction-coupled anaerobic oxidation of methane (AOM) occurs. Accordingly, three sediment layers (16–18.5 cm, 71–73.5 cm, and 161–163.5 cm) from the 1.2 m sediment core were sectioned and named top, middle and bottom, respectively. Total DNA and RNA of each layer were extracted and used for clone libraries and sequence analysis of 16S rRNA genes, the reverse transcription (RT)-PCR products of 16S rRNA and methyl CoM reductase alpha subunit (*mcrA*) genes. Phylogenetic analysis indicated that archaeal communities of the three layers were dominated by the Miscellaneous Crenarchaeotal Group (MCG) whose ecological functions were still unknown. The MCG could be further divided into seven subgroups, named MCG-A, B, C, D, E, F, and G. MCG-A and MCG-G were the most active groups in the estuarine sediments. Known anaerobic methanotrophic archaea (ANMEs) were only found as minor components in these estuarine archaeal communities. This study, together with the studies of deep subsurface sediments, would be a very good start point to target and compare the specific active archaeal groups and their roles in the dark, deep subsurface sediment environments.

Keywords: archaea, methanogen, ANME, SMTZ, anaerobic oxidation of methane, *mcrA*, estuary, microbial community

INTRODUCTION

Marine subsurface sediments probably constitute one of the largest reservoirs of biomass on Earth (Whitman et al., 1998). The diversity of prokaryotic communities in various marine sediments has been studied extensively, but most microbial phylotypes belong to uncultivated groups of unknown physiology and ecological functions (Sørensen and Teske, 2006). Uncultivated archaea, such as Marine Group I (MG-I), Marine Group II (MG-II), Miscellaneous Crenarchaeotic Group (MCG), Marine Benthic Group B (MBGB), Marine Benthic Group D (MBGD) were found not only as dominant groups at some deep-sea sediments, but were also widespread in various environments in nature. These groups were suggested to play important roles in the global cycling of carbon and nitrogen (Orphan et al., 2001; Teske and Sørensen, 2008). However, more investigations were needed to understand the environmental factors associated with their biogeographic distributions, their phylogeny and physiology, and the biogeochemical roles of these archaea in the environment.

Significant amounts of methane are produced in marine sediments. The release of methane to the atmosphere results in the increasing rate of global warming and chemical composition changes (Lelievelda et al., 1993; Hanson and Hanson, 1996). However, nearly all the methane in marine sediments is oxidized before reaching the aerobic waters column and the atmosphere by anaerobic oxidation of methane (AOM) coupled to sulfate reduction catalyzed by microbes in the marine sediments. The main niche for AOM in marine sediments is the sulfate-methane transition zone (SMTZ), where methane produced in the sediments and sulfate from seawater overlap and provide a minimum yield of energy for anaerobic methanotrophs (Knittel and Boetius, 2009). Anaerobic methanotrophic archaea (ANME), named ANME-1, ANME-2, and ANME-3, are believed to be the main players in AOM (Boetius et al., 2000). However, in SMTZs from some deep marine subsurface sediments, such as from Peru Margin sites, ANMEs were not detected, but other uncultivated archaeal groups including South African Gold Mine Euryarchaeotic Group (SAGMEG), MCG and MBGB were found as main components (Inagaki et al., 2006). In a sediment core from Peru Margin site 1227 (Ocean Drilling Program Leg 201), members of MCG and MBGB archaea were found to be more active in the SMTZ than in sediment layers above and below, suggesting either direct or indirect involvement of these archaea in AOM (Sørensen and Teske, 2006).

Estuarine sediments, with complex geochemical profiles, are another important environment that shows high biological activity rates. The archaeal communities in the sediments of tropical,

subtropical and temperate estuaries were dominated by uncultivated archaeal groups, such as MG-I predominant at the near-surface sediments, while MCG distributed throughout the vertical level of the sediment cores (Vieira et al., 2007; Singh et al., 2010; Webster et al., 2010; Jiang et al., 2011). Studies on Pearl River (China) and Santos-Sao Vicente (Brazil) revealed obvious SMTZs in the sediment cores (Saia et al., 2009; Jiang et al., 2011). ANME group ANME-2 was supposed to be the main group with AOM functions in Pearl River estuarine sediment (Jiang et al., 2011). All of these above studies were conducted to investigate the total archaeal community based on the cellular DNA level, which could not exclude the inactive or dead cells persisting in the environments. Here, we aim to investigate the diversity and distribution of both total and active archaeal communities in the sediment of Jiulong River estuary which is located in the southern tropical region in Fujian Province, southern China. The Jiulong River is one of the largest river/estuary systems in southern China with a length of 285 km and an area of 14,741 km^2 (Maskaoui et al., 2002). The river provides large input of freshwater to the Xiamen's coastal waters (**Figure A1**). Our study was designed to: (1) reveal the diversity and abundance of archaea in the Jiulong River estuary by 16S rRNA analysis; (2) reveal the active archaeal communities and their distribution along the sediment core; (3) figure out the vertical distribution profile of archaea involved in the methane cycle by functional methyl co-enzyme M reductase A gene (*mcrA*) analysis. This study would provide more information on the distribution and activity of live archaeal communities in estuarine environments, and would be valuable as an analog of deep subsurface habitats in subsurface microbial investigations.

MATERIALS AND METHODS

STUDY SITE AND SAMPLING

The study site is the Jiulong River estuary (24°24′48.6″ N, 117°56′30.5″ E) in Fujian province, China (**Figure A1**).

A sediment core of 1.2 m was taken using a single-core sampler in December, 2009. The water depth for sampling was about 3.0 m. The bottom water temperature was 13.5°C and the salinity at the sediments surface was 2%. The sediments were mainly composed of sandy clay. The diameter of sediment core was 5.0 cm. The core was sectioned into 2.5 cm slices and transferred to sterile Falcon tubes on a clean bench. Samples were kept at −20°C and then stored at −70°C after back to the laboratory until analysis.

METHANE AND SULFATE CONCENTRATION ANALYSIS

Methane concentrations were measured as following. The subsamples were immediately taken from the central part of the core. Then, 3.0 ml subsamples were transferred with syringes to Bellco anaerobic tubes (Bellco Glass Inc., Vineland, NJ) each containing 6.0 ml of 1 M NaOH. The vials were closed with black butyl rubber stoppers and aluminum crimp seals immediately. After that, the vials were shaken vigorously for 2 min, and 0.5 ml of gas sample from the headspace of each vial was analyzed by the gas chromatograph (Agilent 6820) equipped with a flame ionization detector using a Porapak Q column (2 m × 3 mm). N_2 was the carrier gas with a flow rate of 30 ml/min. Methane peaks were recorded and compared with methane standards. The concentration was recalculated to μmol/l pore water using the sediment volume and the independently determined porosity.

The sulfate concentration was determined by ion chromatography (Dionex DX-600) according to the methods of Jiang et al. (2009).

DNA AND RNA EXTRACTION AND PURIFICATION

In order to avoid contamination, all the DNA and RNA extractions were carried out using the central part of the sediment core with a diameter of around 1 cm. Three parts of sediment core were separated and labeled as: top (16.0–18.5 cm), middle (71.0–73.5 cm) and bottom (161.0–163.5 cm). The DNA was extracted according to the method described earlier (Xu et al., 2007) and the purification was carried out using a Cycle Pure Kit (OMEGA, USA).

RNA was extracted directly from sediment samples using a Soil RNA Kit according to the manufacturer's manual (OMEGA, USA).

CLONE LIBRARIES CONSTRUCTION, RFLP ANALYSIS, AND DNA SEQUENCING

The archaeal 16S rRNA gene fragments were amplified from the three sediment layers by PCR using the primer pair Arch21F (TTCCGGTTGATCCYGCCGGA) and Arch958R (YCCGCGTTGAMTCCAATT) (Lane, 1991; Wagner et al., 1998). The reverse transcription (RT)-PCR of 16S rRNA fragments were carried out using a RevertAid™ First Strand cDNA Synthesis Kit (Fermentas, CAN) by primer Arch958R for the first strand synthesis and PCR amplification by primers Arch21F/Arch958R. For the *mcr*A gene fragments, PCR was performed using the primer pairs ME1 (GCMATGCARATHGGWATGTC) and ME2 (TCATKGCRTAGTTDGGRTAGT) (Hales et al., 1996). The PCR was carried out with the following reaction mix: 100–200 ng sediment DNA, 10.0 pmol of each primer, 10 × PCR reaction buffer, 1.5 mM $MgCl_2$, 200.0 μM dNTP, and 5.0 U Taq polymerase, to give a final volume of 50.0 μl. Thermal cycling was performed with the following protocol: 94°C for 4 min, 30 cycles of 94°C for 1 min, 55°C for 1 min, 72°C for 1 min, and a final step at 72°C for 10 min. The negative controls without DNA were set in parallel.

The amplified fragments were purified using UNIQ-10 PCR product purification kit (Sangon). The fragments were ligated into the pMD18-T vector (TaKaRa) following the manufacturer's instructions and transformed into the competent cells of *Escherichia coli* DH5α. Positive clones were randomly picked for Restriction fragment length polymorphisms (RFLP) analysis.

Cloned PCR products were analyzed by RFLP. The PCR products were purified and digested by restriction enzymes *Rsa*I and *Msp*I. The DNA fragments were separated on 3% (w/v) agarose gel by electrophoresis to screen the clones for grouping into similar clone types. Representative clones with unique RFLP bands were chosen for further sequencing using Sanger sequencing method (Sangon Inc., Shanghai, China).

QUANTITATIVE PCR ANALYSIS OF ARCHAEAL 16S rRNA GENES

The abundance of archaeal and bacterial 16S rRNA genes was evaluated by fluorescence quantitative real-time PCR with the primer sets Arch344f/Arch519r for archaea (Bano et al., 2004) and

Eubac341f/Eubac518r for bacteria (Dilly et al., 2004) on a 7500 Real-time System (Applied Biosystems). Standard curves were constructed by using the method described earlier (Wang et al., 2009). All the amplifications were performed in 20.0 μl reaction mixture with 1.0 μl template DNA, 0.15 μM of each primer, and 10.0 μl of Power SYBR Green PCR Master Mix with ROX and SybrGreen I (Applied Biosystems). Cycle thresholds were set automatically using the 7500 system software, Version 1.3. The average of three replicates was performed.

STATISTICAL AND PHYLOGENETIC ANALYSIS

The coverage of the library was calculated with the formula $C = 1 - (n_1/N)$, where n_1 is the number of single-occurrence phylotypes within a library and N is the total number of clones analyzed (Mullins et al., 1995). The Shannon-Wiener index and Evenness (equitability) were calculated using the equations from Krebs (1989). The richness was estimated by Chao1 estimator (http://www2.biology.ualberta.ca/jbrzusto/rarefact.php).

The 16S rRNA genes retrieved in this study were first submitted to the CHIMERA-CHECK program at the Ribosomal Database Project II (Maidak et al., 2001) to check and remove chimeric sequences. The non-chimeric sequences were submitted to the BLAST search program on the NCBI (National Center for Biotechnology Information) website (http://blast.ncbi.nlm.nih.gov/Blast.cgi) and RDP (Ribosomal Database Project) website (http://rdp.cme.msu.edu/) to identify close relatives. The ARB-software package (Ludwig et al., 2004) and SILVA rRNA sequence database (http://www.arb-silva.de/) were used for sequence alignment. Sequences with identities of greater than 97% were tentatively assigned to one OTU (Operation taxonomic units) using the DOTUR (Schloss and Handelsman, 2005). One sequence per OTU was chosen for the construction of phylogenetic trees. The *mcrA* genes were translated into amino acids at SIB ExPASy (Expert Protein Analysis System) website (http://web.expasy.org/translate/). Sequence alignments with portions of both the 16S rRNA gene and deduced amino acids sequences of McrA were carried out by CLUSTAL X 1.83 software. The phylogenetic trees were constructed by the neighbor-joining and minimum evolution method by Mega 3.1 software (Kumar et al., 2004) with the bootstrap analysis used to estimate the confidence of tree topologies (Saitou and Nei, 1987). The phylogenetic trees presented here were constructed by the neighbor-joining method.

NUCLEOTIDE SEQUENCE ACCESSION NUMBERS

The nucleotide and amino acid sequences obtained in this study were submitted to the NCBI Genbank database with the accession numbers JQ245808–JQ245854 for *mcrA* genes, JQ245855–JQ245893 for RT-PCR products of 16S rRNA and JQ245894–JQ245962 for 16S rRNA genes.

RESULTS

PROFILES OF SULFATE AND METHANE

The concentrations of sulfate and methane along the sediment core were measured as described in the materials and methods section (**Figure 1A**). The sulfate concentration was highest at the sediment surface, and declined with the depth to less than 2.0 mM below 86 cm. The methane concentration was low at the sediment surface and increased rapidly within the interval from 56.0 cm to 76.0 cm; highest concentration of 6.0 mM was reached at 76.0 cm depth. Therefore, the depth between 60.0 and 80.0 cm was defined as SMTZ.

CELL ABUNDANCE AND QUANTIFICATION OF ARCHAEAL 16S rRNA GENES

The archaea and bacteria in the sediment core were quantified by Q-PCR of 16S rRNA genes. The number of bacterial 16S rRNA

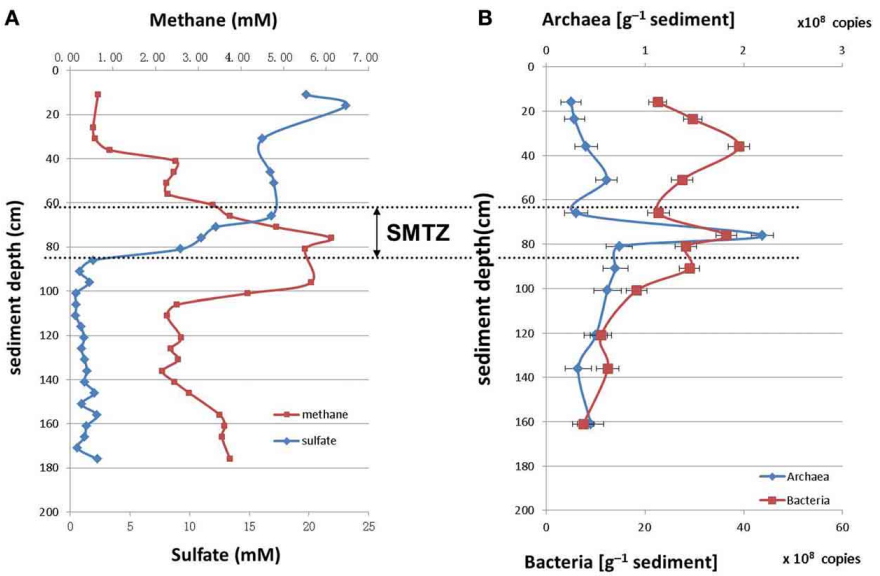

FIGURE 1 | Depth distributions of methane/sulfate concentrations (A) and archaeal/bacterial 16S rRNA gene abundances (number of gene copies/g [wet weight]) (B) in sediments of Jiulong River estuary.

genes varied from 2.52×10^8 to 2.19×10^9 copies/g (wet weight), and that of archaea were from 10^7 to 10^8 copies/g (wet weight) in the sediment core. Overall, the 16S rRNA gene copy number of bacteria was 10 times higher than that of archaea. The archaea reached the highest proportion at the depth between 60.0 and 80.0 cm within the SMTZ (**Figure 1B**).

ARCHAEAL COMMUNITY STRUCTURE

The archaeal communities in the three layers were investigated by library construction and phylogenetic analysis. From each library of the three sediment layers, 50 positive clones were selected randomly for RFLP analysis and sequencing. The coverage values of the 16S rRNA gene libraries were from 85 to 91.5%. According to the Shannon-Wiener index, Simpson's index, Evenness index and Chao-1 estimator, the archaeal diversity in the top layer was higher than the middle and bottom layer (**Table 1**).

BLAST search results showed that most retrieved archaeal 16S rRNA gene sequences were closely related to uncultured archaeal sequences. Phylogenetic analysis indicated the archaeal communities of the three layers were all composed of *Crenarchaeota* and *Euryarchaeota*. MCG were dominant in all libraries, representing more than 50% of the sequenced clones (**Figure 2A**). Methanogens within the order *Methanosarcinales* were detected in every layer, most abundantly in the middle layer. However, the ANME groups which had the function of AOM were not detected in the libraries. MG-I was only detected at the top layer; *Methanocellales* and Lake Valkea Kotinen cluster III (VALIII) groups were found in the middle layer; MBGB were detected at bottom layer; Marine Hydrothermal Vent Group (MHVG) and MBGD were represented in both top and bottom layer, but were absent at the middle layer.

The retrieved crenarchaeal sequences could be classified into MCG, MG-I, and MBGD. Most MCG were closely related to clones from various environments, such as mangrove sediment (GenBank No. FJ477323, DQ363755, DQ363772, and DQ363807), salt marsh sediments (GenBank No. FJ655678 and FJ655681), continental margin sediments (GenBank No. FJ455923 and FJ455926), deep sea sediment with the presence of methane hydrate (GenBank No. EU713901), waste water sludge (GenBank No. CU916834) and petroleum contaminated soil (GenBank No. AB161330, AB161334, and AB161339). According to the previous classification (Jiang et al., 2011), the MCG sequences retrieved from the sediment cores could be assigned to MCG-A, -B, -C, -D, -E, -F, and a new subgroup MCG-G (**Figure 2C**). Other phylogenetic groups represented only small proportions of the three clone libraries, and these sequences were most closely related to clones from deep sea sediments (**Figure A2A**).

Sequences within *Methanosarcinales* were most dominant in *Euryarchaeota* (**Figure A2B**). Related 16S rRNA gene sequences in GenBank originated mostly from wastewater sludge (GenBank No. CU917326), a minerotrophic fen (GenBank No. EU155903 and EU155916), an anaerobic bioreactor (GenBank No. FJ347533), fresh water (GenBank No. AJ937876) and an oil well (GenBank No. EU721747). Clone MID15A was closely related to the cultured species *Methanosarcina horonobensis*, isolated from groundwater in a Miocene subsurface formation (Shimizu et al., 2011). Clones within *Methanocellales*, Terrestrial Miscellaneous Euryarchaeotic Group (TMEG), MBGD, South African Gold Mine Euryarchaeotic Group (SAGMEG) and VALIII were related to clones from a minerotrophic fen (GenBank No. EU155960 and EU155985), a hydrothermal field (GenBank No. AB329758), salt marsh sediments (GenBank No. FJ655585, FJ655615, and FJ655660), and deep-sea methane seep sediments (GenBank No. EU713893).

ACTIVE ARCHAEAL COMMUNITY STRUCTURE

Three 16S rRNA clone libraries were constructed and analyzed in the same way as the 16S rRNA gene clone libraries. The coverage values of the three libraries were from 82.9 to 85.2%. Archaeal diversity in the bottom layer was higher than in the top and middle layer (**Table 1**).

According to the phylogenetic analysis (**Figure 2B**), 16S rRNA sequences were affiliated with the MCG, MBGB, and MHVG within *Crenarchaeota*, and with the *Methanosarcinales*, *Methanomicrobiales*, MBGD and TMEG within the *Euryarchaeota*. Most of the archaeal clones were related to uncultivated archaea.

The top and bottom layers were dominated by MCG archaea, and specifically by sequences within the MCG-A, MCG-B, MCG-E, MCG-F, and MCG-G subgroups (**Figure 2D**). Sequences from MCG-G subgroup accounted for 57% of all MCG clones. These sequences were >95% similar to environmental sequences.

Table 1 | Coverage, diversity, and richness evaluation of constructed libraries.

Library	Layer	Coverage %	Shannon-Wiener index	Simpson's index (1-D)	Evenness	Chao 1 estimator
Archaeal 16S rDNA	Top	85.0	3.230	0.957	0.930	33.1
	Middle	87.5	2.997	0.946	0.910	20.8
	Bottom	91.5	2.761	0.930	0.879	19.6
Archaeal 16S rRNA-based	Top	85.2	2.166	0.859	0.793	13.0
	Middle	82.9	1.952	0.774	0.589	18.0
	Bottom	82.9	2.361	0.875	0.707	23.2
mcrA	Top	86.3	2.762	0.931	0.879	27.0
	Middle	92.7	2.507	0.910	0.876	15.5
	Bottom	90.5	2.479	0.906	0.852	22.0

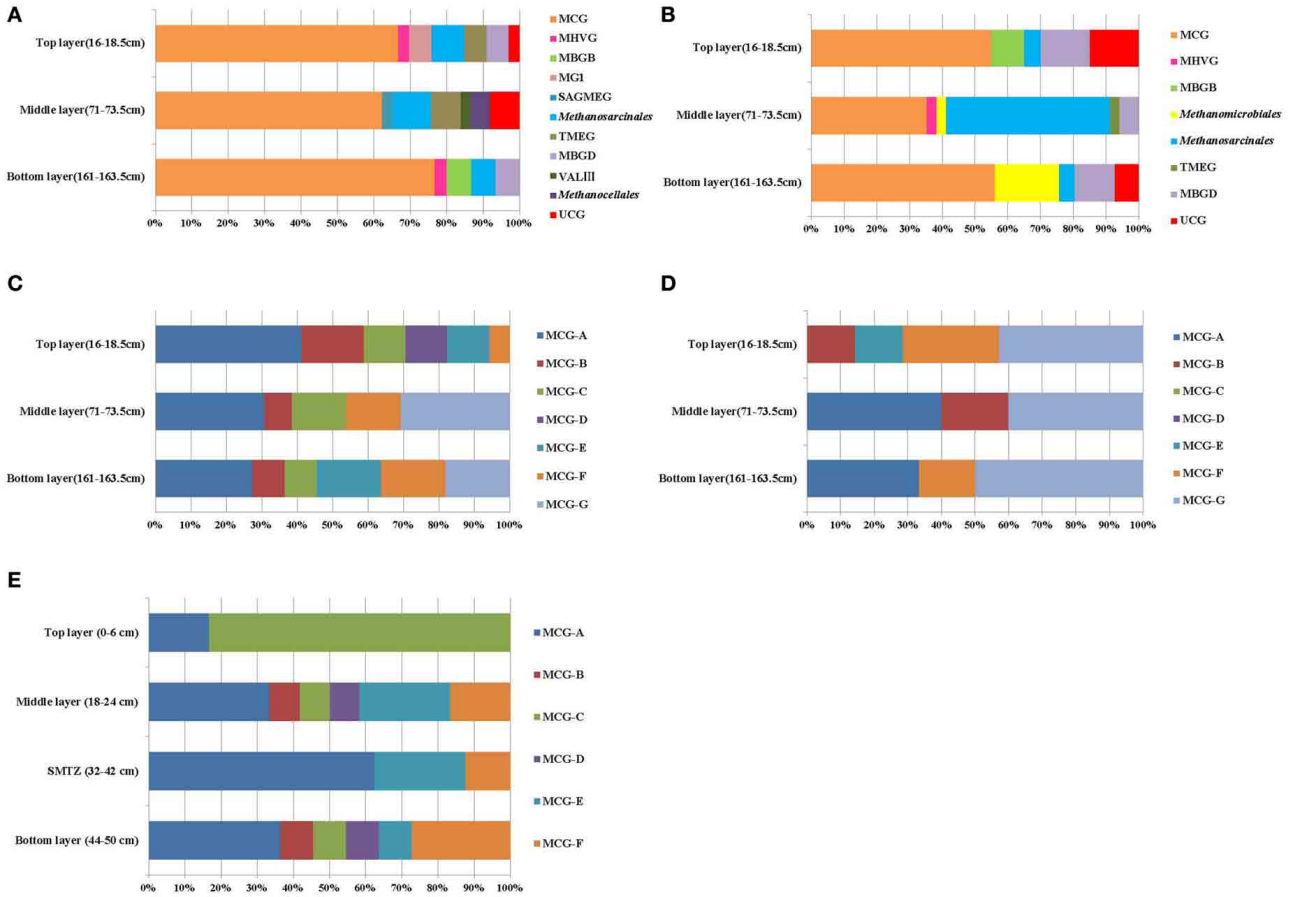

FIGURE 2 | Compositions of archaeal members in 16S rRNA gene clone libraries (A) and 16S rRNA clone libraries (B), MCG subgroups in the 16S rRNA gene clone libraries (C) and 16S rRNA clone libraries (D), and MCG subgroups in 16S rRNA gene clone libraries of Pearl River Estuary (E). Groups shown include Miscellaneous Crenarchaeotal Group (MCG), marine benthic group B (MBGB), Marine Group I (MGI), South African Gold Mine Euryarchaeotic Group (SAGMEG), Terrestrial Miscellaneous Euryarchaeotal Group (TMEG), marine benthic group D (MBGD), Lake Valkea Kotinen cluster III (VALIII), Marine Hydrothermal Vent Group (MHVG), *Methanosarcinales*, *Methanomicrobiales*, and *Methanocellales*.

Sequences of the MCG-A subgroup were detected in middle and bottom layers, while sequences of the MCG-B subgroup were found in the top and middle layers (**Figure A3**).

Among the *Euryarchaeota*, 28% of all clones clustered within the *Methanosarcinales*. Of these, 40% belonged to the ANME-2a branch and originated from the SMTZ. These sequences were closely related to clones from a hydrothermal chimney (GenBank No. AB464787) and marine sediment (GenBank No. AB252424). Clones within the *Methanomicrobiales* and MBGD were also frequently found, and were mostly related to clones from a minerotrophic fen (GenBank No. EU155976, EU155979, and EU155985), salt marsh sediment (GenBank No. FJ655701) and mangrove soil (GenBank No. DQ363830). MBGB was only detected in the top layer (**Figure 3A**).

PHYLOGENETIC ANALYSIS OF *MCRA* GENES

Low diversities were found in the three *mcrA* libraries (**Table 1**), indicating a low diversity of archaea involved in methane cycling in this environment.

Cloned *mcrA* genes belonged to the *Methanomicrobiales*, *Methanosarcinales*, *Methanobacteriales*, and *Methanocellales*. Members of the *Methanomicrobiales* were predominant, and accounted for an average of 80% in all three clone libraries, whereas members of the *Methanosarcinales*, *Methanobacteriales* and *Methanocellales* constituted around 13, 2, and 5%, respectively (**Figure 4**). *mcrA* genes from ANME groups were not detected in the libraries.

Among the *Methanomicrobiales*, 44% of all *mcrA* clones from the top, middle and bottom sediment layers showed over 90% similarity with clones from gassy subsurface sediments of Marennes-Oleron Bay and Fuca Ridge hydrothermal vent (GenBank No. AM942085, AM942099, FJ640793, and FJ640795-FJ640798). Only clone MID_ME_45 was 87% similar to clone mcrA3 from Fuca Ridge hydrothermal vent (Wang et al., 2009). Other retrieved sequences of *Methanomicrobiales* shared highest identity with clones from an oligotrophic fen (GenBank No. AJ489771), brackish lake sediment (GenBank No. AY625601), a solid waste bioreactor (GenBank No. FJ435883) and tidal creek sediment (GenBank No. EU301989).

Sequences among the order *Methanosarcinales* were closely related (91–98% similarity) to clones from rice field soil (GenBank No. AF313863). Clone BOT_ME_23 was most similar with clones from marine sediment, but also shared 92% sequences similarity with *Methanosarcina horonobensis* (Shimizu et al., 2011). Clones within *Methanocellales* were related to *Methanocella paludicola* (GenBank No. AP011532) with low similarities (84–85%), except clone BOT_ME_10 (95%). Sequences within the *Methanobacteriales* were associated with phylotypes from sediment of the Pearl River Estuary (GenBank No. EU681950) and from deep crustal fluid (GenBank No. AY768819) (**Figure 3B**).

DISCUSSION

Most studies on archaeal diversity and distribution were carried out on DNA level, whereas fewer analyses were performed on RNA level to identify active microbial community members (Harrison et al., 2009; Jiang et al., 2011). Here, we investigated not only the abundance and diversity of the archaeal community in the sediments of the Jiulong River estuary, but also the active members by parallel DNA and RNA analysis. Compared with the DNA libraries, the diversity and abundance of clones from RNA-based libraries were lower (**Table 1**), probably reflecting reduced numbers and phylogenetic diversity of active archaeal community members in the environment. According to the phylogenetic analysis, archaeal members of MCG, MHVG, MBGB, TMEG, and *Methanosarcinales* were common groups in DNA and RNA libraries. On the other hand, MG-I, VALIII, *Methanocellales,* and SAGMEG groups were only found at DNA level, while MBGD, ANME-2, and *Methanomicrobiales* groups were only detected at RNA level. The differences of the archaeal compositions found at the DNA and RNA level suggested a difference of archaeal presence and activity in the environment (Sørensen and Teske, 2006).

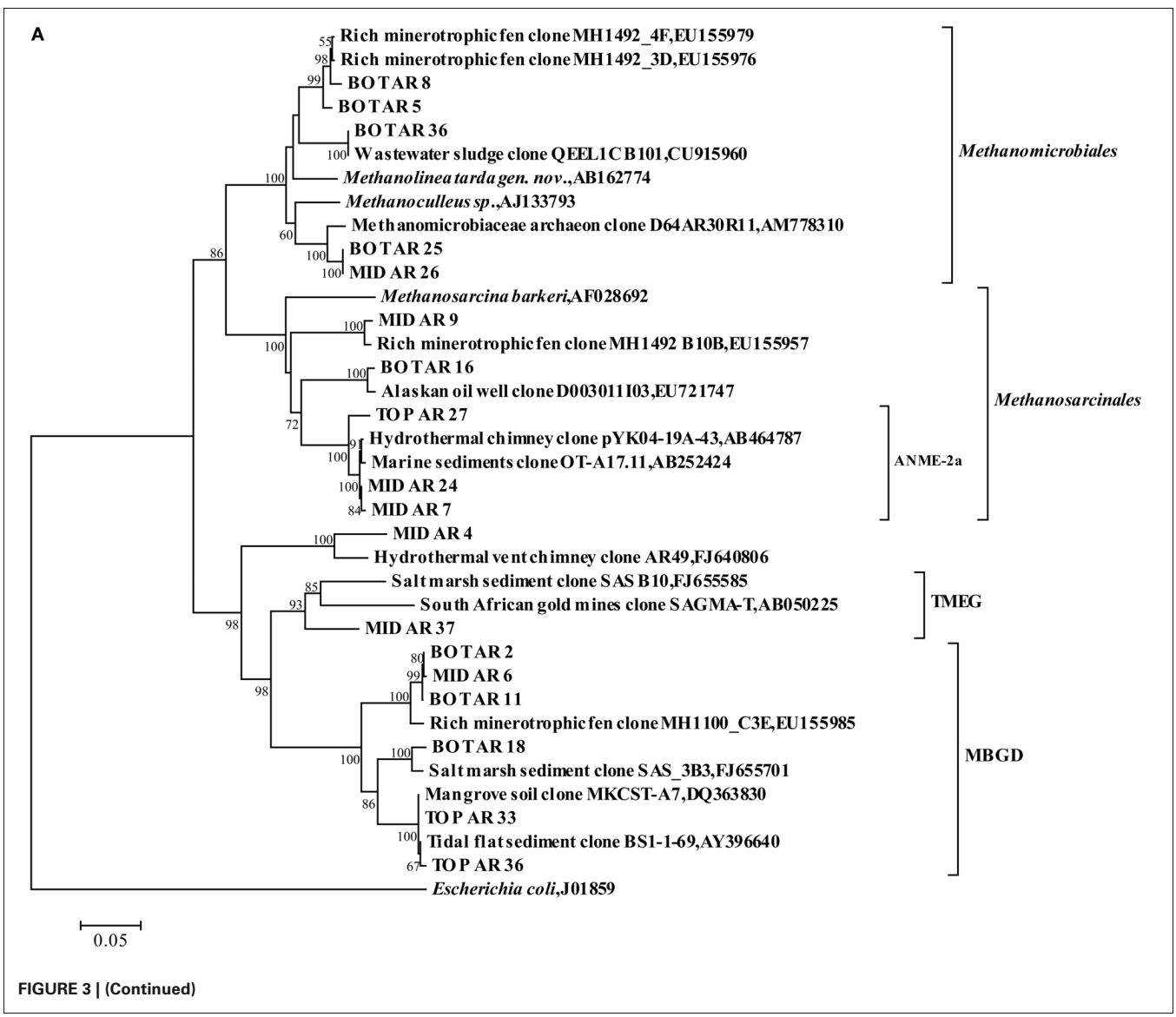

FIGURE 3 | (Continued)

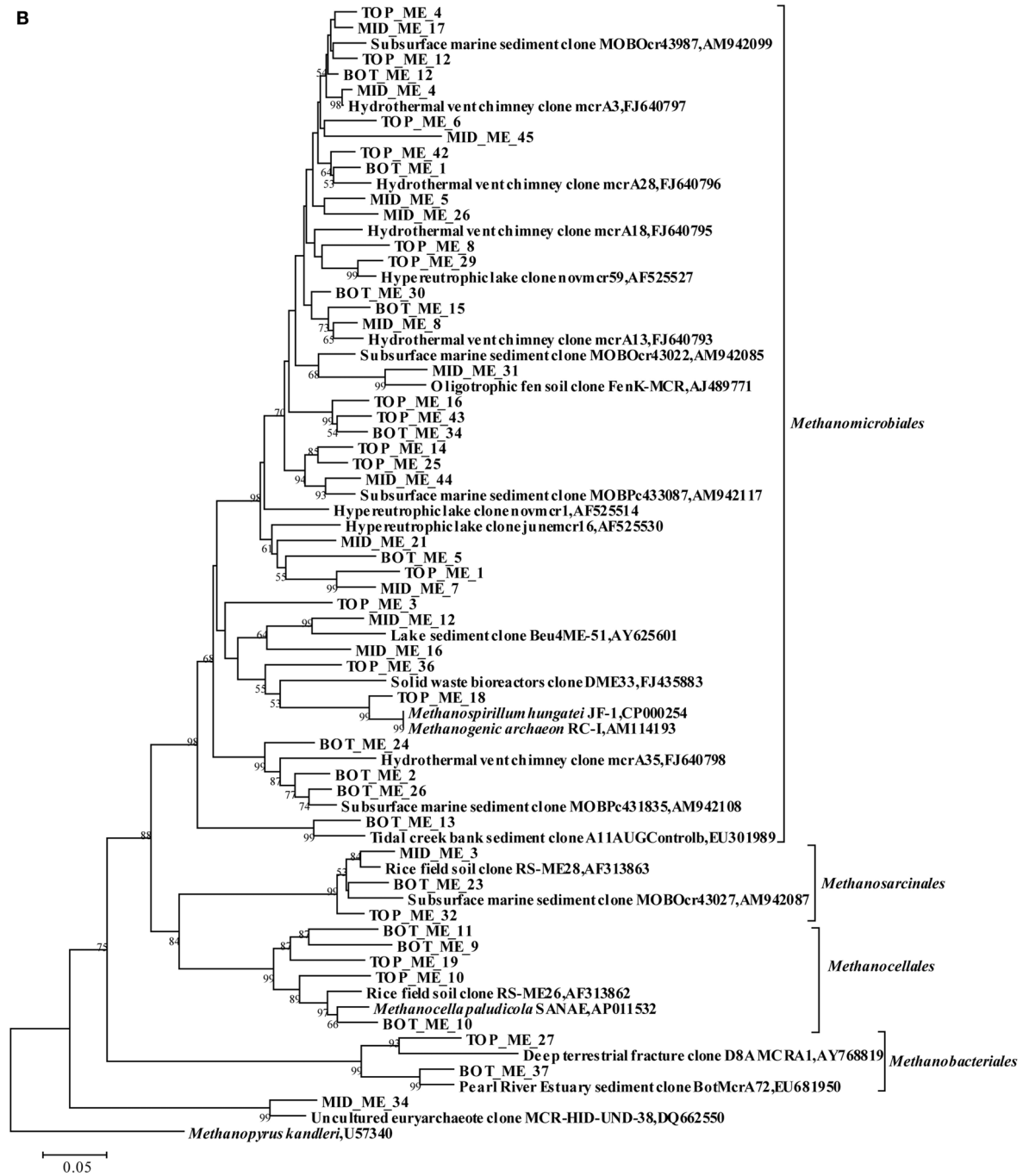

FIGURE 3 | Phylogenetic trees showing the affiliations of euryarchaeal RT-PCR products of 16S rRNA sequences (A) and *mcrA* gene sequences (B) retrieved from this study with selected reference sequences, respectively. The clones from the top, middle and bottom layers are differentiated as TOP, MID, and BOT, respectively. The trees were constructed by neighbor-joining, using nearly full-length aligned nucleotides sequences with *Escherichia coli* J01859 or *methanopyrus* as outgroups, respectively. Bootstrap values are based on 1000 replicates and are shown at the nodes with more than 50% bootstrap support. The scale bars represent 5% sequence divergence. TMEG: Terrestrial Miscellaneous Euryarchaeotal Group; MBGD: Marine Benthic Group D; ANME: anaerobic methane-oxidizing archaea.

MCG was found to be prevalent through the sediment core. Although MCG was frequently detected in marine and terrestrial environments, the ecological function of this group was still poorly constrained; MCG archaea were suggested to represent heterotrophic anaerobes that utilize and assimilate complex organic substrates (Biddle et al., 2006). Jiang et al divided MCG into six subgroups (MCG-A to MCG-F) (Jiang et al., 2011). We found that MCG-C could be further divided into MCG-C

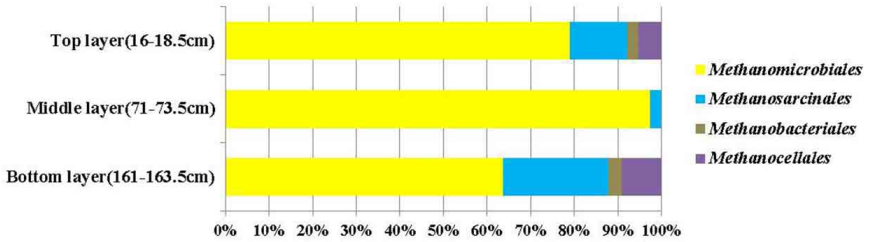

FIGURE 4 | Compositions of *mcrA* gene clone libraries from top, middle (SMTZ) and bottom layers. Groups shown include *Methanomicrobiales*, *Methanosarcinales*, *Methanobacteriales*, and *Methanocellales*.

and MCG-G (**Figure A2A**), and may be further divided into more subgroups when more sequences are available. The MCG-A subgroup was detected most frequently at DNA level, and had the widest distribution among MCG subgroups in all three sediment layers. This result was consistent with the result from that of Pearl River estuarine sediments (**Figure 2E**) where MCG-A was also identified as the most frequently detected archaeal group (Jiang et al., 2011). The DNA sequences retrieved from the Jiulong River estuary and Pearl River Estuary were both related to similar phylotypes from terrestrial habitats, coastal marine sediments and estuarine sediments. However, although MCG-A was predominant at DNA level, MCG-G subgroup was the most frequently detected at RNA level, and should therefore represent the active archaeal subgroup in this estuarine environment. However, only DNA-level diversity analysis has been carried out in the Pearl River estuary (Jiang et al., 2011), and RNA data from this and other estuaries are still missing. The physiology and ecological function of MCG-G is at present unknown, but it was found widespread in various environments including salt mash sediments, mangrove soil, deep-sea sediments, and hydrothermal fluids (Reed et al., 2002; Yan et al., 2006; Kato et al., 2009; Nelson et al., 2009). The distribution, physiology and biogeochemical functions of different MCG subgroups may vary significantly; more careful and intensive studies are required such as designing of specific primers for specific MCG subgroups to monitor their distribution and the correlation with the environments. Other approaches such as metagenomic, metatranscriptomic analysis, in combination with stable isotope probing and/or single cell sequencing and Nano-SIMS would eventually discover the ecological roles of these unknown uncultivated MCG groups.

Within the *Euryarchaeota*, *Methanosarcinales,* and *Methanocellales* were detected in all layers on DNA level. However, no ANME groups were found. At RNA level, *Methanosarcinales* was the major group, especially in the SMTZ; and *Methanomicrobiales* was the second most dominant methanogenic group. The presence of active methanogens (*Methanosarcinales* and *Methanomicrobiales*) in all three layers indicated methanogenic activity in the sediments. Another Euryarchaeal phylotype detected by 16S rRNA and rDNA analysis was MBGD. Although, MBGD sequences in this study were related to counterparts from various marine and terrestrial environments, the MBGD group is generally associated with methane-rich environments (Pachiadaki et al., 2011). The potential role of MBGD in methane metabolism is still unclear.

ANME groups, known as methane-oxidizing archaea, were not detected at DNA level. ANME-1 is distantly affiliated with the *Methanosarcinales* and *Methanomicrobiales*, while ANME-2 and ANME-3 belong to the *Methanosarcinales* (Hinrichs et al., 1999; Orphan et al., 2001; Knittel et al., 2005). At RNA level, 60% of the clones within the order *Methanosarcinales* could be identified as ANME-2, and 40% of these clones were from the SMTZ. No gene expression of *mcrA* was detected, indicating a low proportion of *mcrA* mRNA in the total RNA sample. Nevertheless, the analysis of *mcrA* gene sequences revealed methanogens in this estuarine environment; phylotypes associated with the *Methanomicrobiales* were found dominant, especially in the middle layer. This divergent *mcrA* and 16S rRNA results might be due to the differences in average copy number between the 16S rRNA and *mcrA* genes in the genomes of different methanogens (Nunoura et al., 2008). However, phylotypes associated with ANME groups were not found in the *mcrA* clone library. In this study, ANME-2 was only detected in the 16S rRNA clone library, but absence in 16S rRNA gene library and *mcrA* library, suggesting a very low proportion of ANME in the community. The flack of detection of ANME phylotypes in the *mcrA* DNA library could also have results from limited clone sequencing performed in this study. It is still an open question whether other archaea detected in this environment such as MBGB, MBGD, and MCG play a role in the methane oxidation process.

Knowing the microbes that are alive or active in the deep subsurface sediment environments will help us to figure out the biogeochemical roles of these species. Our study, together with others, would be a good start to understand the specific live archaeal groups and their roles in the deep subsurface sediment environments. Briefly, this is the first step to reveal the active archaeal members in Jiulong River estuarine sediments, and eventually understand their physiology and biogeochemical roles of these largely unknown uncultivated archaea in nature.

ACKNOWLEDGMENTS

This work was supported by National Science Foundation of China (Grant Nos. 40830213, 30821005, and 41006072), a grant from the Science and Technology Commission of Shanghai Municipality (Grant No. 10JC1406700) and a grant from the State Key Laboratory of Ocean Engineering in China (grant no. GKZD010053-1).

REFERENCES

Bano, N., Ruffin, S., Ransom, B., and Hollibaugh, J. T. (2004). Phylogenetic composition of Arctic Ocean archaeal assemblages and comparison with Antarctic assemblages. *Appl. Environ. Microbiol.* 70, 781–789.

Biddle, J. F., Lipp, J. S., Lever, M. A., Lloyd, K. G., Sørensen, K. B., Anderson, R., Fredricks, H. F., Elvert, M., Kelly, T. J., Schrag, D. P., Sogin, M. L., Brenchley, J. E., Teske, A., House, C. H., and Hinrichs, K. U. (2006). Heterotrophic *Archaea* dominate sedimentary subsurface ecosystems off Peru. *Proc. Natl. Acad. Sci. U.S.A.* 103, 3846–3851.

Boetius, A., Ravenschlag, K., Schubert, C. J., Rickert, D., Widdel, F., Gieseke, A., Amann, R., Jorgensen, B. B., Witte, U., and Pfannkuche, O. (2000). A marine microbial consortium apparently mediating anaerobic oxidation of methane. *Nature* 407, 623–626.

Dilly, O., Bloem, J., Vos, A., and Munch, J. C. (2004). Bacterial diversity in agricultural soils during litter decomposition. *Appl. Environ. Microbiol.* 70, 468–474.

Hales, B. A., Edwards, C., Ritchie, D. A., Hall, G., Pickup, R. W., and Saunders, J. R. (1996). Isolation and identification of methanogen-specific DNA from blanket bog peat by PCR amplification and sequence analysis. *Appl. Environ. Microbiol.* 62, 668–675.

Hanson, R. S., and Hanson, T. E. (1996). Methanotrophic bacteria. *Microbiol. Rev.* 60, 439–471.

Harrison, B. K., Zhang, H., Berelson, W., and Orphan, V. J. (2009). Variations in archaeal and bacterial diversity associated with the sulfate-methane transition zone in continental margin sediments (Santa Barbara Basin, California). *Appl. Environ. Microbiol.* 75, 1487–1499.

Hinrichs, K. U., Hayes, J. M., Sylva, S. P., Brewer, P. G., and Delong, E. F. (1999). Methane-consuming archaebacteria in marine sediments. *Nature* 398, 802–805.

Inagaki, F., Nunoura, T., Nakagawa, S., Teske, A., Lever, M., Lauer, A., Suzuki, M., Takai, K., Delwiche, M., Colwell, F. S., Nealson, K. H., Horikoshi, K., D'hondt, S., and Jorgensen, B. B. (2006). Biogeographical distribution and diversity of microbes in methane hydrate-bearing deep marine sediments on the Pacific Ocean margin. *Proc. Natl. Acad. Sci. U.S.A.* 103, 2815–2820.

Jiang, L., Zheng, Y., Chen, J., Xiao, X., and Wang, F. (2011). Stratification of Archaeal communities in shallow sediments of the Pearl River Estuary, Southern China. *Antonie Van Leeuwenhoek* 99, 739–751.

Jiang, L., Zheng, Y., Peng, X., Zhou, H., Zhang, C., Xiao, X., and Wang, F. (2009). Vertical distribution and diversity of sulfate-reducing prokaryotes in the Pearl River estuarine sediments, Southern China. *FEMS Microbiol. Ecol.* 70, 249–262.

Kato, S., Yanagawa, K., Sunamura, M., Takano, Y., Ishibashi, J., Kakegawa, T., Utsumi, M., Yamanaka, T., Toki, T., Noguchi, T., Kobayashi, K., Moroi, A., Kimura, H., Kawarabayasi, Y., Marumo, K., Urabe, T., and Yamagishi, A. (2009). Abundance of *Zetaproteobacteria* within crustal fluids in back-arc hydrothermal fields of the Southern Mariana Trough. *Environ. Microbiol.* 11, 3210–3222.

Knittel, K., and Boetius, A. (2009). Anaerobic oxidation of methane: progress with an unknown process. *Annu. Rev. Microbiol.* 63, 311–334.

Knittel, K., Losekann, T., Boetius, A., Kort, R., and Amann, R. (2005). Diversity and distribution of methanotrophic *Archaea* at cold seeps. *Appl. Environ. Microbiol.* 71, 467–479.

Krebs, C. J. (1989). *Ecological Methodology*. New York, NY: Harper and Row.

Kumar, S., Tamura, K., and Nei, M. (2004). MEGA3, integrated software for molecular evolutionary genetics analysis and sequence alignment. *Brief. Bioinform.* 5, 150–163.

Lane, D. J. (1991). "16S/23S rRNA sequencing," in *Nucleic Acid Techniques in Bacterial Systematics*, eds E. Stackebrandt and M. Goodfellow (Chichester: Wiley), 115–175.

Lelievelda, J., Crutzena, P. J., and Brühla, C. (1993). Climate effects of atmospheric methane. *Chemosphere* 26, 739–768.

Ludwig, W., Strunk, O., Westram, R., Richter, L., Meier, H., Yadhukumar, Buchner, A., Lai, T., Steppi, S., Jobb, G., Forster, W., Brettske, I., Gerber, S., Ginhart, A. W., Gross, O., Grumann, S., Hermann, S., Jost, R., Konig, A., Liss, T., Lussmann, R., May, M., Nonhoff, B., Reichel, B., Strehlow, R., Stamatakis, A., Stuckmann, N., Vilbig, A., Lenke, M., Ludwig, T., Bode, A., and Schleifer, K. H. (2004). ARB: a software environment for sequence data. *Nucleic Acids Res.* 32, 1363–1371.

Maidak, B. L., Cole, J. R., Lilburn, T. G., Parker, C. T. Jr., Saxman, P. R., Farris, R. J., Garrity, G. M., Olsen, G. J., Schmidt, T. M., and Tiedje, J. M. (2001). The RDP-II (Ribosomal Database Project). *Nucleic Acids Res.* 29, 173–174.

Maskaoui, K., Zhou, J. L., Hong, H. S., and Zhang, Z. L. (2002). Contamination by polycyclic aromatic hydrocarbons in the Jiulong River Estuary and Western Xiamen Sea, China. *Environ. Pollut.* 118, 109–122.

Mullins, T. D., Britschgi, T. B., Krest, R. L., and Giovannoni, S. J. (1995). Genetic comparisons reveal the same unknown bacterial lineages in Atlantic and Pacific bacterioplankton communities. *Limnol. Oceanogr.* 40, 148–158.

Nelson, K. A., Moin, N. S., and Bernhard, A. E. (2009). Archaeal diversity and the prevalence of *Crenarchaeota* in salt marsh sediments. *Appl. Environ. Microbiol.* 75, 4211–4215.

Nunoura, T., Oida, H., Miyazaki, J., Miyashita, A., Imachi, H., and Takai, K. (2008). Quantification of *mcrA* by fluorescent PCR in methanogenic and methanotrophic microbial communities. *FEMS Microbiol. Ecol.* 64, 240–247.

Orphan, V. J., House, C. H., Hinrichs, K. U., McKeegan, K. D., and Delong, E. F. (2001). Methane-consuming *Archaea* revealed by directly coupled isotopic and phylogenetic analysis. *Science* 293, 484–487.

Pachiadaki, M. G., Lykousis, V., Stefanou, E. G., and Kormas, K. A. (2011). Prokaryotic community structure and diversity in the sediments of an active submarine mud volcano (Kazan mud volcano, East Mediterranean Sea). *FEMS Microbiol. Ecol.* 72, 429–444.

Reed, D. W., Fujita, Y., Delwiche, M. E., Blackwelder, D. B., Sheridan, P. P., Uchida, T., and Colwell, F. S. (2002). Microbial communities from methane hydrate-bearing deep marine sediments in a forearc basin. *Appl. Environ. Microbiol.* 68, 3759–3770.

Saia, F., Domingues, M., Pellizari, V., and Vazoller, R. (2009). Occurrence of methanogenic *Archaea* in highly polluted sediments of tropical Santos-Sao Vicente Estuary (Sao Paulo, Brazil). *Curr. Microbiol.* 60, 66–70.

Saitou, N., and Nei, M. (1987). The neighbor-joining method: a new method for reconstructing phylogenetic trees. *Mol. Biol. Evol.* 4, 406–425.

Schloss, P. D., and Handelsman, J. (2005). Introducing DOTUR, a computer program for defining operational taxonomic units and estimating species richness. *Appl. Environ. Microbiol.* 71, 1501–1506.

Shimizu, S., Upadhye, R., Ishijima, Y., and Naganuma, T. (2011). *Methanosarcina horonobensis* sp. nov., a methanogenicarchaeon isolated from a deep subsurface Miocene formation. *Int. J. Syst. Evol. Microbiol.* 61, 2503–2507.

Singh, S. K., Verma, P., Ramaiah, N., Chandrashekar, A. A., and Shouche, Y. S. (2010). Phylogenetic diversity of archaeal 16S rRNA and ammonia monooxygenase genes from tropical estuarine sediments on the central west coast of India. *Res. Microbiol.* 161, 177–186.

Sørensen, K. B., and Teske, A. (2006). Stratified communities of active *Archaea* in deep marine subsurface sediments. *Appl. Environ. Microbiol.* 72, 4596–4603.

Teske, A., and Sørensen, K. B. (2008). Uncultured Archaea in deep marine subsurface sediments: have we caught them all? *ISME J.* 2, 3–18.

Vieira, R. P., Clementino, M. M., Cardoso, A. M., Oliveira, D. N., Albano, R. M., Gonzalez, A. M., Paranhos, R., and Martins, O. B. (2007). Archaeal communities in a tropical estuarine ecosystem: Guanabara Bay, Brazil. *Microb. Ecol.* 54, 460–854.

Wagner, M., Roger, A. J., Flax, J. L., Brusseau, G. A., and Stahl, D. A. (1998). Phylogeny of dissimilatory sulfite reductases supports an early origin of sulfate respiration. *J. Bacteriol.* 180, 2975–2982.

Wang, F., Zhou, H., Meng, J., Peng, X., Jiang, L., Sun, P., Zhang, C., Van Nostrand, J. D., Geng, Y., He, Z., Wu, L., Zhou, J., and Xiao, X. (2009). GeoChip-based analysis of metabolic diversity of microbial communities at the Juan de Fuca Ridge hydrothermal vent. *Proc. Natl. Acad. Sci. U.S.A.* 106, 4840–4845.

Webster, G., Rinna, J., Roussel, E. G., Fry, J. C., Weightman, A. J., and Parkes, R. J. (2010). Prokaryotic functional diversity in different biogeochemical depth zones in tidal sediments of the Severn Estuary, UK, revealed by stable-isotope

probing. *FEMS Microbiol. Ecol.* 72, 179–197.

Whitman, W. B., Coleman, D. C., and Wiebe, W. J. (1998). Prokaryotes: the unseen majority. *Proc. Natl. Acad. Sci. U.S.A.* 95, 6578–6583.

Xu, M., Wang, F., Meng, J., and Xiao, X. (2007). Construction and preliminary analysis of a metagenomic library from a deep-sea sediment of east Pacific Nodule Province. *FEMS Microbiol. Ecol.* 62, 233–241.

Yan, B., Hong, K., and Yu, Z. N. (2006). Archaeal communities in mangrove soil characterized by 16S rRNA gene clones. *J. Microbiol.* 44, 566–571.

Conflict of Interest Statement: The authors declare that the research was conducted in the absence of any commercial or financial relationships that could be construed as a potential conflict of interest.

Received: 07 November 2011; accepted: 07 August 2012; published online: 30 August 2012.

Citation: Li Q, Wang F, Chen Z, Yin X and Xiao X (2012) Stratified active archaeal communities in the sediments of Jiulong River estuary, China. Front. Microbio. ***3****:311. doi: 10.3389/fmicb. 2012.00311*

This article was submitted to Frontiers in Extreme Microbiology, a specialty of Frontiers in Microbiology.

APPENDIX

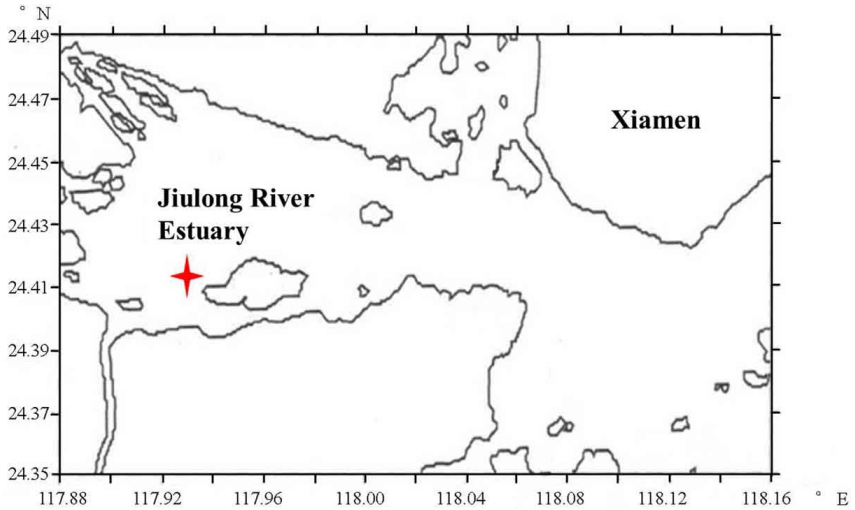

FIGURE A1 | Map of sampling site in the Jiulong River estuary. The asterisk indicates the sampling site (24°24′48.6″ N, 117°56′30.5″ E).

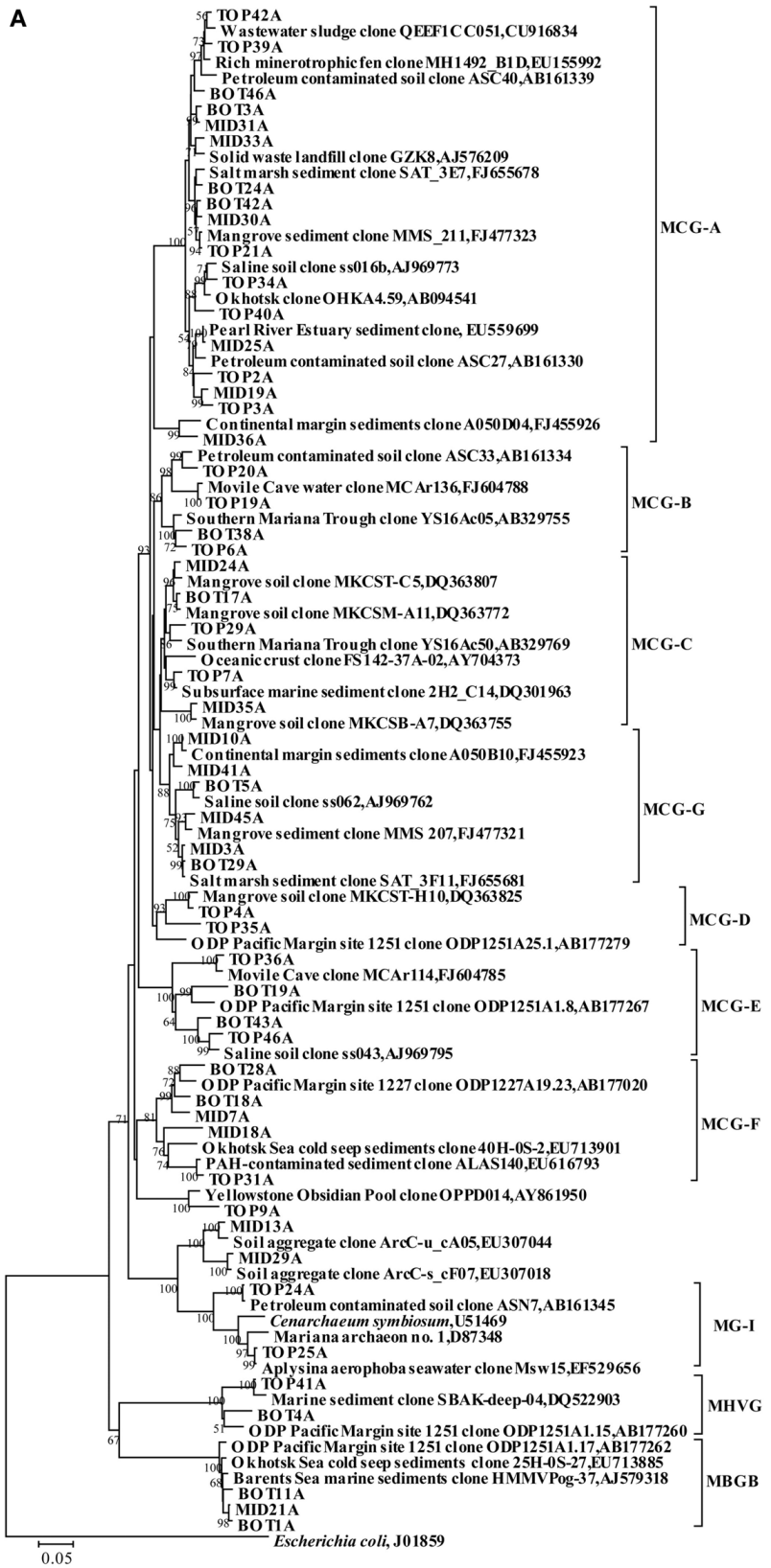

FIGURE A2 | (Continued)

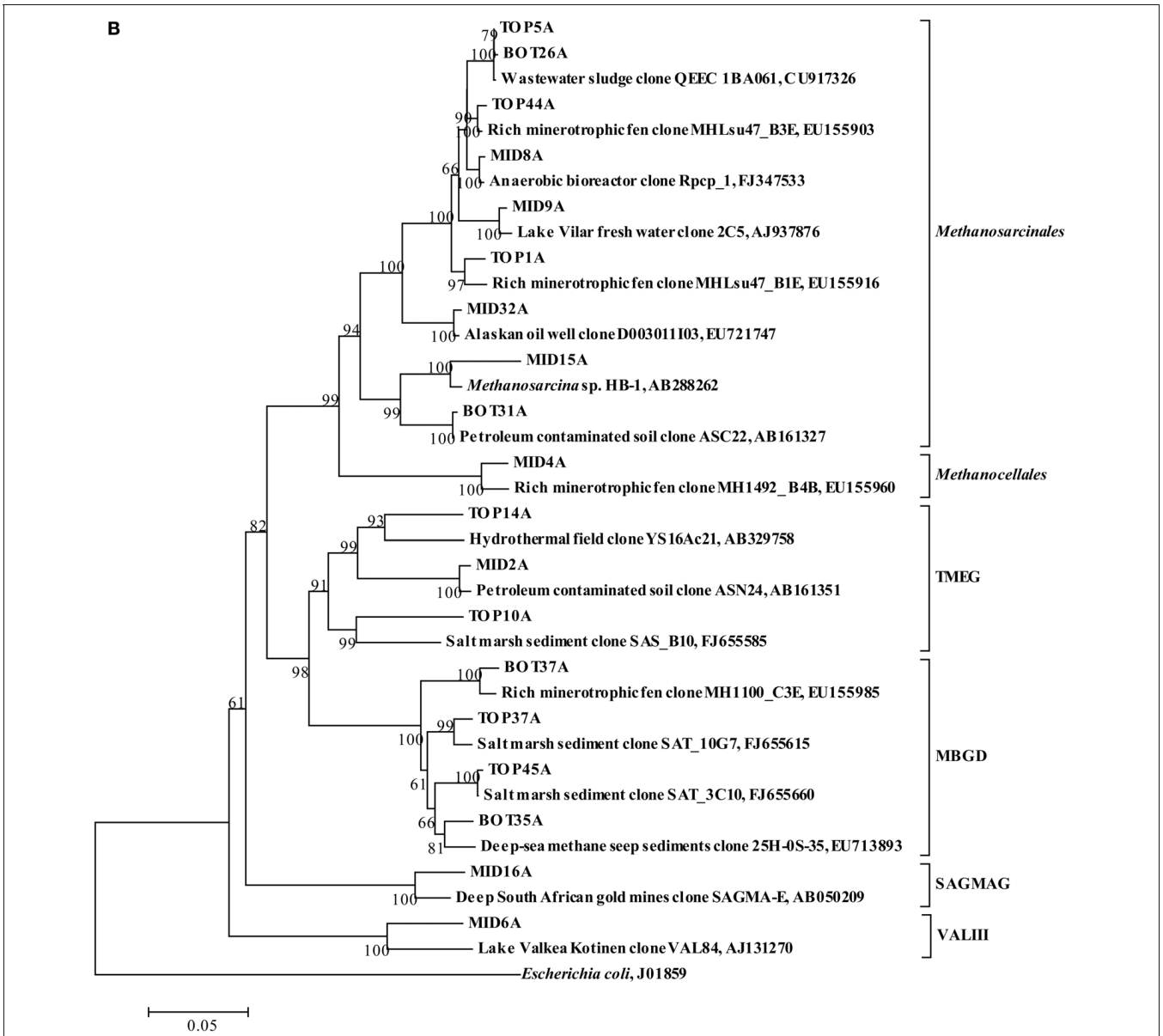

FIGURE A2 | Phylogenetic trees showing the affiliations of crenarchaeal (A) and euryarchaeal (B) 16S rRNA gene sequences retrieved from this study with selected reference sequences. The clones from the top, middle, and bottom layers are differentiated as TOP, MID, and BOT, respectively. The trees were constructed by the neighbor-joining, using nearly full-length aligned nucleotides sequences with *E. coli* J01859 as outgroup. Bootstrap values are based on 1000 replicates and are shown at the nodes with more than 50% bootstrap support. The scale bars represent 5% sequence divergence. MCG: Miscellaneous Crenarchaeotal Group; MHVG: Marine Hydrothermal Vent Group; MG1: Marine Group I; SAGMEG: South African Gold Mine Euryarchaeotic Group; MBGB: Marine Benthic Group B; TMEG: Terrestrial Miscellaneous Euryarchaeotal Group; MBGD: Marine Benthic Group D; VALIII: Lake Valkea Kotinen cluster III.

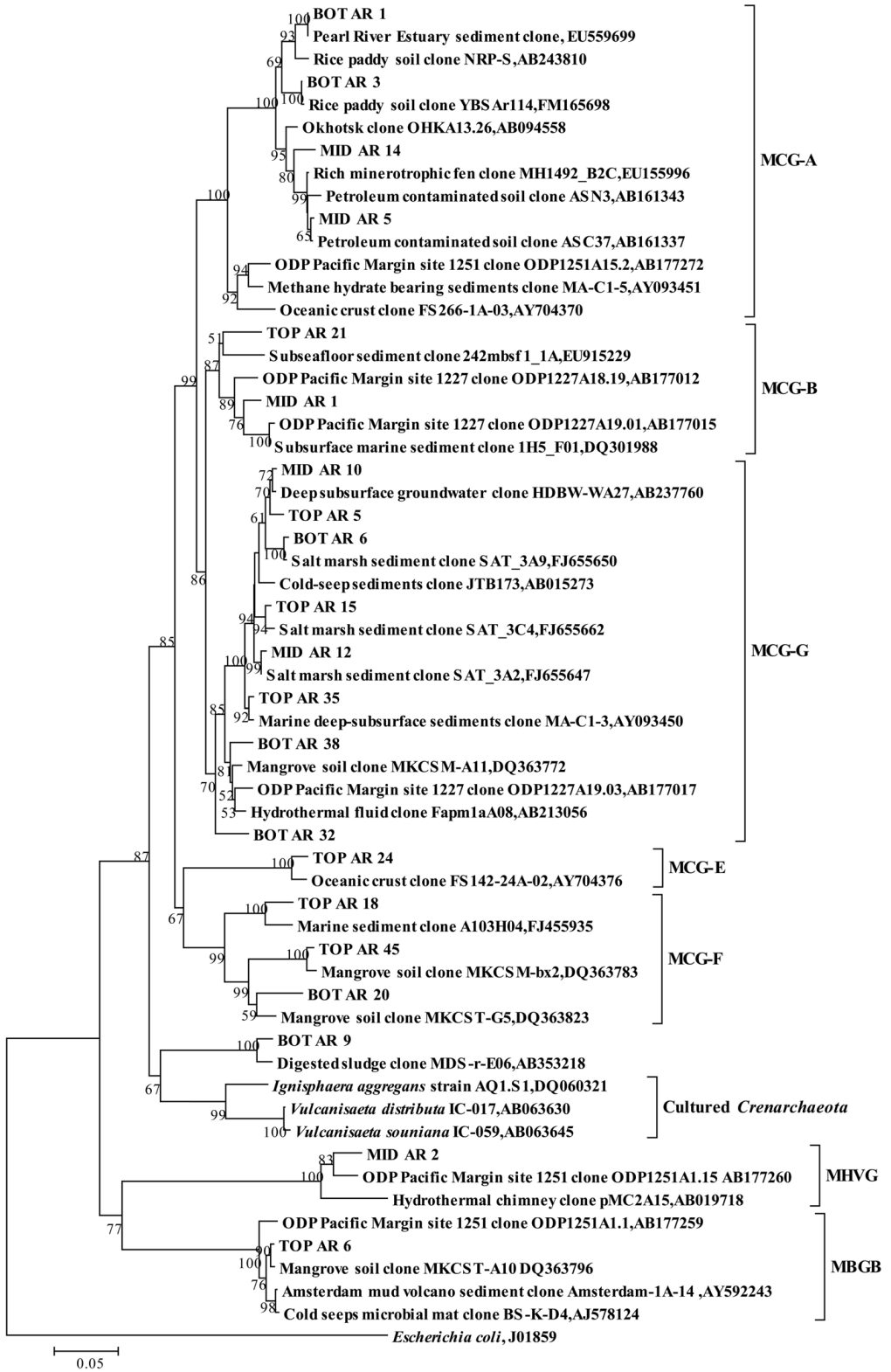

FIGURE A3 | Phylogenetic tree showing the affiliations of crenarchaeal RT-PCR products of 16S rRNA sequences retrieved from this study with selected reference sequences. The clones from the top, middle and bottom layers are differentiated as TOP, MID, and BOT, respectively. The tree was constructed by the neighbor-joining, using nearly full-length aligned nucleotides sequences with *E. coli* J01859 as outgroup. Bootstrap values are based on 1000 replicates and are shown at the nodes with more than 50% bootstrap support. The scale bar represents 5% sequence divergence. MCG: Miscellaneous Crenarchaeotal Group; MHVG: Marine Hydrothermal Vent Group; MBGB: Marine Benthic Group B.

frontiers in
MICROBIOLOGY

EDITORIAL
published: 16 May 2013
doi: 10.3389/fmicb.2013.00122

Deep subsurface microbiology: a guide to the research topic papers

Andreas Teske[1]*, Jennifer F. Biddle[2], Virginia P. Edgcomb[3] and Axel Schippers[4]

[1] *Department of Marine Sciences, University of North Carolina at Chapel Hill, Chapel Hill, NC, USA*
[2] *School of Marine Science and Policy, College of Earth, Ocean, and the Environment, University of Delaware, Lewes, DE, USA*
[3] *220 McLean Laboratory, Department of Geology and Geophysics, Woods Hole Oceanographic Institution, Woods Hole, MA, USA*
[4] *Department of Resource Geochemistry, Federal Institute for Geosciences and Natural Resources (BGR), Hannover, Germany*
**Correspondence: teske@email.unc.edu*

Edited by:
Martin G. Klotz, University of North Carolina at Charlotte, USA

Reviewed by:
Martin G. Klotz, University of North Carolina at Charlotte, USA

Deep subsurface microbiology is a rising field in geomicrobiology, environmental microbiology and microbial ecology that focuses on the molecular detection and quantification, cultivation, biogeographic examination, and distribution of bacteria, archaea, and eukarya that permeate the subsurface biosphere. The deep biosphere includes a variety of subsurface habitats, such as terrestrial deep aquifer systems or mines, deeply buried hydrocarbon reservoirs, marine sediments and the basaltic ocean crust. The deep subsurface biosphere abounds with uncultured, only recently discovered and—at best—incompletely understood microbial populations. So far, microbial cells and DNA remain detectable at sediment depths of more than 1 km and life appears limited mostly by heat in the deep subsurface. Severe energy limitation, either as electron acceptor or donor shortage, and scarcity of microbially degradable organic carbon sources are among the evolutionary pressures that may shape the genomic and physiological repertoire of the deep subsurface biosphere. Its biogeochemical importance in long-term carbon sequestration, subsurface elemental cycling and crustal aging, is a major focus of current research at the interface of microbiology, geochemistry, and biosphere/geosphere evolution. The papers of this Frontiers e-volume bear evidence of the rapid advances in deep subsurface microbiology.

The reader will notice several conspicuous recurring themes in this Frontiers Research topic. This volume opens with a thoroughly argued perspective article on Acetogenesis in the subsurface by Lever (2012), and an accompanying commentary by Oren (2012). Both papers are providing a fresh perspective and a "call to arms" to consider and to investigate acetogenesis as an energetically feasible and widespread pathway that sustains deep subsurface life. These papers argue convincingly that in order to understand the deep subsurface biosphere, major microbial processes in addition to sulfate reduction, methanogenesis and anaerobic methane oxidation have to be explored.

Meanwhile, the microbial cycling of methane and sulfate in the deep subsurface is studied not only with qualitative functional gene surveys but also with functional gene-based molecular quantifications. Schippers et al. (2012) and Blazejak and Schippers (2011) add functional gene qPCR and sequencing to a wide molecular arsenal to quantify and identify the sulfate-reducing and methanogenic microbial communities in organic-rich, reducing marine sediments of Namibia, the Black Sea, and the Peru Margin; the former paper includes an excellent overview on cell counts, qPCR and CARD-FISH quantifications of bacterial and archaeal communities in deep subsurface sediments. In a high-throughput pyrosequencing survey, Mills et al. (2012b) examine the active bacterial community of the methane/sulfate interface in heterotrophic deep marine sediment in the Nankai Trough offshore Japan; by reverse transcription and sequencing of 16S rRNA, they show that the simultaneous presence of methane and sulfate impacts the active bacterial subsurface community only minimally—obviously, other geochemical parameters need to be accounted for. In contrast, hydrocarbon seeps are the extreme endmember of a reducing sedimentary regime that is indeed dominated by microbial sulfate- and methane cycling. Its world-wide distribution remains to be accounted for fully, and is explored here by Siegert et al. (2011) with an Indonesian example. In a combined cultivation-based and functional gene expression study, Ünal et al. (2012) investigated the trace metal requirements and dosage effects on the activity and diversity of methanogen populations in a terrestrial subsurface coal bed. Fichtel et al. (2012) identify chemolithotrophic sulfate-reducing bacteria from deep sediments at the Juan de Fuca Ridge flanks by enrichment, pure culture isolation and physiological testing in the laboratory.

Many microbial groups in the subsurface have no apparent connection to sulfate reduction and methane cycling, but they occur nevertheless in considerable abundance and ubiquity. Two studies of the coastal subsurface—a comprehensive examination of microbial community structure by qPCR, cloning and sequencing of functional and 16S rRNA genes in terrestrial deep sediments near Chesapeake Bay by Breuker et al. (2011), and a reverse transcript analysis of archaea in the methane/sulfate interface of estuarine sediments in Southern China by Li et al. (2012)—focused much of the overall effort on rRNA-based diversity analyses of the Miscellaneous Crenarcheotal Group (MCG), perhaps the most widespread archaeal group in subsurface sediments. The MCG archaea are at present the focus of single-cell sequencing analyses and metagenomic surveys, with the goal of inferring their metabolisms and culture requirements.

Most microbial surveys have focused on organic-rich subsurface sediments in nearshore or continental margin locations where anaerobic processes and populations could be more easily detected. At the opposite end of the spectrum, the oligotrophic subsurface—the organic-lean, non-sulfidic or

oxidized sediments of the open ocean which are representative for most of the seafloor and its sedimentary subsurface—is increasingly scrutinized by microbial community structure analyses, as performed in a pyrosequencing survey by Hoshino et al. (2011) in sediments of the Porcupine bight of the Eastern North Atlantic, and with heterotrophic activity measurements in central North-Atlantic deep sea sediments by Picard and Ferdelman (2011). The oligotrophic subsurface constitutes indeed a biogeochemically and microbiologically distinct habitat: in a theory and hypothesis article, Durbin and Teske (2012) synthesize the evidence for a phylum-level archaeal community shift from organic-rich and reduced sediments to organic-lean and oxidized marine subsurface sediments, and provide detailed phylogenies on many seldom-seen archaeal lineages from organic-lean sediments and hydrothermal vents.

Deep subsurface microbiology does not stop at the sediment/bedrock interface. The basaltic ocean crust is permeated by cracks and fissures that provide microbial habitat and an interface where rock-hosted microbial communities chemically modify the rock matrix. Viewed over long time frames, microbes act as a geological force that catalyzes the chemical alteration of the upper ocean crust, as summarized by Edwards et al. (2012). The energy reservoir of the deep basalt biosphere is demonstrated by a bore hole observatory at Hole ODP896A in the basaltic crust of the Costa Rica Rise; its microbial ecosystem containing a large proportion of autotrophic sulfur oxidizers is sustained by subsurface mixing of reduced formation fluid and oxic seawater—a discovery by Nigro et al. (2012). In a comprehensive metagenomic survey of a different type of rock-hosted microbial ecosystem, Brazelton et al. (2012) are exploring the methanogenic and hydrogenotrophic microbiota fuelled by serpentinization reactions, focusing on terrestrial serpentinite springs on Newfoundland and comparing their metagenomes to those of the previously studied Lost City vents. The rock-hosted terrestrial subsurface biosphere is often more accessible than its marine counterpart, and allows repeated biogeochemical and microbial sampling in mines and boreholes; such accessibility facilitates targeted investigations of specific pathways and processes, for example nitrogen fixation and nitrification in deep granite-hosted ores in Colorado studied by Swanner and Templeton (2011). An overlooked extreme subsurface habitat that requires more microbiological study are mile-deep ice cores; their microbial inhabitants are introduced here by an Ice-binding protein study of a *Flavobacterium* isolated from the deepest ice core segments (close to rock basement) at Station Vostok in Antarctica by Achberger et al. (2011).

Several papers in this volume are addressing methodological advances in deep subsurface microbiology, which are crucial for further progress in this field. New hardware for high-pressure microbial incubations, plus instructions how to build this in your own workshop, is being introduced by Sauer et al. (2012); caution in the long-term storage of microbial samples at 4°C is advocated by Mills et al. (2012a) after they documented storage-related microbial community shifts by high-throughout sequencing; and previously published cell counting protocols for deep subsurface sediments are further refined by Lappé and Kallmeyer (2011) specifically for hydrocarbon-rich sediments.

The volume concludes with papers that provide an evolutionary and genomic perspective on the deep microbial biosphere. Biddle et al. (2012) ponder the future of microbial evolution studies in the subsurface; they advocate to select and study model organisms and phylogenetically defined groups within defined environmental gradients as a promising strategy. To facilitate big-picture genomic surveys, Martino et al. (2012) introduce a novel degenerate PCR primer strategy for metagenomic recovery of unknown microbial communities from the deep subsurface. Anderson et al. (2011) integrate and review the evidence for viral infection of subsurface bacteria and archaea, and for a substantial viral contribution to hydrothermal vent and subsurface metagenomes, while reflecting on the different selection pressures that shape viral communities in these habitats.

This e-volume includes both new methodologies and research strategies that should yield promising results in the future, and expands our current view of deep subsurface microbiology with innovative studies of a wide range of subsurface habitats and microbial ecosystems. There is ample room for further exploration; we note that several areas in subsurface microbiology remain severely understudied. The eukaryotic, mostly fungal subsurface biosphere has only recently been discovered and is being investigated by volume editors Edgcomb and Biddle. The exploration of the deep biosphere in the ocean crust has just started and opens major research opportunities. Unlike marine sediments where photosynthesis-derived buried organic carbon sustains microbial life, inorganic processes in the ocean crusts likely provide the main energy sources for the rock-hosted deep biosphere. The terrestrial deep subsurface and the oceanic crust biosphere remain to be quantified, and overall microbial diversity and function of these microbiota remain to be accounted for across a wide range of geological settings and sampling sites. Everywhere in the subsurface, the study of microbial physiology, the cultivation of novel types of microorganisms, and biochemical analyses of subsurface life strategies remain high on the list of current and future research challenges. Overall, continued in-depth exploration of subsurface biomes will continually yield new insights on microbial adaptation and survival under extreme conditions.

REFERENCES

Achberger, A. M., Brox, T. I., Skidmore, M. L., and Christner, B. C. (2011). Expression and partial characterization of an ice-binding protein from a bacterium isolated at a depth of 3,519 m in the vostok ice core, antarctica. *Front. Microbio.* 2:255. doi: 10.3389/fmicb.2011.00255

Anderson, R. E., Brazelton, W. J., and Baross, J. A. (2011). Is the genetic landscape of the deep subsurface biosphere affected by viruses? *Front. Microbio.* 2:219. doi: 10.3389/fmicb.2011.00219

Biddle, J. F., Sylvan, J. B., Brazelton, W. J., Tully, B. J., Edwards, K. J., Moyer, C. L., et al. (2012). Prospects for the study of evolution in the deep biosphere. *Front. Microbio.* 2:285. doi: 10.3389/fmicb.2011.00285

Blazejak, A., and Schippers, A. (2011). Real-time PCR quantification and diversity analysis of the functional genes aprA and dsrA of sulfate-reducing prokaryotes in marine sediments of the Peru continental margin and the Black Sea. *Front. Microbio.* 2:253. doi: 10.3389/fmicb.2011.00253

Brazelton, W. J., Nelson, B., and Schrenk, M. O. (2012). Metagenomic evidence for H_2 oxidation and H_2 production by serpentinite-hosted subsurface microbial communities.

Front. Microbio. 2:268. doi: 10.3389/fmicb.2011.00268

Breuker, A., Köweker, G., Blazejak, A., and Schippers, A. (2011). The deep biosphere in terrestrial sediments in the chesapeake Bay area, Virginia, USA. *Front. Microbio.* 2:156. doi: 10.3389/fmicb.2011.00156

Durbin, A. M., and Teske, A. (2012). Archaea in organic-lean and organic-rich marine subsurface sediments: an environmental gradient reflected in distinct phylogenetic lineages. *Front. Microbio.* 3:168. doi: 10.3389/fmicb.2012.00168

Edwards, K. J., Fisher, A. T., and Wheat, C. G. (2012). The deep subsurface biosphere in igneous ocean crust: frontier habitats for microbiological exploration. *Front. Microbio.* 3:8. doi: 10.3389/fmicb.2012.00008

Fichtel, K., Mathes, F., Könneke, M., Cypionka, H., and Engelen, B. (2012). Isolation of sulfate-reducing bacteria from sediments above the deep-subseafloor aquifer. *Front. Microbio.* 3:65. doi: 10.3389/fmicb.2012.00065

Hoshino, T., Morono, Y., Terada, T., Imachi, H., Ferdelman, T. G., and Inagaki, F. (2011). Comparative study of subseafloor microbial community structures in deeply buried coral fossils and sediment matrices from the challenger mound in the porcupine seabight. *Front. Microbio.* 2:231. doi: 10.3389/fmicb.2011.00231

Lappé, M., and Kallmeyer, J. (2011). A cell extraction method for oily sediments. *Front. Microbio.* 2:233. doi: 10.3389/fmicb.2011.00233

Lever, M. A. (2012). Acetogenesis in the energy-starved deep biosphere - a paradox? *Front. Microbio.* 2:284. doi: 10.3389/fmicb.2011.00284

Li, Q., Wang, F., Chen, Z., Yin, X., and Xiao, X. (2012). Stratified active archaeal communities in the sediments of Jiulong River estuary, China. *Front. Microbio.* 3:311. doi: 10.3389/fmicb.2012.00311

Martino, A. J., Rhodes, M. E., Biddle, J. F., Brandt, L. D., Tomsho, L. P., and House, C. H. (2012). Novel degenerate PCR method for whole-genome amplification applied to Peru Margin (ODP Leg 201) subsurface samples. *Front. Microbio.* 3:17. doi: 10.3389/fmicb.2012.00017

Mills, H. J., Reese, B. K., and Peter, C. S. (2012a). Characterization of microbial population shifts during sample storage. *Front. Microbio.* 3:49. doi: 10.3389/fmicb.2012.00049

Mills, H. J., Reese, B. K., Shepard, A. K., Riedinger, N., Dowd, S. E., Morono, Y., et al. (2012b). Characterization of metabolically active bacterial populations in subseafloor Nankai Trough sediments above, within, and below the sulfate–methane transition zone. *Front. Microbio.* 3:113. doi: 10.3389/fmicb.2012.00113

Nigro, L. M., Harris, K., Orcutt, B. N., Hyde, A., Clayton-Luce, S., Becker, K., et al. (2012). Microbial communities at the borehole observatory on the costa rica rift flank (Ocean Drilling Program Hole 896A). *Front. Microbio.* 3:232. doi: 10.3389/fmicb.2012.00232

Oren, A. (2012). There must be an acetogen somewhere. *Front. Microbiol.* 3:22. doi: 10.3389/fmicb.2012.00022

Picard, A., and Ferdelman, T. G. (2011). Linking microbial heterotrophic activity and sediment lithology in oxic, oligotrophic sub-seafloor sediments of the North Atlantic Ocean. *Front. Microbio.* 2:263. doi: 10.3389/fmicb.2011.00263

Sauer, P., Glombitza, C., and Kallmeyer, J. (2012). A system for incubations at high gas partial pressure. *Front. Microbio.* 3:25. doi: 10.3389/fmicb.2012.00025

Schippers, A., Kock, D., Höft, C., Köweker, G., and Siegert, M. (2012). Quantification of microbial communities in subsurface marine sediments of the Black Sea and off Namibia. *Front. Microbio.* 3:16. doi: 10.3389/fmicb.2012.00016

Siegert, M., Krüger, M., Teichert, B., Wiedicke, M., and Schippers, A. (2011). Anaerobic oxidation of methane at a marine methane seep in a forearc sediment basin off Sumatra, Indian Ocean. *Front. Microbio.* 2:249. doi: 10.3389/fmicb.2011.00249

Swanner, E. D., and Templeton, A. S. (2011). Potential for nitrogen fixation and nitrification in the granite-hosted subsurface at Henderson Mine, CO. *Front. Microbio.* 2:254. doi: 10.3389/fmicb.2011.00254

Ünal, B., Perry, V. R., Sheth, M., Gomez-Alvarez, V., Chin, K.-J., and Nüsslein, K. (2012). Trace elements affect methanogenic activity and diversity in enrichments from subsurface coal bed produced water. *Front. Microbio.* 3:175. doi: 10.3389/fmicb.2012.00175

Received: 25 April 2013; accepted: 30 April 2013; published online: 16 May 2013.

Citation: Teske A, Biddle JF, Edgcomb VP and Schippers A (2013) Deep subsurface microbiology: a guide to the research topic papers. Front. Microbiol. ***4****:122. doi: 10.3389/fmicb.2013.00122*

This article was submitted to Frontiers in Extreme Microbiology, a specialty of Frontiers in Microbiology.